

# The NJOY Nuclear Data Processing System, Version 2012

Original Author: R. E. MacFarlane  
Theoretical Division  
Los Alamos National Laboratory

Contributing Authors  
D. W. Muir  
R. M. Boicourt  
A. C. Kahler

Current Editor: A. C. Kahler

Original Issue: December 20, 2012

Updated for NJOY2012.50

February 12, 2015

## **Abstract**

The NJOY Nuclear Data Processing System is a comprehensive computer code package for producing pointwise and multigroup cross sections and related quantities from evaluated nuclear data in the ENDF format, including the latest US library, ENDF/B-VII. The NJOY code can work with neutrons, photons, and charged particles, and it can produce libraries for a wide variety of particle transport and reactor analysis codes. NJOY2012 packages all the capabilities of the recent versions of NJOY, plus a few new options, using modern modularized Fortran-90 style.

### **Disclaimer of Liability:**

Neither the United States Government nor the Los Alamos National Security, LLC., nor any of their employees, makes any warranty, express or implied, including the warranties of merchantability and fitness for a particular purpose, or assumes any legal liability or responsibility for the accuracy, completeness, or usefulness of any information, apparatus, product, or process disclosed, or represents that its use would not infringe privately owned rights.

### **Disclaimer of Endorsement:**

Reference herein to any specific commercial products, process, or service by trade name, trademark, manufacturer, or otherwise, does not necessarily constitute or imply its endorsement, recommendation, or favoring by the United States Government or the Los Alamos National Security, LLC. The views and opinions of authors expressed herein do not necessarily state or reflect those of the United States Government or the Los Alamos National Security, LLC., and shall not be used for advertising or product endorsement purposes.

# Contents

|                                                         |            |
|---------------------------------------------------------|------------|
| <b>Contents</b>                                         | <b>iii</b> |
| <b>List of Figures</b>                                  | <b>ix</b>  |
| <b>List of Tables</b>                                   | <b>xii</b> |
| <b>1 INTRODUCTION</b>                                   | <b>1</b>   |
| 1.1 The Modules of NJOY . . . . .                       | 1          |
| 1.2 Data Flow in NJOY . . . . .                         | 3          |
| 1.3 Computer Implementation . . . . .                   | 7          |
| 1.4 History and Acknowledgments . . . . .               | 8          |
| <b>2 NJOY</b>                                           | <b>19</b>  |
| 2.1 The NJOY Program . . . . .                          | 19         |
| 2.2 Interface Files . . . . .                           | 21         |
| 2.3 Free Format Input . . . . .                         | 22         |
| 2.4 ENDF Input-Output . . . . .                         | 23         |
| 2.5 Buffered Binary Scratch Storage . . . . .           | 27         |
| 2.6 Dynamic Storage Allocation . . . . .                | 28         |
| 2.7 ENDF/B Utility Routines . . . . .                   | 28         |
| 2.8 Math Routines . . . . .                             | 29         |
| 2.9 System-Related Utility Routines . . . . .           | 29         |
| 2.10 Error and Warning Messages . . . . .               | 30         |
| 2.11 Coding Details for the NJOY Main Program . . . . . | 33         |
| <b>3 RECONR</b>                                         | <b>43</b>  |
| 3.1 ENDF/B Cross Section Representations . . . . .      | 44         |
| 3.2 Unionization and Linearization Strategy . . . . .   | 45         |
| 3.3 Linearization and Reconstruction Methods . . . . .  | 46         |
| 3.4 Resonance Representations . . . . .                 | 51         |
| 3.5 Code Description . . . . .                          | 65         |
| 3.6 Input Instructions . . . . .                        | 71         |
| 3.7 Error Messages . . . . .                            | 73         |
| 3.8 Input-Output Units . . . . .                        | 75         |
| 3.9 Storage Allocation . . . . .                        | 76         |
| <b>4 BROADR</b>                                         | <b>77</b>  |
| 4.1 Doppler-Broadening Theory . . . . .                 | 78         |
| 4.2 Thermal Quantities . . . . .                        | 83         |
| 4.3 Data-Paging Methodology . . . . .                   | 84         |
| 4.4 Coding Details . . . . .                            | 85         |
| 4.5 User Input . . . . .                                | 88         |
| 4.6 Error Messages . . . . .                            | 91         |
| 4.7 Input/Output Units . . . . .                        | 92         |
| 4.8 Storage Allocation . . . . .                        | 92         |

|          |                                                          |            |
|----------|----------------------------------------------------------|------------|
| <b>5</b> | <b>UNRESR</b>                                            | <b>93</b>  |
| 5.1      | Theory . . . . .                                         | 93         |
| 5.2      | Implementation . . . . .                                 | 106        |
| 5.3      | User Input . . . . .                                     | 109        |
| 5.4      | Output Example . . . . .                                 | 110        |
| 5.5      | Coding Details . . . . .                                 | 111        |
| 5.6      | Error Messages . . . . .                                 | 114        |
| <b>6</b> | <b>HEATR</b>                                             | <b>115</b> |
| 6.1      | Theory of Nuclear Heating . . . . .                      | 115        |
| 6.2      | Theory of Damage Energy . . . . .                        | 119        |
| 6.3      | Computation of KERMA Factors By Energy Balance . . . . . | 121        |
| 6.4      | Kinematic Limits . . . . .                               | 123        |
| 6.5      | Computation of Damage Energy . . . . .                   | 126        |
| 6.6      | Heating and Damage from File 6 . . . . .                 | 129        |
| 6.7      | User Input . . . . .                                     | 132        |
| 6.8      | Reading HEATR Output . . . . .                           | 136        |
| 6.9      | Diagnosing Energy-Balance Problems . . . . .             | 146        |
| 6.10     | Coding Details . . . . .                                 | 150        |
| 6.11     | Error Messages . . . . .                                 | 160        |
| 6.12     | Storage Allocation . . . . .                             | 163        |
| <b>7</b> | <b>THERMR</b>                                            | <b>165</b> |
| 7.1      | Coherent Elastic Scattering . . . . .                    | 166        |
| 7.2      | Incoherent Inelastic Scattering . . . . .                | 168        |
| 7.3      | Incoherent Elastic Scattering . . . . .                  | 174        |
| 7.4      | Coding Details . . . . .                                 | 174        |
| 7.5      | Using the ENDF/B Thermal Data Files . . . . .            | 179        |
| 7.6      | Input Instructions . . . . .                             | 181        |
| 7.7      | Error Messages . . . . .                                 | 184        |
| 7.8      | Input/Output Units . . . . .                             | 186        |
| 7.9      | Storage Allocation . . . . .                             | 186        |
| <b>8</b> | <b>GROUPE</b>                                            | <b>187</b> |
| 8.1      | Multigroup Constants . . . . .                           | 188        |
| 8.2      | Group Ordering . . . . .                                 | 190        |
| 8.3      | Basic ENDF Cross Sections . . . . .                      | 191        |
| 8.4      | Weighting Flux . . . . .                                 | 191        |
| 8.5      | Flux Calculator . . . . .                                | 198        |
| 8.6      | Fission Source . . . . .                                 | 201        |
| 8.7      | Diffusion Cross Sections . . . . .                       | 204        |
| 8.8      | Cross Sections for Transport Theory . . . . .            | 205        |
| 8.9      | Photon Production and Coupled Sets . . . . .             | 207        |
| 8.10     | Thermal Data . . . . .                                   | 209        |
| 8.11     | Generalized Group Integrals . . . . .                    | 211        |
| 8.12     | Two-Body Scattering . . . . .                            | 214        |
| 8.13     | Charged-Particle Elastic Scattering . . . . .            | 217        |
| 8.14     | Continuum Scattering and Fission . . . . .               | 218        |
| 8.15     | File 6 Energy-Angle Distributions . . . . .              | 224        |
| 8.16     | Smoothing . . . . .                                      | 227        |
| 8.17     | GENDF Output . . . . .                                   | 228        |

|           |                                                                                               |            |
|-----------|-----------------------------------------------------------------------------------------------|------------|
| 8.18      | Running GROUPR . . . . .                                                                      | 230        |
| 8.19      | Coding Details . . . . .                                                                      | 251        |
| 8.20      | Error Messages . . . . .                                                                      | 264        |
| <b>9</b>  | <b>GAMINR</b>                                                                                 | <b>271</b> |
| 9.1       | Description of ENDF/B Photon Interaction Files . . . . .                                      | 272        |
| 9.2       | Calculational Method . . . . .                                                                | 273        |
| 9.3       | Integrals Involving Form Factors . . . . .                                                    | 274        |
| 9.4       | Coding Details . . . . .                                                                      | 276        |
| 9.5       | User Input . . . . .                                                                          | 276        |
| 9.6       | Error Messages . . . . .                                                                      | 279        |
| 9.7       | I/O Units . . . . .                                                                           | 282        |
| <b>10</b> | <b>ERRORR</b>                                                                                 | <b>283</b> |
| 10.1      | Introduction . . . . .                                                                        | 283        |
| 10.2      | Definitions of Covariance-Related Quantities . . . . .                                        | 285        |
| 10.3      | Structure of ENDF Files 31, 33, and 40: Energy-Dependent Data . . . . .                       | 287        |
| 10.4      | Resonance-Parameter Formats—File 32 . . . . .                                                 | 292        |
| 10.5      | Secondary Particle Angular Distribution Covariances—File 34 . . . . .                         | 295        |
| 10.6      | Secondary Particle Energy Distribution Covariances—File 35 . . . . .                          | 295        |
| 10.7      | Radioactive Nuclide Production Covariances—File 40 . . . . .                                  | 297        |
| 10.8      | Calculation of Multigroup Fluxes, Cross Sections, and Covariances on the Union Grid . . . . . | 300        |
| 10.9      | Basic Strategy for Collapse to the User Grid . . . . .                                        | 304        |
| 10.10     | Group-Collapse Strategy for Data Derived by Summation . . . . .                               | 305        |
| 10.11     | Processing of Data Derived from Ratio Measurements . . . . .                                  | 308        |
| 10.12     | Multigroup Processing of Resonance-Parameter Uncertainties . . . . .                          | 312        |
| 10.13     | Processing of Lumped-Partial Covariances . . . . .                                            | 313        |
| 10.14     | Input Instructions and Sample Input for ERRORR . . . . .                                      | 313        |
| 10.15     | ERRORR Output File Specification . . . . .                                                    | 334        |
| 10.16     | Error Messages . . . . .                                                                      | 342        |
| 10.17     | Input/Output Units . . . . .                                                                  | 350        |
| <b>11</b> | <b>COVR</b>                                                                                   | <b>353</b> |
| 11.1      | Introduction . . . . .                                                                        | 353        |
| 11.2      | Production of Boxer-Format Libraries . . . . .                                                | 353        |
| 11.3      | Generation of Plots . . . . .                                                                 | 355        |
| 11.4      | Input Instructions for COVR . . . . .                                                         | 358        |
| 11.5      | COVR Example Problem . . . . .                                                                | 364        |
| 11.6      | Error Messages . . . . .                                                                      | 366        |
| 11.7      | Input/Output Units . . . . .                                                                  | 367        |
| 11.8      | Retrieval Program for COVR Output Libraries . . . . .                                         | 368        |
| <b>12</b> | <b>MODER</b>                                                                                  | <b>373</b> |
| 12.1      | Code Description . . . . .                                                                    | 373        |
| 12.2      | Input Instructions . . . . .                                                                  | 373        |
| 12.3      | Sample Input . . . . .                                                                        | 375        |
| 12.4      | Error Messages . . . . .                                                                      | 376        |

|                                                             |            |
|-------------------------------------------------------------|------------|
| <b>13 DTFR</b>                                              | <b>379</b> |
| 13.1 Transport Tables . . . . .                             | 379        |
| 13.2 Data Representations . . . . .                         | 382        |
| 13.3 Plotting . . . . .                                     | 388        |
| 13.4 User Input . . . . .                                   | 391        |
| 13.5 Coding Details . . . . .                               | 396        |
| 13.6 Error Messages . . . . .                               | 398        |
| <b>14 CCCC</b>                                              | <b>399</b> |
| 14.1 Introduction . . . . .                                 | 399        |
| 14.2 CCCC Procedures and Programming Standards . . . . .    | 400        |
| 14.3 The Standard Interface Files . . . . .                 | 403        |
| 14.4 ISOTXS . . . . .                                       | 404        |
| 14.5 BRKOXS . . . . .                                       | 419        |
| 14.6 DLAYXS . . . . .                                       | 426        |
| 14.7 Coding Details . . . . .                               | 431        |
| 14.8 User Input . . . . .                                   | 440        |
| 14.9 Error Messages . . . . .                               | 446        |
| <b>15 MATXSR</b>                                            | <b>449</b> |
| 15.1 Background . . . . .                                   | 449        |
| 15.2 The MATXS Format . . . . .                             | 451        |
| 15.3 Historical Notes . . . . .                             | 470        |
| 15.4 MATXS Libraries . . . . .                              | 471        |
| 15.5 User Input . . . . .                                   | 477        |
| 15.6 Coding Details . . . . .                               | 480        |
| 15.7 Error Messages . . . . .                               | 486        |
| <b>16 RESXSR</b>                                            | <b>489</b> |
| 16.1 Method . . . . .                                       | 489        |
| 16.2 RESXS Format Specification . . . . .                   | 490        |
| 16.3 User Input . . . . .                                   | 493        |
| <b>17 ACER</b>                                              | <b>495</b> |
| 17.1 ACER and ACE Data Classes . . . . .                    | 495        |
| 17.2 Continuous-Energy Neutron Data . . . . .               | 496        |
| 17.3 Energy Grids and Cross Sections . . . . .              | 497        |
| 17.4 Two-Body Scattering Distributions . . . . .            | 500        |
| 17.5 Secondary-Energy Distributions . . . . .               | 501        |
| 17.6 Energy-Angle Distributions . . . . .                   | 501        |
| 17.7 Photon Production . . . . .                            | 506        |
| 17.8 Probability Tables for the Unresolved Region . . . . . | 508        |
| 17.9 Charged-Particle Production . . . . .                  | 508        |
| 17.10 Gas Production . . . . .                              | 509        |
| 17.11 Consistency Checks and Plotting . . . . .             | 510        |
| 17.12 Thermal Cross Sections . . . . .                      | 511        |
| 17.13 Dosimetry Cross Sections . . . . .                    | 515        |
| 17.14 Photoatomic Data . . . . .                            | 516        |
| 17.15 Photonuclear Data . . . . .                           | 517        |
| 17.16 Type 1 and Type 2 . . . . .                           | 518        |
| 17.17 Running ACER . . . . .                                | 519        |

|                                                       |            |
|-------------------------------------------------------|------------|
| 17.18 Coding Details . . . . .                        | 527        |
| 17.19 Error Messages . . . . .                        | 542        |
| <b>18 POWER</b>                                       | <b>547</b> |
| 18.1 Input Instructions . . . . .                     | 547        |
| <b>19 WIMSR</b>                                       | <b>553</b> |
| 19.1 Resonance Integrals . . . . .                    | 553        |
| 19.2 Cross Sections . . . . .                         | 557        |
| 19.3 Burn Data . . . . .                              | 560        |
| 19.4 User Input . . . . .                             | 560        |
| 19.5 Coding Details . . . . .                         | 565        |
| 19.6 WIMS Data File Format . . . . .                  | 568        |
| 19.7 WIMSR Auxiliary Codes . . . . .                  | 572        |
| 19.8 Error Messages . . . . .                         | 572        |
| <b>20 PLOTR</b>                                       | <b>575</b> |
| 20.1 Simple 2-D Plots . . . . .                       | 576        |
| 20.2 Multicurve and Multigroup Plots . . . . .        | 579        |
| 20.3 Right-Hand Axes . . . . .                        | 584        |
| 20.4 Plotting Input Data . . . . .                    | 586        |
| 20.5 Three-D Plots of Angular Distributions . . . . . | 587        |
| 20.6 Three-D Plots of Energy Distributions . . . . .  | 588        |
| 20.7 Two-D Spectra Plots from Files 5 and 6 . . . . . | 590        |
| 20.8 Input Instructions . . . . .                     | 592        |
| 20.9 Coding Details . . . . .                         | 599        |
| 20.10 Storage Allocation . . . . .                    | 601        |
| 20.11 Input and Output Units . . . . .                | 601        |
| 20.12 Error Messages . . . . .                        | 602        |
| <b>21 VIEWR</b>                                       | <b>603</b> |
| 21.1 Modular Structure . . . . .                      | 603        |
| 21.2 Using VIEWR . . . . .                            | 604        |
| 21.3 Input Instructions . . . . .                     | 604        |
| 21.4 Coding Details . . . . .                         | 616        |
| 21.5 The Graphics Module . . . . .                    | 618        |
| 21.6 VIEWR Messages . . . . .                         | 621        |
| <b>22 MIXR</b>                                        | <b>623</b> |
| 22.1 User Input . . . . .                             | 623        |
| 22.2 Coding Details . . . . .                         | 628        |
| 22.3 Error Messages . . . . .                         | 628        |
| <b>23 PURR</b>                                        | <b>631</b> |
| 23.1 Sampling from Ladders . . . . .                  | 631        |
| 23.2 Temperature Correlations . . . . .               | 637        |
| 23.3 Self-Shielded Heating Values . . . . .           | 637        |
| 23.4 Random Numbers . . . . .                         | 638        |
| 23.5 User Input . . . . .                             | 638        |
| 23.6 Coding Details . . . . .                         | 639        |
| 23.7 Error Messages . . . . .                         | 645        |

|                                                |            |
|------------------------------------------------|------------|
| <b>24 LEAPR</b>                                | <b>647</b> |
| 24.1 Theory . . . . .                          | 648        |
| 24.2 Input Instructions . . . . .              | 664        |
| 24.3 LEAPR Examples . . . . .                  | 670        |
| 24.4 Coding Details . . . . .                  | 710        |
| 24.5 Error Messages . . . . .                  | 714        |
| <b>25 GASPR</b>                                | <b>717</b> |
| 25.1 Gas Production . . . . .                  | 717        |
| 25.2 User Input . . . . .                      | 718        |
| 25.3 Coding Details . . . . .                  | 719        |
| 25.4 Error Messages . . . . .                  | 719        |
| <b>26 NJOY Maintenance and Testing</b>         | <b>721</b> |
| 26.1 Code Maintenance with UPD . . . . .       | 721        |
| 26.2 Code Conversion . . . . .                 | 725        |
| 26.3 Standard Test Problems . . . . .          | 725        |
| 26.4 Test Problem 1 . . . . .                  | 727        |
| 26.5 Test Problem 2 . . . . .                  | 731        |
| 26.6 Test Problem 3 . . . . .                  | 734        |
| 26.7 Test Problem 4 . . . . .                  | 736        |
| 26.8 Test Problem 5 . . . . .                  | 737        |
| 26.9 Test Problem 6 . . . . .                  | 739        |
| 26.10 Test Problem 7 . . . . .                 | 741        |
| 26.11 Test Problem 8 . . . . .                 | 743        |
| 26.12 Test Problem 9 . . . . .                 | 744        |
| 26.13 Test Problem 10 . . . . .                | 747        |
| 26.14 Test Problem 11 . . . . .                | 748        |
| 26.15 Test Problem 12 . . . . .                | 751        |
| 26.16 Test Problem 13 . . . . .                | 752        |
| 26.17 Test Problem 14 . . . . .                | 754        |
| 26.18 Test Problem 15 . . . . .                | 755        |
| 26.19 Test Problem 16 . . . . .                | 758        |
| 26.20 Test Problem 17 . . . . .                | 761        |
| 26.21 Test Problem 18 . . . . .                | 764        |
| 26.22 Test Problem 19 . . . . .                | 767        |
| 26.23 Test Problem 20 . . . . .                | 769        |
| 26.24 Application of the NJOY System . . . . . | 770        |
| <b>References</b>                              | <b>775</b> |
| <b>Index</b>                                   | <b>785</b> |



## List of Figures

|    |                                                                                                                            |     |
|----|----------------------------------------------------------------------------------------------------------------------------|-----|
| 1  | RECONR reconstructed xs with smooth, RR and URR regions . . . . .                                                          | 44  |
| 2  | Inverted stack mesh generation description . . . . .                                                                       | 47  |
| 3  | $^{19}\text{F}$ elastic scattering Legendre coefficients from RML data . . . . .                                           | 63  |
| 4  | The $^{10}\text{B}$ (n, $\alpha$ ) cross section versus Doppler broadening temperature . .                                 | 81  |
| 5  | The $^{nat}\text{C}$ elastic scattering cross section versus Doppler broadening temperature . . . . .                      | 82  |
| 6  | The $^{240}\text{Pu}$ low energy (n, $\gamma$ ) cross section versus Doppler broadening temperature . . . . .              | 82  |
| 7  | Energy grid variation with Doppler broadening . . . . .                                                                    | 83  |
| 8  | Components of nuclear heating . . . . .                                                                                    | 116 |
| 9  | Sample recoil energy and lattice displacement data . . . . .                                                               | 120 |
| 10 | Components of radiation damage energy production for $^{27}\text{Al}$ . . . . .                                            | 129 |
| 11 | Total photon energy production and kinematic limits for $^{55}\text{Mn}$ . . . . .                                         | 144 |
| 12 | MT301 and MT443 for $^{59}\text{Co}$ . . . . .                                                                             | 147 |
| 13 | Example of File 3 and File 13 energy grid mis-match . . . . .                                                              | 148 |
| 14 | Example of energy-balance problems . . . . .                                                                               | 148 |
| 15 | Computed photon energy production and kinematic values . . . . .                                                           | 149 |
| 16 | Example of coherent elastic cross section for a crystalline material (graphite)                                            | 167 |
| 17 | Adaptive reconstruction of emission spectra (graphite) . . . . .                                                           | 171 |
| 18 | Neutron distribution for incoherent inelastic scattering from graphite (T = 293.6K) . . . . .                              | 172 |
| 19 | Neutron distribution for incoherent inelastic scattering from graphite (T = 293.6K), expanded view . . . . .               | 172 |
| 20 | Distributions for H in $\text{H}_2\text{O}$ with $E$ - $\mu$ - $E'$ ordering . . . . .                                     | 173 |
| 21 | Incoherent inelastic distribution for H- $\text{H}_2\text{O}$ (expanded view) . . . . .                                    | 183 |
| 22 | Pointwise and multigroup cross section comparison . . . . .                                                                | 192 |
| 23 | The self-shielding effect on the first three $^{238}\text{U}$ capture resonances. . . .                                    | 197 |
| 24 | $^{238}\text{U}$ capture resonance integral versus temperature and background cross section . . . . .                      | 197 |
| 25 | Flux model predictions for $^{238}\text{UO}_2$ in water in the region near the 6.7 eV $^{238}\text{U}$ resonance . . . . . | 200 |
| 26 | Coupled Neutron/Photon Tables . . . . .                                                                                    | 208 |
| 27 | Bragg edges seen in the BeO coherent elastic scattering cross section . .                                                  | 210 |
| 28 | Interpolation along lines of constant energy transfer . . . . .                                                            | 211 |
| 29 | Sample two-body scattering feed function . . . . .                                                                         | 216 |
| 30 | Coordinate mapping between CM and LAB reference frames for A=2 . . . .                                                     | 226 |
| 31 | GROUPR weight functions on a logarithmic flux/unit lethargy scale . . .                                                    | 236 |
| 32 | GROUPR weight functions on a linear energy scale . . . . .                                                                 | 237 |
| 33 | Coupled neutron-proton-photon table . . . . .                                                                              | 250 |
| 34 | Photon coherent scattering angular distributions . . . . .                                                                 | 275 |
| 35 | Photon interaction cross sections for uranium . . . . .                                                                    | 280 |
| 36 | Photon interaction cross sections for hydrogen . . . . .                                                                   | 280 |
| 37 | ENDF/B-VII.0 Uranium photoelectric subshell cross sections . . . . .                                                       | 281 |
| 38 | ENDF/B-VII.0 $^{10}\text{B}$ (n, $\alpha$ ) covariance data . . . . .                                                      | 284 |
| 39 | Example of elastic scattering and (n, $n_1$ ) covariance data . . . . .                                                    | 294 |
| 40 | Example of angular distribution covariance data . . . . .                                                                  | 296 |
| 41 | $^{252}\text{Cf}$ (n,f) spontaneous fission spectrum covariance data . . . . .                                             | 298 |
| 42 | Radioactive nuclide production covariance example . . . . .                                                                | 299 |
| 43 | Illustration of energy grid relations. . . . .                                                                             | 300 |

|    |                                                                                                                                      |     |
|----|--------------------------------------------------------------------------------------------------------------------------------------|-----|
| 44 | Ratioed covariance data for $^{239}\text{Pu}(\text{n},\text{f})$ and $^{241}\text{Am}(\text{n},\text{f})$ cross sections . .         | 311 |
| 45 | $^7\text{Li}$ “Lumped” covariance data . . . . .                                                                                     | 314 |
| 46 | Illustration of Boxer format . . . . .                                                                                               | 356 |
| 47 | Pattern-search logic in used in COVR’s subroutine matshd . . . . .                                                                   | 358 |
| 48 | DTFR cross section plot example . . . . .                                                                                            | 388 |
| 49 | DTFR cross section plot example, expanded energy range . . . . .                                                                     | 389 |
| 50 | DTFR scattering matrix plot example . . . . .                                                                                        | 389 |
| 51 | DTFR photon production matrix plot example . . . . .                                                                                 | 390 |
| 52 | DTFR plot example, multiple plots per frame . . . . .                                                                                | 390 |
| 53 | DTFR plot example, compound edit . . . . .                                                                                           | 394 |
| 54 | Principal cross sections for ENDF/B-VII.0 $^{27}\text{Al}$ . . . . .                                                                 | 511 |
| 55 | Neutron energy distributions from $^{27}\text{Al}(\text{n},\text{n}'\alpha)$ reaction . . . . .                                      | 512 |
| 56 | Neutron scattering distribution from H in $\text{H}_2\text{O}$ . . . . .                                                             | 516 |
| 57 | Sample 2-D plot with default axes . . . . .                                                                                          | 577 |
| 58 | Sample 2-D plot with modified axes . . . . .                                                                                         | 578 |
| 59 | Sample 2-D plot with linear axes . . . . .                                                                                           | 579 |
| 60 | Sample plot with pointwise and multigroup data . . . . .                                                                             | 581 |
| 61 | Sample plot displaying self-shielded cross sections . . . . .                                                                        | 582 |
| 62 | Sample plot with left- and right-hand axes defined . . . . .                                                                         | 584 |
| 63 | Sample plot with user data . . . . .                                                                                                 | 587 |
| 64 | Sample 3-D plot of angular distribution data . . . . .                                                                               | 589 |
| 65 | Sample 3-D plot of neutron secondary-energy distribution data . . . . .                                                              | 590 |
| 66 | Sample 2-D plot of neutron secondary-energy distribution data . . . . .                                                              | 592 |
| 67 | Sample region fill options in VIEWR . . . . .                                                                                        | 614 |
| 68 | Sample 3-D plot with default axis and perspective . . . . .                                                                          | 615 |
| 69 | Sample total cross section probability distributions . . . . .                                                                       | 634 |
| 70 | Bondarenko-style self-shielding . . . . .                                                                                            | 635 |
| 71 | Self-shielding variation with temperature and dilution . . . . .                                                                     | 636 |
| 72 | Graphite phonon frequency spectrum . . . . .                                                                                         | 674 |
| 73 | Coherent elastic scattering cross section for graphite . . . . .                                                                     | 674 |
| 74 | Incoherent elastic scattering cross section for graphite . . . . .                                                                   | 675 |
| 75 | Frequency spectra for $\text{BeO}$ . . . . .                                                                                         | 677 |
| 76 | The frequency spectrum for H in $\text{H}_2\text{O}$ . . . . .                                                                       | 678 |
| 77 | $\mathcal{S}(\alpha, -\beta)$ for H in $\text{H}_2\text{O}$ at room temperature . . . . .                                            | 687 |
| 78 | S-hat vs beta . . . . .                                                                                                              | 688 |
| 79 | Incoherent inelastic spectra for H in $\text{H}_2\text{O}$ . . . . .                                                                 | 688 |
| 80 | Incoherent inelastic spectra for H in $\text{H}_2\text{O}$ , detailed view . . . . .                                                 | 689 |
| 81 | The incoherent inelastic cross section for H in $\text{H}_2\text{O}$ at two temperatures . . . . .                                   | 689 |
| 82 | The incoherent inelastic cross section for H in $\text{H}_2\text{O}$ for higher incident energies . . . . .                          | 690 |
| 83 | The average scattering cosine for H in $\text{H}_2\text{O}$ compared to the static value for scattering from atoms at rest . . . . . | 691 |
| 84 | A perspective view of an angle-energy distribution for H in $\text{H}_2\text{O}$ . . . . .                                           | 692 |
| 85 | A perspective view of the isotropic part of the incoherent inelastic scattering from H in $\text{H}_2\text{O}$ . . . . .             | 692 |
| 86 | Comparison of the ENDF/B-VII.0 thermal cross section for water at lower incident energies with experimental results . . . . .        | 693 |
| 87 | Comparison of the ENDF/B-VII.0 thermal cross section for water at higher incident energies with experimental results . . . . .       | 694 |
| 88 | Harker-Brugger frequency spectrum used for solid methane . . . . .                                                                   | 695 |
| 89 | $\mathcal{S}(\alpha, -\beta)$ for solid methane . . . . .                                                                            | 698 |

|     |                                                                                            |     |
|-----|--------------------------------------------------------------------------------------------|-----|
| 90  | Inelastic and incoherent elastic cross sections for solid methane . . . . .                | 698 |
| 91  | Outgoing neutron spectra for solid methane . . . . .                                       | 699 |
| 92  | Agrawal-Yip frequency spectrum for liquid methane . . . . .                                | 701 |
| 93  | Frequency spectrum for liquid methane with translational and rotational<br>modes . . . . . | 701 |
| 94  | $S(\alpha, \beta)$ for Liquid Methane . . . . .                                            | 703 |
| 95  | Cross section for liquid methane at 100K . . . . .                                         | 704 |
| 96  | Neutron Spectra for liquid methane . . . . .                                               | 704 |
| 97  | Keinert-Sax frequency spectrum . . . . .                                                   | 705 |
| 98  | The static structure factor, $S(\kappa)$ , for liquid hydrogen . . . . .                   | 706 |
| 99  | script-S vs beta for para-hydrogen . . . . .                                               | 706 |
| 100 | script-S vs alpha for para-hydrogen . . . . .                                              | 707 |
| 101 | script-S vs beta for ortho-hydrogen . . . . .                                              | 707 |
| 102 | script-S vs alpha for ortho-hydrogen . . . . .                                             | 708 |
| 103 | Para-hydrogen neutron spectra . . . . .                                                    | 708 |
| 104 | Ortho-hydrogen neutron spectra . . . . .                                                   | 709 |
| 105 | Liquid hydrogen cross sections . . . . .                                                   | 709 |

## List of Tables

|    |                                                                                                               |     |
|----|---------------------------------------------------------------------------------------------------------------|-----|
| 1  | Energy Parameter for Effective Doppler-Broadening . . . . .                                                   | 79  |
| 2  | Atomic Displacement Energy Data for DPA . . . . .                                                             | 120 |
| 3  | ENDF/B-III Thermal Data Files . . . . .                                                                       | 180 |
| 4  | ENDF/B-VII Thermal Data Files . . . . .                                                                       | 180 |
| 5  | Covariance Matrices Affected by Ratio Measurements In ENDF/B-V . .                                            | 310 |
| 6  | Reaction pairs in the ENDF/B-V $^{238}\text{U}$ evaluation . . . . .                                          | 324 |
| 7  | Organization of Data for One Group in a Transport Table . . . . .                                             | 379 |
| 8  | Example of a Transport Table with Internal Edits . . . . .                                                    | 381 |
| 9  | Predefined Edits for DTFR . . . . .                                                                           | 383 |
| 10 | Example of DTFR Transport Tables Using Separate Edits . . . . .                                               | 384 |
| 11 | Thermal Reactions Available to DTFR . . . . .                                                                 | 387 |
| 12 | Standard MATXS particle names . . . . .                                                                       | 452 |
| 13 | Standard MATXS data-type names . . . . .                                                                      | 452 |
| 14 | MATXS neutron emitting reaction names . . . . .                                                               | 453 |
| 15 | MATXS breakup reaction (LR flag) names . . . . .                                                              | 453 |
| 16 | MATXS neutron absorption reaction names . . . . .                                                             | 454 |
| 17 | MATXS fission reaction names . . . . .                                                                        | 454 |
| 18 | Special MATXS NJOY names . . . . .                                                                            | 455 |
| 19 | MATXS gas production names . . . . .                                                                          | 455 |
| 20 | MATXS incident proton reaction names . . . . .                                                                | 456 |
| 21 | MATXS thermal material names (ENDF/B-VII) . . . . .                                                           | 457 |
| 22 | MATXS photoatomic cross section names . . . . .                                                               | 457 |
| 23 | ACE Data Classes and ZAID suffixes . . . . .                                                                  | 496 |
| 24 | Example of union grid size variation in ACER .c files . . . . .                                               | 497 |
| 25 | ENDF/B-VII thermal MT numbers used in ACER and THERMR . . .                                                   | 525 |
| 26 | ACE particle codes for photonuclear files . . . . .                                                           | 541 |
| 27 | Sample Intermediate Resonance $\lambda$ Values . . . . .                                                      | 556 |
| 28 | Conventional thermal material MT numbers used in WIMSR, GROUPR<br>and THERMR . . . . .                        | 564 |
| 29 | Oscillator beta values for $\alpha = 1$ for H in $\text{H}_2\text{O}$ . . . . .                               | 687 |
| 30 | H in $\text{H}_2\text{O}$ SCT effective temperatures . . . . .                                                | 691 |
| 31 | Criticality benchmark results from MCNP5 with NJOY processed<br>ENDF/B-VII.0 data . . . . .                   | 772 |
| 32 | “FAST” criticality benchmark results from TRANSX/PARTISN with<br>NJOY processed ENDF/B-VII.0 data . . . . .   | 772 |
| 33 | “THERMAL” criticality benchmark results from TRANSX/PARTISN<br>and NJOY processed ENDF/B-VII.0 data . . . . . | 772 |

## 1 INTRODUCTION

The NJOY nuclear data processing system[1, 2, 3, 4, 5] is a comprehensive computer code package for producing pointwise and multigroup nuclear cross sections and related quantities from evaluated nuclear data in the ENDF format. The U.S. Evaluated Nuclear Data Files (ENDF) have progressed through a number of versions, notably ENDF/B-III, ENDF/B-IV, ENDF/B-V, ENDF/B-VI, and now ENDF/B-VII[6, 7]. The ENDF format has also evolved through many versions. The format called “ENDF-6” was used for ENDF/B-VI and ENDF/B-VII; the latest version of the format is described in the ENDF-102 document[8, 9]. The ENDF format is also used in other nuclear data libraries such as the JEFF libraries in Europe and the JENDL libraries in Japan, or in specialized libraries distributed through the Nuclear Data Section of the International Atomic Energy Agency (IAEA). These libraries represent the underlying nuclear data from a physics viewpoint, but practical calculations usually require special libraries for particle transport codes or reactor core physics codes. This is the mission of NJOY — to take the basic data from the nuclear data library and convert it into the forms needed for applications.

### 1.1 The Modules of NJOY

The NJOY code consists of a set of main modules, each performing a well-defined processing task. Each of these main modules is essentially a separate computer program. They are linked to one another by input and output files. The main modules are supported by a number of subsidiary modules providing things like physics constants, utility routines, and mathematics subroutines that can be “used” by the main modules. The NJOY modules are grouped as follows:

**NJOY** directs the flow of data through the other modules. Subsidiary modules for locale, ENDF formats, physics constants, utility routines, and math routines are grouped with the NJOY module for descriptive purposes.

**RECONR** reconstructs pointwise (energy-dependent) cross sections from ENDF resonance parameters and interpolation schemes.

**BROADR** Doppler-broadens and thins pointwise cross sections.

**UNRESR** computes effective self-shielded pointwise cross sections in the unresolved energy range.

**HEATR** generates pointwise heat production cross sections (neutron KERMA factors) and radiation damage production cross sections.

- THERMR** produces cross sections and energy-to-energy matrices for free or bound scatterers in the thermal energy range.
- GROUPE** generates self-shielded multigroup cross sections, group-to-group scattering matrices, photon production matrices, and charged-particle multigroup cross sections from pointwise input.
- GAMINR** calculates multigroup photoatomic cross sections, photon KERMA factors, and group-to-group photon scattering matrices.
- ERRORR** computes multigroup covariance matrices from pointwise covariance data.
- COVR** reads the output of ERRORR and performs covariance plotting and output formatting operations.
- MODER** converts ENDF “tapes” back and forth between formatted (that is, ASCII) and blocked binary modes.
- DTFR** formats multigroup data for transport codes that use formats based on the DTF-IV code.
- CCCCR** formats multigroup data for the CCCC standard files ISOTXS, BRKOXS, and DLAYXS.
- MATXSR** formats multigroup data for the newer MATXS cross-section interface file, which works with the TRANSX code to make libraries for many particle transport codes.
- RESXSR** prepares pointwise cross sections in a CCCC-like format for thermal flux calculators.
- ACER** prepares libraries in ACE format for the Los Alamos continuous-energy Monte Carlo MCNP and MCNPX codes. The ACER module is supported by subsidiary modules for the different classes of the ACE format.
- POWR** prepares libraries for the EPRI-CELL and EPRI-CPM codes.
- WIMSR** prepares libraries for the thermal reactor assembly codes WIMS-D and WIMS-E.
- PLOTR** makes plots of cross sections and perspective plots of distributions for both pointwise and multigroup data by generating input for the VIEWR module.
- VIEWR** converts plotting files produced by the other modules into high-quality color Postscript plots.
- MIXR** is used to combine cross sections into elements or mixtures, mainly for plotting.
- PURR** is used to prepare unresolved-region probability tables for the MCNP continuous-energy Monte Carlo code.
- LEAPR** produces thermal scattering data in ENDF-6 File 7 format that can be processed using the THERMR module.
- GASPR** generates gas-production cross sections in the pointwise PENDF format from basic ENDF cross sections.

The methods used in these modules and instructions on how to use them are given in subsequent sections of this report. The sections on the modules are followed by an additional section on NJOY maintenance and testing.

## 1.2 Data Flow in NJOY

The modules of NJOY can be linked in a number of different ways to prepare libraries for various nuclear applications. The following brief summary illustrates the general flow of data in the code.

**RECONR** reads an ENDF file and produces a common energy grid for all reactions (the union grid) such that all cross sections can be obtained to within a specified tolerance by linear interpolation. Resonance cross sections are reconstructed using a method of choosing the energy grid that incorporates control over the number of significant figures generated and a resonance integral criterion to reduce the number of grid points generated for some materials. Summation cross sections (for example, total, inelastic) are reconstructed from their parts. The resulting pointwise cross sections are written onto a “point-ENDF” (PENDF) file for future use. **BROADR** reads a PENDF file and Doppler-broadens the data using the accurate point-kernel method. The union grid allows all resonance reactions to be broadened simultaneously, resulting in a saving of processing time. After broadening and thinning, the summation cross sections are again reconstructed from their parts. The results are written out on a new PENDF file for future use. **UNRESR** produces effective self-shielded pointwise cross sections, versus energy and background cross section, in the unresolved range. This is done for each temperature produced by **BROADR**, using the average resonance parameters from the ENDF evaluation. The results are added to the PENDF file using a special format.

If desired, additional special kinds of data can be added to the PENDF file. **HEATR** computes energy-balance heating, KERMA, and damage energy using reaction kinematics or by applying conservation of energy. The ENDF photon production files can be used in this step, when available. Comparisons of momentum and energy calculations with the photon files can be used to find energy-balance errors in the evaluations. For ENDF-6 formatted data, charged-particle distributions in File 6 are used directly to compute accurate heating and damage parameters. The energy-balance heating results are added to the PENDF file using ENDF reaction numbers in the 300 series; kinematic KERMA uses the special identifier 443, and damage results use the special identifier 444. **THERMR** produces pointwise cross sections in the thermal range. Energy-to-

energy incoherent inelastic scattering matrices can be computed for free-gas scattering or for bound scattering using a precomputed scattering law  $S(\alpha, \beta)$  in ENDF format. The secondary angle and energy grids are determined adaptively so as to represent the function to a desired precision by linear interpolation; the angular representation is then converted to one based on equally probable angles. See the chapter on [THERMR](#) for another possible representation. Coherent-elastic scattering from crystalline materials can be computed using internal lattice information, or for ENDF-6 formatted files, using data from the evaluation directly. The scheme used provides a detailed representation of the delta functions in energy and angle. Incoherent-elastic scattering for hydrogenous materials is represented using equally probable angles computed analytically or using ENDF-6 parameters. The results for all the processes are added to the PENDF file using special formats and special reaction numbers between 221 and 250. Additional reactions describing the production of the gases  $^1\text{H}$ ,  $^2\text{H}$ ,  $^3\text{H}$ ,  $^3\text{He}$ , and  $^4\text{He}$  can be added to the PENDF file with MT=203 – 207 using the [GASPR](#) module.

[GROUPE](#) processes the pointwise cross sections produced by the modules described above into multigroup form. The weighting function for group averaging can be taken to be the Bondarenko form, or it can be computed from the slowing-down equation for a heavy absorber in a light moderator. Self-shielded cross sections, scattering matrices, photon production matrices, charged-particle matrices, and photonuclear matrices are all averaged in a unified way, the only difference being in the function that describes the “feed” into a secondary group  $g'$  with Legendre order  $\ell$  from initial energy  $E$ . The feed function for two-body scattering is computed using a center-of-mass (CM) Gaussian integration scheme, which provides high accuracy even for small Legendre components of the scattering matrix. Special features are included for delayed neutrons, coupled energy-angle distributions (either from [THERMR](#) or from ENDF-6 evaluations using File 6), discrete scattering angles arising from thermal coherent reactions, and charged-particle elastic scattering. Prompt fission is treated with a full group-to-group matrix. The results are written in a special “groupwise-ENDF” format (GENDF) for use by the output formatting modules. [GAMINR](#) uses a specialized version of [GROUPE](#) to compute photoatomic cross sections and group-to-group matrices. Coherent and incoherent atomic form factors are processed in order to extend the useful range of the results to lower energies. Photon heat production cross sections are also generated. The results are saved on a GENDF file.



The covariance module, [ERRORR](#), can either produce its own multigroup cross sections using the methods of [GROUPR](#) or start from a precomputed set. The cross sections and ENDF covariance data are combined in a way that includes the effects of deriving one cross section from several others. Special features are included to process covariances for data given as resonance parameters or ratios (for example, fission  $\bar{\nu}$ ). It is also possible to process covariances for the  $P_1$  component of an angular distribution, a secondary-energy distribution, and radionuclide production. The [COVR](#) module uses the output from [ERRORR](#) together with the [VIEWR](#) module to make publication-quality plots of covariance data; it also provides output in the efficient BOXER format, and it provides a site for user-supplied routines to prepare covariance libraries for various sensitivity systems.

[MODER](#) is often used at the beginning of an NJOY job to convert ENDF library files into binary mode for calculational efficiency, or at the end of a job to obtain a printable version of a result from ENDF, PENDF, or GENDF input. It can also be used to extract desired materials from a multimaterial library, or to combine several materials into a new ENDF, PENDF, or GENDF file. [DTFR](#) is a simple reformatting code that produces cross-section tables acceptable to many discrete-ordinates transport codes. It also converts the GROUPR fission matrix to  $\chi$  and  $\bar{\nu}\sigma_f$  and prepares a photon-production matrix, if desired. The user can define edit cross sections that are any linear combination of the cross sections on the GENDF file. This makes complex edits such as gas production possible. [DTFR](#) also produces plotting files for [VIEWR](#) to use in making routine plots for the cross sections,  $P_0$  scattering matrix, and photon production matrix. This module has become somewhat obsolete with the advent of the MATXS/TRANSX system.

A number of other interface file formats are available from NJOY. The [CC-CCR](#) module is a straightforward reformatting code that supports all the options of the CCCC-IV[10] file specification. In the cross-section file (ISOTXS), the user can choose either isotope  $\chi$  matrices or isotope  $\chi$  vectors collapsed using any specified flux. The BRKOXS file includes the normal self-shielding factors plus self-shielding factors for elastic removal. The DLAYXS provides delayed-neutron data for reactor kinetics codes. Note that some of the cross sections producible with NJOY are not defined in the CCCC files. For that reason, we have introduced the new CCCC-type material cross section file MATXS. The [MATXSR](#) module reformats GENDF data for neutrons, photons, and charged particles into the MATXS format, which is suitable for input to the TRANSX (trans-

port cross section) code[11]. TRANSX can produce libraries for a variety of particle transport codes that have been used over the years, such as ANISN[12], ONEDANT[13], TWODANT[14], and DIF3D[15]. TRANSX has special features to support the latest  $S_N$  transport code from Los Alamos, PARTISN[16]. The MATXS format uses efficient packing techniques and flexible naming conventions that allow it to store all NJOY data types. A companion module, [RESXSR](#), formats pointwise data into a CCCC-like format for use in thermal flux calculators.

Pointwise data can also be fed directly into the [ACER](#) module. This module prepares cross sections and scattering laws in ACE format (A Compact ENDF) for the MCNP code[17]. All the cross sections are represented on a union grid for linear interpolation by taking advantage of the representation used in [RECONR](#) and [BROADR](#). “Laws” for describing scattering and photon production are very detailed, providing a faithful representation of the ENDF-format evaluation with few approximations. The data are organized for random access for purposes of efficiency. MCNP handles self-shielding in the unresolved-energy range using probability tables. The [PURR](#) module of NJOY can be used to prepare these tables and add them to a PENDF file for reading by the [ACER](#) module.

Another alternate path for multigroup data is to use the [POWR](#) module to produce libraries for the power reactor codes EPRI-CELL or EPRI-CPM <sup>1</sup>. Similarly, the [WIMSR](#) module can be used to prepare libraries for the thermal reactor assembly codes WIMS-D and WIMS-E[18].

At the end of any NJOY run, the [PLOTTR](#) and [VIEWR](#) modules can be used to view the results or the original ENDF data. [PLOTTR](#) can prepare 2-D plots with the normal combinations of linear and log axes, including legend blocks or curve tags, titles, and so on. Several curves can be compared on one plot (for example, pointwise data can be compared with multigroup results), and experimental data points with error bars can be superimposed, if desired. Plots can be prepared showing the ratio or percent difference of two cross sections. [PLOTTR](#) can also produce 3-D perspective plots of ENDF and GENDF angle or energy distributions or thermal  $S(\alpha, \beta)$  tables. The output of [PLOTTR](#) is passed to [VIEWR](#), which renders the plotting commands into high-quality color Postscript graphics for printing or for viewing. The [HEATR](#), [COVR](#), [DTFR](#), and [ACER](#) modules also produce plotting files in [VIEWR](#) format that are useful for quality reviews of data-processing results. The [MIXR](#) module can be used

---

<sup>1</sup>EPRI-CELL and EPRI-CPM are proprietary products of the Electric Power Research Institute (EPRI), 3420 Hillview Avenue, Palo Alto, CA 94304.

to combine isotopes into elements for plotting and other purposes. It only works for simple cross sections at the present time.

### 1.3 Computer Implementation

NJOY2012 is written in a modern subset of Fortran-90, stressing the use of modules. This has enabled us to remove all `COMMON` statements, which provides for much safer coding. The modules help to enforce information hiding. Thus, the `RECONR` module only makes the single subroutine `reconr` public; all the internal routines and data structures of the module are protected. The modules also help to promote logical structuring. For example, all of the routines and data structures for working with the ENDF formats, such as subroutine `contio` and the `math,mfh,mth` values are made public by the `endf` module, and they can be easily accessed wherever they are need by the `use endf` statement. As another example, the very large `ACER` module is made more structured by providing subsidiary modules for handling each of the different “classes” of the ACE format (*e.g.* `acefc` for continuous class “c” data, or `acepn` for the new class “u” photonuclear data).

The advanced capabilities that Fortran-90 provides for typing variables (the “kind” property) have enabled us to remove all of the complex short-word/long-word controls from NJOY. Almost all of the internal data in NJOY are handled using 8-byte kinds for real and integer words. These properties are set up in the `locale` module, and they can be changed, if necessary, without touching the balance of the code. An exception is made for the CCC modules `CCCCR`, `MATXSR`, and `RESXSR`, where 4-byte variables and equivalencing are still used to construct records with mixed real, integer, and Hollerith values.

Fortran-90 also provides a capability for the dynamic allocation of memory for data structures. In the past, NJOY used its own `storag` system for this purpose; this system has now been abandoned for the readability, consistency, and exportability provided by the new Fortran standard. We have limited ourselves to the use of “allocatable arrays”. This relieves us of some storage limitations in NJOY, and introduces others.

The earliest versions of NJOY used their own free-form input routine, `FREE`, which was developed long before Fortran supported equivalent capabilities. More recently we have abandoned `FREE` in favor of the standard Fortran `READ*` method. In doing this, we have lost some capabilities (such as the repeat field), but we have gained in transportability. Test fields that were previously delimited with the star character now must be delimited with the single-quote character.

For consistency and convenience, the NJOY modules in previous versions of the code made use of a set of common functions and subroutines located in the **NJOY** module. For NJOY2012, these utility routines have been repackaged into Fortran-90 modules. They include **locale** for localization variables, **physics** for physics constants, **mainio** for input, output, and scratch units, **util** for utility routines like time and date, **endf** for ENDF processing routines and variables, and **math** for mathematics routines. Each of these modules only makes public the minimum set of routines and variables needed by the other modules that “use” them. These modules are described in detail in the **NJOY** chapter of this report.

NJOY is heavily commented. Each module starts with a long block of comment cards that gives a brief description of the module and then gives the current user input instructions. Users should always check the input instructions in the current version of the NJOY source code rather than the instructions summarized in this manual — changes may have been made. For the convenience of users, the input instructions are also available on the web[19]. Furthermore, each function or subroutine starts with a block of comment cards that describes its function and special requirements. Additional lines of comment cards are used inside each procedure to block off its major components.

Typography conventions for Fortran differ from place to place. On most machines at Los Alamos National Laboratory (LANL), Fortran text is given in lowercase. In order to avoid translation problems, previous versions of NJOY avoided using mixed-case text for comments or for labels on graphs. We are gradually moving away from this limiting convention. In this report, Fortran text and variable names are printed using a lowercase **typewriter font**. ENDF-related formats and variables are given using an uppercase **TYPEWRITER FONT**. CCCC formats were traditionally given using uppercase characters, but the usage in this report is mixed.

## 1.4 History and Acknowledgments

NJOY was started as a successor to MINX[20] (A Multigroup Interpretation of Nuclear X-sections) late in 1973 (it was called MINX-II then). The current name was chosen in late 1974 to be evocative of “MINX plus” and to eliminate the reference to “multigroup.” The first goals were to add a photon production capability like that in LAPHAN0[21], to add a photon interaction capability like GAMLEG[22], to provide an easy link to the Los Alamos 30-group libraries of the day using DTF[23] format, and to merge in the capabilities of ETOPL[24] to

produce libraries for the MCN Monte Carlo code (the ancestor of MCNP). Most of the work was done by MacFarlane; Rosemary Boicourt joined the project in 1975. First, the RESEND[25] and SIGMA1[26] modules of MINX were converted to use union grids, and a new method of resonance reconstruction was developed. These steps led to RECONR and BROADR. UNRESR, which was based on methods from ETOX[27], was moved over from MINX with only a few changes. Next, a completely new multigroup averaging program, GROUPE, was developed around the unifying concept of the “feed function,” which handled neutron- and photon-production cross sections in a parallel manner. The CM Gaussian integration for discrete two-body scattering was developed. DTFR was developed as the first NJOY output module. The first versions of the NJOY utility codes were introduced; the new concepts of “structured programming” inspired some of the features of the new NJOY code.

Major influences during this period included Don Harris, Raphe LaBauve, Bob Seamon, and Pat Soran at Los Alamos, and Chuck Weisbin at the Oak Ridge National Laboratory (ORNL). Odelli Ozer at the Brookhaven National Laboratory (and later EPRI) helped with RESEND, and Red Cullen at Lawrence Livermore National Laboratory and John Hancock at Los Alamos helped with the Doppler broadening module. In those days, the development of NJOY was supported by the U.S. Fast Breeder Reactor and Weapons Programs.

Code development continued during 1975. The ERRORR module was added for calculating covariances from ENDF/B files. The ACER module was created by borrowing heavily from ETOPL and Chuck Forrest’s MCPOINT code. Rich Barrett joined the project, and he did most of the work in creating a new CCCC module for NJOY that had several advances over the MINX version and met the CCCC-III standards[28]. By the end of the year, HEATR had also been added to the code (with ideas from Doug Muir). HEATR gave NJOY most of the capabilities of the original KERMA factor code, MACK [29].

During 1976, free-form input and dynamic data storage were added to NJOY. GAMINR was written to complete the original NJOY goal of processing photon interaction cross sections, and the MATXSR module was designed and written, primarily by Rich Barrett. This completed the capability to construct fully coupled cross sections for neutron-photon heating problems. A major new effort was writing the THERMR module to improve upon the thermal moderator scattering cross sections then produced using the FLANGE-II[30] and HEXSCAT[31] codes, and starting the POWER module to produce cross sections for the EPRI-CELL and EPRI-CPM codes used by the U.S. electric utility companies. This

work was funded by the Electric Power Research Institute (EPRI).

The first release of NJOY to what was then called the Radiation Shielding Information Center (RSIC) at Oak Ridge and to the National Energy Software Center (NESC) at Argonne was NJOY77 in the summer of 1977. This version was tested and converted for IBM machines by R. Q. Wright (ORNL). Also, TRANSX was developed during 1977, the MATXS1 30x12 library was produced based on ENDF/B-IV, the flux calculator was added to NJOY to support the EPRI library work, and the first version of the EPRI-CELL library was generated and used.

A second release of NJOY called NJOY78 was made in 1978[32]. In addition, further improvements were made for preparing EPRI cross sections, the MATXS/TRANSX system was improved, and a thermal capability was added to the MCNP Monte Carlo code using cross sections from [THERMR](#) as processed by [ACER](#).

In 1979, the radiation damage calculation was added to [HEATR](#), and the [GROUPT](#) flux calculator was further improved. In 1980, a plotting option was added to [ERRORR](#). During this period, NJOY had become more stable. Changes usually consisted of small improvements or bug fixes instead of major new capabilities. Starting in this period, NJOY received some support from the U.S. Magnetic Fusion Energy Program, mostly for covariance work and TRANSX related library support.

In 1981 and 1982, improvements included the momentum-conservation method for radiative capture in [HEATR](#). Analytic  $\psi\chi$  broadening was added to [RECONR](#) for some cases, and the integral criteria for resonance reconstruction with significant-figure control were installed in [RECONR](#). Several new capabilities were added to [ERRORR](#), and the [COVR](#) module was added to NJOY to handle both [ERRORR](#) plotting and covariance library output. Much of this covariance-related work was done by Doug Muir. Wiley Davidson (LANL) and B.H. Broadhead and R. W. Peele at ORNL were helpful. Some support for the documentation work came from the Paul Scherer Institute (PSI) in Switzerland and OECD Nuclear Energy agency during visits to those institutions. In addition, [CCCCR](#) was updated to the CCCC-IV standards. A new release, NJOY (10/81), was made to the code centers, and the first two volumes of a new NJOY report were written and published. European users began to make important contributions about this time. Enrico Sartori of the NEA Data Bank, then at Saclay in France, Margarete Mattes of the University of Stuttgart in Germany, and Sandro Pelloni of the Paul Scherer Institute in Switzerland deserve mention.

Another major release, NJOY 6/83, was made in 1983. By this time, NJOY was in use in at least 20 laboratories in the United States and around the world. Small improvements continued, such as the kinematic KERMA calculation in [HEATR](#). The temperature dependence of the [BROADR](#) energy grid was introduced early in 1984 based on an observation by Ganesan (India). Volume IV of the NJOY report was published in 1985, and Volume III appeared in 1987.

The next big set of improvements in NJOY was associated with the introduction of the ENDF-6 format. This required significant changes in [RECONR](#) to support new resonance formats like Reich-Moore and Hybrid R-Function (implemented with help from Charlie Dunford of Brookhaven), in [HEATR](#) to implement direct calculations of KERMA and damage from charged-particle and recoil distributions in File 6, in [THERMR](#) to support new formats for File 7, and in [GROUPE](#) to support the group-to-group transfer matrices using energy-angle data from File 6. The [PLOT](#) module was also developed during this period. The result was the release of NJOY89[33] in time for processing the new ENDF/B-VI library and the JEF-2 library (which was also in ENDF-6 format).

During 1989 and 1990, initial processing of ENDF/B-VI and JEF-2 exposed a number of small problems that had to be fixed. In addition, the [ACER](#) module was rewritten to clean it up, to add capabilities to produce ACE dosimetry and photoatomic libraries, and to provide for convenient generation of files in several different formats for users away from LANL. A [MIXR](#) module was added to NJOY, mostly to allow elemental cross sections to be reconstructed from ENDF/B-VI isotopes for plotting purposes. A new technique was introduced into [GROUPE](#) and all the output modules for multigroup data that provided for more efficient processing of fission and photon production matrices with lots of low-energy groups. Major revisions were made to the MATXS format to allow for charged-particle cross sections, to pack matrices with lots of low-energy groups more efficiently, and to make inserting and extracting new materials easier. The [WIMSR](#) module, which had been under development for a number of years in cooperation with WIMS users in Canada and Mexico, was introduced into NJOY. Finally, the [PURR](#) module for generating unresolved-region probability tables for use with MCNP, which had also been under development for many years, was formally added to the code. The result of this year-and-a-half of work was NJOY91.

During the balance of 1991 and 1992, a number of changes were made in response to problems identified by users as ENDF-6 evaluations began to be used in earnest. The first of a number of attempts to handle laboratory-frame



Legendre data in File 6 in MCNP was made — namely, the attempt to convert such sections to use Kalbach systematics. Treatments for phase-space and angle-energy versions of File 6 were added in 1993, as well as improvements in [WIMSR](#) (with contributions of Fortunato Aguilar, ININ, Mexico). Plotting was added for  $S(\alpha, \beta)$  curves from ENDF-6 File 7 and for 2-D and 3-D plots from GENDF data. [HEATR](#) was modified to include incident-energy effects on the fission Q values in 1993. In 1994, we made another attempt to handle the cases of File 6 using laboratory-frame Legendre expansions for MCNP by converting them into the LAW=7 angle-energy format. A fix to the Kalbach option for energy-angle distributions was made based on work by Bob Seamon (LANL). Also, work was done in [HEATR](#) to properly handle the damage energy cutoff at low energies. Quite a bit of work was done during this period to improve the portability of the code by installing it on a variety of systems and using codes like cflint. Other people providing suggestions during this period included Margarete Mattes (Stuttgart), Piet De Leege (Delft), John White (RSIC), and the Petten users. The final version of the NJOY91 series was 91.118 in November 1994, and it was able to process all of the ENDF/B-VI evaluations that had been tried up to that date. A new user manual for NJOY91[3] was released in 1994. This document has remained as the primary reference for NJOY until the release of this report.

NJOY94 was issued at the end of 1994 to clean up 91.118 after 3 years of changes. It also provided a new direct-to-Postscript plotting system by splitting the old PLOTTR module into [PLOTTR](#) and [VIEWWR](#), an updated version of the [PURR](#) module, and a new [LEAPR](#) module for computing thermal scattering functions. In 1995, a new capability was added to handle nuclide production based on a proposed extension to the ENDF-6 File 8, and the new [GASPR](#) module was added to handle gas production. Early in 1996, a capability to pass damage cross sections into MCNP was added. A number of changes were made based on suggestions from users, and based on processing experience with the new 150-MeV evaluations becoming available during this period. A change in the erfc function was made to improve the consistency of  $1/v$  cross sections (problem observed by Cecil Lubitz, KAPL). Late in the year, the plotting system was upgraded to promote color Postscript plotting. In mid 1997, a large update to the [WIMSR](#) module was made based on the work of Andrej Trkov (Slovenia). Problems with calculational accuracy (especially for [BROADR](#)) led to a major upgrade of the math routines. Routines from the SLATEC library were adopted and converted to NJOY style. A new capability was added to



**BROADR** to compute and display some standard thermal quantities, such as thermal cross sections, g factors, and ratio integrals ( $\alpha$ , K1). After some additional bug patches and portability improvements, the NJOY94 series was concluded with the issuance of 94.105 in July of 1997.

NJOY 97.0 was released in October of 1997. The major change was to move to using 8-byte words throughout the code. Modern resonance evaluations push the limit of 6 significant figures available using 32-bit words, and obtaining consistency between people using 32-bit machines and people on 64-bit machines was becoming more and more desirable. Many changes were associated with this, including taking great care with all literal constants in the code, removing Hollerith constants, changing from the **FREE** input routine to a more standard **READ\*** method, and developing the techniques to use either 7-digits or 9-digits in resonance grids, as needed. **SAVE** statements were added to support stack-based compilers. The code now automatically determined the version of ENDF data on the input files, which changed the input a little. Finally, some steps were made to remove statement numbers and move part way to Fortran-90 style without abandoning Fortran-77 compatibility.

A number of changes were made during 1998 to cement the features of the new version. The first new capability added was new conditional probabilities in **PURR** for heating. This feature requires running **HEATR** with partial cross sections for elastic, fission, and capture. Corresponding changes were also made in **ACER**. The tolerances in **RECONR** and **BROADR** were modified to use a tighter tolerance in the thermal range to help preserve the 0.0253-eV cross section and other thermal parameters better (Lubitz). Piet DeLeege (Delft), Sandro Pelloni (PSI), and Andrej Trkov (IJS/Slovenia) were helpful in finding problems during this period. A large number of changes were made based on issues raised by testing the code with the **ftnchek** program. These help for portability between different computer systems. This work was motivated after Giancarlo Panini (Italy) questioned small differences seen using different compilers. Early in 1999, the method for setting the damage threshold in **HEATR** was revised. An internal table of default values was provided, and a new option to allow the user to enter a value for  $E_d$  was added. This change affects the damage near the threshold for elastic displacements. John White (RSIC) helped with this. Based on some code comparisons, Nancy Larson (ORNL) promoted updating the basic constants in the various codes to enhance compatibility, and we followed suit in NJOY. More work was done to enhance activation processing and to provide an automatic loop over all the production reactions for **GROUPT**. Finally, a new

option to properly handle channel spin in Reich-Moore resonance evaluations was added using code contributed by ORNL. The NJOY97 series was frozen in September of 2000.

During the last part of the life of NJOY97, we also had NJOY99 available (dated 31 December 1999). It is a cleaned up version of NJOY97 that moves further toward using block constructs and eliminating statement numbers (but lots of statement numbers are still left). It is compatible with both Fortran-77 and Fortran-90 compilers. Physical constants were moved into a few common blocks and standardized on the 1987 CODATA values from NIST. The NJOY Y2K problem was fixed. The bulk of the changes are in the [ACER](#) module to support new MCNP features, including high-energy data, incident charged particles, and photonuclear data. Before release, this version was tested for a large number of different machine/compiler combinations, including tests on X86 PCs. Compatibility has improved to the point where the unix diff function can be used to compare files and only a small number of very small differences are found. This version was able to process all the materials from ENDF/B-VI Release 5 into a library using the new ACE formats (cumulative elastic distributions, LAW=61, and charged-particle production sections) that were planned to come out with MCNP4c.

We began making patches to NJOY99 in the spring of 2000, starting with fixing a problem with the cold hydrogen and deuterium calculations in [LEAPR](#). This was followed by a number of other small patches. A capability was added for processing anisotropic charged particle emission in [ACER](#). In 2001 the series of MT numbers from 875 – 891 was installed to represent levels in the (n,2n) reaction (needed for a new European  $^9\text{Be}$  evaluation). We added a capability to include delayed neutron data in the ACE files to feed a new capability in MCNP. A photonuclear capability was added to [MATXS](#) — this enables the TRANSX code to generate fully coupled sets for n- $\gamma$  transport. Some coding was added to generate fluorescence data for MCNP using the existing format with new numbers coming from the ENDF/B-VI atomic data. This work does not completely support all the atomic data now available in ENDF/B-VI. The [ACER](#) consistency checks were upgraded to include delayed neutrons, and plots for  $\bar{\nu}$  and the delayed neutron spectra were added. In addition, delayed neutron processing was generalized to allow for 8 time bins as used by the JEFF evaluations.

[PLOT](#) was modified to allow ratio and difference plots using the right-hand scale. The default tolerances used in [RECONR](#) and [BROADR](#) were tightened

up a bit. Some changes to the heating for photoatomic data were provided by Morgan White (LANL). A change was made to [HEATR](#) to provide the photon contribution to heating using a special MT number (442). When passed to MCNP, it allows the code to get good answers for heating even when photons are not being transported. Late in 2002, [LEAPR](#) was updated to include coherent elastic scattering for FCC and BCC crystalline lattices. In 2004, some extensions to the energy grid used for incoherent inelastic scattering were made. A few additional smaller patches were also made during this period.

In 2005, changes proposed for [THERMR](#) and [LEAPR](#) by Margarete Mattes (IKE/ Stuttgart) to support the new IAEA-sponsored evaluations for thermal scattering in water, heavy water, and ZrH were installed. Some additional group structures used in Europe were added. Through this period, we were always increasing the storage space allowed as we adapted to newer and larger evaluations coming out for ENDF/B-VII. During the summer, a number of changes to covariance processing were provided by Andrej Trkov (working at IAEA). Early in 2006, a new sampling scheme for thermal scattering was developed for MCNP that uses continuous distributions for secondary energy instead of the previous discrete values. This removed unsightly artifacts in computed fluxes at low energies, and it alleviated some problems that the cold-neutron-source people were having. More code improvements were made based on detailed compiler checking. Some errors in the treatment of energy-dependent fission  $Q$  were fixed based on a review of the work of Dave Madland (LANL). An approximate treatment for the relativistic gamma in the ENDF/B-VII evaluation for  $n+^1\text{H}$  was added in [HEATR](#) and [GROUPL](#) based on theoretical work from Gerry Hale (LANL). We added a new plot to the [ACER](#) set that shows the recoil part of the heating. This is a sensitive test of energy-balance.

In the summer of 2007, we added some smoothing options to make the low-energy shape of neutron distributions look more like the theoretical shape, namely  $\sqrt{E'}$ . Similar changes were provided for delayed neutron spectra. Additional smoothing was provided for some of the fission spectra at energies above 10 MeV using an exponential shape. A change was made in [GROUPL](#) to override Cartesian interpolation in favor of unit-base interpolation for scattering distributions. This gives smoother scattering source functions and is consistent with what MCNP does.

In 2007, a big change was made to covariance processing by replacing the original NJOY ERRORR module with ERRORJ[34] as contributed to the NJOY project by Japan (Go Chiba). This new module added covariance capabilities

for the more modern resolved-resonance representations, angular distributions, and secondary-energy distributions. A series of additional changes to the new [ERRORR](#) were made over the next couple of years. Go Chiba, Andrej Trkov (IAEA and IJS Slovenia), and Ramon Arcilla (BNL) were involved in this. A capability to handle energy-dependent scattering radius data in the unresolved range was added. In 2008, [ERRORJ](#) work continued. Some work was done in [PLOTTR](#) to implement graphs of [GROUPT](#) emission spectra. In 2009, changes were made for unresolved resonance cross sections to force log-log interpolation to better represent  $1/v$  cross sections. The parameter that looked for steps in the unresolved-range energy grids that were too large was changed from its former value of 3 to 1.26. Some of the steps in ENDF/B-VII are unreasonably large when representing  $1/v$  cross sections. The default energy grid used in the unresolved range was upgraded to one using about 13 points per decade. Additional pages were added to the [ACER](#) plots to display the unresolved-range self-shielded cross sections. This work was influenced by Red Cullen (LLNL). In a related effort, some changes were made in the binning logic for [PURR](#) to improve unresolved-range results. In 2010, changes were made to support the processing of the IRDF international dosimetry file, including the addition of many new reaction MT numbers. Some work was done on the photonuclear options to support the TENDL-2009 library. More [ERRORR](#) changes from Trkov were implemented, and a capability to process the uncertainty in the scattering radius was added. Finally, several updates were submitted by the Japan Atomic Energy Agency (JAEA) related to processing discrete photon data from file 6 into ACE files. NJOY 99.364 was released in February of 2011.

Concurrent with the maintenance of NJOY99, we worked on a new Fortran-90 version of NJOY that took advantage of the module system, the numerical precision system, and the dynamic storage system of Fortran-90. This enabled us to get rid of COMMON statements (always problematic in Fortran) and to obtain a more readable scheme for allocated storage. Additional work was done to upgrade to block structures, but some statement numbers still remain. That new version was called NJOY2010, but was only released to a few in-house (LANL) users, selected external users at Brookhaven, Oak Ridge and Argonne National Laboratories plus the Naval Reactors laboratories, Bettis and KAPL in the United States and to the Atomic Weapons Establishment in the UK. Further code revisions have lead to the current version, NJOY2012, which is described in this report. For most applications, NJOY2012 is compatible with NJOY99. However, there are some new capabilities in NJOY2012 that are not supported

by NJOY99. We borrowed coding from the SAMMY[35] code (thanks are due to Nancy Larson, ORNL) to handle the new Reich-Moore-Limited resonance parameter representation now included in the ENDF-6 format. This coding is used in [RECONR](#) to generate pointwise resonance cross sections and angular distributions. It is used in [ERRORR](#) to generate the sensitivity of resonance cross sections to the resonance parameters for use in calculating cross section uncertainties and covariances in the resonance range. In [THERMR](#), we added an option to construct thermal cross sections using  $(E, \mu, E')$  ordering in addition to the normal  $(E, E', \mu)$  ordering. This ordering is convenient for comparing to experiment, and it is used for thermal sampling in some Monte Carlo codes.



## 2 NJOY

The NJOY module of the NJOY system contains the main program for the system, which directs the sequence of other modules that makes up the desired calculational path. This section of the report also describes a number of subsidiary modules containing common data structures, subroutines, and functions for use in the other modules. This manual describes NJOY version 2012 (or NJOY2012 for short). The differences between this chapter and the corresponding one in the previous report[3] are related to the conversion to Fortran-90 style; to the modularization of the NJOY utility routines and common variables; to changes in free-form input and storage allocation routines; and to the introduction of the new package of mathematics functions.

### 2.1 The NJOY Program

The `njoy` program starts by initializing the page size for blocked-binary ENDF files, opening the output listing file, and writing the NJOY banner on the output listing. It then sets up a loop that simply reads a module name and calls the requested module. The loop continues until the “stop” name is read, and then NJOY exits. The first card read by any module contains the unit numbers for the various input and output files. In this way, the output of one module can be assigned to be the input of another module, thereby linking the modules to perform the desired processing task. An example of the linking procedure is given below:

```

    [mount an ENDF file as tape20]
-- Optional comment card (signified by "dash" "dash" "space")
reconr
20 21
    [input lines for RECONR]
groupr
20 21 0 22
    [input lines for GROUPR]
dtfr
22 23 21
    [input lines for DTFR]
stop
    [DTF-format lines written on tape23]
```

Optional comment cards may only appear at the point in an input deck where a module name is expected. Multiple comment cards are allowed and each must start with the three character string “dash” “dash” “space”. An important feature of a good modular system is that there be a minimum of interactions between the modules in order to reduce side effects. In the NJOY system, modules communicate only by means of the input and output units specified as shown above, and through a limited number of common constants provided by the subsidiary modules. The common constants used in the NJOY main program are in the following modules:

**version** provides the version number string **vers**, initially “2012.0,” and the corresponding date **vday**, initially “ddmmm12,”

**locale** provides localization information, including the laboratory and machine strings, initially “our-lab” and “our-mx,”

**mainio** provides the system unit numbers, **nsysi**, **nsyso**, and **nsyse**,

**endf** provides the page size for blocked-binary ENDF files, **npage**. This value is set in the NJOY main program.

The input instructions for the NJOY module are given as comment cards at the beginning of the module. They are reproduced here for the convenience of the user.

```
!---input specifications (free format)-----
!
! card 1      module option
!
!   module    six character module name, e.g., reconr.
!              it is not necessary to use quotes.
!
!           repeat card 1 for each module desired, and
!           use the name "stop" to terminate the program.
!
! See the comments at the start of each module for its specific input
! instructions.
!
!-----
```

NJOY is usually invoked from a terminal or command window, or from a script. The standard I/O redirection syntax is used to control the choice of an



input file:

```
njoy < test1
```

Of course, the system messages that normally appear in the terminal or command window could be redirected to a file by appending something like “ > out1” to this execution line.

## 2.2 Interface Files

Another requirement of a good modular system is that the input and output files be in a common format so that modules can work with each other’s output in a flexible way. Since NJOY is basically an ENDF processing code, ENDF-compatible formats were chosen for linking modules together. “Input” and “output” modules can be specified to communicate with other formats (the “outside world”). In the example above, `tape23` is an example of such an external file. The other tapes<sup>2</sup> in the example are ENDF-type files, and the sequence shown is fairly typical. If the user in the example needs data at a higher temperature, the `RECONR` point-ENDF, or PENDF, file (`tape21`) can be run through `BROADR` to produce a Doppler-broadened PENDF file for `GROUPR`. Many other combinations are possible simply by rearranging the sequence of module names and changing the unit numbers that link them. These common-format files also provide for convenient restarts at many points in the calculational sequence. For example, if a user is trying to produce pointwise cross sections at 300K, 600K, and 900K and runs out of time while working on 900K, he or she can save the partially completed PENDF file and restart from 600K. Multigroup modules use specially constructed groupwise-ENDF formats (GENDF) that are compatible with the multigroup output modules. A GENDF file from `GROUPR` can be saved in the NJOY data library, run through `CCCCR` to produce one output format, and then run through `MATXSR` for another output format.

In NJOY, unit numbers from 20 through 99 are used for storing results or linking modules, units 10 through 19 are reserved for scratch files, which will be destroyed after a module has completed its job, and units below 10 are reserved for the system. Negative unit numbers indicate binary mode.

<sup>2</sup>The word “tape” will often be used in this report as a synonym for “file”; an actual physical tape is not implied. This is consistent with ENDF custom, where the phrase “ENDF tape” is traditional. Furthermore, in most NJOY installations, the actual files on the machine will have names like “tape23.”

There are special utility routines to open, close, and reposition files. These routines automatically handle the NJOY conventions on positive or negative unit numbers, scratch files, and so on. These routines are available as the following public calls in module `util`:

`openz(lun,new)`

Open the unit=`abs(lun)`. If `lun`  $\geq 0$ , use coded (formatted) mode, and if `lun`  $\leq 0$ , use binary mode. Destroy on close or job termination if `10`  $\leq `lun`  $\leq$  `20`. If `new`=1, destroy the file on this unit (if it exists) and open a new file.$

`closz(lun)`

Close the file with unit=`abs(lun)`. Do nothing if `lun`=0 or if `lun` refers to a scratch file.

`repoz(ntape)`

Rewind the file with unit=`abs(ntape)`. Do nothing if `ntape`=0.

`skiprz(lun,nrec)`

Skip `nrec` records forward or backwards. Caution: Some systems have a call for this option; others can use loops of backspace and dummy reads as given in the NJOY code. Both these operations work well for systems that use “linked-list” data structures for I/O files. On some systems, however, backspace is implemented as a rewind followed by forward dummy reads to the desired location. In such cases (for example, VAX), `skiprz` must be recoded to avoid calling backspace repeatedly. This caution is somewhat moot for current operating systems.

## 2.3 Free Format Input

Free-form input is handled by the standard Fortran-90 `READ*` method. Previous versions of NJOY used a special routine `FREE` for free-form input. This routine was developed before free-form input was routinely available in Fortran, but it has now been retired. Some capabilities that were provided by `FREE`, such as repeat fields, are no longer supported using `READ*`. Basically, users can type in their input quantities separated by spaces. Lines can be terminated early with the slash (/) symbol, leaving any variables not provided at their default values. Text values consisting of single words can be entered without delimiters, but more complex strings containing spaces must be delimited using the single-quote character ('). Real numbers can be entered in a variety of forms; 1, 1., 1.e0, and 1e0 should all be equivalent. Examples of NJOY input will be found throughout this report.

## 2.4 ENDF Input-Output

The ENDF format for evaluated nuclear data is well documented elsewhere,[8] but for the convenience of the reader, some features of the format will be described here.

ENDF “tapes” are subdivided internally into “materials” (MAT), “files” (MF), and “sections” (MT). A MAT contains all data for a particular evaluation for an element or isotope (for example, MAT=825 is an evaluation for  $^{16}\text{O}$  in ENDF/B-VII). A file contains a particular type of data for that MAT: MF=3 is cross-section *versus* energy data; MF=15 contains secondary photon energy distributions. A section refers to a particular reaction [for example, MT=2 is elastic scattering and MT=107 is the  $(n, \alpha)$  reaction]. Every record contains the current MAT, MF and MT values. Two materials are separated by a record with MAT=0 (the material-end or MEND record). Two files are separated by a record with MF=0 (the file-end or FEND record). Two sections are separated by a record with MT=0 (the section-end or SEND record). Finally, the tape is terminated with a record with MAT = -1 (tape-end or TEND record).

NJOY has a set of utility subroutines for locating desired positions on an ENDF tape. They are located in module `endf`, and they can be made available to any other module with the statement “`use endf.`”

`findf(mat,mf,mt,nin)`

Search `nin` backward or forward for the first record with this MAT, MF, MT. Issue a fatal error message if the record is not found.

`tosend(nin,nout,nscr,a)`

`tofend(nin,nout,nscr,a)`

`tomend(nin,nout,nscr,a)`

`totend(nin,nout,nscr,a)`

Skip forward past the next SEND, FEND, MEND, or TEND card on NIN. If `nout` and/or `nscr` are nonzero, copy the records. Input and output files must be in the same mode.

The data on an ENDF tape are written in eight different kinds of “structures”, each of which has a binary and a formatted form. In modern systems, formatted data is normally coded in ASCII. The words “coded,” “formatted”, and “ASCII” will often be used interchangeably here). The structures are: (1) TAPEID, a character-string title for the tape; (2) CONT, a control record (includes SEND, FEND, MEND, and TEND); (3) LIST, a list of data items; (4) HOLL, a list of character-string words (what used to be called Hollerith

data); (5) TAB1, a one-dimensional tabulation of data pairs; (6) TAB2, a two-dimensional tabulation control record; (7) INTG, a special structure of integer fields used for encoding correlation data, and (8) DICT, a directory or index (it used to be called the “dictionary”) to the sections found in the MAT. It should be noted that HOLL is a special case of LIST and DICT is a special case of CONT.

In binary mode, each structure is written as a single logical record as follows:

TAPEID[MAT,MF,MT/A(I),I=1,17] <sup>3</sup>

where MAT=tape number, MF=MT=0, and the character data are 16A4,A2;

CONT[MAT,MF,MT/C1,C2,L1,L2,N1,N2]

LIST[MAT,MF,MT/C1,C2,L1,L2,N1,N2/A(I),I=1,N1]

HOLL[MAT,MF,MT/C1,C2,L1,L2,N1,N2/A(I),I=1,N1]

where MF=1, MT=451, and each line of Hollerith characters is stored in A as 16A4,A2;

TAB1[MAT,MF,MT/C1,C2,L1,L2,N1,N2/NBT(I),JNT(I),I=1,N1

/X(I),Y(I),I=1,N2] where NBT and JNT are the interpolation table and Y(X) is the one-dimensional tabulation;

TAB2[MAT,MF,MT/C1,C2,L1,L2,N1,N2/NBT(I),JNT(I),I=1,N1]

where the interpolation table is to be used to control a series of N2 LIST or TAB1 structures that follow;

INTGIO[MAT,MF,MT/A(I),I=1,NW]

where each line of the array can contain 18 I3 integers, 13 I4 integers, 11 I5 integers, 9 I6 integers, or 8 I7 integers. The specific format is governed by the value of L1 from the CONT record immediately preceding this data structure.

DICT[MAT MF,MT/0.,0.,MFS,MTS,NCS,MODS]

where there is a record for each section in the material (MFS, MTS) giving the card count (NCS) for that section. For ENDF/B-V, MODS indicates the revision number for that section.

The ENDF format manual[8] explains how these structures are combined to represent various physical quantities.

In formatted mode, each structure is broken up into many card images, each containing 6 data words, followed by MAT, MF, MT, and a line sequence number. There is no intrinsic limit to the length of a data structure written in coded form because a program reading the data can normally be coded to use

<sup>3</sup>In ENDF/B manuals, the slash is used as a logical divider. Replace it with a comma and add parentheses when constructing a FORTRAN I/O list.

the data in “pages” of reasonable size. The MINX code[20] (the predecessor of NJOY) was forced to use coded formats to handle the large tabulations found on PENDF tapes. Analysis showed that this code used large amounts of its running time coding and decoding number formats. In order to eliminate this waste, a blocked binary format was developed for the ENDF data structures. A structure is divided up into several logical records of intermediate length (typically about 300 words), each having the following form:

[MAT,MF,MT,NB,NW/A(I),I=1,NW]

where NB is the number of words remaining in the data structure (the last record has NB=0). This type of record is compatible with the official ENDF binary record, but is also adaptable to paging methods. The page size can be chosen to optimize input/output rates for a particular computer system.

A set of utility subroutines has been devised to handle both blocked-binary and paged-BCD input and output. They are also provided by module `endf`.

`contio(nin,nout,nscr,a,nb,nw)`

Read/write a control record from/to `a` (`nb=0`, `nw=6`). `contio` uses `asend`, `amend`, *etc.* for END cards.

`listio(nin,nout,nscr,a,nb,nw)`

Read/write the first record or page of a list record from/to `a`. If `nb` is not zero, continue with `moreio`, as shown in Examples 1 and 2 that follow.

`tab1io(nin,nout,nscr,a,nb,nw)`

Read/write the first record or page of a TAB1 structure. If `nb` is not zero, use `moreio`.

`tab2io(nin,nout,nscr,a,nb,nw)`

Read/write a TAB2 structure (`nb=0`).

`moreio(nin,nout,nscr,a,nb,nw)`

Read/write continuation records or pages from/to the array `a`. Returns `nb=0` after processing the last record or page.

`tpidio(nin,nout,nscr,a,nb,nw)`

Read/write the character-string tape identification record from/to array `a` (`nb=0`, `nw=17`).

`hdatio(nin,nout,nscr,a,nb,nw)`

Read/write the first record or page of the character descriptive data (MF=1, MT=451) from/to `a`, taking account of the 16A4,A2 format needed in ASCII mode. If `nb` is not zero, use `moreio`.

`intgio(nin,nout,nscr,a,nb,nw)`

Read/write an INTG record.

`dictio(nin,nout,nscr,a,nb,nw)`

Read/write the entire material directory from/to `a`. On entry, `nw` is the number of entries in the dictionary. `moreio` is not used.

`asend(nout,ncr)`

`afend(nout,nscr)`

`amend(nout,nscr)`

`atend(nout,nscr)`

Write a section (MT=0), file (MF=MT=0), material (MAT=MF=MT=0) or tape (MAT=-1, MF=MT=0) “end” record on the desired units.

In these calling sequences, the unit numbers can be positive, negative, or zero. Positive numbers mean ASCII mode, negative numbers mean blocked-binary mode, and zero means the file corresponding to this position in the calling sequence is not used. All of these routines use the following variables made public by module `endf`:

`c1h,c2h,l1h,l2h,n1h,n2h,math,mfh,mth,nsh,nsp,nsc`

where `c1h` corresponds to the ENDF C1 field, and so on. The variable `nsh` is the sequence number for `nin`, `nsp` is the sequence number for `nout`, and `nsc` is the sequence number for `nscr`. Two examples may help to make clear the use of these routines.

#### Example 1. Read All Data

```
loc=1
call tablio(nin,0,0,a(loc),nb,nw)
loc=loc+nw
do while (nb.ne.0)
  call moreio(nin,0,0,a(loc),nb,nw)
  loc=loc+nw
enddo
(process data in A)
```

Example 2. Paging

```

      call tablio(nin,0,0,a(1),nb,nw)
110 (process this page of data in A)
      if (nb.eq.0) go to 120
      call moreio(nin,0,0,a(1),nb,nw)
      go to 110
120 continue

```

When **nin** is BCD, paging is automatic. Positive and negative unit numbers can be mixed in **tpidio**, **contio**, **listio**, *etc.*, when mode conversion is desired.

**2.5 Buffered Binary Scratch Storage**

During the execution of a program, large amounts of data often need to be stored in mass storage temporarily. In order to make such scratch storage as efficient as possible, NJOY includes a pair of utility subroutines in module **util** that automatically buffer such data through fast memory to disk.

**loada(i,a,na,ntape,buf,nbuf)**

**finda(i,a,na,ntape,buf,nbuf)**

Load or find data in a buffered binary scratch file. Here **i** is the data point number (**i** must increase, except **i**=1 causes a rewind and **i**<0 flushes the fast memory buffer to mass storage), The array **a** contains data to be stored or provides a destination for data to be read, **na** is the number of words to be transmitted (must be the same for all **i**), **ntape** is the logical unit number of the disk file, **buf** is the fast memory buffer array, and **nbuf** is the length of the buffer array.

When a point is to be saved, **loada** stores it in **buf**. When **buf** becomes full, it is automatically dumped to disk. When a point is to be retrieved, **finda** checks to see whether the desired point is in **buf**. If not, it reads through the disk until the desired point is in memory. It then returns the desired point. When **na** is small with respect to **nbuf**, using **loada/finda** reduces the number of I/O operations dramatically. Sometimes it is necessary to find a particular part of the buffered data. In such cases, use

```

      scana(e,ip,np,na,ntape,buf,nbuf)

```

where **e** is a value for the first of the **na** words, and **ip** points to part of the data whose first word is either equal to **e** or is the first value less than **e**.

## 2.6 Dynamic Storage Allocation

Previous versions of NJOY used an internal package called **storag** for dynamic memory allocation. NJOY2012 uses the standard Fortran-90 storage allocation mechanism. The only feature used is the “allocatable array.” When needed, an array is allocated that will contain a defined number of values. The array can be deallocated when no longer needed, and it will disappear automatically when the scope within which it is defined is exited. This method produces more transparent code than the old **storag** package, because pointers into a single container array are not needed.

## 2.7 ENDF/B Utility Routines

There are several operations performed on ENDF/B data that are needed in so many other modules that it is practical to put them into the **endf** module.

**terp1(x1,y1,x2,y2,x,y,i)**

Interpolate for  $y(x)$  between  $y_1(x_1)$  and  $y_2(x_2)$  using the ENDF interpolation law **i** (**i**=1 means  $y=y_1$ , **i**=2 means  $y$  is linear in  $x$ , **i**=3 means  $y$  is linear in  $\ln(x)$ , **i**=4 means  $\ln(y)$  is linear in  $x$ , **i**=5 means  $\ln(y)$  is linear in  $\ln(x)$ ), and **i**=6 means to interpolate using the charged-particle penetrability with a kinematic threshold of **thr6**.

**terpa(y,x,xnext,idis,a,ip,ir)**

Interpolate for  $y(x)$  in the TAB1 structure in array **a**. The routine searches for the correct interpolation range starting from **ip** and **ir** (initialize to 2 and 1 for first call). It returns **xnext**, the next  $x$  value in the tabulation. **idis** is set to 1 if there is a discontinuity at **xnext**; it is zero otherwise).

**gety1(x,xnext,idis,y1,itape,a)**

**gety2(x,xnext,idis,y1,itape,a)**

Find  $y(x)$  in a TAB1 structure starting at the current location on **itape** by paging the data through array **a**. **gety1** and **gety2** are identical for occasions when two different tapes are being searched at the same time. **xnext** and **idis** behave as in **terpa**. The array **a** must be at least **npage**+50 words in length. These routines are normally used to retrieve cross sections from MF=3.



**gral**(x1,y1,xh,yh,x1,x2,i)

This function returns the integral from  $x_1$  to  $x_2$  of an ENDF function with interpolation law *i* (see **terp1**). **x1**, **y1**, **xh**, and **yh** are the low and high limits of the interpolation panel.

**intega**(f,x1,x2,a,ip,ir)

Integrate the TAB1 function stored in **a** from  $x_1$  to  $x_2$ . The routine automatically determines the correct interpolation law for each panel or fraction of a panel and uses **gral** to compute each part of the integral. Set **ip**=2 and **ir**=1 on the first call to **intega**. In subsequent calls, the previous values of **ip** and **ir** will usually provide a good starting point for searching in the TAB1 structure.

## 2.8 Math Routines

Several mathematics routines are included in the **mathm** module for use by other modules. Most of these routines are based on routines from the SLATEC library converted to NJOY style and Fortran-90.

**legndr**(x,p,np)

Generate Legendre polynomials  $P_\ell(x)$ . The  $\ell = 0$  value is in **p**(1), the  $\ell = 1$  value in **p**(2), etc. **np** is the maximum Legendre order produced, so the largest index for **p** is **np**+1.

**e1**(x)

Compute the first-order exponential integral function  $E_1(x)$ .

**gami**(a,x)

Compute the incomplete gamma function  $\gamma(a, x)$ .

**erfc**(x)

Compute the complementary error function  $\text{erfc}(x)$ .

## 2.9 System-Related Utility Routines

As much as possible, actions that related to system functions have been put into subroutines or functions in the **util** module. The I/O routines have already been discussed. Sometimes these routines might have to be altered for unusual system environments.

**timer**(time)

Returns the run time in seconds. The meaning of this number may vary from system to system. It might be central-processor (CP) time, or at some installations, it may include other factors, such as I/O time or memory

charges. This makes it difficult to compare NJOY runs on different systems. This routine may have to be revised for some systems, because there is no standard Fortran-90 call.

#### **dater(hdate)**

Returns the date as an 8-character string in one of the forms mm/dd/yy or ddmmyy; for example, 11/15/90 or 03jun91. For the Fortran-90 version of NJOY, this is handled using the standard `date_and_time` call.

#### **wclock(htime)**

Returns the “wall clock” time. This is the time of day that the NJOY run started, and it shouldn’t be confused with the elapsed CP time for the run as returned by `timer`. The time is represented as an 8-character string in the form hh:mm:ss; for example, 12:13:47. The user is free to use a 24-hour convention for time. The standard `date_and_time` call is used to retrieve the information from the system.

#### **sigfig(x,ndig,idig)**

Because of the many comparisons and searches that it makes, NJOY often has to match two numbers that are different only in the few least significant bits. This routine is intended to make such numbers exactly equal to each other by truncating the numbers to a given number of digits and removing any low-significance junk resulting from nonterminating binary fractions. The `idig` parameter can be used to move the result up or down by `idig` in the last significant figure. Although this routine was sometimes machine dependent in previous versions of NJOY, the subroutine now used seems to work on all systems tried so far.

#### **a10(x,hx)**

Converts `x` to a 10-column format as a string in `hx` to provide more digits in some NJOY listings without taking too much space. This allows 4, 5, or 6 significant figures to be printed where we previously had four. `hx` has the forms `+1.23456+6`, `+1.2345-38`, or `-1.234+308`.

## **2.10 Error and Warning Messages**

NJOY has a pair of standard routines for printing fatal error messages and warning messages. This helps to enforce consistency in the messages, insulates other subroutines from the complexities of the system (for example, I/O units, “console”, “standard error file”), and provides a site for machine-dependent error handling, including such things as saving “drop files” and generating trace-back listings. These routines are in module `util`.

#### **error(from,mess1,mess2)**

This subroutine should result in a fatal error exit and must be adjusted to reflect the local system. Special features such as traceback information or

saving files for later analysis can be performed here. **from** is a character string containing the name of the procedure that called **error**, and **mess1** and **mess2** are two 60-character strings containing messages describing the error. **mess2** is not printed if it is empty.

**mess(from,mess1,mess2)**

This routine is for nonfatal warning messages. **from** is the routine that called it. It prints **from**, **mess1**, and **mess2** (if not empty), and returns to the calling routine.

The actual error messages produced by functions and subroutines in the NJOY module and the subsidiary modules **util**, **endf**, and **mathm** are listed below, including explanations of the meaning of the errors and suggested steps to alleviate them.

**error in njoy\*\*\*illegal module name**

Check spelling, and check for missing (/) or incorrect item counts in the preceding module. This error message is generated directly by NJOY instead of using **error**.

**error in openz\*\*\*illegal unit number**

**error in closz\*\*\*illegal unit number**

Units less than 10 are reserved for the system.

**error in tomend\*\*\*mode conversion not allowed**

**error in tofend\*\*\*mode conversion not allowed**

**error in tosend\*\*\*mode conversion not allowed**

Input and output units must both be binary or both be BCD. Check the signs of the unit numbers in the input file.

**error in findf\*\*\*mat---mf---mt---not on tape**

Desired section cannot be found. Either the wrong tape was mounted, or there is a mistake in the input deck.

**error in scana\*\*\*initial ip ne 0**

Must be called with **ip=0**.

**error in scana\*\*\*did not find energy ---**

Energy requested is greater than the highest energy in the LOADA/FINDA file.

**error in gral\*\*\*x2 lt x1**

The integration interval is bad.

**error in e1\*\*\*x is 0**

Result is not defined.

**error in gami\*\*\*a must be gt zero**

```

error in gami***x must be gt zero
  Illegal parameter values.
error in dlngam***abs(x) so big dlngam overflows
error in dlngam***x is a negative integer
  Illegal parameter values.
message from dlngam---answer lt half precision...
  Just a warning.
error in csevl***number if terms le 0
error in csevl***number if terms gt 1000
  Won't happen in NJOY.
error in csevl***x outside the interval (-1,1)
  Bad parameter value.
error in d9lgit***x should be gt 0 and le a
error in d9lgit***no convergence in 200 terms...
  Problems computing Tricomi's incomplete gamma function. This error
  should not occur.
message from d9lgit---result less than half precision...
  Just a warning.
error in d9lgmc***x must be ge 10
  Bad parameter value.
error in dgamit***x is negative
  Bad parameter value.
message from dgamit---result less than half precision...
  Just a warning.
error in dgamlm***unable to find xmin
error in dgamlm***unable to find xmax
  Having trouble finding the minimum and maximum bounds for the argu-
  ment in the gamma function.
error in dgamma***x is 0
error in dgamma***x is a negative integer
error in dgamma***x so big gamma overflows
  Bad parameters for the gamma function.
message from dgamma---answer lt half precision...
  Just a warning.
error in d9gmit***x should be gt 0
error in d9gmit***no convergence in 200 terms...
  Problem's with Tricomi's gamma function at small arguments.
error in d9lgic***no convergence in 300 terms...
  Problems with the log complementary incomplete gamma function.

```

## 2.11 Coding Details for the NJOY Main Program

The `njoy` main program of the NJOY code starts with a block of comment cards that gives a short description of the NJOY module and specifications for the user's input lines. (The term "card" is used out of respect for the past; this usage should not be taken to imply that a real card that can be "folded, spindled, or mutilated" has to be used.) These blocks of comments cards occur at the beginning of every NJOY module. It is a good idea to check the input instructions in the comment cards for the current version in order to see whether there have been any changes from the input instructions reproduced in this manual.

The first step in the body of the code is to give "use module" statements for each module that provides a variable or subroutine call to be used here. There are several common variables used in this module. The `vers` string and its associated date string `vday` from the `version` module are important parts of the NJOY Quality Assurance (QA) scheme. They are updated each time a change is made to the code, and they are always printed on the output listing. They are also available to other modules to be written in libraries generated by NJOY or on plots, if desired. The `lab` and `mx` strings are normally used to localize NJOY to a particular institution and to tell what machine was used for an NJOY run when several are available. They are carried in the `locale` module. The quantity `npage` in the `endf` module must be a multiple of 6 (because ENDF records have 6 fields on a line) and 17 (since Hollerith lines use the format "16a4,a2"); therefore, a value of 306 was chosen. If a programmer should desire to use larger pages, the line

```
npage=(npage/102)*102
```

assures that the common divisors of 6 and 17 are preserved. The normal unit numbers for input and terminal output on most systems are `nsysi=5` and `nsyse=6`, as set in module `mainio`. We also define an additional unit with value `nsyso=7` to link to a file called "output" for the main NJOY listing. This file is opened in the main NJOY program.

Next, NJOY writes an "banner" on the output listing file giving the date, time, version, and so on, for this NJOY run. The program now starts an infinite loop, reading in module names, and executing the requested module, until the name "stop" is read.

**Module “locale”** This purpose for this module is to provide localization information for NJOY. Users may find it necessary to change things in this module for their site, machines, or compilers. The public variables provided are

**lab** – a string identifying the user’s institution.

**mx** – a string identifying the machine used, the system, the compiler, or whatever.

**kr** – the kind value for normal real numbers.

**k4** – the kind value for 4-byte real numbers and 4-byte integers (mostly for CCCC records).

**k8** – the kind value for 8-byte Hollerith variables in the CCCC formats.

The default value for **lab** is “our-lab,” and it can be changed to reflect the users site. Up to 8 characters are allowed. The default value for **mx** is “our-mx.” At one time, LANL had a system call that would tell which machine out of a cluster was being used, and this field was used for that. It can also be used to identify the type of machine (*e.g.*, sun, vax, x86, linux) or the compiler used.

NJOY2012 uses the built-in features of Fortran-90 to control the precision of the numbers used internally. This allows us to remove the complex short-word and long-word controls used for the Fortran-77 versions, a great simplification. The normal internal representation used in NJOY2012 is a high-precision one, normally implemented using 64-bit reals and the system default for integers (either 4 or 8 bytes should be OK). The “kind” value to obtain these high-precision reals is returned using the Fortran-90 `selected_real_kind` function, and it should be portable. However, **k4** and **k8** are simply set to the values 4 and 8, respectively. These choices are not standardized by Fortran-90, and the values given here may have to be adjusted for some systems. Anyway, once a proper value of **kr** has been provided, variables, arrays, and constants can be typed using statements like

```
real(kr)::za
real(kr)::elast(20)
real(kr),dimension(:),allocatable::enode
real(kr),parameter::therm=.0253e0_kr
```

**Module “version”** This module provides public version and date strings to any of the other NJOY modules. The initial values are `vers='2012.0'` and

`vday='21dec12'`. It is an important part of the NJOY QA procedure to keep these values up to date as changes are made to the code.

**Module “mainio”** This module provides public values for the system I/O units, namely, `nsysi=5`, `nsyso=7`, and `nsyse=6`. These are the conventional values for these units, but they may have to be changed in some programming environments. Note that these have not been made into constants by setting the “parameter” condition; there are some places where some of these values are temporarily reset.

**Module “physics”** Because NJOY is divided into a number of separate modules, it is important to provide a common set of physical constants to ensure consistency. These constants are as follows:

**pi** – a high precision of 15 digits is provided.

**bk** – Boltzmann’s constant.

**amassn** – the mass of the neutron in AMU.

**amu** – the value of the AMU.

**hbar** – Planck’s constant divided by  $2\pi$ .

**ev** – the value of the electron volt.

**clight** – the velocity of light.

These numbers were obtained from the CODATA’89 set as published by the National Institute of Standards and Technology (NIST). Other NJOY modules can access these values by including the statement “`use physics.`” We have taken pains in NJOY to compute values that can be derived from these standards from these values rather than multiplying the number of physical constants used in the program.

**Module “util”** As outlined above, module `util` makes the following routines public:

**error** – fatal error routine

**mess** – warning message routine

**timer** – CPU elapsed time routine

**dater** – returns a date string

**wclock** – returns a wall-clock time string

**repoz** – repositions a file to the beginning  
**skiprz** – skips records in a file forward and back  
**openz** – opens a new or exiting file  
**closz** – closes a file  
**loada/finda** – a buffered storage system  
**scana** – search in a loada/finda system  
**sigfig** – truncate numbers to a given significance  
**a10** – print real numbers compactly

There are no private subroutines or variables in this module.

The default versions of **error** and **mess** simply write the one or two lines of message characters to the appropriate units. The Fortran-90 `len_trim` function is used to measure the real length of a character string by removing trailing blanks. By changing **nsyse**, messages can be directed to the user's terminal, to a standard error unit, or left to appear on the output file only. The default fatal error exit "**stop 77**" can be sometimes be changed to cause a "traceback" to the subroutine that called **error**, and backward through the stack of subroutines that called it. Also, some systems can cause a drop file or "core" file to be generated for post-mortem analysis with a debugging program.

Subroutines **timer**, **dater**, and **wclock** provide standard interfaces to system routines that sometimes have different names and return different kinds of answers on different computer systems. This is less of a problem with Fortran-90 than it was with previous compilers. The date and wall-clock strings are easy to construct using the standard `date_and_time` call, which is portable to all systems. Some system have an analogous `cpu_time` call, but it is not standard. For other systems, it is necessary to use machine-dependent calls. Some examples of implementing this function on various computer systems are included as UPD machine-dependent idents in the NJOY distribution.

The next four routines in NJOY provide a uniform way of handling input and output files. The unit numbers obey the following convention: zero means do nothing, negative means a binary unit, and positive means a coded unit (ASCII for modern systems.). Unit numbers between 10 and 19 are scratch files, which will be automatically destroyed at the end of the job. Therefore, **repoz** simply takes the absolute value of the unit number and calls `rewind` if it is nonzero. Similarly, **closz** takes the absolute value of the unit number and closes it if nonzero and not a scratch file. Subroutine **skiprz** skips forward with dummy reads of the correct type for the sign of the unit, and it skips backward with backspace. Note that this can be very inefficient for some systems. For example,



the VAX executes backspace by first rewinding and then skipping forward by  $n-1$  records. Making successive calls to backspace, as done in this routine, would be very expensive. It is better to rewind before calling `skiprz`; then only forward skips would be required to get to the desired record. Finally, subroutine `openz` is used to open files with the desired characteristics (that is, binary or formatted, new or old, scratch or permanent). Standard Fortran-90 statements are used. Note that the file names are constructed to have the forms `tape20`, `tape21`, *etc.* Scratch files will have whatever names are standard for the system being used.

The `loada/finda` system was discussed in Section 2.5. The data representation consists of a fairly large buffer array `buf` of length `nbuf`. This buffer contains a number of component blocks, each of length `na`. Therefore, it is easy to compute the location of any block using modular arithmetic on the block index `i`. If the location is currently in the buffer array, the block can be read or written. Otherwise, the associated scratch file `ntape` must be repositioned before being read or written. The files `ntape` have to be written sequentially, but they can be searched in any order. Subroutine `scana` takes advantage of this to locate the block whose first element is closest to the input parameter `e`.

Subroutine `sigfig` is used to control the precision of numbers in several NJOY modules. This is a difficult problem because the true representation of numbers in the machine is as non-terminating binary fractions. In addition, different representations for floating-point numbers are used in different computer systems, and significant-figure truncation can be machine-dependent. The version of `sigfig` used in NJOY2012 seems to be very portable.

Subroutine `a10` is used to make the printing of real numbers on NJOY output listings more compact by stripping off excess characters in the exponent field. It converts the input real number into a 10-character string with the following forms: `+1.23456+6`, `+1.2345-38` and `-1.234+308`. This subroutine is closely related to the private subroutine `a11` in the `endf` module, except for forcing a 10-character field rather than an 11-character field.

**Module “endf”** As discussed in Section 2.4 of this chapter, NJOY uses files in ENDF-like formats for most communications between modules. Subroutines are provided in module `endf` to work with the various ENDF record types. The routines that are public for this module are as follows:

**contio** – to read or write CONT records  
**listio** – to read or write LIST records  
**tablio** – to read or write TAB1 records  
**moreio** – to read or write continuation records  
**tab2io** – to read or write TAB2 records  
**tpidio** – to read or write TAPEID records  
**hdatio** – to read or write character-string records  
**intgio** – to read or write INTG reconrds  
**dictio** – to read or write “dictionary” records  
**tosend** – to read or write to the next SEND record  
**tofend** – to read or write to the next FEND record  
**tomend** – to read or write to the next MEND record  
**totend** – to read or write to the next TEND record  
**asend** – to write SEND record  
**afend** – to write FEND record  
**amend** – to write MEND record  
**atend** – to write TEND record

In addition, the following data words are public for this module:

**c1h** – ENDF C1 field  
**c2h** – ENDF C2 field  
**l1h** – ENDF L1 field  
**l2h** – ENDF L2 field  
**n1h** – ENDF N1 field  
**n2h** – ENDF N2 field  
**math** – ENDF MAT field  
**mf** – ENDF MF field  
**mt** – ENDF MT field  
**nsh** – NS card number (input file)  
**nsp** – NS card number (output file)  
**nsc** – NS card number (scratch file)  
**thr6** – threshold energy for interpolation law 6

There are additional private routines and global variables used inside the module.

Subroutines `contio`, `listio`, `tablio`, `tab2io`, `moreio`, `tpidio`, `hdatio`, `intgio`, and `dictio` are used to read, write, copy, or convert the mode of binary or formatted records on these interface files. They all have similar structures. First, records are read using binary or coded commands, depending on the sign of the unit number. Then the records are written back out, once again using a mode that depends on the sign of the unit number. Unit numbers can be zero, in which case that unit is not used. When these numbers are read, they are converted into integers for the `l1h`, `l2h`, `n1h`, and `n2h` fields using the Fortran nearest-integer function, `nint`. If programmers choose to use a number in the array `a` directly, they should be careful to make the same conversion. Private subroutine `lineio` is used by several of these routines to read or write a line of floating-point numbers. It has two special features. First, any empty fields at the end of a line are filled in with blanks. The second feature is the construction of floating-point numbers without the normal Fortran “E” using subroutine `a11`. Private subroutine `tablio` is used by `tablio` and `tab2io` to read and write ENDF-style interpolation tables. Subroutine `hollio` is used to read or write lines of Hollerith information. Note that Hollerith data are represented using 17 fields per card, but all other ENDF data uses 6 fields per card.

Subroutine `a11` simply breaks up the real-number `x` into a fraction part `f`, a sign part `S`, and an exponent part `n`. The number of digits in the fraction part depends on the number of digits in the exponent part in order to maximize the precision of the formatted representation of `x`. It then constructs a string containing the real number without the normal Fortran “E” and omitting leading zeros in the exponent. If the number being represented has more significant digits than can be represented with the “E” formats, the subroutine automatically shifts to an appropriate “F” format (*e.g.*, F11.8, F11.7, —it etc.) depending on the size of the number. This feature is sometimes needed for the fine texture of resonance data.

As discussed above, ENDF tapes are divided into materials, files, and sections by special end cards with names like MEND, FEND, SEND, and TEND. The subroutines `tosend`, `tofend`, `tomend`, and `totend` can be used to move from the current location to one of these end cards, optionally copying the records as they go. Since these routines do not know the actual structure of the records, they cannot change the mode of the data while copying. They simply read in a record, write it out again if desired, and watch for the specified end card.

The parallel set of routines `asend`, `afend`, `amend`, and `atend` write one of the requested end cards to one or two different output files using the mode defined

by the sign of the unit number. The NJOY convention is to use blanks for the first 66 columns of formatted end cards in order to make them easy to see on ENDF listings. The tapes as received from the National Nuclear Data Center (NNDC) of the Brookhaven National Laboratory may have these fields filled in with numerical values of zero. The **MODER** module automatically changes ENDF tapes from the BNL convention to the NJOY one.

Subroutine **findf** is used very frequently in NJOY modules to search through an ENDF-type tape for a desired section (**mat**, **mf**, **mt**). Since the three numbers that describe sections are always arranged in order, it is possible to search both up and down. On entry, the routine reads the first card and decides if it has to read up or down to find the desired section. It then continues by reading records in the proper direction until it comes to the desired section. It then backs up by one record so that the next read after the call to **findf** will read the first record of the desired section. If the desired section is not found, a fatal error message will be issued. Subroutine **findf** can go into an infinite loop if the MAT number requested is smaller than the number for the first material on the tape (thus **findf** is moving backwards) and the number in the MAT field on the tape identification record is larger than the material number for the first material. Some systems have an “IF (BOI)” function that can be used to detect when the tape is at the “beginning of information.”

Subroutine **terp1** is used to interpolate between two points **x1,y1** and **x2,y2** using ENDF interpolation law **i**. The results for **y** at **x** are given by simple formulas. No tests are made for values that give illegal arguments for the Fortran log and exponent functions. Therefore, fatal arithmetic errors from **terp1** are fairly common. Going slightly out of order, **gral** is a routine that computes integrals inside the endpoints of a segment represented using the ENDF interpolation laws. Once again, simple formulas are used, and it is also possible to get arithmetic errors from the log and exponent functions with this routine.

It is usually necessary to interpolate or integrate functions that involve more than one panel of ENDF interpolated data. Most commonly, this occurs for data in TAB1 format. If the TAB1 record is small enough so that it can fit into an array **a** in memory, subroutine **terpa** can be used to search for the panel that contains **x**, and to interpolate for **y** at **x**. Similarly, **intega** can be used to compute the integral from **x1** to **x2** by integrating over all the panels and parts of panels within these limits. Subroutine **terpa** uses **terp1**, and subroutine **intega** uses **gral**.

NJOY works with some very large TAB1 records that cannot fit into memory. For these cases, **gety1** and **gety2** can be used to interpolate for **y** at **x**. Array **a** only has to be big enough for one page of data (plus a little extra space for parameters like **c1h**, **n2h**, and TAB1 interpolation tables). If the desired **x** is not in memory, new pages of data are read from **itape** until the desired value is found. The subroutine then uses **terp1** to compute **y**. Note that zero is returned if **x** is outside the range of the table, and **xnext=1.e12** when the last point is returned. Subroutines **gety1** and **gety2** are almost identical so that numbers can be retrieved independently from two different input tapes at the same time.

**Module “mathm”** There are several math routines that are needed in various NJOY modules that are provided in this module:

**legndr** – provides Legendre polynomials

**e1** – provides the first-order exponential integral function.

**gami** – provides the incomplete gamma function.

**erfc** – provides the complementary error function.

The last three of these were taken from the SLATEC library, which was developed by the Los Alamos National Laboratory, the Sandia National Laboratory, and the Stanford Linear Accelerator Laboratory. These routines produce very high-precision results as compared to other publicly available routines. They were converted to NJOY conventions and Fortran-90 style for NJOY. This module also contains a large number of private routines that are used in the course of computing the numbers returned by the public routines. Subroutine **legndr** is used to compute Legendre polynomials by recursion. The formulas are as follows:

$$P_0(x) = 1. , \quad (1)$$

$$P_1(x) = x , \quad (2)$$

$$P_{\ell+1}(x) = \frac{(2\ell - 1)xP_\ell(x) - (\ell - 1)P_{\ell-2}}{\ell} , \quad (3)$$

where  $P_0$  is stored in **p(1)**,  $P_1$  is stored in **p(2)**, and so on.



### 3 RECONR

The RECONR module is used to reconstruct resonance cross sections from resonance parameters and to reconstruct cross sections from ENDF nonlinear interpolation schemes. The output is written as a pointwise-ENDF (PENDF) file with all cross sections on a unionized energy grid suitable for linear interpolation to within a specified tolerance. Redundant reactions (for example, total inelastic, charged-particle reactions) are reconstructed to be exactly equal to the sum of their reconstructed and linearized parts at all energies. The resonance parameters are removed from File 2, and the material directory is corrected to reflect all changes. RECONR has the following features:

- Efficient use of dynamic storage allocation and a special stack structure allow very large problems to be run.
- The unionized grid improves the accuracy, usefulness, and ENDF compatibility of the output. All summation cross sections are preserved on the union grid. Up to nine significant figures are allowed.
- A correct directory of the output tape is provided.
- Approximate  $\psi\chi$  Doppler broadening may be used in some cases to speed up reconstruction.
- A resonance-integral criterion is added to the normal linearization criterion in order to reduce the number of points added to the tabulation to represent “unimportant” resonances.
- All ENDF-6 resonance formats currently active are handled, including the calculation of angular distributions from resonance parameters in some cases.

This manual describes RECONR in NJOY 2012.0. The main changes that have been made since the previous report[3] are as follows:

- The change to 7 or 9 significant figures with 64-bit precision (which eliminates the `ndigit` input parameter).
- The addition of new ENDF features, including energy-dependent scattering length, the Reich-Moore channel spin fix, the use of the Reich-Moore-Limited format, computation of angular distributions, and psi-chi broadening for the Multi-Level Breit-Wigner format.
- Expansion of the reaction list to include inelastic levels and charged-particle reactions in addition to the normal elastic, fission, and capture.
- The use of a tighter reconstruction tolerance at thermal energies.
- The change to Fortran-90 style and storage allocation.

### 3.1 ENDF/B Cross Section Representations

A typical cross section derived from an ENDF/B evaluation is shown in Fig. 1. The low-energy cross sections are “smooth”. They are described in File 3 (see Section 2.4 for a review of ENDF/B nomenclature) using cross-section values given on an energy grid with a specified law for interpolation between the points. In the resolved resonance range, resonance parameters are given in File 2, and the cross sections for resonance reactions have to be obtained by adding the contributions of all the resonances to “backgrounds” from File 3. At still higher energies comes the unresolved region where explicit resonances are no longer defined. Instead, the cross section is computed from statistical distributions of the resonance parameters given in File 2 and backgrounds from File 3 (or optionally taken directly from File 3 as for smooth cross sections). Finally, at the highest energies, the smooth File 3 representation is used again.

For light and medium-mass isotopes, the unresolved range is usually omitted. For the lightest isotopes, the resolved range is also omitted, the resonance cross sections being given directly in the “smooth” format. In addition, several different resonance representations are supported (Single-Level Breit-Wigner (SLBW), Multilevel Breit-Wigner (MLBW), Adler-Adler, Hybrid R-Function

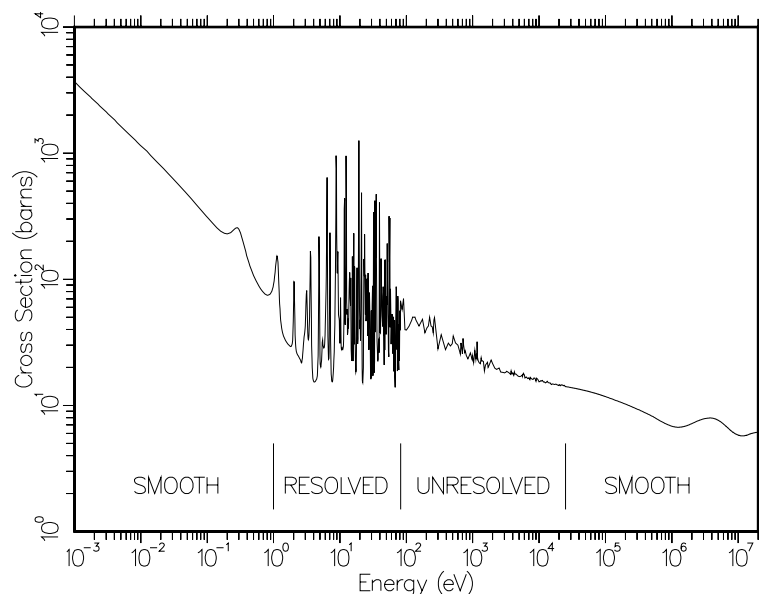


Figure 1: A typical cross section reconstructed from an ENDF/B evaluation using RECONR. The smooth, resolved, and unresolved energy regions use different representations of the cross sections. This is the total cross section for  $^{235}\text{U}$  from ENDF/B-V.



(HRF), Reich-Moore (RM), Reich-Moore-Limited (RML), energy-independent unresolved, and energy-dependent unresolved). The Adler-Adler and Hybrid formats are not being used in modern evaluations. For an increasing number of modern evaluations, the low energy “smooth” region is omitted, and the resolved resonance region is extended to the low energy limit.

RECONR takes these separate representations and produces a simple cross section versus energy representation like the one shown in Fig. 1.

### 3.2 Unionization and Linearization Strategy

Several of the cross sections found in ENDF/B evaluations are summation cross sections (for example, total, inelastic, sometimes (n,2n) or fission, and sometimes charged-particle reactions), and it is important that each summation cross section be equal to the sum of its parts. However, if the partial cross sections are represented with nonlinear interpolation schemes, the sum cannot be represented by any simple interpolation law. A typical case is the sum of elastic scattering (MT=2 interpolated linearly to represent a constant) and radiative capture (MT=102 interpolated log-log to represent  $1/v$ ). The total cross section cannot be represented accurately by either scheme unless the grid points are very close together. This effect leads to significant balance errors in multi-group transport codes and to splitting problems in continuous-energy Monte Carlo codes.

The use of linear-linear interpolation (*i.e.*,  $\sigma$  linear in  $E$ ) can be advantageous in several ways. The data can be plotted easily, they can be integrated easily, cross sections can be Doppler broadened efficiently (see [BROADR](#)), and, linear data can be retrieved efficiently in continuous-energy Monte Carlo codes.

Therefore, RECONR puts all cross sections on a single unionized grid suitable for linear interpolation. As described in more detail below, RECONR makes one pass through the ENDF/B material to select the energy grid, and then a second pass to compute cross sections on this grid. Each cross section on the PENDF file (except for the summation cross sections) is exactly equal to its ENDF/B value. The summation cross sections are then obtained by adding up the partial cross sections at each grid point.

While RECONR is going through the reactions given in the ENDF/B evaluation, it also checks the reaction thresholds against the  $Q$  value and atomic weight ratio to the neutron  $A$  (AWR in the file) given for the reaction. If

$$\text{threshold} \geq \frac{A+1}{A} Q \quad (4)$$

is not true, the threshold energy is moved up to satisfy the condition. This is usually a small change, often only in the least significant digit, and is a consequence of comparing two REAL numbers of finite precision.

If desired, the unionized grid developed from the ENDF/B file can be supplemented with “user grid points” given in the input data. The code automatically adds the conventional thermal point of 0.0253 eV and the 1, 2, and 5 points in each decade to the grid if they are not already present. These simple energy grid points help when comparing materials, and they provide well-controlled starting points for further subdivision of the energy grid.

There are special problems with choosing the energy grid in the unresolved range. In some cases, the unresolved cross section is represented using resonance parameters that are independent of energy. The cross sections are not constant, however, but have a shape determined by the energy variation of neutron wave number, penetrability factors, and so on. RECONR handles this case by choosing a set of energies (about 13 per decade) to be used to calculate the cross sections; the set of energies gives a reasonable approximation to the result intended. For evaluations that use energy-dependent resonance parameters, it is supposed to be sufficient to compute the unresolved cross sections at the given energies and to use interpolation on the cross sections to obtain the appropriate values at other energies. However, some evaluations carried over from earlier versions of ENDF/B were not evaluated using this convention, and cross sections computed using cross-section interpolation are not sufficiently accurate. Even some modern evaluations use inadequate energy grids for the unresolved range. RECONR detects such cases by looking for large steps between the points of the given energy grid. It then adds additional energy grid points using the same 13-per-decade rule used for energy-independent parameters. “Large” is currently defined by `wide` to be a factor of 1.26.

### 3.3 Linearization and Reconstruction Methods

Linearization (`lunion`) and resonance reconstruction (`resxs`) both function by inserting new energy grid points between the points of an original grid using an “inverted stack”. The general concepts involved are illustrated with a simple example shown in Fig. 2.

The stack is first primed with two starting values. For linearization, they will be two adjacent points on the original union grid. For reconstruction, they will usually be the peaks and half-height energies of resonances. The stack is said to be inverted because the lower energy is at the “top” (`I=2`).

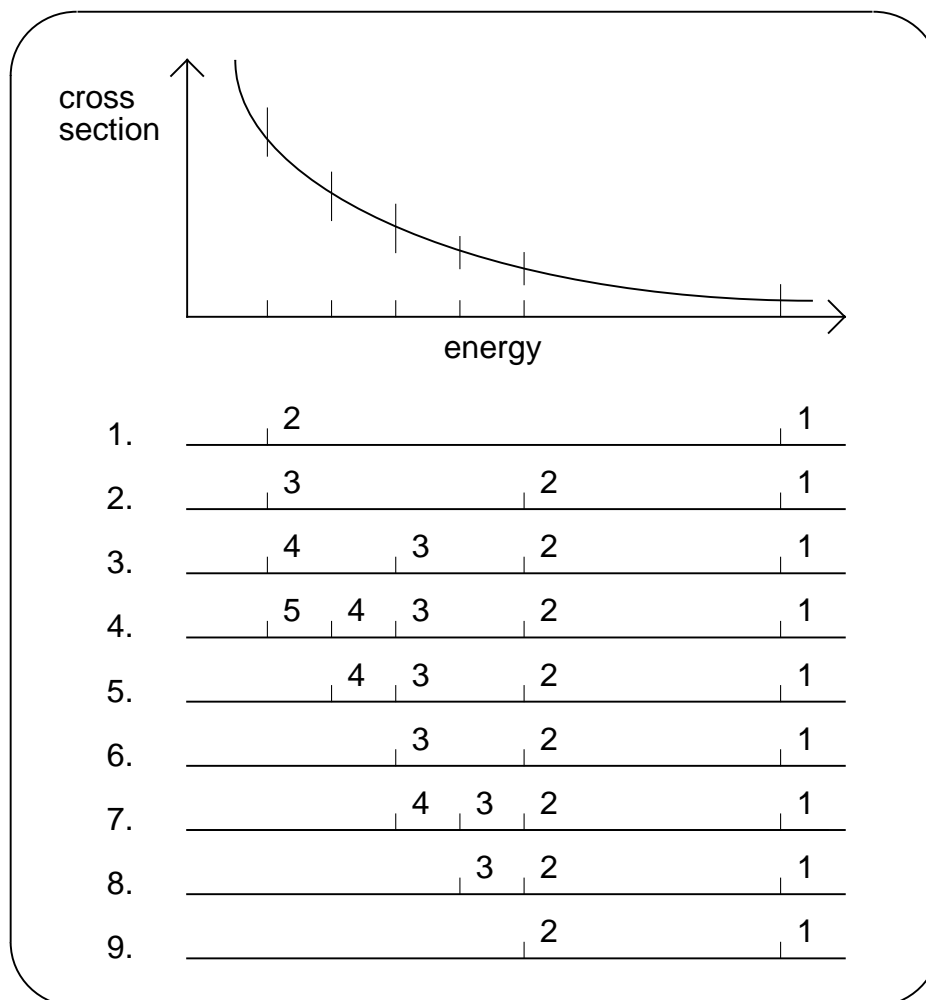


Figure 2: Inverted -stack method used in RECONR and several other places in NJOY. Line 1 shows the two initial points (the lower energy is higher in the stack). In line 2, a new point has been calculated at the midpoint, but the result was not converged, and the new point has been inserted in the stack. In line 3, the midpoint of the top panel has been checked again, found to be not converged, and inserted into the stack. The same thing happens in line 4. In line 5, the top panel is found to be converged, and the top point (5) has been written out. The same thing happens in line 6. In line 7, the top panel is tested and found to be not converged. The midpoint is added to the stack. Finally, in line 8, the top panel is found to be converged, and the top point is written out. This leaves two points in the stack (see line 9). Note that the energy points come off the stack in the desired order of increasing energy, and that only one point has to be moved up in the stack as each new result is inserted.

This interval or panel is now divided into two parts, and the cross section computed at the intermediate point is compared to the result of linear interpolation between the adjacent points. If the two values do not agree within various criteria, the top of the stack is moved up one notch ( $I=3$ ), and the new value is inserted ( $I=2$ ). The code then repeats the checking process for the new (smaller) interval at the top of the stack. The top of the stack rises until convergence is achieved for the top interval. The top energy and cross section are then saved on a scratch file, the stack index is decremented, and the checks are repeated. This process is continued with the top of the stack rising and falling in response to the complexity of the cross section until the entire panel  $\Delta E$  has been converged ( $I=1$ ). The stack is then reprimed with the bounds of the next panel. The process continues until the entire energy range for linearization or reconstruction has been processed.

This stack logic enables a panel to be subdivided into parts as small as  $\Delta E/2^n$  where  $n$  is the stack size, and several different cross sections (elastic, capture, fission) can easily be stored in arrays of this size.

The convergence criterion used for linearization is that the linearized cross section at the intermediate point is within the fractional tolerance `err` (or a small absolute value `errlim`) of the actual cross section specified by the ENDF law. More complicated criteria are used for resonance reconstruction.

There are two basic problems that arise if a simple fractional tolerance test is used to control resonance reconstruction. First, as points are added to the energy grid, adjacent energy values may become so close that they will be rounded to the same number when a formatted output file is produced. There can be serious problems if the code continues to add grid points after this limit is reached. Through the use of dynamic format reconstruction, the energy resolution available for formatted NJOY output (which used ENDF 11-character fields) is 7 significant figures (that is,  $\pm 1.234567 \pm n$ ) rather than the usual 5 or 6 (see Section 2.4). For NJOY2012, the Fortran-90 “kind” parameter is used to assure sufficient precision for this. Even this seven significant figure format is sometimes insufficient for very narrow resonances. If necessary, NJOY can go to nine significant figures by using a Fortran “F” format, *e.g.*,  $\pm 1234.56789$ .

Significant-figure control is implemented as follows: each intermediate energy is first truncated to 7 significant figures before the corresponding cross sections are computed. If the resulting number is equal to either of the adjacent values and convergence has not been obtained, subdivision continues using energies truncated to 9 significant figures. If an energy on this finer grid is equal to

either of the adjacent values, the interval is declared to be converged even though convergence has not been achieved. Thus, no identical energies are produced, but an unpredictable but very small loss in accuracy results.

The second basic problem alluded to above is that a very large number of resonance grid points arise from straightforward linear reconstruction of the resonance cross section of some isotopes. Many of these points come from narrow, weak, high-energy resonances, which do not need to be treated accurately in many applications. As an example, the capture and fission resonance integrals important for thermal reactors must be computed with a  $1/E$  flux weighting. If the resonance reconstruction tolerance is set high (say 1%) to reduce the cost of processing, the resonance integrals will be computed to only 1% accuracy. However, if the reconstruction tolerance were set to a smaller value, like 0.1%, and if the high-energy resonances (whose importance is reduced by the  $1/E$  weight and the  $1/v$  trend of the capture and fission cross sections) were treated with less accuracy than the low-energy resonances, then it is likely that one could achieve an accuracy much better than 1% with an overall reduction in the number of points (hence computing cost). Since  $1/E$  weighting is not realistic in all applications (for example, in fast reactors), user control of this “thinning” operation must be provided.

Based on these arguments, the following approach was chosen to control the problem of very large files. First, panels are subdivided until the elastic, capture, and fission cross sections are converged to within **errmax**, where **errmax**  $\geq$  **err**. These two tolerances are normally chosen to form a reasonable band, such as 1% and 0.1%, to ensure that all resonances are treated at least roughly (for example, for plotting). If the resonance integral ( $1/E$  weight) in some panel is large, the panel is further subdivided to achieve an accuracy of **err** (say 0.1%). However, if the contribution to the resonance integral from any one interval gets small, the interval will be declared converged, and the local value of the cross section will end up with some intermediate accuracy. The contribution to the error in the resonance integral should be less than  $0.5 \times \Delta\sigma \times \Delta E$ . This value is added into an accumulating estimate of the error, and a count of panels truncated by the resonance integral check is incremented.

The problem with this test is that RECONR does not know the value of the resonance integral in advance, so the tolerance parameter **errint** is not the actual allowed fractional error in the integral. Instead, it is more like the resonance integral error per grid point (barns/point). Thus, a choice of **errint**=**err**/10000 with **err**=0.001 would limit the integral error to about 0.001 barn if 10000 points

resulted from reconstruction. Since important resonance integrals vary from a few barns to a few hundred barns, this is a reasonable choice. The integral check can be suppressed by setting **errint** very small or **errmax=err**.

When resonance reconstruction is complete, RECONR provides a summary of the possible resonance integral error due to the integral check over several coarse energy bands. A example from ENDF/B-VII.0  $^{235}\text{U}$  follows:

| estimated maximum error due to<br>resonance integral check (errmax,errint) |                     |                  |                     |                  |                     |                  |
|----------------------------------------------------------------------------|---------------------|------------------|---------------------|------------------|---------------------|------------------|
| upper<br>energy                                                            | elastic<br>integral | percent<br>error | capture<br>integral | percent<br>error | fission<br>integral | percent<br>error |
| 1.00E-05                                                                   |                     |                  |                     |                  |                     |                  |
| 1.00E-04                                                                   | 3.50E+01            | 0.000            | 8.15E+03            | 0.000            | 4.29E+04            | 0.000            |
| 1.00E-03                                                                   | 3.50E+01            | 0.000            | 2.57E+03            | 0.000            | 1.36E+04            | 0.000            |
| 1.00E-02                                                                   | 3.50E+01            | 0.000            | 8.02E+02            | 0.000            | 4.24E+03            | 0.000            |
| 1.00E-01                                                                   | 3.46E+01            | 0.000            | 2.15E+02            | 0.000            | 1.26E+03            | 0.000            |
| 1.00E+00                                                                   | 3.25E+01            | 0.000            | 6.03E+01            | 0.000            | 3.26E+02            | 0.000            |
| 2.00E+00                                                                   | 8.95E+00            | 0.000            | 7.31E+00            | 0.000            | 2.62E+01            | 0.000            |
| 5.00E+00                                                                   | 1.08E+01            | 0.000            | 1.25E+01            | 0.000            | 1.56E+01            | 0.000            |
| 1.00E+01                                                                   | 7.75E+00            | 0.000            | 2.40E+01            | 0.000            | 3.52E+01            | 0.000            |
| 2.00E+01                                                                   | 8.18E+00            | 0.000            | 2.92E+01            | 0.000            | 3.31E+01            | 0.000            |
| 5.00E+01                                                                   | 1.07E+01            | 0.000            | 2.57E+01            | 0.000            | 3.83E+01            | 0.000            |
| 1.00E+02                                                                   | 8.30E+00            | 0.000            | 1.07E+01            | 0.000            | 2.34E+01            | 0.000            |
| 2.00E+02                                                                   | 8.04E+00            | 0.000            | 8.17E+00            | 0.000            | 1.42E+01            | 0.000            |
| 5.00E+02                                                                   | 1.10E+01            | 0.001            | 6.81E+00            | 0.008            | 1.51E+01            | 0.004            |
| 1.00E+03                                                                   | 8.28E+00            | 0.008            | 3.44E+00            | 0.080            | 7.62E+00            | 0.038            |
| 2.00E+03                                                                   | 8.27E+00            | 0.033            | 2.54E+00            | 0.261            | 5.06E+00            | 0.185            |
| points added by resonance reconstruction = 232418                          |                     |                  |                     |                  |                     |                  |
| points affected by resonance integral check = 80445                        |                     |                  |                     |                  |                     |                  |
| final number of resonance points = 242170                                  |                     |                  |                     |                  |                     |                  |
| number of points in final unionized grid = 242600                          |                     |                  |                     |                  |                     |                  |

The parameters **errmax** and **errint**, taken together, should be considered as adjustment “knobs” that can increase or decrease the errors in the “res-int” columns to get an appropriate balance between accuracy and economy for a particular application. The error from significant figure reduction provided by earlier versions of NJOY is no longer needed.

For energies in the thermal range (energies less than `trange=0.5 eV`), the user's reconstruction tolerance is divided by a factor of 5 in order to give better results for several important thermal integrals, especially after Doppler broadening, and to make the 0.0253 eV cross section behave well under Doppler broadening.

### 3.4 Resonance Representations

RECONR uses the resonance formulas as implemented in the original RESEND code[25] with several changes: a more efficient calculation of MLBW cross sections developed by C. R. Lubitz of the Knolls Atomic Power Laboratory (KAPL) and coded by P. Rose of the National Nuclear Data Center (NNDC) at the Brookhaven National Laboratory (BNL), the addition of competitive widths introduced for ENDF/B-V, a  $\psi\chi$  Doppler-broadening calculation for SLBW and Adler-Adler resonance shapes, and a capability to process either the multi-level multi-channel R-matrix Reich-Moore parameters or the multi-level single-channel Hybrid R-Function parameters based on the work of M. Bhat and C. Dunford of the NNDC, an implementation of the GH method for MLBW resonances, which allows psi-chi broadening, and a capability to process the new RML parameters, including resolved resonance energy region angular distributions.

Expanded discussions of the following formulas can be found in the ENDF-6 format manual[8].

**Single-Level Breit-Wigner Representation (SLBW)** The subroutine that computes Single-Level Breit-Wigner cross sections (`csslbw`) uses

$$\begin{aligned} \sigma_n &= \sigma_p \\ &+ \sum_{\ell} \sum_r \sigma_{mr} \left\{ \left[ \cos 2\phi_{\ell} - \left(1 - \frac{\Gamma_{nr}}{\Gamma_r}\right) \right] \psi(\theta, x) \right. \\ &\left. + \sin 2\phi_{\ell} \chi(\theta, x) \right\} , \end{aligned} \quad (5)$$

$$\sigma_f = \sum_{\ell} \sum_r \sigma_{mr} \frac{\Gamma_{fr}}{\Gamma_r} \psi(\theta, x) , \quad (6)$$

$$\sigma_{\gamma} = \sum_{\ell} \sum_r \sigma_{mr} \frac{\Gamma_{\gamma r}}{\Gamma_r} \psi(\theta, x) , \text{ and} \quad (7)$$

$$\sigma_p = \sum_{\ell} \frac{4\pi}{k^2} (2\ell + 1) \sin^2 \theta_{\ell} , \quad (8)$$

where  $\sigma_n$ ,  $\sigma_f$ ,  $\sigma_\gamma$ , and  $\sigma_p$  are the neutron (elastic), fission, radiative capture, and potential scattering components of the cross section arising from the given resonances. There can be “background” cross sections in File 3 that must be added to these values to account for competitive reactions such as inelastic scattering or to correct for the inadequacies of the single-level representation with regard to multilevel effects or missed resonances. The sums extend over all the  $\ell$  values and all the resolved resonances  $r$  with a particular value of  $\ell$ . Each resonance is characterized by its total, neutron, fission, and capture widths ( $\Gamma, \Gamma_n, \Gamma_f, \Gamma_\gamma$ ), by its  $J$  value (AJ in the file), and by its maximum value ( $\mathbf{smax} = \sigma_{mr}/\Gamma_r$  in the code)

$$\sigma_{mr} = \frac{4\pi}{k^2} g_J \frac{\Gamma_{nr}}{\Gamma_r} , \quad (9)$$

where  $g_J$  is the spin statistical factor

$$g_J = \frac{2J+1}{4I+2} , \quad (10)$$

and  $I$  is the total spin (SPI) given in File 2, and  $k$  is the neutron wave number, which depends on incident energy  $E$  and the atomic weight ratio to the neutron for the isotope  $A$  (AWRI in the file), as follows:

$$k = (2.196771 \times 10^{-3}) \frac{A}{A+1} \sqrt{E} . \quad (11)$$

There are two different characteristic lengths that appear in the ENDF resonance formulas: first, there is the “scattering radius”  $\hat{a}$ , which is given directly in File 2 as AP; and second, there is the “channel radius”  $a$ , which is given by

$$a = 0.123 A^{1/3} + 0.08 . \quad (12)$$

If the File 2 parameter NAPS is equal to one,  $a$  is set equal to  $\hat{a}$  in calculating penetrabilities and shift factors (see below). The ENDF-6 option to enter an energy-dependent scattering radius is not supported. The neutron width in the equations for the SLBW cross sections is energy dependent due to the penetration factors  $P_\ell$ ; that is,

$$\Gamma_{nr}(E) = \frac{P_\ell(E) \Gamma_{nr}}{P_\ell(|E_r|)} , \quad (13)$$



where

$$P_0 = \rho , \quad (14)$$

$$P_1 = \frac{\rho^3}{1 + \rho^2} , \quad (15)$$

$$P_2 = \frac{\rho^5}{9 + 3\rho^2 + \rho^4} , \quad (16)$$

$$P_3 = \frac{\rho^7}{225 + 45\rho^2 + 6\rho^4 + \rho^6} , \text{ and} \quad (17)$$

$$P_4 = \frac{\rho^9}{11025 + 1575\rho^2 + 135\rho^4 + 10\rho^6 + \rho^8} , \quad (18)$$

where  $E_r$  is the resonance energy and  $\rho=ka$  depends on the channel radius or the scattering radius as specified by NAPS. The phase shifts are given by

$$\phi_0 = \hat{\rho} , \quad (19)$$

$$\phi_1 = \hat{\rho} - \tan^{-1} \hat{\rho} , \quad (20)$$

$$\phi_2 = \hat{\rho} - \tan^{-1} \frac{3\hat{\rho}}{3 - \hat{\rho}^2} , \quad (21)$$

$$\phi_3 = \hat{\rho} - \tan^{-1} \frac{15\hat{\rho} - \hat{\rho}^3}{15 - 6\hat{\rho}^2} , \text{ and} \quad (22)$$

$$\phi_4 = \hat{\rho} - \tan^{-1} \frac{105\hat{\rho} - 10\hat{\rho}^3}{105 - 45\hat{\rho}^2 + \hat{\rho}^4} , \quad (23)$$

where  $\hat{\rho}=k\hat{a}$  depends on the scattering radius. The final components of the cross section are the actual line shape functions  $\psi$  and  $\chi$ . At zero temperature,

$$\psi = \frac{1}{1 + x^2} , \quad (24)$$

$$\chi = \frac{x}{1 + x^2} , \quad (25)$$

$$x = \frac{2(E - E'_r)}{\Gamma_r} , \quad (26)$$

and

$$E'_r = E_r + \frac{S_\ell(|E_r|) - S_\ell(E)}{2(P_\ell(|E_r|))} \Gamma_{nr}(|E_r|) , \quad (27)$$

in terms of the shift factors

$$S_0 = 0 , \quad (28)$$

$$S_1 = -\frac{1}{1+\rho^2} , \quad (29)$$

$$S_2 = -\frac{18+3\rho^2}{9+3\rho^2+\rho^4} , \quad (30)$$

$$S_3 = -\frac{675+90\rho^2+6\rho^4}{225+45\rho^2+6\rho^4+\rho^6} , \text{ and} \quad (31)$$

$$S_4 = -\frac{44100+4725\rho^2+270\rho^4+10\rho^6}{11025+1575\rho^2+135\rho^4+10\rho^6+\rho^8} . \quad (32)$$

To go to higher temperatures, define

$$\theta = \frac{\Gamma_r}{\sqrt{\frac{4kTE}{A}}} , \quad (33)$$

where  $k$  is the Boltzmann constant and  $T$  is the absolute temperature. The line shapes  $\psi$  and  $\chi$  are now given by

$$\psi = \frac{\sqrt{\pi}}{2} \theta \operatorname{Re} W\left(\frac{\theta x}{2}, \frac{\theta}{2}\right) , \quad (34)$$

and

$$\chi = \frac{\sqrt{\pi}}{2} \theta \operatorname{Im} W\left(\frac{\theta x}{2}, \frac{\theta}{2}\right) , \quad (35)$$

in terms of the complex probability function (see `quickw`, `wtab`, and `w`, which came from the MC<sup>2</sup> code[36])

$$W(x, y) = e^{-z^2} \operatorname{erfc}(-iz) = \frac{i}{\pi} \int_{-\infty}^{\infty} \frac{e^{-t^2}}{z-t} dt , \quad (36)$$

where  $z=x+iy$ . The  $\psi\chi$  method is not as accurate as kernel broadening (see [BROADR](#)) because the backgrounds (which are sometimes quite complex) are not broadened, and terms important for energies less than about  $16kT/A$  are neglected; however, the  $\psi\chi$  method is less expensive than [BROADR](#). Previous versions of RECONR included  $\psi\chi$  broadening for the SLBW and Adler-Adler representations only. This version also allows the method to be used for MLBW cases. The SLBW approach can produce negative elastic cross sections. If found, they are set to a small positive value, and a count is accumulated for a diagnostic in the listing file.

**Multilevel Breit-Wigner Representation (MLBW)** The Lubitz-Rose method used for calculating Multi-Level Breit-Wigner cross sections (`csmlbw`) is formulated as follows:

$$\sigma_n(E) = \frac{\pi}{k^2} \sum_{\ell} \sum_{s=|I-\frac{1}{2}|}^{I+\frac{1}{2}} \sum_{J=|l-s|}^{l+s} g_J |1 - U_{nn}^{\ell s J}(E)|^2, \quad (37)$$

with

$$U_{nn}^{\ell J}(E) = e^{2i\phi_{\ell}} - \sum_r \frac{i\Gamma_{nr}}{E'_r - E - i\Gamma_r/2}, \quad (38)$$

where the other symbols are the same as those used above. Expanding the complex operations gives

$$\begin{aligned} \sigma_n(E) &= \frac{\pi}{k^2} \sum_{\ell} \sum_{s=|I-\frac{1}{2}|}^{I+\frac{1}{2}} \sum_{J=|l-s|}^{l+s} g_J \left\{ \left( 1 - \cos 2\phi_{\ell} - \sum_r \frac{\Gamma_{nr}}{\Gamma_r} \frac{2}{1+x_r^2} \right)^2 \right. \\ &\quad \left. + \left( \sin 2\phi_{\ell} + \sum_r \frac{\Gamma_{nr}}{\Gamma_r} \frac{2x_r}{1+x_r^2} \right)^2 \right\}, \end{aligned} \quad (39)$$

where the sums over  $r$  are limited to resonances in spin sequence  $\ell$  that have the specified value of  $s$  and  $J$ . Unfortunately, the  $s$  dependence of  $\Gamma$  is not known. The file contains only  $\Gamma_J = \Gamma_{s_1 J} + \Gamma_{s_2 J}$ . It is assumed that the  $\Gamma_J$  can be used for one of the two values of  $s$ , and zero is used for the other. Of course, it is important to include both channel-spin terms in the potential scattering. Therefore, the equation is written in the following form:

$$\begin{aligned} \sigma_n(E) &= \frac{\pi}{k^2} \sum_{\ell} \left[ \sum_J g_J \left\{ \left( 1 - \cos 2\phi_{\ell} - \sum_r \frac{\Gamma_{nr}}{\Gamma_r} \frac{2}{1+x_r^2} \right)^2 \right. \right. \\ &\quad \left. \left. + \left( \sin 2\phi_{\ell} + \sum_r \frac{\Gamma_{nr}}{\Gamma_r} \frac{2x_r}{1+x_r^2} \right)^2 \right\} + 2D_{\ell}(1 - \cos 2\phi_{\ell}) \right], \end{aligned} \quad (40)$$

where the summation over  $J$  now runs from

$$||I - \ell| - \frac{1}{2}| \rightarrow I + \ell + \frac{1}{2}, \quad (41)$$

and  $D_{\ell}$  gives the additional contribution to the statistical weight resulting from duplicate  $J$  values not included in the new  $J$  sum; namely,

$$D_\ell = \sum_{s=|I-\frac{1}{2}|}^{I+\frac{1}{2}} \sum_{J=|l-s|}^{l+s} g_J - \sum_{J=||I-\ell|-\frac{1}{2}|}^{I+\ell+\frac{1}{2}} g_J \quad (42)$$

$$= (2\ell + 1) - \sum_{J=||I-\ell|-\frac{1}{2}|}^{I+\ell+\frac{1}{2}} g_J . \quad (43)$$

A case where this correction would appear is the  $\ell=1$  term for a spin-1 nuclide. There will be 5  $J$  values: 1/2, 3/2, and 5/2 for channel spin 3/2; and 1/2 and 3/2 for channel spin 1/2. All five contribute to the potential scattering, but the file will only include resonances for the first three.

The fission and capture cross sections are the same as for the single-level option. The  $\psi\chi$  Doppler-broadening cannot be used with this formulation of the MLBW representation.

However, there is an alternate representation available that does support  $\psi\chi$  broadening:

$$\begin{aligned} \sigma_n &= \sigma_p \\ &+ \sum_\ell \sum_r \sigma_{mr} \left\{ \left[ \cos 2\phi_\ell - \left(1 - \frac{\Gamma_{nr}}{\Gamma_r}\right) + \frac{G_{r\ell}}{\Gamma_{nr}} \right] \psi(\theta, x) \right. \\ &\left. + \left( \sin 2\phi_\ell + \frac{H_{r\ell}}{\Gamma_{nr}} \right) \chi(\theta, x) \right\} , \end{aligned} \quad (44)$$

where

$$G_{r\ell} = \frac{1}{2} \sum_{\substack{r' \neq r \\ J_{r'} \neq J_r}} \Gamma_{nr} \Gamma_{nr'} \frac{\Gamma_r + \Gamma_{r'}}{(E_r - E_{r'})^2 + (\Gamma_r + \Gamma_{r'})^2/4} , \quad (45)$$

and

$$H_{r\ell} = \sum_{\substack{r' \neq r \\ J_{r'} \neq J_r}} \Gamma_{nr} \Gamma_{nr'} \frac{E_r - E_{r'}}{(E_r - E_{r'})^2 + (\Gamma_r + \Gamma_{r'})^2/4} . \quad (46)$$

Nominally, this method is slower than the previous one because it contains a double sum over resonances at each energy. However, it turns out that  $G$  and  $H$  are slowly varying functions of energy, and the calculation can be accelerated by computing them at just a subset of the energies and getting intermediate values by interpolation. It is important to use a large number of  $r'$  values on each side of  $r$ . The GH MLBW method is implemented in `csmlbw2`.

**Adler-Adler Representation (Adler-Adler)** The multilevel Adler-Adler representation (`csaa`) is defined for  $\ell=0$  only. It is useful for fissionable materials. The total cross sections are given by

$$\begin{aligned}\sigma_t(E) = & \frac{4\pi}{k^2} \sin^2 \phi_0 \\ & + \frac{\pi\sqrt{E}}{k^2} \left\{ \sum_r \frac{1}{\nu_r} \left[ (G_r \cos 2\phi_0 + H_r \sin 2\phi_0) \psi(\theta, x) \right. \right. \\ & + \left. \left. (H_r \cos 2\phi_0 - G_r \sin 2\phi_0) \chi(\theta, x) \right] \right. \\ & + \left. A_1 + \frac{A_2}{E} + \frac{A_3}{E^2} + \frac{A_4}{E^3} + B_1 E + B_2 E^2 \right\},\end{aligned}\quad (47)$$

where

$$x = \frac{\mu_r - E}{\nu_r}, \quad (48)$$

and where  $\nu_r$  is the resonance half-width (corresponds to  $\Gamma/2$  in the Breit-Wigner notation),  $\mu_r$  is the resonance energy,  $G_r$  is the symmetric total parameter,  $H_r$  is the asymmetric total parameter, and the  $A_i$  and  $B_i$  are coefficients of the total background correction.

The fission and capture cross section both use the form

$$\begin{aligned}\sigma_x(E) = & \frac{\pi\sqrt{E}}{k^2} \left\{ \sum_r \frac{1}{\nu_r} [G_r \psi(\theta, x) + H_r \chi(\theta, x)] \right. \\ & + \left. A_1 + \frac{A_2}{E} + \frac{A_3}{E^2} + \frac{A_4}{E^4} + B_1 E + B_2 E^2 \right\},\end{aligned}\quad (49)$$

where the values of  $G$ ,  $H$ ,  $A_i$ , and  $B_i$  appropriate for the desired reaction are used.

Doppler-broadening can be applied as for the SLBW case, except note that  $\Gamma_r$  in Eq. 27 must be replaced with  $2\nu_r$ . Doppler-broadened Adler-Adler cross sections are more accurate than SLBW cross sections because the background is smoother. However, cross sections below about  $16kT/A$  will still be inaccurate. The Adler-Adler method is not used in modern evaluations.

**Reich-Moore Representation (RM)** The Reich-Moore representation as implemented in subroutine `csrmat` is a multi-level formulation with two fission channels; hence, it is useful for both structural and fissionable materials. The cross sections are given by

$$\sigma_t = \frac{2\pi}{k^2} \sum_{\ell} \sum_J g_J \left\{ (1 - \text{Re } U_{nn}^{\ell J}) + 2d_{\ell J} [1 - \cos(2\phi_{\ell})] \right\}, \quad (50)$$

$$\sigma_n = \frac{\pi}{k^2} \sum_{\ell} \sum_J g_J \left\{ |1 - U_{nn}^{\ell J}|^2 + 2d_{\ell J} [1 - \cos(2\phi_{\ell})] \right\}, \quad (51)$$

$$\sigma_f = \frac{4\pi}{k^2} \sum_{\ell} \sum_J g_J \sum_c |\mathcal{I}_{nc}^{\ell J}|^2, \text{ and} \quad (52)$$

$$\sigma_{\gamma} = \sigma_t - \sigma_n - \sigma_f, \quad (53)$$

where  $\mathcal{I}_{nc}$  is an element of the inverse of the complex R-matrix and

$$U_{nn}^{\ell J} = e^{2i\phi_{\ell}} \left[ 2\mathcal{I}_{nn} - 1 \right]. \quad (54)$$

The elements of the R-matrix are given by

$$R_{nc}^{\ell J} = \delta_{nc} - \frac{i}{2} \sum_r \frac{\Gamma_{nr}^{1/2} \Gamma_{cr}^{1/2}}{E_r - E - \frac{i}{2} \Gamma_{\gamma r}}. \quad (55)$$

In these equations, “c” stands for the fission channel, “r” indexes the resonances belonging to spin sequence  $(\ell, J)$ , and the other symbols have the same meanings as for SLBW or MLBW. Of course, when fission is not present,  $\sigma_f$  can be ignored. The R-matrix reduces to an R-function, and the matrix inversion normally required to get  $\mathcal{I}_{nn}$  reduces to a simple inversion of a complex number.

As in the MLBW case, the summation over  $J$  runs from

$$||I - \ell| - \frac{1}{2}| \rightarrow I + \ell + \frac{1}{2}. \quad (56)$$

The term  $d_{\ell J}$  in the expressions for the total and elastic cross sections is used to account for the possibility of an additional contribution to the potential scattering cross section from the second channel spin. It is unity if there is a second  $J$  value equal to  $J$ , and zero otherwise. This is just a slightly different approach for making the correction discussed in connection with Eq. (43). Returning to the  $I=1, \ell=1$  example given above,  $d$  will be one for  $J=1/2$  and  $J=3/2$ , and it will be zero for  $J=5/2$ .

ENDF-6 format RM evaluations can contain a parameter LAD that indicates that these parameters can be used to compute an angular distribution for elastic scattering if desired (an approximate angular distribution is still given in File 4 for these cases). The current version of RECONR has such a capability, and it can be used with RM evaluations. Because of channel-spin issues, it works best with RML evaluations. See below for a discussion of angular distributions.

**Hybrid R-Function Representation (HRF)** The Hybrid R-Function representation treats elastic scattering as a multi-level cross section using formulas similar to those given above for the Reich-Moore format in the case where fission is absent. The other reactions are treated with formulas similar to those of the SLBW method. The main use for this format is to provide a better representation of competitive reactions than is provided by any of the other formats described above. This treatment can include a background R-function, tabulated charged-particle penetrabilities, and optical model phase shifts. Following the RM notation, the elastic cross section is given by

$$\sigma_n = \frac{\pi}{k^2} \sum_{\ell} \sum_{s=|I-\frac{1}{2}|}^{I+\frac{1}{2}} \sum_{J=|l-s|}^{l+s} g_J |1 - U_{nn}^{\ell s J}|^2, \quad (57)$$

where the  $U$  function is given by the scalar version of Eq. (54):

$$U_{nn}^{\ell s J} = e^{2i\phi_{\ell}} \left[ \frac{2}{R_{nn}^{\ell s J}} - 1 \right]. \quad (58)$$

The R-function itself is given by

$$R_{nn}^{\ell s J} = 1 - \frac{i}{2} \sum_r \frac{\Gamma_{nr}}{E_r - E - \frac{i}{2}\Gamma_{\gamma r}} - i P_{\ell s J} R_{\ell s J}^0, \quad (59)$$

where  $R_{\ell s J}^0$  is a (complex) background R function and  $P_{\ell s J}$  is a penetrability factor. The background R function can either be read in or set to zero. The penetrability and shift factors are computed from the scattering radius or channel radius as for SLBW. The phase shifts  $\phi_{\ell s J}$  can be computed from the scattering radius as before, or the (complex) phase shifts can be read in from an optical model calculation.

Note that resonance parameters are given explicitly for all three quantum numbers  $\ell$ ,  $s$ , and  $J$ . No correction to the potential scattering cross section from repeated  $J$  values is needed.

Elastic angular distributions can also be computed from HRF parameters if the LAD parameter is set; however, RECONR does not support that.

**Reich-Moore-Limited Representaton (RML)** The Reich-Moore-Limited representation is a more general multilevel and multichannel formulation. In addition to the normal elastic, fission, and capture reactions, it allows for inelastic scattering and Coulomb reactions. Furthermore, it allows resonance angular distributions to be calculated. It is also capable of computing derivatives of cross sections with respect to resonance parameters. See [ERRORR](#). The RML processing in NJOY is based on the SAMMY code[35]. The calculation in RECONR makes use of several subroutines exported by the `samm` module; namely, `s2samm`, `ppsamm`, `rdsamm`, `cssamm`, and `desamm`.

The quantities that are conserved during neutron scattering and reactions are the total angular momentum  $J$  and its associated parity  $\pi$ , and the RML format lumps all the channels with a given  $J^\pi$  into a “spin group.” In each spin group, the reaction channels are defined by  $c = (\alpha, \ell, s, J)$ , where  $\alpha$  stands for the particle pair (masses, charges, spins, parities, and Q-value),  $\ell$  is the orbital angular momentum with associated parity  $(-1)^\ell$ , and  $s$  is the channel spin (the vector sum of the spins of the two particles of the pair). The  $\ell$  and  $s$  values must vector sum to  $J^\pi$  for the spin group. The channels are divided into incident channels and exit channels. Here, the important input channel is defined by the particle pair neutron+target. There can be several such incident channels in a given spin group. The exit channel particle pair defines the reaction taking place. If the exit channel is the same as the incident channel, the reaction is elastic scattering. There can be several exit channels that contribute to a given reaction.

The R-matrix in the Reich-Moore “eliminated width” approximation for a given spin group is given by

$$R_{cc'} = \sum_{\lambda} \frac{\gamma_{\lambda c} \gamma_{\lambda c'}}{E_{\lambda} - E - i\Gamma_{\lambda\gamma}/2} + R_c^b \delta_{cc'}, \quad (60)$$

where  $c$  and  $c'$  are incident and exit channel indexes,  $\lambda$  is the resonance index for resonances in this spin group,  $E_{\lambda}$  is a resonance energy,  $\gamma_{\lambda c}$  is a resonance amplitude, and  $\Gamma_{\lambda\gamma}$  is the “eliminated width,” which normally includes all of the radiation width (capture). The channel indexes runs over the “particle channels” only, which doesn’t include capture. The quantity  $R_c^b$  is the “background R-matrix.”



In order to calculate the contribution of this spin group to the cross sections, we first compute the following quantity:

$$X_{cc'} = P_c^{1/2} L_c^{-1} \sum_{c''} Y_{cc''}^{-1} R_{c''c'} P_{c'}^{1/2}, \quad (61)$$

where

$$Y_{cc''} = L_c^{-1} \delta_{cc''} - R_{cc''}, \quad (62)$$

and

$$L_c = S_c - B_c + iP_c. \quad (63)$$

Here, the  $P_c$  and  $S_c$  are penetrability and shift factors, and the  $B_c$  are boundary constants. The cross sections can now be written down in terms of the  $X_{cc'}$ . For elastic scattering

$$\sigma_{elastic} = \frac{4\pi}{k_\alpha^2} \sum_{J^\pi} \left[ \sin^2 \phi_c (1 - 2X_{cc}^i) - X_{cc}^r \sin(2\phi_c) + \sum_{c'} |X_{cc'}|^2 \right],$$

where  $X_{cc'}^r$  is the real part of  $X_{cc'}$ ,  $X_{cc'}^i$  is the imaginary part,  $\phi_c$  is the phase shift, the sum over  $J^\pi$  is a sum over spin groups, the sum over  $c$  is limited to incident channels in the spin group with particle pair  $\alpha$  equal to neutron+target, and the sum over  $c'$  is limited to exit channels in the spin group with particle pair  $\alpha$ . Similarly, the capture cross section becomes

$$\sigma_{capture} = \frac{4\pi}{k_\alpha^2} \sum_{J^\pi} \sum_c g_{J\alpha} \sum_c \left[ X_{cc}^i - \sum_{c'} |X_{cc'}|^2 \right], \quad (64)$$

where the sum over  $J^\pi$  is a sum over spin groups, the sum over  $c$  is a sum over incident channels in the spin group with particle pair  $\alpha$  equal to neutron+target, and the sum over  $c'$  includes all channels in the spin group. The cross sections for other reactions (if present) are given by

$$\sigma_{reaction} = \frac{4\pi}{k_\alpha^2} \sum_{J^\pi} g_{J\alpha} \sum_c \left[ X_{cc}^i - \sum_{c'} |X_{cc'}|^2 \right], \quad (65)$$

where the sum over  $c$  is limited to channels in the spin group  $J^\pi$  with particle pair  $\alpha$  equal to neutron+target, and the sum over  $c'$  is limited to channels in the spin group with particle pair  $\alpha'$ . The reaction is defined by  $\alpha \rightarrow \alpha'$ . This is one of the strengths of the RML representation. The reaction cross sections can include multiple inelastic levels with full resonance behavior. They can also include cross sections for outgoing charged particles, such as  $(n, \alpha)$  cross sections,

with full resonance behavior. The total cross section can be computed by summing up its parts.

For non-Coulomb channels, the penetrabilities  $P$ , shift factors  $S$ , and phase shift  $\phi$  are the same as those given for the SLBW representation, except if a  $Q$  value is present,  $\rho$  must be modified as follows:

$$\rho = (2.196771 \times 10^{-3}) \frac{A}{A+1} \sqrt{|E + \frac{A+1}{A} Q|} . \quad (66)$$

These factors are a little more complicated for Coulomb channels. See the SAMMY reference for more details.

The RML representation is new to the ENDF format, and it isn't represented by any cases in ENDF/B-VII.0. There are experimental evaluations for  $^{19}\text{F}$  and  $^{35}\text{Cl}$  from ORNL available. However, the RML approach provides a very faithful representation of resonance physics, and it should see increasing use in the future.

**RML Angular Distributions.** One of the physics advances available when using the RML format is the calculation of angular distributions from the resonance parameters. A Legendre representation is used:

$$\frac{d\sigma_{\alpha\alpha'}}{d\Omega_{\text{CM}}} = \sum_L B_{L\alpha\alpha'}(E) P_L(\cos \beta) , \quad (67)$$

where the subscript  $\alpha\alpha'$  indicates the cross section as defined by the two particle pairs,  $P_L$  is the Legendre polynomial of order  $L$ , and  $\beta$  is the angle of the outgoing particle with respect to the incoming neutron in the CM system. The coefficients  $B_{L\alpha\alpha'}(E)$  are given by a complicated six level summation over the elements of the scattering matrix  $U$ , where

$$U_{cc'} = \Omega_c W_{cc'} \Omega_{c'} , \quad (68)$$

where

$$\Omega_c = e^{i(w_c - \phi_c)} , \quad (69)$$

and

$$W = I + 2iX , \quad (70)$$

with  $I$  being the identity matrix and  $X$  having been already given in Eq. 61. The coefficients  $B$  become

$$B_{L\alpha\alpha'}(E) = \frac{1}{4k_\alpha^2} \sum_A \sum_B \sum_C \sum_D \sum_E \sum_F \frac{1}{(2i+1)(2I+1)} \times G_{c_1c'_1;c_2c'_2;L} \text{Re}[(\delta_{c_1c'_1} - U_{c_1c'_1})(\delta_{c_2c'_2} - U_{c_2c'_2}^*)]. \quad (71)$$

The spins  $I$  and  $i$  are for the target and projectile for particle pair  $\alpha$ . The complex expressions for the geometric coefficient  $G$  are given in the SAMMY documentation. The six summations are as follows:

- A sum over spin groups defined by  $J_1^\pi$
- B sum over spin groups defined by  $J_2^\pi$
- C sum over entrance channels  $c_1$  belonging to group  $J_1^\pi$  with particle pair  $\alpha$
- D sum over exit channels  $c'_1$  belonging to group  $J_1^\pi$  with particle pair  $\alpha'$
- E sum over entrance channels  $c_2$  belonging to group  $J_2^\pi$  with particle pair  $\alpha$
- F sum over exit channels  $c'_2$  belonging to group  $J_2^\pi$  with particle pair  $\alpha'$

Fig. 3 shows the first few Legendre coefficients for the elastic scattering cross sections as computed by NJOY from the experimental evaluation for  $^{19}\text{F}$ .

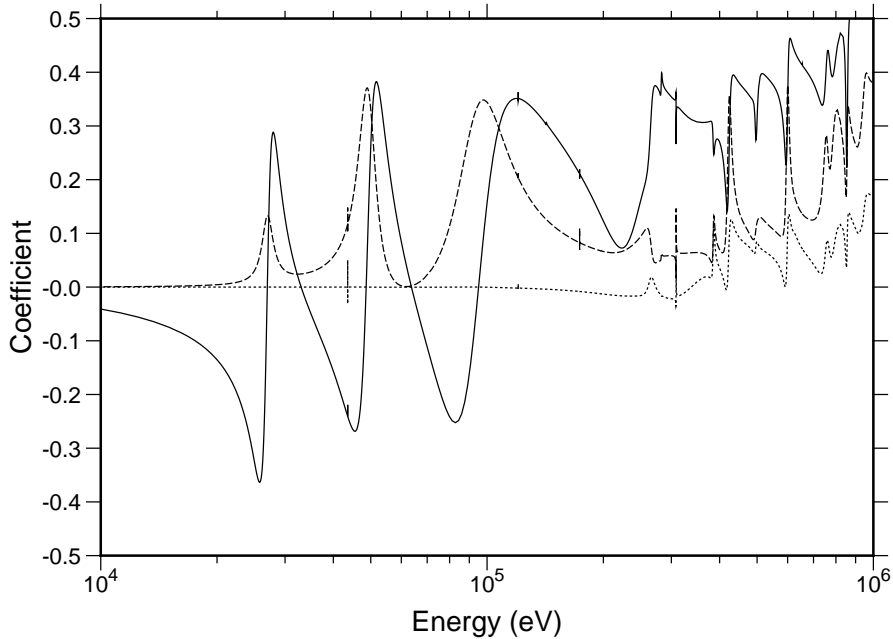


Figure 3: Legendre coefficients of the angular distribution for elastic scattering in  $^{19}\text{F}$  using the RML resonance representation ( $P_1$  solid,  $P_2$  dashed,  $P_3$  dotted).

Because computing resonance angular distributions is a new feature, it is not enabled by default. To activate it, change `Want_Angular_Dist` to true. The Legendre coefficients are written into a section of File 4 on the RECONR PENDF file. Because the normal ENDF File 4 sections are not copied to the PENDF File 4, the presence of File 4 on a PENDF file can be detected by subsequent modules, such as `ACER` or `GROUPE`, and the resonance angular distributions can be used to replace the ENDF File 4 values over the resonance energy range. The default in NJOY2012 is to use the conventional RM processing path for RM parameters. However, there is an option to convert the RM parameters into RML format and process them with the RML methods. If this is done, resonance angular distributions can be computed for an RM evaluation. Change `Want_SAMRML_RM` to true.

**Infinitely-Dilute Unresolved Range Parameters** Infinitely dilute cross sections in the unresolved-energy range are computed in `csunr1` or `csunr2` using average resonance parameters and probability distributions from File 2. With the approximations used, these cross sections are not temperature dependent; therefore, the results are a good match to resolved resonance data generated using `tempr`>0. The formulas used are based on the SLBW approximation with interference.

$$\sigma_n(E) = \sigma_p + \frac{2\pi^2}{k^2} \sum_{\ell,J} \frac{gJ}{D} [\bar{\Gamma}_n^2 R_n - 2\bar{\Gamma}_n \sin^2 \phi_\ell] , \quad (72)$$

$$\sigma_x(E) = \frac{2\pi^2}{k^2} \sum_{\ell,J} \frac{gJ}{D} \bar{\Gamma}_n \bar{\Gamma}_x R_x , \text{ and} \quad (73)$$

$$\sigma_p = \frac{4\pi}{k^2} \sum_{\ell} (2\ell + 1) \sin^2 \phi_\ell , \quad (74)$$

where  $x$  stands for either fission or capture,  $\bar{\Gamma}_i$  and  $\bar{D}$  are the appropriate average widths and spacing for the  $\ell, J$  spin sequence, and  $R_i$  is the fluctuation integral for the reaction and sequence (see `gnr1`). These integrals are simply the averages taken over the chi-square distributions specified in the file; for example,

$$\begin{aligned} \bar{\Gamma}_n \bar{\Gamma}_f R_i &= \left\langle \frac{\Gamma_n \Gamma_f}{\Gamma} \right\rangle \\ &= \int dx_n P_\mu(x_n) \int dx_f P_\nu(x_f) \int dx_c P_\lambda(x_c) \end{aligned} \quad (75)$$

$$\times \frac{\Gamma_n(x_n) \Gamma_f(x_f)}{\Gamma_n(x_n) + \Gamma_f(x_f) + \Gamma_\gamma + \Gamma_c(x_c)} , \quad (76)$$

where  $P_\mu(x)$  is the chi-square distribution for  $\mu$  degrees of freedom. The integrals are evaluated with the quadrature scheme developed by R. Hwang for the MC<sup>2</sup>-2 code[37] giving

$$R_f = \sum_i W_i^\mu \sum_j W_j^\nu \sum_k W_k^\lambda \frac{Q_i^\mu Q_j^\nu}{\bar{\Gamma}_n Q_i^\mu + \bar{\Gamma}_f Q_j^\nu + \Gamma_\gamma + \bar{\Gamma}_c Q_k^\lambda} . \quad (77)$$

The  $W_i^\mu$  and  $Q_i^\mu$  are the appropriate quadrature weights and values for  $\mu$  degrees of freedom, and  $\Gamma_\gamma$  is assumed to be constant (many degrees of freedom). The competitive width  $\bar{\Gamma}_c$  is assumed to affect the fluctuations, but a corresponding cross section is not computed. The entire competitive cross section is supposed to be in the File 3 total cross section as a smooth background.

It should be noted that the reduced average neutron width  $\Gamma_n^0$  (AMUN) is given in the file, and

$$\bar{\Gamma}_n = \Gamma_n^0 \sqrt{E} V_\ell(E) , \quad (78)$$

where the penetrabilities for the unresolved region are defined as

$$V_0 = 1 , \quad (79)$$

$$V_1 = \frac{\rho^2}{1 + \rho^2} , \text{ and} \quad (80)$$

$$V_2 = \frac{\rho^4}{\rho + 3\rho^2 + \rho^4} . \quad (81)$$

Other parameters are defined as for SLBW.

Unresolved resonance parameters can be given as independent of energy, with only fission widths dependent on energy, or as fully energy dependent. The first two options are processed in `csunr1`, and the last one is processed in `csunr2`.

### 3.5 Code Description

RECONR is implemented as a public subroutine `reconr` exported by the Fortran-90 module `reconm` defined by `reconr.f90`.

The first step is to read cards 1, 2, and 3 of the user's input. The TAPEID record of the input file (`nendf`) is read and printed, then the new TAPEID record is written to the output file (`npnd`). RECONR is now ready to enter the loop over the desired materials.

For each material, space is allocated for the energy nodes (`enode`), and `ruin` is called to read cards 4 through 7 of the user's input. If the reconstruction temperature (`tempr`) is greater than zero, a table of  $\psi$  and  $\chi$  functions is generated

(the W table is used; see `wtab` and `quickw`). The `findf` utility routine from module `endf` is then used to find the first card of File 1 (MF=1, MT=451) for the desired material.

File 1 on the input ENDF file is examined to obtain certain constants and flags and to analyze the directory (`anlyzd`). Subroutine `anlyzd` determines which reactions should be considered “redundant”; that is, the reactions that are sums of other reactions and will be included on the output PENDF file. The total cross section (MT=1 for neutrons, MT=501 for photons) will always be included; the nonelastic cross section (MT=3) will be included if it is needed for photon production (that is, MF=12, MT=3 is found); the inelastic cross section (MT=4) will be included if sections with MT in the range 51 – 91 occur in the file, and the total fission reaction (MT=18) will be called redundant if the partial fission representation (MT=19, 20, 21, 38) is found. MT103 (n,p) can be a summation reaction if its partials MT600, MT601, ..., are present, and the same for the other charged-particle absorption reactions. Space for the new material directory is then allocated (`mfs`, `mts`, `ncs`). Section identification and card counts will be entered into these arrays as they are determined.

File 2 on the ENDF file is now checked using `s2sammy` (which was imported from the `samm` module) to see whether the sammy method is needed. This depends on whether RML resonance parameters are found, and whether conversion to RML format has been requested for Reich-Moore or Breit-Wigner data (see `Want_SAMRML_RM` and `Want_SAMRML_BW`). The variable `nmtres` flags the use of SAMMY processing. Because RML evaluations can include more than the normal elastic, fission, and capture reactions, a list of reactions identified is printed. Here is an example for the experimental  $^{19}\text{F}$  evaluation.

```

resonance range information
-----
ier      energy-range      lru lrf  method
1  1.000E-05 1.000E+06    1   7   sammy

samm resonance reactions:    2  102   51   52
samm max legendre order:   7
generating File 4 for resonance angular distributions

```

The next step is to read File 2, which contains resolved and unresolved resonance parameters (if any). The array `res` is allocated to contain the File 2

data and `rdfil2` is called to read them. This routine uses the additional routines `rdf2bw`, `rdf2aa`, `rdf2hy`, `rdsammy`, `rdf2u0`, `rdf2u1`, and `rdf2u2` to read the different types of resonance parameters. The subroutine `rdsammy` is imported from the `samm` module. In addition, another imported routine `ppsammy` is used to prepare for the SAMMY calculation. While the resonance parameters are being stored, RECONR adds each resonance energy to its list of energy nodes (`enode`). In the unresolved energy range, RECONR uses the energies of tabulated parameters or fission widths if available. If the evaluation uses energy-independent parameters, or if the energy steps between the nodes are too large (see `wide`), `rdfil2` creates additional node energies at a density of approximately 13 points per decade (see `egridu`). Note that regions where the unresolved representation for an element overlaps the resolved or smooth ranges are found and marked by negative energy values. The energy nodes are sorted into order and duplications are removed.

If the SAMMY method is active, and if angular distributions have been requested (see `Want_Angular_Dist`), the maximum Legendre order defined by the resonance data is printed out.

If unresolved data are present, subroutine `genunr` is called to compute the infinitely-dilute unresolved average cross sections on the unresolved energy grid using `csunr1` or `csunr2`. Any backgrounds on File 3 are included, except in regions of resolved-unresolved or unresolved-smooth overlap. The computed cross sections are arranged in the order required by the special section with MF=2 and MT=152, which is written onto the PENDF tape by `recout`. Using the normal ENDF style, this format is defined by the following:

```
[MAT,2,152/ZA,AWR,LSSF,0,0,INTUNR]HEAD
[MAT,2,152/0.,0.,5,1,NW,NUNR/
    E1,STOT1,SELAS1,SFIS1,SCAP1,STRN1,
    E2,STOT2,SELAS2,SFIS2,SCAP2,STRN2,
    ...
    ENUNR,STOTNUNR,...]LIST
```

where  $NW = 6 + 6*NUNR$ . The definitions of the energy and cross section entries are fairly obvious, except `STRN` stands for the current-weighted total cross section. This format is specialized to “infinite dilution.” The more general form used for self-shielded effective cross sections will be described in the [UNRESR](#), [PURR](#), and [GROUPR](#) chapters of this manual.

The subroutine **lunion** is used to linearize and unionize the ENDF data. Space is reserved for two buffers to be used by **loada/finda**, for the linearization stack (**x** and **y**), and for the ENDF scratch area (**scr**). The length of the stack (**ndim**) determines the smallest possible subdivision of each panel (energy points as close as  $2^{-\text{ndim}}$  times the panel width can be generated). Since the number of energies in the union grid may soon exceed the capacity of any reasonable memory array, the existing list of energy nodes is copied to binary scratch storage (the **loada/finda** system). This storage system consists of the buffers **bold** and **bnew** and the scratch units **iold** and **inew**. The energy grid points will “ping-pong” back and forth between units 14 and 15 as the union grid is built up. Subroutine **lunion** now starts with **MT=2** and checks each reaction in sequence to determine whether the current grid (on **iold**) is sufficient to represent the reaction to within the desired tolerance using linear interpolation. If not, RECONR adds additional points by adaptively halving the intervals. The new grid is stored on **inew**. The units **inew** and **iold** are swapped, and the next **MT** is processed. When all nonredundant reactions have been examined, the list of energies in **loada/finda** storage is the desired linearized and unionized grid. The storage used is deallocated.

This grid is used as the starting point for resonance reconstruction in **resxs**. Subroutine **resxs** first reserves space for the **loada/finda** buffers **bufr** and **bufg**, the linearization stack (**x** and **y**), and the partial cross sections (**sig**). The length of the stack (**ndim**) determines the smallest possible subdivision of a panel between two nodes (energy points as close as  $2^{-\text{ndim}}$  times the panel width can be generated). Subroutine **resxs** then examines the grid on **ngrid** (**iold** from **lunion**) panel by panel. Grid points are added and cross sections computed until the convergence criteria discussed in Section 3.3 are satisfied. The cross sections are copied to **nout** using **loada**, and **resxs** continues to the next panel. This procedure is continued until all panels are converged. The result is a tape (**nout**) containing the energy grid in the resonance region and the total, elastic, fission, capture, and possibly additional cross sections at each energy point.

Unionization is obtained automatically in the resonance region since all of the partials are computed simultaneously in **sigma**, using **csslbw** for SLBW parameters, **csmlbw** for MLBW parameters, **csaa** for multi-level Adler-Adler parameters, **csrmat** for Reich-Moore parameters, **cshyb** for Hybrid R-Function parameters, **cssammy** for Reich-Moore-Limited parameters, and **sigunr** for unresolved resonance parameters. This last routine retrieves the cross sections from



the table prepared by **genunr**. Subroutine **cssammy** is imported from the **samm** module. A special feature of RECONR is the ability to reconstruct the cross sections at **tempr** by  $\psi\chi$  broadening if SLBW or Adler-Adler parameters are given. This can also be done for MLBW using the GH method implemented by **csmlbw2**. The Doppler-broadened resonance shapes are obtained using **quickw** (see description in the [UNRESR](#) chapter), and the linearization procedure proceeds as before.

The resonance cross sections on **ngrid** are merged with the ENDF cross sections in **emerge**. First, the background grid from **lunion** is merged with the resonance grid from **resxs** and written onto the **loada/finda** file, which will accumulate the total cross section and any other redundant reactions required (**iold/inew**). A loop is then set up over all nonredundant reactions. For each grid point, the ENDF background cross section is obtained by interpolation. If this grid point has a resonance contribution on **nres**, it is added. The resulting net cross section at this point is added into the appropriate redundant cross sections on **iold/inew** and also saved on **ngrid**. When all the energies for this reaction have been processed, the cross sections on **ngrid** are converted into a TAB1 record and written on **nscr**. This loop is continued until all reactions have been processed. When **emerge** is finished, **nscr** contains cross sections for all the nonredundant reactions, and **iold** contains the redundant summation reactions.

Control now passes to **recout**, which writes the new File 1 comments and dictionary. It also writes a default version of the section with MF=2 and MT=151 that gives no resonance parameters. The upper limit of the resolved energy range, **eresh**, is added to the “C2” field of the third card so that [BROADR](#) knows not to broaden into the unresolved energy range. For materials with unresolved data, a specially formatted section (MF=2, MT=152) is written containing the infinitely-dilute unresolved cross sections. This section can be used by [BROADR](#) and [GROUPE](#) to correct for resolved-unresolved overlap effects, if necessary. Subroutine **recout** then steps through the reactions on **nscr** and **iold**. Redundant summation reactions are converted to TAB1 records and inserted in the correct order. Nonredundant reactions are simply copied. Finally, a MEND record is added and control is returned to **reconr**.

Now **reconr** either directs that this process be repeated for another isotope or writes a TEND record and terminates. The result is a new file in ENDF format containing the desired pointwise cross sections. Normally, only Files 1, 2, 3, 10, and 13 are included for neutron files. However, if angular distribution

processing has been requested, a File 4 containing the Legendre coefficients will also be written. Because the original ENDF File 4 was not copied to the PENDF file, the presence of sections of File 4 on the PENDF file provides a flag to subsequent modules that resonance angular distributions have been calculated. Only Files 1 and 23 are included for a photon file.

The SAMMY method is implemented in a separate Fortran-90 module `samm` defined by `sammy.f90`. It exports the subroutines `cssammy` (computes cross sections, angular distributions, and derivatives), `s2sammy` (scans File 2 to see if SAMMY method is needed and measure some sizes), `ppsammy` (sets up SAMMY calculation), `rdsammy` (reads in File 2 data with optional conversion of BW or RM data to RML form), and `desammy` (cleans up after the SAMMY calculation). It also exports some logical parameters, namely, `Want_Partial_Derivs`, `Want_Angular_Dist`, `Want_SAMRML_RM` and `Want_SAMRML_BW`. See [ERRORR](#) for the use of derivatives. If conversion from BW and/or RM was requested, it is possible to get the resulting File 2 values printed out for checking. Just set `imf2` in `sammy.f90` to 1.

The `cssammy` subroutine uses `abpart` to compute some energy-independent pieces of the cross sections and derivatives. The main work for cross sections, angular distributions, and derivatives is done in `cross`. The results for cross sections are returned in `sigp` to be consistent with the other “cs” routines in RECONR. Angular distributions are returned in `sigα`, and sensitivities are returned in `sigd` (derivatives of cross sections with respect to parameters). Subroutine `cross` starts by initializing the quantities being calculated (cross sections, maybe angular distributions, maybe derivatives), and then it sets up a loop over the spin-parity groups. It initializes the results for this spin group and then calls `setr` to compute the elements of the R-matrix (see Eq. 60 and other quantities, such as the Y matrix, penetrabilities (`rootp`), and phase shifts. It then inverts the Y matrix and calculates the X matrix of Eq. 61. See `setxqx`. It can then use the X matrix to compute the contributions to the cross sections (`sectio`), maybe angular distributions (`setleg`), and maybe derivatives from this spin group and add them into the sum over groups. When the loop over spin groups is complete, it normalizes things properly and returns its results.

Going back to subroutine `setr`, it computes the R-matrix first. It then computes the phase shift, penetrabilities, and shift factors. For non-Coulomb cases, the phase shifts come from `sinsix`, and the penetrability  $P$  and boundary condition  $(S - B + iP)^{-1}$  come from `pgh`. For Coulomb cases, subroutine `pghcou`

computes all of these quantities. The penetrability  $P$  is converted to `rootp` for use in Eq. 61.

### 3.6 Input Instructions

The input instructions for each module are given in the code as comment cards at the beginning of the source code for each module. The RECONR instructions are reproduced here for the convenience of the reader.

```
!---input specifications (free format)-----
!
! card 1
!   nendf    unit for endf tape
!   npend    unit for pendf tape
! card 2
!   tlabel   66 character label for new pendf tape
!            delimited with quotes, ended with /.
! card 3
!   mat      material to be reconstructed
!   ncards   number of cards of descriptive data for new mf1
!            (default=0)
!   ngrid    number of user energy grid points to be added.
!            (default=0)
! card 4
!   err      fractional reconstruction tolerance used when
!            resonance-integral error criterion (see errint)
!            is not satisfied.
!   tempr    reconstruction temperature (deg kelvin)
!            (default=0)
!   errmax   fractional reconstruction tolerance used when
!            resonance-integral error criterion is satisfied
!            (errmax.ge.err, default=10*err)
!   errint   maximum resonance-integral error (in barns)
!            per grid point (default=err/20000)
!            (note: the max cross section difference for
!            linearization, errlim, and for reconstruction,
!            errmin, are also tied to errint.  to get maximum
!            accuracy, set errint to a very small number.
!            for economical production, use the defaults.)
! card 5
!   cards    ncards of descriptive comments for mt451
```

```

!           each card delimited with quotes, ended with /.
! card 6
!   enode   users energy grid points
!
!   cards 3, 4, 5, 6 must be input for each material desired
!   mat=0/ terminates execution of reconr.
!
!-----

```

A sample input for processing an isotope from ENDF/B-VII follows (the line numbers are for reference only and are not part of the input). First, mount the ENDF/B-VII file for  $^{235}\text{U}$  on unit 20.

```

1.  reconr
2.  20 21
3.  'pendf tape for U-235 from ENDF/B-VII' /
4.  9228 2/
5.  .001/
6.  '92-U-235 from ENDF/B-VII' /
7.  'processed with NJOY' /
8.  0/

```

Card 2 tells RECONR that the input ENDF tape will be on unit 20, and that the output PENDF tape will be on unit 21. Card 3 is a “TAPEID” label for the output PENDF file. Card 4 gives the MAT number for U-235 and says that two additional comment cards will be given. Card 5 sets the reconstruction tolerance to 0.1% (.001 as a fraction) with all its other parameters defaulted. Cards 6 and 7 are the two comment cards to be inserted into the PENDF files MF1/MT451 section. Finally, the “0/” terminates the RECONR input. The capability to loop over multiple isotopes in RECONR is rarely used for neutron files, but it is useful for photon interaction processing (see GAMINR). The resulting PENDF tape will contain the desired TAPEID card, followed by  $^{235}\text{U}$  data, a MEND card and a TEND card.

### 3.7 Error Messages

error in reconr\*\*\*illegal nsub for reconr

RECONR only processes sublibraries that contain cross section data. Check whether the right input ENDF input tape was mounted.

error in analyzd\*\*\*too many redundant reactions

Increase the global parameter `nmtmax=10`.

error in xxxxxx\*\*\*storage in enode exceeded

Too many energy nodes including the user's nodes and the energies from MF=2. Increase the global parameter `nodmax=800000`. This message can come from `rdf2bw`, `rdf2aa`, `rdf2hy`, `rdf2u0`, `rdf2u1`, or `rdf2u2`.

error in xxxxxx\*\*\*res storage exceeded

Too much resonance data. This should not occur for a conforming ENDF-format file, because `maxres` is computed from the MF=2 line count in the MF=1/MT=451 index. This message can come from `rdfil2`, `rdf2bw`, `rdf2aa`, `rdf2hy`, `rdf2u0`, `rdf2u1`, or `rdf2u2`.

error in xxxxxx\*\*\*storage in eunr exceeded.

Increase the global parameter `maxunr=500`. This message can come from `rdfil2`, `rdf2u1`, or `rdf2u2`.

error in rdfil2\*\*\*illegal resonance mode.

A resonance mode has been requested that RECONR does not understand.

error in rdf2bw\*\*\*energy-dep scattering radius ...

This option is only used in MLBW for current evaluations.

message from rdf2bw\*\*\*calc... of angular distribution not...

This option is only partially available in RECONR. This message can come from `rdf2bw` (for Reich-Moore cases) or from `rdf2hy` (Hybrid R function).

error in rdf2hy\*\*\*hybrid competing reactions not yet added

This option is not yet available in RECONR.

error in lunion\*\*\*ill behaved threshold

The routine is having trouble adjusting the threshold to agree with the Q value. Check the points near the threshold for this evaluation.

error in lunion\*\*\*exceeded stack

Increase length of linearization stack `ndim` (currently 50).

error in resxs\*\*\*stack exceeded

Increase length of reconstruction stack `ndim` (currently 50).

error in sigma\*\*\*general r-matrix not installed.

This option is not yet available in RECONR.

error in sigma\*\*\*illegal option.

There is a problem with the ENDF tape.

error in csmlbw\*\*\*not coded for temperature gt 0 deg k  
 The  $\psi\chi$  Doppler-broadening doesn't work for normal MLBW. This message shouldn't occur, because temperatures greater than zero will cause csmlbw2 to be called.

error in csrmat\*\*\*not coded for temperature gt 0 deg k  
 The  $\psi\chi$  Doppler-broadening doesn't work for RM. Use tempr=0. only.

error in cshybr\*\*\*doppler broad'g not provided for hybrid  
 The  $\psi\chi$  Doppler-broadening doesn't work for hybrid parameters. Use tempr=0. only.

error in csaa\*\*\*bad li value  
 There is an error in the evaluation format.

message from emerge---negative elastic cross sects found  
 Negative elastic cross sections can occur for SLBW evaluations.

error in recout\*\*\*for mf --- mt ---  
 Indexing and pair count for this section do not make sense.

calculation of angular distribution not installed -  
 Message comes from several resonance types that do not support the calculation of angular distributions. Some of them can be used if Want\_SAMRL\_RM or Want\_SAMRML\_BW are true.

message from s2sammy\*\*\*multiple isotopes... -  
 Multiple isotopes for RM sections don't work with the SAMMY method. The code automatically reverts to normal RM processing.

error in s2sammy\*\*\*res storage exceeded. -  
 Storage limited to maxres. Shouldn't occur.

error in s2sammy\*\*\*energy-dep scattering length... -  
 This only works for MLBW parameters.

error in rearrange\*\*\*nres fault -  
 Trouble while rearranging resonances into spin-group order.

errorr in findsp\*\*\*quantum numbers in file 2 do not... -  
 Problems with the quantum numbers for the evaluation.

error in checkqn\*\*\*error in quantum numbers -  
 Problems with the quantum numbers for the evaluation.

error in lmaxxx\*\*\*l1lmax limit to 51 -  
 Problems with the Clebsch-Gordan coefficients for the angular distributions.

error in clbsch\*\*\*did not count correctly -  
 Problems with the Clebsch-Gordan coefficients for the angular distributions.

error in pspcou\*\*\*llmax larger than 100 -  
 Problem computing the Coulomb phase shifts.

error in bigeta\*\*\*I0 sum failed -  
 Problem for the Coulomb routine.

error in bigeta\*\*\*K0 sum failed -  
 Problem for the Coulomb routine.

error in bigeta\*\*\*L1 sum failed -  
 Problem for the Coulomb routine.

error in bigeta\*\*\*K1 sum failed -  
 Problem for the Coulomb routine.

error in setleg\*\*\*nppx too large -  
 Problem generating Legendre polynomials.

### 3.8 Input-Output Units

The following logical units are used:

- 10 `nscr1` in `reconr`, `nout` in `lunion`, and `nin` in `emerge`. Contains copy of nonredundant sections from original ENDF tape.
- 11 `nscr2` in `reconr`; `ngrid` in `lunion`, `resxs`, and `emerge`. Contains union grid for ENDF tape (not counting resonances).
- 12 `nscr3` in `reconr`, `nout` in `resxs`, and `nres` in `emerge`. Contains resonance grid and cross sections.
- 13 `nscr4` in `reconr` is used for two separate purposes. In `resxs` it is a binary scratch file `nscr` used for the unthinned resonance data. In `emerge` and `recout`, it is `nmerge` and contains the nonredundant reactions on the union grid.
- 14/15 `iold/inew` in `lunion`. Are used locally only to accumulate union grid for ENDF cross sections. Destroy after use.
- 14/15 `iold/inew` in `emerge`. Are used locally only to accumulate summation cross sections on union grid.
- 20-99 User's choice for ENDF (`nendf`) and PENDF (`npend`) tape numbers to link RECONR with other NJOY modules.
- 5,6,7 See the [NJOY](#) chapter for a description of the I/O units.

Note that 11, 12, 14, and 15 are always binary. Unit 10 has the same mode as `nendf`. Unit 13 is binary when used in RESXS, and it has the same mode as `npend` elsewhere. `npend` can have a different mode than `nendf`.

### 3.9 Storage Allocation

Storage allocation in RECONR is sensitive to (1) the amount of resonance parameter data, (2) the number of energy-grid node values, (3) the size of the resonance reconstruction stack, (4) the use of  $\psi\chi$  broadening, and (5) the sizes of the `loada/finda` buffers. Other storage requirements are minor.

Buffer sizes can be reduced or increased at will. The result is a storage/speed tradeoff with no change in capability or accuracy. See the global parameters `nbufg=2000`, `nbufr=2000`, and `nbuf=2000` at the beginning of the `reconm` module.

The  $\psi\chi$  broadening option requires 7688 words of additional storage. Therefore, memory use can be reduced if  $\psi\chi$  is not required. No code changes are needed — just avoid `tempr` greater than zero.

Resonance reconstruction in `resxs` uses  $5 \times \text{ndim}$  words. The parameter `ndim` determines the smallest subdivision of a panel that can be obtained. Using `ndim=30` allows points to be generated with spacing as small as one-billionth of the panel size ( $2^{30}$ ).

The code currently allows for `nodmax=800000` energy nodes and `maxunr=500` unresolved points. These values tend to increase as additional very detailed resonance evaluations appear, but the current values seem to be sufficient for the evaluations existing as of this writing.



## 4 BROADR

BROADR module generates Doppler-broadened cross sections in PENDF format starting from piecewise linear cross sections in PENDF format. The input cross sections can be from RECONR or from a previous BROADR run. The code is based on SIGMA1[26] by D. E. Cullen. The method is often called “kernel broadening” because it uses a detailed integration of the integral equation defining the effective cross section. It is a fully accurate method, treating all resonance and non-resonance cross sections including multilevel effects. BROADR has the following features:

- An alternate calculation is used for low energies and high temperatures that corrects a numerical problem of the original SIGMA1. (This problem has been corrected in another way in later versions of SIGMA1.)
- Dynamic storage allocation is used, which allows the code to be run on large or small machines with full use of whatever storage is made available.
- All low-threshold reactions are broadened in parallel on a union grid.
- The union grid is constructed adaptively to give a linearized representation of the broadened cross section with tolerances consistent with those used in RECONR. Energy points may be added to or removed from the input grid as required for the best possible representation. Precision up to 9 significant figures is allowed for energies.
- The summation cross sections such as total, nonelastic, and sometimes fission or (n,2n) are reconstructed to equal the sum of their parts.
- Standard thermal cross sections, integrals, and ratios are computed when the temperature is 293.6K (0.0253 eV).
- The file directory (actually an index to the reactions present) is updated.

This report describes the BROADR module in NJOY 2012.0. The main changes from the version reported previously[3] are as follows:

- the use of 7 or 9 significant figures together with the use of 64-bit precision for consistency with RECONR,
- the restriction that `ntemp2` be less than or equal to 10 has been eliminated,
- the calculation of standard thermal cross sections and integral parameters when the base temperature requested is 293.6K (0.0253 eV),
- the use of an enhanced reconstruction tolerance in the thermal range, and
- the conversion to Fortran-90 style.

### 4.1 Doppler-Broadening Theory

The effective cross section for a material at temperature  $T$  is defined to be that cross section that gives the same reaction rate for stationary target nuclei as the real cross section gives for moving nuclei. Therefore,

$$\rho v \bar{\sigma}(v, T) = \int d\mathbf{v}' \rho |\mathbf{v} - \mathbf{v}'| \sigma(|\mathbf{v} - \mathbf{v}'|) P(\mathbf{v}', T) , \quad (82)$$

where  $\mathbf{v}$  is the velocity of the incident particles,  $\mathbf{v}'$  is the velocity of the target,  $\rho$  is the density of target nuclei,  $\sigma$  is the cross section for stationary nuclei, and  $P(\mathbf{v}', T)$  is the distribution of target velocities in the laboratory system. For many cases of interest, the target motion is isotropic and the distribution of velocities can be described by the Maxwell-Boltzmann function

$$P(\mathbf{v}', T) d\mathbf{v}' = \frac{\alpha^{3/2}}{\pi^{3/2}} \exp(-\alpha v'^2) d\mathbf{v}' , \quad (83)$$

where  $\alpha = M/(2kT)$ ,  $k$  is Boltzmann's constant, and  $M$  is the target mass.

Eq. 82 can be partially integrated in terms of the relative speed  $V = |\mathbf{v} - \mathbf{v}'|$  to give the standard form of the Doppler-broadened cross section:

$$\bar{\sigma}(v) = \frac{\alpha^{1/2}}{\phi^{1/2} v^2} \int_0^\infty dV \sigma(V) V^2 \left\{ e^{-\alpha(V-v)^2} - e^{-\alpha(V+v)^2} \right\} . \quad (84)$$

It is instructive to break this up into two parts:

$$\bar{\sigma}(v) = \sigma^*(v) - \sigma^*(-v) , \quad (85)$$

where

$$\sigma^*(v) = \frac{\alpha^{1/2}}{\pi^{1/2} v^2} \int_0^\infty dV \sigma(V) V^2 e^{-\alpha(V-v)^2} . \quad (86)$$

The exponential function in Eq. (86) limits the significant part of the integral to the range

$$v - \frac{4}{\sqrt{\alpha}} < V < v + \frac{4}{\sqrt{\alpha}} .$$

For  $\sigma^*(-v)$ , the integral depends only on velocities satisfying

$$0 \leq V < \frac{4}{\sqrt{\alpha}} .$$

Table 1: Energy Parameter for Effective Doppler-Broadening

| Target           | Temperature | Energy Parameter ( $E_m$ ) |
|------------------|-------------|----------------------------|
| $^2\text{H}$     | 300K        | 0.2 eV                     |
| $^{235}\text{U}$ | 300K        | 0.0017 eV                  |
| $^{235}\text{U}$ | 1.0 keV     | 69 eV                      |

These results can be converted to energy units using

$$E_m = \frac{1}{2}m\left(\frac{4}{\sqrt{\alpha}}\right)^2 = \frac{16kT}{A}.$$

Some examples are given in Table 1. Doppler-broadening effects will be important below this energy and for any features such as resonances, thresholds, or artificial discontinuities in evaluations that are not slowly varying with respect to  $2\sqrt{E_m E}$ . As an example, for  $^{235}\text{U}$  at 100 eV, Doppler effects are important for features smaller than about 0.8 eV.

The numerical evaluation of Eq. (86) developed for SIGMA1 assumes that the cross section can be represented by a piecewise linear function of energy to acceptable accuracy. This is just the form of the NJOY PENDF files (see RECONR). Defining the reduced variables  $y = \sqrt{\alpha x}$  and  $x = \sqrt{\alpha V}$ , the cross section becomes

$$\sigma(x) = \sigma_i + s_i(x^2 - x_i^2), \quad (87)$$

with slope  $s_i = (\sigma_{i+1} - \sigma_i)/(x_{i+1}^2 - x_i^2)$ . Eq. (86) can now be written as

$$\sigma^*(y) = \frac{1}{\pi^{1/2}y^2} \sum_{i=0}^N \int_{x_i}^{x_{i+1}} \sigma(x) x^2 e^{-(x-y)^2} dx = \sum_i \{A_i [\sigma_i - s_i x_i^2] + B_i s_i\}, \quad (88)$$

where

$$\begin{aligned} x_0 &= 0, \\ x_{N+1} &= \infty, \\ A_i &= \frac{1}{y^2}H_2 + \frac{2}{y}H_1 + H_0, \text{ and} \\ B_i &= \frac{1}{y^2}H_4 + \frac{4}{y}H_3 + 6H_2 + 4yH_1 + y^2H_0, \end{aligned}$$

and where  $H_n$  is shorthand for  $H_n(x_i - y, x_{i+1} - y)$ . The extrapolations to zero and infinity assume a constant cross section ( $s_0 = s_N = 0$ ). The  $H$  functions are

the incomplete probability integrals defined by

$$H_n(a, b) = \frac{1}{\sqrt{\pi}} \int_a^b z^n e^{-z^2} dz . \quad (89)$$

These functions can be computed in two ways. First,

$$H_n(a, b) = F_n(a) - F_n(b) , \quad (90)$$

where

$$F_n(a) = \frac{1}{\sqrt{\pi}} \int_a^\infty z^n e^{-z^2} dz . \quad (91)$$

These functions satisfy a recursion relation that can be used to obtain

$$F_0(a) = \frac{1}{2} \text{erfc}(a) , \quad (92)$$

$$F_1(a) = \frac{1}{2\sqrt{\pi}} \exp(-a^2) , \text{ and} \quad (93)$$

$$F_n(a) = \frac{n-1}{2} F_{n-2}(a) + a^{n-1} F_1(a) , \quad (94)$$

where  $\text{erfc}(a)$  denotes the complementary error function

$$\text{erfc}(a) = \frac{2}{\sqrt{\pi}} \int_a^\infty e^{-z^2} dz . \quad (95)$$

However, when  $F_n(a) \approx F_n(b)$ , the difference in Eq. (90) may lose significance. In such cases,  $H_n(a, b)$  can be computed by a second method based on a direct Taylor expansion of the defining integral. Write

$$H_n(a, b) = \frac{1}{\sqrt{\pi}} \int_0^b z^n e^{-z^2} dz - \frac{1}{\sqrt{\pi}} \int_0^a z^n e^{-z^2} dz = G_n(b) - G_n(a) . \quad (96)$$

But by Taylor's Theorem,

$$G_n(b) - G_n(a) = \frac{b-a}{1!} G'_n(a) + \dots + \frac{(b-a)^m}{m!} G_n^{(m)}(a) + \dots . \quad (97)$$

Also,

$$G_n^{(m)}(x) = \frac{d^{m-1}}{dx^{m-1}} [x^n e^{-x^2}] = e^{-x^2} P_n^m(x) , \quad (98)$$

where  $P_n^m(x)$  is a polynomial with recursion relation

$$P_n^m(x) = \frac{d}{dx} P_n^{m-1}(x) - 2x P_n^{m-1}(x) , \quad (99)$$

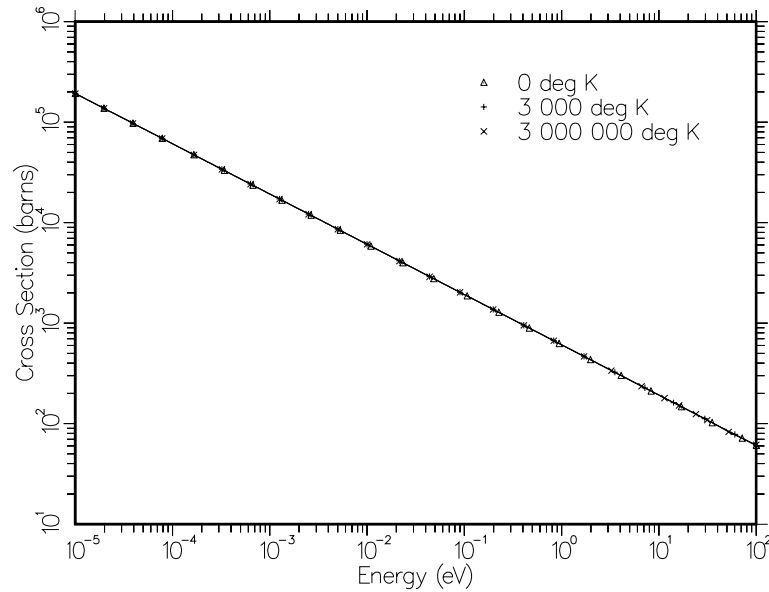


Figure 4: The  $(n,\alpha)$  cross section for  $^{10}\text{B}$  from ENDF/B-V for three different temperatures showing that a  $1/v$  cross section is invariant under Doppler-broadening.

with  $P_n^1 = x^n$ . From this point, it is straightforward to generate terms until the desired number of significant figures is obtained.

When interpreting BROADR output, it is useful to remember several important features of the Doppler-broadening process. A  $1/v$  cross section remains unchanged. Contrary to “popular knowledge”, the area under a resonance does not remain unchanged unless  $E \gg kT/A$ . In fact, each resonance develops a new  $1/v$  tail. Finally, a constant cross section (for example, elastic scattering) develops a  $1/v$  tail at low energies after Doppler-broadening. These effects are shown in Figs. 4, 5, and 6; they can be best understood by noting that the Doppler process preserves reaction rate  $v\sigma(v)$  according to Eq. (82), and a finite reaction rate is expected for  $T > 0\text{K}$  even as  $v \rightarrow 0$ .

Earlier versions of BROADR and SIGMA1 assumed that the input energy grid from RECONR could also be used to represent the Doppler-broadened cross section before thinning. The grid was then thinned to take advantage of the smoothing effect of Doppler broadening. Unfortunately, this assumption is inadequate. The reconstruction process in RECONR places many points near the center of a resonance to represent its sharp sides. After broadening, the cross section in this energy region becomes rather smooth; the sharp sides are moved out to energies where RECONR provides few points. At still higher energies, the resonance line shape returns to its asymptotic value, and the RECONR grid

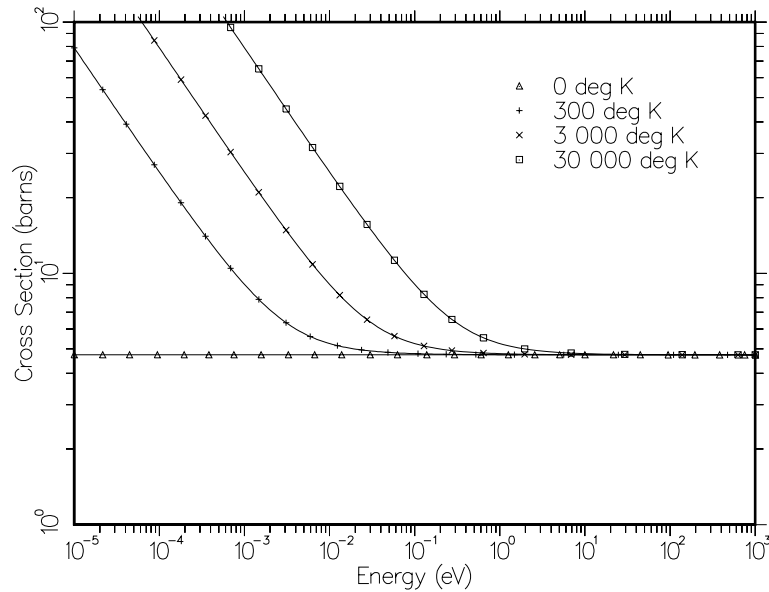


Figure 5: The elastic cross section for carbon from ENDF/B-V showing that Doppler-broadening a constant cross section adds a  $1/v$  tail.

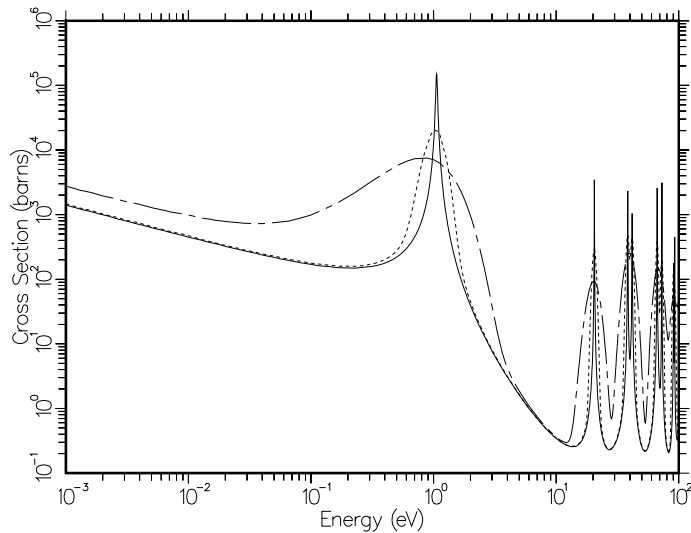


Figure 6: The  $(n, \gamma)$  cross section for  $^{240}\text{Pu}$  for several temperatures showing the effects of Doppler broadening on resonances. The temperatures are 0K (solid), 30 000K (dotted), and 300 000K (dash-dot). The higher resonances behave in the classical manner even at 30 000K; note that the line shape returns to the asymptotic value in the wings of the resonance. All resonances at 300 000K (and to a lesser extent the first resonance for 30 000K) show the additional  $1/v$  component that appears when  $kT/A$  is large with respect to the resonance energy.

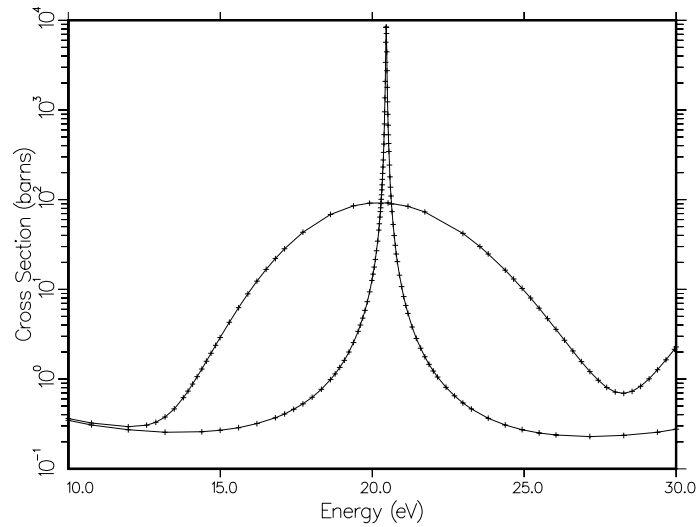


Figure 7: An expanded plot of the 20 eV resonance from Fig. 6 showing both thinning and “thickening” of the energy grid produced adaptively by BROADR. The two curves show the capture cross section at 0K and 300 000K. Note that the high-temperature curve has fewer points than the 0K curve near the peak at 20 eV and more points in the wings near 15 eV and 25 eV. Clearly, using the 0K grid to represent the broadened cross section in the wings of this resonance would give poor results.

is adequate once more. The more recent versions of BROADR check the cross section between points of the incoming energy grid, and add additional grid points if they are necessary to represent the broadened line shape to the desired accuracy. This effect is illustrated in Fig. 7.

## 4.2 Thermal Quantities

In thermal-reactor work, people make very effective use of a few standard thermal constants to characterize nuclear systems. These parameters include the cross sections at the standard thermal value of 0.0253 eV (2200 m/s), the integrals of the cross sections against a Maxwellian distribution for 0.0253 eV, the g-factors (which express the ratio between a Maxwellian integral and the corresponding thermal cross section),  $\eta$ ,  $\alpha$ , and K1. Here,  $\eta$  is the Maxwellian-weighted average of  $(\bar{\nu})\sigma_f/(\sigma_f + \sigma_c)$ ,  $\alpha$  is the average of  $\sigma_c/\sigma_f$ , and K1 is the average of  $(\bar{\nu} - 1)\sigma_f - \sigma_c$ . If BROADR is run for a temperature close to 293.6K (which is equivalent to 0.0253 eV), these thermal quantities are automatically calculated and displayed. Here is a sample output for  $^{235}\text{U}$  from ENDF/B-VII:

```

thermal quantities at 293.6 K = 0.0253 eV
-----
      thermal fission xsec:  5.8490E+02
      thermal fission nubar: 2.4367E+00
      thermal capture xsec:  9.8665E+01
      thermal capture g-factor: 9.9086E-01
      thermal capture integral: 8.6639E+01
      capture resonance integral: 1.4043E+02
      thermal fission integral: 5.0605E+02
      thermal fission g-factor: 9.7628E-01
      thermal alpha integral:  1.6828E-01
      thermal eta integral:  2.0859E+00
      thermal k1 integral:  6.4040E+02
      equivalent k1:  7.2262E+02
      fission resonance integral: 2.7596E+02
-----

```

### 4.3 Data-Paging Methodology

A piecewise linear representation of a reaction cross section of a resonance material may require a very large number of energy points. For example, ENDF/B-VII  $^{238}\text{U}$  (MAT9237) requires 167 000 points for the total cross section for 0.1% precision (`errmax=err`). It is impractical to load all these points into memory simultaneously. However, the discussion following Eq. (86) in the theory section shows that only a limited energy range around the point of interest is required.

The strategy used is to stage the cross-section data into three “pages” of `npage` points each. Points in the center page can then be broadened using the `npage` or more points on each side of the point of interest. If  $v - 4/\sqrt{\alpha}$  and  $v + 4/\sqrt{\alpha}$  are both included in the three-page range, accurate broadening can be performed. If not, a diagnostic warning is printed; the user should repeat the calculation with a smaller temperature step or a larger page size.

There are many different reaction cross sections for each material. However, the cross sections for high velocities are normally smooth with respect to  $32kT/A$  for any temperatures outside of stellar photospheres; therefore, they do not show significant Doppler effects. The upper energy limit for Doppler broadening is the smallest of (i) the input value `thnmax`, (ii) the upper limit of the



resolved-resonance energy range, (iii) the lowest threshold (often, but not always  $>100$  keV), or (iv) 1.0 MeV (the default input value for `thnmax`). No Doppler broadening or energy-grid reconstruction is performed above that energy. Under most conditions, and what users typically expect as the default action, the second condition sets the Doppler broadening upper limit. However, users are cautioned that the third condition may cause Doppler broadening to cease at unexpectedly low energies, well below the upper limit of the resolved-resonance energy range. For example, recent JENDL (JENDL-3.3 and JENDL-4.0 as of this writing) evaluations for  $^{235}\text{U}$  include a resolved-resonance range upper limit of 2.25 keV, but also include non-zero cross sections for an inelastic level with a 77 eV threshold. Under the rules itemized above, Doppler broadening of these data stops at 77 eV. Other evaluations (*e.g.*, ENDF/B-VI, ENDF/B-VII and JEFF-3.1) share the same resolved-resonance range data but have zeroed out this inelastic cross section from 77 eV to 2.25 keV and so Doppler broadening of these files occurs throughout the resolved-resonance range, as most users expect. As noted in the BROADR module source code comments, users may specify a negative value for `thnmax` to override these selection rules and force Doppler broadening to an upper energy of `abs(thnmax)` eV.

Finally, we note that the  $A_i$  and  $B_i$  factors in Eq. (88) depend only on the energy (or velocity) values and not on the cross sections. Since the  $A_i$  and  $B_i$  are expensive to compute, the code computes them only once for the points of a unionized energy grid. The sum of Eq. (88) is accumulated for all the non-threshold reactions simultaneously. This feature helps make BROADR run faster.

#### 4.4 Coding Details

The main subroutine for BROADR is `broadr` from module `broadm`. The code begins by reading the user's input (see Section 4.5). Storage is then allocated for the `loada/finda` buffers (`ibufo` and `ibufn`) and for the scratch storage (`iscr`). The buffer length `nbuf` can be changed at will (currently `nbuf` is 1000).

The input PENDF tape is searched for the desired material (`mat1`). If the restart option is set (`istart=1`), the temperatures less than or equal to `temp1` for `mat1` are assumed to have been broadened previously, and they are copied to the output file. In either case, the files for `temp1` are copied to a scratch file on unit `nscr1`.

Next, `nscr1` is rewound and examined reaction by reaction. The energy grid from the total cross section (MT1) is saved on scratch storage using `loada`. If

the input tape has not been through [RECONR](#), the *BROADR* module will still run, but at possibly reduced accuracy. The next low-threshold reaction (that is, the next reaction with a threshold less than `emin`, which is currently 1 eV) is located on `nscr1`. The energy points are retrieved from scratch file `iold` (12 or 13) using `finda`, the cross sections for this reaction are computed on this grid, and the results are stored on scratch file `inew` (13 or 12) using `loada`. The units for `iold` and `inew` are then exchanged, and the entire process is repeated for the next low-threshold reaction.

The final result of this process is a list of `nreac` low-threshold-reaction types in `mtr` (usually MT2, MT18, and MT102), the threshold value for the first high-threshold reaction (or the input value) in `thnmax`, and scratch file `iold` containing the energy grid and all the low-threshold reactions (there are `n2in` points).

Now that the number of reactions to be broadened simultaneously is known (`nreac`), storage for data paging can be assigned. The total amount of storage available is `namax`. The value of `namax` should be as large as possible (current value is 15 000 000). This space is divided up into the largest possible page size, `npage`. An overflow region `nstack` is also allocated. Now that the page size is known, the code allocates three pages for energies (`e`), three pages for each reaction cross section (`s`), one extended page for the broadened energy grid (`eb`), and three extended pages for the broadened cross section (`sb`). This system is designed to use the available storage with maximum efficiency.

The cross sections on `iold` are now broadened by `bfile3` (see below) and the results are written on scratch unit `inew` using `loada`.

The directory from `nscr1` is revised to reflect any thinning or thickening and written on the output PENDF tape (`nout`). Note that the new temperature is written into the first word of the Hollerith data record to simplify later searching.

The broadened cross sections are now converted into ENDF TAB1 records and merged with the unbroadened cross sections on `nscr1`. The total cross section (and sometimes nonelastic, inelastic, fission, (n,2n), or charged-particle reactions) is reconstructed to equal the sum of its parts. The new Doppler-broadened “MAT” on `NOUT` is a legal PENDF file with the same MAT number as the original data but with a new temperature.

The process is now repeated for each of the `ntemp2` final temperatures `temp2` requested. Note that after each step `inew` contains the new data and `iold` contains the previous data. If the “bootstrap” option is set (`istrap=1`), these units are interchanged. For this option, `stemp2(it)` is always obtained from

`temp2(it-1)`. Because of the thinning effect of Doppler-broadening, the broadening runs faster at each step. The accumulation of error is usually not a problem. For `istrap=0`, `temp1` is used for the starting temperature every time.

The broadening and energy-grid reconstruction are directed by `bfile3`. The routine loads data into the appropriate memory pages from scratch file `iold` and then either calls `broadn` to broaden it (with thinning or thickening of the grid as necessary) or calls `thinb` to thin it without broadening. The results are written onto scratch file `inew`.

In `broadn`, the energy grid points just loaded into `e` by `bfile3` are converted to the dimensionless variables `x` and `y` [see Eq. (87)]. An adaptive reconstruction of the Doppler broadened cross section is then performed for the energy range in the center page using an inverted stack algorithm like the one described for [RECONR](#). The upper limit of each panel is taken to be a point from the input grid, but in order to allow for thinning, up to `nmax=10` of the input grid points can be skipped before the actual upper limit is selected. In addition, the energy of the upper limit cannot be more than `step=2.01` times the energy of the preceding point. The cross sections are now computed at the midpoint of the top panel in the stack using `bsigma`. If the results differ from the values obtained by interpolation by more than the specified tolerance, the new point is added to the stack, and the tests are repeated. Otherwise, the top point in the stack is converged. A backward check is made to see if some of the previous points can be removed based on the new value, the new value is stored in the output array, and the height of the stack is reduced by one. The routine now tries to subdivide the new panel at the top of the stack in the same way. When the stack has been reduced to one element, a new upper limit is chosen from the input energy grid as described above, and the entire process is repeated. The reconstruction logic in *BROADR* uses the same integral tests as [RECONR](#). Refer to the [RECONR](#) chapter for more details.

Subroutine `bsigma` is used to calculate the actual broadened cross section at an energy point using the data in the three pages. First, the routine locates the energy panel containing the desired energy `en`. It then loops over intervals below the current point adding in contributions to  $\bar{\sigma}$  from the  $V-v$  term of Eq. (84) until the contributions to the cross section become small. If the lower limit of the bottom page is reached before convergence, a warning message is issued. The routine then loops over intervals above the current point until convergence. Once again, a warning is issued if necessary. Finally, the low-energy term [the one involving  $V+v$  in Eq. (84)] is added, if applicable.

Subroutine **thinb** is provided for cases where the input cross section set is to be thinned only. This routine uses the original SIGMA1 method. The first input point is always kept. The routine then loops over higher energy values. For each grid point, all the points from there back to the last accepted point are checked for their deviation from a straight line. If they all can be removed without violating the specified tolerance, the interval is extended to the next higher point and the tests are repeated. If any point in the range is too far from the linear approximation, the last point in the range is accepted as an output point, and the testing process is repeated starting from this new lower limit. The procedure terminates when all of the points in the middle page have been thinned, and control is returned to **bfile3** to get the next page of data.

Subroutine **hunky** has been modified from the original SIGMA1 version to implement the alternate  $H_n(a, b)$  calculation when necessary (see **hnabb**). When using the direct method,  $F_n$  values from the previous step are used in the difference of Eq. (90), and **funky** is called to get the new values. The  $A_i$  and  $B_i$  of Eq. (88) are related to the **s1** and **s2** here.

Subroutine **funky** evaluates  $F_n(a)$  by the recursion formula of Eq. (94) using the very accurate SLATEC version of the reduced complementary error function from the NJOY2012 math module.

Function **hnabb** implements the alternate calculation described by Eqs. (96)-(99). The series expansion is continued until about six significant figures are guaranteed (see **eps** and **hnabb**). Currently, **hnabb** is called when only four significant figures are reliable in **hunky** (see **toler** in **hunky**).

## 4.5 User Input

The following input instructions have been copied from the comment cards at the start of BROADR.

```
!---input specifications (free format)-----
!
! card 1
!   nendf   input endf tape (for thermal nubar only)
!   nin     input pendf tape
!   nout    output pendf tape
!
! card 2
!   mat1    material to broadened and thinned
!   ntemp2  number of final temperatures (default=1)
```

```

!   istart  restart (0 no, 1 yes, default 0)
!   istrap  bootstrap (0 no, 1 yes, default 0
!   temp1   starting temperature from nin (default=0K)
!
! card 3
!   errthn  fractional tolerance for thinning
!   thnmax  max. energy for broadening and thinning
!           (default=1 MeV)
!   errmax  fractional tolerance used when integral criterion
!           is satisfied (same usage as in reconr)
!           (errmax.ge.errthn, default=10*errthn)
!   errint  parameter to control integral thinning
!           (usage as in reconr) (default=errthn/20000)
!           set very small to turn off integral thinning.
!   (A good choice for the convergence parameters
!   errthn, errmax, and errint is the same set of
!   values used in reconr)
!
! card 4
!   temp2   final temperatures (deg Kelvin)
!
! card 5
!   mat1    next MAT number to be processed with these
!           parameters.  Terminate with mat1=0.
!
!----input options-----
!
! The output tape will contain the ntemp2 final temperatures
! specified.  It is necessary to have temp1.le.temp2(1).
! if temp2.eq.temp1, the data will be thinned only.
!
! restart   Continue broadening an existing pendf tape.  All
!           temperatures are copied through temp1.  Additional
!           final temperatures are added by starting with the
!           data at temp1.
!
! bootstrap If bootstrap is not requested, each final tempera-
!           ture is generated by broadening directly from temp1
!           to temp2.  If bootstrap is requested, each final temp-
!           erature is broadened from the preceding temperature.
!           Bootstrapping is faster due to the thinning in the
!           previous step.  However, errors accumulate.

```

```

!
! thnmax      A possible upper limit for broadening and thinning.
!              The actual upper limit is the lowest of (i) this input
!              value; (ii) the end of the resolved resonance range;
!              (iii) the lowest reaction threshold; or (iv) 1.0 MeV.
!
!              A negative value for thnmax forces the Doppler
!              broadening upper limit to be abs(thnmax) irrespective
!              of the other conditions.
!
!              Caution:  this may cause one or more threshold
!              reactions to be broadened.  The magnitude of
!              thnmax must be chosen to keep the number of
!              broadenable reactions less than or equal to the
!              maximum of ntt (160).
!
!              Caution: for use in transport codes, it is recommended
!              to use the program default.  We don't know how
!              to compute the spectrum of scattered neutrons from
!              a broadened inelastic level in the current generation
!              of codes.  Broadened cross sections for threshold
!              reactions may be useful for other purposes.
!
!-----

```

Note that `temp1` need not occur on `nout` if `istart=0`. The restart option (`istart=1`) enables the user to add new temperatures to the end of an existing PENDF tape. This option is also useful if a job runs out of time while processing, for example, the fifth temperature in a job requesting six or more final temperatures. The job can be restarted from the `nout`. The first four temperatures will be copied to the new `nout` and broadening will continue for temperature five. The bootstrap option speeds up the code by using the broadened result for `temp2(i-1)` as the starting point to obtain `temp2(i)`. The `thnmax` parameters can be used to speed up a calculation or to prevent the broadening of inappropriate data such as sharp steps or triangles in an evaluated cross section (for example, ENDF/B-V lead).

The following example prepares a broadened PENDF file for  $^{235}\text{U}$  from ENDF/B-VII at two temperatures. The line numbers are for reference only; they are not part of the input.

```

1.  broadr
2.  20 21 22
3.  9228 2/
4.  .001/
5.  300. 1200.
6.  0/

```

On line 2, unit 20 should contain the ENDF file and unit 21 should a [RECONR](#)-generated ASCII PENDF file of 0K cross sections for the isotope. Two materials will be generated on unit 21 with 0.1% accuracy. First will be the 300K data, followed by a MEND record, followed by the 1200K data, followed by MEND and and TEND records. Best results are obtained when the error tolerance `errthn` and the optional integral-thinning controls `errmax` and `errint` are the same as those used for the [RECONR](#) run.

#### 4.6 Error Messages

**error in broadr\*\*\*nin and nout must be same mode**

Use coded to coded, or blocked binary to blocked binary. The latter is faster due to the several tape copies performed in BROADR.

**error in broadr\*\*\*too many low threshold reactions**

The current limit is set by the global parameter `ntt=180`. Check `tt`, `mtr`, and `ntt` in `broadr`, `tt` in `bfile3`, and `sbt` in `broadn`.

**message from broadr---desired mat and temp not on tape**

Check the input PENDF file and the user input.

**message from broadr---no broadenable reactions**

No low threshold reactions were found.

**error in broadr\*\*\*storage exceeded**

Insufficient storage to update directory. Increase `nwscr=1000` in `broadr`.

**message from stounx---sigma zero data removed ...**

The input PENDF tape already contained a special unresolved section in File 2. It has been removed. Rerun [UNRESR](#) if necessary.

**message from bsigma---broadening truncated at a=----**

The page is too small for the temperature difference requested. Increase total storage available (`namax`) or repeat the calculation with smaller temperature steps and `istrap=1`. The normal maximum size of `a` is 4.0 and `a` is inversely proportional to  $T_i - T_{i-1}$ .

## 4.7 Input/Output Units

The following units are used for input and output by *BROADR*.

- 10     **nscr1** in *BROADR*. Contains the ENDF/B data at the initial temperature.
- 12/13   **io1d/inew** in *BROADR*. Contains union grid and low threshold reactions.
- 20-99   User's choice for **nin** and **nout** to link with other modules.

Units 12 and 13 will always be binary. Unit 10 will have the same mode as **nin** and **nout**.

## 4.8 Storage Allocation

All storage is divided in the most efficient way possible. The container array size **namax** should be made as large as possible. The value of **nbuf** can be increased or decreased at will — larger values will give faster execution. The value for **nwscr** depends on the size of the ENDF/B dictionary, and 1000 words is sufficient for all current evaluations.



## 5 UNRESR

The UNRESR module is used to produce effective self-shielded cross sections for resonance reactions in the unresolved energy range. In ENDF-format evaluations, the unresolved range begins at an energy where it is difficult to measure individual resonances and extends to an energy where the effects of fluctuations in the resonance cross sections become unimportant for practical calculations. As described in the ENDF format manual,[8] resonance information for this energy range is given as average values for resonance widths and spacings together with distribution functions for the widths and spacings. This representation can be converted into effective cross sections suitable for codes that use the background cross section method, often called the Bondarenko method,[38] using a method originally developed for the MC2 code[36] and extended for the ETOX code[27]. This unresolved-resonance method has the following features:

- Flux-weighted cross sections are produced for the total, elastic, fission, and capture cross sections, including competition with inelastic scattering.
- A current-weighted total cross section is produced for calculating the effective self-shielded transport cross section.
- The energy grid used is consistent with the grid used by [RECONR](#).
- The computed effective cross sections are written on the PENDF tape in a specially defined section (MF2, MT152) for use by other modules.
- The accurate quadrature scheme from the MC2-2 code[37] is used for computing averages over the ENDF statistical distribution functions.

This report describes UNRESR in NJOY 2012.0. The main changes from the version reported previously[3] are as follows:

- the generation of a refined energy grid for some evaluations
- elimination of the restriction that `ntemp` and `nsigz` be less than or equal to 10, and
- the conversion to Fortran-90 style and storage allocation.

### 5.1 Theory

In the unresolved energy range, it is not possible to define precise values for the cross sections of the resonance reactions  $\sigma_x(E)$ , where  $x$  stands for the reaction

type (total, elastic, fission, or capture). It is only possible to define average values. Of course, these average values should try to preserve the reaction rate:

$$\bar{\sigma}_{0x}(E^*) = \frac{\int_{E_1}^{E_2} \sigma_x(E) \phi_0(E) dE}{\int_{E_1}^{E_2} \phi_0(E) dE} , \quad (100)$$

where  $\phi_0(E)$  is the scalar flux,  $E^*$  is an effective energy in the range  $[E_1, E_2]$ , and the range  $[E_1, E_2]$  is large enough to hold many resonances but small with respect to slowly varying functions of  $E$ . In order to calculate effective values for the transport cross section, it is necessary to compute the current-weighted total cross section also. It is given by

$$\bar{\sigma}_{1t}(E^*) = \frac{\int_{E_1}^{E_2} \sigma_x(E) \phi_1(E) dE}{\int_{E_1}^{E_2} \phi_1(E) dE} , \quad (101)$$

where the  $P_1$  component of the neutron flux,  $\phi_1(E)$ , is proportional to the neutron current. To proceed farther, it is necessary to choose a model for the shape of  $\phi_\ell(E)$  in the vicinity of  $E^*$ . The model used in UNRESR is based on the  $B_0$  approximation for large homogeneous systems and narrow resonances:

$$\phi_\ell(E) = \frac{C(E)}{[\Sigma_t(E)]^\ell} , \quad (102)$$

where  $C(E)$  is a slowly varying function of  $E$ , and  $\Sigma_t(E)$  is the macroscopic total cross section for the system. In order to use this result in Eq. 100, it is further assumed that the effects of other isotopes in the mixture can be approximated by a constant called  $\sigma_0$  in the range  $[E_1, E_2]$ , or

$$\phi_\ell(E) = \frac{C(E)}{[\sigma_0 + \sigma_t(E)]^\ell} . \quad (103)$$

Therefore, the effective cross sections in the unresolved range are represented by

$$\bar{\sigma}_{0x}(E^*) = \frac{\int_{E_1}^{E_2} \frac{\sigma_x(E)}{\sigma_0 + \sigma_t(E)} C(E) dE}{\int_{E_1}^{E_2} \frac{1}{\sigma_0 + \sigma_t(E)} C(E) dE} , \quad (104)$$

with  $x$  being  $t$  for total,  $e$  for elastic,  $f$  for fission, and  $\gamma$  for capture, and

$$\bar{\sigma}_{1t}(E^*) = \frac{\int_{E_1}^{E_2} \frac{\sigma_x(E)}{[\sigma_0 + \sigma_t(E)]^2} C(E) dE}{\int_{E_1}^{E_2} \frac{1}{[\sigma_0 + \sigma_t(E)]^2} C(E) dE} . \quad (105)$$

This equation can also be written in the equivalent form

$$\bar{\sigma}_{1t}(E^*) = \frac{\int_{E_1}^{E_2} \frac{1}{\sigma_0 + \sigma_t(E)} C(E) dE}{\int_{E_1}^{E_2} \frac{1}{[\sigma_0 + \sigma_t(E)]^2} C(E) dE} - \sigma_0 . \quad (106)$$

The parameter  $\sigma_0$  in Eq. 103 deserves more discussion. It can be looked at as a parameter that controls the depth of resonance dips in the flux. When  $\sigma_0$  is large with respect to the peak cross sections of resonances in  $\sigma_t(E)$ , the shape of the flux is essentially  $C(E)$ . For smaller values of  $\sigma_0$ , dips will develop in the flux that correspond to peaks in  $\sigma_t$ . These dips will cancel out part of the reaction rate in the region of the peaks, thus leading to self-shielding of the cross section. Analysis shows that it is possible to use this single parameter to represent the effects of admixed materials or the effects of neutron escape from an absorbing region. See the [GROUPR](#) chapter of this manual for additional details.

The cross sections that appear in the above integrals can be written as the sum of a resonant part and a smooth part as follows:

$$\sigma_x(E) = b_x + \sigma_{Rx}(E) = b_x + \sum_s \sum_r \sigma_{xsr}(E - E_{sr}) , \quad (107)$$

where  $s$  is an index to a spin sequence,  $r$  is an index to a particular resonance in that spin sequence, and  $E_{sr}$  is the center energy for that resonance. The smooth part  $b_x$  can come from a smooth background given in the ENDF file, and it also includes the potential scattering cross section  $\sigma_p$  for the elastic and total cross sections ( $x=t$  and  $x=e$ ). In terms of the smooth and resonant parts, the effective cross sections become

$$\bar{\sigma}_{0x}(E^*) = b_x + \frac{\int_{E_1}^{E_2} \frac{\sigma_{Rx}(E)}{\bar{\sigma} + \sigma_{Rt}(E)} C(E) dE}{\int_{E_1}^{E_2} \frac{1}{\bar{\sigma} + \sigma_{Rt}(E)} C(E) dE} , \quad (108)$$

and

$$\bar{\sigma}_{1t}(E^*) = \frac{\int_{E_1}^{E_2} \frac{1}{\bar{\sigma} + \sigma_{Rt}(E)} C(E) dE}{\int_{E_1}^{E_2} \frac{1}{[\bar{\sigma} + \sigma_{Rt}(E)]^2} C(E) dE} - \sigma_0 , \quad (109)$$

where  $\bar{\sigma} = b_t + \sigma_0$ . It is convenient to transform the denominators of Eqs. 108 and 109 into

$$\int \frac{1}{\bar{\sigma} + \sigma_t} C dE = \frac{1}{\bar{\sigma}} \left\{ \int C dE - \int \frac{\sigma_t}{\bar{\sigma} + \sigma_t} C dE \right\} , \quad (110)$$

and

$$\int \frac{1}{[\bar{\sigma} + \sigma_t]^2} C dE = \frac{1}{\bar{\sigma}^2} \left\{ \int C dE - \int \frac{\sigma_t}{\bar{\sigma} + \sigma_t} C dE - \int \frac{\bar{\sigma}\sigma_t}{[\bar{\sigma} + \sigma_t]^2} C dE \right\} . \quad (111)$$

Furthermore, since  $C(E)$  is assumed to be a slowly-varying function of  $E$ , it can be pulled out through all integrals and dropped. The average cross sections become

$$\bar{\sigma}_{0x} = b_x + \frac{\bar{\sigma} I_{0x}}{1 - I_{0t}} , \quad (112)$$

and

$$\bar{\sigma}_{1t} = b_t + \frac{\bar{\sigma} I_{1t}}{1 - I_{0t} - I_{1t}} . \quad (113)$$

The last equation can also be written in the form

$$\bar{\sigma}_{1t} = \bar{\sigma} \left[ \frac{1 - I_{0t}}{1 - I_{0t} - I_{1t}} \right] - \sigma_0 . \quad (114)$$

The average cross sections are thereby seen to depend on two types of “fluctuation integrals:”

$$I_{0x} = \frac{1}{E_2 - E_1} \int_{E_1}^{E_2} \frac{\sigma_{Rx}(E)}{\bar{\sigma} + \sigma_{Rt}(E)} dE , \quad (115)$$

and

$$I_{1t} = \frac{1}{E_2 - E_1} \int_{E_1}^{E_2} \frac{\bar{\sigma}\sigma_{Rt}(E)}{[\bar{\sigma} + \sigma_{Rt}(E)]^2} dE , \quad (116)$$

where  $x$  can take on the values  $t$ ,  $n$ ,  $f$ , or  $\gamma$ . Note that  $I_{1t} \leq I_{0t}$ , the difference increasing as  $\sigma_0$  decreases from infinity.

Inserting the actual sums over resonances into the formula for  $I_{0x}$  gives

$$I_{0x} = \frac{1}{E_2 - E_1} \int_{E_1}^{E_2} \frac{\sum_{sr} \sigma_{xsr}(E - E_{sr})}{\bar{\sigma} + \sum_{sr} \sigma_{tsr}(E - E_{sr})} dE . \quad (117)$$

If the resonances were widely separated, only the “self” term would be important, and one would obtain

$$I_{0x} = \sum_{sr} \frac{1}{E_2 - E_1} \int_{E_1}^{E_2} \frac{\sigma_{xsr}(E - E_{sr})}{\bar{\sigma} + \sigma_{tsr}(E - E_{sr})} dE . \quad (118)$$

Since the range of integration is large with respect to the width of any one resonance, the variable of integration can be changed to  $\xi = E - E_{sr}$ , and the limits on  $\xi$  can be extended to infinity. For any one sequence, the interval  $E_2 - E_1$  is equal to the average spacing of resonances in that sequence times the number of resonances in the interval. Therefore,

$$I_{0x}^I = \sum_s \frac{1}{D_s} \frac{1}{N_s} \sum_r \int_{-\infty}^{\infty} \frac{\sigma_{xsr}(\xi)}{\bar{\sigma} + \sigma_{tsr}(\xi)} d\xi \quad (119)$$

where  $D_s$  is the average spacing, and the “I” superscript indicates that this is the “isolated resonance” result. Because there are assumed to be many resonances in the interval, the sum over resonances can be changed to a multiple integration over some characteristic set of parameters (such as widths) times the probability of finding a resonance with some particular values of the parameters:

$$\frac{1}{N} \sum_{r \in s} f_r = \langle f \rangle_s = \int d\alpha P_s(\alpha) \int d\beta P_s(\beta) \cdots f(\alpha, \beta, \cdots) . \quad (120)$$

In the following text, this multiple integral (up to four fold) will be abbreviated by writing the  $\alpha$  integral only. The final results for isolated resonances are as follows:

$$I_{0x}^I = \sum_s \frac{1}{D_s} \int P(\alpha) \int_{-\infty}^{\infty} \frac{\sigma_{xs\alpha}(\xi)}{\bar{\sigma} + \sigma_{ts\alpha}(\xi)} d\xi d\alpha , \quad (121)$$

and

$$I_{1t}^I = \sum_s \frac{1}{D_s} \int P(\alpha) \int_{-\infty}^{\infty} \frac{\bar{\sigma} \sigma_{ts\alpha}(\xi)}{[\bar{\sigma} + \sigma_{ts\alpha}(\xi)]^2} d\xi d\alpha . \quad (122)$$

If the effects of overlap are too large to be neglected, overlap corrections to the isolated resonance result can be constructed using the continued-fraction generator

$$\frac{1}{a+b} = \frac{1}{a} \left( 1 - \frac{b}{a+b} \right). \quad (123)$$

Starting with the  $I_0$  integrals,

$$\begin{aligned} \frac{\sum_{sr} \sigma_{xsr}}{\bar{\sigma} + \sum_{sr} \sigma_{tsr}} &= \sum_{sr} \frac{\sigma_{xsr}}{\bar{\sigma} + \sigma_{tsr}} \left\{ 1 \right. \\ &\quad \left. - \sum_{r' \neq r} \frac{\sigma_{tsr'}}{\bar{\sigma} + \sum_{tsr}} - \sum_{s' \neq s} \sum_{r'} \frac{\sigma_{ts'r'}}{\bar{\sigma} + \sum_{tsr}} \right\}. \end{aligned} \quad (124)$$

Expand the second term in the braces to get

$$\begin{aligned} \frac{\sum_{sr} \sigma_{xsr}}{\bar{\sigma} + \sum_{sr} \sigma_{tsr}} &= \sum_{sr} \frac{\sigma_{xsr}}{\bar{\sigma} + \sigma_{tsr}} \left\{ 1 \right. \\ &\quad - \sum_{r' \neq r} \frac{\sigma_{tsr'}}{\bar{\sigma} + \sigma_{tsr} + \sigma_{tsr'}} \\ &\quad \left\{ 1 - \sum_{\substack{r'' \neq r \\ r'' \neq r'}} \frac{\sigma_{tsr''}}{\bar{\sigma} + \sum_{tsr}} - \sum_{s' \neq s} \sum_{r'} \frac{\sigma_{ts'r'}}{\bar{\sigma} + \sum_{tsr}} \right\} \\ &\quad \left. - \sum_{s' \neq s} \sum_{r'} \frac{\sigma_{ts'r'}}{\bar{\sigma} + \sum_{tsr}} \right\}. \end{aligned} \quad (125)$$

Neglecting the products of three *different* resonances in sequence  $s$  gives

$$\begin{aligned} \frac{\sum_{sr} \sigma_{xsr}}{\bar{\sigma} + \sum_{sr} \sigma_{tsr}} &= \sum_{sr} \frac{\sigma_{xsr}}{\bar{\sigma} + \sigma_{tsr}} \\ &\quad \times \left\{ 1 - \sum_{r' \neq r} \frac{\sigma_{tsr'}}{\bar{\sigma} + \sigma_{tsr} + \sigma_{tsr'}} \right\} \\ &\quad \times \left[ 1 - \sum_{s' \neq s} \sum_{r'} \frac{\sigma_{ts'r'}}{\bar{\sigma} + \sum_{tsr}} \right]. \end{aligned} \quad (126)$$

The factor before the opening brace is the isolated resonance result, the factor in braces is the in-sequence overlap correction, and the factor in brackets is the sequence-sequence overlap correction. Note that recursion can be used to refine the sequence-sequence correction to any desired accuracy. Similarly, the

$I_1$  integral requires

$$\frac{\sum_{sr} \bar{\sigma} \sigma_{xsr}}{[\bar{\sigma} + \sum_{sr} \sigma_{tsr}]^2} = \sum_{sr} \frac{\bar{\sigma} \sigma_{xsr}}{[\bar{\sigma} + \sigma_{tsr}]^2} \left[ 1 - \sum_{r' \neq r} \frac{\sigma_{tsr'}}{\bar{\sigma} + \sum \sigma_{tsr}} - \sum_{s' \neq s} \sum_{r'} \frac{\sigma_{ts'r'}}{\bar{\sigma} + \sum \sigma_{tsr}} \right]^2. \quad (127)$$

Once more, we expand the fraction and neglect terms that will result in products of three or more different resonances in the same sequence. The result is

$$\begin{aligned} \frac{\sum_{sr} \bar{\sigma} \sigma_{xsr}}{[\bar{\sigma} + \sum_{sr} \sigma_{tsr}]^2} &= \sum_{sr} \frac{\bar{\sigma} \sigma_{xsr}}{[\bar{\sigma} + \sigma_{tsr}]^2} \\ &\times \left\{ 1 - 2 \sum_{r' \neq r} \frac{\sigma_{tsr'}}{\bar{\sigma} + \sigma_{tsr} + \sigma_{tsr'}} + \sum_{r' \neq r} \left( \frac{\sigma_{tsr'}}{\bar{\sigma} + \sigma_{tsr} + \sigma_{tsr'}} \right)^2 \right\} \\ &\times \left[ 1 - \sum_{s' \neq s} \sum_{r'} \frac{\sigma_{ts'r'}}{\bar{\sigma} + \sum \sigma_{tsr}} \right], \end{aligned} \quad (128)$$

where in-sequence and sequence-sequence overlap terms have been factored out.

The next step is to substitute these results back into the fluctuation integrals  $I_0$  and  $I_1$ . The integrals over energy and the sums over different resonances in each sequence can be handled as described above for isolated resonances. This procedure will result in three different kinds of integrals. The first kind includes the isolated resonance integrals already considered above

$$\begin{aligned} B_{xs} &= \frac{1}{E_2 - E_1} \int_{E_1}^{E_2} \sum_r \frac{\sigma_{xsr}}{\bar{\sigma} + \sigma_{tsr}} dE \\ &= \frac{1}{D_s} \int P(\alpha) \int_{-\infty}^{\infty} \frac{\sigma_{xs\alpha}(\xi)}{\bar{\sigma} + \sigma_{ts\alpha}(\xi)} d\xi d\alpha, \end{aligned} \quad (129)$$

and

$$\begin{aligned} D_{ts} &= \frac{1}{E_2 - E_1} \int_{E_1}^{E_2} \sum_r \frac{\bar{\sigma} \sigma_{tsr}}{[\bar{\sigma} + \sigma_{tsr}]^2} dE \\ &= \frac{1}{D_s} \int P(\alpha) \int_{-\infty}^{\infty} \frac{\bar{\sigma} \sigma_{ts\alpha}(\xi)}{[\bar{\sigma} + \sigma_{ts\alpha}(\xi)]^2} d\xi d\alpha. \end{aligned} \quad (130)$$

Note that  $D_t \leq B_t$ , the difference increasing as  $\sigma_0$  decreases from infinity.

The next kind are the in-sequence overlap integrals. The sum over  $r'$  is replaced by integrals over the probabilities of finding each partial width and the probability of finding a resonance  $r'$  at a distance  $\eta$  from resonance  $r$ .

$$\begin{aligned}
V_{0xs} &= \frac{1}{E_2 - E_1} \int_{E_1}^{E_2} \sum_r \sum_{r' \neq r} \frac{\sigma_{xsr}}{\bar{\sigma} + \sigma_{tsr}} \frac{\sigma_{tsr'}}{\bar{\sigma} + \sigma_{tsr} + \sigma_{tsr'}} dE \\
&= \frac{1}{D_s^2} \int P(\alpha) \int P(\beta) \int \int \Omega(\eta) \frac{\sigma_{xs\alpha}(\xi)}{\bar{\sigma} + \sigma_{ts\alpha}(\xi)} \\
&\quad \frac{\sigma_{ts\beta}(\xi - \eta)}{\bar{\sigma} + \sigma_{ts\alpha}(\xi) + \sigma_{ts\beta}(\xi - \eta)} d\eta d\xi d\beta d\alpha , \tag{131}
\end{aligned}$$

where  $\xi = E - E_{sr}$  and  $\eta = E_{sr'} - E_{sr}$ . Similarly,

$$\begin{aligned}
V_{1ts} &= \frac{1}{E_2 - E_1} \int_{E_1}^{E_2} \sum_r \sum_{r' \neq r} \frac{\bar{\sigma} \sigma_{tsr}}{[\bar{\sigma} + \sigma_{tsr}]^2} \left\{ 2 \frac{\sigma_{tsr'}}{\bar{\sigma} + \sigma_{tsr} + \sigma_{tsr'}} \right. \\
&\quad \left. - \left( \frac{\sigma_{tsr'}}{\bar{\sigma} + \sigma_{tsr} + \sigma_{tsr'}} \right)^2 \right\} dE \\
&= \frac{1}{D_s^2} \int P(\alpha) \int P(\beta) \int \int \Omega(\eta) \frac{\bar{\sigma} \sigma_{ts\alpha}(\xi)}{[\bar{\sigma} + \sigma_{ts\alpha}(\xi)]^2} \\
&\quad \left\{ 2 \frac{\sigma_{ts\beta}(\xi - \eta)}{\bar{\sigma} + \sigma_{ts\alpha}(\xi) + \sigma_{ts\beta}(\xi - \eta)} \right. \\
&\quad \left. - \left[ \frac{\sigma_{ts\beta}(\xi - \eta)}{\bar{\sigma} + \sigma_{ts\alpha}(\xi) + \sigma_{ts\beta}(\xi - \eta)} \right]^2 \right\} d\eta d\xi d\beta d\alpha . \tag{132}
\end{aligned}$$

The final class of integrals includes the sequence-sequence overlap corrections. They are simplified by noting that the positions of resonances in different spin sequences are uncorrelated. Therefore,  $\Omega(\eta)=1$ , and the integral of the product reduces to the product of the integrals.

Using the results and definitions from above, the fluctuation integrals become

$$I_{0x} = \sum_s A_{xs} , \tag{133}$$

$$A_{xs} = (B_{xs} - V_{0xs}) \left[ 1 - \sum_{s' \neq s} A_{ts'} \right] , \tag{134}$$

and

$$I_{1t} = \sum_s (D_{ts} - V_{1ts}) \left[ 1 - \sum_{s' \neq s} A_{ts'} \right]^2 , \tag{135}$$



where Eq. 134 provides a recursive definition of the  $A_{ts}$  for the sequence-sequence corrections as well as the normal value of  $A_{xs}$ .

These equations are formally exact for the sequence-sequence overlaps, but in-sequence overlaps only include the interactions between pairs of resonances. Three different approximations to this result are currently in use.

**The MC2/ETOX Approximation** The MC2 and ETOX codes use similar approximations to the results above, except that MC2 does not include a calculation of the current-weighted total cross section. Both codes explicitly neglect the in-sequence overlap corrections. This approximation was based on the assumption that resonance repulsion would reduce the overlap between resonances in a particular spin sequence, leaving the accidental close spacing of resonances in different sequences as the dominant overlap effect. In addition, both codes stop the recursion of Eq. 134 at  $A_t = B_t$ . Thus,

$$I_{0x} = \sum_s B_{xs} \left( 1 - \sum_{s' \neq s} B_{ts'} \right), \quad (136)$$

and

$$I_{1t} = \sum_s D_{ts} \left( 1 - \sum_{s' \neq s} B_{ts'} \right)^2. \quad (137)$$

The equations for the effective cross sections in the MC2/ETOX approximation become

$$\bar{\sigma}_{0x} = b_x + \frac{\bar{\sigma} \sum_s B_{xs} \left( 1 - \sum_{s' \neq s} B_{ts'} \right)}{1 - \sum_s B_{ts} \left( 1 - \sum_{s' \neq s} B_{ts'} \right)}, \quad (138)$$

and

$$\bar{\sigma}_{1t} = b_t + \frac{\bar{\sigma} \sum_s D_{ts} \left( 1 - \sum_{s' \neq s} B_{ts'} \right)^2}{1 - \sum_s B_{ts} \left( 1 - \sum_{s' \neq s} B_{ts'} \right) - \sum_s D_{ts} \left( 1 - \sum_{s' \neq s} B_{ts'} \right)^2}, \quad (139)$$

or

$$\bar{\sigma}_{1t} = \bar{\sigma} \left[ \frac{1 - \sum_s B_{ts} \left( 1 - \sum_{s' \neq s} B_{ts'} \right)}{1 - \sum_s B_{ts} \left( 1 - \sum_{s' \neq s} B_{ts'} \right) - \sum_s D_{ts} \left( 1 - \sum_{s' \neq s} B_{ts'} \right)^2} \right] - \sigma_0 . \quad (140)$$

These are the equations that are used in the UNRESR module of NJOY. Note that the equation in the ETOX code and report corresponding to Eq. 140 is incorrect. The following equation was used in the ETOX code:

$$\bar{\sigma}_{1t} = \bar{\sigma} \left[ \frac{1 - \sum_s B_{ts} \left( 1 - \sum_{s' \neq s} B_{ts'} \right)}{1 - \sum_s C_{ts} \left( 1 - \sum_{s' \neq s} C_{ts'} \right)} \right] - \sigma_0 , \quad (141)$$

with  $C_{ts} = B_{ts} + D_{ts}$ .

**The MC2-2 Approximation** The MC2-2 code includes the in-sequence overlap corrections, which the authors found to be more important than previously thought. It uses additional approximations to obtain the equivalent of

$$\bar{\sigma}_{0x} = b_x + \bar{\sigma} \sum_s \frac{B_{xs} - V_{0xs}}{1 - B_{ts} + V_{0ts}} . \quad (142)$$

The additional approximations used are

1. Set  $A_{ts} = B_{ts} - V_{0ts}$  (first-order sequence-sequence overlap),
2. Neglect the factor  $(1 - \sum_{s' \neq s} A_{ts'})$  in the denominator, and
3. Use the approximation  $1 - \sum_i f_i \approx \prod_i (1 - f_i)$  on the numerator and denominator.

These simplifications result in a loss of accuracy for the sequence-sequence overlap correction at relatively low values of  $\sigma_0$ . The  $\bar{\sigma}_{1t}$  term is not calculated.

**The UXSR Approximation** The experimental UXSR module was developed at Oak Ridge (with some contributions from LANL) based on coding from the Argonne National Laboratory (ANL) in an attempt to include the sophisticated in-sequence overlap corrections from MC2-2 without approximating the sequence-sequence corrections so badly. It also implemented a calculation of the

current-weighted total cross section, which was omitted in MC2-2. The additional cost of using the full expressions for Eqs. 133 and 135 is minimal, and effective cross sections can be computed for lower values of  $\sigma_0$  when in-sequence overlap is small (*e.g.*,  $^{238}\text{U}$ ).

Now that expressions have been chosen for computing the cross sections in terms of the isolated-resonance integrals, it is necessary to select an efficient numerical method for computing them. The resonant parts of the cross sections are given by

$$\sigma_{xsr}(E-E_{sr}) = \left[ \sigma_m \frac{\Gamma_x}{\Gamma} \psi(\theta, X) \right]_{sr} , \quad (143)$$

and

$$\sigma_{tsr}(E-E_{sr}) = [ \sigma_m \{ \cos 2\phi_\ell \psi(\theta, X) + \sin 2\phi_\ell \chi(\theta, X) \} ]_{sr} , \quad (144)$$

where  $x$  takes on the values  $\gamma$ ,  $f$ , or  $c$  for capture, fission, or competition, and

$$\sigma_m = \frac{4\pi g_J}{k^2} \frac{\Gamma_n}{\Gamma} , \quad (145)$$

$$\theta = \sqrt{\frac{A}{4kTE_0}} \Gamma , \quad (146)$$

$$X = \frac{2(E-E_0)}{\Gamma} , \quad (147)$$

$$g_J = \frac{2J+1}{2(2I+1)} , \text{ and} \quad (148)$$

$$k = 2.196771 \times 10^{-3} \frac{A}{1+A} \sqrt{E} . \quad (149)$$

The functions  $\psi$  and  $\chi$  are the symmetric and antisymmetric components of the broadened resonance line shape:

$$\psi(\theta, X) = \frac{\theta\sqrt{\pi}}{2} \text{Re}W \left( \frac{\theta X}{2}, \frac{\theta}{2} \right) , \quad (150)$$

and

$$\chi(\theta, X) = \theta\sqrt{\pi} \text{Im}W \left( \frac{\theta X}{2}, \frac{\theta}{2} \right) , \quad (151)$$

where

$$W(x, y) = \exp[-(x + iy)^2] \operatorname{erfc}[-i(x + iy)] \quad (152)$$

is the complex probability integral. The methods for computing  $\psi$  and  $\chi$  are well known (see **quikw**).

The first integral needed is

$$\begin{aligned} B_{xs} &= \frac{1}{D_s} \int P(\alpha) \int \frac{\sigma_{xs\alpha}(\xi)}{\bar{\sigma} + \sigma_{ts\alpha}(\xi)} d\xi d\alpha \\ &= \frac{1}{D_s} \int P(\alpha) \int \frac{\sigma_m(\Gamma_x/\Gamma) \psi(\theta, X)}{\bar{\sigma} + \sigma_m\{\cos 2\phi_\ell \psi(\theta, X) + \sin 2\phi_\ell \chi(\theta, X)\}} d\xi d\alpha \\ &= \frac{1}{D_s} \int P(\alpha) \frac{\Gamma_x}{2 \cos 2\phi_\ell} \int \frac{\psi(\theta, X)}{\beta + \psi(\theta, X) + \tan 2\phi_\ell \chi(\theta, X)} dX d\alpha \end{aligned} \quad (153)$$

where

$$\beta = \frac{\bar{\sigma}}{\sigma_m \cos 2\phi_\ell} . \quad (154)$$

The second integral needed is

$$\begin{aligned} B_{ts} &= \frac{1}{D_s} \int P(\alpha) \int \frac{\sigma_{ts\alpha}(\xi)}{\bar{\sigma} + \sigma_{ts\alpha}(\xi)} d\xi d\alpha \\ &= \frac{1}{D_s} \int P(\alpha) \frac{\Gamma}{2} \int \frac{\psi(\theta, X) + \tan 2\phi_\ell \chi(\theta, X)}{\beta + \psi(\theta, X) + \tan 2\phi_\ell \chi(\theta, X)} dX d\alpha . \end{aligned} \quad (155)$$

Both of these integrals can be expressed in terms of the basic  $J$  integral:

$$\begin{aligned} B_{xs} &= \frac{1}{D_s} \int P(\alpha) \frac{\Gamma}{\cos 2\phi_\ell} J(\beta, \theta, \tan 2\phi_\ell, 0) d\alpha , \text{ and} \\ B_{ts} &= \frac{1}{D_s} \int P(\alpha) \Gamma J(\beta, \theta, \tan 2\phi_\ell, \tan 2\phi_\ell) d\alpha , \end{aligned} \quad (156)$$

where

$$J(\beta, \theta, a, b) = \frac{1}{2} \int_{-\infty}^{\infty} \frac{\psi(\theta, X) + b \chi(\theta, X)}{\beta + \psi(\theta, X) + a \chi(\theta, X)} dX . \quad (157)$$

The  $D$  integral can be handled in the same way, but only total reaction is required.

$$\begin{aligned}
D_{ts} &= \frac{1}{D_s} \int P(\alpha) \int \frac{\bar{\sigma} \sigma_{ts\alpha}(\xi)}{[\bar{\sigma} + \sigma_{ts\alpha}(\xi)]^2} d\xi d\alpha \\
&= \frac{1}{D_s} \int P(\alpha) \frac{\Gamma}{2} \int \frac{\beta \psi(\theta, X) + \tan 2\phi_\ell \chi(\theta, X)}{[\beta + \psi(\theta, X) + \tan 2\phi_\ell \chi(\theta, X)]^2} dX d\alpha \\
&= \frac{1}{D_s} \int P(\alpha) \Gamma K(\beta, \theta, \tan 2\phi_\ell, \tan 2\phi_\ell) d\alpha, \tag{158}
\end{aligned}$$

where

$$K(\beta, \theta, a, b) = \frac{1}{2} \int_{-\infty}^{\infty} \frac{\beta [\psi(\theta, X) + b \chi(\theta, X)]}{[\beta + \psi(\theta, X) + a \chi(\theta, X)]^2} dX. \tag{159}$$

A method for computing  $J$ , including the interference effects, has been developed by Hwang for MC2-2[37]. However, this method was not available in the days when MC2 and ETOX were developed. Therefore, UNRESR uses only  $J(\beta, \theta, 0, 0)$  and  $K(\beta, \theta, 0, 0)$  in computing the isolated-resonance fluctuation integrals. A direct integration is used over most of the  $X$  range, but the part of the integral arising from large  $X$  is handled using analytic integrations of the asymptotic forms of the arguments (see [ajku](#)).

The final step is to do the  $n$ -fold integration over the probability distributions for the resonance widths. This integration has been abbreviated as a single integration over  $\alpha$  in the above equations. The method used was originally developed for MC2-2 and is based on Gauss-Jacobi quadratures. A set of 10 quadrature points and weights is provided for each of the  $\chi^2$  probability distributions with 1 through 4 degrees of freedom. These quadratures convert the  $n$ -fold integral into an  $n$ -fold summation. The value of  $n$  can be as large as 4 when  $\Gamma_n$ ,  $\Gamma_f$ ,  $\Gamma_\gamma$ , and  $\Gamma_c$  (competitive width) are all present.

Although UNRESR neglects the effects of overlap between resonances in the same spin sequence and the effects of interference in the elastic and total cross sections, it still gives reasonable results for the background cross section values needed for most practical problems. Modern evaluations are steadily reducing the need for accurate unresolved calculations by extending the resolved resonance range to higher and higher energies. Ultimately, UNRESR should be upgraded to use the UXSR approach. Another alternative is to generate self-shielded effective cross sections from ladders of resonances chosen statistically (see [PURR](#)). This avoids many of the approximations in the overlap corrections.

In NJOY2012, running the [PURR](#) module after UNRESR overwrites the UNRESR output with the [PURR](#) results. In fact, UNRESR can be omitted

from the processing stream. To use UNRESR results, either omit [PURR](#) from the processing stream or run it before running UNRESR.

## 5.2 Implementation

In implementing this theory in UNRESR, there are special considerations involving the choice of an incident energy grid, what to do if the unresolved range overlaps the resolved range or the range of smooth cross sections, the choice of the  $\sigma_0$  grid, how to interpolate on  $\sigma_0$ , and how to communicate the results to other modules.

**Choice of Energy Grid.** The same logic is used to choose the incident energy grid in UNRESR and [RECONR](#). It is complicated, because of the several different representations available for unresolved data, and because of the existence of evaluations that have been carried over from previous versions of ENDF/B or ENDF/B-VII evaluations with inadequate energy grids. Even many modern evaluations have inadequate energy grids.

For evaluations that give energy-independent unresolved-resonance parameters, there is still an energy dependence to the cross sections. Because this dependence is normally somewhere between constant and a  $1/v$  law, a fairly coarse grid with about 13 points per decade should be sufficient to allow the cross sections to be computed reliably using linear-linear interpolation.

If the evaluation uses energy-dependent parameters, the normal rule would be to use the energies that were provided by the evaluator and to obtain intermediate cross sections by interpolation. Unfortunately, some of the evaluations carried over from earlier days contain some energy intervals that are quite large (for example, steps by factors of 10). The evaluators for these isotopes assumed that the user would use parameter interpolation and compute the cross sections at a number of intermediate energies in these long steps. Even some newer evaluations contain large jumps in the energy grid. UNRESR will detect such evaluations and add additional energy points in the large energy steps using an algorithm similar to the one used for the cases with energy-independent parameters. For NJOY2012, large jumps in the energy grid are any with step ratios greater than `wide`, which is currently set to 1.26.

The final energy grid can be observed by scanning the printed output from UNRESR.

**Resolved-Unresolved Overlap.** Elemental evaluations include separate energy ranges in MF2/MT151 for each of the isotopes of the element, and these energy ranges do not have to be the same for each isotope. This means that the lower end of an unresolved range may overlap the resolved range from another isotope, and the upper end of the unresolved range for an isotope can overlap the smooth range of another isotope. These overlap regions are detected by UNRESR as the resonance data are read in, and they are marked by making the sign of the incident energy value negative.

**Choosing a  $\sigma_0$  Grid.** There are two factors to consider, namely, choosing values that will represent the shape adequately, and limiting the range of  $\sigma_0$  to the region where the theory is valid. The  $\sigma_x(\sigma_0)$  curves start out decreasing from the infinite dilution value as  $1/\sigma_0$  as  $\sigma_0$  decreases from infinity ( $1 \times 10^{10}$  in the code). The curve eventually goes through an inflection point at some characteristic value of  $\sigma_0$ , becomes concave upward, and approaches a limiting value at small  $\sigma_0$  that is smaller than the infinite-dilution value. Decade steps are often used, but the user should try to select values that include the inflection point and not waste values on the  $1/\sigma_0$  region. Half-decade values are useful near the inflection point (*e.g.*, 100, 300, 1000 for  $^{235}\text{U}$ ). The grid interval chosen should be consistent with the interpolation method used (see below).

Choosing the lower limit for  $\sigma_0$  is a more difficult problem. As shown in the theory section (5.1), resonance overlap effects are developed as a series in  $1/\sigma_0$ , and the series is truncated after only one step of recursion in Eq. 134. This means that the overlap correction should be most accurate for large  $\sigma_0$  and gradually get worse as  $\sigma_0$  decreases. Experience shows that the correction can actually get large enough to produce negative cross sections for small  $\sigma_0$ . (This problem can also show up as a failure in interpolation when a log scheme has been selected.) For isotopes that have relatively narrow resonances spaced relatively widely, such as  $^{238}\text{U}$ , UNRESR gives reasonable results to  $\sigma_0$  values as low as 0.1. For materials with stronger overlap, such as  $^{235}\text{U}$ , a lower limit around 100 is more reasonable. A few of the heavy actinide evaluations have been seen to break down for  $\sigma_0$  values lower than 1000. This problem is not too serious in practice. The fertile materials, which appear in large concentrations in reactors, allow the necessary small values of  $\sigma_0$ . The fissile materials have to be more dilute, and the larger  $\sigma_0$  limit needed for them is not usually a problem.

The UXSR approximation discussed above allows one to reach somewhat smaller  $\sigma_0$  values.

**Interpolating on  $\sigma_0$ .** It turns out that these functions are difficult to interpolate because they have a limited radius of convergence. Although approximate schemes have been developed based on using functions of similar shape such as the tanh function[39], better results can be obtained by using different interpolation schemes for the low- and high- $\sigma_0$  ranges. The TRANSX-CTR code[11] used interpolation in  $1/\sigma_0$  for high  $\sigma_0$ , Lagrangian interpolation of  $\ln\sigma_x$  vs  $\ln\sigma_0$ , for intermediate values, and a  $\sigma_0^2$  extrapolation for very low  $\sigma_0$ . Unfortunately, schemes like this sometimes give ridiculous interpolation excursions when the polynomials are not suitable. Therefore, TRANSX-2[40] has had to revert to using simple linear interpolation, which is always bounded and predictable, but which requires relatively fine  $\sigma_0$  grids.

**Communicating Results to Other Modules.** NJOY tries to use ENDF-like files for all communications between the different calculational modules. Because the unresolved effective cross sections were originally derived from the resonance parameters in File 2, it seemed reasonable to create a new section in File 2 to carry the unresolved cross sections onto other modules, and a special MT number of 152 was selected for this purpose. RECONR creates an MT152 that contains only the infinitely-dilute unresolved cross sections. UNRESR overwrites it with self-shielded unresolved cross sections. GROUPT can then use these cross sections in its calculation of the multigroup constants. The format used for MT152 is given below using the conventional ENDF style.

```
[MAT,2,152/ ZA, AWR, LSSF, 0, 0, INTUNR ] HEAD
[MAT,2,152/ TEMZ, 0, NREAC, NSIGZ, NW, NUNR/
  SIGZ(1), SIGZ(2),...,SIGZ(NSIGZ),
  EUNR(1),
  SIGU(1,1,1), SIGU(1,2,1),...,SIGU(1,NSIGZ,1),
  SIGU(2,1,1),...
  ...
  SIGU(NREAC,1,1),...,SIGU(NREAC,NSIGZ,1),
  EUNR(2),...
  <continue for energies through EUNR(NUNR)>
  ...SIGU(NREAC,NSIGZ,NUNR) ] LIST
```

where NREAC is always 5 (for the total, elastic, fission, capture, and current-weighted total reactions, in that order), NSIGZ is the number of  $\sigma_0$  values, NUNR is the number of unresolved energy grid points, and NW is given by



```
NW=NSIGZ+NUNR*(1+5*NSIGZ)
```

### 5.3 User Input

The following summary of the user input instructions was copied from the comment cards at the beginning of the UNRESR module in the NJOY2012 source file.

```
!---input specifications (free format)-----
!
! card 1
!   nendf   unit for endf tape
!   nin     unit for input pendf tape
!   nout    unit for output pendf tape
! card 2
!   matd    material to be processed
!   ntemp   no. of temperatures (default=1)
!   nsigz   no. of sigma zeroes (default=1)
!   iprint  print option (0=min, 1=max) (default=0)
! card 3
!   temp    temperatures in Kelvin (including zero)
! card 4
!   sigz    sigma zero values (including infinity)
!           cards 2, 3, 4 must be input for each material desired
!           matd=0/ terminates execution of unresr.
!
!-----
```

Card 1, as usual, specifies the input and output units for the module. The input PENDF file on **nin** must have been processed through [RECONR](#) and [BROADR](#). It will contain default versions of the special unresolved section with MF=2 and MT=152 that gives the infinitely-dilute unresolved cross sections for each temperature. The output PENDF file **nout** will contain revised sections MF2, MT152 that give effective cross sections *vs*  $\sigma_0$  for all temperatures.

Card 2 is used to specify the material desired (**matd**), the number of temperatures and background cross sections desired (**ntemp** and **nsigz**), and the print

option (iprint). The actual temperature and  $\sigma_0$  values are given on Cards 3 and 4. Temperatures should be chosen to be adequate for the planned applications. The temperature dependence of the effective cross sections is usually monotonic and fairly smooth. Polynomial interpolation schemes using  $T$  are often used, and roughly uniform spacing for the temperature grid (or spacing that increases modestly as  $T$  increases) is usually suitable.

The choice of a grid for  $\sigma_0$  is more difficult. The curves of cross section versus  $\sigma_0$  have an inflection point, and it is important to choose the grid to represent the inflection point fairly well. A log spacing for  $\sigma_0$  is recommended. Very small values of  $\sigma_0$  should not be used. These considerations are discussed in more detail in the “Implementation” section (5.2) above. Unfortunately, the best choice for a grid can only be found by trial and error.

## 5.4 Output Example

The following portion of UNRESR output is for  $^{238}\text{U}$  from ENDF/B-VII.0.

```

unresr...calculation of unresolved resonance cross sections          494.4s

                                storage   8/   20000

unit for input endf/b tape ..... -21
unit for input pendf tape ..... -23
unit for output pendf tape ..... -24

temperatures ..... 2.936E+02
                   4.000E+02
                   ...
sigma zero values ..... 1.000E+10
                       1.000E+03
                       1.000E+02
                       5.000E+01
                       2.000E+01
                       1.000E+01
                       5.000E+00
                       2.000E+00
                       1.000E+00
                       5.000E-01

print option (0 min., 1 max.) ..... 1

```

|                                       |                  |     |           |           |           |           |
|---------------------------------------|------------------|-----|-----------|-----------|-----------|-----------|
| mat = 9237                            | temp = 2.936E+02 |     |           |           |           | 494.4s    |
| energy = 2.0000E+04                   |                  |     |           |           |           |           |
| 1.433E+01                             | 1.428E+01        | ... | 1.311E+01 | 1.297E+01 | 1.291E+01 | 1.288E+01 |
| 1.380E+01                             | 1.375E+01        | ... | 1.264E+01 | 1.252E+01 | 1.247E+01 | 1.244E+01 |
| 0.000E+00                             | 0.000E+00        | ... | 0.000E+00 | 0.000E+00 | 0.000E+00 | 0.000E+00 |
| 5.294E-01                             | 5.280E-01        | ... | 4.654E-01 | 4.540E-01 | 4.491E-01 | 4.464E-01 |
| 1.433E+01                             | 1.424E+01        | ... | 1.246E+01 | 1.230E+01 | 1.223E+01 | 1.220E+01 |
| energy = 2.3000E+04                   |                  |     |           |           |           |           |
| 1.414E+01                             | 1.411E+01        | ... | 1.307E+01 | 1.293E+01 | 1.288E+01 | 1.285E+01 |
| 1.364E+01                             | 1.361E+01        | ... | 1.262E+01 | 1.250E+01 | 1.245E+01 | 1.242E+01 |
| 0.000E+00                             | 0.000E+00        | ... | 0.000E+00 | 0.000E+00 | 0.000E+00 | 0.000E+00 |
| 4.962E-01                             | 4.951E-01        | ... | 4.426E-01 | 4.325E-01 | 4.281E-01 | 4.257E-01 |
| 1.414E+01                             | 1.407E+01        | ... | 1.246E+01 | 1.229E+01 | 1.223E+01 | 1.219E+01 |
| ...                                   |                  |     |           |           |           |           |
| energy = 1.4903E+05                   |                  |     |           |           |           |           |
| 1.140E+01                             | 1.140E+01        | ... | 1.124E+01 | 1.118E+01 | 1.115E+01 | 1.113E+01 |
| 1.126E+01                             | 1.126E+01        | ... | 1.110E+01 | 1.104E+01 | 1.101E+01 | 1.099E+01 |
| 0.000E+00                             | 0.000E+00        | ... | 0.000E+00 | 0.000E+00 | 0.000E+00 | 0.000E+00 |
| 1.427E-01                             | 1.427E-01        | ... | 1.406E-01 | 1.386E-01 | 1.374E-01 | 1.367E-01 |
| 1.213E+01                             | 1.212E+01        | ... | 1.174E+01 | 1.156E+01 | 1.147E+01 | 1.141E+01 |
| generated cross sections at 18 points |                  |     |           |           |           | 494.9s    |

The display of the cross section table for each energy has  $\sigma_0$  reading across (in decreasing order) and reaction type reading down (in the order of total, elastic, fission, capture, and current-weighted total). Four  $\sigma_0$  values were removed from the table to make it narrower for this report.

## 5.5 Coding Details

The main entry point for UNRESR is subroutine **unresr**, which is exported by module **unresm**. The subroutine starts by reading in the user's input and output unit numbers and opening the files that will be needed during the UNRESR run. After printing the introductory timer line, storage is allocated for an array **scr**, which will be used for reading in ENDF records. The default size of this array is **maxscr**=1000, which has proved sufficient for all evaluations tried so far. UNRESR now prints out the user's unit numbers on the output listing and calls **uwtab** to prepare internal tables used by **uw** to compute the real and imaginary parts of the complex probability integral.

The next step is to read in the `tapeid` records of the ENDF and PENDF tapes. The loop over materials starts at statement number 110 by reading in the user's values for the ENDF MAT number, number of temperatures `ntemp`, number of  $\sigma_0$  values `nsigz`, and print flag `iprint`. If this is not the end of the material loop (`mat=0`), the actual values of the temperatures and background cross sections are read into the arrays `temp` and `sigz`. The input quantities are echoed to the output listing to help detect input errors.

The code then begins a loop over the requested temperatures. It writes the current values of material ID, temperature, and time on the output listing. It then reads the resonance parameters from the section with MT=151 in File 2 of the ENDF tape using `rdunf2`. The arrays `eunr` with length `maxeunr=150` and `array` with length `maxarray=10000` are used to store these data. Next, it reads the background cross sections from File 3 for each of the resonance reactions using `rdunf3`. Here, `sb` is used to store the data. The array `b` is allocated with length `nb=5000` to build an output record to be written in MT=152 on the new PENDF file.

The next loop is over all the energy grid points at this temperature. The grid points were determined in `rdunf2`, and the `nunr` points are stored in the array `eunr`. The background cross sections are stored in an array `sb(ie,ix)`. The energy index takes on `nunr` values, and the reaction index `ix` takes on four values. The calculation of the actual effective cross sections takes place in `unres1`. The results for each energy appear in the array `sigu(ix,is)`, where `is` takes on `nsigz` values. Each `unres1` array is stored into the accumulating output array `b` and printed on the output listing.

At this point, UNRESR checks to see if there is a previous version of MT152 on the PENDF tape. If so, these new data will replace it. If not, a new section with MT=152 will be created. In either case, a new section MT451 in File 1 is generated containing the current temperature and the correct entry in the directory for the PENDF tape. Finally, the new MT152 for this temperature is copied onto the output file from the `b` array, and the rest of the contents of this temperature on the old PENDF file are copied to the new PENDF file. After writing a report on the number of resonance points generated and the amount of computer time used, UNRESR branches back to continue the temperature loop. When the last temperature has been processed, the code closes the files, writes a final report on the output listing, and terminates.

Note that UNRESR takes special branches for materials with no resonance parameters or materials with no unresolved parameters. Therefore, the user can

freely request an UNRESR run even when there are no unresolved resonance data present on the ENDF tape. UNRESR simply copies **nin** to **nout** in this case.

The subroutine **rdunf2** is used to read in the unresolved resonance parameters from File 2 of the input ENDF tape. It is very similar to the corresponding coding in **RECONR**. The array **scr** is used to read in the ENDF record, the resonance parameter data are stored in the array **arry**, and the final grid of energy values is stored in **eunr**. Note that **rdunf2** will add extra energy nodes for evaluations with energy-independent parameters or for energy-dependent evaluations that have energy steps larger than the factor **wide**, which is currently set to 1.26. The subroutine also discovers resolved-unresolved or unresolved-smooth overlap, flags those energy values, and prints messages to the user on the output listing.

Subroutine **ilist** is used to insert a new energy into a list of energies in ascending order. It is used to manage the accumulation of the grid of energy nodes.

Subroutine **rdunf3** is used to read in the background cross sections in the unresolved range from File 3. The unresolved energy grid determined by **rdunf2** is used for the background cross sections.

The main calculation of the effective cross sections for the unresolved range is performed in subroutine **unres1**. The calculation is done in two passes: first, the potential scattering cross section is computed; second, the unresolved cross sections are computed. The passes are controlled by the parameter **ispot**. In both cases, resonance parameter data stored in **arry** by **rdunf2** are used. The coding is similar to that used in **RECONR** down to the point where the ETOX statistical averages are computed. The three loops over **kf**, **kn**, and **kl** carry out the n-fold quadrature represented as integrals over  $\alpha$  in the text. They account for variations in the fission width, neutron width, and competitive width. The capture width is assumed to be constant. Note that **ajku** is called in the innermost loop to compute the  $J$  and  $K$  integrals in **xj** and **xk**, respectively. The  $K$  integral returned by this routine is actually  $J + K$  in our notation. The final quantities are computed in the loops over **itp** and **is0**. Note that **tk** is equivalent to  $B_{ts} + D_{ts}$  in our notation. Similarly, **t1** is equivalent to  $B_{xs}$ , and **tj** is equivalent to  $B_{ts}$ . The last step in this subroutine is to compute the average cross sections by summing over spin sequences. The loop over **ks** computes **xj** as  $\sum_s B_{ts}$  and **xk** as  $\sum_s C_{ts}$ . With these quantities available, it is easy to finish the calculation of the effective cross sections as given by Eq. 138 and Eq. 140.

The subroutines `unfac`, `intrf`, and `intr` are similar to corresponding routines from `RECONR` and don't require further discussion here. Subroutine `ajku` is used to compute the  $J$  and  $K$  integrals without interference corrections. The subroutines `quikw`, `uwtab`, and `uw` implement a package for computing the complex probability integral efficiently. It was originally developed at ANL for the MC2 code. When it is used, a pair of  $62 \times 62$  tables for the real and imaginary parts of the complex probability integral are precomputed using `uwtab` and `uw`. Values of  $W$  for small arguments are obtained by interpolating in these pre-computed tables. Values of  $W$  for larger arguments are obtained using various asymptotic formulas.

## 5.6 Error Messages

**error in unresr\*\*\*mode conversion between nin and nout**

Input and output files must both be in ASCII mode (positive unit numbers), or they must both be in binary mode (negative unit numbers).

**error in unresr\*\*\*storage exceeded**

There is not enough room in the `b` array. Increase `nb`, which currently is 5000.

**error in rdunf2\*\*\*storage exceeded**

There is not enough room in `array`. Increase the value of `maxarray`, which currently is 10000.

**error in unresl\*\*\*storage exceeded**

The code is currently limited to 50 spin sequences. For more spin sequences, it will be necessary to increase the dimensions of several arrays in this subroutine.

## 6 HEATR

The HEATR module generates pointwise heat production cross sections and radiation damage energy production for specified reactions and adds them to an existing PENDF file. The heating and damage numbers can then be easily group averaged, plotted, or reformatted for other purposes. An option of use to evaluators checks ENDF/B files for neutron/photon energy-balance consistency. The advantages of HEATR include

- Heating and damage are computed in a consistent way.
- All ENDF/B neutron and photon data are used.
- ENDF/B-6 charged-particle distributions are used when available.
- Kinematic checks are available to improve future evaluations.
- Both energy-balance and kinematic KERMA factors can be produced.

This chapter describes HEATR in NJOY 2012.0. Changes since the version reported previously[3] include

- a provision for entering a value for the damage displacement energy or taking an appropriate default,
- the introduction of the “photon momentum recoil” calculation and the “one-particle recoil approximation” for incomplete sections of File 6,
- preparing [VIEWR](#) input for plots of the heating and photon production compared to their kinematic limits, and
- conversion to Fortran-90 style.

### 6.1 Theory of Nuclear Heating

Heating is an important parameter of any nuclear system. It may represent the product being sold – as in a power reactor – or it may affect the design of peripheral systems such as shields and structural components.

Nuclear heating can be conveniently divided into neutron heating and photon heating (see Fig. 8). Neutron heating at a given location is proportional to the local neutron flux and arises from the kinetic energy of the charged products of a neutron induced reaction (including both charged secondary particles and the recoil nucleus itself). Similarly, photon heating is proportional to the flux of secondary photons transported from the site of previous neutron reactions. It is also traceable to the kinetic energy of charged particles (for example, electron-positron pairs and recoil induced by photoelectric capture).

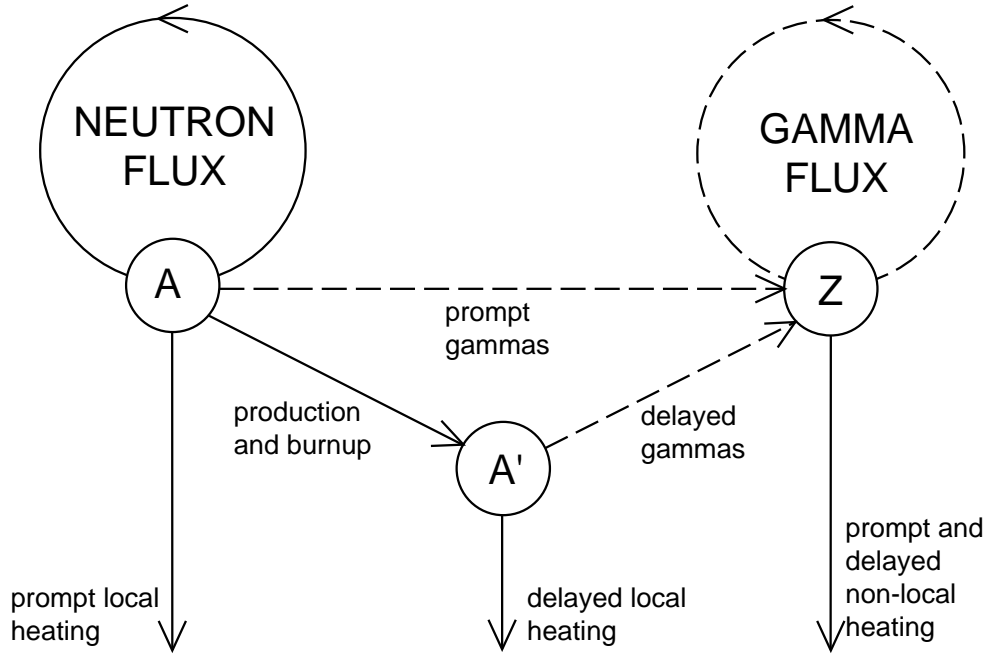


Figure 8: Components of nuclear heating. HEATR treats the prompt local neutron heating only. Gamma heating is computed in [GAMINR](#). Delayed local heating and photon production are not treated by NJOY, and they must be added at a later stage.

Heating, therefore, is often described by KERMA[29] (Kinetic Energy Release in Materials) coefficients  $k_{ij}(E)$  defined such that the heating rate in a mixture is given by

$$H(E) = \sum_i \sum_j \rho_i k_{ij}(E) \phi(E) , \quad (160)$$

where  $\rho_i$  is the number density of material  $i$ ,  $k_{ij}(E)$  is the KERMA coefficient for material  $i$  and reaction  $j$  at incident energy  $E$ , and  $\phi(E)$  is the neutron or photon scalar flux at  $E$ . KERMA is used just like a microscopic reaction cross section except that its units are energy  $\times$  cross section (eV-barns for HEATR). When multiplied by a flux and number density, the result would give heating in eV/s.

The “direct method” for computing the KERMA coefficient is

$$k_{ij}(E) = \sum_{\ell} \bar{E}_{ij\ell}(E) \sigma_{ij}(E) , \quad (161)$$

where the sum is carried out over all charged products of the reaction including the recoil nucleus, and  $\bar{E}_{ij\ell}$  is the total kinetic energy carried away by the  $\ell^{th}$



species of secondary particle. These kinds of data are now becoming available for some materials with the advent of ENDF/B-VI and ENDF/B-VII, but earlier ENDF/B versions did not include the detailed spectral information needed to evaluate Eq. 161.

For this reason, NJOY computes KERMA factors for many materials by the “energy-balance method” [41]. The energy allocated to neutrons and photons is simply subtracted from the available energy to obtain the energy carried away by charged particles:

$$k_{ij}(E) = \left( E + Q_{ij} - \bar{E}_{ijn} - \bar{E}_{ij\gamma} \right) \sigma_{ij}(E) , \quad (162)$$

where  $Q_{ij}$  is the mass-difference Q value for material  $i$  and reaction  $j$ ,  $\bar{E}_n$  is the total energy of secondary neutrons including multiplicity, and  $\bar{E}_\gamma$  is the energy of secondary photons including photon yields.

This method was well suited for use with ENDF/B-V, or any other evaluation containing neutron and photon spectral data, but not the particle spectra required by the direct method. The disadvantage of this method is that the KERMA factor sometimes depends on a difference between large numbers. In order to obtain accurate results, care must be taken by the evaluator to ensure that photon and neutron yields and average energies are consistent. In fact, the lack of consistency in ENDF/B-V often revealed itself as negative KERMA coefficients [42].

However, a negative KERMA coefficient is not always the defect it seems to be. It must be remembered that heating has both neutron and photon components. A negative KERMA might indicate that too much energy has been included with the photon production in the evaluation. This will result in excessive photon heating if most of the photons stay in the system. However, the negative KERMA will have just the right magnitude to cancel this excess heating. The energy-balance method guarantees conservation of total energy in large homogeneous systems.

In this context, large and homogeneous means that most neutrons and photons stay in their source regions. It is clear that energy-balance errors in the evaluation affect the spatial distribution of heat and not the total system heating when the energy-balance method is employed.

A final problem with the energy-balance method occurs for the elemental evaluations common in earlier versions of ENDF/B. Isotopic Q values and cross sections are not available in the files. It will usually be possible to define ad-

equate cross sections, yields, and spectra for the element. However, it is clear that the available energy should be computed with an effective  $Q$  given by

$$\bar{Q} = \frac{\sum_i \rho_i \sigma_i Q_i}{\sum_i \rho_i \sigma_i}, \quad (163)$$

where  $\rho_i$  is the atomic fraction of isotope  $i$  in the element. This number is energy dependent and can be represented only approximately by the single constant  $Q$  allowed in ENDF/B. HEATR allows the user to input an auxiliary energy-dependent  $Q$  for elements.

For elastic and discrete-level inelastic scattering, the neutron KERMA coefficient can be evaluated directly without reference to photon data. For other reactions, conservation of momentum and energy can be used to estimate the KERMA or to compute minimum and maximum limits for the heating. HEATR includes an option that tests the energy-balance KERMA factors against these kinematic limits, thereby providing a valuable test of the neutron-photon consistency of the evaluation. If the energy-balance heating numbers for a particular isotope should fail these tests, and if the isotope is important for a “small” system, an improved evaluation is probably required. The alternative of making *ad hoc* fixes to improve the local heat production is dangerous because the faults in the neutron and/or photon data revealed by the tests may lead to significant errors in neutron transport and/or photon dose and nonlocal energy deposition.

In practice, an exception to this conclusion must be made for the radiative capture reaction  $(n,\gamma)$ . The difference between the available energy  $E+Q$  and the total energy of the emitted photons is such a small fraction of  $E+Q$  that it is difficult to hold enough precision to get reasonable recoil energies. Moreover, the emitted photons cause a component of recoil whose effect is not normally included in evaluated capture spectra. Finally, the “element problem” cited above is especially troublesome for capture because the available energy may change by several MeV between energies dominated by resonances in different isotopes of the element, giving rise to many negative or absurdly large heating numbers. These problems are more important for damage calculations (see below) where the entire effect comes from recoil and the compensation provided by later deposition of the photon energy is absent.

For these reasons, HEATR estimates the recoil due to radiative capture using conservation of momentum. The recoil is the vector sum of the “kick” caused by the incident neutron and the kicks due to the emission of all subsequent

photons. Assuming that all photon emission is isotropic and that the directions of photon emission are uncorrelated, the photon component of recoil depends on the average of  $E_\gamma^2$  over the entire photon spectrum

$$E_R = \frac{E}{A+1} + \frac{\overline{E_\gamma^2}}{2(A+1)mc^2} , \quad (164)$$

where  $mc^2$  is the neutron mass energy. The second term is important below 25 – 100 keV. This formula gives an estimate that works for both isotopes and elements and has no precision problems. However, it does not explicitly conserve energy, and isotopes with bad capture photon data can still cause problems.

## 6.2 Theory of Damage Energy

Damage to materials caused by neutron irradiation is an important design consideration in fission reactors and is expected to be an even more important problem in fusion power systems. There are many radiation effects that may cause damage, for example, direct heating, gas production (*e.g.*, helium embrittlement), and the production of lattice defects.

A large cluster of lattice defects can be produced by the primary recoil nucleus of a nuclear reaction as it slows down in a lattice. It has been shown that there is an empirical correlation between the number of displaced atoms (DPA, displacements per atom) and various properties of metals, such as elasticity. The number of displaced atoms depends on the total available energy  $E_a$  and the energy required to displace an atom from its lattice position  $E_d$ . Since the available energy is used up by producing pairs,

$$\text{DPA} = \frac{E_a}{2E_d} . \quad (165)$$

The values of  $E_d$  used in practice are chosen to represent the empirical correlations, and a wide range of values is found in the literature[43, 44, 45]. Table 2 gives the default values used in NJOY2012. The energy available to cause displacements is what HEATR calculates. It depend on the recoil spectrum and the partition of recoil energy between electronic excitations and atomic motion. The partition function used is given by Robinson[46] based on the electronic screening theory of Lindhard[47] (see Fig. 9).

The damage output from HEATR is the damage energy production cross section (eV-barns). As in Eq. 160, multiplying by the density and flux gives

Table 2: Typical Values for the Atomic Displacement Energy Needed to Compute DPA[45].

| Element | $E_d$ , eV | Element | $E_d$ , eV |
|---------|------------|---------|------------|
| Be      | 31         | Co      | 40         |
| C       | 31         | Ni      | 40         |
| Mg      | 25         | Cu      | 40         |
| Al      | 27         | Zr      | 40         |
| Si      | 25         | Nb      | 40         |
| Ca      | 40         | Mo      | 60         |
| Ti      | 40         | Ag      | 60         |
| V       | 40         | Ta      | 90         |
| Cr      | 40         | W       | 90         |
| Mn      | 40         | Au      | 30         |
| Fe      | 40         | Pb      | 25         |

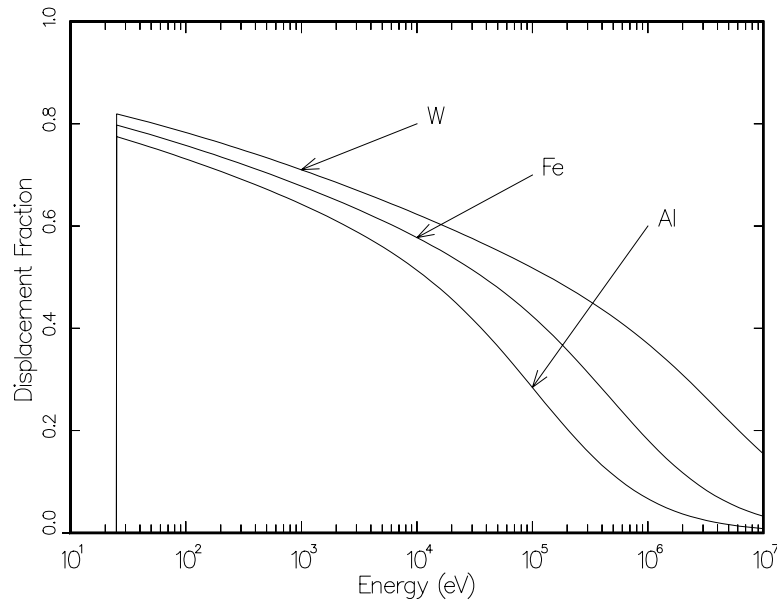


Figure 9: Examples of the portion of the primary recoil energy that is available to cause lattice displacements in metallic lattices. The remaining energy leads to electronic excitation. The quantity plotted is  $P(E)$  from Eq. 195 divided by  $E$ . The 25 eV cutoff is also discussed in connection with Eq. 195.

eV/s. Dividing by  $2E_d$  gives displacements/s. This result is often reduced by an efficiency factor (say 80%) to improve the fit to the empirical correlations.

### 6.3 Computation of KERMA Factors By Energy Balance

The older ENDF/B files do not usually give photon production data for all partial reactions. Summation reactions such as nonelastic (MT=3) and inelastic (MT=4) are often used. It is still possible to compute partial KERMA factors for those summation reactions by reordering Eq. 162 as follows:

$$k_{ij} = \sum_{j \in J} k_{ij}^n(E) - \sum_{\ell \in J} \bar{E}_{i\ell\gamma} \sigma_{i\ell}(E) , \quad (166)$$

where  $j$  runs over all neutron partials contained in  $J$ , and  $\ell$  runs over all photon partials in  $J$ . The total KERMA is well defined, but partial KERMA factors should be used only with caution.

HEATR loops through all the neutron reactions on the ENDF/B tape. If energy balance is to be used, it computes the neutron contributions needed for the first term. These are

$$k_{ij}^n(E) = \left[ E + Q_{ij} - \bar{E}_{ijn}(E) \right] \sigma_{ij}(E) . \quad (167)$$

The  $Q$  value is zero for elastic and inelastic scattering. For (n,n') particle reactions represented by scattering with an LR flag set,  $Q$  is the ENDF "C1" field from MF=3. For most other reactions,  $Q$  is the "C2" field from MF=3. HEATR allows users to override any  $Q$  value with their own numbers.

There are some special problems with obtaining the  $Q$  value for fission. First, the fission  $Q$  value given in the C1 field of MF=3 includes delayed contributions, and second, the  $Q$  value for fission is energy dependent. The energy dependence can be seen by writing the mass balance equation for the reaction. In energy units,

$$Q = m_A + m_n - m_{fp} - \bar{\nu} m_n , \quad (168)$$

where  $m_A$  is the mass energy of the target,  $m_n$  is the mass energy of the neutron,  $m_{fp}$  is the total mass energy of the fission products, and  $\bar{\nu}$  is the fission neutron yield. Both  $m_{fp}$  and  $\bar{\nu}$  are energy dependent. It is also necessary to account for the energy dependence of neutrino emission. Values for some of these terms and estimates for the energy dependence are given in MF=1/MT=458 and the discussion of that section in the ENDF format manual, ENDF-102[8]. We have

chosen to ignore the energy dependence of delayed beta and gamma emission because we don't yet treat it in subsequent codes. Therefore, the following corrections are made to get an effective  $Q$  for fission in HEATR:

$$Q' = Q - 8.07E6(\bar{\nu}(E) - \bar{\nu}(0)) + .307E - E_{\beta D} - E_{\gamma D} , \quad (169)$$

where  $E_{\beta D}$  and  $E_{\gamma D}$  are the delayed beta and gamma energies from MT=458. The term  $.307E$  is an estimate of the energy dependence of the terms  $m_{fp}$  and  $m_n$ .

The  $\bar{E}_n$  value as used in Eq. 167 is defined to include multiplicity. The multiplicity is either implicit — for example, 2 for (n,2n) — or is retrieved from the ENDF/B file (fission  $\bar{\nu}$ ). The average energy per neutron is computed differently for discrete two-body reactions and continuum reactions.

For elastic and discrete inelastic scattering (MT=2, 51-90),

$$\bar{E}_n = \frac{E}{(A+1)^2} (1 + 2Rf_1 + R^2) , \quad (170)$$

where  $f_1$  is the center-of-mass (CM) average scattering cosine from MF=4 and  $R$  is the effective mass ratio. For elastic scattering,  $R=A$ , but for threshold scattering,

$$R = A \sqrt{1 - \frac{(A+1)S}{AE}} , \quad (171)$$

where  $S$  is the negative of the C2 field from MF=3.

For continuum scattering, the average energy per neutron is computed from the secondary neutron spectrum,  $g$ , in MF=5 using

$$\bar{E}_n(E) = \int_0^U E' g(E, E') dE' , \quad (172)$$

where  $U$  is defined in MF=5. If  $g$  is tabulated (LAW=1 or LAW=5), the integral is carried out analytically for each panel by making use of the ENDF/B interpolation laws. For the simple analytic representations (LAW=7, 9, or 11), the average energies are known[8].

The neutron cross sections required by Eq. 167 are obtained from an existing PENDF file (see RECONR, and BROADR).

When the neutron sum in Eq. 166 is complete, the code processes the photon production files. If the evaluation does not include photon data, HEATR returns only the first sum. This is equivalent to assuming that all photon energy is deposited locally, consistent with the fact that there will be no contribution to

the photon transport source from this material. The same result can be forced by using the `local` parameter (see “User Input”, Section 6.7, below).

Discrete photon yields and energies are obtained from MF=12 or 13. Continuum photon data are obtained from MF=15, and the average photon energy and  $\overline{E_\gamma^2}$  are computed. For radiative capture, the photon term becomes

$$E_\gamma \sigma_\gamma = \left( E + Q - \frac{E}{A+1} + \frac{\overline{E_\gamma^2}}{2(A+1)mc^2} Y_\gamma \right) \sigma_\gamma , \quad (173)$$

[8] where  $Y_\gamma$  is the capture photon yield from MF=12. This corrects the capture contribution from Eq. 167 by conservation of momentum. For other reactions, Eq. 167 is sufficient, and the product of  $\overline{E_\gamma}$ ,  $Y_\gamma$ , and  $\sigma_\gamma$  is subtracted from the neutron contribution.

#### 6.4 Kinematic Limits

As an option provided mainly as an aid to evaluators, HEATR will compute the kinematic maximum and minimum KERMA coefficients and compare them with the energy-balance results. The formulas are as follows. For elastic scattering (MT=2), the expected recoil energy is

$$\overline{E_R} = \frac{2AE}{(A+1)^2} (1 - f_1) . \quad (174)$$

For discrete-inelastic scattering (MT=51-90), the photon momentum is neglected to obtain

$$\overline{E_R} = \frac{2AE}{(A+1)^2} \left[ 1 - f_1 \sqrt{1 - \frac{(A+1)E_\gamma}{AE}} \right] - \frac{E_\gamma}{A+1} , \quad (175)$$

where  $E_\gamma = -C2$  from MF=3. For continuum inelastic scattering (MT=91), secondary neutrons are assumed to be isotropic in the laboratory system (LAB) giving

$$\overline{E_R} = \frac{E - E_n}{A} , \quad (176)$$

and

$$\overline{E_\gamma} = \frac{(A-1)E - (A+1)\overline{E_n}}{A} , \quad (177)$$

where  $\overline{E}_\gamma$  is the average photon energy expected for this representation. For radiative capture (MT=102),

$$\overline{E}_R = \frac{E}{A+1} + E_K \quad (178)$$

and

$$\overline{E}_\gamma = Q + \frac{AE}{A+1} - E_K, \quad (179)$$

where

$$E_K = \frac{1}{2M_R c^2} \left[ \frac{AE}{A+1} + Q \right]^2 \left\{ 1 - \frac{1}{M_R c^2} \left[ \frac{AE}{A+1} + Q \right] \right\}, \quad (180)$$

with

$$M_R c^2 = (939.565 \times 10^6)(A+1) - Q \quad (181)$$

being the mass energy in eV. The value of this constant is actually computed from fundamental constants in NJOY2012.

For two-body scattering followed by particle emission (MT=51-91, LR flag set), a minimum and maximum can be defined:

$$(E'_R + E_x)_{\min} = \overline{E}_R, \text{ and} \quad (182)$$

$$(E'_R + E_x)_{\max} = \overline{E}_R + Q + (E_\gamma)_{\max}, \quad (183)$$

where  $\overline{E}_R$  is the value from Eq. 175 or (176),  $Q$  is the C2 field from File 3, and  $(E_\gamma)_{\max}$  is the negative of the C2 field from File 3. In these equations,  $E'_R$  is the recoil energy and  $E_x$  is the energy of the charged product. For absorption followed by particle emission (MT=103-120),

$$(E_R + E_x)_{\min} = \frac{E}{A+1-x}, \quad (184)$$

$$(E_\gamma)_{\max} = Q + \frac{A-x}{A+1-x} E, \text{ and} \quad (185)$$

$$(E_R + E_x)_{\max} = E + Q, \quad (186)$$

where  $Q$  is the C2 field from MF=3 and  $x$  is the particle mass ratio ( $x=1$  gives a minimum for all reactions). For (n,2n) reactions,



$$(E_R)_{\min} = 0 , \text{ and} \quad (187)$$

$$(E_R)_{\max} = \frac{E + \bar{E}_n}{A - 1} , \quad (188)$$

and for (n,3n) reactions,

$$(E_R)_{\min} = 0 , \text{ and} \quad (189)$$

$$(E_R)_{\max} = \frac{E + 2\bar{E}_n}{A - 2} . \quad (190)$$

For both (n,2n) and (n,3n), if  $(E_R)_{\max}$  is greater than  $E_R$ , it is set equal to  $E_R$ . In addition, these formulas are not used for  $A < 10$ ;  $(E_R)_{\max}$  is set to  $E_R$ . For other neutron continuum scattering reactions (MT=22-45),

$$(E_R + E_x)_{\min} = 0 , \text{ and} \quad (191)$$

$$(E_R + E_x)_{\max} = E + Q - \bar{E}_n , \quad (192)$$

where  $Q$  is the C2 field from File 3. Finally, for fission (MT=18-21, 38), the limits are

$$(E_R)_{\min} = E + Q - \frac{1}{2}\bar{E}_n - 15 \times 10^6 \text{ eV} , \text{ and} \quad (193)$$

$$(E_R)_{\max} = E + Q - \bar{E}_n , \quad (194)$$

where  $Q$  is the prompt fission  $Q$ -value less neutrinos. It is determined by taking the total (less neutrinos) value from File 3 and subtracting the delayed energy obtained from  $MF=1/MT=458$ .

These values are intended to be very conservative. Note that  $E_K$  is only significant at very low neutron energy. In order to reduce unimportant error messages, a tolerance band is applied to the above limits. If all checks are satisfied, the resulting KERMA coefficients should give good local heating results even when 99.8% of the photons escape the local region. More information on using the kinematic checks to diagnose energy-balance problems in evaluations will be found in “Diagnosing Energy-Balance Problems”, Section 6.9.

The upper kinematic limit can also be written out to the output tape as MT=443 if desired. It is similar to the KERMA factors generated by the MACK code[29], and it is sometimes preferable to the energy-balance KERMA for calculating local heating for evaluations with severe energy-balance problems. The kinematic value in MT=443 is useful for plots (see the examples in this report).

## 6.5 Computation of Damage Energy

The formulas used for calculating damage energy are derived from the same sources as the heating formulas given above, except in this case, the effects of scattering angle do not result in simple factors like  $f_1$  because the Robinson partition function is not linear. Instead, it is calculated as follows:

$$P(E) = \frac{E_R}{1 + F_L(3.4008\epsilon^{1/6} + 0.40244\epsilon^{3/4} + \epsilon)} , \quad (195)$$

if  $E_R \geq 25.0$  eV, and zero otherwise. In Eq. 195,  $E_R$  is the primary recoil energy,

$$\epsilon = \frac{E_R}{E_L} , \quad (196)$$

$$E_L = 30.724 Z_R Z_L \left( Z_R^{2/3} + Z_L^{2/3} \right)^{1/2} (A_R + A_L) / A_L , \text{ and} \quad (197)$$

$$F_L = \frac{0.0793 Z_R^{2/3} Z_L^{1/2} (A_R + A_L)^{3/2}}{\left( Z_R^{2/3} + Z_L^{2/3} \right)^{3/4} A_R^{3/2} A_L^{1/2}} , \quad (198)$$

and  $Z_i$  and  $A_i$  refer to the charge and atomic number of the lattice nuclei (L) and the recoil nuclei (R). The function behaves like  $E_R$  at low recoil energies and then levels out at higher energies. Therefore, the damage-energy production cross section is always less than the heat production cross section. See Fig. 9 for examples.

For elastic and two-body discrete-level inelastic scattering,

$$E_R(E, \mu) = \frac{AE}{(A+1)^2} \left( 1 - 2R\mu + R^2 \right) , \quad (199)$$

where the “effective mass” is given by

$$R = \sqrt{1 - \frac{(A+1)(-Q)}{AE}} , \quad (200)$$

and  $\mu$  is the CM scattering cosine. The damage energy production cross section is then obtained from

$$D(E) = \sigma(E) \int_{-1}^1 f(E, \mu) P(E_R[E, \mu]) d\mu , \quad (201)$$

where  $f$  is the angular distribution from the ENDF/B File 4. This integration is performed with a 20-point Gauss-Legendre quadrature. Discrete-level reactions with LR flags to indicate, for example,  $(n, n')\alpha$  reactions, are treated in the same way at present. The additional emitted particles are ignored.

Continuum reactions like  $(n, n')$  give a recoil spectrum

$$E_R(E, E', \mu) = \frac{1}{A} \left( E - 2\sqrt{EE'}\mu + E' \right) , \quad (202)$$

where  $E'$  is the secondary neutron energy,  $\mu$  is the laboratory cosine, and the photon momentum has been neglected. The damage becomes

$$D(E) = \sigma(E) \int_0^\infty dE' \int_{-1}^1 d\mu f(E, \mu) g(E, E') P(E_R[E, E', \mu]) , \quad (203)$$

where  $g$  is the secondary energy distribution from File 5. In the code, the angular distribution is defaulted to isotropic, and a 4-point Gaussian quadrature is used for the angular integration. For analytic representations of  $g$ , an adaptive integration to 5% accuracy is used for  $E'$ ; for tabulated File 5 data, a trapezoidal integration is performed using the energy grid of the file. The same procedure is used for  $(n, 2n)$ ,  $(n, 3n)$ , etc., but it is not realistic for reactions like  $(n, n')p$  or  $(n, n')\alpha$ . The neutron in these types of reactions can get out of the nucleus quite easily; thus, much of the energy available to secondary particles is typically carried away by the charged particles[48]. HEATR treats these reactions in the same way as  $(n, p)$  or  $(n, \alpha)$ .

The recoil for radiative capture must include the momentum of the emitted photons below 25 – 100 keV giving

$$E_R = \frac{E}{A+1} - 2\sqrt{\frac{E}{A+1}} \sqrt{\frac{E_\gamma^2}{2(A+1)mc^2}} \cos \phi + \frac{\overline{E_\gamma^2}}{2(A+1)mc^2} , \quad (204)$$

where  $\phi$  is the angle between the incident neutron direction and emitted photon direction. If subsequent photons are emitted in a cascade, each one will add an additional term of  $\overline{E_\gamma^2}$  and an additional angle. A complete averaging of

Eq. 204 with respect to  $P(E_R)$  would be very difficult and would require angular correlations not present in ENDF/B evaluations. However, damage calculations are still fairly crude, and an estimate for the damage obtained by treating the neutron “kick” and all the photon kicks independently should give a reasonable upper limit because

$$\int_{-1}^1 D(E_R) d\cos\phi \leq D\left(\frac{E}{A+1}\right) + \sum_{\gamma} D\left(\frac{\overline{E_{\gamma}^2}}{2M_R c^2}\right). \quad (205)$$

The actual formula used in the code is

$$\begin{aligned} D(E) = & D\left(\frac{E}{A+1}\right) + D\left(\frac{1}{2M_R c^2} \left[\frac{AE}{A+1} + Q\right]^2\right) \\ & + \sum_{\gamma} D\left(\frac{\overline{E_{\gamma}^2}}{2M_R c^2}\right) - D\left(\frac{1}{2M_R c^2} \left[\frac{AE}{A+1} + Q\right]^2\right), \end{aligned} \quad (206)$$

where the first line is computed in the neutron section, and the second line is computed in the photon section. This form also provides a reasonable default when no photons are given.

Finally, for the (n,particle) reactions, the primary recoil is given by

$$E_R = \frac{1}{A+1} \left( E^* - 2\sqrt{aE^*E_a} \cos\phi + aE_a \right), \quad (207)$$

where  $a$  is the mass ratio of the emitted particle to the neutron,  $E^*$  is given by

$$E^* = \frac{A+1-a}{A+1} E, \quad (208)$$

and the particle energy  $E_a$  is approximated as being equal to the smaller of the available energy

$$Q + \frac{AE}{A+1}, \quad (209)$$

or the Coulomb barrier energy

$$\frac{1.029 \times 10^6 zZ}{a^{1/3} + A^{1/3}} \text{ in eV}, \quad (210)$$

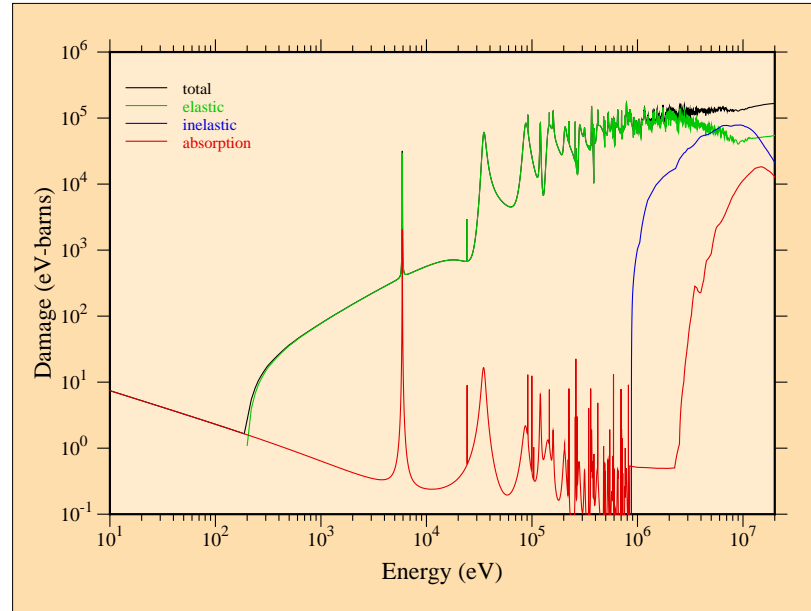


Figure 10: Components of radiation damage energy production for  $^{27}\text{Al}$  from ENDF/B-VII.0. Note that capture dominates at very low energies, then elastic dominates, and finally inelastic begins to contribute at very high energies.

where  $z$  is the charge of the emitted particle and  $Z$  is the charge of the target. A more reasonable distribution would be desirable[48], but this one has the advantage of eliminating an integration, and most results are dominated by the kick imparted by the incident neutron anyway. The angular distribution for the emitted particle is taken as isotropic in the lab. At high incident energies, direct interaction processes would be expected to give rise to a forward-peaked distribution, thereby reducing the damage. However, the importance of this effect is also reduced by the dominance of the neutron kick.

Fig. 10 gives a typical result for a damage energy production calculation, showing the separate contributions of elastic, inelastic, and absorption processes.

## 6.6 Heating and Damage from File 6

A number of the new evaluations in ENDF/B-VI and -VII include complete energy-angle distributions for all of the particles produced by a reaction, including the residual nucleus. In these cases, HEATR can compute the contributions to KERMA by calculating the average energy in the spectrum of each outgoing charged particle or residual nucleus and using Eq. 161.

A fully-populated section of File 6 contains subsections for all of the particles and photons produced by the reaction, including the recoil nucleus. There are a number of different schemes used to represent the energy-angle distributions for these outgoing particles. The most important ones for HEATR follow:

- *No distribution.* In this case, the subsection is inadequate for use in heating and damage calculations. A warning message is issued.
- *Two-body angular distribution.* These are basically the same as distributions in File 4.
- *Recoil distribution.* This particle is a recoil nucleus from a two-body reaction. Its angular distribution is assumed to be the complement of the angular distribution for the first subsection in this section.
- *CM Kalbach distribution.* This format is often used by LANL evaluations, and transformation to the laboratory frame is required. The looping order for the data is  $E, E', \mu$ .
- *LAB Legendre distribution.* This format is used in most of the ORNL evaluations for ENDF/B-VI. It is already in the laboratory frame, and the angular information can be simply ignored.
- *LAB angle-energy distribution.* This format is used for the  $^9\text{Be}$  evaluation of ENDF/B-VI by LLNL. The looping order is  $E, \mu, E'$ .

The normal procedure is to loop through all of these subsections. The subsections producing neutrons are processed to be used in a total energy check, but they contribute nothing to the heating or to the damage. Subsections describing charged particles and residual nuclei are processed into heating and damage contributions. Finally, the photon subsection is processed for the photon energy check and the total energy check, even though it does not affect either heating or damage. Any remaining difference between the eV-barns available for the reaction and the eV-barns carried away by the neutrons, photons, particles, and recoil is added into the heating to help preserve the total energy deposition in the spirit of the energy-balance method.

For “two-body” sections, the emitted particle energy is given by

$$E' = \frac{A'E}{A+1} \left( 1 + 2R\mu + R^2 \right), \quad (211)$$

where

$$R = \sqrt{\frac{A(A+1-A')}{A'}}, \quad (212)$$

and  $A'$  is the ratio of the mass of the outgoing particle to that of the incident particle. The heating is obtained by doing a simple integral over  $\mu$ , and the damage is computed using the integral over  $\mu$  given in Eq. 201. In both cases, the integrals are performed using either a 20-point Gauss-Legendre quadrature (for Legendre representations) or a trapezoidal integration (for tabulated data).

For “recoil” sections, the code backs up to the particle distribution and calculates the recoil using the same method described above with the sign of  $\mu$  changed.

For laboratory distributions that use the  $E, E', \mu$  ordering, the angular part can be ignored, and the heating and damage become

$$K(E) = \int g(E \rightarrow E') E' dE' , \quad (213)$$

and

$$D(E) = \int g(E \rightarrow E') P(E') dE' , \quad (214)$$

where  $g(E \rightarrow E')$  is the angle-integrated energy distribution from File 6, and  $P(E')$  is the damage partition function. Trapezoidal integration is used for the continuum, and the integrand is simply added into the sum for the delta functions (if any).

Heating for subsections that use the ordering  $E, \mu, E'$  is computed using the formula

$$K(E) = \int \left\{ \int g(E \rightarrow E', \mu) E' dE' \right\} d\mu , \quad (215)$$

where an inner integral is performed using trapezoidal integration for each value in the  $\mu$  grid. The results are then used in a second trapezoidal integration over  $\mu$ . The damage integral is performed at the same time in a parallel manner.

The problem is somewhat more difficult for subsections represented in the center-of-mass frame. The definitions for  $K(E)$  and  $D(E)$  are the same as those given above, except that the quantity  $g(E \rightarrow E')$  has to be generated in the lab system. The methods used to do the transformation are basically the same in HEATR and GROUPR. The first step is to set up an adaptive integration over  $E'$ . The first value needed to prime the stack is obtained by calling `h6cm` with  $E'=0$ . It returns the corresponding value of  $g$  in the lab system and a value for `epnext`. The second value for the stack is computed for  $E=\text{epnext}$ . The routine then subdivides this interval until 2% convergence is achieved, accumulating the

contributions to the heating and damage integrals as it goes. It then moves up to a new panel. This process continues until the entire range of  $E'$  has been covered.

The key to this process is `h6cm`. As described in more detail in the [GROUPR](#) chapter of this manual, it performs integrals of the form

$$g_L(E \rightarrow E'_L) = \int_{\mu_{\min}}^{+1} g_C(E \rightarrow E'_C, \mu_C) J d\mu_L, \quad (216)$$

where  $L$  and  $C$  denote the laboratory and center-of-mass systems, respectively, and  $J$  is the Jacobian for the transformation. The contours in the  $E'_C, \mu_C$  frame that are used for these integrals have constant  $E'_L$ . The limiting cosine,  $\mu_{\min}$ , depends on kinematic factors and the maximum possible value for  $E'_C$  in the File 6 tabulation.

The ENDF/B-VII library contains a few abbreviated versions of File 6 that contain an energy-angle distribution for neutron emission, but no recoil or photon data. In order to get semi-reasonable results for both heating and damage for such cases, HEATR applies a “one-particle recoil approximation,” where the first particle emitted is assumed to induce all the recoil. There are also some cases where capture photons are described in MF=6/MT=102 with no corresponding recoil data. Here, the recoil can be added using the same logic described above for capture represented using File 15. The difference between the eV-barns available for the reaction and the energy accounted for by the emitted neutrons, photons, particles, and the approximated recoil is added into the heating in order to preserve the total heating in the spirit of the energy-balance method.

## 6.7 User Input

The input instructions that follow were reproduced from the comment cards in the current version of HEATR.

```
!---input specifications (free format)-----
!
! card 1
!   nendf    unit for endf tape
!   nin      unit for input pendf tape
!   nout     unit for output pendf tape
!   nplot    unit for graphical check output
! card 2
```



```

!   matd      material to be processed
!   npk       number of partial kermas desired (default=0)
!   nqa       number of user q values (default=0)
!   ntemp     number of temperatures to process
!             (default=0, meaning all on pendf)
!   local     0/1=gamma rays transported/deposited locally
!             (default=0)
!   iprint    print (0 min, 1 max, 2 check) (default=0)
!   ed        displacement energy for damage
!             (default from built-in table)
! card 3      for npk gt 0 only
!   mtk       mt numbers for partial kermas desired
!             total (mt301) will be provided automatically.
!             partial kerma for reaction mt is mt+300
!             and may not be properly defined unless
!             a gamma file for mt is on endf tape.
!             special values allowed--
!             303   non-elastic (all but mt2)
!             304   inelastic (mt51 thru 91)
!             318   fission (mt18 or mt19, 20, 21, 38)
!             401   disappearance (mt102 thru 120)
!             442   total ev-barns
!             443   total kinematic kerma (high limit)
!             damage energy production values--
!             444   total
!             445   elastic (mt2)
!             446   inelastic (mt51 thru 91)
!             447   disappearance (mt102 thru 120)
!             cards 4 and 5 for nqa gt 0 only
! card 4
!   mta       mt numbers for users q values
! card 5
!   qa        user specified q values (ev)
!             (if qa.ge.99.e6, read in variable qbar
!             for this reaction)
! card 5a     variable qbar (for reactions with qa flag only)
!   qbar      tab1 record giving qbar versus e (1000 words max)
!
!-----

```

Card 1 specifies the input and output units for HEATR. They are all ENDF-type files. The input PENDF file has normally been through [RECONR](#) and [BROADR](#), but it is possible to run HEATR directly on an ENDF file in order to do kinematic checks. In this case, the results in the resonance range should be ignored. Defining `nplot` will produce a file of input for the [VIEWR](#) module containing detailed energy-balance test results. This option should only be used together with `iprint=2`.

On Card 2, the default value for `npk` is zero, which instructs the code to process the energy-balance total KERMA (MT=301) only. Most often, the user will also want to include MT=443 and MT=444 (`npk=2`). The kinematic KERMA computed when MT=443 is requested is very useful for judging the energy-balance consistency of an evaluation (see the subsection on “Diagnosing Energy-Balance Problems”, Section 6.9, below). It can also be used instead of the energy-balance value in MT=301 when local heating effects are important and the evaluation scores poorly in an energy-balance check. Damage energy production cross sections (MT=444) should be computed for important structural materials; this expensive calculation can be omitted for other materials.

When kinematic checks are desired, a number of additional `npk` values can be included. They can be determined by checking the evaluation to see what partial KERMA factors are well defined. For old-style evaluations that do not use File 6, look for the MT values used in Files 12 and 13. Many evaluations use only MT=3 and MT=102 (or 3, 18, and 102 for fissionable materials); in these cases, the only `mtk` values that make sense are 302, 303, and 402 (or 302, 303, 318, and 402 for fissionable materials). Caution: in many evaluations, MT=102 is used at low energies and taken to zero at some breakpoint. MT=3 is used at higher energies. In these evaluations, the partial KERMA MT=402 does not make sense above the breakpoint, and MT=3 does not make sense below it.

More complicated photon-production evaluations may include MT=4 and/or discrete-photon data in MT=51-90. In these cases, the user can request `mtk=304`. The same kind of energy-range restriction discussed for MT=102 can occur for the inelastic contributions. Other evaluations give additional partial reactions that can be used to check the photon production and energy-balance consistency of an evaluation in detail. Unfortunately, HEATR can only handle 6 additional reactions at a time. Multiple runs may be necessary in complex cases.

Note that several special `mtk` values are provided for the components of the damage-energy production cross section. They were used to prepare Fig. 10, and may be of interest to specialists, but they are not needed for most libraries.

In a few cases in the past, it has been necessary to change the Q values that are normally retrieved from the ENDF tape. In addition, it is sometimes necessary to replace the single Q value supplied in MF=3 with an energy-dependent Q function for an element. One example of the former occurred for  $^{16}\text{O}$  for ENDF/B-V. The first inelastic level (MT=51) decays by pair production rather than the more normal mode of photon emission. In order to get the correct heating, it was necessary to change the Q value by giving Card 4 and Card 5 as follows:

```
51
-5.0294e6
```

That is, the Q value is increased by twice the electron energy of 0.511 MeV. Another example is the sequential (n,2n) reaction for  $^9\text{Be}$  in ENDF/B-V. It is necessary to include 4 changes to the Q values:

```
46 47 48 49/
-1.6651e6 -1.6651e6 -1.6651e6 -1.6651e6/
```

The next example illustrates using energy-dependent Q values for elemental titanium. Set nqa equal to 3 and give the following values on Cards 4, 5, and 5a:

```
16 103 107/
99e6 99e6 99e6/
0. 0. 0 0 1 8
8 2
8.0e6 -8.14e6 9.0e6 -8.14e6 1.1e7 -8.38e6
1.2e7 -8.74e6 1.3e7 -1.03e7 1.4e7 -1.091e7
1.5e7 -1.11e7 2.0e7 -1.125e7/
0. 0. 0 0 1 9
9 2
1.0e-5 1.82e5 4.0e6 1.82e5 5.0e6 -1.19e6
6.0e6 -2.01e6 7.0e6 -2.20e6 8.0e6 -2.27e6
1.4e7 -2.35e6 1.7e6 -2.43e6 2.0e7 -2.37e6/
0. 0. 0 0 1 9
9 2
```

```

1.0e-5 2.182e6 6.0e6 2.182e6 7.0e6 2.10e6
8.0e6 -3.11e5 9.0e6 -9.90e5 1.0e7 -1.20e6
1.1e7 -1.27e6 1.4e6 -1.32e6 2.0e7 -1.48e6/

```

The next parameter on Card 2 is **ntemp**. For normal runs, use zero, and all the temperatures on the input PENDF tape will be processed. For kinematic check runs, use **ntemp**=1. The **local** parameter suppresses the processing of the photon-production files, if any. The photon energy appears in the KERMA factors as if the photons had very short range. A useful way to use the **iprint** parameter is to set it to zero for normal runs, which produce heating and damage values at all temperatures, and to use **iprint**=2 for the energy-balance check run, which is performed for the first temperature on **nin** only.

Card 3 gives the partial KERMA and damage selection MT numbers. Note that the user does not include MT=301 in this list. It is always inserted as the first value automatically. Giving MT=301 in this list will cause an informative message to be issued.

Cards 4, 5, and 5a give the user's changes to the ENDF Q values. The way in which to use these cards was described in connection with **nqa** on Card 2.

## 6.8 Reading HEATR Output

When full output and/or kinematic checks have been requested, HEATR loops through the reactions found in Files 3, 12, and 13. For each reaction, it prints out information about the energies, yields, cross sections, and contributions to heating. The energy grid used is a subset of the PENDF grid. At present, decade steps are used below 1 eV, factor-of-two steps are used from 1 eV to 100 keV, quarter-lethargy steps are used above 100 keV, and approximately 1 MeV steps are used above 2 MeV. An example of this printout for elastic scattering in ENDF/B-VII <sup>27</sup>Al is shown below:

| neutron heating for mt 2 |            | q0 = 0.0000E+00 | q = 0.0000E+00 |            |            |
|--------------------------|------------|-----------------|----------------|------------|------------|
| e                        | ebar       | ...             | xsec           | heating    | damage     |
| 1.0000E-05               | 9.3052E-06 | ...             | 1.5694E+01     | 1.0903E-05 | 0.0000E+00 |
| 1.0000E-04               | 9.3052E-05 | ...             | 5.1179E+00     | 3.5557E-05 | 0.0000E+00 |
| 1.0000E-03               | 9.3052E-04 | ...             | 2.0644E+00     | 1.4342E-04 | 0.0000E+00 |
| 1.0000E-02               | 9.3052E-03 | ...             | 1.4925E+00     | 1.0369E-03 | 0.0000E+00 |
| 1.0000E-01               | 9.3052E-02 | ...             | 1.4318E+00     | 9.9474E-03 | 0.0000E+00 |
| ...                      |            |                 |                |            |            |

|            |            |     |            |            |            |
|------------|------------|-----|------------|------------|------------|
| 1.0000E+03 | 9.3052E+02 | ... | 1.3662E+00 | 9.4914E+01 | 7.7171E+01 |
| 2.0000E+03 | 1.8610E+03 | ... | 1.3196E+00 | 1.8337E+02 | 1.5115E+02 |
| 5.0000E+03 | 4.6526E+03 | ... | 1.2130E+00 | 4.2136E+02 | 3.3998E+02 |
| 1.0000E+04 | 9.3052E+03 | ... | 1.0367E+00 | 7.2028E+02 | 5.6725E+02 |
| 2.0000E+04 | 1.8610E+04 | ... | 6.6204E-01 | 9.1991E+02 | 7.0347E+02 |
| 5.0000E+04 | 4.6526E+04 | ... | 2.3220E+00 | 8.0660E+03 | 5.8732E+03 |
| 1.0000E+05 | 9.3052E+04 | ... | 5.2976E+00 | 3.6805E+04 | 2.5521E+04 |
| ...        |            |     |            |            |            |
| 1.0000E+07 | 9.7233E+06 | ... | 7.4942E-01 | 2.0738E+05 | 4.5689E+04 |
| 1.1000E+07 | 1.0699E+07 | ... | 7.4953E-01 | 2.2576E+05 | 4.7347E+04 |
| 1.2000E+07 | 1.1682E+07 | ... | 7.6363E-01 | 2.4286E+05 | 4.9202E+04 |
| 1.3000E+07 | 1.2673E+07 | ... | 7.6329E-01 | 2.4980E+05 | 4.9559E+04 |
| 1.4000E+07 | 1.3670E+07 | ... | 7.7918E-01 | 2.5737E+05 | 5.0566E+04 |
| 1.5000E+07 | 1.4671E+07 | ... | 7.9297E-01 | 2.6088E+05 | 5.1189E+04 |
| 1.6000E+07 | 1.5676E+07 | ... | 8.1414E-01 | 2.6347E+05 | 5.1973E+04 |
| 1.7000E+07 | 1.6681E+07 | ... | 8.3429E-01 | 2.6577E+05 | 5.2680E+04 |
| 1.8000E+07 | 1.7689E+07 | ... | 8.4524E-01 | 2.6246E+05 | 5.2747E+04 |
| 1.9000E+07 | 1.8695E+07 | ... | 8.7093E-01 | 2.6568E+05 | 5.3787E+04 |
| 2.0000E+07 | 1.9703E+07 | ... | 8.9326E-01 | 2.6547E+05 | 5.4573E+04 |
| ...        |            |     |            |            |            |
| 1.4000E+08 | 1.3985E+08 | ... | 2.9730E-01 | 4.3523E+04 | 1.4994E+04 |
| 1.4600E+08 | 1.4585E+08 | ... | 2.7580E-01 | 4.1851E+04 | 1.3890E+04 |
| 1.5000E+08 | 1.4984E+08 | ... | 2.6510E-01 | 4.1161E+04 | 1.3339E+04 |

Note the identification and Q information printed on the first line; q is the ENDF Q value from File 3, and q0 is the corresponding mass-difference Q value needed for Eq. 162. The ebar, yield (which was replaced by “...” to make this listing fit better), and xsec columns contain  $\bar{E}_n$ , Y, and  $\sigma$ , respectively. The heating column is just  $(E+Q-Y\bar{E}_n)\sigma$ . The results are similar for discrete inelastic levels represented using File 4. The heating due to the associated photons will be subtracted later while MF=12 or MF=13 is being processed. However, if an LR flag is set, the residual nucleus from the (n,n') reaction breaks up by emitting additional particles. This extra breakup energy changes the q0 value. An example of such a section for  $^{27}\text{Al}(n,n_{25})p$  from ENDF/B-V follows:

| neutron heating for mt 75    q0 = -8.2710e+06    q = -1.0750e+07 |            |            |            |            |
|------------------------------------------------------------------|------------|------------|------------|------------|
| e                                                                | ebars      | yield      | xsec       | heating    |
| 1.2000e+07                                                       | 7.8653e+05 | 1.0000e+00 | 8.2242e-02 | 2.4199e+05 |
| 1.3000e+07                                                       | 1.7116e+06 | 1.0000e+00 | 8.0121e-02 | 2.4176e+05 |

|            |            |            |            |            |
|------------|------------|------------|------------|------------|
| 1.4000e+07 | 2.6427e+06 | 1.0000e+00 | 5.9282e-02 | 1.8296e+05 |
| 1.5000e+07 | 3.5864e+06 | 1.0000e+00 | 4.1834e-02 | 1.3147e+05 |
| 1.6000e+07 | 4.5096e+06 | 1.0000e+00 | 2.8880e-02 | 9.2977e+04 |
| 1.7000e+07 | 5.4335e+06 | 1.0000e+00 | 1.9867e-02 | 6.5472e+04 |
| 1.8000e+07 | 6.3848e+06 | 1.0000e+00 | 1.3677e-02 | 4.5739e+04 |
| 1.9000e+07 | 7.2944e+06 | 1.0000e+00 | 9.4771e-03 | 3.2550e+04 |
| 2.0000e+07 | 8.2479e+06 | 1.0000e+00 | 6.6142e-03 | 2.3025e+04 |

Starting with ENDF/B-VI, discrete-inelastic sections may also be given in File 6. Such sections contain their own photon production data, and the **heating** column will represent the entire recoil energy as in Eq. 175. (See below for detailed discussion of ENDF/B-VI output.)

For continuum reactions that use MF=4 and MF=5, such as (n,n') or (n,2n), the neutron part of the display looks like this:

| neutron heating for mt 16    q0 = -1.3057e+07    q = -1.3057e+07 |            |            |            |            |
|------------------------------------------------------------------|------------|------------|------------|------------|
| e                                                                | ebar       | yield      | xsec       | heating    |
| 1.4000e+07                                                       | 1.9960e+05 | 2.0000e+00 | 2.4000e-02 | 1.3051e+04 |
| 1.5000e+07                                                       | 6.6850e+05 | 2.0000e+00 | 1.2320e-01 | 7.4659e+04 |
| 1.6000e+07                                                       | 1.0855e+06 | 2.0000e+00 | 2.0710e-01 | 1.5987e+05 |
| 1.7000e+07                                                       | 1.4308e+06 | 2.0000e+00 | 2.6510e-01 | 2.8667e+05 |
| 1.8000e+07                                                       | 1.6379e+06 | 2.0000e+00 | 3.0300e-01 | 5.0518e+05 |
| 1.9000e+07                                                       | 1.7659e+06 | 2.0000e+00 | 3.3000e-01 | 7.9567e+05 |
| 2.0000e+07                                                       | 1.8755e+06 | 2.0000e+00 | 3.5000e-01 | 1.1172e+06 |

Once again, the photon effects will be subtracted later.

Absorption reactions such as (n, $\gamma$ ) or (n,p), lead to similar displays, but the particle **ebar** columns will always be set to zero (no emitted neutrons). An example follows:

| neutron heating for mt103    q0 = -1.8278e+06    q = -1.8278e+06 |            |            |            |            |
|------------------------------------------------------------------|------------|------------|------------|------------|
| e                                                                | ebar       | yield      | xsec       | heating    |
| 2.5000E+06                                                       | 0.0000E+00 | 1.0000E+00 | 3.2800E-05 | 2.2048E+01 |
| 3.0000E+06                                                       | 0.0000E+00 | 1.0000E+00 | 1.3300E-03 | 1.5590E+03 |
| 3.5000E+06                                                       | 0.0000E+00 | 1.0000E+00 | 1.0100E-02 | 1.6889E+04 |
| 4.0000E+06                                                       | 0.0000E+00 | 1.0000E+00 | 6.9667E-03 | 1.5133E+04 |
| 4.5000E+06                                                       | 0.0000E+00 | 1.0000E+00 | 1.7000E-02 | 4.5427E+04 |
| 5.0000E+06                                                       | 0.0000E+00 | 1.0000E+00 | 2.3300E-02 | 7.3912E+04 |

```

...
1.7000E+07  0.0000E+00  1.0000E+00  5.5200E-02  8.3751E+05
1.8000E+07  0.0000E+00  1.0000E+00  4.7800E-02  7.7303E+05
1.9000E+07  0.0000E+00  1.0000E+00  4.0200E-02  6.9032E+05
2.0000E+07  0.0000E+00  1.0000E+00  3.2200E-02  5.8514E+05

```

If File 6 is present (which happens for evaluations in ENDF-6 format only, such as the evaluations in ENDFB-VII), each reaction will be divided into subsections, one for each emitted particle. The neutron subsections are displayed as part of the energy-balance checks, but they do not contribute to KERMA or damage. The subsection for each charged particle or residual nucleus will give the incident energy, average energy for the emitted particle, cross section, heating contribution, and (optionally) damage contribution as follows:

```

file six heating for mt 28, particle =    1      q = -8.2721E+06
      e      ebar      yield      xsec      heating
9.0000E+06  1.2303E+05  1.0000E+00  1.0385E-03  0.0000E+00
1.0000E+07  4.6746E+05  1.0000E+00  1.3526E-02  0.0000E+00
...
1.8000E+07  3.1862E+06  1.0000E+00  3.7721E-01  0.0000E+00
1.9000E+07  3.4535E+06  1.0000E+00  3.7577E-01  0.0000E+00
2.0000E+07  3.7207E+06  1.0000E+00  3.7434E-01  0.0000E+00

file six heating for mt 28, particle = 1001      q = -8.2721E+06
      e      ebar      yield      xsec      heating
9.0000E+06  4.5909E+05  1.0000E+00  1.0385E-03  4.7677E+02
1.0000E+07  8.9616E+05  1.0000E+00  1.3526E-02  1.2121E+04
...
1.8000E+07  3.5193E+06  1.0000E+00  3.7721E-01  1.3275E+06
1.9000E+07  3.8257E+06  1.0000E+00  3.7577E-01  1.4376E+06
2.0000E+07  4.1321E+06  1.0000E+00  3.7434E-01  1.5468E+06

file six heating for mt 28, particle = 12026      q = -8.2721E+06
      e      ebar      yield      xsec      heating
9.0000E+06  3.2104E+05  1.0000E+00  1.0385E-03  3.3340E+02
1.0000E+07  3.8540E+05  1.0000E+00  1.3526E-02  5.2128E+03
...
1.8000E+07  8.0820E+05  1.0000E+00  3.7721E-01  3.0486E+05
1.9000E+07  8.6147E+05  1.0000E+00  3.7577E-01  3.2372E+05
2.0000E+07  9.1475E+05  1.0000E+00  3.7434E-01  3.4243E+05

```

```

file six heating for mt 28, particle =    0    q = -8.2721E+06
      e      ebar      yield      xsec      heating
9.0000E+06  1.8347E+05  2.8104E-06  1.0385E-03  0.0000E+00
                        ebal -1.8204E+02
1.0000E+07  4.4913E+05  3.0441E-05  1.3526E-02  0.0000E+00
                        ebal -2.8626E+02
...
1.8000E+07  1.8309E+06  1.2028E+00  3.7721E-01  0.0000E+00
                        ebal  4.5397E+03
1.9000E+07  1.8856E+06  1.3695E+00  3.7577E-01  0.0000E+00
                        ebal  1.8336E+03
2.0000E+07  1.9403E+06  1.5363E+00  3.7434E-01  0.0000E+00
                        ebal -7.6798E+03

```

Note that the last subsection in this example was for emitted photons. Photons do not contribute to the KERMA or damage, but this information is used to check the total energy conservation for this reaction. The **ebal** lines show the difference between the available energy and the sum over all the outgoing particles. The values should be a small percentage of the total heating. If the **ebal** values are too large, there may be an error in the evaluation, or it may be necessary to refine the energy grids in the distributions. In addition, this photon production information is needed later for the photon energy check.

After all the sections corresponding to MT numbers in File 3 have been processed (using the File 4, File 4/5, or File 6 method as appropriate), the photon production sections in Files 12 and 13 are processed, if present. File 12 data are usually present for radiative capture (MT=102), at least at low energies. Simple files normally give a tabulated photon spectrum. The display gives the average energy for this spectrum in the **ebar** column and the negative contribution to the heating computed with Eq. 173 in the **heating** column. The **edam** column contains the  $\overline{E_\gamma^2}$  term needed to compute the photon contribution to the damage, which is given in the **damage** column. See Eq. 206. The display also has an extra line for each incident energy containing the percent error “--- pc” between the total photon energy as computed from File 12 and the value  $E+Q-E/(A+1)$  computed from File 3. As discussed above, HEATR does not guarantee energy balance in large systems if this error occurs. The following example shows some large errors due to mistakes in the ENDF/B-V evaluation for  $^{55}\text{Mn}$ . Two columns labeled **edam** and **xsec** have been removed to show the



heating and damage columns. The text has also been shifted to the left of its normal position to fit better on the printed page.

```

photon energy (from yields) mf12, mt102
      e      ebar/err      egam ...      yield      heating      damage
1  continuum gammas
1.0000e-05  4.5088e+06  2.4237e+02 ...  2.4791e+00 -4.8477e+09  5.4975e+04
1.0000e-05      53.7 pc
1.0703e-04  4.5088e+06  2.4237e+02 ...  2.4791e+00 -1.4819e+09  1.6806e+04
1.0703e-04      53.7 pc
1.2520e-03  4.5088e+06  2.4237e+02 ...  2.4791e+00 -4.3347e+08  4.9159e+03
1.2520e-03      53.7 pc
...
1.3571e+04  4.4522e+06  2.3887e+02 ...  2.4836e+00 -7.3869e+03 -1.2406e-01
1.3571e+04      51.8 pc
2.7142e+04  4.3957e+06  2.3536e+02 ...  2.4881e+00 -3.7037e+05 -1.6487e+01
2.7142e+04      49.9 pc
5.4287e+04  4.2826e+06  2.2834e+02 ...  2.4972e+00 -2.5604e+04 -2.5340e+00
5.4287e+04      46.0 pc
1.0858e+05  4.0563e+06  2.1430e+02 ...  2.5154e+00 -1.3327e+04 -2.7289e+00
1.0858e+05      38.3 pc

```

Many MF=12, MT=102 sections give multiplicities for the production of discrete photons. In these cases, HEATR prints out data for all of the parts, and it provides a sum at the end. The balance error is printed with the sum. The following example shows a case with discrete photons. The last two columns have been removed (**heating**, **damage**), and the text has been compacted and shifted to the left to fit on the printed page.

```

photon energy (from yields) mf12, mt102
      e      ebar/err      egam      edam      xsec      yield
1  7.7260E+06 ev gamma
1.0000e-05  7.7260e+06  1.1448e+03  8.9780e+02  1.1677e+01  3.0000e-01
1.1406e-04  7.7260e+06  1.1448e+03  8.9780e+02  3.4574e+00  3.0000e-01
1.1406e-03  7.7260e+06  1.1448e+03  8.9780e+02  1.0934e+00  3.0000e-01
...
2.0000e+07  2.7005e+07  1.1448e+03  8.9780e+02  1.0000e-03  3.0000e-01
2  7.6950e+06 ev gamma
1.0000e-05  7.6950e+06  1.1356e+03  8.9091e+02  1.1677e+01  5.0000e-02

```

|            |            |            |            |            |            |
|------------|------------|------------|------------|------------|------------|
| 1.1406e-04 | 7.6950e+06 | 1.1356e+03 | 8.9091e+02 | 3.4574e+00 | 5.0000e-02 |
| ...        |            |            |            |            |            |
| 2.0000e+07 | 2.6974e+07 | 1.1356e+03 | 8.9091e+02 | 1.0000e-03 | 5.0000e-02 |
| 3          | 6.8630e+06 | ev gamma   |            |            |            |
| 1.0000e-05 | 6.8630e+06 | 9.0330e+02 | 7.1515e+02 | 1.1677e+01 | 1.2000e-03 |
| 1.1406e-04 | 6.8630e+06 | 9.0330e+02 | 7.1515e+02 | 3.4574e+00 | 1.2000e-03 |
| 1.1406e-03 | 6.8630e+06 | 9.0330e+02 | 7.1515e+02 | 1.0934e+00 | 1.2000e-03 |
| ...        |            |            |            |            |            |
| 89         | 3.1000e+04 | eV gamma   |            |            |            |
| 1.0000e-05 | 3.1000e+04 | 1.8430e-02 | 0.0000e+00 | 1.1677e+01 | 2.8884e-01 |
| 1.0000e-05 | 0.0        | pc         |            |            |            |
| 1.1406e-04 | 3.1000e+04 | 1.8430e-02 | 0.0000e+00 | 3.4574e+00 | 2.8884e-01 |
| 1.1406e-04 | 0.0        | pc         |            |            |            |
| 1.1406e-03 | 3.1000e+04 | 1.8430e-02 | 0.0000e+00 | 1.0934e+00 | 2.8884e-01 |
| 1.1406e-03 | 0.0        | pc         |            |            |            |
| 1.1912e-02 | 3.1000e+04 | 1.8430e-02 | 0.0000e+00 | 3.3832e-01 | 2.8884e-01 |
| 1.1912e-02 | 0.0        | pc         |            |            |            |
| ...        |            |            |            |            |            |
| 2.0000e+07 | 3.1000e+04 | 1.8430e-02 | 0.0000e+00 | 1.0000e-03 | 2.8884e-01 |
| 2.0000e+07 | 0.0        | pc         |            |            |            |

In this case ( $^{27}\text{Al}$ ), the capture energy production checks out perfectly for the sum of all 89 discrete photons.

Other sections using either File 12 or File 13 generate displays similar to the following:

| photon energy (from xsecs) mf13, mt 3 |                  |            |            |            |             |
|---------------------------------------|------------------|------------|------------|------------|-------------|
|                                       | e                | ebar       | xsec       | energy     | heating     |
| 1                                     | continuum gammas |            |            |            |             |
|                                       | 2.0000e+05       | 3.6753e+06 | 4.2076e-03 | 1.5464e+04 | -1.5464e+04 |
|                                       | 4.0500e+05       | 3.3863e+06 | 5.2873e-03 | 1.7904e+04 | -1.7904e+04 |
|                                       | 6.0031e+05       | 3.1097e+06 | 6.4478e-03 | 2.0051e+04 | -2.0051e+04 |
|                                       | 8.0182e+05       | 2.0089e+06 | 9.3236e-02 | 1.8730e+05 | -1.8730e+05 |
|                                       | 1.0000e+06       | 9.2622e+05 | 1.7859e-01 | 1.6541e+05 | -1.6541e+05 |
|                                       | 1.2000e+06       | 9.6151e+05 | 2.8329e-01 | 2.7239e+05 | -2.7239e+05 |
|                                       | ...              |            |            |            |             |

Note that the photon  $\overline{E}\sigma$  is simply subtracted from the **heating** column for each incident energy.

If the partial KERMA `mtk=443` was requested in the user's input, HEATR will print out a special section that tests the total photon energy production against the kinematic limits (see Section 6.4 above for the formulas used). An example follows:

```

photon energy production check
      e      ev-barns      min      max
1.0000e-05  9.0215e+07  9.0187e+07  9.0200e+07
1.1406e-04  2.6712e+07  2.6704e+07  2.6708e+07
1.1406e-03  8.4479e+06  8.4453e+06  8.4466e+06
1.1912e-02  2.6138e+06  2.6130e+06  2.6134e+06
1.2812e-01  7.9895e+05  7.9871e+05  7.9883e+05
1.2812e+00  2.5211e+05  2.5203e+05  2.5207e+05
2.6875e+00  1.7420e+05  1.7415e+05  1.7417e+05
5.5000e+00  1.2186e+05  1.2182e+05  1.2184e+05
1.1406e+01  8.4662e+04  8.4636e+04  8.4648e+04
2.4062e+01  5.8231e+04  5.8213e+04  5.8222e+04
4.9375e+01  4.0614e+04  4.0601e+04  4.0607e+04
1.0000e+02  2.8522e+04  2.8514e+04  2.8518e+04
...
8.0000e+06  3.8972e+06  3.7964e+06  4.4880e+06
9.0000e+06  4.4782e+06  4.4401e+06  5.4986e+06
1.0000e+07  4.9645e+06  5.2078e+06  6.6176e+06
1.1000e+07  5.3712e+06  6.1302e+06  7.8374e+06 ----
1.2000e+07  5.3212e+06  5.8699e+06  8.0618e+06
1.3000e+07  5.0984e+06  5.9333e+06  8.5312e+06 ----
1.4000e+07  4.7415e+06  5.7172e+06  8.6605e+06 ----
1.5000e+07  4.0795e+06  4.7419e+06  8.0409e+06 ----
1.6000e+07  3.2521e+06  3.6806e+06  7.2734e+06 ----
1.7000e+07  2.8079e+06  2.8418e+06  6.6927e+06
1.8000e+07  2.7492e+06  2.2915e+06  6.2850e+06
1.9000e+07  2.9626e+06  1.9674e+06  6.2330e+06
2.0000e+07  3.4419e+06  1.7938e+06  6.1994e+06

```

The low and high kinematic limits will be the same at low energies where only kinematics affect the calculations. They may be the same for all energies for ENDF/B-VII evaluations that provide complete distributions for all outgoing charged particles and recoil nuclei. Normally, the limits diverge above the threshold for continuum reactions. Note that HEATR marks lines where the

computed value goes more than a little way outside the limits with the symbols ++++ or ----. It is often convenient to extract these numbers from the output listing and plot them (see Fig. 11). Although the energy grid is a little coarse, such plots can often be useful (see below).

The last part of a full HEATR output listing is a tabulation of the computed KERMA and damage coefficients on the normal coarse energy grid. Columns are provided for the total KERMA and for each of the partial KERMA results requested with `mtk` values in the user's input. If kinematic checks were requested, the check values are written just above and below the corresponding partial KERMA values. In addition, `low` and `high` messages are written just above or just below the kinematic limits in every column where a significant violation of the limits occurs. Caution: if summation reactions (MT=3, MT=4) were used to define the photon production over some parts of the energy range, the partial KERMA results may not make sense at some energies. For example, consider the common pattern in ENDF/B-V where MT=102 is used for capture at low energies, but at higher energies, it is set to zero, and the capture contribution is included in MT=3 (nonelastic). Clearly, the partial KERMA MT=402 doesn't make sense above this breakpoint. The following example shows part of the final KERMA listing for ENDF/B-V.1  $^{55}\text{Mn}$ . The damage column was removed and the columns compressed to fit on the printed page.

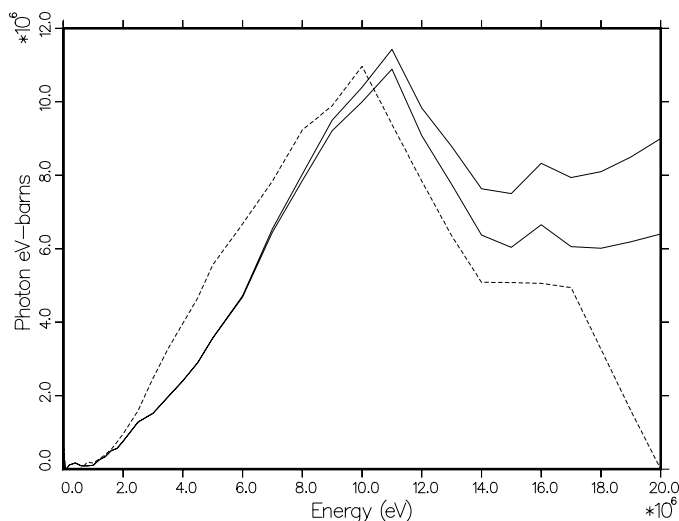


Figure 11: Example of a plot comparing the total photon energy production for  $^{55}\text{Mn}$  from ENDF/B-V.1 (dashed) with the kinematic limits (solid).

| final kerma factors |     |             |            |             |            |            |
|---------------------|-----|-------------|------------|-------------|------------|------------|
|                     | e   | 301         | 302        | 303         | 402        | 443        |
|                     | min | 1.2400e-04  | 3.7775e-06 | 1.2022e-04  | 1.2022e-04 |            |
| 1.0000e-05          |     | 4.0068e+05  | 3.7775e-06 | 4.0068e+05  | 4.0068e+05 | 4.0068e+05 |
|                     | max | 3.3820e+05  | 3.7775e-06 | 3.3820e+05  | 3.3820e+05 |            |
|                     |     | high        |            | high        | high       |            |
| ...                 |     |             |            |             |            |            |
|                     | min | 3.2373e+04  | 2.3497e+04 | 8.8759e+03  | 4.1114e+01 |            |
| 6.0031e+05          |     | 1.0017e+05  | 2.3497e+04 | 7.6673e+04  | 2.9899e+04 | 3.2375e+04 |
|                     | max | 3.2375e+04  | 2.3497e+04 | 8.8781e+03  | 4.3366e+01 |            |
|                     |     | high        |            | high        | high       |            |
|                     |     | low         |            | low         |            |            |
|                     | min | 7.3041e+04  | 5.9403e+04 | 1.3638e+04  | 4.4748e+01 |            |
| 8.0182e+05          |     | -2.4355e+04 | 5.9403e+04 | -8.3758e+04 | 2.4987e+04 | 7.3043e+04 |
|                     | max | 7.3043e+04  | 5.9403e+04 | 1.3640e+04  | 4.6676e+01 |            |
|                     |     |             |            |             | high       |            |
|                     |     | low         |            | low         |            |            |
|                     | min | 9.8973e+04  | 7.7075e+04 | 2.1898e+04  | 4.7777e+01 |            |
| 1.0000e+06          |     | 3.7682e+04  | 7.7075e+04 | -3.9393e+04 | 2.1917e+04 | 9.8974e+04 |
|                     | max | 9.8974e+04  | 7.7075e+04 | 2.1900e+04  | 4.9509e+01 |            |
|                     |     |             |            |             | high       |            |
|                     |     | low         |            | low         |            |            |
|                     | min | 1.1397e+05  | 7.7800e+04 | 3.6168e+04  | 4.9760e+01 |            |
| 1.2000e+06          |     | 9.5321e+04  | 7.7800e+04 | 1.7521e+04  | 1.9482e+04 | 1.1397e+05 |
|                     | max | 1.1397e+05  | 7.7800e+04 | 3.6169e+04  | 5.1335e+01 |            |
|                     |     |             |            |             | high       |            |
|                     |     | low         |            | low         |            |            |
|                     | min | 1.4632e+05  | 1.0192e+05 | 4.4402e+04  | 5.3005e+01 |            |
| 1.4000e+06          |     | 9.8251e+04  | 1.0192e+05 | -3.6667e+03 | 1.8208e+04 | 1.4632e+05 |
|                     | max | 1.4632e+05  | 1.0192e+05 | 4.4403e+04  | 5.4511e+01 |            |
|                     |     |             |            |             | high       |            |
| ...                 |     |             |            |             |            |            |

|            |     |            |            |            |            |            |
|------------|-----|------------|------------|------------|------------|------------|
|            | min | 2.3650e+05 | 1.6907e+05 | 6.7426e+04 | 1.7607e+02 |            |
| 1.9000e+07 |     | 7.1384e+06 | 1.6907e+05 | 6.9693e+06 | 1.3503e+04 | 2.5435e+06 |
|            | max | 2.5435e+06 | 1.6907e+05 | 2.3744e+06 | 1.7939e+02 |            |
|            |     | high       |            | high       | high       |            |
|            | min | 2.4001e+05 | 1.8261e+05 | 5.7406e+04 | 1.4423e+02 |            |
| 2.0000e+07 |     | 9.2369e+06 | 1.8261e+05 | 9.0543e+06 | 1.0908e+04 | 2.8385e+06 |
|            | max | 2.8385e+06 | 1.8261e+05 | 2.6559e+06 | 1.4701e+02 |            |
|            |     | high       |            | high       | high       |            |

The following subsection discusses how to analyze the “check” output of HEATR in order to diagnose energy-balance errors in ENDF-format evaluations. The examples are drawn from ENDF/B-V testing[42]. In general, results like these are less likely to occur in modern evaluations.

## 6.9 Diagnosing Energy-Balance Problems

The analysis should start with MT=102, because if it is wrong, the guarantee of energy conservation for large systems breaks down. If the display for MF=12, MT=102 shows messages of the form “--- pc”, there may be a problem. If these messages only show up at the higher energies, and if the size of the error increases with energy, it is probable that the evaluator has used a thermal spectrum over the entire energy range (this is very common). Of course, the total photon energy production from radiative capture should equal

$$\frac{A}{A+1}E + Q, \quad (217)$$

where the rest of the total energy  $E+Q$  is carried away by recoil. If only a thermal spectrum is given, the  $E$  term is being neglected, and errors will normally appear above about 1 MeV. The  $E$  term can be included in evaluations that use tabulated data by giving  $E$ -dependent spectra in File 15; and it can be included for evaluations that use discrete photons by setting the “primary photon” flags in File 12 properly. In practice, the capture cross sections above 1 MeV are often comparatively small due to the  $1/v$  tendency of capture, and the errors introduced by neglecting the  $E$  term can be ignored.

If the MT=102 errors show up at low energies, there is probably an error in the average photon yield from File 12, in the average energy computed from File 15, or both. In the  $^{55}\text{Mn}$  case shown above, the yield had been incorrectly

entered. In addition, the spectrum didn't agree with the experimental data because the bin boundaries were shifted. Each case must be inspected in detail to find the problems.

The next common source of energy-balance errors in ENDF files arises from the representation used for inelastic scattering. Typically, the neutron scattering is described in detail using up to 40 levels for the  $(n,n')$  reaction. However, the photon production is often described using MF=13/MT=3 or MF=13/MT=4 and rather coarse energy resolution. As a result, it is possible to find photons for  $(n,n_1)$  being produced for incident neutron energies slightly below the MT=51 threshold! These photons would lead to a spike of negative KERMA factors. A more common effect of the coarse grid used for photon production is to lead to an underestimate or overestimate of the photon production by not following the detailed shape of the inelastic cross section. The HEATR "kinematic KERMA" is correct in this range since only two-body reactions are active. Therefore, a plot of MT=301 and MT=443 on the same frame normally shows these effects in detail. Fig. 12 is an example of such a plot.

Fig. 13 shows both the inelastic cross section from File 3 and the photon production cross section from File 13 to demonstrate the mismatch in the energy grids that contributes to the energy-balance errors. These kinds of errors are best removed by changing to a representation that uses File 12 to give photon

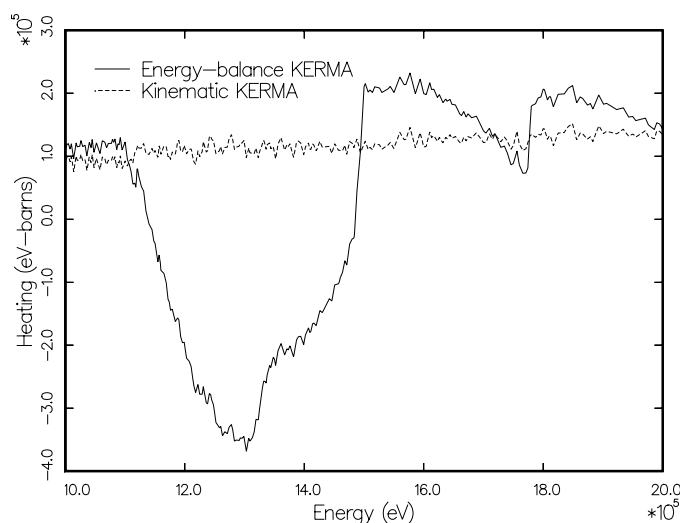


Figure 12: Comparison of MT=301 with MT=443 for the region of the discrete-inelastic thresholds for  $^{59}\text{Co}$  from ENDF/B-V.2. Note the large region of negative KERMA. The best way to remove this kind of problem is by using yields in File 12, MT=51, 52, 53, ... to represent the photon production.

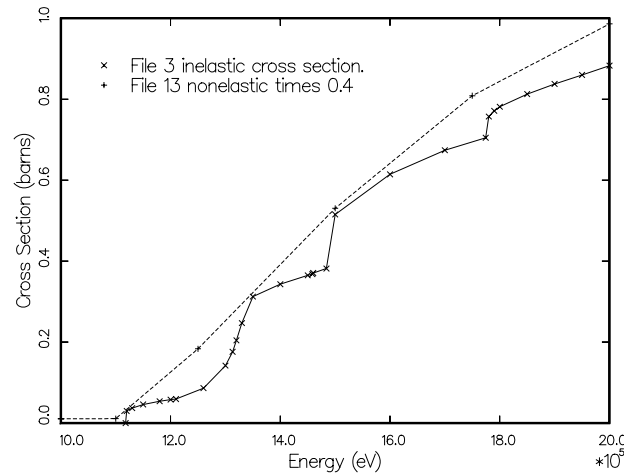


Figure 13: Plot showing the mismatch between the energy grids used for File 3 and File 13 in the region of the thresholds for discrete-inelastic scattering levels for the case shown in Fig. 12. The cross and ex symbols show the actual grid energies in the evaluation.

production yields for the separate reactions MT=51, MT=52, etc. This representation makes full use of the File 3 cross sections, and as long as each section of File 12 conserves energy, the total inelastic reaction is guaranteed to conserve energy, even at the finest energy resolution.

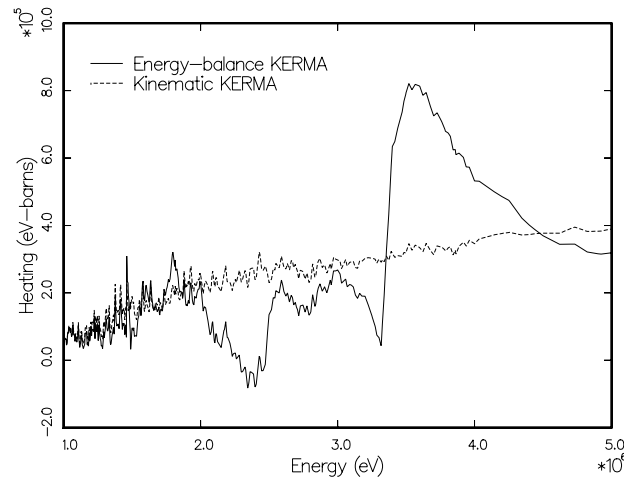


Figure 14: Typical energy-balance problems between points where balance is satisfied. Discrete photons were used below about 2 MeV, and energy balance is reasonably good there. The energy points in MF=13 for the continuum part are at 2, 3, and 5 MeV, and the balance is also good at those energies. Clearly, a grid in File 13 that used steps of about 0.25 MeV between 2 and 4 MeV would reduce the size of the deviations substantially and remove the negative KERMA factors.



A method that is frequently used by evaluators of photon production files is to select a number of nonelastic photon spectra on a fairly coarse incident-energy grid using theory or experiment, and then to readjust the photon yield on this energy grid so as to conserve energy at each grid point. However, the results do not, in general, conserve energy at intermediate points. If a very coarse energy grid is used for File 13, quite large deviations between MT=301 and MT=443 can result. Fig. 14 shows such a case. The solution to this kind of violation of energy balance is to add intermediate points in Files 13 and 15 until the magnitude of the deviations is small enough for practical calculations.

Especially large energy-balance errors of this type are caused by interpolating across the minimum formed by the decreasing capture heating and the increasing inelastic heating. Fig. 15 shows a dramatic example using a photon energy production comparison.

For energies above the threshold for continuum reactions like (n,n') or (n,2n), it is difficult to use the results of the kinematic checks to fix evaluations. The representation of Eqs. 176 and 177 for continuum inelastic scattering is very rough. Comparison to other more accurate methods suggests that a CM formula

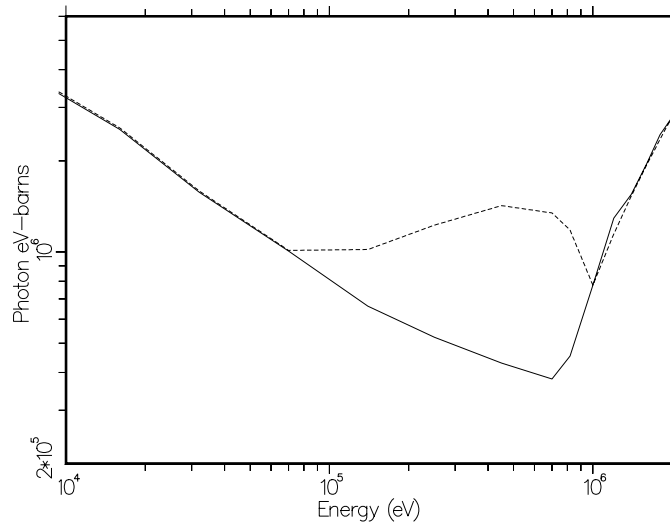


Figure 15: Computed photon energy production (dashed) compared with the kinematic value (solid) for  $^{93}\text{Nb}$  from ENDF/B-V. The original File 13 has grid points at 100 keV and 1 MeV. Interpolating across that wide bin gives a photon production rate that is much too large for energies in the vicinity of a few hundred keV. This will result in a large region of negative heating numbers. Since this is just the region of the peak flux in a fast reactor, niobium-clad regions could be cooled instead of heated!

would be better here[49], even though the ENDF file says “lab.” Most other reactions give very wide low and high limits. Two exceptions are (n,2n) and (n,3n). If they dominate the cross section, the kinematic limits will be fairly close together. In the 14 MeV range, energy errors could be in the photon data, the neutron data, or both. The best way to eliminate balance errors is to construct a new evaluation based on up-to-date nuclear model codes.

## 6.10 Coding Details

The main subroutine is `heatr`, which is exported by module `heatm`. It starts by reading the user’s input and locating the desired material on the PENDF file. The main loop is over temperature. For each temperature, a check is made to see if the user provided a value for the damage displacement energy. If not, a default value is provided. Next, `hinit` is called to examine the directory. Flags are set if MF=12 or 13 is present, if MT=18 or 19 is used, and if MT=458 is present (see `mgam`, `mt19`, and `mt458`). The flags `mt103`, `mt104`, `mt105`, `mt106` and `mt107` are set if the corresponding particle production levels are present. The MT numbers used for the levels depend on whether the input file used version 6 format or one of the earlier formats. For example, `mt103` is set if MT=600-649 is found for ENDF-6 data, or if MT=700-719 is found for earlier versions. The code also checks to see if the corresponding angular distribution data are present (see `nmiss4`). If any are not present, the code will assume they are isotropic. Note that `hinit` also collects a list of the File 6 MT numbers in `mt6(i6)`. For fissionable materials, the delayed fission energy values are retrieved from MF=1/MT=458, and the correction, `qdel`, is computed for later use when calculating the heating from prompt fission.

The next step in `hinit` is to make a copy of File 6 on a scratch file (if any sections of File 6 were found). While doing this, it searches through the subsections for each reaction accumulating the ZA residual remaining after each particle is given. If it comes to the photons (`zap=0`), which should be last, and there is still a ZA residual left, then it concludes that there is no subsection describing the residual. It loads a value into `mt6no(ii6)` that is the index to the subsection that the recoil should have followed had it been present. If it comes to the end of the subsection list without finding photons and still has a ZA residual, it sets `mt6no(ii6)` to `nk`; that is, the residual missing should follow the last subsection. In either case, the routine prints out messages about “photon recoil correction” or “one-particle recoil approximation.”

Finally, `hinit` makes a standardized copy of the ENDF tape using `hconvr`, and it also saves the grid of the total cross section (MT=1) on the `loada/finda` scratch file that will be used to accumulate the KERMA factors, damage, and kinematic checks (if requested). Note also `mt303`, which tells which of the requested edits is for nonelastic heating, MT=303. This is used later for writing out the photon energy production check.

Now `nheat` is called. Its basic function is to loop over the “nonredundant” reactions in File 3, and to accumulate the corresponding contributions to the partial heating and partial damage values into the appropriate elements of the `c` array on the `loada/finda` file. Redundant reactions are reactions that duplicate or include effects that can be obtained from another MT number. They are determined using a set of `if` statements just after the entry to the reaction loop at statement number 105. The structure of the `c` array depends on whether kinematic checks are being accumulated or not and whether photon production files are present. If neither occurs, the structure has `npk+1` elements as follows:

| Element            | Contents                |
|--------------------|-------------------------|
| 1                  | energy                  |
| 2                  | total heating           |
| 3                  | value for first partial |
| ...                |                         |
| <code>npk+1</code> | value for last partial  |

where `npk` is the number of partial KERMA or damage values being accumulated, including the total. If checks are being accumulated, the `c` array has the following  $3*\text{npk}+1$  elements:

| Element          | Contents                                |
|------------------|-----------------------------------------|
| 1                | energy                                  |
| 2                | total heating                           |
| 3                | value for first partial                 |
| ...              |                                         |
| $2+\text{npk}$   | lower kinematic limit for total         |
| $3+\text{npk}$   | lower kinematic limit for first partial |
| ...              |                                         |
| $2+2*\text{npk}$ | upper kinematic limit for total         |
| $3+2*\text{npk}$ | upper kinematic limit for first partial |
| ...              |                                         |
| $3*\text{npk}+1$ | upper kinematic limit for last partial  |

If photon production files are present in the evaluation, the total length of the `c` array increases by the following three words (`len` is the old length from above plus three):

| Element            | Contents                        |
|--------------------|---------------------------------|
| <code>len-2</code> | photon capture correction       |
| <code>len-1</code> | total photon eV-barns           |
| <code>len</code>   | total energy yield for “subtot” |

Back inside the loop over nonredundant reactions, subroutine `gety1` is initialized for this reaction. The code checks to see if this section uses File 6 for its distributions; if so, it arranges to make multiple passes through the reaction’s energy grid, one pass for each subsection of the MF=6 section, and perhaps one additional pass to synthesize the missing recoil subsection. It is now possible to select the appropriate Q value and particle yield, and to initialize the appropriate calculational routine. This routine will be `sixbar` for all reactions described in File 6, `disbar` for two-body reactions using File 4 (including charged-particle reactions in the 600 or 700 series of MT numbers), `conbar` for continuum reactions represented using File 5, and `capdam` for the neutron disappearance reactions (MT=102, 103, *etc.*) and the charged-particle continuum reactions from the 600 or 700 series of MT numbers. The last step before beginning the energy loop for this reaction is to call `indx`, which determines which element of the `c` array is to receive the heating or damage contribution from this reaction (see below).

The energy loop in `nheat` goes through statement number 190. For each energy, `finda` is called to retrieve the current values for the energy [see `c(1)`] and the partial heating and damage values as accumulated so far. On the first pass through the scratch file, the list of energies to be used for printing information on the listing is established in `elist` using a few `if` statements based on the range of the energy variable `e`. For each energy, the corresponding cross section is retrieved using `gety1` and the appropriate  $\bar{E}$  and damage numbers are computed by calling `getsix`, `disbar`, `conbar`, or `capdam`. The heating contribution is computed from the appropriate formula, and the heating and damage numbers are summed into the `c` array at location `index`. If requested, the kinematic limits on the heating are computed and summed into the `c` array at `index+npk` and `index+2*npk`. The completed results for this energy and reaction are written out onto the `loada/finda` scratch file, and the energy loop is continued.

When the energy loop is complete, the subroutine jumps to the next section (or subsection in the case of File 6) and repeats the entire energy loop for that reaction (or particle from File 6).

Subroutine `indx` is used to select what element of the `c` array is to receive the heating or damage contribution for a section with a particular MT number. The meaning of each element of the `c` array is obtained from the `mtp` array. Normally, a reaction MT contributes to the partial heating element with `mtp(i)=MT+300`. But it can also contribute to several other elements of `c`, such as nonelastic (MT=303), inelastic (MT=304), etc. Therefore, `indx` returns the count of reactions contributed to by `mt` in `nmt` and the indexes for the `c` array in `imt(nmt)`.

Subroutine `capdam` is used to compute the damage energy for neutron capture (or disappearance) reactions; that is, for MT=102, 103, etc. On the initialization entry (`ee=0.0`), the routine sets up various kinematics parameters, such as `zx` and `ax` to describe the outgoing particle, and initializes `df`. In order to save time, the routine only calculates the damage on a grid that increases by steps of 10%. Intermediate values are obtained by interpolation (see `e1`, `dam1`, `en`, and `damn`). The values at the grid points are computed using

$$D \left( \frac{E}{A+1} \right) + D \left( \frac{1}{2M_R c^2} \left[ \frac{AE}{A+1} + Q \right]^2 \right) \quad (218)$$

for radiative capture (the corrections for multiple photon emission will be made later), or using Eq. 201 with  $E_R$  from Eq. 207 and a 4-point Gauss-Legendre quadrature. The angular distribution for particle emission is taken to be isotropic.

Subroutine `disbar` is used by `nheat` to compute the average secondary energy and damage energy for elastic scattering (MT=2), discrete-inelastic scattering (MT=51-90), or discrete-level particle production (MT=600-648, 650-698, etc. for ENDF/B-VI or ENDF/B-VII, or MT=700-717, 720-737, etc. for earlier versions). It starts by initializing `hgtfle` (which is very similar to `getfle` in the GROUPR module), determining kinematic parameters like `awp` (the mass ratio to the neutron for the emitted particle), and initializing `df`. In order to save time, it only computes the heating and damage on a grid based on steps by a factor of 1.1 and the `enext` values from `hgtfle`. On a normal entry, it interpolates between these values (see `e1`, `c1`, `dam1`, `en`, `cn`, and `damn`). When the desired `ee` exceeds `en`, the old high values are moved down to the low positions, and new high values are calculated. The calculation of `cn` follows Eq. 170. The calculation of `damn` uses Eq. 201 with a 20-point Gauss-Legendre quadrature (see `nq`, `qp`, and `qw`).

Function **df** is used to compute the damage partition function given in Eq. 195. The constants that depend on the recoil atom or particle type and lattice type (see **zr**, **ar**, **z1**, **a1**) are computed in an initialization call with **e**=0.0. Thereafter, it can be called with any other value of **e**.

Similarly, **conbar** computes the average secondary energy and damage energy for continuous distributions described in File 5. Analytic representations use simple formulas coded into **anabar** or a combination of adaptive and Gaussian quadrature in **anadam**. Tabulated data are interpolated from the File 5 table using **tabbar** or integrated using trapezoidal and Gaussian quadratures in **tabdam**. As usual, the routine is initialized by calling it with **e**=0.0. The secondary-particle yield is either chosen from the MT number, or **hgtlyd** is initialized. The desired section of File 5 is located on the input ENDF tape, and the kinematic constants are computed. The reactions with MT=22, 28, 32, 33, and 34 will be treated using the **capdam** method; if **mtd** has one of these values (see **mtt**), **capdam** is initialized. As is the case for **getsed** in the **GROUPT** module, this routine can handle some sections of File 5 that contain multiple subsections, but the analytic subsections must come first. As each analytic subsection is read, appropriate data are stored in the external array **c** using pointers saved in the array **loc**. Only the first energy is read and stored for a tabulated subsection (**lf**=1). The idea is to have only two energy values in memory at a time in order to save storage; the second subsection will be read during the first normal entry to the subroutine. The final step in the initialization pass is to initialize **df**. For a normal entry into **conbar**, the energy-dependent fission yield is retrieved, if needed, and the loop over subsections is entered. Each subsection in File 5 starts with a fractional-probability record. The desired value for energy **e** is computed by interpolation using the standard **NJOY** utility routine **terpa**. For analytic subsections, the routine uses **anabar** to compute  $\overline{E_n}$ , and **anadam** or **capdam** to compute the damage energy. Note that in order to save time, **anadam** is only calculated on a fairly coarse grid based on steps by a factor of 1.5. The intermediate values are obtained by interpolation using **terp1**. For tabulated subsections, **ebar** and **dame** values are normally obtained by interpolation (see **elo**, **flo**, **dlo**, **ehi**, **fhi**, and **dhi**). However, for the first entry, or whenever **e** reaches **ehi**, the high data are moved into the low positions, new high data are read from the File 5 subsection, and the values for heating and damage are computed at **ehi** using **tabbar** and either **tabdam** or **capdam**.

Subroutine **hgtlyd** is similar to **getyld** in the **GROUPT** module. It finds the required section on the ENDF tape and reads the entire LIST or TAB1

record into memory. On normal entries, it either computes the yield using the polynomial formula with constants from the LIST record, or it uses **terpa** to interpolate for the yield in the TAB1 data.

Subroutine **anabar** is used to compute the average energy for a neutron described by an analytic subsection of File 5. The simple formulas used are tabulated in the ENDF format manual[8]. Similarly, **anadam** is used to compute the damage energy for an analytic subsection of File 5. Only LF=9 (the Simple Maxwellian Distribution) is supported; the routine returns zero for other laws. Note that a statement function is defined to compute the secondary energy distribution for this law (see **sed**). For each incident energy, the spectrum temperature **theta** is retrieved using **terpa**, and an adaptive integration stack is initialized with points at four secondary energies, namely, 1.,  $.5(E-U)$ ,  $\theta$ , and  $E-U$ , where  $U$  is a parameter that sets the maximum possible value of  $E'$ . The adaptive procedure proceeds to solve Eq. 203 by subdividing this starting grid until trapezoidal integration can be used on each panel. The inner integral over emission cosine  $\mu$  is performed using a 4-point Gauss-Legendre quadrature for each point on the adaptive grid. The function **sed** is used to compute  $g(E')$ , and **df** is used to compute the partition function.

Subroutine **tabbar** is used to compute the average energy of the emitted neutron for a tabulated subsection of File 5. It can also be used for a tabulated subsection of File 6. This option is flagged by **law** negative. The trick is to set the “stride” or “cycle” through the file to be larger than 2 (see **ncyc**). The angular part of the  $g(E \rightarrow E')$  table is skipped, and only the  $E'$  and  $g$  values are retrieved. For File 5, this routine only works for laws 1 and 5; others cause a fatal error message to be issued. In both of these cases, the integral over  $E'$  needed to compute the average energy is done analytically for each panel in the input data using a different formula for each interpolation scheme **int**.

Subroutine **tabdam** is used to compute the damage energy for a tabulated subsection of File 5. The integration that is needed is given in Eq. 203. The energy grid of the tabulation is assumed to be good enough to allow trapezoidal integration to be used for  $E'$ , and a 4-point Gauss-Legendre quadrature is used for  $\mu$ .

Subroutine **sixbar** is used to compute charged-particle average energy and damage energy represented by using a subsection of File 6. As is common with NJOY subroutines, **sixbar** is initialized by calling it with **e**=0.0. The initialization path is controlled by **j6**, which is the index to the current subsection in File 6; by **irec**, which is 1 when a recoil response is to be calculated, and by

`jrec`, which tells the routine how to get back to the next subsection after a recoil calculation. If this is not a recoil subsection, the routine jumps to statement 110 and starts reading in the data for the desired subsection. If it is flagged as a recoil (see `irec`), the routine backs up to the subsection describing the particle that induced the recoil and then continues by reading in the data for that particle.

The first step is to read in the TAB1 record that contains the particle yield, identity (`zap` and `awp`), and representation `law`. If this law describes a two-body recoil distribution, the routine sets `jrec` for a proper return, sets `irec` to back up to the corresponding direct emission subsection, and jumps back to the beginning of the routine to do the recoil calculation.

When the code finally arrives at statement number 210, it is ready to start processing the current subsection. It reads in the parameters for laws 3 and 6, or the TAB2 record and the data for the first energy point for the other laws. With the data in place, it computes the corresponding values for mean energy and damage energy using `getsix` or `tabsq6` and returns.

In the special case where the section contains only a single subsection that describes a neutron, the data stored in memory will be the data for that subsection, and the subroutine `tabbar` with a negative value for the law is used to produce the low values.

On a normal entry (`e>0`), `sixbar` checks to see whether `e` is in the current interpolation range. If it is, the code jumps to statement number 400. For the analytic laws (`law=3` and `law=6`), it uses a direct call to `getsix` to compute the mean energy and damage energy. For the tabulated laws, it interpolates for the results using the low and high data (see `elo`, `flo`, `dlo`, `ehi`, `fhi`, and `dhi`). On the first entry, or whenever `e` increases to `ehi`, the code moves the high data to the low positions, and then it reads in the data for the next energy and computes a new set of high values for mean energy and damage using `getsix` or `tabsq6`.

Subroutine `getsix` is used to compute the mean energy and damage energy for one particular incident energy in a subsection of File 6. The method used depends on the value of `law` and the reference frame for the subsection. The first case in the coding is for `law=1` with data in the CM system.

This case uses Eqs. 213 and 214 with an adaptive integration over  $E'$ . The integration stack is contained in the arrays `x` and `y`. It is primed with `x(2)=0`, and `h6cm` is called to compute `y(2)` and the next grid point `epnext`. The first panel is completed by calculating `y(1)` and `x(1)=epnext`. The panel is then



divided in half, and the midpoint is tested to see if it is within `tol=0.02` (*i.e.*, 2%) of the linearly interpolated value. If not, the midpoint is inserted in `x` and `y`, and the new top panel [that is `x(2)-x(3)`] is tested. This continues until convergence is achieved in the top panel. The contributions to the heating and damage are added into the accumulating integrals at statement number 190, and `i` is decremented so that the process can be repeated for the next panel down. When `i` decreases to one, the current value of `epnext` is used to start the next higher  $E'$  panel. This loop over panels continues until the entire  $E'$  range has been integrated.

The next special case is for tabulated distributions that use  $E$ ,  $E'$ ,  $\mu$  ordering in the lab system. The angular part is ignored. A simple loop over the NEP points in  $g(E \rightarrow E')$  is carried out. Trapezoidal integration is used for each panel for both heating and damage (`h` and `d`). If `nd>0`, the first `nd` entries are discrete energies, and the values of the integrand at those energies are added into `h` and `d`. Finally, `h` and `d` are copied into `ebar` and `dame`.

The block of coding starting at statement number 450 is used to compute particle mean energies for the emitted particles from two-body reactions, or to compute the mean recoil energy for a two-body reaction (see `irec>0`). The calculation follows Eq. 211. Note that the kinematic factors include `awp`, the mass ratio of the emitted particle to the incident particle. The parameter `beta` here is the same as  $R$  in Eq. 212. If the angular distribution in File 6 is in Legendre form, the heating and damage integrals are performed using a 20-point Gauss-Legendre quadrature (see `nq`, `qp`, and `qw`). If the angular distribution is tabulated as  $f(\mu)$  versus  $\mu$ , a trapezoidal integration is used for both heating and damage.

The final option in `getsix` is for lab distributions that use  $E$ ,  $\mu$ ,  $E'$  ordering. See Eq. 215. The inner integrals are computed using trapezoidal integration. The outer integral over  $\mu$  also uses trapezoidal integration on the results of the inner integrals for each  $\mu$  grid point.

Note that `getsix` has an `irec` parameter in its calling list. When this parameter is greater than zero, the angular distribution is complemented and the charge and mass of the particle are modified to represent the recoil species. The value of `irec` is controlled by `sixbar`.

Subroutine `h6cm` is used by `getsix` to compute the lab distribution  $g(E \rightarrow E'_L)$  of Eq. 216 using the CM data in File 6. This subroutine uses `h6dis`, `h6ddx` and `h6psp` to retrieve the CM discrete, tabulated or phase-space data from the file.

These routines are basically the same as `f6cm`, `f6dis`, `f6ddx` and `f6psp`. See [GROUPE](#) for more details.

Subroutine `gheat` is used to correct the heating and damage values accumulated during the pass through the neutron sections. It loops through all of the reactions in File 12 and File 13 using two ENDF-type tapes. One is the input PENDF tape, which is used to retrieve cross sections for use with the photon multiplicities in File 12. The other is a version of the input ENDF tape that has been passed through `hconvr` to put the photon data in a standard form (see Chapter 8 ([GROUPE](#)) of this manual for a more detailed discussion of `conver`). This scratch tape is used to retrieve the File 12 and File 13 data. It is very common to find reaction MT=3 (nonelastic) in File 12, but this reaction has been removed from the PENDF tape because it is redundant; that is, it is equal to MT1–MT2. Therefore, two passes are made through the File 12 data for MT=3, an addition pass with MT=1 from the PENDF tape, and a subtraction pass with MT=2 from the PENDF tape. Once the desired sections on the two tapes have been found, the subroutines `gambar`, `capdam`, and `disgam` are initialized.

The energy loop for `gheat` goes through statement number 190. For each energy, `finda` is used to retrieve the partial KERMA factors as computed from the pass through the neutron files. The yield or cross section is retrieved using `gety1` into the variable `y`. If necessary, the corresponding cross section `x` is retrieved using `gety2`. For cases where an energy-dependent  $Q$  is available, it is retrieved using `terp1` on the data stored at `lqx`. The next two lines correct the energy of “primary” photons (`lp=2`).

For radiative capture represented in File 12 (MT=102), `gambar`, `disgam`, and/or `capdam` are called to return  $\overline{E}_\gamma$  and  $\overline{E}_\gamma^2/(2m_Rc^2)$  for this photon spectrum or discrete photon and to correct the heating and values in the `c` array using Eq. 173 and the second line of Eq. 206. The capture contribution to the total photon eV-barns is added into `c(npkk-1)` and the photon energy yield is loaded into `c(npkk)` for each subsection. When the last subsection is reached, the capture energy check is made using this subtotal. Note that the capture error is loaded into `c(npkk-2)` for later use in calculating the kinematic limits for photon energy production.

For other photon-production reactions, the photon eV-barns contribution is subtracted from the energy-balance heating position, added into the total photon energy value in `c(npkk-1)`, and added into `c(npkk)` for the subtotal for a section with multiple subsections. After all the corrections have been completed for this

energy, the revised values are written out using `loada`. The code then moves on to the next reaction and repeats the entire process.

When the reaction loop has been finished, `gheat` checks to see if it can print out a photon energy production check. It can do this if kinematic checks have been requested and if MT=303 was requested in the user's list of partial KERMA calculations. The code reads through the `loada/finda` file one more time. For each energy in `elist`, it prints out the total photon eV-barns from `c(npkk-1)` and the kinematic limits `elo` and `ehi`. If the limits are violated by more than 10%, alarms consisting of the strings `++++` or `----` are printed after the eV-barns values.

Subroutine `gambar` is used to compute the mean energy for continuous photon spectra and the photon recoil correction for capture. When called with `e=0.0`, it locates the desired section of File 15 on the ENDF tape and reads in the first incident energy. On a normal entry, it checks to see if `e` is in the range of the data already computed (`elo`, `ehi`, etc.), and if so, it interpolates for the desired results. If not (or on the first real entry), it moves the high data down to the low positions, reads in the next energy from File 15, prepares new values at the new `ehi`, and checks the energy range again. The photon `ebar` is returned by `tabbar`, and the corrections to the heating value (`esqb`) and damage value (`esqd`) from photon production are generated using `tabsqr`.

Subroutine `tabsqr` is used to compute the average recoil energy

$$\frac{\overline{E_\gamma^2}}{2M_R c^2} \quad (219)$$

for radiative capture for a tabulated subsection of File 15. The corresponding damage energy is computed at the same time. The basic secondary-energy integral is over the panels defined by the grid points given in File 15. Inside each panel, the integral is computed using a 4-point Gauss-Legendre quadrature.

Subroutine `disgam` is used to compute the  $\overline{E_\gamma^2}$  and corresponding damage energy for a discrete capture photon. The rest-mass constant is computed by calling `disgam` once with `e=0`.

Subroutine `hout` writes the new PENDF tape with the desired heating and damage MT numbers added. It also corrects the directory in MF=1/MT=451, and it prepares the output listing for printing. The first step is to loop through the partial KERMA factors requested and to write the data on the `loada/finda` file onto a scratch tape in ENDF File 3 format. While the first partial is being prepared, the code matches energies in `c(1)` against the energy list for printing

in `elist`. When a match is found, the partial KERMA factors are checked against the kinematic limits, and the variables `klo` or `khi` are set if any of the comparisons are out of bounds. The KERMA factors, kinematic limits, and error flags are then printed on the output listing. When all of the new sections for File 3 have been prepared, the code updates the contents of the File 1 directory. It then loops through the rest of the input PENDF tapes copying sections to the output and inserting the new sections in the appropriate places. When the new PENDF file has been completed, `hout` makes `VIEWR` input for a set of plots showing the total heating and the photon production compared to their kinematic limits in both lin-lin and log-log forms. The lin-lin plots show the high-energy range better, and the log-log plots expand the low-energy range.

### 6.11 Error Messages

`error in heatr***requested too many kerma mts`

6 values in addition to MT=301 are allowed with kinematic checks; otherwise, 25 can be requested. See `npkmax=28`. When checks are requested, the number of words needed is  $3*\text{npk}+7$ ; otherwise,  $\text{npk}+3$  are needed.

`error in heatr***requested too many q values`

Limited to 30 by the global parameter `nqamax=30`.

`error in heatr***too much energy-dependent q data`

Limited to `maxqbar=10000`.

`error in heatr***mode conversion not allowed...`

Both units must be BCD (positive) or blocked binary (negative).

`error in hinit***too many mf6 reactions`

A maximum of 320 reactions are allowed. See the global parameter `maxmf6=320`.

`message from heatr---mt301 always calculated`

MT=301 was given in the input list of partial KERMA factors. This is not necessary; it is always inserted automatically.

`message from hinit---mf4 and 6 missing, isotropy...`

Cross sections were found for charged-particle levels in the 600 or 700 series of MT numbers, but no corresponding angular distributions were found. Isotropy is assumed to enable the calculation to proceed, but this evaluation should be upgraded to include the proper sections of File 4 or 6.

`message from hinit---mt18 is redundant...`

If MT=19 is present, MT=18 will be ignored.

`message from hinit---mt19 has no spectrum...`

In some evaluations, the partial fission reactions MT=19, 20, 21, and 38 are given in File 3, but no corresponding distributions are given. In these

cases, it is assumed that MT=18 should be used for the fission neutron distributions.

message from hinit---mt458 is missing for this mat

The fission Q value cannot be adjusted for delayed effects.

message from hinit---photon momentum recoil used

message from hinit---one-particle recoil approx. used

message from nheat---changed Q from --- to ---

The fission Q value is adjusted from the total (non-neutrino) value given in File 3 to a prompt value using the delayed neutron energy from MF=1/MT=458.

error in nheat\*\*\*binding energy for sequential...

The user must enter special Q values for the ENDF/B evaluation for  $^9\text{Be}$ . See the discussion in Section 6.7.

error in nheat\*\*\*storage exceeded

Insufficient storage for diagnostic energy grid. See the global parameter ilmax=100 at the start of the module.

error in conbar\*\*\*nktot gt nkmax

More than 12 subsections found. See the parameter nkmax=12.

error in conbar\*\*\*insufficient storage for raw endf...

The allocatable array a in nheat is too small. Increase na=10000.

error in hgtyld\*\*\*storage exceeded

Increase nwmax in nheat. Currently 7000.

error in tabbar\*\*\*coded for lf=1 and lf=5 only

Self-explanatory. Should not occur.

message from sixbar---no distribution for mt --- ...

The ENDF-6 format allows the evaluator to describe a subsection of File 6 with "law=0"; that is, no distribution is given. Such sections are fine for giving particle yields for gas production and similar applications, but they are not adequate for computing heating and damage.

error in h6ddx\*\*\*too many legendre terms

See nlmax=65 in h6ddx.

error in h6ddx\*\*\*illegal lang

The allowed values for the angular law flag are 1, 2, and 11–15.

message from h6ddx---vertical segment(s) in distribution...

The distribution contains some discontinuities that make  $y(x)$  ill-defined. The second point is moved up slightly.

error in h6dis\*\*\*illegal lang

The allowed values for the angular law flag are 1, 2, and 11–15.

error in bacha\*\*\*dominant isotope not known for...

The Kalbach-systematics approach to computing angular distributions for particle emission requires the separation energy as computed by the liquid drop model. If the target for an evaluation is an element, it is necessary to choose a dominant isotope that adequately represents the effect for this element. Dominant isotopes for materials often evaluated as elements are given in if statements in this routine. If the desired value is missing, it must be added, and NJOY will have to be recompiled. See the corresponding routines in [GROUPE](#) and [ACER](#) as well.

error in h6psp\*\*\*3, 4, or 5 particles only

The phase-space law is defined for 3, 4, or 5 particles only.

message from hgtfile---lab distribution changed to cm...

ENDF procedures require that two-body reactions be described in the CM system. Some earlier evaluations claim to be in the lab system. However, they are for relatively heavy targets, and changing to the CM frame will cause only a small change in the results.

error in hgtfile\*\*\*desired energy above highest energy...

Fault in the evaluation.

error in getco\*\*\*limited to 64 legendre coefficients

The upgraded ENDF limit.

error in getco\*\*\*lab to cm conversion not coded

Discrete scattering data should be in the CM system already.

message from hconvr---gamma prod patch made for mt ---

This reflects some problems in the old ENDF-III evaluations for Cl and K, which were also carried over to later ENDF versions.

error in hconvr\*\*\*too many lo=2 gammas

See lmax=500.

error in hconvr\*\*\*exceeded storage for nubar

See nnu=6000.

error in gheat\*\*\*lo=2 not coded

Will not occur since lo=2 data have been transformed to lo=1 format by hconvr.

message from gheat---no file 12 for this material

Information only.

message from gheat---skipping ... processed in mf6

NJOY has found photon data for a given mt in both mf6 and mf12 - mf15. Only the mf6 data are used.

error in gambar\*\*\*storage exceeded in a

Increase nd=10000 in gheat.

error in gambar\*\*\*requested energy gt highest given

Probably reflects an error in the evaluation.

### 6.12 Storage Allocation

Allocatable arrays are used for most large data blocks. Storage requirements are dominated by the length of File 5 or File 15 for the evaluation. The `loada/finda` buffer size `nbuf` may be decreased or increased at will. The code is currently dimensioned as follows:

|       |                                                       |
|-------|-------------------------------------------------------|
| 100   | coarse grid points                                    |
| 30    | auxiliary Q values                                    |
| 25    | partial KERMA (7 when kinematic limits are requested) |
| 10000 | words of energy-dependent Q data                      |
| 10000 | maximum for File 5 or 15 raw data                     |
| 7000  | maximum for fission yield data                        |
| 320   | File 6 reactions                                      |





## 7 THERMR

The THERMR module generates pointwise neutron scattering cross sections in the thermal energy range and adds them to an existing PENDF file. The cross sections can then be group-averaged, plotted, or reformatted in subsequent modules. THERMR works with either the original ENDF/B-III thermal format[50] and data files[51] (which were also used for ENDF/B-IV and -V), or the newer ENDF-6 format[8]. Coherent elastic cross sections are generated for crystalline materials using either parameters given in an ENDF-6 format evaluation or an extended version of the method of HEXSCAT[31]. Incoherent elastic cross sections for non-crystalline materials such as polyethylene and ZrH can be generated either from parameters in an ENDF-6 format file or by direct evaluation using parameters included in the THERMR coding. Inelastic cross sections and energy-to-energy transfer matrices can be produced for a gas of free atoms, or for bound scatterers when ENDF  $S(\alpha, \beta)$  scattering functions are available. This function has previously been performed using FLANGE-II[30]. THERMR has the following features:

- The energy grid for coherent elastic scattering is produced adaptively so as to represent the cross section between the sharp Bragg edges to a specified tolerance using linear interpolation.
- The secondary energy grid for inelastic incoherent scattering when using  $E$ - $E'$ - $\mu$  ordering is produced adaptively so as to represent all structure with linear interpolation. Discrete-angle representations are used to avoid the limitations of Legendre expansions.
- An option to use  $E$ - $\mu$ - $E'$  ordering is available. Dependences on  $\mu$  and  $E'$  are constructed adaptively.
- Incoherent cross sections are computed by integrating the incoherent distributions for consistency.
- Free-atom incoherent scattering is normalized to the Doppler broadened elastic scattering cross section in order to provide an approximate representation of resonance scattering and to preserve the correct total cross section.
- Hard-to-find parameters for the ENDF/B-III evaluations are included in the code for the user's convenience.
- ENDF-6 format files can be processed. This gives the evaluator more control over the final results, because all parameters needed to compute the cross sections are contained in the file.

This report describes THERMR in NJOY 2012.0. The differences from the previously reported version[3] are related to the change to Fortran-90 style and

memory allocation, to the addition of the  $E$ - $\mu$ - $E'$  ordering option, and to changes in the energy grid for free-gas scattering at high temperatures.

### 7.1 Coherent Elastic Scattering

In crystalline solids consisting of coherent scatters — for example, graphite — the so-called “zero-phonon term” leads to interference scattering from the various planes of atoms of the crystals making up the solid. There is no energy loss in such scattering, and the ENDF term for the reaction is coherent elastic scattering. The cross section may be represented as follows:

$$\sigma^{\text{coh}}(E, E', \mu) = \frac{\sigma_c}{E} \sum_{E_i > E} f_i e^{-2W E_i} \delta(\mu - \mu_0) \delta(E - E') , \quad (220)$$

where

$$\mu_0 = 1 - 2 \frac{E_i}{E} , \quad (221)$$

and the integrated cross section is given by

$$\sigma^{\text{coh}} = \frac{\sigma_c}{E} \sum_{E_i > E} f_i e^{-2W E_i} . \quad (222)$$

In these equations,  $E$  is the incident neutron energy,  $E'$  is the secondary neutron energy,  $\mu$  is the scattering cosine in the laboratory (LAB) reference system,  $\sigma_c$  is the characteristic coherent cross section for the material,  $W$  is the effective Debye-Waller coefficient (which is a function of temperature), the  $E_i$  are the so-called “Bragg edges”, and the  $f_i$  are related to the crystallographic structure factors.

It can be seen from Eq. 222 and the example in Fig. 16 that the coherent elastic cross section is zero before the first Bragg edge,  $E_1$  (typically about 2 to 5 meV). It then jumps sharply to a value determined by  $f_1$  and the Debye-Waller term. At higher energies, the cross section drops off as  $1/E$  until  $E=E_2$ . It then takes another jump and resumes its  $1/E$  drop-off. The sizes of the steps in the cross section gradually get smaller, and at high energies there is nothing left but an asymptotic  $1/E$  decrease (typically above 1 to 2 eV).

For evaluations in the ENDF-6 format, the section MF=7/MT=2 contains the quantity  $E\sigma^{\text{coh}}(E)$  as a function of energy and temperature. The energy dependence is given as a histogram with breaks at the Bragg energies. The cross section is easily recovered from this representation by dividing by  $E$ . The

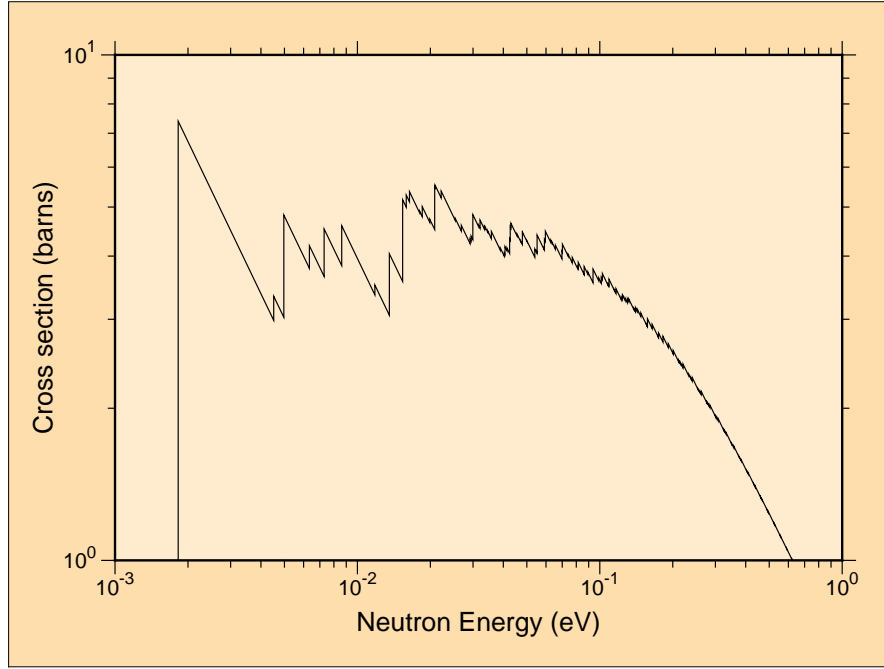


Figure 16: Typical behavior of the coherent elastic scattering cross section for a crystalline material as computed by THERMR. This cross section is for graphite at 293.6K.

$E_i$  are easily found as the tabulation points of the function, and the  $f_i$  for a point can be obtained by subtracting the value at the previous point.

For evaluations using the older ENDF/B-III thermal format, it is necessary to compute the  $E_i$  and  $f_i$  in THERMR. The methods used are based on HEXSCAT and work only for the hexagonal materials graphite, Be, and BeO. The Bragg edges are given by

$$E_i = \frac{\hbar^2 \tau_i^2}{8m}, \quad (223)$$

where  $\tau_i$  is the length of the vectors of one particular “shell” of the reciprocal lattice, and  $m$  is the neutron mass. The  $f_i$  factors are given by

$$f_i = \frac{\pi^2 \hbar^2}{2mNV} \sum_{\text{shell}} |F(\tau)|^2, \quad (224)$$

where the shell sum extends over all reciprocal lattice vectors of the given length,  $N$  is the number of atoms in the unit cell, and  $F$  is the crystallographic structure factor. The calculation works by preparing a sorted list of precomputed  $\tau_i$  and  $f_i$  values. As  $\tau_i$  gets large, the values of  $\tau_i$  get more and more closely spaced. In order to save storage and run time, a range of  $\tau$  values can be lumped together

to give a single effective  $\tau_i$  and  $f_i$ . This device washes out the Bragg edges at high energies while preserving the proper average cross section and angular dependence. The current grouping factor is 5% (see `eps` in `sigcoh`).

Lattice constants (given in `sigcoh` for graphite, Be, and BeO), form factor formulas (see `form`), Debye-Waller coefficients, and methods for computing reciprocal lattice vectors were borrowed directly from HEXSCAT.

The energy grid for  $E$  is obtained adaptively (see `coh`). A panel extending from just above one Bragg edge to just below the next higher edge is subdivided by successive halving until linear interpolation is within a specified fractional tolerance (`tol`) of the exact cross section at every point. This procedure is repeated for every panel from the first Bragg edge to the specified maximum energy for the thermal treatment (`emax`).

The code usually computes and writes out the cross section of Eq. 222, the average over  $\mu$  of Eq. 220, which is sometimes called the  $P_0$  cross section. Subsequent modules can deduce the correct discrete scattering angles  $\mu_0$  from the location of the Bragg edges  $E_i$  and the factors  $f_i$  from the cross section steps at the Bragg edges (see `GROUPE`). Legendre cross sections can also be computed by making a small change to the code. It is not necessary to give the  $P_1$ ,  $P_2$ , and  $P_3$  cross sections explicitly as was done in some earlier codes or in File 4 of the ENDF thermal tapes.

## 7.2 Incoherent Inelastic Scattering

In ENDF/B notation, the thermal incoherent scattering cross section is given by

$$\sigma^{\text{inc}}(E, E', \mu) = \frac{\sigma_b}{2kT} \sqrt{\frac{E'}{E}} e^{-\beta/2} S(\alpha, \beta) , \quad (225)$$

where  $E$  is the initial neutron energy,  $E'$  is the energy of the scattered neutron,  $\mu$  is the scattering cosine in the laboratory system,  $\sigma_b$  is the characteristic bound incoherent cross section for the nuclide,  $T$  is the Kelvin temperature,  $\beta$  is the dimensionless energy transfer,

$$\beta = \frac{E' - E}{kT} , \quad (226)$$

$\alpha$  is the dimensionless momentum transfer,

$$\alpha = \frac{E' + E - 2\mu\sqrt{EE'}}{AkT} , \quad (227)$$

$k$  is Boltzmann's constant, and  $A$  is the ratio of the scatter mass to the neutron mass. The bound scattering cross section is usually given in terms of the characteristic free cross section,  $\sigma_f$ ,

$$\sigma_b = \sigma_f \frac{(A+1)^2}{A^2} . \quad (228)$$

The scattering law  $S(\alpha, \beta)$  describes the binding of the scattering atom in a material. For a free gas of scatterers with no internal structure

$$S(\alpha, \beta) = \frac{1}{\sqrt{4\pi\alpha}} \exp \left\{ -\frac{\alpha^2 + \beta^2}{4\alpha} \right\} . \quad (229)$$

For binding in solids and liquids,  $S(\alpha, \beta)$  for a number of important moderator materials is available in ENDF/B File 7 format. The scattering law is given as tables of  $S$  versus  $\alpha$  for various values of  $\beta$ . Values of  $S$  for other values of  $\alpha$  and  $\beta$  can be obtained by interpolation. The scattering law is normally symmetric in  $\beta$  and only has to be tabulated for positive values, but for materials like orthohydrogen and parahydrogen of interest for cold moderators at neutron scattering facilities, this is not true. These kinds of materials are identified by the ENDF-6 LASYM option, and THERMR assumes that the scattering law is given explicitly for both positive and negative values of  $\beta$ .

If the  $\alpha$  or  $\beta$  required is outside the range of the table in File 7, the differential scattering cross section can be computed using the short collision time (SCT) approximation

$$\sigma^{\text{SCT}}(E, E', \mu) = \frac{\sigma_b}{2kT} \frac{\sqrt{E'/E}}{\sqrt{4\pi\alpha T_{\text{eff}}/T}} \exp \left\{ -\frac{(\alpha - |\beta|)^2}{4\alpha} \frac{T}{T_{\text{eff}}} - \frac{\beta + |\beta|}{2} \right\} , \quad (230)$$

where  $T_{\text{eff}}$  is the effective temperature for the SCT approximation. These temperatures are available[51] for the older ENDF/B-III evaluations; they are usually somewhat larger than the corresponding Maxwellian temperature  $T$ . For the convenience of the user, the values of  $T_{\text{eff}}$  for the common moderators are included as defaults (see input instructions). For the newer ENDF-6 format, the effective temperatures are included in the data file. However, there is a complication. Some evaluations give  $S(\alpha, \beta)$  for a molecule or compound (in the ENDF/B-III files, these cases are BeO and C<sub>6</sub>H<sub>6</sub>). The corresponding SCT approximation must contain terms for both atoms. The two sets of bound cross sections and effective temperatures are included in the data statements in THERMR, and they can be given in the new ENDF-6 format if desired.

THERMR expects the requested temperature  $T$  to be one of the temperatures included on the ENDF/B thermal file, or within a few degrees of that value (296K is used if 300K is requested). Intermediate temperatures should be obtained by interpolating between the resulting cross sections and not by interpolating  $S(\alpha, \beta)$ .

The cross sections for incoherent inelastic scattering are computed in the `calcem` subroutine. There are two possible orderings of the basic variables allowed (see `iform`). For  $E-E'-\mu$  ordering, the secondary energy grid for incoherent scattering is obtained adaptively. A stack is first primed with the point at zero and the first point above zero that can be derived from the positive and negative values of  $\beta$  from the evaluator's  $\beta$  grid using Eq. 226. (For free-gas scattering, the  $\beta$  grid is taken to have nine entries between 0.0 eV and 25.0 eV). This interval is then subdivided by successive halving until the cross section obtained by linear interpolation is within the specified tolerance of the correct cross section (from `sig1`). The next highest energy derived from the  $\beta$  grid is then calculated, and the subdivision process is repeated for this new interval. This process is continued until the  $\beta$  grid has been exhausted. Excess points with zero cross section are removed before writing the spectrum into File 6. This procedure is sure to pick up all the structure in the evaluation; giving points related to the  $\beta$  grid avoids excessive work in trying to fit sharp corners introduced by breaks in the interpolation of  $S(\alpha, \beta)$ . Fig. 17 shows how the procedure picks up features resulting from the sharp excitation features in the graphite phonon frequency distribution.

The result of this adaptive reconstruction is easily integrated by the trapezoid rule to find the incoherent cross section at energy  $E$ .

The cross section for one particular  $E \rightarrow E'$  is the integral over the angular variable of Eq. 225. The angular dependence is obtained by adaptively subdividing the cosine range until the actual angular function (see `sig`) is represented by linear interpolation to within a specified tolerance. The integral under this curve is used in calculating the secondary-energy dependence as described above. Rather than providing the traditional Legendre coefficients, THERMR divides the angular range into equally probable cosine bins and then selects the single cosine in each bin that preserves the average cosine in the bin. These equally probable cosines can be converted to Legendre coefficients easily when producing group constants, and they are suitable for direct use in Monte Carlo codes. For strongly peaked functions, such as scattering for  $E \gg kT$  when the result begins to look “elastic”, all the discrete angles will be bunched together near

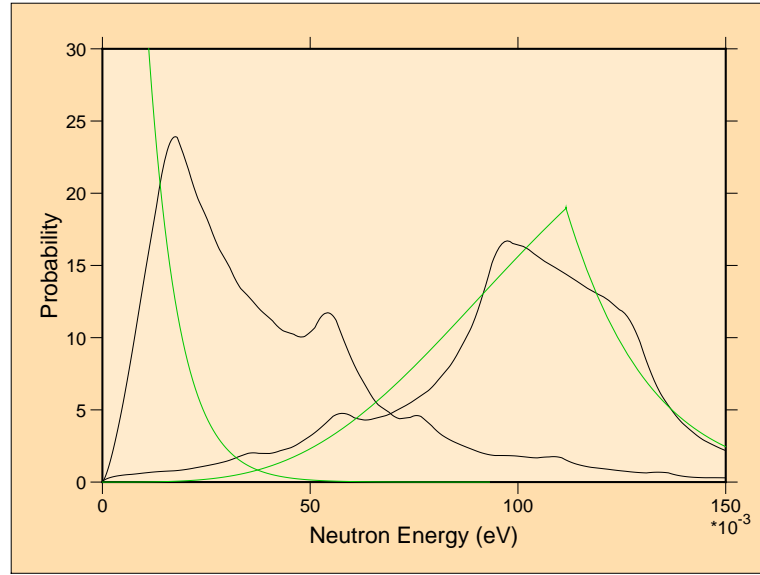


Figure 17: Adaptive reconstruction of two of the emission curves for graphite at 293.6K ( $E=.00016$  eV to the left, and  $E=.1116$  eV to the right). Note the presence of excitation features from the phonon frequency spectrum for both upscatter and downscatter. The breaks in the curves are due to  $\beta$  interpolation in  $S(\alpha, \beta)$  and not to the tolerances in the reconstruction process. The green curves are the corresponding free gas results.

the scattering angle defined by ordinary kinematics. This behavior cannot be obtained with ordinary  $P_3$  Legendre coefficients. Conversely, if such angles are converted to Legendre form, very high orders can be used. If a direct calculation of Legendre components is desired, reverse the sign of `nnl` in `calcem`.

The incident energy grid is currently stored directly in the code (see `egrid` in `calcem`). The choice of grid for  $\sigma^{\text{inc}}(E)$  is not critical since the cross section is a slowly varying function of  $E$ . However, the energy grid would seem to be important for the emission spectra. In order to demonstrate the problem, two perspective plots of the full energy distribution of incoherent inelastic scattering from graphite at 293.6K are shown in Figs. 18 and 19. The second plot is simply an expansion of the high-energy region of the distribution.

It is clear that  $\sigma^{\text{inc}}(E, E')$  for one value of  $E'$  is a very strongly energy-dependent function for the higher incident energies. However, as shown in Fig. 19, the shape of the secondary energy distribution changes more slowly, with the peak tending to follow the line  $E'=E$ . This behavior implies that a relatively coarse incident energy grid might prove adequate if a suitable method is used to interpolate between the shapes at adjacent  $E$  values. One such in-

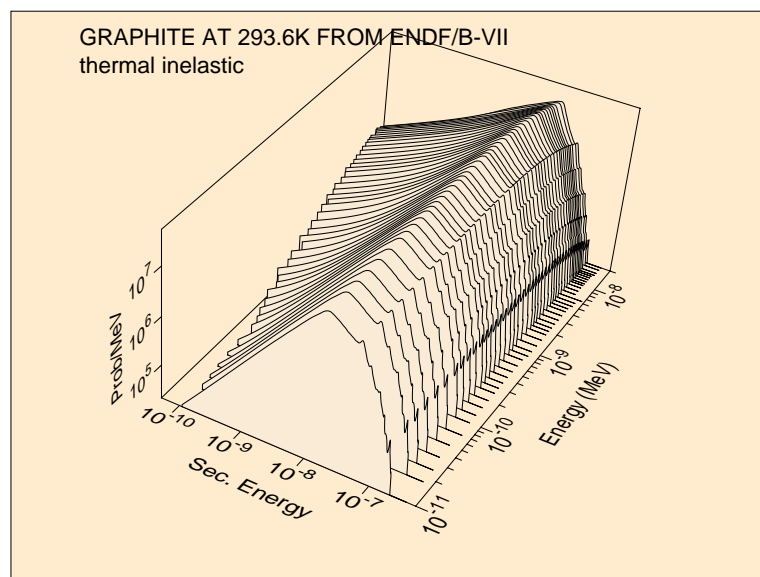


Figure 18: Neutron distribution for incoherent inelastic scattering from graphite ( $T = 293.6\text{K}$ ).

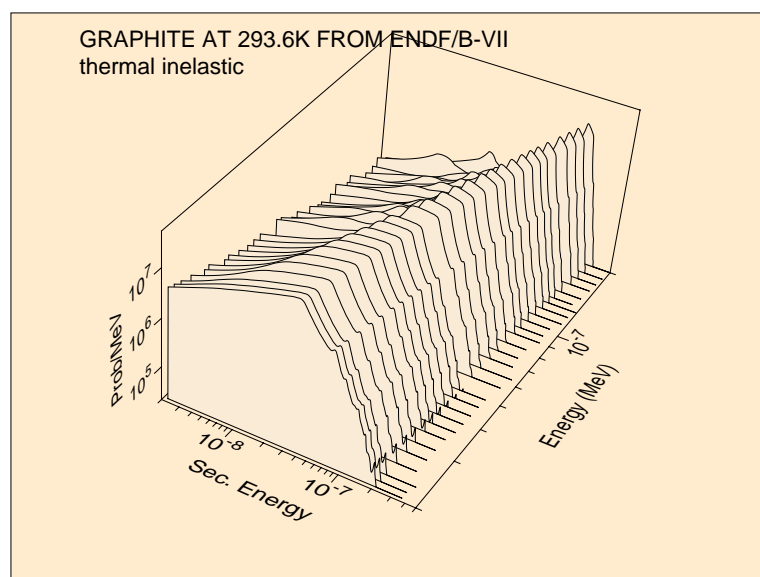


Figure 19: Expanded view of the high-energy region of the graphite incoherent inelastic distribution.

terpolation scheme is implemented in [GROUPR](#). The use of discrete angles is especially suitable for this interpolation scheme.

Strictly speaking, the scattering law for free-gas scattering given in Eq. [229](#) is only applicable to scatterers with no internal structure. However, many ma-



materials of interest in reactor physics have strong scattering resonances in the thermal range (for example,  $^{240}\text{Pu}$  and  $^{135}\text{Xe}$ ). The Doppler broadened elastic cross section produced by BROADR is formally correct for a gas of resonant scatterers, but the cross section resulting from Eq. 229 is not. In order to allow for resonance scattering in a way that at least provides the correct total cross section, THERMR renormalizes the free-atom scattering to the broadened elastic cross section. The secondary energy distribution will still be incorrect.

The built-in grid for incident neutron energies is suitable for normal temperatures found in reactors. For higher temperatures (higher than `break=3000`), the grid values are scaled up to span the kinds of energies expected.

If the  $E$ - $\mu$ - $E'$  option is selected (`iform=1`), an adaptive reconstruction of the angular cross section  $\sigma(E, \mu)$  is performed. For each  $\mu$  value, the secondary energy spectrum is generated adaptively, and the integral over that spectrum is saved as  $\sigma(E, \mu)$ . The results are written out using the ENDF-6 format File 6/law 7 option. This ordering is more like the results of experiments, and the THERMR results can be used to compare to experiment. See Fig. 20 for a figure based on this kind of ordering.

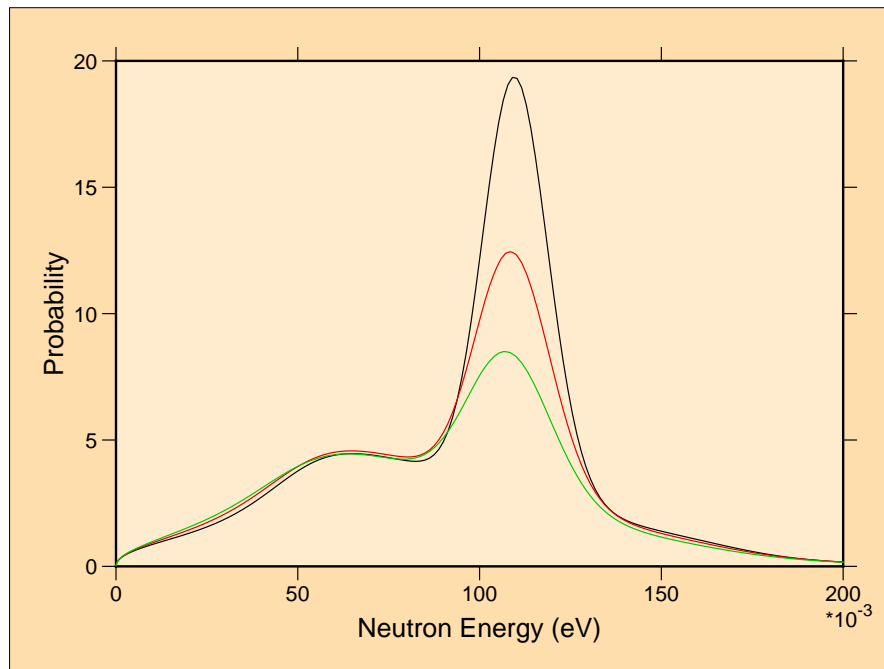


Figure 20: Example of distributions for H in  $\text{H}_2\text{O}$  with  $E$ - $\mu$ - $E'$  ordering. The incident energy is 0.115 eV. The black curve is at 51.3 deg, the red curve is at 60 deg, and the green curve is at 68 deg.

### 7.3 Incoherent Elastic Scattering

In hydrogenous solids, there is an elastic (no energy loss) component of scattering arising from the zero-phonon term that can be treated in the incoherent approximation because of the large incoherent cross section of hydrogen. The ENDF term for this process is incoherent elastic scattering, and it is found in the materials polyethylene and zirconium hydride. The differential cross section is given by

$$\sigma^{\text{iel}}(E, E', \mu) = \frac{\sigma_b}{2} e^{-2WE(1-\mu)} \delta(E - E') , \quad (231)$$

where  $\sigma_b$  is the characteristic bound cross section and  $W$  is the Debye-Waller coefficient. The energy grid of the elastic cross section is used for  $E$ , and the average cross section and equally probable angles are computed using

$$\sigma^{\text{iel}}(E) = \frac{\sigma_b}{2} \left\{ \frac{1 - e^{-4WE}}{2WE} \right\} , \quad (232)$$

and

$$\begin{aligned} \bar{\mu}_i &= \frac{N}{2WE} \left[ e^{-2WE(1-\mu_i)} (2WE\mu_i - 1) \right. \\ &\quad \left. - e^{-2WE(1-\mu_{i-1})} (2WE\mu_{i-1} - 1) \right] / (1 - e^{-4WE}) , \end{aligned} \quad (233)$$

where

$$\mu_i = 1 + \frac{1}{2WE} \ln \left[ \frac{1 - e^{-4WE}}{N} + e^{-2WE(1-\mu_{i-1})} \right] \quad (234)$$

is the upper limit of one equal probability bin and  $\bar{\mu}_i$  is the selected discrete cosine in this bin. Here  $N$  is the number of bins and  $\mu_0$  is  $-1$ .

The characteristic bound cross sections and the Debye-Waller coefficients can be read from MF=7/MT=2 of an ENDF-6 format evaluation, or obtained directly from data statements in the code for the older format.

### 7.4 Coding Details

The `thermr` routine comes from module `thrmr`. The procedure begins with the reading of the user's input. The required ENDF tape (`nendf`) is only used for MF=7 data; it can be set to zero if only free-gas scattering is needed. Similarly, `matde` is the material number for the File 7 tape and can be set to zero for

free-atom problems. The ENDF File 7 format only gives “ $M_0 \sigma_{f0}$ ”, the product of the free scattering cross section for the principal scatterer and the number of principal scatterer atoms in the molecule. As a result, THERMR needs the parameter **natom** to obtain the effective microscopic cross section (for example, for H in H<sub>2</sub>O, use **natom**=2). For ENDF/B-III format files, default parameters are supplied for mixed moderators (BeO and benzene) and effective temperatures, if needed.

Continuing, **thermr** finds the desired material on the input PENDF and ENDF tapes. It will automatically loop over **ntemp** materials on **nin**. The input tape must have been through **BROADR**. The elastic cross section at the current temperature is saved on a **loada/finda** scratch file to be used for normalizing free-atom scattering if necessary. For ENDF-6 format materials, the parameters for the elastic calculation are read in using **rdelas**. Next, **thermr** computes elastic and/or inelastic cross sections by calls to **coh**, **iel**, and **calcem**. Finally, the results are written onto the output PENDF tape by **tpend**.

Some alteration of ENDF/B formats and conventions was required to accommodate thermal cross sections. The incoherent inelastic cross sections fit well into MF=3 using MT=**mtref** (see user input). The coherent or incoherent elastic cross section (if present) uses **mtref**+1. Other modules of NJOY expect that thermal MT numbers will be between 221 and 250. The incoherent energy-to-energy matrix is stored in MF=6 (coupled angle-energy distributions). Before the introduction of the ENDF-6 format, the ENDF File 6 formats were not well-suited to this application because secondary angle and energy were not tightly coupled as required by the physics of the problem. Therefore, three new formats were defined for File 6: LTT=5 for discrete-angle inelastic transfer cross sections, LTT=6 for discrete-angle elastic data, and LTT=7 for coherent elastic reactions. The format for LTT=5 follows in the notation of ENDF-102[50]:

```

MAT,6,MT [ ZA, AWR, 0, LTT, 0, 0 ] CONT  LTT=5
MAT,6,MT [ T, 0., 0, 1, NNE / NNE, 2 ] TAB2
MAT,6,MT [ 0., EN, 0, 0, NEP*(NL+1), NL+1 /
          EP(1), PP(1), EPM(1,1), ...
          EP(2), PP(2), ... ] LIST
... repeat the LIST for the NNE values of EN ...
MAT,6,0 [ 0., 0., 0, 0, 0, 0 ] SEND

```

There is a list record for each of the NNE values of incident energy. Each list record gives the normalized secondary energy distribution as NEP values of PP vs.  $E'$ , and for each value of  $E'$ , the record gives NL equally probable cosines, EPM. Similarly, the format for LTT=6 is:

```

MAT,6,MT [ ZA, AWR, 0, LTT, 0, 0 ] CONT LTT=6
MAT,6,MT [ T, 0., 0, 1, NNE / NNE, 2 ] TAB2
MAT,6,MT [ 0., EN, 0, 0, NU+2, NU+2 /
          EN, 1., U(1), U(2), ... ] LIST
... repeat the LIST for the NNE values of EN ...
MAT,6,0 [ 0., 0., 0, 0, 0, 0 ] SEND

```

Here, there is just a set of NU equally probable cosines given for each incident energy. Note that this format was designed to look like that for LTT=5 with NEP=1. Finally, the format for LTT=7 is:

```

MAT,6,MT [ ZA, AWR, 0, LTT, 0, 0 ] CONT LTT=7
MAT,6,MT [ 0., 0., 0, 0, 0, 0, NBRAGG ] CONT
MAT,6,0 [ 0., 0., 0, 0, 0, 0 ] SEND

```

In this case, all the important information is in File 3 under MT=**mtref**+1. For convenience, the number of Bragg edges used is given here in File 6 as NBRAGG.

In subroutine **coh**, the energy grid is determined adaptively and stored into the same **loada/finda** scratch file used for the elastic cross section. The elastic cross section is converted to the coherent grid using Lagrangian interpolation (see **terp**). The structure of the record stored on the scratch file is [energy / static elastic / incoherent inelastic / coherent elastic].

Coherent cross sections at a given energy  $E$  are computed by **sigcoh**. If this is the first entry ( $E=0$ ) for an ENDF-III type material, the appropriate lattice constants are selected and the Debye-Waller coefficient is obtained for the desired temperature by interpolation. Then the reciprocal lattice wave vectors and structure factors are computed, sorted into shells, and stored for later use. On a normal entry ( $E>0$ ), the stored list is used to compute the cross section. For ENDF-6 format materials, the initialization step is used to organize the data already read from MF=7/MT=2 by **rdelas**, and subsequent entries are used to compute the cross section.

Incoherent elastic cross sections are computed in subroutine `iel`. The appropriate bound cross sections and Debye-Waller coefficients are either extracted from the data already read from an ENDF-6 format MF=7/MT=2 by `rdelas`, or they are extracted from data statements in `iel` and then adjusted to the specified temperature using `terp` or `terpa`. The angle-integrated cross section is computed analytically on the grid of the static elastic cross section and written back onto the `loada/finda` scratch file in the same slot used for coherent elastic as described above (both never occur simultaneously in the same material). The discrete equally probable cosines are cast into LTT=7 format and written onto a scratch tape for use by `tpend`.

Incoherent cross sections and distributions are generated in `calcem`. On the first entry, the ENDF/B scattering law is read in or parameters are set for free-atom scattering. For ENDF-6 files, the effective temperatures for the SCT approximation are read in. For the older formats, these numbers were either read in or set to default values during the user input process. The calculation for  $E$ - $E'$ - $\mu$  ordering (`iform`=0) goes through statement 300. An adaptive loop to determine the secondary energy grid is carried out. The required cross sections and discrete cosines are returned by `sigl`, which uses `sig` to compute the differential cross sections. Because the spectrum curve will have discontinuities in slope at energies corresponding to the break points of the  $\beta$  grid, it is important to use these energies as the starting points for the adaptive reconstruction. The first panel starts at  $E' = 0$  and ends at the first energy greater than zero that can be derived from the  $\beta$  grid. This will normally be a negative  $\beta$  value corresponding to  $E' < E$ . These two energies and their corresponding cross sections are loaded into an inverted stack like the one used in `RECONR`. Next, the top interval in the stack is divided in half, and new cross sections are computed at this midpoint. If the new cross section is not within the desired tolerance of the value obtained by linear interpolation between the adjacent points, the new value is inserted into the stack. Otherwise, the top value in the stack is converged and can be saved to the location where the spectrum is accumulating. Each time the stack gets down to a single element, a new point is calculated from the next  $\beta$  value in the evaluator's  $\beta$  grid, and the subdivision process is continued. During this reconstruction process, the integrated cross section is computed by adding in each trapezoid. In addition, note is taken of the last nonzero cross section value in order to remove excess zero values from the end

of the record. The  $\sigma$  vs.  $E'$  curve is complete when the  $\beta$  grid has been exhausted (the highest positive value). The result is put directly into the modified MF=6 format and written onto a scratch file.

When all the desired incident energies have been processed, the incoherent cross section is calculated on the File 3 energy grid by interpolating in the table of values computed by the reconstruction process. The results are stored on the `loada/finda` tape. If free-atom scattering has been selected, the elastic cross section is stored in the incoherent slot.

Incoherent inelastic scattering cross sections and discrete cosines are computed in `sigl`. The stack for the adaptive reconstruction of the angular distribution for a given  $E \rightarrow E'$  is primed with  $\mu = -1$ ,  $\mu = +1$ , and the angle for static scattering. The top interval on the stack is subdivided by halving until the actual cross section computed by `sig` is within a specified tolerance of a linear interpolate. As each panel is converged, its area is added to the accumulating cross section. On convergence, the fraction of the cross section corresponding to each equally probable bin is computed, and the linearization process is repeated to find the bin boundaries and discrete cosines. Note that Legendre coefficients can be computed in this routine from the discrete cosines.

Subroutine `sig` is used to compute the actual double-differential cross section for a given value of  $E$ ,  $E'$ , and  $\mu$ . This is done using  $S(\alpha, \beta)$  (with the possible use of the SCT approximation for large values of  $\alpha$  or  $\beta$ ), or using the free-gas scattering law. Normally,  $s(\alpha, \beta)$  is symmetrical in  $\beta$  and results are extracted from the table at `isab` using  $|\beta|$ . However, this is not true for materials like orthohydrogen and parahydrogen. In these cases, the LASYM parameter is set, and explicit  $S(\alpha, \beta)$  values are given for both negative and positive  $\beta$ . For liquids, the presence of diffusion leads to a singularity for  $\beta = 0$  and small  $\alpha$  (the quasi-elastic scattering peak). The normal ENDF interpolation laws do not represent  $S(\alpha, \beta)$  well in this region. Therefore, THERMR tries to determine if the material is a liquid by looking at the small- $\alpha$  behavior of the  $\beta = 0$  curve (see `cliq`). It then extrapolates low- $\beta$  curves to low- $\alpha$  values using a  $\beta^2/\alpha$  law.

The calculation for  $E-\mu-E'$  ordering starts at statement number 510. In a loop over incident energies, subroutine `sigu` is called to reconstruct  $\sigma(E, \mu)$  adaptively. The method used is the same as that described above for the energy distribution, and the result represents the angular cross section to within a desired tolerance. The inelastic cross section is obtained as the integral over the angular cross section. Subroutine `sigu` obtains the secondary energy spectrum corresponding to  $E$  and  $\mu$  adaptively. It uses the beta values from the evaluation

as starting points for subdivision, just as described above for  $E$ - $E'$ - $\mu$  ordering. It uses `sig` to obtain the cross section for a given  $E$ ,  $E'$ , and  $\mu$ . The results of this calculation are written onto `nscr` using the ENDF-6 File 6/Law 7 format and passed to `tpend`.

Finally, `tpend` is called to prepare the output tape. The File 1 directory is updated to account for the new sections that are being added. File 3 is located and the cross sections stored on the `loada/finda` scratch file are retrieved, formatted, and written to the output tape. Note that the elastic cross section in MT=2 and the total cross section in MT=1 are not changed from their static values, nor is the union grid updated. As a result, MT=221 – 250 must be considered supplemental. Subsequent modules could ignore them or use them in place of the static values. Also note that it is possible to run THERMR several times with different values of `mtref`. The result would be one PENDF tape containing static cross sections and cross sections for several different binding states that can be selected at will (for example, MT=2 for static hydrogen, MT=221 for free hydrogen, MT=222 for hydrogen in water, and MT=223 and MT=224 for hydrogen in polyethylene, all on one PENDF tape).

File 6 distributions are read from a scratch file (`nscr`) in ENDF format, normalized, and written back onto the final tape. Since free incoherent scattering was set equal to elastic scattering in `calcem`, the approximate resonance correction of the matrix is now complete.

## 7.5 Using the ENDF/B Thermal Data Files

The thermal data files originally prepared for ENDF/B-III were also used for ENDF/B-IV and ENDF/B-V.<sup>4</sup> Table 3 summarizes the contents of these data tapes.

For most of these evaluations, THERMR will produce cross sections appropriate for the major scattering atom bound in a particular material, for example, hydrogen bound in water, or Zr bound in ZrH. In these cases, the cross sections are combined later (for example, hydrogen bound in water would be combined with free-gas oxygen, and Zr bound in ZrH would be combined with H bound in ZrH). The treatment to be used for the secondary scattering atoms for each evaluation is indicated in the table.

In two cases – BeO and Benzene – the scattering laws  $S(\alpha, \beta)$  for the two component atoms have been combined into a single scattering law normalized to

---

<sup>4</sup>The data files and the reference manual[51] are available from the National Nuclear Data Center, Brookhaven National Laboratory, Upton, NY 11973. Request Tapes 320 through 325 and report ENDF-269.

Table 3: Moderator Materials on ENDF/B-III Thermal Data Tapes Showing Their MAT Numbers and Distribution Tape Numbers

| Material                      | MAT  | Tape | MTs     | elastic | secondary |
|-------------------------------|------|------|---------|---------|-----------|
| Be                            | 1064 | 321  | 231,232 | coh     |           |
| BeO                           | 1099 | 321  | 233,234 | coh     | none      |
| C (graphite)                  | 1065 | 322  | 229,230 | coh     |           |
| H(CH <sub>2</sub> )           | 1114 | 322  | 223     | iel     | free C    |
| C <sub>6</sub> H <sub>6</sub> | 1095 | 325  | 227     |         | none      |
| D(D <sub>2</sub> O)           | 1004 | 320  | 228     |         | free O    |
| H(H <sub>2</sub> O)           | 1002 | 320  | 222     |         | free O    |
| Zr(ZrH <sub>n</sub> )         | 1096 | 323  | 235,236 | iel     | 1097      |
| H(ZrH <sub>n</sub> )          | 1097 | 323  | 225,226 | iel     | 1096      |

be used with the cross section of the primary scattering atom. For these cases, THERMR produces a cross section for the molecule or compound directly. In making a macroscopic cross section for BeO, the user would multiply the thermal

Table 4: ENDF/B-VII Moderator Materials with Their MAT and MT Numbers

| Material                      | MAT | MTs     | elastic | secondary |
|-------------------------------|-----|---------|---------|-----------|
| Al                            | 45  | 243,244 | coh     |           |
| Be                            | 26  | 231,232 | coh     |           |
| Be(BeO)                       | 27  | 233,234 | coh     |           |
| O(BeO)                        | 28  | 237,238 | coh     |           |
| C(graphite)                   | 31  | 229,230 | coh     |           |
| Fe                            | 56  | 245,246 | coh     |           |
| H(CH <sub>2</sub> )           | 37  | 223     | iel     | free C    |
| H(liquidCH <sub>4</sub> )     | 33  |         |         |           |
| H(solidCH <sub>4</sub> )      | 34  |         |         |           |
| C <sub>6</sub> H <sub>6</sub> | 40  | 227     |         | none      |
| D(D <sub>2</sub> O)           | 11  | 228     |         | free O    |
| D(paraD <sub>2</sub> )        | 12  |         |         |           |
| D(orthoD <sub>2</sub> )       | 13  |         |         |           |
| H(H <sub>2</sub> O)           | 1   | 222     |         |           |
| H(paraH <sub>2</sub> )        | 2   |         |         |           |
| H(orthoH <sub>2</sub> )       | 3   |         |         |           |
| Zr(ZrH <sub>n</sub> )         | 58  | 235,236 | iel     |           |
| H(ZrH <sub>n</sub> )          | 7   | 225,226 | iel     |           |
| U(UO <sub>2</sub> )           | 76  | 241,242 | coh     |           |
| O(UO <sub>2</sub> )           | 75  | 239,240 | coh     |           |



BeO cross section from THERMR by the atomic density of Be, taking care not to add any additional thermal contribution for the oxygen.

THERMR labels the thermal cross sections that it generates with specially defined MT numbers. The particular numbers shown in the table are recognized by the reaction naming logic in MATXS. Note that two numbers are defined for materials that have both inelastic and elastic components; the first number is for inelastic, and the second for elastic.

For ENDF/B-VII, there are additional thermal materials available, and the numbering has changed. See Table 4.

## 7.6 Input Instructions

The following input instructions have been copied from the comment cards in THERMR:

```

!---input specifications (free format)-----
!
!  card 1
!      nendf      endf tape for mf7 data
!      nin        old pendf tape
!      nout       new pendf tape
!  card 2
!      matde      material desired on endf tape
!      matdp      material desired on pendf tape
!      nbin       number of equi-probable angles
!      ntemp      number of temperatures (default=1)
!      iin        inelastic options
!                0      none
!                1      compute as free gas
!                2      read s(a,b) and compute matrix
!      icoh       elastic options
!                0      none
!                1      compute using ENDF6 format data
!                -----or for earlier formats
!                1      graphite
!                2      beryllium
!                3      beryllium oxide
!                11     polyethylene
!                12     h(zrh)
!                13     zr(zrh)

```

```

!      iform      output format for inelastic distributions
!                  0      E-E'-mu ordering (MF6 special)
!                  1      E-mu-E' ordering (MF6/Law7)
!      natom      number of principal atoms
!      mtref      mt for inelastic reaction (221-250 only)
!      iprint      print option (0=minimum, 1=maximum,
!                  2=max. normal + intermediate results)
!                  (default=0)
!      card 3
!      tempr      temperatures (kelvin)
!      card 4
!      tol        tolerance
!      emax        maximum energy for thermal treatment
!                  (for temperatures greater than 3000,
!                  emax and the energy grid are scaled by
!                  temp/300. free gas only.)
!
!      nendf can be endf-6 format (e.g., from leapr) while
!      nin and nout are endf-4 or 5 format, if desired.
!
!-----

```

The following sample problem illustrates the production of thermal cross sections for hydrogen in water.

```

thermr
20 21 22 /
1 125 8 2 2 0 0 2 222 0
293.6 500/
.01 4.6
stop

```

It is assumed that ENDF/B-VII evaluation for H in H<sub>2</sub>O is mounted on unit 20, and that a previously prepared PENDF file for <sup>1</sup>H (MAT125) is mounted on unit 21. The thermal cross sections for hydrogen in water will be written on unit 22 using `mtref=222`. Note that the parameter `natom` is set to 2 because the water molecule H<sub>2</sub>O contains two hydrogen atoms. In addition, `icoh=0` for hydrogen in water, and `iform=0` for  $E$ - $E'$ - $\mu$  ordering. The higher-energy parts

of the neutron emission curves for this example are shown in Fig. 21. The sharp peak at  $E=E'$  is quasi-elastic scattering broadened by diffusion.

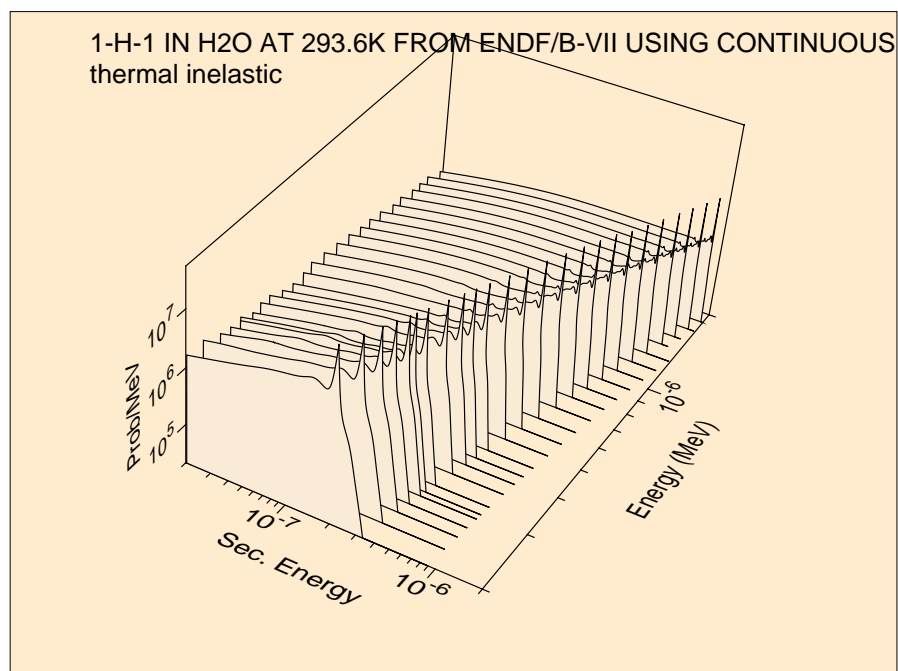


Figure 21: Expanded view of the high-energy region for the incoherent inelastic distribution of hydrogen bound in water. Note the sharp quasi-elastic peak at  $E=E'$ .

A calculation of both free and graphite cross sections for ENDF/B-VII carbon would go as follows:

```
reconr
20 22 / tape20 is carbon
/
600 1/
.001/
'6-C-nat from ENDF/B-VII'/
0/
broadr
20 22 23
600 1/
.001/
293.6
0/
thermr
0 23 24
```

```

0 600 8 1 2 0 0 1 221 0
293.6
.005 5
thermr
26 24 25 / tape 26 is ENDF/B-VII graphite
31 600 8 1 2 1 0 1 229 0
293.6
.005 5
stop

```

First, ENDF/B-VII carbon must be mounted on unit 20. At LANL this is done by copying it to a file named `tape20` in the user's local file space. Similarly, ENDF/B-VII graphite must be copied to `tape26`. Next, `RECONR` is run to linearize the evaluation, and `BROADR` is run to prepare 293.6K cross sections. The first THERMR run is for free-gas scattering (`mtref=221`), and the second run is for carbon bound in graphite (`mtref=229`). Note that `natom` is now 1, and that 8 discrete angles were requested in both cases. For graphite, `icoh` is set to 1 in order to request the calculation of coherent elastic scattering like that shown in Fig. 16. The coherent results will use MF=3 and MT=230. Distributions will be calculated to 0.5% accuracy for energies up to 5 eV. The final PENDF file will be `tape25`.

## 7.7 Error Messages

`error in thermr***nin=0`

An input PENDF tape is required.

`error in thermr***mode conversion not allowed`

`nin` and `nout` must both be binary or both be coded.

`error in thermr***illegal reference mt`

Restricted to MT=221–250. User's should note that Card 2 has an additional input parameter, `iform`, in NJOY2012. Unmodified NJOY99 input decks will produce this error message.

`error in thermr***desired material not on pendf tape`

Check input instructions against contents of thermal tape.

`error in thermr***desired temperature not on tape`

Check input instructions against contents of thermal tape.

`error in rdelas***too much elastic data`

There is not enough space in the allocatable array `a`. See `na=10000`.

error in rdelas\*\*\*desired temp not found

The temperatures requested in THERMR must be the same as the temperatures on the input PENDF tape.

error in coh\*\*\*too many legendre orders

The code currently computes only  $P_0$ , but `nl=1` in `coh` can be changed if desired. Code is currently limited to 6 ( $P_5$ ). If more coefficients are desired, increase `nlmax` and the dimensions of the variables `s`, `ej`, and `ex` in `coh`, `calcem`, and `tpend`.

error in sigcoh\*\*\*storage exceeded

Not enough room for lattice factors. Increase `nw` which is currently 10000.

error in sigcoh\*\*\*illegal lat

Only three lattices are coded so far. To add others, insert the constants in `sigcoh` and form factor formulas in `form`.

error in iel\*\*\*bad temperature for debye-waller factor

Shouldn't occur unless new materials are added incorrectly.

error in iel\*\*\*unknown material identifier

Only three options are coded so far. To add others, insert data statements for the Debye-Waller integrals and values for the bound cross sections.

error in calcem\*\*\*nl too large for binning

Increase the value of the parameter `nlmax` which is currently 33.

error in calcem\*\*\*storage exceeded

There is not enough space in the global scratch array. Increase `nwscr`, which is currently 99000, in `thermr`.

error in calcem\*\*\*desired temperature not found

Any temperature requested in THERMR must be on the input PENDF tape.

error in calcem\*\*\*bad temperature for teff

error in calcem\*\*\*bad temperature for teff2

Data for effective temperatures use a temperature grid that is not consistent with the  $S(\alpha, \beta)$  data.

error in calcem\*\*\*isabt=1 pendf tape found

THERMR cannot process this format.

error in calcem\*\*\*only 2 sct atoms allowed

For mixed moderators, such as BeO and Benzene, the SCT contribution from each atom must be included. The code only allows for 2.

error in calcem\*\*\*too many angles

For  $E-\mu-E'$  ordering, there are more than `mumax=300` angles being generated.

error in sig\*\*\*illegal option

Only tabulated  $S(\alpha, \beta)$  and free gas are coded at this time.

error in sigl\*\*\*no legal solution

message from sigl---disc=ffff, set to abs value....

error in sigl\*\*\*no legal solution (quadratic path)

The code has trouble solving the equation for the boundary of a bin.

error in tpend\*\*\*storage exceeded

Increase nwscr in thermr.

error in tpend\*\*\*cross section = 0

Thermal cross section of zero cannot be used to normalize the distribution.

## 7.8 Input/Output Units

The following logical units are used.

- 10/11    `iold/inew` in `thermr`. Also used in `coh`, `calcem`, and `tpend`. Used for the `loada/finda` scratch file that saves the energy grid and reaction cross sections.
- 12      `nscr` in `thermr`. Also used in `calcem` and `tpend`. Contains the scattering matrix before normalization.
- 13      `nscr2` in `thermr` and `tpend`. Contains data from `nin` that are to be simply copied to `nout`.
- 20-99   `User's choice for nendf, nin, nout, and nread (iinc=2 only) to link with other modules. No mode conversion between nin and nout allowed.`

Units 10 and 11 are always binary. Units 12 and 13 have the same mode as `nin` and `nout`. The user can choose the modes for `nendf`, `nin`, `nout`, except `nin` and `nout` must have the same mode.

## 7.9 Storage Allocation

The storage allocated in THERMR is for the `loada/finda` buffers and a scratch array. The value of `nbuf` may be changed at will; larger values increase I/O efficiency. The variable `nwscr` controls the maximum size of the TAB1 records of  $\sigma(E \rightarrow E')$  versus  $E'$  for incoherent scattering. Hence it interacts with `tol`. The linearization stack (`stk`) in `coh` is controlled by `imax` and the number of Legendre components requested (always 1 in the standard version). The current value of `imax` (20) is sufficient to divide each panel into parts as small as one-millionth of the panel size. The length of the list of lattice factors (`f1`) in `sigcoh` is controlled by the size of the ENDF/B File 7, and `nw=10000` must be big enough for the problem.

## 8 GROUPR

GROUPR computes group-to-group scattering matrices, and anisotropic photon production matrices for neutrons from ENDF/B-IV, -V, -VI, or -VII evaluated nuclear data. With ENDF-6 format files, photonuclear data and incoming and outgoing charged particles can also be handled. Special features are provided for ratio quantities (for example,  $\bar{\mu}$ ,  $\bar{\nu}$ , or photon yield), inverse velocity, delayed neutron spectra by time group, and anisotropic thermal neutron scattering. Fission is represented as a group-to-group matrix for full generality. Scattering matrices and photon production matrices may be self-shielded if desired.

The Bondarenko narrow-resonance weighting scheme[38] is normally used. Optionally, a weighting flux can be computed for various mixtures of heavy absorbers with light moderators. An accurate pointwise solution of the integral slowing down equation is used. This option is normally called on to account for intermediate resonance effects in the epithermal range.

Neutron data and photon-production data are processed in a parallel manner using the same weight function and quadrature scheme. This assures consistent cross sections for coupled neutron-photon problems. Two-body scattering is computed with a center-of-mass (CM) Gaussian quadrature, which gives accurate results even for small Legendre components of the group-to-group matrix.

User conveniences include free-form input and complete control over which reactions are processed. The neutron group structure, photon group structure, and weight function can each be read in or set to one of the internal options. Output can be printed and/or written to an output “groupwise-ENDF” (GENDF) file for further processing by a formatting module ([DTFR](#), [CCCCR](#), [MATXSR](#), [WIMSR](#)), by the covariance module ([ERRORR](#)), or by the MCNP continuous-energy Monte Carlo module ([ACER](#)).

This section describes GROUPR in NJOY 2012.2. The main differences between this version and the version previously reported [3] follow:

- elimination of the restriction that `ntemp` and `nsigz` be less than or equal to 10, and
- tabulated angular distributions are now included for discrete scattering,
- Legendre orders to 64 and the ENDF LTT=3 option where distributions have separate low- and high-energy treatments are now handled,
- an extended system for treating nuclide production has been added,
- additional group structures and weight functions are included, and
- the coding has been converted to Fortran-90 style and memory allocation.

### 8.1 Multigroup Constants

Multigroup constants are normally used by computer codes that calculate the distributions of neutrons and/or photons in space and energy, and that compute various responses to these distributions, such as criticality, dose to personnel, or activation of materials. These distributions are solutions of the neutral particle transport equation.<sup>5</sup>

$$\begin{aligned} \mu \frac{\partial}{\partial x} \phi(x, \mu, E) &+ \sigma_t(x, E) \phi(x, \mu, E) \\ &= \int d\Omega' \int dE' \sigma_X(x, E' \rightarrow E, \Omega' \rightarrow \Omega) \phi(x, \mu', E') \\ &+ Q(x, \mu, E) , \end{aligned} \quad (235)$$

where the flux  $\phi$  is allowed to vary with position  $x$ , direction  $\Omega$  with polar cosine  $\mu$ , and energy  $E$ . Similarly, the macroscopic total cross section  $\sigma_t$  varies with position and energy. The right-hand side of the equation contains the source due to transfers from other directions  $\Omega'$  and energies  $E'$  (as described by the macroscopic transfer cross section  $\sigma_X$ ), and a fixed or external source  $Q$ .

The macroscopic cross sections (in units of  $\text{cm}^{-1}$ ) in Eq. 235 can be calculated from microscopic cross sections for the component isotopes or elements (in barns) using

$$\sigma_t(x, E) = \sum_i \rho_i(x) \sigma_t^i(T[x], E) , \quad (236)$$

where  $\rho_i$  is the number density for a constituent (in  $\text{barns}^{-1}\text{cm}^{-1}$ ), which may vary with position, and  $T$  is the temperature, which may also vary with position. A similar formula holds for  $\sigma_X$ .

The transfer cross section  $\sigma_X$  (which includes both scattering and fission processes) is normally assumed to depend only on the cosine of the scattering angle,  $\mu_0 = \Omega \cdot \Omega'$ . This allows  $\sigma_X$  to be expanded using Legendre polynomials

$$\sigma_X(x, E' \rightarrow E, \Omega' \rightarrow \Omega) = \sum_{\ell=0}^{\infty} \frac{2\ell+1}{4\pi} \sigma_{X\ell}(x, E' \rightarrow E) P_{\ell}(\mu_0) . \quad (237)$$

Application of the addition theorem and integration over azimuthal angle then gives

---

<sup>5</sup>The following development uses a notation based on Bell and Glasstone[52], where the lower-case sigma is used for both macroscopic and microscopic cross sections, depending on the context. One-dimensional slab geometry is used throughout for simplicity.



$$\begin{aligned}
\mu \frac{\partial}{\partial x} \phi(x, \mu, E) &+ \sigma_t(x, E) \phi(x, \mu, E) \\
&= \sum_{\ell=0}^{\infty} \frac{2\ell+1}{2} P_{\ell}(\mu) \int \sigma_{X\ell}(x, E' \rightarrow E) \phi_{\ell}(x, E') dE' \\
&+ Q(x, \mu, E) ,
\end{aligned} \tag{238}$$

where

$$\phi_{\ell}(x, E) = \int P_{\ell}(\mu) \phi(x, \mu, E) d\mu . \tag{239}$$

The desired responses are then given by

$$R(x) = \int \sigma_r(x, E) \phi_0(x, E) dE , \tag{240}$$

where  $\sigma_r$  is the reaction cross section for the response. The next step is to integrate Eqs. 238 and 240 over a range of energies chosen to lie in group  $g$ . The results are

$$\begin{aligned}
\mu \frac{\partial}{\partial x} \phi_g(x, \mu) &+ \sum_{\ell=0}^{\infty} P_{\ell}(\mu) \sigma_{t\ell g}(x) \phi_{\ell g}(x) \\
&= \sum_{\ell=0}^{\infty} \frac{2\ell+1}{2} P_{\ell}(\mu) \sum_{g'} \sigma_{X\ell g' \rightarrow g}(x) \phi_{\ell g'}(x) + Q_g(x, \mu) ,
\end{aligned} \tag{241}$$

and

$$R(x) = \sum_g \sigma_{rg}(x) \phi_{0g}(x) , \tag{242}$$

where

$$\phi_{\ell g}(x) = \int_g \phi_{\ell}(x, E) dE , \tag{243}$$

$$\sigma_{t\ell g}(x) = \frac{\int_g \sigma_t(x, E) \phi_{\ell}(x, E) dE}{\int_g \phi_{\ell}(x, E) dE} , \tag{244}$$

$$\sigma_r(x) = \frac{\int_g \sigma_r(x, E) \phi_0(x, E) dE}{\int_g \phi_0(x, E) dE} , \quad (245)$$

and

$$\sigma_{X\ell g' \rightarrow g} = \frac{\int_g dE \int_{g'} dE' \sigma_{X\ell}(x, E' \rightarrow E) \phi_\ell(x, E)}{\int_g \phi_\ell(x, E) dE} . \quad (246)$$

The last three equations provide the fundamental definitions for the multi-group cross sections and the group-to-group matrix. Note that the values of the group constants depend upon the basic energy-dependent cross sections obtained from an ENDF-format evaluation by way of the [RECONR](#), [BROADR](#), [UNRESR](#), [HEATR](#), [THERMR](#), and [PURR](#) modules of NJOY, and the shape of  $\phi$  within the group.

## 8.2 Group Ordering

Since neutrons normally lose energy in scattering, the scattering source into group  $g$  depends on the flux at higher-energy groups  $g'$  and the cross section for transferring neutrons from  $g'$  to  $g$ . For this reason, Eq. 241 is usually solved by sweeping from high energies to low energies. (Any thermal upscatter or fission is handled by iteration.) Data libraries for use with transport codes normally number the groups such that group 1 is the highest-energy group, and all the scattering matrix elements that transfer neutrons into group 1 are given first, followed by those for scattering into group 2, and so on.

However, in ENDF files the evaluated nuclear data are always given in order of increasing incident energy, and secondary neutron distributions are described by giving emission spectra for given incident energies. Therefore, GROUPR numbers its groups such that group 1 is the lowest-energy group, and it calculates that scattering out of group 1, followed by the scattering out of group 2, and so on.

The “backward” energy-group numbering convention used by GROUPR is a possible source of confusion in interpreting output produced by the various modules of NJOY. All group indices printed by GROUPR or written to the GROUPR output file use the increasing-energy order. The covariance modules and photon interaction module follow the GROUPR ordering convention. Output modules such as [DTFR](#), [CCCCR](#), [MATXS](#), and [WIMSR](#) invert the group

order and rearrange the scattering matrices from the GROUPR outscatter organization to the “transport” inscatter form. Any group indices printed by these three output modules will be in the conventional transport decreasing-energy order.

### 8.3 Basic ENDF Cross Sections

The basic energy-dependent cross sections and energy-angle distributions needed for Eqs. 244, 245, and 246 are obtained from evaluated nuclear data in ENDF format[8]. These data are indexed by material (MAT), type of information (MF), and reaction (MT). Materials can be single isotopes, elements, or compounds. Type of information includes energy-dependent cross section (MF=3), angular distributions (MF=4), secondary energy distributions (MF=5), and energy-angle distributions (MF=6). Reactions include the total (MT=1) required for Eq. 244, the partial scattering reactions that must be summed for Eq. 246 [that is, elastic (MT=2), discrete-level inelastic (MT=51 – 90), (n,2n) (MT=16), *etc.*], and the many partial reactions that can be used to calculate responses [for example, (n,2n) or (n, $\alpha$ ) for activation, gas production, heat production (KERMA), radiation damage (DPA), *etc.*].

Before using GROUPR, the basic ENDF/B cross sections should have been converted into energy- and temperature-dependent pointwise cross sections in PENDF (pointwise ENDF) format using RECONR and BROADR. For heavy isotopes, unresolved self-shielding data should have been added to the PENDF tape<sup>6</sup> using UNRESR or PURR. If requested, heat production cross sections (KERMA), radiation damage production (or DPA), and thermal upscatter data can also have been added to the PENDF tape using HEATR and THERMR. See the chapters on these other modules for more information.

The detailed methods used for evaluating Eqs. 244, 245, and 246 from ENDF and PENDF tapes are given below (see Sections 8.11 through 8.15). An example of an ENDF pointwise cross section compared with group-averaged cross sections from GROUPR is given in Fig. 22.

### 8.4 Weighting Flux

In general, the weighting flux  $\phi$  is not known; it is, after all, the particle distribution being sought in the transport calculation. However, it is often possible to obtain fairly accurate group constants for a particular application if the shape

---

<sup>6</sup>The term “tape” is used loosely in this report to refer to any input or output file. Of course, such files would be on disk storage in a modern system.

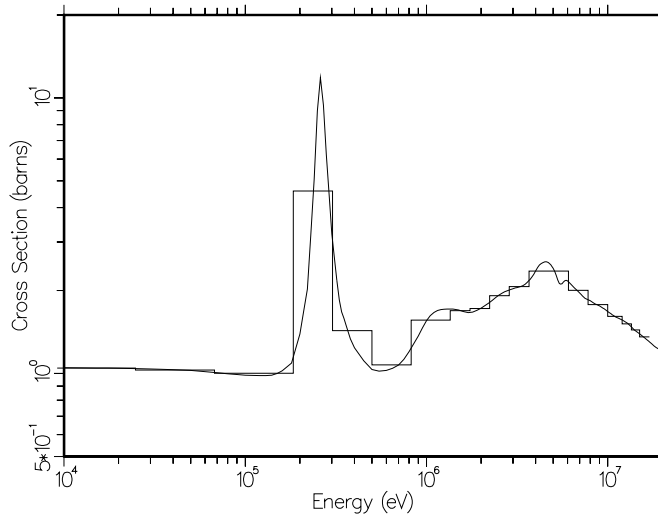


Figure 22: A comparison of the pointwise and multigroup representations for the total cross section of  ${}^7\text{Li}$ . The Los Alamos 30-group structure is shown.

of the flux is reasonably well known over the broad energy ranges of a particular few-group structure (for example, a fission spectrum, thermal Maxwellian, or  $1/E$  slowing-down spectrum). Alternatively, one can use many small groups so that mistakes in guessing the shape inside the group are not very important. The key to using the multigroup method effectively is balancing the tradeoffs between the choice of weight function and the number of groups used for each different class of problem being solved.

In many cases of practical interest, the flux  $\phi$  will contain dips corresponding to the absorption resonances of the various materials. In the reaction rate  $\sigma(E) \times \phi(E)$ , these dips clearly reduce (self-shield) the effect of the corresponding resonance. GROUPR provides two methods to estimate the effect of this self-shielding: the Bondarenko model and the flux calculator.

In the Bondarenko model[38], the narrow resonance (NR) approximation, and the  $B_N$  approximation for large systems[52] are invoked to obtain

$$\phi_\ell(E) = \frac{W_\ell(E)}{[\sigma_t(E)]^{\ell+1}}, \quad (247)$$

where  $\phi_\ell$  is the  $\ell$ -th Legendre component of the angular flux, the  $W_\ell(E)$  are smooth functions of energy (such as  $1/E$ +fission), and  $\sigma_t(E)$  is the total macroscopic cross section for the material. GROUPR takes all of the  $W_\ell$  to be equal to the single function  $C(E)$ , where  $C(E)$  can be read in or set to one of several internally defined functions. It is further assumed that the important self-shielding

effect of the flux can be obtained for isotope  $i$  by representing all the other isotopes with a constant “background cross section”,  $\sigma_0$ . Therefore,

$$\phi_\ell^i(E) = \frac{C(E)}{[\sigma_t^i(E) + \sigma_0^i]^{\ell+1}} , \quad (248)$$

where  $\sigma_t^i$  is the microscopic total cross section for isotope  $i$ . The qualitative behavior of Eq. 248 is easy to understand. If  $\sigma_0$  is larger than the tallest peaks in  $\sigma_t$ , the weighting flux  $\phi$  is approximately proportional to the smooth weighting function  $C(E)$ . This is called infinite dilution; the cross section in the material of interest has little or no effect on the flux. On the other hand, if  $\sigma_0$  is small with respect to  $\sigma_t$ , the weighting flux will have large dips at the locations of the peaks in  $\sigma_t$ , and a large self-shielding effect will be expected.

Each component material of a mixture has a different weight function. The macroscopic total cross sections are given by

$$\sigma_{t\ell g} = \sum_i \rho_i \sigma_{t\ell g}^i(\sigma_0^i, T) , \quad (249)$$

where

$$\sigma_{t\ell g}^i(\sigma_0, T) = \frac{\int_g \frac{\sigma_t^i(E, T)}{[\sigma_0 + \sigma_t^i]^{\ell+1}} C(E) dE}{\int_g \frac{1}{[\sigma_0 + \sigma_t^i]^{\ell+1}} C(E) dE} . \quad (250)$$

Similar equations are used for  $\sigma_R$  and  $\sigma_{X\ell g \rightarrow g'}$ . On the GROUPR level,  $\sigma_0$  and  $T$  are simply parameters. Subsequent codes, such as 1DX[53] or TRANSX[11, 40], can compute an appropriate value for  $\sigma_0$ , and then interpolate in tables of cross section versus  $\sigma_0$  and  $T$  to get the desired self-shielded group constants.

The appropriate value for  $\sigma_0^i$  is obvious when a single resonance material is mixed with a moderator material (for example,  $^{238}\text{UO}_2$ ), because the admixed materials typically have a constant cross section in the energy range where the heavy isotopes have resonances. For a mixture of resonance materials, the normal procedure is to preserve the average of Eq. 248 in each group by using

$$\sigma_{0g}^i = \frac{1}{\rho_i} \sum_{j \neq i} \rho_j \sigma_{t0g}^j(\sigma_{0g}^j, T) , \quad (251)$$

where the  $\rho_i$  are atomic densities or atomic fractions. Eq. 251 is solved by iteration. Interference between resonances in different materials is handled in an average sense only.

In the unresolved energy range (see [UNRESR](#) and [PURR](#)), the explicit dependence of cross section on energy is not known. The integrands are replaced by their expected values

$$\sigma_{x\ell g}(\sigma_0) = \frac{\int_g \left\langle \frac{\sigma_x}{[\sigma_0 + \sigma_t]^{\ell+1}} \right\rangle W_\ell dE}{\int_g \left\langle \frac{1}{[\sigma_0 + \sigma_t]^{\ell+1}} \right\rangle W_\ell dE}, \quad (252)$$

where the expected values are averages over the distributions of resonance position and width expected in the vicinity of energy  $E$ . The [UNRESR](#) and [PURR](#) modules produce effective self-shielded point cross sections defined by

$$\langle \sigma_x \rangle_\ell = \frac{\left\langle \frac{\sigma_x}{[\sigma_0 + \sigma_t]^{\ell+1}} \right\rangle}{\left\langle \frac{1}{[\sigma_0 + \sigma_t]^{\ell+1}} \right\rangle}. \quad (253)$$

Substituting Eq. 253 into Eq. 252 gives an equation of the form of Eqs. 244 and 245, except that  $\sigma$  is replaced by  $\langle \sigma \rangle$ , and the flux is replaced by an average effective flux. This effective flux can be obtained by manipulating the effective total cross section as follows:

$$\langle \sigma_t \rangle_\ell = \frac{\left\langle \frac{\sigma_0 + \sigma_t - \sigma_0}{[\sigma_0 + \sigma_t]^{\ell+1}} \right\rangle}{\left\langle \frac{1}{[\sigma_0 + \sigma_t]^{\ell+1}} \right\rangle} = \frac{\left\langle \frac{1}{[\sigma_0 + \sigma_t]^\ell} \right\rangle}{\left\langle \frac{1}{[\sigma_0 + \sigma_t]^{\ell+1}} \right\rangle} - \sigma_0, \quad (254)$$

from which

$$\left\langle \frac{1}{[\sigma_0 + \sigma_t]^{\ell+1}} \right\rangle = \frac{\left\langle \frac{1}{[\sigma_0 + \sigma_t]^\ell} \right\rangle}{\sigma_0 + \langle \sigma_t \rangle_k}. \quad (255)$$

Eq. 255 defines a recursion relation which can be used to compute the effective flux to any order

$$\left\langle \frac{1}{[\sigma_0 + \sigma_t]^{\ell+1}} \right\rangle = \prod_{k=0}^{\ell} \frac{1}{\sigma_0 + \langle \sigma_t \rangle_k}, \quad (256)$$

This equation reduces to Eq. 248 in the resolved range. It is the formula used in `genflx` to compute  $\phi_\ell(E)$  for the Bondarenko option.

When heterogeneity effects are important, the background cross section method can be extended as follows. In an infinite system of two regions (fuel and moderator), the neutron balance equations are

$$V_f \sigma_f \phi_f = (1 - P_f) V_f S_f + P_m V_m S_m , \quad (257)$$

and

$$V_m \sigma_m \phi_m = P_f V_f S_f + (1 - P_m) V_m S_m , \quad (258)$$

where  $V_f$  and  $V_m$  are the region volumes,  $\sigma_f$  and  $\sigma_m$  are the corresponding total macroscopic cross sections,  $S_f$  and  $S_m$  are the sources per unit volume in each region,  $P_f$  is the probability that a neutron born in the fuel will suffer its next collision in the moderator, and  $P_m$  is the probability that a neutron born in the moderator will suffer its next collision in the fuel. As usual, use is made of the reciprocity theorem,

$$V_f \sigma_f P_f = V_m \sigma_m P_m , \quad (259)$$

and the Wigner rational approximation to the fuel escape probability,

$$P_f = \frac{\sigma_e}{\sigma_e + \sigma_f} , \quad (260)$$

where  $\sigma_e$  is a slowly varying function of energy called the escape cross section, to obtain an equation for the fuel flux in the form

$$(\sigma_f + \sigma_e) \phi_f = \frac{\sigma_e S_m}{\sigma_m} + S_f . \quad (261)$$

In the limit where the resonances are narrow with respect to both fuel and moderator scattering, the source terms  $S_f$  and  $S_m$  take on their asymptotic forms of  $\sigma_p/E$  and  $\sigma_m/E$  respectively, and this equation becomes equivalent to the Bondarenko model quoted above with

$$\sigma_0^f = \frac{\sigma_e}{\rho_f} , \quad (262)$$

and

$$C(E) = \frac{\sigma_e + \sigma_p}{\rho_f E} . \quad (263)$$

Note that a large escape cross section (a sample that is small relative to the

average distance to collision), corresponds to infinite dilution as discussed above. To illustrate the general case, consider a neutron traveling through a lump of uranium oxide with an energy close to a resonance energy. If the neutron scatters from an oxygen nucleus, it will lose enough energy so that it can no longer react with the uranium resonance. Similarly, if the neutron escapes from the lump, it can no longer react with the uranium resonance. The processes of moderator scattering and escape are equivalent in some way. Comparing Eq. 262 with Eq. 251 gives an “equivalence principle” that says that a lump of particular dimensions and a mixture of particular composition will have the same self-shielded cross sections when the narrow resonance approximation is valid. The effects of material mixing and escape can simply be added to obtain the effective  $\sigma_0$  for a lump containing admixed moderator material. Therefore, Eq. 251 is extended to read

$$\sigma_{0g}^i = \frac{1}{\rho_i} \left\{ \sigma_e + \sum_{j \neq i} \rho_j \sigma_{t0g}^j(\sigma_{0g}^j, T) \right\}, \quad (264)$$

where the escape cross section for simple convex objects (such as plates, spheres, or cylinders) is given by  $(4V/S)^{-1}$ , where  $V$  and  $S$  are the volume and surface area of the object, respectively. Many codes that use the background cross section method modify the escape cross section as defined above to correct for errors in the Wigner rational approximation (“Bell factor”, “Levine factor”), or to correct for the interaction between different lumps in the moderating region (“Dancoff corrections”). These enhancements will not be discussed here.

As an example of self-shielded cross sections and how they vary with the background cross section, Fig. 23 shows the first three capture resonances of  $^{238}\text{U}$  (which are very important for thermal power reactors) at room temperature for  $\sigma_0$  values ranging from infinity down to 10 barns. Background cross sections that range between 20 and 50 barns are typical for uranium-oxide pin cells.

The **BROADR** chapter of this report showed its capability to compute standard resonance integrals. However, when self shielding and material temperature come into play, the effective resonance integral changes. GROUPE can calculate these quantities by doing one-group calculations with  $1/E$  weighting over a standard energy range. Using the range 0.5 eV to the upper limit of the evaluation will match what **BROADR** does. Fig. 24 shows the temperature dependence of the capture resonance integral for  $^{238}\text{U}$  from ENDF/B-VII at several different background cross sections. The range between 20 and 50 barns is typical for reactor pin cells.



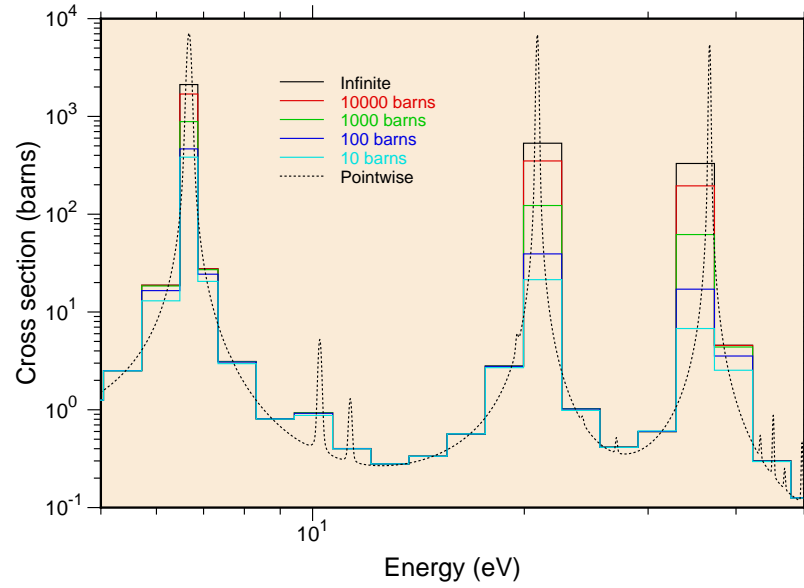


Figure 23: The self-shielding effect on the first three  $^{238}\text{U}$  capture resonances at room temperature in the 5 to 50 eV range. The multigroup boundaries are from the Los Alamos 187-group structure.

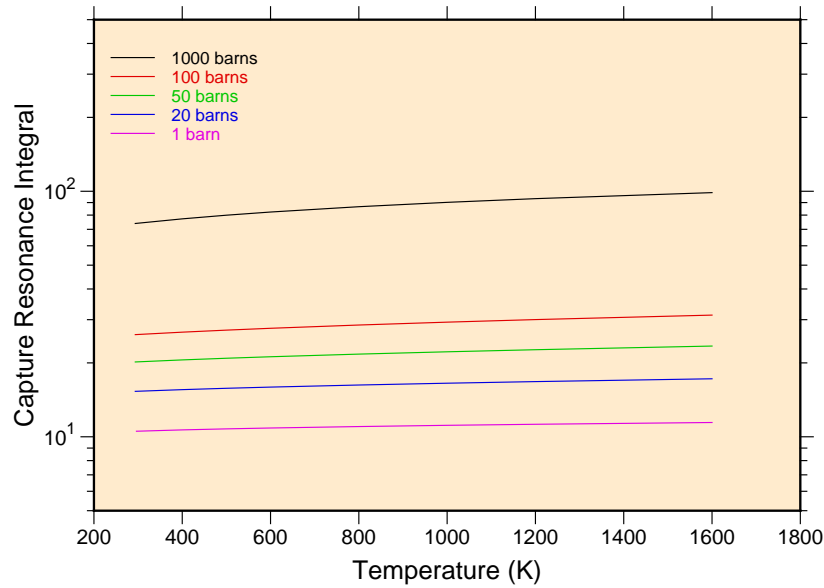


Figure 24: The capture resonance integral for  $^{238}\text{U}$  showing its variation with temperature and background cross section  $\sigma_0$ . The resonance integral at infinite dilution is 275.58 barns. Note the slope with temperature, which helps to produce a negative temperature coefficient for uranium systems.

### 8.5 Flux Calculator

This narrow-resonance approach is quite useful for practical fast reactor problems. However, for nuclear systems sensitive to energies from 1 to 500 eV, there are many broad- and intermediate-width resonances which cannot be self-shielded with sufficient accuracy using the Bondarenko approach. The GROUPR flux calculator is designed for just such problems.

Consider an infinite homogeneous mixture of two materials and assume isotropic scattering in the center-of-mass system. The integral slowing-down equation becomes

$$\begin{aligned} \sigma(E) \phi(E) &= \int_E^{E/\alpha_1} \frac{\sigma_{s1}(E')}{(1 - \alpha_1)E'} \phi(E') dE' \\ &+ \int_E^{E/\alpha_2} \frac{\sigma_{s2}(E')}{(1 - \alpha_2)E'} \phi(E') dE' . \end{aligned} \quad (265)$$

Furthermore, assume that material 1 is a pure scatterer with constant cross section and transform to the  $\sigma_0$  representation. The integral equation becomes

$$\begin{aligned} [\sigma_0 + \sigma_{t2}(E)] \phi(E) &= \int_E^{E/\alpha_1} \frac{\sigma_0}{(1 - \alpha_1)E'} \phi(E') dE' \\ &+ \int_E^{E/\alpha_2} \frac{\sigma_{s2}(E')}{(1 - \alpha_2)E'} \phi(E') dE' . \end{aligned} \quad (266)$$

Finally, assume that the moderator (material 1) is light enough so that all the resonances of material 2 are narrow with respect to scattering from material 1. This allows the first integral to be approximated by its asymptotic form,  $1/E$ . More generally, the integral is assumed to be a smooth function of  $E$  given by  $C(E)$ . In this way, material 1 can represent a mixture of other materials just as in the Bondarenko method. Fission source and thermal upscatter effects can also be lumped in  $C(E)$ . The integral equation has now been reduced to

$$[\sigma_0 + \sigma_t(E)] \phi(E) = C(E) \sigma_0 + \int_E^{E/\alpha} \frac{\sigma_s(E')}{(1 - \alpha)E'} \phi(E') dE' . \quad (267)$$

This is the simplest problem that can be solved using the flux calculator. The results still depend on the single parameter  $\sigma_0$ , and they can be used easily by codes that accept Bondarenko cross sections.

For heterogeneous problems, when the narrow-resonance approximation fails, both  $S_f$  and  $S_m$  in Eq. 261 will show resonance features. To proceed further with the solution of this equation, it is necessary to eliminate the moderator flux that is implicit in  $S_m$ . As a sample case, consider a fuel pin immersed in a large region of water. The fission neutrons appear at high energies, escape from the pin, slow down in the moderator (giving a  $1/E$  flux), and are absorbed by the resonances in the pin. In this limit, any dips in the moderator flux caused by resonances in the fuel are small. On the other hand, in a closely packed lattice, the flux in the moderator is very similar to the flux in the fuel, and resonance dips in the moderator flux become very evident. Intermediate cases can be approximated[54] by assuming

$$\phi_m = (1 - \beta) C(E) + \beta \phi_f , \quad (268)$$

where  $\beta$  is a heterogeneity parameter given by

$$\beta = \frac{V_f \sigma_e}{V_m \sigma_m} . \quad (269)$$

Note that  $\beta \rightarrow 0$  gives the isolated rod limit and  $\beta \rightarrow 1$  gives the close-packed lattice limit. This substitution reduces the calculation of the fuel flux to

$$(\sigma_f + \sigma_e) \phi_f = (1 - \beta) C(E) \sigma_e + S_\beta , \quad (270)$$

where  $S_\beta$  is the source term corresponding to a homogeneous mixture of the fuel isotopes with the isotopes from the moderator region changed by the factor  $\beta \sigma_e / \sigma_m$ . If the fuel and moderator each consisted of a single isotope and for isotropic scattering in the center-of-mass system, the integral equation would become

$$\begin{aligned} [\sigma_0 + \sigma_t(E)] \phi_f(E) &= (1 - \beta) C(E) \sigma_0 \\ &+ \int_E^{E/\alpha_m} \frac{\beta \sigma_0}{(1 - \alpha_m) E'} \phi_f(E') dE' \\ &+ \int_E^{E/\alpha_f} \frac{\sigma_{sf}(E')}{(1 - \alpha_f) E'} \phi_f(E') dE' , \end{aligned} \quad (271)$$

where  $\sigma_0$  is  $\sigma_e$  divided by the fuel density (units are barns/atom),  $\alpha_m$  and  $\alpha_f$  are the maximum fractional energy change in scattering for the two isotopes, and  $\sigma_{sf}(E')$  is the fuel scattering cross section.

This result has a form parallel to that of Eq. 267, but the solution depends on the two parameters  $\beta$  and  $\sigma_0$ . For any given data set,  $\beta$  must be chosen in advance. This might not be difficult if the data are to be used for one particular system, such as pressurized water reactors. The routine also has the capability to include one more moderator integral with a different  $\alpha$  value and a constant cross section. The full equation is

$$\begin{aligned}
 [\sigma_0 + \sigma_t(E)] \phi_f(E) &= (1 - \beta) C(E) \sigma_0 \\
 &+ \int_E^{E/\alpha_3} \frac{\beta(1 - \gamma)(\sigma_0 - \sigma_{am})}{(1 - \alpha_3)E'} \phi_f(E') dE' \\
 &+ \int_E^{E/\alpha_2} \frac{\sigma_{am} + \beta\gamma(\sigma_0 - \sigma_{am})}{(1 - \alpha_2)E'} \phi_f(E') dE' \\
 &+ \int_E^{E/\alpha_f} \frac{\sigma_{sf}(E')}{(1 - \alpha_f)E'} \phi_f(E') dE' , \quad (272)
 \end{aligned}$$

where  $\sigma_{am}$  is the cross section of the admixed moderator (with energy loss  $\alpha_2$ ), and  $\gamma$  is the fraction of the admixed moderator that is mixed with the external moderator (which has energy loss  $\alpha_3$ ). This allows calculations with H<sub>2</sub>O as the moderator and an oxide as the fuel. The flux calculator can thus obtain quite realistic flux shapes for a variety of fuel, admixed moderator and external moderator combinations. An example comparing the Bondarenko flux with a more realistic computed flux is given in Fig. 25.

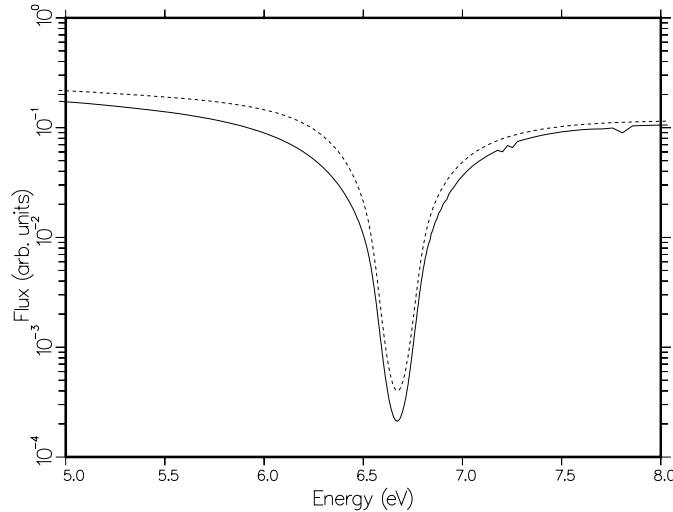


Figure 25: A comparison of the Bondarenko flux model (dashed) with a realistic computed flux (solid) for a <sup>238</sup>U oxide pin in water in the region of the 6.7 eV resonance.

In practice, a fuel rod rarely contains only one resonance isotope. As an example, consider a mixture of a few percent of  $^{239}\text{Pu}$  with  $^{238}\text{U}$  as the major component. There will be a strong dip in the flux associated with the 6.7 eV  $^{238}\text{U}$  resonance that will affect the flux in the region of the 7.8 eV  $^{239}\text{Pu}$  resonance (the interference effect), and there will also be a dip in the flux corresponding to the 7.8 eV resonance (the self-shielding effect). This additional complication in the flux shape would be expected to change the group constants for  $^{239}\text{Pu}$  since both features lie in the same group for typical group structures. However, the effect of the  $^{239}\text{Pu}$  on the  $^{238}\text{U}$  group constants should be minimal. This argument suggests that the full flux calculation be used for  $^{238}\text{U}$  as a single resonance material. The resulting flux would then be used to estimate the flux to be used in averaging the  $^{239}\text{Pu}$  cross sections as follows:

$$\phi_{239}(E, \sigma_0) = \frac{\phi_{238}(E, 50)}{\sigma_0 + \frac{\sigma_{239}(E)}{1 + \frac{\sigma_{238}(E)}{50}}} , \quad (273)$$

where the  $^{238}\text{U}$  flux is characteristic of a background of 50 barns/atom, which is representative of many thermal reactor systems. This formula assumes that the effect of  $^{239}\text{Pu}$  on the scattering source for the mixture is small, but it retains the absorption effects. The self-shielding of  $^{239}\text{Pu}$  is treated in the narrow resonance approximation only. The GROUPR flux calculator includes an option to write out a file containing the calculated flux and cross section needed for this formula (*e.g.*, for  $^{238}\text{U}$ ) and another option to skip the flux calculation and use the formula above to obtain the weighting flux (*e.g.*, for  $^{239}\text{Pu}$ ).

The slowing-down integral equation of Eq. 267 or 271 is solved point by point (see subroutine **genflx**) using the total and elastic cross sections on the PENDF tape produced by **RECONR**. In order to keep this task within bounds, the flux is computed from the lower limit of the first group to a specified energy **fehi** or until **nfmax** values have been computed. The flux at higher energies is continued using the Bondarenko model described above.

## 8.6 Fission Source

The fission source was included in the transfer cross section  $\sigma_X$  in the development above. It is usually convenient to separate fission from scattering. Assum-

ing isotropy, the source of fission neutrons into group  $g$  is given by

$$S_g = \sum_{g'} \sigma_{fg' \rightarrow g} \phi_{0g'} , \quad (274)$$

where the group-to-group matrix for fission is defined as in Eq. 246, but with  $\ell$  equal to zero. Most existing transport codes do not use this matrix form directly because the upscatter is expensive to handle and a reasonably accurate alternative exists. Except for relatively high neutron energies, the spectrum of fission neutrons is only weakly dependent on initial energy. Therefore, the fission source can be written

$$S_g = \chi_g \sum_{g'} \bar{\nu}_{g'} \sigma_{fg'} \phi_{0g'} , \quad (275)$$

where  $\bar{\nu}_g$  is the fission neutron yield,  $\sigma_{fg}$  is the fission cross section, and  $\chi_g$  is the average fission spectrum (the familiar “chi” vector), which can be defined by

$$\chi_g = \frac{\sum_{g'} \sigma_{fg' \rightarrow g} \phi_{0g'}}{\sum_g \sum_{g'} \sigma_{fg' \rightarrow g} \phi_{0g'}} . \quad (276)$$

The fission neutron yield is given by

$$\bar{\nu}_g = \sum_{g'} \sigma_{fg \rightarrow g'} / \sigma_{fg} . \quad (277)$$

Clearly,  $\chi_g$  as given by Eq. 276 depends on the flux in the system of interest. The dependence is weak except for high incident energies, and a rough guess for  $\phi_{0g}$  usually gives an accurate spectrum. When this is not the case, the problem can be iterated, or the full matrix representation can be used.

It is possible to take advantage of the weak energy dependence of the shape of the fission spectrum at low energies to reduce the time required to process fission data, and to reduce the size of the fission data on the output file. GROUPR determines a break energy from File 5 such that the fission spectrum is constant below this energy. It only has to make a single calculation of this spectrum  $\chi_g^{LE}$ . Then it computes a fission neutron production cross section  $\sigma_{fPg}^{HE}$  for groups below the break energy using the normal cross section processing methods. A full matrix  $\sigma_{fg' \rightarrow g}^{HE}$  is computed for groups above the break point. As an example, consider using the GROUPR 187-group structure and finding that there are

130 constant groups. The  $187 \times 187$  matrix is reduced to a  $57 \times 187$  matrix, a 187-element spectrum vector, and a 130-group production vector, for a total reduction in size of 68%. The effective fission matrix is given by

$$\sigma_{fg' \rightarrow g} = \sigma_{fg' \rightarrow g}^{HE} + \chi_g^{LE} \sigma_{fPg'}^{LE} . \quad (278)$$

The fission matrix computed by GROUPR represents the prompt part of fission only. The delayed component of fission is represented by a delayed-neutron yield  $\bar{\nu}_g^D$ , decay constants for six (or sometimes 8) time groups,  $\lambda_i^D$ , and emission probability spectra for six (or 8) time groups,  $\chi_{ig}^D$ . Steady-state fission can be obtained using

$$\bar{\nu}_g^{SS} = \bar{\nu}_g + \bar{\nu}_g^D , \quad (279)$$

and

$$\chi_g^{SS} = \frac{\sum_{g'} \sigma_{fg' \rightarrow g} \phi_{0g'} + \chi_g^D \sum_{g'} \bar{\nu}_{g'}^D \sigma_{fg'} \phi_{0g'}}{\sum_g \sum_{g'} \sigma_{fg' \rightarrow g} \phi_{0g'} + \sum_{g'} \bar{\nu}_{g'}^D \sigma_{fg'} \phi_{0g'}} , \quad (280)$$

where

$$\chi_g^D = \sum_i \chi_{ig}^D . \quad (281)$$

Note that  $\chi_g^D$  sums to unity, but the  $\chi$  for each time group sums to the fraction of the delayed neutron yield that appears in that time group.

In ENDF-format files, the total fission reaction is represented by MT=18. Important isotopes also give the partial fission reactions (n,f), (n,n'f), (n,2nf), and sometimes (n,3nf) using MT=19, 20, 21, and 38 respectively. The MT=18 representation is adequate for most fission reactor applications, but the partial reactions should be processed for applications with significant flux above 6 MeV. Caution: although the cross section for MT=18 equals the sum of its parts, the group-to-group fission matrix  $\sigma_{fg \rightarrow g'}$  computed from MT=18 will not, in general, equal the sum of the partial matrices for MT=19, 20, 21, and 38 above the 6-MeV threshold for second-chance fission. The breakup into partial fission matrices has not been used in recent ENDF/B-VII evaluations. The delayed neutron data are given in MT=455. Sample input instructions for processing the various combinations of fission reactions used in ENDF/B will be found in

Section 8.14. GROUPR outputs all the components of fission separately in order to give succeeding modules or codes complete flexibility.

## 8.7 Diffusion Cross Sections

The diffusion equation is often used in reactor physics calculations. Starting with Eq. 241, use the Legendre expansion for  $\phi_g$  in the derivative term, and make use of the recursion relation for  $\mu P_\ell(\mu)$  and the orthogonality relation for the Legendre polynomials to obtain the transport equation in spherical-harmonic form

$$\begin{aligned} \frac{n+1}{2n+1} \frac{\partial \phi_{n+1,g}}{\partial x} + \frac{n}{2n+1} \frac{\partial \phi_{n-1,g}}{\partial x} \sigma_{tn,g} \phi_{ng} \\ = \sum_{g'} \sigma_{sng' \rightarrow g} \phi_{ng'} + S_{fg} + Q_{ng} , \end{aligned} \quad (282)$$

where the transfer term has been separated into a scattering term with cross section  $\sigma_s$ , and a fission source term  $S_f$ . When this set of equations is truncated at  $n = N$ , the results are usually called the “P<sub>N</sub> equations”. For now, all terms with  $n > 1$  are dropped, and  $Q$  is assumed to be isotropic. Thus,

$$\frac{\partial \phi_{1g}}{\partial x} + \sigma_{t0g} \phi_{0g} = \sum_{g'} \sigma_{s0g' \rightarrow g} \phi_{0g'} + S_{fg} + Q_{0g} , \quad (283)$$

and

$$\frac{1}{3} \frac{\partial \phi_{0g}}{\partial x} + \sigma_{t1g} \phi_{1g} = \sum_{g'} \sigma_{s1g' \rightarrow g} \phi_{1g'} . \quad (284)$$

The second equation can be written in the form of Fick’s Law as follows:

$$\phi_{1g} = -D_g \frac{\partial \phi_{0g}}{\partial x} , \quad (285)$$

$$D_g = \frac{1}{3} \frac{1}{\sigma_{t1g} - \sum_{g'} \sigma_{s1g' \rightarrow g} \phi_{1g'} / \phi_{1g}} , \quad (286)$$

where  $D_g$  is the diffusion constant. The term in the denominator of the second factor is the transport cross section for diffusion,  $\sigma_{trD}$ . Unfortunately, it depends on a fairly complete knowledge of the neutron current in the system, perhaps



from a previous calculation. However, for many problems,  $\sigma_{trD}$  can be simplified by assuming that

$$\sum_{g'} \sigma_{s1g' \rightarrow g} \phi_{1g'} \approx \sum_{g'} \sigma_{s1g \rightarrow g'} \phi_{1g} , \quad (287)$$

with the result that

$$\sigma_{trD,g} = \sigma_{t1g} - \sum_{g'} \sigma_{s1g \rightarrow g'} , \quad (288)$$

or

$$\sigma_{trD,g} = \sigma_{t1g} - \bar{\mu}_g \sigma_{s0g} , \quad (289)$$

where  $\bar{\mu}_g$  is the average scattering cosine for neutrons in group  $g$ . These forms depend only on the shape of the weighting flux within the group, as usual. Substituting for  $\phi_{1g}$  in Eq. 283 gives

$$\frac{\partial}{\partial x} \left( -D_g \frac{\partial \phi_{0g}}{\partial x} \right) + \sigma_{0tg} \phi_{0g} = \sum_{g'} \sigma_{s0g' \rightarrow g} \phi_{0g'} + S_{fg} + Q_{0g} , \quad (290)$$

which is the standard diffusion equation in slab geometry. Neither the diffusion coefficient nor the transport cross section for diffusion is produced directly by GROUPR. However, the components such as  $\sigma_{t\ell}$  and  $\sigma_{s0g' \rightarrow g}$  are made available to subsequent modules.

## 8.8 Cross Sections for Transport Theory

The  $S_N$  (discrete ordinates) transport codes solve the equation

$$\begin{aligned} \mu \frac{\partial}{\partial x} \phi_g(\mu, x) &+ \sigma_g^{SN} \phi_g(\mu, x) \\ &= \sum_{\ell=0}^N \frac{2\ell+1}{2} P_\ell(\mu) \sum_{g'} \sigma_{s\ell g' \rightarrow g}^{SN}(x) \phi_{\ell g'} \\ &+ S_{fg} + Q_g(\mu, x) , \end{aligned} \quad (291)$$

where once again one-dimensional slab geometry has been used for simplicity.<sup>7</sup>

By comparing Eq. 291 with Eq. 241, it is seen that the  $S_N$  equations require the

---

<sup>7</sup>The following development is based on the work of Bell, Hansen, and Sandmeier[55].

following cross sections:

$$\sigma_{slg' \rightarrow g}^{SN} = \sigma_{slg' \rightarrow g}, \quad g' \neq g, \quad (292)$$

and

$$\sigma_{slg \rightarrow g}^{SN} = \sigma_{slg \rightarrow g} - \sigma_{tlg} + \sigma_g^{SN}, \quad (293)$$

where  $\sigma_g^{SN}$  is not determined and can be chosen to improve the convergence of the  $S_N$  calculation. A particular choice of  $\sigma_g^{SN}$  gives rise to a “transport approximation”, and various recipes are in use, such as:

Consistent-P approximation:

$$\sigma_g^{SN} = \sigma_{t0g}. \quad (294)$$

Inconsistent-P approximation:

$$\sigma_g^{SN} = \sigma_{t,N+1,g}. \quad (295)$$

Diagonal transport approximation:

$$\sigma_g^{SN} = \sigma_{t,N+1,g} - \sigma_{s,N+1,g \rightarrow g}. \quad (296)$$

Bell-Hansen-Sandmeier (BHS) or extended transport approximation:

$$\sigma_g^{SN} = \sigma_{t,N+1,g} - \sum_{g'} \sigma_{s,N+1,g \rightarrow g'}. \quad (297)$$

Inflow transport approximation:

$$\sigma_g^{SN} = \sigma_{t,N+1,g} - \frac{\sum_{g'} \sigma_{s,N+1,g' \rightarrow g} \phi_{N+1,g'}}{\phi_{N+1,g}}. \quad (298)$$

The first two approximations are most appropriate when the scattering orders above  $N$  are small. The inconsistent option removes most of the delta function of forward scattering introduced by the correction for the anisotropy of the total scattering rate, and should normally be more convergent than the consistent option. The diagonal and BHS recipes make an attempt to correct for anisotropy in the scattering matrix and are especially effective for forward-peaked scattering. The BHS form is more often used, but the diagonal option can be substituted when BHS produces negative values. The inflow recipe makes the  $N+1$  term

of the  $P_N$  expansion vanish, but it requires a good knowledge of the  $N+1$  flux moment from some previous calculation. Inflow reduces to BHS for systems in equilibrium by detail balance (*i.e.*, the thermal region). In the absence of self-shielding (that is,  $\sigma_0 \rightarrow \infty$ ), the distinction between  $\sigma_{t1}$  and  $\sigma_{t0}$  disappears, and so does the distinction between the inconsistent-P and consistent-P options. Also note that the inflow and BHS versions of  $\sigma_g$  are equivalent to the definitions of  $\sigma_{trD,g}$  given in Eqs. 286 and 288, respectively, when  $N=0$ .

The transport-corrected cross sections are not computed directly by GROUPE, but the components needed are written to the GROUPE output file for use by subsequent modules.

## 8.9 Photon Production and Coupled Sets

Photon transport is treated with an equation similar to Eq. 241, except that the flux, cross sections, and groups are all referred to photon interactions and photon energies instead of to the corresponding neutron quantities. Methods of producing the photon interaction cross sections are described in GAMINR. The external photon source  $Q_g$  depends on the neutron flux and the photon production cross sections through

$$Q_g(x, \mu) = \sum_{\ell=0}^{\infty} \frac{2\ell+1}{2} P_{\ell}(\mu) \sum_{g'} \sigma_{\gamma\ell g' \rightarrow g}(x) \phi_{\ell g'}(x) , \quad (299)$$

where  $\sigma_{\gamma\ell g' \rightarrow g}$  is defined by Eq. 246 with X replaced by  $\gamma$ . The ENDF files define  $\sigma_{\gamma}$  using a combination of photon production cross sections (MF=13), photon yields (MF=12) with respect to neutron cross sections (MF=3), discrete lines (MF=12 and 13), and continuous  $\gamma$  distributions (MF=15). Methods for working with these representations will be discussed in more detail below.

The low-energy groups for fission and capture normally have photon emission spectra whose shapes do not change with energy. The same method used for reducing the size of the fission matrix (see Section 8.6) can be used for these photon production matrices. In mathematical form,

$$\sigma_{\gamma g' \rightarrow g} = \sigma_{\gamma g' \rightarrow g}^{HE} + s_{\gamma}^{LE} g \sigma_{\gamma P g}^{LE} , \quad (300)$$

where  $s_{\gamma}^{LE} g$  is the normalized emission spectrum, and  $\sigma_{\gamma P g}^{LE}$  is the associated production cross section.

For many practical problems, it is convenient to combine the neutron and photon transport calculations into a single application of Eq. 241 where the photons are treated as additional groups of low-energy neutrons. Since  $(\gamma, n)$  events are not usually very important, the downscattering structure (see Section 8.2) of the transport calculation is preserved for both  $n \rightarrow \gamma$  and  $n \rightarrow n$  events. Cross sections for this application are called “coupled sets”. Coupled sets are not produced directly by GROUPR, but the  $n \rightarrow n$  and  $n \rightarrow \gamma$  components are made available to the other modules where they can be combined with  $\gamma \rightarrow \gamma$  cross sections from GAMINR. As an example, the MATXSR module can format data for the TRANSX code, which can, in turn, prepare coupled sets for use by standard transport codes such as ONEDANT[13] or PARTISN[16]. The normal arrangement of data in a coupled set is shown schematically in Fig. 26.

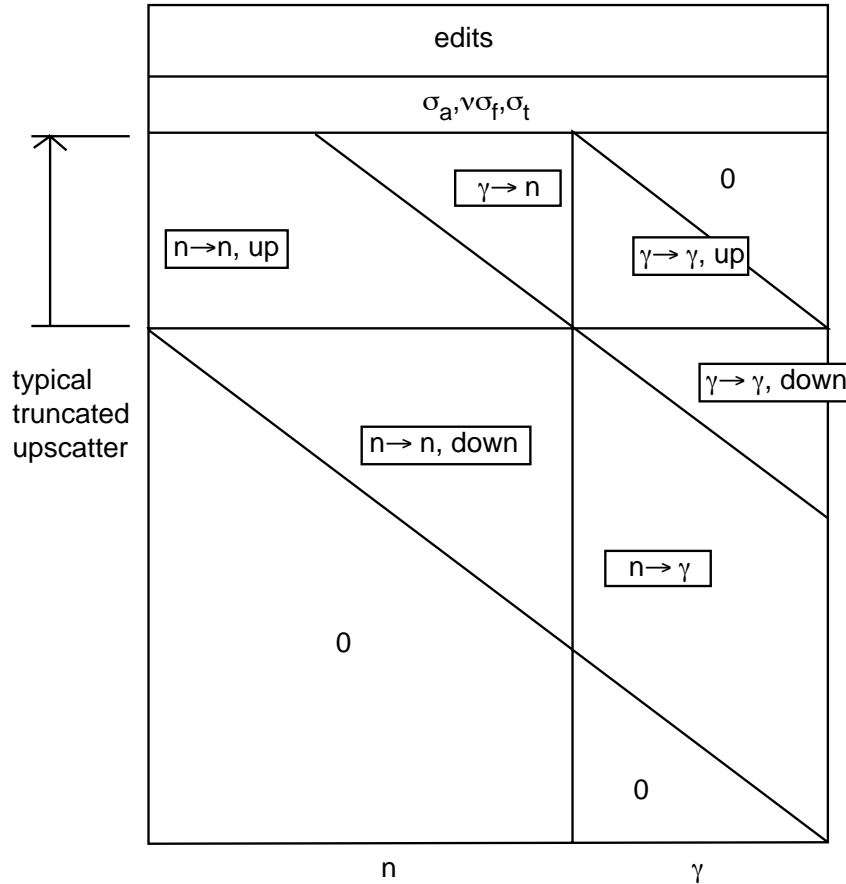


Figure 26: Arrangement of neutron (n) and photon (γ) cross sections in a coupled transport table. The group index increases from left to right, and the position index increases from top to bottom. The  $\gamma \rightarrow n$  and  $\gamma \rightarrow \gamma$  upscatter blocks are normally empty.

### 8.10 Thermal Data

GROUPR uses the thermal data written onto the PENDF tape by the [THERMR](#) module. It does not process ENDF File-7 data directly. Three different representations of thermal scattering are used in ENDF.

For crystalline materials like graphite, coherent elastic (with zero energy change) scattering can take place. The cross section for this process shows well-defined Bragg edges at energies that correspond to the various lattice-plane spacings in the crystalline powder. As shown in [THERMR](#), the angular dependence of the coherent elastic cross section can be written as

$$\sigma^{coh}(E, \mu) = \sum_i \frac{b_i}{E} \delta(\mu - \mu_i) , \quad (301)$$

where

$$\mu_i = 1 - 2 \frac{E_i}{E} , \quad (302)$$

and where the  $E_i$  are the energies of the Bragg edges. [THERMR](#) integrates Eq. 301 over all angles, and writes the result to the PENDF tape. Clearly, the  $b_i$  can be recovered from

$$E \sigma^{coh}(E) = \sum_i' b_i , \quad (303)$$

where the primed sum is over all  $i$  such that  $E_i < E$ . It is only necessary to locate the steps in  $E \sigma^{coh}(E)$ . The size of the step gives  $b_i$ , and the  $E$  for the step gives  $E_i$ . The Legendre cross sections become

$$\sigma_\ell^{coh}(E) = \sum_i' \frac{b_i}{E} P_\ell(\mu_i) , \quad (304)$$

where any terms with  $\mu_i < -1$  are omitted from the primed sum. An example of a pointwise cross section for coherent elastic scattering is given in Fig. 27.

For hydrogenous solids like polyethylene and zirconium hydride, the process of incoherent elastic scattering is important. Here the angular cross section is given by

$$\sigma^{iel}(E, \mu) = \frac{\sigma_b}{2} \exp \left[ -\frac{2EW}{A} (1 - \mu) \right] . \quad (305)$$

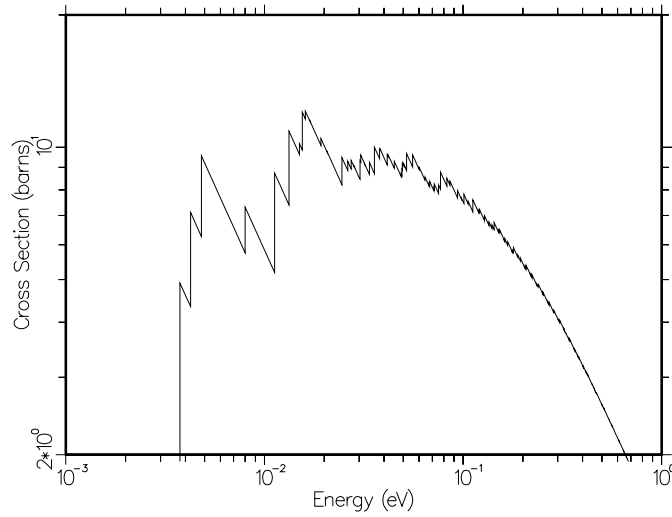


Figure 27: The coherent elastic scattering cross section for BeO showing the Bragg edges. The shape of  $\sigma(E)$  between edges is  $1/E$ . Therefore, the function  $E\sigma(E)$  is a stair-step function, where the height of each step depends on the structure factor for scattering from that set of lattice planes (see Eq. 303).

**THERMR** converts this into an integrated cross section,  $\sigma^{iel}(E)$ , and a set of  $N$  equally probable emission cosines,  $\bar{\mu}_i$ . These angles are present in File 6 on the PENDF tape. GROUPR can easily determine the Legendre components of the scattering cross section using

$$\sigma_\ell^{iel}(E) = \sigma^{iel}(E) \frac{1}{N} \sum_{i=1}^N P_\ell(\mu_i) . \quad (306)$$

The third thermal process is incoherent inelastic scattering. Here the neutron energy can either increase or decrease. The data from **THERMR** are given as a cross section in File 3 and an energy-angle distribution using a special form of File 6. The distribution is represented by sets of secondary-energy values  $E'$  for particular incident energies  $E$ . For each  $E \rightarrow E'$ , a scattering probability  $f^{inc}(E \rightarrow E')$  and a set of equally probable cosines  $\mu_i(E \rightarrow E')$  are given. The scattering probabilities for each value of  $E$  integrate to unity. Although the thermal scattering cross section is a smooth function of incident neutron energy, this is not true for the scattering from  $E$  to one particular final energy group  $g'$ , since the differential cross section tends to peak along the line  $E' = E$  and at energy-transfer values corresponding to well-defined excitations in the molecule or lattice. If interpolation between adjacent values of  $E$  were to be performed along lines of constant  $E'$ , the excitation peaks and the  $E = E'$  feature would

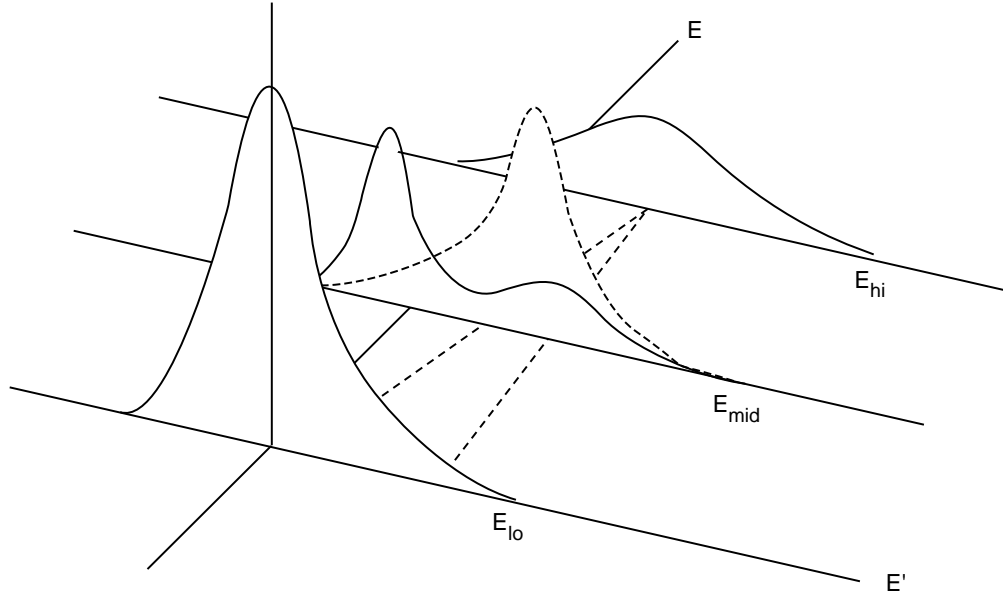


Figure 28: Illustration of thermal interpolation showing the double-humped curve resulting from simple Cartesian interpolation for a discrete excitation (solid) and the more realistic curve obtained by interpolating along lines of constant energy transfer (dashed).

produce double features in the intermediate spectrum, as shown in Fig. 28. To avoid this problem, while still using a relatively sparse incident energy grid, GROUPR interpolates between  $E$  and  $E'$  along lines of constant energy transfer. Of course, this breaks down at low values of  $E'$ , because one of the spectra will go to zero before the other one does. In this range, GROUPR transforms the low-energy parts of the two spectra onto a “unit base,” combines them in fractions that depend on  $E$ , and scales the result back out to the interpolated value of  $E'$  corresponding to  $E$ .

### 8.11 Generalized Group Integrals

In order to unify many formerly different processing tasks, GROUPR uses the concept of a generalized group integral

$$\sigma_g = \frac{\int_g \mathcal{F}(E) \sigma(E) \phi(E) dE}{\int_g \phi(E) dE}, \quad (307)$$

where the integrals are over all initial neutron energies in group  $g$ ,  $\sigma(E)$  is a cross section at  $E$ , and  $\phi(E)$  is an estimate of the flux at  $E$ . The function  $\mathcal{F}(E)$  is called the “feed function”. It alone changes for different data types. To average a neutron cross section,  $\mathcal{F}$  is set to 1. To average a ratio quantity like  $\bar{\mu}$  with respect to elastic scattering,  $\mathcal{F}$  is set to  $\bar{\mu}$ . For photon production,  $\mathcal{F}$  is the photon yield. For matrices,  $\mathcal{F}$  is the  $\ell$ -th Legendre component of the normalized probability of scattering into secondary energy group  $g'$  from initial energy  $E$ . This definition is clearly independent of whether the secondary particle is a neutron or a photon.

The question of integration grid or quadrature scheme is important for the evaluation of Eq. 307. Each factor in the integrands has its own characteristic features, and it is important to account for them all. First, a grid must be established for each factor. As an example, the grid of  $\sigma(E)$  is generated in *RECONR* such that sigma can be obtained to within a given tolerance by linear interpolation. *GROU*PR contains a subroutine *getsig* which carries out this interpolation at  $E$  and also returns the next grid energy in *enext*. Subroutines *getflx* and *getff* perform similar functions for the flux and feed function. It is now easy to generate a union grid for the three-factor integrand using the following Fortran:

```
...
call getsig(e,enext,...)
call getflx(e,en,...)
if (en.lt.enext) enext=en
call getff(e,en,...)
if (en.lt.enext) enext=en
...
```

On occasion, there will be a discontinuity at *enext* for one of the factors. In order to flag such a case, each “get” routine also sets a discontinuity flag *idisc*. The grid logic actually used throughout *NJOY* is as follows:

```
...
call getsig(e,enext,idisc,...)
call getflx(e,en,idis,...)
if (en.eq.enext.and.idis.gt.idisc) idisc=idis
if (en.lt.enext) idisc=idis
if (en.lt.enext) enext=en
call getff(e,en,idis,...)
if (en.eq.enext.and.idis.gt.idisc) idisc=idis
```



```

      if (en.lt.enext) idisc=idis
      if (en.lt.enext) enext=en
      ...

```

This union grid for the integrand in the numerator is used to subdivide the generalized group integral of Eq. 307 into “panels”. The main program of GROUPR carries out the integrals with the following logic:

```

      ...
      elo=egn(ig)
      ehi=egn(ig+1)
      enext=ehi
230  call panel(elo,enext,...)
      if (enext.eq.ehi) go to 240
      elo=enext
      enext=ehi
      go to 230
240  continue
      ...

```

A panel is first defined by the energy bounds of group  $g$ . Subroutine `panel` is called to sum in the contributions from this panel. However, `panel` discovers that the integrand has a grid point at `enext` less than `ehi`. It adds in the contributions for the smaller panel `elo` to `enext` and returns. GROUPR now sees that `enext` is less than `ehi`, so it tries a new panel from the top of the last panel (`elo=enext`) to `ehi`. This loop continues until a panel with `ehi` as its upper bound is summed in. The integral for this group is then complete.

In this simple way, the algorithm accounts for the user’s group structure and for all structure in the integrand. The method used for establishing the [RE-CONR](#) grid makes this integration algorithm equivalent to adaptive integration as used in MINX[20]. It has the great advantage that no “stack” of intermediate results is carried along. This single-pass feature of the quadrature scheme allows many different integrals to be accumulated simultaneously within reasonable storage limits. In this way, GROUPR accumulates cross sections for all values of  $\sigma_0$  simultaneously. Similarly, group-to-group cross sections are computed for all secondary energy groups and all Legendre orders simultaneously.

Any degree of complexity can be used for the integral over each subpanel. Because  $\sigma(E)$  has been linearized, `panel` is based on trapezoidal integration. Both  $\phi(E)$  and  $R(E) = \sigma(E) \times \phi(E)$  are assumed to vary linearly across each panel. In some cases, the feed function is oscillatory over a certain energy range

(see Two-Body Scattering, Section 8.12). It is then convenient to integrate inside the panel using Lobatto quadrature[56] (note the variable **nq** in **panel1**). As discussed in more detail later, this method can obtain accurate results for an oscillatory function whose integral is small with respect to its magnitude. This behavior is characteristic of the higher Legendre components of two-body scattering cross sections.

The generalized integration scheme discussed here is also used by the **GAM-INR** and **ERRORR** modules.

## 8.12 Two-Body Scattering

Elastic scattering (ENDF/B MT=2) and discrete inelastic neutron scattering (with MT=51 – 90) are both examples of two-body kinematics and are treated together by GROUPR. Some other cases that occur for charged particles or in File 6 will be discussed later. The feed function required for the group-to-group matrix calculation may be written

$$\mathcal{F}_{\ell g'}(E) = \int_{g'} dE' \int_{-1}^{+1} d\omega f(E \rightarrow E', \omega) P_{\ell}(\mu[\omega]) , \quad (308)$$

where  $f(E \rightarrow E', \omega)$  is the probability of scattering from  $E$  to  $E'$  through a center-of-mass cosine  $\omega$  and  $P_{\ell}$  is a Legendre polynomial for laboratory cosine  $\mu$ . The laboratory cosine corresponding to  $\omega$  is given by

$$\mu = \frac{1 + R\omega}{\sqrt{1 + R^2 + 2R\omega}} , \quad (309)$$

and the cosine  $\omega$  is related to secondary energy  $E'$  by

$$\omega = \frac{E'(1 + A)^2/A' - E(1 + R^2)}{2RE} , \quad (310)$$

where  $A'$  is the ratio of the emitted particle mass to the incident particle mass ( $A'=1$  for neutron scattering). In Eqs. 309 and 310,  $R$  is the effective mass ratio

$$R = \sqrt{\frac{A(A + 1 - A')}{A'}} \sqrt{1 - \frac{(A + 1)(-Q)}{AE}} , \quad (311)$$

where  $A$  is the ratio of target mass to neutron mass, and  $-Q$  is the energy level of the excited nucleus ( $Q=0$  for elastic scattering). Integrating Eq. 308 over secondary energy gives

$$\mathcal{F}_{\ell g'}(E) = \int_{\omega_1}^{\omega_2} f(E, \omega) P_{\ell}(\mu[\omega]) d\omega , \quad (312)$$

where  $\omega_1$  and  $\omega_2$  are evaluated using Eq. 310 for  $E'$  equal to the upper and lower bounds of  $g'$ , respectively. The scattering probability is given by

$$f(E, \omega) = \sum_{\ell=0}^L f_{\ell}(E) P_{\ell}(\omega) , \quad (313)$$

where the Legendre coefficients are either retrieved directly from the ENDF File 4 or computed from File 4 tabulated angular distributions (see subroutines `getfle` and `getco`).

The integration in Eq. 312 is performed (see subroutine `getdis`) simultaneously for all Legendre components using Gaussian quadrature[56]. The quadrature order is selected based on the estimated polynomial order of the integrand. A reasonable estimate is given by

$$ND + NL + \log(300/A) , \quad (314)$$

where ND is the number of Legendre components desired for the feed function, and NL is the number of components required to represent  $f(E, \omega)$ . The log term approximates the number of additional components required to represent the center-of-mass to lab transformation.

The two-body feed function for higher Legendre orders is a strongly oscillatory function in some energy ranges. An example is shown in Fig. 29. Furthermore, the integral of the oscillatory part is often small with respect to the magnitude of the function. Such functions are very difficult to integrate with adaptive techniques, which converge to some fraction of the integral of the absolute value. This is the reason that MINX[20] gave poor answers for small Legendre components of the scattering matrix. Gaussian methods, on the other hand, are capable of integrating such oscillatory functions exactly if they are polynomials. Since a polynomial representation of the feed function is fairly accurate, a Gaussian quadrature scheme was chosen. The scheme used is also well adapted to performing many integrals in parallel. In GROUPR, all Legendre components and all final groups are accumulated simultaneously (see `panel`).

The boundaries of the various regions of the feed function are called “critical points.” Between critical points, the feed function is a smooth analytic function of approximately known polynomial order. It is only necessary to add these critical points to the incident energy grid of the feed function (the `enext` variable) and to tell `panel` what quadrature order (`nq`) to use. The critical points are determined in `getff` by solving Eq. 310 for the values of  $E$  for which  $\omega = +1$

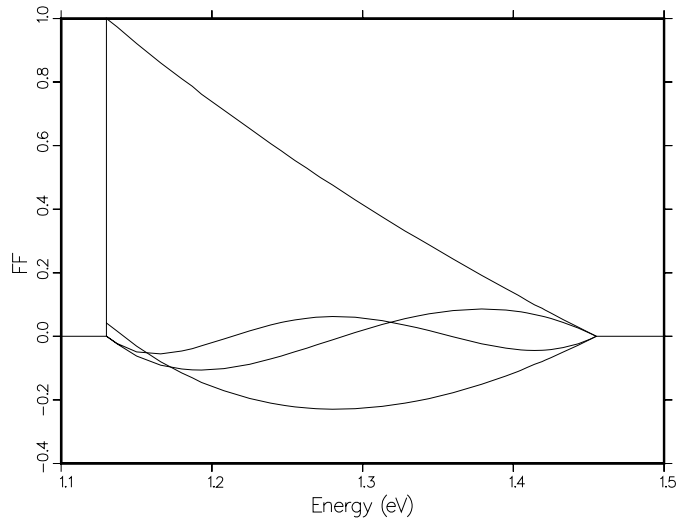


Figure 29: A typical feed function for two-body scattering showing the oscillations that must be treated correctly by the integration over incident energy.

and  $\omega = -1$  when  $E'$  is equal to the various group boundaries. This can be done by writing

$$\frac{E_g}{E} = \frac{1}{(1+A)^2} [R^2 \pm 2R + 1] , \quad (315)$$

substituting for  $E$  using Eq. 311, and then solving for  $R$ . The result is

$$E_{crit} = \frac{\frac{(A+1)(-Q)}{A}}{1 - \frac{A'F^2}{A(A+1-A')}} , \quad (316)$$

where

$$F = \frac{1 \pm \sqrt{D}}{1 + \frac{E_F}{(-Q)}} , \quad (317)$$

$$D = \left[ \frac{A(A+1-A')}{A'} \left( 1 + \frac{E_F}{(-Q)} \right) - 1 \right] \frac{E_F}{(-Q)} , \quad (318)$$

and

$$E_F = \frac{1+A}{A+1-A'} E_g . \quad (319)$$

File 4 can also contain angular distributions for charged-particle emission through discrete levels (for ENDF/B-VI and later see MT=600 – 648 for protons, MT=650 – 698 for deuterons, and so on; the elastic case, MT=2, is discussed in the next section). Moreover, File 6 can contain angular distributions for discrete two-body scattering (see Law 3). It can also declare that a particular particle is the recoil particle from a two-body reaction (Law 4), in which case the appropriate angular distribution is obtained from the corresponding Law 3 subsection by complementing the angle. The representation of the angular distribution for these laws is almost identical to that in File 4, and the calculation is done in `getdis` using much of the File 4 coding. The effects on the kinematics of the difference in the mass of the emitted and incident particles are handled by the variable  $A'$  in the above equations.

### 8.13 Charged-Particle Elastic Scattering

Coulomb scattering only occurs in the elastic channel, and this calculation also uses the `getdis` subroutine. The problem with Coulomb scattering is that the basic Rutherford formula becomes singular at small angles. In practice, this singularity is removed by the screening effects of the atomic electrons. The forward transport of charged particles in this screening regime is usually handled by continuous-slowing-down theory by using a “stopping power”. The new ENDF-6 format allows for three different ways to handle the large-angle scattering regime. First and most general is the nuclear amplitude expansion:

$$\begin{aligned}\sigma &= |\text{nucl} + \text{coul}|^2 \\ &= \sigma_{\text{nucl}} + \sigma_{\text{coul}} + \text{interference}\end{aligned}\tag{320}$$

The Coulomb term is given by the Rutherford formula, a Legendre expansion is defined for the nuclear term, and a complex Legendre expansion is defined for the interference term. This representation cannot be generated directly from experimental data; an R-matrix or phase-shift analysis is necessary.

A method very closely related to experiment ( $\sigma_{\text{exp}}$ ) is the nuclear plus interference (NI) formula:

$$\sigma_{\text{NI}}(\mu, E) = \sigma_{\text{exp}}(\mu, E) - \sigma_{\text{coul}}(\mu, E),\tag{321}$$

where the function is only defined for angles with cosines  $\mu < \mu_{\text{max}}$ . The mini-

mum angle is usually taken to be somewhere around 20 degrees (GROUPR uses  $\mu_{\max}=0.96$ ). This function is still ill-behaved near the cutoff, and it must be tabulated. The third option is the residual cross section expansion:

$$\sigma_R(\mu, E) = (1 - \mu) [\sigma_{\text{exp}}(\mu, E) - \sigma_{\text{coul}}(\mu, E)]. \quad (322)$$

The  $(1 - \mu)$  term removes the pole at the origin. The residual is uncertain, but it is usually small enough that the entire curve can be fitted with Legendre polynomials without worrying about what happens at small angles. In practice, both the nuclear amplitude expansion and the nuclear plus interference representation are converted to the residual cross section representation in subroutine `conver`. As a result, `getdis` only has to cope with the one representation.

## 8.14 Continuum Scattering and Fission

In ENDF evaluations, scattering from many closely-spaced levels or multibody scattering such as  $(n,2n)$ ,  $(n,n'\alpha)$  or fission is often represented using a separable function of scattering cosine and secondary neutron energy

$$f(E \rightarrow E', \mu) = F(E, \mu) g(E \rightarrow E'), \quad (323)$$

where  $F$  is the probability that a neutron will scatter through a laboratory angle with cosine  $\mu$  irrespective of final energy  $E'$ . It is obtained from MF=4. Similarly,  $g$  is the probability that a neutron's energy will change from  $E$  to  $E'$  irrespective of the scattering angle, and it is given in MF=5. Continuum reactions are mostly identified by MT numbers of 6 – 49 and 91. Recently, previously unused MT numbers, 152 through 200, were assigned to additional continuum reactions that are beginning to appear in specialized evaluated files that extend beyond 20 MeV (*e.g.*, the International Reactor Dosimetry and Fusion File). Secondary-energy distributions, whether found in MF=5 or MF=6 are represented by “Laws” as follows:

| Law | Description                                                       |
|-----|-------------------------------------------------------------------|
| 1   | Arbitrary tabulated function                                      |
| 5   | General evaporation spectrum<br>(Used for delayed neutrons only.) |
| 7   | Simple Maxwellian fission spectrum                                |
| 9   | Evaporation spectrum                                              |
| 11  | Energy-dependent Watt fission spectrum                            |
| 12  | Energy-dependent spectrum of Madland and Nix                      |

The feed functions for continuum scattering are simply

$$\mathcal{F}_{\ell g'}(E') = \int_{-1}^{+1} P_{\ell}(\mu) f(E, \mu) d\mu \int_{g'} g(E, E') dE' . \quad (324)$$

The first integral is returned by **getfle** [“fle” for  $f_{\ell}(E)$ ] as described above, and the second integral is returned by **getsed** (“sed” for secondary-energy distribution).

For Law 1,  $g$  is given as a tabulated function of  $E'$  for various values of  $E$ . When  $E_1 \leq E < E_2$ , the term  $\int_{g'} g(E, E') dE'$  is obtained by interpolating between precomputed values of  $\int_{g'} g(E_1, E') dE'$  and  $\int_{g'} g(E_2, E') dE'$  in subroutine **getsed**. Except in the case of fission, any apparent upscatter produced by the “stairstep” treatment near  $E=E'$  is added to the in-group scattering term ( $g'=g$ ).

For Law 5,  $g(x)$  is given versus  $x = E'/\theta(E)$  and  $\theta(E)$  is given vs.  $E$  in File 5. This secondary neutron distribution leads to the following group integral:

$$\int_{g'} g(E, E') dE' = \theta(E) \int_{E_1/\theta}^{E_2/\theta} g(x) dx , \quad (325)$$

with  $E_1$  and  $E_2$  being the lower and upper boundary energies for group  $g'$ .

For Law 7, the secondary-energy distribution is given by

$$g(E, E') = \frac{\sqrt{E'}}{I} \exp\left(-\frac{E'}{\theta(E)}\right) , \quad (326)$$

where the effective temperature  $\theta(E)$  is tabulated in File 5 and the normalization factor is given by

$$I = \theta^{3/2} \left[ \sqrt{\frac{\pi}{4}} \operatorname{erf}(x) - x e^{-x} \right] , \quad (327)$$

where

$$x = \frac{E - U}{\theta} . \quad (328)$$

Here  $U$  is a constant used to define the upper limit of secondary neutron energy  $\theta \leq E' \leq E - U$ . The desired group integral is given by

$$\begin{aligned}
\int_{g'} g(E, E') dE' &= \int_{E_1}^{E_2} g(E, E') dE' \\
&= \frac{X_1 - X_2 - Y_1 + Y_2}{\sqrt{\pi/4 - Y - X}} ,
\end{aligned} \tag{329}$$

where

$$X = \sqrt{x} e^{-x} , \tag{330}$$

$$Y = \sqrt{\frac{\pi}{4}} \operatorname{erfc}(\sqrt{x}) , \tag{331}$$

and where  $X_1$ ,  $Y_1$ ,  $X_2$ , and  $Y_2$  refer to  $X$  and  $Y$  evaluated at  $E_1/\theta$  and  $E_2/\theta$ . The integral of Eq. 329 is computed in **anased** (“ana” for analytic). The function “erfc” is the reduced complementary error function[56].

For Law 9, the secondary-energy distribution is given by

$$g(E, E') = \frac{E'}{I} \exp\left(-\frac{E'}{\theta(E)}\right) , \tag{332}$$

where

$$I = \theta^2 [1 - e^{-x}(1 + x)] . \tag{333}$$

Here  $x$  has the same meaning as above – see Eq. 328. The group integral is

$$\int_{g'} g(E, E') dE' = \frac{(1 + x_1)e^{-x_1} - (1 + x_2)e^{-x_2}}{1 - (1 + x)e^{-x}} , \tag{334}$$

where  $x_1$  and  $x_2$  refer to  $E_1/\theta$  and  $E_2/\theta$ , respectively. This result is also computed in **anased**.

For Law 11, the secondary-energy distribution is given by

$$g(E, E') = \frac{e^{-E'/a}}{I} \sinh(\sqrt{bE'}) , \tag{335}$$

where

$$I = \frac{1}{2} \sqrt{\frac{\pi a^3 b}{4}} e^{x_0} [\operatorname{erf}(\sqrt{x} - \sqrt{x_0}) + \operatorname{erf}(\sqrt{x} + \sqrt{x_0})] - a e^{-x \sinh(abx)} . \tag{336}$$



In this case,  $a(E)$  and  $b(E)$  are given in File 5,

$$x = \frac{E - U}{a} , \quad (337)$$

and

$$x_0 = \frac{ab}{4} . \quad (338)$$

The group integrals are given by

$$\int_{g'} g(E, E') = \frac{H(x_1, x_2, x_0)}{H(0, x, x_0)} , \quad (339)$$

where

$$\begin{aligned} H(x_1, x_2, x_0) &= H_2(\sqrt{x_1} - \sqrt{x_0}, \sqrt{x_2} - \sqrt{x_0}) \\ &+ \sqrt{x_0} H_1(\sqrt{x_1} - \sqrt{x_0}, \sqrt{x_2} - \sqrt{x_0}) \\ &- H_2(\sqrt{x_1} + \sqrt{x_0}, \sqrt{x_2} + \sqrt{x_0}) \\ &+ \sqrt{x_0} H_1(\sqrt{x_1} + \sqrt{x_0}, \sqrt{x_2} + \sqrt{x_0}) , \end{aligned} \quad (340)$$

and where

$$H_n(a, b) = \frac{1}{\pi} \int_a^b z^n e^{-z^2} dz . \quad (341)$$

The methods for computing  $H_n$  are described in [BROADR](#). When  $\sqrt{x_2} < .01$ , a short-cut calculation can be used for the numerator of Eq. 339

$$\frac{4\sqrt{x_0}e^{-x_0}}{3\sqrt{\pi/4}} [x_2^{3/2} - x_1^{3/2}] . \quad (342)$$

For Law 12, the Madland-Nix option, the secondary-energy distribution is given by

$$g(E, E') = \frac{1}{2} [G(E', E_{fl}) + G(E', E_{fh})] , \quad (343)$$

where

$$\begin{aligned}
G(E', E_f) \\
= \frac{1}{3\sqrt{E_f T_m}} \left[ u_2^{3/2} E_1(u_2) - u_1^{3/2} E_1(u_1) + \gamma(3/2, u_2) - \gamma(3/2, u_1) \right],
\end{aligned} \tag{344}$$

$$u_1 = (\sqrt{E'} - \sqrt{E_f})^2 / T_m, \text{ and} \tag{345}$$

$$u_2 = (\sqrt{E'} + \sqrt{E_f})^2 / T_m, \tag{346}$$

and where  $E_{fl}$ ,  $E_{fh}$ , and  $T_m(E)$  are given in File 5. The special functions used are the first-order exponential integral,  $E_1(x)$ , and the incomplete gamma function,  $\gamma(n, x)$ . The group integrals of this function are very complex[57]. Let

$$\alpha = \sqrt{T_m}, \tag{347}$$

$$\beta = \sqrt{E_f}, \tag{348}$$

$$A = \frac{(\sqrt{E_1} + \beta)^2}{\alpha^2}, \tag{349}$$

$$B = \frac{(\sqrt{E_2} + \beta)^2}{\alpha^2}, \tag{350}$$

$$A' = \frac{(\sqrt{E_1} - \beta)^2}{\alpha^2}, \text{ and} \tag{351}$$

$$B' = \frac{(\sqrt{E_2} - \beta)^2}{\alpha^2}. \tag{352}$$

Then the integral over the range  $(E_1, E_2)$  of  $G$  is given by one of the following three expression, depending on the region of integration in which  $E_1$  and  $E_2$  lie.

Region I ( $E_1 \geq E_f, E_2 > E_f$ )

$$\begin{aligned}
& 3\sqrt{E_f T_m} \int_{E_1}^{E_2} G(E', E_f) dE' \\
&= \left[ \left( \frac{2}{5} \alpha^2 B^{5/2} - \frac{1}{2} \alpha \beta B^2 \right) E_1(B) - \left( \frac{2}{5} \alpha^2 A^{5/2} - \frac{1}{2} \alpha \beta A^2 \right) E_1(A) \right] \\
&- \left[ \left( \frac{2}{5} \alpha^2 B'^{5/2} + \frac{1}{2} \alpha \beta B'^2 \right) E_1(B') - \left( \frac{2}{5} \alpha^2 A'^{5/2} + \frac{1}{2} \alpha \beta A'^2 \right) E_1(A') \right] \\
&+ \left[ (\alpha^2 B - 2\alpha \beta B^{1/2}) \gamma(3/2, B) - (\alpha^2 A - 2\alpha \beta A^{1/2}) \gamma(3/2, A) \right] \\
&- \left[ (\alpha^2 B' + 2\alpha \beta B'^{1/2}) \gamma(3/2, B') - (\alpha^2 A' + 2\alpha \beta A'^{1/2}) \gamma(3/2, A') \right] \\
&- \frac{3}{5} \alpha^2 [\gamma(5/2, B) - \gamma(5/2, A) - \gamma(5/2, B') + \gamma(5/2, A')] \\
&- \frac{3}{2} \alpha \beta [e^{-B}(1+B) - e^{-A}(1+A) + e^{-B'}(1+B') - e^{-A'}(1+A')] .
\end{aligned} \tag{353}$$

Region II ( $E_1 < E_f, E_2 \leq E_f$ )

$$\begin{aligned}
& 3\sqrt{E_f T_m} \int_{E_1}^{E_2} G(E', E_f) dE' \\
&= \left[ \left( \frac{2}{5} \alpha^2 B^{5/2} - \frac{1}{2} \alpha \beta B^2 \right) E_1(B) - \left( \frac{2}{5} \alpha^2 A^{5/2} - \frac{1}{2} \alpha \beta A^2 \right) E_1(A) \right] \\
&- \left[ \left( \frac{2}{5} \alpha^2 B'^2 \right) E_1(B') - \left( \frac{2}{5} \alpha^2 A'^{5/2} - \frac{1}{2} \alpha \beta A'^2 \right) E_1(A') \right] \\
&+ \left[ (\alpha^2 B - 2\alpha \beta B^{1/2}) \gamma(3/2, B) - (\alpha^2 A - 2\alpha \beta A^{1/2}) \gamma(3/2, A) \right] \\
&- \left[ (\alpha^2 B' - 2\alpha \beta B'^{1/2}) \gamma(3/2, B') - (\alpha^2 A' - 2\alpha \beta A'^{1/2}) \gamma(3/2, A') \right] \\
&- \frac{3}{5} \alpha \beta [\gamma(5/2, B) - \gamma(5/2, A) - \gamma(5/2, B') + \gamma(5/2, A')] \\
&- \frac{3}{2} \alpha \beta [e^{-B}(1+B) - e^{-A}(1+A) - e^{-B'}(1+B') + e^{-A'}(1+A')] .
\end{aligned} \tag{354}$$

Region III ( $E_1 < E_f, E_2 > E_f$ )

$$\begin{aligned}
& 3\sqrt{E_f T_m} \int_{E_1}^{E_2} G(E', E_f) dE' \\
&= \left[ \left( \frac{2}{5} \alpha^2 B^{5/2} - \frac{1}{2} \alpha \beta B^2 \right) E_1(B) - \left( \frac{2}{5} \alpha^2 A^{5/2} - \frac{1}{2} \alpha \beta A^2 \right) E_1(A) \right] \\
&- \left[ \left( \frac{2}{5} \alpha^2 B'^{5/2} + \frac{1}{2} \alpha \beta B'^2 \right) E_1(B') - \left( \frac{2}{5} \alpha^2 A'^{5/2} - \frac{1}{2} \alpha \beta A'^2 \right) E_1(A') \right] \\
&+ \left[ (\alpha^2 B - 2\alpha \beta B^{1/2}) \gamma(3/2, B) - (\alpha^2 A - 2\alpha \beta A^{1/2}) \gamma(3/2, A) \right] \\
&- \left[ (\alpha^2 B' + 2\alpha \beta B'^{1/2}) \gamma(3/2, B') - (\alpha^2 A' - 2\alpha \beta A'^{1/2}) \gamma(3/2, A') \right] \\
&- \frac{3}{5} \alpha^2 [\gamma(5/2, B) - \gamma(5/2, A) - \gamma(5/2, B') + \gamma(5/2, A')] \\
&- \frac{3}{2} \alpha \beta [e^{-B}(1+B) - e^{-A}(1+A) + e^{-B'}(1+B') + e^{-A'}(1+A') - 2] .
\end{aligned} \tag{355}$$

### 8.15 File 6 Energy-Angle Distributions

If the File 6 data are expressed as a continuous energy-angle distribution (Law 1) in the laboratory system, it is fairly easy to generate the multigroup transfer matrix. As usual for GROUPR, the task is to calculate the “feed function” (the Legendre moments for transferring to all possible secondary-energy groups starting with incident energy  $E$ ). The  $E'$  integration is controlled by the `getmf6` subroutine, which calls `f6lab` to generate the integrands. This routine expects data in Law-1 format, where the looping order is  $E$ ,  $E'$ ,  $\mu$ . The only problems here are handling the new ENDF-6 interpolation laws for two-dimensional tabulations (for example, unit base) and converting tabulated angle functions for  $E \rightarrow E'$  into Legendre coefficients (which is done with a Gauss-Legendre quadrature of order  $\sim 8$ ).

If the File 6 data are given in the energy-angle form of Law 7 (where the looping order is  $E$ ,  $\mu$ ,  $E'$ ), GROUPR converts it to the Law 1 form using subroutine `l12lab`. It does this by stepping through an  $E'$  grid that is the union of the  $E'$  grids for all the different angles given. At each of these union  $E'$  values, it calculates the Legendre coefficients using a Gauss-Legendre quadrature of order 8, and it checks back to see if the preceding point is still needed to represent the distribution to the desired degree of accuracy. Now `getmf6` and `f6lab` can be used to complete the calculation as above.

If the File 6 data are expressed in the CM system, or if the phase-space option is used, more processing is necessary to convert to the LAB system. This conversion is done for each incident energy  $E$  given in the file. The grid for laboratory secondary energy  $E'_L$  is obtained by doing an adaptive reconstruction of the emission probability  $p_{L\ell}(E, E'_L)$  such that each Legendre order can be expressed as a linear-linear function of  $E'_L$ . This part is done in subroutine `cm2lab`. The values for  $p_{L\ell}(E, E'_L)$  are obtained in subroutine `f6cm` by doing an adaptive integration along the contour  $E'_L = \text{const}$  in the  $E'_C, \mu_C$  plane using  $\mu_L$  as the variable of integration:

$$p_{L\ell}(E, E'_L) = \int_{\mu_{\min}}^{+1} p_C(E, E'_C, \mu_C) P_\ell(\mu_L) J d\mu_L , \quad (356)$$

where  $\mu$  is a scattering cosine and  $L$  and  $C$  denote the laboratory and center-of-mass (CM) systems, respectively. The Jacobian is given by

$$J = \sqrt{\frac{E'_L}{E'_C}} = \frac{1}{\sqrt{1 + c^2 - 2c\mu_L}} , \quad (357)$$

and the cosine transformation is given by

$$\mu_C = J(\mu_L - c) . \quad (358)$$

The constant  $c$  is given by

$$c = \sqrt{\frac{A'}{(A+1)^2}} \sqrt{\frac{E}{E'_L}} , \quad (359)$$

where  $A$  is the ratio of the atomic weight of the target to the atomic weight of the projectile, and  $A'$  is the ratio of the atomic weight of the emitted particle to the atomic weight of the projectile. The lower limit of the integral depends on the maximum possible value for the center-of-mass (CM) secondary energy as follows:

$$\mu_{\min} = \frac{1}{2c} \left( 1 + c^2 - \frac{E'_{C\max}}{E'_L} \right), \quad (360)$$

where

$$E'_{L\max} = E \left( \sqrt{\frac{E'_{C\max}}{E}} + \sqrt{\frac{A'}{(A+1)^2}} \right)^2 . \quad (361)$$

An example of the integration contours for this coordinate transformation is given in Fig. 30.

The CM energy-angle distribution can be given as a set of Legendre coefficients or a tabulated angular distribution for each possible energy transfer  $E \rightarrow E'$ , as a “precompound fraction”  $r(E, E')$  for use with the Kalbach-Mann[58] or Kalbach[59] angular distributions, or as parameters for a phase-space distribution. The first three options are processed using **f6ddx**, and the last using **f6psp**. The Kalbach option leads to a very compact representation. Kalbach and Mann examined large number of experimental angular distributions for neutrons and charged particles. They noticed that each distribution could be divided into two parts: an equilibrium part symmetric in  $\mu$ , and a forward-peaked preequilibrium part. The relative amount of the two parts depended on a parameter  $r$ , the preequilibrium fraction, that varies from zero for low  $E'$  to 1.0 for large  $E'$ . The shapes of the two parts of the distributions depended most directly on  $E'$ . This representation is very useful for preequilibrium statistical-model codes like GNASH[60], because they can compute the parameter  $r$ , and all the rest of the

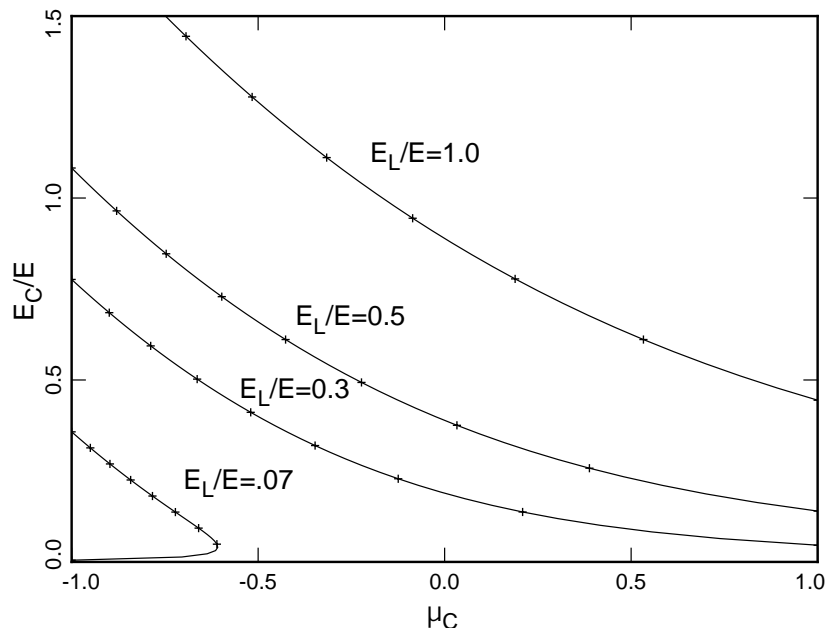


Figure 30: Coordinate mapping between CM and laboratory reference frames for  $A=2$ . The parameters  $E_L$  and  $E_C$  are the secondary energies in the Lab and CM frames. The crosses on the curves are at  $\mu_L$  values of  $-1.0, -0.75, -0.50, \dots, 0.75$ , and  $1.0$ . This figure also illustrates the advantage of integrating over  $\mu_L$  for the contour in the lower-left corner. The values of  $E_C$  and  $\mu_C$  are single-values functions of  $\mu_L$ .

angular information comes from simple universal functions. More specifically, Kalbach’s latest work says that

$$f(\mu) = \frac{a}{2 \sinh(a)} \left[ \cosh(a\mu) + r \sinh(a\mu) \right], \quad (362)$$

where  $a$  is a simple function of  $E$ ,  $E'$ , and  $B_b$ , the separation energy of the emitted particle from the liquid-drop model without pairing and shell terms. The separation energies are computed by formulas in **bach**. There is a problem for elemental evaluations, because the calculations needs an  $A$  value for the element, and it is difficult to guess which  $A$  value is most characteristic of the element. A short table is included in the routine, and an “**error in bach**” will result if the function is called for an element that doesn’t appear in the table. Similar routines appear in **HEATR** and **ACER**. A better long-range solution would be desirable. Fortunately, elemental evaluations are rare in modern evaluated libraries.

The File 6 processing methods in GROUPR apply equally well to neutrons, photonuclear photons, and charged particles. The effects on the kinematics due to the difference in mass between the incident particle and the emitted particle are handled by the variable  $A'$  in the above equations.

### 8.16 Smoothing

For continuum CM distributions in File 6, the low-energy shape should go like  $\sqrt{E'_C}$ . From Eq. 357, we see that the low-energy shape for the Lab distribution would then go like  $\sqrt{E'_L}$ . However, ENDF/B-VII evaluations for File 6 were normally prepared using advanced nuclear model codes, such as GNASH from LANL. These codes naturally produce spectra represented with histogram bins, and these bins normally give a constant probability from zero energy to the next bin boundary. This is certainly not a  $\sqrt{E}$  shape! The histogram shape can cause trouble with the CM-Lab transformation if some care is not taken. Clearly, the histogram grossly overestimates the probability of scattering to very low energies. This apparent problem is somewhat alleviated by the fact that the total probability of that lowest histogram bin is usually quite small. However, in order to get better looking shapes, GROUPR has coding that replaces the coarse histogram with a finer histogram chosen to represent a  $\sqrt{E}$  shape more closely. This smoothing coding scans up through the histogram distribution from the evaluation to find the region that behaves like  $\sqrt{E}$ . It then uses a recursive procedure to subdivide the region using a given factor until it reaches a fairly low energy (currently 40 eV).

A similar procedure is used to provide a  $\sqrt{E}$  shape at low energies for delayed neutron spectra.

For a few of the ENDF/B-VII actinides, the energy grid used to represent the fission spectrum becomes too coarse above 10 MeV. If that situation is found, GROUPR changes the interpolation law from the given lin-lin option to lin-log — that is, an exponential tail is assumed for the high energies. This assumption is consistent with the original evaluations. This modification can be important for reaction rates of high-threshold reactions.

These smoothing options are controlled by the global parameter `ismooth`, which is turned on by default (in contrast to NJOY99 where it is turned off by default).

### 8.17 GENDF Output

The group constants produced by GROUPE are normally written to an output file in GENDF (groupwise ENDF) format for use by other modules of NJOY. For example, [DTFR](#) can be used to convert a GENDF material to DTF (or “transport”) format; [CCCCR](#) produces the standard interface files[10] ISOTXS, BRKOXS, and DLAYXS; [MATXS](#) produces a file in MATXS format[11]; and [POWR](#) produces libraries for the Electric Power Research Institute (EPRI) codes EPRI-CELL and EPRI-CPM. Other formats can easily be produced by new modules, and some functions such as group collapse, are conveniently performed directly in GENDF format. The GENDF format is also used for [GAMINR](#) output, and both [ACER](#) and [ERRORR](#) use GENDF input for some purposes.

Depending on the sign of `ngout2` (see below), the GENDF file will be written in either coded mode (*e.g.*, ASCII) or in the special NJOY blocked-binary mode. Conversion between these modes can be performed subsequently by the [MODER](#) module.

The GENDF material begins with a header record (MF=1, MT=451), but the format of this first section is different from MT=451 on an ENDF or PENDF tape. The section consists of a “CONT” record, containing

|     |                                   |
|-----|-----------------------------------|
| ZA  | Standard 1000*Z+A value           |
| AWR | Atomic weight ratio to neutron    |
| 0   | Zero                              |
| NZ  | Number of $\sigma_0$ values       |
| -1  | Identifies a GENDF-type data file |
| NTW | Number of words in title          |

and a single “LIST” record, containing

|        |                                                     |
|--------|-----------------------------------------------------|
| TEMPIN | Material temperature (Kelvin)                       |
| 0.     | Zero                                                |
| NGN    | Number of neutron groups                            |
| NGG    | Number of photon groups                             |
| NW     | Number of words in LIST                             |
| 0      | Zero                                                |
| TITLE  | Title from GROUPE input (NTW words)                 |
| SIGZ   | Sigma-zero values (NZ words)                        |
| EGN    | Neutron group boundaries, low to high (NGN+1 words) |
| EGG    | Photon group boundaries, low to high (NGG+1 words). |



For photoatomic GENDF files produced by the [GAMINR](#) module, the photon group structure is stored in **ngn** and **egn**, and the number of photon groups is given as **ngg**=0. The word count is  $NW = NTW + NZ + NGN + 1 + NGG + 1$ . The LIST record is followed by a standard ENDF file-end record (FEND). The normal ENDF section-end (SEND) is omitted.

This header is followed by a series of records for reactions. The ENDF ordering requirements are relaxed, and MF and MT values can occur in any order. Each section starts with a “CONT” record.

|        |                                   |
|--------|-----------------------------------|
| ZA     | Standard $1000 \cdot Z + A$ value |
| AWR    | Standard atomic weight ratio      |
| NL     | Number of Legendre components     |
| NZ     | Number of sigma-zero values       |
| LRFLAG | Break-up identifier flag          |
| NGN    | Number of groups                  |

It is followed by a series of LIST records, one for every incident-energy group with nonzero result,

|       |                               |
|-------|-------------------------------|
| TEMP  | Material temperature (Kelvin) |
| 0.    | Zero                          |
| NG2   | Number of secondary positions |
| IG2LO | Index to lowest nonzero group |
| NW    | Number of words in LIST       |
| IG    | Group index for this record   |
| A(NW) | Data for LIST (NW words),     |

where  $NW = NL \cdot NZ \cdot NG2$ . The last LIST record in the sequence is the one with  $IG = NGN$ . It must be given even if its contents are zero. The last LIST record is followed by a SEND record.

The contents of A(NW) change for various types of data. For simple cross section “vectors” (MF=3), NG2 is 2, and A contains the two Fortran arrays

FLUX(NL,NZ), SIGMA(NL,NZ)

in that order. For ratio quantities like fission  $\bar{\nu}$ , NG2 is 3, and A contains

FLUX(NL,NZ), RATIO(NL,NZ), SIGMA(NL,NZ).

For transfer matrices (MF=6, 16, 21, *etc.*), A contains

FLUX(NL,NZ), MATRIX(NL,NZ,NG2-1).

The actual secondary group indices for the last index of MATRIX are usually IG2LO, IG2LO+1, *etc.*, using the GROUPE convention of labeling groups in order of increasing energy. If the low-energy part of the fission matrix (or the

fission or capture photon production matrices) uses the special format described in Section 8.6, the spectrum will be found in a LIST record with IG=0 and the production cross section will be found in a series of records with IG2L0=0. The group range for the spectrum ranges from IG2L0 to IG2L0+NG2-1. For IG2L0=0, NG2 will be 2 as for a normal cross section, and the two values will be the flux for group IG and the corresponding production cross section.

Finally, for delayed neutron spectra (MF=5), NL is used to index the time groups, NZ is 1, and there is only one incident energy record (IG=IGN). The array A contains

LAMBDA(NL), CHID(NL,NG2-1),

where LAMBDA contains the delayed-neutron time constants and CHID contains the spectra.

The GENDF material ends with a material-end (MEND) record, and the GENDF tape ends with a tape-end (TEND) record.

## 8.18 Running GROUPR

GROUPR's input instructions follow. They are reproduced from the comment cards at the beginning of the 2012.0 version of the GROUPR module. Because the code changes from time to time, it is a good idea to check these comment cards in the current version to obtain up-to-date input instructions.

```
!---input specifications (free format)-----
!
! card1
!   nendf   unit for endf tape
!   npend   unit for pendf tape
!   ngout1  unit for input gout tape (default=0)
!   ngout2  unit for output gout tape (default=0)
! card2
!   matb    material to be processed
!           if ngout=0, matb<0 is an option to automatically
!           process all the mats on the endf input tape.
!           otherwise, matb<0 is a flag to add mts to and/or
!           replace individual mts on gout1.
!   ign     neutron group structure option
!   igg     gamma group structure option
!   iwt     weight function option
!   lord    legendre order
!   ntemp   number of temperatures (default=1)
```

```

!   nsigz   number of sigma zeroes (default=1)
!   iprint  long print option (0/1=minimum/maximum)
!           (default=1)
! card3
!   title   run label (up to 80 characters delimited by quotes,
!           ended with /) (default=blank)
! card4
!   temp    temperatures in kelvin
! card5
!   sigz    sigma zero values (including infinity)
!
!           if ign=1, read neutron group structure (6a and 6b)
! card6a
!   ngm     number of groups
! card6b
!   egm     ngm+1 group breaks (ev)
!
!           if igg=1, read gamma group structure (7a and 7b)
! card7a
!   ngg     number of groups
! card7b
!   egg     ngg+1 group breaks (ev)
!
!           weight function options (8a,8b,8c,8d)
! card8a    flux calculator parameters (iwt.lt.0 only)
!   fehi    break between computed flux and bondarenko flux
!           (must be in resolved resonance range)
!   sigpot  estimate of potential scattering cross section
!   nflmax  maximum number of computed flux points
!   ninwt   tape unit for new flux parameters (default=0)
!   jsigz   index of reference sigma zero in sigz array
!           (default=0)
!   alpha2  alpha for admixed moderator (def=0=none)
!   sam     admixed moderator xsec in barns per absorber
!           atom (def=0=none)
!   beta    heterogeneity parameter (def=0=none)
!   alpha3  alpha for external moderator (def=0=none)
!   gamma   fraction of admixed moderator cross section in
!           external moderator cross section (def=0)
! card8b    tabulated (iwt=1 or -1 only)
!   wght    read weight function as tab1 record.
!           end with a /.

```

```

! card8c      analytic flux parameters (iwt=4 or -4 only)
!   eb        thermal break (ev)
!   tb        thermal temperature (ev)
!   ec        fission break (ev)
!   tc        fission temperature (ev)
! card8d      input resonance flux (iwt=0 only)
!   ninwt     tape unit for flux parameters
!
! card9
!   mfd       file to be processed
!   mtd       section to be processed
!   mtname    description of section to be processed
!             repeat for all reactions desired
!             mfd=0/ terminates this temperature/material.
! card10
!   matd      next mat number to be processed
!             matd=0/ terminates groupr run.
!
!---options for input variables-----
!
!   ign       meaning
!   ---       -----
!   1         arbitrary structure (read in)
!   2         csewg 239-group structure
!   3         lanl 30-group structure
!   4         anl 27-group structure
!   5         rrd 50-group structure
!   6         gam-i 68-group structure
!   7         gam-ii 100-group structure
!   8         laser-thermos 35-group structure
!   9         epri-cpm 69-group structure
!   10        lanl 187-group structure
!   11        lanl 70-group structure
!   12        sand-ii 620-group structure
!   13        lanl 80-group structure
!   14        eurlib 100-group structure
!   15        sand-ia 640-group structure
!   16        vitamin-e 174-group structure
!   17        vitamin-j 175-group structure
!   18        xmas nea-lanl
!   all new additional group structure with 7 significant
!   decimal digits compatible with calendf

```

|   |     |                                              |
|---|-----|----------------------------------------------|
| ! | 19  | ecco 33-group structure                      |
| ! | 20  | ecco 1968-group structure                    |
| ! | 21  | tripoli 315-group structure                  |
| ! | 22  | xmas lwpc 172-group structure                |
| ! | 23  | vit-j lwpc 175-group structure               |
| ! |     |                                              |
| ! | igg | meaning                                      |
| ! | --- | -----                                        |
| ! | 0   | none                                         |
| ! | 1   | arbitrary structure (read in)                |
| ! | 2   | csewg 94-group structure                     |
| ! | 3   | lanl 12-group structure                      |
| ! | 4   | steiner 21-group gamma-ray structure         |
| ! | 5   | straker 22-group structure                   |
| ! | 6   | lanl 48-group structure                      |
| ! | 7   | lanl 24-group structure                      |
| ! | 8   | vitamin-c 36-group structure                 |
| ! | 9   | vitamin-e 38-group structure                 |
| ! | 10  | vitamin-j 42-group structure                 |
| ! |     |                                              |
| ! | iwt | meaning                                      |
| ! | --- | -----                                        |
| ! | 1   | read in smooth weight function               |
| ! | 2   | constant                                     |
| ! | 3   | 1/e                                          |
| ! | 4   | 1/e + fission spectrum + thermal maxwellian  |
| ! | 5   | epri-cell lwr                                |
| ! | 6   | (thermal) -- (1/e) -- (fission + fusion)     |
| ! | 7   | same with t-dep thermal part                 |
| ! | 8   | thermal--1/e--fast reactor--fission + fusion |
| ! | 9   | claw weight function                         |
| ! | 10  | claw with t-dependent thermal part           |
| ! | 11  | vitamin-e weight function (ornl-5505)        |
| ! | 12  | vit-e with t-dep thermal part                |
| ! | -n  | compute flux with weight n                   |
| ! | 0   | read in resonance flux from ninwt            |
| ! |     |                                              |
| ! | mfd | meaning                                      |
| ! | --- | -----                                        |
| ! | 3   | cross section or yield vector                |
| ! | 5   | fission chi by short-cut method              |
| ! | 6   | neutron-neutron matrix (mf4/5)               |

```

!      8      neutron-neutron matrix (mf6)
!     12      photon prod. xsec (photon yields given, mf12)
!     13      photon prod. xsec (photon xsecs given, mf13)
!     16      neutron-gamma matrix (photon yields given)
!     17      neutron-gamma matrix (photon xsecs given)
!     18      neutron-gamma matrix (mf6)
!           note: if necessary, mfd=13 will automatically change
!           to 12 and mfd=16 will automatically change to 17 or 18.
!     21      proton production matrix (mf6)
!     22      deuteron production (mf6)
!     23      triton production (mf6)
!     24      he-3 production (mf6)
!     25      alpha production (mf6)
!     26      residual nucleus (a>4) production (mf6)
!     31      proton production matrix (mf4)
!     32      deuteron production (mf4)
!     33      triton production (mf4)
!     34      he-3 production (mf4)
!     35      alpha production (mf4)
!     36      residual nucleus (a>4) production (mf4)
!           note: if necessary, mfd=21-26 will
!           automatically change to 31-36.
! 1zzzaaam    nuclide production for zzzaaam
!              subsection from file 3
! 2zzzaaam    nuclide production for zzzaaam
!              subsection from file 6
! 3zzzaaam    nuclide production for zzzaaam
!              subsection from file 9
! 4zzzaaam    nuclide production for zzzaaam
!              subsection from file 10
!
!   mtd       meaning
!   ---       -----
!   -n        process all mt numbers from the previous
!              entry to n inclusive
!   221-250    reserved for thermal scattering
!   258        average lethargy
!   259        average inverse velocity (m/sec)
!
!   automatic reaction processing options
!   -----
!       3/      do all reactions in file3 on input pendf

```

```

!      6/      do all matrix reactions in endf dictionary
!     10/      do all isotope productions using mf8
!     13/      do all photon production cross sections
!     16/      do all photon production matrices
!     21/      do all proton production matrices
!     22/      do all deuteron production matrices
!     23/      do all triton production matrices
!     24/      do all he-3 production matrices
!     25/      do all alpha production matrices
!     26/      do all a>4 production matrices
!
!-----

```

In these instructions, **card1** defines the input and output units for GROUPR. The module requires both ENDF and PENDF input tapes, because the PENDF tapes produced by [RECONR](#), [BROADR](#) *etc.*, do not contain angle (MF=4), energy (MF=5), or photon (MF=12, 15) distributions. For materials that do not use resonance parameters to represent part of the cross section, it is possible to use a copy of the ENDF tape in place of the PENDF tape. The normal mode for GROUPR is to use **ngout1=0**; however, sometimes it is convenient to add a new material or reaction to an existing GENDF tape. The old GENDF tape is then mounted on unit **ngout1**, and the revised GENDF tape will be written to **ngout2**.

Card 2 selects the first material to be processed (**matb**) and sets up the group structures, weighting option, Legendre order, and self-shielding parameters for all the materials to be processed in this run.

The names of the available group structures are given in the input instructions. Energy bounds or lethargy bounds can be found in the source code. Of course, it is always possible to read in an arbitrary group structure (see **card6a** through **card7b**). The energies must be given in increasing order (note that this is opposite from the usual convention). Here is an example of the input cards for the conventional 4-group structure historically used in some thermal reactor codes:

```

4/ card6a
1e-5 .625 5530 .821e6 10e6 / card6b

```

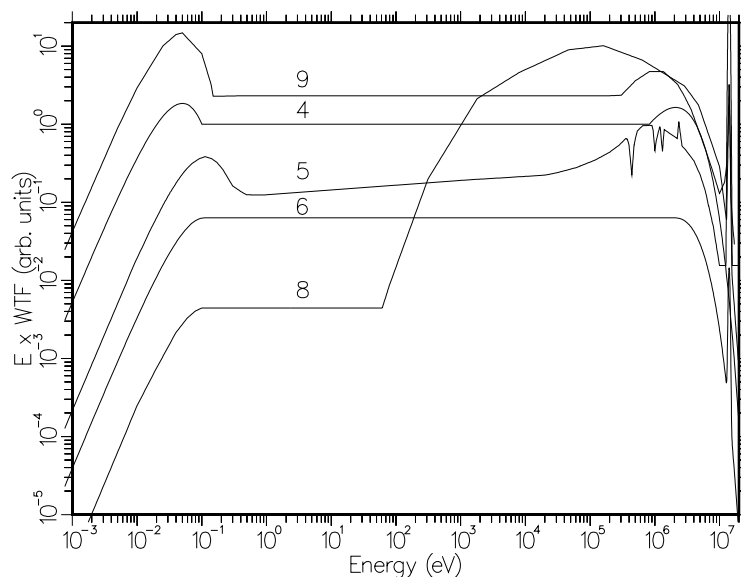


Figure 31: Built-in neutron weight functions of GROUPR on a logarithmic flux-per-unit-lethargy plot that emphasizes the low energy range.

These cards are read by the standard Fortran READ\* method. Fields are delimited by space, and “/” terminates the processing of input on a card. Anything after the slash is a comment.

The available weight function options are listed in the input instructions under `iwt`. See Fig. 31 and Fig. 32. Here are brief descriptions of the options:

**IWT=2** The weight function is constant (not shown in the Figures). This option is usually chosen for very fine group structures such as the 620-group or 640-group dosimetry structures.

**IWT=3** The weight function is proportional to  $1/E$ . The slowing-down of neutrons in water gives a  $1/E$  flux from about 1 eV up to 100 keV, or so. This weight function is traditionally used for calculating resonance integrals, but it is not useful at the lower and higher energies needed for a full set of transport constants. Although not shown, the graph of this function is a flat line on a flux-per-unit-lethargy plot, such as the one in Fig. 31.

**IWT=4** This weight function combines a thermal Maxwellian at low energies, a  $1/E$  function at intermediate energies, and a fission spectrum at high energies to obtain a function appropriate for several different applications. The temperatures of the Maxwellian and fission parts and the energies where the components join can be chosen by the user. Therefore, option 4 can be used to produce typical thermal reactor weight functions like those shown in Figures 31 and 32, a pure fission spectrum for calculating some



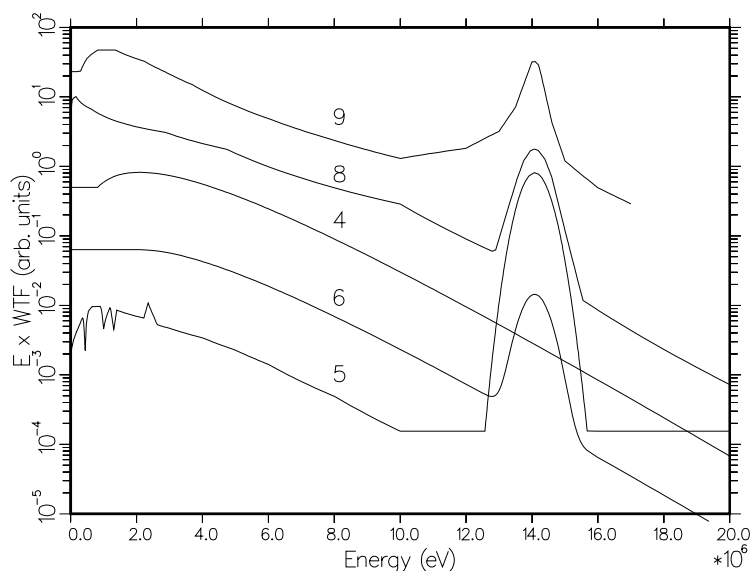


Figure 32: Built-in neutron weight functions on a linear plot that emphasizes the high-energy range.

kinds of dosimetry cross sections, or a pure thermal spectrum for getting effective thermal average cross sections. The function for IWT=4 shown in the figure was produced using a thermal temperature of 0.025 eV joined to  $1/E$  at 0.1 eV, and a fission temperature of 1.40 MeV joined to  $1/E$  at 820.3 keV.

**IWT=5** This is a mid-life PWR (pressurized water reactor) flux spectrum with a fusion peak added (see below for a discussion of the fusion peak used). Note the peaks and dips resulting from oxygen resonances and windows at high energies, and the hardening apparent in the epithermal region. The thermal part of the function is also hardened with respect to a simple Maxwellian shape. The dips that should show up in the eV range due to resonances and  $^{238}\text{U}$  have been removed to allow the self-shielding method to work without risk of counting the shielding effects twice. This weight function has been used for several libraries[61] prepared for the Electric Power Research Institute (EPRI), and for the MATXS7 library used with the TRANSX code.

**IWT=6** This function is similar to option 4, but the breakpoints were chosen to keep the curves continuous. The thermal Maxwellian is calculated for 300K. In this case, the fusion peak (see below) was added to the high-energy tail of the fission spectrum for smoothness.

**IWT=7** This option is reserved for future use.

**IWT=8** This function is intended for cross sections libraries used for fast reactor analysis (typically, fast breeder designs), but is also useful for fusion-blanket problems. It has a fusion peak at high energies, followed by a fission

spectrum, a slowing-down spectrum typical of a fast reactor, and a thermal tail. The tail is provided to help give reasonable results in shields far from the core; its characteristic temperature is 300K. Note the sharp drop in the flux as energy decreases from 19 keV. This region is important for  $^{238}\text{U}$  absorption, and this drop-off helps to give good group constants for fast reactors. Of course, it would be entirely wrong for a thermal reactor.

IWT=9 This is another typical thermal+ $1/E$ +fission+fusion function that has been used for many libraries at LANL in the 30-group structure. The CLAW-3 and CLAW-4 libraries are available from the Radiation Shielding Information Computational Center at ORNL.

IWT=10 This is the same as the CLAW weight function (IWT=9), but the shape of the thermal part is automatically recalculated to follow a Maxwellian law for temperature  $T$ .

IWT=11 This is the weight function used in the VITAMIN-E library. It has the following segments: a .0253-eV thermal Maxwellian below 0.414 eV, a  $1/E$  law from .414 eV to 2.12 MeV, a 1.415-MeV fission spectrum from 2.12 to 10 MeV, another  $1/E$  section from 10 to 12.52 MeV, a fusion peak (25 keV width) between 12.52 and 15.68 MeV, and a final  $1/E$  section for all higher energies. The shape of the fusion peak is almost identical to IWT=5 (see Fig. 32). The low-energy part of this weight function is not shown.

Just as in the case of group structures, an arbitrary weight function can be read in (see card8b). This function is presented to GROUPE as an ENDF/B “TAB1” record. This means that a count of  $E, C(E)$  pairs and one or more interpolation schemes are given. For the case of a single interpolation scheme, the input cards would be

```
0. 0. 0 0 1 N N INT
E1 C(E1) E2 C(E2) ... / card8b
```

where N is the count of  $E, C(E)$  pairs, and INT specifies the interpolation law to be used for values of  $E$  between the grid values  $E_1, E_2, \dots$  according to the following schemes:

| INT | Meaning       |
|-----|---------------|
| 1   | histogram     |
| 2   | linear-linear |
| 3   | linear-log    |
| 4   | log-linear    |
| 5   | log-log       |

For example, INT=5 specifies that  $\ln C$  is a linear function of  $\ln E$  in each panel  $E_i \leq E < E_j$ . Similarly, INT=4 specifies that  $\ln C$  is a linear function of  $E$  in each panel. As many physical lines as are needed can be used for “card8b”, as long as the terminating slash is included.

One of the weighting options, IWT=4, is a generalized “1/ $E$ +fission+thermal” function where the thermal temperature, fission temperature, and breakpoint energies (all in eV) are given on card8c. The weight function for the Los Alamos LIB-IV cross section library[62] used

```
.10 .025 820.3e3 1.4e6 / card8c
```

See Figures 31 and 32 for a plot of this function.

Several of these weight functions include a fusion peak. Because of the finite width of the distribution of ion energies in a D-T fusion plasma, the emitted 14-MeV neutrons clearly will not have a delta-function energy spectrum. In fact, owing to the presence of a cross-product term in the kinematic relations, the typical ion-energy spread of a few tens of kilovolts is magnified into a neutron-energy spread of around 1 MeV. For an assumed isotropic Maxwellian plasma, the neutron peak shape (for example, see the review article by Lehner[63]) is

$$S(E) = C \int_0^\infty \exp\{-b[v^2 + v_0(g)^2] - cg^2\} \sinh(2bv v_0) \frac{g^3 \sigma(g)}{v_0(g)} dg . \quad (363)$$

Here  $S(E)$  is the number of neutrons emitted with laboratory energy between  $E$  and  $E + dE$ ,  $C$  is a normalization factor,  $v$  is the laboratory velocity corresponding to energy  $E$ , and  $v_0$  is the velocity of the neutron in the CM system. Both  $v_0$  and the fusion cross section  $\sigma$  are determined by the relative velocity  $g$  of the reacting ions, the integration variable in Eq. 363. The coefficient  $b$  is equal to  $M/2kT$ , where  $M$  is the total mass of the reacting ions and  $kT$  is the plasma temperature. Similarly,  $c$  is  $\mu/2kT$ , where  $\mu$  is the reduced mass of the ion system. The only approximation involved in Lehner’s derivation of Eq. 363 is that all particles may be treated nonrelativistically. At 14 MeV, the relativistic factor

$$\gamma = \frac{1}{\sqrt{1 - v^2/c^2}} , \quad (364)$$

is very close to unity (1.015), and it varies negligibly over the range of interest (say, 13 to 17 MeV). It is sufficient then to invoke relativistic mechanics in defining the location of the 14-MeV peak but not in discussing the shape. This effect moves the peak toward lower neutron energies, but only by about 20 keV. Although the expression for  $S(E)$  in Eq. 363 is accurate, it has the disadvantage of requiring a numerical integration at each point  $E$  in the energy spectrum. For this reason, we consider what simplifications can be made without serious loss of accuracy. In the energy range around the 14-MeV peak, the product  $2bv v_0$  in Eq. 363 has a numerical value of about 6000. Thus, the hyperbolic sine can obviously be replaced by just the positive exponential term. If we make this change in Eq. 363, we can write the following, still nearly exact, expression for the neutron spectrum:

$$S_1(E) = C_1 \int_0^\infty \exp[-b(v - v_0)^2] P(v_0) dv_0 . \quad (365)$$

Here we also have inverted the function  $v_0(g)$  and changed the integration variable. The spectrum then is a linear superposition of velocity exponentials with slightly different peak locations. For normal plasma temperatures, the velocity distribution  $P(v_0)$  is very narrow, since the expression for  $v_0$  is dominated by the nuclear Q-value (17.586 MeV) rather than the contribution from the ion kinetic energy (typically around 50 keV). Thus, it seems reasonable to approximate  $P(v_0)$  as delta function

$$P(v_0) \approx \delta(v_0 - v_p) . \quad (366)$$

This gives a second approximate form,

$$S_2(E) = C_2 \exp[-b(v - v_p)^2] , \quad (367)$$

where  $v_p$  has the obvious meaning of the laboratory neutron velocity at the center of the peak. We shall refer to this as the velocity exponential form of the neutron energy spectrum. An expression essentially identical to Eq. 367 was given in an early paper by Nagle and coworkers[64]. In order to examine the accuracy of the velocity exponential form, we have calculated  $S(E)$  from Eq. 363 and  $S_2(E)$  from Eq. 367 at 20 keV, a typical plasma temperature in current fusion-reactor concepts. In performing the numerical integration over  $g$  in Eq. 363, we used numerical values for the D-T fusion cross section taken from the compilation by Jarmie and Seagrave[65]. In evaluating  $S_2(E)$  using Eq. 367,

a value of  $v_p$  was chosen so as to force agreement between  $S_2(E)$  and  $S(E)$  at 17 MeV. As discussed by Muir[66], the overall agreement is remarkably good, the maximum error over the range from 13.5 to 17 MeV being about 2%. The value of  $v_p$  thus derived corresponds to a peak-center energy  $E_p$  of 14.07 MeV. This value includes the small ( $\sim 20$  keV) relativistic correction mentioned above. If we approximate the mass of the D+T system as 5 times the neutron mass, then we obtain the recommended peak shape

$$S_{\text{rec}}(E) = \exp\left[-\frac{5}{kT}(\sqrt{E} - \sqrt{E_p})^2\right], \quad (368)$$

where  $E_p=14.07$  MeV. The functional form in Eq. 368 was used to calculate the fusion peak shapes appearing in two of the data statements in `genwtf` (namely, those utilized for IWT=5 and 8) and is also used explicitly in `getwtf` to calculate analytically the weight function for IWT=6. In all three cases,  $kT=25$  keV is used as an average or typical fusion-reactor plasma temperature. See Fig. 32 for a graphical display of the resulting weight functions in the 14-MeV region.

The GROUPR flux calculator is selected by a negative sign on `iwt`. The additional `card8a` is then read. The calculator option used is determined by the number of parameters given and their values. The parameters `fehi` and `nflmax` are used to select the energy range for the flux calculation, and they also determine the cost in time and storage. The actual value for `sigpot` is not very critical – a number near 10 barns is typical for fissionable materials.

Nonzero values for `ninwt` and `jsigz` will cause the computed flux for a given fissionable isotope (such as  $^{238}\text{U}$ ) to be written out onto a file. This saved flux can be used as input for a subsequent run for a fissile material (such as  $^{239}\text{Pu}$ ) with `iwt=0` to get an approximate correction for resonance-resonance interference. See Eq. 273.

Nonzero values for some of the last five parameters on `card8a` select the extended flux calculation of Eq. 271. The simplest such calculation is for an isolated pin containing a heavy absorber with an admixed moderator. For  $^{238}\text{UO}_2$ , the card might be

```
400 10.6 5000 0 0 .7768 7.5 / card8a
```

where 7.5 barns is twice the oxygen cross section and  $\alpha$  is computed from  $[(A-1)/(A+1)]^2$  with  $A = 15.858$ . A more general case would be a PWR-like lattice of  $^{238}\text{UO}_2$  fuel rods in water:

```
400 10.6 5000 0 0 .7768 7.5 .40 1.7e-7 .086 / card8a
```

where .086 is computed using 3.75 barns for O and 40 barns for the two H atoms bound in water; that is,

$$\gamma = \frac{3.75}{2 * 20 + 3.75} = .086 . \quad (369)$$

A third example would compute the flux for a homogeneous mixture of  $^{238}\text{U}$  and hydrogen

```
400 10.6 5000 0 0 0 0 1. 1.7e-7 / card8a
```

As a final example, consider a homogeneous mixture of uranium and water. This requires **beta**=1 and **sam**=0. Thus,

```
400 10.6 5000 0 0 .7768 0. 1. 1.7e-7 .086 / card8a
```

The maximum Legendre expansion order used for scattering matrices is set by **lord**. The number of tables produced is **lord**+1; that is,  $\ell = 0, 1, \dots, \text{lord}$ . When more than 1 value of  $\sigma_0$  is requested, both the  $\ell=0$  and  $\ell=1$  components of the total cross section are produced.

Card 3 contains a short descriptive title that is printed on the listing and added to the output GENDF tape. Card 4 gives the **ntemp** values of temperature for the run. They must be in ascending order, and if unresolved data are included on the PENDF tape, the temperatures in this list must match the first **ntemp** values in MF=2, MT=152 from **UNRESR** or **PURR** (see **stounr** and **getunr**). Card 5 gives the  $\sigma_0$  values for the run in descending order, starting with infinity (represented by  $10^{10}$  barns).

This completes the description of the global input parameters for GROU<sup>PR</sup>. The rest of the input cards request reactions to be processed for the various temperatures and materials desired. Because of the many types of data that it can process, GROU<sup>PR</sup> does not have a completely automatic mode for choosing

reactions to be processed. On the basic level, it asks the user to request each separate cross section or group-to-group matrix using the parameters **mfd**, **mtd**, and **mtname**. However, simplified input modes are also available. For example, the one “**card9**” containing

```
3/
```

will process the cross section “vectors” for all of the reaction MT numbers found on the PENDF tape.

For completeness, the full input for **matd**, **mfd**, and **mtname** will be described first. Most readers can skip to the description of automated processing below. The value of **mfd** depends on the output desired (vector, matrix) and the form of the data on the ENDF evaluation. Simple cross section “vectors”  $\sigma_{xg}$  are requested using **mfd**=3 and the **mtd** numbers desired from the list of reactions available in the evaluation (check the directory in MF=1,MT=451 of the ENDF and PENDF tapes for the reactions available). A typical example would be

```
3  1 'total'/
3  2 'elastic'/
3 16 '(n,2n)'/
3 51 '(n,nprime)first'/
3 -66 '(n,nprime)next'/
3 91 '(n,nprime)continuum'/
3 102 'radiative capture'/
```

The combinations of “3 51” followed by “3 -66” means process all the reactions from 51 through 66; that is,  $(n,n'_1)$ ,  $(n,n'_2)$ ,  $\dots$ ,  $(n,n'_{16})$ . If self-shielding is requested, the following reactions will be processed using **nsigz** values of background cross section: total (MT=1), elastic (MT=2), fission (MT=18 and 19), radiative capture (MT=102), heat production (MT=301), kinematic KERMA (MT=443), and damage energy production (MT=444). The other File-3 reactions will be computed at  $\sigma_0=\infty$  only. This list of reactions can be altered by small changes in **init** if desired.

There are several special options for **mtd** available when processing cross section vectors:

| <u>mtd</u> | <u>Option</u>                                                                                                                                                                                                                                   |
|------------|-------------------------------------------------------------------------------------------------------------------------------------------------------------------------------------------------------------------------------------------------|
| 259        | Average inverse neutron velocity for group in s/m.                                                                                                                                                                                              |
| 258        | Average lethargy for group.                                                                                                                                                                                                                     |
| 251        | Average elastic scattering cosine $\bar{\mu}$ computed from File 4.                                                                                                                                                                             |
| 252        | Continuous-slowing-down parameter $\bar{\xi}$ (average logarithmic energy decrement for elastic scattering) computed from File 4.                                                                                                               |
| 253        | Continuous-slowing-down parameter $\bar{\gamma}$ (the average of the square of the logarithmic energy decrement for elastic scattering, divided by twice the average logarithmic energy decrement for elastic scattering) computed from File 4. |
| 452        | $\bar{\nu}$ : the average total fission yield computed from MF=1 and MF=3.                                                                                                                                                                      |
| 455        | $\bar{\nu}^D$ : the average delayed neutron yield computed from MF=1 and MF=3.                                                                                                                                                                  |
| 456        | $\bar{\nu}^P$ : the average prompt fission neutron yield computed from MF=1 and MF=3.                                                                                                                                                           |

There are also some special options for **mfd** that can be used when processing cross sections:

| <u>mfd</u> | <u>Option</u>                                                                                                                              |
|------------|--------------------------------------------------------------------------------------------------------------------------------------------|
| 12         | Photon production cross section computed from File 12 and File 3.                                                                          |
| 13         | Photon production cross section computed from File 13. Recent versions of GROUPR will automatically shift between 12 and 13, if necessary. |
| 1zzzaaam   | nuclide production for zzzzaaam from a subsection of MF=3                                                                                  |
| 2zzzaaam   | nuclide production for zzzzaaam from a subsection of MF=6                                                                                  |
| 3zzzaaam   | nuclide production for zzzzaaam from a subsection of MF=9                                                                                  |
| 4zzzaaam   | nuclide production for zzzzaaam from a subsection of MF=10                                                                                 |

An example of the isomer production capability would be the radiative capture reaction of ENDF/B-V  $^{109}\text{Ag}(n,\gamma)$  from Tape 532:

```
30471090 102 '(n,g) T0 g.s.'/
30471091 102 '(n,n) to isomer'/'
```



The next class of reactions usually processed is the group-to-group neutron scattering matrices. The complete list of `mtd` values is most easily found under File 4 in the MF=1,MT=451 “dictionary” section of the evaluation. An example follows:

```
6  2 'elastic matrix'/
6 16 '(n,2n) matrix'/
6 51 '(n,nprime)first matrix'/
6 -66 '(n,nprime)next matrix'/
6 91 '(n,nprime)continuum matrix'/ .
```

Using `mfd=6` implies that File 4, or File 4 and File 5, will be used to generate the group-to-group matrix. The elastic matrix will be computed for `nsigz` values of background cross section, but the other reactions will be computed for  $\sigma_0=\infty$  only. The list of matrices to be self-shielded can be altered by changing `init`.

Fission is more complex. For the minor isotopes, only the total fission reaction is used, and the following input is appropriate for the prompt component:

```
3 18 'fission xsec'/
6 18 'prompt fission matrix'/
```

For the important isotopes, partial fission reactions are given. They are really not needed for most fission reactor problems, and the input above is adequate. However, for problems where high-energy neutrons are important, the following input should be used:

```
3 18 'total fission'/
3 19 '(n,f)'/
3 20 '(n,nf)'/
3 21 '(n,2nf)'/
3 38 '(n,3nf)'/
6 19 '(n,f)'/
6 20 '(n,nf)'/
6 21 '(n,2nf)'/
6 38 '(n,3nf)'/
```

Note that “6 18” is omitted because it will, in general, be different from the sum of the partial matrices (see Section 8.6). Some materials don’t have data for (n,3nf); in these cases, omit the two lines with `mtd=38` from the input. The fission matrix is not self-shielded. Since resonance-to-resonance fission-spectrum variations are not described in the ENDF format, it is sufficient to self-shield the cross section and then to use the self-shielding factor for the cross section to self-shield the fission neutron production.

Delayed fission data are available for the important actinide isotopes, and the following input to GROUPR is used to process them:

```
3 455 'delayed nubar'/
5 455 'delayed spectra'/
```

The line for `mfd=5` automatically requests spectra for all time groups of delayed neutrons. The time constants are also extracted from the evaluation. As discussed in Section 8.6, formatting modules such as [DTFR](#) and [CCCCR](#) must combine the prompt and delayed fission data written onto the GENDF tape in order to obtain steady-state fission parameters for use in transport codes.

Starting with the ENDF-6 format, neutron production data may also be found in File 6, and `mfd=8` is used to tell the code to use MF6 for this `mtd`. When using full input, the user will have to check the File 1 directory and determine what subsections occur in File 6.

Photon production reactions can be found in the ENDF dictionary under MF=12 and 13. To request a neutron-to-photon matrix, add 4 to this number.<sup>8</sup> For example,

```
17 3 'nonelastic photons'/
16 4 'inelastic photons'/
16 18 'fission photons'/
16 102 'capture photons'/
```

Yields (MF=12) are normally used with resonance reactions (MT=18 or MT=102), or for low-lying inelastic levels (MT=51, 52, ....). MT=3 is often used by evaluators as a catch-all reaction at high energies where it is difficult to separate

<sup>8</sup>In recent versions of NJOY, GROUPR will automatically shift between 16 and 17 using data read from the ENDF dictionary by the `conver` subroutine. Thus, use of `mfd=17` is no longer necessary.

the source reactions in total photon emission measurements. In these cases, photon production cross sections from other reactions like MT=102 are normally set equal to zero at high energies. The general rule for photon emission is that the total production is equal to the sum of all the partial production reactions given in the evaluation. Starting with the ENDF-6 format, photon production may also appear in File 6. Use `mfd=18` to process these contributions. Since resonance-to-resonance variations in photon spectra are not given in ENDF evaluations, GROUPR does not normally self-shield the photon production matrices (although this can be done if desired by making a small change in `init`); instead, it is assumed that only the corresponding cross section needs to be shielded. Subsequent codes can use the cross section self-shielding factor with the infinite-dilution photon production matrix to obtain self-shielded photon production numbers.

This version of GROUPR can also generate group-to-group matrices for charged-particle production from neutron reactions and for all kinds of matrices for incident charged particles. The incident particle is determined by the input tape mounted. The identity of the secondary particle is chosen by using one of the following special `mfd` values:

For distributions given in File 6 (energy-angle):

| <code>mfd</code> | Meaning                           |
|------------------|-----------------------------------|
| 21               | proton production                 |
| 22               | deuteron production               |
| 23               | triton production                 |
| 24               | <sup>3</sup> He production        |
| 25               | alpha production                  |
| 26               | residual nucleus (A>4) production |

For distributions given in File 4 (angle only):

| <code>mfd</code> | Meaning                           |
|------------------|-----------------------------------|
| 31               | proton production                 |
| 32               | deuteron production               |
| 33               | triton production                 |
| 34               | <sup>3</sup> He production        |
| 35               | alpha production                  |
| 36               | residual nucleus (A>4) production |

If necessary, `mfd=21-26` will automatically change to 31-36.

The user will normally process all reactions of interest at the first temperature (for example, 300K). At higher temperatures, the threshold reactions should be omitted, because their cross sections do not change significantly with temperature except at the most extreme conditions. This means that only the following reactions should be included for the higher temperatures (if present): total (MT=1), elastic (MT=2), fission (MT=18), radiative capture (MT=102), heating (MT=301), kinematic KERMA (MT=443), damage (MT=444), and any thermal cross sections (MT=221-250). Only the elastic and thermal matrices should be included at the higher temperatures.

Warning: when using the explicit-input option, it is a fatal error to request a reaction that does not appear in the evaluation, cannot be computed from the evaluation, or was not added to the PENDF tape by a previous module. Reactions with thresholds above the upper boundary of the highest energy group will be skipped after printing a message on the output file.

Automated processing of essentially all reactions included in an ENDF/B evaluation is also available. As mentioned previously, the single card

3/

will process all the reactions found in File 3 of the input PENDF tape. However, this list excludes thermal data (MT=221-250) and special options such as `mtd=251-253, 258-259, and 452-456`. If any of these reactions are needed, they should be given explicitly (see example below). Similarly, the single card

6/

will process the group-to-group matrices for all reactions appearing in File 4 of the ENDF/B tape, except for MT=103-107 and thermal scattering matrices (MT=221-250). If MT=18 and 19 are both present, only MT=19 will be processed into a fission matrix. For ENDF-6 evaluations, the “8/” option will also process every neutron-producing subsection in File 6. Photon production cross sections are requested using

13/

and photon-production matrices are requested with the single card

```
16/
```

In both cases, all reactions in both File 12 and File 13 will be processed without the need for using `mfd=12` or `mfd=17`. For ENDF-6 libraries, this option will also process all photon-production subsections in File 6. There is no automatic option for delayed neutron data. An example of a processing run for a fissionable isotope with thermal cross sections follows:

```
3/
3 221/ thermal xsec
3 229/ average inverse velocity
3 455/ delayed nubar
5 455/ delayed spectra
6/
6 221/ thermal matrix
16/ photon production matrix
```

An example of charged-particle processing for the incident-neutron part of a coupled n-p- $\gamma$  library follows:

```
3/ cross sections
6/ neutron production matrix
16/ photon production matrix
21/ proton production matrix
```

The layout of data in a n-p- $\gamma$  coupled set is shown in Figure 33.

There is a new ENDF format now becoming available that helps to describe the production of all isotopes and isomers in a given system. It uses a directory in File 8 to direct the code to productions represented by MF=3, by MF=9 times MF=3, by MF=10, or by sections of MF=6 times MF=3. When this format is used, it is possible to give the simple command

```
10/
```



### 8.19 Coding Details

The `group` subroutine is exported by the `groupm` module. GROUPR begins by reading most of the user's input (see `ruinb`). It then locates the desired material and temperature on the input ENDF, PENDF, and GENDF tapes, and reads in the self-shielded unresolved cross sections (if any) from the PENDF tape using `stounr`. If self-shielding was requested, `genflx` is used to compute the weighting flux as described in Section 8.4. The next step is to write the header record for this material on the output GENDF tape.

The code is now ready to begin the loop over reactions for this material and temperature. Either an input card is read to get `mfd`, `mtd` and `mtname` (the reaction name), or the next reaction in an automatic sequence is selected. First, the default Legendre order, secondary group count, and  $\sigma_0$  count are selected for the reaction in `init`, and the retrieval routines are initialized. `group` then processes the reaction using the `panel` logic described in Section 8.11. If a "shortcut" fission spectrum was requested (`mfd=5`), for delayed fission, and for the low-energy "constant" spectra, the spectrum is calculated directly using `getff`. As the cross sections for each group are obtained, they are printed out (see `displa`) and written to the GENDF tape. When the last group has been processed, `group` loops back to read a new input card for a new reaction.

This loop over reactions continues until a terminating "0/" card is read. `group` then proceeds to the next temperature, if any, and repeats the loop over reactions. After the last temperature has been processed for the first material, an opportunity is provided to change to a new material, keeping all the other input parameters unchanged. A "0/" card at this point causes all the files to be closed, prints out the final messages, and terminates the `group` run.

Automatic choice of the next reaction to be processed is done in one of two ways. For a simple range of MT numbers, such as the example 51 - 66 used above, the negative value is stored in the variable `mtdp` in the `group` subroutine. When `mtdp` is negative, `mtd` is incremented after each reaction until it is greater than the absolute value of `mtdp`. `mtdp` is then reset to one, and the code proceeds to the next input card. When processing photon data, `mfd=16` will automatically change to 17, if necessary. Similarly, `mfd=21, 22, ...` will automatically change to `mfd=31, 32, ...`. A more automatic method is triggered by `mtd=0`. In this case, a subroutine called `nextr` is called to return the next value of `mtd` to be used, and a subroutine called `namer` is called to generate the reaction name. For `mfd=3`, `nextr` finds the next reaction in File 3 on the input PENDF tape. MT=251-253 and thermal data (MT=221-250) are excluded. The MT values

for the special options (258, 259, *etc.*) do not appear on the PENDF tape, and they must be requested explicitly. For matrices, GROUPR works with a set of lists loaded into global arrays by `conver`. The list `mf4` contains all the neutron-scattering MT numbers that appear in the File 4 part of the directory on the ENDF tape, and the list `mf6` contains all the MT numbers of sections of File 6 that contain subsections that produce neutrons. Therefore, reading through these two lists returns all the neutron-producing matrix reactions. Similarly, the list `mf12` contains all the File 12 entries from the directory, `mf13` contains the File 13 entries, and `mf18` contains all the MT values for sections in File 6 that contain subsections for photon production. Scanning through these three lists produces all the photon production matrix reactions. Two arrays are used for charged-particle producing reactions; the first index runs through the charged particles in the order p, d, t,  $^3\text{He}$ ,  $\alpha$ , recoil. Taking proton production as an example, the list elements `mf6p(1,i)` contain the MT numbers of sections in File 6 that contain subsections that produce protons. The list elements `mf4r(1,i)` contain MT numbers from File 4 for two-body reactions that produce protons; namely, MT600 - MT648. `next` scans through both of these lists to return indexes to all the reactions that produce protons. The same procedure is used for the other charged particles. The arrays `mf10s` and `mf10i` are used in a similar way for nuclide production.

Subroutine `namer` generates name strings with up to 15 Hollerith words with 4 characters each (60 characters). The names depend on the “ZA” of the projectile and the MT number for the reaction. The parameter `mf d` is used to choose between the suffixes “cross section” and “matrix”. Some examples of the names produced follow:

| Name        | Name        | Name      |
|-------------|-------------|-----------|
| (n,total)   | (n,heat)    | (p,p02)   |
| (n,elastic) | (n,p02)     | (p,n00)   |
| (n,2n)      | (p,elastic) | (g,total) |
| (n,n01)     | (p,2n)      | (g,pair)  |

Subroutines `mfchk` and `mfchk2` are used with the full input for reaction selection in GROUPR to check whether `mf d=17` is needed when `mf d=16` was requested, or whether one of the charged-particle File 4 values `mf d=31-36` is needed when `mf d=21-26` were requested. The lists in global variables like `mf12` are used, just as for `next`.

Subroutine `gengpn` generates the group bounds in the global array `egn` for the neutron group structure from input cards, from data statements, or by



calculation. Some of the data statements use energies in eV and some use lethargy. Similarly, **gengpg** generates the photon group structure in global array **egg** from input cards or data statements; in this case, all bounds are in eV.

Subroutine **genwtf** sets up the weight function option requested with **iwt** by reading the input cards into **weights**, transferring numbers from data statements to **weights**, or simply reporting the analytic weight option requested. Subroutine **getwtf** returns the values of the weight function at energy  $E$  by calculation or by interpolation in the table established by **genwtf**. The current version returns the same value for all Legendre orders. Choosing **enext** is difficult for **getwtf** because the functions have not been explicitly linearized. It is important to generate extra grid points in energy regions where the weight function may vary faster than the cross section (for example, in the fusion peak).

Subroutine **genflx** computes the self-shielded weighting flux using either the Bondarenko model or the flux calculator, and it writes the result on a scratch tape using the **loada** utility routine. When fluxes are needed for the generalized group integrals, they are read from this scratch file using **finda** (see **getflx**). Subroutine **genflx** starts by checking for the weighting option. If the Bondarenko model was selected, it initializes **gety1** and **getwtf** to read the total cross section from the PENDF tape and the smooth weighting function  $C(E)$  set up by **genwtf**. It then steps through the union grid of  $\sigma_t(E)$  and  $C(E)$  computing the flux vs.  $\sigma_0$  and Legendre order by means of Eq. 248. In the unresolved energy range, **getunr** is used to retrieve the unresolved cross sections as a function of  $\sigma_0$ , and Eq. 256 is used to compute the weighting flux. In both cases, the data at each energy are stored as the  $1+(\text{lord}+1)*\text{nsigz}$  components

**e**, **phi(il,iz)**,

where **il** runs from 1 to **lord**+1 and **iz** runs from 1 to **nsigz**.

If the flux calculator option was requested, **genflx** sets up the parameters for the calculation and requests needed storage space. Next, the cross section retrieval routines **gety1** and **gety2** are set up to return total and elastic cross sections from the PENDF tape. A lower energy limit, **felo**, is chosen, and the cross sections are read into storage until a maximum energy, **fehi**, or a maximum number of points, **nemax**, is reached.

The slowing-down equation, either Eq. 267 or Eq. 271, is then solved from the break energy down to **felo**. The scattering source from energies above the break is based on the NR approximation. When the calculation is finished, fluxes from  $10^{-5}$  eV to **felo** are written to the scratch file using **loada** in the

same format used for the Bondarenko option. From **felo** to the energy break point, fluxes are transferred from memory to the **loada** file. Finally, above the break point, fluxes are computed and saved using the Bondarenko model.

Subroutine **init** is used to set up the number of  $\sigma_0$  values, secondary energy groups, and Legendre components for each combination of **mfd** and **mtd**. If **mfd**=8, a special copy of File 6 is made for use in **getaed**. The list of reactions to be self-shielded can be changed if desired. The number of secondary groups **ng** helps determine the storage required for the accumulating group integrals (see allocatable array **ans**) in **grouppr**. For simple cross section vectors, **ng**=2. The **nz**\***nl** flux components are stored first, followed by the **nz**\***nl** cross section components. When all the panels for one group have been processed, dividing position 2 by position 1 gives the group-averaged cross section. For ratio quantities like  $\bar{\nu}$  and  $\bar{\mu}$  (**mtd**=251-253, 452, 455, 456), **ng** is 3. Once again, the flux components are stored first, followed by the **nl**\***nz** components of **ratio**\***sigma**, followed by the components of the cross section. This arrangement allows for the calculation of group-averaged values of **ratio**\***sigma**, **ratio**, or cross section by dividing position 2 by 1, position 2 by 3, or position 3 by 1, respectively. For matrices, **ng** is set to one more than the number of secondary groups (**ngn** or **ngg**). The **nl**\***nz** flux components are stored first, followed by the **nl**\***nz** integrals for each secondary-energy group in turn.

Subroutine **panel** performs the generalized group integrals using the logic described in Section 8.11. For most calls to **panel**, the lower point of each “panel” was computed as the upper point of the previous panel. Therefore, **panel** is careful to save these previous values. However, if the bottom of the panel is just above a discontinuity, new values of cross section and flux are retrieved. Once the values at the lower boundary of the panel are in place, new values for the top of the panel are retrieved (see **flux**, **sig**). If the top of the panel is at a discontinuity in  $\sigma$  or at a group boundary, the energy used is just below the nominal top of the panel. “Just below” and “just above” are determined by **rndoff** and **delta**. For maximum accuracy, these numbers should be chosen such that **rndoff**>1, **delta**<1, and **rndoff**\***delta**<1 for the precision of the machine being used.

For simple average cross sections, the integrals of  $\sigma \times \phi$  and  $\phi$  are computed for the panel using trapezoids. This is justified by the linearization of  $\sigma$ ; the value of  $\sigma \times \phi$  at the midpoint is too uncertain to justify a more complex treatment. For two-body scattering, the feed function is far from linear over the panel. In fact, it can show oscillations as described in Section 8.12. The integral of the

triple product  $\mathcal{F} \times \sigma \times \phi$  is obtained by Lobatto quadrature of order 6 or 10 using the quadrature points and weights given in the parameter statements (see `qp6`, `qw6`, `qp10`, `qw10`). The cross section and reaction rate are determined at each quadrature point by interpolation, and the feed function is obtained by `getff`. For many reactions, `ff` will be nonzero for only a certain range of secondary groups. The value `ig1` is the index to the first nonzero result, and `ng1` is the number of nonzero values of `ff` in the range. Subroutine `panel` maintains the two corresponding values `iglo` and `ng` to specify the nonzero range of values in array `ans`. Finally, the flux and cross section at the top of the panel are transferred to `flst` and `slst`, and control is returned to the panel loop in `groupr`.

Subroutine `displa` is used to print cross sections and group-to-group matrices on the output listing (`nsyso`). Small values are removed for efficiency. Note that different formats are used in different circumstances. Infinitely dilute data are printed without  $\sigma_0$  labels. Isotropic matrices are printed with several final groups on each line. Delayed neutron spectra are printed using the Legendre order variable for time groups and with the time constants given on a heading line.

Subroutine `getflx` returns `nl*nz` components of the weighting flux. If `nsigz` is 1, the flux is computed using `getwtf`, and all Legendre orders are taken to be equal. When self-shielding has been requested, the flux components are obtained by interpolating between adjacent values retrieved with `finda` from the scratch tape written by `genflx`. The grid energies found on the scratch tape are used to get `enext`. The flux is taken to be continuous, so `idis` is always set to zero.

Subroutine `getyld` returns the yield needed by `getff` for fission (MT=452, 455, or 456 from File 1) or radionuclide production yields from File 9 (using `mfd=3zzzaaam`). This routine also retrieves the delayed neutron time constants when `mtd=455`. Tabulated yields are obtained by interpolation using the utility routine `terpa`. Polynomial data are expanded by direct computation.

Subroutine `getsig` returns `nl*nz` components of the cross section using point data from the PENDF tape and self-shielded unresolved data, if present, from `getunr`. The routine starts by adjusting MF and MT for the special options (`mtd=258-259`, `mfd=3zzzaaam`, *etc.*) and locating the desired section on the PENDF tape. Subroutine `getsig` is then called for each desired energy value  $E$  in increasing order. For `mtd=258` or `259`, the appropriate velocity or lethargy is computed from  $E$  and returned. In the more general cases, `gety1` is used to retrieve the pointwise cross section from the PENDF tape, and `getunr` is called to replace this value with self-shielded unresolved cross sections if necessary.

The unresolved cross sections are handled using **stounr** and **getunr**. Subroutine **stounr** locates the desired material and temperature in MF=2, MT=152 of the PENDF tape, and then it copies the data into the global allocatable storage array **unr**. The  $\sigma_0$  grid on the PENDF tape does not have to agree with the list requested for **groupr**, but a diagnostic message will be printed if they are different. However, the **ntemp** values of temperature requested by **groupr** must agree with the first **ntemp** temperatures on the PENDF tape, or a fatal error will result. Subroutine **getunr** checks whether  $E$  is in the unresolved energy range and whether MT is one of the resonance reactions. If so, it locates the desired interpolation range in the **unr** array, and interpolates for the self-shielded cross sections. If this is an energy range where resolved and unresolved ranges overlap, the resolved part is added to the background  $\sigma_0$  before interpolation. The subroutine **terpu** is used for interpolating in the unresolved cross section tables. The special value MT=261 is used to select the  $\ell=1$  component of the total cross section. Note that **getsig** also uses this  $\ell=1$  value for  $\ell=2, 3, \dots$

Subroutine **getff** returns the feed function **ff** using different portions of the coding for different options. The first section is used for cross sections and ratio quantities. The same yield **yld** is returned for every  $\ell$ -component in **ff**.

The second section of **getff** is for neutron continuum transfer matrices. The yield is either determined from MT [for example, **yld**=2 for MT=16, the (n,2n) reaction], or it is obtained using **getyld** for fission. Next, the angular distribution is obtained using **getfle** (see  $F$  in Eq. 323), and the secondary energy distribution is obtained using **getsed** (see  $g$  in Eq. 323). Finally, the product of the three factors is loaded in **ff**. Note that the range of groups returned extends from **iglo**=1 to the highest nonzero result, for a total of **ng** groups. Since **ff** for these reactions is a smooth function of incident energy, **nq** is set to zero, and no additional quadrature points will be used in **panel**.

The third section of **getff** is for gamma production matrices. The photon yields are obtained using **getyld**. In general, there are **nyl** different yields, each one corresponding to a different discrete gamma ray, or to the continuum. The angular distributions for these gamma rays are obtained using **getgfl** (most ENDF/B photons are given as isotropic). The energy distribution for the continuum (if any) is obtained by **getsed**. Now, the code loops through the photon group structure placing each discrete photon in the appropriate group and adding in the continuum part. During this loop, the range of nonzero values (**iglo**, **ighi**) is determined. Finally, the nonzero values are packed into **ff**, and **iglo** and **ng** are returned to describe the distribution. Again, **nq**=0 is used.

The fourth section of **getff** handles two-body scattering, either elastic or discrete-level inelastic, and both neutrons and charged particles. First, subroutine **parts** is called to set up the particle type,  $A'$  value, and the scattering law for reactions that use File 4. Then **getdis** is called to finish the processing.

The fifth section handles thermal-neutron scattering. The bulk of the work is done by **getaed**, which is discussed below. Subroutine **getff** takes the output of **getaed** and packs it into the final result, **ff**.

The last two sections of **getff** are used to process energy-angle distributions from ENDF-6 format sections of File 6. The subroutine simply calls **getmf6**.

Subroutine **parts** is used to set up particles for reactions that use File 4. Different branches are used for ENDF-6 and earlier ENDF versions because the MT numbers used for charged-particle discrete levels have been changed. For example, proton levels use MT=600-649 in ENDF-6 libraries, but MT=700-719 in earlier libraries. If **mfd**=3, no action is taken. For other **mfd** values, the routine determines **zap**, **aprime**, and **law**. The result depends on whether File 4 or File 6 data are to be used.

Subroutine **getmf6** is used to compute the feed function for reactions represented in File 6. As is common with NJOY subroutines, it is called with **ed**=0 to initialize the subroutine. The first step is to locate the desired section of File 6 on the input ENDF tape. It then sets the parameter **zad** (for ZA desired) based on the input value **mfd** and searches through the section for the desired subsection. If this subsection has **law**=4, it defines a recoil particle; the code backs up to the first subsection in the section, which is assumed to be the subsection describing the emitted particle. The subroutine has now arrived at statement number 140, where it decides whether to branch to special coding for two-body reactions (statement number 500) or phase-space reactions (statement number 150). All the other options have a TAB2 record at this point that defines the incident energy grid. For **law**=1, the data for the first incident energy are read in and converted to the Lab frame by **cm2lab**. Similarly, for **law**=7, the data are read in and converted to a **law**=1 format by **l12lab**.

For a normal entry, **getmf6** interpolates for the particle yield for the current particle. For all of the laws except 2-5 (discrete two-body laws), it then checks to see whether the energy **ed** is in the current panel (or if this is the first time in the first panel). If not, it moves the high data to the low position and reads in new high data. Of course, it also converts the new high data to the correct form with **cm2lab** or **l12lab**. Once **ed** is in the current panel, the code reaches statement number 300, which sets up the loop over secondary energy

by initializing **f6lab**. This loop uses a grid that consists of the **epnext** values returned by **f6lab** and the group bounds **eg(i)**. The actual integral over  $E'_L$  inside each group uses trapezoidal integration. The last step for laws 1, 6, and 7 is to add in the contributions to the feed function from discrete energies in File 6. For the discrete two-body laws (2-5), the routine goes through statement number 500, which simply calls **getdis**. For all laws, the last step is to check the normalization of the feed function. If the error is large, a message is printed out. In any case, the results are adjusted to preserve exact normalization.

Subroutine **cm2lab** is used to convert a CM distribution starting at **inow** in **cnow** into a Lab distribution, which will be stored starting at **jnow**. This routine generates a grid for the Lab secondary energy  $E'_L$  by adaptive reconstruction. The reconstruction stack is first primed with  $p_{L\ell}(E, 0)$  as computed by **f6cm** and  $p_{L\ell}(E, E'_{\text{next}})$  (also from **f6cm**), where the value  $E'_{\text{next}}$  is the value **epnext** returned by the first call to **f6cm**. This panel is then divided in half, and the value returned by **f6cm** is compared with the linear interpolate. If they agree within 0.5% (see **tol**), this panel is converged. Otherwise, it is subdivided further. When convergence has been achieved for this panel, a new panel is chosen, and it is subdivided to convergence. When the entire range for  $E'_L$  has been processed, the final parameters are loaded into the new File 6 record for  $p_{L\ell}(E, E'_L)$  (which starts at **jnow** in **cnow**), and the routine returns to **getmf6**.

Subroutine **f6cm** is used to compute the Legendre coefficients of the double-differential scattering function  $p_{\ell}(E \rightarrow E')$  in the Lab system from data given in File 6 in the CM frame. The memory area **cnow** contains the raw data. It is necessary to call the routine **ep=0** for each new value of  $E$ . Thereafter, values of **ep** can be requested in any order. This is required by the adaptive scheme used to generate the Lab  $E'$  grid in **cm2lab**. The conversion uses Eqs. 356 - 361. On a normal entry with  $E'_L > 0$ , the code computes the lower limit of the integral  $\mu_{\text{min}}$ . It then sets up an adaptive integration over a panel starting at  $\mu=1$ . The value for  $E'_C$  is computed using

$$E'_C = (1 + c^2 - 2c\mu_L)E'_L, \quad (370)$$

which is based on Eq. 357, and either **f6ddx** or **f6psp** is called to compute  $p_C(E, E'_C, \mu_C)$  and **epnext**. The lower limit of the integration panel is then computed by setting  $E'_C$  equal to **epnext** and solving for the CM cosine using

$$\mu_C = \frac{\mu_L - c}{\sqrt{1 + c^2 - 2c\mu_L}}. \quad (371)$$

Of course, the larger of this result and  $\mu_{\min}$  is used as the lower bound of the panel. Therefore, the adaptive integration operates on a nice continuous function. It continues subdividing the  $\mu_C$  grid in this panel until convergence is achieved within 0.5% for all Legendre orders. The lower bound of this panel becomes the upper bound of a new panel, and a new lower bound is selected as above. The integration is carried out over successive panels until  $\mu_{\min}$  is reached. When the calculation of the continuum part of  $p_{L\ell}$  is finished for these values of  $E$  and  $E'_L$ , the routine checks for possible contributions from delta functions. Next, the routine scans through the computed coefficients and zeros out any small ones that may just be noise. Finally, it chooses a value for `epnext` and returns.

Function `f6ddx` is used to compute the double-differential scattering function  $f(E \rightarrow E', \omega)$ , where secondary energy  $E'$  and scattering cosine  $\omega$  are in the CM system. On entry, `cnow` contains the File 6 data for a particular value of  $E$ , and `f6ddx` must be called once with `ep=0` for each new value of  $E$ . Thereafter, `ep` values can be requested in any order (this is required by the adaptive scheme used to convert to the Lab system in `f6cm`). For a normal entry with `ep>0`, the code searches for the panel in the data that contain the requested value of  $E'$ . If `lang=1` for this subsection of File 6, the data are already given as Legendre coefficients, and the code simply interpolates for the desired results. If `lang=2`, the data use the Kalbach-Mann scheme for representing the energy-angle distribution. This routine includes both the original Kalbach-Mann representation[58] and the newer Kalbach representation[59]. It has been set to use the latter by the parameter statement `k86=1`. The code interpolates for the model parameters at  $E'$  and computes the desired answer with the model's formulas. The ENDF-6 format also allows CM distributions given as values tabulated versus scattering cosine (see `lang=11-15`). Note that there is a "stub" to take special action at low energies. It is currently disabled by the statement `efirst=0.0`, but it may be used sometime in the future to account for the fact that the low-energy dependence of the scattering function must vary as  $f(E') = c * \sqrt{E'}$ .

Function `bach` computes the Kalbach-86  $a$  parameter, which depends on the neutron separation energy for the target `izat` using the liquid-drop model without pairing and shell terms. The formula used describes the reaction  $a+B \rightarrow C+d$ :

$$\begin{aligned}
E_{sep} = & 15.68(A_C - A_B) \\
& - 28.07\left(\frac{(N_C - Z_C)^2}{A_C} - \frac{(N_B - Z_B)^2}{A_B}\right) \\
& - 18.56(A_C^{2/3} - A_B^{2/3}) \\
& + 33.22\left(\frac{(N_C - Z_C)^2}{A_C^{4/3}} - \frac{(N_B - Z_B)^2}{A_B^{4/3}}\right) \\
& - 0.717\left(\frac{Z_C^2}{A_C^{1/3}} - \frac{Z_B^2}{A_B^{1/3}}\right) \\
& + 1.211\left(\frac{Z_C^2}{A_C} - \frac{Z_B^2}{A_B}\right), \tag{372}
\end{aligned}$$

where  $A$  stands for atomic weight,  $Z$  for charge number, and  $N$  for neutron number. Note that, even for reactions like (n,2n),  $C$  is the residual nucleus resulting from the removal of one particle,  $d$ ; it is not necessarily the real physical residual nucleus for the reaction. If the target **izat** is an element,  $E_{sep}$  has to be computed for some dominant isotope in the element. Dominant isotopes are assigned in this routine for some materials that often appear as elements in ENDF evaluations; if the particular target required does not appear, a fatal error message is issued. The user will have to add a line to the routine for the material and reassemble the code.

Subroutine **1121ab** converts File 6 from Law-7 format to Law-1 format using the laboratory Legendre representation. Law 7 represents the double-differential scattering distribution  $f(E \rightarrow E', \mu)$  by giving a series of tables of  $f(E \rightarrow E')$  for series of  $\mu$  values. On entry, the entire Law-7 section is stored in **c** starting at **inow**. The code loops through a set of  $E'$  values chosen to be the union of all the  $E'$  grids for all the different  $\mu$  values. For each point on this union grid, the code interpolates for all the corresponding  $f(\mu)$  values, and it uses them to compute **n1** Legendre coefficients  $f_\ell(E')$ . After completing the calculation for a new value of  $E'$ , it checks the normalization of the result, and then it checks back to see whether the previous value is still needed to represent the curves  $f_\ell(E')$  within a tolerance of 0.5%. The results are written in **c** starting at **jnow**. They have the Law-1 Legendre form, namely, sets of values  $E'$ ,  $f_0(E')$ ,  $f_1(E')$ ,  $\dots$ ,  $f_{NL-1}(E')$ , given for a series of  $E'$  values starting with zero.

Subroutine **f61ab** is used to return the Legendre coefficients of the double-differential scattering function  $f_\ell(E \rightarrow E')$  for particular values of  $E$  and  $E'$  in the Lab system (see **e** and **ep**) from a part of File 6 in Law-1 format. Since Law-



7 sections have been converted to Law-1 format using `l12lab`, and since CM sections in Law-1 format have been converted to the Lab frame using `cm2lab`, the only two roles left for this subroutine are interpolation to the desired values of  $E$  and  $E'$  and preparation of Legendre coefficients for sections that use the File-6 variant with `law=1` and `lang=11-15` (laboratory distributions tabulated) vs.  $\mu$ . Only the continuum portion of the distribution is processed here; any delta functions given in File 6 must be handled separately. The routine is initialized by calling it with `ep=0`. Data for the two incident energy values that bracket  $E$  are already present in `clo` and `chi`. Then the routine extracts various parameters from the `c` array and prepares the variables used to control interpolation. These variables are complicated, because this routine handles three different interpolation schemes: “cartesian”, “unit base”, and “corresponding point” (see the ENDF-6 manual[8] for more details). For a normal entry, the code searches the data in `clo` and `chi` for the intervals containing  $E'$ . If `lang=1`, it performs a two-dimensional interpolation for the `n1` coefficients at  $E$  and  $E'$ . For `lang>1`, it computes the Legendre coefficients from the File 6 data, and then does the two-dimensional interpolation. Finally, it computes `epnext` and returns.

Subroutine `getdis` is used to compute the feed function for elastic or discrete inelastic scattering of neutrons or charged particles using either File 4 or File 6 data. First, the angular distribution is retrieved with `getfle`, and an appropriate quadrature order is selected using Eq. 314. Then, a group loop from low energy to high energy is used to compute the  $\omega_1$  and  $\omega_2$  limits of Eq. 312, and the range  $(\omega_1, \omega_2)$  is subdivided using the appropriate Gauss-Legendre quadrature points (see `qp4`, `qp8`, `qp12`, and `qp20`). The function  $f(E, \omega)$  is computed at each of these quadrature points using Eq. 313 and the angular distribution previously returned by `getfle`. The laboratory cosine at the quadrature point,  $\mu[\omega]$ , is computed using Eq. 309. Finally, the integrand of Eq. 312 is multiplied by the appropriate quadrature weight (`qw4`, `qw8`, `qw12`, or `qw20`) and added into the accumulating integral. This continues until  $\omega_2 = 1$ . The nonzero values of `ff` and the parameters `iglo` and `ng` are then complete for this value of  $E$ .

The next step is to determine `enext` based on the next critical point as given by Eqs. 316 - 319. Special cases are used for elastic scattering to avoid numerical problems. Note that the discontinuity flag `idisc` is set for critical points. The `nq` variable is also set to force `panel` to subdivide the initial-energy integration.

Subroutine `getfle` retrieves or computes the Legendre coefficients for the angular distribution of a reaction at incident energy  $E$ . When called with `e=0`,

`getfile` requests storage for the raw data, reads in the File 4 information for the first two incident energies on the file, and then uses `getco` to retrieve the corresponding coefficients. On subsequent entries with  $e > 0$ , `getfile` simply interpolates for the desired coefficients. When  $e$  exceeds the upper energy in storage, the values for the upper energy are moved to the lower positions, and new upper values are read and converted to coefficients. An isotropic distribution is returned if  $e$  is outside the range of the angular data from File 4.

Subroutine `getaed` retrieves angle-energy data for thermal scattering reactions. For coherent elastic scattering, the routine reads through the cross section on the PENDF tape using `gety1` and locates the Bragg edges. On each subsequent call to `getaed`, the Legendre components of the cross section are computed using Eq. 304. For incoherent elastic scattering, the routine is first initialized by reading in the raw data for the first energy. On subsequent entries, a test is made to see whether  $e$  is in the range  $e_{lo}$  to  $e_{hi}$ . If not, the high data are moved to the low positions, and new high data are read. The Legendre components are then computed using Eq. 306. For incoherent inelastic scattering, `getaed` is initialized by reading in the raw data for the first two incident energies. On subsequent entries, the subroutine checks to see whether  $e$  is between  $e_{lo}$  and  $e_{hi}$ . If not, the data for  $e_{hi}$  are moved to the low positions, and new raw data are read from File 6 and binned. Once the correct data are in place, the desired energy-angle distribution is computed by using a combination of interpolation along lines of constant energy transfer and unit-base interpolation.

Subroutine `getgfl` returns the Legendre coefficients for the angular distributions for all discrete and continuum photons for a reaction simultaneously. When called with  $ed = 0$ , the routine reads File 14 into scratch storage and finds the starting location for the subsection describing each photon. On subsequent entries with  $ed > 0$ , `getgfl` sets up a loop over the  $ng$  photons on this section of File 14. For each photon, it searches for the energy panel that contains  $ed$ , uses `getco` to retrieve or compute the Legendre coefficients at the upper and lower File 14 energies, and interpolates for the desired coefficients at  $ed$  using `terp1`. Since most ENDF photons are represented as isotropic, a special short-cut calculation is provided for that case. Isotropic results are also returned if  $ed$  is outside the range of the data in File 14.

Subroutine `getco` is used by both `getfile` and `getgfl` to retrieve or compute Legendre coefficients from data in File 4 or File 14 format. The user can request output in either the Lab or CM system, and the raw data can be either Legendre coefficients or tabulated probability versus emission cosine. However, if the raw

data are in the laboratory system, CM coefficients cannot be produced. If the raw data are already in the form of coefficients in the desired system, **getco** simply checks for the maximum Legendre order needed using a tolerance of **toler=1e-6** and returns the coefficients in **f1** and the order in **n1**. If coordinate conversion is required, or if the raw data are tabulated, **getco** sets up the integral over cosine using Gauss-Legendre quadrature of order 20 (see **qp** and **qw**). The scattering probability for the quadrature point is computed from the coefficients or obtained by interpolating in the tabulation. The Legendre polynomials in the desired reference system are then computed. If the raw data are in the CM system ( $\omega$ ) and the result is to be in the Lab system ( $\mu$ ), the desired polynomials are  $P_\ell(\mu[\omega])$ ; otherwise, the quadrature angle is used directly to compute the polynomials. Once the coefficients have been computed, they are checked using **toler** to determine the maximum order, **n1**, and the results are returned in **f1**.

Subroutine **getgyl** is used to retrieve the yields for all photons emitted in a specified reaction simultaneously. The raw data are obtained from the ENDF/B tape as either yields (MF=12) or production cross section (MF=13). In the latter case, **getgyl** actually returns the fraction of the total yield assigned to each photon. The cross section returned by **getsig** is the total photon production cross section from MF=13 on the PENDF tape, which makes the resulting integral correct. Using the normal GROUPE procedure, **getgyl** is initialized by calling it with **ed=0**. The entire File 12 or File 13 is read into scratch storage, and the starting location for each subsection is determined. On subsequent entries (**ed>0**), the routine loops over the **ny1** photons found, and uses **terpa** to compute the yield at **ed**. If this is a primary photon, a discontinuity is set up at the energy where the photon will change groups. For MF=12, the calculation is finished. For MF=13, the numbers calculated above are converted to fractions of the total yield by dividing by the total production subsection from File 13. This routine does not handle ENDF/B transition probability arrays directly, because they will have been converted to File 12 yields by **conver**.

Subroutine **conver** converts ENDF/B evaluations to a standard form. If transition probability arrays were used in File 12, they are converted to yields and written back into File 12. If a section with MF=1 and MT=456 is missing from the evaluation, a copy of MT=452 is added to the tape as MT=456. In addition, a second copy of the modified tape is made on unit **nscr**. While **conver** is reading through the tape, lists of the reactions in File 4, File 12, and File 13 are written to global arrays for use by the automatic reaction selection logic in **nexttr**. For ENDF-6 evaluations containing File 6, the routine scans through File

6 looking for sections that produce neutrons, photons, or charged particles. The MT numbers for these sections are stored into **mf6**, **mf18**, and **mf6p**. The routine also checks for sections of File 4 containing charged-particle angular distributions and records their MT numbers in **mf4r**. Finally, if the section MF=6/MT=2 contains charged-particle elastic scattering information given using the nuclear-plus-interference format, it is converted into the residual-cross-section format for **getdis**.

Subroutine **getsed** returns the secondary-energy distribution for neutrons or continuum photons for all groups simultaneously. Both tabulated and analytic functions are handled. **getsed** is initialized for a particular reaction by calling it with **ed**=0. First, scratch storage is allocated, and all the subsections are read in. Analytic subsections are left in their raw form, but tabulated subsections are averaged over outgoing energy groups for each of the given incident energies. The array **loc** contains pointers for each subsection. On subsequent entries (**ed**>0), **getsed** loops over the subsections for this reaction. It first retrieves the fractional probability for the subsection using **terpa**. If an analytic law is specified, **anased** is used to compute the group integral for each secondary-energy group. Each integral is multiplied by the fractional probability for the law and accumulated into **sed**. For tabulated data, the routine simply interpolates between the two values for the group integrals using **terp1**, and accumulates them into **sed**. Note that various restrictions on the ordering of subsections and prohibition of multiple tabulated subsections needed for earlier versions of GROUPR are no longer required. Upscatter is not allowed in secondary-energy distributions except for fission or photon production. If found, it is put into the “in-group” ( $g'=g$ ).

Subroutine **anased** is used to calculate the integral from **e1** to **e2** for one of the analytic laws (see Eqs. 326 - 355). The routine uses the SLATEC version of the reduced complementary error function from the NJOY2012 math module. The resulting integral is returned in **g**.

Subroutine **hnab** is used to compute the special functions required for analytic law 11, the energy-dependent Watt spectrum. The method used is described in the **BROADR** chapter of this manual.

## 8.20 Error Messages

The fatal error messages and warning message from GROUPR are listed below, along with recommended actions to recover from the problem.

error in groupr\*\*\*unable to find mat=---, t=---.

Check for input error or wrong PENDF tape mounted.

error in groupr\*\*\*photons not allowed with igg=0.

In order to produce photon data, a photon group structure must be requested. Check the input on card 2.

error in groupr\*\*\*illegal mfd.

Check input mfd; legal values are 3, 5, 6, 8, 12, 13, 16, 17, 18, 21-26, 31-36, and the isotope production values like Xzzzaaam for X = 1, 2, 3 or 4.

message from groupr---auto finds no reactions for mf=--.

An automatic reaction selection card of the form "mfd" was given in the input, but the ENDF and PENDF tapes do not contain any sections that would produce the desired cross sections or matrices.

error in groupr\*\*\*unable to find next temp.

The current material ended before the requested temperature was found.

error in ruinb\*\*\*ntemp=0 not allowed.

There must be at least one temperature requested.

error in ruinb\*\*\*nsigz=0 not allowed.

There must be at least one background cross section. The first input value is automatically changed to 1e10.

error in gengpn\*\*\*read-in group structure is out of order.

Group structures must be given in ascending energy order.

error in gengpn\*\*\*illegal group structure.

Check input; current legal values are 1 through 23.

error in gengpg\*\*\*illegal group structure.

Check input; current legal values are 1 through 10.

error in genwtf\*\*\*exceeded storage reading user weight ...

See the allocatable array tmp with length ntmp=10000.

error in genwtf\*\*\*illegal weight function requested.

Check input; current legal values are -12 through +12.

error in genflx\*\*\*total not defined over energy range.

A complete total cross section is needed for self-shielding. This means that "dosimetry" and "activation" tapes, which normally give only a few key reactions, can only be processed using nsigz=1 (infinite dilution).

error in getfwt\*\*\*e outside range of data.

A premature end-of-file was found on the input flux tape when using the iwt=0 option. Check to be sure the tape was the output from a legal flux calculator run.

error in getfwt\*\*\*requested e is out of order.

The cause could be an improper input tape. Check as above.

`error in panel***elo.gt.ehi.`

This indicates some error in the energy grid for `panel`. It usually occurs if `rndoff` and `delta` are incorrect for your machine. Make sure that `rndoff>1`, that `delta<1`, and that the product `rndoff*delta<1` when evaluated on your machine (for example, 1.00000001 is not greater than unity on a 32-bit machine).

`error in panel***bad nq`

The `nq` parameter can be 2, 6, or 10 with the currently installed quadratures.

`error in getyld***illegal lnd.`

The maximum number of time groups is 8. See global array `dntc(8)`.

`error in getyld***requested nuclide not found.`

Unable to find requested nuclide production yield.

`error in getsig***illegal mt.`

Check input for `mtd`.

`error in getsig***desired lfs not found.`

Check input for `mfd` greater than 10000000.

`message from stounr---no unresolved sigma zero data....`

This message probably means that `UNRESR` or `PURR` was never run for this material. Infinitely dilute values will be used.

`message from stounr---sigma zero grids do not match....`

The unresolved calculations will probably work best if the  $\sigma_0$  grid in GROUPR matches the one in `UNRESR` or `PURR`. However, this is not necessary. `getunr` will interpolate to get values on the GROUPR grid from the `UNRESR` or `PURR` grid. A message is issued in case this isn't what the user really intended.

`error in stounr***storage exceeded.`

There is not enough storage for unresolved cross section data on PENDF tape. The allocatable array `tmp` has length `ntmp=10000`.

`error in stounr***cannot find temp=---`

The list of temperatures requested for the GROUPR run must agree with the first `ntemp` temperatures on the PENDF tape. Check your `BROADR` and `UNRESR` or `PURR` runs.

`error in getff***do not know how to handle ...`

The `getff` routine branches to different blocks of coding for different combinations of `mfd` and `mtd`, but if no appropriate branch is found for the current values, this error message is issued. It probably indicates an error in the evaluation.

`error in getmf6***desired particle not found.`

The outgoing particle for a group-to-group matrix is implied by the value of `mfd` (for example, protons for `mfd=21`). This message means that the

section of File 6 requested with `mfd` and `mtd` does not contain a subsection that produces that particle. Check the user input. This message should not occur with automatic reaction selection.

`error in getmf6***illegal law.`

The value of the `law` parameter is greater than 7. This implies an error in the evaluation.

`error in getmf6***too many subsection energy points.`

Limited by the parameter `maxss=500`.

`error in getmf6***storage exceeded.`

See the allocatable array `temp` with length `ntmp=990000`.

`message from getmf6---bad grids for corresponding point....`

Corresponding-point interpolation won't work correctly unless the two grids above and below the point of interest have the same number of points. This message means that there is an error in the evaluation.

`error in getmf6***too many subsections for one particle.`

We currently allow for no more than three. See `iyss(3)`, `izss(3)`, and `jss(3)`.

`error in cm2lab***storage exceeded.`

This means that the allocatable array `tmp` with length `ntmp=990000` in subroutine `getmf6` has run out of space.

`error in f6ddx***illegal lang.`

The value of `lang` for tabulated angular distributions must be in the range 11-15.

`error in bach***dominant isotope not known.`

The calculation of the neutron separation energy needed for the Kalbach model for particle energy-angle distributions needs a value for the dominant isotope in an element. It will have to be added to the code. The same problem will occur with the parallel routines in [HEATR](#) and [ACER](#).

`error in l12lab***storage exceeded.`

This means that the allocatable array `tmp` with length `ntmp=990000` in subroutine `getmf6` has run out of space.

`error in f6cm***nl>mxlg`

The current limit is `mxlg=65`.

`error in f6ddx***nl>mxlg`

The current limit is `mxlg=65`.

`error in f6lab***illegal lang.`

The value of `lang` must be in the range 11-15 for tabulated angular distributions.

`error in getdis***illegal nqp`

The allowed quadrature orders are 4, 8, 12, and 20.

error in getfle\*\*\*desired energy above highest energy...

Should not occur for well-constructed ENDF files. Check the evaluation to be sure File 3 and File 4 are consistent.

message from getfle---lab distribution changed to cm.

Angular distributions for two-body reactions are supposed to be given in the CM frame by ENDF conventions. Some old evaluations for heavy materials violate this rule; changing to the CM frame has little effect on the answers.

error in getaed\*\*\*thermal mf6/law7 not coded

This subroutine can't handle the  $E-\mu-E'$  ordering option provided by [THERMR](#).

error in getaed\*\*\*storage exceeded.

This refers to the allocatable array `aes` with length `maxaes=200000`.

error in getgfl\*\*\*too many gammas.

See the parameter `maxgfl=500`.

error in getgfl\*\*\*storage exceeded.

See the parameter `ntmp=10000`.

error in getgfl\*\*\*desired energy at highest given energy.

This problem should not occur in a well-constructed ENDF file. Check Files 3, 12, 13, and 14 for consistency.

error in getco\*\*\*limited to 64 legendre coefficients.

See `nlmax=65` and `P(65)`.

error in getco\*\*\*lab to cm conversion not coded.

The need for this type of conversion rarely occurs on the current ENDF evaluations, because CM is consistently used for two-body reactions, and the laboratory frame is consistently used for continuum reactions. There are a few exceptions for the heavy isotopes, where CM and lab are essentially equivalent, but they were errors when the files were generated.

error in getgyl\*\*\*lo=2 not coded.

This message should not occur, because any transition probability arrays on the ENDF tape should have been converted to yields by `conver`.

error in getgyl\*\*\*too many gammas.

The current limit is 550 photons. See the parameter `nylmax=550`.

error in getgyl\*\*\*storage exceeded.

This refers to the allocatable array `tmp` with length `ntmp=15000`.

message from conver---cannot do complete particle production...

With the advent of the ENDF-6 format, it is possible to make evaluations that fully describe all the products of a nuclear reaction. Some carry-over evaluations from earlier ENDF/B versions also have this capability, but many do not. This message is intended to goad evaluators to improve things!



message from conver---gamma production patch made for ...

This patch is used to correct the old ENDF/B-III evaluations for MAT=1149 and MAT=1150 (chlorine and potassium).

error in conver\*\*\*nnth too large

See mxnnth=350.

error in conver\*\*\*too many lo=2 gammas.

The LO=2 processing uses a set of allocatable arrays that are sized using lmax=500. That number can be increased freely, if necessary.

error in conver\*\*\*storage for fission nu exceeded.

The storage in the allocatable array nu is sized using nnu=6000, which can be increased freely.

error in conver\*\*\*xxxx to big.

The automatic processing of reactions is controlled by lists stored in global arrays like mf4 or mf6p. This error occurs when one of the particular indexes, indicated by "xxx" exceeds maxr1=500. The arrays for MF=10 (see imf10) have a limit of maxr2=500.

error in getsed\*\*\*too many subsections.

The current limit is 20. See the parameter nkmax=20.

error in getsed\*\*\*storage n tmp exceeded.

The input ENDF data are stored in the allocatable array tmp with length ntmp=50000.

message from getsed---upscatter correction....

This reaction should not have upscatter. The error is placed into the in-group element.

error in anased\*\*\*illegal lf.

Legal values are 5, 7, 9, 11, and 12.

error in f6psp\*\*\*3, 4, or 5 particles only.

Phase-space formulas for 3, 4, or 5 particles are provided in this routine. Check for an error in the evaluation.



## 9 GAMINR

The GAMINR module of NJOY is designed to produce complete and accurate multigroup photoatomic (but not photonuclear) cross sections from ENDF/B-IV, -V -VI or -VII data[67]. It will also work with the newer formats developed for ENDF/B-VII. Total, coherent, incoherent, pair-production, and photoelectric cross sections can be averaged using a variety of group structures and weighting functions. The Legendre components of the group-to-group coherent and incoherent scattering cross sections are calculated using the form factors[68] now available in ENDF/B. These form factors account for the binding of the electron in its atom. Consequently, the cross sections are accurate for energies as low as 1 keV. GAMINR also computes partial heating cross sections or kinetic energy release in materials (KERMA) factors for each reaction and sums them to obtain the total heating factor. The resulting multigroup constants are written on an intermediate interface file for later conversion to any desired format. Photonuclear reactions such as  $(\gamma, n)$  are not computed by this module.

GAMINR differs from the previously used GAMLEG code[22] in the following ways:

- Coherent form factors are processed thereby allowing higher Legendre components of the coherent scattering cross section to be produced. GAMLEG processed the  $P_0$  cross section only.
- Incoherent structure factors are processed giving accurate results at low energies where the Klein-Nishina formula fails.
- Heat-production cross sections (KERMA factors) are generated.
- Variable dimensioning and dynamic storage allocation allow arbitrarily complex problems to be run.
- GAMINR is much slower than GAMLEG since charge scaling of the incoherent matrix can no longer be used at all energies.

This chapter describes GAMINR in version 2012.0. The only differences between this version and the one reported previously[3] are the addition of additional group structures and weight functions and the conversion to Fortran-90 style and memory allocation.

### 9.1 Description of ENDF/B Photon Interaction Files

In the ENDF/B-IV and later photon interaction files, the coherent scattering of photons by electrons is represented by

$$\sigma_C(E, E', \mu) dE' d\mu = \frac{3\sigma_T}{8} (1 + \mu^2) |F(q, Z)|^2 \delta(E - E') dE' d\mu , \quad (373)$$

where  $E$  is the energy of the incident photon,  $E'$  is the energy of the scattered photon,  $\mu$  is the scattering cosine,  $\sigma_T$  is the classical Thomson cross section (0.66524486 b),  $Z$  is the atomic number of the scattering atom, and  $F$  is the atomic form factor. The coherent form factor is a function of momentum transfer  $q$  given by

$$q = 2k \sqrt{\frac{1 - \mu}{2}} , \quad (374)$$

where  $k$  is the energy in free-electron units ( $k = E/511003.4$  eV), but  $F$  is actually tabulated versus the quantity  $x = 20.60744q$ . The coherent form factor is given as MT=502 in File 27.

Incoherent scattering is represented by the expression

$$\sigma_I(E, E', \mu) dE' d\mu = S(q, Z) \sigma_{KN}(E, E', \mu) dE' d\mu , \quad (375)$$

where  $S$  is the incoherent scattering function and  $\sigma_{KN}$  is the free-electron Klein-Nishina cross section

$$\sigma_{KN}(E, E', \mu) = \frac{3\sigma_T}{8k^2} \left[ \frac{k}{k'} + \frac{k'}{k} + 2 \left( \frac{1}{k} - \frac{1}{k'} \right) + \left( \frac{1}{k} - \frac{1}{k'} \right)^2 \right] . \quad (376)$$

The scattering angle and momentum transfer for incoherent scattering are given by

$$\mu = 1 + \frac{1}{k} - \frac{1}{k'} , \quad (377)$$

and

$$q = 2k \sqrt{\frac{1 - \mu}{2}} \frac{\sqrt{1 + (k^2 + 2k)(1 - \mu)/2}}{1 + k(1 - \mu)} . \quad (378)$$

As was the case for coherent scattering,  $S(q, Z)$  is actually tabulated *vs.*  $x = 20.60744q$ . It is important to note that  $S$  is essentially equal to  $Z$  for  $x$  greater than  $Z$ . The incoherent scattering function is given as MT=504 in File 27.

The ENDF/B-IV, -V, -VI, and -VII photon interaction files also contain tabulated cross sections for total, coherent, incoherent, pair production, and photoelectric reactions. They are given in File 23 as MT=501, 502, 504, 516, and 602 respectively (note however, starting with the ENDF/B-VI files, MT=602 data appear in MT=522). The coherent and incoherent cross sections were obtained by the evaluator by integrating Eqs. 373 and 375 and are therefore redundant. Due care must be taken to avoid introducing inconsistencies. Starting with ENDF/B-VI, there are additional cross sections given for the partial photoelectric reactions starting with MT=534.

## 9.2 Calculational Method

The multigroup cross sections produced by GAMINR are defined as follows:

$$\sigma_{xg} = \frac{\int_g \sigma_x \phi_0(E) dE}{\int_g \phi_0(E) dE}, \quad (379)$$

$$\sigma_{T\ell g} = \frac{\int_g \sigma_T(E) \phi_\ell(E) dE}{\int_g \phi_\ell(E) dE}, \text{ and} \quad (380)$$

$$\sigma_{x\ell g \rightarrow g'} = \frac{\int_g \mathcal{F}_{x\ell g'}(E) \sigma_x(E) \phi_\ell(E) dE}{\int_g \phi_\ell(E) dE}. \quad (381)$$

In these expressions,  $g$  represents an energy group for the initial energy  $E$ ,  $g'$  is a group of final energies  $E'$ ,  $x$  stands for one of the reaction types,  $T$  denotes the total, and  $\phi_\ell$  is a Legendre component of a guess for the photon flux. In the last equation,  $\mathcal{F}$  is the “feed function”; that is, the total normalized probability of scattering from  $E$  into group  $g'$ . The feed function for coherent scattering is

$$\begin{aligned} \mathcal{F}_{C\ell g'}(E) &= \frac{\int_{-1}^{+1} \sigma_C(E, E', \mu) P_\ell(\mu) d\mu}{\sigma_C(E)} \\ &= \frac{\int_{-1}^{+1} (1 - \mu^2) |F(x)|^2 P_\ell(\mu) d\mu}{\int_{-1}^{+1} (1 - \mu^2) |F(x)|^2 d\mu}, \end{aligned} \quad (382)$$

for  $E$  in  $g'$  and zero elsewhere.

Here  $P_\ell(\mu)$  is a Legendre polynomial. Note that  $\mathcal{F}_{C0g'} = 1$ ; this form assures that the coherent scattering cross sections are consistent with the values tabulated in File 23.

For incoherent scattering,

$$\mathcal{F}_{I\ell g'} = \frac{\int_{g'} S(q, Z) \sigma_{KN}(E, E', \mu) P_\ell(\mu) dE'}{\int_{g'} S(q, Z) \sigma_{KN}(E, E', \mu) dE'} . \quad (383)$$

Because  $S$  is simply equal to  $Z$  for high values of  $q$ , it is not necessary to completely recompute the incoherent matrix when processing a series of elements in the order of increasing  $Z$ . GAMINR automatically determines that some groups for element  $Z_{now}$  can be obtained from element  $Z_{last}$  by scaling by  $Z_{now}/Z_{last}$ .

Finally, pair-production is represented as a  $(\gamma, 2\gamma)$  scattering event, where

$$\mathcal{F}_{PP\ell g'}(E) = \begin{cases} 2, & \text{if } g' \text{ includes } 511003.4 \text{ eV;} \\ 0, & \text{otherwise .} \end{cases} \quad (384)$$

In addition, GAMINR computes multigroup heating cross sections or KERMA factors as follows:

$$\sigma_{Hxg} = \frac{\int_g [E - \bar{E}_x(E)] \sigma_x(E) \phi_0(E) dE}{\int_g \phi_o(E) dE} , \quad (385)$$

where  $\bar{E}_x(E)$  is the average energy of photons scattered from  $E$  by reaction type  $x$ . The average energies are computed using

$$\bar{E}_C = E , \quad (386)$$

$$\bar{E}_{PP} = 1.022007 * 10^6 \text{ eV} , \quad (387)$$

$$\bar{E}_{PE} = 0, \text{ and} \quad (388)$$

$$\bar{E}_I(E) = \int_0^\infty E' \sigma_I(E, E', \mu) dE' / \sigma_I(E) . \quad (389)$$

These separate contributions to the heating cross section are summed to get a quantity that can be combined with a calculated flux to obtain the total heating rate.

### 9.3 Integrals Involving Form Factors

The integrals of Eqs. 382 and 383 that involve the form factors are very difficult to perform because of the extreme forward peaking of the scattering at high energies. Fig. 34 illustrates the problem for coherent scattering.

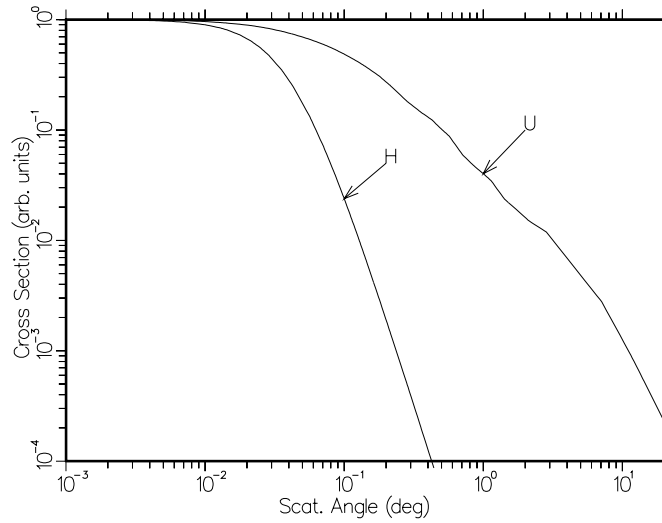


Figure 34: Angular distribution for coherent scattering from hydrogen and uranium at high photon energy.

For coherent scattering, the integral of Eq. 382 is broken up into panels by the tabulation values of  $x$ . Each panel is integrated in the  $x$  domain using Lobatto quadrature of order 6 for  $\ell = 3$  or less and order 10 for larger Legendre orders. Eq. 374 is used to compute the  $\mu$  value for each  $x$  and to obtain the Jacobian required.

Since  $\mu$  is quadratic in  $x$ , the polynomial order of the integrand in the numerator of Eq. 382 is  $2\ell + 2$  plus twice the polynomial order of  $F$  in the panel. For  $\ell = 3$ , the theory of Gaussian quadrature implies that the integral will be exact if  $F$  can be represented as a quadratic function over the panel.

The incoherent integral of Eq. 383 is also broken up into panels, but here the panels are defined by the union of the tabulation values of  $x$  and the momenta corresponding to the secondary-energy group bounds. The relationship between  $x$ ,  $\mu$ , and secondary energy is given in Eqs. 377 and 378. This time, the integral is performed *vs.*  $E'$  using Lobatto quadrature of order 6 for  $\ell$  less than or equal to 5 and order 10 for larger  $\ell$  values.

All form factors and structure factors are interpolated using ENDF/B log-log interpolation as specified by the format. However, the cross sections in the file were evaluated using a special log-log-quadratic scheme. Ignoring this complication may lead to a 5% error in the incoherent cross section at 0.1 keV with a negligible error at the higher energies that are of most practical concern[68].

## 9.4 Coding Details

The main entry point is subroutine `gaminr` exported by module `gaminm`. The code begins by reading the user's input. It then locates the position for the new material on the old GENDF tape (if any) and copies the earlier results to the new output tape. The desired material is also located on the input PENDF tape prepared previously using `RECONR`. A new material header is then written onto the output tape leaving the code ready to begin the loop over reaction types.

For each of the preset reaction types, GAMINR uses the panel logic of `GROUPT` to average the cross sections (see the “panel” discussion in Section 8.11). If this is the first material in a series of elements, the incoherent matrix is saved to a scratch area. For subsequent materials, the higher energy matrix elements are obtained by scaling these saved values by the appropriate  $Z$  ratio. The resulting cross sections and group-to-group matrix elements are then printed out and written to the output tape. The heat production contribution from each reaction is summed into a storage area. After all reactions have been processed for this material, a special pass through the output logic is used to create a heating section using MT=525 for ENDF/B-VI and later files or MT=525 for earlier ENDF/B files. Finally, the rest of the old output tape is copied to the new output tape. A description of the format of the multigroup output tape will be found in the `GROUPT` chapter (see Section 8.17).

As with `panel` in `GROUPT`, `gpanel` integrates the triple product  $\mathcal{F} \cdot \sigma \cdot \phi$ . The feed into secondary group  $g'$  for Legendre order  $\ell$  from initial energy  $E$  is computed in `gtff` as described in Section 9.3 above. Cross sections are read from the PENDF tape (see `gtsig`). Flux can be read in, constant, or  $1/E$  with high and low energy roll-offs (see `gnwtf` and `gtflx`).

## 9.5 User Input

The following description of the user input is reproduced from the comment cards at the beginning of the GAMINR module.

```
!---input specifications (free format)-----
!
! card1
!      nendf    unit for endf tape
!      npend    unit for pendf tape
!      ngam1    unit for input ngam tape (default=0)
!      ngam2    unit for output ngam tape (default=0)
```



```

! card2
!   matb   material to be processed
!           input materials in ascending order
!   igg     gamma group structure option
!   iwt     weight function option
!   lord    legendre order
!   iprint  print option (0/1=minimum/maximum) (default=1)
! card3
!   title   run label up to 80 characters (delimited by ',
!           ended with /)
! card4     (igg=1 only)
!   ngg     number of groups
!   egg     ngg+1 group bounds (ev)
! card5     (iwt=1 only)
!   wght    weight function as tab1 record
! card6
!   mfd     file to be processed
!   mtd     section to be processed
!   mtname  description of section to be processed
!           repeat for all reactions desired
!           mfd=0/ terminates this material
!           mfd=-1/ is a flag to process all sections present
!           for this material (termination is automatic)
! card7
!   matd    next mat number to be processed
!           terminate gaminr run with matd=0.
!
! ---options for input variables-----
!
!           igg     meaning
!           ---     -----
!           0       none
!           1       arbitrary structure (read in)
!           2       csewg 94-group structure
!           3       lanl 12-group structure
!           4       steiner 21-group gamma-ray structure
!           5       straker 22-group structure
!           6       lanl 48-group structure
!           7       lanl 24-group structure
!           8       vitamin-c 36-group structure
!           9       vitamin-e 38-group structure
!           10      vitamin-j 42-group structure

```

```

!
!      iwt      meaning
!      ---      -
!      1      read in
!      2      constant
!      3      1/e + rolloffs
!
!-----

```

Note that both an ENDF/B tape and a PENDF tape from [RECONR](#) are required. Older, pre-ENDF/B-VI, photon interaction tapes are available from the Radiation Shielding Information Computational Center (RSICC) at ORNL as DLC7E (for ENDF/B-IV) or DLC-99/HUGO (for ENDF/B-V). A photoatomic library in ENDF-6 format based on DLC-99 is available from the National Nuclear Data Center (NNDC) at the Brookhaven National Laboratory. The latest ENDF/B-VII photoatomic library is also available from the NNDC. Material numbers (`matb`) are simply the element  $Z$  number for versions IV and V; they are equal to  $100*Z$  for ENDF-6 formatted files. The values of `matd` on card 7 should be given in increasing order for maximum economy. The normal mode of operation uses `mfd` = -1. This automatically processes MT=501, 502, 504, 516, 522, and 525. For pre-ENDF-6 formatted files, the photoelectric cross section is changed from 522 to 602, and the heating cross section is changed from 525 to 621.

The following sample run prepares a GENDF tape for two elements. The numbers on the left are for reference; they are not part of the input.

```

1.  reconr
2.  20 21
3.  'pendf tape for 2 elements from ENDF/B-VII'/
4.  100 1 0/
5.  .001 0./
6.  '1-hydrogen'/
7.  9200 1 0/
8.  .001 0./
9.  '92-uranium'/
10. 0/
11. gaminr
12. 20 21 0 22

```

```

13.  100 7 3 4 0
14.  '24-group photon interaction library'/
15.  -1/
16.  9200
17.  -1/
18.  0/
19.  stop

```

On line 2, an ENDF/B tape containing File 23 has been mounted on logical unit 20. The title on line 3 will appear on the PENDF tape. Material 100 is hydrogen (lines 4-6) and material 9200 is uranium (lines 7-9). The element names on lines 8 and 11 will appear on the PENDF tape in MF=1,MT=451. Linearization is accurate to better than 0.1%. A more complete description of [RECONR's](#) input may be found in Section 3.6.

GAMINR uses the same ENDF tape as [RECONR](#) (actually only MF=27 is read by GAMINR), but GAMINR also reads the [RECONR](#) output tape on unit 21. The GAMINR GENDF tape will be on unit 22. Card 13 specifies hydrogen as the first material, 24 groups,  $1/E$  weight with roll-offs, Legendre components through  $P_3$ , and the full printed output. Cards 16 and 17 select the default list of reaction types. Card 16 specifies uranium as the second material to be processed, and line 18 terminates the element loop and the GAMINR run.

Figs. 35 and 36 illustrate plots of the results of this sample run. These graphs were made using the [DTFR](#) and [VIEWR](#) modules.

Starting with ENDF/B-VI, the photon interaction (or photoatomic) files contain detailed photoelectric cross sections, not just the MT=522 total photoelectric cross section. These photoelectric cross sections have MT numbers starting with 534. As an example, Fig. 37 shows the first 9 partial cross sections for uranium — the K, L, and M subshells — taken from ENDF/B-VII. GAMINR input is somewhat more complicated when these reactions are included because they are different for every element.

## 9.6 Error Messages

```

error in genggp***illegal group structure
      Values of IGG must lie between 1 and 10.

```

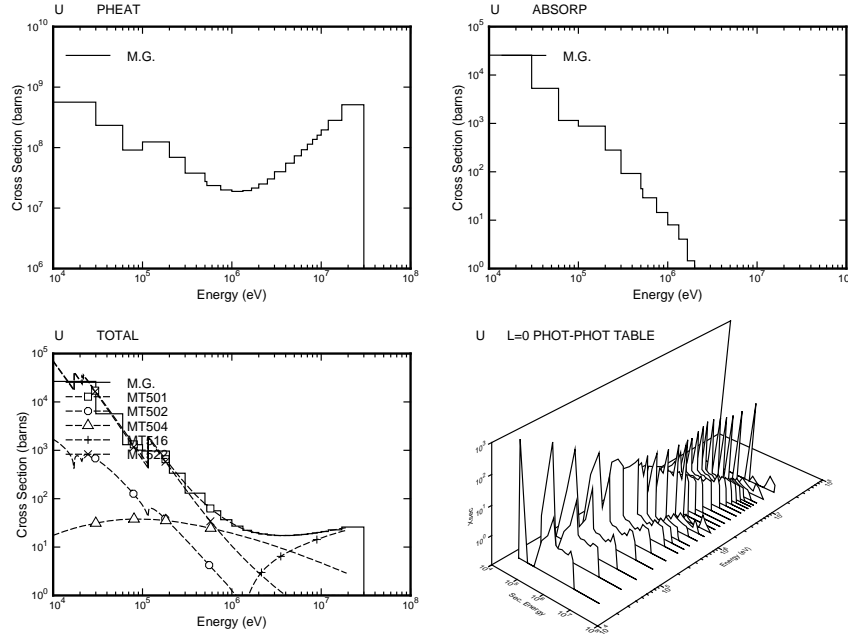


Figure 35: Plots of the photon interaction cross sections and the photon scattering distribution for uranium showing both 24-group and continuous cross sections. Note the prominent photoelectric absorption edge near 100 keV.

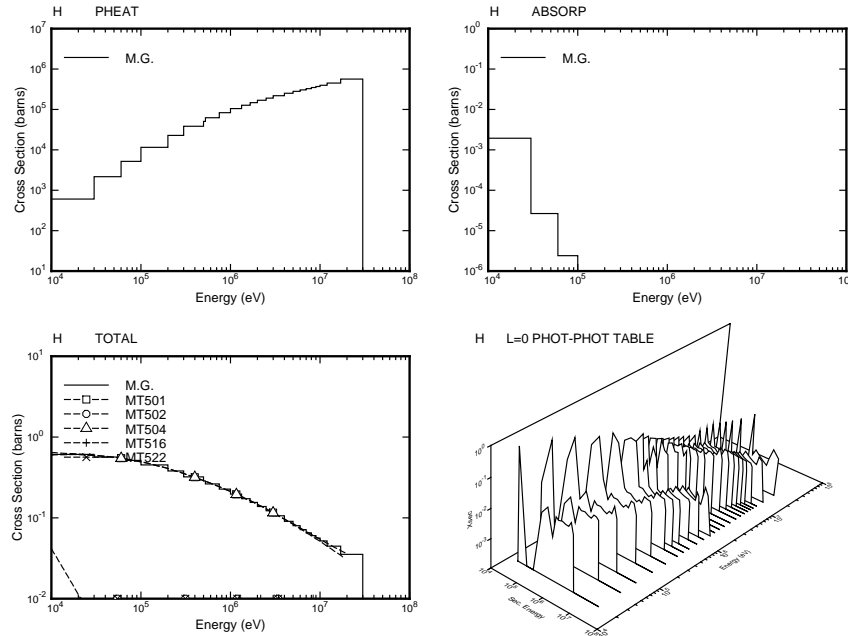


Figure 36: Plots of the photon interaction cross sections and the photon scattering distribution for hydrogen showing both 24-group and continuous cross sections. The cross sections are simpler for this case.

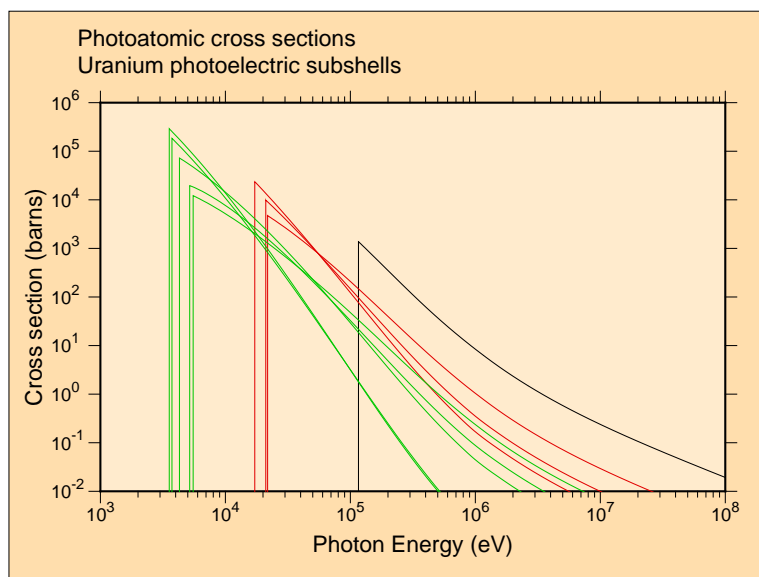


Figure 37: The first nine photoelectric subshell cross sections for uranium from ENDF/B-VII.0. Black is the S subshell ( $1s^{1/2}$ ), red is the L1, L2, and L3 subshells ( $2s^{1/2}$ ,  $2p^{1/2}$ ,  $2p^{3/2}$ ), and green is the M1 through M5 subshells ( $3s^{1/2}$ ,  $3p^{1/2}$ ,  $3p^{3/2}$ ,  $3d^{3/2}$ ,  $3d^{5/2}$ ).

error in genggp\*\*\*too many groups.

Increase the size of the global array `egg` by changing the parameter `ngmax=400` located at the start of the module.

error in gnwtf\*\*\*illegal iwt

Values of `iwt` must lie between 1 and 3.

error in gpanel\*\*\*elo gt ehi.

There is something wrong with the energy grids during integration over incident energy. This usually means there is a problem with the choice of `rndoff` and/or `delta`. Be sure that `rndoff`<1, `delta`>1, and `rndoff*delta`<1 as represented on your machine.

ERROR IN GTFF\*\*\*ILLEGAL FILE TYPE.

Only files 23 and 26 can be requested.

error in gtff\*\*\*illegal reaction for cross section=---

Only reactions 501, 502, 504, 516, 602, and 621 (heat) can be requested for ENDF/B-IV or -V, or only 501, 502, 504, 516, 522, and 525 for ENDF/B-VI or VII.

error in gtff\*\*\*insufficient storage for form factor.

This refers to the allocatable array `pff` with size `nwpff=5000` defined in the main `gaminr` routine.

## 9.7 I/O Units

There are no scratch files used in GAMINR. The only restriction on the files assigned on line 1 of the user input is that `ngam1` and `ngam2` must be in the same mode (that is, both binary or both formatted).

## 10 ERRORR

The ERRORR module is used to produce cross section and distribution covariances from error files in ENDF format. This chapter describes ERRORR in NJOY 2012.0. There are many differences from the version reported previously[3], including those connected with the conversion to Fortran-90 style and storage allocation, advanced methods for handling resonance covariances, covariances for angular distributions, covariances for energy distributions, and covariances for radionuclide production.

### 10.1 Introduction

After evaluators have completed their review of the available measurements of various nuclear data (having true values  $\sigma_1, \sigma_2, \sigma_3, \dots$ ) and the theoretical analysis, they will have formed at least a subjective opinion of the joint probability distribution of the data examined; that is, the probability

$$P(\sigma_1, \sigma_2, \dots) d\sigma_1 d\sigma_2 \dots$$

that the true value of  $\sigma_1$  lies in the range  $(\sigma_1, \sigma_1 + d\sigma_1)$ , and that  $\sigma_2$  lies in the range  $(\sigma_2, \sigma_2 + d\sigma_2)$ , etc. In the early versions of the ENDF format, only the first moments (expectation values) of this probability distribution could be included in the numerical data files. However, beginning with ENDF/B-IV and expanding significantly in ENDF/B-V ENDF/B-VI and ENDF/B-VII, the second moments of the data probability distributions have been included in many of the files. As discussed in Section 10.2, these second moments (or “data covariances”) contain information on the uncertainty of individual data, as well as correlations that may exist. Fig. 38 shows an example of this for  $^{10}\text{B}$  from ENDF/B-VII.0. The top plot shows the first moment (the percent standard deviation) of the uncertainty in the  $(n, \alpha)$  cross section. The right-hand plot shows the cross section. The center plot shows the correlations between the  $(n, \alpha)$  cross section at one energy to itself at other energies.

Data covariances have many applications. For example, they can be combined with sensitivity coefficients to obtain the uncertainty, due to the data, in calculated quantities of applied interest[69]. This information can be used in turn to judge the adequacy of the data for that application.

The availability of data covariances also makes it possible to use the generalized method of least squares to improve the data evaluation after new integral or

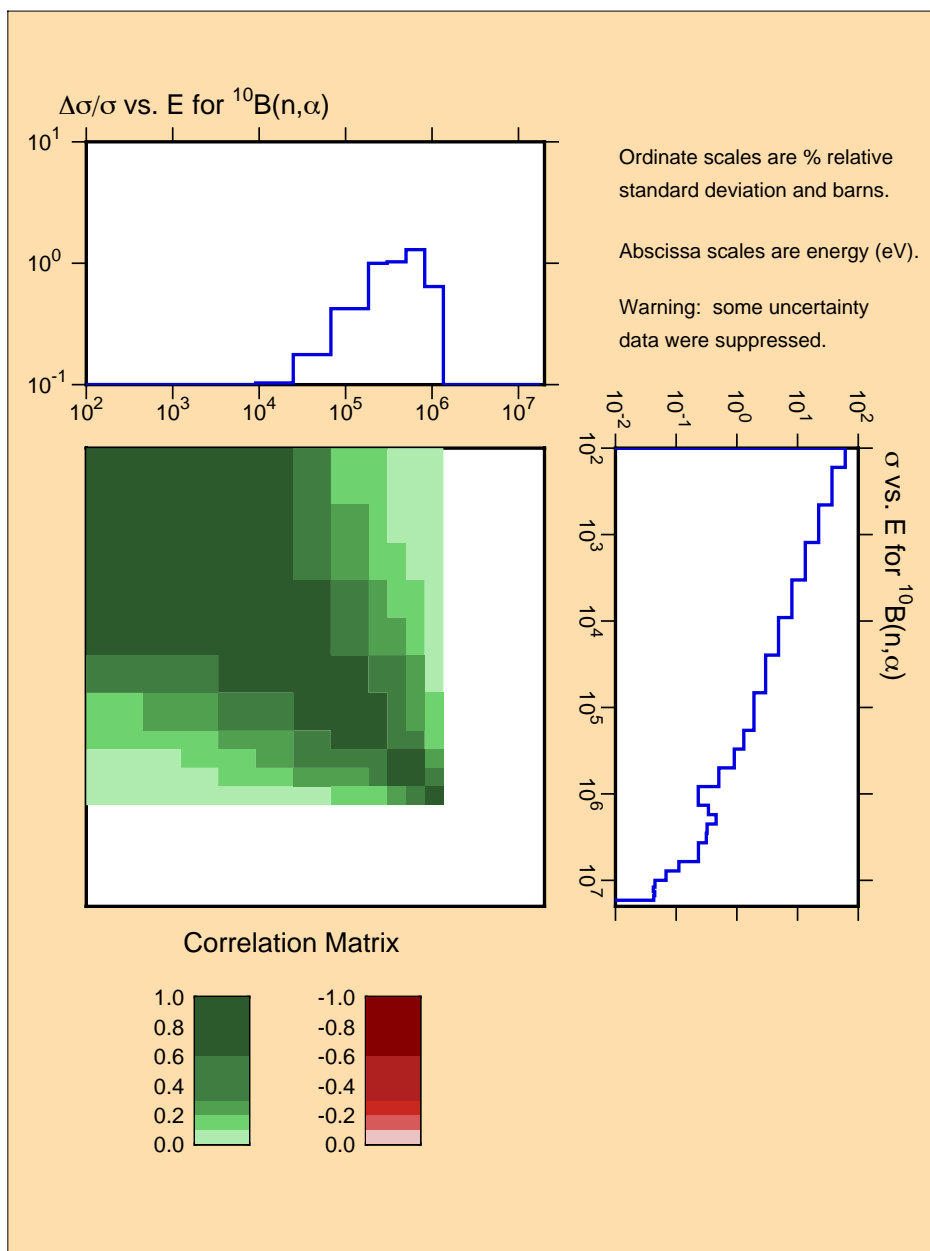


Figure 38: Covariance plot for  $^{10}\text{B}(n,\alpha)$  from ENDF/B-VII.0. This reaction is used as a standard in the ENDF system.

differential measurements have been performed[70]. The least-squares method requires only data covariances (not the full probability distribution), and the improved, or adjusted, data are guaranteed[71] to have the smallest possible uncertainties, regardless of the actual shape of the underlying probability distribution function,  $P(\sigma_1, \sigma_2, \dots)$ . Thus, the ENDF-formatted covariance files



contain, in about as compact a form as possible, a statement about the quality of the data, as well as sufficient information (in principle) to carry out future improvements on an objective basis.

In many of these applications, it is necessary to begin by converting energy-dependent covariance information in ENDF format[8] into multigroup form. This task can be performed conveniently in the NJOY environment, using the ERRORR module. In particular, ERRORR calculates the uncertainty in infinitely dilute multigroup cross sections (or multigroup  $\bar{\nu}$  values), as well as the associated correlation coefficients. These data are obtained by combining absolute or relative covariances from ENDF Files 31, 32, 33, 34, 35 and 40 with multigroup  $\bar{\nu}$  data, cross section data, angular distribution data, fission spectra data or radionuclide production data. These multigroup data are obtained from **GROUPR** processing, or in some instances are calculated within ERRORR. ERRORR is coded to treat all approved ENDF-4, -5, and -6 covariance formats for these files. ERRORR can also treat resolved-resonance covariances given in File 32 using the old Breit-Wigner resolved-resonance parameter uncertainties (LRF=1 and 2) in Version-5 format, the “Version-5 compatible” option of Version 6 (LCOMP=0) using the new formats that include resonance-resonance covariances, and the newest format based on Reich-Moore-Limited parameters that include resonance-resonance correlations between different reactions.

The methodology of ERRORR assumes that the weighting flux used to convert energy-dependent cross sections into multigroup averages is free of uncertainty. In cases in which the cross-section information is obtained from an existing multigroup library, it is usually necessary to make assumptions about the shape of the cross section and the weight function within certain input energy groups.

## 10.2 Definitions of Covariance-Related Quantities

For convenient reference in discussing the methodology and input requirements of the ERRORR module, we next review the basic definitions of covariance-related quantities. Let  $x_0$  and  $y_0$  be the evaluated values of  $x$  and  $y$ , respectively:

$$x_0 \equiv E[x] , \quad (390)$$

and

$$y_0 \equiv E[y] . \quad (391)$$

Here  $E$  is the expectation operator, which performs an average over the joint probability distribution of  $x$  and  $y$ . The second moment of this distribution is called the covariance of  $x$  with  $y$ :

$$\text{cov}(x, y) \equiv E[(x - x_0)(y - y_0)] . \quad (392)$$

Covariance is a measure of the degree to which  $x$  and  $y$  are both affected by the same sources of error. The covariance of  $x$  with itself is called the variance of  $x$ :

$$\text{var}(x) \equiv \text{cov}(x, x) = E[(x - x_0)^2] . \quad (393)$$

The more familiar standard deviation  $\Delta x$  (also called the “uncertainty”) is simply

$$\Delta x \equiv [\text{var}(x)]^{1/2} = [\text{cov}(x, x)]^{1/2} . \quad (394)$$

The correlation between  $x$  and  $y$  (also called the correlation coefficient) is defined as

$$\text{corr}(x, y) \equiv \frac{\text{cov}(x, y)}{\Delta x \Delta y} . \quad (395)$$

The absolute value of a correlation coefficient is guaranteed to be less than or equal to unity. Another useful quantity is the relative covariance of  $x$  with  $y$ ,

$$\text{rcov}(x, y) \equiv \frac{\text{cov}(x, y)}{x_0 y_0} . \quad (396)$$

Unlike  $\text{cov}(x, y)$ , the relative covariance  $\text{rcov}(x, y)$  is a dimensionless quantity. Closely related to the relative covariance is the relative standard deviation,

$$\frac{\Delta x}{x_0} = \frac{[\text{cov}(x, x)]^{1/2}}{x_0} , \quad (397)$$

which, from Eq. 396, can be written as

$$\frac{\Delta x}{x_0} = [\text{rcov}(x, x)]^{1/2} . \quad (398)$$

Combining Eqs. 395 and 396, we have another useful result,

$$\text{corr}(x, y) = \frac{\text{rcov}(x, y)}{(\Delta x/x_0)(\Delta y/y_0)} . \quad (399)$$

While it is customary to speak of uncertainties and correlations as separate entities, these are actually just two different aspects of the covariance. If one has

a set of absolute covariances for various reactions, including the self-covariance, then Eqs. 394 and 395 can be used to calculate  $\Delta x$  and  $\text{corr}(x, y)$ . Similarly, if one has a set of relative covariances, one can use Eqs. 398 and 399 to calculate  $\Delta x/x_0$  and  $\text{corr}(x, y)$ .

Consider now a set of nuclear data  $\sigma_i$  with uncertainties characterized by the covariances  $\text{cov}(\sigma_i, \sigma_j)$ . Let  $A$  and  $B$  be two linear functions of the  $\sigma_i$ ,

$$A = \sum_i a_i \sigma_i \quad (400)$$

and

$$B = \sum_j b_j \sigma_j, \quad (401)$$

where the  $a_i$  and  $b_j$  are sets of known constants. The above definitions can be used to calculate the covariances of the functions  $A$  and  $B$  induced by the covariances of the data. From Eq. 392,

$$\begin{aligned} \text{cov}(A, B) &= \text{E} \left\{ \left( \sum_i a_i \sigma_i - \sum_i a_i \text{E}(\sigma_i) \right) \left( \sum_j b_j \sigma_j - \sum_j b_j \text{E}(\sigma_j) \right) \right\} \\ &= \sum_{i,j} a_i b_j \text{E} \left\{ \left( \sigma_i - \text{E}(\sigma_i) \right) \left( \sigma_j - \text{E}(\sigma_j) \right) \right\}, \end{aligned} \quad (402)$$

so that

$$\text{cov}(A, B) = \sum_{i,j} a_i b_j \text{cov}(\sigma_i, \sigma_j) \quad (403)$$

This result, called the “propagation of errors” formula, is fundamental to the subject of multigroup processing of ENDF covariance data and will be referenced frequently in later sections of this chapter.

### 10.3 Structure of ENDF Files 31, 33, and 40: Energy-Dependent Data

Data in ENDF format are stored in various numbered “files,” where the file number depends on the type of information contained. For example, the covariances of  $\bar{\nu}(E)$  (the average number of neutrons per fission, which is a function of the incident neutron energy) are stored in File 31, where the possible “reaction”

types are prompt  $\bar{\nu}$ , delayed  $\bar{\nu}$ , and total  $\bar{\nu}$ . File 33 contains the covariances of energy-dependent cross sections. In general, for data given in File N, covariance data are given in File (N+30). The structures of Files 31, 33, and 40 are identical and will be described first.

Files 31, 33, and 40 describe the covariances of energy-dependent data. To expand on this point, we recall that the full energy dependence of a cross section  $\sigma(E)$ , for example, is described in the ENDF File 3 by specifying the cross-section values at a relatively small number of energy points and then providing a set of interpolation laws to be used in reconstructing the actual cross section at any intermediate energy. Somewhat the same philosophy is used to describe the two-dimensional energy dependence of data covariances in Files 31, 33, and 40. That is, one specifies a set of numerical data and a set of formulae, which together can be used to compute  $\text{cov}(x, y)$  for any desired pair of energies,  $E_x$  and  $E_y$ . Although the interpolation laws are presently restricted to the simple forms described below, it is not true (as sometimes stated) that ENDF contains multigroup covariances. The expression “multigroup covariance” refers to the covariance of one multigroup-averaged quantity with another averaged quantity, whereas ENDF contains the covariances between point-energy data. It is precisely the task of *ERRORR* to compute multigroup covariances, starting from point covariances.

Files 31, 33, and 40 of an evaluation for material **MAT** are divided into “sections,” indexed by the reaction type **MT**. A section (**MAT**,**MT**) is further subdivided into “subsections.” As described in the ENDF formats manual, a subsection is the repository for all explicit statements of the two-dimensional energy dependence of the covariances of reaction (**MAT**,**MT**) with another reaction (**MAT1**,**MT1**). Because covariances are symmetric, a subsection with **MAT1**=**MAT** and **MT1**<**MT** would be redundant with a subsection in an earlier section, and such data are, by convention, omitted from the ENDF files.

Subsections are further divided into “sub-subsections.” Two different types of sub-subsections are used in the ENDF-5 and ENDF-6 formats. *ERRORR* also treats data covariances in the earlier ENDF-4 format, but this is of little practical interest since only three covariance evaluations were released in the Version-4 format. “NI-type” sub-subsections are used to express covariances explicitly, while “NC-type” sub-subsections are used to indicate the existence of connections between various data that result in “implicit” covariance contributions for various reaction pairs. We shall return to this point when discussing NC-Type Sub-Subsections.

**NI-Type Sub-Subsections.** Multiple NI-type sub-subsections are used to describe multiple, statistically independent sources of uncertainty for a given reaction pair. If  $\text{cov}(x, y)_n$  is the covariance computed from the data in one sub-subsection, then, because the uncertainties in different sub-subsections are uncorrelated,

$$\text{cov}(x, y) = \sum_{n=1}^{\text{NI}} \text{cov}(x, y)_n ,$$

where NI is the number of NI-type sub-subsections in the current subsection. The numerical content of one NI-type sub-subsection consists of either one or two energy grids, a collection of constants, and a parameter LB. The parameter LB governs how the energies and constants are to be used in constructing the covariance in various rectangular regions of  $E_x - E_y$  space. For LB=0, 1, 2 and 8, a single table containing pairs  $(E_i, F_i)$  is given. For LB=3 and LB=4, two such tables are given. For LB=5, a single set of energies  $E_i$  is given, along with an associated square matrix of constants  $G_{ij}$ . Finally, for LB=6, two energy grids are given, along with an associated rectangular matrix of constants  $G'_{ij}$ .

The first of these tables  $(E_i, F_i)$  defines a function  $f(E)$  that is constant except for discrete steps at energies  $E_i$ ,

$$f(E) = F_i, \text{ if } E_i \leq E < E_{i+1} . \quad (404)$$

Similarly, if there is a second table,

$$f'(E) = F'_j, \text{ if } E'_j \leq E < E'_{j+1} . \quad (405)$$

The LB=5 matrix data  $G_{ij}$  also define a function,

$$g(E_x, E_y) = G_{ij}, \text{ if } E_i \leq E_x < E_{i+1} \text{ and } E_j , \quad (406)$$

and similarly for LB=6

$$g'(E_x, E_y) = G'_{ij}, \text{ if } E_i \leq E_x < E_{i+1} \text{ and } E_j \leq E_y < E'_{j+1} . \quad (407)$$

These functions are simply histograms in either one or two dimensions. Using the functions  $f$ ,  $f'$ ,  $g$ , and  $g'$  thus defined, we can list the formulae in Eq. 408, which are used to specify energy-dependent covariances for the different allowed

values of LB. Thus, if  $x$  is the value of the cross section or of the  $\bar{\nu}$  value for the reaction (MAT,MT) that determines the ENDF/B section, and if  $y$  is the value for the reaction (MAT1,MT1) that determines the subsection, then for

$$\begin{aligned}
 \text{LB} &= 0, & \text{cov}(x, y)_n &= f(E_x) \delta(E_x, E_y) \\
 \text{LB} &= 1, & \text{rcov}(x, y)_n &= f(E_x) \delta(E_x, E_y) \\
 \text{LB} &= 2, & \text{rcov}(x, y)_n &= f(E_x) f(E_y) \\
 \text{LB} &= 3, & \text{rcov}(x, y)_n &= f(E_x) f'(E_y) \\
 \text{LB} &= 4, & \text{rcov}(x, y)_n &= f(E_x) \delta(E_x, E_y) f'(E_x) f'(E_y) \\
 \text{LB} &= 5, & \text{rcov}(x, y)_n &= g(E_x, E_y) \\
 \text{LB} &= 6, & \text{rcov}(x, y)_n &= g'(E_x, E_y) .
 \end{aligned} \tag{408}$$

The symbol  $\delta(E_x, E_y)$  has the following meaning:  $\delta(E_x, E_y)=1$  if  $E_x$  and  $E_y$  fall in the same energy interval of the first table ( $E_i, F_i$ ), and  $\delta(E_x, E_y)=0$  otherwise.

The final covariance law, LB=8, is an exceptional case that cannot be expressed in terms of point covariances. LB=8 is used primarily to represent uncertainty effects due to suspected, but unresolved, energy-dependent structure in a given cross section. If  $\Delta E_j$  is the energy width of the  $j$ -th “union” energy group (see the discussion of union groups in Section 10.8), and if this group lies within the  $k$ -th range ( $E_k, E_{k+1}$ ) of an ENDF LB=8 energy grid, then the effect of the LB=8 subsection is to trigger the addition of an uncorrelated contribution of  $F_k (E_{k+1} - E_k) / \Delta E_j$  to the (absolute) variance of the  $j$ -th union-group cross section. No contributions to off-diagonal elements of the multigroup covariance matrix are generated by an LB=8 sub-subsection.

**NC-Type Sub-Subsections.** NC-type sub-subsections, which describe covariances indirectly, are used in several evaluation situations, which are flagged by different values of the parameter LTY. The first situation, LTY=0, occurs when the following two conditions are met: (a) the covariances of a given reaction MT, both with itself and with other reactions, can be deduced in an energy range (E1, E2) solely from the application of a cross-section “derivation relation,”

$$x(\text{MAT}, \text{MT}; E) = \sum_i C_i x(\text{MAT}, \text{MT}_i; E), \tag{409}$$

and (b) the covariances of all of the reaction cross sections on the right-hand side of Eq. 409 have been given directly (that is, using only NI-type sub-subsections) throughout the range (E1, E2). The energy boundaries E1 and E2, the constants

$C_i$ , and the reaction identifiers  $MT_i$  are specified in an NC-type sub-subsection with  $LTY=0$ . This format is widely used in the ENDF/B library, and it makes possible the elimination of large volumes of otherwise redundant data. It also introduces considerable complexity in the multigroup processing, as discussed in Section 10.8, and adds to the computer running times. The presence of this one short sub-subsection affects the calculation of the covariances for many different reaction pairs, such as  $x(MAT, MT)$  with  $x(MAT, MT_i)$ . Less widely used are NC-type sub-subsections with  $LTY=1$ . These are employed when a reaction  $MT$  in material  $MAT$  is evaluated in some energy range ( $E1$ ,  $E2$ ) as a ratio to a standard reaction  $MTS$  in some other material  $MATS$ . That is,

$$x(MAT, MT; E) = R(E) x(MATS, MTS; E). \quad (410)$$

In practical evaluation situations, the uncertainty of  $R$  is almost never correlated with that of  $x(MATS, MTS)$ . Because of this, the relative uncertainty in  $R$  is treated simply as one independent component of the relative uncertainty in  $x(MAT, MT)$ , and it is described using normal NI-type sub-subsections. On the other hand, the contribution from uncertainty in  $x(MATS, MTS)$  is represented with an NC-type sub-subsection with  $LTY=1$ , which contains, in ENDF/B-V, only  $E1$ ,  $E2$ ,  $MATS$ , and  $MTS$ . The actual numerical covariance information must be read from the evaluation for the standard material  $MATS$ , which usually resides on an entirely different ENDF tape. An NC-type sub-subsection with  $LTY=1$ , which occurs in a given subsection ( $MAT, MT$ ;  $MAT, MT$ ), affects the calculation of the covariances only for the current reaction pair (reaction  $MT$  with itself) and, in this respect, is more like an NI-type sub-subsection than, for example, an NC-type sub-subsection with  $LTY=0$ . This similarity is exploited in the processing of ratio covariances, as discussed in Section 10.11.

An NC-type sub-subsection with  $LTY=2$  is used, in a similar way, to describe the covariances of  $x(MAT, MT)$  with  $x(MATS, MTS)$ . As in the  $LTY=1$  case, an  $LTY=2$  sub-subsection contains only  $E1$ ,  $E2$ ,  $MATS$ , and  $MTS$ .

An NC-type sub-subsection with  $LTY=3$  is included in material  $MATS$  to describe the (redundant) covariances of  $x(MATS, MTS)$  with  $x(MAT, MT)$ . The numerical information contained here is the same as for  $LTY=1$  and  $LTY=2$ . As discussed in Section 10.11, an important function of  $LTY=3$  data is to help locate reactions other than ( $MAT, MT$ ) that have been measured relative to the same standard ( $MATS, MTS$ ).

#### 10.4 Resonance-Parameter Formats—File 32

File 32 contains covariances of resonance parameters from File 2. Older versions of ERRORR could only handle the ENDF-5 format (now called the “Version-5 compatible” format). Current versions can handle the newer ENDF-6 formats that include resonance-resonance correlations.

**ENDF-5 Type Resonance Formats.** With these formats (LCOMP=0), ERRORR processes File 32 in the following limited sense: when infinite-dilution cross-section covariances are processed (see previous section) from File 33, the diagonal elements of the resulting (self-reaction) multigroup covariance matrices are augmented by contributions based on the parameter covariances in File 32. These methods were sufficient for processing the covariance files in ENDF/B-VI.

For either of the permitted resolved resonance formalisms (LRF=1 or LRF=2), the parameters considered in File 32 are the resonance energy  $E_r$ , the neutron width  $\Gamma_n$ , the radiative capture width  $\Gamma_\gamma$ , the fission width  $\Gamma_f$ , and (in Version 5 only) the total angular momentum  $J$ . All cross-parameter relative covariances, such as  $\text{rcov}(\Gamma_n, \Gamma_\gamma)$ , are included, with the exception of the covariances of  $E_r$  with the remaining parameters, which are assumed to be negligible. Cross-resonance covariances, such as  $\text{cov}(E_r^i, E_r^j)$ , where  $i$  and  $j$  refer to different resonances, are omitted in the LCOMP=0 option.

**ENDF/B-VII Resonance Covariances.** For ENDF/B-VII, a number of evaluations include covariance formats that represent the correlations between resonance parameters for a given resonance and between different resonances. In later versions of NJOY99, these cases are handled by the ERRORJ[34] module, which was developed in Japan and contributed to the NJOY project. For NJOY2012, the ERRORJ coding was integrated into the ERRORR module. The ERRORJ approach is based on computing the sensitivity of a cross section to a give resonance by numerical differencing and then combining these sensitivities with parameter covariances from the evaluation.

There are three basic covariance format options, governed by the LCOMP and/or LRU flags. The LRU flag distinguishes between resolved resonance (LRU=1) and unresolved resonance (LRU=2) data. For LCOMP=1/LRU=1, there may be two classes of data, designated as NSRS or NLRS sub-subsections. NSRS sub-subsections provide covariance data among parameters of specified resolved resonances. Covariances may be given for all ENDF recognized resolved resonance formats (as specified via the LRF flag). NLRS sub-subsections provide long-range



parameter covariances. These data are allowed for all resolved resonance formats. At present there are no NLRS sub-subsection data in ENDF/B-VII, and NJOY does not process these data.

The LCOMP=2/LRU=1 format provides a combination of resolved resonance parameters and their uncertainties plus a correlation matrix. The correlation matrix is given in a special packed form using the ENDF INTG record format with matrix elements consisting of as few as 2 to as many as 6 digits. Covariance matrix elements,  $V_{ij}$  can be reconstructed as

$$V_{ij} = D_i C_{ij} D_j \quad (411)$$

where  $D_i$  is the uncertainty on parameter  $i$  and  $C_{ij}$  is the correlation matrix element relating parameters  $i$  and  $j$ . Since the correlation matrix is symmetric, and its diagonal terms are unity, only the upper triangle of matrix elements is given in the ENDF file. This more compact representation of the covariances helps for materials with large numbers of resonances.

Finally, the LRU=2 (LCOMP is not defined and its location in the ENDF file is typically set to zero) format is used to define covariances for unresolved resonance parameters. The data represent an energy independent relative covariance matrix even if the underlying unresolved resonance parameters are energy dependent. This is a symmetric matrix and so only the upper triangular portion of the matrix is provided in the ENDF file.

The original covariance data formats did not allow the evaluator to define an uncertainty in the scattering radius (only for resonance energy and the total or partial resonance widths). This deficiency was eliminated in 2009, but until new evaluations are released there are no scattering radius uncertainty data in current evaluated library files. NJOY can include scattering radius uncertainty effects if such data are given in the evaluated file. In addition, users can specify an uncertainty in the ERRORR input so that this important component to the cross section uncertainty is considered when processing existing files that lack these data (see the description for `dap` on Card 7 in Section 10.14 below).

**Reich-Moore-Limited Covariance Representations.** The current ENDF-6 format also allows resonances using the LRF=7 Reich-Moore-Limited (RML) representation. In addition to the covariances described above, the RML approach can define channel-channel covariances properly. There are two experimental evaluations currently available that use this approach. The  $^{19}\text{F}$  evaluation from the ORNL represents the four reactions elastic, capture, (n,n<sub>1</sub>), and

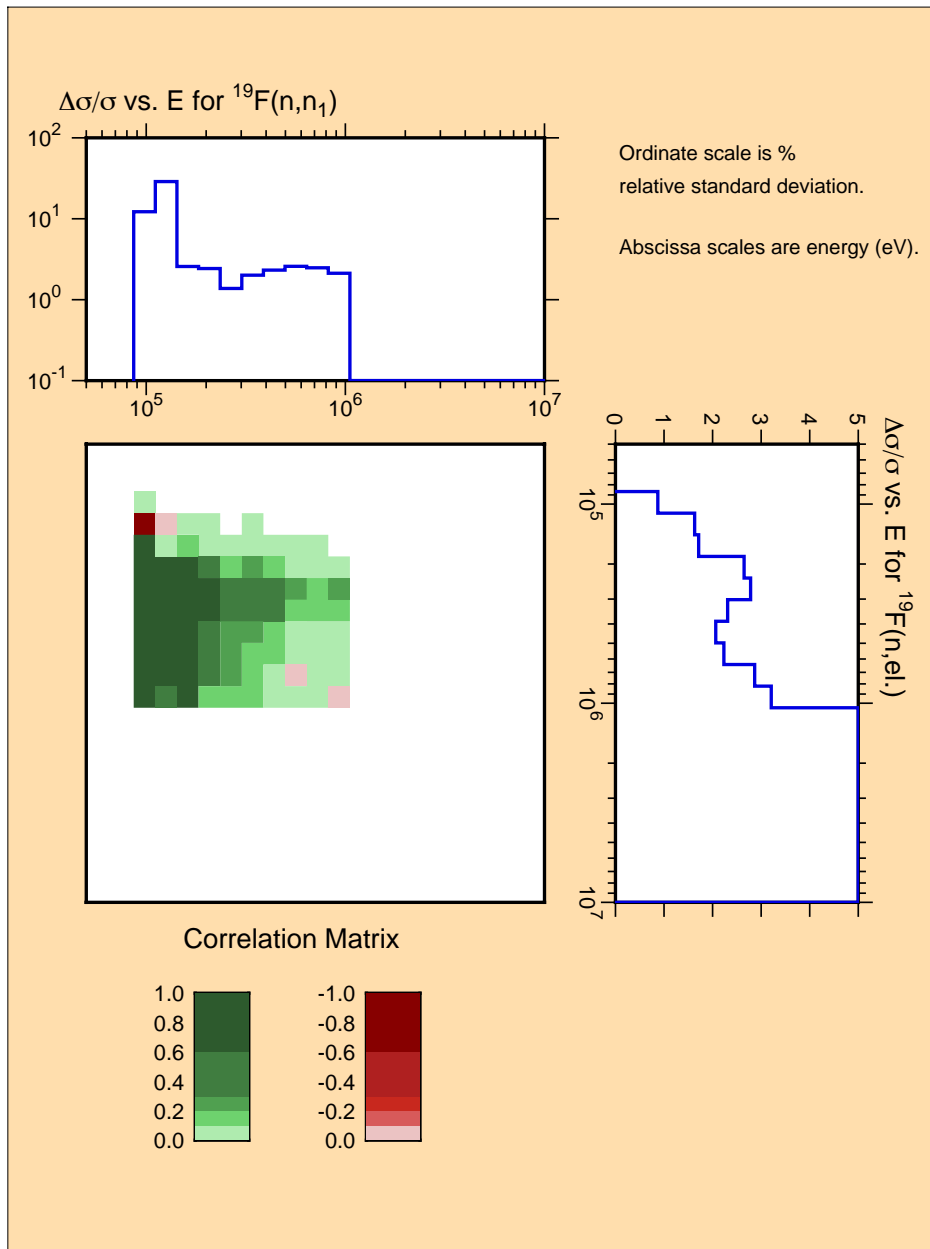


Figure 39: Covariance plot for the elastic and  $(n,n_1)$  reactions in the experimental evaluation for  $^{19}\text{F}$ , demonstrating the channel-channel covariances possible when using the Reich-Moore-Limited resonance representation.

$(n,n_2)$ . Fig. 39 shows that ERRORR can generate the covariances between elastic and  $(n,n_1)$ . The  $^{35}\text{Cl}$  evaluation from ORNL represents the reactions elastic, capture, and  $(n,\alpha)$ . The coding in NJOY2012 to handle these cases uses analytic calculations for the parameter sensitivities borrowed from SAMMY[35].

### 10.5 Secondary Particle Angular Distribution Covariances—File 34

File 34 contains covariances for angular distributions of secondary particles. While the underlying angular distribution data in File 4 may be given as tabulated distributions or as Legendre polynomial coefficients, File 34's covariance data are only given for Legendre coefficients. At present there is no provision to specify covariances between cross sections from File 3 and angular distributions from File 4, nor to specify angular distribution covariances between different materials. The data format is governed by the LB flag discussed above in Section 10.3 with LB values of 0, 1, 2, 5 and 6 allowed.

File 34 in the ENDF file may include covariance data for any MT reaction defined in File 4, but currently NJOY only processes the  $P_1$  component of MT=2 (elastic scattering).

Fig. 40 shows an example of the covariances computed from File 34 for  $^{238}\text{U}$  from JENDL-3.3. As usual, there are three components to this plot. On the right side, we illustrate  $\bar{\mu}$  vs energy, which displays the expected forward-peaked characteristic with increasing energy; on the top is the uncertainty in  $\bar{\mu}$  vs energy; and in the center is the correlation matrix. The ERRORR input for this case will be presented below.

### 10.6 Secondary Particle Energy Distribution Covariances—File 35

File 35 contains covariance matrices for the energy distributions of secondary particles given in File 5. If the spectral distributions are correlated with angular distributions and given in File 6, the covariance information still appears in File 35 (the MT section identifier is the common datum relating these data) and refers to the angle-integrated distributions only. The secondary energy distribution is usually defined on a relatively fine energy grid, and multiple distributions are given as a function of increasing incident particle energy. Since the uncertainties in secondary distributions are usually highly correlated as a function of incident particle energy, it is generally sufficient to only define a few covariance matrices over relatively broad incident energy groups. There is no provision to specify covariances between these groups nor with data from other files such as File 3 cross sections or File 1 prompt, delayed or total  $\bar{\nu}$ .

File 35 covariance data are given in a series of NK subsections, with each subsection covering a unique incident particle energy range. The lowest energy

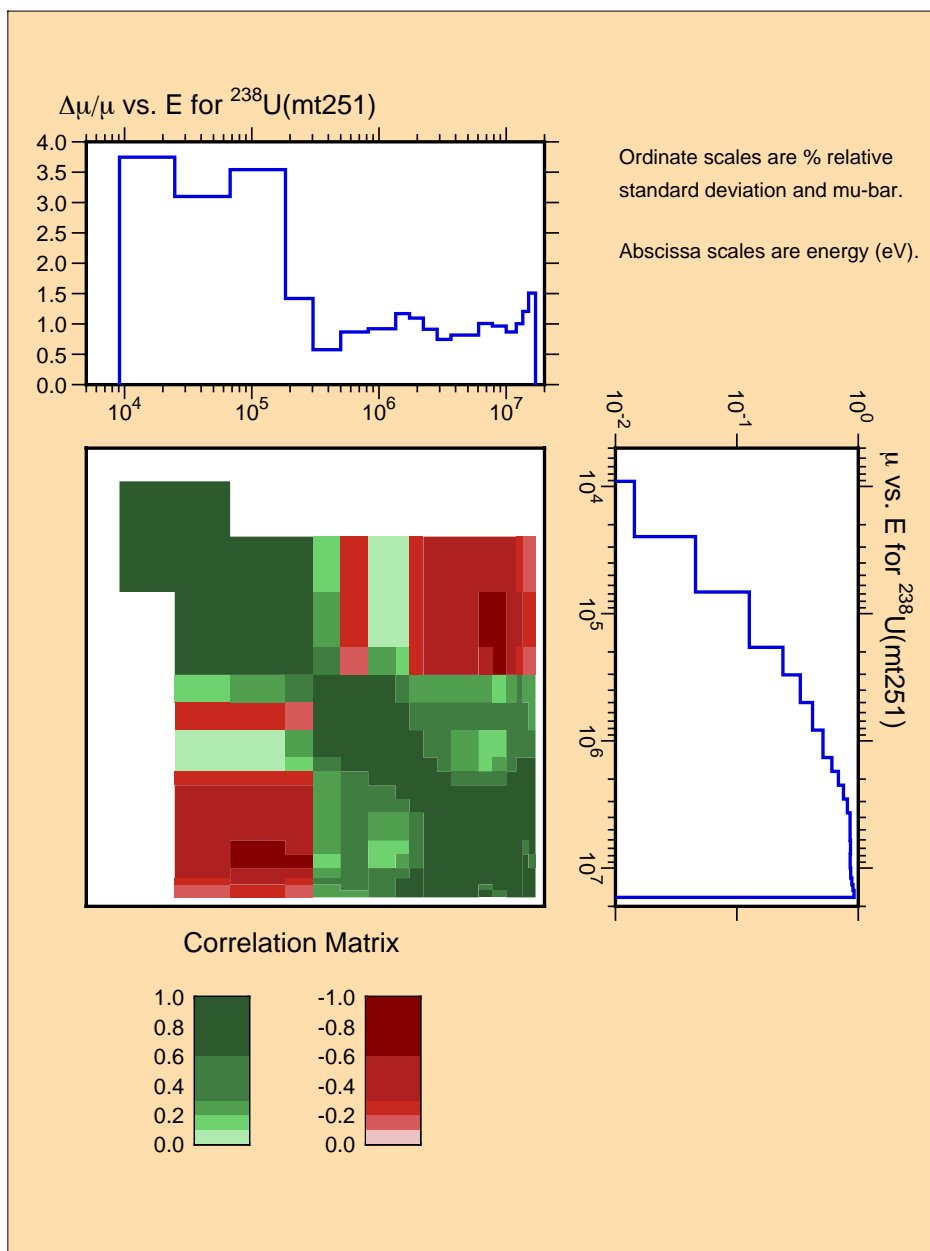


Figure 40: Example of angular distribution covariance data.

of the first subsection and the highest energy of the last subsection must cover the entire incident particle energy range from File 5 (or File 6). When processing MF35 data, the user can specify the incident particle energy of interest (**efmean** on Card 7). NJOY will process the  $NK^{\text{th}}$  subsection whose energy is closest to, but less than, **efmean**. The data tabulated in the ENDF file are normalized probabilities of absolute covariances identified as an LB=7 subsection. LB=7 is

identical to LB=5 defined in Section 10.3 except that these data are now absolute rather than relative covariances.

The ENDF format manual notes these matrices are probability distributions that must remain normalized to unity and therefore the elements in these symmetric matrices are constrained such that the sum of the elements in any row (or column) must be zero. This is sometimes referred to as the “zero sum” rule. Of course, when dealing with real numbers of finite precision whose values can vary by orders of magnitude it is virtually impossible to rigorously conform to this rule. Therefore, if the sum is sufficiently small, the rule is judged to be satisfied. If not, the ENDF manual provides a correction formula to apply to all matrix elements. When processing File 35 data NJOY, checks this summation requirement and, if necessary, applies the required correction. NJOY uses the “sufficiently small” criteria specified in the Format manual for this check.

At present there are no File 35 data in ENDF/B-VII.0 neutron files, but the  $^{252}\text{Cf}$  decay file does contain such data. Also, these data are becoming available in preliminary ENDF/B-VII.1 files available from the National Nuclear Data Center (NNDC) at Brookhaven National Laboratory (BNL). These files follow the “zero sum” rule discussed above, but users are cautioned that other internationally distributed files, particularly those from JENDL-3.3, may provide File 35 data in an alternate format. The matrix elements in the JENDL-3.3 files have been divided by the group energy width to yield energy-group averaged probability distributions, as this is the data representation expected by the Japanese ERRORJ code[34]. A conversion code, chmf35, has been developed and is available from the Nuclear Energy Agency <sup>9</sup> to reformat these files so that they are suitable for processing by NJOY.

Fig. 41 shows the results of processing the fictitious  $^{252}\text{Cf}$  evaluation. The ERRORR input for this job will be presented below.

## 10.7 Radioactive Nuclide Production Covariances–File 40

There is only one file in ENDF/B-VII.0 that includes File 40 covariance data –  $^{93}\text{Nb}$ . The input for calculating the  $^{93m}\text{Nb}$  production uncertainty will be shown below, but the resulting covariances are shown here in Fig. 42. The form of the graphical output obtained when processing File 40 is identical to that produced when processing File 33; with the cross section shown to the right, the uncertainty shown to the top and the correlation matrix shown in the center.

That these are File 40 data can be determined from the label on the uncertainty

<sup>9</sup>chmf35 may be downloaded from <http://www.nea.fr/dbprog/Njoy/chmf35.for>

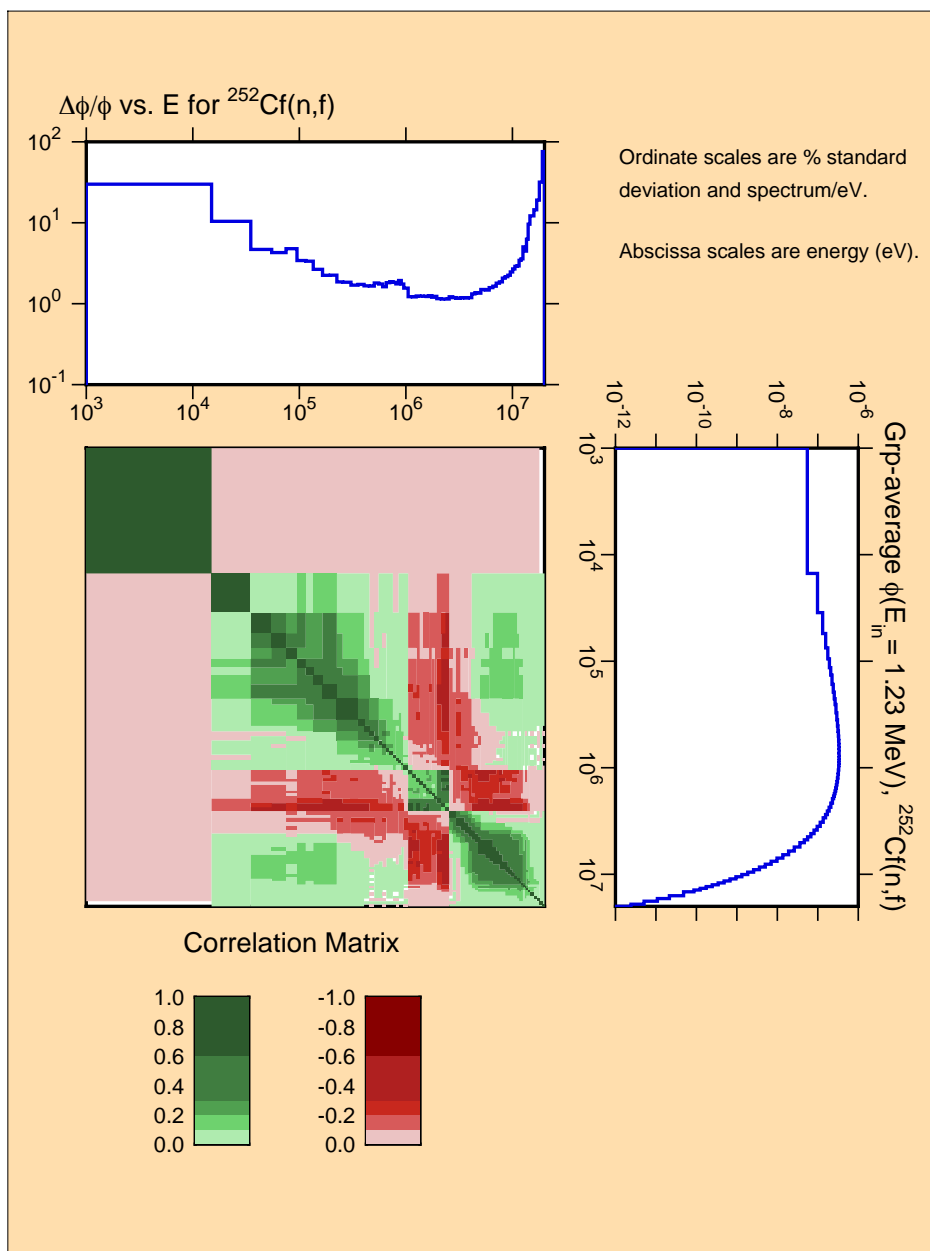


Figure 41: Example of energy distribution covariances. The appearance of negative correlations results from the requirement for preserving normalization.

portion of the plot. In 2009, the File 40 format was modified to include the **IZAP** parameter that identifies the daughter product. We include this **IZAP** value in the plot label so that the user can more fully identify these data. If an older File 40 file is processed that does not define **IZAP**, then the text string “MF40” will appear in the title. In the example shown here we have modified the original

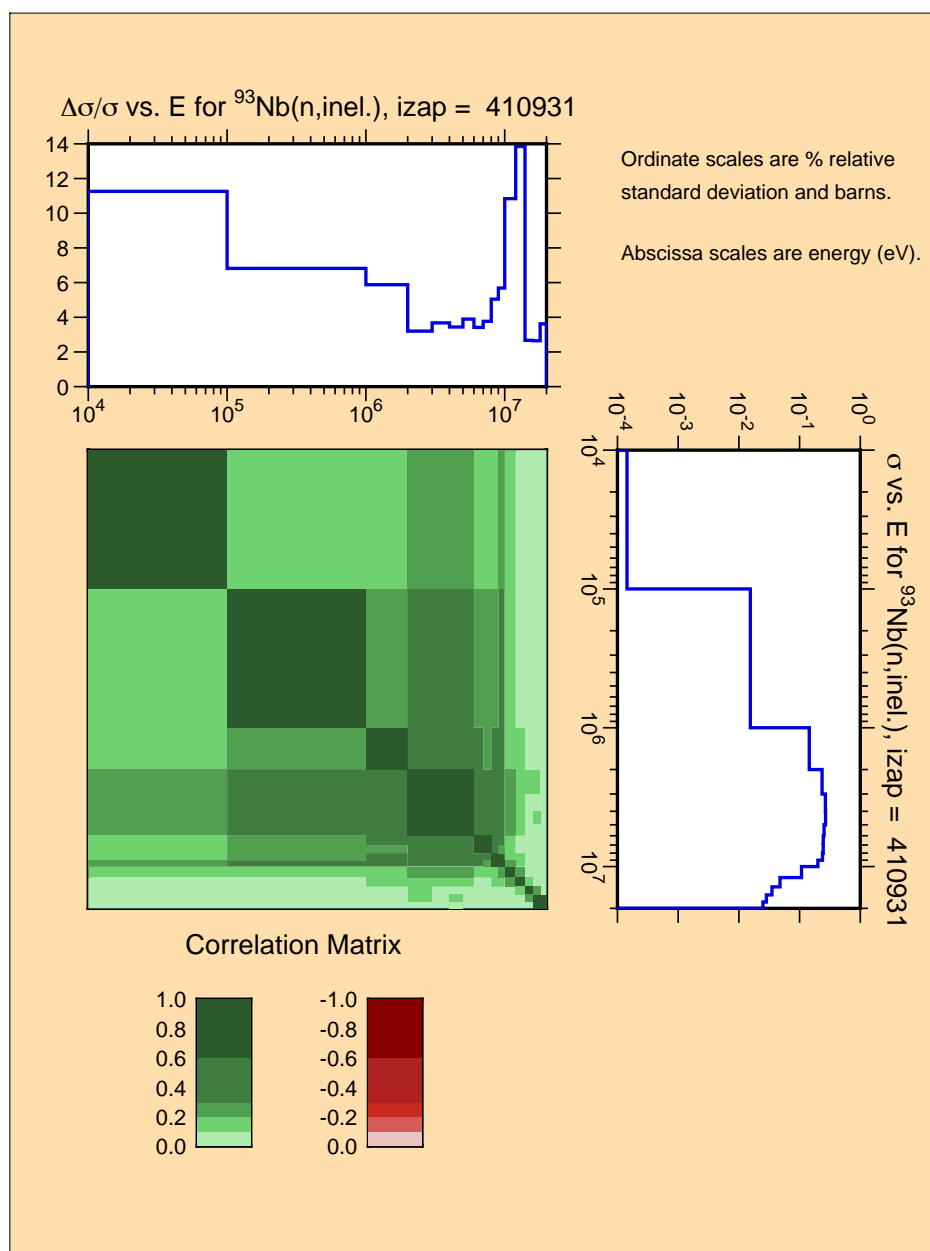


Figure 42: Example of radioactive nuclide production covariances.

ENDF/B-VII.0  $^{93}\text{Nb}$  file to include the proper IZAP value in File 40, which then appears in the plot title.

## 10.8 Calculation of Multigroup Fluxes, Cross Sections, and Covariances on the Union Grid

As mentioned before, the main function of the ERRORR module is to calculate the uncertainty in group-averaged cross sections at infinite dilution due to uncertainty in the ENDF point data. In this and the following sections, we describe the procedures used in performing this task.

In order to proceed, it is necessary to introduce into the discussion three different energy grids, namely, the user grid, the ENDF grid, and the union grid. The relationship of these three grids is shown in Fig. 43. The user grid is the multigroup structure in which the output multigroup covariances are to be produced. The ENDF grid is the collection of energies obtained (in subroutines `gridd` and `grist`) by forming the union of (a) all energy “lists” appearing in any NI-type sub-subsection of any subsection to be processed in the current ENDF material, and (b) all energy pairs used to define the range of effectiveness of any NC-type sub-subsection of any subsection to be processed. The union grid, on the other hand, is simply the union of the user grid and ENDF grid. The utility of the union grid is that (a) the covariances are particularly simple to calculate in this grid, as discussed below, and (b) the multigroup covariances needed by the user are then easily obtained by a straightforward collapse from this to the user grid. In fact, the design of the current ENDF covariance format was strongly influenced by the desire to employ this particular procedure for multigroup processing[72, 73].

After the union grid is formed in subroutine `uniong`, the cross sections  $x(E)$  and weighting flux  $\phi(E)$  are integrated to produce  $x_I$  and  $\phi_I$ , multigrouped on this grid. If point cross sections are supplied, an exact integration is done in subroutine `grpav`. If, on the other hand, a multigroup cross-section library is supplied, then subroutine `colaps` is used. If a library group is subdivided by a union-group boundary, then over the span of that library group, the unknown energy dependencies of  $x(E)$  and  $\phi(E)$ , which are needed to calculate  $x_I$  and  $\phi_I$ , are approximated in subroutine `colaps` by constants. Normally, the effect

|            |  |               |  |               |  |
|------------|--|---------------|--|---------------|--|
| User Grid  |  | $\phi_1, X_1$ |  | $\phi_2, X_2$ |  |
| ENDF Grid  |  | $F_1$         |  | $F_2$         |  |
| Union Grid |  | $\phi_1, x_1$ |  | $\phi_2, x_1$ |  |
|            |  |               |  | $\phi_3, x_3$ |  |
|            |  |               |  |               |  |
|            |  |               |  | $\phi_4, x_4$ |  |

Figure 43: Illustration of energy grid relations.



of this approximation is not large and, in any case, can be reduced or eliminated by increasing the number of groups in the input library.

We next consider the theoretical basis for the calculation of union-grid multi-group covariances, as performed in subroutine `covcal`. By definition,  $x_I$  is just the average of  $x(E)$  over union group I,

$$x_I \equiv \frac{\int_I \phi(E) x(E) dE}{\int_I \phi(E) dE} , \quad (412)$$

where  $\phi(E)$  is the flux “model” assumed for the multigroup calculations. Let  $y_J$  denote similarly the average of  $y(E)$  over union group  $J$ .

Let us imagine that these groups are subdivided into many subintervals of infinitesimal width, so that in the  $i^{\text{th}}$  subinterval of group I, for example,  $x(E)$  can be well approximated by the constant  $x_i$ . By this device, the integrals that define  $x_I$  and  $y_J$  can be converted to discrete sums:

$$x_I = \frac{\sum_{i \in I} \phi_i x_i}{\phi_I} = \sum_{i \in I} \alpha_{Ii} x_i , \quad (413)$$

where

$$\phi_i = \int_i \phi(E) dE , \quad (414)$$

$$\phi_I = \sum_{i \in I} \phi_i = \int_I \phi(E) dE , \quad (415)$$

and

$$\alpha_{Ii} \equiv \frac{\phi_i}{\phi_I} . \quad (416)$$

From these definitions, clearly

$$\sum_{i \in I} \alpha_{Ii} = 1 . \quad (417)$$

Similarly for  $y$ ,

$$y_J = \sum_{j \in J} \alpha_{Jj} y_j , \quad (418)$$

and

$$\sum_{j \in J} \alpha_{Jj} = 1 . \quad (419)$$

The methodology of *ERRORR* assumes that  $\phi(E)$  in Eq. 412 is free of uncertainty. Under this assumption, the terms  $\alpha_{Ii}$  and  $\alpha_{Jj}$  are simply known constants. The covariance of  $x_I$  with  $y_J$  can then be calculated using the propagation-of-errors formula, Eq. 403, together with Eqs. 413 and 418.

$$\begin{aligned} \text{cov}(x_I, y_J) &= \sum_{\substack{i \in I \\ j \in J}} \alpha_{Ii} \alpha_{Jj} \text{cov}(x_i, y_j) \\ &= \sum_{\substack{i \in I \\ j \in J}} \alpha_{Ii} \alpha_{Jj} \sum_n \text{cov}(x_i, y_j)_n , \end{aligned} \quad (420)$$

where the summation over  $n$  results from the different independent contributions to the ENDF point covariances coming from the different NI-type sub-subsections. Changing the order of summation, we obtain

$$\text{cov}(x_I, y_J) = \sum_n \text{cov}(x_I, y_J)_n , \quad (421)$$

where

$$\text{cov}(x_I, y_J)_n = \sum_{\substack{i \in I \\ j \in J}} \alpha_{Ii} \alpha_{Jj} \text{cov}(x_i, y_j)_n . \quad (422)$$

To evaluate the sum in Eq. 422, we make use of the fact that union groups  $I$  and  $J$  do not cross any ENDF grid boundaries. Recalling the discussion of NI-type sub-subsections (and excluding for the moment the case where sub-subsections with  $\text{LB}=8$  are present), there are only two possibilities for the energy dependence of the covariance between ENDF grid points; thus, over the limits of the sum, either  $\text{cov}(x_i, y_j)_n$  is independent of  $i$  and  $j$  (if  $\text{LB}=0$ ) or  $\text{rcov}(x_i, y_j)_n$  is independent of  $i$  and  $j$  (if  $1 \leq \text{LB} \leq 6$ ). We consider first the constant-absolute-

covariance case, LB=0. Eq. 422 can then be rewritten as follows:

$$\text{cov}(x_I, y_J)_n = \text{cov}(x, y)_n \sum_{\substack{i \in I \\ j \in J}} \alpha_{Ii} \alpha_{Jj} = \text{cov}(x, y)_n \left( \sum_{i \in I} \alpha_{Ii} \right) \left( \sum_{j \in J} \alpha_{Jj} \right). \quad (423)$$

Invoking Eqs. 417 and 419, we obtain

$$\text{cov}(x_I, y_J)_n = \text{cov}(x, y)_n \quad (\text{LB} = 0). \quad (424)$$

For LB-values ranging from 1 to 6, the relative covariance is constant over each union group, so we rewrite Eq. 422 in the form

$$\begin{aligned} \text{cov}(x_I, y_J)_n &= \sum_{\substack{i \in I \\ j \in J}} \alpha_{Ii} \alpha_{Jj} x_i x_j \text{rcov}(x_i, x_j)_n \\ &= \text{rcov}(x, y)_n \sum_{\substack{i \in I \\ j \in J}} (\alpha_{Ii} x_i) (\alpha_{Jj} y_j) \\ &= \text{rcov}(x, y)_n \left( \sum_{i \in I} \alpha_{Ii} x_i \right) \left( \sum_{j \in J} \alpha_{Jj} y_j \right). \end{aligned} \quad (425)$$

Substituting here from Eqs. 413 and 418, we obtain

$$\text{cov}(x_I, y_J)_n = x_I y_J \text{rcov}(x, y)_n \quad (1 \leq \text{LB} \leq 6). \quad (426)$$

The final union-group multigroup covariance is obtained by inserting these results, Eqs. 424 and 426, back into Eq. 421

$$\text{cov}(x_I, y_J) = \sum_{n(\text{LB}=0)} \text{cov}(x, y)_n + \sum_{n(\text{LB}=1,6)} x_I y_J \text{rcov}(x, y)_n, \quad (427)$$

where the first sum runs over all sub-subsections with LB=0 and the second runs over all sub-subsections with LB=1 through 6. The quantities  $\text{cov}(x, y)_n$  and  $\text{rcov}(x, y)_n$  here are simply the point-energy covariances from the ENDF covariance file, as described in Eqs. 404 through 408. Equation 427 then is the basic equation used in subroutine `covcal` to calculate the desired union-group covariances.

The final step, if sub-subsections with LB=8 are present, is to increment the diagonal elements (variances) as follows:

$$\text{cov}(x_I, x_I) = \text{cov}(x_I, x_I) + F_k (E_{k+1} - E_k) / \Delta E_I , \quad (428)$$

where  $k$  indexes the range of the LB=8 energy grid that includes union group  $I$ .

## 10.9 Basic Strategy for Collapse to the User Grid

The union-group fluxes  $\phi_I$  are used, in subroutine **sigc**, to collapse the union-group cross sections to the coarser user grid. Changing notation slightly, let us denote by  $x_I(a)$  the cross section in union group  $I$  for reaction  $a$ , and similarly let  $X_K(a)$  be the cross section in user group  $K$  for the same reaction. In complete analogy with Eq. 413,

$$X_K(a) = \frac{\sum_{I \in K} \phi_I x_I(a)}{\phi_K} = \sum_{I \in K} A_{KI} x_I(a) , \quad (429)$$

where

$$\phi_K = \sum_{I \in K} \phi_I , \quad (430)$$

and

$$A_{KI} = \frac{\phi_I}{\phi_K} . \quad (431)$$

Applying the propagation-of-errors formula again gives

$$\text{cov} [X_K(a), X_L(b)] = \sum_{\substack{I \in K \\ J \in L}} A_{KI} A_{LJ} \text{cov}[x_I(a), x_J(b)] . \quad (432)$$

An alternative expression, obtained by simply rearranging coefficients, is

$$\text{cov} [X_K(a), X_L(b)] = \frac{1}{\phi_K \phi_L} \sum_{\substack{I \in K \\ J \in L}} T_{IJ}(a, b) , \quad (433)$$

where

$$T_{IJ}(a, b) = \phi_I \phi_J \text{cov}[x_I(a), x_J(b)] . \quad (434)$$

Eqs. 433 and 434 provide the basic framework in the ERRORR module for the production of multigroup covariances in the coarse user-group structure. Finally, if requested, the Eq. 433 absolute covariances are converted to relative form,

$$\text{rcov}[X_K(a), X_L(b)] = \frac{\text{cov}[X_K(a), X_L(b)]}{X_K(a) X_L(b)} . \quad (435)$$

### 10.10 Group-Collapse Strategy for Data Derived by Summation

The procedure described in the previous section must be modified if, in some energy range, either reaction  $a$  or  $b$  is a “derived” quantity in the sense of Eq. 409 or Eq. 410. In such a case, one cannot apply Eq. 427 directly to the calculation of  $\text{cov}[x_I(a), x_J(b)]$ , because the covariances on the right-hand side of Eq. 427 will be missing from the ENDF file in the affected energy region.

We consider first the case in which some cross sections are evaluated (“derived”) by simply summing other evaluated cross sections, as in Eq. 409. Equation 428 can then be rewritten as

$$X_K(a) = \sum_{I \in K} A_{KI} \left\{ \sum_{\text{all } c} C_I(a, c) x_I(c) \right\} , \quad (436)$$

where the quantity in curly brackets is the value of the derived cross section “a” in union group  $I$ , as reconstructed from the directly evaluated cross sections  $x_I(c)$ . The derivation coefficients  $C_I(a, c)$  depend on the union-group index  $I$ , because the evaluator is permitted to employ different derivation strategies in different energy ranges in order to simplify and shorten the covariance files.

To expand on this last point, suppose there are only three reactions, and suppose that the cross sections  $x(1)$  and  $x(2)$  rigorously sum to  $x(3)$  at all energies. Further suppose that within the energy range covered by the first union group, the cross-section evaluator has used this logical connection in order to “derive”  $x(3)$ , that is to evaluate  $x(3)$ , by summing the existing evaluations for  $x(1)$  and  $x(2)$ ,

$$x_1(3) = x_1(1) + x_1(2) . \quad (437)$$

Further suppose that in the range of union group 2,  $x(1)$  is derived by employing the same logical connection, but in a different way,

$$x_2(1) = x_2(3) - x_2(2) , \quad (438)$$

and in union group 3, all three reactions are directly evaluated.

In this example  $C_I(a, c)$  has the following values:

$$\begin{array}{lll} C_1(1,1) = 1 & C_1(1,2) = 0 & C_1(1,3) = 0 \\ C_1(2,1) = 0 & C_1(2,2) = 1 & C_1(2,3) = 0 \\ C_1(3,1) = 1 & C_1(3,2) = 1 & C_1(3,3) = 0 \end{array}$$

$$\begin{array}{lll} C_2(1,1) = 0 & C_2(1,2) = -1 & C_2(1,3) = 1 \\ C_2(2,1) = 0 & C_2(2,2) = 1 & C_2(2,3) = 0 \\ C_2(3,1) = 0 & C_2(3,2) = 0 & C_2(3,3) = 1 \end{array}$$

$$\begin{array}{lll} C_3(1,1) = 1 & C_3(1,2) = 0 & C_3(1,3) = 0 \\ C_3(2,1) = 0 & C_3(2,2) = 1 & C_3(2,3) = 0 \\ C_3(3,1) = 0 & C_3(3,2) = 0 & C_3(3,3) = 1 \end{array}$$

Note that in all cases we have formally considered the evaluated cross sections to be derived from themselves,  $C_I(a, c)|_{\text{eval}} = \delta_{ac}$ . This device allows us to use Eq. 435 for all reactions, regardless of whether they are derived or evaluated. Note that, in every case where reaction  $c$  is derived in group  $I$ ,  $C_I(a, c) = 0$ . (See boxed submatrices.) This null “sensitivity coefficient” is important, because it means that Eq. 435 remains a linear relation involving only dependent quantities with known covariances (the evaluated subset of the union-group cross sections) on the right. This allows us once again to use the propagation-of-errors formula to obtain the desired user-group covariances.

$$\text{cov}[X_K, (a), X_L(b)] = \sum_{\substack{\text{all } c \\ \text{all } d}} \sum_{\substack{I \in K \\ J \in L}} A_{KI} C_I(a, c) A_{LJ} C_J(b, d) \text{cov}[x_I(c), x_J(d)] , \quad (439)$$

or, alternatively,

$$\text{cov}[X_K, (a), X_L(b)] = \frac{1}{\phi_K \phi_L} \sum_{\substack{\text{all } c \\ \text{all } d}} \sum_{\substack{I \in K \\ J \in L}} C_I(a, c) C_J(b, d) T_{IJ}(c, d) , \quad (440)$$

where

$$T_{IJ}(c, d) = \phi_I \phi_J \text{cov}[x_I(c), x_J(d)] . \quad (441)$$

In subroutine `covcal`, the flux-covariance product  $T_{IJ}$  is calculated for all evaluated reaction pairs and written to a “scratch” binary disk file, unit 11. (For diagnostic purposes, it is possible to change this to a formatted scratch

file by manually resetting the variable `imode` to +1 in the main program.) In the subsequent collapse to the user's group structure in subroutine `covout`, the user-group covariances  $\text{cov}[X_K(a), X_L(b)]$  for one specific a-b reaction pair, for all "MT1" energy groups L, and for as large a range of "MT" energy groups K as possible, are calculated simultaneously in memory.

In `covout`, the disk file (unit 11) is rewound and read completely through, once in each range of MT groups for each a-b reaction pair, to access the union-group covariances for the evaluated reactions. As the union-group data pass through memory, contributions to the user-group covariances are accumulated using Eq. 439.

In the fairly common situation where cross sections  $x(a)$  and  $x(b)$  are directly evaluated over the whole energy range of the data file,

$$C_I(a, c) = \delta_{ac}, \text{ for all } I, \quad (442)$$

and

$$C_J(b, d) = \delta_{bd}, \text{ for all } J. \quad (443)$$

In this case, Eq. 439 can be greatly simplified.

$$\begin{aligned} \text{cov}[X_K(a), X_L(b)] &= \frac{1}{\phi_K \phi_L} \sum_{\substack{\text{all } c \\ \text{all } d}} \sum_{\substack{I \in K \\ J \in L}} \delta_{ac} \delta_{bd} T_{IJ}(c, d) \\ &= \frac{1}{\phi_K \phi_L} \sum_{\substack{I \in K \\ J \in L}} T_{IJ}(a, b). \end{aligned} \quad (444)$$

This result, which is identical to Eq. 432, suggests a shortcut calculational path, which is followed in subroutine `covout` whenever both reactions are directly evaluated. In preparation for this situation, a second copy of the `covcal` binary output file is generated when `covout` is first called. The second copy, on unit 12, is read only in the trivial derivation cases just described (flagged in the code by setting `isd=1`). Unit 12 is not rewound before processing a given reaction pair a-b, since earlier reaction pairs on the file do not contribute to the sum in Eq. 439 in these cases. Reading of the second copy stops after the union-group covariances for reaction pair a-b are found, because the later reaction pairs do not contribute either.

### 10.11 Processing of Data Derived from Ratio Measurements

The treatment of implicit covariances that arise from ratio measurements, as in Eq. 410, is totally different from the treatment of data derived by summation, Eq. 409, discussed in the previous section. Before discussing the processing details, it is helpful first to review the subject of ratio evaluations generally. Returning to the “x-y” notation of Section 10.2, let  $x(E_x)$  be the value of the cross section for reaction  $x$  at energy  $E_x$ , and  $y(E_y)$  the cross section for reaction  $y$  at energy  $E_y$ . In some energy region  $(L_x, H_x)$ , suppose that the best knowledge of  $x(E_x)$  is obtained through the application of a measured ratio,  $u(E_x)$ :

$$x(E_x) = u(E_x) z(E_x), \text{ if } L_x \leq E_x \leq H_x, \quad (445)$$

where reaction  $z$  is some well-known cross section, possibly one of the official ENDF/B standard cross sections. Similarly, suppose  $y$  is derived from the same standard, over a possibly different energy range:

$$y(E_y) = v(E_y) z(E_y), \text{ if } L_y \leq E_y \leq H_y. \quad (446)$$

By performing a first-order Taylor-series expansion and then applying the formula for propagation of errors, one can obtain an expression for the contribution to the relative covariance,  $\text{rcov}[x(E_x), y(E_y)]$ , that is attributable to these ratio measurements. In the usual case, where the ratios  $u$  and  $v$  are only weakly correlated with the standard cross section  $z$ , the result is quite simple:

$$\text{rcov}[x(E_x), y(E_y)]_{\text{ratio}} = \text{rcov}[u(E_x), v(E_y)] + \text{rcov}[z(E_x), z(E_y)] \quad (447)$$

if  $L_x \leq E_x \leq H_x$  and  $L_y \leq E_y \leq H_y$ , and

$$\text{rcov}[x(E_x), y(E_y)]_{\text{ratio}} = 0 \text{ otherwise.} \quad (448)$$

Thus, in this fairly common evaluation situation, the covariance separates naturally into a part involving only the measured ratios and a part involving only the standard. Because the second contribution,  $\text{cov}(\text{MT}_z, \text{MT}_z)$ , can be read directly from the NI-type sub-subsections in evaluation for the standard, it is not included explicitly in the ENDF subsections for the derived quantities,  $\text{cov}(\text{MT}_x, \text{MT}_x)$  or  $\text{cov}(\text{MT}_y, \text{MT}_y)$ . Instead, the existence of this additional contribution to the covariance is signalled by the presence of an NC-type sub-subsection.



The strategy adopted for processing this information in subroutine **stand** is to load the NI-type sub-subsections from the evaluation of the standard into the same storage array that is used to store NI-type covariances from the evaluation for reaction  $x$ . From that point on, the data from the standard are handled just as if they had come from the evaluation for  $x$ , but with one exception. As indicated by Eq. 448, the covariance contribution  $\text{cov}[z(E_x), z(E_y)]$  is not added into the total covariance matrix for the current reaction pair if either  $E_x$  or  $E_y$  lies outside the corresponding energy “window”  $(L_x, H_x)$  or  $(L_y, H_y)$ , respectively.

As discussed in Section 10.3, in addition to identifying the standard reaction, the NC-type sub-subsection contains a control parameter **LTY** and two energies **EL** and **EH** whose significance depends on **LTY**. **LTY** is used to identify particular evaluation scenarios: reaction  $x$  is the same as reaction  $y$  (or at least they are derived from  $z$  over the same energy range) (**LTY**=1);  $y$  is identical to the standard (**LTY**=2); or  $x$  is identical to the standard (**LTY**=3). A fourth possibility, namely, that  $x$ ,  $y$ , and  $z$  are entirely distinct, cannot presently be treated with a single NC-type sub-subsection; that is, there is no **LTY** value defined for this case. However, as discussed later, it is still possible to process covariances for this situation by combining information from sub-subsections in two different evaluations. For convenience, we shall refer to this fourth case as **LTY**=4.

The interrelationship of **LTY**, **EL**, **EH**, and the windows  $(L_x, H_x)$  and  $(L_y, H_y)$  used in **ERRORR** for the “zeroing-out” operation of Eq. 448, is summarized below:

$$\begin{aligned}
 \text{LTY} = 1 & \\
 & (L_x, H_x) = (L_y, H_y) = (\text{EL}, \text{EH}) \\
 \text{LTY} = 2 & \\
 & (L_x, H_x) = (\text{EL}, \text{EH}) \\
 & (L_y, H_y) = (10^{-5} \text{ eV}, 20 \text{ MeV}) \\
 \text{LTY} = 3 & \\
 & (L_x, H_x) = (10^{-5} \text{ eV}, 20 \text{ MeV}) \\
 & (L_y, H_y) = (\text{EL}, \text{EH}) \\
 \text{LTY} = 4 & \\
 & (L_x, H_x) = (\text{EL}, \text{EH}) \\
 & (L_y, H_y) = (\text{EL}', \text{EH}') .
 \end{aligned} \tag{449}$$

Table 5: Covariance Matrices Affected by Ratio Measurements In ENDF/B-V

|                        | <sup>10</sup> B | <sup>238</sup> U | <sup>235</sup> U | <sup>239</sup> Pu | <sup>239</sup> Pu | <sup>241</sup> Am | <sup>242</sup> Pu |
|------------------------|-----------------|------------------|------------------|-------------------|-------------------|-------------------|-------------------|
|                        | (n,α)           | (n,γ)            | (n,f)            | (n,f)             | (n,γ)             | (n,f)             | (n,f)             |
| <sup>10</sup> B(n,α)   | *               | 3                |                  |                   |                   |                   |                   |
| <sup>238</sup> U(n,γ)  | 2               | 1                |                  |                   |                   |                   |                   |
| <sup>235</sup> U(n,f)  |                 |                  | *                | 3                 | 3                 | 3                 | 3                 |
| <sup>239</sup> Pu(n,f) |                 |                  | 2                | 1                 | 1                 | 4                 | 4                 |
| <sup>239</sup> Pu(n,γ) |                 |                  | 2                | 1                 | 1                 | 4                 | 4                 |
| <sup>241</sup> Am(n,f) |                 |                  | 2                | 4                 | 4                 | 1                 | 4                 |
| <sup>242</sup> Pu(n,f) |                 |                  | 2                | 4                 | 4                 | 4                 | 1                 |

\* = standard

Integer = LTY value (see text)

If the user requests covariance data,  $\text{cov}(x, y)$ , where  $x$  and  $y$  are different and both are distinct from the standard (LTY=4), the ERRORR module obtains (EL,EH) from the LTY=2 subsection in the evaluation for  $x$  that “points” to  $z$ . Then, the covariance file for  $z$  is read to obtain both (a) the explicit covariances  $\text{cov}(z, z)$  and (b) the second energy window (EL', EH'), the latter being found in the LTY=3 sub-subsection that points back to  $y$ .

We will illustrate ratio covariance processing using data from ENDF/B-V. Table 5 lists all ENDF/B-V reactions that contain ratio-to-standard covariance data. The symbols entered in the reaction-by-reaction matrix indicate which reactions are referenced as standards (\*), and which reaction pairs have implicit nonzero covariances (LTY). ERRORR will produce multigroup covariances for any of the reaction pairs in Table 5 that are marked with (\*) or (LTY). The cross-material covariances (LTY=2, 3, or 4) must be requested individually using the IREAD=2 option (see Section 10.14, especially the discussion of Cards 10 and 11). An attempt to process covariances for any of the cases LTY=1 through 4 without supplying a separate ENDF tape containing the needed standard will result in an error stop in subroutine **gridd**. The error diagnostic, however, will supply the details of the corrective action required. (See general discussion of diagnostic messages in Section 10.16.)

As an example of the ratio-data capabilities of ERRORR, Fig. 44 shows the covariances between the fission cross sections of <sup>239</sup>Pu (reaction  $x$ ) and those of the important actinide <sup>241</sup>Am (reaction  $y$ ). This is an LTY=4 case where  $(L_x, H_x) = (0.2 \text{ MeV}, 15 \text{ MeV})$  and  $(L_y, H_y) = (0.2 \text{ MeV}, 20 \text{ MeV})$ . The effect of using two different windows is apparent in the lower right corner of the

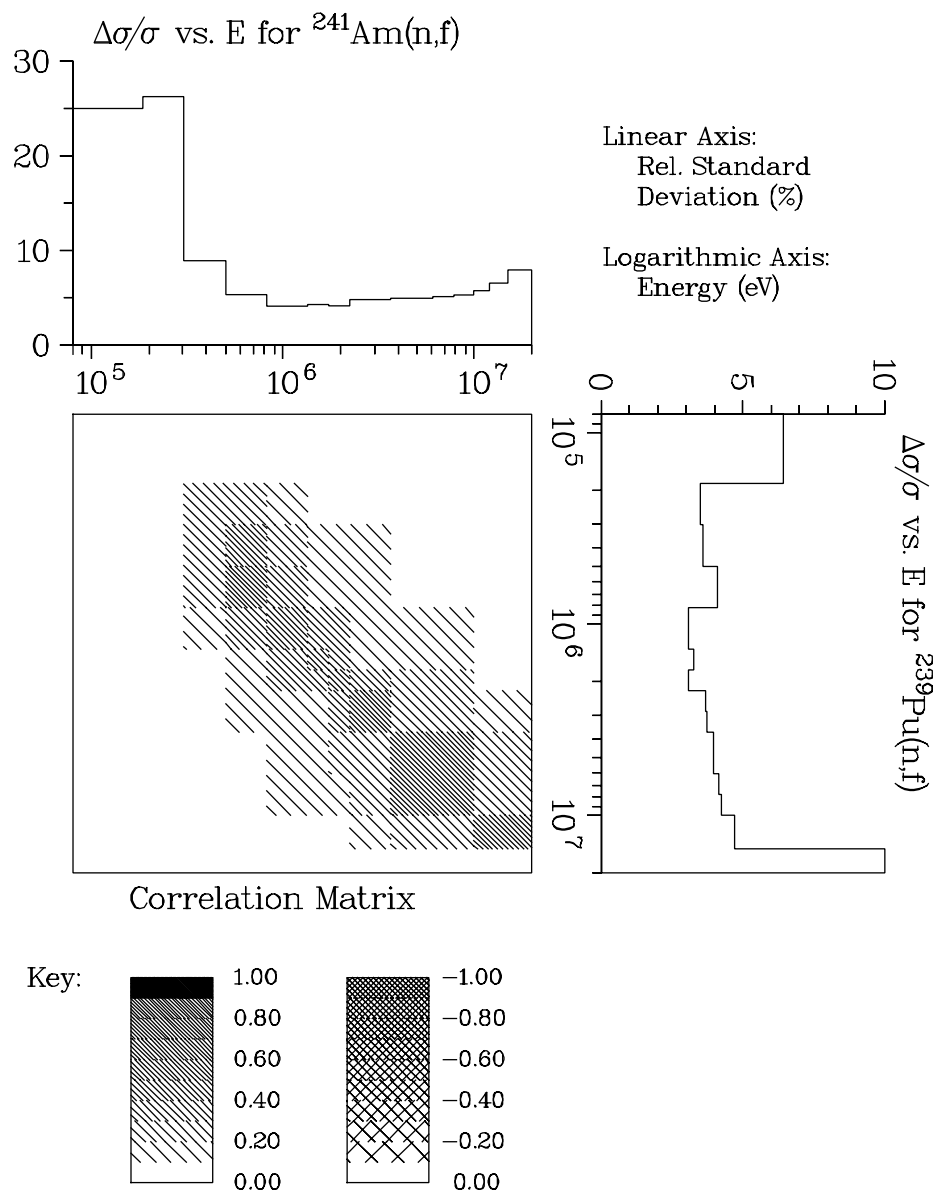


Figure 44: Covariance data for  $^{239}\text{Pu}(n,f)$  with  $^{241}\text{Am}(n,f)$ . This older figure illustrates the black & white option for covariance plots using hatching to represent levels of correlation.

correlation matrix. The plot itself was produced with NJOY's [COVER](#) module. The complete input needed to compute and plot these data is given below (see the fourth input example in [Section 10.14](#)).

## 10.12 Multigroup Processing of Resonance-Parameter Uncertainties

In some materials, and in certain energy regions, the cross-section uncertainty is dominated by the uncertainty in resolved resonance parameters. As described above, there are several formats available in the ENDF-6 format for describing resonance covariances. When using the early ENDF-5 format (which is available in the ENDF-6 format as LCOMP=0) the resonance-parameter contribution to the uncertainty in infinite-dilution fission and capture cross sections is included automatically when cross-section covariances are processed. The contribution is obtained from the Breit-Wigner formulae for the fission and capture areas of a resonance,  $A_f$  and  $A_\gamma$ . By differentiating these formulae with respect to the resonance parameters, one obtains a set of sensitivities. With these sensitivities and the covariance matrix of the parameters from MF32, one can apply the propagation-of-errors formula to obtain the covariances  $\text{cov}(A_\gamma, A_\gamma)$ ,  $\text{cov}(A_\gamma, A_f)$ , and  $\text{cov}(A_f, A_f)$ .

The resonance contribution is properly weighted with the isotopic abundance and the ratio of the weight function at the resonance to the average weight in the group. It is assumed, however, that the area of a resonance lies entirely within the group that contains the resonance energy  $E_r$ . Because of this assumption, and because ENDF-5 and the LCOMP=0 option of ENDF-6 provide no correlations between parameters of different resonances, the calculated resonance-parameter contribution affects only the diagonal elements of the affected matrices,  $\text{cov}[X_K(a), X_K(b)]$ .

When one of the more advanced options (LCOMP=1 or LCOMP=2) is found in MF32, and for Single-Level Breit-Wigner, Multi-Level Breit-Wigner, or Reich-Moore resonance parameters, the ERRORR code branches to the ERRORJ logic. The resonance cross sections are computed on a special grid and group averaged. Then each parameter is changed in turn to generate new cross sections. Sensitivity parameters are computed from the differences. These sensitivity coefficients are then combined with the covariances of the parameters to obtain covariances on the multigroup cross sections. The matrices are very large in many cases, and the folding is time consuming. There are two formats in use for the parameter covariances. One gives each value in a full computer word. With many resonances, this can become very bulky. The other uses a more compact representation based on the correlations. Just a few digits are used for each correlation, thus reducing the size of the evaluation. The coding must reconstruct the actual covariance values before folding them with the sensitivities, so this

economization doesn't help with the time required to fold the data in the final cross section covariances.

If Reich-Moore-Limited resonances are found (LRF=7, a different branch is taken. In this case, it is possible to use analytic formulas to compute the cross section sensitivities to the parameters. These formulas are given in detail in the SAMMY reference[35]. These sensitivities are computed on a special energy grid and group averaged. They are then folded with the parameter covariances as described above to obtain the cross section covariances.

### 10.13 Processing of Lumped-Partial Covariances

The lumped-partial covariance format, allows the evaluator to specify a group of nuclear reactions and to give the uncertainty only in the sum of the cross sections for that group of reactions. One can, for example, replace 30 or 40 discrete-level inelastic cross sections with 5 or 6 lumped cross sections when constructing the covariance files. Because the volume of the covariance data varies, in general, as the square of the number of reactions, this lumping can greatly reduce the size of the files.

The first ENDF evaluation to employ the lumped-partial format was Young's evaluation[74, 75] for  $^7\text{Li}$  (ENDF/B-V, Rev. 2). All covariance data for this evaluation have been successfully processed into multigroup form using ERRORR. The covariances for MT854 (a single real level with an excitation energy of 4.63 MeV) with MT855 (6 lumped pseudo-levels, with excitation energies ranging from 4.75 MeV to 6.75 MeV) have been plotted in Fig. 45. The large negative correlations along the diagonal result from the fact that, below 10 MeV, these inelastic reactions are the major contributors to the relatively well-known tritium production cross section. An upward variation in one reaction at a given energy must be accompanied by a downward change in the other reaction. As shown in the plot, the magnitude of this negative correlation diminishes at higher energies, as other reactions begin to contribute significantly to the tritium-production cross section. Plots of this type, prepared using ERRORR and COVR, have proved to be useful tools in the validation of the covariance files of new evaluations[76].

### 10.14 Input Instructions and Sample Input for ERRORR

As an aid to discussions of the user input to ERRORR, we list below the input instructions that appear as comment cards at the beginning of the current version of this module. Since the code and, hence, the instructions change from

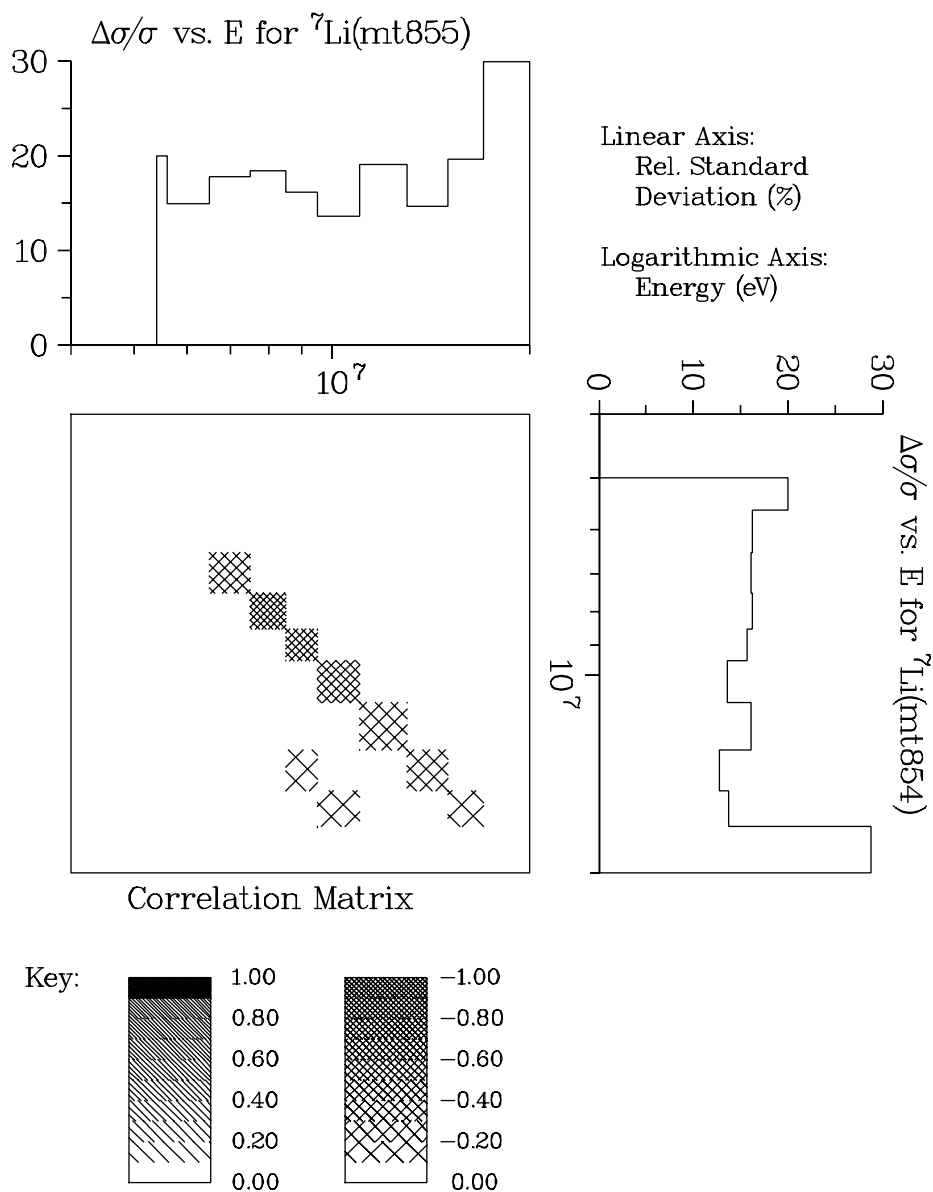


Figure 45: Covariance data for  ${}^7\text{Li}$  (MT854) with  ${}^7\text{Li}$  (MT855).

time to time, it is always advisable to consult the comment-card instructions contained in the version of the code actually being used and not to rely on the instructions published in any document, including this one. Note that the word “tape” is used in the instructions to refer to an input or output file, regardless of the actual storage medium.

```

!---input specifications (free format)-----
!
!  card 1
!    nendf  unit for endf tape
!    npend  unit for pendf tape
!    ngout  unit for input group xsec (gendf) tape
!           (if zero, group xsecs will be calculated)
!           (if iread eq 2 or if mfcov eq 31, 35 or 40 (see
!            card 7), then ngout cannot be zero)
!           (if mfcov eq 35 (see card 7),
!            ngout cannot be zero)
!           (default=0)
!    nout   unit for output covariance tape (default=0)
!    nin    unit for input covariance tape (default=0)
!           (nin and nout must be both coded or both binary)
!    nstan  unit for ratio-to-standard tape (default=0)
!  card 2
!    matd   material to be processed
!    ign    neutron group option
!           (ign definition same as groupr, except ign=19,
!            which means read in an energy grid, as in ign=1,
!            and supplement this with the endf covariance grid
!            within the range of the user-specified energies)
!           (default=1)
!    iwt    weight function option (default=6)
!    iprint print option (0/1=minimum/maximum) (default=1)
!    irelco covariance form (0/1=absolute/relative) (default=1)
!  card 3  (** REQUIRED for njoy2012 **)
!    mprint print option for group averaging (0/1=min (default)/max)
!    tempin temperature (default=300)
!
!---for endf/b version 4 (iverf=4) only-----
!
!  card 4
!    nek    number of derived xsec energy ranges
!           (if zero, all xsecs are independent)
!  card 5  (omit if nek=0)
!    ek     nek+1 derived xsec energy bounds
!  card 6  (omit if nek=0)
!    akxy   derived cross section coefficients, one row/line

```

```

!
!---for endf/b version 5 or 6 (iverf=5 or 6) only-----
!
! card 7
!   iread  0/1/2=program calculated mts/input mts and eks/
!           calculated mts plus extra mat1-mt1 pairs from input
!           (default=0)
!   mfcov  endf covariance file (31, 33, 34, 35 or 40) to be
!           processed (default=33).
!           note--contribution to group cross section
!           covariances from resonance-parameter uncertainties
!           (mf=32) is included when mfcov=33 is specified.
!           (mf=-33) high speed calc for test case
!           (mf=333) hight speed calc for test case (faster)
!   irespr  processing for resonance parameter covariances
!           (mf=32) (default=1)
!           0 = area sensitivity method
!           1 = 1\% sensitivity method
!   legord  legendre order for calculating covariances (default=1)
!           (if mfcov is not 34, legord is ignored)
!   ifissp  subsection of the fission spectrum covariance
!           matrix to process (default=-1 which means process
!           the subsection that includes efmean). The value
!           for ifissp that appears in njoy's standard output
!           will equal the subsection containing efmean.
!           (if mfcov is not 35, ifissp is ignored)
!   efmean  incident neutron energy (eV). Process the covar-
!           iance matrix subsection whose energy interval in-
!           cludes efmean. if ifissp=-1 and efmean is not
!           specified, set efmean=2.e6_kr. But if there is only
!           one subsection, process it and if the input efmean
!           was not within this subsection's energy range then
!           redefine efmean to equal the average energy for
!           this subsection.
!           (if mfcov is not 35, efmean is ignored)
!   dap     user specified scattering radius uncertainty, given
!           as a fraction (i.e., dap=0.1 means 10\% uncertainty
!           in the scattering radius). The default value is
!           zero. This variable is only defined for mfcov=33
!           and if non-zero will be used in lieu of any data
!           that might have been read from the nendf tape.
!

```



```

! following cards only if iread eq 1
! card 8
!   nmt      no. mts to be processed
!   nek      no. derived cross section energy ranges
!             (if zero, all xsecs are independent)
! card 8a
!   mts      nmt mts
! card 8b    (omit if nek=0)
!   ek      nek+1 derived cross section energy bounds
! card 9     (omit if nek=0)
!   akxy     derived cross section coefficients, one row/line
!
! following card only if iread eq 2
! card 10
!   mat1     cross-material reaction to be added to
!   mt1      covariance reaction list.
!             repeat for all mat1-mt1 pairs desired
!             terminate with mat1=0.
!
! following card only if nstan ne 0
! card 11
!   matb     standards reaction referenced
!   mtb      in matd.
!   matc     standards reaction to be
!   mtc      used instead.
!             repeat for all standard reactions to be redefined.
!             terminate with matb=0.
! note.  if matb(1) and mtb(1) are negative, then matc(1) and
!         mtc(1) identify a third reaction, correlated with matd thru
!         the use of the same standard.  covariances of all reactions
!         in matd (which reference the standard) with the reaction
!         matc(1)-mtc(1) will be produced.  the standard reaction
!         must be identified on card 10 and repeated as the negative
!         entries on card 11.  the group xsec tape ngout must include
!         all covariance reactions in matd, plus matc(1)-mtc(1).
!
! card 12a (for ign eq 1 or ign eq 19)
!   ngm      number of groups
! card 12b
!   egm      ngm+1 group bounds (ev)
! card 13 (for iwt eq 1 only)
!   wght     weight function as a tab1 record

```

```

! card 13b analytic flux parameters (iwt=4 only)
!   eb      thermal break (ev)
!   tb      thermal temperature (ev)
!   ec      fission break (ev)
!   tc      fission temperature (ev)
!
! ---options for input variables-----
!
!   ign      meaning
!   ---      -----
!   1        arbitrary structure (read in)
!   2        csewg 239-group structure
!   3        lanl 30-group structure
!   4        anl 27-group structure
!   5        rrd 50-group structure
!   6        gam-i 68-group structure
!   7        gam-ii 100-group structure
!   8        laser-thermos 35-group structure
!   9        epri-cpm 69-group structure
!   10       lanl 187-group structure
!   11       lanl 70-group structure
!   12       sand-ii 620-group structure
!   13       lanl 80-group structure
!   14       eurlib 100-group structure
!   15       sand-ia 640-group structure
!   16       vitamin-e 174-group structure
!   17       vitamin-j 175-group structure
!   18       xmas 172-group structure
!   19       read in, supplemented with endf covariance grid
!
!   iwt      meaning
!   ---      -----
!   1        read in smooth weight function
!   2        constant
!   3        1/e
!   4        1/e + fission spectrum + thermal maxwellian
!   5        epri-cell lwr
!   6        (thermal) -- (1/e) -- (fission + fusion)
!   7        same with t-dep thermal part
!   8        thermal--1/e--fast reactor--fission + fusion
!   9        claw weight function
!   10       claw with t-dependent thermal part

```

```

!      11      vitamin-e weight function (ornl-5505)
!      12      vit-e with t-dep thermal part
!
!-----

```

As an example of the use of these commands, here is the input used to produce Fig. 38, the covariance plot for  $^{10}\text{B}$  from ENDF/B-VII.0.

```

1. errorr
2. 31 32 0 33/
3. 525 3 9 1 1/
4. 0 0./
5. 0 33/
6. covr
7. 33 0 34/
8. 1/
9. /
10. /
11. 525/
12. viewr
13. 34 35/
14. stop

```

The line numbers are for reference and are not part of the input. Identical versions of the ENDF/B-VII.0 file for  $^{10}\text{B}$  can be copied to **tape31** and **tape32**. The ERRORR output will appear on **tape33**. In this sample input deck, that file is the input file to **COVR** which generates the plot instructions that are subsequently written to **tape34**. Line 3 defines the material to be processed (525, or  $^{10}\text{B}$ ), the group structure, the weight function, the listing option, and requests relative covariances. Line 4 turns off printing for the group averaging and requests zero temperature. Users are cautioned that line 4 is now required in all ERRORR input decks whereas in *njoy99* it is only required when *ngout* is zero. Line 5 asks the program to calculate the MT numbers to be processed and to work with File 33. The **COVR** and **VIEWR** input in lines 6 through 13 act to prepare the graph as seen in Fig. 38.

The following paragraphs give more detail on how the various input parameters are used.

**npnd**, **ngout** ... The user must supply either a PENDF tape on unit **npnd** or a GENDF tape on unit **ngout**. If present, the **npnd** tape should contain pointwise (resonance-reconstructed, but not multigroup) data and is normally produced with the **RECONR** module. If the resonance region is of no interest, a simple copy of the ENDF tape will suffice for this purpose. The GENDF tape, if present, should contain multigroup cross sections and/or  $\bar{\nu}$  values, produced by the **GROUPE** module, for all reactions for which multigroup covariances are needed. Group cross sections need not be in the same group structure as the requested output covariances, although if the input group structure is much coarser than the output structure, rather crude approximations will be made in deriving an effective set of fine-group cross sections and fluxes from the coarse input data. Certain types of covariance calculations related to fission data or the computation of cross-material covariances require the user to supply a GENDF tape on **ngout** (that is, **npnd** must be zero).

**nin**, **nout** ... Input and output covariance tapes in the user's group structure may either be both formatted or both binary. Although ERRORR lacks an explicit multimaterial loop, the same effect can be achieved by executing a series of ERRORR runs, with the output of one run becoming the input of the next. Only two unit numbers need be employed, with the data going back and forth between them until the multimaterial library is complete. To save time, binary files should be used for this purpose. **MODER** can be used to convert the final output tape from binary to formatted form, if desired.

**nstan** ... This tape is needed if covariances are requested for a reaction pair that is related by ratio measurements, as discussed in Section 10.11. The ENDF subsection for such a pair will contain an NC-type sub-subsection with **LTY**=1, 2, or 3. The specific pairs in ENDF/B-V that require a standards tape are tabulated in Table 5 (Section 10.11). For other evaluations, one can assume **nstan** is not needed. The code will stop with a clear error message if this assumption proves incorrect.

**iread** ... For ENDF/B versions 5 and 6, the list of reactions for which covariances are produced is constructed in one of several ways, depending on the value of **iread**. If **iread**=0, which is the generally recommended choice, the reaction list is assumed to be identical to the list of sections contained in the ENDF/B covariance file (see **mfcov** below). Although **iread**=0 is the most convenient option for constructing the list of covariance reactions, it leads to a problem if some covariance reactions have thresholds above the highest group boundary of the user's structure. These reactions will have zero cross sections

in all groups and thus will be omitted from **ngout**. To avoid this difficulty, **ERRORR** automatically resets the user's highest group boundary to 20 MeV whenever **iread**=0. By judicious choice of weighting functions, one can minimize the effect of this resetting on the other cross sections and their covariances.

If **iread**=1, only the covariance reactions specifically named by the user will be included in the reaction list. For certain applications, this option can save considerable execution time. However, to take advantage of this option, the user must examine the ENDF evaluation visually to determine which reactions are derived from other reactions in each energy region. As discussed in Section 10.3, this information is contained in NC-type sub-subsections with **LTY**=0. Incorrect results will be obtained if one requests processing for a given reaction without processing all of the reactions from which the given reaction is derived in the energy region spanned by the output group structure. The inclusion of those reactions may require, in turn, additional inclusions as well. In addition, the user must extract from the file (and enter into the input) the appropriate derivation coefficients and the energy ranges over which they apply. An example of the required input is presented below in the discussion of the parameters **nmt**, **nek**, **mts**, **ek**, and **akxy**.

If **iread**=0 or 1, a complete set of covariance matrices is written. That is, covariance matrices are produced for every reaction-pair combination that can be formed from the given reaction list. For those reaction pairs where the evaluator has not specified the covariances, the output matrix contains only zeros.

In the evaluation containing cross-material covariances, subsections involving the other materials will be ignored if **iread**=0 or 1. These subsections can be selectively processed by specifying **iread**=2. If **iread**=2, the reaction list is initially constructed in the same way as for **iread**=0. This list is then supplemented with a list of extra reactions (**MAT**1<sub>*k*</sub>, **MT**1<sub>*k*</sub>) (where (**MAT**1<sub>*k*</sub> ≠ **MATD**), specified by the user. The output in this case contains matrices for all of the (**MATD**, **MT**<sub>*i*</sub>; **MATD**, **MT**<sub>*j*</sub>) combinations, as before, plus matrices for all (**MATD**, **MT**<sub>*i*</sub>; **MAT**1<sub>*k*</sub>, **MT**1<sub>*k*</sub>) combinations. However, covariances among the extra reactions, for example (**MAT**1<sub>*k*</sub>, **MT**1<sub>*k*</sub>; **MAT**1<sub>*m*</sub>, **MT**1<sub>*m*</sub>), are not computed. Input for an example problem that illustrates the use of **iread**=2 is given below, in the discussion of **mfcov**. That discussion also includes an illustration of the set of **MAT**/**MT** combinations that are processed when **iread**=2.

**mfcov** ... is used to specify whether covariances of  $\bar{\nu}$  (**mfcov**=31), cross sections (**mfcov**=33), angular distributions (**mfcov**=34), secondary energy distri-

butions (**mf**cov=35), or radioactive nuclide production (**mf**cov=40) are needed. If **mf**cov=31, 35, or 40, it is necessary to supply multigrouped cross sections and  $\bar{\nu}$  values on a GENDF tape that is, **np**end must be 0); the sample problem below shows the calculational sequence required. The parameter **mf**cov=32 is reserved for a planned future capability to compute uncertainties in self-shielded cross sections. If **mf**cov=33, the contribution of the uncertainty in individual resonance parameters (File 32) is included in the calculated uncertainty in infinite-dilution group cross sections. Given below is the complete NJOY input for a calculation of a multigroup  $\bar{\nu}$  covariance library for  $^{238}\text{U}$ , including five cross-material reactions.

```

moder / mount ENDF tapes 515, 516, and 555 on units 20, 21, and 22.
1 -23
'ENDF/B-V NUBAR COVARIANCE MATERIALS'/
20 1380
20 1381
21 1390
22 1395
22 1398
20 1399
0/
moder / copy ENDF for use as a PENDF.
-23 -24
groupr / prepare GENDF with multigrouped nubars.
-23 -24 0 25
1380 3 0 3 0 1 1 0
'BIG3 + 2 NUBAR'/
0.
1.e10
3 452 'TOTAL NUBAR'/
0/
1381
3 452 'TOTAL NUBAR'/
0/
1390
3 452 'TOTAL NUBAR'/
0/
1395
3 452 'TOTAL NUBAR'/
0/

```

```

1398
3 452 'TOTAL NUBAR' /
3 455 'DELAYED NUBAR' /
3 456 'PROMPT NUBAR' /
0 /
1399
3 452 'TOTAL NUBAR' /
0 /
0 /
errorr / prepare multigroup nubar covariance library.
-23 0 25 26 /
1398 19 1 1
0 0. /
2 31
1380 452
1381 452
1390 452
1395 452
1399 452
0 /
1
1.e7 1.7e7
stop

```

Note the use of the [MODER](#) module to prepare a special ENDF tape containing selected evaluations from other ENDF tapes. Because only high-energy  $\bar{\nu}$  data are requested (10 – 17 MeV), it is unnecessary to use [RECONR](#) to prepare a PENDF tape for [GROUPT](#). A copy of the ENDF tape is used instead.

Following the prescription given in the discussion of the `iread=2` option, with this particular input, covariance matrices will be produced for those reaction pairs marked with an X in Table 6. The remaining non-redundant possibilities (dashes) can be filled in with successive ERRORR runs with `MATD=1380, 1381, etc.`

`nwt, nek, mts, ek, akxy ...` For ENDF/B version 5, if `iread=1`, the user specifies a subset of the evaluator's covariance reactions (that is, a subset of the sections of `mf cov`), as the particular set of reactions for which processing is requested. These `nmt` desired reactions are entered in the array `mts`. As mentioned in the discussion of `iread` above, one must also include in the `mts` array all reactions from which the desired reactions are derived.

Table 6: Reaction pairs in the ENDF/B-V  $^{238}\text{U}$  evaluation

|                | a | b | c | d | e | f | g | h | i |
|----------------|---|---|---|---|---|---|---|---|---|
| a = (1398,452) | X | X | X | X | X | X | X | X | X |
| b = (1398,455) |   | X | X | X | X | X | X | X | X |
| c = (1398,456) |   |   | X | X | X | X | X | X | X |
| d = (1380,452) |   |   |   | — | — | — | — | — | — |
| e = (1381,452) |   |   |   |   | — | — | — | — | — |
| f = (1390,452) |   |   |   |   |   | — | — | — | — |
| g = (1395,452) |   |   |   |   |   |   | — | — | — |
| h = (1398,452) |   |   |   |   |   |   |   | — | — |
| i = (1399,452) |   |   |   |   |   |   |   |   | — |

Another requirement of the `iread=1` option is that the actual derivation coefficients, called `akxy` in the code, but called  $C_I(a, c)$  in the discussion in Section 10.10, must be entered in the ERRORR input for `nek` energy ranges spanning the output group structure. Adjacent ENDF derivation ranges may be merged into a single range if the derivation-coefficient matrix for the `nm`t explicitly requested reactions is the same in each of the adjacent ranges. The ordering of the  $C_I(a, c)$  data is as follows: on one line of input the coefficients are specified for a fixed  $a$ -value and for all  $c$ -values ranging from 1 to `nm`t. One such line is given for each  $a$ -value. Finally, there is an outer loop over the `nek` energy ranges. An example of the input that is required for `iread=1` is given below for the case of ENDF/B-V carbon `MAT=1306`. It will be necessary to examine File 33 of the evaluation (which is available on the ENDF/B-V standards file, Tape 511), in order to understand the details of this example.

```

moder
20- 21
moder / copy ENDF for use as a PENDF.
-21 -22/
errorr
-21 -22 0 -23/
1306 3 1/
2 0 0
1 33
7 3
1 2 4 102 103 104 107
1.e-5 2e6 4.812e6 2e7

```



```

0 1 0 1 0 0 0
0 1 0 0 0 0 0
0 0 1 0 0 0 0
0 0 0 1 0 0 0
0 0 0 0 1 0 0
0 0 0 0 0 1 0
0 0 0 0 0 0 1
1 0 0 0 0 0 0
0 1 0 0 0 0 0
0 0 1 0 0 0 0
0 0 0 1 0 0 0
0 0 0 0 1 0 0
0 0 0 0 0 1 0
0 0 0 0 0 0 1
1 0 0 0 0 0 0
0 1 0 0 0 0 0
1 -1 0 -1 -1 -1 -1
0 0 0 1 0 0 0
0 0 0 0 1 0 0
0 0 0 0 0 1 0
0 0 0 0 0 0 1
stop

```

Note that here, even if the user wanted to process only  $M=2$  and  $MT=4$ , for example, it is nevertheless necessary to include  $MT=1$ ,  $MT=102$ ,  $MT=103$ ,  $MT=104$ , and  $MT=107$ , because the `ign=3` group structure extends to 17.0 MeV, and above 4.812 MeV,  $MT=4$  is derived from the relation

$$\sigma_4 = \sigma_1 - \sigma_2 - \sigma_{102} - \sigma_{103} - \sigma_{104} - \sigma_{107} . \quad (450)$$

See the corresponding  $C_I(a, c)$  matrix in the input above (the last 7 lines before `stop`).

`matb`, `mtb`, `matc`, `mtc` ... Card 11 provides a capability to remap all references to a given standards reaction (`matb`, `mtb`) appearing in NC-type sub-subsections with `lty=1`, `2`, or `3` into references to a different reaction (`matc`, `mtc`). (See the discussion of ratio measurements in Section 10.11.) This facility is useful if the evaluation (`matb`, `mtb`) is for some reason unavailable. Up to 5 such standards can be redefined. As explained in the note on the input instructions at the beginning of this section, Card 11 is also used, if `matb(1)` and `mtb(1)` are

negative, to process covariances between two distinct reactions, both measured relative to a common standards reaction. This was referred to as the `lty=4` case in Section 10.11. A separate ERRORR run is required for each requested `lty=4` reaction pair.

This second use of Card 11 is illustrated in the sample NJOY input listed below, which is the input used to generate and plot the data shown in Fig. 44. The input to the COVR module contained in the sample is explained in the following chapter.

```

mount T562 on tape30
mount T563 on tape40
mount T560 on tape50

moder
1 -31
'U235 FROM T562'/
30 1395
0/
moder
1 -21
'AM241 FROM T560 AND PU239 FROM T563'/
50 1361/ AM241
40 1399/ PU239
0/
reconr
-21 -22
'10 PERCENT PENDF FOR AM241 AND PU239'/
1361/
.1/
1399/
.1/
0/
GROUPR
-21 -22 0 -24
1361 3 0 2 0 1 1 0
'30 GROUP XSECS FOR AM241 AND PU239'/
0
1e10
3 1/
3 2/
3 4/

```

```

3 16/
3 17/
3 18/
3 102/
0/
1399
3 18/
3 102/
0/
0/
errorr
-21 0 -24 -25 0 -31
1361 3 1 1
0 0. /
0 33
0/
errorr
-21 0 -24 -28 -25 -31
1399 3 1 1
0 0. /
2 33
1395 18
0/
-1395 -18 1361 18
0/
covr
-28/
0 0 0 8e4
1 1 0 0 2
1399 18 1361 18
stop

```

The input for a File 34 case preparing covariances for an angular distribution is shown below. This is the input that produced Fig. 40 shown above. This deck runs a job sequence that includes **MODER** (ASCII-to-binary conversion), **RECONR** and **BROADR** (cross section reconstruction to 300K), **GROUPL** (unweighted, infinitely dilute multigroup cross sections plus average  $\bar{\mu}$ ), **ERRORR** (specifying **mf cov=34** for  $\bar{\mu}$  covariance processing), and **COVR** and **VIEWR** (for plot generation and conversion to Postscript format). The input on **tape20** was the JENDL-3.3 evaluation for  $^{238}\text{U}$ .

```

moder
  20 -21 /
reconr
  -21 -22 /
  'processing jendl-3.3 u-238.'
  9237 0 0 /
  0.001 /
  0 /
broadr
  -21 -22 -23 /
  9237 1 0 0 0 /
  0.001 /
  300. /
  0 /
groupr
  -21 -23 0 91 /
  9237 3 0 2 1 1 1 0 /
  'test'
  300. /
  1.0e10 /
  3 /
  3 251 'mubar' /
  0 /
  0 /
--
-- process mf34
errorr
  -21 0 91 27 0 0 /
  9237 3 2 1 1 /
  0 300. /
  0 34 1 1 -1 /
--
-- make mf34 plot file.
covr
  27 0 37 /
  1 /
  /
  /
  9237 /
--

```

```

-- make mf34 postscript file.
viewr
  37 47 /
stop

```

The input for the File 35 case that produced the plot of secondary energy covariances seen in Fig. 41 is given below. This is a problem taken from the NJOY test suite that uses a fictitious input file for  $^{252}\text{Cf}$ . The [GROUPE](#) and [ERRORR](#) inputs specify a user-defined group structure that corresponds to the energies listed in File 1 of the evaluation with the uncertainties provided by the evaluator. This makes it easy to verify that the results agree with the evaluator's intent.

```

--
-- Copy ascii input to binary.
moder
  20 -21 /
--
-- Resonance reconstruction, to 0.1\%.
reconr
  -21 -22 /
  'processing e70 252Cf with decay mf5/mt18 & mf35/mt18'
  9999 0 0 /
  0.001 /
  0 /
--
-- Doppler broaden to 300K.
broadr
  -21 -22 -23 /
  9999 1 0 0 0 /
  0.001 /
  300. /
  0 /
--
-- Group average, 300K with mf35 group structure.
-- - All file 3 cross sections plus fission spectrum.
groupr
  -21 -23 0 91 /
  9999 1 0 2 1 1 1 1 /
  'test'

```

```

300. /
1.0e10 /
71 / # of groups, energy boundaries follow:
1.000000-5 1.500000+4 3.500000+4 5.500000+4 7.500000+4
9.500000+4 1.150000+5 1.350000+5 1.650000+5 1.950000+5
2.250000+5 2.550000+5 3.050000+5 3.550000+5 4.050000+5
4.550000+5 5.050000+5 5.550000+5 6.050000+5 6.550000+5
7.050000+5 7.550000+5 8.050000+5 8.550000+5 9.050000+5
9.550000+5 1.050000+6 1.150000+6 1.250000+6 1.350000+6
1.450000+6 1.550000+6 1.650000+6 1.750000+6 1.850000+6
1.950000+6 2.150000+6 2.350000+6 2.550000+6 2.750000+6
2.950000+6 3.250000+6 3.550000+6 3.850000+6 4.150000+6
4.450000+6 4.750000+6 5.050000+6 5.550000+6 6.050000+6
6.550000+6 7.050000+6 7.550000+6 8.050000+6 8.550000+6
9.050000+6 9.550000+6 1.005000+7 1.055000+7 1.105000+7
1.155000+7 1.205000+7 1.255000+7 1.305000+7 1.355000+7
1.405000+7 1.460000+7 1.590000+7 1.690000+7 1.790000+7
1.910000+7 2.000000+7
3 /
5 18 'chi' /
0 /
0 /
--
-- ERRORJ, mf35
errorr
20 0 91 28 0 0 /
9999 1 2 1 1 /
0 300. /
0 35 1 1 -1 1.23e6 /
71 / # of groups, energy boundaries follow:
1.000000-5 1.500000+4 3.500000+4 5.500000+4 7.500000+4
9.500000+4 1.150000+5 1.350000+5 1.650000+5 1.950000+5
2.250000+5 2.550000+5 3.050000+5 3.550000+5 4.050000+5
4.550000+5 5.050000+5 5.550000+5 6.050000+5 6.550000+5
7.050000+5 7.550000+5 8.050000+5 8.550000+5 9.050000+5
9.550000+5 1.050000+6 1.150000+6 1.250000+6 1.350000+6
1.450000+6 1.550000+6 1.650000+6 1.750000+6 1.850000+6
1.950000+6 2.150000+6 2.350000+6 2.550000+6 2.750000+6
2.950000+6 3.250000+6 3.550000+6 3.850000+6 4.150000+6
4.450000+6 4.750000+6 5.050000+6 5.550000+6 6.050000+6
6.550000+6 7.050000+6 7.550000+6 8.050000+6 8.550000+6
9.050000+6 9.550000+6 1.005000+7 1.055000+7 1.105000+7

```

```

1.155000+7 1.205000+7 1.255000+7 1.305000+7 1.355000+7
1.405000+7 1.460000+7 1.590000+7 1.690000+7 1.790000+7
1.910000+7 2.000000+7
--
-- make plot file.
covr
28 0 38 /
1 /
1.e3 /
/
9999 /
--
-- make postscript file.
viewr
38 39 /
stop

```

The final example gives the input used to prepare Fig. 42 showing the uncertainties in radionuclide production for  $^{93}\text{Nb}$ . This is a fairly elaborate input deck, as it includes [GROUPR/ERRORR/](#) [COVR/VIEWR](#) processing for both File 3 and File 10.

```

-- Extract/convert neutron evaluated data
moder
1 -21
'41-Nb-93 from e70'/
20 4125
0/
--
-- Make an ASCII copy
moder
-21 41 /
--
-- Reconstruct xs
reconr
41 42
'pendf for 41-Nb-93'/
4125 2/
0.001 0. 0.003/
'41-Nb-93 from e70'/
'Processed with NJOY'/

```

```

0/
--
-- Doppler broaden xs
broadr
41 42 43
4125 1 0 0 0./
0.001 2.0e6 0.003/
300.
0/
--
-- groupr, process all file 3 reactions:
groupr
41 43 0 44 /
4125 1 0 6 0 1 1 1 /
'41-Nb-93 from e70 with NJOY'/
300. /
1.e10 /
21 /
1.e-5 0.625 10.7 100.0 1.e3 1.e4 1.e5 1.e6
2.e6 3.e6 4.e6 5.e6 6.e6 7.e6 8.e6 9.e6 10.e6
12.e6 14.e6 16.e6 18.e6 20.e6 /
3 /
0/
0/
--
-- errorrj, process all file 3 reaction uncertainties:
errorr
41 43 44 45/
4125 1 6 1 1 /
0 300. /
0 33 /
21 /
1.e-5 0.625 10.7 100.0 1.e3 1.e4 1.e5 1.e6
2.e6 3.e6 4.e6 5.e6 6.e6 7.e6 8.e6 9.e6 10.e6
12.e6 14.e6 16.e6 18.e6 20.e6 /
--
-- create plot of mf33 uncertainty data
covr
45 0 55 /
1 /
1.e-1 /
/

```



```

4125 /
viewr
55 65 /
--
-- groupr, process all file 10 reactions:
groupr
41 43 0 46 /
4125 1 0 6 0 1 1 1 /
'41-Nb-93 from e70 with NJOY'/
300. /
1.e10 /
21 /
1.e-5 0.625 10.7 100.0 1.e3 1.e4 1.e5 1.e6
2.e6 3.e6 4.e6 5.e6 6.e6 7.e6 8.e6 9.e6 10.e6
12.e6 14.e6 16.e6 18.e6 20.e6 /
10 /
0/
0/
--
-- errorrj, process all file 10 reaction uncertainties:
errorr
41 43 46 47/
4125 1 6 1 1 /
0 300. /
0 40 /
21 /
1.e-5 0.625 10.7 100.0 1.e3 1.e4 1.e5 1.e6
2.e6 3.e6 4.e6 5.e6 6.e6 7.e6 8.e6 9.e6 10.e6
12.e6 14.e6 16.e6 18.e6 20.e6 /
--
-- create plot of mf40 uncertainty data
covr
47 0 57 /
1 /
1.e3 /
/
4125 /
viewr
57 67 /
stop

```

### 10.15 ERRORR Output File Specification

The results from ERRORR are written to an output file on unit **nout**, provided that the input parameter **nout** is nonzero. This file contains the user's group structure, the multigroup cross sections, and either absolute (**irelco**=0) or relative (**irelco**=1) covariances. If **nout** is positive, then a formatted (card-image) file is written, and, if negative, a binary file is written. In either case, the output is written with the standard **NJOY** I/O utilities, and the result has an ENDF-like structure. As is the case for ENDF, PENDF, and GENDF files, ERRORR output files can be converted from binary to formatted form (and *vice versa*) by using the **MODER** module. The energy-group ordering of the data written to **nout** follows the ENDF convention, that is, low-energy groups precede high-energy groups.

It is occasionally of interest to examine a formatted ERRORR output file visually. For this and other reasons, we describe below the detailed form of the formatted output file. To assist in the description, we give below an example listing of such a file, which was produced during the processing of COVILS-2[77].

The data in the listing are written in the form of standard, 80-column card-images consisting of 10 data fields. As in ENDF, the first 6 fields are 11 characters wide and are used for either floating-point numbers or integers. The seventh, eighth, ninth, and tenth fields are 4, 2, 3, and 5 characters wide, respectively, and are used for integers only. The four digits in Field 7 are the **MAT**, or material number, of the isotope or element; the two digits in Field 8 are the **MF**, or file number, which indicates the general type of data (for example, cross-section data *vs.* covariance data); the three digits in Field 9 are the **MT**, or section number, which indicates the particular nuclear reaction; and finally, the five digits in Field 10 are **NSEQ**, the card sequence number. As usual, sections are terminated by zeros in the **MT** field, files by zeros in the **MF** field, and materials by zeros in the **MAT** field.

Following an initial tape header record, the second card shown in the listing is the first data card for the material **MAT**=1326, which is ENDF/B-V elemental iron. Note that on this card the number  $2.6 \times 10^4$  appears in the first field and 55.365 in the second field. These are the “ZA” ( $1000 \times Z - A$ ) and “AWR” (atomic weight relative to the neutron) numbers taken directly from the ENDF file. The fact that ZA is 26 000 (suggesting that  $A = 0$ ) is a convention that means that the data are for the natural element, Fe, rather than for a single isotope. The value of -11 appearing in Field 5 is a flag (read by the **MODER**

module, for example) that identifies the present file format as the ERRORR output format.

Also note that MF=1 and MT=451 on cards NSEQ=1 - 15. This MF, MT combination is used in the ENDF format for descriptive Hollerith information, but it is used here to specify the boundaries of the multigroup structure used for the processed data to follow. On Card 2, note the number 74 in Field 3 and the number 75 in Field 5, which indicate, respectively, the number of energy groups and the number of energy-group boundaries in the multigroup set. The values of the group boundaries, given in eV from low to high energy, follow in Cards 3 through 15. Cards 16 and 17 are section and file terminators, respectively.

Multigroup cross-section data are given in barns on Cards 18 through 631. This file, denoted by MF=3, corresponds to the smooth cross-section file in ENDF. The MT-numbers (Field 9) can be identified with particular nuclear reactions by consulting Appendix B of the ENDF format manual [8]. Note that cross sections for the lumped-partial reaction MT=851 have been constructed by ERRORR according to the directions given in the ENDF file.

#### Example of ERRORR Output Data File

|            |            |            |            |            |            |      |       |      |   |    |  |
|------------|------------|------------|------------|------------|------------|------|-------|------|---|----|--|
|            |            |            |            |            |            |      | 1     | 0    | 0 | 0  |  |
| 2.600000+4 | 5.536500+1 | 0          | 0          | -11        |            |      | 01326 | 1451 |   | 1  |  |
| 0.000000+0 | 0.000000+0 | 74         | 0          | 75         |            |      | 01326 | 1451 |   | 2  |  |
| 1.000000-5 | 7.602200-4 | 1.239500-2 | 4.275500-2 | 8.196800-2 | 1.523000-1 | 1326 | 1451  |      |   | 3  |  |
| 4.139900-1 | 8.764200-1 | 1.125400+0 | 1.855400+0 | 3.927900+0 | 5.043500+0 | 1326 | 1451  |      |   | 4  |  |
| 8.315300+0 | 1.760300+1 | 3.726700+1 | 7.889300+1 | 1.013000+2 | 1.670200+2 | 1326 | 1451  |      |   | 5  |  |
| 3.535800+2 | 7.485200+2 | 1.584600+3 | 3.354600+3 | 7.101700+3 | 9.118800+3 | 1326 | 1451  |      |   | 6  |  |
| 1.503400+4 | 2.478800+4 | 2.605800+4 | 2.808800+4 | 3.182800+4 | 4.086800+4 | 1326 | 1451  |      |   | 7  |  |
| 5.247500+4 | 6.737900+4 | 8.651700+4 | 1.110900+5 | 1.426400+5 | 1.831600+5 | 1326 | 1451  |      |   | 8  |  |
| 2.351800+5 | 3.019700+5 | 3.877400+5 | 4.393700+5 | 4.978700+5 | 5.641600+5 | 1326 | 1451  |      |   | 9  |  |
| 6.392800+5 | 7.244000+5 | 8.208500+5 | 1.054000+6 | 1.194300+6 | 1.353400+6 | 1326 | 1451  |      |   | 10 |  |
| 1.737700+6 | 1.969100+6 | 2.231300+6 | 2.528400+6 | 2.865000+6 | 3.246500+6 | 1326 | 1451  |      |   | 11 |  |
| 3.678800+6 | 4.168600+6 | 4.723700+6 | 5.352600+6 | 6.065300+6 | 6.872900+6 | 1326 | 1451  |      |   | 12 |  |
| 7.788000+6 | 8.825000+6 | 1.000000+7 | 1.100000+7 | 1.200000+7 | 1.300000+7 | 1326 | 1451  |      |   | 13 |  |
| 1.350000+7 | 1.375000+7 | 1.394000+7 | 1.420000+7 | 1.442000+7 | 1.464000+7 | 1326 | 1451  |      |   | 14 |  |
| 1.500000+7 | 1.600000+7 | 2.000000+7 |            |            |            | 1326 | 1451  |      |   | 15 |  |
|            |            |            |            |            |            | 1326 | 1     | 0    |   | 16 |  |
|            |            |            |            |            |            | 1326 | 0     | 0    |   | 17 |  |
| 0.000000+0 | 0.000000+0 | 0          | 0          | 74         |            |      | 01326 | 3    | 1 | 18 |  |
| 3.242538+1 | 1.638221+1 | 1.395614+1 | 1.310400+1 | 1.266828+1 | 1.222209+1 | 1326 | 3     | 1    |   | 19 |  |
| 1.192867+1 | 1.180887+1 | 1.173992+1 | 1.164882+1 | 1.159180+1 | 1.155850+1 | 1326 | 3     | 1    |   | 20 |  |
| 1.151292+1 | 1.146973+1 | 1.143331+1 | 1.140845+1 | 1.137811+1 | 1.103735+1 | 1326 | 3     | 1    |   | 21 |  |

|            |            |            |            |            |            |      |      |     |    |
|------------|------------|------------|------------|------------|------------|------|------|-----|----|
| 1.031032+1 | 9.276154+0 | 7.382612+0 | 7.137478+0 | 1.602539+1 | 4.178159+0 | 1326 | 3    | 1   | 22 |
| 1.482726+0 | 1.406100+0 | 3.875233+1 | 3.832471+1 | 8.517735+0 | 5.325881+0 | 1326 | 3    | 1   | 23 |
| 4.200487+0 | 6.723474+0 | 4.481126+0 | 3.610952+0 | 3.923129+0 | 4.868550+0 | 1326 | 3    | 1   | 24 |
| 2.836503+0 | 3.245566+0 | 4.853495+0 | 3.640536+0 | 3.205600+0 | 2.250606+0 | 1326 | 3    | 1   | 25 |
| 2.732808+0 | 3.895072+0 | 2.571093+0 | 2.501068+0 | 2.958182+0 | 2.985432+0 | 1326 | 3    | 1   | 26 |
| 2.899251+0 | 3.213480+0 | 3.189247+0 | 3.477117+0 | 3.389077+0 | 3.403654+0 | 1326 | 3    | 1   | 27 |
| 3.625322+0 | 3.668095+0 | 3.697471+0 | 3.674937+0 | 3.632669+0 | 3.545578+0 | 1326 | 3    | 1   | 28 |
| 3.383465+0 | 3.214864+0 | 3.053930+0 | 2.905813+0 | 2.743816+0 | 2.674006+0 | 1326 | 3    | 1   | 29 |
| 2.635890+0 | 2.613351+0 | 2.590513+0 | 2.567519+0 | 2.547020+0 | 2.517568+0 | 1326 | 3    | 1   | 30 |
| 2.457292+0 | 2.307503+0 |            |            |            |            | 1326 | 3    | 1   | 31 |
|            |            |            |            |            |            | 1326 | 3    | 0   | 32 |
| 0.000000+0 | 0.000000+0 | 0          | 0          | 74         | 01326      | 3    | 2    | 33  |    |
| 1.140000+1 | 1.140000+1 | 1.139999+1 | 1.139998+1 | 1.139996+1 | 1.139991+1 | 1326 | 3    | 2   | 34 |
| 1.139978+1 | 1.139964+1 | 1.139947+1 | 1.139900+1 | 1.139839+1 | 1.139764+1 | 1326 | 3    | 2   | 35 |
| 1.139553+1 | 1.139053+1 | 1.137995+1 | 1.136763+1 | 1.134459+1 | 1.101228+1 | 1326 | 3    | 2   | 36 |
| 1.029462+1 | 9.055728+0 | 7.376526+0 | 7.127705+0 | 1.599799+1 | 4.168132+0 | 1326 | 3    | 2   | 37 |
| 1.450895+0 | 1.368534+0 | 3.867417+1 | 3.827977+1 | 8.473823+0 | 5.294164+0 | 1326 | 3    | 2   | 38 |
| 4.169383+0 | 6.691388+0 | 4.451224+0 | 3.586689+0 | 3.901454+0 | 4.844768+0 | 1326 | 3    | 2   | 39 |
| 2.815969+0 | 3.225118+0 | 4.830640+0 | 3.616074+0 | 3.180014+0 | 2.223638+0 | 1326 | 3    | 2   | 40 |
| 2.703083+0 | 3.863693+0 | 2.346491+0 | 2.057345+0 | 2.535809+0 | 2.262868+0 | 1326 | 3    | 2   | 41 |
| 2.127090+0 | 2.261804+0 | 2.256791+0 | 2.533315+0 | 2.231035+0 | 2.144008+0 | 1326 | 3    | 2   | 42 |
| 2.151420+0 | 2.170908+0 | 2.095557+0 | 2.088164+0 | 2.073116+0 | 2.006202+0 | 1326 | 3    | 2   | 43 |
| 1.857245+0 | 1.711327+0 | 1.565212+0 | 1.419054+0 | 1.283900+0 | 1.274210+0 | 1326 | 3    | 2   | 44 |
| 1.266290+0 | 1.253001+0 | 1.238749+0 | 1.224132+0 | 1.210283+0 | 1.196914+0 | 1326 | 3    | 2   | 45 |
| 1.165341+0 | 1.042323+0 |            |            |            |            | 1326 | 3    | 2   | 46 |
|            |            |            |            |            |            | 1326 | 3    | 0   | 47 |
| .          | .          |            |            |            |            |      |      |     |    |
| 0.000000+0 | 0.000000+0 | 0          | 0          | 74         | 01326      | 3107 | 603  |     |    |
| 0.000000+0 | 0.000000+0 | 0.000000+0 | 0.000000+0 | 0.000000+0 | 0.000000+0 | 1326 | 3107 | 604 |    |
| 0.000000+0 | 0.000000+0 | 0.000000+0 | 0.000000+0 | 0.000000+0 | 0.000000+0 | 1326 | 3107 | 605 |    |
| 0.000000+0 | 0.000000+0 | 0.000000+0 | 0.000000+0 | 0.000000+0 | 0.000000+0 | 1326 | 3107 | 606 |    |
| 0.000000+0 | 0.000000+0 | 0.000000+0 | 0.000000+0 | 0.000000+0 | 0.000000+0 | 1326 | 3107 | 607 |    |
| 0.000000+0 | 0.000000+0 | 0.000000+0 | 0.000000+0 | 0.000000+0 | 0.000000+0 | 1326 | 3107 | 608 |    |
| 0.000000+0 | 0.000000+0 | 0.000000+0 | 0.000000+0 | 0.000000+0 | 0.000000+0 | 1326 | 3107 | 609 |    |
| 0.000000+0 | 0.000000+0 | 0.000000+0 | 0.000000+0 | 0.000000+0 | 0.000000+0 | 1326 | 3107 | 610 |    |
| 0.000000+0 | 0.000000+0 | 0.000000+0 | 0.000000+0 | 0.000000+0 | 0.000000+0 | 1326 | 3107 | 611 |    |
| 0.000000+0 | 0.000000+0 | 0.000000+0 | 0.000000+0 | 5.054213-6 | 3.154394-5 | 1326 | 3107 | 612 |    |
| 6.536392-5 | 1.636755-4 | 4.937945-4 | 1.599742-3 | 4.467725-3 | 9.026301-3 | 1326 | 3107 | 613 |    |
| 1.492042-2 | 2.174807-2 | 2.912657-2 | 3.467999-2 | 3.849531-2 | 3.982821-2 | 1326 | 3107 | 614 |    |
| 3.986411-2 | 3.988542-2 | 3.971171-2 | 3.918684-2 | 3.866013-2 | 3.800829-2 | 1326 | 3107 | 615 |    |
| 3.513214-2 | 1.922833-2 |            |            |            |            | 1326 | 3107 | 616 |    |

|            |            |            |            |            |                     |          |      |
|------------|------------|------------|------------|------------|---------------------|----------|------|
|            |            |            |            |            |                     | 1326 3 0 | 617  |
| 0.000000+0 | 0.000000+0 | 0          | 0          | 74         | 01326 3851          |          | 618  |
| 0.000000+0 | 0.000000+0 | 0.000000+0 | 0.000000+0 | 0.000000+0 | 0.000000+01326 3851 |          | 619  |
| 0.000000+0 | 0.000000+0 | 0.000000+0 | 0.000000+0 | 0.000000+0 | 0.000000+01326 3851 |          | 620  |
| 0.000000+0 | 0.000000+0 | 0.000000+0 | 0.000000+0 | 0.000000+0 | 0.000000+01326 3851 |          | 621  |
| 0.000000+0 | 0.000000+0 | 0.000000+0 | 0.000000+0 | 0.000000+0 | 1.713016-41326 3851 |          | 622  |
| 2.605423-2 | 2.747897-2 | 2.715636-2 | 2.656936-2 | 2.500170-2 | 2.240780-21326 3851 |          | 623  |
| 2.044663-2 | 1.866612-2 | 1.650006-2 | 1.483479-2 | 1.452751-2 | 1.445474-21326 3851 |          | 624  |
| 1.484054-2 | 1.514701-2 | 1.823890-2 | 1.948106-2 | 2.054081-2 | 2.151007-21326 3851 |          | 625  |
| 2.239315-2 | 2.355651-2 | 2.568895-2 | 2.711755-2 | 2.775385-2 | 2.831557-21326 3851 |          | 626  |
| 2.892825-2 | 2.891470-2 | 2.891944-2 | 2.909114-2 | 2.816820-2 | 2.648783-21326 3851 |          | 627  |
| 2.379156-2 | 2.036489-2 | 1.658885-2 | 1.236790-2 | 8.719756-3 | 5.515926-31326 3851 |          | 628  |
| 2.789373-3 | 1.967219-3 | 1.199289-3 | 5.263406-4 | 1.809961-4 | 1.629883-41326 3851 |          | 629  |
| 1.542762-4 | 1.491088-4 | 1.438805-4 | 1.385182-4 | 1.332255-4 | 1.265700-41326 3851 |          | 630  |
| 1.111753-4 | 5.198675-5 |            |            |            | 1326 3851           |          | 631  |
|            |            |            |            |            | 1326 3 0            |          | 632  |
|            |            |            |            |            | 1326 0 0            |          | 633  |
| 2.600000+4 | 5.536500+1 | 0          | 0          | 0          | 41132633            | 1        | 634  |
| 0.000000+0 | 0.000000+0 | 0          | 1          | 0          | 74132633            | 1        | 635  |
| 0.000000+0 | 0.000000+0 | 17         | 1          | 17         | 1132633             | 1        | 636  |
| 4.771962-4 | 6.905149-4 | 7.654629-4 | 7.983731-4 | 8.169108-4 | 8.372624-4132633    | 1        | 637  |
| 8.514704-4 | 8.574701-4 | 8.609741-4 | 8.656539-4 | 8.686033-4 | 8.703185-4132633    | 1        | 638  |
| 8.707277-4 | 8.728724-4 | 8.748390-4 | 8.757964-4 | 7.461125-4 | 132633              | 1        | 639  |
| 0.000000+0 | 0.000000+0 | 17         | 1          | 17         | 2132633             | 1        | 640  |
| 6.905149-4 | 1.247608-3 | 1.443338-3 | 1.529285-3 | 1.577697-3 | 1.630846-3132633    | 1        | 641  |
| 1.667951-3 | 1.683619-3 | 1.692770-3 | 1.704992-3 | 1.712694-3 | 1.717174-3132633    | 1        | 642  |
| 1.722305-3 | 1.727680-3 | 1.731573-3 | 1.733468-3 | 1.476784-3 | 132633              | 1        | 643  |
| 0.000000+0 | 0.000000+0 | 17         | 1          | 17         | 3132633             | 1        | 644  |
| 7.654629-4 | 1.443338-3 | 1.681504-3 | 1.786085-3 | 1.844993-3 | 1.909666-3132633    | 1        | 645  |
| 1.954815-3 | 1.973881-3 | 1.985016-3 | 1.999887-3 | 2.009259-3 | 2.014710-3132633    | 1        | 646  |
| 2.021500-3 | 2.028010-3 | 2.032580-3 | 2.034804-3 | 1.733500-3 | 132633              | 1        | 647  |
| 0.000000+0 | 0.000000+0 | 17         | 1          | 17         | 4132633             | 1        | 648  |
| 7.983731-4 | 1.529285-3 | 1.786085-3 | 1.898848-3 | 1.962365-3 | 2.032098-3132633    | 1        | 649  |
| 2.080780-3 | 2.101337-3 | 2.113343-3 | 2.129378-3 | 2.139484-3 | 2.145360-3132633    | 1        | 650  |
| 2.152879-3 | 2.159888-3 | 2.164754-3 | 2.167123-3 | 1.846226-3 | 132633              | 1        | 651  |
| .          |            |            |            |            |                     |          |      |
| .          |            |            |            |            |                     |          |      |
| 0.000000+0 | 0.000000+0 | 0          | 102        | 0          | 74132633            | 1        | 1738 |
| 0.000000+0 | 0.000000+0 | 13         | 1          | 13         | 1132633             | 1        | 1739 |
| 2.593694-4 | 2.593694-4 | 2.593694-4 | 2.593694-4 | 2.593694-4 | 2.593694-4132633    | 1        | 1740 |
| 2.593694-4 | 2.593694-4 | 2.593694-4 | 2.593694-4 | 2.593694-4 | 2.593694-4132633    | 1        | 1741 |
| 7.341822-5 |            |            |            |            | 132633              | 1        | 1742 |

|            |            |            |            |            |            |        |        |
|------------|------------|------------|------------|------------|------------|--------|--------|
| 0.000000+0 | 0.000000+0 | 13         | 1          | 13         | 2132633    | 1      | 1743   |
| 1.216493-4 | 1.216493-4 | 1.216493-4 | 1.216493-4 | 1.216493-4 | 1.216493-4 | 132633 | 1 1744 |
| 1.216493-4 | 1.216493-4 | 1.216493-4 | 1.216493-4 | 1.216493-4 | 1.216493-4 | 132633 | 1 1745 |
| 3.443457-5 |            |            |            |            |            | 132633 | 1 1746 |
| 0.000000+0 | 0.000000+0 | 13         | 1          | 13         | 3132633    | 1      | 1747   |
| 7.326236-5 | 7.326236-5 | 7.326236-5 | 7.326236-5 | 7.326236-5 | 7.326236-5 | 132633 | 1 1748 |
| 7.326236-5 | 7.326236-5 | 7.326236-5 | 7.326236-5 | 7.326236-5 | 7.326236-5 | 132633 | 1 1749 |
| 2.073796-5 |            |            |            |            |            | 132633 | 1 1750 |
| 0.000000+0 | 0.000000+0 | 13         | 1          | 13         | 4132633    | 1      | 1751   |
| 5.201525-5 | 5.201525-5 | 5.201525-5 | 5.201525-5 | 5.201525-5 | 5.201525-5 | 132633 | 1 1752 |
| 5.201525-5 | 5.201525-5 | 5.201525-5 | 5.201525-5 | 5.201525-5 | 5.201525-5 | 132633 | 1 1753 |
| 1.472366-5 |            |            |            |            |            | 132633 | 1 1754 |
| 0.000000+0 | 0.000000+0 | 13         | 1          | 13         | 5132633    | 1      | 1755   |
| 4.004717-5 | 4.004717-5 | 4.004717-5 | 4.004717-5 | 4.004717-5 | 4.004717-5 | 132633 | 1 1756 |
| 4.004717-5 | 4.004717-5 | 4.004717-5 | 4.004717-5 | 4.004717-5 | 4.004717-5 | 132633 | 1 1757 |
| 1.133592-5 |            |            |            |            |            | 132633 | 1 1758 |
| 0.000000+0 | 0.000000+0 | 13         | 1          | 13         | 6132633    | 1      | 1759   |
| 2.690806-5 | 2.690806-5 | 2.690806-5 | 2.690806-5 | 2.690806-5 | 2.690806-5 | 132633 | 1 1760 |
| 2.690806-5 | 2.690806-5 | 2.690806-5 | 2.690806-5 | 2.690806-5 | 2.690806-5 | 132633 | 1 1761 |
| 7.616711-6 |            |            |            |            |            | 132633 | 1 1762 |
| 0.000000+0 | 0.000000+0 | 13         | 1          | 13         | 7132633    | 1      | 1763   |
| 1.773523-5 | 1.773523-5 | 1.773523-5 | 1.773523-5 | 1.773523-5 | 1.773523-5 | 132633 | 1 1764 |
| 1.773523-5 | 1.773523-5 | 1.773523-5 | 1.773523-5 | 1.773523-5 | 1.773523-5 | 132633 | 1 1765 |
| 5.020211-6 |            |            |            |            |            | 132633 | 1 1766 |
| 0.000000+0 | 0.000000+0 | 13         | 1          | 13         | 8132633    | 1      | 1767   |
| 1.386183-5 | 1.386183-5 | 1.386183-5 | 1.386183-5 | 1.386183-5 | 1.386183-5 | 132633 | 1 1768 |
| 1.386183-5 | 1.386183-5 | 1.386183-5 | 1.386183-5 | 1.386183-5 | 1.386183-5 | 132633 | 1 1769 |
| 3.923789-6 |            |            |            |            |            | 132633 | 1 1770 |
| 0.000000+0 | 0.000000+0 | 13         | 1          | 13         | 9132633    | 1      | 1771   |
| 1.159959-5 | 1.159959-5 | 1.159959-5 | 1.159959-5 | 1.159959-5 | 1.159959-5 | 132633 | 1 1772 |
| 1.159959-5 | 1.159959-5 | 1.159959-5 | 1.159959-5 | 1.159959-5 | 1.159959-5 | 132633 | 1 1773 |
| 3.283431-6 |            |            |            |            |            | 132633 | 1 1774 |
| 0.000000+0 | 0.000000+0 | 13         | 1          | 13         | 10132633   | 1      | 1775   |
| 8.578299-6 | 8.578299-6 | 8.578299-6 | 8.578299-6 | 8.578299-6 | 8.578299-6 | 132633 | 1 1776 |
| 8.578299-6 | 8.578299-6 | 8.578299-6 | 8.578299-6 | 8.578299-6 | 8.578299-6 | 132633 | 1 1777 |
| 2.428210-6 |            |            |            |            |            | 132633 | 1 1778 |
| 0.000000+0 | 0.000000+0 | 13         | 1          | 13         | 11132633   | 1      | 1779   |
| 6.674139-6 | 6.674139-6 | 6.674139-6 | 6.674139-6 | 6.674139-6 | 6.674139-6 | 132633 | 1 1780 |
| 6.674139-6 | 6.674139-6 | 6.674139-6 | 6.674139-6 | 6.674139-6 | 6.674139-6 | 132633 | 1 1781 |
| 1.889210-6 |            |            |            |            |            | 132633 | 1 1782 |
| 0.000000+0 | 0.000000+0 | 13         | 1          | 13         | 12132633   | 1      | 1783   |
| 5.566800-6 | 5.566800-6 | 5.566800-6 | 5.566800-6 | 5.566800-6 | 5.566800-6 | 132633 | 1 1784 |

|            |            |            |            |            |            |          |   |      |
|------------|------------|------------|------------|------------|------------|----------|---|------|
| 5.566800-6 | 5.566800-6 | 5.566800-6 | 5.566800-6 | 5.566800-6 | 5.566800-6 | 132633   | 1 | 1785 |
| 1.575762-6 |            |            |            |            |            | 132633   | 1 | 1786 |
| 0.000000+0 | 0.000000+0 | 17         | 1          | 17         |            | 13132633 | 1 | 1787 |
| 1.154480-6 | 1.154480-6 | 1.154480-6 | 1.154480-6 | 1.154480-6 | 1.154480-6 | 132633   | 1 | 1788 |
| 1.154480-6 | 1.154480-6 | 1.154480-6 | 1.154480-6 | 1.154480-6 | 1.154480-6 | 132633   | 1 | 1789 |
| 1.342892-5 | 1.827518-5 | 1.827518-5 | 1.827518-5 | 1.584766-5 |            | 132633   | 1 | 1790 |
| 0.000000+0 | 0.000000+0 | 5          | 13         | 5          |            | 14132633 | 1 | 1791 |
| 1.237530-5 | 1.726138-5 | 1.726138-5 | 1.726138-5 | 1.496853-5 |            | 132633   | 1 | 1792 |
| 0.000000+0 | 0.000000+0 | 5          | 13         | 5          |            | 15132633 | 1 | 1793 |
| 8.364854-6 | 1.166751-5 | 1.166751-5 | 1.166751-5 | 1.011770-5 |            | 132633   | 1 | 1794 |
| 0.000000+0 | 0.000000+0 | 5          | 13         | 5          |            | 16132633 | 1 | 1795 |
| 6.412509-6 | 8.944329-6 | 8.944329-6 | 8.944329-6 | 7.756243-6 |            | 132633   | 1 | 1796 |
| 0.000000+0 | 0.000000+0 | 27         | 13         | 27         |            | 17132633 | 1 | 1797 |
| 4.578647-6 | 6.386412-6 | 6.386412-6 | 6.386412-6 | 6.057870-6 | 3.913034-6 | 132633   | 1 | 1798 |
| 3.913034-6 | 3.913034-6 | 3.913034-6 | 3.913034-6 | 3.913034-6 | 3.913034-6 | 132633   | 1 | 1799 |
| 3.913034-6 | 3.913034-6 | 3.913034-6 | 3.913034-6 | 3.913034-6 | 3.913034-6 | 132633   | 1 | 1800 |
| 3.913034-6 | 3.913034-6 | 3.913034-6 | 3.913034-6 | 3.913034-6 | 3.913034-6 | 132633   | 1 | 1801 |
| 3.913034-6 | 3.913034-6 | 7.376951-7 |            |            |            | 132633   | 1 | 1802 |
| 0.000000+0 | 0.000000+0 | 23         | 17         | 23         |            | 18132633 | 1 | 1803 |
| 3.017049-6 | 2.271340-5 | 2.271340-5 | 2.271340-5 | 2.271340-5 | 2.271340-5 | 132633   | 1 | 1804 |
| 2.271340-5 | 2.271340-5 | 2.271340-5 | 2.271340-5 | 2.271340-5 | 2.271340-5 | 132633   | 1 | 1805 |
| 2.271340-5 | 2.271340-5 | 2.271340-5 | 2.271340-5 | 2.271340-5 | 2.271340-5 | 132633   | 1 | 1806 |
| 2.271340-5 | 2.271340-5 | 2.271340-5 | 2.271340-5 | 4.281989-6 |            | 132633   | 1 | 1807 |
| 0.000000+0 | 0.000000+0 | 23         | 17         | 23         |            | 19132633 | 1 | 1808 |
| 2.023187-6 | 1.523126-5 | 1.523126-5 | 1.523126-5 | 1.523126-5 | 1.523126-5 | 132633   | 1 | 1809 |
| 1.523126-5 | 1.523126-5 | 1.523126-5 | 1.523126-5 | 1.523126-5 | 1.523126-5 | 132633   | 1 | 1810 |
| 1.523126-5 | 1.523126-5 | 1.523126-5 | 1.523126-5 | 1.523126-5 | 1.523126-5 | 132633   | 1 | 1811 |
| 1.523126-5 | 1.523126-5 | 1.523126-5 | 1.523126-5 | 2.871437-6 |            | 132633   | 1 | 1812 |
| 0.000000+0 | 0.000000+0 | 23         | 17         | 23         |            | 20132633 | 1 | 1813 |
| 3.156422-5 | 2.376265-4 | 2.376265-4 | 2.376265-4 | 2.376265-4 | 2.376265-4 | 132633   | 1 | 1814 |
| 2.376265-4 | 2.376265-4 | 2.376265-4 | 2.376265-4 | 2.376265-4 | 2.376265-4 | 132633   | 1 | 1815 |
| 2.376265-4 | 2.376265-4 | 2.376265-4 | 2.376265-4 | 2.376265-4 | 2.376265-4 | 132633   | 1 | 1816 |
| 2.376265-4 | 2.376265-4 | 2.376265-4 | 2.376265-4 | 4.479796-5 |            | 132633   | 1 | 1817 |
| .          |            |            |            |            |            |          |   |      |
| .          |            |            |            |            |            |          |   |      |
| 2.666295-6 | 2.007280-5 | 2.007280-5 | 2.007280-5 | 2.007280-5 | 2.007280-5 | 132633   | 1 | 1899 |
| 2.007280-5 | 2.007280-5 | 2.007280-5 | 2.007280-5 | 2.007280-5 | 2.007280-5 | 132633   | 1 | 1900 |
| 2.007280-5 | 2.007280-5 | 2.007280-5 | 2.007280-5 | 2.007280-5 | 2.007280-5 | 132633   | 1 | 1901 |
| 2.007280-5 | 2.007280-5 | 2.007280-5 | 2.007280-5 | 3.784176-6 |            | 132633   | 1 | 1902 |
| 0.000000+0 | 0.000000+0 | 23         | 17         | 23         |            | 38132633 | 1 | 1903 |
| 2.169670-6 | 1.633404-5 | 1.633404-5 | 1.633404-5 | 1.633404-5 | 1.633404-5 | 132633   | 1 | 1904 |
| 1.633404-5 | 1.633404-5 | 1.633404-5 | 1.633404-5 | 1.633404-5 | 1.633404-5 | 132633   | 1 | 1905 |

|            |            |            |            |            |            |          |   |      |
|------------|------------|------------|------------|------------|------------|----------|---|------|
| 1.633404-5 | 1.633404-5 | 1.633404-5 | 1.633404-5 | 1.633404-5 | 1.633404-5 | 132633   | 1 | 1906 |
| 1.633404-5 | 1.633404-5 | 1.633404-5 | 1.633404-5 | 3.079335-6 |            | 132633   | 1 | 1907 |
| 0.000000+0 | 0.000000+0 | 23         | 17         | 23         |            | 39132633 | 1 | 1908 |
| 2.382007-7 | 1.793258-6 | 1.793258-6 | 1.793258-6 | 1.793258-6 | 1.793258-6 | 132633   | 1 | 1909 |
| 1.793258-6 | 1.793258-6 | 1.793258-6 | 1.793258-6 | 1.793258-6 | 1.793258-6 | 132633   | 1 | 1910 |
| 1.793258-6 | 1.793258-6 | 1.793258-6 | 1.793258-6 | 1.793258-6 | 1.793258-6 | 132633   | 1 | 1911 |
| 1.793258-6 | 1.793258-6 | 1.793258-6 | 1.793258-6 | 3.380696-7 |            | 132633   | 1 | 1912 |
| 0.000000+0 | 0.000000+0 | 1          | 74         | 1          |            | 74132633 | 1 | 1913 |
| 0.000000+0 |            |            |            |            |            | 132633   | 1 | 1914 |
| 0.000000+0 | 0.000000+0 | 0          | 103        | 0          |            | 74132633 | 1 | 1915 |
| 0.000000+0 | 0.000000+0 | 1          | 74         | 1          |            | 74132633 | 1 | 1916 |
| 0.000000+0 |            |            |            |            |            | 132633   | 1 | 1917 |
| 0.000000+0 | 0.000000+0 | 0          | 104        | 0          |            | 74132633 | 1 | 1918 |
| 0.000000+0 | 0.000000+0 | 1          | 74         | 1          |            | 74132633 | 1 | 1919 |
| 0.000000+0 |            |            |            |            |            | 132633   | 1 | 1920 |
| 0.000000+0 | 0.000000+0 | 0          | 105        | 0          |            | 74132633 | 1 | 1921 |
| 0.000000+0 | 0.000000+0 | 1          | 74         | 1          |            | 74132633 | 1 | 1922 |
| 0.000000+0 |            |            |            |            |            | 132633   | 1 | 1923 |
| 0.000000+0 | 0.000000+0 | 0          | 106        | 0          |            | 74132633 | 1 | 1924 |
| 0.000000+0 | 0.000000+0 | 1          | 74         | 1          |            | 74132633 | 1 | 1925 |
| 0.000000+0 |            |            |            |            |            | 132633   | 1 | 1926 |
| 0.000000+0 | 0.000000+0 | 0          | 107        | 0          |            | 74132633 | 1 | 1927 |
| 0.000000+0 | 0.000000+0 | 1          | 74         | 1          |            | 74132633 | 1 | 1928 |
| 0.000000+0 |            |            |            |            |            | 132633   | 1 | 1929 |
| 0.000000+0 | 0.000000+0 | 0          | 851        | 0          |            | 74132633 | 1 | 1930 |
| 0.000000+0 | 0.000000+0 | 1          | 74         | 1          |            | 74132633 | 1 | 1931 |
| 0.000000+0 |            |            |            |            |            | 132633   | 1 | 1932 |
|            |            |            |            |            |            | 132633   | 0 | 1933 |
| 2.600000+4 | 5.536500+1 | 0          | 0          | 0          |            | 40132633 | 2 | 1934 |
| 0.000000+0 | 0.000000+0 | 0          | 2          | 0          |            | 74132633 | 2 | 1935 |
| 0.000000+0 | 0.000000+0 | 17         | 1          | 17         |            | 1132633  | 2 | 1936 |
| 2.500000-3 | 2.500000-3 | 2.500000-3 | 2.500000-3 | 2.500000-3 | 2.500000-3 | 132633   | 2 | 1937 |
| 2.500000-3 | 2.500000-3 | 2.500000-3 | 2.500000-3 | 2.500000-3 | 2.500000-3 | 132633   | 2 | 1938 |
| 2.500000-3 | 2.500000-3 | 2.500000-3 | 2.500000-3 | 2.128462-3 |            | 132633   | 2 | 1939 |
| 0.000000+0 | 0.000000+0 | 17         | 1          | 17         |            | 2132633  | 2 | 1940 |
| 2.500000-3 | 2.500000-3 | 2.500000-3 | 2.500000-3 | 2.500000-3 | 2.500000-3 | 132633   | 2 | 1941 |
| 2.500000-3 | 2.500000-3 | 2.500000-3 | 2.500000-3 | 2.500000-3 | 2.500000-3 | 132633   | 2 | 1942 |
| 2.500000-3 | 2.500000-3 | 2.500000-3 | 2.500000-3 | 2.128462-3 |            | 132633   | 2 | 1943 |
| 0.000000+0 | 0.000000+0 | 17         | 1          | 17         |            | 3132633  | 2 | 1944 |
| 2.500000-3 | 2.500000-3 | 2.500000-3 | 2.500000-3 | 2.500000-3 | 2.500000-3 | 132633   | 2 | 1945 |
| 2.500000-3 | 2.500000-3 | 2.500000-3 | 2.500000-3 | 2.500000-3 | 2.500000-3 | 132633   | 2 | 1946 |
| 2.500000-3 | 2.500000-3 | 2.500000-3 | 2.500000-3 | 2.128462-3 |            | 132633   | 2 | 1947 |



```

0.000000+0 0.000000+0          17          1          17          4132633  2 1948
2.500000-3 2.500000-3 2.500000-3 2.500000-3 2.500000-3 2.500000-3132633  2 1949
2.500000-3 2.500000-3 2.500000-3 2.500000-3 2.500000-3 2.500000-3132633  2 1950
2.500000-3 2.500000-3 2.500000-3 2.500000-3 2.128462-3          132633  2 1951
.
.

```

The processed multigroup covariance data for MAT=1326 begin with Card 634. The designation of MF=33 in Field 8 is the value of `mfcov`, as discussed in Section 10.14. Card 634 repeats the ZA and AWR numbers in Fields 1 and 2, and the number 41 in Field 6 indicates that covariance matrices follow for 41 reaction pairs. The number 1 in the MT field (Field 9) indicates that all 41 reaction-pairs have MT=1 as the first reaction.

The data for one such reaction pair begin at Card 1738. Field 4 of Card 1738 (a CONT record) contains the number 102, so the second reaction here is MT1=102. In other words, the data to follow refer to the covariance matrix of the iron total cross section (MT=1) with the iron radiative capture reaction (MT1=102). This is followed by 74 LIST records, one for each group. The occurrence of the number 14 in Field 6 of Card 1791 indicates that the block of data starting there refers to Group 14 of MT=1, *i.e.*, the fourteenth row of the covariance matrix. The number 5 in Field 3 of Card 1791 indicates that there are 5 consecutive groups of MT1=102 for which covariances will be given explicitly. The first covariance applies to group 13 of MT1=102, as indicated by the number 13 in Field 4. Then, in referring to the entry in the fifth field of Card 1792, for example, one would say that the relative covariance of the iron total cross section in Group 14 (17.603 – 37.267 eV) with the iron radiative capture cross section in Group 17 (101.3 – 167.02 eV) is  $1.496853 \times 10^{-5}$ .

Any row of a covariance matrix, or any part of a row, that contains only zeros is omitted from the ERRORR output file. The only exception is that the last row (Group 74 here) is always given explicitly, even if it does contain only zeros. The occurrence of the last row terminates a given covariance matrix and signals that the next card will name a new reaction pair. These two conventions are applied simultaneously in Cards 1915 – 1917 to compactly represent the covariance matrix for a reaction pair (1, 103) having only zero covariances; a judgement made by the evaluator.

Although the output file in this example contained no cross-material covariances, the only difference in the file structure in the cross-material case is that MAT1 is specified in the integer field just preceding MT1, for example, in Field

3 on Card 1738. The entry MAT1=0 in that position is a flag to indicate that MAT1=MAT=1326.

## 10.16 Error Messages

**error in errorr\*\*\*error in 999 option**

If an input tape contains MF=32 data but no MF=33 data, the user must create a new tape with MF=33 placeholder data. This is done by specifying the input and output tapes and up to five cards with individual MT numbers. If the user attempts to specify more than 5 MT values, this error message occurs.

**error in errorr\*\*\*nstand should be different from nendf**

Check the input files.

**error in errorr\*\*\*illegal iread=---**

Currently defined values are 0, 1, and 2.

**error in errorr\*\*\*ngout must be nonzero when ...**

The ngout unit must be used mfcov=31, 35, or 40.

**error in errorr\*\*\*mfcov=35 requested but no spectra present**

The ENDF data doesn't support a request for mfcov=35.

**error in errorr\*\*\*User ifissp -- not found.**

When processing MF=35 data, the original tape shall contain information for a number of energy intervals. "ifissp" is the user specified energy interval to process and, if greater than zero, must be less than or equal to the number of intervals on the tape.

**error in errorj\*\*\*storage exceeded.**

Can occur in a number of ERRORR's routines, not just errorj. The source code should be examined to see what array needs to be increased.

**error in errorr\*\*\*no covariance data found for user ifissp.**

When processing MF=35 data, the original tape shall contain information for a number of energy intervals. The user may specify an energy interval with ifissp or define ifissp=-1 and then specify a specific mean energy efmean. If the specified energy is outside the range of the energy intervals on the input tape, this message results.

**error in errorr\*\*\*nendf-to-nendf2 copy for matd failed.**

This error should not occur. It means that an attempt to create a scratch tape for the required MATD from the original input tape has failed. Check that the input tape is not corrupted.

**error in errorr\*\*\*not coded for mfcov=---**

Allowed values are 31, 33, 34, 35, and 40.

**error in errorr\*\*\*not enough space for endf dictionary.**

The allocatable array dict has length nwi=4000. It needs to be increased.

error in errorr\*\*\*too many reaction types.

This error occurs in runs with `iverf=4` if the number of requested covariance reactions is more than 60. A possible solution is to use the `iread=1` option to select only the most needed reactions. This error also occurs in runs where internal group averaging is requested (`ngout=0`) if there are more than 200 sections in `MF=33`. An alternative is to run `GROUPR` first, then `ERRORR` with `ngout.gt.0`.

error in errorr\*\*\*only --- ek energies allowed.

The number of derived-cross-section energy-range boundaries is limited to `nkmax=50`.

error in errorr\*\*\*too many standards redefined.

Limit is 5. See input for `nstan.ne.0`.

error in gridd\*\*\*not coded for `nmt1>1` of `mf34`

When processing angular distribution uncertainty data (`MF=34`), `ERRORR` can only handle Legendre coefficient uncertainty data (`LTT=1`).

error in gridd\*\*\*illegal `mt1=0`.

Probably a fault in the evaluation.

error in gridd\*\*\*mt --- referenced in derivation ....

There is a fault in the evaluation or input.

error in gridd\*\*\*too many formulas in nc-type sub-sub ....

Limit is `irmax=80`.

error in gridd\*\*\*too many mt-numbers in nc-type sub-sub ....

Limit is `nmtmax=150`.

error in gridd\*\*\*cannot calculate covariance of reaction....

This message is self-explanatory.

error in gridd\*\*\*covariances of reaction....

There is a fault in the evaluation.

error in gridd\*\*\*nc subsection too big....

Increase `nwscr` in this subroutine.

error in gridd\*\*\*ni subsection too big....

Increase `nwscr` in this subroutine.

error in gridd\*\*\*too many reaction types.

This error occurs if `iverf=5` and if the requested number of covariance reactions is greater than 60. If cross-material covariances are not needed, then a possible solution is to use the `iread=1` option to select only the most needed reactions.

error in gridd\*\*\*illegal `mt1=0`.

There is fault in the evaluation. Evaluator may have meant to indicate `MT1=MT`. If so, change the data value for `MT1` on `NENDF` from 0 to `MT` and resubmit.

**error in merge\*\*\*storage exceeded.**

Either the number of points in the x grid exceeds `nxmax=5000` or the number in the y grid exceeds `nenimx=5000`.

**error in merge\*\*\*y(---)=--- lt y(---)=---**

This problem should not occur.

**error in grist\*\*\*standards tape bad.**

There is a fault in the evaluation. Standards reactions must have at least one subsection; that is, they may not be components of a lumped reaction.

**error in grist\*\*\*illegal lb=0.**

There is a fault in the evaluation. Absolute covariances are not permitted in the standards.

**error in grist\*\*\*illegal ni=0 in the standard,...**

There is a fault in the evaluation. Standards reactions may not be derived from other reactions.

**error in lumpmt\*\*\*storage exceeded.**

The number of component reactions of a lumped reaction is limited to `nlmt=50`.

**error in covcal\*\*\*storage exceeded in loc.**

The number of NI-type sub-subsections in any subsection is limited to `locm=30`.

**error in covcal\*\*\*lb=--- when lt=---**

There is a fault in the evaluation. The (lb, lt) combination is not defined.

**error in covcal\*\*\*not coded for lb=---**

Currently defined values are 0 through 6 and 8.

**error in covcal\*\*\*storage exceeded in egt.**

Should not occur, these arrays are now allocated based upon known storage requirements for this job.

**error in covcal\*\*\*mfcov mt found not equal to input mt.**

There is a conflict between internal list of covariance reactions and the reactions encountered in the ENDF file. This problem should not occur.

**error in covcal\*\*\*storage exceeded in scr.**

There is insufficient space to store the information from NI-type sub-subsections. Increase the size of `namx=2000000`.

**error in covcal\*\*\*illegal mt1=0.**

See similar diagnostic in subroutine `gridd` above.

**error in covcal\*\*\*data in scr(loci) are illegal.**

There is a fault in the evaluation. The ratio-to-standard data are bad. Either `LTY` is outside the legal ENDF range of 1 – 3 or the energies (`EL`, `EH`) are negative or out of order.

error in covcal\*\*\*must request mat1=--- and mt1=--- on ....

There is an input error in requesting covariances of X with Y when both are measured relative to Z. The standard Z must be specified on Card 10 and must appear as negative entries on Card 11.

error in covcal\*\*\*unpermitted for lb=--.

When processing MF34 data, LB values less than 0, or 3, 4, 7, and 8 are not supported.

error in sumchk\*\*\*endf file error....

The MF=35 matrix must be symmetric and the lb flag must be 7.

error in sumchk\*\*\*ne, ncove mismatch.

This error should not occur. It means that the number of elements NE that define the covariance matrix and that was saved in a working array does not match the number of elements now being processed to verify the "zero sum rule." The LOC(LI) array may be corrupted.

error in spcint\*\*\*no mf5 or mf6, mt=--- spectrum on nendf2.

This error should not occur. When processing MF=35 data, it means that the underlying spectrum data for this MT value (normally found in File 5 or File 6) is not present. The scratch copy nendf2 of the original input tape has been corrupted.

error in spcint\*\*\*not ready for lf = --.

We can only calculate the spectrum integral for lf=1 at this time.

error in spcint\*\*\*array overflow.

nnw, currently 10000, needs to be increased.

error in spcint\*\*\*looking for mf=6,mt=--.

Spectrum data from File 6 are ordered by increasing IZAP value, with the IZAP=1=neutron spectrum expected to occur first. For this MT, the initial spectrum was not for neutrons.

error in spcint\*\*\*not ready for mf=6, mt=---, law=--.

We can only calculate the spectrum integral for LAW=1 at this time.

error in rdgout\*\*\*mat --- not found.

Cannot find MAT on multigroup library.

error in rdgout\*\*\*mf---, mt--- not found.

Cannot find requested group structure or cross sections on multigroup library.

error in rdgout\*\*\*bad index for b equivalent to sig(ig).

This problem should not occur.

error in resprx\*\*\*illegal or no coding data structure ...

Only certain combinations of lru and lrf are supported. For lru=1, lrf=1, 2, 3, and 7 work. For lru=2, lrf=1 and 2 work.

error in resprx\*\*\*illegal or unrecognized data struct ....  
 nro .ne. 0 is not supported.

error in resprx\*\*\*cannot handle lrf=7 RML resonance rep....  
 You must set isammy=1 to enable the calculation of the derivatives using  
 the SAMMY method to process RML resonances.

error in resprx\*\*\*not ready for isr=1, lrf=--.  
 Option not yet coded.

error in resprx\*\*\*mf2/mf32 l-state mismatch ...  
 The nls value for mf32 URR data is larger than that specified in mf2. This  
 is likely an evaluation file error.

message from resprx---mf2 nls=I, but mf32 nls=J ...  
 The nls value for mf32 URR data is smaller than that specified in mf2.  
 Processing will continue but covariance data for the complete set of mf2  
 URR parameters is incomplete.

error in resprx\*\*\*illegal isr.  
 Only isr=0 allowed.

error in rpxsamm\*\*\*storage exceeded.  
 Increase nwds, currently 1500000, in covout.

error in rpxlc0\*\*\*storage exceeded.  
 See maxnls=10.

error in rpxlc0\*\*\*not allowed lrf.  
 Only lrf=1 or 2 allowed here.

error in rpxlc0\*\*\*number of pointwise xsec ... exceeded....  
 See maxe=600000.

error in rpxlc0\*\*\*bad covariance data for....  
 Wrong number of resonance parameters, negative diagonal elements, etc.

error in rpxlc12\*\*\*cannot hand RML with isammy=0.  
 You must set isammy=1 to get the derivatives for RML parameters.

error in rpxlc12\*\*\*different type of resonance for....  
 Much of the resonance parameter data found in MF=2 and MF=32 are re-  
 dundant, but in this instance, the expected redundant data were not found.  
 This indicates an error in the original evaluated file.

error in rpxlc12\*\*\*b array storage exceeded....  
 See maxb=30000.

error in rpxlc12\*\*\*a array storage exceeded....  
 Increase nwds, currently 1500000, in covout.

error in rpxlc12\*\*\*storage exceeded....  
 See mxnpar=7000.

error in rpxlc12\*\*\*mpar.gt.4.and.lrf.le.2 not coded.  
 Format not supported.

error in rpxlc12\*\*\*lcomp=1 general form.  
 This value of lrf is not coded.

error in rpxlc12\*\*\*problem.  
 Resonance parameter data were read from MF=32, but no corresponding resonance is defined in MF=2. This indicates an error in the original evaluated file.

error in rpxlc12\*\*\*a array for nlrs stroage exceeded.  
 Increase nwds, currently 1500000, in covout.

error in rpxlc12\*\*\*nlrs>0 not coded.  
 Option not supported.

error in rpxlc2\*\*\*a array storage exceeded.  
 Increase nwds, currently 1500000, in covout.

error in rpxlc2\*\*\*no RR uncertainties in mf32.  
 Check the evaluation for uncertainty data.

error in rpxlc2\*\*\*illegal value of ndigit.  
 The ndigit value can vary from 2 through 6.

error in rpxunr\*\*\*storage exceeded (lru=2)  
 See mxnpar=100. Note, perhaps not the best coding practice but mxnpar can be assigned different values in different subroutines; currently its 7000 elsewhere but 100 here.

error in rpxunr\*\*\*number of pointwise xsec of res excede...  
 See maxe=600000.

error in respend\*\*\*number of pointwise xsec of re excede...  
 See maxe=600000.

error in resdumr\*\*\*lru=2/lrf=1/lfw=0: amu? no coding.  
 Obsolete message.

error in resdumr\*\*\*lru=2/lrf=1/lfw=1: amu? no coding.  
 Obsolete message.

error in resdumr\*\*\*lru=---, lrf=-- no coding.  
 Option not supported.

error in resdumr\*\*\*nlru2 exceeeded mxlru2  
 See mxlru2=100.

error in rxgrpg\*\*\*i0>ipoint not coded.  
 This is a poorly worded message that essentially means that the previously calculated pointwise cross sections do not span the energy interval for this multigroup, and therefore it is not possible to internally calculate the necessary group average data needed for covariance processing.

error in skiprp\*\*\*no coding type lrf=--.  
The lrf value is limited to 1 through 3.

error in grpav4\*\*\*not coded for multimaterial group av'g.  
Single material mfcov=34 data only.

error in alsigc\*\*\*no coded for lump xsec.  
Cannot handle lumped cross sections for mfcov=34 data.

error in egtlgc\*\*\*no coded for ltt=2.  
Option not supported.

error in covout\*\*\*illegal condition for sad.  
Bad combination of options.

error in covout\*\*\*unable to find iy or iyp from mts array.  
There is a conflict between the internal list of covariance reactions and the reactions encountered on the union-group covariance file produced in covcal. This problem should not occur.

error in covout\*\*\*unexpectedly, ix ne iy or ixp ne iyp.  
This problem should not occur.

error in covout\*\*\*please check isd=1.  
Covariances between different MT values are not supported for MF=34.  
This is likely a fault in the evaluation.

error in sigc\*\*\*covariance reaction missing from lump'g ....  
A covariance reaction in the mt 851 to 870 range cannot be found in the lumped reaction definition tables. This problem should not occur.

error in resrp\*\*\*illegal or unrecognized ... in mf=32...  
There is a fault in the evaluation. Allowed values of lrf are 1 and 2 (single- and multi-level Breit-Wigner representations).

error in resrp\*\*\*bad covariance data for res params....  
There is a fault in the evaluation. Covariance matrix of the parameters has negative variances, infinite correlation coefficients, or correlation coefficients greater than 2.0. Data may be out of order.

error in resrp\*\*\*unresolved energy range was illegal.  
Check evaluation.

error in resrp\*\*\*storage exceeded.  
Increase nwds, currently 1500000, in covout.

error in resrp\*\*\*storage exceeded (lru=2).  
Increase nwds, currently 1500000, in covout.

error in resrp\*\*\*mpar=-- was not coded.  
Option not supported.

error in resrp\*\*\*storage exceeded for rel. covariance.  
See nparmx=60.



error in resprp\*\*\*bad rel. covariance data for ....  
 Negative diagonal element.

error in resprp\*\*\*storage exceeded for sensitivities.  
 See igumax=20.

message from grpav---mf --- mt --- has thresh gt highest ...  
 Though not a fatal error, this message often precedes an abort in covcal caused by the absence of this reaction on ngout. If iread=1, then delete this reaction from the requested list of covariance reactions.

error in grpav\*\*\*unable to find temp=---.  
 The program cannot locate requested material and temperature on npend.

error in grpav\*\*\*cannot group-average mt=---. use groupr....  
 The mfcov=31 and ngout=0 options are not compatible.

error in grpav\*\*\*not coded for multimat group averaging....  
 The iread=2 and ngout=0 options are not compatible.

error in colaps\*\*\*ngout is not a groupr output tape.  
 Check your input.

error in colaps\*\*\*storage exceeded.  
 Check nwscr. This error should not occur as the array allocation is made based upon known storage requirements.

error in colaps\*\*\*did not find expected mf1 mt451.  
 Multigroup libraries produced with the [GROUPE](#) module always contain the group structure in MF=1, MT=451.

error in colaps\*\*\*ngout group structure does not span ....  
 The supplied library must cover the entire energy range of the union grid, which is the same as the energy range of the user's grid.

error in colaps\*\*\*not coded for multiple sigma zeroes ...  
 Should not occur in njoy2012 which automatically converts general formatted gendf files to the more restricted format expected by ERRORR.

error in colaps\*\*\*not ready for file 6.  
 We can only handle spectra in file 5 currently.

error in uniong\*\*\*exceeded storage in mfcov energy grid.  
 Applies only if iverf=4. See nenimx=5000.

error in uniong\*\*\*energies out of order. --- lt ---.  
 Applies only if iverf=4.

error in uniong\*\*\*exceeded storage in union grid.  
 Insufficient space to store the union grid. Increase nunmax=5000.

error in egngpn\*\*\*read-in group structure is out of order.  
 With the ign=1 option, the supplied group structure must be in increasing order.

error in egngpn\*\*\*illegal group structure requested.

Allowed values of **ign** are 1-17 and 19.

error in egntwf\*\*\*illegal weight function requested.

Allowed values of **iwt** are 1-12.

error in egtsig\*\*\*mt=0

In the **ngout=0** option, a point cross section has been requested by **grpav** for an illegal MT number. In this context, the allowed values of **MT** are 1-200, 251-253, and 600-799. MT numbers 600-699 are not defined in ENDF-5, but may be used on ENDF and PENDF files specially prepared as input to ERRORR, to allow processing of nonstandard reaction types.

message from egtwf---xs energy range exceeds ...

The cross section multigroup energy range extends beyond the energy range defined for the weight function. Cross section values in the undefined region will be wrong or **nan**.

## 10.17 Input/Output Units

The following logical units are used:

- 10 ngout** in **grpav** and **ntp** in **colaps**. Contains the union group cross sections for all reactions with covariances. If the user input value of **ngout** is zero, point data are read from **npend** and written to **ngout=-10** in **grpav**. If the input value **ngout** is not zero, coarse group multigroup data are read from the user's **ngout** in **colaps** and written to **ntp=-10**. When **colaps** is finished, **ngout** is reset to -10.
- 11 nscr** in **covcal** and **covout**. Contains the union-group multigroup covariances for the directly evaluated reactions.
- 12 nscr2** in **covout**. This is a second copy of **nscr**, which is read only for the "trivial" derivation case, **isd=1**. Saves execution time by eliminating the calculation of many zero contributions.
- 13 nscrg** in the **covcal** and **rdgout**. This unit is used to extract a single MAT from a multimaterial **ngout**.
- 15 nscr** in **lumpmt** and **lumpxs**. This unit is used if MT numbers in the 851-870 range (lumped reactions) are found in ENDF covariance file to keep a copy of the covariance file.
- 20-99** Users can choose any of these numbers for **nendf**, **npend**, **ngout**, **nout**, **nin**, and **nstan**.

Units 11 and 12 are normally binary, although they can be switched to formatted mode by changing the value of the variable **imode** in the main program to +1. Unit 13 has the same mode as **ngout**. The user can choose the modes for **nendf**,

`npend`, `ngout`, `nout`, `nin`, and `nstan`, except that `nout` and `nin` must have the same mode.



## 11 COVR

### 11.1 Introduction

The COVR module of NJOY is an editing module that post processes the output of [ERRORR](#) in a manner analogous to the way [MATXS](#) and [DTFR](#) post process the output of [GROUPL](#). COVR performs two quite separate functions using the multigroup covariance file from [ERRORR](#) as input. First, it can prepare a new covariance library in a highly compressed card-image format, which is suitable for use as input to sensitivity analysis programs[78, 79]. Data in this form can also be copied to the system output file to obtain a compact printed summary of an [ERRORR](#) run without using the sometimes bulky long-print option in [ERRORR](#). Such a summary can also provide information on standard deviations and correlation coefficients, neither of which are printed by [ERRORR](#). The second main function of COVR is to produce publication-quality plots[76] of the multigroup covariance information.

This section describes COVR in NJOY 2012.0. The difference between this version and the one reported previously[3] include:

- new plotting capabilities using the [VIEWR](#) module to produce high-quality Postscript output,
- an option to display the plots in color, including the use of shades of green and shades of red, with user specified color boundaries, to represent positive and negative correlations, and
- differences due to the change to Fortran-90 style and memory allocation.

### 11.2 Production of Boxer-Format Libraries

As discussed in the [ERRORR](#) section of this manual, the output file of that module contains the group structure, cross sections, and either absolute (`irelco=0`) or relative (`irelco=1`) covariances for one or more materials, in either card-image or NJOY blocked-binary form. If the COVR user-input parameter `nout` is greater than zero, COVR reads an [ERRORR](#) output file from unit `nin` and produces a new multigroup covariance library on unit `nout`. COVR performs only sorting and reformatting operations on the [ERRORR](#) data.

In COVR, as well as [ERRORR](#), the ENDF energy ordering is followed. That is, low group indices correspond to low energies, high indices to high energies. Regarding group structures, in the library mode of operation COVR (like [ERRORR](#)) makes extensive use of external (disk) storage so that even on machines

that have a relatively small central memory very large group structures (up to 640 groups) can be handled successfully. (See, however, the comments at the end of Section 11.3 regarding group-number limitations in the plot mode.)

The material and reaction coverage of COVR post-processing is determined by a set of reaction pairs (`mat,mt;mat1,mt1`) supplied by the user (see input Card 4 in the input instructions and the corresponding discussion that follows in Section 11.4). At the beginning of the output library, the group structure is given. Then, for each specified reaction pair, the output library contains either a covariance matrix or a correlation matrix, depending on the output option (`matype`) selected. In the case that covariances are requested (`matype=3`), the type of data on `nout` (absolute *vs.* relative) is governed by the covariance type present on `nin`. In addition, whenever `mat1=mat` and `mt1=mt`, the group-cross-section vector and the (absolute/relative) standard-deviation vector for that particular reaction are written to `nout` just before the matrix itself. All data (group structure, cross sections, standard deviations, and matrices) are written to `nout` using a highly compressed, card-image format.

The design of this format, called the BOXER format, proceeds from a simple fact: as discussed in the [ERRORR](#) section of this manual, most of the ENDF covariance formats define certain rectangular regions (boxes) in energy “space,” over which the relative covariance is constant. (The ENDF format allowing a constant absolute covariance is only rarely used.) The coordinate axes of the two-dimensional energy space in question are  $E_x$  and  $E_y$ , where  $x$  and  $y$  indicate the particular reaction pair to which the ENDF covariances apply. Because of this feature of the basic evaluations, one expects that an element of a multigroup relative covariance matrix, derived from the ENDF data for a given reaction pair, frequently will be identical either to the element before it in the same row ( $E_x$  constant,  $E_y$  varying) or to the element above it in the same column ( $E_y$  constant,  $E_x$  varying). Thus, the Boxer format allows a combination of horizontal and vertical repeat operations.

Even though the [ERRORR](#) output format already suppresses zero covariances, very large data compression factors can be achieved in transforming data from the [ERRORR](#) format to the Boxer format. As one example, the [ERRORR](#) output file for a particular 137-group reactor-dosimetry library[80] contained 38 000 card images, while the corresponding COVR output file contained fewer than 1000 card images.

In the BOXER format, data are stored as a list of numerical data values (*e.g.*, relative covariances), together with a list of integers that control the loading of

these data into the reconstructed array  $C(i, j)$ . A negative control integer,  $-n$ , indicates that the next value in the data list is to be loaded into the next  $n$  columns ( $j$ -locations) of the current row of  $C(i, j)$ . A positive integer  $m$ , on the other hand, means that, for the next  $m$   $j$ -values, the value to be loaded is to be carried down from the row above,

$$C(i, j) = C(i-1, j) . \quad (451)$$

For the first row ( $i = 1$ ), the row above is defined to contain all zeros.

In constructing the compressed data set in subroutine **press**, the choice between using the “repeat-new-value” method or the “carry-down” method is made dynamically on the basis of taking the longest possible step. If  $m = n$ , the carry-down method is chosen, as it does not require an entry in the data list.

As an additional compression feature of the format, one may indicate by a “flag” that the matrix  $C(i, j)$  is symmetric; hence, explicit instructions are provided in the compressed data library for the reconstruction of only the upper right triangle of  $C(i, j)$ . These various aspects of the Boxer format are illustrated by a simple example in Fig. 46. Here  $a, b, c$  and  $d$  are arbitrary, nonzero, unequal data values.

Before the data values are tested in **press** to see if they are indeed equal, the **NJOY** utility **sigfig** is called to round off the trailing digits that would not appear on the formatted output anyway. Relative covariances, for example, are written to **nout** in 1P8E10.3 format, which has only four significant figures. Thus, the three data values 0.036126, 0.036130, and 0.036134 would all be judged to be equal by this logic.

### 11.3 Generation of Plots

The COVR plot mode, which is requested by specifying **nout=0**, is used to generate publication-quality plots of multigroup covariance data from a card-image or binary **ERRORR** output file. Examples of plots produced by COVR can be seen in the **ERRORR** section of this manual. In addition to their usefulness in preparing publications, the plots have proved to be a useful tool for checking the reasonableness and mechanical correctness of new covariance evaluations. One can, for example, execute **ERRORR** and COVR in tandem, using the evaluator’s energy grid as the user group structure (**ERRORR** input option **ign=19**). The output of such a run is a series of plots showing all important features of the covariance evaluation.

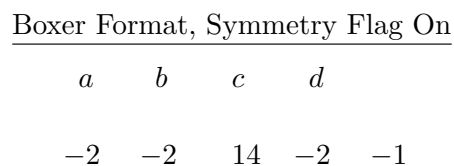
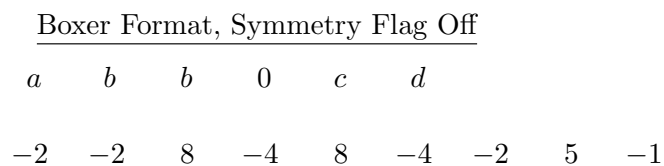
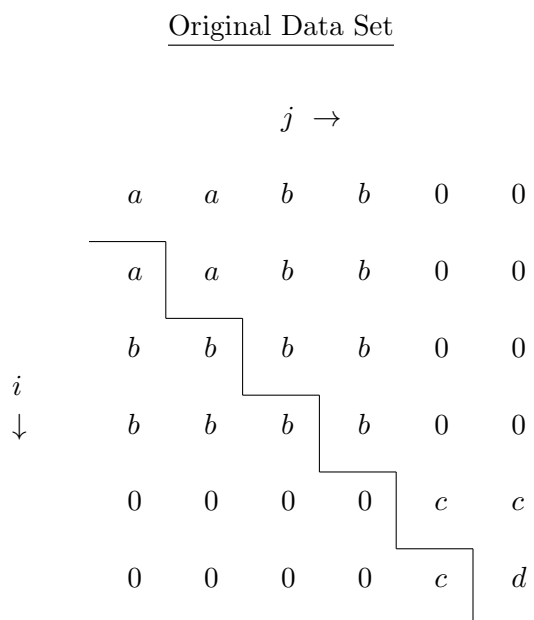


Figure 46: Illustration of Boxer format

As can be seen in the examples mentioned above, each plot contains a shaded contour map of the correlation matrix. If black & white plots are needed, positive-correlation regions are shaded with parallel straight lines (hatching), while negative correlations are indicated by cross-hatching. When color is requested (see the second card in the input instructions, the positive correlations are represented by shades of green, and the negative correlations are represented by shades of red. The plots also contain two additional inset graphs giving the energy dependence of the associated standard deviation vectors. One of the vec-



tor plots is rotated by 90 degrees, so that the logarithmic energy scales for the vector plots can be aligned with the corresponding scales for the matrix plot. When `MAT=MAT1` and `MT=MT1`, we plot the cross section rather than repeating the standard deviation plot.

This type of plot presents the covariance data in a more lucid manner than most alternative plotting packages. However, use of this option does require the sophisticated capabilities of the [VIEWR](#) module to create rotated subplots and to fill regions with colors or hatching patterns. See the [VIEWR](#) section of this report for more details.

Just as in the library mode, the material and reaction coverage of the sequence of plots generated in the plot mode is determined by the reaction pairs specified by the user on input Card 4. Other input, specific to the generation of plots, is described in Section 11.4. We next discuss some aspects of the plot-generation coding.

After a covariance matrix is read in subroutine `covard`, it is converted to a correlation matrix in subroutine `corr`. The correlation matrix is then scanned in subroutine `matshd` to find a set of boundary curves that divide  $E_x - E_y$  energy space into a small number of connected regions of nearly constant correlation strength. Here the phrase “nearly constant” refers to the subdivision of the range of possible correlation values ( $-1.0$  to  $+1.0$ ) into a number of equal-width bands, the fineness of the subdivision being controlled by the user-input parameter `ndiv`. Two regions have nearly equal correlations if the correlations fall into the same band. As each boundary curve is located, the enclosed region is shaded (with a line density proportional to the band correlation magnitude) with direct writes to the [VIEWR](#) file.

The algorithm used to find the maximum extent of a region of nearly constant correlation is best described by referring to the simple example in Fig. 47. After locating the upper left corner of a new correlation region, for example at point  $a$  in the figure, the search proceeds as far as possible down the first column ( $E_y$  held constant) to point  $b$ . New columns are scanned in the same way:  $c-d$ ,  $e-f$ ,  $g-h$ . Having found that the pattern does continue into column  $e-f$ , for the sake of simplicity, the algorithm ignores the possibility of additional, disjoint, continuations of the pattern elsewhere in the same column (such as at  $e'-f'$ ), and region I is ended at  $h$ . (Region II will be found and correctly shaded at a later stage of the calculation.)

As the plot option is presently coded, the entire correlation matrix must reside in memory during the pattern-search operation just described.

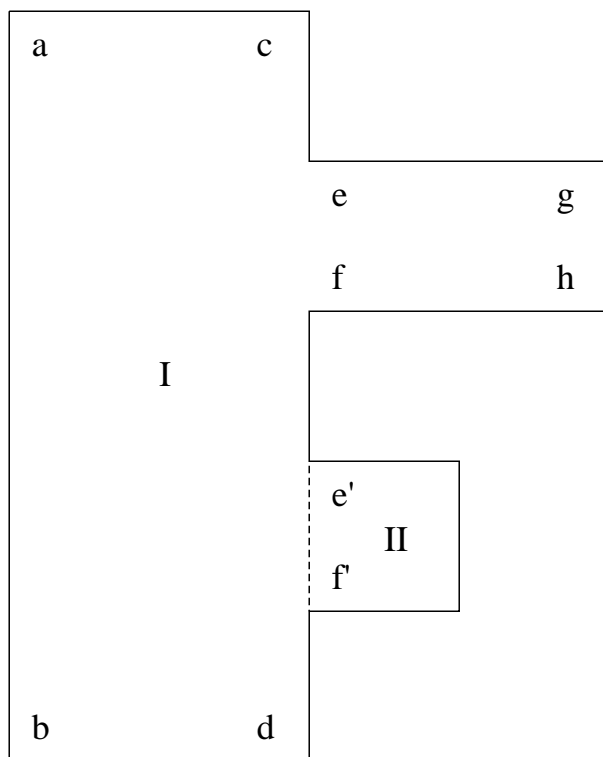


Figure 47: Pattern-search logic in subroutine matshd.

#### 11.4 Input Instructions for COVR

As an aid to discussions of the user input to COVR, we list below the input instructions that appear as comment cards at the beginning of the current version of this module. It is always advisable to consult the comment-card instructions embedded in the version of the code actually being used and not to rely on the instructions published in any document, including this one. Following the listing are further remarks on several of the input items; the remarks supplement the comment cards below. See especially the lengthy discussion of the parameters on Card 4.

```
!---input specifications (free format)-----
!
! card 1
!   nin          input tape unit
!   nout         output tape unit
!               (default=0=none)
!   nplot        viewr output unit
```

```

!                                     (default=0=none)
!
!   ---cards 2, 2a, and 3a for nout.ne.0 only (plot option)
!
! card 2
!   icolor          select color or monochrome style
!                   0=monochrome (uses cross hatching)
!                   1=color background and contours
!                   2=color background and contours plus
!                   card 2' follows.
!                   (default=0)
! card 2' (only when icolor=2)
!   nlev,(tlev(i),i=1,nlev)
!                   defines the number of correlation matrix
!                   intervals and their boundaries. Zero is
!                   assumed as the lower limit of the first
!                   boundary, but the User must specify unity
!                   as the upper limit of the last boundary.
!                   nlev is a positive integer .le. 9.
!                   default values (when icolor=1) are:
!                   6,0.001,0.1,0.2,0.3,0.6,1.0
! card 2a
!   epmin           lowest energy of interest (default=0.)
! card 3a
!   irelco          type of covariances present on nin
!                   0/1=absolute/relative covariances
!                   (default=1)
!   ncase           no. cases to be run (maximum=40)
!                   (default=1)
!   noleg           plot legend option
!                   -1/0/1=legend for first subcase only/
!                   legend for all plots/no legends
!                   (default=0)
!   nstart          sequential figure number
!                   0/n=not needed/first figure is figure n.
!                   (default=1)
!   ndiv            no. of subdivisions of each of the
!                   gray shades (default=1)
!
!   ---cards 2b, 3b, and 3c for nout gt 0 (library option) only--
!
! card 2b

```

```

!      matype          output library matrix option
!                      3/4=covariances/correlations
!                      (default=3)
!      ncase           no. cases to be run (maximum=40)
!                      (default=1)
!      card 3b
!      hlibid          up to 6 characters for identification
!      card 3c
!      hdescr          up to 21 characters of descriptive
!                      information
!
!      ---cards 4 for both options---
!
!      card 4
!      mat             desired mat number
!      mt              desired mt number
!      mat1            desired mat1 number
!      mt1             desired mt1 number
!                      (default for mt, mat1 and mt1 are 0,0,0
!                      meaning process all mts for this mat
!                      with mat1=mat)
!                      (neg. values for mt, mat1, and mt1 mean
!                      process all mts for this mat, except for
!                      the mt-numbers -mt, -mat1, and -mt1. in
!                      general, -n will strip both mt=1 and mt=n.
!                      -4 will strip mt=1, mt=3, and mt=4, and
!                      -62, for example, will strip mt=1, mt=62,
!                      mt=63, ... up to and incl. mt=90.)
!      repeat card 4 ncase times
!
!      note---if more than one material appears on the input tape,
!      the mat numbers must be in ascending order.
!
!-----

```

**icolor** ... This parameter is used to specify creation of monochrome (cross-hatched) or color correlation matrix plots. Although the default setting is **icolor=0** (to produce monochrome plots) the capabilities of modern printers and display terminals makes creation of color plots the more common option. If **icolor=1** a default six-interval color pattern is used when creating the correla-

tion matrix; if `icolor=2` then input card 2' is required where the user specifies the number of color intervals (an integer, `nlev`, where `nlev` is a positive non-zero integer  $< 10$ ) plus `nlev` real numbers that define the color boundaries, `tlev(i)`,  $i=1, nlev$ . `tlev(nlev)` must be unity. Users are cautioned that use of too many intervals may require an increase in the value of `ipat` in subroutine `matshd`.

`epmin` ... This parameter is used to eliminate uninteresting energy regions from the correlation and standard deviation plots, or to display high-energy regions with greater resolution.

`irelco` ... This parameter must match the value used in the [ERRORR](#) run that produced the covariances to be plotted.

`ncase` ... This is the number of cases, or occurrences of Card 4. See the discussion of input parameters `mat`, `mt`, `mat1`, and `mt1` below. Presently, `ncase` is limited to 60. Problems larger than this can be run as a series of COVR jobs, each processing a batch of up to 60 cases. See also the parameter `nstart` below.

`noleg` ... "Legend" here refers to the gray-shading scale (key) as well as the figure caption. `noleg=1` is used as a rough-draft mode to display plots quickly.

`nstart` ... Unless `nstart=0`, the plots are assigned a sequential figure number, beginning at `nstart`, and a list of figures is drawn on the final plot frame.

`ndiv` ... One gray-shade step equals 0.20 in correlation magnitude if `ndiv=1`. Finer gradations are possible with `ndiv` greater than 1. The plots appearing in the [ERRORR](#) section of this manual were generated with `ndiv=2`.

`hlibid` ... This is a 6-character string, normally containing the name of the output covariance library. It is written on the header records present at the beginning of each output data block.

`hdescr` ... This contains additional information, for example, on where and when the library was produced; it is also written on the data header records.

`mat`, `mt`, `mat1`, `mt1` ... The information contained in the output library or plot file is controlled by means of these parameters on input Card 4. If `mt` is positive, then a single covariance matrix for reaction (`mat`,`mt`) with reaction (`mat1`,`mt1`) will be read from `nin` and processed. On unit `nin` (and, in the library option, on unit `nout`), the rapidly varying, or column, index is the group index of (`mat1`,`mt1`), and the slowly varying, or row, index is the group index of (`mat`,`mt`). If `mat1` is different from `mat`, COVR will expect to find separate materials (produced by separate [ERRORR](#) runs) for both `mat` and `mat1` on `nin`. The `mat` numbers must occur on `nin` in ascending order. In the case of positive

`mt`, the entries `mat1=0` and `mt1=0` are shorthand for `mat1=mat` and `mt1=mt`, respectively. If, on the other hand, `mt` is zero, negative, or defaulted, Card 4 becomes a kind of macro-instruction that is expanded by subroutine `expndo` into a request for many `(mt, mt1)` pairs, all with `mat1=mat`. If, for example, Card 4 contains the entry

```
MAT/
```

or, equivalently,

```
MAT 0 0 0
```

first the cross-section file, `MF=3`, for material `MAT` is read from the input covariance tape on unit `nin` to obtain the list of reactions present. Then, all possible reaction combinations `(mt, mt1)` are formed in ENDF order. Thus, for example, if the reactions present are `MT=1, 2, 3`, and `16`, then the behavior of the code is the same as if the following input were specified:

```
MAT 1 0 1
MAT 1 0 2
MAT 1 0 3
MAT 1 0 16
MAT 2 0 2
MAT 2 0 3
MAT 2 0 16
MAT 3 0 3
MAT 3 0 16
MAT 16 0 16
```

Because of the clear labor-saving advantage of this feature, especially if there are many reactions, enhancements have been added to permit its use in the additional situation in which many, but not all, combinations are desired. As discussed in some detail in the input instructions, it is possible to strip selected reactions out of the list before the `(mt, mt1)` combinations are formed. For example, if the reactions present are once again `1, 2, 3`, and `16`, then a Card 4 containing

```
MAT -3/
```

would produce the same output as the following three cards:

```
MAT 2 0 2
MAT 2 0 16
MAT 16 0 16
```

The stripping of the higher inelastic levels, mentioned in the input instructions, is useful because [ERRORR](#) automatically resets the highest user-group energy to 20 MeV whenever `IREAD=0`, and this can result in the inclusion of unwanted high-threshold reactions on the [ERRORR](#) output file.

For one of several reasons, a requested reaction pair (`mat,mt; mat1,mt1`) may be absent from the COVR output. The usual reason that this occurs is that the normal `iread` option for the [ERRORR](#) module is `iread=0`, and this results in the generation of an output matrix for every possible reaction-pair combination. For those combinations that do not occur in the ENDF evaluation, the [ERRORR](#) output matrix contains only zeroes. These null matrices are omitted at the COVR output stage, in both the library and plot modes.

Additionally, in the plot mode, the correlations may be nonzero, but everywhere less than  $0.2/\text{ndiv}$  in absolute magnitude. In this case, the entire correlation plot would consist of a single blank region. These rather uninteresting plots having small correlations are also omitted from the plot file. A final, similar category is the class of “empty” plots. Because parallel lines to achieve a gray effect when color is not used have limited resolution, there is clearly some lower limit, for a given value of the correlation magnitude, on the physical size of a region that can be sensibly shaded. COVR does not attempt to shade regions that are smaller than this limit. If a correlation matrix does contain some plottable data (magnitudes exceeding  $0.2/\text{ndiv}$ ), but all plottable regions are smaller than the size limit discussed above, then an empty plot will be generated on the plot file. As a convenience in discarding these empty plots at the time a report is produced, no caption is written on such plots and the figure number is not advanced. Also, these plots are omitted from the list of figures prepared at the end of a plot run. (See the discussion of user-input parameter `nstart`.)

In the library mode, each omission of a requested, but null, matrix is noted on the **output** file with an informative diagnostic. In the plot mode, a summary table is printed at the end of the run to identify all requested matrices that were omitted because they were null or small, as well as those that were plotted, but empty.

### 11.5 COVR Example Problem

In this section we discuss the production of a particular COVR output library, both to illustrate the input and as a supplement to the general discussion of BOXER format libraries in Section 11.2. In the **ERRORR** chapter of this report (the second input set in Section 10.14), we gave the complete NJOY input for producing a 7-reaction, 30-group covariance library in **ERRORR** output format for  $^{12}\text{C}$ . By appending the following lines to that input (just before the **stop** card), one can produce, in addition, a 2-reaction COVR output library in BOXER format.

```

covr
-23 24
3 3
' LIB'
'MAT1306 COVR EXAMPLE'/
1306 2 0 2
1306 2 0 4
1306 4 0 4

```

The resulting library occupies only 49 lines and is listed below.

```

0  LIB-A- 30 MAT1306 COVR EXAMPLE 1306 2 1306 2 31 10 31 3 0 31 1
1.390E-04 1.520E-01 4.140E-01 1.130E+00 3.060E+00 8.320E+00 2.260E+01 6.140E+01
1.670E+02 4.540E+02 1.235E+03 3.350E+03 9.120E+03 2.480E+04 6.760E+04 1.840E+05
3.030E+05 5.000E+05 8.230E+05 1.353E+06 1.738E+06 2.232E+06 2.865E+06 3.680E+06
6.070E+06 7.790E+06 1.000E+07 1.200E+07 1.350E+07 1.500E+07 1.700E+07
-1 -1 -1 -1 -1 -1 -1 -1 -1 -1 -1 -1 -1 -1 -1 -1 -1 -1 -1 -1 -1 -1
-1 -1 -1 -1 -1
1  LIB-A- 30 MAT1306 COVR EXAMPLE 1306 2 1306 2 23 10 23 3 0 30 1
4.739E+00 4.738E+00 4.735E+00 4.729E+00 4.712E+00 4.676E+00 4.579E+00 4.332E+00
4.002E+00 3.619E+00 3.103E+00 2.477E+00 1.998E+00 1.820E+00 1.710E+00 2.256E+00
1.447E+00 9.921E-01 8.223E-01 7.627E-01 8.631E-01 8.228E-01 8.845E-01
-8 -1 -1 -1 -1 -1 -1 -1 -1 -1 -1 -1 -1 -1 -1 -1 -1 -1 -1 -1 -1 -1

```



```

2  LIB-A- 30 MAT1306 COVR EXAMPLE 1306 2 1306 2 18 10 18 3 0 30 1
2.000E-03 1.964E-03 4.583E-03 3.822E-03 4.583E-03 4.288E-03 3.730E-03 4.141E-03
6.501E-03 1.011E-02 9.558E-03 9.981E-03 1.806E-02 1.854E-02 3.296E-02 3.760E-02
4.255E-02 7.632E-02
-9 -1 -5 -1 -1 -1 -1 -1 -1 -1 -1 -1 -1 -1 -1 -1
3  LIB-A- 30 MAT1306 COVR EXAMPLE 1306 2 1306 2 43 10 58 4 0 30 0
4.000E-06 2.797E-06 3.856E-06 6.317E-06 4.613E-06 2.407E-06 1.229E-06 2.100E-05
1.534E-05 8.000E-06 4.087E-06 1.461E-05 1.366E-05 2.100E-05 1.838E-05 9.004E-06
1.391E-05 8.934E-06 1.715E-05 4.447E-06 4.227E-05 4.373E-05 2.446E-05 1.980E-05
1.223E-05 1.022E-04 6.116E-05 4.048E-05 2.500E-05 9.136E-05 4.572E-05 9.962E-05
6.641E-05 6.308E-05 3.260E-04 1.614E-04 3.437E-04 1.086E-03 4.250E-04 1.413E-03
7.052E-04 1.811E-03 5.825E-03
-9 -1 224 -1 -5 -1 -4 -1 9 -5 -1 -4 -1 79 -1 -1 13 -1 13 -1
-1 11 -1 -1 10 -1 -1 9 -1 -1 -1 -1 -6 -1 -1 -1 -6 -1 -1 6
-1 -1 -1 4 -1 -1 4 -1 4 -1 -2 1 -1 -1 1 -1 1 -1
3  LIB-A- 30 MAT1306 COVR EXAMPLE 1306 2 1306 4 38 10 47 4 0 30 30
-1.106E-04-4.897E-05-3.047E-05-2.164E-05-2.630E-05-2.337E-05-2.192E-05-2.261E-04
-1.001E-04-6.228E-05-4.423E-05-5.376E-05-4.777E-05-4.481E-05-1.441E-03-2.659E-04
-1.571E-04-1.210E-03-1.305E-03-4.021E-04-1.131E-03-6.462E-04-8.562E-04-2.261E-04
-1.001E-04-6.228E-05-1.922E-03-9.140E-04-8.121E-04-7.520E-04-3.040E-03-1.348E-03
-1.517E-03-3.460E-03-4.423E-05-5.376E-05-4.777E-05-1.044E-02
623 -1 -1 -1 -1 -1 -1 -1 23 -1 -1 -1 -1 -1 -1 -1 53 -1 -1 -1
27 -1 -1 -1 27 -1 -1 -1 27 -1 -1 -1 -1 -1 -1 27 -1 -1 -1 28
-1 -1 27 -1 -1 -1 -1
1  LIB-A- 30 MAT1306 COVR EXAMPLE 1306 4 1306 4 7 10 8 3 0 30 1
6.091E-02 2.478E-01 3.301E-01 4.310E-01 4.013E-01 4.306E-01 4.935E-01
23 -1 -1 -1 -1 -1 -1 -1
2  LIB-A- 30 MAT1306 COVR EXAMPLE 1306 4 1306 4 7 10 8 3 0 30 1
2.499E-01 1.085E-01 9.724E-02 9.806E-02 1.358E-01 1.263E-01 2.177E-01
23 -1 -1 -1 -1 -1 -1 -1
3  LIB-A- 30 MAT1306 COVR EXAMPLE 1306 4 1306 4 28 10 29 4 0 30 0
6.245E-02 7.530E-03 3.823E-03 1.154E-03 1.338E-03 1.211E-03 1.155E-03 1.176E-02
2.311E-03 5.938E-04 6.451E-04 5.843E-04 5.578E-04 9.455E-03 1.887E-03 4.735E-04
4.295E-04 4.106E-04 9.617E-03 1.872E-03 1.670E-03 3.033E-04 1.844E-02 5.214E-03
3.493E-04 1.596E-02 5.253E-03 4.741E-02
437 -1 -1 -1 -1 -1 -1 -1 -1 -1 -1 -1 -1 -1 -1 -1 -1 -1 -1
-1 -1 -1 -1 -1 -1 -1 -1 -1

```

Note that the header card at the start of each data block contains an integer `itype`, specifying the type of data contained in the current block, a 12-character library name (“LIB-A- 30” in this case), 21 characters of user-supplied descriptive information, `mat`, `mt`, `mat1`, `mt1`, and a set of 7 integers. The meaning

of the various values of `itype` is as follows: 0 = group boundaries, 1 = cross sections, 2 = standard deviations, 3 = covariances, and 4 = correlations. The library name is generated within COVR by adding either “-A-” (for a covariance library) or “-B-” (for a correlation library), together with the number of energy groups, to the user-supplied library name `hlibid`. (The `ERRORR` input option `ign=3` used in this example specifies a built-in 30-group structure). The final seven integers on the header card indicate the number and format of the data values, the number and format of the control integers (called “*m*” and “*n*” in the discussion in Section 11.2), a data paging flag, and the dimensions of the reconstructed data array,  $C(i, j)$ .

In order to clarify the process of reconstructing a full matrix from data in BOXER format, we list in Section 11.8 a short retrieval program, BOXR. With very few modifications, this program could be incorporated into a sensitivity analysis program, for example, to allow direct access to covariance libraries[77] in this compact format. Alternatively, it could be used to translate COVR libraries into other desired forms. In any case, an examination of the retrieval program should clarify the meaning of the various integer parameters on the header cards in a COVR output library.

## 11.6 Error Messages

`error in covr***requested too many cases.`

`ncase` is limited to 40. Note that a case refers to one input Card 4, which may request processing of either a single reaction pair or a whole series of reaction pairs. See input instructions for Card 4 and the comments that follow.

`error in expndo***storage exceeded.`

Should not occur since array space is allocated based upon known storage needs.

`error in corr***group structures do not agree.`

This problem should not occur.

`error in covard***storage exceeded.`

Should not occur since array space is allocated based upon known storage needs.

`error in covard***did not find file 77 subsection...`

Requested reaction *y* of the current *x-y* pair is not found on `nin`.

`error in trunc***bad data.`

Either all cross sections are very small (less than `xslim` =  $10^{-4}$  barn) or `epmin` is larger than the highest group boundary.

**error in matshd\*\*\*ipat gt 99999.**

Maximum number of correlation patterns is 99999. Reduce **ndiv** to 1 or raise **epmin** in order to reduce the complexity of the correlation plot.

**error in matshd\*\*\*storage exceeded.**

**nwig**=2\*(**ixmax**+1)+600 words are available for storing the boundary curve of a constant-correlation region. This will not be exceeded for any practical number of groups **ixmax**.

**error in level\*\*\*coefficient = --- out of range.**

The absolute magnitude of a computed correlation coefficient is greater than 2. The input covariance file may be faulty.

**error in finds\*\*\*mat --- mf --- mt --- not on tape.**

Requested reaction **x** of the current **x-y** pair is not found on **nin**.

**error in press\*\*\*storage exceeded.**

This problem should not occur.

**error in press\*\*\*matrix not symmetric....**

Symmetric-matrix format is requested for a matrix that is asymmetric. This problem should not occur.

**error in setfor\*\*\*nvf (= ---) or ncf (= ---) is illegal.**

This problem should not occur.

## 11.7 Input/Output Units

The following logical units are used:

**10** **nin** in **corr** and **covard**, **nscr** in other routines. These units are used to extract either one or two (if **mat1**≠**mat**) materials from the input covariance tape.

**11** **nscr1** in the plot mode. These units are used to document null and small covariance matrices and empty plots.

**11/12** **nscr1/nscr2** in the library mode. In **covard**, the input covariances for the current reaction pair are read from unit 10 and written to **nscr2** (= 12). If the output library is to contain correlation coefficients (**matype** = 4), then in **corr** the covariances are read from **nscr2**, and the calculated correlations are written to **nscr1** (= 11). If output covariances are requested (**matype** = 3), the value of **nscr1** is simply reset to **nscr2** (= 12). In either case, **press** reads the data from unit **nscr1** and writes the compressed data to **nout**.

**20-99** User's choice for **nin** and **nout**.

Unit 10 has the same mode as **nin**. Unit **nout**, if used, is always formatted.

Unit 11 is formatted in the plot option and it is binary in the library option.

Unit 12, if used, is always binary.

## 11.8 Retrieval Program for COVR Output Libraries

```

PROGRAM BOXR
C *****
C FUNCTION OF PROGRAM.  READ DATA FROM UNIT NIN IN THE COMPRESSED
C *BOXER* FORMAT PRODUCED BY THE COVR MODULE OF NJOY, AND LOAD THE
C FULL, RECONSTRUCTED MATRIX INTO C(I,J).  THEN WRITE THE RESULT ON
C UNIT NOUT IN HIGH-TO-LOW ENERGY ORDER.  FAILURE TO FIND A
C REQUESTED DATA SET RESULTS IN AN ERROR STOP.
C
C      ITYPE  DATA TYPE REQUESTED,
C              = -1, TO WRITE A TABLE OF CONTENTS OF NIN, IN THE
C                  FORMAT OF BOXR INPUT INSTRUCTIONS, ON UNIT NTAB.
C              = 0, FOR GROUP BOUNDARIES,
C              = 1, FOR CROSS SECTIONS,
C              = 2, FOR STANDARD DEVIATIONS,
C              = 3, FOR COVARIANCE MATRIX,
C              = 4, FOR CORRELATION MATRIX, OR (IF MT1 IS ZERO)
C                  TRANSFER MATRIX FROM COVFILS2.
C      ITYPEH  VALUE OF ITYPE ON CURRENT DATA HEADER CARD.
C
C      (MAT,MT,MAT1,MT1)  REQUESTED REACTION PAIR.
C      (MATH,MTH,MAT1H,MT1H) CURRENT REACTION PAIR.
C      (XVAL(IV),IV=1,NVAL) DATA VALUE ARRAY IN THE *BOXER* FORMAT.
C      NVMAX              MAXIMUM ALLOWABLE VALUE OF NVAL.
C      (ICON(IC),IC=1,NCON) CONTROL-PARAMETER ARRAY IN *BOXER* FORMAT.
C      NCMAX              MAXIMUM ALLOWABLE VALUE OF NCON.
C
C      I          ROW INDEX OF MATRIX C(I,J), NORMALLY THE ENERGY GROUP
C                  OF THE REACTION (MAT,MT).
C      NROW       NUMBER OF ROWS IN C(I,J).
C      NROWH      VALUE OF NROW ON DATA HEADER CARD.
C      NROWM      CONTINUATION FLAG, = 0 FOR FINAL DATA BLOCK OF CURRENT
C                  REACTION PAIR.
C      J          COLUMN INDEX OF C(I,J), FOR MATRIX DATA THE ENERGY GROUP
C                  OF THE REACTION (MAT1,MT1), = 1 FOR VECTORS.
C      NCOL       NUMBER OF COLUMNS IN C(I,J).
C      NCOLH      VALUE OF NCOL ON DATA HEADER CARD, = 0 IF C(I,J) IS A
C                  SYMMETRIC MATRIX REPRESENTED IN THE *BOXER* FORMAT BY
C                  JUST THE UPPER RIGHT TRIANGLE (J.GE.I).
C      NGMAX      MAXIMUM ALLOWABLE VALUE OF NROW AND NCOL.

```

```

C      *****
C      DIMENSION IVFT(3), ICFT(3), IA(9), IB(9)
C      DIMENSION C(200,200), CR(200), XVAL(880), ICON(900)
C      DATA NGMAX /200/, NVMAX /880/, NCMAX /900/, IDASH /4H----/
C      DATA NINPUT /5/, NIN /20/, NOUT /21/, NTAB /22/, IZERO /0/
C
C      ***READ USER-SUPPLIED REACTION-TYPE AND MAT-MT INFORMATION.
10  READ (NINPUT,190) ITYPE,MAT,MT,MAT1,MT1
C      INPUT IS TERMINATED BY ENTERING (0,0).
C      IF (ITYPE.GE.0.AND.MAT.EQ.0) STOP
C
C      ***RETRIEVE REQUESTED DATA FROM UNIT NIN.
20  READ (NIN,210,END=900) ITYPEH,(IA(K),K=1,9),MATH,MTH,MAT1H,MT1H
C      1 ,NVAL,NVF,NCON,NCF,NROWM,NROWH,NCOLH
C
C      ***IN COVFILS2, ITYPEH=9 IS USED AS A TERMINATOR.
30  IF (ITYPEH.EQ.9) GO TO 900
C      IF (ITYPE.EQ.-1.AND.MATH.EQ.0) MATH=1
C      IF (ITYPE.EQ.-1.AND.IA(2).NE.IDASH)
C      1 WRITE (NTAB,190) ITYPEH,MATH,MTH,MAT1H,MT1H
C      IF (NVAL.GT.NVMAX) STOP 3
C      IF (NCON.GT.NCMAX) STOP 4
C      SET FORMATS, THEN READ BOXER DATA.
C      CALL SETFOR (NVF,NCF,NOUT,IVFT,ICFT)
C      IF (NVAL.GT.0) READ (NIN,IVFT) (XVAL(K),K=1,NVAL)
C      IF (NCON.GT.0) READ (NIN,ICFT) (ICON(K),K=1,NCON)
C      TEST IF THESE ARE THE DESIRED DATA.  FOR THE GROUP BOUNDARIES
C      ONLY, THE VALUES MATH, MTH, MAT1H, AND MT1H ON THE HEADER CARD
C      ARE IGNORED.  FOR ITYPE=1 OR 2, MAT1H AND MT1H ARE IGNORED.
C      FOR MATRIX DATA, ITYPE=3 OR 4, A COMPLETE MATCH IS REQUIRED.
C      IF (ITYPEH.NE.ITYPE) GO TO 20
C      IF (ITYPE.EQ.0) GO TO 40
C      IF (MATH.NE.MAT.OR.MTH.NE.MT) GO TO 20
C      IF (ITYPE.EQ.1.OR.ITYPE.EQ.2) GO TO 40
C      IF (MAT1H.NE.MAT1.OR.MT1H.NE.MT1) GO TO 20
C      INITIALIZE
40  NX=0
C      I=1
C      ISTART=1
C      J=0
50  NROW=NROWH
C      NCOL=NCOLH

```

```

      IV=0
      NSYM=0
      IF (NCOL.EQ.0) NSYM=1
      IF (NCOL.EQ.0) NCOL=NROW
      IF (NROW.GT.NGMAX.OR.NCOL.GT.NGMAX) GO TO 910
C
C      ***LOAD DATA FROM XVAL INTO C(I,J) AS DIRECTED BY ICON.
      DO 110 IC=1,NCON
      IF (ICON(IC).LT.0) GO TO 60
      IF (ICON(IC).EQ.0) STOP 6
      NLOAD=ICON(IC)
      GO TO 70
60  NLOAD=-ICON(IC)
      IV=IV+1
      IF (IV.GT.NVAL) STOP 7
      CLOAD=XVAL(IV)
70  CONTINUE
      DO 100 N=1,NLOAD
      J=J+1
      IF (J.LE.NCOL) GO TO 80
C      START NEW ROW
      I=I+1
      IF (I.GT.NROW) STOP 10
      J=1
      IF (NSYM.EQ.1) J=I
80  IF (ICON(IC).LE.0) GO TO 90
      CLOAD=0.
      IF (I.GT.ISTART) CLOAD=C(I-1,J)
90  C(I,J)=CLOAD
      NX=NX+1
      IF (NSYM.EQ.0.OR.I.EQ.J) GO TO 100
      C(J,I)=CLOAD
      NX=NX+1
100 CONTINUE
110 CONTINUE
      IF (NROWM.EQ.0) GO TO 120
C      READ IN NEW PAGE OF DATA FROM NIN
      IF (J.NE.NCOL) STOP 11
      READ (NIN,210) IYPEH,(IB(K),K=1,9),MATH,MTH,MAT1H,MT1H,NVAL,NVF
1  ,NCON,NCF,NROWM,NROWH,NCOLH
      CALL SETFOR (NVF,NCF,NOUT,IVFT,ICFT)
      IF (NVAL.GT.0) READ (NIN,IVFT) (XVAL(K),K=1,NVAL)

```

```

      IF (NCON.GT.0) READ (NIN,ICFT) (ICON(K),K=1,NCON)
      ISTART=I+1
      GO TO 50
120  CONTINUE
C     FINISHED LOADING C(I,J)
      IF (NX.NE.NROW*NCOL) STOP 12
C
C     ***WRITE C(I,J) TO NOUT IN HIGH-TO-LOW ENERGY ORDER.
      WRITE (NOUT,220)
      WRITE (NOUT,210) IYPEH,(IA(K),K=1,9),MATH,MTH,MAT1H,MT1H,NVAL,NVF
1    ,NCON,NCF,NROWM,NROWH,NCOLH
      IF (NCOL.EQ.1) GO TO 150
      DO 140 I=1,NROW
      IR=NROW+1-I
C     IN COVFILS2, TRANSFER MATRICES ARE ALREADY IN HIGH-TO-LOW ORDER
      IF (ITYPE.EQ.4.AND.MT1.EQ.0) IR=I
      DO 130 J=1,NCOL
      JR=NCOL+1-J
      IF (ITYPE.EQ.4.AND.MT1.EQ.0) JR=J
130  CR(J)=C(IR,JR)
140  WRITE (NOUT,200) (CR(L),L=1,NCOL)
      GO TO 10
150  DO 160 I=1,NROW
      IR=NROW+1-I
160  CR(I)=C(IR,1)
      WRITE (NOUT,200) (CR(K),K=1,NROW)
      GO TO 10
C
C     ***PRINT ERROR MESSAGES.
900  IF (ITYPE.NE.-1) WRITE (NOUT,901) ITYPE,MAT,MT,MAT1,MT1
901  FORMAT (/50H ***ERROR IN BOXR***CANNOT FIND ITYPE,MAT,MT,MAT1,
1    ,5HMT1 =,5I5)
      IF (ITYPE.EQ.-1) WRITE(NTAB,190) IZERO,IZERO
      STOP
910  WRITE (NOUT,911) NGMAX
911  FORMAT (/45H ***ERROR IN BOXR*** NUMBER OF GROUPS EXCEEDS,I4)
      STOP
C
190  FORMAT (5I6)
200  FORMAT (1P8E10.3)
210  FORMAT (I1,A3,8A4,2(I5,I4),2(I4,I3),3I4)
220  FORMAT (///)

```

```

      END
      SUBROUTINE SETFOR (NVF,NCF,NOUT,IVFT,ICFT)
C      *****
C      SET *BOXER* INPUT/OUTPUT FORMATS.
C      *****
      DIMENSION IFT(3,14), IVFT(3), ICFT(3)
      DATA IFT /4H(80I,4H1) ,4H ,4H(40I,4H2) ,4H ,4H(26I,4H3) ,
1 4H ,4H(20I,4H4) ,4H ,4H(16I,4H5) ,4H ,4H(13I,4H6) ,4H
2 ,4H(11F,4H7.4),4H ,4H(10F,4H8.5),4H ,4H(1P8,4HE9.2,4H)
3 ,4H(1P8,4HE10.,4H3) ,4H(1P7,4HE11.,4H4) ,4H(1P6,4HE12.,4H5) ,4
4 H(1P6,4HE13.,4H6) ,4H(1P5,4HE14.,4H7) /
C
      IF (NVF.LT.7.OR.NVF.GT.14) GO TO 900
      IF (NCF.LT.1.OR.NCF.GT.6) GO TO 900
C
C      ***SET FORMATS
      DO 10 I=1,3
      IVFT(I)=IFT(I,NVF)
10 ICFT(I)=IFT(I,NCF)
      RETURN
C
C      ERROR MESSAGE
900 WRITE (NOUT,901) NVF,NCF
901 FORMAT (/28H ***ERROR IN SETFOR***NVF (=:I3,11H) OR NCF (=:I3,13H)
1 IS ILLEGAL.)
      STOP
      END

```



## 12 MODER

The MODER module is used to convert ENDF, PENDF, and GENDF tapes from the NJOY blocked-binary mode to formatted mode (ASCII on modern computers), and *vice versa*. It can also be used to copy data from one logical unit to another without change of mode, or to make a new tape containing selected materials from one or more ENDF, PENDF, or GENDF tapes. MODER handles all ENDF-4 through ENDF-6 formats, plus special-purpose formats developed for NJOY, such as the **GROUPR** and **ERRORR** output formats. This section describes MODER in NJOY 2012.0. The differences between this version and the one previously reported[3] are connected with the conversion to Fortran-90 style, some changes in File 6 formats for thermal data, and the implementation of new covariance formats, including the INTG record.

### 12.1 Code Description

The main subroutine **moder** is exported by the module **modem**. At the beginning of execution, MODER rewinds the output tape **nout**. Additionally, each time a new input tape **nin** is specified, that unit is rewound. MODER then processes **nin** one file at a time, either for all materials on **nin**, or optionally (see following section) for a single specified material. As each file is identified, the main program calls a subroutine dedicated to that file. Each subroutine makes the series of calls to **contio**, **listio**, etc., that is appropriate to that file.

If **nin** and **nout** are of opposite sign, then mode conversion is performed automatically by the utility I/O subroutines. If **nin** and **nout** have the same sign, then no mode conversion is performed; runs of this type can be used simply to make an extra copy of the input tape or to retrieve selected materials without mode change. Only a little more than one page of scratch storage is needed, so there are no limitations on which tapes can be processed.

### 12.2 Input Instructions

As an aid to discussions of the user input to MODER, the input instructions that appear as comment cards at the beginning of the current version of this module are listed below. Since code changes are possible, it is always advisable to consult the comment-card instructions contained in the version of the code actually being used before proceeding with an actual calculation.

```

!---input specifications (free format)-----
!
! card 1      unit numbers
!      nin    input unit
!      nout   output unit
!
! a positive unit is coded (mode 3).
! a negative unit is blocked binary (njoy mode).
!
! note: abs(nin) ge 1 and le 19 is a flag to select various
!       materials from one or more input tapes, with or
!       without mode conversion. the kind of data to be
!       processed is keyed to nin as follows:
!           nin=1, for endf or pendf input and output,
!           2, for gendf input and output,
!           3, for errorr-format input and output.
!
!       cards 2 and 3 for abs (nin) ge 1 and le 19 only.
!
! card 2
!      tpid   tapeid for nout. 66 characters allowed
!             (delimited with ', ended with /)
! card 3
!      nin    input unit
!             terminate moder by setting nin=0
!      matd   material on this tape to add to nout
!-----

```

The contents of **nin** and **nout** are positive or negative logical unit numbers, with absolute magnitudes normally in the range 20-99, inclusive. Positive unit numbers refer to formatted tapes, and negative unit numbers refer to blocked-binary tapes. No other input is required to copy or convert the entire contents of the data file on unit **nin**, writing the results to unit **nout**.

A positive value of **nin** in the range 1-3 is used as a trigger to specify that the data to be copied or converted are not the contents of a single tape, but, instead, they are selected materials from one or more input tapes. The type of data to be processed (ENDF/PENDF *vs.* GENDF *vs.* [ERRORR](#)-format) is keyed to the value of **nin**, as detailed in the instructions above. If **nin** is in the

range 1-3, and only in this case, additional input is supplied to specify (on card 2) the tape-identification information to be written on the first record of the output tape and to specify (on card 3) both the **mat**-numbers of the materials to be included and the logical units where each of the desired materials are to be found. Note that the slash terminating the Hollerith information on card 2 is required. In the case of GENDF processing of a material **matd**, which is present on the specified input tape at a series of temperatures, a single card 3 causes the retrieval of all temperatures. Card 3 is repeated as many times as needed, and input is terminated with a card containing 0/.

### 12.3 Sample Input

It is good practice to convert the mode of the ENDF/B tape before proceeding with any NJOY run. The time spent in MODER is normally much less than the time saved by the subsequent modules. The required input for this is extremely simple. In this first example, an ENDF-formatted file, designated “tape20” is copied to a binary-formatted file designated “tape21”. This file is subsequently used as input to [RECONR](#).

```
moder
20 -21
reconr
-21 -22
...
```

For older versions of ENDF/B, the released “tapes” usually contained multiple materials. In the following example we specify that a single material, 1305, be extracted from “tape20” and written to “tape21”. Subsequent use of “tape21” will be more efficient since only the material of interest is on that tape.

```
moder
1 -21
'B-10'/
20 1305
0/
reconr
-21 -22
```

...

The final example (taken from one of the standard sample problems) shows the use of MODER to prepare a special multimaterial ENDF tape for a covariance calculation involving the 5 primary fissionable isotopes. Since, in this particular example problem, the resonance region is of no interest, a copy of the ENDF serves as the PENDF for later modules. Mount ENDF Tape 515, 516, and 555 on units 20, 21, and 22.

```

moder
1 -23
'endf/b-v nubar covariance materials'/
20 1380
20 1381
21 1390
22 1395
22 1398
20 1399
0/
moder
-23 -24
group
-23 -24 0 25
...
```

The second moder run copies the ENDF file to use as a PENDF file for [GROUPR](#).

## 12.4 Error Messages

error in moder\*\*\*endf materials must be in ascending order

This is a problem with the material ordering for the input tape.

message from moder---mat nnnn not found on gendf tape

Check the matd value on input card 3 and make sure that the correct input tape was mounted.

error in moder\*\*\*this material is not a gendf material

Input file contains an illegal mixture of data, namely, an initial GENDF material, followed by the indicated non-GENDF mat.

error in moder\*\*\*input is not an errorr output tape  
 User has requested **ERRORR**-format processing, but input data file is not a **ERRORR**-format tape.

error in moder\*\*\*input is not an endf or pendf tape  
 User has specified **nin**=1 on card 1, thereby requesting selective multitape ENDF or PENDF processing, but input data file on the unit **nin** specified on card 3 is not an ENDF/PENDF file.

error in moder\*\*\*input is not an endf tape  
 See comments above.

error in moder\*\*\*input is not a gendf tape  
 User has requested GENDF processing, but input data file is not a GENDF tape.

error in moder\*\*\*conversion not coded for mf=nn  
 There is an illegal or unrecognizable **mf** value on **nin**.

error in moder\*\*\*should have found send card  
 MODER is lost. The listed data display the contents of the last card read. Input data file may be bad.

error in moder\*\*\*illegal covariance mf=nn  
**ERRORR**-format file is missing the required **mf**=3. ENDF and PENDF tapes must be **mat** ordered.

error in file2\*\*\*illegal mt  
 Only the standard **mt**=151 and the NJOY special values of **mt**=152 and 153 are allowed in File 2.

error in file5\*\*\*illegal lf  
 The File 5 **lf** value is outside the legal range 1-12.

error in file6\*\*\*illegal ltt  
 This message comes from the branch used for ENDF-5 format or for thermal data generated by the **THERMR** module. Check the format of the File 6 sections.

error in file6\*\*\*illegal endf6 law  
 This message comes from the branch used for ENDF-6 tapes. Check the values for the **law** parameter in the sections of File 6.

error in file7\*\*\*illegal mt=nnn  
 Only **mt**=2 and **mt**=4 are allowed in File 7 for the ENDF-6 format.

error in file7\*\*\*illegal value of lthr=n  
 Only values of 1 or 2 are allowed for **lthr** in ENDF-6.

error in file15\*\*\*illegal lf  
 Only **lf**=1 and the special **lanl** format **lf**=2 are allowed



## 13 DTFR

This module is used to prepare libraries for discrete-ordinates transport codes that accept the format designed for the  $S_N$  code DTF-IV[23]. As this was one of the early discrete-ordinates codes, many newer  $S_N$  and diffusion codes allow DTF format as an input option. DTFR also contains a simple plotting capability for providing a quick look at its output. DTFR was the first output module written for the NJOY system, and it has been largely superseded by the MATXS/TRANSX system. But DTFR is still useful for some purposes because of its simplicity. This section describes DTFR 2012.0. There are two main differences between this version and the one reported previously[3]:

- the conversion to Fortran-90 style and memory allocation, and
- a new plotting system that prepares input for the [VIEWR](#) module to make higher quality Postscript plots.

### 13.1 Transport Tables

Transport tables in DTF format are organized to mirror the structure of the data inside a discrete-ordinates transport code. These codes start with the highest energy group and work downward. (The conventional order for group indices is to increase as energy decreases.) Therefore, for each group  $g$ , the data required are the reaction cross sections for group  $g$  and the scattering cross sections to  $g$  from other groups  $g'$ . Each data element is said to occupy a “position” in the table for group  $g$ . The organization is shown in Table 7.

Table 7: Organization of Data for One Group in a Transport Table

| Position | Meaning                                    |
|----------|--------------------------------------------|
| 1        | edit cross sections                        |
| ...      | (if any)                                   |
| iptotl-3 | last special edit                          |
| iptotl-2 | particle-balance absorption                |
| iptotl-1 | fission neutron production                 |
| iptotl   | total cross section                        |
| iptotl+1 | upscatter $g \leftarrow g'$ ( $g' > g$ )   |
| ...      | (if any)                                   |
| ipingp   | ingroup scattering $g \leftarrow g$        |
| ...      | downscatter $g \leftarrow g'$ ( $g' < g$ ) |
| itabl    | end of table                               |

The basic table consists of the three standard edits, namely, particle balance absorption ( $\sigma_a$ ), fission neutron production cross section ( $\bar{\nu}\sigma_f$ ), and total cross section ( $\sigma_t$ ). These standard edits are followed by the group-to-group scattering cross sections. If desired, the standard edits can be preceded by `iptotl-3` special edits, which can be used in the transport code to calculate various responses of the system (for example, heating, activation, or gas production). If `iptotl` is the position of the total cross section, the positions of the three standard edits will be `iptotl-2`, `ipingp-1`, and `iptotl`, respectively. The positions of the special edits (if `iptotl>3`) will be 1, 2, ... `iptotl-3`.

Most transport tables describe only downscatter. In such cases, the position of the ingroup element is `ipingp=iptotl+1`. Position `iptotl+1` would contain  $\sigma_{g \leftarrow (g-1)}$ , and so on. If thermal upscatter is present, the `nup` upscatter cross sections are between the total cross section element and the ingroup element. Therefore, position `iptotl-1` contains  $\sigma_{g \leftarrow (g+1)}$ , and so on. The position parameters must satisfy the following conditions:

$$\begin{aligned} \text{iptotl} &\geq 3 \quad , \text{ and} \\ \text{ipingp} &= \text{iptotl} + \text{nup} + 1 . \end{aligned}$$

The number of positions for a group is called the table length. A full table will have the table length given by

$$\text{itabl} = \text{iptotl-3} + 3 + \text{nup} + \text{ng} \quad ,$$

where `ng` is the total number of groups in the set. Table lengths can be truncated in some cases. If this is done correctly, the important cross sections will be conserved, and valid results can still be obtained.

An example of a transport table is given in Table 8. This table was generated with DTFR for ENDF/B-VI  $^{235}\text{U}$  (`mat=9228`). It contains three special edits: the (n,2n) cross section, the fission cross section, and the radiative capture cross section. These are followed by the three standard edits, and then by the ingroup scattering for group 1. Since this is the highest energy group, there is no downscatter to this group from groups above, and the rest of the positions are filled with zeros. Group 2 starts on line 8 with the six edit cross sections. The seventh number is the ingroup cross section, and the eighth is the scattering from group 1 to group 2. Continuing to lines 14 and 15, there are now two downscatter elements: two to three and one to three. Note that there is an entire table for each Legendre order, and that each table has a header card that describes its contents. The ellipses were added to mark removed lines.



Table 8: Example of a Transport Table with Internal Edits

```

IL= 1 TABLE 30 GP 36 POS, MAT= 9228 IZ= 1 TEMP= 3.00000E+02
 3.2597E-01 2.0823E+00 6.1629E-04 1.3965E+00 9.7755E+00 5.9989E+00
 3.1734E+00 0.0000E+00 0.0000E+00 0.0000E+00 0.0000E+00 0.0000E+00
 0.0000E+00 0.0000E+00 0.0000E+00 0.0000E+00 0.0000E+00 0.0000E+00
 0.0000E+00 0.0000E+00 0.0000E+00 0.0000E+00 0.0000E+00 0.0000E+00
 0.0000E+00 0.0000E+00 0.0000E+00 0.0000E+00 0.0000E+00 0.0000E+00
 0.0000E+00 0.0000E+00 0.0000E+00 0.0000E+00 0.0000E+00 0.0000E+00
 4.9950E-01 2.0532E+00 1.1756E-03 1.4681E+00 9.1321E+00 5.8659E+00
 3.0495E+00 1.1523E-01 0.0000E+00 0.0000E+00 0.0000E+00 0.0000E+00
 0.0000E+00 0.0000E+00 0.0000E+00 0.0000E+00 0.0000E+00 0.0000E+00
 0.0000E+00 0.0000E+00 0.0000E+00 0.0000E+00 0.0000E+00 0.0000E+00
 0.0000E+00 0.0000E+00 0.0000E+00 0.0000E+00 0.0000E+00 0.0000E+00
 0.0000E+00 0.0000E+00 0.0000E+00 0.0000E+00 0.0000E+00 0.0000E+00
 6.8192E-01 1.8830E+00 1.5668E-03 1.1928E+00 8.0521E+00 5.7877E+00
 2.9838E+00 8.2484E-02 3.1214E-02 0.0000E+00 0.0000E+00 0.0000E+00
...
IL= 2 TABLE 30 GP 36 POS, MAT= 9228 IZ= 1 TEMP= 3.00000E+02
 0.0000E+00 0.0000E+00 0.0000E+00 0.0000E+00 0.0000E+00 0.0000E+00
 2.8003E+00 0.0000E+00 0.0000E+00 0.0000E+00 0.0000E+00 0.0000E+00
 0.0000E+00 0.0000E+00 0.0000E+00 0.0000E+00 0.0000E+00 0.0000E+00
 0.0000E+00 0.0000E+00 0.0000E+00 0.0000E+00 0.0000E+00 0.0000E+00
 0.0000E+00 0.0000E+00 0.0000E+00 0.0000E+00 0.0000E+00 0.0000E+00
 0.0000E+00 0.0000E+00 0.0000E+00 0.0000E+00 0.0000E+00 0.0000E+00
 0.0000E+00 0.0000E+00 0.0000E+00 0.0000E+00 0.0000E+00 0.0000E+00
 2.5972E+00 3.8535E-02 0.0000E+00 0.0000E+00 0.0000E+00 0.0000E+00
 0.0000E+00 0.0000E+00 0.0000E+00 0.0000E+00 0.0000E+00 0.0000E+00
 0.0000E+00 0.0000E+00 0.0000E+00 0.0000E+00 0.0000E+00 0.0000E+00
 0.0000E+00 0.0000E+00 0.0000E+00 0.0000E+00 0.0000E+00 0.0000E+00
 0.0000E+00 0.0000E+00 0.0000E+00 0.0000E+00 0.0000E+00 0.0000E+00
 0.0000E+00 0.0000E+00 0.0000E+00 0.0000E+00 0.0000E+00 0.0000E+00
 2.4730E+00 2.3851E-02 7.4855E-03 0.0000E+00 0.0000E+00 0.0000E+00
...
IP= 1 TABLE 30 GP 12 POS, MAT= 9228 IZ= 1 TEMP= 3.00000E+02
 0.0000E+00 0.0000E+00 1.1808E-02 2.0992E-02 2.4928E-02 5.7726E-02
 6.0219E-01 1.8328E+00 5.5365E+00 7.5176E+00 1.0018E+01 2.0404E+00
 0.0000E+00 0.0000E+00 1.0938E-02 1.9445E-02 2.4306E-02 5.8998E-02
 5.7158E-01 1.7441E+00 5.2857E+00 7.2063E+00 9.5514E+00 1.9537E+00
 0.0000E+00 0.0000E+00 8.6352E-03 1.5352E-02 2.6314E-02 7.8974E-02
 5.3190E-01 1.6485E+00 5.0937E+00 7.1114E+00 9.1307E+00 1.9158E+00
 0.0000E+00 0.0000E+00 5.0549E-03 8.9865E-03 2.9371E-02 1.0974E-01
 4.6950E-01 1.4973E+00 4.7871E+00 6.9512E+00 8.4624E+00 1.8534E+00
.....

```

The last table in this example describes the photon production matrix. There are 30 neutron groups and 12 photon groups. The photon group index replaces

the position index used in the neutron tables. Therefore, the first 12 numbers in this table correspond to photon production from neutron group 1. The photon groups are arranged in order of decreasing energy.

The header lines at the start of each table in this example give the Legendre order, number of groups, number of positions, MAT number,  $\sigma_0$  number, and temperature.

DTFR will also produce a variant of the transport tables that was used for Los Alamos libraries in years past. These are sometimes called “CLAW Libraries” after the CLAW-III and CLAW-IV libraries available from the Radiation Safety Information Computational Center (RSICC) at the Oak Ridge National Laboratory. Although CLAW-IV uses a version of this format, it was actually generated using MATXS cross sections and the TRANSX code[81, 11].

The key feature of the CLAW tables is that the edits are removed from their normal position at the beginning of each group in the transport table and written out on separate lines. The format specified a particular list of reactions (see Table 9) that is defined using data statements in DTFR. In addition, thermal upscatter is not allowed in this format. An example of this style of transport table is given in Table 10. Note that eye-readable identifiers were added to the right-hand edge of each card by DTFR. The card labels contain the first two letters of the material name, the reaction name or the Legendre order, and a sequence number. The format of the header lines at the start of each table is different from the last example. The quantity in parentheses on the “EDIT XSEC” card is groups by number of edit reactions. For the neutron tables, it is table length by groups. For the gamma table, it is gamma groups by neutron groups.

## 13.2 Data Representations

The data stored into the transport tables are obtained from [GROUPT](#). Since all the scattering matrix reactions are kept separate in the multigroup processing, it is necessary to add them up to compute the DTF scattering matrix. They are obtained from the sections with `mf=6` on the input GENDF tape. Similarly, all the photon production matrices have to be added up to obtain the final DTF photon production table. These sections have `mf=16`.

Table 9: Predefined Edits for DTFR

| Reaction Name | Position | Reaction | Multiplicity |
|---------------|----------|----------|--------------|
| els           | 1        | 2        | 1            |
| ins           | 2        | 4        | 1            |
| n2n           | 3        | 16       | 1            |
|               | 3        | 6        | 1            |
|               | 3        | 7        | 1            |
|               | 3        | 8        | 1            |
|               | 3        | 9        | 1            |
| n3n           | 4        | 17       | 1            |
| ngm           | 5        | 102      | 1            |
| nal           | 6        | 107      | 1            |
| np            | 7        | 103      | 1            |
| fdir          | 8        | 19       | 1            |
| nnf           | 9        | 20       | 1            |
| n2nf          | 10       | 21       | 1            |
| ftot          | 11       | 18       | 1            |
| nd            | 12       | 104      | 1            |
| nt            | 13       | 105      | 1            |
| nhe3          | 14       | 106      | 1            |
| n2p           | 15       | 111      | 1            |
| npa           | 16       | 112      | 1            |
| nt2a          | 17       | 113      | 1            |
| nd2a          | 18       | 114      | 1            |
| n2a           | 19       | 108      | 1            |
| n3a           | 20       | 109      | 1            |
| nnd           | 21       | 32       | 1            |
| nnd2a         | 22       | 35       | 1            |
| nnhe3         | 23       | 34       | 1            |
| nna           | 24       | 22       | 1            |
| n2na          | 25       | 24       | 1            |
| nn3a          | 26       | 23       | 1            |
| n3na          | 27       | 25       | 1            |
| nnp           | 28       | 28       | 1            |
| nn2a          | 29       | 29       | 1            |
| n2n2a         | 30       | 30       | 1            |
| nnt           | 31       | 33       | 1            |
| nnt2a         | 32       | 36       | 1            |
| n4n           | 33       | 37       | 1            |
| n3nf          | 34       | 38       | 1            |
| chi           | 35       | 470      | 1            |
| chid          | 36       | 471      | 1            |
| nud           | 37       | 455      | 1            |
| phi           | 38       | 300      | 1            |
| theat         | 39       | 301      | 1            |
|               | 39       | 443      | 0            |
| kerma         | 40       | 443      | 1            |
| tdame         | 41       | 444      | 1            |
| nusf          | 42       | 1        | 1            |
| totl          | 43       | 452      | 1            |

Table 10: Example of DTFR Transport Tables Using Separate Edits

```

U235      EDIT XSEC ( 30X 48) PROC BY NJOY1  ON 05/03/90
 3.03110E+00 2.85141E+00 2.75464E+00 2.66464E+00 2.87622E+00 3.56158E+00U2  ELS
 4.43195E+00 4.38571E+00 3.94779E+00 3.53864E+00 3.34261E+00 3.61868E+00U2  ELS
 4.74566E+00 6.13164E+00 7.65700E+00 9.34710E+00 1.08466E+01 1.16438E+01U2  ELS
 1.19400E+01 1.28024E+01 1.32190E+01 1.31520E+01 1.29202E+01 1.30545E+01U2  ELS
 1.27990E+01 1.19229E+01 1.32489E+01 1.41192E+01 1.47783E+01 1.54225E+01U2  ELS
 3.78514E-01 4.17166E-01 4.61638E-01 5.44816E-01 8.11127E-01 1.37822E+00U2  INS
 2.20958E+00 2.30405E+00 2.34199E+00 2.28404E+00 2.14540E+00 1.90879E+00U2  INS
 1.60448E+00 1.29695E+00 9.63151E-01 4.00064E-01 4.54497E-02 3.03043E-03U2  INS
 1.87467E-06 7.26072E-08 0.00000E+00 0.00000E+00 0.00000E+00 0.00000E+00U2  INS
 0.00000E+00 0.00000E+00 0.00000E+00 0.00000E+00 0.00000E+00 0.00000E+00U2  INS
 3.25966E-01 4.99502E-01 6.81925E-01 8.22064E-01 6.05949E-01 3.47278E-01U2  N2N
 8.86188E-03 0.00000E+00 0.00000E+00 0.00000E+00 0.00000E+00 0.00000E+00U2  N2N
 0.00000E+00 0.00000E+00 0.00000E+00 0.00000E+00 0.00000E+00 0.00000E+00U2  N2N
...
U235      L=0 N-N TABLE ( 33X 30)
 1.39646E+00 9.77549E+00 5.99892E+00 3.17345E+00 0.00000E+00 0.00000E+00U2  0
 0.00000E+00 0.00000E+00 0.00000E+00 0.00000E+00 0.00000E+00 0.00000E+00U2  0
 0.00000E+00 0.00000E+00 0.00000E+00 0.00000E+00 0.00000E+00 0.00000E+00U2  0
 0.00000E+00 0.00000E+00 0.00000E+00 0.00000E+00 0.00000E+00 0.00000E+00U2  0
 0.00000E+00 0.00000E+00 0.00000E+00 0.00000E+00 0.00000E+00 0.00000E+00U2  0
 0.00000E+00 0.00000E+00 0.00000E+00 1.46808E+00 9.13206E+00 5.86594E+00U2  0
 3.04950E+00 1.15234E-01 0.00000E+00 0.00000E+00 0.00000E+00 0.00000E+00U2  0
 0.00000E+00 0.00000E+00 0.00000E+00 0.00000E+00 0.00000E+00 0.00000E+00U2  0
...
U235      L=1 N-N TABLE ( 33X 30)
 0.00000E+00 0.00000E+00 0.00000E+00 2.80033E+00 0.00000E+00 0.00000E+00U2  1
 0.00000E+00 0.00000E+00 0.00000E+00 0.00000E+00 0.00000E+00 0.00000E+00U2  1
 0.00000E+00 0.00000E+00 0.00000E+00 0.00000E+00 0.00000E+00 0.00000E+00U2  1
 0.00000E+00 0.00000E+00 0.00000E+00 0.00000E+00 0.00000E+00 0.00000E+00U2  1
 0.00000E+00 0.00000E+00 0.00000E+00 0.00000E+00 0.00000E+00 0.00000E+00U2  1
 0.00000E+00 0.00000E+00 0.00000E+00 0.00000E+00 0.00000E+00 0.00000E+00U2  1
 2.59724E+00 3.85346E-02 0.00000E+00 0.00000E+00 0.00000E+00 0.00000E+00U2  1
 0.00000E+00 0.00000E+00 0.00000E+00 0.00000E+00 0.00000E+00 0.00000E+00U2  1
...
U235      L=0 N-P TABLE ( 12X 30)
 0.00000E+00 0.00000E+00 1.18077E-02 2.09916E-02 2.49277E-02 5.77264E-02U2  0
 6.02189E-01 1.83282E+00 5.53653E+00 7.51757E+00 1.00182E+01 2.04037E+00U2  0
 0.00000E+00 0.00000E+00 1.09379E-02 1.94453E-02 2.43062E-02 5.89981E-02U2  0
 5.71583E-01 1.74411E+00 5.28569E+00 7.20630E+00 9.55138E+00 1.95373E+00U2  0
 0.00000E+00 0.00000E+00 8.63521E-03 1.53515E-02 2.63136E-02 7.89737E-02U2  0
 5.31904E-01 1.64847E+00 5.09371E+00 7.11139E+00 9.13067E+00 1.91577E+00U2  0
 0.00000E+00 0.00000E+00 5.05490E-03 8.98652E-03 2.93715E-02 1.09745E-01U2  0
.....

```

The standard edit called particle-balance absorption is used in discrete-ordinates transport codes to calculate the balance table. The most fundamental definition for this quantity is

$$\sigma_{a,g} = \sigma_{t,g} - \sum_{g'} \sigma_{s,g' \leftarrow g} . \quad (452)$$

The total cross section is obtained from **mf**=3, **mt**=1 on the input GENDF tape. The scattering matrix is obtained by adding all the matrix reactions found in File 6 on the input tape. The absorption edit is often written in the form

$$\sigma_{a,g} = \sigma_{\gamma,g} + \sigma_{f,g} - \sigma_{n2n,g} , \quad (453)$$

which is good up to the threshold for other multiparticle reactions. Because of the presence of the (n,2n) term, the  $\sigma_a$  parameter is not equal to the real neutron absorption for high-energy groups. In fact, it is often negative.

The next standard edit is used to compute the fission neutron production rate when constructing a fission source. It is used together with a fission spectrum, which can be included in the specials edits (see below). The fission contributions from the GENDF tape are complicated. First, the prompt fission matrix may be given in **mt**=18 (total fission), or in the partial fission reactions **mt**=19, **mt**=20, **mt**=21, and **mt**=38, which stand for (n,f), (n,n'f), (n,2nf), and (n,3nf). Second, each of these matrices may take advantage of the fact that the shape of the fission spectrum is constant at low energies. Thus, fission can be represented using single fission  $\chi_g^{LE}$  vector with this shape at low energies, with an accompanying fission neutron production cross section  $\sigma_{Pfg}^{LE}$  at low energies, and with a rectangular fission matrix  $\sigma_{g,g \rightarrow g'}^{HE}$  at high energies. The third complication is the presence of delayed fission neutron emission. The delayed neutron yield  $\bar{\nu}_g^D$  is retrieved from **mf**=3, **mt**=455, and the delayed neutron spectrum  $\chi_g^D$  is obtained by adding up the spectra for the time groups in **mf**=5, **mt**=455. The following equation shows how these separate terms are combined into the steady-state fission neutron production edit:

$$\bar{\nu}_g^{SS} \sigma_{fg} = \sum_{g'} \sigma_{fg \rightarrow g'}^{HE} + \sigma_{Pfg}^{LE} + \bar{\nu}_g^D \sigma_{fg} . \quad (454)$$

The associated steady-state fission spectrum is given by

$$\chi_{g'}^{SS} = \frac{\sum_g \sigma_{fg \rightarrow g'}^{HE} \phi_g + \chi_{g'}^{LE} \sum_g \sigma_{Pfg}^{LE} \phi_g + \chi_{g'}^D \sum_g \bar{\nu}_g^D \sigma_{fg} \phi_g}{\text{NORM}}, \quad (455)$$

where NORM is the quantity that will normalize the spectrum, namely, the sum of the numerator over all  $g'$ .

The total cross section is read directly from **mf**=3, **mt**=1. No transport corrections are made. The normal convention for libraries made with DTFR in the past was to supply P<sub>4</sub> tables and let the application code construct transport-corrected P<sub>3</sub> tables if it wanted them.

A flexible scheme is provided for constructing special edit cross sections. Each position can contain any of the cross sections available in File 3 of the GENDF tape, or a position can contain a combination of several cross sections weighted by multiplicities. For example, the ENDF/B-IV evaluation for <sup>12</sup>C contains the two reactions (n,α) (in **mf**=3, **mt**=107) and (n,n')3α (in **mf**=3, **mt**=91). To obtain the helium production cross section, it is only necessary to request an edit made up as follows:

$$1 \times \text{MT107} + 3 \times \text{MT91} .$$

Most of the reactions for these special edits are requested by giving their ENDF MT numbers. The following special MT values are used to request some special quantities:

| Special MT | Meaning                                                  |
|------------|----------------------------------------------------------|
| 300        | weighting flux (from <b>mf</b> =3, <b>mt</b> =1)         |
| 455        | delayed neutron yield ( <b>mf</b> =3, <b>mt</b> =455)    |
| 470        | steady-state spectrum (see Eq. 455)                      |
| 471        | delayed neutron spectrum ( <b>mf</b> =5, <b>mt</b> =455) |

See Section 13.4 on user input for more details.

DTFR can also construct transport tables suitable for calculations in the thermal range. These tables allow for upscatter, and the user can specify that bound scattering cross sections be used in the thermal range instead of the normal static elastic scattering reaction. The NJOY thermal capabilities are described in more detail in the [THERMR](#) and [GROUPE](#) sections of this report. In brief, NJOY can provide thermal scattering cross sections and matrices for any material treated as a free gas in thermal equilibrium (a Maxwell-Boltzmann

Table 11: Thermal Reactions Available to DTFR when using the ENDF/B-VII.0 Thermal Evaluations

| MTI | MTC | Thermal Binding Condition            |
|-----|-----|--------------------------------------|
| 221 |     | free gas                             |
| 222 |     | H in H <sub>2</sub> O                |
| 223 | 224 | H in polyethylene (CH <sub>2</sub> ) |
| 225 | 226 | H in ZrH                             |
| 227 |     | Benzene                              |
| 228 |     | D in D <sub>2</sub> O                |
| 229 | 230 | C in graphite                        |
| 231 | 232 | Be metal                             |
| 233 | 234 | Be in BeO                            |
| 235 | 236 | Zr in ZrH                            |
| 237 | 238 | O in BeO                             |
| 239 | 240 | O in UO <sub>2</sub>                 |
| 241 | 242 | U in UO <sub>2</sub>                 |
| 243 | 244 | Al metal                             |
| 245 | 246 | Fe metal                             |

distribution), or it can provide data for a number of important moderator materials whose scattering laws  $S(\alpha, \beta)$  are available in the ENDF/B-VII libraries. These thermal “materials” look like different reactions for the dominant scattering isotope after being processed by [GROUPT](#). Table 11 lists the different binding states that are available for ENDF/B-VII and the MT numbers used to request them. Materials like “H in H<sub>2</sub>O” give the scattering for the principal scattering isotope only; the other isotope should be treated using free-gas scattering. There is an exception: benzene was evaluated as a complete molecule, and the results were renormalized to be used with the cross section for the dominant isotope <sup>1</sup>H. Therefore, this material should be used with the density corresponding to the dominant isotope, and no thermal contribution from the other isotope should be included at all (set both `mti` and `mtc` to zero).

As described in more detail in the subsection on user input, DTFR has an input parameter called `ntherm` that specifies the number of incident-energy groups to be treated using thermal cross sections; this parameter determines the breakpoint between the thermal treatment and the normal static treatment. DTFR subtracts the static elastic cross section (`mt=2`) from both the total and absorption edits in this group range, and it adds the `mti` and `mtc` cross sections to these positions. Similarly, it omits the contributions from the `mt=2` matrix for these final-energy groups, and it adds in the contributions from `mti` and `mtc`. The user is free to use a number of upscatter positions less than `ntherm`. The

code will truncate the table in a way that preserves the total thermal scattering cross section.

### 13.3 Plotting

Plots of the output data from a formatting program like DTFR are useful in two ways: first, they provide a nice summary of the library and help its users to understand the trends in the data easily, and second, they are helpful in quality control as an aid to finding errors in processing. This versions replaces the old-style plotting from the original version of DTFR with a nicer system making use of the NJOY VIEWR module to produce attractive Postscript plots.

DTFR automatically makes two-dimensional log-log graphs for all the special edit positions and the three standard edit positions. If available (see `npend`), pointwise cross sections are plotted on the same frame as the group cross sections. If the multigroup cross section is a combination of several reactions, the pointwise cross sections for all of the components are plotted. An example of this will be found below. DTFR also prepares three-dimensional isometric projections of the  $P_0$  scattering matrix and the  $P_0$  photon-production table. The user can request that one reaction be plotted per page, or that four reactions be drawn on the same page. Examples of these plots are given in Figures 48–52.

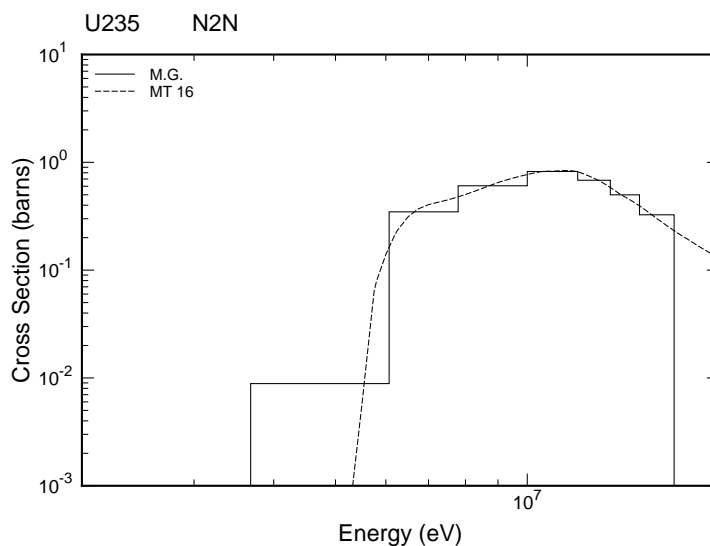


Figure 48: An example of DTFR plotting for the (n,2n) reaction of ENDF/B-VI  $^{235}\text{U}$ . This plot was prepared using `ifilm=1` and in-table edits. All the threshold reactions are shown using the same energy range to make comparisons easy.



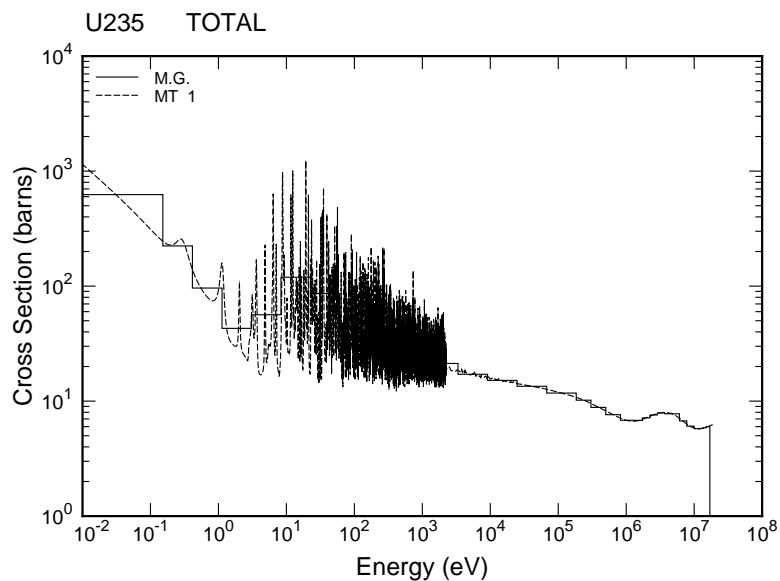


Figure 49: This is the total cross section for ENDF/B-VI  $^{235}\text{U}$  from the same run as the previous plot. The energy range from  $1 \times 10^{-5}$  eV to  $1 \times 10^{-2}$  eV was removed to expand the rest of the energy scale.

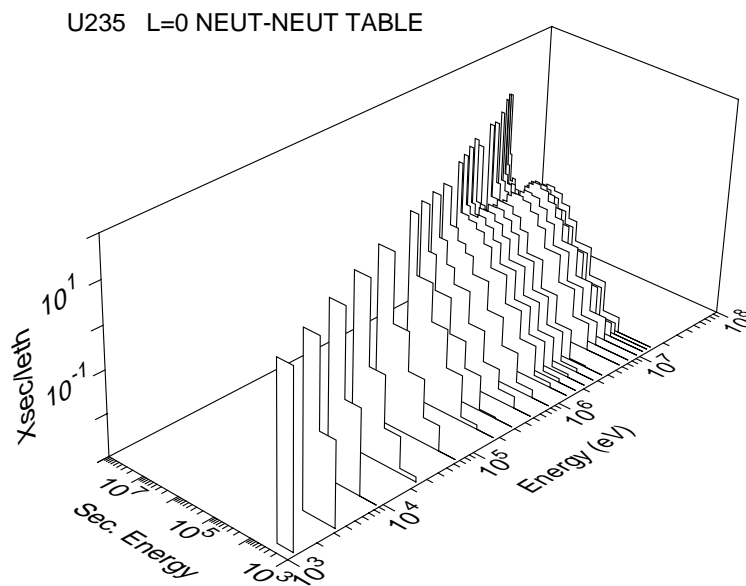


Figure 50: This plot shows the  $P_0$  scattering matrix for ENDF/B-VI  $^{235}\text{U}$  by incident and secondary energy.

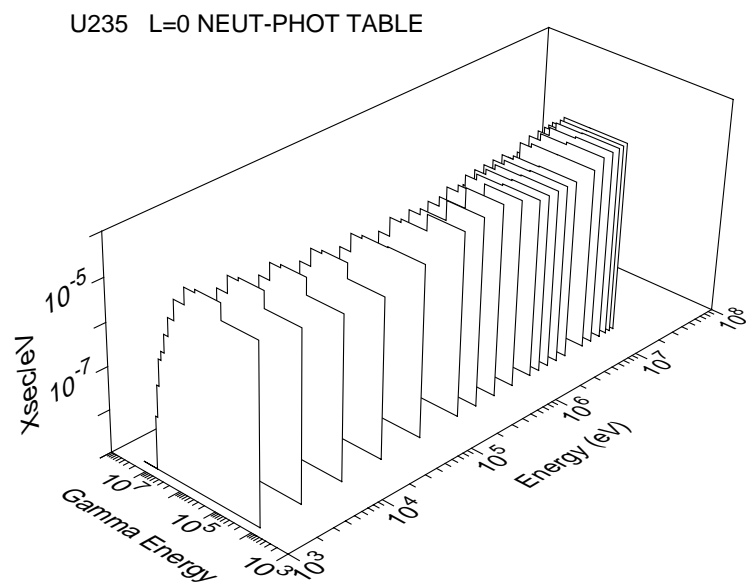


Figure 51: The  $30 \times 12$   $P_0$  photon production matrix for  $^{235}\text{U}$  is plotted versus neutron energy and photon energy.

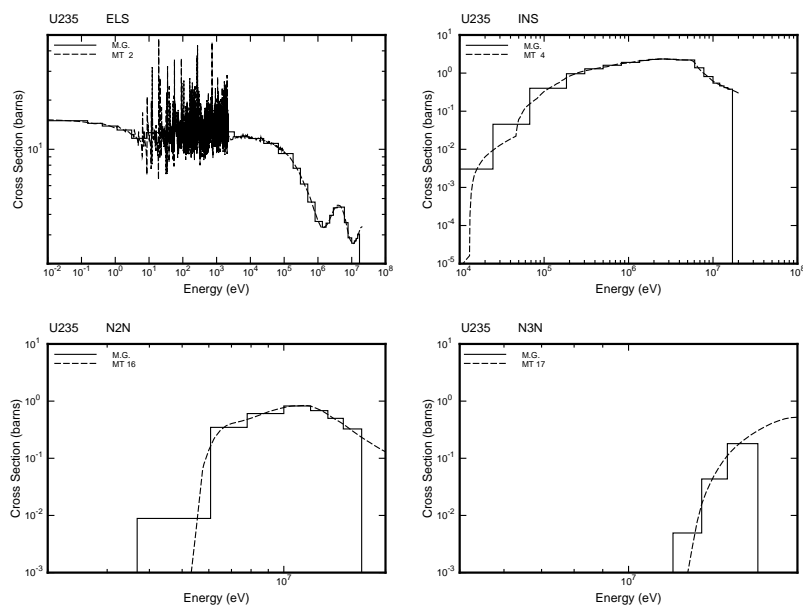


Figure 52: An example of DTFR plotting using `ifilm=2` for ENDF/B-VI  $^{235}\text{U}$  for some of the standard edits with `iedit=1`.

### 13.4 User Input

The following user input specifications were copied from the comment cards at the beginning of the DTFR module source code.

```

!---input specifications (free format)-----
!
! card 1      units
!   nin      input unit with data from groupr (binary).
!   nout     output unit containing dtf tables (coded).
!            (default=0=none)
!   npend    input unit with pendf tape for point plots.
!            (default=0=none)
!   nplot    output plot info for plotr module
!            (default=0=none)
! card 2      options
!   iprint   print control (0 minimum, 1 maximum)
!   ifilm    film control (0/1/2=no/yes with 1 plot per frame/
!            yes with 4 plots per frame (default=0)
!   iedit    edit control (0/1=in table/separate) (default=0)
!
!            cards 3 through 5 only for iedit=0
!
! card 3      neutron tables
!   nlmax    number of neutron tables desired.
!   ng       number of neutron groups
!   iptotl   position of total cross section
!   ipingp   position of in-group scattering cross section.
!   itabl    neutron table length desired.
!   ned      number of entries in edit table (default=0).
!   ntherm   number of thermal groups (default=0).
! card 3a only for ntherm ne 0
! card 3a     thermal incoherent and coherent mts
!   mti      mt for thermal incoherent data
!   mtc      mt for thermal coherent data (default=0)
!   nlc      no. coherent legendre orders (default=0)
! card 4      edit names
!            six character hollerith names for edits for as many
!            cards as needed.  there will be iptotl-3 names read.
!            each name is delimited with '.
! card 5      edit specifications
!            ned triplets of numbers on as many cards as needed.

```

```

!      positions can appear more than once.
!      reaction types can appear more than once.
!      jpos      position of edit quantity.
!      mt        endf reaction number.
!      mult      multiplicity to be used when adding this mt.
!
!      card 6 for iedit=1
!
! card 6      claw-format tables
!      nlmax     number of neutron tables (def=5)
!      ng        number of neutron groups (def=30)
!                (number of thermal groups is zero)
!
! card 7      gamma ray tables
!      nptabl     number of gamma tables desired (default=0)
!      ngp        number of gamma groups (default=0)
! card 8      material description
!      one card for each table set desired.
!      empty card (/) terminates execution of dtfr.
!      hisnam     6-character isotope name
!      mat        material number as in endf (default=0)
!      jsigz      index number of sigma-zero desired (default=1)
!      dtemp      temperature desired (default=300)
!
!-----

```

As usual, card 1 is used to assign the input and output units for the module. `nin` must be an output tape from [GROUPE](#), and it can be in either binary or coded mode. The output file `nout` must be in coded mode. It will contain the DTF-format card images. File `npend` should be the same PENDF tape that was used in [GROUPE](#) when `nin` was made. It is only needed if plots are requested. The `nplot` file will contain the input lines that [VIEWR](#) will use to prepare the Postscript plots of the DTFR results. Card 2 starts out with the print flag `iprint`, which is usually set to 1. The parameter `ifilm` can be used to suppress plotting, or to request plots with either 1 or 4 graphs per frame. Examples of the DTFR plotting capability were given above. The value of `iprint` is used to control the output format. If it is equal to zero, a conventional DTF-type table is produced. If any edits were requested, they are given in the table using the first few positions in the table. The separate-edits option is used to produce cross

sections in the “CLAW” format. In this format, the edits are extracted from the table and written out separately with identification information appended to the right side of each card image. The scattering tables have only the standard 3 edits, and they also have standard identification fields added to the right side of each card. Examples of both styles were given above.

Cards 3 through 5 are used for `iedit=0` only. The first parameter is `ilmax`. It is the number of Legendre tables desired; that is, it would be 4 for a  $P_3$  set. The number of groups `ng` must agree with the number on the input tape from `GROUPT`. The value of `iptotl` is used to determine both the position of the total cross section in the table and the number of special edit positions at the front of the table (`iptotl-3`, which can be zero). Note that `ned` is not the number of edit positions; it is the number of edit specification triplets to be read. Therefore, `ned ≥ iptotl-3`. Also `ipingp=iptotl+1` if there is no upscatter, and `ipingp=iptotl+nup+1` when the total number of upscatter groups is `nup`. (The parameter `nup` is not actually given in the input; it is always equal to `ipingp-iptotl-1`.) The length of a full table is given by

$$\begin{array}{rcl}
 & & \text{iptotl-3} \\
 + & 3 & \\
 + & \text{nup} & \\
 + & \text{ng} & \\
 \hline
 & \text{itable} &
 \end{array}$$

However, smaller table lengths can be requested; truncation will be performed in a way that preserves the production cross sections. The parameter `ntherm` can be set to zero if no thermal upscatter cross sections are desired. If nonzero, it refers to the number of incident thermal groups, and it is used to define the breakpoint between the thermal and epithermal treatments. It is not necessarily equal to `nup`.

Card 3a is only given if `ntherm>0`. It gives the `mt` numbers for the thermal incoherent and coherent cross sections to be extracted from the GENDF tape. Examples might include 221 and zero for free-gas scattering, or 229 and 230 for graphite. `NLC` can be used to truncate the anisotropy of the coherent term, if desired. For thermal cases, DTFR subtracts the static elastic scattering from both the total and absorption positions for the lowest `ntherm` groups, and then it adds in the cross sections corresponding to `mti` and `mtc` for these thermal groups. When reading through the matrices, it omits all the contributions from the static elastic matrix for the thermal groups, and adds in the `mti` and `mtc` contributions for these groups instead.

Card 4 gives Hollerith names for the edit cross sections. These **ned** names will appear on the output listing, but they are not passed on to the output file.

Card 5 specifies the contents of each of the special edit fields. Note that each edit can be any linear combination of the cross sections on the input GENDF tape. This feature can be used to produce complex edits like gas production. An example follows:

```

1.  ...
2.  n.he4 kerma fiss
3.  1 107/
4.  1 91 3/
5.  2 301/
6.  3 444/
7.  ....

```

The line numbers are not part of the input. Line 1 represents all the input cards before card 4, and line 7 represents all the cards after card 5. This input is for ENDF/B-IV  $^{12}\text{C}$ . Lines 3 and 4 construct a helium-production cross section as the sum of  $(n,\alpha)$  and three times  $(n,n')3\alpha$ . Lines 5 and 6 assign two more edit positions for heating and damage, respectively. The MT numbers used for

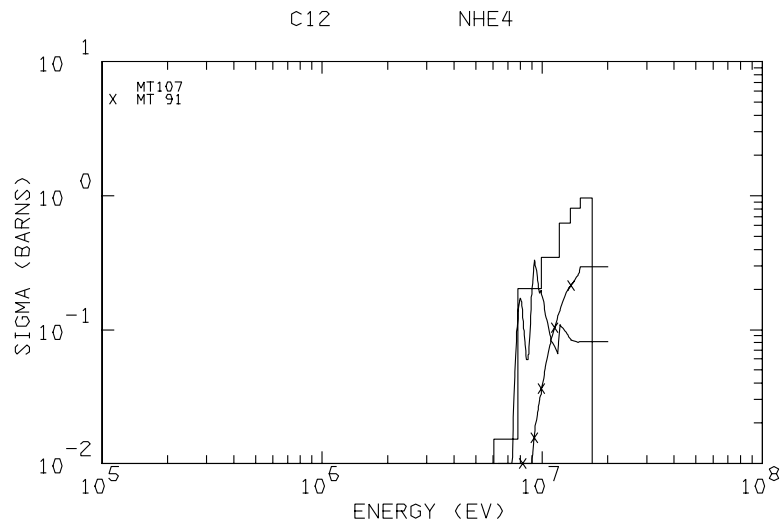


Figure 53: An example of a DTFR edit plot showing multiple pointwise curves that are the components of a compound edit. This graph is for ENDF/B-IV  $^{12}\text{C}$  helium production. The histogram gives the sum of the  $(n,\alpha)$  cross section and three times the  $(n,n')3\alpha$  cross section.

the `mt` field on card 5 are usually just the ENDF MT numbers for the reaction. However, there are special values available to request the weighting flux, the steady-state and delayed components of the fission neutron spectrum, or the delayed fission neutron yield. Remember that the steady-state fission neutron production cross section will be found in position `iptot1-1` of the transport table.

When a multigroup edit is a combination of several cross sections as in this example, the plot of the edit includes the pointwise cross sections for all of the component reactions. Figure 53 illustrates this for the  $^{12}\text{C}$  helium-production reaction. Another useful technique is to build up a compound edit out of two reactions using a multiplicity of zero for the second reaction. This causes the second reaction to be plotted but not included in the edit cross section. This method can be used to compare the energy-balance (`mt=301`) and kinematic (`mt=443`) versions of the KERMA factor. The appropriate input lines are

```
...
heat/
1 301 1 1 443 0/
...
```

Note that this method is used in the predefined edits associated with `iedit=1` (see Table 9).

Card 6 is used instead if `iedit=1`. As described above, the list of special edit cross sections is fixed for the CLAW format. Therefore, it is only necessary to give `nlmax` and `ng`. The number of thermal groups is automatically set to zero.

The next card read for either choice of output format is card 6, which controls the generation of a photon production matrix. The number of photon production tables is usually zero (none), or one. Only a few materials in the ENDF/B libraries have anisotropic photon production data. Of course, `ngp` must agree with the photon group structure used in [GROUPR](#).

The input deck ends with a material description card for each material to be processed. These materials must all be on the input GENDF tape. (Multi-MAT GENDF tapes can be prepared using [MODER](#) from single-material [GROUPR](#) output files, but since it is easy to combine materials at the DTF-format stage, DTFR is usually run for one MAT at a time.) The Hollerith material names given will appear in the comment cards before tables and in the special labels added to the right-hand edge of each card. The material numbers `mat` are the

same ENDF MAT numbers used when preparing the multigroup cross sections. DTFR has only a limited capability for handling self-shielded cross sections. The user can specify that a given set of tables be prepared using one particular temperature `dtemp` and one particular background cross section, the `jsigz`<sup>th</sup> value in the set.

### 13.5 Coding Details

The main entry point for DTFR is `dtfr` from module `dtfm`, which starts by calling `ruin` to read the user's input. Note that the special set of edits used when `iedit=1` is specified using parameter arrays in `ruin` (see `kmted`, `kjped`, `kmultd`, and `kmtid`). The next steps are to open a scratch file `nscr` and to initialize the plotting output.

The main loop over materials, dilution values, and temperatures goes through statement number 105. This is where input card number 8 is read (see input instructions) to identify the material to be processed. The input GENDF tape is then rewound, and `nin` is searched for the material and temperature. If a PENDF input tape has been mounted, the corresponding material and temperature are located on `npnd`. Note that the materials in the input file do not have to be in the same order as the materials on either `nin` or `npnd`. If a requested material or temperature is not found, a fatal error message is issued.

When the input files have been properly positioned, `dtfr` checks to see if there is enough storage for the tables. The limit `nwsmax=500000` is large enough for any reasonable multigroup set. If larger sets are desired, increase the value of this variable which will automatically increase the dimension of the global array `sig(nwsmax)`. The loop over reactions and groups in a reaction goes through statement number 150. Once the cross sections have been read off the input tape, the code branches to different sections to process different kinds of data. The first of these processes the File 3 neutron cross sections. Note that the total cross section is stored in both `iptot1` and `iptot1-2`. In addition, the `GROUPR` weighting flux can be extracted from the section `mf=3`, `mt=1` and stored into a special edit requested using `mt=300`. Special edit cross sections are weighted with the specified multiplicities and summed into the specified edit positions in the “do `ied=1`, `ned`” loop. Thermal corrections to static scattering are made at statement number 260. The method used is to subtract `mt=2` and add `mti` and `mtc` to both the total and absorption positions.

The block of coding starting with statement number 300 is used to accumulate the total scattering matrix. Most numbers are simply added into the correct



position in the transport table. The operation specified by Eq. 452 is performed by subtracting all matrix elements from the absorption position. In addition, in the thermal range, the `mti` and `mtc` data are used instead of the `mt=2` data.

The prompt part of fission is handled starting at statement number 340. Note that a check is made to see if `MT=18` was already processed if `mt=19` is found. This results in a fatal error, so the user must be careful to process only one of these representations in `GROUPT`. The special cases `ig=0` and `ig21o=0` flag the presence of the low-energy constant spectrum or production cross section, respectively. Delayed fission contributions are handled by the next block of coding. The method used for combining the fission matrix, the constant-spectrum part, and the delayed parts are defined by Eqs. 454 and 455. The normalization parameter needed to fix up  $\chi$  is accumulated in the variable `cnorm`.

The photon-production matrix is accumulated starting at statement number 600. It is a very simple process of adding all the partial matrices with `mf=16` on the input `GENDF` file. When all the reactions and groups for this material and temperature have been processed, `dtfr` calls the subroutine `dtfout` to prepare the tables and plots, and then it loops back to statement number 105 for the next requested material. After all the materials, temperatures, and background cross sections have been written out, the plotting system is terminated (see below), files are closed, a final message is printed, and control is returned to `njoy`.

Subroutine `dtfout` controls the preparation of the output DTF tables on `nout`, the printing of the tables on the user's output device, and the preparation of plots. This is a simple routine with separate paths for in-table edits and separate edits. Plotting is handled using different subroutines for the edits, the neutron table, and the photon-production table.

Subroutine `plotted` is used to prepare plots of all the special and standard edit positions, including overlay plots of `PENDF` cross sections if `npend` is available. Subroutine `histod` is used to convert the multigroup values into a pointwise cross section with steps at each of the group boundary energies; that is, into histogram form. Subroutine `dpend` prepares the `PENDF` part of the plot by thinning the original `PENDF` grid down to a new grid with  $x$  spacing something like the resolution of a typical screen. In addition, it "thickens" reactions, if necessary, so that there are enough points to properly follow the curve on the final log-log plot. Both the histogram and `PENDF` data arrays are written on the `nplot` unit as simple text commands in `VIEWR` format.

Subroutine `plotnn` is used to plot an isometric view of the neutron table. This is done by removing the edits from the table and then writing lines to

`nplot`. Note that the energies corresponding to the groups are used in the `VIEWR` commands, thus producing more realistic pictures than the older DTFR methods was able to make. A similar process is performed in `plotnp` for the photon-production matrix.

### 13.6 Error Messages

`error in dtfr***number of neutron groups disagrees with...`

The value of `ng` in the input must be consistent with the number of groups on the input GENDF tape. Check the input, and check whether the correct tape was mounted.

`error in dtfr***number of gamma groups disagrees with...`

Same as above, except check the number of gamma groups `ngp`.

`error in dtfr***desired temperature not on pendf`

Code is unable to find `mat` and `dtemp` on the input PENDF tape `npend`. Check the input information and check whether the correct PENDF tape was mounted.

`error in dtfr***not enough storage for table`

There is not enough space in the `sig` array to construct a table with so many positions and groups. See the global parameter `nwsmax=500000`.

`error in dtfr***not enough storage for record`

There is not enough space in the `a` array to read in the data on the GENDF tape. See the global parameter `nwamax=40000`.

`error in dtfr***mt18 already processed//mt19 not allowed`

Make sure that `GROUPE` processes the fission matrix using either `mt=18` only, or `mt=19, 20, 21, and 38`, but not both.

`error in dtfr***delayed nubar required to add delayed ....`

The delayed neutron yield must have been processed in `GROUPE` (`mfd=3`, `mtd=455`), or DTFR will be unable to construct the steady-state fission vectors.

`error in ruin***iping.le.iptotl`

The ingroup position `iping` is normally `iptotl+1`, and it will be larger still if thermal upscatter is to be included. Check input card number 3.

`error in ruin***not enough storage for edits`

See the global parameter `nedmax=50`.

`error in dpend***npts exceeds ndim`

The thinning/thickening process has produced too many points for the arrays `x` and `y`. These are global arrays dimensioned at by the global parameter `ndim=7000`.

## 14 CCCCCR

This module is used to produce the standard CCCC interface files ISOTXS, BRKOXS, and DLAYXS from [GROUPE](#) output. This chapter describes CCCCCR in NJOY 2012.0. The only differences between this version and the one reported previously[3] have to do with the conversion to Fortran-90 style and memory allocation.

### 14.1 Introduction

The CCCC interface files (commonly pronounced “four cees”) were developed by the Committee for Computer Code Coordination for the US Fast Breeder Reactor Program. When the members of this committee started work in 1970, they noted that because of the large variety of computers and computer systems, computer codes developed at one laboratory were often incompatible with computers at other laboratories. Major rewrites of codes or wasteful duplicate efforts were common. They hoped to create a system that would allow different laboratories to create codes that could be moved to other sites more easily. Moreover, they hoped that the codes developed at different laboratories could easily work together, thereby achieving larger and more capable calculational systems than any one laboratory could hope to develop by itself.

They approached this problem in two ways. First, they tried to establish general programming standards that would make computer codes more portable. And second, they tried to establish standard interface files for reactor physics codes that would make it easier for computer codes to communicate with each other. The results of this work appeared in fullest form as the CCCC-III and CCCC-IV standards[28, 10].

The MINX code[20], which was the predecessor of NJOY, was able to produce libraries [62] that used the CCCC-III interface formats. The LINX and BINX library management codes[82] and the CINX group collapse code[83] were also released during this period. Major codes that used data in CCCC-format included SPHINX[84] from Westinghouse, TDOWN[85] from General Electric, DIF3D[15] from Argonne National Laboratory, and ONEDANT[13] from LANL. It was indeed found that codes could be moved more easily than before. Analysts could use ONEDANT and DIF3D on similar problems; they could even use one code to generate utility files (for example, mixture and geometry files) that would work with the other code! When NJOY was developed, it first produced version III formats and was later upgraded to the CCCC-IV standard.

With the demise of the breeder reactor program, development of the CCCC system has stopped. However, many good programs are still available that make use of CCCC files and programming standards. The LANL DANDE system[86] was an example of how the use of standard interface files can be used to couple several reactor physics programs together into an easy-to-use and powerful product. In areas where the CCCC standards were not very successful, such as gamma ray cross sections and cross sections for the fusion energy range, the MATXS format is available as an alternative. This generalized material cross section library format uses CCCC-type techniques. The modern  $S_N$  code PARTISN[16] makes very heavy use of both standard and non-standard CCCC files. Thus, the CCCC spirit is not dead.

## 14.2 CCCC Procedures and Programming Standards

Although the CCCC programming standards went so far as to give advice on program structure, documentation, and good coding practice, their main purpose was to make it easier to move computer codes from one machine to another. The main problems in those days were the slightly different implementations of input/output on CDC and IBM machines, the different word size on CDC and IBM machines, and the relatively small size of the main memory on the CDC 7600. The last of these problems was attacked by limiting the maximum memory requirements for CCCC-compliant codes. This problem has disappeared for modern computers.

The word-size problem has three components. First, it is often necessary to change the statements that allocate space for variables and arrays [for example, “`DIMENSION A(10)`” might have to be changed to “`REAL*8 A(10)`” when moving from a long-word machine (CDC, Cray) to a short-word machine (IBM, VAX, Sun)]. Second, the names of functions that work with double-precision variables normally must be changed (for example, `ALOG10` to `DLOG10`). And third, the word boundaries of double-precision variables must be properly aligned in common blocks and equivalenced arrays. The standard CCCC method for handling name changes has been based on using standard control cards. As an example, a code for a long-word machine might contain the following code fragment:

```

CSW
C      REAL*8 HA(10)
CSW
CLW
      INTEGER HA(10)
CLW

```

The variable `HA` is intended to hold 10 words of Hollerith information using the standard CCCC 6-character word length. Such a variable must be declared as double precision on short-word machines, which typically allow four Hollerith characters per word. To change this code to its short-word version, a special utility code reads through each line removing the comment “C” from lines bracketed by the “SW” comments and inserting a “C” in column 1 for all lines bracketed by “LW” comments. Early versions of NJOY used this scheme; later versions used UPD[87] conditional statements instead. For example, the source file contained

```

*IF SW
      REAL*8 HA(10)
*ELSE
      INTEGER HA(10)
*ENDIF

```

and the compile file produced by UPD had only one of the two alternatives activated, depending on whether `SW` has been set or not. NJOY2012 uses built-in features of Fortran-90 to handle this problem. The `locale` module defines a special “kind” for the Hollerith data that is packed into CCCC records.

The word-alignment problem requires that some care be used in allocating arrays and common blocks. For example,

```

REAL*8 HA
COMMON/BAD/IA(3),HA(10)

```

should be avoided; it would be OK with `IA(4)`. Most CCCC records contain

mixtures of Hollerith, floating-point, and integer variables. The desired data is normally extracted by making use of equivalenced arrays. For example, a code could contain the following declarations:

```
REAL*8 HA(10)
DIMENSION A(20),IA(20)
EQUIVALENCE (HA(1),A(1)),(IA(1),A(1))
```

Assume that a record containing 2 Hollerith variables (which require two single-precision variables each), 2 floating-point numbers (at single precision), and 2 integers has been read into array **A**. How do you extract the first of the integers? The solution depends on defining a CCCC-standard quantity called **mult**, which is 1 for long-word machines and 2 for short-word machines. Now, the desired value can be obtained with an expression of the form

```
I1=IA(2*MULT+3)
```

The second Hollerith variable would be extracted using the simple expression

```
H2=HA(2)
```

Changing the value of **mult** when transporting a code to a different machine is easily handled using control-card brackets or UPD conditionals as described above.

In NJOY2012, common blocks are no longer used, but equivalencing is still used to pack Hollerith (or character), integer, and real data into the CCCC records.

The remaining feature of the CCCC programming standards that is used in codes like PARTISN is the concept of standardized input/output subroutines. The CCCC interface files are sequential binary files (binary for efficiency and sequential for simplicity). The interface formats are arranged so that the length of any record can be calculated using parameters already read from previous records. It is convenient to insulate CCCC input/output from system variations by defining two standard routines:

**REED(NREF, IREC, ARRAY, NWDS, MODE)**

Read record **IREC** from unit **NREF** into **ARRAY**. The record has length **NWDS** in single-precision words. The **MODE** parameter is used to control I/O buffering, and it is not used in **NJOY**. Records can be read out of sequence; the routine does any record skipping (forward or backward) needed to arrive at record number **IREC**.

**RITE(NREF, IREC, ARRAY, NWDS, MODE)**

Write record **IREC** onto unit **NREF** using the data in **ARRAY**. The first **NWDS** single-precision words will be written. The **MODE** parameter is ignored. The records **NREF** must be written in sequence. The unit will be rewound if **IREC=1**.

When transporting a code between different computer systems, it is only necessary to have (or prepare) operational versions of **REED** and **RITE** for the target machine.

In the conversion to Fortran-90 style, we tried to avoid all these tricks. The reading and writing of CCCC records was coded in directly to avoid word-length problems (no more **REED** or **RITE**). All internal variable and data read from the GENDF file use 8-byte words. It is only at the last stage when the data are stored into the CCCC records that the 8-byte data are converted to 4-byte words. Thus, **mult** is always equal to 2. In general, the accuracy obtained with 4-byte words is sufficient for multigroup data.

### 14.3 The Standard Interface Files

The CCCCCR module produces data libraries that use three of the CCCC-IV standard interface files, namely:

**ISOTXS** for nuclide (isotope)-ordered multigroup neutron cross sections including cross section versus energy functions for the principal cross sections, group-to-group scattering matrices, and fission neutron production and spectra tables;

**BRKOXS** for Bondarenko-type self-shielding factors versus energy group, temperature, and background cross section for the reactions with major resonance contributions; and

**DLAYXS** for delayed-neutron precursor yields, emission spectra, and decay constants for the major fissionable isotopes.

The format of each of these files, the definition of the types of data included, and the uses and weaknesses of these three standard file formats are discussed in the following three sections.

As mentioned in the preceding section, the normal form of the CCCC files is binary and sequential. CCCCCR writes its output in this binary mode. Of course, coded versions (ASCII for modern systems) are needed to move library files between different machines, and the formats used for the coded versions are given in the file descriptions below. A separate program, BINX[82], is used to convert back and forth between coded and binary modes. BINX can also be used to prepare an interpreted listing of a library. CCCCCR can prepare an entire multimaterial library in one run if a multimaterial GENDF file is available. It can also be used to prepare an interface file containing only one material. These one-material files can be merged into multimaterial libraries using the LINX code[82].

#### 14.4 ISOTXS

The format for the ISOTXS material (isotope)-ordered cross section file is given below. This computer-text format is standard for the CCCC interface files. Of course, if these lines were to be inserted into an F90 computer code, the initial "C" would have to be changed to "!".

```

C*****
C              REVISED 11/30/76              -
C              -                              -
CF          ISOTXS-IV                        -
CE          MICROSCOPIC GROUP NEUTRON CROSS SECTIONS -
C              -                              -
CN              THIS FILE PROVIDES A BASIC BROAD GROUP -
CN              LIBRARY, ORDERED BY ISOTOPE -
CN              FORMATS GIVEN ARE FOR FILE EXCHANGE PURPOSES -
CN              ONLY. -
C              -
C*****

C-----
CS          FILE STRUCTURE -
CS              -                              -
CS          RECORD TYPE                PRESENT IF -
CS          =====                ===== -
CS          FILE IDENTIFICATION        ALWAYS -
CS          FILE CONTROL                ALWAYS -
CS          FILE DATA                  ALWAYS -

```



```

CS          FILE-WIDE CHI DATA                      ICHIST.GT.1      -
CS  ***** (REPEAT FOR ALL ISOTOPES)                -
CS  *          ISOTOPE CONTROL AND GROUP                -
CS  *                      INDEPENDENT DATA    ALWAYS                -
CS  *          PRINCIPAL CROSS SECTIONS                ALWAYS                -
CS  *          ISOTOPE CHI DATA                      ICHI.GT.1      -
CS  *  ***** (REPEAT TO NSCMAX SCATTERING BLOCKS)    -
CS  *  *  ***** (REPEAT FROM 1 TO NSBLOK)            -
CS  *  *  *  SCATTERING SUB-BLOCK                      LORD(N).GT.0    -
CS  *****                                           -
C                                           -
C-----

C-----

CR          FILE IDENTIFICATION                        -
C                                           -
CL  HNAME,(HUSE(I),I=1,2),IVERS                    -
C                                           -
CW  1+3*MULT=NUMBER OF WORDS                        -
C                                           -
CB  FORMAT(11H OV ISOTXS ,1H*,2A6,1H*,I6)            -
C                                           -
CD  HNAME          HOLLERITH FILE NAME - ISOTXS -    -
CD  HUSE(I)        HOLLERITH USER IDENTIFICATION (A6) -
CD  IVERS          FILE VERSION NUMBER                -
CD  MULT           DOUBLE PRECISION PARAMETER          -
CD                      1- A6 WORD IS SINGLE WORD      -
CD                      2- A6 WORD IS DOUBLE PRECISION WORD -
C                                           -
C-----

C-----

CR          FILE CONTROL      (1D RECORD)                -
C                                           -
CL  NGROUP,NISO,MAXUP,MAXDN,MAXORD,ICHIST,NSCMAX,NSBLOK -
C                                           -
CW  8=NUMBER OF WORDS                        -
C                                           -
CB  FORMAT(4H 1D ,8I6)                        -
C                                           -
CD  NGROUP          NUMBER OF ENERGY GROUPS IN FILE    -
CD  NISO            NUMBER OF ISOTOPES IN FILE          -

```

|    |                                                  |                                                    |   |
|----|--------------------------------------------------|----------------------------------------------------|---|
| CD | MAXUP                                            | MAXIMUM NUMBER OF UPSCATTER GROUPS                 | - |
| CD | MAXDN                                            | MAXIMUM NUMBER OF DOWNSCATTER GROUPS               | - |
| CD | MAXORD                                           | MAXIMUM SCATTERING ORDER (MAXIMUM VALUE OF         | - |
| CD |                                                  | LEGENDRE EXPANSION INDEX USED IN FILE).            | - |
| CD | ICHIST                                           | FILE-WIDE FISSION SPECTRUM FLAG                    | - |
| CD |                                                  | ICHIST.EQ.0, NO FILE-WIDE SPECTRUM                 | - |
| CD |                                                  | ICHIST.EQ.1, FILE-WIDE CHI VECTOR                  | - |
| CD |                                                  | ICHIST.GT.1, FILE-WIDE CHI MATRIX                  | - |
| CD | NSCMAX                                           | MAXIMUM NUMBER OF BLOCKS OF SCATTERING DATA        | - |
| CD | NSBLOK                                           | SUBBLOCKING CONTROL FOR SCATTER MATRICES. THE      | - |
| CD |                                                  | SCATTERING DATA ARE SUBBLOCKED INTO NSBLOK         | - |
| CD |                                                  | RECORDS (SUBBLOCKS) PER SCATTERING BLOCK.          | - |
| C  |                                                  |                                                    | - |
| C  | -----                                            |                                                    |   |
| C  | -----                                            |                                                    |   |
| CR | FILE DATA                                        | (2D RECORD)                                        | - |
| C  |                                                  |                                                    | - |
| CL | (HSETID(I),I=1,12),(HISONM(I),I=1,NISO),         |                                                    | - |
| CL | 1(CHI(J),J=1,NGROUP),(VEL(J),J=1,NGROUP),        |                                                    | - |
| CL | 2(EMAX(J),J=1,NGROUP),EMIN,(LOCA(I),I=1,NISO)    |                                                    | - |
| C  |                                                  |                                                    | - |
| CW | (NISO+12)*MULT+1+NISO                            |                                                    | - |
| CW | +NGROUP*(2+ICHIST*(2/ICHIST+1)))=NUMBER OF WORDS |                                                    | - |
| C  |                                                  |                                                    | - |
| CB | FORMAT(4H 2D ,1H*,11A6,1H*/                      | HSETID,HISONM                                      | - |
| CB | 11H*,A6,1H*,9(1X,A6)/(10(1X,A6)))                |                                                    | - |
| CB | FORMAT(6E12.5)                                   | CHI (PRESENT IF ICHIST.EQ.1)                       | - |
| CD | FORMAT(6E12.5)                                   | VEL,EMAX,EMIN                                      | - |
| CD | FORMAT(12I6)                                     | LOCA                                               | - |
| C  |                                                  |                                                    | - |
| CD | HSETID(I)                                        | HOLLERITH IDENTIFICATION OF FILE (A6)              | - |
| CD | HISONM(I)                                        | HOLLERITH ISOTOPE LABEL FOR ISOTOPE I (A6)         | - |
| CD | CHI(J)                                           | FILE-WIDE FISSION SPECTRUM(PRESENT IF ICHIST.EQ.1) | - |
| CD | VEL(J)                                           | MEAN NEUTRON VELOCITY IN GROUP J (CM/SEC)          | - |
| CD | EMAX(J)                                          | MAXIMUM ENERGY BOUND OF GROUP J (EV)               | - |
| CD | EMIN                                             | MINIMUM ENERGY BOUND OF SET (EV)                   | - |
| CD | LOCA(I)                                          | NUMBER OF RECORDS TO BE SKIPPED TO READ DATA FOR   | - |
| CD |                                                  | ISOTOPE I. LOCA(1)=0                               | - |
| C  |                                                  |                                                    | - |
| C  | -----                                            |                                                    |   |

```

C-----
CR          FILE-WIDE CHI DATA    (3D RECORD)          -
C                                                    -
CC          PRESENT IF ICHIST.GT.1                      -
C                                                    -
CL          ((CHI(K,J),K=1,ICHIST),J=1,NGROUP),(ISSPEC(I),I=1,NGROUP) -
C                                                    -
CW          NGROUP*(ICHIST+1)=NUMBER OF WORDS          -
C                                                    -
CB          FORMAT(4H 3D ,5E12.5/(6E12.5))    CHI        -
CB          FORMAT(12I6)                      ISSPEC      -
C                                                    -
CD          CHI(K,J)      FRACTION OF NEUTRONS EMITTED INTO GROUP J AS A -
CD                        RESULT OF FISSION IN ANY GROUP,USING SPECTRUM K -
CD          ISSPEC(I)      ISSPEC(I)=K IMPLIES THAT SPECTRUM K IS USED -
CD                        TO CALCULATE EMISSION SPECTRUM FROM FISSION -
CD                        IN GROUP I                    -
C                                                    -
C-----

C-----
CR          ISOTOPE CONTROL AND GROUP INDEPENDENT DATA    (4D RECORD) -
C                                                    -
CL          HABSID,HIDENT,HMAT,AMASS,EFISS,ECAPT,TEMP,SIGPOT,ADENS,KBR,ICHI, -
CL          1IFIS,IALF,INP,IN2N,IND,INT,LTOT,LTRN,ISTRPD, -
CL          2(IDSCT(N),N=1,NSCMAX),(LORD(N),N=1,NSCMAX), -
CL          3((JBAND(J,N),J=1,NGROUP),N=1,NSCMAX), -
CL          4((IJJ(J,N),J=1,NGROUP),N=1,NSCMAX) -
C                                                    -
CW          3*MULT+17+NSCMAX*(2*NGROUP+2)=NUMBER OF WORDS -
C                                                    -
CB          FORMAT(4H 4D ,3(1X,A6)/6E12.5/ -
CB          1(12I6)) -
C                                                    -
CD          HABSID      HOLLERITH ABSOLUTE ISOTOPE LABEL - SAME FOR ALL -
CD                        VERSIONS OF THE SAME ISOTOPE IN FILE (A6)-
CD          HIDENT      IDENTIFIER OF LIBRARY FROM WHICH BASIC DATA -
CD                        CAME (E.G. ENDF/B) (A6) -
CD          HMAT        ISOTOPE IDENTIFICATION (E.G. ENDF/B MAT NO.) (A6) -
CD          AMASS        GRAM ATOMIC WEIGHT -
CD          EFISS        TOTAL THERMAL ENERGY YIELD/FISSION (W.SEC/FISS) -
CD          ECAPT        TOTAL THERMAL ENERGY YIELD/CAPTURE (W.SEC/CAPT) -

```

|    |          |                                                   |   |
|----|----------|---------------------------------------------------|---|
| CD | TEMP     | ISOTOPE TEMPERATURE (DEGREES KELVIN)              | - |
| CD | SIGPOT   | AVERAGE EFFECTIVE POTENTIAL SCATTERING IN         | - |
| CD |          | RESONANCE RANGE (BARNS/ATOM)                      | - |
| CD | ADENS    | DENSITY OF ISOTOPE IN MIXTURE IN WHICH ISOTOPE    | - |
| CD |          | CROSS SECTIONS WERE GENERATED (A/BARN-CM)-        | - |
| CD | KBR      | ISOTOPE CLASSIFICATION                            | - |
| CD |          | 0=UNDEFINED                                       | - |
| CD |          | 1=FISSILE                                         | - |
| CD |          | 2=FERTILE                                         | - |
| CD |          | 3=OTHER ACTINIDE                                  | - |
| CD |          | 4=FISSION PRODUCT                                 | - |
| CD |          | 5=STRUCTURE                                       | - |
| CD |          | 6=COOLANT                                         | - |
| CD |          | 7=CONTROL                                         | - |
| CD | ICHI     | ISOTOPE FISSION SPECTRUM FLAG                     | - |
| CD |          | ICHI.EQ.0, USE FILE-WIDE CHI                      | - |
| CD |          | ICHI.EQ.1, ISOTOPE CHI VECTOR                     | - |
| CD |          | ICHI.GT.1, ISOTOPE CHI MATRIX                     | - |
| CD | IFIS     | (N,F) CROSS SECTION FLAG                          | - |
| CD |          | IFIS=0, NO FISSION DATA IN PRINCIPAL CROSS        | - |
| CD |          | SECTION RECORD                                    | - |
| CD |          | =1, FISSION DATA PRESENT IN PRINCIPAL             | - |
| CD |          | CROSS SECTION RECORD                              | - |
| CD | IALF     | (N,ALPHA) CROSS SECTION FLAG                      | - |
| CD |          | SAME OPTIONS AS IFIS                              | - |
| CD | INP      | (N,P) CROSS SECTION FLAG                          | - |
| CD |          | SAME OPTIONS AS IFIS                              | - |
| CD | IN2N     | (N,2N) CROSS SECTION FLAG                         | - |
| CD |          | SAME OPTIONS AS IFIS                              | - |
| CD | IND      | (N,D) CROSS SECTION FLAG                          | - |
| CD |          | SAME OPTIONS AS IFIS                              | - |
| CD | INT      | (N,T) CROSS SECTION FLAG                          | - |
| CD |          | SAME OPTIONS AS IFIS                              | - |
| CD | LTOT     | NUMBER OF MOMENTS OF TOTAL CROSS SECTION PROVIDED | - |
| CD |          | IN PRINCIPAL CROSS SECTIONS RECORD                | - |
| CD | LTRN     | NUMBER OF MOMENTS OF TRANSPORT CROSS SECTION      | - |
| CD |          | PROVIDED IN PRINCIPAL CROSS SECTION RECORD        | - |
| CD | ISTRPD   | NUMBER OF COORDINATE DIRECTIONS FOR WHICH         | - |
| CD |          | COORDINATE DEPENDENT TRANSPORT CROSS SECTIONS     | - |
| CD |          | ARE GIVEN, IS ISTRPD=0, NO COORDINATE DEPENDENT   | - |
| CD |          | TRANSPORT CROSS SECTIONS ARE GIVEN.               | - |
| CD | IDSCT(N) | SCATTERING MATRIX TYPE IDENTIFICATION FOR         | - |

```

CD          SCATTERING BLOCK N, SIGNIFICANT ONLY IF      -
CD          LORD(N).GT.0                                  -
CD          IDSCT(N)=000 + NN, TOTAL SCATTERING, (SUM OF   -
CD          ELASTIC, INELASTIC, AND N2N SCATTERING        -
CD          MATRIX TERMS),                                -
CD          =100 + NN, ELASTIC SCATTERING                  -
CD          =200 + NN, INELASTIC SCATTERING                -
CD          =300 + NN, (N,2N) SCATTERING,----SEE         -
CD          NOTE BELOW----                                -
CD          WHERE NN IS THE LEGENDRE EXPANSION INDEX OF THE -
CD          FIRST MATRIX IN BLOCK N                        -
CD  LORD(N)  NUMBER OF SCATTERING ORDERS IN BLOCK N.  IF  -
CD          LORD(N)=0, THIS BLOCK IS NOT PRESENT FOR THIS  -
CD          ISOTOPE.  IF NN IS THE VALUE TAKEN FROM       -
CD          IDSCT(N), THEN THE MATRICES IN THIS BLOCK     -
CD          HAVE LEGENDRE EXPANSION INDICES OF NN,NN+1,   -
CD          NN+2,...,NN+LORD(N)-1                          -
CD  JBAND(J,N)  NUMBER OF GROUPS THAT SCATTER INTO GROUP J, -
CD          INCLUDING SELF-SCATTER, IN SCATTERING BLOCK N. -
CD          IF JBAND(J,N)=0, NO SCATTER DATA IS PRESENT IN -
CD          BLOCK N                                         -
CD  IJJ(J,N)   POSITION OF IN-GROUP SCATTERING CROSS SECTION IN -
CD          SCATTERING DATA FOR GROUP J, SCATTERING BLOCK -
CD          N, COUNTED FROM THE FIRST WORD OF GROUP J DATA. -
CD          IF JBAND(J,N).NE.0 THEN IJJ(J,N) MUST SATISFY -
CD          THE RELATION 1.LE.IJJ(J,N).LE.JBAND(J,N)      -
C                                                    -
CD          NOTE- FOR N,2N SCATTER, THE MATRIX CONTAINS TERMS -
CD          SCAT(J TO G), WHICH ARE EMISSION (PRODUCTION)- -
CD          BASED, I.E., ARE DEFINED SUCH THAT MACROSCOPIC -
CD          SCAT(J TO G) TIMES THE FLUX IN GROUP J GIVES   -
CD          THE RATE OF EMISSION (PRODUCTION) OF NEUTRONS -
CD          INTO GROUP G.                                  -
C                                                    -
C-----
C-----
CR          PRINCIPAL CROSS SECTIONS    (5D RECORD)      -
C                                                    -
CL          ((STRPL(J,L),J=1,NGROUP),L=1,LTRN),          -
CL          1((STOTPL(J,L),J=1,NGROUP),L=1,LTOT),(SNGAM(J),J=1,NGROUP). -
CL          2(SFIS(J),J=1,NGROUP),(SNUTOT(J),J=1,NGROUP), -

```

```

CL  3(CHISO(J),J=1,NGROUP),(SNALF(J),J=1,NGROUP),      -
CL  4(SNP(J),J=1,NGROUP),(SN2N(J),J=1,NGROUP),          -
CL  5(SND(J),J=1,NGROUP),(SNT(J),J=1,NGROUP),          -
CL  6((STRPD(J,I),J=1,NGROUP),I=1,ISTRPD)              -
C                                                         -
CW  (1+LTRN+LTOT+IALF+INP+IN2N+IND+ISTRPD+2*IFIS+      -
CW  ICHI*(2/(ICHI+1)))*NGROUP=NUMBER OF WORDS          -
C                                                         -
CB  FORMAT(4H 5D ,5E12.5/(6E12.5)) LENGTH OF LIST AS ABOVE -
C                                                         -
CD  STRPL(J,L)    PL WEIGHTED TRANSPORT CROSS SECTION  -
CD                THE FIRST ELEMENT OF ARRAY STRPL IS THE -
CD                CURRENT (P1) WEIGHTED TRANSPORT CROSS SECTION -
CD                THE LEGENDRE EXPANSION COEFFICIENT FACTOR (2L+1) -
CD                IS NOT INCLUDED IN STRPL(J,L).          -
CD  STOTPL(J,L)   PL WEIGHTED TOTAL CROSS SECTION       -
CD                THE FIRST ELEMENT OF ARRAY STOTPL IS THE -
CD                FLUX (P0) WEIGHTED TOTAL CROSS SECTION -
CD                THE LEGENDRE EXPANSION COEFFICIENT FACTOR (2L+1) -
CD                IS NOT INCLUDED IN STOTPL(J,L).          -
CD  SNGAM(J)      (N,GAMMA)                             -
CD  SFIS(J)       (N,F)          (PRESENT IF IFIS.GT.0)  -
CD  SNUTOT(J)     TOTAL NEUTRON YIELD/FISSION (PRESENT IF IFIS.GT.0) -
CD  CHISO(J)I     ISOTOPE CHI  (PRESENT IF ICHI.EQ.1)    -
CD  SNALF(J)      (N,ALPHA)    (PRESENT IF IALF.GT.0)    -
CD  SNP(J)        (N,P)        (PRESENT IF INP.GT.0)     -
CD  SN2N(J)       (N,2N)       (PRESENT IF IN2N.GT.0)    ----SEE -
CD                NOTE-----                             -
CD  SND(J)        (N,D)        (PRESENT IF IND.GT.0)     -
CD  SNT(J)        (N,T)        (PRESENT IF INT.GT.0)     -
CD  STRPD(J,I)    COORDINATE DIRECTION I TRANSPORT CROSS SECTION -
CD                (PRESENT IF ISTRPD.GT.0)                -
C                                                         -
CN                NOTE - THE PRINCIPAL N,2N CROSS SECTION SN2N(J) -
CN                IS DEFINED AS THE N,2N REACTION CROSS SECTION, -
CN                I.E., SUCH THAT MACROSCOPIC SN2N(J) TIMES THE -
CN                FLUX IN GROUP J GIVES THE RATE AT WHICH N,2N -
CN                REACTIONS OCCUR IN GROUP J.  THUS, FOR N,2N -
CN                SCATTERING, SN2N(J) = 0.5*(SUM OF SCAT(J TO G) -
CN                SUMMED OVER ALL G).                      -
C                                                         -
C-----

```

```

C-----
CR          ISOTOPE CHI DATA    (6D RECORD)          -
C                                                    -
CC          PRESENT IF ICHI.GT.1                      -
C                                                    -
CL          ((CHIISO(K,J),K=1,ICHI),J=1,NGROUP),(ISOPEC(I),I=1,NGROUP) -
C                                                    -
CW          NGROUP*(ICHI+1)=NUMBER OF WORDS           -
C                                                    -
CB          FORMAT(4H 6D ,5E12.5/(6E12.5))    CHIISO   -
CB          FORMAT(12I6)                      ISOPEC    -
C                                                    -
CD          CHIISO(K,J)    FRACTION OF NEUTRONS EMITTED INTO GROUP J AS -
CD                               RESULT OF FISSION IN ANY GROUP,USING SPECTRUM K -
CD          ISOPEC(I)      ISOPEC(I)=K IMPLIES THAT SPECTRUM K IS USED -
CD                               TO CALCULATE EMISSION SPECTRUM FROM FISSION -
CD                               IN GROUP I              -
C                                                    -
C-----

C-----
CR          SCATTERING SUB-BLOCK    (7D RECORD)          -
C                                                    -
CC          PRESENT IF LORD(N).GT.0                  -
C                                                    -
CL          ((SCAT(K,L),K=1,KMAX),L=1,LORDN)          -
C                                                    -
CC          KMAX=SUM OVER J OF JBAND(J,N) WITHIN THE J-GROUP RANGE OF THIS -
CC          SUB-BLOCK.  IF M IS THE INDEX OF THE SUB-BLOCK, THE J-GROUP -
CC          RANGE CONTAINED WITHIN THIS SUB-BLOCK IS -
CC          JL=(M-1)*((NGROUP-1)/NSBLOK+1 TO JU=MINO(NGROUP,JUP), -
CC          WHERE JUP=M*((NGROUP-1)/NSBLOK+1).         -
C                                                    -
CC          LORDN=LORD(N)                             -
CC          N IS THE INDEX FOR THE LOOP OVER NSCMAX (SEE FILE STRUCTURE) -
C                                                    -
CW          KMAX*LORDN=NUMBER OF WORDS                -
C                                                    -
CB          FORMAT(4H 7D ,5E12.5/(6E12.5))          -
C                                                    -
CD          SCAT(K,L)      SCATTERING MATRIX OF SCATTERING ORDER L, FOR -

```

|    |                                                   |   |
|----|---------------------------------------------------|---|
| CD | REACTION TYPE IDENTIFIED BY IDSCT(N) FOR THIS     | - |
| CD | BLOCK, JBAND(J,N) VALUES FOR SCATTERING INTO      | - |
| CD | GROUP J ARE STORED AT LOCATIONS K=SUM FROM 1      | - |
| CD | TO (J-1) OF JBAND(J,N) PLUS 1 TO K-1+JBAND(J,N).  | - |
| CD | THE SUM IS ZERO WHEN J=1, J-TO-J SCATTER IS       | - |
| CD | THE IJJ(J,N)-TH ENTRY IN THE RANGE JBAND(J,N),    | - |
| CD | VALUES ARE STORED IN THE ORDER (J+JUP),           | - |
| CD | (J+JUP-1), ..., (J+1), J, (J-1), ..., (J-JDN),    | - |
| CD | WHERE JUP=IJJ(J,N)-1 AND JDN=JBAND(J,N)-IJJ(J,N)- | - |
| C  |                                                   | - |
| C  | -----                                             | - |

Most of the variables in the “File Identification and File Control” record are taken from the user’s input. Note that **MAXUP** is always set to zero. CCCCCR does not process the NJOY thermal data at the present time. The **ICHIST** parameter will always be zero. CCCCCR does not produce a file-wide fission spectrum or matrix. The old practice of using a single fission spectrum for all calculations is inaccurate and obsolete. Actually, the effective fission spectrum depends on the mixture of isotopes and the flux. Any file-wide spectrum would have to be at least problem dependent, and it should also be region dependent. The parameters **NSCMAX** and **NSBLOK** in the “File Control” record will be discussed in connection with the scattering matrix format.

In the “File Data” record, the Hollerith set identification and the isotope names are taken from the user’s input. As mentioned above, the file-wide fission spectrum **CHI** never appears. The mean neutron velocities by group (**VEL**) are obtained from the inverse velocities computed by **GROUPR**:

$$\left\langle \frac{1}{v} \right\rangle_g = \frac{\int_g \frac{1}{v} \phi(E) dE}{\int_g \phi(E) dE}, \quad (456)$$

where  $g$  is the group index,  $\phi(E)$  is the **GROUPR** weighting spectrum, and  $v$  is the neutron velocity, which is computed from the neutron mass and energy using  $v = \sqrt{2E/m}$ . The units of these quantities are s/m; they are converted to cm/s for ISOTXS by inverting and multiplying by 100. The group structure [see **EMAX(J)** and **EMIN**] is obtained directly from **mf=1**, **mt=451** on the GENDF tape. Note that **GROUPR** energy groups are given in order of increasing energy



and ISOTXS energy groups are given in order of decreasing energy. CCCCCR handles the conversion.

The “File-Wide Chi Data” record never appears; see the discussion above for the reasons.

In the “Isotope Control and Group Independent Data” record, the first ten parameters are taken from the user’s input. The gram atomic weight for the material (**AMASS**) can be computed from the ENDF AWR parameter available on the GENDF file using the gram atomic weight of the neutron as a multiplier. The energy-release parameters **EFISS** and **ECAPT** must also be computed by the user. The **ECAPT** values are normally based on the ENDF Q values given in File 3, but, in some cases, it is also necessary to add additional decay energy coming from short-lived activation steps. For example, the **ECAPT** value for  $^{238}\text{U}$  should include the energy for the  $^{239}\text{U}$   $\beta$ -decay step, and perhaps even the energy from the  $^{239}\text{Np}$   $\beta$  decay. The values for **EFISS** should be based on the total non-neutrino energy release, which can be obtained from **mf**=3, **mt**=18 or **mf**=1, **mt**=458 on the ENDF tape. The **TEMP** parameter is normally set to 300K. The value of **SIGPOT** can be computed from the scattering-radius parameter **AP** in File 2 of the ENDF tape using  $\sigma_p = 4\pi a^2$ . The parameter **ADENS** is usually set to zero to imply infinite dilution. **KBR** can be chosen based on the normal use of the material by the community for which the library is being produced.

The **ICHI** parameter is related to the **ichix** parameter in the user’s input. As discussed above, the option **ICHI**=0 is never used by CCCCCR. Beyond that, the **NJOY** user has the option of producing a fission  $\chi$  vector using the default **GROU**PR flux (which is available on the GENDF tape) or a user-supplied weighting flux **SPEC**. This enables the user to produce an ISOTXS library appropriate to a class of problems with a flux similar to **SPEC**. In general, the incident-energy dependence of the fission spectrum is weak, so the choice of this weighting spectrum is not critical. Noticeable differences might be expected between a thermal spectrum on the one hand and a fast-reactor or fusion-blanket spectrum on the other. The  $\chi$  vector is defined as follows:

$$\chi_{g'} = \frac{\sum_g \sigma_{fg \rightarrow g'} \phi_g}{\sum_{g'} \sum_g \sigma_{fg \rightarrow g'} \phi_g}, \quad (457)$$

where  $\sigma_f$  is the fission group-to-group matrix from **GROU**PR,  $\phi_g$  is either the model flux or **SPEC**, and the denominator assures that  $\chi_{g'}$  will be normalized. Actually, the calculation is more complicated than that because of the necessity

to include delayed-neutron production. A “steady-state” value for the fission spectrum can be obtained as follows:

$$\chi_{g'}^{SS} = \frac{\sum_g \sigma_{fg \rightarrow g'} \phi_g + \chi_{g'}^D \sum_g \bar{\nu}_g^D \sigma_{fg} \phi_g}{\sum_{g'} \sum_g \sigma_{fg \rightarrow g'} \phi_g + \sum_g \bar{\nu}_g^D \sigma_{fg} \phi_g}, \quad (458)$$

where  $\bar{\nu}_g^D$  is the delayed-neutron yield obtained from `mf=3, mt=455` on the GENDF tape,  $\chi_{g'}^D$  is the total delayed-neutron spectrum obtained by summing over the time groups in `mf=5, mt=455`, and  $\sigma_{fg}$  is the fission cross section for group  $g$  obtained from `mf=3, mt=18`.

This is still not the end of the complications of fission. If the partial fission reactions MT=19, 20, 21, and 38 are present, the fission matrix term in the above equations is obtained by adding the contributions from all the partial reactions found. In these cases, a matrix for MT=18 will normally not be present on the GENDF tape. If it is, it will be ignored. Beginning with NJOY 91.0, a new and more efficient representation is used for the fission matrix computed in [GROUPR](#). It is well known that the shape of the fission spectrum is independent of energy up to energies of several hundred keV. [GROUPR](#) takes advantage of this by computing this low-energy spectrum only once. It then computes a fission neutron production cross section for all the groups up to the energy at which significant energy dependence starts. At higher energies, the full group-to-group fission matrix is computed as in earlier versions of NJOY. Therefore, it is now necessary to compute the values of  $\sigma_{fg \rightarrow g'}$  as used in the above equations using

$$\sigma_{fg \rightarrow g'} = \chi_{g'}^{LE} (\bar{\nu} \sigma_f)_g^{LE} + \sigma_{fg \rightarrow g'}^{HE}, \quad (459)$$

where LE stands for low energy, HE stands for high energy; the low-energy production cross sections written as  $\nu \sigma_f$  will be found on the GENDF tape using the special flag `IG2L0=0`, and the low-energy  $\chi$  will be found on the GENDF tape with `IG=0`.

In order to obtain still better accuracy, CCCCCR can produce a fission  $\chi$  matrix instead of the vector. Using the above notation, the full  $\chi$  matrix becomes

$$\chi_{g \rightarrow g'}^{SS} = \frac{\chi_{g'}^{LE} (\bar{\nu} \sigma_f)_g^{LE} + \sigma_{fg \rightarrow g'}^{HE} + \chi_{g'}^D \bar{\nu}_g^D \sigma_{fg}}{\text{NORM}}, \quad (460)$$

where NORM is just the value that normalizes the  $\chi$  matrix; that is, the sum of the numerator over all  $g'$ . Note that the “Isotope Chi Data” record allows for a rectangular fission matrix similar to the one produced by [GROUPR](#). It is obtained by using the input SPEC array to define the range of groups that will be averaged into each of the final ICHIX spectra. For example, to collapse a ten-group  $\chi$  matrix into a five-group matrix, SPEC might contain the ten values 1, 2, 3, 4, 5, 5, 5, 5, 5, 5. More formally,

$$\chi_{k \rightarrow g'}^{SS} = \frac{\sum_{s(g)=k} (\chi_{g'}^{LE} (\bar{\nu} \sigma_f)_g^{LE} + \sigma_{fg \rightarrow g'}^{HE} + \chi_{g'}^D \bar{\nu}_g^D \sigma_{fg}) \phi_g}{\text{NORM}}, \quad (461)$$

where  $\phi_g$  is the default weighting function from the GENDF tape,  $s(g)$  is the SPEC array provided by the user, and the summation is over all groups  $g$  satisfying the condition that  $s(g)=k$ . Future versions of CCCCCR could construct the SPEC array automatically using the information in the new GENDF format.

Continuing with the description of the “Isotope Control and Group Independent Data” record, the next 9 parameters are flags that tell what reactions will be described in the “Principal Cross Sections” record. They will be described below. Similarly, the parameters IDSCT, LORDN, JBAND, and IJJ will be described later in connection with the “Scattering Sub-Block” records.

The ISOTXS format allows for a fixed set of principal cross sections that was chosen based on the needs of fission reactor calculations. This is one of its main defects; the list does not allow for other reactions that become important above 6–10 MeV, and it does not allow for other quantities of interest, such as gas production, KERMA factors, and radiation damage production cross sections. Most of the reactions are simply copied from `mf=3` on the GENDF tape with the group order inverted — this is true for `SNGAM`, the  $(n, \gamma)$  cross section, which is taken from `mt=102`; for `SFIS`, the  $(n, f)$  cross section, which is taken from `mt=18`; for `SNALF`, the  $(n, \alpha)$  cross section, which is taken from `mt=107`; for `SNP`, the  $(n, p)$  cross section, which is taken from `mt=103`; for `SND`, the  $(n, d)$  cross section, which is taken from `mt=104`; and for `SNT`, the  $(n, t)$  cross section, which is taken from `mt=105`. The  $(n, 2n)$  cross section, `SN2N`, is normally taken from `mt=16`. However, earlier versions of ENDF represented the sequential  $(n, 2n)$  reaction in  $^9\text{Be}$  using `mt=6, 7, 8, and 9`. If present, these partial  $(n, 2n)$  reactions are added into `SN2N`. The flags `IFIS`, `IALF`, `INP`, `IN2N`, `IND`, and `INT` in the “Isotope Control and Group Independent Data” record are set to indicate which of these reactions have been found for this material.

In going from version III of the CCCC specifications to version IV, there was some controversy over the appropriate definition for the (n,2n) cross section and matrix. It was decided that the quantity in **SN2N** would be the (n,2n) reaction cross section; that is, it would define the probability that an (n,2n) reaction takes place. The (n,2n) matrix would be defined such that the sum over all secondary groups would produce the (n,2n) production cross section, which is two times larger than the reaction cross section.

The **CHISO** vector, which contains the fission spectrum vector (if any), was discussed above. A complete calculation of the fission source also requires the fission yield, **SNUTOT**, which can be used together with the fission cross section to calculate the fission neutron production cross section,  $\bar{\nu}\sigma_f$ . The fission yield can be calculated from the **GROUPE** fission matrix using

$$\bar{\nu}_g = \frac{\sum_{g'} \sigma_{fg \rightarrow g'}}{\sigma_{fg}} . \quad (462)$$

Adding delayed neutron contributions and accounting for the partition of the fission matrix into low-energy and high-energy parts (see the discussion of  $\chi$  above) gives the equation actually used by CCCC:

$$\bar{\nu}_g^{SS} = \frac{\sum_{g'} \sigma_{fg \rightarrow g'}^{HE} + (\bar{\nu}\sigma_f)_g^{LE} + \bar{\nu}_g^D \sigma_{fg}}{\sigma_{fg}} . \quad (463)$$

The total cross section produced by **GROUPE** contains two components: the flux-weighted or  $P_0$  total cross section, and the current-weighted or  $P_1$  total cross section. The  $P_0$  part is stored into **STOTPL**, and the **LTOT** flag is set to 1. **STRPL** contains the transport cross section used by diffusion codes; this is,

$$\sigma_{tr,g} = \sigma_{t1,g} - \sum_{g'} \sigma_{e1,g \rightarrow g'} , \quad (464)$$

where  $\sigma_{t1,g}$  is the  $P_1$  total cross section and  $\sigma_{e1,g \rightarrow g'}$  is the  $P_1$  component of the elastic scattering matrix, which is obtained from **mf=6**, **mt=2** on the GENDF tape from **GROUPE**. The flag **LTRN** is set to 1; that is, no higher-order transport corrections are provided. Direction-dependent transport cross sections are not computed by CCCC; therefore, **ISTRPD** is always zero, and the **STRPD** vectors are missing.

As discussed above, the “Isotope Chi Data” record may be present if the user set ICHIX>1 and supplied a SPEC vector to define how the full  $\chi$  matrix is to be collapsed into a rectangular  $\chi$  matrix.

The treatment of scattering matrices in the ISOTXS format is complex and has lots of possible variations. Only the variations supported by CCCCCR will be described here. First of all, the scattering data are divided into blocks and subblocks. A block is either one of the designated scattering reactions [that is, total, elastic, inelastic, or (n,2n)] and contains all the group-to-group elements and Legendre orders for that reaction (IFOPT=1), or it is one particular Legendre order for one of the designated reactions and contains all the group-to-group elements for that order and reaction (IFOPT=2). Its actual content is determined by IDSCT and LORDN. If IFOPT=1 has been selected, IDSCT(1)=100 and LORDN(1)=4 would designate a block for the elastic scattering matrix of order P<sub>3</sub> that contains all 4 Legendre orders and all group-to-group elements. If IFOPT=2 has been selected, IDSCT(1)=100 with LORDN(1)=1 would designate a block containing all group-to-group elements for the P<sub>0</sub> elastic matrix, IDSCT(2)=101 with LORDN(2)=1 would designate a block containing the P<sub>1</sub> elastic matrix, and so on. In CCCCCR, LORDN is always equal to 1 for IFOPT=2.

The ISOTXS format attempts to pack scattering matrices efficiently. First, all the scattering matrices treated here are triangular because only downscatter is present. And second, because of the limited range of elastic downscatter, only a limited range of groups above the inscatter group will contribute to the scattering into a given secondary-energy group. Therefore, ISOTXS removes zero cross sections by defining bands of incident energy groups that contribute to each final energy group. The bands are defined by JBAND, the number of initial energy groups in the band, and IJJ, an index to identify the position of the ingroup element in the band. The following table illustrates banding for a hypothetical elastic scattering reaction:

| Band | Element | JBAND | IJJ |
|------|---------|-------|-----|
| 1    | 1→1     | 1     | 1   |
| 2    | 2→2     | 2     | 1   |
|      | 1→2     |       |     |
| 3    | 3→3     | 2     | 1   |
|      | 2→3     |       |     |
| 4    | 4→4     | 2     | 1   |
|      | 3→4     |       |     |

Note that IJJ is always 1 in the absence of upscatter. This scheme is efficient for elastic scattering, but it is not efficient for threshold reactions because the ingroup element must always be included in the band. This means that lots of zeros must be given for final energy groups below the threshold group. An improved and simplified scheme is used in the MATXS format.

For IFOPT=2, the elements in the table above would be stored in the sequence shown, top to bottom. Each Legendre order would have its own block arranged in the same order. For IFOPT=1, the Legendre order data are intermixed with the group-to-group data. In each band, the elements for all initial groups for  $P_0$  are given, then all initial groups for  $P_1$ , and so on through LORDN Legendre orders.

Scattering matrices can be very large. For example, an 80-group elastic matrix can have as many as  $80 \times 79/2 = 3160$  elements per Legendre order. That would be 12 640 words for a  $P_3$  block using IFOPT=1, or four blocks of 3160 words each for IFOPT=2. The latter is practical; the former is not <sup>10</sup>. The corresponding numbers for 200 groups would be 79 600 and 19 900. Both of these numbers are clearly impractical as record sizes. This is where subblocking comes in. If each block is divided up so that there is one subblock for each energy group, the maximum record size is reduced substantially. For IFOPT=1, the maximum record size is equal to the number of groups times the number of Legendre orders, or 800 for the 200-group  $P_3$  case. For IFOPT=2, the maximum record size is just equal to the number of groups. Although the ISOTXS formats allows subblocks to contain several groups, CCCC does not. The possible values of NSBLOK are limited to 1 and NGROUP. In summary, the CCCC user has four matrix blocking options:

1. *IFOPT=1 and NSBLOK=1*. This produces a single block and a single subblock for each reaction. It is probably the best choice for small group structures (up to about 30 groups). The maximum record size is  $n_\ell \times n_g(n_g-1)/2$ .
2. *IFOPT=1 and NSBLOK=NGROUP*. This produces a block for each reaction, and each block contains  $n_g$  subblocks. The maximum record size is  $n_\ell \times n_g$ . This is a good choice for larger group structures because it keeps the record size up as compared with option 4 below.
3. *IFOPT=2 and NSBLOK=1*. This produces  $n_\ell$  blocks and subblocks for each reaction. The maximum record size is  $n_g(n_g-1)/2$ . It has only a

<sup>10</sup>At least it was not practical many years ago. However we see no benefit in revising the existing algorithm, and so keep this description

modest advantage in the maximum number of groups over option 1. Unless the application that uses the library finds it convenient to read one Legendre order at a time, the user might just as well choose option 2 if option 1 produces records that are too large.

4. *IFOPT=2 and NSBLOK=NGROUP*. This produces  $n_\ell$  blocks for each reaction, each with  $n_g$  subblocks. The maximum record size is  $n_g$ . The number of groups would have to be on the order of 1000 before this option would be preferred to option 2.

If CCCCCR does not have enough memory to process option 1 or 3, the code automatically sets NSBLOK to NGROUP, thereby activating option 2 or 4, respectively.

Note that the ISOTXS format specifies that the total scattering matrix is the sum of the elastic, inelastic, and (n,2n) matrices [see the definition of IDSCT(N)]. This implies that the inelastic matrix must contain the normal (n,n') reactions from *mt*=51-91, and also any other neutron-producing reactions that might be present. Examples are (n,n' $\alpha$ ), (n,n'p), and (n,3n).

## 14.5 BRKOXS

The format for the BRKOXS Bondarenko-type self-shielding factor file is given below in the standard format.

```

C*****
C                      REVISED 11/30/76                      -
C                                                              -
CF          BRKOXS-IV                                         -
CE          MICROSCOPIC GROUP DELAYED NEUTRON PRECURSOR DATA -
C                                                              -
CN                      THIS FILE PROVIDES DATA NECESSARY FOR -
CN                      BONDARENKO TREATMENT IN ADDITION TO   -
CN                      THOSE DATA IN FILE ISOTXS            -
CN                      FORMATS GIVEN ARE FOR FILE EXCHANGE PURPOSES -
CN                      ONLY.                                  -
C                                                              -
C*****
C-----
CS          FILE STRUCTURE                                     -
CS                                                              -
CS          RECORD TYPE                                         PRESENT IF -
CS          =====
```

|    |                                                             |        |   |
|----|-------------------------------------------------------------|--------|---|
| CS | FILE IDENTIFICATION                                         | ALWAYS | - |
| CS | FILE CONTROL                                                | ALWAYS | - |
| CS | FILE DATA                                                   | ALWAYS | - |
| CS | ***** (REPEAT FROM 1 TO NISOSH)                             |        | - |
| CS | * SELF-SHIELDING FACTORS                                    | ALWAYS | - |
| CS | * CROSS SECTIONS                                            | ALWAYS | - |
| CS | *****                                                       |        | - |
| C  |                                                             |        | - |
| C  | -----                                                       |        |   |
| C  | -----                                                       |        |   |
| CR | FILE IDENTIFICATION                                         |        | - |
| C  |                                                             |        | - |
| CL | HNAME, (HUSE(I), I=1, 2), IVERS                             |        | - |
| C  |                                                             |        | - |
| CW | 1+3*MULT=NUMBER OF WORDS                                    |        | - |
| C  |                                                             |        | - |
| CB | FORMAT(11H OV BRKX , 1H*, 2A6, 1H*, I6)                     |        | - |
| C  |                                                             |        | - |
| CD | HNAME HOLLERITH FILE NAME - BRKX -                          |        | - |
| CD | HUSE(I) HOLLERITH USER IDENTIFICATION (A6)                  |        | - |
| CD | IVERS FILE VERSION NUMBER                                   |        | - |
| CD | MULT DOUBLE PRECISION PARAMETER                             |        | - |
| CD | 1- A6 WORD IS SINGLE WORD                                   |        | - |
| CD | 2- A6 WORD IS DOUBLE PRECISION WORD                         |        | - |
| C  |                                                             |        | - |
| C  | -----                                                       |        |   |
| C  | -----                                                       |        |   |
| CR | FILE CONTROL (1D RECORD)                                    |        | - |
| C  |                                                             |        | - |
| CL | NGROUP, NISOSH, NSIGPT, NTEMPT, NREACT, IBLK                |        | - |
| C  |                                                             |        | - |
| CW | 6 = NUMBER OF WORDS                                         |        | - |
| C  |                                                             |        | - |
| CB | FORMAT(4H 1D , 6I6)                                         |        | - |
| C  |                                                             |        | - |
| CD | NGROUP NUMBER OF ENERGY GROUPS IN SET                       |        | - |
| CD | NISOSH NUMBER OF ISOTOPES WITH SELF-SHIELDING FACTORS       |        | - |
| CD | NSIGPT TOTAL NUMBER OF VALUES OF VARIABLE X (SEE FILE DATA- |        | - |
| CD | RECORD) WHICH ARE GIVEN. NSIGPT IS EQUAL TO                 |        | - |
| CD | THE SUM FROM 1 TO NISOSH OF NTABP(I)                        |        | - |



```

CD   NTEMPT      TOTAL NUMBER OF VALUES OF VARIABLE TB (SEE FILE -
CD                  DATA RECORD) WHICH ARE GIVEN. NTEMPT IS EQUAL -
CD                  TO THE SUM FROM 1 TO NISOSH OF NTABT(I) -
CD   NREACT      NUMBER OF REACTION TYPES FOR WHICH SELF-SHIELDING -
CD                  FACTORS ARE GIVEN (IN PREVIOUS VERSIONS OF THIS -
CD                  FILES NREACT HAS BEEN IMPLICITLY SET TO 5). -
CD   IBLK        BLOCKING OPTION FLAG FOR SELF-SHIELDING FACTORS, -
CD                  IBLK=0, FACTORS NOT BLOCKED BY REACTION TYPE, -
CD                  IBLK=1, FACTORS ARE BLOCKED BY REACTION TYPE. -
C -
C-----
C-----
CR          FILE DATA   (2D RECORD) -
C -
CL   (HISONM(I),I=NISOSH),(X(K),K=1,NSIGPT),(TB(K),K=1,NTEMPT), -
CL   1(EMAX(J),J=1,NGROUP),EMIN,(JBFL(I),I=1,NISOSH), -
CL   2(JBFH(I),I=NISOSH),(NTABP(I),I=1,NISOSH),(NTABT(I),I=1,NISOSH) -
C -
CW   (4+MULT)*NISOSH+NSIGPT+NTEMPT+NGROUP+1=NUMBER OF WORDS -
C -
CB   FORMAT(4H 2D ,9(1X,A6)/          HISONM -
CB   1(10(1X,A6))) -
CB   FORMAT(6E12.5)          X,TB,EMAX,EMIN -
CB   FORMAT(12I6)          JBFL,JBFH,NTABP,NTABT -
C -
CD   HISONM(I)      HOLLERITH ISOTOPE LABEL FOR ISOTOPE I (A6). THESE -
CD                  LABELS MUST BE A SUBSET OF THOSE IN FILE ISOTXS -
CD                  OR GRUPXS, IN THE CORRESPONDING ARRAY. -
CD   X(K)           ARRAY OF LN(SIGPO)/LN(10) VALUES FOR ALL ISOTOPES, -
CD                  WHERE SIGPO IS THE TOTAL CROSS SECTION OF THE -
CD                  OTHER ISOTOPES IN THE MIXTURE IN BARNS PER ATOM -
CD                  OF THIS ISOTOPE. FOR ISOTOPE I, THE NTABP(I) -
CD                  VALUES OF X FOR WHICH SELF-SHIELDING FACTORS -
CD                  ARE GIVEN ARE STORED STARTING AT LOCATION L=1+ -
CD                  SUM FROM 1 TO I-1 OF NTABP(K). -
CD   TB(K)          ARRAY OF TEMPERATURES (DEGREES C) FOR ALL ISOTOPES. -
CD                  FOR ISOTOPE I, THE NTBT(I) VALUES OF TB FOR -
CD                  WHICH SELF-SHIELDING FACTORS ARE GIVEN ARE -
CD                  STORED AT LOCATION L=1+SUM FROM 1 TO I-1 OF -
CD                  NTABT(K). -
CD   EMAX(J)        MAXIMUM ENERGY BOUND OF GROUP J (EV) -

```

```

CD      EMIN          MINIMUM ENERGY BOUND OF SET (EV)          -
CD      JBFL(I)       LOWEST NUMBERED OF HIGHEST ENERGY GROUP FOR WHICH -
CD                        SELF-SHIELDING FACTORS ARE GIVEN          -
CD      JBFH(I)       HIGHEST NUMBERED OR LOWEST ENERGY GROUP FOR WHICH -
CD                        SELF-SHIELDING FACTORS ARE GIVEN          -
CD      NTABP(I)      NUMBER OF SIGPO VALUES FOR WHICH SELF-SHIELDING -
CD                        FACTORS ARE GIVEN FOR ISOTOPE I.          -
CD      NTABT(I)      NUMBER OF TEMPERATURE VALUES FOR WHICH SELF- -
CD                        SHIELDING FACTORS ARE GIVEN FOR ISOTOPE I. -
C                                              -
C-----
C-----
CR          SELF-SHIELDING FACTORS      (3D RECORD)          -
C                                              -
CL      (((FFACT(N,K,J,M),N=1,NBINT),K=1,NBTEM),J=JBFLI,JBFHI),M=ML,MU) -
CL                        ----- SEE DESCRIPTION BELOW ----- -
C                                              -
CC      NBINT=NTABP(I)          -
CC      NBTEM=NTABT(I)          -
CC      JBFLI=JBFL(I)          -
CC      JBFHI=JBFH(I)          -
CC      FOR ML, MU SEE STRUCTURE BELOW          -
C                                              -
CW      NBINT*NBTEM*(JBFHI-JBFLI+1)*(MU-ML+1) = NUMBER OF WORDS -
C                                              -
CB      FORMAT(4H 3D ,5E12.5/(6E12.5))          -
C                                              -
CC      DO 1 L=1,NBLOK          -
CC      1 READ(N) *LIST AS ABOVE*          -
C                                              -
CC          IF IBLK=0, NBLOK=1, ML=1, MU=NREACT          -
CC          IF IBLK=1, NBLOK=NREACT, ML=MU=L, WHERE L IS THE BLOCK -
C                                              -
CD      FFACT(N,K,J,M)      SELF-SHIELDING FACTOR EVALUATED AT X(N) AND -
CD                        TB(K) FOR ENERGY GROUP J, THE M INDEX IS -
CD                        A DUMMY INDEX TO DENOTE THE REACTION TYPE, -
CD                        THE FIRST FIVE REACTION TYPES ARE, IN -
CD                        ORDER, TOTAL, CAPTURE, FISSION, TRANSPORT, -
CD                        AND ELASTIC.          -
C                                              -
CB          NOTE THAT IS IBLK=1, EACH REACTION TYPE WILL CONSTITUTE -

```

|    |                                                                |   |
|----|----------------------------------------------------------------|---|
| CB | A SEPARATE DATA BLOCK.                                         | - |
| C  |                                                                | - |
| C  | -----                                                          |   |
| C  | -----                                                          |   |
| CR | CROSS SECTIONS (4D RECORD)                                     | - |
| C  |                                                                | - |
| CL | (XSPO(J),J=1,NGROUP),(XSIN(J),J=1,NGROUP),(XSE(J),J=1,NGROUP), | - |
| CL | 1(XSMU(J),J=1,NGROUP),(XSED(J),J=1,NGROUP),(XSX(J),J=1,NGROUP) | - |
| C  |                                                                | - |
| CW | 6*NGROUP=NUMBER OF WORDS                                       | - |
| C  |                                                                | - |
| CB | FORMAT(4H 4D ,5E12.5/(6E12.5))                                 | - |
| C  |                                                                | - |
| CD | XSPO(J) POTENTIAL SCATTERING CROSS SECTION (BARNs)             | - |
| CD | XSIN(J) INELASTIC CROSS SECTION (BARNs)                        | - |
| CD | XSE(J) ELASTIC CROSS SECTION (BARNs)                           | - |
| CD | XSMU(J) AVERAGE COSINE OF ELASTIC SCATTERING ANGLE             | - |
| CD | XSED(J) ELASTIC DOWN-SCATTERING TO ADJACENT GROUP              | - |
| CD | XSXI(J) AVERAGE ELASTIC SCATTERING LETHARGY INCREMENT          | - |
| C  |                                                                | - |
| C  | -----                                                          |   |

The BRKXOS file is used to supply self-shielding factors for use with the Bondarenko method[38] for calculating effective macroscopic cross sections for the components of nuclear systems. As discussed in detail in the [GROUPR](#) chapter of this manual, this system is based on using a model flux for isotope  $i$  of the form

$$\phi_{\ell}^i(E, T) = \frac{C(E)}{[\sigma_0^i + \sigma_t^i(E, T)]^{\ell+1}}, \quad (465)$$

where  $C(E)$  is a smooth weighting flux,  $\sigma_t^i(E, T)$  is the total cross section for material  $i$  at temperature  $T$ ,  $\ell$  is the Legendre order, and  $\sigma_0^i$  is a parameter that can be used to account for the presence of other materials and the possibility of escape from the absorbing region (heterogeneity). [GROUPR](#) uses this model flux to calculate effective multigroup cross sections for the resonance-region reactions (total, elastic, fission, capture) for user specified values of  $\sigma_0$  and  $T$ .

When  $\sigma_0$  is large with respect to the highest peaks in  $\sigma_t$ , the flux is essentially proportional to  $C(E)$ . This is called infinite dilution, and the corresponding

cross sections are appropriate for an absorber in a dilute mixture or for a very thin sample of the absorber. As  $\sigma_0$  decreases, the flux  $\phi(E)$  develops dips where  $\sigma_t$  has peaks. These dips cancel out part of the effect of the corresponding peaks in the resonance cross sections, thereby reducing, or self-shielding, the reaction rate. It is convenient to represent this effect as a self-shielding factor; that is,

$$\sigma_{xg}(T, \sigma_0) = f_{xg}(T, \sigma_0) \times \sigma_{xg}(300^\circ K, \infty) . \quad (466)$$

In the CCCC system, the f-factors are stored in the BRKOXS file and the infinitely dilute cross sections are stored in the ISOTXS file. A code that prepares effective cross sections, such as SPHINX[84] or 1DX[53], determines the appropriate  $T$  and  $\sigma_0$  values for each region and group in a reactor problem, using equivalence theory together with the user's specifications for composition and geometry. It then reads in the cross sections and f-factors from the ISOTXS and BRKOXS files, interpolates in the  $T$  and  $\sigma_0$  tables to obtain the desired f-factors, and multiplies to obtain the effective cross sections.

In the BRKOXS file specification given above, the components of the “File Identification” record are the same as for ISOTXS. The parameters in the “File Control” record are used to calculate the sizes and locations of data in the records to follow. The “File Data” record contains all the isotope names, all the  $\sigma_0$  values for every isotope, all the  $T$  values for every isotope, the group structure, and several arrays used for unpacking the other data. The Hollerith material names in HISONM are the same as those used in ISOTXS, and they are obtained from the user's input. The  $\sigma_0$  values are packed into  $X(K)$  using  $NTABP(I)$ . Note that the base-10 logarithm of  $\sigma_0$  is stored. Therefore, a typical library might contain the following:

| material I | NTABP(I) | X(K)                        |
|------------|----------|-----------------------------|
| 1          | 3        | 3.0 2.0 1.0                 |
| 2          | 7        | 4.0 3.0 2.0 1.477 1. 0. -1. |
| 3          | 5        | 4.0 3.0 2.0 1.0 0.0         |
| ...        | ...      | ...                         |

Similarly, the  $T$  values are stored in  $TB(K)$  using  $NTABT(I)$ . The absolute temperatures used by **GROUPR** must be changed to  $^\circ\text{C}$  before being stored. The energy bounds for the group structure found on the GENDF tape are stored in  $EMAX(J)$  and  $EMIN$ . As discussed in connection with the ISOTXS format, group boundaries are stored in order of decreasing energy in the BRKOXS file.

The self-shielding factor approach is designed to account for resonance self-shielding. It is not necessarily appropriate for low energies if only broad resonance features are apparent, or for high energies where only small residual fluctuations in the cross section are seen. For this reason, the BRKOXS format provides the JBFL(I) and JBFH(I) arrays in the “File Data” record. They are used to limit the range of the numbers given in the “Self-Shielding Factors” record. The reactions that are active in the resonance energy range usually include only the total, elastic, fission, and capture channels. The total cross section is usually computed for the two Legendre orders  $\ell=0$  and  $\ell=1$ . This second value is often called the current-weighted total cross section, and it is needed to compute the self-shielded diffusion coefficient. [GROUPE](#) also computes a self-shielded elastic scattering matrix. It can be used to provide two quantities for the BRKOXS file. First, the diffusion coefficient requires the calculation of a transport cross section for diffusion. The relationships are as follows:

$$D_g = \frac{1}{3\sigma_{tr,g}} , \quad (467)$$

and

$$\sigma_{tr,g} = \sigma_{t1,g} - \sum_{g'} \sigma_{e1,g \rightarrow g'} . \quad (468)$$

Therefore, the current-weighted  $P_1$  elastic cross section contributes to the transport self-shielding factor. The second use for the self-shielded elastic scattering matrix is to compute a self-shielding factor for elastic removal. For heavy isotopes, the energy lost in elastic scattering is small, and all the removal is normally to one group. The format requires that at least the five standard reactions be given in a specified order. NJOY is able to add one more as follows:

1. total ( $P_0$  weighted),
2. capture ( $P_0$ ),
3. fission ( $P_0$ ),
4. transport ( $P_1$ ),
5. elastic ( $P_0$ ), and
6. elastic removal ( $P_0$ )

The normal pattern for the BRKOXS file expects that there will be one record of self-shielding factors for each material. Such a record could get quite large. For example, with 6 reactions, 6 temperatures, 6  $\sigma_0$  values, and 100 resonance

groups, a “Self-Shielding Factors” record could have over 20 000 words. This number can be made more manageable by setting the `IBLK` flag in the “File Control” record to 1. Then there will be a separate record of self-shielding factors for each reaction; this would reduce the record size for the example to a more reasonable 3600 words.

The actual self-shielding factors are computed from the cross sections given on the GENDF tape and stored into the `FFACT(N,K,J,M)` array of the “Self-Shielding Factors” record with group order converted to the standard decreasing-energy convention. Following the FORTRAN convention, `N` is the fastest varying index in this array, `K` is the next fastest varying index, and so on. The identities of these indices are

`N`  $\sigma_0$ ,  
`K` temperature  $T$ ,  
`J` group, and  
`M` reaction

The “Cross Sections” record contains some additional cross sections and special parameters that are often used in self-shielding codes and are not included in the ISOTXS file. The `XSP0` cross section is taken to be constant and equal to the CCCR input parameter `XSP0`, which is computed as  $4\pi a^2$ . The `XSIN` cross section is obtained by summing over the final group index for every group-to-group matrix in File 6 except elastic,  $(n,2n)$ , and fission. Therefore, it may contain effects of multiplicities greater than 1 if reactions like  $(n,3n)$  or  $(n,2n\alpha)$  are active for the material. It may be slightly larger in high-energy groups than the cross section that would be obtained using the same sum over reactions in File 3. The `XSE` cross section is obtained from `mf=6`, `mt=2` on the GENDF tape by summing over final groups. The parameters for continuous slowing down theory, `XSMU` and `XSXI`, are obtained from `mt=251` and `mt=252`, respectively. The methods used for calculating these quantities are described in the [GROUPR](#) section of this report. Finally, the elastic downscattering cross section is obtained from the elastic matrix on the GENDF tape (`mf=6`, `mt=2`).

## 14.6 DLAYXS

The format for the DLAYXS delayed-neutron data file is given below in the standard format.

```

C*****
C              REVISED 11/30/76              -
C              -                              -
CF          DLAYXS-IV                        -
CE          MICROSCOPIC GROUP DELAYED NEUTRON PRECURSOR DATA -
C              -                              -
CN              THIS FILE PROVIDES PRECURSOR YIELDS,      -
CN              EMISSION SPECTRA, AND DECAY CONSTANTS     -
CN              ORDERED BY ISOTOPE. ISOTOPES ARE IDENTIFIED -
CN              BY ABSOLUTE ISOTOPE LABELS FOR RELATION TO -
CN              ISOTOPES IN EITHER FILE ISOTXS OR GRUPXS.  -
CN              FORMATS GIVEN ARE FOR FILE EXCHANGE PURPOSES -
CN              ONLY.                                     -
C              -                              -
C*****

C-----
CS          FILE STRUCTURE                      -
CS              -                              -
CS          RECORD TYPE                        PRESENT IF -
CS          =====                          ===== -
CS          FILE IDENTIFICATION                ALWAYS     -
CS          FILE CONTROL                      ALWAYS     -
CS          FILE DATA, DECAY CONSTANTS, AND -
CS          EMISSION SPECTRA                  ALWAYS     -
CS          ***** (REPEAT TO NISOD)         -
CS          *          DELAYED NEUTRON PRECURSOR -
CS          *          YIELD DATA              ALWAYS     -
CS          *****                          -
C              -                              -
C-----

C-----
CR          FILE IDENTIFICATION                  -
C              -                              -
CL          HNAME,(HUSE(I),I=1,2),IVERS        -
C              -                              -
CW          1+3*MULT=NUMBER OF WORDS           -
C              -                              -
CB          FORMAT(11H 0V DLAYXS ,1H*,2A6,1H*,I6) -

```

```

C -
CD  HNAME      HOLLERITH FILE NAME - DLAYXS - -
CD  HUSE(I)    HOLLERITH USER IDENTIFICATION (A6) -
CD  IVERS      FILE VERSION NUMBER -
CD  MULT       DOUBLE PRECISION PARAMETER -
CD              1- A6 WORD IS SINGLE WORD -
CD              2- A6 WORD IS DOUBLE PRECISION WORD -
C -
C-----

C-----

CR          FILE CONTROL    (1D RECORD) -
C -
CL  NGROUP,NISOD,NFAM,IDUM -
C -
CW  4=NUMBER OF WORDS -
C -
CB  FORMAT(4H 1D ,4I6) -
C -
CD  NGROUP      NUMBER OF NEUTRON ENERGY GROUPS IN SET -
CD  NISOD       NUMBER OF ISOTOPES IN DELAYED NEUTRON SET -
CD  NFAM        NUMBER OF DELAYED NEUTRON FAMILIES IN SET -
CD  IDUM        DUMMY TO MAKE UP FOUR-WORD RECORD -
C -
C-----

C-----

CR          FILE DATA, DECAY CONSTANTS, AND EMISSION SPECTRA -
C              (2D RECORD) -
C -
CL  (HABSID(I),I=1,NISOD),(FLAM(N),N=1,FAM),((CHID(J,N),J=1,NGROUP), -
CL  N=1,NFAM),(EMAX(J),J=1,NGROUP),EMIN,(NKFAM(I),I=1,NISOD), -
CL  (LOCA(I),I=1,NISOD) -
C -
CW  (2+MULT)*NISOD+(NGROUP+1)*(NFAM+1)=NUMBER OF WORDS -
C -
CB  FORMAT(4H 2D ,9(1X,A6))          HABSID -
CB  1(10(1X,A6))) -
CB  FORMAT(6E12.5)          FLAM,CHID,EMAX,EMIN -
CB  FORMAT(12I6)          NKFAM,LOCA -
C -
CD  HABSID(I)    HOLLERITH ABSOLUTE ISOTOPE LABEL FOR ISOTOPE I (A6)-

```



|    |                                                             |                                                   |   |
|----|-------------------------------------------------------------|---------------------------------------------------|---|
| CD | FLAM(N)                                                     | DELAYED NEUTRON PRECURSOR DECAY CONSTANT          | - |
| CD |                                                             | FOR FAMILY N                                      | - |
| CD | CHID(J,N)                                                   | FRACTION OF DELAYED NEUTRONS EMITTED INTO NEUTRON | - |
| CD |                                                             | ENERGY GROUP J FROM PRECURSOR FAMILY N            | - |
| CD | EMAX(J)                                                     | MAXIMUM ENERGY BOUND OF GROUP J (EV)              | - |
| CD | EMIN                                                        | MINIMUM ENERGY BOUND OF SET (EV)                  | - |
| CD | NKFAM(I)                                                    | NUMBER OF FAMILIES TO WHICH FISSION IN ISOTOPE I  | - |
| CD |                                                             | CONTRIBUTES DELAYED NEUTRON PRECURSORS            | - |
| CD | LOCA(I)                                                     | NUMBER OF RECORDS TO BE SKIPPED TO READ DATA FOR  | - |
| CD |                                                             | ISOTOPE I, LOCA(1)=0                              | - |
| C  |                                                             |                                                   | - |
| C  | -----                                                       |                                                   |   |
| C  | -----                                                       |                                                   |   |
| CR |                                                             | DELAYED NEUTRON PRECURSOR YIELD DATA (3D RECORD)  | - |
| C  |                                                             |                                                   | - |
| CL | (SNUDEL(J,K),J=1,NGROUP),K=1,NKFAMI),(NUMFAM(K),K=1,NKFAMI) |                                                   | - |
| C  |                                                             |                                                   | - |
| CC | NKFAMI=NKFAM(I)                                             |                                                   | - |
| C  |                                                             |                                                   | - |
| CW | (NGROUP+1)*NKFAMI=NUMBER OF WORDS                           |                                                   | - |
| C  |                                                             |                                                   | - |
| CB | FORMAT(4H 3D ,5E12.5/(6E12.5))                              | SNUDEL                                            | - |
| CB | FORMAT(12I6)                                                | NUMFAM                                            | - |
| C  |                                                             |                                                   | - |
| CD | SNUDEL(J,K)                                                 | NUMBER OF DELAYED NEUTRON PRECURSORS PRODUCED IN  | - |
| CD |                                                             | FAMILY NUMBER NUMFAM(K) PER FISSION IN            | - |
| CD |                                                             | GROUP J                                           | - |
| CD | NUMFAM(K)                                                   | FAMILY NUMBER OF THE K-TH YIELD VECTOR IN         | - |
| CD |                                                             | ARRAY SNUDEL(J,K)                                 | - |
| C  |                                                             |                                                   | - |
| C  | -----                                                       |                                                   |   |

This file is used to communicate delayed-neutron data to reactor kinetics codes. The ENDF files give a total delayed-neutron yield  $\bar{\nu}_d$  in the section labeled **mf=1**, **mt=455**. **GROUPR** averages this yield for each neutron group  $g$

using

$$\bar{\nu}_g^D = \frac{\int_g \nu_d(E) \sigma_f(E) \phi(E) dE}{\int_g \sigma_f(E) \phi(E) dE} . \quad (469)$$

This same section of the ENDF tape contains the decay constants for the delayed-neutron time groups. These numbers are passed on to the **GROUPR** routine that averages the delayed-neutron spectra, and they end up in the **mf=5** record on the GENDF tape. The ENDF evaluations give the delayed-neutron spectra for the time groups in **mf=5**, **mt=455**. These spectra are not separately normalized. Rather, the sum over all time groups is normalized, but the integral of any one of the spectra gives the “delayed fraction” for that time group. **GROUPR** simply averages these spectra using the specified neutron group structure. The resulting group spectra (and the decay constants from File 1) are written onto the GENDF tape.

Returning to the DLAYXS format description, the parameters in the “File Identification” record are obtained from the user’s input, just as for ISOTXS and BRKOXS. The parameter **NGROUP** is also a user input quantity. **NISOD** is determined after the entire GENDF tape has been searched for isotopes that are on the user’s list of **NISO** materials and that have delayed-neutron data. The **NFAM** parameter needs some additional explanation. A “family” for the DLAYXS file is actually an index that selects one particular spectrum from the **CHID** array. It could correspond to an actual delayed-neutron precursor isotope left after a fission event. In such a case, there would be many “families” corresponding to the many possible fission fragment isotopes. The **SNUDEL** yields would be analogous to fission product yields. The ENDF evaluations take a more macroscopic approach. Spectra are chosen to include all the emissions from a group of delayed-neutron precursors for a particular fissioning nucleus with similar decay constants. In this representation, the DLAYXS “family” corresponds to a particular decay constant and spectrum for a particular target isotope. Therefore, the number of families is simply six or eight times the number of isotopes, *e.g.*, **NFAM=6\*NISOD**.

In the “File Data, Decay Constants, and Emission Spectra” record, the Holterith isotope names **HABSID** are obtained from the names in the user’s input. The **FLAM** values come directly from the decay constant values originally extracted from File 1 of the ENDF tape. The family index for isotope **ISO** and time group **I** is simply computed as **6\*(ISO-1)+I** or **8\*(ISO-1)+I**. The **CHID** array

is loaded from the `mf=5, mt=455` section on the GENDF tape using the family index and the group index. As usual, the order of groups has to be changed from the GROUPT convention with increasing-energy order to the CCCC convention with decreasing-energy order. The group structure itself is obtained from the GENDF header record and stored into `EMAX` and `EMIN` in the conventional order. The value of `NKFAM` is simply 6 or 8 for every isotope. The `LOCA` values are also easy to compute; they are just `ISO` minus 1.

The delayed-neutron yields versus incident neutron energy group and family index are given in the “Delayed Neutron Precursor Yield Data” record. As mentioned above, the total yield is given in `mf=3` of the GENDF tape, and the delayed fractions can be computed by summing the spectrum for each time group over the energy group index. The array `SNUDEL` in this `DLAYXS` record contains the product of these values. Note that there is one of these yield records for each delayed-neutron isotope, and each record contains six or eight families. The `NKFAM` vector is used to establish the correspondence between these families and the entire list of families used in the file data record. As an example, `NUMFAM(1)` would contain 1, 2, 3, 4, 5, 6; `NUMFAM(2)` would contain 7, 8, 9, 10, 11, 12, and so on.

## 14.7 Coding Details

Subroutine `ccccr` is the only public call for module `ccccm`. The module has a number of global variables and arrays defined. One key set of variables and arrays provides the area for accumulating the CCCC data. It provides a set of equivalenced arrays so that integers, reals, and Hollerith strings can all be stored in the same binary records. It sets up both integers and reals to be 4-byte quantities. Hollerith words (with up to 8 characters each) are 8-byte quantities. The CCCC `mult` value is set to 2. See `a(50000)`, `ia(50000)`, and `ha(25000)`. The parameter `isiza=50000` defines the size of these equivalenced arrays in 4-byte units.

The main subroutine of CCCCCR starts by allocating an array `maxe` for reading in data from the input ENDF-format files. Note that this array uses 8-byte words. The values read in will be converted to the 4-byte words used in the CCCC `a,ia,ha` set as necessary. Note the variable `next`. It will keep track of the next available location in the `a,ia,ha` area.

Next, the unit numbers for input and output are read. The signs given for CCCC units are ignored; they are opened as binary files. The subroutine continues by reading input cards 2 through 5. At this point, CCCCCR branches

to different subroutines for each of the three interface file types that have been requested (see `cisotx`, `cbrkxs`, and `cdlyxs`). Each of these routines is paired with a print routine that is called if the `iprint` flag has been set to 1 (see `pisotx`, `pbrkxs`, and `pdlyxs`). When the last of these routines returns, CCCCC closes its active I/O units, writes a report, and terminates.

**ISOTXS File Preparation.** The `cisotx` routine starts by calling `ruinis` to read in the portion of the user's input specific to the ISOTXS file. It then calls `isxdatt` to read through the input GENDF file and extract the ISOTXS data.

Subroutine `ISXDATT` starts by setting up pointers in the `a,ia,ha` area for the different types of data to be read in. These pointers are identified in the comments at the start of the subroutine. The routine then reads the GENDF header record for the first material and extracts the group boundary energies. If the group structure found does not match the one requested in the user's input, an error message is issued. Otherwise, the order of the groups is changed from the `GROUPE`/ENDF convention of increasing energy to the CCCC convention of decreasing energy (which is the normal ordering for application programs) as the 8-byte GENDF data are copied into the 4-byte words of the `a` array. The routine then begins a loop over all the materials (isotopes) requested (see `do 300 i=1,niso`). It searches through the input GENDF tape for the first material with the requested MAT number (that is, the first temperature for the MAT) and copies it to a scratch file. Note that materials are written in the order requested by the user's input material list, not in the order that they are found on the GENDF tape.

This scratch tape is scanned for the ISOTXS principal cross section data in `prinxs`. This process is fairly simple for most of the ENDF File 3 cross sections. Each MT number in File 3 is compared to the list of desired principal cross sections in `nstx`; if a match is found, the corresponding element of `iflag` is set, and the cross section table is copied into memory using a pointer from the `iptr` array. The (n,2n) reaction is a special case. In addition to `mt=16`, the routine watches for the partial (n,2n) representation used in the ENDF/B-IV and -V evaluations for  $^9\text{Be}$  (namely, `mt=6, 7, 8, and 9`), and adds them into the appropriate memory locations. Fission is obtained from `mt=18`, but if the partial fission reactions are present (`mt=19, 20, 21, 38`), the flag `mt=19` is set. Average neutron velocities are obtained from the special `GROUPE`-produced section labeled by `mt=259`. These are inverse velocities in s/m, and `prinxs` inverts them and multiplies by 100 to get velocities in cm/s. In addition to

the normal flux-weighted total cross section, the routine also stores the current-weighted, or  $P_1$ , cross section for use in calculating the transport cross section (see below). Finally, File 3 may also contain `mt=455`, the delayed-neutron  $\bar{\nu}$  parameter. The GENDF record for this parameter also contains  $\sigma_f$  and the flux for each group. The delayed-neutron production rate  $\bar{\nu}_d\sigma_f$  is stored for use in calculating the total  $\bar{\nu}$  parameter, and  $\bar{\nu}_d\sigma_f\phi$  is added into the `dnorm` array for later use in normalizing the total fission spectrum,  $\chi$ . Note that there are two options for the flux used in this normalization: it can be the default library flux found on each record of the GENDF file, or it can be a flux spectrum `spec` provided by the user.

While reading through the scratch tape, `prinxs` also watches for the elastic scattering matrix (`mf=6, mt=2`). The total  $P_1$  elastic cross section is calculated by summing over all secondary neutron groups, and the result is subtracted from the current-weighted total cross section to obtain the transport cross section.

The processing of the fission matrix (`mf=6, mt=18`) and the delayed-fission spectra (`mf=5, mt=455`) depend on the `ichix` option. The  $\bar{\nu}$  parameter `SNUTOT` is always calculated for fissionable isotopes. `CHISO` is only calculated if the vector representation was requested; in addition, it can be calculated using the flux from GENDF or using the input flux in `SPECT`. Starting with NJOY 91.0, the fission matrix is represented by a real group-to-group matrix at high energies, and by a single spectrum (with `IG=0`) and an associated production cross section (with `IG2L0=0`) at low energies. This representation can lead to great savings for libraries with many low-energy groups. The contributions to `SNUTOT` from the low-energy range are easily obtained by adding in the production cross section. At high energies, the sum of the group-to-group matrix over all secondary-energy groups is added in. After `mf=3, mt=455` and `mf=6, mt=18` have been processed, it is only necessary to divide the total production rate in memory by the fission cross section to obtain the required total  $\bar{\nu}$  values.

The prompt part of the fission  $\chi$  vector or matrix is obtained from `mf=6, mt=18`, or if the `MT=19` flag was set while reading File 3, from `mt=19, 20, 21, and 38`. The code starts at statement number 207, and it is fairly complicated because it has to cope with the following options:

1.  $\chi$  vector versus  $\chi$  matrix,
2. default weighting for the vector versus input weighting,
3. square matrix versus collapsed rectangular matrix, and
4. constant and matrix parts of `mf=6` GENDF record.

Note that separate normalization sums are accumulated in `cnorm(ispec)` for the chi vector or for each column of the matrix while the  $\chi$  elements are being stored. The delayed contributions to the fission  $\chi$  vector or matrix are taken from `mf=5`, `mt=455` (see statement number 230). The time group spectra are added and multiplied by the delayed neutron production rate `dnorm` (which can be incident energy dependent through the `ispec` index if a matrix is being constructed). The delayed contributions to the normalization sum for the  $\chi$  vector or for each column of the  $\chi$  matrix are added into `cnorm` during this step. After all the components of the fission spectrum have been read from the GENDF file, the  $\chi$  vector or the columns of the  $\chi$  matrix are normalized using this quantity.

When all sections of the scratch tape have been processed, `prinxs` goes through the principal cross section block, removing any parts that have zero cross sections. The resulting block is written to scratch file `nsCRT2`. Finally, it writes the chi matrix data, if any, to the same scratch file and returns to `isxdAT`.

Subroutine `isomtx` is then called to read through the scratch tape and process the group-to-group matrices into CCCC format. In order to allow large matrices to be processed on machines with limited memory, one or more passes can be made through the scratch tape (see `do 400 nj=1,npass`). The number of passes used depends upon the amount of space available in scratch array `b` and on the subblocking option requested by the user. The four options supported by CCCCCR were discussed in connection with the ISOTXS format description. Only one pass is required for the first option. In the other cases, the length of one subblock is divided into the length of the scratch array to determine the number of subblocks that can be accumulated on one pass (`nrec`) and the number of passes required (`npass`).

Four matrix reactions are extracted from the scratch tape (see `do 500 i=1,4`). The total matrix is obtained by adding all matrices found on the GENDF tape except the fission matrices. The elastic matrix is obtained from `mt=2` only. The  $(n,2n)$  matrix is normally obtained from `MT=16`, but the sum of `mt=6`, 7, 8, 9, 46, 47, 48, and 49 will be used for the old  $^9\text{Be}$  representation, if found. The inelastic matrix is the sum of everything else; that is, it includes the normal inelastic reactions `mt=51-91`, and it also includes other neutron-producing reactions like  $(n,3n)$ ,  $(n,n'p)$ , and  $(n,n'\alpha)$ . Each GENDF section found is passed to `shuff1`, which rearranges the input data into the CCCC order in scratch array `b`, and then to `wrtmtx`, which repacks the data into banded form and writes the results to `nsCRT2`.

Subroutine **shuffl** reads each of the group-to-group cross sections for a given reaction (MT) and calculates a location for each cross section in the scratch array (**noloc**). Different formulas are used for the location of the two allowed values of **IFOPT**. For **IFOPT=1**, the data are stored with incident group index **ig1** changing fastest, then Legendre index **il**, and with final group index **ig2** changing slowest. Note that the indexing scheme only stores the triangle of the matrix corresponding to ingroup scattering and downscatter (that is,  $ig2 \geq ig1$ ). In addition, the first group in a subblocking range **ng2z** is used. This means that values of **ig2** less than **ng2z** will result in storage locations less than **irsize**, and they will not be stored (see statement 200). Groups with **ig2** above the subblock might be stored in memory, or they might end up above the upper limit of the memory area and be suppressed by statement number 200. Similarly, the data for **IFOPT=2** are stored with **ig1** as the fastest varying index, then **ig2**, and finally with **il** as the slowest varying index. Here also, the storage pointer **noloc** is calculated so that only elements with  $ig2 \geq ig1$  are stored, and elements that are outside of a given subblock are removed if they fall outside the bounds of the memory array.

Subroutine **wrtmtx** searches through the memory area loaded in **shuffl** to find the bands of group-to-group elements that will be written on the final ISOTXS file. The calculation of locations in the memory array depends on the blocking and subblocking options selected. In general, the routine calculates locations **NOLOCA** and tests the cross section found there against the value **eps=1.E-10**. The highest index that violates this test for a given final energy group determines the bandwidth for that group. (Remember that the in-scattering group is always kept, even if it has zero cross section.) Once the band limits have been found, the subroutine loops back through the memory area and squeezes out the locations that are not included in the bands. At this point, all the elements of the “Scattering Sub-Block” are in their final locations, and the record is written out to scratch tape **nsCRT2**.

When **isomtx** returns to **isxdat**, the “Isotope Control and Group Independent Data” record is completed by filling in the values of **IDSCT** and **IJJ**, and the record is written to scratch tape **nsCRT3**. The **LOCA** values for the “File Date” record are also calculated at this point. They remain in memory at 119. Once the “do 300” loop over the requested isotopes has finished, the **isxdat** routine returns.

Back in **cisotx**, all the data needed for the ISOTXS file are now in memory or on one of the CCCC-style scratch files **nsCRT2** or **nsCRT3**. The routine simply

steps through the ISOTXS records and either constructs them or copies them from a scratch file. When the file has been written, the routine returns to `cccr`, which checks the print flag, and calls `pisotx`, if requested.

Subroutine `pisotx` is a fairly simple routine. It reads through the ISOTXS file produced by CCCR and prepares an interpreted listing of the data.

**BRKOXS File Preparation.** Subroutine `cbrkxs` is used to prepare the BRKOXS file, if requested. Following the same pattern as `cisotx`, it calls `ruinbr` to read the user's input, then it calls `brkdat` to extract the desired data from the GENDF file, and finally it writes the output BRKOXS file using data stored in memory and on a scratch tape by `brkdat`.

The storage locations used by `brkdat` are outlined in the comment cards at the beginning of the subroutine. The subroutine now opens the input GENDF file and reads in the header record. After checking for possibly incompatible group structures, it reverses the order of the group bounds and loads them into the `emax` and `emin` arrays. The data block starting at 119 is sized to hold 13 infinitely dilute cross section vectors that will either be needed during the processing (vectors 1 through 7) or will be written into the "Cross Sections" record. These 13 quantities are

1.  $P_0$  total cross section,
2. capture cross section,
3. fission cross section,
4.  $P_1$  total -  $P_1$  elastic,
5. elastic cross section,
6.  $P_1$  total cross section,
7.  $P_1$  flux,
8.  $XSP_0$ ,
9. inelastic cross section,
10. elastic cross section,
11. average elastic scattering cosine  $\bar{\mu}$ ,
12. elastic downscatter to adjacent group, and
13. average elastic lethargy increment  $\xi$ .

Pointer 120 defines the balance of the available memory.

The next step is to determine whether it is necessary to subblock the self-shielding factor record. The amount of space available in the memory area is



compared with the maximum amount of memory required for the f-factors. If there is not enough space, **nsblk** is increased to **nreact**; otherwise, it is left at 1. The value of **nsblk** is stored into the IBLK field of the BRKOXS “File Control” record.

The isotope loop is complicated because CCCCCR allows the materials on the GENDF tape to be in any order, but it arranges things so that the materials on the BRKOXS files are in the order that the materials are named in the user’s input. The main loop is controlled by `do 370 i=1,niso`. For each pass, the input GENDF tape is rewound and searched for isotope I (see `do 170 j=1,niso`). Once a desired material has been found, the  $\sigma_0$  list in the header record is examined. Either the first **abs(nzi)** values are extracted (for **nzi** negative), or the particular values that occur on the input **asig** list are extracted (for **nzi** positive). In either case, **nzj** is the number of  $\sigma_0$  values found, **isig** contains the pointers to the values selected, and **csig** contains the actual values of  $\sigma_0$ .

GENDF tapes contain one or more temperatures for each material recorded as consecutive MATs. Starting at statement number 190, **brkdat** reads through all the materials with the current MAT number selecting the desired temperatures and copying them to a scratch file **nsCRT1**. The procedure used to select temperatures is similar to the one used to select  $\sigma_0$  values. If **nti** is negative, the first **abs(nti)** temperatures are extracted. If **nti** is positive, only temperatures on the list in **atem** are extracted. In either case, **ntj** is the number of temperatures found for this material, **item** contains indices to those temperatures, and **ctem** contains the actual temperature values.

In the loop beginning at `do 340 nsb=1,nsblk`, a pass through the scratch tape is made for each subblock (1 or **nreact**). Each section of the GENDF format is located, and either **xsproc** (for **mf=3**) or **mxproc** (for **mf=6**) is called to process the data in the section.

Subroutine **xsproc** is called once for each reaction in File 3 of the GENDF tape. It reads in all the data, checks which reaction is present, and stores the data in one of the 13 cross section locations (see 119), or in one of the f-factor locations (see 120). If the denominator for the f-factor calculation is zero, the division is skipped, and a warning message is issued.

Subroutine **mxproc** is called once for each reaction in File 6 of the GENDF tape. It loops through statement number 120 to read all of the incident groups, and then it uses different sections of coding to fill in or fix up the rest of the 13 elements in the infinitely dilute cross section block at 119. These quantities include the elastic and inelastic cross sections, the transport cross section, and

the removal cross section. This routine also computes the elastic removal self-shielding factors from `mf=6`, `mt=2`, and stores the results in the f-factor area at 120.

Back in `brkdat`, the self-shielded transport cross sections are converted into f-factors. A check is then made to see if the transport values were properly computed. This requires that a self-shielded elastic matrix was available for all the higher temperatures. A warning message is issued if the required data were not present. The last 6 of the 13 vectors stored starting at 119 are the data needed for the “Cross Sections” record; that block is written to scratch file `nsCRT2`. Next, the accumulated f-factor data at 120 are written to `nsCRT2`, and the `NTABP` and `NTABT` arrays are stored at 114 and 115, respectively.

The last step inside the isotope loop is to call `thnwrt` to thin out the f-factor data and write the results onto scratch file `nsCRT3`. It starts by reading the cross section data from `nsCRT2` into memory. Then it reads the f-factor data into memory and repacks it to take account of the group range for interesting self-shielding factors, namely, `JBFL` to `JBFH`. When this is finished, it writes the f-factor array out to `nsCRT3`, and then it writes the unchanged cross section block out to `nsCRT3`. Note that these two records are now in the correct order to be copied to the `BRKOXS` file.

Subroutine `thnwrt` now returns control to `brkdat`. When the “do 370” loop has finished, the routine cleans up the “File Data” information in memory and returns to the main `BRKOXS` routine. At this point, all the information required to construct the output file is present in memory or on scratch tape `nsCRT3`. The routine steps through the records of the `BRKOXS` format constructing them or copying them from the CCCC-style scratch file. It then returns to `ccccr`, which checks to see whether `pbrkxs` should be called.

Subroutine `pbrkxs` is a fairly simple routine. It reads through the `BRKOXS` file produced by `ccccr` and prepares an interpreted listing of the data.

**DLAYXS File Preparation.** Subroutine `cdlyxs` is used to prepare a `DLAYXS` file, if requested. It starts by calling `dldata` to extract the delayed-neutron data from the input `GENDF` file. Since all the data are stored into memory, `cdlyxs` continues by simply writing out the required “File Identification”, “File Control”, “File Data, Decay Constants, and Emission Spectra”, and “Delayed Neutron Precursor Yield Data” records. If no delayed-neutron data are found, `cdlyxs` issues a fatal error message. The coding can handle either the traditional 6 time groups of `ENDF/B` or the 8 time groups used in some other

evaluation systems. For convenience, the following discussion will just use the 6 time groups.

Subroutine `dldata` starts by reserving space for the dynamic arrays used to store the delayed-neutron data; the purpose for each of these arrays is summarized in the comment block at the beginning of the subroutine. ENDF delayed-neutron files are based on the traditional 6 time groups; therefore, CCCCCR makes each time group for each isotope correspond to one DLAYXS “delayed-neutron family” (see `NFAM=6*NISOD`). Next, `dldata` starts reading through the materials on the GENDF tape and looking at each material requested in the user’s input (the material loop goes through statement 110). For the first material, it reads the header record, checks that the group structure is compatible with the user’s input value `ngroup`, and stores the structure in `EMAX` and `EMIN` in the conventional decreasing-energy order. For all materials, it watches for sections with `mf=3, mt=455` or `mf=5, mt=455`.

When `mf=3/mt=455` is found (see statement 310), `dldata` stores the total delayed-neutron yield from `GROUPR` in the `snudel` array (pointer 18) using an offset computed from the time group index (which varies from 1 to 6), the group index, and the isotope index. (The group index goes through statement 130). For the present, the same value is stored for every time group.

When `mf=5/mt=455` is found (see statement 410), the rest of the data for this isotope are stored into memory. The `HABSID` field is obtained from the isotope name in the user’s input. The `LOCA` field is easy to calculate from the isotope index. The decay constants for each of the time groups are copied into `FLAM` from the GENDF record. The number of families for this isotope is simply 6; this number is loaded into the location corresponding to `NKFAM`. Finally, the actual delayed-neutron spectra for each time group are loaded into the `CHID` area using energy group and family number as indexes. At this point, the spectrum for each time group is summed over group index to determine the delayed fraction for that time group [see `FRACT(I)`]. Then this fraction is used to change the total delayed-neutron yield for each time group in the `SNUDEL` area into the fractional delayed-neutron yield for that time group (family).

When all the isotopes containing delayed-neutron data have been processed, `dldata` returns to `cdlyxs`. When `cdlyxs` returns to the main subroutine of CCCCCR after writing the DLAYXS file, the print routine `pdlyxs` may be called. This is a fairly simple routine that reads through a file in DLAYXS format and prepares an interpreted listing.

## 14.8 User Input

The user input instructions copied from the comment cards at the beginning of the CCCR source code are given below. It is always a good idea to check the comments cards in the current version of the code in case there have been any changes.

```

!---input specifications (free format)-----
!
!-cccr-
! card 1 units
!   nin      input unit for data from groupr
!   nisot     output unit for isotxs (0 if isotxs not wanted)
!   nbrks     output unit for brkoxs (0 if brkoxs not wanted)
!   ndlay     output unit for dlayxs (0 if dlayxs not wanted)
! card 2 identification
!   lprint    print flag (0/1=not print/printed)
!   ivers     file version number (default=0)
!   huse       user identification (12 characters)
!              delimited by *, ended by /.
!              (default=blank)
! card 3
!   hsetid     hollerith identification of set (12 characters)
!              delimited by *, ended by /.
!              (default=blank)
! card 4 file control
!   ngroup     number of neutron energy groups
!   nggrup     number of gamma energy groups
!   niso       number of isotopes desire
!   maxord     maximum legendre order
!   ifopt      matrix blocking option (1/2=blocking by
!              reaction/legendre order)
! card 5 isotope parameters (one card per isotope)
!   (first four words are hollerith, up to six characters
!   each, delimited by *)
!   hisnm      hollerith isotope label
!   habsid     hollerith absolute isotope label
!   hident     identifier of data source library (endf)
!   hmat       isotope identification
!   imat       numerical isotope identifier (endf mat number)
!   xspo       average potential scattering cross sect. (brkoxs)

```

```

!-cisotx- (only if nisot.gt.0)
! card 1 file control
!   nsblok      subblocking option for scattering matrix
!               (1 or ngroup sub-blocks allowed)
!   maxup       maximum number of upscatter groups (always zero)
!   maxdn       maximum number of downscatter groups
!   ichix       fission chi representation
!               -1   vector (using groupr flux)
!               0   none
!               +1   vector (using input flux)
!               .gt.1 matrix
! card 2 chi vector control (ichix=1 only)
!   spec        ngroup flux values used to collapse the groupr
!               fission matrix into a chi vector
! card 3 chi matrix control (ichix.gt.1 only)
!   spec        ngroup values of spec(i)=k define the range of
!               groups i to be averaged to obtain spectrum k.
!               index k ranges from 1 to ichi.
!               the model flux is used to weight each group i.
! card 4 isotope control (one card per isotope)
!   kbr         isotope classification
!   amass       gram atomic weight
!   efiss       total thermal energy/fission
!   ecapt       total thermal energy/capture
!   temp        isotope temperature
!   sigpot      average effective potential scattering
!   adens       density of isotope in mixture
!
!-cbrkxs- (only if nbrks.gt.0)
! card 1 (2i6) file data
!   nti         number of temperatures desired
!               (-n means accept first n temperatures)
!   nzi         number of sigpo values desire
!               (-n means accept first n dilution factors)
! card 2 (not needed if nti.lt.0)
!   atem(nti)   values of desired temperatures
! card 3 (not needed if nzi.lt.0)
!   asig(nzi)   values of desired sigpo
!
!-cdlayx-- no input required
!-----

```

These instructions are divided into four parts. First, there is a general section that applies to all three interface files following `-cccr-`. Second, there is a section of special parameters for ISOTXS following `-cisotx-`. Third, there is a section of special parameters for BRKOXS following `-cbrkxs-`. And fourth, there is a comment following `-cdlaxs-` noting that no special input is required for the DLAYXS file.

In the `-cccr-` section, Card 1 is used to read in the unit numbers for input and output. `nin` must be a GENDF tape prepared using [GROUPE](#), and it can have either binary (`nin<0`) or ASCII (`nin>0`) mode. The units for the output ISOTXS, BRKOXS, and DLAYXS files are all binary, but either sign can be used on the unit numbers. If any unit number is given as zero, the corresponding CCCC interface file will not be generated. On Card 2, the `lprint=1` is used to request a full printout of all the CCCC files generated. The file version number `ivers` can be used to distinguish between different libraries generated using NJOY. The user identification field `huse` can contain any desired 12-character string. An example of Card 2 might be

```
0 7 'T2 LANL NJOY' /
```

Card 3 contains a description of the library using up to 72 characters (12 standard CCCC words of 6 characters each). For example,

```
'LIB-IV 50-GROUP LMFBR LIBRARY FROM ENDF/B-IV (1976)' /
```

On Card 4, the values given for `ngroup` must agree with the number of groups on the input GENDF tape or a fatal error message will be issued. `nggroup` is not used. `niso` is the total number of materials or isotopes to be searched for on the GENDF tape. The value of `maxord` should be less than or equal to the maximum Legendre order used in the [GROUPE](#) run. The use of the matrix blocking parameter `ifopt` was discussed in detail in connection with the description of the ISOTXS format above. A value of 1 has been normally used for Los Alamos libraries.

A line using the Card 5 format is given for each of the `niso` isotopes or materials to be processed. The Hollerith isotope label and the Hollerith absolute isotope label have normally been set to the conventional isotope name at Los

Alamos; for example, `u235` or `cnat`. The library name in `habsid` can vary quite a lot now that many other libraries are available in ENDF format. The values of `hmat` and `imat` will normally be derived from the MAT number characteristic of all libraries in ENDF format. Unfortunately, `xspo`, the average potential scattering cross section, must be entered by hand. It can be obtained from `mf=2`, `mt=151` on the ENDF file for the material by determining the scattering radius  $a$  from the AP field and computing  $\sigma_p = 4\pi a^2$ . The following fragment of an ENDF/B evaluation shows the vicinity of AP:

```

...
9.223500+4 2.330248+2      0      0      1      09228 2151
9.223500+4 1.000000+0      0      1      2      09228 2151
1.000000-5 2.250000+3      1      3      0      19228 2151
3.500000+0 9.602000-1      0      0      1      39228 2151
2.330200+2 9.602000-1      0      0     19158     31939228 2151
-2.038300+3 3.000000+0 1.970300-2 3.379200-2-4.665200-2-1.008800-19228 2151
...

```

The scattering radius is the second number on the fourth card in the section `mf=2`, `mt=151`. Using it as  $a$  gives  $4\pi(0.96020)^2 = 11.582$  barns for the value of `xspo`. An example of Card 5 follows:

```
U235 U235 ENDF6 '9228' 9228 11.582
```

Note that the Hollerith string “9228” had to be delimited by quotes because it does not begin with a letter. The delimiters are optional for the other Hollerith variables.

The next block of input cards is specific to ISOTXS and only appears if ISOTXS processing was requested with a nonzero value for `nisot`. The first parameter on Card 1 is `nsblok`, which was discussed in connection with matrix blocking and subblocking. `nsblok` and `ifopt` work together to control how a large scattering matrix is broken up into smaller records on the ISOTXS interface file. The important factor is the maximum size of the binary records. They should be small enough to fit into a reasonable amount of memory in any application codes that use ISOTXS files, but they should be large enough to

keep the number of I/O operations to a minimum. The maximum record size for each option is repeated below for the convenience of the reader:

1. `ifopt=1` and `nsblok=1`:  $n_\ell \times n_g(n_g-1)/2$ ,
2. `ifopt=1` and `nsblok=ngroup`:  $n_\ell \times n_g$ ,
3. `ifopt=2` and `nsblok=1`:  $n_g(n_g-1)/2$ ,
4. `ifopt=2` and `nsblok=ngroup`:  $n_g$ ,

where  $n_\ell$  is the number of Legendre orders and  $n_g$  is the number of groups. If the user specifies `nsblok=1` and the resulting output record is too large for the available memory, `nsblok` will be changed to `ngroup` automatically.

Card 1 of the ISOTXS section continues with `maxup`. This parameter is always zero for CCCCCR; thermal upscatter matrices are not processed. The normal value of `maxdn` is `ngroup`, but it can be made smaller to reduce the size of the matrices. The cross section for any removed downscatter groups will be lumped into the last group in order to preserve the production cross section. The `ichix` is used to control the generation of fission  $\chi$  vectors and matrices. The representations allowed were discussed above in connection with the description of the ISOTXS format (see Section 14.4). The most commonly used option has been `ichix=-1` because most application codes cannot handle fission  $\chi$  matrices. The `GROUPE` flux is normally chosen to be characteristic of the class of problems a given library is intended to treat; therefore, it is rarely necessary to supply an input weighting spectrum (see `ichix=+1` and `spec`). The following scenario illustrates a case where this option might be useful. Assume that an 80-group library is made using the `GROUPE` fast reactor weight function (`iwt=8`), which contains a shape in the fission range typical of both fast reactors and fusion blankets plus a fusion peak at 14 MeV. This GENDF library could be used to generate two different ISOTXS libraries, one using the default flux and useful for fusion problems, and one using a spectrum `spec` from which the fusion peak has been removed. The latter would be better for fast reactor analysis because the  $\chi$  vectors would not contain the component of high-energy fission from the 14 MeV range. Card 2 is used to input the user's choice for `spec`.

CCCCCR can also produce fission  $\chi$  matrices for codes that can use them. These matrices can be rectangular to take advantage of the fact that the  $\chi_{g \rightarrow g'}$  function is basically independent of  $g$  at low energies (large values of  $g$ ). Taking the `GROUPE` 30-group structure as an example, if the energy at which significant incident-energy dependence begins is taken to be about 100 keV, then



groups 16 through 30 will have identical  $\chi$  vectors. The value of `ichix` should be set to 16, and the `spec` vector of Card 3 should be set to

```
1 2 3 4 5 6 7 8 9 10 11 12 13 14 15
16 16 16 16 16 16 16 16 16 16 16 16 16 16 16/
```

The resulting  $\chi$  matrix will be rectangular with  $16 \times 30$  elements.

Card 4 completes the input specific to ISOTXS. The value of `kbr` can be set to reflect the normal use of this material in the applications that this library is intended to treat. The `amass` parameter has units of gram atomic weight. It can be calculated from the normal ENDF AWR parameter (the atomic weight ratio to the neutron) by multiplying by the gram atomic weight of the neutron. `temp` was historically 300K for NJOY CCCC libraries. The same value can be used for `sigpot` and `xspo` (see above). The `adens` parameter has no meaning for CCCCCR; it can be set to zero to imply infinite dilution.

The choice of values for `efiss` and `ecapt` is more complicated. As discussed in Section 14.4, `efiss` is basically the total non-neutrino energy released by a fission reaction. It is available in eV as the pseudo Q value in `mf=3`, `mt=18` (the energy release from fission is given in more detail in `mf=1`, `mt=458`). The following fragment of the ENDF/B-VI evaluation for  $^{235}\text{U}$  shows how to find the Q value:

```
...
                                     9228 3 0 4413
9.223500+4 2.330250+2                0      0      0      09228 3 18 4414
1.937200+8 1.937200+8                0      0      1      3339228 3 18 4415
      333      2                                     9228 3 18 4416
1.000000-5 0.000000+0 7.712960+1 0.000000+0 2.250000+3 0.000000+09228 3 18 4417
2.250000+3 5.362770+0 2.300000+3 5.396710+0 2.500000+3 5.957280+09228 3 18 4418
...
```

The Q value is the second number on the second card of the section `mf=3`, `mt=18`. Converting to CCCC units gives

$$193.72 \times 10^6 \text{ eV} \times 1.602 \times 10^{-19} \text{ watt-s/eV} = .31034 \times 10^{-10} \text{ watt-s/fission}$$

The value for `ecapt` is determined from the Q value for `mf=3`, `mt=102`, the radiative capture reaction. However, if the isotope remaining after capture has a relatively short half-life, the energy of the decays leading to the final stable

daughter should be added onto the capture Q value. (The meaning of “stable” may vary from application to application). As an example, consider aluminum. The  $^{28}\text{Al}$  capture product decays with a half-life of 2.24 minutes producing 9.31 MeV of  $\beta^-$  energy and a 1.779 MeV photon. Therefore, the actual value of `ecapt` should be calculated as follows:

$$\begin{array}{rcl}
 7.724 \text{ MeV} & \text{mt=102 prompt Q value} & \\
 9.310 \text{ MeV} & \beta^- \text{ energy} & \\
 1.779 \text{ MeV} & \text{delayed-}\gamma \text{ energy} & \\
 \hline
 18.813 \text{ MeV} & & \\
 \times 1.602 \times 10^{-13} & & \\
 \hline
 .3014 \times 10^{-11} & \text{in watt-s/capture} &
 \end{array}$$

The next section of the input file is specific to BRKXOS. Card 1 enables the user to just accept all or part of the temperatures and sigma-zero values on the input GENDF tape. If the value of `nti` is negative, the first `abs(nti)`  $T$  values for each material will be used. If fewer values are available, only those will be used. If `nti` is positive, input Card 2 will be read for a list of  $T$  values, and only data with temperatures on that list will be extracted from the GENDF tape. The parameter `nzi` and the list of  $\sigma_0$  values on Card 3 work in the same way.

No additional input is required for DLAYXS files.

## 14.9 Error Messages

### `error in isxdat***incompatible group structures`

The number of groups on the input GENDF tape must match the number of groups specified in the CCCCC input. Check whether the correct input file was mounted.

### `error in isomtx***input record too large`

There is not enough space in the scratch array `b` to read in the input records from the GENDF tape. The only solution is to increase the size of the main CCCC equivalenced array set. See `a,ia,ha` with `isiza=50000` at the beginning of the `ccccm` module.

### `error in isomtx***output record too large`

There is not enough space in the scratch array `b` for the output subblock record, even with `nsblok` changed to `ngroup`. The only solution is to increase the size of the main CCCC equivalenced array set. See `a,ia,ha` with `isiza=50000` at the beginning of the `ccccm` module.

### `error in shuffl***sigze of endf input array exceeded`

See the global parameter `maxe=8000` at the start of the module.

**error in pisotx\*\*\*input record too large**

One of the binary records on the ISOTXS file is too large for the memory available to prinxs. This should not occur because there was enough memory to create the record in the first place.

**error in brkdat\*\*\*incompatible group structures**

The number of groups on the input GENDF tape must match the number of groups specified in the CCCCCR input. Check whether the correct input file was mounted.

**error in brkdat\*\*\*max size of endf record exceeded.**

See the global parameter maxe=8000 at the start of the module.

**message from brkdat---all available mats have been processed**

This message is issued when all the materials on the GENDF file have been processed, but one or more of the materials requested in the user's input were not found. Check the input material list, and check which materials were written onto the input GENDF file.

**message from brkdat---no temperatures for mat=nnnn**

This means that none of the requested temperatures were found for this MAT. This makes it impossible to include the material in the BRKOXS file. The warning message is issued, and all references to this material are thinned out of the BRKOXS records.

**message from brkdat---need elastic matrices at higher temps**

The self-shielded transport cross section requires self-shielded  $P_1$  elastic scattering matrices for accurate results. This means that mf=6, mt=2 should be available on the GENDF tape for all temperatures. If this scattering matrix is missing for the higher temperatures, this warning message is issued.

**error in xsproc\*\*\*max size of endf record exceeded.**

See the global parameter maxe=8000 at the start of the module.

**message from xsproc---infinite f-factor mt jg jz temp**

The calculation of an f-factor requires division by the infinitely dilute cross section. This message means that the divisor was zero for reaction mt, group jg, background cross section jz, and temperature temp. The division is skipped, and the numerator is used unchanged.

**error in mxproc\*\*\*max size of endf record exceeded.**

See the global parameter maxe=8000 at the start of the module.

**error in pbrkxs\*\*\*input record too large**

One of the binary records on the BRKOXS file is too large for the memory available to pbrkxs. This should not occur because there was enough memory to create the record in the first place.

**message from cdlyxs---no delayed neutron data found**

There was no delayed-neutron data found by DLDATA. Make sure that `mf=3`, `mt=455` and `mf=5`, `mt=455` were requested during the [GROUPR](#) run and that the delayed-neutron isotopes were included in the material list given in the CCCR input.

`error in dlldata***max size of endf record exceeded.`

See the global parameter `maxe=8000` at the start of the module.

`error in dlldata***incompatible group structures`

The number of groups on the input GENDF tape must match the number of groups specified in the CCCR input. Check whether the correct input file was mounted.

`error in pdlyxs***input record too large`

One of the binary records on the DLAYXS file is too large for the memory available to `pdlyxs`. This should not occur because there was enough memory to create the record in the first place.

## 15 MATXS

The MATXS material cross section format is a generalized CCCC-type interface format for neutron, photon, and charged-particle data, including cross sections, group-to-group matrices, temperature variations, self-shielding, and time-dependence. The CCCC standards are discussed in more detail in the CCCC chapter of this manual and in the CCCC-III and CCCC-IV reports[28, 10]. MATXS libraries can be used with the TRANSX code[11, 40] to produce effective cross sections for a wide variety of application codes. This chapter describes MATXS in NJOY 2012.0. It differs from the version reported previously[3] in the following ways:

- the removal of the internal capability to print MATXS files (use an external listing code),
- the addition of the nuclide production capability, and
- the conversion to Fortran-90 style and memory allocation.

### 15.1 Background

Even the very best nuclear cross section processing code would be useless if it were unable to deliver its products to users. This is the role of the interface file. There have been interface files since the beginning of calculational neutronics; examples include the DTF format (see the [DTFR](#) chapter of this manual) that was devised for the early discrete-ordinates transport code DTF-IV[23], and the CCCC ISOTXS format[10] (see the [CCCCR](#) section of this manual). Both of these interface formats are still in use today, but both of them have problems and show their age. Some of these problems result from the increase in the capabilities of computer systems (capabilities that allow us to consider much more complex problems), some arise from the many new kinds of nuclear systems that are being studied today, and some come from 20/20 hindsight, which makes it easy to see the design flaws in earlier formats.

Based on the problems seen with existing interface files, an ideal interface file should be

**extendable**, so that new cross section types, new incident or secondary particle types, or new energy ranges are easy to add without changing the basic format;

- comprehensive**, in order to be able to handle as many of the kinds of data produced by the processing code as possible (results should not be lost just because there are no places for them);
- generalizable**, to allow common methods to be used for similar kinds of data (for example,  $nn$  matrices and  $\gamma\gamma$  matrices) in order to transfer the experience gained in one field to another, and in order to simplify coding by allowing components to be reused;
- self-contained**, because it should not be necessary to provide additional information that is not in the file in order to use or interpret the file;
- compact**, because nuclear data often have many zeros or very small numbers in tables (for example, threshold reactions, scattering matrices), and these zeros must be removed effectively for economic storage and fast transfer of libraries; and
- efficient**, thus implying that binary mode should be used, that the records have a well-defined maximum size, and that there is a minimum number of records to reduce the number of I/O operations.

Comparing the DTF format to these principles gives the following results: it is fairly *extendable* because it has no fixed particles, energy limits, or reaction types; it is not very *comprehensive* because it can only transmit the total scattering matrix; it is fairly *generalizable* because of the lack of fixed types; it is not at all *self-contained* in that it requires outside definitions like table length, position of the total, group structure, and identity of edit cross sections; it is not very *compact* because most zeros must be given explicitly in the tables; and it is not very *efficient* because it uses coded card-image records.

Similarly, studying the ISOTXS format gives the following results: it is not *extendable* because it works for neutrons only and allows only very limited types of reactions to be included; it is not *comprehensive* because it works for neutrons only and allows only very limited types of reactions to be included; it is not *generalizable* because of its specialization to fast-reactor problems (as proof, note that the CCCC files for  $\gamma$  cross sections use completely different formats); it is reasonably *self-contained* because all the parameters are internal, the group structure is given, and all names needed for labeling an interpreted listing are well determined; it is fairly *compact* because many zeros are removed (but too many still remain); it is fairly *efficient* because it uses binary mode, but record sizes are poorly predictable and very nonuniform, thereby needlessly increasing the size of application codes and the number of I/O operations.

## 15.2 The MATXS Format

Following these general principles, the MATXS material cross section file was designed to extend and generalize the existing interface formats while still using the CCCC approach for efficiency and familiarity (see the CCCCCR section of this report for more details). The first design principle was that all information would be identified using lists of Hollerith names. As an example, if the list of reactions included in the file contains entries such as **nf**, **ng**, and **n2n**, it is trivial to add additional reactions such as **kerma** or **dpa**. This approach is much more extendable than the fixed set of reaction flags used in ISOTXS. The second design principle was that the file would be designed to hold sets of vectors and rectangular matrices and that the same format would be used regardless of the contents of the vectors and matrices. As a consequence, once a code can handle  $n \rightarrow n$ , it can also handle  $\gamma \rightarrow \gamma$ ; once a code can handle  $n \rightarrow \gamma$ , it can also handle  $\gamma \rightarrow n$ ,  $n \rightarrow \beta$ , or even  $d \rightarrow p$ . This approach is an example of generalization. Each material is now divided into data types identified by input and output particle. As an example,  $n \rightarrow \gamma$  is a data type characterized by input particle equals neutron, and output particle equals photon. The matrices for this data type contain cross sections for producing photons in photon group  $\gamma$  due to reactions of neutrons in group  $n$ . The vectors, if any, would contain photon production cross sections versus neutron group. The use of completely general data types helps make the format comprehensive.

The names for materials are written in the forms **u235**, **fe56**, **tinat**, or **h2a**. Note that “**nat**” is used explicitly for elements; names like **be** or **c** should be avoided. Suffixes “**a**”, “**b**”, or “**c**” are used to label different versions of a material in a library. In order to keep names to six characters, isomers should be identified by incrementing the “thousands” digit in the atomic number field; for example, **nb193a** would be the second version of the first isomer of  $^{93}\text{Nb}$ . The standard names for MATXS particles are given in Table 12.

The standard names for the data types (**h<sub>type</sub>**) are mostly based on these particle names; the use of the terms **scat**, **dk**, **therm** are exceptions. Table 13 illustrates the scheme used.

Reactions names are constructed in MATXSR from the ENDF MT number, the LR flag (if present), and the incident particle name. Examples of the standard names are given in Tables 14–22. Note that the first **n** is omitted from the last three reactions in Table 14. It is implicit in the data-type name. This convention saves space in the name for possible breakup products (see Table 15). The first **n** is also implicit in the reactions of Table 15. No multiplicity is used

Table 12: Standard Particle Names

| Name     | Particle                                    |
|----------|---------------------------------------------|
| <b>n</b> | neutron                                     |
| <b>g</b> | gamma                                       |
| <b>p</b> | proton                                      |
| <b>d</b> | deuteron                                    |
| <b>t</b> | triton                                      |
| <b>h</b> | $^3\text{He}$ nucleus                       |
| <b>a</b> | alpha                                       |
| <b>b</b> | beta                                        |
| <b>r</b> | residual or recoil (heavier than $\alpha$ ) |

in the breakup product strings in order to avoid possible confusions with the discrete-level number; just count the like letters to get the multiplicity. The names used for the most common neutron absorption reactions are given in Table 16, and the names used for the fission reactions are given in Table 17. MATXS libraries typically give the total fission cross section and all the partial cross sections (when available) in the vector blocks, but they do not give the total fission matrix when the partial matrices are available.

Table 18 gives some additional reaction names, some of which are special NJOY names. As discussed in the GROUPE chapter of this report, the total cross section can be averaged with the  $\ell$ th order of the flux to obtain the multi-

Table 13: Standard Data-Type Names

| Name          | Data Type                         |
|---------------|-----------------------------------|
| <b>nscat</b>  | neutron scattering                |
| <b>ng</b>     | neutron-induced gamma production  |
| <b>np</b>     | neutron-induced proton production |
| <b>nr</b>     | neutron-to-recoil matrix          |
| <b>gscat</b>  | gamma scattering                  |
| <b>pscat</b>  | proton scattering                 |
| <b>pn</b>     | proton-induced neutron production |
| ...           | ...                               |
| <b>ntherm</b> | thermal scattering data           |
| <b>dkn</b>    | delayed-neutron data              |
| <b>dkhg</b>   | decay heat and gamma data         |
| <b>dkb</b>    | decay beta data                   |



Table 14: Simple Neutron-Emitting Reactions

| Name          | MT | Description                      |
|---------------|----|----------------------------------|
| <b>nelas</b>  | 2  | neutron elastic scattering       |
| <b>nnonel</b> | 3  | neutron nonelastic (MT=1–MT=2)   |
| <b>ninel</b>  | 4  | neutron inelastic sum (MT=51–91) |
| <b>n2n</b>    | 16 | (n,2n)                           |
| <b>n3n</b>    | 17 | (n,3n)                           |
| <b>nna</b>    | 22 | (n,n' $\alpha$ )                 |
| <b>nnp</b>    | 28 | (n,n' $p$ )                      |
| <b>n01</b>    | 51 | (n,n <sub>1</sub> )              |
| <b>n02</b>    | 52 | (n,n <sub>2</sub> )              |
| <b>ncn</b>    | 91 | (n,n') to continuum              |

group total cross section components  $\sigma_{t\ell,g}$ . These total cross section components and the corresponding Legendre fluxes are given names like the first four shown in Table 18. Related names with first letters **g**, **p**, **d**, *etc.*, will also be found in MATXS libraries. The average inverse velocities are defined to preserve the time term of the time-dependent Boltzmann equation:

$$\left\langle \frac{1}{v} \right\rangle = \frac{\int_g (1/v) \phi(E) dE}{\int_g \phi(E) dE} . \quad (470)$$

The meaning of the terms energy-balance heat production and kinematic KERMA factor are discussed in more detail in the [HEATR](#) chapter of this manual. Briefly, the energy-balance heating (**mt**=301) is computed by subtracting the energy carried away by neutrons and photons from the energy available for a reaction. The result should be the energy deposited by charged particles and the recoil nucleus,

Table 15: Breakup Reactions (LR flags)

| Name          | MT | LR | Description                   |
|---------------|----|----|-------------------------------|
| <b>n07a</b>   | 57 | 22 | (n,n <sub>7</sub> ) $\alpha$  |
| <b>n51p</b>   | 65 | 28 | (n,n <sub>15</sub> ) $p$      |
| <b>n02aa</b>  | 52 | 29 | (n,n <sub>2</sub> )2 $\alpha$ |
| <b>ncnaaa</b> | 91 | 23 | (n,n')3 $\alpha$              |
| <b>n06na</b>  | 56 | 24 | (n,n <sub>5</sub> )n $\alpha$ |
| <b>n01ee</b>  | 51 | 40 | (n,n <sub>1</sub> )ee         |

Table 16: Neutron-Absorption Reactions

| Name        | MT  | Description       |
|-------------|-----|-------------------|
| <b>nabs</b> | 101 | total absorption  |
| <b>ng</b>   | 102 | radiative capture |
| <b>np</b>   | 103 | (n,p)             |
| <b>na</b>   | 107 | (n, $\alpha$ )    |

that is, the local heating. Unfortunately, problems with the energy-balance consistency of evaluations, the difficulty of determining the available energy for elements, and the inaccuracy in the difference between relatively large numbers sometimes cause this value to have unphysical values (for example, negative heating). These values do have the property of always conserving energy for large systems. The kinematic value (**mt**=443) is computed from reaction kinematics alone. It is very accurate at low energies, but when three or more particles are involved in the reaction, it begins to fail. The results in **kerma** are always larger than the correct heating value. Comparing the two estimates for the local heating can reveal problems in the evaluations[42, 88]. The MATXS user is free to choose whichever number is more appropriate for the problem. The reaction **dame** is also generated using data from **HEATR**. As discussed in the **HEATR** section of this report, this “damage-energy production” cross section can be used to obtain the DPA (displacements per atom) parameter used in radiation damage studies.

The gas-production reaction names given in Table 19 can also appear with other particle names before the decimal point. The names for reactions induced by incident charged particles follow the neutron names in most cases, except that the first letter is changed to indicate the incident particle type. Discrete-

Table 17: Fission Reactions

| Name         | MT  | Description                     |
|--------------|-----|---------------------------------|
| <b>nftot</b> | 18  | total fission                   |
| <b>nf</b>    | 19  | (n,f) first-chance fission      |
| <b>nnf</b>   | 20  | (n,n'f) second-chance fission   |
| <b>n2nf</b>  | 21  | (n,n2f) third-chance fission    |
| <b>n3nf</b>  | 38  | (n,n3f) fourth-chance fission   |
| <b>nudel</b> | 455 | delayed-neutron yield (MF=3)    |
| <b>chid</b>  | 455 | delayed-neutron spectrum (MF=5) |

Table 18: Special NJOY Names

| Name         | MT  | Description                           |
|--------------|-----|---------------------------------------|
| <b>ntot0</b> | 1   | P <sub>0</sub> total cross section    |
| <b>ntot1</b> | 1   | P <sub>1</sub> total cross section    |
| <b>nwt0</b>  | 1   | P <sub>0</sub> weight function (flux) |
| <b>nwt1</b>  | 1   | P <sub>1</sub> weight function (flux) |
| <b>mubar</b> | 251 | scattering $\bar{\mu}$                |
| <b>xi</b>    | 252 | scattering $\xi$                      |
| <b>invel</b> | 259 | inverse velocity (sec/m)              |
| <b>heat</b>  | 301 | energy-balance heat production        |
| <b>kerma</b> | 443 | kinematic KERMA factor                |
| <b>dame</b>  | 444 | damage-energy production              |

level scattering reactions are exceptions; **n01** is used for both (n,n<sub>1</sub>) and (p,n<sub>1</sub>). Also note the **n00** cannot be used for incident neutrons; the name **nelas** is used instead. Similarly, **p00** is not used for incident protons.

As discussed in more detail below, scattering from thermal moderators is treated like *materials* in ENDF/B libraries, but it is treated like *reactions* on the GENDF files. The free-gas scattering reaction can appear in any material, but the other thermal MT numbers can only appear in the material corresponding to the dominant scattering isotope. For example, **hh2o** only appears in <sup>1</sup>H. There are two versions of **zrhyd**; one appears in <sup>1</sup>H and the other in Zr. The coherent and incoherent terms in the thermal cross section are kept separate for the convenience of applications; all the coherent names end with \$. Note that MATXS files contain two different representations for the scattering cross sections at low energies:

Table 19: Gas-Production Reactions

| Name          | MT  | Description               |
|---------------|-----|---------------------------|
| <b>n.neut</b> | 201 | total neutron production  |
| <b>n.gam</b>  | 202 | total $\gamma$ production |
| <b>n.h1</b>   | 203 | hydrogen production       |
| <b>n.h3</b>   | 205 | tritium production        |
| <b>n.HE4</b>  | 207 | helium production         |

Table 20: Incident-Proton Reactions

| Name         | MT  | Description                                   |
|--------------|-----|-----------------------------------------------|
| <b>pelas</b> | 2   | proton elastic scattering                     |
| <b>p01</b>   | 601 | discrete-level (p,p <sub>1</sub> ) scattering |
| <b>n00</b>   | 50  | discrete-level (p,n <sub>0</sub> )            |
| <b>n01</b>   | 51  | discrete-level (p,n <sub>1</sub> )            |
| <b>p2n</b>   | 16  | (p,2n)                                        |
| <b>pg</b>    | 102 | (p, $\gamma$ )                                |
| <b>pt</b>    | 104 | (p,t)                                         |

**static**, where the cross section and group-to-group matrix are obtained from **nscat**, which is derived from **mt=2** on the ENDF evaluation. (This is scattering for “static” nuclei; energy loss from recoil is included.); and

**thermal**, where the cross section and group-to-group matrix are obtained from one of the thermal reactions in the **ntherm** data type. (The scattering nuclei are in motion with a distribution described by the Maxwell-Boltzmann law; both energy loss and energy gain events are possible.)

The TRANSX code gives the user the choice of static or thermal scattering, and it also allows the user to choose which binding state is desired for a particular moderator material.

The ENDF representation of photoatomic reactions was described in the **GAMINR** chapter. The **gheat** reaction, constructed in **GAMINR**, represents the local heating from atomic recoil and photo-electric electron production. Fluorescence photons from photoelectric interactions are assumed to deposit their energy locally.

**GROUPT** and MATXSR are capable of supporting a new experimental capability for generating nuclide production cross sections. This capability is most useful for radionuclides and isomers, but it is general enough to handle all the possible heavy products of a nuclear reaction. The input GENDF file may contain several different sections that produce a given nuclide. MATXSR adds them up into a single named reaction. The naming convention used for capture reactions is **cZZAAA**, where Z and A are the charge and mass numbers for the nuclide. Isomers are handled by incrementing the first position of the “AAA” field. Products of other reactions are named using the pattern **rZZAAA**, with the same convention used for isomers. The reason that capture products are distinguished from those from other reactions is that the former may have to be self shielded.

Table 21: Thermal Material Names for ENDF/B-VII

| Name  | MT  | Description                                     |
|-------|-----|-------------------------------------------------|
| free  | 221 | free-gas scattering                             |
| h2o   | 222 | H in H <sub>2</sub> O                           |
| poly  | 223 | H in polyethylene (CH <sub>2</sub> ) incoherent |
| poly  | 224 | H in polyethylene (CH <sub>2</sub> ) coherent   |
| hzrh  | 225 | H in ZrH incoherent                             |
| hzrh  | 226 | H in ZrH coherent                               |
| benz  | 227 | Benzene incoherent                              |
| d2o   | 228 | D in D <sub>2</sub> O                           |
| graph | 229 | C in graphite incoherent                        |
| graph | 230 | C in graphite coherent                          |
| be    | 231 | Be metal incoherent                             |
| be    | 232 | Be metal coherent                               |
| bebeo | 233 | Be in BeO incoherent                            |
| bebeo | 234 | Be in BeO coherent                              |
| zrzrh | 235 | Zr in ZrH incoherent                            |
| zrzrh | 236 | Zr in ZrH coherent                              |
| obeo  | 237 | O in BeO incoherent                             |
| obeo  | 238 | O in BeO coherent                               |
| ouo2  | 239 | O in UO <sub>2</sub> incoherent                 |
| ouo2  | 240 | O in UO <sub>2</sub> coherent                   |
| uuo2  | 241 | U in UO <sub>2</sub> incoherent                 |
| uuo2  | 242 | U in UO <sub>2</sub> coherent                   |
| al    | 243 | Al metal incoherent                             |
| al    | 244 | Al metal coherent                               |
| fe    | 245 | Fe metal incoherent                             |
| fe    | 246 | Fe metal coherent                               |

Table 22: Photoatomic Cross Sections

| Name  | MT  | Description                              |
|-------|-----|------------------------------------------|
| gtot0 | 501 | P <sub>0</sub> total                     |
| gwt0  | 501 | P <sub>0</sub> weight function (flux)    |
| gcoh  | 502 | coherent scattering                      |
| ginch | 504 | incoherent scattering                    |
| gpair | 516 | pair production ( $\gamma$ , $2\gamma$ ) |
| gabs  | 522 | photoelectric absorption                 |
| gheat | 525 | heating                                  |

The CCCC standards have always used 6-character Hollerith strings for names. These kinds of names are represented as “REAL\*8” double precision variables on 32-bit machines (IBM, VAX, Sun, *etc.*) and as single-precision variables on 60- to 64-bit machines (CDC, Cray). However, a double-precision variable on a short-word machine can hold 8 characters. So can single-precision

variables on CDC and Cray machines. There do not seem to be any computer systems currently in use that require 6-character words. Therefore, the latest versions of the MATXS format and the MATXSR module have been written to handle 8-character names.

The formal format specification for the MATXS material cross section file follows, using the standard CCCC presentation (except for the ! before the c):

```

!           Standardized CCCC format listing for MATXS file
!c
!c*****
!c           proposed 09/09/77
!c           (modified 09/80)
!c           (nomenclature changed 06/88)
!c           (modified for const sub-blocks 06/90)
!c           (ordering changed 10/90)
!c      c           (bcd format changed 12/21/91)
!c
!cf      matxs
!ce      material cross section file
!c
!cn           this file contains cross section
!cn           vectors and matrices for all
!cn           particles, materials, and reactions;
!cn           delayed neutron spectra by time group;
!cn           and decay heat and photon spectra.
!c
!cn      formats given are for file exchange only
!c
!c*****
!c
!c-----
!cs      file structure
!cs
!cs      record type           present if
!cs      =====
!cs      file identification      always
!cs      file control             always
!cs      set hollerith identification  always
!cs      file data                always
!cs

```

```

!cs ***** (repeat for all particles)
!cs *          group structures          always
!cs *****
!cs
!cs ***** (repeat for all materials)
!cs *          material control          always
!cs *
!cs * ***** (repeat for all submaterials)
!cs * *          vector control          n1db.gt.0
!cs * *
!cs * * ***** (repeat for all vector blocks)
!cs * * *          vector block          n1db.gt.0
!cs * * *****
!cs * *
!cs * * ***** (repeat for all matrix blocks)
!cs * * *          matrix control          n2d.gt.0
!cs * * *
!cs * * * ***** (repeat for all sub-blocks)
!cs * * * *          matrix sub-block          n2d.gt.0
!cs * * * *****
!cs * * *
!cs * * *          constant sub-block          jconst.gt.0
!cs * * *
!cs *****
!c
!c-----
!c
!c
!c-----
!cr          file identification
!c
!cl  hname,(huse(i),i=1,2),ivers
!c
!cw  1+3*mult
!c
!cb  format(4h 0v ,a8,1h*,2a8,1h*,i6)
!c
!cd  hname          hollerith file name - matxs - (a8)
!cd  huse          hollerith user identification (a8)
!cd  ivers          file version number
!cd  mult          double precision parameter
!cd                  1- a8 word is single word

```

```

!cd                2- a8 word is double precision word
!c
!c-----
!c
!c
!c-----
!cr                file control
!c
!cl    npart,ntype,nholl,nmat,maxw,length
!c
!cw    6
!c
!cb    format(6h 1d    ,6i6)
!c
!cd    npart        number of particles for which group
!cd                      structures are given
!cd    ntype        number of data types present in set
!cd    nholl        number of words in set hollerith
!cd                      identification record
!cd    nmat         number of materials on file
!cd    maxw         maximum record size for sub-blocking
!cd    length       length of file
!c
!c-----
!c
!c
!c-----
!cr                set hollerith identification
!c
!cl    (hsetid(i),i=1,nholl)
!c
!cw    nholl*mult
!c
!cb    format(4h 2d /(9a8))
!c
!cd    hsetid        hollerith identification of set (a8)
!cd                      (to be edited out 72 characters per line)
!c
!c-----
!c
!c
!c-----

```



```

!cr      file data
!c
!cl      (hprr(j),j=1,npart),(hrr(k),k=1,nrr),(hrrn(i),i=1,nrrn),
!cl      1(nrrp(j),j=1,npart),(jrrn(k),k=1,nrr),(jrrtp(k),k=1,nrr),
!cl      2(nrrbm(i),i=1,nrrn),(lrrm(i),i=1,nrrn)
!c
!cw      (npart+nrr+nrrn)*mult+2*nrr+npart+2*nrrn
!c
!cb      format(4h 3d ,4x,8a8/(9a8))      hrr,hrr,hrrn
!cb      format(12i6)                      nrrp,jrrn,jrrtp,nrrbm,lrrm
!c
!cd      hrr(j)      hrrrith rrtrification for rrtrrr j
!cd                      n      rrtrrr
!cd                      g      gamma
!cd                      p      rrtrrr
!cd                      d      rrtrrrn
!cd                      t      rrtrrr
!cd                      h      rr-3 rrtrrr
!cd                      a      alpha (rr-4 rrtrrr)
!cd                      b      rrtr
!cd                      r      rrtrrr or rrtrrr
!cd                      (rrtrrr rrtrrr alpha)
!cd      hrr(k)      hrrrith rrtrification for rrtr rrtr k
!cd                      nrrat      rrtrrr rrtrrrrr
!cd                      nr      rrtrrr rrtrrrrr rrtrrrrr rrtrrrrr
!cd                      grrat      gamma rrtrrrrr
!cd                      pr      rrtrrr rrtrrr rrtrrr rrtrrrrr
!cd                      .      .
!cd                      .      .
!cd                      .      .
!cd                      dkn      rrtrrr rrtrrr rrtrrr
!cd                      dkhr      rrtr rrtr and gamma rrtrrr
!cd                      dkb      rrtr rrtr rrtrrr
!cd      hrrn(i)      hrrrith rrtrification for rrtrrrrr i
!cd      nrrp(j)      nrtrrr of rrtrrr rrtrrr for rrtrrr j
!cd      jrrn(k)      rrtrrr of rrtrrrrr rrtrrrrr rrtrrrrr rrtrrrrr
!cd                      rrtrrr rrtr k.  for dk rrtrrr rrtrrr, jrrn is 0.
!cd      jrrtp(k)      rrtrrr of rrtrrrrr rrtrrrrr rrtrrrrr rrtrrrrr
!cd                      rrtrrr rrtrrr k
!cd      nrrbm(i)      nrtrrr of rrtrrrrrrrrrrr for rrtrrrrrrr i
!cd      lrrm(i)      rrtrrrrr of rrtrrrrrrr i
!c

```

```

!c-----
!c
!c
!c-----
!cr          group structure
!c
!cl      (gpb(i),i=1,ngr),emin
!c
!cc      ngr=ngrp(j)
!c
!cw      ngrp(j)+1
!c
!cb      format(4h 4d ,8x,1p,5e12.5/(6e12.5))
!c
!cd      gpb(i)          maximum energy bound for group i for particle j
!cd      emin            minimum energy bound for particle j
!c
!c-----
!c
!c
!c-----
!cr          material control
!c
!cl      hmat,amass,(temp(i),sigz(i),itype(i),n1d(i),n2d(i),
!cl      1locs(i),i=1,nsubm)
!c
!cw      mult+1+6*nsubm
!c
!cb      format(4h 5d ,a8,1p,2e12.5/(2e12.5,5i6))
!c
!cd      hmat            hollerith material identifier
!cd      amass           atomic weight ratio
!cd      temp            ambient temperature or other parameters for
!cd                      submaterial i
!cd      sigz            dilution factor or other parameters for
!cd                      submaterial i
!cd      itype           data type for submaterial i
!cd      n1d             number of vectors for submaterial i
!cd      n2d             number of matrix blocks for submaterial i
!cd      locs            location of submaterial i
!c
!c-----

```

```

!c
!c
!c-----
!cr          vector control
!c
!cl      (hvps(i),i=1,n1d),(nfg(i),i=1,n1d),(nlg(i),i=1,n1d)
!c
!cw      (mult+2)*n1d
!c
!cb      format(4h 6d ,4x,8a8/(9a8))      hvps
!cb      format(12i6)                      iblk,nfg,nlg
!c
!cd      hvps(i)      hollerith identifier of vector
!cd                      nelas      neutron elastic scattering
!cd                      n2n        (n,2n)
!cd                      nnf        second chance fission
!cd                      gabs       gamma absorption
!cd                      p2n        protons in, 2 neutrons out
!cd                      .          .
!cd                      .          .
!cd                      .          .
!cd      nfg(i)      number of first group in band for vector i
!cd      nlg(i)      number of last group in band for vector i
!c
!c-----
!c
!c
!c-----
!cr          vector block
!c
!cl      (vps(i),i=1,kmax)
!c
!cc      kmax=sum over group band for each vector in block j
!c
!cw      kmax
!c
!cb      format(4h 7d ,8x,1p,5e12.5/(6e12.5))
!c
!cd      vps(i)      data for group bands for vectors in block j.
!cd                      block size is determined by taking all the group
!cd                      bands that have a total length less than or equal
!cd                      to maxw.

```

```

!c
!c-----
!c
!c
!c-----
!cr      scattering matrix control
!c
!cl      hmtx,lord,jconst,
!cl      1(jband(1),l=1,noutg(k)),(ijj(1),l=1,noutg(k))
!c
!cw      mult+2+2*noutg(k)
!c
!cb      format(4h 8d ,4x,a8/(12i6))      hmtx,lord,jconst,
!cb                                           jband,ijj
!c
!cd      hmtx      hollerith identification of block
!cd      lord      number of orders present
!cd      jconst     number of groups with constant spectrum
!cd      jband(1)   bandwidth for group 1
!cd      ij(1)      lowest group in band for group 1
!c
!c-----
!c
!c
!c-----
!cr      scattering sub-block
!c
!cl      (scat(k),k=1,kmax)
!c
!cc      kmax=lord times the sum over all jband in the group range of
!cc      this sub-block
!c
!cb      format(4h 9d ,8x,1p,5e12.5/(6e12.5))
!c
!cw      kmax
!c
!cd      scat(k)    matrix data given as bands of elements for initial
!cd                  groups that lead to each final group.  the order
!cd                  of the elements is as follows:  band for p0 of
!cd                  group i, band for p1 of group i, ... , band for p0
!cd                  of group i+1, band for p1 of group i+1, etc.  the
!cd                  groups in each band are given in descending order.

```

```

!cd          the size of each sub-block is determined by the
!cd          total length of a group of bands that is less than
!cd          or equal to maxw.
!cd
!cd          if jconst.gt.0, the contributions from the jconst
!cd          low-energy groups are given separately.
!c
!c-----
!c
!c
!c
!c-----
!cr          constant sub-block
!c
!cl    (spec(l),l=1,noutg(k)),(prod(l),l=l1,ning(k))
!c
!cc    l1=ning(k)-jconst+1
!c
!cw    noutg(k)+jconst
!c
!cb    format(4h10d ,8x,1p,5e12.5/(6e12.5))
!c
!cd    spec          normalized spectrum of final particles for initial
!cd                   particles in groups l1 to ning(k)
!cd    prod          production cross section (e.g., nu*sigf) for
!cd                   initial groups l1 through ning(k)
!cd
!cd          this option is normally used for the energy-independent
!cd          neutron and photon spectra from fission and radiative
!cd          capture usually seen at low energies.
!c
!c-----

```

The MATXS format is intended to communicate multigroup cross sections and matrices for all reaction types, incident particles, and outgoing particles from a nuclear data processing code to applications. It also includes temperature and self-shielding effects, delayed-neutron data, and a limited format for decay heat and delayed photon or particle emission. As shown in the “File Structure” presentation above, the main loop is over material. Materials are subdivided into submaterials, which usually correspond to different data types, temperatures,

and background cross section ( $\sigma_0$ ) values. Each submaterial can contain a series of “Vector Blocks” giving cross section versus energy for one of the allowed group structures and incident particles, and it can contain a series of matrix blocks and subblocks giving the cross sections for group-to-group transfers.

The “File Identification” record is the same for all CCCC files. It gives the Hollerith name for the file (which is always **matxs**), a version number **ivers**, which can be used to distinguish between different libraries in this format, and a Hollerith identification string **huse**, which can be used for entries like “T2 LANL NJOY”.

The “File Control” record contains parameters that are needed to compute the lengths of the following records. The meaning of the various names is well explained in the format specification, and the values of the parameters are obtained from the user’s input. The purpose of **maxw** is to tell application codes how much memory they will need to read through the records on these MATXS files. It is used for both vector blocks and matrix subblocks when deciding how to break them up. The MATXSR value is 5000 words. The code tries to make as many records as possible that have nearly this size in order to minimize the number of I/O operations. The parameter **length** is used to help find the end of the file when appending a new material to an existing file. Its units are left unspecified in the format. It is usually the length in records, in which case record skipping can be used to find the end. Or it could be the length in words on computer systems that allow direct word-addressed I/O operations (this used to be possible using CTSS on Cray computers).

The “Set Hollerith Identification” record comes next. It contains an arbitrary amount of Hollerith text to describe the contents of the library. The description comes from the user’s input.

The “File Data” record contains a number of important arrays that define the structure of data types and the location of materials. The parameter **hprt** contains the standard names for the **npart** particles. The standard names for particles were discussed above. The standard names for the data types and materials (**htype** and **hmatn**) were also discussed above. The next three parameters are used to complete the specification of the data types included in this MATXS library. **ngrp** just gives the number of groups used for each particle type; for example, the traditional Los Alamos  $30 \times 12$  library (with 30 neutron groups and 12 photon groups) would have **ngrp**(1)=30 and **ngrp**(2)=12. Using the same example, the **nscat** data type would have **jinp**(1)=1 and **joutp**(1)=1; the **ng** data type would have **jinp**(2)=1 and **joutp**(2)=2; and the **gscat** data type

would have `jinp(3)=2` and `joutp(3)=2`. The information for these 6 arrays is given in the user's input.

The final two parameters in the "File Data" record are `nsubm` and `locm`. The value of `nsubm` depends on the number of data types, the number of temperatures, and the number of background cross sections found on the input GENDF tapes. The value for `locm(i)` is usually the record index for material `i`. A code can then jump directly to a desired material using record skipping (forward or backward). However, the units for `locm` have been left unspecified to allow direct random access for systems that use word-addressable random-access I/O operations.

The "Group Structure" records give the energy bounds for `npart` group structures. Following the normal convention for application codes, the energy bounds are given in the order of decreasing energy. The numbers are obtained from `mf=1, mt=451` on the GENDF tape. The `GROUPR` module currently uses one group structure for all particles (`n`, `p`,  $\alpha$ , *etc.*), and another for photons ( $\gamma$ ).

Inside the material loop, there is a "Material Control" record for each material. The choice of names for `hmat` was discussed above. The `amass` parameter is the same as the ENDF AWR parameter; that is, it is the ratio of the target mass to the neutron mass. Temperatures `temp` are given in degrees Kelvin, and background cross sections for self-shielding codes (`sigz`, or  $\sigma_0$ ) are given in barns. The parameter `itype` tells which data-type each submaterial belongs to using the data type codes defined by `htype`. Although it is not specified in the format description, the order that MATXSR loops through submaterials is as follows: the outer loop is over data type, the next loop is over temperature, and the innermost loop is over background cross section. The number of cross section vector reactions and matrix reactions for each submaterial are given in `n1d` and `n2d`. Finally, `locs(i)` normally gives the record index for submaterial `i`. A code can search the arrays `temp`, `sigz`, and `itype` for a desired submaterial, and then jump right to the desired submaterial using record skipping. Alternatively, a version that uses word addresses in `locs` could use random-access methods to jump to the desired submaterial.

Each submaterial that contains vectors (`n1d>0`) starts with a "Vector Control" record. This record gives a list of reaction names in `hvps`. MATXSR constructs these reaction names automatically based on the MT number, ENDF "LR flag" (if any), and the incident particle type. Examples of these names were given above. The parameters `nfg` and `nlg` are used to remove unnecessary leading or trailing zeros in reaction cross section vectors. The zeroes are usually

due to thresholds. For example, an  $(n,2n)$  reaction might only have nonzero cross sections for groups 1 through 5 out of an 80-group structure. Storing only the 5-element band will save 75 words on the MATXS file. Even with the zeros removed, the number of words of vector cross section data for a submaterial can be quite large. Therefore, the MATXS format provides a way to break the vector data into a number of vector blocks. The idea is to sum up the bandwidths for each reaction (that is,  $\mathbf{nlg}(i) - \mathbf{nfg}(i) + 1$ ) in order to find the largest number of reactions that will fit within a block of length less than or equal to **maxw**. The data for this block are written to the output file, and then the next group of reactions is found. This continues until all the vector data have been written out as a series of “Vector Block” records with lengths less than **maxw** (5000 words in MATXSR). This method minimizes the number of records on the file while allowing the application codes that read MATXS libraries to allocate space for reading the records economically.

Most submaterials will contain **n2b** “Scattering Matrix Control” records. The convention for the reaction names used in **hmtx** were discussed above. **lord** gives the *number* of Legendre orders present for this reaction; that is, **lord**=4 for a  $P_3$  matrix. Matrices are compacted for efficient storage and data transfer using two techniques. First, unnecessary leading and trailing zeros for group-to-group transfers into a particular final group are removed by banding. **jband**(*i*) gives the number of incident groups in the band for final group *i*, and **ijj**(*i*) gives the group index for the lowest-energy group (highest group index) in the band for group *i*. For example, consider an isotropic  $(n,2n)$  reaction with a threshold in group 3 of a 30-group structure. The values for **jband** and **ijj** for group 20 might well be 3 and 3, respectively. That is, groups 1 through 3 scatter into group 20. The order of storage for this matrix would be as follows:

| Band | Element | jband | ijj |
|------|---------|-------|-----|
| 1    | 1→1     | 1     | 1   |
| 2    | 2→2     | 2     | 2   |
|      | 1→2     |       |     |
| 3    | 3→3     | 3     | 3   |
|      | 2→3     |       |     |
|      | 1→3     |       |     |
| 4    | 3→4     | 3     | 3   |
|      | 2→4     |       |     |
|      | 1→4     |       |     |
| ...  | ...     |       |     |



Note that this scheme is more efficient than the similar one used for the CCCC ISOTXS file, because that method required that the ingroup element had to be included in the band. For anisotropic matrices, the `lord` Legendre components are stored with the source-group elements. Thus, there are `lord(i)*jband(i)` elements in each band, and they are stored in the following order (assuming a  $P_1$  matrix):

| Band | Element | Order | jband | ijj |
|------|---------|-------|-------|-----|
| 1    | 1→1     | 0     | 1     | 1   |
|      | 1→1     | 1     |       |     |
| 2    | 2→2     | 0     | 2     | 2   |
|      | 1→2     | 0     |       |     |
|      | 2→2     | 1     |       |     |
|      | 1→2     | 1     |       |     |
|      | 2→2     | 1     |       |     |
| 3    | 3→3     | 0     | 3     | 3   |
|      | 2→3     | 0     |       |     |
|      | 1→3     | 0     |       |     |
|      | 3→3     | 1     |       |     |
| ...  | ...     |       |       |     |

This kind of matrix block can be subdivided into subblocks using a method similar to the one described above for vector cross sections. The code starts summing the product of `jband` and `lord` for the final energy groups until the data for the next band will cause the sum to exceed `maxw` (5000 words in MATXSR). These data are then written out as a matrix subblock. The code then repeats the process for the rest of the group ranges. The result is a minimal number of “Scattering Sub-Blocks,” none of which has a size larger than the file limit.

The second method used to compact scattering matrices is based on the observation that the shape of the outgoing neutron or photon spectrum from fission and radiative capture reactions tends to be independent of energy at low neutron energies. `GROUPE` determines the group where significant energy dependence begins. Below this point, it computes a single spectrum to describe the outgoing neutron or photon distribution and a production cross section to go with it. At high energies, it produces a group-to-group matrix. This method can lead to appreciable reductions in storage requirements. For example, consider the 187-group structure, which has many low-energy groups. The fission spectrum for  $^{235}\text{U}$  doesn’t begin to show significant energy dependence until an energy of about 9 keV. This means that there are 118 constant groups. A  $187 \times 187$  matrix is thereby reduced to a  $187 \times 69$  matrix, and 187-group vector,

and a 118-group vector — a 62 % reduction in storage requirements. Even larger reductions in size are obtained in more favorable cases. The parameter `jconst` gives the number of low-energy groups having a constant spectrum. If `jconst`>0, a single “Constant Sub-Block” record will be given after the regular “Scattering Sub-Block” records. This record will contain the spectrum `spec` and the production cross section `prod` needed to reconstruct the low-energy part of the full matrix. In mathematical form,

$$\sigma_{x,g \rightarrow g'} = \chi_{g'}^{LE} \sigma_{Px,g}^{LE} + \sigma_{x,g \rightarrow g'}^{HE} , \quad (471)$$

where LE stands for low energy, HE stands for high energy,  $\chi^{LE}$  is the constant spectrum,  $\sigma_{Px}^{LE}$  is the production cross section for reaction  $x$ , and  $\sigma^{HE}$  is the normal group-to-group matrix.

### 15.3 Historical Notes

The original version of the MATXS specification was constructed in September, 1977. The “Matrix Control” record in this original version contained the names and banding parameters for every group of every reaction. As a result, the record could become very large for libraries with many groups. The MATXS format was modified in September of 1980 to have a different “Matrix Control” record for each reaction. For several years following this date, NJOY contained both MATXSR and NMATXS modules, and two different versions of TRANSX were in use. All traces of the original version of the format have now disappeared.

Changes beginning in the late 1980’s were introduced to make MATXSR able to handle data types with either incoming or outgoing charged particles. Actually, the format wasn’t changed. The particle, data type, and reaction name conventions described in Tables 12 – 22 were chosen, and these new names required some corresponding changes in the code. The TRANSX code also had to be modified to recognize the new names and to work with multiparticle coupled sets.

The concept of using constant subblocks to reduce the size of GENDF and MATXS files is actually quite old. Various versions of updates to install the scheme were written over about a 5-year period. It was finally decided to permanently install the scheme in June of 1990. The changes required to [GROUPR](#), [DTFR](#), [CCCCR](#), [MATXSR](#), [POWR](#), and [WIMSR](#). In addition, TRANSX had to be

changed to accept the new constant subblocks. Unfortunately, this change was large enough to impact all MATXS users.

If many users were to be impacted, other nagging problems with the code could also be corrected at that time. With the original format, it was always very difficult to add, replace, or extract a material. The data type loop was outside the material loop, and the pieces for a given material were scattered throughout the file. Therefore, the ordering of the file was changed to put the data type loop inside the material loop along with the other submaterials. With this change, it was easy to rewrite the BBC library maintenance code from the TRANSX package to be able to insert a new material at any point in the library. It was also easy to give BBC the capability of extracting a short library containing only selected materials from a large MATXS library. Using the short library can significantly speed up TRANSX runs to prepare data for reactor design problems. The only disadvantage of the new ordering is that identical photoatomic data blocks have to be given for each isotope of an element. However, these data are not too bulky, and the additional overhead is manageable. This arrangement might make it easier to add photonuclear data in the future.

Finally, the current scheme of dividing the vector and matrix data into subblocks was added. The goal was to keep the record size below some fairly large maximum value (5000 words is currently being used). This kind of limit makes it easier to design application codes that make efficient use of memory. In addition, using as few records as possible reduces the number of I/O operations needed for a trip through the library, thereby improving execution time. The new subblocking scheme is also very simple.

## 15.4 MATXS Libraries

The normal process for preparing a MATXS library using NJOY starts with a series of runs to prepare PENDF tapes for each of the materials of interest. For incident neutrons, these PENDF runs normally involve running the modules [RECONR](#), [BROADR](#), [UNRESR](#), [HEATR](#), and [THERMR](#). For incident photons and charged particles, only [RECONR](#) is needed. The next step is to run [GROUPE](#) for each material and incident particle. Each [GROUPE](#) run can produce data for all outgoing particles and for photons. As an example, consider the problem of producing data for a coupled neutron-photon-proton library. [GROUPE](#) would be run using the ENDF-6 incident-neutron data and requesting `mfd` values of 3 (cross sections), 6 (neutron matrices,  $nn$ ), 16 (photon

production matrices,  $n\gamma$ ), and 21 (proton production matrices,  $np$ ). **GAMINR** would be run to produce the photoatomic cross sections and  $\gamma\gamma$  matrices. **GROUPE** can be used to produce  $\gamma n$  and  $\gamma p$  matrices. **GROUPE** would be run again for the ENDF-6 format proton sublibrary, requesting **mf** values of 3 (cross sections), 6 (neutron production,  $pn$ ), 16 (photon production,  $p\gamma$ ), and 21 (proton scattering and production,  $pp$ ).

Once all the GENDF fragments from all these **GROUPE** and **GAMINR** runs are available, they can be merged into multimaterial GENDF tapes using **MODER**. For the example above, three multimaterial GENDF tapes should be prepared: one for incident neutrons, one for incident photons, and one for incident protons. The input description in the following section shows how the unit numbers for these three GENDF files are given to MATXSR.

When the MATXSR run is made, the code scans through all the input GENDF tapes searching for the specified materials. For each material, it extracts all the data types requested in the MATXSR input and appearing on the input tapes. In addition, it extracts every temperature,  $\sigma_0$  value, reaction, and Legendre order found on the input tapes. The following paragraphs describe various special features of the formatting process.

**Normal Neutron and Photon Data.** Normal, infinitely dilute cross sections and group-to-group matrices for neutron reactions, photon production, and photonuclear reactions are read from the input tapes and stored in the MATXS file using the formats described above. Almost all partial reactions are kept. Reaction names are constructed automatically; a number of examples were given above in Tables 14 – 22. The total cross section and weighting flux from **GROUPE** are given in the section **mf**=3, **mt**=1 with both  $P_0$  and  $P_1$  components. All four vectors are written to the MATXS file. A similar treatment is used for **mt**=501 in the photoatomic case, except that only  $P_0$  terms are saved.

The treatment of fission is also special. ENDF libraries sometimes use only **mt**=18, the total fission reaction, for both cross section and emission spectrum data; sometimes the partial fission cross sections  $(n,f)$ ,  $(n,n'f)$ ,  $(n,2nf)$ , and  $(n,3nf)$  are also given in File 3 (**mt**=19, 20, 21, and 38); and sometimes the partial reactions are also used to describe the neutron emission matrix. If the last case is found, the **mt**=18 matrix may not be complete above the threshold for second-chance fission, and it should be ignored. Normally, it would not be processed in **GROUPE**, but just in case, MATXSR will ignore it. Delayed-neutron spectra processed in **GROUPE** are written into the section labeled **mf**=5, **mt**=455 on

the GENDF tape, and this section includes data for all time groups. MATXSR adds up these separate time-group spectra to produce a single delayed-neutron spectrum for the MATXS vector data blocks. Application codes can use the fission data in the MATXS library to construct steady-state fission vectors as follows:

$$\bar{\nu}_g^{SS} = \frac{\sum_{g'} \sigma_{fg \rightarrow g'}^{HE} + \sigma_{Pfg}^{LE} + \bar{\nu}_g^D \sigma_{fg}}{\sigma_{fg}} , \quad (472)$$

where  $\sigma^{HE}$  is the matrix part of the prompt fission reaction,  $\sigma_{Pfg}^{LE}$  is the low-energy production cross section for fission neutrons,  $\bar{\nu}^D$  is the total delayed-neutron yield, and  $\sigma_{fg}$  is the fission cross section. If partial fission matrices are available, the first two terms in the denominator would also have to be summed over the reactions present. Continuing,

$$\chi_{g'}^{SS} = \frac{\sum_g \sigma_{fg \rightarrow g'}^{HE} \phi_g + \chi_{g'}^{LE} \sum_g \sigma_{Pfg}^{LE} \phi_g + \chi_{g'}^D \sum_g \bar{\nu}_g^D \sigma_{fg} \phi_g}{\text{NORM}} , \quad (473)$$

where  $\chi^{LE}$  is the constant-spectrum part of the fission reaction,  $\chi^D$  is the total delayed-neutron spectrum, and NORM is the quantity that normalizes  $\chi^{SS}$ , namely, the sum of the numerator over all  $g'$ . The weighting flux  $\phi_g$  would normally be problem- and region-dependent in the application code.

**Self-Shielding Data.** If higher temperatures and  $\sigma_0$  values are found on the input GENDF file, MATXSR automatically prepares submaterials for them. This self-shielding information can be used by application codes to prepare effective cross sections for mixtures of materials in various geometrical arrangements using equivalence theory. This approach is often called the Bondarenko method[38].

As discussed in more detail in the [GROUPR](#) section of this report, this system is based on using a model flux for isotope  $i$  of the form

$$\phi_\ell^i(E, T) = \frac{C(E)}{[\sigma_0^i + \sigma_t^i(E, T)]^{\ell+1}} , \quad (474)$$

where  $C(E)$  is a smooth weighting flux,  $\sigma_t^i(E, T)$  is the total cross section for material  $i$  at temperature  $T$ ,  $\ell$  is the Legendre order, and  $\sigma_0^i$  is a parameter that

can be used to account for the presence of other materials and the possibility of escape from the absorbing region (heterogeneity). **GROU**PR uses this model flux to calculate effective multigroup cross sections for the resonance-region reactions (total, elastic, fission, capture) for several values of  $\sigma_0$  and several values of  $T$ .

When  $\sigma_0$  is large with respect to the highest peaks in  $\sigma_t$ , the flux is essentially proportional to  $C(E)$ . This is called infinite dilution, and the corresponding cross sections are appropriate for an absorber in a dilute mixture or for a very thin sample of the absorber. As  $\sigma_0$  decreases, the flux  $\phi(E)$  develops dips where  $\sigma_t$  has peaks. These dips cancel out part of the effect of the corresponding peaks in the resonance cross sections, thereby reducing, or self-shielding the reaction rate. In the MATXS format, these effects are represented by differences instead of the f-factors used in earlier formats (see the description of the BRKOXS file in the **CCCCR** section of this report). That is, the submaterial corresponding to temperature  $T$  and background cross section  $\sigma_0$  contains the differences between the cross sections found on the GENDF tape for those parameters and the infinitely dilute values found in the first submaterial (normally,  $T=300\text{K}$  and  $\sigma_0=1\times 10^{10}\text{barns}$ ).

This approach has two advantages. First, data for groups with no self-shielding are automatically removed from MATXS vectors and matrices by the banding process without having to violate the principle of *generalization* and define a special format for neglecting values of “1.0” instead of values of “0.0.” Second, effective cross sections can be accumulated by simply adding the self-shielding effects multiplied by appropriate interpolation weights to an accumulating sum that starts out equal to the infinitely dilute cross section. With f-factors, it is necessary to save the infinitely dilute cross sections during each step so that they can be multiplied by the f-factors. Thus, using differences is more economical in coding and in storage space requirements. The TRANSX code makes good use of this feature.

**Thermal Data.** ENDF-6 thermal data comes from a thermal sublibrary. In this sublibrary, the various material configurations are handled as separate materials. However, after the ENDF data have been processed by the **THERMR** module, the different thermal materials are handled as reactions. Table 21 gives the correspondence between the special NJOY thermal MT numbers and the actual thermal materials. These are the names that work for ENDF/B-VII[6]. If MATXSR is used for ENDF/B-VII (or earlier) materials, the name for BeO will be slightly wrong, but it could be fixed by hand editing of the MATXS file.

Each of these thermal reactions corresponds to a particular dominant material. For example,  $\text{mt}=222$  gives the thermal cross section for hydrogen bound in water. It will only appear in the material H1 in a MATXS library. Similarly,  $\text{mt}=223\text{--}227$  will only appear in  $^1\text{H}$ ,  $\text{mt}=228$  will only appear in  $^2\text{H}$ ,  $\text{mt}=229\text{--}230$  will only appear in  $^{nat}\text{C}$ ,  $\text{mt}=231\text{--}234$  will only appear in  $^9\text{Be}$ , and  $\text{mt}=235\text{--}236$  will only appear in  $^{nat}\text{Zr}$ . Free-gas scattering ( $\text{mt}=221$ ) will appear in all materials.

Many of these materials describe the scattering from one atom of a compound bound in that compound; for example, H in  $\text{H}_2\text{O}$ , D in  $\text{D}_2\text{O}$ , or Zr in  $\text{ZrH}$ . The application code using this data is expected to add on the effects of scattering from the other atoms of the compound. For water, the scattering from free oxygen is added to the “H in  $\text{H}_2\text{O}$ ” scattering. For zirconium, the scattering for “H in  $\text{ZrH}$ ” is added to the scattering from “Zr in  $\text{ZrH}$ ”. There are two exceptions in the existing ENDF/B evaluations. The benzene data set contains the entire scattering from the  $\text{C}_6\text{H}_6$  molecule normalized to the hydrogen cross section. Therefore, if an application code specifies H1 with the benzene scattering option and the correct density for H1 in the system, the result will contain all of the benzene scattering effect. No additional scattering is to be added for the carbon atoms. Similarly, BeO contains all the scattering from the compound normalized to the beryllium cross section. Check the [THERMR](#) section of this report for more information.

Six of these materials have names ending with \$. These reactions represent coherent elastic scattering from crystalline powdered materials (C, Be, BeO) or incoherent elastic scattering from solids containing hydrogen (polyethylene,  $\text{ZrH}$ ). These reactions contain ingroup elements only in the scattering matrices; that is, they cause angular redistribution without energy loss in scattering. Each \$ reaction should be added to the corresponding inelastic reaction by the application code. This part of the scattering can lead to difficulties with transport corrections in discrete-ordinates transport codes.

The final unique aspects of the thermal data are that the matrices show upscatter, and they are only defined below some maximum energy. The energy range aspect is easily handled by the banding method used to reduce the size of the vector blocks. The upscatter aspect is handled by **jband** and **ijj**. The order of storage for a simple thermal case with only 2 upscatter groups would be as follows:

| Band | Element | jband | ijj |
|------|---------|-------|-----|
| ...  | ...     |       |     |
| 27   | 27→27   | 2     | 27  |
|      | 26→27   |       |     |
| 28   | 29→28   | 3     | 29  |
|      | 28→28   |       |     |
|      | 27→28   |       |     |
| 29   | 30→29   | 3     | 30  |
|      | 29→29   |       |     |
|      | 28→29   |       |     |
| 30   | 30→30   | 2     | 30  |
|      | 29→30   |       |     |

**Charged-Particle Data.** The treatment of data for incident charged particles is very similar to that used for neutron data, except for charged-particle elastic scattering. The elastic channel has contributions from Coulomb scattering that become infinite as the scattering angle goes to zero. In nature, this singularity is removed by electronic screening, but some other approach is needed for a data set that concentrates on isolated nuclear reactions. The approach selected is used in some existing applications. The elastic scattering distribution is broken up into two parts: (1) a normal angular distribution for angles from some low cutoff, say 20°, back to 180°, and (2) a straight-ahead continuous slowing-down contribution to represent the effects of angles below the cutoff. The continuous slowing-down part is closely related to the normal “stopping power” for charged particles. The large-angle part can be converted into a normal scattering matrix (see the discussion of charged-particle elastic scattering in the [GROUPR](#) chapter of this manual for more details).

Discrete-ordinates transport codes can often be modified to handle charged-particle data in this form, but they require an effective total cross section. The ENDF-6 format for charged-particle data does not define a total cross section because of the singularity in the elastic contribution. However, for application purposes, a reasonable definition of an effective total cross section is that it is the sum of all the partial reaction cross sections including the cross section obtained for the truncated elastic scattering reaction. This is the method that MATXSR uses to compute the quantities `ptot0`, `dtot0`, `ttot0`, *etc.*



**Delayed-Neutron Data.** Delayed-neutron yields, spectra, and decay constants by time group are required by reactor kinetics codes. The previous CCCC format for these data was DLAYXS (see the CCCCCR chapter of this manual). Because of the generalization inherent in the MATXS format, these data can be added without any changes in the structure of the file. This option has not yet been added to MATXS<sub>R</sub>, and the procedures used will be described in a future version of this report.

**Decay-Photon and Decay-Heat Data.** Many nuclear reactions leave radioactive products. These products may be simple daughter isotopes that decay in a few steps to a stable final state with the emission of a few photons and electrons (or heat), or they may be a complex array of fission product isotopes that emit a complex spectrum of photons and electrons (or heat) showing many time constants. Procedures to store these data in MATXS libraries will be included in a future version of this report.

## 15.5 User Input

The user input specifications below were copied from the comment cards at the beginning of the MATXS<sub>R</sub> module. It is always a good idea to check the comment cards in the current version of the code for possible changes.

```
!---input specifications (free format)-----
!
! card 1 units
!   ngen1      input unit for data from groupr
!   ngen2      input unit for data from gaminr
!   nmatx      output unit for matxs
!   ngen3      incident proton data from groupr (default=0)
!   ngen4      incident deuteron data from groupr (default=0)
!   ngen5      incident triton data from groupr (default=0)
!   ngen6      incident he3 data from groupr (default=0)
!   ngen7      incident alpha data from groupr (default=0)
! card 2 user identification
!   ivers      file version number (default=0)
!   huse       user id (up to 16 characters, delimited by ',
!              ended by /) (default=blank)
! card 3 file control
!   npart      number of particles for which group
!              structures are given
```

```

!   ntype      number of data types in set
!   nholl      number of cards to be read for hollerith
!               identification record.
!   nmat       number of materials desired
! card 4 set hollerith identification
!   hsetid     hollerith identification of set
!               (each line can be up to 72 characters,
!               delimited with ', ended by /)
! card 5 particle identifiers
!   hpart      hollerith identifiers for particles
!               (up to 8 characters each)
! card 6 energy groups
!   ngrp       number of groups for each particle
! card 7 data type identifiers
!   htype      hollerith identifiers for data types
!               (up to 8 characters each)
! card 8 input particle ids
!   jinp       input particle id for each data type
! card 9 output particle ids
!   joutp      output particle id for each data type
! card 10 material data (one card per material)
!   hmat       hollerith material identifier
!               (up to 8 characters each)
!   matno      integer material identifier
!               (endf mat number)
!   matgg      mat number for photoatomic data
!               (default=100*(matno/100) as in endf-6)
!
!-----

```

Card 1 is used to specify the units for the input GENDF tapes and the output MATXS library. As usual, the sign of a GENDF unit number is used to determine its mode; negative numbers mean binary, and positive numbers mean coded (*i.e.*, ASCII). The output file is always binary, and its sign is ignored. The most common MATXSR runs are for neutron and photon data only. In these cases, card 1 can be truncated after the **nmatx**. If incident charged-particle GENDF files are available, any of the units **ngen3** through **ngen7** can be assigned.

Card 2 is used to control the MATXSR print option **iprint** and to provide the information for the MATXS “User Identification” record. An example for

Card 2 follows:

```
0 17 'T2 LANL NJOY'/'
```

Card 3 is used to input the counts for the “File Control” record and to tell the user input routine how many quantities to read in subsequent input cards. Card 4 is repeated `nho11` times to give the Hollerith description for the library. Each line must be delimited by quote characters and terminated by `/`. For example,

```
' MATXS17                                27 FEB 91 '/
' 69-GROUP THERMAL LIBRARY FROM ENDF/B-VI      '/
'   THIS LIBRARY INCLUDES NEUTRON, PHOTON, AND  '/
'   THERMAL SCATTERING DATA FOR 133 MATERIALS.  '/
```

The lines are written out on the MATXS file as given, except that the maximum length for each line is 72 characters.

Card 5 is used to read in the Hollerith names for the `npart` particles for this library. The standard names for the particles were given above in Table 12. The number of groups desired for each particle are given on card 6. The data-type names (see Table 13) are given on Card 7. Cards 8 and 9 are used to specify the input and output particles for each data type. The user should take care that the number of groups given for each particle is consistent with the input data, and that the particle assignments to data type names (`jinp` and `joutp`) are consistent with the names. The code does not check.

Card 10 is repeated `nmat` times to specify the materials to be written out on the library. The rules for constructing the material names `hmat` were given in Section 15.2. The `matno` parameter is the ENDF MAT number for this material as used on the input GENDF files. For ENDF/B-VI, the MAT number is the same for all sublibraries (that is, for incident neutrons, photons, protons, *etc.*), and only one value is needed to specify the desired material. However, photoatomic data are atomic in character, and the MAT numbers always refer to the element. For example, `MAT=2600` for the photoatomic data of iron. **MATXSR** reads a second MAT number field, `matgg`, for the photoatomic data. Its default value is given by

```
100*(MATNO/100)
```

and it is, therefore, not usually needed. The normal form for card 10 would be as follows:

```
FE56 2631/
```

However, the photoatomic libraries for earlier versions of the ENDF/B files used MAT numbers like 26 for elements. The `matgg` parameter can be used to process data from these older libraries. Note that delimiting quote characters are not required for Hollerith names that are single words and start with a letter.

MATXSR always processes all submaterials found on all the nonzero GENDF units `ngen1` through `ngen7`. It processes every temperature and  $\sigma_0$  value found. It processes (almost) every reaction cross section and matrix found, and it processes every Legendre order given. The only way to control the contents of the MATXS library is through the input to `GROUPE` or `GAMINR` and by the materials included when building the input GENDF files. A convenient way to handle this task is to assemble the results of a number of single-material `GROUPE` runs into composite GENDF tapes using `MODER`.

## 15.6 Coding Details

Subroutine `matxsr` is the only public call for module `matxsm`. The module has a number of global variables and arrays defined. One key set of variables and arrays provides the area for accumulating the MATXS data. It provides a set of equivalenced arrays so that integers, reals, and Hollerith strings can all be stored in the same binary records. It sets up both integers and reals to be 4-byte quantities. Hollerith words (with up to 8 characters each) are 8-byte quantities. The CCCC `mult` value is set to 2. See `a(200000)`, `ia(200000)`, and `ha(100000)`. The parameter `isiza=200000` defines the size of these equivalenced arrays in 4-byte units.

The internal representation for all the elements of the MATXS file and for GENDF data uses 8-byte quantities.

The next step in subroutine `matxsr` is to read in the unit numbers for the input and output files and to open the files. Note that the sign for `nmatx` is

ignored. It will always be binary. Several binary scratch files are also opened. Next, the user input for the “File Identification” record is read (see card 2 in the user input description), and the `cmatxs` routine is called to read the input GENDF files and construct the output MATXS file. When `cmatxs` returns, the main routine closes the units, prints its final timer line, and returns to the NJOY program.

Subroutine `cmatxs` starts by defining three constants:

`nsubmx=100` is the maximum number of submaterials allowed for a material, including data types, temperatures, and background cross sections;  
`maxord=5` is the maximum Legendre order (that is,  $P_5$  allowed for group-to-group matrices; and  
`maxw=5000` is the maximum size for vector block and matrix subblock records on the MATXS file.

It continues by calling `ruinm` to read the user’s input. Some of the quantities read by `ruinm` are stored directly into `ia`, `a`, and `ha` using pointers like `icont` and `iholl`. Note the use of `mult=2` to compute the jump in the index when Hollerith items are stored, and note the the variable `next` keeps track of the current location in the MATXS equivalenced arrays. Subroutine `ruinm` returns to `cmatxs` after loading the “File Data” record.

The next step is to call subroutine `mtxdat` to read the input GENDF data and write it to the scratch tapes used later in this subroutine. The first step is to set up an area at pointer `igrup` for the `npart` group structures and to calculate its length. Note that the number of words reserved is forced to be even in order to avoid possible word-alignment problems for these 4-byte words. With the current version of `GROUPR`, all particles are assumed to use the same group structure. Photons have a different one. It is only necessary to look through the unit numbers from input card 1 and find the first one that contains data. The group structures are then read in from `mf=1,mt=451` and reversed to have the conventional decreasing-energy order. The subroutine now reserves space for the “Material Control” record starting at `imatc` with length `nwmc` and begins the material loop (see `do 700 im=1,nmat`). Note how the Hollerith material name is loaded into the “Material Control” record storage area by making use of the `mult` parameter and the equivalence between the arrays `a` and `ha`.

The first loop inside the material loop is the data-type loop (see `do 600 i=1, ntype`). The same MAT number is used for all particles, but a different one is used for photoatomic data. The input unit to be used depends on the identity

of the incident particle. Since these comparisons use constants like `hprot` with values like “6hp,” it is important to use the standard names in the user input (see Table 12). The identity of the outgoing particle for the data type determines the MF number for the matrices on the GENDF tape, `mfm`. As described in the [GROUPE](#) section of this report, the MF assignments are as follows:

| MF value | Outgoing Particle         |
|----------|---------------------------|
| 6        | neutrons                  |
| 16       | photons                   |
| 21       | protons                   |
| 22       | deuterons                 |
| 23       | tritons                   |
| 24       | <sup>3</sup> He particles |
| 25       | alphas                    |
| 26       | photoatomic data          |

The MF number for the vector data (`mfv`) is 3, except for the photoatomic case, where it is 23.

The next step is to search for the desired material `imat` on the current input tape. When the first occurrence of `imat` has been found, `mtxdat` reads in its head record, and then it sets up a loop over all the temperatures for this material (the loop goes through statement number 300). As it reads through each temperature, it copies the results to scratch file `nscr`. The data for the first temperature is also copied to scratch file `iref`. File `iref` will be used for the higher temperature and  $\sigma_0$  values to calculate the delta-sigma values. While the data are being copied, `mtxdat` counts the number of one-dimensional reactions, `noned`, and the number of two-dimensional reactions, `ntwod`, for each value of the background cross section,  $\sigma_0$ . When the scratch tapes are complete, the subroutine starts a loop over  $\sigma_0$  for this material and temperature; it calls `vector` to produce the vector cross sections, it calls `matrix` to produce the matrix cross sections, and it loads the information on this submaterial into the “Material Control” record. When the  $\sigma_0$  loop is complete, the code jumps back to statement number 300 to get the next temperature. When all the temperatures have been processed, it reaches statement number 600 and goes back through the entire process again for the next data type. When the “do 600” loop exits, the entire “Material Control” block has been filled in, and the subroutine writes the record to scratch file `nscrt6`.

At this point, the processing for material `imat` is complete. The “do 700” loop continues until all the requested materials have been found and processed.

Subroutine **findg** is used to search GENDF file **ntape** for a specified section (**mat**, **mf**, **mt**). If it does not find the requested section, a fatal error message is issued. Materials (**mat**) do not have to be in order on a GENDF tape. Therefore, this routine simply reads forward until it comes to the first record matching the requested **mat**, **mf**, and **mt** values. If the section is not found, it rewinds once and searches again. When the section is found, it backspaces by one record so that the next record read will be the desired record.

Subroutine **hname** is used to construct a Hollerith reaction name **hreact** from an ENDF MT number (**mt**), an ENDF “LR flag” (**lr**), and an incident particle name (**hp**). The definitions of the names were discussed above in connection with Tables 14–22, and the actual MT numbers and strings used are given in parameter arrays in this subroutine. If no preset name is found for an MT number, a default name of the form **MTnnn** is constructed.

Subroutine **vector** reads the cross section vectors for one submaterial (that is, one data type, one temperature, and one  $\sigma_0$ ). It starts by clearing some flags that are used to detect the occurrence of particular reactions. For example, **k107** is set if the  $(n,\alpha)$  reaction (**mt**=107) is found. Pointers are assigned for the vector control and vector data arrays (see **ivcon**, **ivdat**). Note that there must be enough container memory available to hold all the vector data (**ning**\***nld** words). The routine now starts up a loop over sections on the input scratch tape (the loop goes through statement number 115). The sections that it processes are determined by the value of **mf**, which will be 3, except for photoatomic data, when it will be 23. Delayed fission  $\chi$  is a special case; it will be found in the section with an MT value of **mf**+2. As each interesting section is found, the Hollerith name for the reaction is constructed, and the location of the reaction relative to **ivdat** is computed. When the total cross section is found (**mt**=1), names and locations are set up for the  $P_\ell$  components of the weight function (for example, **nwt0** and **nwt1**) and for the  $P_\ell$  components of the total cross section (**ntot0** and **ntot1**). If appropriate, the first letter of these names might be **p**, **d**, *etc.*, depending on the incident particle. When the total photoatomic cross section is found (**mt**=501), names and locations are defined for the  $\gamma$  weight and the  $P_0$  cross section (**gwt0** and **gtot0**). When the charged-particle elastic cross section is found for particle **x** (**mt**=2), names and locations are set up for the weight function **xwt0** and the effective charged-particle total cross section **xtot0**. Once the name and location have been selected, the code reads the data for all groups from file **nscr** and stores them at the selected location. If this submaterial corresponds to a higher temperature or  $\sigma_0$ , the corresponding data

is also read from file `iref` and subtracted from the `nscr` data. As a result, self-shielding information in the MATXS file is given as differences rather than f-factors as in the previous CCCC self-shielding file, BRKOXS. The delayed-neutron spectra are read from `mf=5`, `mt=455`; the spectra from the time groups on the GENDF tape are added to obtain a single spectrum  $\chi_d$ .

There is a special feature in `vector` for incident charged-particle reactions. Although discrete-ordinates transport codes require a total cross section, it is not actually possible to compute a total cross section for charged-particle reactions because Coulomb scattering is singular for straight-ahead scattering (at least in the absence of electronic screening). The solution to this problem used by `GROUPE` is to exclude a range of forward angles from the charged-particle elastic matrix (this angular range is handled by continuous-slowing-down theory in the application codes). Therefore, MATXSR can construct an effective total cross section by adding all the reaction cross sections found to this truncated elastic cross section. However, it must be careful to watch for possibly redundant cross sections that must be omitted from the sum; for example, if the total  $(x,p)$  cross section (`mt=103`) is present for incident particle  $x$ , the discrete-level  $(x,p_n)$  cross sections and the  $(x,p)$  continuum reactions (`mt=600-649`) must be omitted from the sum. This is the function of flags like `k103`.

There is another special feature for nuclide production data. When using this experimental ENDF format, there may be a number of different sections on the GENDF file producing the same product. These separate contributions are added up into one single production cross section in the block of coding starting at statement number 410.

When all the reactions have been entered, subroutine `vector` thins the vector data just loaded by removing unneeded leading or trailing zeros (actually, numbers less than `small=1.e-30`) from each reaction. These zeros can arise from thresholds and upper limits for thermal-range reactions. In addition, since data for the higher temperatures and  $\sigma_0$  values are stored as differences, zero (or very small) elements can imply that there is no significant temperature or  $\sigma_0$  dependence. The subroutine simply steps through the `ivdat` data block to find the band limits `nfg` and `nlg` for each reaction, to squeeze out the zeros, and to record the band limits in the vector control block at `ivcon`. When all of the `n1d` reactions have been processed, the resulting vector data is written out as a series of “Vector Block” records on scratch tape `nscr3`. The subblocking is controlled by `maxw` (5000 words). The code just steps through the cross section bands until the next reaction will cause the sum to exceed `maxw`. It then writes



these reactions to the scratch file, and it repeats the process for the next group of reactions. Each record will have fewer than **maxw** words, and the minimum number of records will be produced within the restriction that no reaction is broken up between records. The last step in the subroutine is to write the “Vector Control” record for this submaterial to scratch file **nsct2**.

Subroutine **matrix** reads the group-to-group matrix data for this submaterial, converts it to MATXS format, and writes the results to a scratch file. The pointer **imcon** is used to accumulate matrix control information, pointer **icdat** is used for the low-energy constant spectrum data (if any), **ijg11** is used for banding information, and pointer **imdat** for the actual matrix data. The main loop is over the **n2d** matrix reaction types. The head card for the reaction is read in from **nsct**, and for higher temperatures and  $\sigma_0$  values, from **iref** also. Subroutine **hname** is called to construct the Hollerith reaction name, subroutine **band** is called to read through the data and determine the banding parameters used to remove excess zero elements, and subroutine **shuf1** is called to read through the input scratch file again and load the data into memory in its final compact form.

Subroutine **band** is fairly simple. It loops over all the groups for this reaction on **nsct** and/or **iref**. When the loop is finished, **jg1lo(i)** and **jg1hi(e)** contain lowest and highest initial-group indices found for each final group **i**. Note that the actual cross section for a matrix element (or the cross section difference when **iref** is being used) is not checked; it is assumed that **GROUPR** has done a good job removing excess zeros. This should be improved in a future version. Before returning, these limiting group indices are used to compute the MATXS parameters **jband** and **ijj**, and to insert them into the accumulating matrix control block at pointer **imcon**.

Subroutine **shuf1** starts by initializing a loop through statement number 100 that will be used to produce “Matrix Sub-Block” records. Inside this loop, the code sums the bandwidths found by **band** to find out how many final-energy group bands can fit in a subblock with length less than or equal to **maxw** words. The result is a pair of group indices **i0** and **imax** that define the range of groups to be included in the subblock. Subroutine **shuf1** now makes a pass through scratch file **nsct**, and also through scratch file **iref** for higher temperatures and  $\sigma_0$  values. It stores away the constant subblock data (**ig=0** for the constant spectrum and **ig21o=0** for the production cross section), if found. For each group-to-group element, it computes the final group index **jg2**. If the group is in the allowed range for this subblock, it computes the output location **no1oc**

and stores the element in memory. For higher temperatures and  $\sigma_0$  values, it subtracts the base value found on file `iref`. (This step is normally needed for neutron elastic scattering only.) When the group loops for `nscr` and `iref` are complete, the subroutine writes out the “Matrix Sub-Block” record on a scratch file, resets the `ng2z` parameter to the top group of the subblock, and continues the loop through statement number 100 to produce the rest of the subblocks for this reaction. The resulting series of subblock records on the scratch file are all less than `maxw` words in length, and the number of records is minimal within the restriction that bands are not split between records.

Returning to `matrix`, data already in memory are used to complete the “Matrix Control” record, which is written out onto `nsCRT2`. If no matrix data were found by `band` and `shuf1`, a dummy matrix control record is written on `nsCRT2` and a dummy matrix data record is written on `nsCRT3`. Finally, the constant subblock data saved in `shuf1` (if any) is written to `nsCRT3`.

Returning to subroutine `cmatx`, after the call to `mtxdat`, the data stored in the `a,ia,ha` equivalenced arrays are written to the output file for the “File Identification,” “File Control,” “Set Hollerith Identification,” “File Data,” and “Group Structure” records. In a loop over materials, the “Material Control” record is copied from `nsCRT6` to the output file. Then, in a loop over the submaterials for this material, the “Vector Control” records are copied from `nsCRT2`, the “Vector Blocks” are copied from `nsCRT3`, the “Matrix Control” blocks are copied from `nsCRT2`, and the “Matrix Subblocks” are copied from `nsCRT3`. Subroutine `cmatx` then returns to the main MATXSR routine, files are closed, and the MATXSR run is complete.

## 15.7 Error Messages

The fatal-error and warning messages generated by MATXSR are given below, along with suggested actions to alleviate the problem.

`error in mtxdat***input error (nin=0)`

No input GENDF tape has been given. Check Card 1 of the user input.

`error in mtxdat***too many submaterials`

The code is currently limited to 100 submaterials per material. See `nsubmx=100` in `cmatxs`.

`error in findg***mat or mf or mt le 0 not allowed`

Subroutine `findg` has been asked to search for an illegal section on the GENDF tape.

error in findg\*\*\*mat=nnnn mf=nn mt=nnn not on tape

The requested section was not found on the input GENDF tape. Check that the correct tape was mounted.

error in vector\*\*\*exceed input data array size.

Check the parameter maxb=30000 in vector.

error in band\*\*\*input too large

Check the parameter maxb=30000 in matrix.

error in shufl\*\*\*input too large

Check the parameter maxb=30000 in shufl.

error in lstlio\*\*\*storage exceeded

See nbmax=2000 in mtxdatt, the size of the array b.



## 16 RESXSR

In thermal reactor systems, resonance self-shielding in the near epithermal range (*e.g.*, 4-200 eV) is often poorly represented by the simple Bondarenko model[38]. The normal form of this model as used by the TRANSX code[40] assumes that all the absorber resonances are narrow with respect to the energy lost in neutron scattering. In this near epithermal range, many resonances have widths that violate this assumption. A number of ways exist to try to compensate for this problem, one example being intermediate-resonance theory as discussed in the [WIMSR](#) chapter of this manual. The [GROUPR](#) flux calculator can also be used to compensate for wide and intermediate resonances, but only for homogeneous systems or idealized reactor cells.

One way to solve this problem accurately is to move the flux calculation into TRANSX, where full information on material mixtures and geometry can be made available. To test this concept, an experimental version of TRANSX was created that could do a full pointwise flux solution using collision probabilities for cylindrical systems with an arbitrary number and arrangement of shells. It could then take the computed flux by region and generate new, accurate, self-shielded cross sections for the groups in the near epithermal range.

Of course, this experimental code required pointwise cross sections in the epithermal range to do these calculations. Since TRANSX uses CCCC standard interface files[10] for all other communication to the outside world, it was decided to define an interface format for resonance-region pointwise cross sections, or RESXS. This RESXSR module was written to produce the RESXS file from PENDF tapes produced using the other modules of NJOY.

This module and the RESXS format may be of use for other applications besides TRANSX.

### 16.1 Method

For each material, the data for elastic (`mt=2`), fission (`mt=18`), if present, and capture (`mt=102`) for the desired energy range and for all the desired temperatures are read in and interpolated onto a single union grid. This large set of cross sections is then thinned down using an input tolerance `EPS`. Using a union grid for all reactions and temperatures makes temperature interpolation and reconstruction of the total cross section easy.

These data are then written out in the specially defined RESXS format. The key to this format is the “Cross Section Block.” For each incident energy, it is

necessary to give two or three cross sections for each temperature. If all the many energy points were given in one record, the record could be many thousands of words in length. Therefore, the cross section data are broken up into a set of blocks, where each block contains NBLOK records, except the last block can be shorter.

## 16.2 RESXS Format Specification

The specification for the RESXS format follows in the standard CCCC style[10]. These card images were copied from the comment cards at the beginning of the RESXSR source.

```

!*****
!           proposed 09/24/90
!
!f          resxs
!e          resonance cross section file
!
!n          this file contains pointwise cross
!n          sections for the epithermal resonance
!n          range to be used for hyper-fine flux
!n          calculations.  elastic, fission, and
!n          capture cross sections are given vs
!n          temperature.  linear interpolation is
!n          assumed.
!
!n          formats given are for file exchange only
!
!*****
!
!
!-----
!s          file structure
!s
!s          record type           present if
!s          =====
!s          file identification    always
!s          file control           always
!s          set hollerith identification  always
!s          file data              always
!s

```

```

!s ***** (repeat for all materials) -
!s *          material control          always -
!s * -
!s * ***** (repeat for all cross section blocks) -
!s * *          cross section block          always -
!s * ***** -
!s ***** -
! -
!-----
!
!
!-----
!r          file identification -
! -
!l  hname,(huse(i),i=1,2),ivers -
! -
!w  1+3*mult -
! -
!b  format(4h ov ,a8,1h*,2a8,1h*,i6) -
! -
!d  hname          hollerith file name - resxs - (a8) -
!d  huse          hollerith user identification (a8) -
!d  ivers          file version number -
!d  mult          double precision parameter -
!d                  1- a8 word is single word -
!d                  2- a8 word is double precision word -
! -
!-----
!
!
!-----
!r          file control -
! -
!l  efirst,elast,nholl,nmat,nblok -
! -
!w  5 -
! -
!b  format(4h 1d ,2i6) -
! -
!d  efirst          lowest energy on file (ev) -
!d  elast          highest enery on file (ev) -
!d  nholl          number of words in set hollerith -

```

```

!d          identification record          -
!d  nmat      number of materials on file  -
!d  nblok     energy blocking factor       -
!          -
!-----
!
!
!-----
!r          set hollerith identification   -
!          -
!l  (hsetid(i),i=1,nholl)                 -
!          -
!w  nholl*mult                             -
!          -
!b  format(4h 2d ,8a8/(9a8))              -
!          -
!d  hsetid     hollerith identification of set (a8) -
!d          (to be edited out 72 characters per line) -
!          -
!-----
!
!
!-----
!r          file data                     -
!          -
!l  (hmatn(i),i=1,nmat),(ntemp(i),i=1,nmat),(locm(i),i=1,nmat) -
!          -
!w  (mult+2)*nmat                         -
!          -
!b  format(4h 3d ,8a8/(9a8))      hmatn    -
!b  format(12i6)                  ntemp,locm -
!          -
!d  hmatn(i)    hollerith identification for material i -
!d  ntemp(i)    number of temperatures for material i -
!d  locm(i)     location of material i -
!          -
!-----
!
!
!-----
!r          material control              -
!          -

```



```

!l      hmat,amass,(temp(i),i=1,ntemp),nreac,nener      -
!
!w      mult+3+ntemp      -
!
!b      format(4h 6d ,a8,1h*,1p1e12.5/(6e12.5))      hmat,temp      -
!b      format(2i6)      nener,blok      -
!
!d      hmat      hollerith material identifier      -
!d      amass      atomic weight ratio      -
!d      temp      temperature values for this material      -
!d      nreac      number of reactions for this material      -
!d      (3 for fissionable, 2 for nonfissionable)      -
!d      nener      number of energies for this material      -
!
!-----
!
!
!-----
!r      cross section block      -
!
!l      (xsb(i),i=1,imax)      -
!
!c      imax=3*ntemp*(number of energies in the block)      -
!
!w      imax      -
!
!b      format(4h 8d ,1p5e12.5/(6e12.5))      -
!
!d      xsb(i)      data for a block of nblok or fewer point energy      -
!d      values. the data values given for each energy      -
!d      are nelas, nfis, and ng at temp(1), followed by      -
!d      nelas, nfis, and ng at temp(2), and so on.      -
!
!-----

```

### 16.3 User Input

The following input specifications were taken from the comment cards at the beginning of the RESXSR source. It is always a good idea to check the comment cards in the current version in case there have been changes.

```

! User input:
!
! card 1  units
!      nout      output unit
!
! card 2  control
!      nmat      number of materials
!      maxt      max. number of temperatures
!      nholl     number of lines of descriptive comments
!      efirst    lower energy limit (ev)
!      elast     upper energy limit
!      eps       thinning tolerance
!
! card 3  user id
!      huse      hollerith user identification (up to 16 chars)
!      ivers     file version number
!
! card 4  descriptive data (repeat nholl times)
!      holl      line of hollerith data (72 chars max)
!
! card 5  material specifications (repeat nmat times)
!      hmat      hollerith name for material (up to 8 chars)
!      mat       endf mat number for material
!      unit      njoy unit number for pendf data
!

```

The only difficulty in constructing the input file for RESXSR is in choosing **efirst**, **last**, and **eps**. The goal is to get a set that can be used to generate reasonably good fluxes and cross sections without being too expensive. Also, the energy limits should be consistent with the group bounds that will be used for the multigroup part of the calculation. However, the upper energy limit should be enough above the highest group to be treated with this method that “Placek” oscillations from the discontinuity in the source from higher energies have some chance to die out. It is possible that the values of **eps** could be somewhat larger than the value used in [RECONR](#) and [BROADR](#) to attain additional economy. In practice, it may be necessary to iterate a few times to get a good compromise.

## 17 ACER

The ACER module prepares libraries in ACE format (A Compact ENDF) for the MCNP continuous-energy neutron-photon Monte Carlo code[17]. One of the design goals for MCNP has been to use the most detailed representation of the physics of a problem that is practical. Therefore, the ACE format has evolved to include all the details of the ENDF[8] representations for neutron and photon data. However, for the sake of efficiency, the representation of data in ACE is quite different from that in ENDF. The fundamental difference is the use of random access with pointers to the various parts of the data. Other key differences include the use of union energy grids, equal-probability bins, and cumulative probability distributions.

This chapter describes ACER from NJOY 2012.0. It differs from the version reported previously[3] in a number of ways.

- Probability tables for self shielding in the unresolved energy range are now included.
- Incident energy thinning for angle and energy distributions is no longer supported.
- A new cumulative distribution format is available for angular distributions.
- A new representation is available for energy-angle distributions using cumulative distributions for both emission energy and emission cosine (LAW=61).
- A new option for photonuclear data is now available.
- A detailed format for the production of particles other than the incident particle has been added to support n-particle transport.
- ACE files can now be produced for incident charged particles.
- Extensive consistency checking and a capability to produce color Postscript plots of the ACE data have been added.
- Fortran-90 style and storage allocation are now used. ACER has been reorganized to use separate modules for the different classes of ACE data with another module used for supporting routines.

### 17.1 ACER and ACE Data Classes

The ACE format provides for several different “classes” of data, the most popular being the “continuous-energy neutron” class. Others include photo-atomic data, thermal data, and photo-nuclear data. Files for each class of data are distinguished by a code letter at the end of the ZAIID identifier for each material. For example, a file with a ZAIID identifier of “13027.00c” would

Table 23: ACE Data Classes and ZAID suffixes

| Suffix | ACE Data Class                       |
|--------|--------------------------------------|
| c      | continuous-energy neutron data       |
| t      | thermal $S(\alpha, \beta)$ data      |
| y      | dosimetry data                       |
| p      | photo-atomic data (incomplete)       |
| u      | photonuclear data                    |
| h      | continuous-energy proton data        |
| o      | continuous-energy deuteron data      |
| r      | continuous-energy triton data        |
| s      | continuous-energy $^3\text{He}$ data |
| a      | continuous-energy alpha data         |

contain continuous-energy neutron data. The data classes currently handled by ACER and the class suffixes are given in Table 23.

For the Fortran-90 version of ACER, each different class of ACE data is handled by a different sub-module; the module `acefc` handles the continuous-energy neutron data class (and also incident charged particles), the module `aceth` handles thermal data, the module `acepa` handles photo-atomic data, and the module `acepn` handles photonuclear data. There is also an `acem` module containing routines common to more than one of the ACER sub-modules. The main ACER module itself `acem` is used to read in the user's input commands and then to call the main subroutines from the appropriate sub-module to carry out the ACE library production desired. The following sections of this chapter will describe the methods used to construct data for each of these classes, discuss the user input and how to set up ACER jobs, and give coding details for the ACER set of modules.

## 17.2 Continuous-Energy Neutron Data

The next few sections will discuss the details of preparing data for this very important class of ACE data. The module `acefc` exports two subroutine calls; namely, `acetop` for producing the continuous-energy data file, and `acefix` for printing or editing continuous-energy data files. The latter function also includes consistency checking and plotting.

### 17.3 Energy Grids and Cross Sections

MCNP requires that all the cross sections be given on a single union energy grid suitable for linear interpolation. This was also true of its predecessor MCN[89], and this is one of the reasons that the [RECONR](#) and [BROADR](#) modules of NJOY are also organized around union grids and linear interpolation.

The energy grid and cross section data on an NJOY PENDF tape are basically consistent with the requirements of MCNP. In the still recent past, when computers were smaller, there was a problem that many ENDF evaluations (especially ENDF/B-VI evaluations) produced energy grids with very large numbers of points. A few examples from early ENDF/B-VI releases are shown in Table 24. Thus, it was considered useful to reduce the size of these data sets by reducing the number of energy points in the union grid. This kind of thinning is no longer routinely done for libraries produced by LANL, but it is still available, if needed.

Of course, any thinning of the energy grid will result in a loss of accuracy. The goal is to control the accuracy loss and balance it against the memory requirements. This balance will vary from application to application. For example, a user doing fusion calculations may be able to drastically reduce the number of resonance points at low energies without affecting the results significantly. Similarly, a thermal-reactor designer may be able to reduce the number of energy points used above 100 to 200 eV with minimal impact on the answers.

The `acefc` module provides two different thinning algorithms (implemented in `unionx`). First, the code can do a very crude removal of points; for example, it can remove 2 out of every 3 points for all energies between `E1` and `E2`. This is called the “energy skip” option. It is now obsolete, and it is not recommended.

The second thinning option is “integral fraction” thinning. The idea here is to attempt to preserve the resonance integral. Two weighting functions are provided:  $1/E$  and flat. The former is best for thermal-type problems, and the

Table 24: Union Energy Grid Sizes for Some Evaluations from ENDF/B-V and ENDF/B-VI

| Evaluation                                    | Union Grid |
|-----------------------------------------------|------------|
| $^{235}\text{U}$ , ENDF/B-V at 300K and 0.5%  | 7 200      |
| $^{235}\text{U}$ , ENDF/B-VI at 300K and 0.5% | 49 100     |
| $^{238}\text{U}$ , ENDF/B-V at 300K and 0.5%  | 30 900     |
| $^{238}\text{U}$ , ENDF/B-VI at 300K and 0.5% | 58 300     |

latter preserves more points in the high-energy range. The user specifies a target number of points for the final energy grid. The code uses this target number to estimate an initial thinning tolerance, and it starts moving through the energy grid and calculating the contributions to the total and capture resonance integrals from each energy panel. Panels whose contributions to both integrals are small with respect to the current tolerance are candidates for rejection. The code has additional tolerances designed to preserve major features and to preserve a reasonable minimum lethargy step; these features keep some of the points from being rejected. When the entire energy range has been scanned, the code checks the resulting number of points against the user's target. If the goal has not been reached, it doubles the tolerance and repeats the entire process. When the target has been reached, it prints out the new and original values for the resonance integrals for several subranges of the total energy range. If the errors introduced by thinning are too large, the user will have to repeat the ACER run using a larger target for the final number of energy points. An example of the printout provided with integral thinning is given below.

```
original grid= 19585 with integrals    5.9781e+07  2.1716e+04
```

```
new grid= 18809 with integrals    5.9782e+07  2.1720e+04
```

```
new grid= 17842 with integrals    5.9782e+07  2.1724e+04
```

```
new grid= 16227 with integrals    5.9782e+07  2.1735e+04
```

```
new grid= 13786 with integrals    5.9783e+07  2.1727e+04
```

```
new grid= 11033 with integrals    5.9785e+07  2.1762e+04
```

```
total
```

|            |            |     |     |     |     |     |
|------------|------------|-----|-----|-----|-----|-----|
| 8.0942e+04 | 5.4213e+05 | 0.0 | 0.0 | 0.0 | 0.0 | 0.0 |
| 1.7327e+05 | 4.1284e+05 | 0.0 | 0.0 | 0.0 | 0.0 | 0.1 |
| 2.5257e+05 | 3.0142e+05 | 0.0 | 0.0 | 0.0 | 0.1 | 0.1 |
| 3.2191e+05 | 1.8647e+05 | 0.0 | 0.0 | 0.0 | 0.1 | 0.3 |
| 4.4842e+05 | 5.0962e+05 | 0.0 | 0.0 | 0.0 | 0.0 | 0.1 |
| 5.5888e+05 | 3.5549e+05 | 0.0 | 0.0 | 0.0 | 0.0 | 0.1 |
| 6.5861e+05 | 2.0999e+05 | 0.0 | 0.0 | 0.0 | 0.1 | 0.3 |
| 7.8043e+05 | 4.1624e+05 | 0.0 | 0.0 | 0.0 | 0.0 | 0.1 |
| 1.1206e+06 | 9.0192e+05 | 0.1 | 0.1 | 0.1 | 0.1 | 0.1 |
| 2.0000e+07 | 5.5945e+07 | 0.0 | 0.0 | 0.0 | 0.0 | 0.0 |

|            |            |     |     |     |      |     |      |      |      |
|------------|------------|-----|-----|-----|------|-----|------|------|------|
| capture    |            |     |     |     |      |     |      |      |      |
| 8.0942e+04 | 1.0141e+03 | 0.3 | 0.4 | 0.8 | -0.5 | 1.5 |      |      |      |
| 1.7327e+05 | 7.3599e+02 | 0.0 | 0.2 | 0.5 | 0.0  | 0.2 |      |      |      |
| 2.5257e+05 | 5.4686e+02 | 0.0 | 0.0 | 0.3 | 0.5  | 1.3 |      |      |      |
| 3.2191e+05 | 4.2149e+02 | 0.0 | 0.1 | 0.3 | 1.0  | 1.4 |      |      |      |
| 4.4842e+05 | 5.9879e+02 | 0.0 | 0.1 | 0.2 | 0.4  | 0.7 |      |      |      |
| 5.5888e+05 | 5.7626e+02 | 0.0 | 0.0 | 0.1 | 0.2  | 0.4 |      |      |      |
| 6.5861e+05 | 5.5110e+02 | 0.0 | 0.1 | 0.3 | 0.5  | 0.8 |      |      |      |
| 7.8043e+05 | 8.4225e+02 | 0.0 | 0.0 | 0.1 | 0.2  | 0.4 |      |      |      |
| 1.1206e+06 | 1.3748e+03 | 0.0 | 0.0 | 0.0 | 0.0  | 0.1 |      |      |      |
| 2.0000e+07 | 1.5054e+04 | 0.0 | 0.0 | 0.0 | 0.0  | 0.0 |      |      |      |
|            |            |     |     |     |      |     |      |      |      |
| 861        | 827        | 825 | 739 | 983 | 1137 | 867 | 1262 | 1575 | 1956 |

The numbers at the ends of the first few lines of this listing are the total and capture resonance integrals computed by ACER. The sections starting with the words **total** and **capture** give the resonance integrals for a few energy ranges, and they also show the percentage change caused by thinning for each step of the process. This sample shows that the capture integral increases by as much as 1.5% after thinning to 11 000 points. If this seems too large, the user can repeat the run using a target of 15 000 points; the maximum capture error will be reduced to 1%. The last line of the listing shows the number of points remaining in each energy interval with the intervals listed horizontally. In this case, the original number of points was about 1958 for each interval. The high energy band has not been thinned much at all, but the low energy band has lost 56% of its points.

The formats for storing energy grid and cross section data in an ACE library are completely described in Appendix F of the MCNP manual, but they will also be reviewed briefly here for the reader's convenience. The principal cross sections are given in the ESZ block. First, the NES energy values of the union grid are given, then the NES values of the total cross section. These are followed by the absorption cross section, elastic cross section, and average heating numbers. The cross sections for the other NTR reaction types are controlled by a set of blocks called MTR, LQR, TYR, and LSIG that contain the reaction ENDF MT numbers, the Q values, the reaction types, and pointers to the cross section data for each reaction, respectively. The cross section segments addressed by the pointers in the LSIG block contain a count of values, the energy index from

the main energy grid for the first value, and the actual cross sections for the reaction.

The energy and cross section values from the input PENDF tape are copied onto the grid of the total cross section in subroutine `unionx`. This routine also handles the thinning as described above. The results are written onto a scratch tape and passed on to subroutine `acelod`, which reads in the cross sections and stores them into the ACE-format blocks. Note that all energy values in the ACE libraries are given in MeV. The ACE heating numbers are computed by dividing the heat production cross sections from MT=301 on the PENDF tape by the corresponding total cross sections to obtain heating in MeV per reaction. Damage values from MT=444 are converted to MeV-barns. Sometimes additional cross sections, such as nonelastic or inelastic are needed, and they are added at the end of the reaction list. Note that there are two reaction counters used in the ACE format: NTR is the total number of reactions, and NR is the number of reactions that participate in the transport (*i.e.*, that add up to the total cross section). Reactions with index values above NR and up to NRT can be used for tallies. This can include reactions like damage or gas production.

## 17.4 Two-Body Scattering Distributions

Reactions like elastic and discrete-level inelastic scattering are completely described by their reaction cross sections, Q values, and angular distributions in the center-of-mass (CM) system. The ACE locations for the cross sections and Q values were noted above. The angular distributions are stored in the AND block using a set of pointers stored in the LAND block. Two different representations for angular distributions are provided: equally probable cosine bins, and cumulative distributions. In the older format, which is supported by all versions of MCNP, the angular distributions are represented by 32 equally probable cosine bins for each incident energy (except for isotropic cases). The methods for doing this calculation in ACER were borrowed from ETOPL[24]. The calculation is driven by `topfil`, which uses `ptleg` for distributions represented using Legendre coefficients and `pttab` for distributions given as tabulations of scattering probability versus scattering cosine  $P(\mu)$ . The ENDF angular distributions are obtained from File 4 on the input ENDF tape.

The newer representation for angular distributions has been available in MCNP since version 4C. The ENDF data are converted into cumulative density functions (CDF) and the corresponding probability density functions (PDF) versus scattering cosine. This option is triggered by `newfor=1` in the User's



ACER input, and the work is done in subroutine `acensd` (“nsd” for neutron scattering distributions) using `ptleg2` for Legendre coefficient data and `pttab2` for tabulated data. This representation is superior to the 32-bin one for high-energy evaluations (those that go beyond 20 MeV), which have very sharply forward-peaked shapes. It also reduces biases in the average cosine for scattering at lower energies. Even though it is sometimes more bulky than the 32-bin representation, the newer cumulative format is now the default.

## 17.5 Secondary-Energy Distributions

In earlier versions of MCNP, and in the original MCN code, tabulated energy distributions for secondary neutrons from multi-body reactions like  $(n, 2n)$  or composite reactions like  $(n, n'_c)$  were represented using equally probable bins (see LAW=1 in the DLW block). This representation turned out to be poor because it didn’t sample low-probability important events like those in the high-energy tails of energy distributions. The current standard representation for tabulated energy distributions is LAW=4, the “Continuous Tabular Distribution.” This scheme is based on sampling from a cumulative density distribution  $C(E')$ , which gives the probability that the energy of the emitted particle will be less than  $E'$ . Since this probability runs from 0 to 1, it is easy to select a random number in this range and interpolate for the corresponding value of  $E'$ . The differential density distribution  $P(E')$  is also given for use in MCNP’s interpolation scheme. These quantities are computed in subroutine `acelod` using `acelf5` and stored into the ACE DLW block using pointers stored in the LDLW block.

Analytic energy distribution laws, such as the LF=7 simple Maxwellian fission spectrum, the LF=9 evaporation spectrum, or the LF=11 energy-dependent Watt spectrum, are also stored into the DLW and LDLW blocks. The ACE representation is a faithful image of the ENDF representation, so `acelod` simply stores the various fields into the correct locations in memory.

## 17.6 Energy-Angle Distributions

A new feature of the ENDF-6 format is coupled energy-angle distributions in File 6. (There was a File 6 format available in earlier versions of the ENDF format, but it was never used. The new ENDF-6 MF=6 format is different.) For neutrons, there are four different representations to be considered:

- The Kalbach law for  $\sigma(E \rightarrow E')$  angular distributions as used in ENDF/B-VI and later evaluations from Los Alamos;

- Legendre coefficients for  $\sigma(E \rightarrow E')$  in the laboratory system as used in ENDF/B-VI and later evaluations from Oak Ridge;
- Secondary-energy distributions versus laboratory scattering cosine as used in the Livermore evaluation of  $^9\text{Be}$  in ENDF/B-VI; and
- The phase-space distribution as used in the Los Alamos evaluation of the  $(n, 2n)$  reaction for  $^2\text{H}$  in ENDF/B-VI.

New evaluations using tabulations of angular distributions in the laboratory frame, or coefficients or tabulations in the CM frame, are expected to appear soon.

**Kalbach Systematics.** Kalbach and Mann[58] examined a large number of experimental angular distributions for neutrons and charged particles. They noticed that each distribution could be divided into two parts: an equilibrium part symmetric in  $\mu$ , and a forward-peaked pre-equilibrium part. The relative amount of the two parts depended on a parameter  $r$ , the pre-equilibrium fraction, that varied from zero for low  $E'$  to 1.0 for large  $E'$ . The shapes of the two parts of the distributions depended most directly on  $E'$ . This representation is very useful for pre-equilibrium statistical-model codes like GNASH[60], because they can compute the parameter  $r$ , and all the rest of the angular information comes from simple universal functions. More specifically, Kalbach's latest work[59] says that

$$f(\mu) = \frac{a}{2 \sinh(a)} \left[ \cosh(a\mu) + r \sinh(a\mu) \right], \quad (475)$$

where  $a$  is a simple function of  $E$ ,  $E'$ , and  $B_b$ , the separation energy of the emitted particle from the liquid-drop model without pairing and shell terms. The values for  $a$  are computed by subroutine `bachaa` from the common module `acecm`.

A special sampling scheme has been developed for this case. The MCNP code already had logic to select a secondary energy  $E'$  from a distribution. The problem was to select an emission cosine  $\mu$  for this  $E'$ . First, the Kalbach distribution is written in the form

$$f(\mu) = \frac{a}{2 \sinh(a)} \left[ (1 - r) \cosh(a\mu) + r e^{a\mu} \right]. \quad (476)$$

Now select a random number  $R_1$ . If  $R_1 < r$ , use the first distribution in Eq. 476. Select a second random number  $R_2$ , where

$$R_2 = \int_{-1}^{\mu} \frac{a \cosh(ax)}{2 \sinh(a)} dx = \frac{\sinh(a\mu)}{2 \sinh(a)} + \frac{1}{2} . \quad (477)$$

Therefore, the emission cosine is

$$\mu = \frac{1}{a} \sinh^{-1} \left[ (2R_2 - 1) \sinh(a) \right] . \quad (478)$$

If  $R_1 \leq r$ , use the second distribution in Eq. 476. Select a random number  $R_2$ , where

$$R_2 = \int_{-1}^{\mu} \frac{ae^{ax}}{2 \sinh(a)} dx = \frac{e^{a\mu} - e^{-a}}{e^a - e^{-a}} , \quad (479)$$

and emit a particle with cosine

$$\mu = \frac{1}{a} \ln \left[ R_2 e^a + (1 - R_2) e^{-a} \right] . \quad (480)$$

The ACE format for the Kalbach File 6 data is similar to the LAW=4 format used for other continuous energy distributions, namely, cumulative distribution functions. To this are added tables for the pre-equilibrium ratio  $r$  and the Kalbach slope parameter  $a$ . The result is the LAW=44 format.

**Legendre or Tabulated Distributions for E to E'.** This option is used in many of the newer Oak Ridge evaluations, such as the isotopes of chromium,  $^{55}\text{Mn}$ , the isotopes of iron, the isotopes of nickel, the isotopes of copper, and the isotopes of lead. The distribution for outgoing neutrons is given as a set of normalized emission spectra  $g(E, E')$  for various incident energies  $E$ . In addition, an angular distribution is given for each  $E \rightarrow E'$  as a Legendre expansion. Emission energy and angle are given in the laboratory frame. Some recent European evaluations use a similar representation in the CM frame.

The last few versions of ACER tried various ways to handle these formats within the limitations of versions of MCNP up to 4B, but none of them were very satisfactory. Therefore, we added a new representation for MCNP4C called LAW=61. This law uses the cumulative density approach for sampling for  $E'$ , just as in LAW=4 or 44. In addition, it gives a cumulative type distribution

in the emission cosine for each  $E'$ . This is a bulky representation, but it has the advantage of not forcing any approximations on MCNP. This format is also selected by giving `newfor=1`, which is now the default for ACER.

For users who prefer to use the older versions of MCNP with the older representation, the option `newfor=0` can be selected. ACER will try to convert the Legendre data into an equivalent section using ENDF MF=6 format with 33 cosines. This section can then be processed into ACE LAW=67 format as described below. This process is reasonably straightforward for laboratory data. If necessary, ACER does attempt to convert CM data to the lab frame when building one of these MF=6 representations, but the methods used are fairly rough and approximate. See `fix6`.

**Laboratory Angle-Energy Distributions.** The ENDF/B-VI evaluation for  $^9\text{Be}$  prepared at the Lawrence Livermore National Laboratory uses the angle-energy option. That is, the outer loop is on incident energy  $E$ , the next loop is on laboratory scattering cosine  $\mu$ , and the inner loop is on secondary energy  $E'$ . In order to sample from data in this form, the first step is to integrate over  $E'$  for each  $\mu$  in order to obtain the differential angular distribution  $f(E, \mu)$ . This angular distribution is converted into 32 equally probable bins and stored into the ACE file using the same format used for two-body angular distributions. The emission spectra for the individual  $\mu$  values are normalized and stored into the file using a format called LAW=67 (named for ENDF File 6, Law 7). MCNP can sample from this representation as follows: for each emission, first sample from  $f(\mu)$  to get an emission angle, then find the corresponding spectrum and sample from its cumulative probability distribution to get the value of  $E'$ .

**N-Body Phase-Space Distributions.** The phase-space distribution for particle  $i$  in the CM system is given by

$$P_i^{\text{CM}}(\mu, E, E') = C_n \sqrt{E'} (E_i^{\text{max}} - E')^{3n/2-4}, \quad (481)$$

where  $E_i^{\text{max}}$  is the maximum possible CM energy for particle  $i$ ,  $\mu$  and  $E'$  are in the CM system, and the  $C_n$  are normalization constants. The value of  $E_i^{\text{max}}$  is a fraction of the energy available in the CM:

$$E_i^{\text{max}} = \frac{M - m_i}{M} E_a, \quad (482)$$

where  $M$  is the total mass of the  $n$  particles being treated by this law, and

$$E_a = \frac{m_T}{m_p + m_T} E + Q. \quad (483)$$

Here,  $m_T$  is the target mass, and  $m_p$  is the projectile mass. In summary, the data items required for the phase-space law are

| Symbol | ENDF | Location                            |
|--------|------|-------------------------------------|
| $n$    | NPSX | N2 field of the MF=6 CONT for LAW=6 |
| $m_i$  | AWI  | C1 field of third card in MF=1      |
| $m_p$  | AWP  | C2 field of LAW=6 TAB1 record       |
| $m_T$  | AWR  | C2 field of section HEAD record     |
| $M$    | APSX | C1 field of LAW=6 CONT record       |
| $Q$    | Q    | C1 field of the MF=3 TAB1 record    |

These equations are sampled with a compact numerical scheme similar to LAW=4. Note that all the spectra scale with the maximum possible outgoing energy. Therefore, it is easy to construct a single normalized distribution with  $E_i^{\max}=1$  with a reasonable number of  $x = E'/E_i^{\max}$  points and then to construct a cumulative distribution function for it. The grid uses uniform spacing above  $x = 0.10$  and log spacing below. The  $x$  grid, the probability density values  $P(x)$ , the cumulative densities  $C(x)$ , NPSX, and APSX are stored in the Law=66 format. For any given  $E$ , the cumulative distribution function is sampled with a random number between 0 and 1. The resulting  $x$  value is then multiplied by  $E_i^{\max}$  to get the emitted  $E'$  value. The corresponding CM cosine value is obtained by sampling uniformly in the interval  $[-1, 1]$ .

The CM to lab transformation is carried out by adding the CM velocity of the initial collision to the emitted particle velocity.

$$E'_{\text{LAB}} = E_{\text{CM}} + E'_{\text{CM}} + 2\mu_{\text{CM}}\sqrt{E_{\text{CM}}E'_{\text{CM}}}, \quad (484)$$

and

$$\mu_{\text{LAB}} = \frac{\sqrt{E'_{\text{CM}}}\mu_{\text{CM}} + \sqrt{E_{\text{CM}}}}{\sqrt{E'_{\text{LAB}}}}, \quad (485)$$

where the CM energy is

$$E_{\text{CM}} = \frac{A}{A+1} E. \quad (486)$$

**Smoothing.** For a number of important ENDF/B-VII evaluations (including main actinides), the spectra from continuous reactions like MT=91 are given in histogram form. This is a natural result of the nuclear model codes used to generate the evaluations. At low energies, you will typically see one histogram bin extending from zero energy to keV energies; that is, the emission probability will be constant in that range. From physics, we expect that the limiting shape at low emission energies in the CM frame will be  $\sqrt{E'_{CM}}$  (implying a  $\sqrt{E'_{LAB}}$  shape in the laboratory). Therefore, the histogram shape greatly overestimates the source into low energies. This problem is somewhat alleviated by the low probability for scattering into this lowest bin, and the evaluations that use this representation give good results for criticality calculations. However to improve the physical consistency of the emission spectra, ACER has an option to convert the low energy part of the spectra into a new histogram representation with finer steps that does a better job of approximating the  $\sqrt{E'_{CM}}$  shape. We call this “smoothing” and it is controlled by the parameter `ismooth`. For NJOY2012 the default is to carry out the smoothing operation. Users are cautioned that this is opposite the NJOY99.x default setting.

A similar smoothing operation is applied to the low-energy bin of the delayed neutron spectra for fission when `ismooth` is set. A somewhat different problem occurs at energies above 10 MeV for some of the MF=5 fission spectrum sections. The energy grid shifts from a reasonable size below 10 MeV to one that is too coarse above there. The expected shape of the fission spectrum on the high-energy side is nearly exponential. ACER inserts additional grid points between the ones in the evaluation using linear-in-E and log-in-probability interpolation when `ismooth` is set. Without smoothing the coarse high energy mesh can cause significant errors in reaction rates for high-threshold reactions.

## 17.7 Photon Production

Earlier versions of MCNP used a very simple representation for photon production from neutron reactions. There was a single total photon production cross section on the same union grid as the neutron data, and there were 600 words of data describing the spectrum of outgoing neutrons. This table contained 20 equally likely outgoing photon energies for each of 30 incident neutron groups. This representation did not achieve the MCNP goal of providing the best possible representation of the physics of the problem. It was inadequate in representing discrete photons because their real energies were often lost, and it was inadequate in representing low-probability events from the tails of distri-

butions. This was especially noticeable in capture events because of the high photon energies possible. It is still possible to use this representation, but it is no longer recommended. The newer “Expanded Photon Production Data” option is preferred.

**Photon Production Cross Section.** In the earlier versions of the ENDF format, photon production cross section information was given in File 13 (photon production cross sections), or as a combination of File 3 (reaction cross sections) and File 12 (photon production yields). With the ENDF-6 format, photon production can also be computed using a combination of File 3 and File 6 (product yields and energy-angle distributions).

The first step in photon production processing takes place in subroutine `convr`. MF=12 on the ENDF tape is examined for transition probability arrays (LO=2). If they are found, they are converted into the photon yield format (LO=1). The final photon yield data are written onto a scratch tape. Next, the MF=13 data are copied, and MF=14 (photon angular distributions) is updated to reflect the changes made in MF=12. Finally, if File 6 is present, any photon production subsections found are converted into a special MF=16 format on the scratch tape. The next step is performed in `gamsum`. The scratch tape from `convr` is used together with the input PENDF tape to calculate the sum of MF=13, MF=12×MF=3, and MF=16×MF=3 for all the photon reactions on the normal union energy grid. Later, this total photon production cross section is written into the ACE GPD block in `acelod`.

**Photon Production Matrix.** The 30-by-20 photon production matrix is computed from input multi-group data. Therefore, it is necessary to execute the `GROUPT` module prior to ACER. This run should use the 30-group option for neutrons and a photon group structure with many groups (the CSEWG 94-group structure is normally used). The `gamout` routine reads the multi-group data and adds up all the reactions. It then integrates through the photon groups for each neutron group and finds the equal-probability boundaries. For each of these equally probable bins, it selects a single photon energy that preserves the average energy for the bin. The results are written on a scratch tape in a special ENDF-type format and passed to `acelod` to be inserted into the GPD block.

**Expanded Photon Production Data.** This newer representation allows each discrete photon to be treated with its proper energy, and it allows for a

much better representation of the spectrum of continuum photons. In the ACE representation, the MTRP block lists all the photon reactions included by ENDF MT number. Since some reactions may describe more than one photon (for example, radiative capture reactions usually describe many discrete photons), the identifier numbers are given as  $1000 \times \text{MT}$  plus a photon index. Thus 102002 would stand for the second photon described under radiative capture (MT=102). Each of the NMTR photons listed in the MTRP block can have its own cross section or yield as described in the SIGP and LSIGP blocks, its own angular distribution as described in the ANDP and LANDP blocks, and its own energy distribution as described in the DLWP and LDLWP blocks. In addition, the YP block contains a list of reaction MT numbers that are needed as photon production yield multipliers.

These expanded photon production data are stored into the ACE-format blocks in `acelod` using the information written on a scratch file by `convr`.

## 17.8 Probability Tables for the Unresolved Region

Starting with Version 4B, MCNP has been able to make use of cross section probability tables for energies in the unresolved resonance range to get proper self-shielding effects. These tables are produced by the `PURR` module of NJOY. The tables provide a cumulative density function that gives the probability that the total cross section observed at some energy  $E$  in the unresolved resonance range will be less than some particular values. MCNP can then throw a random number and search this table to get a sample value for the total cross section at each collision. The probability tables also include conditional probability distributions that give values for scattering, fission, capture, and heating for each particular value of the total. The probability tables are read from the input PENDF file and stored into the ACE format in `acelod`.

## 17.9 Charged-Particle Production

Another recent addition to the continuous-energy neutron data class for MCNP is a detailed representation of the emission of light charged particles from neutron-induced reactions. These kinds of data are now available for a number of materials in ENDF/B evaluations, including the large set of evaluations originally added for ENDF/B-VI Release 6 that go to incident neutron energies of 150 MeV.



When present, the charged-particle production data reside in a set of ACE blocks at the end of the ACE file. There is a set of data given for each charged particle produced: protons, deuterons, tritons,  $^3\text{He}$ 's, and alphas. These data sets give a production cross section and a heating value referenced to the standard union energy grid from the ESZ block, and they also give the fraction of the production coming from each reaction producing the particle, together with the associated angle and energy distribution data for the reaction. These data are loaded into the ACE format using subroutine `acelcp`, which support most of the formats described above, including LAWs 44 and 61.

These charged particle production distributions will be used in advanced versions of MCNP to provide the source from neutron reactions for subsequent charged-particle transport, thus providing a true n-particle Monte Carlo capability.

Care must be taken to handle heating correctly in n-particle transport calculations. The heating value in the main ESZ block of the ACE format contains energy deposition resulting from all the charged particles resulting from nuclear reactions. If a user wants to do a coupled neutron-gamma-proton calculation, it is necessary to subtract the proton heating from the main heating value first. The subsequent non-local energy deposition from the transported protons will be handled directly. This is why the new charged-particle blocks include the separate heating contribution associated with each particle.

### 17.10 Gas Production

During the NJOY run that makes the input for ACER processing, the user can choose to run the `GASPR` module. It goes through all the reactions given on its input ENDF and PENDF files and constructs reaction cross sections for the production of the light charged particles (p, d, t,  $^3\text{He}$ , and alpha) and writes them on a new version of the PENDF file. When `acelod` processes this PENDF file, the cross sections are made available in the ACE file for use in MCNP tallies. Watch for reaction names like “(n,Xp).”

These gas production cross sections are basically the same as the charged-particle production cross sections in the new charged-particle sections on the ACE file (except for reactions using the ENDF LR flags), but the latter are not available for simple tallies.

### 17.11 Consistency Checks and Plotting

As part of the Quality Assurance (QA) process for producing ACE library files, ACER has the capability to read in an ACE file and check the data for some common problems. These are called “consistency checks,” and the checks are provided for class “c” libraries are as follows:

- check reaction thresholds against Q values,
- check the main energy grid is monotonic,
- check angular distributions for correct reference frame,
- check angular distributions for unreasonable cosine values ( $\mu$  out of range,  $\mu$  values not monotonic, cumulative probability out of range, cumulative probabilities not monotonic)
- check energy distributions (illegal interpolation,  $E'$  greater than the maximum possible value, bad cumulative probability, decreasing cumulative probability, bad Kalbach  $r$ , bad angular cumulative probability, decreasing angular commutative probability),
- check photon production sum,
- check photon production distributions (bad cumulative probability, decreasing cumulative probability), and
- check particle production sections (bad LAW=4 cumulative probability, decreasing LAW=4 cumulative probability, bad LAW=44 cumulative probability, decreasing LAW=44 cumulative probability, bad LAW=44 Kalbach  $r$ , bad LAW=61 cumulative probability, decreasing LAW=61 cumulative probability, bad LAW=61 angular cumulative probability, decreasing angular cumulative probability)

When  $E'$  values greater than the expected limit are found, the consistency-check routine can correct them. See the sections on running ACER for the details.

Another important part of the ACE QA procedure is to prepare an extensive set of plots and to scan through them for possible problems. The `aplots` routine does this, together with a number of subsidiary routines. The plots are generated in the form of an input file for the `VIEWR` module, which can then prepare the final plots as color Postscript files. The plots include pages showing the principle ACE cross sections (total, elastic, absorption, photon production), non-threshold reactions (such as capture and heating), and threshold reactions in log form (to feature the low-energy region) and linear form (for higher energies). Several reactions are given per page. The routine also prepares expanded views of the cross sections in the resonance range to make the details of prominent

resonances more apparent. In addition, the plots include 3-D perspective views of angular distributions for the new format. The 32-bin representation of the angular distributions is shown as contour plots. The energy and energy-angle distributions for tabulated representations are also shown as 3-D perspective plots. Finally, the particle production data, if present, are shown using similar 2-D and 3-D plots. Fig. 54 is an example of the log plot for the principal cross sections, and Fig. 55 is an example of a 3-D plot for particle emission.

### 17.12 Thermal Cross Sections

Thermal data is the second class of ACE data to be considered, and they are handled by the `aceth` module. This module exports two subroutines: `acesix` to process the data into ACE format, and `thrfix` for edits, listings, and plots.

For energies below several eV, the thermal motions of nuclei can lead to significant energy gains in neutron scattering. In addition, the binding of atoms into liquids and solids begins to affect the scattering cross section and the distribution of scattered neutrons in angle and energy. MCNP can handle thermal

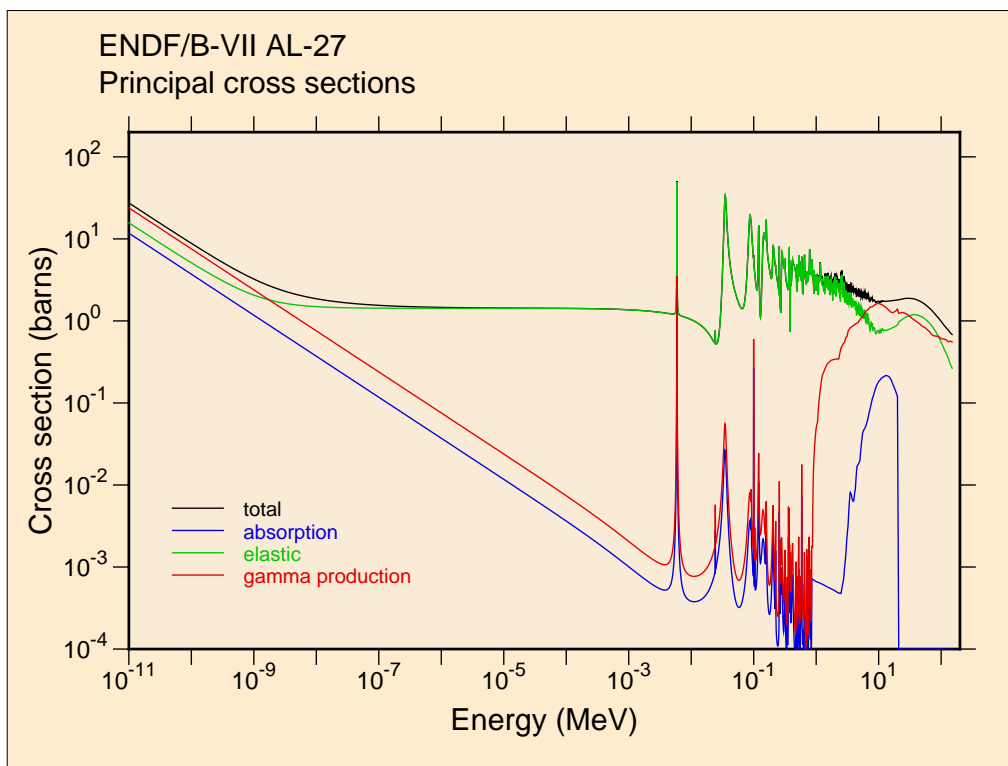


Figure 54: A log plot of the ACE principal cross sections for  $^{27}\text{Al}$  from ENDF/B-VII.0. Note the extension beyond 20 MeV to 150 MeV.

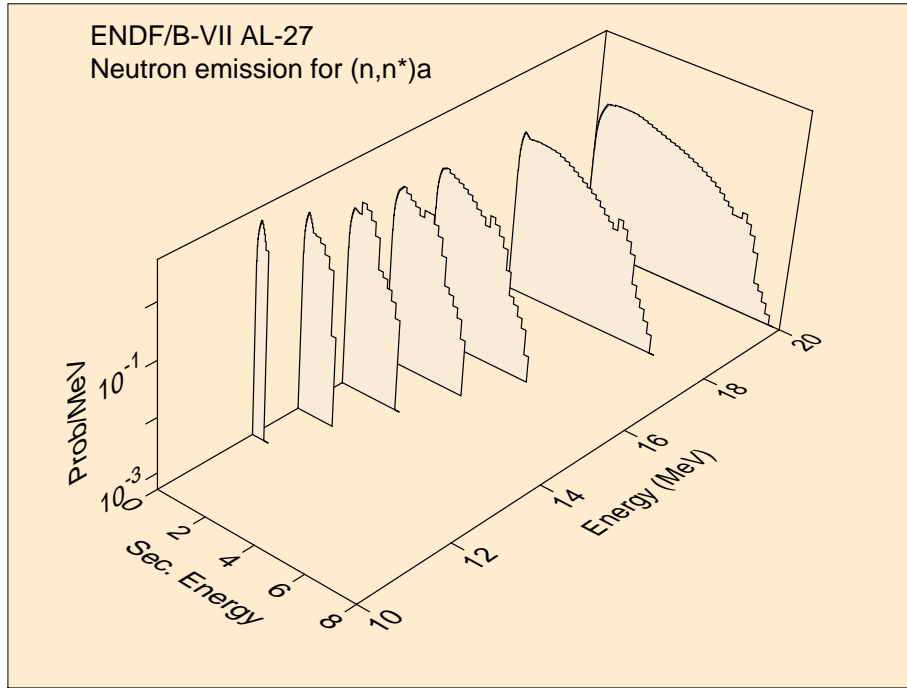


Figure 55: A 3-D view of the energy distribution for neutrons emitted from the  $(n,n'\alpha)$  reaction on  $^{27}\text{Al}$  from ENDF/B-VII.

neutron scattering from the atoms of a free gas using internal kinematic formulas that assume a Boltzmann distribution. The bound-atom effects are treated using thermal data from ENDF evaluations stored in a special MCNP thermal library.

The ENDF format allows for several thermal processes. Thermal inelastic scattering is represented using the scattering law  $S(\alpha, \beta)$ , where  $\alpha$  and  $\beta$  are dimensionless momentum and energy transfer parameters, respectively:

$$\sigma(E \rightarrow E', \mu) = \frac{\sigma_b}{4\pi T} \sqrt{\frac{E'}{E}} e^{-\beta/2} S(\alpha, \beta), \quad (487)$$

where

$$\alpha = \frac{E' + E - 2\mu\sqrt{EE'}}{AkT}, \quad (488)$$

and

$$\beta = \frac{E' - E}{kT}. \quad (489)$$

$E$  and  $E'$  are the incident and outgoing neutron energies,  $\mu$  is the scattering cosine,  $T$  is the absolute temperature,  $A$  is the mass ratio to the neutron of the scatterer, and  $k$  is Boltzmann's constant. This process occurs in all the ENDF thermal materials, such as water, heavy water, graphite, beryllium, beryllium oxide, polyethylene, benzene, and zirconium hydride.

The **THERMR** module of NJOY uses this equation and evaluated  $S(\alpha, \beta)$  data from an ENDF-format evaluation to compute  $\sigma(E \rightarrow E', \mu)$ . The  $E'$  dependence of the integral over  $\mu$  is computed adaptively so as to represent the function using linear interpolation within a specified tolerance. The angular distribution at each of these  $E'$  values is then calculated in a similar way, but the curve of  $\sigma$  vs.  $\mu$  is then converted into equally probable bins (typically 8), and a discrete angle is selected for each bin that preserves the average scattering cosine for that bin. The data are written onto the PENDF tape using special MF=6-like formats.

The **acesix** subroutine reads this thermal section on the input PENDF file. In older versions of this method, the energy distribution  $\sigma(E \rightarrow E')$  is converted into equally probable bins (typically 16), and a discrete energy is chosen for each bin that preserves the average energy in that bin. The result of this process is a set of equally probable events (typically  $8 \times 16 = 128$  events) in  $E', \mu$  space for each incident energy. It is very easy to sample from this representation, and it is fairly compact. See **iwt=0** in the input instructions.

However, it must be recognized that this scheme is only reasonable if each neutron undergoes several scattering events before being detected. The artificial discrete lines must be averaged out. Be careful when using this method to analyze experimental arrangements using optically thin elements and small-angle detectors. In addition, as in all equal-probability bin schemes, the wings of functions (which may be unlikely but important) are not well sampled. ACER includes a variation to partially relieve this problem: instead of equal bin weights, the pattern 1, 4, 10, 10, ..., 10, 4, 1 is used (see "variable weighting" in the input instructions). This approach produces some samples fairly far out on the wings of the energy distribution. Angles are still equally weighted. See **iwt=1** in the input instructions.

In practice, this method using discrete energies can still leave some artificial peaks in typical thermal neutron spectra. These peaks don't have much effect on average quantities for most applications, but they are visually offensive. The newer versions of MCNP (version 5.1.50 and later) support continuous distributions of  $\sigma(E \rightarrow E')$  with PDF and CDF values to drive the sampling. See

`iwt=2` in the input instructions. This is the preferred representation. The thermal inelastic data prepared by `acesix` is loaded into the ACE blocks ITIE and ITXE by `thr1od`.

The second ENDF process to consider is “coherent elastic” scattering. This process occurs in powdered crystalline materials, such as graphite, beryllium, and beryllium oxide. Bragg scattering from the crystal planes leads to jumps in the cross section vs. energy curve as scattering from each new set of planes becomes possible. The formula for this process can be written in the following form:

$$\sigma(E, \mu) = \sigma_c \frac{\pi \hbar^2}{4MEV} \sum_{\tau \neq 0}^{\tau < \tau_{\max}} f(\tau) \delta(\mu - \mu_0[\tau]) , \quad (490)$$

where

$$\tau_{\max} = \sqrt{\frac{8ME}{\hbar^2}} , \quad (491)$$

and

$$\mu_0 = 1 - \frac{\hbar^2 \tau^2}{4ME} , \quad (492)$$

and where  $E$  is the incident neutron energy,  $E'$  is the outgoing neutron energy,  $\mu$  is the scattering cosine,  $\sigma_c$  is the characteristic coherent scattering cross section for the material,  $M$  is the target mass,  $V$  is the volume of the unit cell,  $\tau$  is the radius of one of the reciprocal lattice shells, and  $f(\tau)$  is the effective structure factor for that shell.

Examination of these equations shows that the angle-integrated cross section will go through a jump proportional to  $f(\mu)$  when  $E$  gets large enough so that  $\mu_0 = -1$  for a given value of  $\tau$ . At this energy, a backward directed component of discrete-angle scattering will appear. As the energy increases, this discrete-angle line will shift toward the forward direction. It is clear that the only information that MCNP needs to represent this process in complete detail is a histogram  $P(E)$  tabulated at the values of  $E$  where the cross section jumps. The cross section will then be given by  $P(E)/E$ . The intensity and angle of each of the discrete lines can be deduced from the sizes of the steps in  $P(E)$  and the  $E$  values where the steps take place.

The  $P(E)$  function is computed from  $\sigma(E)$  in `acesix`. Subroutine `thr1od` stores the number of Bragg edges, the Bragg energies, and the  $P$  values at the Bragg edges into the ACE-format ITCE block.

The third ENDF thermal process is incoherent elastic scattering. It occurs for hydrogenous solids like polyethylene and zirconium hydride by virtue of the large incoherent scattering length and small coherent scattering length of hydrogen. The equation describing this process is

$$\sigma(E, \mu) = \frac{\sigma_b}{2} e^{-2EW(1-\mu)/A}, \quad (493)$$

where  $\sigma_b$  is the characteristic bound cross section, and  $W$  is the Debye-Waller integral. The **THERMR** module of NJOY computes the integrated cross section  $\sigma(E)$  for this process and a set of equally probable cosines for each incident energy  $E$ ; it writes them onto the PENDF tape using a special format. These quantities are copied into the ITCE and ITCA blocks of the ACE format in subroutine **thr1od**.

No consistency checking is currently available for thermal files, but a set of plots is provided to help with QA. The plots are prepared as input for the **VIEWR** module, which can generate the final color Postscript files for plotting. A log plot of the total, inelastic, and elastic (if present) cross sections is given first, followed by plots of the average scattering cosine,  $\mu_{bar}$ , and the average energy of the scattering neutrons,  $e_{bar}$ . Perspective views of the energy spectrum for thermal neutron scattering are provided, and several plots of the angle-energy emission for different incident energies are also present. Fig. 56 shows an example of an angular distribution plot.

### 17.13 Dosimetry Cross Sections

The ACE dosimetry data forms another class of MCNP data, and they are handled by the **acedo** sub-module of the ACER group. This class of library provides cross sections to be used for response functions in MCNP; the data cannot be used for actual neutron transport. The information on a dosimetry file is limited to an MTR block, which describes the reactions included in the set, an LSIG block containing pointers to the cross section data for the reactions, and the SIGD block, which contains the actual data. The format for dosimetry cross section storage is different from the format for neutron cross sections. The union grid for linear interpolation is not used; instead, the cross sections are stored with their ENDF interpolation laws. If the file mounted as the input PENDF tape is a real PENDF tape (that is, if it has been through **RECONR**), all the reactions are already linearized, and the interpolation information stored in the SIGD block will indicate linear interpolation for a single interpolation range.

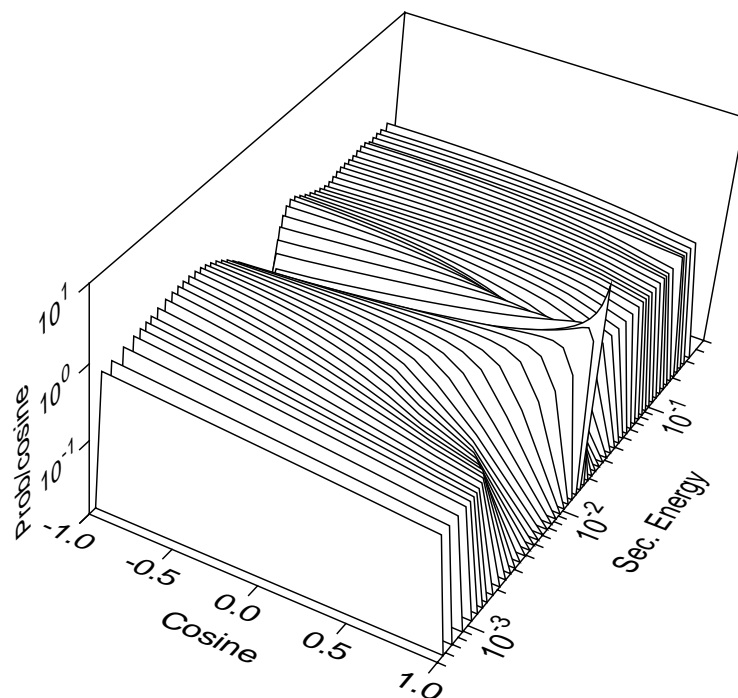


Figure 56: A perspective view of an angle-energy distribution for H in H<sub>2</sub>O.

However, if the file mounted as NPEND is actually an ENDF file, the SIGD block may indicate multiple interpolation ranges with nonlinear interpolation laws.

#### 17.14 Photoatomic Data

Photoatomic data form another ACE class. The data are processed using the `acepa` module, which exports the subroutine `acepho` for formatting the data, and the subroutine `phofix` for editing, listing, consistency checks, and plots.

Photons from direct sources and photons produced by neutron reactions are scattered and absorbed by atomic processes, producing heat at the same time. The existing MCNP “photon interaction” libraries were based on fairly old cross section data and assembled by hand[90, 91]. This version of ACER contains the beginnings of an automated capability to produce these libraries from the latest ENDF/B photoatomic data.

The cross sections for the basic photoatomic process incoherent scattering, coherent scattering, pair production, and photoelectric absorption are given on a union energy grid. Actually, the energies and the cross sections are stored as



logarithms, and MCNP uses linear interpolation on them; therefore, the effective interpolation law is log-log. MCNP determines the mean-free-path to a reaction using the sum of these partial cross sections instead of a total cross section.

If the reaction is incoherent (Compton) scattering, the scattering is assumed to be given by the product of the free-electron Klein-Nishina cross section and the incoherent scattering function,  $I(v)$ . MCNP assumes that this function is tabulated on a given 21-point grid of  $v$  values, where  $v$  is the momentum of the recoil electron given in inverse angstroms. It is easy to extract the scattering function from the section MF=26, MT=504 of the photoatomic ENDF library and to interpolate the function onto the required  $v$  grid.

If the reaction is coherent (Thomson) scattering, the photon will be scattered without energy loss, and the scattering distribution is given by the Thomson cross section times the coherent form factor. The sampling scheme used in MCNP requires the coherent form factor tabulated on a predefined set of 55  $v$  values, and it also requires integrated form factors tabulated at 55 values of  $v^2$ , where the  $v$  values are the same set used for the form factors. These values are extracted from the section MF=26, MT=502, and the integrals are done using the standard NJOY routine `intega`.

Photoelectric absorption results in the emission of a complex pattern of discrete “fluorescence” photons and electrons (which lead to heating) due to the cascades through the atomic levels as the atom de-excites.

The fluorescence part is not coded yet. This section will be completed when the new fluorescence methods have been developed and installed in MCNP. In the meantime, ambitious users may be able to meld the new cross sections computed by the methods discussed in this section with the fluorescence data from the current MCNP library.

### 17.15 Photonuclear Data

Photonuclear data forms a new class of ACE data that has just become available in recent years. These data are handled by the module `acepn`, which exports the call `acephn` for processing the data into ACE format, and the call `phnfix` for editing, listing, consistency checks, and plots. A fairly large number of photonuclear evaluations is available as of this writing. They were originally collected by the Data Section of the IAEA, and they then migrated into ENDF/B-VII.0.

The new ACE photonuclear format differs in some ways from the more familiar continuous-energy format (class “c”). In this format, all emissions (neutrons, photons, and charged particles) are treated symmetrically using blocks with the

style of the particle production blocks from the class “c” format. Each possible reaction product is described by a production cross section, a partial heating value, fractions represented by different reaction channels, and angle, energy, or energy-angle distributions for each reaction channel.

One class of the new evaluations consists of those performed at LANL and a large set of materials using the same methods generated at the Korea Atomic Energy Research Institute (KAERI). These evaluations lump all the photonuclear processes into a single reaction with MT=5 and use subsections of MF=6/MT=5 to represent all the neutrons, photons, and charged particles produced. These are processed by using the energy grid of MT=5 as the union grid. The ACE total and heating values are constructed on this grid. Then the sections of File 6 are processed to generate production cross sections and partial heating values for each of the emitted species. Each emitted neutron or charged particle also has an energy-angle distribution associated with it, represented using the Kalbach LAW=44 format, and emitted photons are represented using LAW=4.

### 17.16 Type 1 and Type 2

ACE library files come in two different types in order to allow for efficiency and portability.

- Type 1 is a simple formatted file suitable for exchanging ACE libraries between different computers.
- Type 2 is a FORTRAN-77 direct-access binary file for efficient use during actual MCNP runs.

There used to be Type 3 using word-addressable random access methods, but these methods were machine specific, and the type has been abandoned. ACER stores all values in memory as real numbers, and it is easy to write them out in Type-2 format, because all fields in that format are also represented by real numbers (except for some of the fields in the header record). The Type 1 format requires that fields that represent integers must be written in integer format, that is, right justified and without decimal points. The output routines in the ACER submodules contain logic to perform this step (see `aceout`, `throu`, `dosout`, `phoout`, and `phnout`).

The ACER user can prepare libraries using either Type 1 or Type 2 output. The advantage of Type 1 is that the files can be easily moved to other machines or laboratories. The advantage of Type 2 is that it is more compact and can be used directly by MCNP with no performance penalties. At any time, ACER can

be used to convert one format to another, or to make a listing of the data from any of the formats (see `iopt` values from 7 through 9 in the input instructions).

### 17.17 Running ACER

The following input instructions are copied from the comment cards at the beginning of the ACER module. Users should always check the actual comment cards for the current version to see if there have been any changes.

```
!---input specifications (free format)-----
!
! card 1
!   nendf    unit for input endf tape
!   npend    unit for input pendf tape
!   ngend    unit for input multigroup photon data
!   nace     unit for output ace tape
!   ndir     unit for output mcnp directory
! card 2
!   iopt     type of acer run option
!             1   fast data
!             2   thermal data
!             3   dosimetry data
!             4   photo-atomic data
!             5   photo-nuclear data
!             7   read type 1 ace files to print or edit
!             8   read type 2 ace files to print or edit
!             set iopt negative for mcnp format
!   iprint   print control (0 min, 1 max, default=1)
!   itype    ace output type (1, or 2, default=1)
!   suff     id suffix for zaid (default=.00)
!   nxtra    number of iz,aw pairs to read in (default=0)
! card 3
!   hk       descriptive character string (70 char max)
!             delimited by quotes
! card 4 (nxtra.gt.0 only)
!   iz,aw    nxtra pairs of iz and aw
!
!   --- fast data (iopt=1 only) ---
!
! card 5
!   matd     material to be processed
```

```

!   tempd   temperature desired (kelvin) (default=300)
! card 6
!   newfor   use new cumulative angle distributions,
!             law 61, and outgoing particle distributions.
!             (0=no, 1=yes, default=1)
!   iopp     detailed photons (0=no, 1=yes, default=1)
! card 7
!   type of thinning is determined by sign of thin(1)
!   (pos. or zero/neg.=energy skip/integral fraction)
!   (all entries defaulted=no thinning)
!   thin(1)  e1 energy below which to use all energies (ev)
!             or iwt weighting option (1=flat,2=1/e)
!             (1/e actually has weight=10 when e lt .1)
!   thin(2)  e2 energy above which to use all energies
!             or target number of points
!   thin(3)  iskf skip factor--use every iskf-th energy
!             between e1 and e2, or rsigz reference sigma zero
!
!   --- thermal data (iopt=2 only) ---
!
! card 8
!   matd     material to be processed
!   tempd     temperature desired (kelvin) (default=300)
!   tname     thermal zaid name ( 6 char max, def=za)
! card 8a
!   iza01     moderator component za value
!   iza02     moderator component za value (def=0)
!   iza03     moderator component za value (def=0)
! card 9
!   mti       mt for thermal incoherent data
!   nbint     number of bins for incoherent scattering
!   mte       mt for thermal elastic data
!   ielas    0/1=coherent/incoherent elastic
!   nmix      number of atom types in mixed moderator
!             (default=1, not mixed)
!             (example, 2 for beo or c6h6)
!   emax      maximum energy for thermal treatment (ev)
!             (default=1000.=determined from mf3, mti)
!   iwt       weighting option
!             0/1/2=variable/constant/tabulated (default=variable)
!
!   --- dosimetry data (iopt=3 only) ---

```

```

!
! card 10
!   matd      material to be processed
!   tempd     temperature desired (kelvin) (default=300)
!
!   --- photo-atomic data (iopt=4 only) ---
!
! card 11
!   matd      material to be processed
!
!   --- photo-nuclear data (iopt=5 only) ---
!
! card 11
!   matd      material to be processed
!
!   --- print or edit existing files (iopt=7-9) ---
!
!   No additional input cards are required.  Mount the old
!   ace tape on "npend".  The code can modify zaid, hk,
!   the (iz,aw) list, and the type of the file.  Use suff<0
!   to leave the old zaid unchanged.  Use just "/" on
!   card 3 to leave the comment field hk unchanged.  Use
!   nxtra=0 to leave the old iz,aw list unchanged.  The
!   code can modify zaid, hk, and type of file.
!
!   Exhaustive consistency checks are automatically made on
!   the input file.  If ngend.ne.0, a set of standard ACE plots
!   are prepared on unit ngend as plotr input instructions.
!
!-----

```

**Card 1.** ACER uses the information from the ENDF tape mounted on unit `nendf` for angle, energy, energy-angle, and photon emission distributions, and it uses the data on `npend` for the unionized and linearized cross sections. The latter file should have been processed through [RECONR](#), and maybe [BROADR](#). If it wasn't, ACER will still work, but the energy grids may not be quite right. The `ngend` unit is only needed for input if the old 30×20 photon production matrix is to be constructed; otherwise, set it to zero. In addition, `ngend` is used for plotting output (if available) when one of the print or edit options is selected

(see `iopt=7` below; set it to zero to suppress plotting output. Unit `nace` is the main output tape for the ACE-format library, and unit `ndir` will contain a single line of text intended to be edited and incorporated into a directory for a big multi-material ACE library.

**Card 2.** The value of `iopt` specifies the kind of ACE data being produced, as indicated in the instructions. The long print option, `iprint=1`, produces a complete, interpreted listing of the ACE data. The shorter print options just put out progress information from the ACER job and a brief listing of the header information for the library that was generated. The `ntype` parameter specifies whether the output library will be in ASCII or binary form. In MCNP jobs, materials are identified by their “zaid” numbers (rhymes with “staid”); they are constructed by using the value  $1000 \times Z + A$ , appending the value of `suff` (the suffix), and then adding a letter that indicates the library class (“c” for continuous, “t” for thermal, *etc.* (see Table 23). For example, 92235.70c denotes a continuous (fast data) library entry for  $^{235}\text{U}$  from ENDF/B-VII. Thermal zaid numbers are actually alphanumeric before the dot; see Card 8. Finally, `nextra` is the number of extra `iz`, `aw` pairs of values to be read in on Card 4.

**Card 3.** This card contains a descriptive character string up to 70 characters long. It must be delimited by ‘ characters and terminated by the / character.

**Card 4.** Read in `nextra` pairs of numbers `iz` and `aw` for photoatomic data. Use as many cards as necessary.

**Card 5.** This is the first card for a fast data library run. It specifies the ENDF MAT number and the absolute temperature for the material to be processed. ENDF MAT numbers are 4-digit numbers. For the earlier versions of ENDF/B, they were assigned in an arbitrary way; for example, 1276 was  $^{16}\text{O}$  for ENDF/B-IV and 1395 represented  $^{235}\text{U}$  for ENDF/B-V. For ENDF/B-VI and later, a systematic scheme has been selected that allows the same MAT number to be used for all the various sub-libraries (for example, neutron data, thermal data, incident proton data, *etc.*). This scheme is based on using  $Z$  to get the first two digits. The second two digits are chosen to be zero for elements, and for normal isotopes, they step in units of 3 up and down around 25, the value for the lowest isotope of the normal stable group of isotopes. This leaves room for two isomers for each isotope in between. Examples include 9225 for  $^{234}\text{U}$ , 9228 for  $^{235}\text{U}$ , and

2200 for natural Ti. If the temperature is greater than zero, the input PENDF tape must have been run through [BROADR](#).

**Card 6.** The flag **newfor** is equal to 1 if the new cumulative format for angular distributions, the LAW=61 format for energy-angle data, and the particle production sections are desired; otherwise, it is zero. The default is **newfor**=1, suitable for use with MCNP4C and subsequent versions. The flag **iopp** determines whether the newer detailed photon data option is used (preferred), or whether the older 30×20 photon production matrices are to be generated. Remember that if the latter option is selected, [GROUPT](#) must be run before ACER to generate multigroup versions of the photon production matrices for all reactions, and the resulting GENDF tape must be coupled to ACER using the **ngend** input parameter.

**Card 7.** Thinning of the union energy grid can be performed using several options as described in detail in Section [17.1](#) above. Defaulting the entire card by entering only / results in no thinning. This is preferred.

**Card 8.** This card starts the input of parameters for the thermal library option. The material MAT number and absolute temperature are given. The default temperature is 293.6K and the default **tname** is generated from ZA. Therefore, the simplest version of this card would consist of a MAT number followed by /. Check the discussion above for Card 5. In almost all cases, an entry for **tname** is desirable. Examples are “LWTR” for H in light water (or “HH2O” for hydrogen in water), “GRAPH” for graphite, “ZRZRH” for zirconium in zirconium hydride, and so on.

**Card 8a.** MCNP needs to know the **zaid** values to get the fast data needed to go with a particular set of thermal data. For a thermal set like HH2O, only **iza01**=1001 would be needed. For a mixed moderator like benzene, values for both **iza01** and **iza02** must be given (*e.g.*, 1001 and 6000). See **nmix** below. The third input parameter allows for the aliases 6012 and 6000, if needed.

**Card 9.** The value **mti** must correspond to one of the values used for this material in the [THERMR](#) runs that generated the input PENDF tape (see Table [25](#)). The number of bins to use for the equally probable bins for the outgoing neutron spectra is defined by **nbint**; the default value is 16. The parameter **mte**

defaults to zero; a nonzero value is only needed for materials that show elastic scattering (see Table 25). The value `ielas` indicates whether this elastic scattering is coherent or incoherent. In the ENDF/B thermal evaluations, some isotopes for mixtures are represented like water, which describes the scattering from hydrogen bound in water, and some are given like benzene, which describes the scattering from the benzene molecule normalized to the hydrogen cross section. The parameter `nmix` is used to tell ACER about this effect. For the existing ENDF/B evaluations, the user should use `nmix=2` for benzene; the user should use `nmix=1` for all other materials. The parameter `emax` defines the maximum energy to be used for the thermal scattering treatment. This value should be coordinated with the value of `emax` in `THERMR`. A number around 4 eV is reasonable for most problems. The default for this parameter is 1000., which means that the code will determine the upper limit from the data in MF=3 on the PENDF tape. Thus, the value used in `THERMR` is passed into ACER without the user having to check it. The last parameter on Card 9 is `iwt`. As described in Section 17.12, the weighting pattern for probability bins for emitted thermal neutrons can be flat (that is, equally probable bins), or it can be variable in the pattern 1, 4, 10, 10,..., 10, 4, 1 in order to better sample the outlying wings of the energy distribution. The default is variable. Better yet, for modern MCNP 5.1.50 and later, use `iwt=2`, which gives a continuous distribution in outgoing energy, eliminating the discrete energy spikes.

The simplest version of Card 9 would contain only `mti` followed by `/`. This works for many materials, including water, heavy water, and benzene, but if an elastic (coherent or incoherent) component is present then the appropriate `mte` value must also appear.

**Card 10.** This card is used for dosimetry libraries only. It specifies the material MAT number and absolute temperatures. See the discussion of `mat` and `tempd` for the fast (continuous) libraries.

**Card 11.** Photoatomic libraries require only the single parameter `matd`. For ENDF/B-VII input, this will be a number like 100 for hydrogen or 9200 for uranium.

**Card 12.** Photonuclear libraries require only the single parameter `matd`. See the discussion of `mat` for the fast (continuous) libraries.



Table 25: Conventional values for the thermal MT numbers (MTI and MTE) used in ACER and [THERMR](#) for ENDF/B-VII

| Thermal Material      | MTI Value | MTE Value |
|-----------------------|-----------|-----------|
| H in H <sub>2</sub> O | 222       |           |
| D in D <sub>2</sub> O | 228       |           |
| Be metal              | 231       | 232       |
| Graphite              | 229       | 230       |
| Benzine               | 227       |           |
| Zr in ZrH             | 235       | 236       |
| H in ZrH              | 225       | 226       |
| Be(BeO)               | 233       | 234       |
| O(BeO)                | 237       | 238       |
| H in Polyethylene     | 223       | 224       |
| U(UO <sub>2</sub> )   | 241       | 242       |
| O(UO <sub>2</sub> )   | 239       | 240       |
| Al                    | 243       | 244       |
| Fe                    | 245       | 246       |

**Editing Runs.** No special input cards are required for editing runs. The class of data in the library is automatically determined from the ZAID suffix. The type of the output library is determined by **ntype** on Card 2. Changes can be made in the fields **zaid**, **hk**, and in the (**iz**,**aw**) list. One common use for these editing parameters would be as follows. A user runs several isotopes, one at a time, using the default ZAID of “.00c”, and 1/E integral thinning. Later, the user decides that all these materials should go into a particular library with the suffix “.77c” and the comment field “ENDF/B-VII library 7 for thermal reactor applications.” ACER can handle these changes.

The following is a typical ACER input deck for producing a continuous-energy file (class “c”):

```
acer
20 21 0 31 32
1 0 1/
'ENDF/B-VII U-238'/
9237 293.6/
/
/
acer
```

```

0 31 33 34 35
7 1 1/
'ENDF/B-VII U-238'/
viewr
33 36/
stop

```

It assumes that the ENDF file for  $^{238}\text{U}$  from ENDF/B-VII has been mounted on unit 20 (**tape20**) and that the corresponding PENDF tape (after running through **RECONR**, **BROADR**, *etc.*) has been mounted on unit 21 (**tape21**). We have used **iopt**=1 for fast continuous data, suppressed the output listing with **iprint**=1, and requested Type-1 output (**itype**=1). Any desired descriptive line may be used, but some library schemes might like to define special arrangements of text. The proper ENDF MAT number for  $^{238}\text{U}$  is 9237, and we are taking the first temperature produced in the **BROADR** run, namely, 293.6K. This corresponds to 0.0253e-6 MeV, the standard base temperature for MCNP data files. We have taken the default values for **newfor** and **iopp**, so we expect to see the new formats and the detailed photon data. We have also taken the default of no thinning, which is preferred with modern large computers. The output ACE file and XSDIR line will appear on **tape31** and **tape32**. The second ACER run is used to provide QA checks. It reads in the Type-1 file from **tape31** and writes out a new Type-1 file and a new XSDIR line on **tape34** and **tape35**, respectively. While doing this, it runs the consistency checks and makes a set of plots on **tape33**. If the consistency plots find an  $E' > E'_{max}$  error that can be repaired, the modified result will be on **tape34**. Finally, the **VIEWR** module is run to convert the information on **tape33** into color Postscript plots on **tape36**. The actual step of reading the ACE file is a useful QA step, as are the consistency checks and plots. In addition, it is good practice to run the output ACE file immediately into a simple MCNP test job to see if it really scans correctly. This is easy to do by incorporating the input example above and the MCNP test input into a single script.

The second input example for ACER is for producing a thermal class “t” library for hydrogen in water at a temperature of 800K using continuous energy distributions:

```

acer
20 21 0 31 32

```

```

2 0/
'1-h-1 in h2o at 800k from endf-vii'/
125 800 'hh2o'/
1001/
222 64 0 0 2/
acer
0 31 22 33 34/
7 1/
'1-h-1 in h2o at 800k from endf-vii'/
viewr
22 23/
stop

```

Here we have the additional entry `tname='hh2o'`, which is used to construct the ZAID value (which will be “hh2o.00t”). We have used `mti=222`, the standard value for hydrogen in water (see Table 25) and requested 64 bins with the continuous tabulated data the outgoing neutron spectrum. Experience has shown that more bins than the default of 16 are often desirable.

### 17.18 Coding Details

ACER begins in the `acer` routine provided by module `acem` by reading the user’s input. The input varies according to whether “fast”, “thermal”, “dosimetry”, “photoatomic”, or photonuclear” data are wanted, or if editing or type conversion is desired. See `iopt`. For regular processing runs (`iopt=1-5`), input ENDF and PENDF tapes are required, the input GENDF tape is only needed if a photon production matrix is to be constructed. For edit runs, the input ACE file is mounted on the PENDF unit, and the GENDF unit is used for plotting output, if desired. The code then branches to a different subroutine (in a different module) for each different value of `iopt`.

Processing of fast data is controlled by `acetop` (which is in the `acefc` module). It begins by opening the ENDF, PENDF, and GENDF units, and by opening a scratch file MSCR used to accumulate the input for the `acelod` procedure. Subroutine `first` is then called to read the MF=1 and MF=2 data from the input tapes and to prepare the corresponding data on MSCR. It copies the TAPEID record and Hollerith descriptive data on the PENDF tape to MSCR, and it processes the directory on the ENDF tape in order to set flags that depend on which reactions and data types are present. For example, `mt19` is

set if a distribution is provided for MT=19, in addition or instead of the more standard MT=18. The global variables **nf12s**, **mf1x**, and **gmt** are used to keep track of the reactions involved in computing photon production. For the new format (**newfor**=1), the MT=3 reactions that imply the production of neutrons or charged particles (either directly or as a residual) are identified. The MF, MT, and product identity for each such reaction is stored in the arrays **kprod**, **mprod**, and **iprod**, respectively, for a total of **nprod** items. Subroutine **first** continues by standardizing and copying the fission neutron yield sections (see **tabize**), by writing a dummy File 2 on **mscr**, and by copying the probability tables in MT=153, if present. The next step is to read through File 3 on the input PENDF tape to make an ordered list of all the thresholds in the array **ethr**. The thresholds for each particle production are also determined (see **t201**, **t203**, **t204**, *etc.*, for neutrons, protons, deuterons, *etc.*). The last step is only performed if the **newfor** option has been selected. The routine reads through the subsections of File 6 on the input ENDF tape and adds any additional particle production sections found into the arrays **kprod**, **mprod**, and **iprod**, and it updates the production thresholds **t201**, **t203**, *etc.*. The final total of **nprod** elements are sorted into order by first MT and then particle identity, and subroutine **first** returns.

If necessary, **convr** is called next. It converts MF=12 photon transition probability arrays (**lo**=2), if present, into the photon yield format (**lo**=1) by tracing all the cascades through the photon level structure. The results are written on NSCR2. Sections of File 13 are simply copied to the scratch tape. While working, the routine adds any additional thresholds associated with photons in MF=13 to the **ethr** list, and it stores any discontinuities found in **disc**. It is important to make sure these discontinuities appear in the final energy grid as sharp steps. If MF=12 was converted, corresponding isotropic photon angular distribution sections are constructed and written into File 14 on the scratch tape. Other sections of File 14 are copied. If File 6 is present (ENDF-6 format evaluations only), **convr** checks to see whether photon production subsections are present. If so, it converts them into specially defined MF=16 sections on the scratch tape. The resulting scratch tape contains sections for MF=12, MF=13, MF=14, and MF=16. The updated list of threshold and the list of are sorted into order, and the discontinuities are printed out on the listing for the user's information.

Returning to **acetop**, subroutine **unionx** is called to construct the union energy grid. It starts by checking the probability tables, if present, and setting

the flag `mtcomp` if an overlap with `MT=4` is indicated. It continues by reading in the energy grid of the total cross section on the PENDF tape. In the process, it watches for energies from the lists of thresholds and photon discontinuities and adds corresponding sharp steps by plus and minus one in the seventh significant figure to the ACE energy grid. If integral thinning was requested, it computes the starting weighted integrals for the total cross section. Note that the energy grid, the total cross sections, and the weighted integrals are stored on a `loada/finda` tape for later use. If `RECONR` and `BROADR` were used to produce the PENDF tape, this is the desired union grid. If another file is used for PENDF input, ACER will still work, but the grid might not be really correct. If integral thinning was requested, subroutine `unionx` now reads forward on the PENDF tape to find the capture cross section, `MT=102`, and read through the section computing the capture integrals and storing them on the `loada/finda` tape. After printing out the original integrals, it carries out the integral thinning procedure described in Section 17.3, taking care not to remove the breaks at the thresholds and photon-production discontinuities. When an energy grid has been found that satisfies the input target, `UNIONX` prints out a table of the final resonance integrals by energy bands. This thinning process is somewhat obsolete with modern large computers, and it probably will not be maintained in the future.

A different process is used in `unionx` to generate a union grid for incident charged-particle data classes. The `RECONR` module is not used for incident charged particles, so the routine reads through File 3 and constructs a unionized grid appropriate for linear-linear interpolation. It then searches forward to find `MF=6/MT=2` and adds in the energy points found there. It then reads back through the energy grid obtained so far and adds additional energy points to large intervals. The parameter `step=1.2` is used to add these additional grid energies. The input PENDF file is backed up to `MF=3` for the next step.

Now that the complete union energy grid has been determined, `unionx` reads through File 3 to write all the other desired reactions onto this new energy grid. Some reactions are eliminated as “redundant;” for example, `MT=4` (total inelastic) can be removed, unless it will be needed later for photon production. MCNP is sensitive to errors in the reaction thresholds. `RECONR` normally makes sure the the threshold is slightly greater than the theoretical value. This routine will print out a message if it finds a reaction threshold that is lower than the theoretical value. While writing out the new sections of File 3, the total cross section is recomputed to be exactly equal to the sum over the partial reactions

at each energy grid point and stored using `loada/finda`. When this process is complete, the file `nscr` contains all the unionized reaction cross sections. Subroutine `unionx` now writes out the new total cross section on the file `mscr`, and then copies over all the new reaction sections from `nscr`. The file `mscr` now has a complete File 3.

Next, `acetop` calls `topfil` to prepare new versions of MF=4, MF=5, and MF=6 on `mscr`. First, `ptinit` is called to precalculate some of the constants needed for converting angular distributions to equally probable bins. After the constants have been calculated, `topfil` starts a loop over all the sections for Files 4, 5, and 6 on the ENDF tape. Some reactions are just skipped entirely; for example, if `first` found a distribution for MF=19 and set the `mt19` flag, the distribution for MT=18 is removed. For the new format (`newfor=1`), sections of File 4 (angular distributions) are simply copied for later processing. For the old format, the sections are converted into a representation giving 32 equally probable cosine bins for each incident energy (with appropriate exceptions for completely isotropic sections or energy values). Angular distributions using Legendre coefficients are converted using `ptleg`, and tabulated distributions are converted using `pttab`. A special ENDF option, flagged by `lft3=3`, directs that the section is divided into low- and high-energy parts. The high-energy part is always tabulated.

Continuing with `topfil`, sections of File 5 are just copied for more processing later. For sections of File 6 with the old format requested (`newfor=0`), sections are scanned to see if any use tabulated sections with laws other than the Kalbach representation (`lf=1` and `lang=2`). If so, the routine backs up and calls `fix6` to convert the distribution into `lf=7` form, a form the older versions of MCNP can understand.

Subroutine `fix6` produces a section with the  $E, \mu, E'$  ordering in the laboratory frame using 33 equally spaced cosine values for each incident energy. The original data can be in either Legendre coefficient form or in tabulated form. If the data are given in the CM frame, a conversion to the laboratory frame is carried out, but no attempt is made to refine the energy and cosine grids to provide a really good representation in the laboratory. If the input data are sufficiently dense, the results are not too bad.

Returning to `topfil` at “work on file 6,” data for LF=6 (phase-space distributions) are just copied. Sections with LF=1 (tabulated) are also just copied, except if there is more than one interpolation range, or if nonlinear interpolation is specified, `cptab` is called to linearize the representation and reduce it to one

interpolation range as required by the ACE format. For LF=2 (two-body angular distributions) when the new formats have been requested (`newfor=1`), the ENDF data are just copied to the `mscr` file. For the old formats, the data are converted into 32 equally probable cosine bins using either `ptleg` for Legendre data or `pttab` for tabulated distributions. LF=5 sections (charged-particle elastic scattering) are copied. For LF=7 (either original  $E, \mu, E'$  data from ENDF or data converted using `fix6`), the overall angular distribution is computed by integrating over all outgoing energies. The TAB2 record that defines the loop over incident energies in the ENDF format is converted to a TAB1 record to hold the new overall angular distribution. For the old format (`newfor=0`), this angular distribution is converted into 32 equally probable cosine bins using `pttab`. The TAB1 records for the various cosines described by LF=7 are copied to the output file. Thus, the LF=7 sections on `mscr` are almost in standard form, except for the extra overall angular distribution.

When `topfil` is complete, `acetop` calls `gamsum`, which computes the total photon production cross section on the union grid. It does this by adding the contributions from the MF=12 photon yields times the corresponding MF=3 cross sections, the MF=13 photon production cross sections, and MF=16 yields times the corresponding MF=3 cross sections. The results are written out using MF=13, MT=1.

Next, subroutine `gamout` is called to add the photon distribution information to the main scratch tape. If no GENDF tape is available, `gamout` simply copies MF=14, MF=15, and MF=16 from the scratch tape prepared by `convr`. However, if the GENDF tape is present, it prepares the 600-word photon production matrix. The first step is to read through the input tape extracting the photon group boundaries and adding up all the photon production reactions into one matrix. The code then loops over neutron groups converting the outgoing photon groups into equal-probability bins and computing the single discrete photon in each bin that conserves energy. Finally, the resulting 30-by-20 matrix is written onto the output tape using the identification MF=15, MT=1. This process is now obsolete and may not be maintained in future versions.

Upon returning to `acetop`, the tape `mscr` is completed by adding a material-end, or MEND, record. Subroutine `acelod` is called with `mscr` as its input file. It reads through the file in order and stores the numbers into memory in ACE format. The first step is to define the ACE `zaid` value based on  $1000 \cdot Z + A$  for this material, plus a numerical suffix provided by the user (the default is “.00”), plus a letter suffix appropriate for this class of data (see Table 23). For

the **acefc** module, the data class is completely determined by identity of the incident particle in **izai**. The routine then counts all the reactions that survived **unionx**, using slightly different rules for the different incident particles. Here, **ntr** is the count of all the reactions present on the input **mscr** file, and **nr** is the subset of reactions that actually determines the transport and contributes to the total reaction cross section. The routine then reads through File 1 and stores the total and prompt fission  $\bar{\nu}$  data, if present, into the temporary areas **nut** and **nup** for future use. The routine also reads through File 2 and stores in unresolved-range probability tables, if present, into a temporary area **urd**.

Next, the energy grid of the total cross section from MF=3 is read in starting at pointer **esz**. This determines the number of energy points in the union grid, **nes**, which can then be used to compute the pointers to the other cross sections in the main cross section block (namely, **it** for total, **ic** for absorption, **ie** for elastic, and **ih** for heating). The blocks for supplemental cross sections can also be assigned; for example, **lqr** for reaction Q values, or **lsig** for reaction cross section pointers. With all these pointers computed, **acelod** can simply read through File 3 and store all the cross sections, Q values, and cross section locators in their assigned slots. The total and absorption cross sections are summed up from their parts during this process. Because of the complexities of handling the various possible incident particles, this process is divided into three parts: a loop over reactions producing the incident particle, a loop over reactions that do not produce the incident particle, and a pass to go back and add MT=3 (nonelastic) and MT=4 (inelastic), if they are needed for photon production. After MF=3 has been read, the fission  $\bar{\nu}$  data can be stored in the main memory block.

The next step is to assign the LAND and AND blocks after the cross section data, and to read in the angular distribution data, store them in the AND block, and save the pointers in the LAND block. Coupled energy-angle sections from File 6 with LF=1 or LF=6 don't have separate angular distributions, and they are flagged by putting the value -1 in the LAND block for the reaction. For the remaining reactions, the TYR block is filled in with the particle yield for the reaction — for example, 2 for an (n,2n) reaction — and the sign of the TYR entry is adjusted to be positive for laboratory-frame distributions and negative for CM-frame distributions. Sections that are completely isotropic are flagged by putting 0 in the LAND block for the reaction, and anisotropic sections are processed by calling **acensd** (for neutron scattering distributions) or **acecpe** (for charged-particle elastic distributions).



In `acensd`, a loop is set up over the incident energies in the section. For the old format, the first record has always been adjusted to be a TAB1 record containing the 32-bin angular distribution, and it can be stored directly into the cells of the ACE image. For the new format, there are several possibilities. If `LF=7`, the distribution in the TAB1 record is already in the desired form. For tabulated `MF=4` data, `pttab2` is called to produce a properly normalized distribution. For `MF=4` Legendre coefficient data, `ptleg2` is called to reconstruct the pointwise angular distribution adaptively and make sure it is properly normalized. For Legendre data in File 6, `ptleg2` is used in the same way. For tabulated data in File 6, the LIST representation is transformed into a TAB1 representation, and `pttab2` is used to produce the properly normalized distribution. With a simple tabulated distribution in place, `acensd` can now integrate to form the cumulative density distribution, double check the normalization, and write the results into the proper ACE memory locations. Allowance is made for the `LTT=3` format, where separate low- and high-energy sections are given, and distributions that are found to be completely isotropic are removed by setting their entry to zero in the LAND block.

Subroutine `acecpe` handles charged-particle elastic scattering, supporting the new ACER capability to produce libraries using charged-particle classes. As this option is fairly new, the routine prints out a number of intermediate results on the output listing after the header “working on charged-particle elastic,”

Next, the LDLW and DLW blocks are assigned following the angular data, and the energy distribution data are read and stored. Reactions from the different ENDF files are processed through different paths. Sections of File 5 go to `acelf5`. Sections of File 6 go to `acelf6`. Sections of File 4 (except for elastic scattering) are represented by `LAW=3` discrete-level distributions that provide the parameters that MCNP uses to compute emission energy after discrete-inelastic scattering.

In `acelf5`, each section of energy distribution data is examined for its “LAW” and stored accordingly. The analytic laws from ENDF File 5 are simple to store; there is basically a one-to-one correspondence between the ENDF quantities and their ACE equivalents (except, eV are converted to MeV). Tabulated sections in File 5 (`LF=1`) are converted into the `LAW=4` cumulative density function format by computing the cumulative probability function and storing tables of  $E'$ ,  $P(E')$ , and  $C(E')$  for each  $E$ .

Subroutine `acelf6` is used to process energy-angle distributions from sections of File 6. The particle yield for data from `MF=5` is determined by the MT

number; for example, the yield is 2 for MT=16, the (n,2n) reaction. On the other hand, subsections of File 6 contain explicit values for the particle yield, and the yield may vary with  $E$ . In addition, there may be more than one subsection describing emission for a particle. An example of this is  $^{19}\text{F}$  from ENDF/B-VI, which has two subsections for emitted neutrons (first neutron and second neutron). To handle all these complications, ACER reads through the entire section of MF=6 data for a given reaction, looks at all the yield tabulations, and computes the total yield for the reaction. It types out messages if multiple subsections are found for one particle, if energy-dependent yields are found, or if noninteger yields are found.

The case of constant integer yields is simple; the value is stored in the **tyr** array just as for MF=5 reactions. The sign of the yield in **tyr** is positive for laboratory data and negative for CM data.

Generalized yield data are stored as a table of  $E$  and  $Y(E)$  starting at location **ntyr** with respect to the start of the DLW block. The value of **ntyr** is stored in the **tyr** array as  $100+\text{ntyr}$ . The sign of this value is positive for laboratory data and negative for CM data. The code then repositions the input file to the start of the section for the current reaction in order to read in the distributions.

As each subsection is read, the yield tabulation is converted into a fractional probability for this subsection by dividing by the generalized yield. There are five different types of secondary particle distributions that must be processed: Legendre data (LAW=1, LANG=1), Kalbach data (LAW=1, LANG=2), tabulated data (LAW=1, LANG>2), angle-energy data (LAW=7), and phase-space data (LAW=6).

The first three share the same loop over incident energy  $E$ . For each secondary energy  $E'$ , the probability  $P(E')$  and the angular representation are read from the input file, and the cumulative probability density  $C(E')$  is computed. For Kalbach data, the only angular parameter is the pre-equilibrium fraction  $r$ . The corresponding slope parameter  $a$  is computed using the function **bachaa**, and both  $r$  and  $a$  are stored in the table using the ACE Law 44 format.

Neither Legendre data nor tabulated angular distributions will appear for the old format (**newfor**=0), because such sections were intercepted and converted to LF=7 in **topfil**. For the new format, the Legendre distributions are converted to tabulated form using **ptleg2** and the tabulated distributions are converted to properly normalized tabulations. In both cases, the result is integrated to obtain the cumulative density function. The result is stored using the new ACE format, LAW=61.

LAW=7 data are handled in a separate incident-energy loop, which stores data using the ACE Law 67 format. The individual energy distributions on the input file have already been normalized and are ready to be stored in the `xss` array. Note that the values of `intmu` and `nmu` were passed to this part of the code using two nonstandard locations in the TAB1 record that was originally the TAB2 record controlling the loop over  $\mu$  but now contains the angular distribution in 32 equal-probability bins.

The phase-space distribution doesn't need an incident-energy loop. It is only necessary to store the values of `apsx` and `npxs` into the `xss` array and to compute a single set of  $E'$ ,  $P(E')$ , and  $C(E')$  values for  $E'_{\max} = 1$ . The normalization factor  $C_n$  is obtained from the integration over  $E'$  in order to guarantee that  $C(E'_{\max} = 1)$ .

Once the secondary-particle energy distributions and angle-energy distributions have all been stored, the GPD pointer is computed to point to the start of the photon production data. The total photon production cross section itself is simply read from the section MF=13, MT=1 on the input tape and stored starting at GPD. The next step depends on whether photon production matrices were requested by giving ACER a nonzero value for the input GENDF tape. If so, the matrix is read from the section MF=15, MT=1 on the input tape and stored in memory just after the photon production cross section. If not, a dummy matrix of 600 zeros is stored. The ACE fast library is finished.

At this point, `ntrp` is set, `acelod` calls `acelpp` to store detailed photon data. The code goes through the main energy grid changing eV to MeV with all energies adjusted to have a maximum of nine significant figures. The summation cross sections, total and absorption, are also truncated to nine-digit precision.

The final step in `acelod` is to call `acelcp` to load the particle production data. For incident neutrons, these are charged-particle production blocks, but for incident charged particles, these blocks are for all particles not the same as the incident particle, and neutron emission is included.

Now that all the fast ACE data have been stored into memory, `acetop` calls `aceprt` to print the data on the output listing file. The amount of information printed depends on the value of the input parameter `iprint`. Finally, `acetop` calls `aceout` to write out the ACE fast library.

The output library file can be written in Type-1 or Type-2 format, depending on the value of `itype`. As described above, Type 1 is a simple formatted file suitable for exchanging ACE libraries between different computers, and Type 2 is a Fortran direct-access binary file. The problem here is that Type 2 files are

written with all data as real numbers (except for some of the fields in the header record). Some of these numbers represent integers, and the Type 1 format requires that these numbers be written into their fields in integer format, that is, right justified and without decimal points. In order to handle both these file types in a portable way, subroutine **acelod** first stores all values into memory as real numbers in the array **xss**. Therefore, the contents of memory can be written out in Type 2 format with no further processing. In order to convert to Type-1 formats, subroutine **change** is used. Subroutine **change** knows the type (real or integer) of every word in the ACE format. When converting from internal Type-2 data to Type-1 output, it uses **typen** to write the number directly to **nout** using the appropriate format (I20 or 1PE20.12).

Processing of thermal data is controlled by subroutine **acesix** from module **aceth**. It starts by finding the desired temperature on the input PENDF tape. The inelastic and elastic cross sections are copied to a scratch file **nscr**. The scratch file is then rewound, and the inelastic cross section is read again to determine the maximum thermal energy **emax**.

If the elastic component is coherent, the input cross sections from **nin** are divided by  $E$  to get a stair-step function, which is written to the output file. If the elastic component is incoherent, the incident energies and equally probable emission cosines are read from MF=6 on **nin** and the corresponding cross sections are read from MF=3 on **nscr**. All data are stored into memory in ACE format and then written onto **nout**.

The processing of inelastic scattering is more complex. After the proper section on File 6 is located, a uniform or variable pattern of weights is constructed in **wt(i)**. The energy grid is obtained from File 6 on **nin**, and the corresponding cross sections are read from MF=3 on **nscr**. The secondary-energy spectrum for each incident energy is converted into bins using the weight pattern in **wt(i)**, and the single  $E'$  that conserves the average energy for the bin is computed. The **nang** equally probable cosines for this new  $E'$  are obtained by interpolation. Once all of the **nbin\*nang** events have been computed and stored in memory, they are copied out to **nout**.

At this point, all the thermal data have been computed, and **nout** is passed to subroutine **thrlod** for storing into memory in ACE format. This memory image is then printed out using subroutine **thrprt**, if desired, and written to the final Type-1 or Type-2 output file using **throu**.

Subroutine **thrfix** is the other call exported by module **aceth**, and it can be called from ACER for editing or listing thermal files that have already been

produced. It begins by reading the input Type-1 or Type-2 file into memory. It then allows for editing the ZAID value, the descriptive string, or the (iz,aw) list. The thermal ACE file can be printed out by using `thrprt`, and the file can be written out in either Type-1 or Type-2 format using `thrwrt`. If the input unit normally called `ngend` is nonzero, it is interpreted as `nplot` and used by subroutine `tplots` to output a file for `VIEWR` that will generate a set of color Postscript plots of the thermal scattering data.

Processing of dosimetry data is controlled by subroutine `acedos` from module `acedo`. It begins by allocating space for the main ACE container array `xss(nxss)` and a scratch array `scr` that will be used to read in the ENDF data records. It then opens the input file, determines what ENDF version is being used, and searches for the desired MAT and temperature (`matd` and `tempd`). This option is normally used directly on ENDF-style evaluations for dosimetry cross sections that just give the cross sections and omit the additional distributions needed for full transport calculations. These are usually threshold reactions, and zero temperature works fine. The dosimetry option can also be used with PENDF-style input containing broadened capture cross sections, and in this case, a non-zero value for `tempd` would be appropriate.

The `acedos` routine searches for the first reaction in File 3, defines locators for the MTR, LSIG, and SIG blocks by assuming that there are no more than `nmax=100` reactions present, and it begins a loop over all the reactions in File 3.

For each reaction, its MT identifier is stored in the MTR block, the current pointer value is stored in the LSIG block, and the interpolation table and cross sections are stored in the SIGD block starting at the current pointer value. The pointer is then increased by the number of words stored, and the reaction loop continues. Note that if the input tape is real PENDF tape (that is, if it has been through `RECONR`), the cross sections will have been linearized onto a union grid. There will only be a single interpolation range for each reaction. However, if the input file was an ENDF tape, there may be several interpolation ranges specifying nonlinear interpolation laws for a given reaction, and the energy grids for different reactions may be different.

When the reaction loop has been completed, the excess space in the MTR and LSIG blocks is squeezed out, and the scratch storage array is deallocated. The final steps are to construct the ZAID value for the material using the “y” class, to call `dosprt` to print the results, and to call `dosout` to write the ACE dosimetry library file.

Subroutine **dosfix** is the other call exported by module **acedo**. It is used when the user requests editing or printing of an ACE dosimetry file separate from the production of the file. The routine reads in input Type-1 or Type-2 ACE file into memory and allows the user to adjust the ZAID value for the material or to change the comment string and (iz,aw) list. It calls **dosprt** to print the file and **dosout** to write out the modified file. Note that the type of the ACE file can be changed from 1 to 2 or from 2 to 1 at this point. No consistency checks or cross-section plots are currently provided for dosimetry libraries.

The **dosout** routine calls **typen** directly to cause Type 1 fields to be written in the proper floating-point or integer format, if requested.

Processing of photoatomic data is controlled by subroutine **acepho** in module **acepa**. It starts by allocating an area for scratch storage **scr** and the main ACE container array **xss**. The input file is opened and scanned to determine what ENDF version is being used. The requested material **matd** is then located, and **acepho** reads in the energy grid for the total cross section, **mt=501**, which will be used as the union grid for all the photoatomic reactions, starting at pointer **esz**. The number of energy points in the union grid is **nes**, and that value can now be used to compute the pointers **iinc**, **icoh**, **iabs**, and **ipair**, representing incoherent scattering, coherent scattering, photoelectric absorption, and pair production, respectively. The **acepho** routine then reads through File 23 on the input tape, extracts the cross sections for each of the reactions using the energy points of the union grid, and stores the cross sections at the appropriate pointer values. Note that the cross sections and energies have not been converted to log form at this point, but the energies have been converted to MeV. The detailed sub-shell cross section for photo-ionization supported by the most recent version of the ENDF-6 photoatomic format are not supported in this version of **acepho**.

The pointers to the **jinc** block for incoherent scattering functions, the **jcoh** block for coherent form factors, the **jflo** block for fluorescence data, and the **lhnm** block for heating numbers are now computed in the storage area just following the cross sections.

The **jcoh** block uses a fixed grid of 55 values for the momentum transfer of the recoil electron (in inverse Angstroms) specified in the parameter array **vc**. The code first reads through MF=27, MT=502 and interpolates for the values of the coherent form factor at these 55 recoil values. They are stored in the **jcoh** block as the second block of 55 numbers. The code then loops through the 55 recoil values again, computing the cumulative integral of the coherent form factor for each recoil value and storing them as the first group of 55 words

in `jcoh`. The anomalous form factors supported by the latest version of the ENDF-6 format are not yet supported by this version.

The incoherent scattering function is tabulated on a fixed grid of 21 values for the momentum of the recoil electron (in inverse Angstroms) that is given in the parameter array `vi`. The values are obtained by interpolating in the section MF=27, MT=504 from the input file. At the same time, the contribution to the heating from incoherent photon scattering is computed on the union grid with subroutine `iheat`.

The calculation of fluorescence data for photoelectric absorption is not complete in this version. A message to the user is provided.

Finally, the scratch storage is deallocated, the ZAID value is generated for class “p”, `phoprt` is called to prepare the output listing for the photoatomic data, and `phoout` is called to prepare the output library file. Note that `typen` is called for each field in order to write it out in Type 1 format with the proper floating or integer format, if requested.

Subroutine `iheat` is used to calculate the local heating associated with incoherent photon scattering.

The other call exported by module `phopa` is `phofix`, which provides for editing or printing photoatomic libraries when requested by the user from `acer`. It reads in the Type-1 or Type-2 input file, and allows the ZAID value, the comment string, or the (iz,aw) list to be changed, if desired. A listing of the file can be obtained using `phoprt`, and the modified ACE file can be written using `phoout`. Note the the ACE file type can be changed from 1 to 2, or from 2 to 1 at this point. No consistency checks or plots are currently provided for photoatomic libraries.

Processing of photonuclear data is controlled by subroutine `acephn` in module `acepn`. The photonuclear format is a little different from the more familiar class “c” format used for incident neutrons and charged particles. In the class “c” format, sections describing the emission of the particle that matches the input particle are treated specially, and photon production is treated specially. The other emissions are lumped together in the particle production sections. In the photonuclear format, all the products (neutron, photon, charged particles) are treated symmetrically, and they all are given in blocks similar to the particle production blocks used for class “c.”

To begin, storage is allocated for the scratch array used to read in ENDF records, the ENDF version being used is determined, and the location of the desired material on the input file is found. The routine then reads through the

ENDF “dictionary,” sets some flags to indicate the presence of some kinds of data, and save a list of the reactions found (see `mfm`, `mtm`, and `nr6`). If fission nubar data are available on the input file, they are read into the `fnubar` array. There is no real distinction made between total and prompt nubar in current photonuclear evaluations.

The energy grid is taken from the first section of File 3 found. For Los Alamos evaluations, and others that use that same style, this is `MT=5`, and that value is stored in `mttot`. Some other evaluations will start with `MT=1` or `MT=3`, and that value is stored in `mttot`. It is now possible to define the cross section locators for the ACE file, namely, `esz` (always 1), `tot`, `non`, `els`, and `thn`. The pointer for the elastic cross section, `els`, is set to zero if elastic data do not occur on the input file (see `ielas`). The routine can now assign locators for the partial cross sections, including `mtr` for the MT value, `lqr` for the Q value, and `lsig` for pointers to the data in the data block starting at `sig`. It reads through File 3 on the input file, stores each cross section in the appropriate locations, and computes a correct total that is the sum of all the partial cross sections.

With the cross sections in place, `aceph` makes a pass through the distributions of the input file to count the different particles produced (see `nneut`, `nphot`, `nprot`, *etc.*), to determine the production thresholds (see `tneut`, `tphot`, `tprot`, *etc.*), and to accumulate the heating from any recoils described in File 6. For the latter, the average energy of the recoil distribution is computed on its natural energy grid, and then the results are interpolated onto the ACE energy grid, converted to “per reaction” units by dividing by the total cross section, and added into the accumulating total heating at index `thn`. For photonuclear capture (`MT=102`) when no recoil is given, or for sections of File 6 that don’t define the recoil spectrum, the corresponding recoil energy per reaction is added into the accumulating heating.

At this point, there is enough information to set up the IXS block and to fill in the elements that define the particle types emitted and the number of reactions that contribute to that particle production. The numeric codes used for the various particles in the ACE file are shown in Table 26.

Now a loop is set up over the particle types that have been found to be available for this material in the order neutrons, photons, protons, and so on. For each particle, additional entries are made into the IXS block: the pointer to the data for the particle `pxs`, the pointer to the list of MT numbers contributing `mtrp`, the pointer to the list of yield/system values `tyrp`, the pointer to the list of cross section pointers `lsigp`, and the pointer to the list of cross section



Table 26: ACE Particle Codes for Photonuclear Files

| Code | Particle Data Class |
|------|---------------------|
| 1    | neutrons            |
| 2    | photons             |
| 9    | protons             |
| 31   | deuterons           |
| 32   | tritons data        |
| 33   | $^3\text{He}$       |
| 34   | alphas              |

data blocks **sigp**. The first two elements in the **sigp** segment are filled in: the index to the threshold for the production from the main energy grid **it**, and the count of production cross section values (from **it** to **nes**). The code now loops through the File 4 and/or File 6 again and treats each section or subsection that contributes for this particular particle. In each case, the contribution is summed into the accumulating production cross sections, the data giving the fractional yield for this reaction to the total production of this particle is stored, and the heating contribution from this reaction for this particle is added in.

Now that the **sigp** data are complete, the code can compute the pointer to the list of LANDP entries and the pointer to the ANDP data block and store them in the IXS block. It continues by reading through the sections that contribute angular distributions, storing the data in the normal ACE-format slots, and adding in the appropriate contributions to the accumulating heating cross section. Angular distributions are stored using the “new formats”, LAW=61. They are generated with the help of subroutines **ptleg2** and **pttab2**, just as described above for class “c” files.

The locators for energy distributions can now be defined and stored into the IXS block (see **ldlwp** and **dlwp**). Subroutine **acephn** searches through Files 4, 5, and 6 to find sections that contribute energy distributions. Each such distribution is stored using the appropriate ACE law, and the contribution to the heating from the distribution is added into the accumulating heating cross section. The methods are similar to those described for energy and energy-angle distributions above.

When the loop over all the particle types is complete, the routine converts the main energy grid to MeV and adjusts the precision of the energies and the heating to 7 digits. The ZAID value for this material is generated using a class suffix of “u,” and the results are written to the output file.

The other call exported by module `acepn` is `phnfix`, which provides for editing or printing photonuclear libraries when requested by the user from `acer`. It reads in the Type-1 or Type-2 ACE files, and allows for adjustments of the ZAID value, the descriptive text string, or the (iz,aw) list. The ACE photonuclear file can be printed using `phnpri`. The data file can be written out in either Type-1 or Type-2 format using `phnout`. And an input file for the `VIEWR` module can be produced that will generate color Postscript plots of all the photonuclear cross sections, the heating value, the individual particle production and heating values, and angle or energy distributions as 3-D perspective plots.

## 17.19 Error Messages

**error in acer\*\*\*illegal iopt**

IOPT must be between 1 and 5, 7 and 9.

**error in first\*\*\*desired temperature not found**

Desired temperature was not found on the input PENDF tape. Check for an input error or whether the wrong tape was mounted.

**error in first\*\*\*storage exceeded**

This can result if there are more than `maxpp=250` sections in File 12 on the input ENDF tape (`maxpp` is a global parameter at the beginning of module `acefc`) or if there are more than `ngmtmx=500` different gamma rays described in the evaluation (`ngmtmx` is defined in subroutine `first`).

**error in first\*\*\*too many production items**

There isn't enough space in the global arrays that accumulate particle production information. See the global parameter `maxpr=300` and the beginning of module `acefc`.

**error in first\*\*\*too many threshold**

See `nethr=300` in `first`.

**error in topfil\*\*\*nxc.gt.nxcmax**

More than 500 reactions have been found on the input ENDF tape. See the global parameter `nxcmax=500` at the start of module `acefc`.

**error in pttab\*\*\*storage exceeded**

This routine can process up to 300 secondary angles. See the parameter `npmax=300`.

**error in pttab\*\*\*tab ang dis has more than one terp range**

Only one interpolation range is allowed when processing tabulated angular distributions in `pttab`. In some cases, two ranges are allowed; see `chekit`.

**error in pttab\*\*\*tab ang dist not allowed for**

Interpolation schemes that use logs for the scattering cosine (`int=3` or `5`) are not allowed because  $\mu$  can take on negative values.

error in chekit\*\*\*wrong type of nr=2 file 5 mt  
Only certain types can be handled here.

error in fix6\*\*\*storage in a exceeded  
See the parameter namax=9000.

error in gamsum\*\*\*exceeded storage in dictionary  
Limited by the global parameter nxcmax=500 at the beginning of module acefc.

error in convr\*\*\*storage exceeded for photon data  
There is not enough room in the allocatable array tot for the total photon yield array from MF=12 or MF=13. See nwtot=5000.

error in convr\*\*\*storage exceeded for edis  
The list of discontinuity energies is limited to nned=50 elements in convr.

error in convr\*\*\*too many lo=2 photons  
See lmax=100 in convr.

error in convr\*\*\*only law=1 allowed for endf6 file6 photons  
Photon sections in File 6 should use the tabulated representation only.

error in gamout\*\*\*expected send card while reading mf14  
Sequence of ENDF records is off.

error in gamout\*\*\*mat not found  
The desired material was not found on the input GENDF tape. Make sure that the correct file was mounted.

error in gamout\*\*\*storage in a exceeded  
Storage exceeded in the dynamic array scr. Check the value for nwamax in this subroutine.

error in gamout\*\*\*no gamma groups on ngend  
The input GENDF tape does not contain a photon group structure. Remember that using the 30×20 matrix option for photon emission requires that a [GROUPE](#) run be made to produce multigroup cross sections for all of the photon production reactions.

error in gamout\*\*\*storage in sig exceeded  
Storage limit for the allocatable array sig has been exceeded. See nsmax=5000.

error in aceout\*\*\*not coded for this incident particle  
Neutrons, protons, deuterons, tritons, He-3, or alpha are allowed.

error in acelod\*\*\*insufficient storage for esz block  
The ESZ block contains 5×NES words, and this value must be less than the limit of nxss=7 000 000 words, which is set in the global variables at the start of the acefc module.

error in acelod\*\*\*insufficient space for cross sections  
There is not enough space for the SIG block in the container array xss. See the discussion for the ESZ block above.

`error in acensd***insufficient storage for angular...`

There is not enough space for the angular data block in the container array `xss`. See the discussion for the ESZ block above.

`error in acelod***insufficient space for energy dist`

There is not enough space for the DLW block in `xss`. See the discussion for the ESZ block above.

`error in acelod***insufficient space for photon spectra`

There is not enough space in `xss`. See the discussion for the ESZ block above.

`error in acelod***30 groups are required for ...`

The photon production neutron group structure must be 30 groups.

`error in acelod***insufficient storage for energy dist`

There is not enough space in `xss`. See the discussion for the ESZ block above.

`error in acelf5***insufficient space for energy dist`

There is not enough space for the DLW block in `xss`. See the discussion for the ESZ block above.

`error in acelf5***scratch storage exceeded reading lf=1`

See `nwscr=5000`.

`error in acelf5***sorry acer cannot handle lf=5...`

This evaluation contains a bad representation.

`error in acelf5***illegal lf=...`

The `acelf5` routine can process `LF=1, 5, 7, 9, and 11` from ENDF File 5.

`error in acelf6***illegal law for endf6 file6 neutrons`

Only `lf=1, 6, or 7` are allowed here.

`error in acelf6***insufficient space for mf6 tab2`

There is not enough space in `xss`. See the discussion for the ESZ block above.

`error in acelf6***insufficient space for mf6 neutron yield`

There is not enough space in `xss`. See the discussion for the ESZ block above.

`error in acelf6***exceeded scratch storage`

There is not enough space in `xss`. See the discussion for the ESZ block above.

`error in acelf6***storage exceeded for generalized yield`

See `ishift=500`.

`error in acelf6***only lang=1, 2, 11-13 allowed ...`

Others aren't expected here.

**error in ptlegc\*\*\*too many coulomb angles**  
 The parameter `maxang=2000` needs to be adjusted.

**error in acelp\*\*\*insufficient space for photon production**  
 There is not enough space in `xss`. See the discussion for the ESZ block above.

**error in acelp\*\*\*no. of gamma energies not complete**  
 There is something wrong with the data for this reaction on the main ACER scratch file.

**error in acelp\*\*\*insufficient storage for input photon**  
 There is not enough storage in the dynamic array `SCR`. This size is controlled by the statement `nwscr=150 000` in subroutine `acelp`.

**error in bachaa\*\*\*dominant isotope not known for ...**  
 The separation energy calculation only works for isotopes. This routine contains a small table of the dominant isotope in elements that sometimes appear in evaluations. This message means that the dominant isotope is not known for this element, and that the table must be extended.

**error in acelcp\*\*\*exceeded scratch storage**  
 See `nwscr=5000` in `acelcp`.

**error in acelcp\*\*\*insufficient storage for angular dist...**  
 There is not enough space in `xss`. See the discussion for the ESZ block above.

**error in acelcp\*\*\*unsupported law and lang**  
 Only some combinations of `LF=1` and `LF=2` are currently handled.

**error in acelcp\*\*\*scratch array overflowing ...**  
 Reduce the number of energy points.

**error in acefix\*\*\*problem with particle id in zaid**  
 Unknown particle type.

**error in acefix\*\*\*illegal file type**  
 Only files of class "c" can be handled here.

**error in aplof4\*\*\*too many e values in angular distribution**  
 Up to 1200 allowed. See parameter `maxe=1200`.

**error in acesix\*\*\*storage exceeded for coherent reactions**  
 There is insufficient space in the `six` array for the coherent or incoherent data, respectively. This is a space of 50 000 words. This value is set by the statement `ninmax=50 000` at the beginning of the `acesix` routine.

**error in acesix\*\*\*exceeded storage for incoherent reactions**  
 See the explanations above.

**error in acesix\*\*\*exceeded storage for incoherent elastic**  
 See the explanations above.

**error in acesix\*\*\*coded for equiprobable angles only**

The input thermal File 6 (a nonstandard format) must use the equiprobable angle format. Since this is currently the only format produced by [THERMR](#), this error should not occur.

**error in acesix\*\*\*solution out of range**

The routine is not able to find a legal solution while trying to find the equiprobable bins for inelastic scattering.

**error in acedos\*\*\*desired mat and temp not found**

The requested material and temperature were not found on the input photo-atomic PENDF file. Check for an input error, and make sure that the correct file has been mounted as **npndf**. Remember that this is normally the output of a [RECONR](#) run to assure correct unionization and linearization.

**error in acedos\*\*\*too many reactions, need ...**

The number of mt values in the ACE output file exceeds acedos's internal limits. Increase the value of **nmax**.

**message from acepho---photoelectric processing not complete**

This version doesn't handle fluorescence data as yet.

**error in acephn\*\*\*too many reactions in mtr list**

See the parameter **mmax=80**.

**error in acephn\*\*\*mf=6/mt=201-207 not supported...**

Some of the first-generation of photonuclear evaluations represented particle production from photonuclear reactions using MT=201 through 207, as for gas production. This does not conform to the ENDF-6 format and cannot be processed here.

**error in acephn\*\*\*insufficient storage for angular dist...**

More space is needed in the main **xss** array. Adjust the parameter **nxss=999000**.

**error in acephn\*\*\*file 5 law not ready**

The code can only handle laws 1, 7, and 9 from File 5.

**error in phnpvt\*\*\*law not installed**

The routine can currently handle the following ACE laws: 4, 7, 9, 33, and 44

## 18 POWR

The POWR module is used to prepare libraries for the Electric Power Research Institute (EPRI) reactor analysis codes EPRI-CELL and EPRI-CPM.<sup>11</sup> These codes were originally developed to provide an alternative to the reactor manufacturers' computer codes for calculating reactor core performance as required for operating and reloading power reactors run by US electric utility companies. Because these codes require up-to-date accurate cross sections that were not controlled by the reactor manufacturers, EPRI contracted with the Los Alamos National Laboratory to generate new libraries based on the US-standard Evaluated Nuclear Data Files (ENDF). With this funding, we were able to develop the [THERMR](#) module and the associated thermal multigroup methods in [GROUPE](#). We also developed this POWR module to format cross section data in GENDF format for use in CELL or CPM. In addition, it was necessary to make a number of modifications to EPRI-CELL to make it perform well with unadjusted cross sections. The results of all this work were reported in 1984[61].

This module has not been used at Los Alamos since 1984, although we have had scattered reports of use elsewhere. A list of the input instructions, without further comment, follows.

### 18.1 Input Instructions

As an aid to discussions of the user input to POWR, the input instructions that appear as comment cards at the beginning of the current version of this module are listed below. Since code changes are possible, albeit unlikely for this module, it is always advisable to consult the comment-card instructions contained in the version of the code actually being used before proceeding with an actual calculation.

```
!---input specifications (free format)-----
!
! card 1
!   ngendf  unit for input gout tape
!   nout    unit for output tape
! card 2
!   lib     library option (1=fast, 2=thermal, 3=cpm)
```

<sup>11</sup>EPRI-CELL and EPRI-CPM are proprietary products of the Electric Power Research Institute, 3420 Hillview Avenue, Palo Alto, CA 94304. For more information, please contact the owners.

```

!   iprint  print option (0=minimum, 1=maximum)
!           (default=0)
!   iclaps  group collapsing option (0=collapse from 185 group
!           to desired group structure, 1=no collapse)
!           (default=0)
!
!-----for lib=1-----
!
! card 3
!   matd    material to be processed
!           if matd lt 0, read-in absorption data only for
!           this material with mat=abs(matd) directly from
!           input deck (see card 6)
!   following three parameters irrelevant for matd lt 0
!   rtemp   reference temperature (degrees kelvin)
!           (default=300  k)
!   iff     f-factor option
!           (0/1=do not calculate f-factors/calculate if found)
!           (default=1)
!   nsgz    no. of sigma zeroes to process for this material
!           (default=0=all found on input tape)
!   izref   ref. sigzero for elastic matrix (default=1)
! cards 4 and 5 for normal run only (matd gt 0)
! card 4
!   word    description of nuclide (up to 16 characters,
!           delimited with *, ended with /) (default=blank)
! card 5
!   fsn     title of fission spectrum (up to 40 characters,
!           delimited with *, ended with /0 (default=blank)
!           delimited with *, ended with /) (default=blank)
! card 6 for reading in absorption data only
!   abs     ngnd absorption values (default values=0)
! repeat cards 3 through 6 for each material desired.
! terminate with matd=0/ (i.e., a 0/ card).
!
!-----for lib=2-----
!
! card 3
!   matd    material to be processed
!   idtemp  temperature id (default=300  k)
!   name    hollerith name of isotope (up to 10 characters,
!           delimited with *, ended with /) (default=blank)

```



```

! card 4      default for all values=0.
!   itrc      transport correction option (0 no, 1 yes)
!   mti       thermal inelastic mt
!   mtc       thermal elastic mt
! card 5      default for all values=0.
!   xi
!   alpha
!   mubar
!   nu
!   kappa fission
!   kappa capture
!   lambda
!   sigma s   if 0, set to scattering cross section at group 35
! repeat cards 3 thru 5 for each material and temperature desired
! (maximum number of temperatures allowed is 7.)
! terminate with matd=0/ (i.e., a 0/ card).
!
!----for lib=3-----
!
! card 3
!   nlib      number of library.
!   idat      date library is written (i format).
!   newmat    number of materials to be added.
!   iopt      add option (0=mats will be read in,
!               1=use all mats found on gendf).
!   mode      0/1/2=replace isotope(2) in cpmlib/
!               add/create a new library (default=0)
!   if5       file5 (burnup data) option
!               0/1/2=do not process file5 burnup data/
!               process burnup data along with rest of data/
!               process burnup data only (default=0)
!               (default=0)
!   if4       file4 (cross section data) option
!               0/1=do not process/process
!               (default=1)
! card 4 for iopt=0 only
!   mat       endf mat number of all desired materials.
!               for materials not on gendf tape, use ident for mat.
!               if mat lt 0, add 100 to output ident
!               (for second isomer of an isotope)
! card 5
!   nina      nina indicator.

```

```

!           0/1/2/3=normal/
!           no file2 data, calculate absorption in file4/
!           no file2 data, read in absorption in file4/
!           read in all file2 and file4 data.
!   ntemp   no. of temperatures to process for this material
!           (default=0=all found on input tape)
!   nsigz   no. of sigma zeroes to process for this material
!           (default=0=all found on input tape)
!   sgref   reference sigma zero
!   following 2 parameters are for nina=0 or nina=3.
!   ires    resonance absorber indicator (0/1=no/yes)
!   sigp    potential cross section from endf.
!   following 5 parameters are for ntapea=0 only
!   mti     thermal inelastic mt
!   mtc     thermal elastic mt
!   ip1opt  0/1=calculate p1 matrices/
!           correct p0 scattering matrix ingroups.
!   *****if a p1 matrix is calculated for one of the isotopes
!           having a p1 matrix on the old library, file 6 on the
!           new library will be completely replaced.*****
!   inorf   0/1=include resonance fission if found/
!           do not include
!   following two parameters for mode=0 only
!   pos     position of this isotope in cpmlib
!   posr    (for ires=1) position of this isotope in resonance
!           tabulation in cpmlib
!   repeat card 5 for each nuclide.
!   following three cards are for if5 gt 0 only
!   card 6
!   ntis    no. time-dependent isotopes
!   nfis    no. fissionable burnup isotopes
!   card 7
!   identb  ident of each of the nfis isotopes
!   card 8
!   identa  ident of time-dependent isotope
!   decay   decay constant (default=0.)
!   yield   nfis yields (default=0.)
!   repeat card 8 for each of the ntis isotopes.
!   card 9 for if5=2 only
!   aw      atomic weight
!   indfis  fission indicator
!   ntemp   no. temperatures on old library

```

```

! repeat card 9 for each of the ntis isotopes.
! card 10
!   lambda  resonance group goldstein lambdas
!   *****remember that the 69-group structure has 13 resonance
!   groups while the collapsed 185-group structure has 15.
!   use a slash at end of each line of card 10 input.*****
! repeat card 10 for each nuclide having nina=0, nina=3, or
!   ires=1.
! cards 11 and 11a for nuclides having nina=3 only.
! card 11
!   resnu    nrg nus values to go with the lambda values
! card 11a
!   tot      nrg total xsec values to go with the lambda values
! read cards 11 and 11a for each nuclide having nina=3.
! cards 12 for nina gt 2 only
!   aw       atomic weight
!   temp     temperature
!   fpa      ngnd absorption values (default=0.)
! cards 12a, 12b, 12c for nuclides having nina=3 only.
! card 12a
!   nus      ngnd nus values
!   fis      ngnd fission values
!   xtr      ngnd transport values
! card 12b
!   ia       group.  0 means no scattering from this group
!   l1       lowest group to which scattering occurs
!   l2       highest group to which scattering occurs
! card 12c  for ia gt 0 only
!   scat     l2-l1+1 scattering values
! repeat card 12b and 12c for each group
! repeat cards 12 for each of the nina gt 2 nuclides
!
!-----

```



## 19 WIMSR

The WIMSR module is used to prepare libraries for the reactor-physics code WIMS[18]. WIMS stands for “Winfrith improved multigroup scheme;” it has been developed through its various versions at the UK laboratory AEE/Winfrith. WIMS-E was the Winfrith version *circa* 1990, and it was distributed commercially. WIMS-D is an older version that is freely available through various distribution centers; therefore, it is very popular all around the world.

WIMS uses collision-probability methods for computing fluxes in reactor pin cells and more complicated geometrical arrangements. Therefore, it requires transport, fission, and capture cross sections, a transfer matrix for epithermal neutrons, fission-source information ( $\bar{\nu}$  and  $\chi$ ), and a bound-atom scattering matrix for thermal neutrons. Self-shielded cross sections are obtained using equivalence theory from tabulated resonance integrals with intermediate resonance corrections. The resonance integrals can be obtained from the self-shielded cross sections produced by [GROUPR](#), and the intermediate-resonance  $\lambda$  values by group can be computed using the NJOY flux calculator. WIMS libraries normally use a standard 69-group structure with 14 fast groups, 13 resonance groups, and 42 thermal groups.

This chapter of the report describes WIMSR in NJOY 2012.0. It differs from the version previously reported[3] because of the change to Fortran-90 style and storage allocation.

### 19.1 Resonance Integrals

WIMS computes the self-shielded cross sections for a wide range of mixtures and fuel geometries using equivalence theory. The [GROUPR](#) chapter of this report describes the narrow-resonance (NR) version of equivalence theory; that is, all systems with the same value for the “sigma-zero,”

$$\sigma_{0i} = \frac{1}{n_i} \left\{ \sum_{j \neq i} n_j \sigma_{tj} + \sigma_e \right\}, \quad (494)$$

in a group have the same self-shielded cross section in that group. Here,  $n_j$  is the number density for material  $j$  with cross section  $\sigma_{tj}$ , and  $\sigma_e$  is the escape cross section (which takes care of the geometry of the fuel).

However, in the near epithermal range (*e.g.*, 4-100 eV), some resonances are too wide for the NR approximation to apply well. For these resonances, the effect of a moderator material is reduced, because collisions with the moderator

do not always result in enough energy loss to remove the neutron from the resonance. For this reason, WIMS uses an intermediate-resonance (IR) extension to equivalence theory in which the background cross section is taken to be the following:

$$\sigma_{Pi} = \frac{1}{n_i} \left\{ \sum_j n_j \lambda_j \sigma_{pj} + \sigma_e \right\} , \quad (495)$$

where the  $\lambda$  factors are numbers between zero and one. Note that  $\sigma_p$ , the potential scattering cross section, is used here, and that the sum is now over all materials. The basic concept is the same: all systems with the same value of the IR “sigma-P” for a group will have the same self-shielded cross sections for that group.

WIMS takes the additional step of expressing the self-shielding data in terms of “resonance integrals,” instead of using the self-shielded cross sections produced by [GROUPR](#). That is

$$\sigma_x(\sigma_0) = \frac{\sigma_P I_x(\sigma_P)}{\sigma_P - I_a(\sigma_P)} , \quad (496)$$

and

$$I_x(\sigma_P) = \frac{\sigma_P \sigma_x(\sigma_0)}{\sigma_P + \sigma_a(\sigma_0)} , \quad (497)$$

where  $x$  denotes the reaction, either “a” for absorption or “nf” for nu\*fission, and  $I_x$  is the corresponding resonance integral.

In order to clarify the meaning of this pair of equations, consider a homogeneous mixture of  $^{238}\text{U}$  and hydrogen with concentrations such that there are 50 barns of hydrogen scattering per atom of uranium. The [GROUPR](#) flux calculator can be used to solve for the flux in this mixture, and [GROUPR](#) can then calculate the corresponding absorption cross section for  $^{238}\text{U}$ . Assuming that  $\lambda = 0.1$  and  $\sigma_p = 10$  for the uranium, the numbers being appropriate for WIMS group 25, we get  $\sigma_P = 51$ . This value of  $\sigma_p$  goes into the `sigz` array in the resonance-integral block on the WIMS library, and the corresponding  $I_a$  goes into the `resa` array.

At some later time, a WIMS user runs a problem for a homogeneous mixture of  $^{238}\text{U}$  and hydrogen that matches these specifications. WIMS will compute a

value of  $\sigma_P$  of 51.0, interpolate in the table of resonance integrals, and compute a new absorption cross section that is exactly equal to the accurate computed result from the original [GROUPE](#) flux-calculator run.

This argument can be extended to more complex systems. For example, the assembly calculated using the flux calculator could represent an enriched uranium-oxide fuel pin of a size typical of a user's reactor system with a water moderator. The computed absorption cross section is converted to a resonance integral and stored with the computed value of  $\sigma_P$ . In any later calculation that happens to mimic the same composition and geometry, WIMS will return the accurate calculated absorption cross section. Equivalence theory, with all its approximations, is only used to interpolate and extrapolate around these calculated values. This is a powerful approach, because it allows a user to optimize the library in order to obtain very accurate results for a limited range of systems without having to modify the methods used in the lattice-physics code. Unfortunately, the present version of WIMSR does not allow you to enter  $\sigma_P$  directly; it computes it from input data that only consider one material at a time. A future version may include the more general capabilities described in this paragraph.

Let us call the homogeneous uranium-hydrogen case discussed above "case 0." Now, consider a homogeneous mixture of  $^{238}\text{U}$ , oxygen, and hydrogen. Ratio the number densities to the uranium density such that there is 1 barn/atom of oxygen scattering and 50 barn/atom of hydrogen scattering. Carry out an accurate flux calculation for the mixture, and call the result "case 1." Also do an accurate flux calculation with only hydrogen, but at a density corresponding to 51 barns/atom. Call this result "case 2." The IR lambda value for oxygen is then given by

$$\lambda = \frac{\sigma_a(1) - \sigma_a(0)}{\sigma_a(2) - \sigma_a(0)} . \quad (498)$$

Note that  $\lambda$  will be 1 if the oxygen and hydrogen have exactly the same effect on the absorption cross section. In practice,  $\lambda = .91$  for WIMS group 27 (which contains the large 6.7 eV resonance of  $^{238}\text{U}$ ), and  $\lambda = 1$  for all the other resonance groups. That is, all the resonances above the 6.7 eV resonance are effectively narrow with respect to oxygen scattering.

Similarly, do a flux-calculator solution for a homogeneous mixture of  $^{238}\text{U}$  combined with 1 barn/atom of  $^{235}\text{U}$  and 50 barn/atom of hydrogen. Call the

result “case 3.” Now, the lambda value for  $^{235}\text{U}$  is given by

$$\lambda = \frac{\sigma_a(3) - \sigma_a(0)}{\sigma_a(2) - \sigma_a(0)}. \quad (499)$$

The actual value obtained for WIMS group 27 is .035. Group 26 gives 0.50, and group 25 gives 0.09. An examination of the flux-calculator equations in the [GROUPE](#) chapter of this manual shows that the effect of the “admixed” moderator term depends only on its atomic mass (through the  $\alpha$  value); therefore, the IR  $\lambda$  values will be the same for all uranium isotopes (and the same values should work for all the actinides). This conclusion neglects the small effects of absorption in the admixed isotope on the intraresonance flux for one resonance.

This process can be continued for additional admixed materials from each important range of atomic mass. The result is the table of  $\lambda_{gi}$  values needed as WIMSR input.

What are the implications of this discussion? Foremost is the observation that the lambda values for the isotopes are a function of the composition of the mixture that was used for the base calculation. To make the effect of this clear, let us consider two different types of cells:

1. a homogeneous mixture of  $^{238}\text{U}$  and hydrogen, and
2. a homogeneous mixture of  $^{235}\text{U}$  and hydrogen.

A look at the pointwise cross sections in group 27 shows very different pictures for the two uranium isotopes. The  $^{238}\text{U}$  cross section has one large, fairly wide resonance at 6.7 eV, and the  $^{235}\text{U}$  cross section has several narrower resonances scattered across the group. If the lambda values are computed for these two different situations, the results in Table [27](#) are obtained.

Table 27: IR  $\lambda$  Values for Several Resonance Groups and Two Different Reactor Systems

| WIMS<br>group | $\lambda(\text{U})$         | $\lambda(\text{O})$         | $\lambda(\text{U})$          | $\lambda(\text{O})$          |
|---------------|-----------------------------|-----------------------------|------------------------------|------------------------------|
|               | $^{238}\text{U}@50\text{b}$ | $^{238}\text{U}@50\text{b}$ | $^{235}\text{U}@200\text{b}$ | $^{235}\text{U}@200\text{b}$ |
| 27            | .035                        | .91                         | 0.20                         | 1.00                         |
| 26            | .50                         | 1.00                        | .38                          | 1.00                         |
| 25            | .092                        | 1.00                        | .44                          | 1.00                         |
| 24            | .090                        | 1.00                        | .55                          | 1.00                         |
| 23            | .29                         | 1.00                        | .46                          | 1.00                         |



It is clear that the energy dependence of the two lambda sets is quite different. This is because of the difference in the resonance structure between  $^{238}\text{U}$  and  $^{235}\text{U}$ . Clearly, the one resonance in group 27 in  $^{238}\text{U}$  is effectively wider than the group of resonances in group 27 for  $^{235}\text{U}$ . Group 26 has essentially no resonance character for  $^{238}\text{U}$ , which reverses the sense of the difference. In groups 24 and 25, the  $^{235}\text{U}$  resonances become more narrow, while the  $^{238}\text{U}$  resonances stay fairly wide. Finally, in group 23, the  $^{238}\text{U}$  resonances begin to get narrower.

These results imply that completely different sets of lambda values should be used for different fuel/moderator systems, such as  $^{238}\text{U}$ /water,  $^{235}\text{U}$ /water, or  $^{238}\text{U}$ /graphite. In practice, this is rarely done.

The remaining question is, “How should the self-shielded cross sections for the minor isotopes be calculated?” Formally, the best approach using NJOY would be to first do an accurate flux calculation for pure  $^{238}\text{U}$  mixed with hydrogen (or to be really accurate, a typical reactor cell containing pure  $^{238}\text{U}$  oxide), and to save the resulting flux on a scratch file. This flux would then be used as input for the  $^{235}\text{U}$  calculation. See the [GROUPR](#) chapter for details. This approach takes care of all the complexities of resonance-resonance interference, the drop in the average flux across the group caused by accumulated  $^{238}\text{U}$  absorptions, and so on. In practice, this is rarely done. Since the self-shielding effects in the minor actinides are much smaller than those in the main absorber, it is usually sufficient to do a simple NR calculation for the minor actinides and to convert them into WIMS resonance integrals with the normal lambda values for heavy isotopes.

## 19.2 Cross Sections

The first part of the WIMS cross section data contains  $\sigma_p$  for the resonance groups (15-27 in the normal 69-group structure), the scattering power per unit lethargy for the resonance groups, the transport cross section for the non-thermal groups (1-27 normally), the absorption cross section for the non-thermal groups, an obsolete quantity for the resonance groups (set to zero), and the intermediate-resonance  $\lambda$  values for the resonance groups. For WIMS-E, the (n,2n) cross section is added between the slowing-down power and the transport cross section.

The  $\sigma_p$  value is assumed to be constant (see `sigp` in the user input instructions). It must be obtained by finding the scattering length  $a$  in the ENDF file and computing  $\sigma_p = 4\pi a^2$ . The scattering power per unit lethargy is  $\xi\sigma_s/\tau$ , where  $\xi$  is the log energy loss parameter given as MT=252 on the GENDF file,  $\sigma_s$  is the elastic scattering cross section (MT=2), and  $\tau$  is the lethargy

width for the group, which can be calculated from the group structure given in MF=1/MT=451 on the GENDF file. The (n,2n) cross section is obtained from MF=3/MT=16 on the GENDF file. The absorption cross section is computed by adding up the fission cross section (MT=18) and all the cross sections given with MT=102-150. The (n,2n) cross section (MT=16) is then subtracted from the sum. Finally, the  $\lambda$  values are obtained from the user's input. See Section 19.1 for more details on these intermediate-resonance corrections.

The next part of the WIMS data file contains the fission neutron production cross section  $\bar{\nu}\sigma_f$  and the fission cross section  $\sigma_f$  for the non-thermal groups (1-27 normally). The cross section is always obtained from MT=18 on the GENDF file, but there are several complications involved in getting  $\bar{\nu}$ .

A shortcut for obtaining the fission data is to run MFD=3/MTD=452 and MFD=5/MTD=452 in [GROUPE](#). This approach ignores the energy dependence of fission neutron emission at high energies and the effects of delayed neutrons on the fission spectrum. If these options are used in [GROUPE](#), it is important not to use the other options described below at the same time. When WIMSR finds a section on the GENDF file with MF=3/MT=452, it can read in  $\bar{\nu}\sigma_f$  directly.

A better approach to fission in [GROUPE](#) is to prepare a full fission matrix for MT=18, or to prepare matrices for all the partial fission reactions, MT=19, 20, 21, and 38. The latter is the recommended approach for evaluations with both MT=18 and MT=19 given in File 5. See the [GROUPE](#) chapter for more details. WIMSR reads in the data given in MF=6/MT=18, or in MF=6/MT=19,20,..., and sums over all secondary-energy groups to obtain the prompt part of  $\bar{\nu}\sigma_f$ . It adds in the delayed part of  $\bar{\nu}\sigma_f$  from MF=3/MT=455. If the input GENDF file contains both MT=18 and partial fission matrices, a diagnostic message will be printed, and the partial-fission representation will be used.

The next section of the WIMS data file contains the non-thermal  $P_0$  scattering matrix for incident-energy groups in the non-thermal range (1-27 normally). This matrix is loaded by summing over all of the reactions found on the GENDF tape except the thermal reactions `mti` and `mtc`. If requested, this matrix is transport corrected by subtracting the sum over secondary-energy groups of the  $P_1$  matrix for each primary group. When the individual reactions are read, they are loaded into "full" matrix (typically 69×69). At the same time, a record is kept of the lowest and highest secondary groups found for each primary group. These limits are then used to pack the scattering matrix into a more compact form.

The scattering matrix is not actively self-shielded in WIMS, but WIMSR allows the user to request that the elastic component be evaluated at some reference  $\sigma_0$  value different from infinity. This option can be useful for the major fertile component of reactor fuel, that is, for  $^{238}\text{U}$  in pins of a uranium system, or for  $^{232}\text{Th}$  for fuel in a Thorium/ $^{233}\text{U}$  system.

Because the thermal scattering matrix depends on temperature, the next component of the WIMSR data contains the **ntemp** versions of the basic cross sections and the  $P_0$  scattering matrix for the thermal groups (28-69 normally). The cross sections included are transport, absorption,  $\nu^*\text{fission}$ , and fission. The transport positions contain the sum of the thermal inelastic cross section obtained by summing up the  $P_0$  matrix (MF=6/MT=MTI), the thermal elastic cross section from the diagonal elements of the  $P_0$  matrix (MF=6/MT=MTC), if present, and the absorption cross section. If separate  $P_1$  matrices are not given for this material, the  $P_1$  cross section obtained by summing the  $P_1$  matrices over secondary groups for each primary group is subtracted. The matrix data are read from sections on the GENDF file with MF=6/MT=MTI and MF=6/MT=MTC (if present). As for the temperature-independent matrices, they can be transport-corrected by subtracting the sum over secondary groups of the  $P_1$  matrix for each primary group from the self-scatter position. Also, minimum and maximum limits on the secondary group are determined for each primary group, and the matrix is compacted for efficiency.

The next part of the WIMS data file contains the resonance data, which were discussed in Section 19.1. In some cases, these resonance data are followed by a fission spectrum block. The complications of obtaining the fission spectrum are the same as those described above for obtaining the fission neutron production cross section,  $\bar{\nu}\sigma_f$ . If the short-cut option was used in **GROUPR**, the fission spectrum can be read directly from MF=5/MT=452 on the GENDF file. The sum over groups is also accumulated in **cnorm** in order to allow the final spectrum to be normalized accurately. The shortcut approach neglects the effects of delayed neutron emission on the fission spectrum.

If fission matrices are available (either MT=18, or MT=19+20+21...), the prompt part of the fission spectrum is obtained by summing  $\sigma_{gg'}\phi_g$  over all primary groups,  $g$ . These numbers are also summed into **cnorm** for use later in normalizing  $\chi$ . The delayed part is obtained as

$$\left\{ \sum_g \nu_d \sigma_{fg} \phi_g \right\} \chi_{dg'} , \quad (500)$$

which also contributes to the normalization. Note that the energy dependence of the fission matrix is factored into the final  $\chi$  in proportion to the weighting flux used in [GROUPR](#) to prepare the WIMSR input file. For thermal reactor problems, it is easy to provide a good estimate for this weighting flux.

The final block on the WIMS data tape is optional. If present, it contains  $P_1$  scattering matrices for each temperature. These matrices are defined over the entire group range (normally 1-69), and they contain both the temperature-independent and temperature-dependent reactions in each matrix. The methods used to build up these matrices are parallel to those discussed above for the  $P_0$  matrices. Note that if  $P_1$  matrices are given, the transport corrections are not included in the transport cross sections or  $P_0$  matrices.

### 19.3 Burn Data

WIMS uses a simplified burn model for tracking the production and depletion of actinides and fission products, and the chains used are hard-wired into the code. WIMSR provides a method to enter new fission-yield data into the WIMS library format, but it has not been used or tested very much so far.

### 19.4 User Input

The following user input specifications were copied from the comment cards at the beginning of the WIMSR source. It is always a good idea to check the comment cards in the current version to see if there have been any changes.

```
!-----
!  
! Format multigroup cross sections from groupr for WIMS.  
!  
!---input specifications (free format)----  
!  
! card 1  
!   ngendf  unit for input gendf tape  
!   nout    unit for output wims tape  
!  
! card 2  
!   iprint  print option  
!           0=minimum (default)  
!           1=regular  
!           2=1+intermediate results
```

```

!      iverw      wims version
!                  4=wims-d (default)
!                  5=wims-e
!      igroup    group option
!                  0=69 groups (default)
!                  9=user's choice
!
! card 2a (igroup.eq.9 only)
!      ngnd      number of groups
!      nfg       number of fast groups
!      nrg       number of resonance groups
!      igref     reference group (default is last fast group)
!
! card 3
!      mat       endf mat number of the material to be processed
!      nfid      not used
!      rdfid     identification of material for the wims library
!      iburn     burnup data option
!                  -1=suppress printout of burnup data
!                  0=no burnup data is provided (default)
!                  1=burnup data is provided in cards 5 and 6
!
! card 4
!      ntemp     no. of temperatures to process for this material
!                  in the thermal energy range
!                  (0=all found on input tape)
!      nsigz     no. of sigma zeroes to process for this material
!                  (0=all found on input tape)
!      sgref     reference sigma zero
!                  (.ge. 1.e10 to select all cross sect. at inf.dil.*
!                      but fully shielded elastic x-sect,
!                  .lt. 1.e10 to select all x-sect at inf.dil.
!                  =sig0      from the list on groupr input to
!                      select all x-sect. at that sig0)
!      ires      resonance absorber indicator
!                  0=no resonance tables
!                  >0=ires temperatures processed
!      sigp      potential cross section from endf.
!                  (if zero, replace by the elastic cross section)
!      mti       thermal inelastic mt (default=0=none)
!      mtc       thermal elastic mt (default=0=none)
!      iplopt    include p1 matrices

```

```

!           0=yes
!           1=no, correct p0 ingroups (default)
!   inorf   resonance fission (if found)
!           0=include resonance fission (default)
!           1=do not include
!   isof    fission spectrum
!           0=do not include fission spectrum (default)
!           1=include fission spectrum
!   ifprod  fission product flag
!           0=not a fission product (default)
!           1=fission product, no resonance tables
!           2=fission product, resonance tables
!   jp1     transport correction neutron current spectrum flag
!           0=use p1-flux for transport correction (default)
!           >0=read in jp1 values of the neutron current
!           spectrum from input
!
!   the following cards 5 and 6 are for iburn gt 0 only
! card 5
!   ntis    no. of time-dependent isotopes
!           for burnable materials ntis=2
!           for fissile materials ntis>2 when fission product
!           yields are given.
!   efiss   energy released per fission
!
! card 6a
!   identa  ident of capture product isotope
!   yield   yield of product identa from capture
!
! card 6b
!   identa  ident of decay product isotope (zero if stable)
!   lambda  decay constant (s-1)
!
! card 6c (repeated ntis-2 times, if necessary)
!   identa  ident of fission product isotope
!   yield   fission yield of identa from burnup of mat
!
! card 7
!   lambda  resonance-group goldstein lambdas (13 for
!           default 69-group structure, nrg otherwise).
!
! card 8    (only when jp1>0)

```

```
!    p1flx    current spectrum (jp1 entries read, the rest are
!              set with the default p1-flux calculated by njoy).
!-----
```

The first card specifies the input and output unit numbers, as is normal for NJOY modules. **ngendf** comes from a previous **GROUPE** run, and it can be in either binary or ASCII mode. **nout** is always in ASCII mode.

The options card allows the user to select how much detail will be printed on the output listing (**iprint**), whether the output is intended for WIMS-D or WIMS-E (**iverw**), and how many groups are desired. Currently, the only difference between WIMS-D and WIMS-E output is that some additional reaction cross sections are included for the latter. If the user selects some group structure different from the standard 69-group structure, an additional input card is required to give the number of groups (**ngnd**), the number of fast groups (**nfg**, 14 for 69 groups), the number of resonance groups (**nrg**, 13 for 69 groups), and the reference group used for normalizing the flux (**igref**, normally the low-energy group of the fast groups).

Card 3 is required. It gives the ENDF MAT number for the materials to be processed. If this MAT doesn't appear on the GENDF tape, a fatal error message will be issued. **nfid** will be the identification number for this material used on the output WIMS library, and **rdfid** will be the identification number for the resonance data. Formally, WIMS libraries allow for data sets with more than one version of the resonance-integral tabulation. The last parameter on this card is **iburn** to flag whether burn data are included in the input stream.

Card 4 starts out with **ntemp** and **nsigz**, which define the size of the resonance-integral tables. They are normally both set to zero; the code then uses all of the values computed by **GROUPE**. The reference sigma-zero value, **sgref**, is used for the elastic cross section and matrix, because these quantities are not normally self-shielded by WIMS. Normally, **1e10** is appropriate, but for the major fissionable material in the reactor (*i.e.*,  $^{238}\text{U}$  or  $^{232}\text{Th}$ ), it may be better to use a realistic number like **sgref=50**. WIMSR assumes that the potential scattering cross section for the material is constant, but this constant value is not available from the **GROUPE** output. The WIMSR user will have to look in the ENDF-formatted evaluation for the scattering length  $a$ , compute  $\sigma_p = 4\pi a^2$ , and enter the value as **sigp**. As shown in the following ENDF-formatted file fragment, the scattering length (9.56630- 1 in this case) is the second item on the fourth line in MF=2, MT=151.

|            |            |   |   |     |         |      |
|------------|------------|---|---|-----|---------|------|
| ...        |            |   |   |     |         |      |
| 9.22350+ 4 | 2.33025+ 2 | 0 | 0 | 1   | 01395   | 2151 |
| 9.22350+ 4 | 1.00000+ 0 | 0 | 1 | 2   | 01395   | 2151 |
| 1.00000+ 0 | 8.20000+ 1 | 1 | 1 | 0   | 01395   | 2151 |
| 3.50000+ 0 | 9.56630- 1 | 0 | 0 | 1   | 01395   | 2151 |
| 2.33025+ 2 | 0.00000+ 0 | 0 | 0 | 780 | 1301395 | 2151 |
| ...        |            |   |   |     |         |      |

The parameters `mti` and `mtc` select the thermal inelastic and elastic data from the sections that might be available on the GENDF tape. Most materials have only free-gas scattering available, and the appropriate values would be `mti`=221 and `mtc`=0. The conventional values to use for reactor moderator materials are given in Table 28.

Continuing with Card 4, WIMSR allows  $P_1$  scattering to be treated in two ways. If `ip1opt`=0, the  $P_1$  matrix for the material is written to the WIMS output file explicitly. This option is normally used only for major moderator materials, such as the components of water. The other option, `ip1opt`=1, instructs the code to use the  $P_1$  data to transport-correct the  $P_0$  elastic scattering

Table 28: Conventional values for thermal MT numbers (`mti` and `mtc`) used in WIMSR, [GROUPE](#), and [THERMR](#)

| Thermal Material      | MTI Value | MTC Value |
|-----------------------|-----------|-----------|
| H in H <sub>2</sub> O | 222       |           |
| D in D <sub>2</sub> O | 228       |           |
| Be metal              | 231       | 232       |
| Graphite              | 229       | 230       |
| Benzene               | 227       |           |
| Zr in ZrH             | 235       | 236       |
| H in ZrH              | 225       | 226       |
| Be(BeO)               | 233       | 234       |
| O(BeO)                | 237       | 238       |
| O(UO <sub>2</sub> )   | 239       | 240       |
| U(UO <sub>2</sub> )   | 241       | 242       |
| H in Polyethylene     | 223       | 224       |
| Al metal              | 243       | 244       |
| Fe metal              | 245       | 246       |



matrix; that is, the ingroup elements of the  $P_0$  matrix are reduced by the sum over all outgoing groups of the  $P_1$  matrix for that ingoing group.

The `inorf` parameter can be set to 1 to eliminate the resonance-integral table for `nu*fission` from the WIMS output. Some of the higher actinides are treated this way for some WIMS libraries. The `isof` flag is set to 1 to tell WIMSR to produce a fission spectrum. This is usually done for main fissile materials, such as  $^{235}\text{U}$  and  $^{239}\text{Pu}$ . The `ifprod` flag is used to control whether resonance tables are included for fission products.

WIMSR has some capability to format burn data for incorporation into a WIMS library (see cards 5 and 6). This part of the code has not been used or tested very much.

The final card gives the intermediate-resonance  $\lambda$  values for each of the resonance groups. Methods for obtaining these quantities with NJOY are outlined in Section 19.1.

## 19.5 Coding Details

The main entry point for WIMSR is subroutine `wimsr` exported by module `wimsr`. WIMSR starts by reserving the scratch files with unit numbers from 10 through 14. The next step is to read and echo the user's input. Note that the array `scr` is allocated. The code will issue error messages if more than the default `nwscr=30000` words are needed. Subroutine `wmunit` is then called. It looks at the record `MF=1/MT=451` for the desired material on the input GENDF tape to obtain the group structure. It then reads through the entire GENDF tape for this material to set the fission flags `i318` and `i618` and to count the number of temperatures that are available. The fission flag is used to handle cases where both `MT=18` and the partial fission representation (`MT=19, 20, ...`) appear on the GENDF tape.

Subroutine `resint` is called next to compute the WIMS resonance integrals from the `GROUPT` self-shielded cross sections. It reads through the entire GENDF tape and extracts the flux, absorption cross section, fission cross section, and elastic cross section versus temperature and sigma-zero for all of the resonance groups. It also extracts the reference-group flux versus temperature and sigma-zero and the fission  $\bar{\nu}$  value. The latter is computed from File 6 with delayed contributions from `MT=455` in File 3. Once all the data are in place, `resint` uses the  $\bar{\nu}$  values to convert the self-shielded fission cross sections into self-shielded  $\bar{\nu}\sigma_f$  values.

If the user has asked for a value of `ntemp` that is larger than the number of temperatures on the GENDF tape for this material, `resint` will duplicate the values from the last temperature given into the higher temperature positions for the flux and the absorption cross section.

The final step in `wminit` is to convert the self-shielded cross sections into resonance integrals using the method described in Section 19.1. These resonance integrals are written out to a scratch file and displayed on the output listing using subroutine `rsiout`. The elastic resonance integrals are only written for WIMS-E.

Next, the main program calls `xssecs` to process the cross sections. The outermost loop is over temperature. A distinction has to be made between the temperature-independent matrix data, such as (n,2n) and (n,n') reactions, and the temperature-dependent matrix data, such as thermal scattering. While reading through the GENDF tape, the following quantities are extracted and stored using the allocatable arrays indicated:

|                   |                                                                                                                                                            |
|-------------------|------------------------------------------------------------------------------------------------------------------------------------------------------------|
| <code>abs1</code> | radiative capture (MT=102);                                                                                                                                |
| <code>abs2</code> | other absorption reactions (MT=103-150);                                                                                                                   |
| <code>sf0</code>  | the fission cross section (MT=18);                                                                                                                         |
| <code>ab0</code>  | also the fission cross section (MT=18);                                                                                                                    |
| <code>sn2n</code> | the (n,2n) cross section;                                                                                                                                  |
| <code>scat</code> | the elastic scattering cross section (MT=2), possibly using the value corresponding to the reference sigma-zero value instead of infinite dilution;        |
| <code>xi</code>   | the log slowing down $\xi$ (MT=252);                                                                                                                       |
| <code>snus</code> | the fission yield $\bar{\nu}\sigma_f$ computed from either 3/452 or File 6 plus the delayed part from 3/455;                                               |
| <code>chi</code>  | the fission spectrum $\chi$ computed from either 5/455 or File 6 plus the delayed contributions from MT=455;                                               |
| <code>xs</code>   | the temperature-dependent scattering matrix, containing <code>mti</code> and <code>mtc</code> , the thermal inelastic and elastic reactions, respectively; |
| <code>l1</code>   | the smallest group number for a nonzero element of the nonelastic part of the matrix stored in <code>xs</code> ;                                           |
| <code>l1e</code>  | the smallest group number for a nonzero element of the elastic part of the matrix stored in <code>xs</code> ;                                              |
| <code>l2</code>   | the largest group number for a nonzero element of the nonelastic part of the matrix stored in <code>xs</code> ;                                            |

|             |                                                                                                                                   |
|-------------|-----------------------------------------------------------------------------------------------------------------------------------|
| <b>12e</b>  | the largest group number for a nonzero element of the elastic part of the matrix stored in <b>xs</b> ; and                        |
| <b>csp1</b> | the $P_1$ cross section for the thermal matrix obtained by summing over the $P_1$ matrix elements for scattering from each group. |

Once all the data for a temperature have been stored in memory, several additional operations are performed on them. The initial absorption cross section in **ab0** contains the fission cross section. The final value is formed by adding the data in **abs1** and **abs2**, and then subtracting the (n,2n) cross section in **sn2n**. The final transport cross section in **xtr** is formed by adding the absorption and subtracting the transport correction (**csp1**). The slowing-down power per unit lethargy is computed from  $\xi$ ,  $\sigma_{scat}$ , and the group boundary energies at **iegb**.

As usual, the treatment of fission is more complex. For some combinations of options,  $\bar{\nu}$  is computed by dividing the fission neutron production cross section by the fission cross section, and for others, the value of  $\bar{\nu}\sigma_f$  has to be computed from  $\bar{\nu}$  and  $\sigma_f$ . In addition, the fission spectrum, if requested, is normalized.

Subroutine **xsco** starts with a section that writes and prints the temperature-independent part of the WIMS data. This section is skipped when **xsco** is called with **itemp**>1. It first processes the temperature-independent vectors: potential scattering, slowing-down power, transport, absorption, IR lambda, and sometimes (n,2n). Next, it processes the fission vectors **nu\*sigf** and **sigf**. The temperature-independent part of the scattering matrix includes the fast groups and the resonance groups (this normally totals 27 groups). It is packed by retrieving the low (**lone**) and high (**ltwo**) limits for each band of nonzero elements from **l1** and **l2**, which were loaded in **xsecs**. They are used to compute the number of elements in the band and the location of the self-scatter element in the band (always 1 for this part of the matrix, because there is no upscatter). They are also used to direct how the numbers in **xs** are moved into **scr** with the zeros outside of the band removed. Note that the data are stored as follows: location of self-scatter for group 1, number of elements in band for group 1, the band of elements for group 1, location of self-scatter for group 2, number of elements in group 2, the band of elements for group 2, *etc.* If the number of elements in a band is zero, the two counts are there, but no band data are given. After being printed, the temperature-independent part of the matrix is written out on a scratch file **nscr2**.

The next part of **xsco** is executed for **itemp**=1 and all the higher temperatures. It prints and writes the temperature-dependent transport, and absorption

cross sections (they are defined in the thermal range only, normally groups 28-69). Note that the absorption cross section is also written out on scratch file **nscr3**. If available, the temperature-dependent fission neutron production cross section and fission cross section are also printed and written. The temperature-dependent scattering matrix is processed as described above, except that the incident-neutron group range is limited to the thermal range (normally 28-69). Note that the location of the self-scatter element will no longer be 1 for these data, because of the presence of upscatter. The packed matrix length and the packed data are written out to scratch file **nscr3**.

If the user has requested that  $P_1$  scattering matrices be constructed for the material, subroutine **p1scat** is called. It uses methods similar to those described above. The results are printed and written onto **nscr4** by **p1sout**.

The last step in WIMSR is to call **wimout** to prepare the final WIMS data library. The first card on **nout** is slightly different for WIMS-D and WIMS-E. It is followed by lines for the burnup data using numbers obtained from common storage.

The data needed for the material identifier card are available in global storage. The temperature-independent data are read from **nscr2** and written to **nout**. Similarly, the temperature-dependent data are read from **nscr3** (although the **tempr** array is obtained from global storage). For WIMS-D, a record mark is written at this point.

The resonance data, if needed, are read from **nscr1** and written to **nout**. The format is slightly different for WIMS-D and WIMS-E. The WIMS-D version has extra lines containing **ntnp**, the product of the number of temperatures and the number of sigma-zero values, and it has a record mark after the resonance data block. The WIMS-E version has an extra section of resonance-integral data for computing the self-shielded elastic scattering cross section.

If a fission spectrum was requested, it is written out next by using data from the allocatable array **uff**. If a  $P_1$  matrix was requested, it is read in from **nscr4** and written out onto **nout**.

This completes the entire WIMS library. The final step takes place in the main WIMSR program, where the normal timing and storage usage messages are printed.

## 19.6 WIMS Data File Format

The following section describes the WIMS data output provided by WIMSR. It consists of a number of logical blocks of information written out in coded form.

The output is intended to be used by a library maintenance code to prepare a binary library for use by the WIMS code.

#### Library Header (2I5)

|      |                                                                                      |
|------|--------------------------------------------------------------------------------------|
| NFID | material identifier                                                                  |
| NPOS | position to insert material on a large multimaterial library (given for WIMS-E only) |

#### Burnup Data (3(1PE15.8,I6))

(YIELD(I), IFISP(I), I=1, JCC/2 fission yields and fission product flag

#### Material Identifier Data (I6,1PE15.8,5I6)

|        |                                                                                                                                                                                                                                                                                               |
|--------|-----------------------------------------------------------------------------------------------------------------------------------------------------------------------------------------------------------------------------------------------------------------------------------------------|
| IDENT  | material identifier                                                                                                                                                                                                                                                                           |
| AWR    | atomic weight ratio to neutron                                                                                                                                                                                                                                                                |
| IZNUM  | atomic charge number $Z$ for this material                                                                                                                                                                                                                                                    |
| IFIS   | fission and resonance flag: 0=non-fissile with no resonance tabulation, 1=non-fissile with resonance absorption only, 2=fissile with resonance absorption only ( <i>e.g.</i> , $^{240}\text{Pu}$ ), 3=fissile with resonance absorption and fission, 4=fissile with no resonance tabulations. |
| NTEMP  | number of temperatures                                                                                                                                                                                                                                                                        |
| NRESTB | number of resonance tables included (0 or 1)                                                                                                                                                                                                                                                  |
| ISOF   | fission spectrum flag (0=no, 1=yes)                                                                                                                                                                                                                                                           |

#### Temperature-Independent Vectors (1P5E15.8)

|                      |                                                        |
|----------------------|--------------------------------------------------------|
| (SIGP(I), I=1, N2)   | $\sigma_p$ for resonance groups                        |
| (XX(I), I=1, N2)     | $\xi\sigma_s/\tau$ for resonance groups                |
| (XTR(I), I=1, N1+N2) | transport cross section for fast and resonance groups  |
| (ABS(I), I=N1+N2)    | absorption cross section for fast and resonance groups |
| (DUM, I=1, N2)       | unused dummy for resonance groups                      |
| (ALAM(I), I=1, N2)   | IR $\lambda$ values for resonance groups               |

#### Temperature-Independent Fission (IFIS>1 only) (1P5E15.8)

|                     |                                                   |
|---------------------|---------------------------------------------------|
| (NSIGF(I), I=1, N1) | $\bar{\nu}\sigma_f$ for fast and resonance groups |
|---------------------|---------------------------------------------------|

(SIGF(I), I=1, N1)  $\sigma_f$  for fast and resonance groups

#### P<sub>0</sub> Matrix Length (I15)

NDAT length of P<sub>0</sub> scattering block to follow

#### Temperature-Independent P<sub>0</sub> Matrix (1PE15.8)

(XS(I), I=1, NDAT) packed scattering data: IS for group 1, NS for group 1, NS scattering elements for group 1, IS for group 2, NS for group 2, *etc.*, through all of the fast and resonance groups (normally through group 27). IS is the position of self-scatter in the band of scattering elements (always 1 here), and NS is the number of elements in the band.

#### Temperature Values (1PE15.8)

(TEMP(I), I=1, NTEMP) temperatures in Kelvin

*Repeat the following 4 blocks for each of the NTEMP temperatures.*

#### Temperature-Dependent Transport and Absorption (1PE15.8)

(XTR(I), I=1, N3) transport cross section for thermal groups

(ABS(I), I=1, N3) absorption cross section for thermal groups

#### Temperature-Dependent Fission Vectors (1PE15.8)

(NSIGF(I), I=1, N3) fission neutron production cross section  $\bar{\nu}\sigma_f$  for thermal groups

(SIGF(I), I=1, N3) fission cross section  $\sigma_f$  for thermal groups

#### Temperature-Dependent P<sub>0</sub> Matrix Length (I15)

NDAT length of P<sub>0</sub> scattering block

#### Temperature-Dependent P<sub>0</sub> Matrix (1PE15.8)

XS(I), I=1, NDAT packed scattering data: IS for group N, NS for group N, NS scattering elements for group N, IS for group N+1, NS for group N+1, *etc.* through the last group (normally group 69). IS is the position of self-scatter in the band of scattering

elements, and NS is the number of elements in the band.

Record Mark ( ' 999999999999' ), WIMS-D only

Resonance Control Data

|       |                                               |
|-------|-----------------------------------------------|
| RID   | resonance set identifier                      |
| NTEMP | number of temperatures for this resonance set |
| NSIGZ | number of background cross section values     |

Absorption Resonance Data

|                             |                                 |
|-----------------------------|---------------------------------|
| (TEMP(I), I=1, NTEMP)       | temperatures                    |
| (SIGZ(I), I=1, NSIGZ)       | background cross section values |
| (RESA(I), I=1, NTEMP*NSIGZ) | absorption resonance integrals  |

Nu\*fission Resonance Data

|                              |                                 |
|------------------------------|---------------------------------|
| (TEMP(I), I=1, NTEMP)        | temperatures                    |
| (SIGZ(I), I=1, NSIGZ)        | background cross section values |
| (RESNF(I), I=1, NTEMP*NSIGZ) | nu*fission resonance integrals  |

Scattering Resonance Data, WIMS-E only

|                             |                                 |
|-----------------------------|---------------------------------|
| (TEMP(I), I=1, NTEMP)       | temperatures                    |
| (SIGZ(I), I=1, NSIGZ)       | background cross section values |
| (RESS(I), I=1, NTEMP*NSIGZ) | scattering resonance integrals  |

Record Mark ( ' 999999999999' ), WIMS-D only

Fission Spectrum

|                        |                         |
|------------------------|-------------------------|
| (FSPECT(I), I=1, NGND) | fission spectrum $\chi$ |
|------------------------|-------------------------|

*Repeat the following two blocks  
for each of NTEMP temperatures.*

P<sub>1</sub> Matrix Length (I15)

|      |                                           |
|------|-------------------------------------------|
| NDAT | length of P <sub>1</sub> scattering block |
|------|-------------------------------------------|

P<sub>1</sub> Matrix (1PE15.8)

XS(I), I=1,NDAT)      packed scattering data: IS for group 1, NS for group 1, NS scattering elements for group 1, IS for group 2, NS for group 2, *etc.*, through the last group (normally group 69). IS is the position of self-scatter in the band of scattering elements, and NS is the number of elements in the band.

**19.7 WIMSR Auxiliary Codes**

The WIMSR output as described above is not directly usable by WIMS. Two library-maintenance codes are used at Los Alamos. An unpublished code called FIXER is used to modify (fix up) an existing WIMS-D library, or to create a new one, using WIMSR output. It processes burnup data, main data, resonance data, and P<sub>1</sub> matrices. In its fix-up mode, it can replace, delete, or add a material. another unpublished code called WRITER is a code to read a WIMS-D library in coded form, convert it to binary form, and list it in a user readable form.

**19.8 Error Messages**

error in wimsr\*\*\*too many time dependent isotopes

See nymax=100 in the global variables at the beginning of the wimsm module.

error in wminit\*\*\*desired material is not on gendf tape

Check whether the right input GENDF input tape was mounted.

error in wminit\*\*\*incorrect group structure

The group structure on the input GENDF file does not agree with the one specified in the WIMSR input deck.

message from wminit---mat xxxx mf xx has both mt18 and ...

If both MT=18 and MT=19 are present in File 3 or File 6, WIMSR must make a choice of which to use. For materials with partial fission reactions, **GROUPR** normally does not process the fission matrix from MT=18. It is more accurate to use the sum of the partial fission matrices.

message from wminit---mat xxxx has no mf3, mt252 ...

In the absence of an input section for  $\bar{\mu}$ , it will be computed assuming isotropic CM scattering.



error in resint\*\*\*storage exceeded

The size of the allocatable scratch array is set by the global parameter  
nwscr=30000.

error in xsecs\*\*\*storage exceeded

The size of the allocatable scratch array is set by the global parameter  
nwscr=30000.

message from xsecs---ref sig0 xxx not on list...

In this case, the first entry will be used as the default.

message from xsecs---nu-bar calculated from fission ....

This is just to alert the user to this situation.

message from xsecs---use only xx temps for mat xxxx

The thermal inelastic sections are missing from some of the higher temperatures on the input GENDF tape. This message tells you how many temperatures can be used correctly. Check the [THERMR](#) and [GROUPE](#) runs if more temperatures are needed.

error in xseco\*\*\*scratch storage exceeded

The size of the allocatable scratch array is set by the global parameter  
nwscr=30000.

error in plscat\*\*\*storage exceeded

The size of the allocatable scratch array is set by the global parameter  
nwscr=30000.

error in plscat\*\*\*no p1 matrices found for mat xxxx

Check the [GROUPE](#) run to make sure that  $P_1$  matrices have been requested for the desired materials.

error in plscat\*\*\*no temperature-dependent reactions ...

Check the [GROUPE](#) run to make sure that the elastic scattering matrix was requested.



## 20 PLOTR

The PLOTR module provides a general-purpose plotting capability for ENDF, PENDF, and GENDF files by generating files that [VIEWR](#) can use to generate high-quality Postscript plots. The following kinds of plots are produced:

- conventional 2-D plots (for example, cross section *vs* energy) of ENDF, PENDF, or GENDF data with the normal combinations of linear and log scales, automatic or user-specified ranges and labels, an optional alternate right-hand axis, and with one or two title lines;
- a set of experimental data by itself or superimposed on ENDF, PENDF, or GENDF curves;
- curves of various patterns, labeled with tags and arrows or described in a legend block;
- data points given with a variety of symbols with error bars (they can be identified in a legend block);
- detailed 3-D perspective plots of File 4 or File 6 angular distributions with a choice of a linear or a log axes for incident energy and a choice of energy range and viewpoint;
- selected 2-D plots of File 5 and File 15 emission spectra for specified incident energies, and selected 2-D emission spectra for given energies and particle types for File 6 data;
- detailed 3-D perspective plots of File 5, 6, or 15 energy distributions with a choice of log or linear axes and viewpoint (both  $EE'\theta$  and  $E\theta E'$  laws are supported);
- 3-D plots of GENDF data; and
- various 2-D plots for File 7 data, including both symmetric and asymmetric  $S(\alpha, \beta)$  *vs* either  $\alpha$  or  $\beta$ .

This section describes PLOTR in NJOY 2012.0. The PLOTR module described previously[3] included both the capability to parse data in ENDF formats and the basic plotting calls. In this version, the basic plotting calls have been moved to the new [VIEWR](#) module, and the PLOTR module concentrates exclusively on constructing plots from the data files. The coding has been converted into a modular Fortran-90 style.

Methods for generating these types of plots will be given in the following subsections. An attempt has been made to keep the input as simple as possible by moving the less common options to the right-hand side of each input line so that they can be easily defaulted. A complete copy of the input instructions will be found in Section [20.8](#). It may be useful to refer to it occasionally while reading the following sections.

## 20.1 Simple 2-D Plots

The simplest kind of 2-D plot is for a single reaction from an ENDF, PENDF, or GENDF file using automatic scales and default labels. For example, to plot the total cross section of carbon from ENDF/B-VII, use the following input (don't type the line numbers; they are inserted here for reference):

```
1.  plotr
2.  31/
3.  /
4.  1/
5.  '<endf/b-vii carbon'/
6.  '<t>otal <c>ross <s>ection'/
7.  4/
8.  /
9.  /
10. /
11. /
12. 6 20 600 3 1/ tape20 is ENDF/B-VII carbon
13. /
14. 99/
15. stop
```

The data to be plotted are selected in line 12 using the normal MAT, MF, MT notation of ENDF. The “slash” at the end of the line hides several defaults, the first of which is the temperature, which defaults to 0K. The “4” in line 7 selects log-log axes (a number of other options are defaulted here also). Lines 8 through 11 are blank, resulting in the choice of automatically defined ranges and default labels. Two title lines are given on lines 5 and 6. Note the use of special shift characters to change between lowercase and uppercase. The file on tape31 should be sent through [VIEWR](#) to generate the Postscript plot. The result is shown in Fig. [57](#).

In many cases, the default scales will give reasonable plots. However, in this case, the low-energy portion of the plot is approximately constant. It makes sense to change the lower limit of the  $x$  axis in order to expand the amount of detail shown at higher energies. A slight change in the lower limit of the  $y$  axis would also be beneficial. It is only necessary to change two lines as follows:

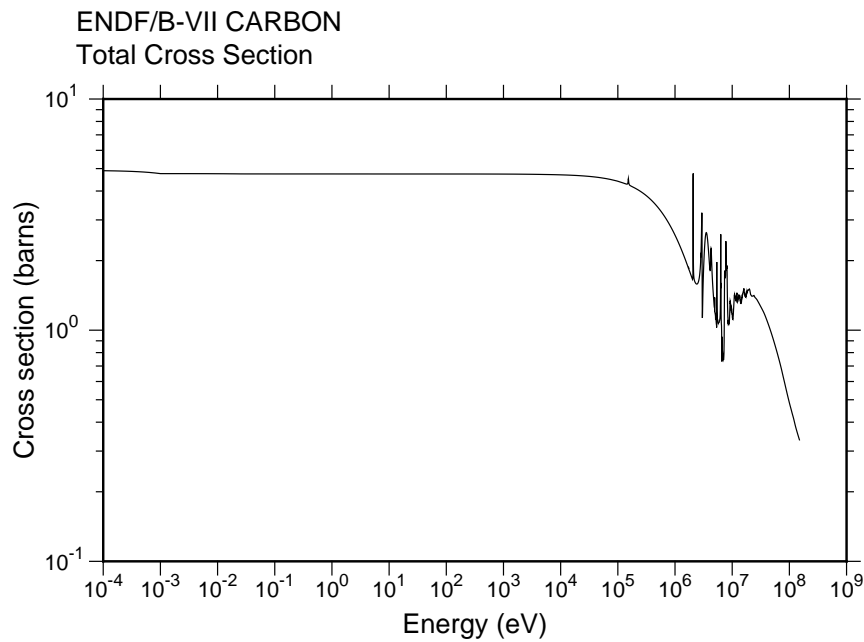


Figure 57: Simple 2-D plot of the total cross section of ENDF/B-VII carbon using automatic log-log axes.

```

8.  1e3 2e7/
10.  .5 10/

```

Note that the third parameter on these axes cards should always be defaulted for log scales. The results are shown in Fig. 58. This is a better balanced plot.

If the user needs to emphasize the high-energy region, linear scales are more appropriate. In addition, some people may prefer a different font. The following input gives the results shown in Fig. 59. Note how the new font is specified in line 3. The linear-linear axes option is selected in line 7.

```

1.  plotr
2.  31/
3.  1 1/
4.  1/
5.  '<endf/b-vii carbon'/
6.  '<t>otal <c>ross <s>ection'/
7.  1/

```

```

8.  /
9.  /
10. /
11. /
12. 6 20 600 3 1/ tape20 is ENDF/B-VII carbon
13. /
14. 99/
15. stop

```

The limits for the linear  $x$  axis in this example could have been specified by the user with a card of the form

```
8. 0 1e7 2e6/
```

The general rule for linear axes is either give all three parameters explicitly, or default all three parameters. For log axes, either give the first two parameters and default the third, or default all three parameters.

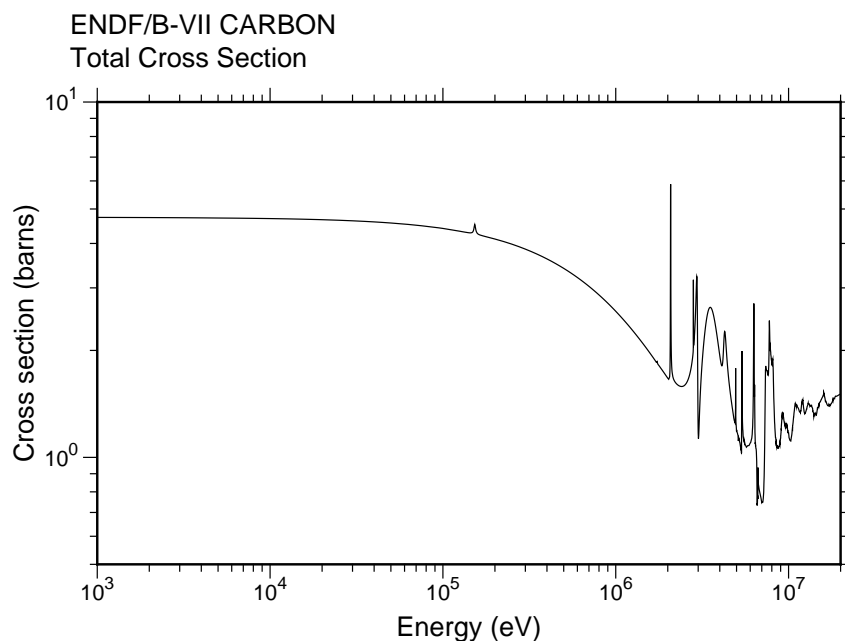


Figure 58: Simple 2-D plot of the total cross section of ENDF/B-VII carbon using log-log axes with user-selected ranges.

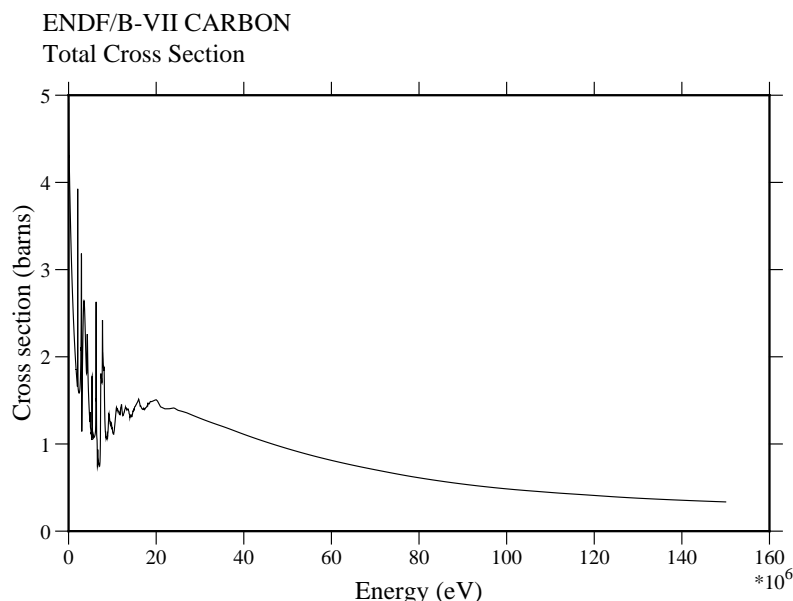


Figure 59: Simple 2-D plot of the total cross section of ENDF/B-VII.0 carbon using linear axes to emphasize the high-energy region and a more elaborate font.

Most ENDF or PENDF reactions will have many more energy points than can be shown on a graph like those in these figures. Therefore, PLOTR “thins” the grid down until there are fewer than `max` points on the plot (`max` is currently 10 000). On the other hand, at some energies some ENDF reactions are described on fairly coarse energy grids using interpolation laws like “lin-lin” or “log-log”. These representations will look as the evaluator intended if they are plotted using corresponding scales (for example, log-log interpolation on log-log scales, or log-lin interpolation on log-lin scales), but if they were to be plotted on a different set of axes, the cross sections between the grid points would be different from those intended. Therefore, PLOTR “thickens” the energy grid by adding additional energy points between the grid points of the evaluation and computing the cross section at each of these points from the given interpolation law. The resulting curves will be faithful to the evaluation, but they may exhibit unphysical bumps and cusps in certain modes of presentation.

## 20.2 Multicurve and Multigroup Plots

Several curves can be drawn on each set of axes, and each curve can be taken from a different data source. The following input deck demonstrates how GENDF data can be compared with PENDF data by overplotting:

```

1.  plotr
2.  31/
3.  /
4.  1/
5.  'ENDF/B-VII #EH.5>241#EXHX>Pu' /
6.  /
7.  4 0 2 1 5e3 500/
8.  .1 2e7/
9.  /
10. 1 1e4/
11. /
12. 6 23 9443 3 18 293.6/
13. /
14. 'pointwise fission'/
15. 2/
16. 1 24 9443 3 18 293.6 1 1 1/
17. 0 0 1/
18. 'multigroup fission'/
19. 99/
20. stop

```

The result is shown in Fig. 60. The PENDF data are requested on Card 12, and the GENDF data are requested on Card 16. Note the use of `ivers=1` to denote GENDF data, and also note the settings for `nth`, `ntp`, and `nh` necessary to select the  $P_0$  infinitely dilute cross section for plotting. The GENDF-format data are automatically converted into histogram form for plotting. This example also demonstrates using a “legend” block to identify the two curves. The position for the legend is given on Card 7. These values are normally determined by trial and error. Note also the presence of a superscript in the title. The superscript depends on the [VIEWR](#) “instruction” mode, which is described in the [VIEWR](#) section of this report.

As another example of a plot of multigroup data, Fig. 61 shows both infinitely dilute and self-shielded cross sections, and the plot also compares them with the pointwise cross section. In order to distinguish better between the different curves, color and double width are used. Here are the curve colors currently allowed:



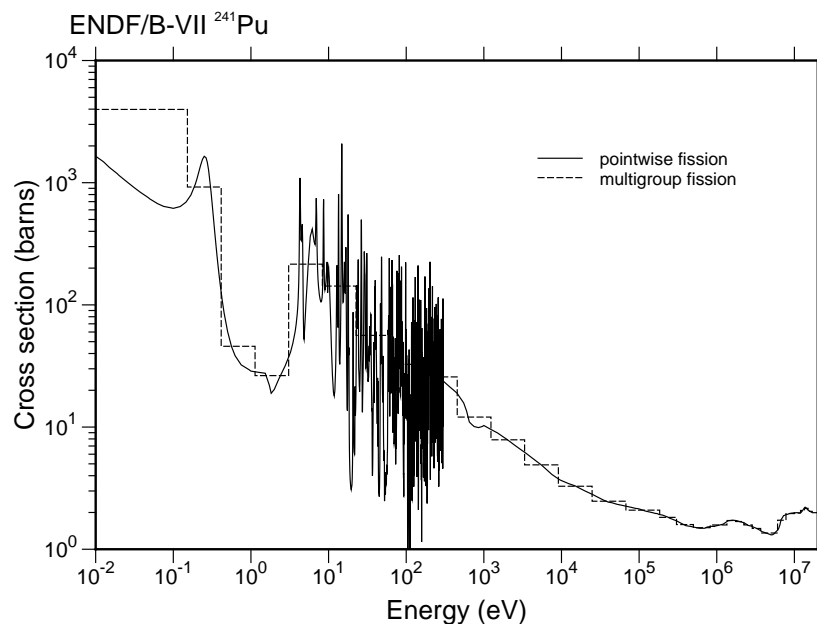


Figure 60: Comparison of the multigroup fission cross section of ENDF/B-VII.0  $^{241}\text{Pu}$  (dashed curve) with the corresponding pointwise cross section from the PENDF tape (solid curve).

curve color (def=black)

0=black  
 1=red  
 2=green  
 3=blue  
 4=magenta  
 5=cyan  
 6=brown  
 7=purple  
 8=orange

In addition, this plot uses “tags” and arrows to identify the different curves. The position of the tags and the  $x$  location for the arrowhead usually must be determined by trial and error. See lines 15, 20 and 25, which give the  $x$  and  $y$  coordinates of the tag and  $x$  coordinate where the arrow head meets the curve. The input for this example follows:

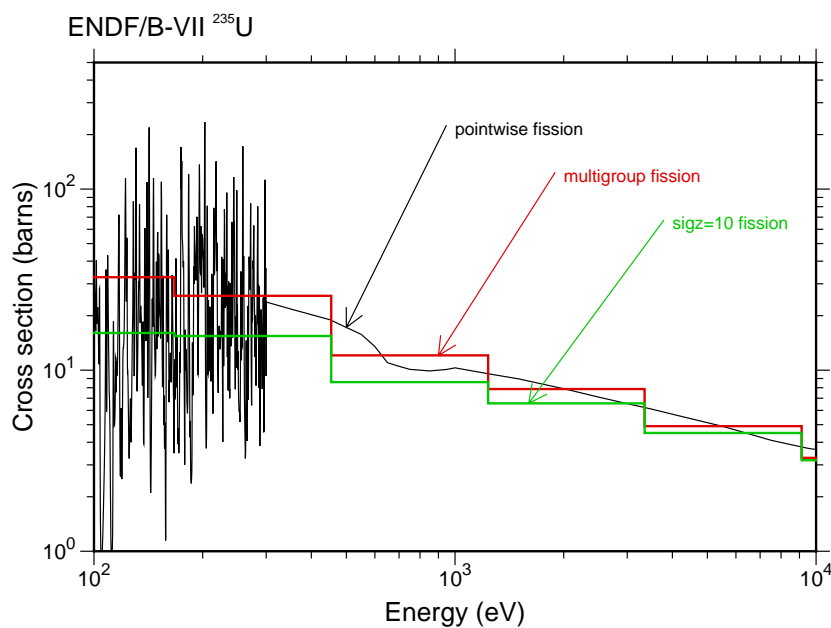


Figure 61: Multigroup fission cross sections of ENDF/B-VII.0  $^{235}\text{U}$  for infinite dilution and a 10-barn background compared with the corresponding pointwise cross section.

```

1.  plotr
2.  31/
3.  /
4.  1/
5.  'ENDF/B-VII #EH.5>235#EXHX>U' /
6.  /
7.  4 0 2 2/
8.  100 10000/
9.  /
10. 1 500/
11. /
12. 6 23 9443 3 18 293.6/
13. /
14. 'pointwise fission'/
15. 1000 200 500/
16. 2/
17. 1 24 9228 3 18 293.6 1 1 1/
18. 0 0 1 2/
19. 'multigroup fission'/

```

```

20. 2000 110 900/
21. 3/
22. 1 24 9228 3 18 293.6 1 3 1/
23. 0 0 2 2/
24. ']'#S+LH.5>0#LXHX>=10 fission'/
25. 4000 60 1600/
26. 99/
27. stop

```

This example requires 293.6K PENDF data for  $^{235}\text{U}$  on the input file **tape23** and 293.6K multigroup data for  $\sigma_0 = \infty$ ,  $\sigma_0 = 500$  barns, and  $\sigma_0 = 10$  barns on **tape24**. These tapes can be generated with the following NJOY input deck:

```

1. reconr
2. 20 21/ tape20 is U-235
3. /
4. 9228/
5. .1/
6. 0/
7. broadr
8. 20 21 22
9. 9228 1/
10. .1/
11. 293.6
12. 0/
13. unresr
14. 20 22 23
15. 9228 1 3 1
16. 293.6
17. 1e10 500 10
18. 0/
19. groupr
20. 20 23 0 24
21. 9228 3 0 3 1 1 3 1
22. /
23. 293.6
24. 1e10 500 10
25. 3 1/
26. 3 18/
27. 3 102/

```

```

28.  0/
29.  0/
30.  stop

```

### 20.3 Right-Hand Axes

PLOTR supports the capability to have different ordinate scales on the left and right sides of a graph. One place where this can be used is plotting a data curve and the ratio of another data curve to the first curve. An example of this is shown in Fig. 62. The input file used to make this plot is shown below. The [RECONR](#) module is run twice to make zero °K PENDF files for plotting. Note the minus signs on lines 28 and 35 — this selects the right-hand scale for those sections of the input. In line 36, the value of `nth` of 3 request the ratio calculation, and the additional input card in line 37 is read to access the second material for the ratio.

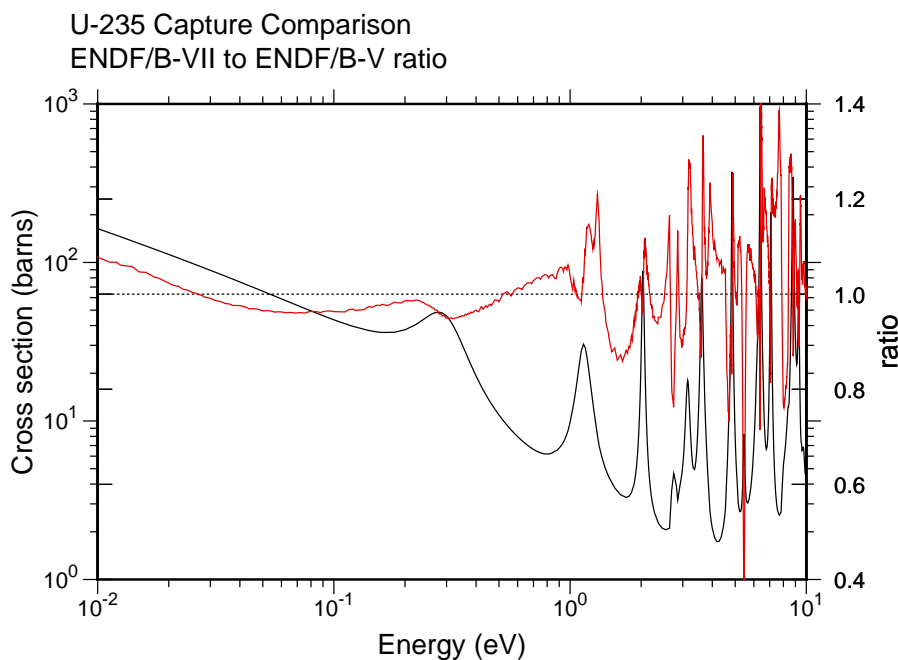


Figure 62: Using a right-hand axis to plot the ratio of the ENDF/B-VII.0 capture cross section for  $^{235}\text{U}$  to the ENDF/B-V value. The black curve is the ENDF/B-V cross section, and the red curve is the ratio (right-hand axis).

```
1. reconr
2. 20 22/ tape20 ENDF/B-V U-235
3. /
4. 1395/
5. .02/
6. 0/
7. reconr
8. 21 23/ tape20 ENDF/B-VII U-235
9. /
10. 9228/
11. .02/
12. 0/
13. plotr
14. 31/
15. /
16. 1/
17. 'U-235 Capture Comparison'/
18. 'ENDF/B-VII to ENDF/B-V ratio'/
19. 4 1/
20. 1e-2 10/
21. /
22. /
23. /
24. 0.4 1.4 .2/
25. 'ratio'/
26. 5 22 1395 3 102/ tape20 is carbon from V
27. /
28. -2/
29. 0/
30. 0 0 4/
31. 0/
32. 1e-2 1./
33. 10. 1./
34. /
35. -3/
36. 5 22 1395 3 102 0. 1 3/ tape20 is carbon from V
37. 6 23 9228 3 102 0./
38. 0 0 0 1/
39. 99/
40. stop
```

## 20.4 Plotting Input Data

PLOTR allows the user to insert data directly into the input deck. The main use of this is to superimpose experimental data over curves obtained from ENDF, PENDF or GENDF tapes, but reading data directly from the input deck can also be used to add precalculated curves or eye guides to plots, or to add special features such as vertical lines to separate regions on plots. Experimental data points can be plotted with a variety of symbols, and  $x$  and/or  $y$  error bars can be included if desired. The error bars can be either symmetric or asymmetric. For experimental data, the curves and various sets of data points are normally identified using a legend block. The following input produces a typical example of this type of plot:

```

1.  plotr
2.  31/
3.  /
4.  1/
5.  'ENDF/B-VII CARBON'/
6.  '(n,l,a>) with fake data'/
7.  1 0 2 1 1.3e7 .25/
8.  6e6 18e6/
9.  /
10. /
11. /
12. 6 20 600 3 107/
13. /
14. 'ENDF/B-VII MAT 600'/
15. 2/
16. 0/
17. -1 0/
18. '<s>mith & <s>mith 1914'/
19. 0/
20. 1.1e7 .08 .05 .05/
21. 1.2e7 .10 .05 .05/
22. 1.3e7 .09 .04 .04/
23. 1.4e7 .08 .03 .03/
24. /
25. 3/
26. 0/
27. -1 2/
28. 'Black & Blue 2008'/

```

```

29.  0/
30.  1.15e7 .07 .02 0. .2e6 0./
31.  1.25e7 .11 .02 0. .2e6 0./
32.  1.35e7 .08 .015 0. .2e6 0./
33.  1.45e7 .075 .01 0. .2e6 0./
34.  /
35.  99/
36.  stop

```

The results are shown in Fig. 63. The error bars for both of these simulated data sets are symmetric, as indicated explicitly in Cards 20 through 23, or by the zeroes in Cards 30 through 33. They can also be asymmetric if the lower and upper (or right and left) values are nonzero and different.

## 20.5 Three-D Plots of Angular Distributions

ENDF angular distribution data, whether given in File 4 or File 6, can be very bulky. Therefore, it is useful to present them in the form of a perspective plot

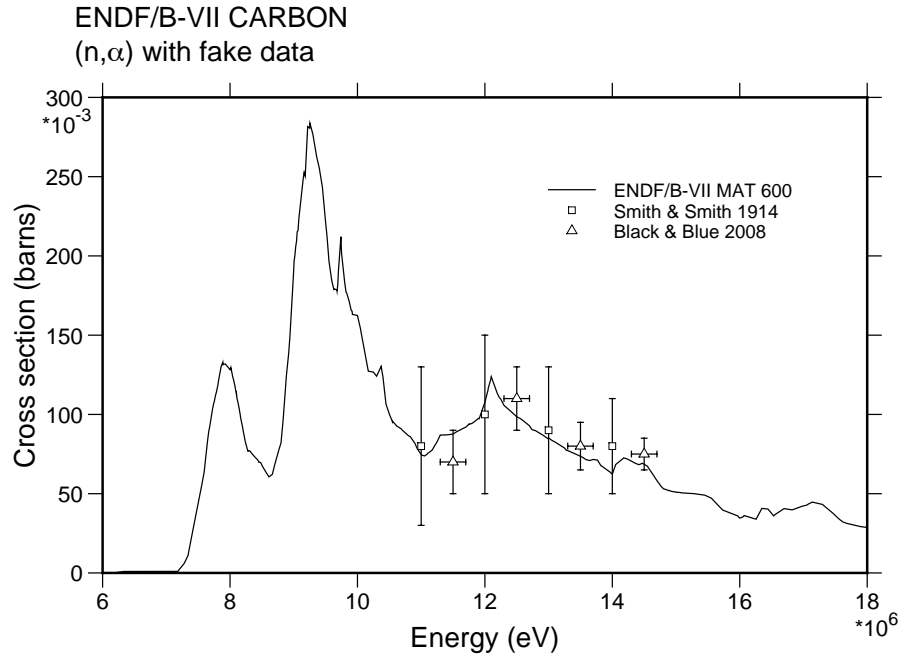


Figure 63: Carbon (n, $\alpha$ ) cross section compared with two sets of simulated experimental data represented with two types of error bars.

showing a family of angular distribution curves for each value of incident particle energy. An input deck to make such a perspective plot follows:

```

1.  plotr
2.  31/
3.  /
4.  1/
5.  'ENDF/B-V CARBON'/
6.  'Elastic MF4'/
7.  -1 2/
8.  /
9.  /
10. 1e6 5e6 1e6/
11. /
12. /
13. /
14. 5 20 1306 4 2/
15. /
16. 99/
17. stop

```

Fig. 64 shows the result using a linear axis for incident energy. This axis is the  $y$  axis, and its range has been limited to expand a particular part of the distribution. A linear scale emphasizes the high-energy region.

## 20.6 Three-D Plots of Energy Distributions

Three-D perspective plots are also useful for energy distributions. For the ENDF-5 and earlier formats, neutron secondary-energy distributions are given in File 5. The following input deck shows how to request a 3-D plot for File 5:

```

1.  plotr
2.  31/
3.  /
4.  1/
5.  'ENDF/B-V Li-6'/
6.  '(n,2n)]a neutron distribution'/
7.  -1 2 1/
8.  /
9.  /
10. 4e6 20e6 2e6/

```



```

11.  /
12.  5 20 1303 5 24/
13.  /
14.  99/
15.  stop

```

Grids lines have been requested in Card 7. The result is shown in Fig. 65. Similar methods can be used to plot photon emission distributions from File 15.

The new ENDF-6 format also provides for giving distributions for other emitted particles, such as protons, alphas, photons, and even recoil nuclei. This complicates the task of selecting which distribution is to be extracted from File 6. The user must specify the index for the particular outgoing particle to be considered (see `nkh`). Line 12 might become, for example,

```

12.  6 20 2437 103 0. 0 0 1/

```

which would request a plot of the proton distribution for the (n,p) reaction of  $^{54}\text{Cr}$  from ENDF/B-VI.

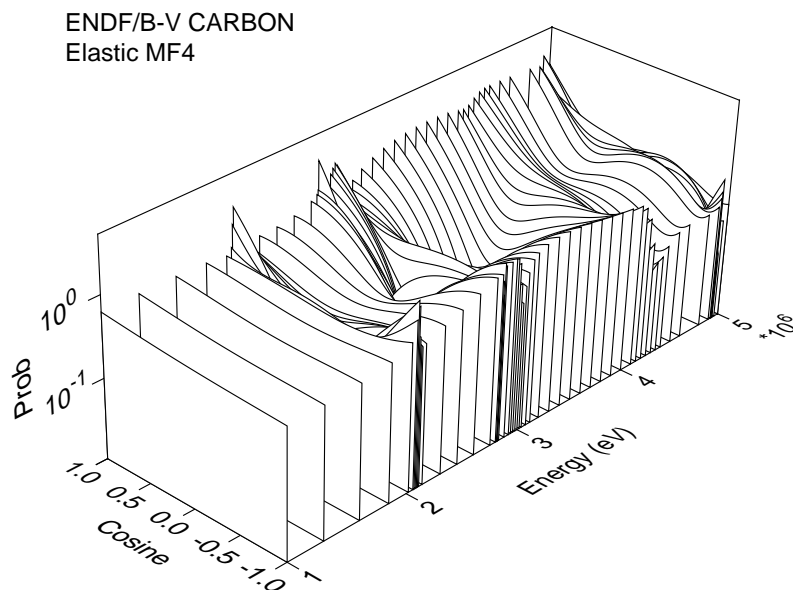


Figure 64: Perspective view of carbon elastic scattering angular distribution.

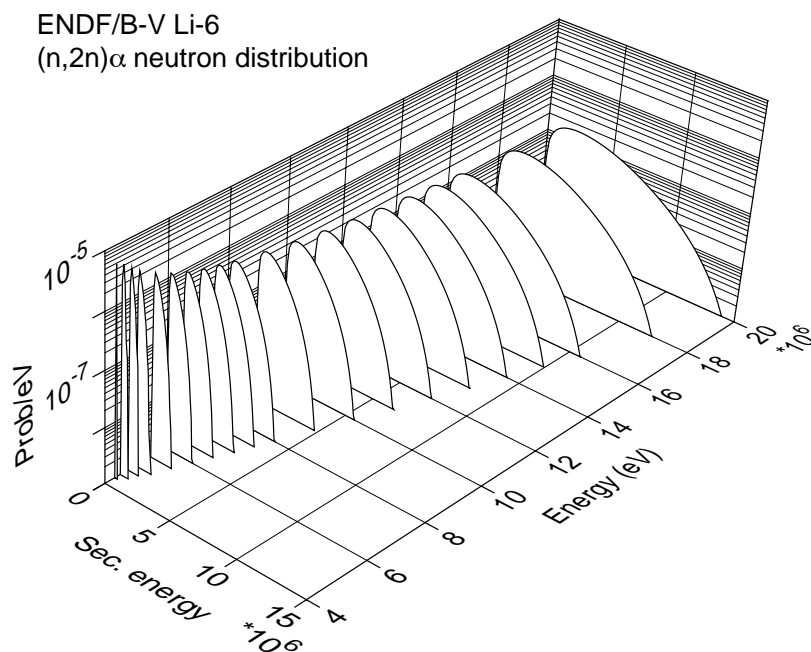


Figure 65: Perspective plot of  ${}^6\text{Li}$  (n,2n) $\alpha$  neutron secondary-energy distributions.

For some evaluations, File 6 uses Law 7, where the energy-angle distribution is represented as  $E \rightarrow E'$  distributions for several emission cosines  $\mu$ . In these cases, the `ntp` parameter may be used to select one of the emission angles, and the 3-D plot shows the distribution for that angle.

## 20.7 Two-D Spectra Plots from Files 5 and 6

It is difficult to see real detail on 3-D plots, and the emission spectra cannot be compared with measurements. Therefore, PLOTR has the capability to extract the spectrum for a particular particle and incident energy. The following input deck shows how several such spectra can be plotted on one graph.

```

1.  plotr
2.  31/
3.  /
4.  1/
5.  'ENDF/B-V Li-6'/
6.  '(n,2n)]a >neutron spectra vs <E>' /
7.  4 0 2 2/
8.  10. 2.e7/

```

```

9.  /
10. 1e-11 1e-6/
11. '<c>ross <s>ection (barns/e<V>)' /
12. 5 20 1303 5 24 0. 12/
13. /
14. '10 <m>e<v>' /
15. 1e3 2e-11 1e2/
16. 2/
17. 5 20 1303 5 24 0. 16/
18. /
19. '14 <m>e<v>' /
20. 1e4 2e-10 2e3/
21. 3/
22. 5 20 1303 5 24 0. 20/
23. /
24. '20 <m>e<v>' /
25. 1e5 2e-9 4e4/
26. 99/
27. stop

```

The results are shown in Fig. 66. “Tags” are used to distinguish between the different incident energy values.

The method used for selecting which curve is to be plotted is awkward in the current version of PLOTR. The user must give the index number of the incident energy desired (like the value 12 in line 12 of this example).

When an ENDF-6 format File 6 is available, emission spectra will normally be given for several emitted particles, photons, and recoil nuclei. In addition, angular data may be given for various  $E \rightarrow E'$  transfers using several different representations. This complicates the task of selecting which curve is to be extracted from File 6. For Law 1 data, the user must specify the particular outgoing particle to be considered (see **nk**), the index for the incident energy desired (see **nth**), and the dependent variable to plot (see **ntp**). The result depends on the representation used. In every case, **ntp**=1 gives the cross section versus  $E'$ , but for Legendre polynomials, **ntp**=2 gives the  $P_1$  component versus  $E'$ , and for Kalbach-Mann, **ntp**=2 gives the preequilibrium ratio versus  $E'$ . For Law 7, **ntp** specifies the emission angle. The graph will show a spectrum versus  $E'$  for the specified angle, specified incident energy  $E$ , and specified particle.

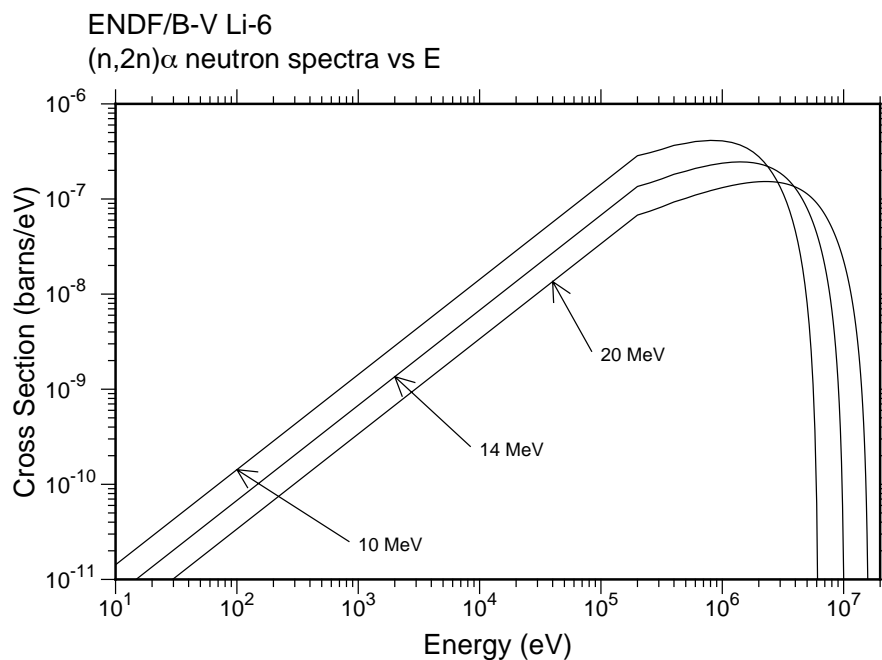


Figure 66: Two-D plot of selected secondary neutron spectra for the  ${}^6\text{Li}$  (n,2n) $\alpha$  reaction.

## 20.8 Input Instructions

```
!---input-----
!
! card 0
!   nplt          unit for output plot commands
!   nplt0         unit for input plot commands
!                 default=0=none
!                 output plot commands are appended
!                 to the input plot commands, if any.
! card 1
!   lori          page orientation (def=1)
!                 0 portrait (7.5x10in)
!                 1 landscape (10x7.5in)
!   istyle        character style (def=2)
!                 1 = roman
!                 2 = swiss
!   size          character size option
!                 pos = height in page units
!                 neg = height as fraction of subplot size
```

```

!               (default=0.30)
!   ipcol       page color (def=white)
!               0=white
!               1=navajo white
!               2=blanched almond
!               3=antique white
!               4=very pale yellow
!               5=very pale rose
!               6=very pale green
!               7=very pale blue
!
! -----repeat cards 2 through 13 for each curve-----
!
!   card 2
!   iplot       plot index
!               99 = terminate plotting job
!               1 = new axes, new page
!               -1 = new axes, existing page
!               n = nth additional plot on existing axes
!               -n = start a new set of curves using
!                   the alternate y axis
!               default = 1
!   iwcol       window color (def=white)
!               color list same as for ipcol above
!   factx       factor for energies (default=1.)
!   facty       factor for cross-sections (default=1.)
!   xll,yll     lower-left corner of plot area
!   ww,wh,wr    window width, height, and rotation angle
!               (plot area defaults to one plot per page)
!
! -----cards 3 thru 7 for iplot = 1 or -1 only-----
!
!   card 3
!   t1          first line of title
!               60 characters allowed.
!               default=none
!
!   card 3a
!   t2          second line of title
!               60 characters allowed.
!               default=none
!

```

```

! card 4
!   itype           type for primary axes
!                   1 = linear x - linear y
!                   2 = linear x - log y
!                   3 = log x - linear y
!                   4 = log x - log y
!                   set negative for 3d axes
!                   default=4
!   jtype           type for alternate y axis or z axis
!                   0 = none
!                   1 = linear
!                   2 = log
!                   default=0
!   igrd            grid and tic mark control
!                   0 = no grid lines or tic marks
!                   1 = grid lines
!                   2 = tic marks on outside
!                   3 = tic marks on inside
!                   default=2
!   ileg            option to write a legend.
!                   0 = none
!                   1 = write a legend block with upper left
!                       corner at xtag,ytag (see below)
!                   2 = use tag labels on each curve with
!                       a vector from the tag to the curve
!                   default=0
!   xtag            x coordinate of upper left corner
!                   of legend block
!   ytag            y coord of upper left corner
!                   default=upper left corner of plot
!
! card 5
!   el              lowest energy to be plotted
!   eh              highest energy to be plotted
!   xstep           x axis step
!                   default = automatic scales
!                   (default all 3, or none)
!                   (the actual value of xstep is
!                     ignored for log scales)
!
! card 5a
!   xlabel          label for x axis

```

```

!          60 characters allowed.
!          default="energy (ev)"
!
! card 6
!   yl          lowest value of y axis.
!   yh          highest value of y axis.
!   ystep       step for y axis (linear scales only)
!               default = automatic scales
!               (default all 3, or none)
!               (the actual value of ystep is
!               ignored for log scales)
!
! card 6a
!   ylabl       label for y axis
!               60 characters allowed.
!               default="cross section (barns)"
!
! card 7  (jtype.gt.0 only)
!   rbot        lowest value of secondary y axis or z axis
!   rtop        highest value of secondary y axis or z axis
!   rstep       step for secondary y axis or z axis
!               default for last three = automatic
!
! card 7a  (jtype.gt.0 only)
!   rl          label for alternate y axis or z axis
!               60 characters allowed.
!               default=blank
!
! -----cards 8 thru 9 are always given-----
!
! card 8
!   iverf       version of endf tape
!               set to zero for data on input file
!               and ignore rest of parameters on card
!               set to 1 for gendf data
!   nin         input tape
!               can change for every curve if desired.
!   matd        desired material
!   mfd         desired file
!   mtd         desired section
!               mtd=0 means loop over all reactions in mfd
!               (usually one page per mt, but for mf=3,

```

```

!               resonance reactions may have several pages)
!   temper      temperature for endf data (degK, default=0.)
!   nth,ntp,nkh see below (defaults=1)
!
!   special meanings for nth,ntp,nkh for file 3 or 5 data
!       nth      number of subsection to plot
!           (works for isomer prod, delayed n, etc.)
!       ntp      not used
!       nkh      not used
!
!   special meanings for nth for file 4 Legendre data
!       nth      index for Legendre coefficient (p1, p2, ...)
!
!   special meanings for nth,ntp,nkh for file 6 data
!       nth      index for incident energy
!       ntp      number of dep. variable in cyle to plot
!           (or angle number for law 7)
!       nkh      number of outgoing particle to plot
!
!   special meanings for nth,ntp,nkh for gendf mf=3 data
!       nth=0 for flux per unit lethargy
!       nth=1 for cross section (default)
!       ntp=1 for infinite dilution (default)
!       ntp=2 for next lowest sigma-zero values, etc.
!       nkh=1 for p0 weighting (default)
!       nkh=2 for p1 weighting (total only)
!
!   special meaning for nth for gendf mf=6 data
!       nth=1 plot 2-d spectrum for group 1
!       nth=2 plot 2-d spectrum for group 2
!       etc.
!       no special flags are needed for mf=6 3d plots
!
!   special meanings for nth and ntp for mf7 plots
!       nth is index for indep. variable (alpha or beta)
!       ntp=1 selects alpha as indep. variable (default)
!       ntp=2 selects beta as indep. variable
!       nkh=1 selects normal s(alpha,beta)
!       nkh=2 selects script s(alpha,-beta)
!       nkh=3 selects script s(alpha,beta)
!
!   -----cards 9 and 10 for 2d plots only-----

```



```

!
! card 9
! icon symbol and connection option
! 0 = points connected, no symbols
! -i = points not connected, symbol at every
! ith point
! i = points connected, symbol at every ith
! points
! default=0
! isym no. of symbol to be used
! 0 = square
! 1 = octagon
! 2 = triangle
! 3 = cross
! 4 = ex
! 5 = diamond
! 6 = inverted triangle
! 7 = exed square
! 8 = crossed ex
! 9 = crossed diamond
! 10 = crossed octagon
! 11 = double triangle
! 12 = crossed square
! 13 = exed octagon
! 14 = triangle and square
! 15 = filled circle
! 16 = open circle
! 17 = open square
! 18 = filled square
! default=0
! idash type of line to plot
! 0 = solid
! 1 = dashed
! 2 = chain dash
! 3 = chain dot
! 4 = dot
! default=0
! iccol curve color (def=black)
! 0=black
! 1=red
! 2=green
! 3=blue

```

```

!           4=magenta
!           5=cyan
!           6=brown
!           7=purple
!           8=orange
!   ithick   thickness of curve (def=1)
!           0 = invisible (for shaded areas)
!   ishade   shade pattern
!           0 = none
!           1 to 10 = 10\% to 100\% gray
!           11 to 20 = 45 deg right hatching
!           21 to 30 = 45 deg left hatching
!           31 to 40 = 45 deg cross hatching
!           41 to 50 = shades of green
!           51 to 60 = shades of red
!           61 to 70 = shades of brown
!           71 to 80 = shades of blue
!           default=0
!
! card 10 ---ileg.ne.0 only---
!   aleg     title for curve tag or legend block
!           60 characters allowed.
!           default=blank
!
! card 10a ---ileg.eq.2 only---
!   xtag     x position of tag title
!   ytag     y position of tag title
!   xpoint   x coordinate of vector point
!           (.le.0 to omit vector)
!
! -----card 11 for 3d plots only-----
!
! card 11
!   xv,yv,zv  abs. coords of view point
!           defaults=15.,-15.,15.
!   x3,y3,z3  abs. sides of work box volume
!           defaults=2.5,6.5,2.5
!
!           set x3 or y3 negative to flip the order of the
!           axis on that side of the work box.
!
! -----cards 12 thru 13 for iverf = 0 only-----

```

```

!
!  card 12
!      nform          format code for input data
!                      0 = free format input with
!                      optional x and y error bars
!
!  card 13  ---nform = 0 only---
!      xdata          dependent value
!                      terminate with empty card (/)
!      ydata          independent value
!      yerr1          lower y error limit
!                      no y error bar if zero
!      yerr2          upper y error limit
!                      if zero, equals yerr1
!      xerr1          x left error limit
!                      no x error bar if zero
!      xerr2          x right error limit
!                      if zero, equals xerr1
!
!  all curves contain at least 10 points per decade (see delta).
!  code can plot curves containing fewer than 2000 points (see
!  max) without thinning.  curves with more points are thinned
!  based on a minimum spacing determined from max and the
!  length of the x axis.
!
!-----

```

## 20.9 Coding Details

Subroutine `plotr` is the only public call in the module `plotm`. It starts by setting up the default paper size, margins, working box, and view point. It then reads in the first two input cards to define the unit for Postscript output and the parameters for the graphics page, such as orientation, font style, font size, and page color. The routine can then start the main loop over plots, subplots, and curves (see statement number 110). The next card is read, which gives the value of `iplot`. If `iplot=99`, the job is complete and the code exits through statement number 700 by writing an end “99” on the plot file and closing the open units.

The next step is to start reading the user’s input. For each input line, the defaults are set and the standard Fortran `READ*` method is used to read the

input. Once all the input parameters have been read, the code branches to different regions for different data types.

For ENDF and PENDF data, PLOTR reads the first part of File 1 and searches for the desired temperature. It then uses `findf` to locate the desired material and reaction. Note that there is an option for an automatic reaction loop that enters at statement number 320. When `mtd=0`, `plotr` automatically loops over all the MT numbers that it finds in the current file. For 2-D plots, it is necessary to extract the desired  $x$  and  $y$  values out of a TAB1 or a LIST record. It is fairly tricky finding this record because of the large number of possible formats in Files 3, 5, 6, 7, and 15. Some improvements are needed here to allow PLOTR to construct angular distributions from File 4 and to allow access by actual values rather than the indexes `nth`, `ntp`, and `nkh`.

Once the appropriate record has been located, PLOTR sets up a process to extract the  $x$  and  $y$  values from the record either thinning or thickening the given  $x$  grid as necessary to get a good plot. After all the values have been computed, the code ends up at statement number 610, and the `VIEWR` instructions to make the 2-D plot are written to the output file `nplt`. Control then loops back to either statement number 110 (ordinary manual reaction specification) or to statement number 320 (automatic reaction loop).

For 3-D ENDF or PENDF plots, the code first skips to the desired subsection of File 4, 5, 6, 15, etc. The structure of a subsection varies with the law used to describe the data. The format for File 4 and File 6 two-body angular distribution data is similar, so a common procedure `ad3d` can be used for these two Files. At each incident energy, the angular distribution is either obtained by interpolation in the given tabulation, or it is computed from the given Legendre coefficients. Once all the numbers have been loaded into the `aa` array, they are written to the output `nplot` file in `VIEWR` format.

For Files 5, 6, and 15 3-D plots, control is passed to subroutine `ed3d`. The data from the desired subsection are extracted and loaded into the `aa` array. During this process, the maximum and minimum values on the various axes are determined. The code determines an appropriate vertical axis range of about 3 decades. It then writes out the `VIEWR` file for the 3-D energy plot, removing any  $z$  values that are too small.

For GENDF 2-D data, PLOTR searches the GENDF tape for the requested material and temperature. It then reads in the entire MT=451 header record and sets pointers to the energy boundaries for the particle and photon group structures. The next step is to loop through the records on the file looking for

the desired reaction. The cross section values are read from the list records, and energy values for the histogram break points are computed from the group structure information. The resulting  $x$  and  $y$  arrays are passed to statement number 610 and written to the **VIEWR** file.

For 3-D GENDF plots, subroutine **gg3d** is used to extract the data for the distribution, add in the group-boundary energies, set up the axis limits, and write out the resulting distribution in **VIEWR** format.

Experimental data are read directly into the  $x$  and  $y$  arrays from the input deck. If error bars are present, they are read into the arrays **dxm**, **dxp**, **dym**, and **dyp**. The  $x$  and  $y$  arrays are passed to statement number 610 and written out in **VIEWR** format.

There are several remaining routines in PLOTR. Subroutine **gety6** is used to page in data from an ENDF-6 format File 6. Subroutine **fix17** is used to transform File 6 Law 7 into Law 1 form for plotting. This requires putting the spectra for all angles onto a common secondary-energy grid, and then integrating over angle for each energy of this common grid. The result is a  $P_0$  energy distribution ready for plotting. Subroutine **rname** constructs reaction names from ENDF MT numbers. Subroutine **ascale** constructs good axis limits and step sizes for linear axes.

## 20.10 Storage Allocation

The array **a**(30000) with length **nwamax**=30 000 words is used for reading in ENDF-format records. The main container array is **aa**(100000) with length **maxaa**=100 000. The maximum number of  $x, y$  pairs in any plot is set by data **max**=10 000. There are several arrays of this length equivalenced to various regions of the container array **aa**. See **x**(10000), **y**(10000), **b**(10000), **dxm**(10000), **dxp**(10000), **dym**(10000), and **dyp**(10000). These assignments could be changed, if necessary, for a very high resolution device. The arrays used to map coordinate values to curves for 3-D plots are limited to 200. This could be a problem if an evaluation had more than 200 incident energies in File 4, 5, or 6. There is a limit of 400 incident or outgoing energy groups for GENDF 3-D distributions.

## 20.11 Input and Output Units

PLOTR doesn't use any internal scratch units. The only units used are those mentioned on cards 0 and 8, and they can be either ASCII (**nin** positive) or

blocked binary (*nin* negative) as desired. ASCII and blocked binary units can be mixed on a single plot if necessary.

## 20.12 Error Messages

**error in plotr\*\*\*error in axis input**

Check your input Cards 5, 6, and/or 7. Remember that the easiest thing to do with *xstep*, *ystep*, or *rstep* for log axes is to take the default value. For linear scales, either give all three parameters, or default all three. Usually this message means some previous card is missing.

**error in plotr\*\*\*desired mat and temp not found a**

Check the input cards against the input tape mounted.

**error in plotr\*\*\*lf=1 only for mf5 or 15.**

The analytic secondary distribution laws are not supported by PLOTR.

**error in plotr\*\*\*lf=1 or 7 only for file 6.**

Two-D plots from File 6 are currently limited to laws 1 and 7.

**error in plotr\*\*\*illegal ntd for mf7.**

The requested value of *nth* is larger than the number of beta values available in File 7.

**error in plotr\*\*\*temperature not found.**

The requested temperature is not available in File 7.

**error in plotr\*\*\*storage exceeded.**

Either there is an undiscovered error in the thinning/thickening logic, or an attempt has been made to read a GENDF reaction with more than *nwamax*=30 000 words.

**error in plotr\*\*\*illegal mf6 law.**

Only laws 0, 1, 2, 3, 4, and 7 are currently supported.

**error in plotr\*\*\*3d mf7 plots not available.**

This would be a desirable extension for PLOTR.

**message from plotr---no distribution, no plot**

No distribution was found on the input tape.

**error in gg3d\*\*\*too many incident groups for 3d gendf plot**

This is limited to *maxx3*=400 groups.

**error in gg3d\*\*\*too many data for 3d gendf plot**

More than *maxaa*=100 000 words of GENDF data are needed.

**error in gg3d\*\*\*too many secondary groups for 3d gendf plot**

This is controlled by *maxy3*=400.

**error in fixl7\*\*\*not enough storage to convert file 7**

Up to *nw7max*=6000 words are made available out the the *aa* array for converting File 7.

## 21 VIEWR

The VIEWR module provides a general-purpose plotting capability for NJOY. It reads in user commands that define a variety of 2-D and 3-D graphs, and then it writes a Postscript file to display the graphs with high quality. Some of the capabilities of VIEWR include

- conventional 2-D plots (for example, cross section *vs* energy) with the normal combinations of linear and log scales, automatic or user-specified ranges and labels, an optional alternate right-hand axis, and with one or two title lines;
- curves of various line patterns, labeled with tags and arrows or described in a legend block;
- data points given with a variety of symbols with error bars (they can be identified in a legend block);
- the superposition of several plots on a given set of axes;
- detailed 3-D perspective plots for data such as angular distributions or energy distributions, with a choice of linear or log axes, with a choice of working area and viewpoint, and with one or two title lines;
- color can be used to distinguish between different curves, and the graphics window area and page background can also have selected colors;
- closed regions can be displayed with various kinds of cross hatching for filled with selected colors; and
- multiple plots can be put on each page.

Many examples of graphs generated by VIEWR can be found elsewhere in this report. This section describes VIEWR in NJOY 2012.0. When the previous report[3] was prepared, the module called “PLOTTR” included the capabilities now supported by the NJOY2012 PLOTTR module and the NJOY2012 VIEWR module. The original PLOTTR module was split up into one part that contains the logic needed to extract data from ENDF, PENDF, and GENDF files (the new [PLOTTR](#)) and another part containing the logic to convert the user’s commands and data values into the desired Postscript file (the new VIEWR). Therefore, this chapter is completely new.

### 21.1 Modular Structure

The `viewr` subroutine is encapsulated into a Fortran-90 module that only makes public that one subroutine call. This module is supported by module `graph`, which makes a number of calls and data structures public. The features in

**graph** provide the low-level capabilities for generating Postscript graphics that are used by the routines in VIEWR. We will first describe VIEWR by giving the user-input specifications and describing the details of the VIEWR coding. Finally, we will describe the details of the graphics calls as implemented in the separate **graph** module.

## 21.2 Using VIEWR

The VIEWR module can be used as a general-purpose plotting engine by constructing input for it by hand. However, it is more commonly used to display data assembled by other NJOY modules. For example, **PLOTR** reads data in ENDF, PENDF, or GENDF formats and constructs an output file in VIEWR format. **COVR** constructs an elaborate set of plots of cross-section covariance data using color contour maps and rotated subplots. **HEATR** can produce graphs showing the heating value, the photon energy production, and their associated kinematic limits. **DTFR** and **ACER** both are capable of generating VIEWR files that show the cross sections and distributions contained in the libraries that they produce. See the writeups for these various modules for examples of these kinds of plots.

## 21.3 Input Instructions

There is actually only one line of input for the VIEWR module itself:

```
!---input-----
!  
!  card 1  
!      infile          input file  
!      nps             postscript output file  
!
```

The plotting commands and data are provided on an input file to VIEWR that use the following format:

```
!---data file format-----
!  
!  card 1  
!      lori            page orientation (def=1)
```



```

!           0  portrait (7.5x10in)
!           1  landscape (10x7.5in)
!   istyle   character style (def=2)
!           1  roman
!           2  swiss
!   size     character size option
!           pos = height in page units
!           neg = height as fraction of subplot size
!           (default=.30)
!   ipcol     page color (def=white)
!           0=white
!           1=navajo white
!           2=blanched almond
!           3=antique white
!           4=very pale yellow
!           5=very pale rose
!           6=very pale green
!           7=very pale blue
!
! -----repeat cards 2 through 13 for each curve-----
!
!   card 2
!   iplot     plot index
!           99 = terminate plotting job
!           1  = new axes, new page
!          -1  = new axes, existing page
!           n  = nth additional plot on existing axes
!          -n  = start a new set of curves using
!                the alternate y axis
!           default = 1
!   iwcol     window color (def=white)
!           color list same as for ipcol above
!   factx     factor for energies (default=1.)
!   facty     factor for cross-sections (default=1.)
!   xll,yll   lower-left corner of plot area
!   ww,wh,wr  window width, height, and rotation angle
!           (plot area defaults to one plot per page)
!
! -----cards 3 thru 7 for iplot = 1 or -1 only-----
!
!   card 3
!   t1        first line of title

```

```

!           60 characters allowed.
!           default=none
!
!   card 3a
!       t2           second line of title
!           60 characters allowed.
!           default=none
!
!   card 4
!       itype        type for primary axes
!                   1 = linear x - linear y
!                   2 = linear x - log y
!                   3 = log x - linear y
!                   4 = log x - log y
!                   set negative for 3d axes
!                   0 = no plot, titles only
!                   default=4
!       jtype        type for alternate y axis or z axis
!                   0 = none
!                   1 = linear
!                   2 = log
!                   default=0
!       igrd         grid and tic mark control
!                   0 = no grid lines or tic marks
!                   1 = grid lines
!                   2 = tic marks on outside
!                   3 = tic marks on inside
!                   default=2
!       ileg         option to write a legend.
!                   0 = none
!                   1 = write a legend block with upper left
!                       corner at xtag,ytag (see below)
!                   2 = use tag labels on each curve with
!                       a vector from the tag to the curve
!                   default=0
!       xtag         x coordinate of upper left corner
!                   of legend block
!       ytag         y coord of upper left corner
!                   default=upper left corner of plot
!
!   card 5
!       xmin         lowest energy to be plotted

```

```

!      xmax      highest energy to be plotted
!      xstep      x axis step
!
!      default = automatic scales
!      (for linear, give all 3, or none)
!      (for log, give first 2, or none)
!
!      card 5a
!      xlabl      label for x axis
!
!      60 characters allowed.
!
!      (default = no label, no numbering)
!
!      card 6
!      ymin      lowest value of y axis.
!      ymax      highest value of y axis.
!      ystep      step for y axis (linear scales only)
!
!      default = automatic scales
!      (for linear, give all 3, or none)
!      (for log, give first 2, or none)
!
!      card 6a
!      ylabl      label for y axis
!
!      60 characters allowed.
!
!      (default = no label, no numbering)
!
!      card 7  (jtype.gt.0 only)
!      rmin      lowest value of secondary y axis or z axis
!      rmax      highest value of secondary y axis or z axis
!      rstep      step for secondary y axis or z axis
!
!      (default = automatic scale)
!
!      (for linear, give all 3, or none)
!      (for log, give first 2, or none)
!
!      card 7a  (jtype.gt.0 only)
!      rl        label for alternate y axis or z axis
!
!      60 characters allowed.
!
!      (default = no label, no numbering)
!
!      card 8  -- dummy input card for consistency with plotr
!
!      it always should be 0/
!
!      -----cards 9 and 10 for 2d plots only-----
!

```

```

!   card 9
!       icon           symbol and connection option
!                       0 = points connected, no symbols
!                       -i = points not connected, symbol at every
!                           ith point
!                       i = points connected, symbol at every ith
!                           points
!                       default=0
!       isym           no. of symbol to be used
!                       0 = square
!                       1 = octagon
!                       2 = triangle
!                       3 = cross
!                       4 = ex
!                       5 = diamond
!                       6 = inverted triangle
!                       7 = exed square
!                       8 = crossed ex
!                       9 = crossed diamond
!                       10 = crossed octagon
!                       11 = double triangle
!                       12 = crossed square
!                       13 = exed octagon
!                       14 = triangle and square
!                       15 = filled circle
!                       16 = open circle
!                       17 = open square
!                       18 = filled square
!                       19 = filled diamond
!                       20 = filled triangle
!                       21 = filled inverted triangle
!                       22 = crossed circle
!                       23 = exed circle
!                       24 = exed diamond
!                       default=0
!       idash          type of line to plot
!                       0 = solid
!                       1 = dashed
!                       2 = chain dash
!                       3 = chain dot
!                       4 = dot
!                       5 = invisible

```

```

!               default=0
!   iccol       curve color (def=black)
!               0=black
!               1=red
!               2=green
!               3=blue
!               4=magenta
!               5=cyan
!               6=brown
!               7=purple
!               8=orange
!   ithick      controls thickness of curve
!               0 = invisible (for shaded areas)
!               (default=1)
!   ishade      shade pattern
!               0 = none
!               1 to 10 = 10\% to 100\% gray
!               11 to 20 = 45 deg right hatching
!               21 to 30 = 45 deg left hatching
!               31 to 40 = 45 deg cross hatching
!               41 to 50 = shades of green
!               51 to 60 = shades of red
!               61 to 70 = shades of brown
!               71 to 80 = shades of blue
!               default=0
!
!   card 10    ---ileg.ne.0 only---
!   aleg       title for curve tag or legend block
!               60 characters allowed.
!               default=blank
!
!   card 10a   ---ileg.eq.2 only---
!   xtag       x position of tag title
!   ytag       y position of tag title
!   xpoint     x coordinate of vector point
!               (.le.0 to omit vector)
!
!   -----card 11 for 3d plots only-----
!
!   card 11
!   xv,yv,zv   abs. coords of view point
!               defaults= 15.,-15.,15.

```

```

!      x3,y3,z3      abs. sides of work box volume
!                      defaults=2.5,6.5,2.5
!
!          set x3 negative to flip the order of the axis on
!          that side of the box (secondary energy, cosine).
!
! card 12
!      nform          format code for input data
!                      0 = free format input with
!                      optional x and y error bars
!                      1 = free format input for a
!                      3d family of curves z(x) vs y
!
! card 13  ---nform = 0 only---  2-d data
!      xdata          independent value
!                      terminate with empty card (/)
!      ydata          dependent value
!      yerr1          lower y error limit
!                      no y error bar if zero
!      yerr2          upper y error limit
!                      if zero, equals yerr1
!      xerr1          x left error limit
!                      no x error bar if zero
!      xerr2          x right error limit
!                      if zero, equals xerr1
!
! card 14  ---nform = 1 only---  3-d data
!      y              y value for curve
!                      repeat cards 13 and 13a for each curve
!                      terminate with empty card (/)
!
! card14a  ---nform = 1 only---
!      x              x value
!      z              z value
!                      repeat card 13a for each point in curve
!                      terminate with empty card (/)
!                      disspla version requires same x grid
!                      for each value of y.
!
!-----

```

Card 1 in the data file format sets up the specifications for the graphics page. The orientation can be either portrait or landscape. Characters can use a serif style “roman,” implemented by the Postscript Times-Roman font, or sans-serif “swiss,” implemented by the Postscript Helvetica font. The character size can be specified in inches or as a fraction of the subplot size. The latter is handy when subplots are shrunk down to just a fraction of the page. The default character size is 0.30 inches. The page color set here is the color of the overall page. See below for the color inside the frame of a subplot. We have provided a set of pale colors here for these backgrounds.

Card 2 starts a new plot, subplot, or curve on an existing plot. It also provides the flag indicating the the plotting job is finished; namely, `iplot=99/`. The value for `n` when its magnitude is greater than one is arbitrary, but we often use 2, 3, *etc.*, to indicate the second, third, *etc.*, curves on a set of axes. You could just use the value `n=2` for every additional curve, and it would still work. The window color `ipcol` refers to the color inside the axes frame for 2-D plots and to the color used for the various slices of the function for 3-D plots. The same set of light colors described for the page background is used here, and the pages look good if different colors are selected for the page color and the window color. The parameters `factx` and `facty` are handy for changing the x or y units for a plot or for scaling curves on a multi-curve graph to be closer to each other. The last few parameters on this card are only needed when several small subplots are put onto one page. They define the position, size, and rotation of the subplot. The covariance plots from [COVR](#) make use of this feature.

The next few lines of input are only given for new plots or subplots. There can be zero, one, or two lines of titles provided above the graph. The size of the plot readjusts to use the space not used by titles. The titles (and all the other labels in VIEWR) can use some special characters to trigger effects like subscript, superscript, symbol characters, size changes, or font changes. The rules for this are defined in the source listing as follows:

```
!
! Character specifications are similar to DISSPLA, except that
! the default case is lower instead of upper. This allows
! mixed-case strings to be used in Postscript mode. The
! following shift characters are used:
!     < = upper-case standard
!     > = lower-case or mixed-case standard
!     [ = upper-case greek
```

```

!      ] = lower-case or mixed-case greek
!      # = instructions
! Give one of the shift characters twice to get it instead of
! its action. The following instructions are supported:
!      Ev = elevate by v as a fraction of the height
!           if v is missing or D is given, use .5
!      Lv = lower by v as a fraction of the height
!           if v is missing or D is given, use .5
!      Hv = change height by v as a fraction of the height
!           if v is missing or D is given, use .5
!      Fi = change to font number i
!      Mi = change mode number, where mode 0 is the lower 128
!           postscript characters and mode 1 is the upper 128
!      X  = reset E, L, or H. Font and Mode must be
!           reset explicitly.
!      c is a real number, i is an integer.
!

```

Normal characters are just entered using mixed upper and lower case as desired. If desired, upper case can be forced using the trigger character. For example,

```
<p>u-239 from <endf/b-vi>
```

will have the indicated characters displayed in upper case. Similarly, Greek letters can be entered using mixed upper and lower case, or they can be given in all lower case and then forced to upper case with the trigger character:

```

Display ]a> and ]b>, then ]G> and ]D>
Display ]a< and ]b>, then [g> and [d>

```

Subscripts and superscripts use the “instruction” trigger character. For example,

```
ENDF/B-VI #EH<3#HXEX<h>e
```

displays the isotope name for  ${}^3\text{He}$  correctly with a subscript one-half the size of the main characters. Subscripts lowered by one-quarter of the character size



and with height equal to three-quarters of the character size could be obtained using

```
X#L.25H.75<min#HXLX<
```

For the mapping of the symbols and the other special characters available by shifting to the upper 128 characters in each font, check the Postscript Red Book[92].

Returning to the input data, Card 4 sets up the axes for the plot using `itype` and `jtype`. Several choices are allowed for adding grid lines to the axes. There are two ways available to label the curves in multi-curve graphs, namely, legend blocks, and curve tags. The default location for the legend block is the upper left corner of the graph area, but it can be positioned wherever desired using `xtag` and `ytag`. These values use coordinate units. The legend block contains a line for each curve giving the plotting symbol, curve style or color, and an identifying string entered below (see `aleg`). Curve tags are defined below.

Cards 5, 5a, 6, 6a, 7, and 7a define the axis limits, step sizes, and labels. The limits and step sizes are defined automatically based on the data, but they can also be defined manually to better control the display. This is often necessary for multi-curve plots, because the axes are chosen based on the extent of the first curve, which may not be suitable for all the curves in the graph. The graph scales are sometimes scaled with a power of ten, and these powers are always chosen to be divisible by three. Thus, you might have a scale labeled barns with a factor of  $10^{-3}$  indicated; the numbers on the scale would then be milli-barns. Note that when no label is given, the numbering for the axis is also omitted.

Card 8 is a dummy card that is only used to make the VIEWR input more compatible with the `PLOTR` input. As indicated, it should always contain 0/.

Cards 9, 10, and 10a are used for curves on 2-D plots. You can use the `icon` connection parameter to choose simple curves, sets of symbols, or symbols connected by curves. A variety of symbols and curve types are provided, and curves can be rendered in color if desired. The colors provided are all darker than the light backgrounds provided. We do not allow for the light curves on dark backgrounds that some people like. Another way to distinguish between different curves is with the weight of the curve (see `ithick`). If the curve being plotted is closed, it can be filled with hatching patterns, shades of gray, or colors (shades of green, red, brown, or blue). The shades of gray could be used to show

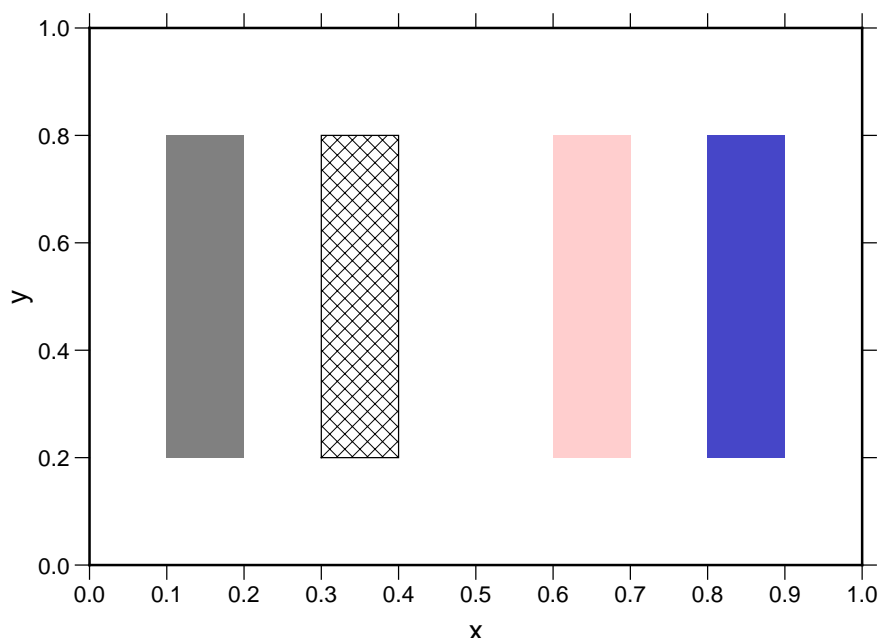


Figure 67: Examples of regions filled with gray, cross hatching and outlined, pink, and dark blue.

a variance band around a curve. The colors are used for the contour plots of covariances produced by [COVR](#), and many other uses are possible. See Fig. [67](#) for examples of fills.

Card 10 gives `aleg`, the identifying string for the curve that is used if legend blocks or curve tags were requested. The location for the curve tag and the point where the arrow point touches the curve are defined on Card 10a. The arrow from the tag to the curve can be omitted, if desired.

Card 11 is only given for 3-D plots. It defines the imaginary work box that contains the perspective view of the 3-D function, and it defines the view point outside of the box where your eye goes. The perspective distortion will be greater for close viewpoints and less for distant ones. The 3-D coding is not very sophisticated, and it is best to keep the view point in the octant defined by the defaults  $x,y,z=(15,-15,15)$ . That is, you are looking in along the  $x$  and  $z$  axes and the  $y$  axis is running away from you. You have the option of flipping the sense of the  $x$  axis, which is along the front of the work box as seen from the view point. This makes it possible to see features on either side of the slices of the function that are given for different discrete values of  $y$ . Fig. [68](#) may help to clarify the coordinate system used.

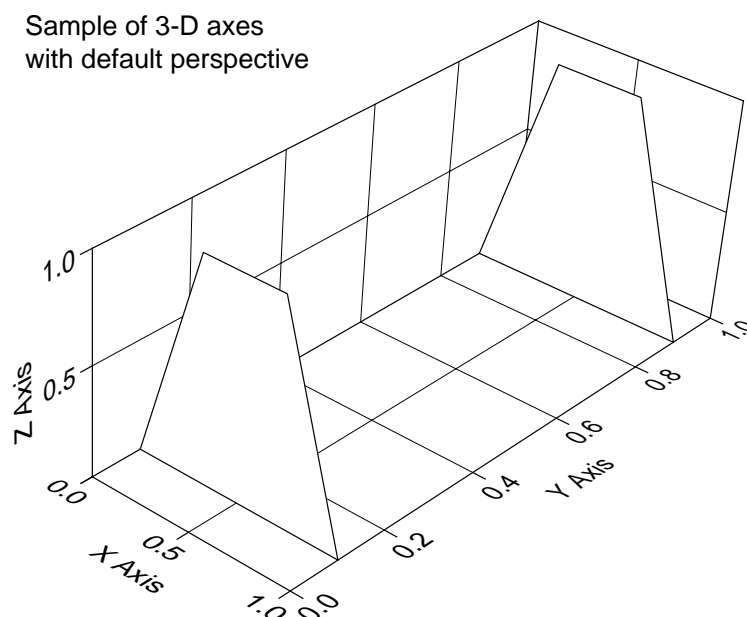


Figure 68: The 3-D coordinate system using the default work box and view point.

At this point, all the specifications for the 2-D or 3-D graph have been entered, and it is only necessary to enter the actual values to be plotted. The format to be used is controlled by **nform**, which currently has only two options. Option **nform=0** is used for 2-D curves with optional error bars. In order to make the input simple for simple cases, the sequence of the possible  $x$  and  $y$  values is arranged to be defaulted at various points. For a simple curve, you can just give  $x$  and  $y$ , and then terminate the line with  $/$ . For the most common case of error bars (symmetric  $y$  errors), just give  $x$ ,  $y$ ,  $\Delta y$ , and the terminating slash. The next step allows for asymmetric  $y$  error bars, then symmetric  $x$  error bars, and finally asymmetric  $x$  error bars. Terminate the list with an empty line (only  $/$ ).

For 3-D views, the function is represented by giving a set of curves  $z(x)$  for given values of  $y$ . The  $y$  values are given in increasing order, and each  $y$  value is followed by lines of  $x$  and  $z$  values terminated by  $/$ . The set of lines for each  $y$  is terminated by an empty card (only  $/$ ). The  $y$  list is also terminated by an empty line, so there are two lines with only  $/$  given at the end of the **nform=1** structure.

After the input data are given, the code loops back to search for another **iplot** value. If **iplot=99**, the job is finished.

## 21.4 Coding Details

The main entry for VIEWR is subroutine `viewr`, which is exported by module `viewm`. It starts up by setting the default values for paper size, margins, font size, line width, work box, and viewpoint. Sizes are currently given in inches (with apologies to the rest of the world). The first part of the input is read in to determine the page parameters, and then subroutine `gplot` from the `graph` module is called to initialize the plotting system.

The next step is to start the main loop over various plots, subplots, and curves in plots. The key to this is `iplot`, and this loop continues until `iplot=99`. For other values of `iplot`, the code reads in the user's input and stores the values in global variables for the `viewm` module. When all of the input values have been read for this particular plot, subplot, or curve, subroutine `viewr` call either `set2d` or `set3d` to do the work, and then loops back for the next case. When it sees `iplot=99`, it closes the current window (`endw`), closes the current page (`endp`), shuts down the plotting system (`gdone`), and exits from the VIEWR module.

Subroutine `set2d` is used to prepare a 2-D plot or subplot, or to add another curve to an existing set of 2-D axes. The information on the particular curve being plotted is passed in as parameters to the subroutine, and the other parameters that describe the plot or curve are available in the global variables (see the beginning of module `viewm`). For new plots, the code calls `initp` from the `graph` module to initialize a new page. Then for either a new plot or a new subplot on this page, it calls `init2` to initialize the graph area for a 2-D plot.

The next step takes place if automatic scaling has been requested by leaving the axis limits blank. The code reads through the input data to find the minimum and maximum values on the axis or axes being scaled. It then choose the axis limits and step size to have nice even values using either `ascalv` for linear axes or direct determination of the axis decades for log scales. With the axes determined, it calls `axis2` to construct and label the axes and to draw the line and tic marks on the opposite sides to complete the 2-D graph area. If a right-side axis has been requested, it adds it also. The legend block, if requested, is located inside the graph frame using either the default location (upper left corner) or the user's `xtag,ytag` choice.

Next, subroutine `frame2` is called, which establishes a clipping path just outside of the frame formed by the axes. This allows for a hint to suggest that a curve passes outside the specified graph area. Subroutine `erbar` is called to draw on the error bars, if any. Subroutine `curv2` is called to draw on the curves or the

plotting symbols. Subroutine `legndb` is called if a legend block was requested, or `tagit` is called if curve tags were desired instead. Finally, `endfr` is called to close out this graph frame, and subroutine `set2d` returns to the VIEWR main routine.

Subroutine `erbar` draws error bars, either x or y, and either symmetric or asymmetric. Note that they are drawn before the plotting symbol is drawn. This makes the opaque plotting symbol appear on top of the error bars for the expected appearance. The cap size for the error bars is set in this routine as `capd=0.02` in inches. Conversion between the user's data coordinates and absolute plot units is done using `xscale` and `yscale`. The error bars and caps are drawn using the routine `vect3`, which is actually drawing in two dimensions because the z coordinate is set to `zero`.

Subroutine `legndb` constructs the legend block or adds an additional line to an existing block. Subroutine `tagit` places a tag string at the desired location `xtag,ytag` and optionally draws an arrow from the tag string to meet the curve at `xpoint`. The routine interpolates for the y value corresponding to `xpoint` to define the position for the point of the arrow.

Subroutine `set3d` is used to construct a 3-D perspective plot. It first calls `initp` to initialize the graphics page, and then it calls `init3` to set up the 3-D perspective projection. Next, it reads through the input data to find the x, y, and z limits, and to adjust for nice scales. When this is complete, `set3d` can start to construct the scales and the opposite axes to complete the entire 3-D plotting frame. Grids can be added to the bottom and to the back two sides, if desired.

With the frame in place, subroutine `curv3` is called to produce the  $z(x)$  curve for each  $y$  value. The routine starts at the largest  $y$  value and works forward. Each  $z(x)$  curve is converted to an opaque panel by completing the polygon to the bottom and side of the graph area and filling with the window color. In this way, the curve for each lower value of  $y$  simply paints over the higher values, and no sophisticated hidden-line removal procedure is required.

Subroutine `ascalv` is used to adjust the minimum and maximum values for an axis to nice even values and to choose an appropriate step size. The routine is set up to prefer multiples of  $10^3$  for axis limits to suggest our normal micro, milli, kilo, and mega preferences for numbers, and it tries to use integer type labels rather than floating-point ones when possible.

## 21.5 The Graphics Module

The basic graphics calls used by VIEWR are provided by module **graph**. This section will describe how they work. There are two logical levels included in the module. The higher level works with windows, frames, user coordinates, and the like. Most of these routines are made public by the module. The lower level works to write the Postscript text itself, and most of these routines are not public.

Module **graph** uses a large number of global variables and arrays. They are not public, and they are accessed from the outside through various public subroutines. Note especially the values that describe the fonts, including the three font names (“Times-Roman,” “Helvetica,” and “Symbol”). There are tables of character widths for each of the fonts (**cs1**, **cw2**, *etc.*). Also note the tables that define the light colors for backgrounds and the darker colors for foregrounds. They are given using RGB values, and they could be customized to improve the artistic appearance of things.

The graphing logic uses a hierarchy of objects to represent a graph. The highest level is the graphing “page,” which is initialized by subroutine **initp** and ended by subroutine **endp**. A page is defined by its size, orientation, font style, font height normal line weight, and page background color. The user’s choices come in through the parameters to the subroutine, and they are used to set the appropriate internal global variables. The low-level routine **newp** is called to increment the Postscript page number and to write the corresponding Postscript “Page” comment. A page border is drawn using the low-level command **poly2** and the page area is filled with the defined page color.

The next level in the hierarchy is the “window,” which defines the area enclosing the graph, its titles, and its axis labels. It can have its own border (see **ibord**) and it sets up its own clipping path to protect other windows on the page. A window is initialized using **window** and ended using **endw**. Note that **endw** calls the low-level routine **gend** to end the clipping path and to write a “gend” comment on the Postscript file. The titles for the plot or subplot are drawn by **window**. There is also a subroutine called **transw** associated with a window. It transforms between the units inside the window and the actual units on the page, thus allowing for the possibility that the window has been rotated.

The third level of the hierarchy is related to the actual 2-D or 3-D plots. Subroutine **init2** is used to initialize a 2-D plot by choosing an origin and axis lengths to nicely position the graph in the window. It sets the coordinate transformation to turn off 3-D perspective. Finally, it draws the graph frame

(see `wframe=0.005`) and fills it with the specified window color. The 2-D plots also use a “frame.” Subroutine `frame2` initializes a frame by setting a clipping path just outside the frame boundary. This margin is controlled by `grace`. A frame is ended by calling `endfr`.

A 3-D plot is initialized by calling `init3`. It sets the color of the 3-D slices to the window color, sets up the axis parameters, and sets up the 3-D perspective transformation. It then adjusts the scale and position for the 3-D view to center the projection in the window. The key to transforming coordinates is subroutine `trans3`. It converts `x,y,z` coordinates in 3-space into `u,v` coordinates in the corresponding view plane. Note that `trans3` also gets called for lots of 2-D work, but the parameters that control the transformation are set to appropriate 2-D values by `init2` in those cases.

To draw a 2-D vector, `vect2` just calls `vect3` with the `z` coordinate set to zero. The subroutine `vect3` uses `trans3` to go from `x1,y1,z1` to window coordinates `wu1,wv1`. Then, `transw` is used to go from `wu1,wv1` to real page coordinates `u1,v1`, thereby accounting for any possible rotation of the window on the page. The point `u1,v1` is then passed to the low-level Postscript routine `moveh`, which moves the current position to `u1,v1`. The same process is used for the other end of the vector, and the low-level routine `drawh` is used to draw the line with width `w`. If this is an arrow (see `ivec`), the head can be constructed using suitable geometry.

Similarly, to draw a 2-D axis, `axis2` just calls `axis3` with the `z`-axis elements of the unit vectors set to zero. Subroutine `axis3` is a general routine to draw an axis projected into 3-D perspective. The line of the axis is defined by its length `asize`, its `x,y,z` origin, a unit vector along the length of the axis, and a unit vector defining the vertical direction for the characters. The subdivision of linear axis is defined by the minimum value, maximum value, and step size (`amin`, `amax`, and `astp`), but log axes need only the minimum and maximum values. Other options control the numbering, the label, and the tic marks. The `axis3` routine also sets up the constants that control the scaling subroutines `xscale`, `yscale`, and `zscale`, which are used to convert user coordinates into axis coordinates for plotting curves in either 2-D or 3-D displays. The reverse transformation can be done in 2-D using `xinvrs` and `yinvrs`.

Subroutine `grid2` is used to generate a grid for a 2-D case using the 3-D call with `z`-axis parameters set to zero. Subroutine `grid3` is used to draw a grid in a plane projected by perspective. The grid can be drawn perpendicular to the `x`, the `y`, or the `z` axis. It can be located at the minimum or the maximum. This

allows it to be used to subdivide all the back 3 surfaces of the 3-D perspective box. Both log and linear subdivision is possible. The log grids subdivide each decade at the 2, 3, 4, 5, *etc.* values.

Subroutine `curv2` is used to draw a curve or plot symbols on a 2-D plot. It uses the standard `trans3` and `transw` transformations to come up with the low-level u,v coordinates that go to the Postscript routines. It can also be used to fill a curve with color or hatching (see `fillh` and `hatch`). Subroutine `curv3` draws a 3-D curve by making the perspective transformation, completing the polygon to the working box bottom and back, and filling the polygon with the window color to make it opaque.

Subroutine `poly2` draws a filled 2-D polygon, with or without an outline. Similarly, `poly3` draws a 3-D polygon. Subroutine `hatch` will fill the current path with hatching or cross hatching. The options are left-leaning lines at 45 degrees, right-leaning lines at 45 degrees, or both superimposed.

Subroutine `text2` draws a 2-D text string using the 3-D call in the normal pattern of this module. Subroutine `text3` draws a text string projected by perspective into a 3-D space. The string starts at `xo,yo,zo`, and its orientation is controlled by one unit vector along the string, and a second unit vector that defines the vertical direction for the characters. This routine is complicated because it watches for a variety of trigger characters that enable things like subscript, superscript, size changes, font changes, and special characters. Subroutine `txtlen` is almost identical, but instead of drawing the string, it calculates the space that it will take to help with functions like centering labels. It uses a private routine `ssum` to add up character widths. These routines also use `rget` to decode real numbers out of a string.

The rest of the routines in module `graph` are the Postscript-dependent plotting package. The package begins with the public routine `gplot`, which sets up for “US letter” (8.5 inches by 11.0 inches) size, defines the page orientation (portrait or landscape), opens the Postscript output unit (`nps`), and writes the Postscript bounding box and page orientation comments. This routine pairs with `gdone`, which writes some closing Postscript comments and closes the Postscript output unit.

Subroutine `gset` sets up a clipping path, and subroutine `gend` closes a clipping path.

Subroutine `newp` starts a new Postscript page, including writing the “Page” comment that is needed by programs such as `ghostview` to make it easy to scan through Postscript files containing many plots (such as [ACER](#) output). It is



paired with **endp** to write the Postscript command “showpage” at the end of each page.

Subroutines **moveh** and **drawh** are routines for drawing lines on the page. This includes making various kinds of dashed lines, and doing the coordinate conversion between portrait and landscape orientations. Subroutine **fillh** is used to fill the current path with a color. The colors available for filling were defined in some global arrays as described above.

Subroutine **cclip** is used to set up a clipping path on the current path, and **nclip** is used to terminate it. Subroutine **ncurve** is used to cancel the current curve path in order to make a shaded region that doesn’t have a border.

Subroutine **dsym** is used to generate the symbols used for plotting by drawing them with low-level Postscript commands. The symbols are made opaque by filling them with the window color, or filled symbols can be made by filling polygons with the foreground color. A small routine called **circle** is used here. Subroutine **dchr** is used to draw a Postscript character in perspective by using basic Postscript transformations. This routine also sets the desired font and uses the octal character notation to get special characters. Subroutine **charw** is also needed for handling character strings; it returns the width for characters in the built-in fonts using the information from the global arrays of character widths.

The module ends with subroutine **stripv**, which is used to strip leading and trailing blanks from character strings and to return the actual number of characters found.

## 21.6 VIEWR Messages

message from viewr\*\*\*too much 3d data...

The amount of 3-D data allowed is controlled by **maxaa=200 000** and the array **aa(200000)**.

message from set3d\*\*\*curve truncated.

The 3-D plots are limited to **kmax=1999** elements. See **x(2000)**, **y(2000)**, and **z(2000)**.



## 22 MIXR

The MIXR module will construct a new PENDF tape with a specified set of reactions that are linear combinations of the cross sections on the input tapes. MIXR can also be used for ENDF tapes, but the input interpolation laws are ignored. The output file contains ENDF File 1 and File 3 sections only, and linear-linear interpolation is assumed.

MIXR can be used for several purposes. When combined with [PLOTTR](#), it can be used to construct mixed cross sections for plotting with [VIEWR](#). One example would be to combine the isotopic cross sections given in modern evaluations into elemental cross sections for comparison with older evaluated elemental data such as found, for example, in ENDF/B-V. Such an example is provided in the sample deck below. Another would be to compute the difference between two versions of a particular reaction; plots that simultaneously show one version of a function and the difference between that version and another are sometimes very revealing. In both cases, the mixed cross section is computed on the union grid of its components, and all details are preserved.

Another use for MIXR would be to prepare a new ENDF material to represent a particular “enriched uranium,” having a particular amount of  $^{235}\text{U}$  mixed with  $^{238}\text{U}$ . This file could then be run through the [GROUPT](#) flux calculator to generate an accurate pointwise flux for enriched uranium mixed with water, or for pins of enriched uranium in a typical reactor lattice. This computed flux could then be used as the weighting flux for computing the self-shielded cross sections of both  $^{235}\text{U}$  and  $^{238}\text{U}$  in two subsequent [GROUPT](#) runs. This approach handles the interference between resonances in  $^{235}\text{U}$  and  $^{238}\text{U}$  accurately, including proper treatment of all wide and intermediate resonance effects.

This section describes MIXR in NJOY 2012.3.

### 22.1 User Input

The following input instructions were copied from the comment cards at the beginning of the MIXR source. It is always a good idea to check the cards in the current version of the program for possible changes.

```

! user input --
!
! card 1  --  units
!      nout      output unit for mixed cross sections
!      nin1      first input unit (endf or pendf)
!      nin2      second input unit
!      ...      continue for nnin<=nninmx (=10) input units
!
! card 2  --  reaction list
!      mtn      list of nmt<=nmtmx (=20) mt numbers for
!              the output reactions
!
! card 3  --  material list
!      matn,     list of nmat<=nmatmx (=nninmx=10) pairs (matn,wtn)
!      wtn,     of material numbers and associated weighting factors
!
! card 4  --  temperature
!      temp     temperature (use zero except for pendf tapes)
!
! card 5  --  output material
!      matd     material number
!      za      za value
!      awr     awr value
!
! card 6  --  file 1 comment card
!      des     description (66 char max)
!
!-----

```

**Card 1.** This card gives the unit numbers for the output that will contain the mixed cross sections and the input files that contain the materials to be mixed together. Note that there is a limit of **nninmx**, currently 10, input files.

**Card 2.** The code currently allows up to **nmtmx**, currently 20, mixed reactions to be generated. This card contains a list of the MT numbers for these reactions. The number of reactions is counted automatically.

**Card 3.** This card (it may continue onto several lines) contains the MAT numbers and weights for the materials to be mixed. The first pair **matn**, **wtn** refers to the data on input file **nin1**; the next pair is for **nin2**, etc.

**Card 4.** The same temperature is used for all of the materials, and its value is given on this card in Kelvin. The appropriate value for ENDF tapes is zero. The temperatures used for PENDF cases must be in the set included on the PENDF tape.

**Card 5.** This card gives some values that are needed to construct the ENDF or PENDF file for the output material. **matd** is the conventional material number. **za** is  $1000 * Z + A$ , where  $Z$  is the charge number and  $A$  is the atomic mass number for the mixture. Finally, **awr** is the mass ratio to the neutron for the mixture.

**Card 6.** This card contains one line of text to be used for the Hollerith descriptive information in MF=1/MT=451 on the new ENDF tape for the fixture. The final tape on NOUT will contain the section MF=1/MT=451 and sections MF=3/MT=MT<sub>n</sub> only.

The following sample input deck combines the four isotopes of iron to generate plots for the total cross section (MT=1), the energy-balance heating cross section (MT=301), and the radiation damage cross section (MT=444). See the [PLOT](#) section of this report for more information on the part of the input deck that produces the actual graphs.

```
cfs get tape21:/pendf/5/fe/natr2
cfs get tape22:/pendf/6/fe/54
cfs get tape23:/pendf/6/fe/56
cfs get tape24:/pendf/6/fe/57
cfs get tape25:/pendf/6/fe/58
cat>input <<EOF
mixr
20 -22 -23 -24 -25/
1 301 444/
2625 .0590
2631 .9172
2634 .0210
2637 .0028/
```

```

300/
2600 26000 56.
'Fe-nat for ENDF/B-VI from MIXR'/
plotr
31/
/
1/
'ENDF/B-VI IRON'/
'TOTAL'/
1 0 2 1 13e6 9./
0 20e6 2e6/
/
0 10 2/
/
6 20 2600 3 1 300/
/
'ENDF/B-VI'/
2/
5 -21 1326 3 1 300/
0 0 4/
'ENDF/B-V'/
1/
'ENDF/B-VI IRON'/
'TOTAL'/
4 0 2 1/
1e2 1e5/
/
/
/
6 20 2600 3 1 300/
/
'ENDF/B-VI'/
2/
5 -21 1326 3 1 300/
0 0 4/
'ENDF/B-V'/
1/
'ENDF/B-VI IRON'/
'HEATING CHECK'/
1 0 2 1 1e6 2.7e6/
0 20e6 2e6/
/

```

```

0 3e6 .5e6/
*Heating (eV-barns)'/
6 20 2600 3 301 300/
/
'ENDF/B-VI'/'
3/
5 -21 1326 3 301 300/
0 0 4/
'ENDF/B-V'/'
1/
'ENDF/B-VI IRON'/'
'DAMAGE CHECK'/'
1 0 2 1 13e6 7e4/
0 20e6 2e6/
/
0 35e4 5e4/
'Damage (eV-barns)'/
6 20 2600 3 444 300/
/
'ENDF/B-VI'/'
3/
5 -21 1326 3 444 300/
0 0 4/
'ENDF/B-V'/'
99/
viewr
31 32
stop
EOF
xnjoy<input
cfs store plot:/pendf/6/fe/natplot

```

The first few lines retrieve ENDF/B-V version of  $^{nat}\text{Fe}$ , and the four iron isotopes for ENDF/B-VI. A c-shell “here file” is then created with the input for MIXR, [PLOT](#)R, and [VIEW](#)R. The lines after the EOF line take care of executing NJOY and saving the plot file for future use.

Returning to the actual NJOY input cards, note that the MIXR output will be on **tape20** in ASCII mode, and the four isotopic input files (in binary mode) will be on **tape22** through **tape25**. The next input card lists the three reaction types to be written onto the output file; it is followed by four cards giving the

isotope MAT numbers and the atomic fractions that they are to have in the mixture. These mix-specification cards are then followed by a card asking for a temperature of 300K.

The last two cards in the MIXR section specify the ENDF parameters for the mixed material that will be written on **tape20**. The MAT number is to be 2600 (the standard ENDF-6 value for natural iron), the ZA value is to be 26000, and the AWR value is to be 56.0000 (a rather crude choice). The text line shown will appear in MF=1/MT=451 on the output tape.

At this point, the MIXR module will run and produce its output file. The rest of the input deck reads in this output file and makes a graphical comparison of the mixed elemental cross section with the corresponding elemental values from ENDF/B-V.

## 22.2 Coding Details

Subroutine **mixr** is exported by module **mixm**. The heart of MIXR is subroutine **gety**. It is similar to **gety1** in the **endf** module, except that it works with several TAB1 records in parallel. The routine is initialized for up to **nmtmx** input TAB1 records on up to **nninmx** input tapes by calling it with **x=0** for each tape. It returns the value of **xnext** for each tabulation. The calling program can compare these **xnext** values to determine the lowest energy point for the mixed reaction (the threshold).

On subsequent calls with **x>0**, MIXR returns the value of **y** corresponding to **x** for the specified tabulation, and it also computes **xnext** for this tabulation. The calling program can loop through all the input tapes, compute the mixed value of **y** as a linear combination of the separate **gety** results, and compute the next energy grid point as the lowest of the values of **xnext** returned by the separate **gety** calls. In this way, the mixed results are obtained on a unionized grid, and no features are lost.

To do its job, **gety** has to keep tables of the current location and related parameters on each of the input tapes. These tables will be found in the subroutine, all with dimension **nninmx**.

## 22.3 Error Messages

**error in mixr\*\*\*mat and temp not found**

There is an inconsistency between the requested **matn** and **temp** values and the materials found on the input files **nin1**, **nin2**, ....



message from mixr\*\*\*mt=xxx not present for mat=xxxx

This message is just information. If the user asked for construction of, for example, an (n,2n) reaction for an element, and if one of the isotopes did not have an (n,2n) reaction, this message would be issued.

error in gety\*\*\*not properly initialized

The subroutine `gety` has to be called with `x=0` for each material/section combination to be introduced into the mixed reaction before it is called with `x>0`.



## 23 PURR

The unresolved self-shielding data generated by [UNRESR](#) are suitable for use in multigroup methods after processing by [GROUPT](#), but the so-called Bondarenko method[38] is not very useful for continuous-energy Monte Carlo codes like MCNP[17]. As pointed out by Levitt[93], the natural approach for treating unresolved-resonance self-shielding for Monte Carlo codes is the “Probability Table” method. The method requires tables of the probability that the total cross section will be less than some value  $\sigma_t$  for a number of incident energies. Then, when the Monte Carlo code needs the cross section at  $E$ , it selects a random number between 0 and 1 and looks up the corresponding  $\sigma_t$  in the appropriate probability table. The corresponding capture and fission cross sections are obtained from conditional probability tables that give  $\sigma_\gamma$  and  $\sigma_f$  versus  $\sigma_t$ . This approach allows geometry and mix effects on self-shielding to arise naturally during the Monte Carlo calculation, and it supplies reasonable variances for the tallies. The probability table method has been used successfully in a number of applications, notably the VIM continuous-energy Monte Carlo code[94], which was developed to solve fast-reactor problems where unresolved effects become very important.

The PURR module produces probability tables that can be used in versions of MCNP from 4B on to treat unresolved-resonance self-shielding.

In recent versions of NJOY, the Bondarenko self-shielded cross sections from PURR will override any previous self-shielded data on the PENDF file coming from [UNRESR](#).

This document describes PURR in NJOY 2012.0.

### 23.1 Sampling from Ladders

In the unresolved range, we don’t know the real center energy of any of the resonances, and we don’t know the partial widths that determine the shape and strength of any particular resonance. However, the ENDF evaluation provides us with mean values for the resonance spacings, the probability distribution for the spacings (the Wigner distribution), the mean values for the resonance partial widths, and the distributions for the partial widths (chi-square distributions for various numbers of degrees of freedom). These quantities are given for several different spin sequences, which are statistically independent, and for a number of energies spaced through the unresolved energy range. A “narrow-resonance assumption” is always made in the unresolved range; that is, the energy loss in

scattering in the system is assumed to be large with respect to the width of any of the resonances. Thus, neutrons arrive at random energies that are not correlated with the resonance structure. The effective cross sections at one of the energies in the ENDF unresolved grid then depend on a number of resonances in the vicinity of that energy, all of which are assumed to have resonance parameters characteristic of that grid energy value.

This allows us to define a plausible set of cross sections in the vicinity of one of the grid energies. We first define an energy range that will hold a specified number of resonances, and we randomly choose a set of sampling energies in this range, avoiding the ends of the range to reduce truncation effects. For each spin sequence, we start by choosing a center for the starting resonance from a uniform distribution (this provides a random offset between the various spin sequences in the ladder). We then choose a set of partial widths for this resonance drawn from the appropriate distributions. A second resonance is then chosen above the first using the distribution for resonance spacings, and partial widths are randomly chosen for it. Then a third resonance is chosen, and so on, until the energy range defined for the ladder has been filled. We can now compute the cross section contributions from this spin sequence at each of the sampling energies. We then step to the next spin sequence and repeat the process. After looping through all the spin sequences, the accumulated cross sections are one possible set of plausible cross sections that obey the defined statistics for the unresolved range.

We can now go through this set of sampled cross sections, determine how many values of the total cross section hit each bin, and compute the conditional average for the elastic, fission, and capture cross sections for samples where the total ends up in each bin. This is the contribution to the probability table from the particular resonance ladder. However, using only one ladder could result in average cross sections that differ dramatically from the expected infinitely dilute averages computed directly from the resonance parameters. Therefore, the whole sampling process is repeated again for a user-selected number of different ladders. When enough ladders have been processed, the average cross sections will begin to converge to the expected results. The following piece of a PURR output listing shows 16 ladders being processed for  $^{235}\text{U}$  from ENDF/B-VII.0:

```

e= 2.2500E+03   spot= 1.1700E+01   dbar= 1.6137E-01   sigx= 0.0000E+00
      total      elastic      fission      capture
  1  1.9471E+01  1.2074E+01  5.3460E+00  2.0507E+00
  2  1.9617E+01  1.2041E+01  5.6196E+00  1.9566E+00
  3  1.9559E+01  1.2075E+01  5.4597E+00  2.0245E+00
  4  1.9458E+01  1.2000E+01  5.5723E+00  1.8859E+00
  ...
 14  1.9456E+01  1.2102E+01  5.3632E+00  1.9905E+00
 15  1.9660E+01  1.2082E+01  5.4429E+00  2.1354E+00
 16  1.9363E+01  1.2019E+01  5.3736E+00  1.9710E+00
bkgd 0.0000E+00  0.0000E+00  0.0000E+00  0.0000E+00
infd 1.9778E+01  1.2105E+01  5.6364E+00  2.0363E+00
aver 1.9567E+01  1.2068E+01  5.5030E+00  1.9964E+00
pcsd      1.38      0.32      3.28      4.97
nres      3664

```

Some steps have been eliminated for brevity. The “aver” values computed from the sampling have converged to be fairly close to the infinitely dilute values “infd” computed from the resonance parameters. Here **spot** is the potential scattering cross section, **dbar** is the average resonance spacing, and **sigx** is the competitive cross section.

The probability table can be used to generate a picture of the probability distribution for the total cross section as shown in Fig. 69. This example is for  $^{238}\text{U}$ . It demonstrates how the fluctuations get smaller as energy increases, which means that the self-shielding effect also gets smaller.

The statements that generate the **VIEWR** input for this kind of plot are normally commented out.

During the sampling process, **PURR** also computes Bondarenko-style self-shielded cross sections just like those produced by **UNRESR**. These values are printed out so that they can be compared with the results from other methods. For recent versions of **NJOY**, the Bondarenko self-shielded cross sections replace any previous values on the PENDF file from **UNRESR**. The Bondarenko cross

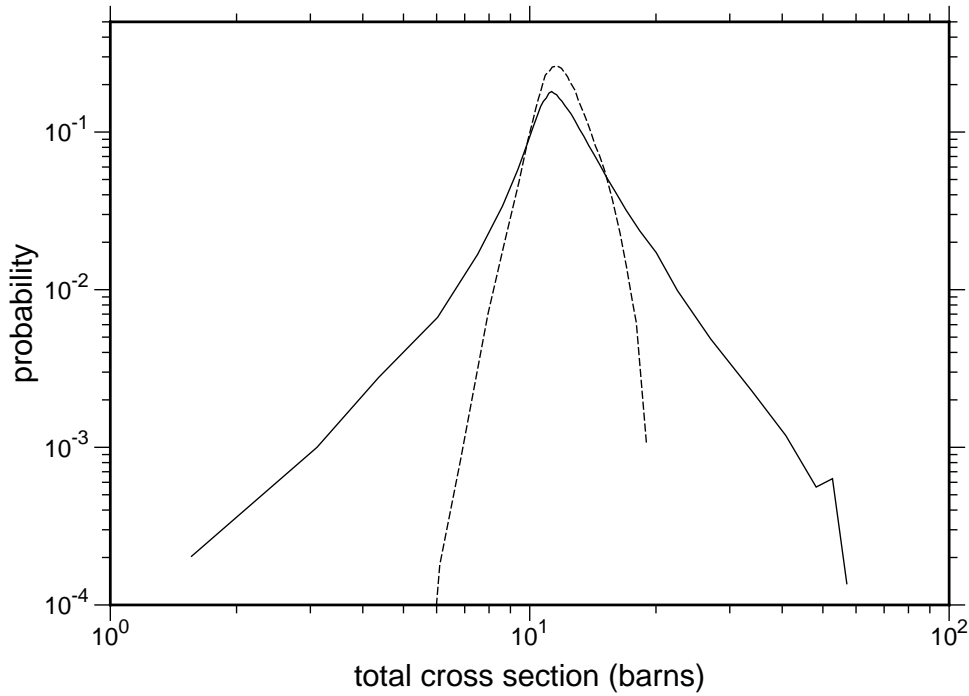


Figure 69: The probability distribution for the total cross section at 20 keV (solid) and 140 keV (dashed) in the unresolved resonance range of  $^{238}\text{U}$ .

sections can also be computed directly from the probability table using

$$\sigma_x(E) = \frac{\sum_i \frac{P_i(E)\sigma_{xi}(E)}{\sigma_0 + \sigma_{ti}(E)}}{\sum_i \frac{P_i(E)}{\sigma_0 + \sigma_{ti}}}, \quad (501)$$

where  $x$  can be  $t$  for total,  $n$  for elastic,  $f$  for fission, or  $\gamma$  for capture. These values are also printed out. They can be compared to the Bondarenko values from direct sampling to help judge whether adequate convergence has been obtained.

Fig. 70 shows Bondarenko-style self-shielded curves from PURR for the total cross section for  $^{238}\text{U}$  in the unresolved region at three different values of the dilution. This kind of plot is included in the standard graphs generated by ACER. Most of the self shielding comes from the elastic channel in this case. Fig. 71 shows how the total self-shielding factor for  $^{238}\text{U}$  varies with temperature and dilution at an energy of 20 keV.

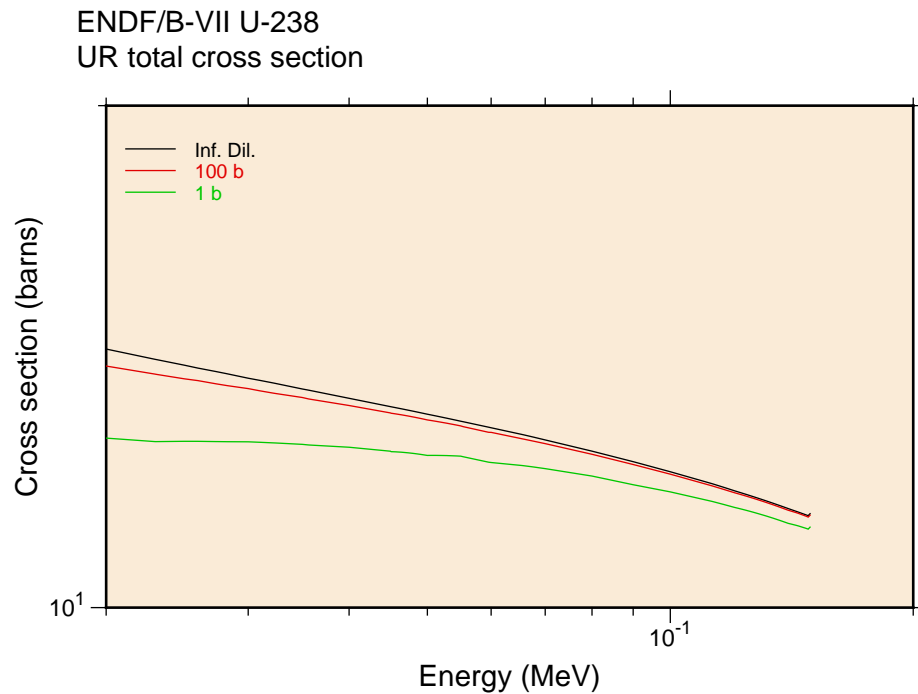


Figure 70: Bondarenko-style self-shielded cross sections for the total cross section of  $^{238}\text{U}$  in the unresolved resonance region at three different dilutions.

PURR uses the Single-Level Breit-Wigner (SLBW) approximation to calculate cross sections (as specified for ENDF unresolved data), and it uses the  $\psi$ - $\chi$  method to compute the Doppler broadened values. As is well known, this method doesn't always produce reasonable results for the small cross sections between resonances due to the neglect of interference and multi-channel effects. It is even possible to get negative elastic cross sections. When comparing Bondarenko results from PURR with those from [UNRESR](#), several factors should be considered. The PURR results may be more reliable at low  $\sigma_0$  values than [UNRESR](#) results because of the more complete treatment of resonance overlap effects, but the unrealistic cross sections in the dips between resonances will eventually make even the PURR results suspect at low values. This effect may be especially apparent for the current-weighted total cross section, which is especially sensitive to the low cross sections between resonances.

The following piece of a PURR output listing shows the probability table for the  $^{235}\text{U}$  example at an energy of 2.25 keV:

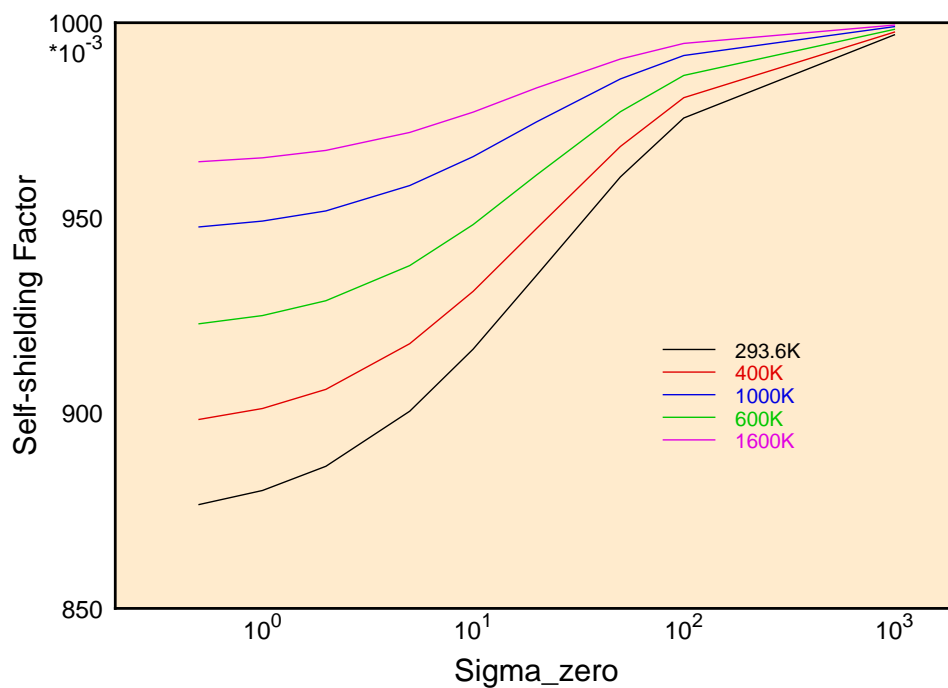


Figure 71: Self-shielding factors for the total cross section of  $^{238}\text{U}$  at 20 keV showing the variation with temperature and background cross section (dilution).

| probability table |           |           |           |           |           |     |
|-------------------|-----------|-----------|-----------|-----------|-----------|-----|
| tmin              | 1.162E+01 |           |           |           |           |     |
| tmax              | 1.352E+01 | 1.428E+01 | 1.509E+01 | 1.594E+01 | 1.683E+01 | ... |
|                   | 2.339E+01 | 2.471E+01 | 2.611E+01 | 2.758E+01 | 2.913E+01 | ... |
| prob              | 2.084E-02 | 3.597E-02 | 5.978E-02 | 8.244E-02 | 9.788E-02 | ... |
|                   | 6.094E-02 | 5.269E-02 | 4.169E-02 | 3.112E-02 | 1.806E-02 | ... |
| tot 2.936E+02     | 1.308E+01 | 1.393E+01 | 1.469E+01 | 1.552E+01 | 1.639E+01 | ... |
|                   | 2.275E+01 | 2.403E+01 | 2.537E+01 | 2.680E+01 | 2.832E+01 | ... |
| els 2.936E+02     | 1.114E+01 | 1.132E+01 | 1.144E+01 | 1.151E+01 | 1.161E+01 | ... |
|                   | 1.220E+01 | 1.230E+01 | 1.262E+01 | 1.274E+01 | 1.287E+01 | ... |
| fis 2.936E+02     | 1.486E+00 | 1.976E+00 | 2.444E+00 | 3.002E+00 | 3.582E+00 | ... |
|                   | 7.838E+00 | 8.607E+00 | 9.206E+00 | 1.023E+01 | 1.104E+01 | ... |
| cap 2.936E+02     | 4.574E-01 | 6.334E-01 | 8.095E-01 | 1.005E+00 | 1.202E+00 | ... |
|                   | 2.711E+00 | 3.121E+00 | 3.543E+00 | 3.832E+00 | 4.417E+00 | ... |

The columns give the results for the 20 probability bins, but the rightmost 5 columns of numbers have been removed to make the lines fit this page. Thus,



we are seeing bins 1-5 and 11-15. The rows for **tmax** give the upper bounds for the total cross section bins, and **prob** gives the probability that the total cross section lies in the bin. The **tot**, **els**, **fis**, and **cap** lines give the average cross section seen when the total lies in that bin, all for a temperature of 293.6K.

The ENDF format contains an option called LSSF. When LSSF=1, the resonance parameters are to be used to compute a fluctuation factor or self-shielding factor that is to be applied to the cross section given in File 3 of the ENDF tape. When LSSF=0, the parameters are used to compute cross sections that are to be added to any possible background corrections that may be given in File 3. The presence of this option doesn't effect the table printed out by PURR, but when LSSF=1, all the cross section values are divided by the corresponding infinitely dilute cross sections before the output file is written. The bins then contain dimensionless fluctuation factors instead of cross sections in barns.

## 23.2 Temperature Correlations

One important feature of PURR is its ability to handle temperature correlations. If the Monte Carlo code is tracking a particle through a system, it periodically checks for a total cross section to calculate the range to the next collision. Consider a collision that takes place in a region at a particular temperature. The Monte Carlo code samples from the probability table, getting a low cross section. The mean free path then takes the particle into another region at a different temperature that contains the same material. The sampled total cross section there cannot be independent from the first; the resulting cross section must also be low. PURR handles this kind of correlation. When a particular ladder of resonances is sampled to obtain a probability table, all the different temperatures are sampled simultaneously at the same energies to preserve the correlations. In the Monte Carlo code, it is only necessary to use the same random number to sample for the cross section in the two different regions to preserve the proper correlations.

## 23.3 Self-Shielded Heating Values

PURR can also provide self-shielding effects for the heating if partial heating cross sections are provided to it from [HEATR](#). Of course, there are no resonance parameters for heating, but the heating value does depend on the elastic, fission, and capture cross sections in the unresolved range. It may also have a contribution from competitive reactions, such as MT=51 discrete inelastic scattering or

(n,p) absorption. The general idea is to extract the portion of the heating corresponding to elastic, fission, and heating, and to apply the fluctuations in the probability table to them in order to get an estimate for the possible fluctuations in the total heating. This requires that [HEATR](#) be run to generate the partial heating values MT=302 (elastic), MT=318 (fission), and MT=402 (capture), in addition to the normal MT=301 (total heating). With these present, each partial heating value (eV-barns) can be divided by the corresponding infinitely-dilute reaction cross section to get eV/reaction for that reaction channel. These numbers can then be multiplied by the corresponding conditional cross section in each bin of the probability table and added to the eV-barns from the competitive reaction, if any, to get a value for heating in eV-barns in each bin. Finally, these values can be divided by the average total for the bin to get a heating value in eV/reaction that MCNP can use with sampled values of the total cross section to produce contributions to heating tallies.

### 23.4 Random Numbers

The version of PURR in NJOY 2012.0 introduces its own Fortran-based random number generator `rann`. Earlier versions relied on random number generators from the host systems, but this resulted in different answers from every machine and made it hard to do Quality Assurance (QA) on PURR results. The new approach allows the comparisons to be made with methods such as `unix diff`. Different machines should give the same results unless real changes are made.

### 23.5 User Input

The following user input specification was copied from the comment cards at the beginning of the PURR source. It is always a good idea to check these comments in the current version in case there have been changes.

```
! card 1
!   nendf    unit for endf tape
!   nin      unit for input pendf tape
!   nout     unit for output pendf tape
! card 2
!   matd     material to be processed
!           matd=0 terminates purr
!   ntemp    no. of temperatures (default=1)
!   nsigz    no of sigma zeros (default=1)
```

```

!   nbin    no. of probability bins
!   nladr    no. of resonance ladders
!   iprint  print option (0=min, 1=max, def=1)
!   nunx    no. of energy points desired (def=0=all)
! card 3
!   temp    temperatures in Kelvin (including zero)
! card 4
!   sigz    sigma zero values (including infinity)

```

The following is an example of [HEATR](#) and [PURR](#) input for a full calculation of the probability tables for a fissionable material. This would be just a small part of a sequence for producing a [PENDF](#) file for  $^{235}\text{U}$ .

```

...
heatr
-21 -24 -25/
9228 5/
302 318 402 443 444/
purrr
-21 -25 -26
9228 8 7 20 32/
293.6 400 600 800 1000 1200 1600 2000/
1e10 1e4 1e3 300 100 30 10/
0/
...

```

The [HEATR](#) run requests partial heating for elastic, fission, capture, kinematic total, and damage. The total heating, MT=301, is always produced automatically. The [PURR](#) run requests 20 bins for the probability table, and 32 ladders are to be used.

## 23.6 Coding Details

Subroutine `purrr` is the only exported routine of module `purrm`. It starts by setting various parameters, like `nermax`, `nsamp`, and `maxscr`, by reading the first card of the user input, and by calling `uwtab2` to compute the constants needed for calculating the table for the complex probability integral  $w$ . The calculation of the  $w$  table is the same as in [UNRESR](#). The routine now opens the requested

units and makes the first call to the random number generator **rann** to initialize the random number sequence.

Now **purr** can begin the loop over requested materials. Card 2 from the user input is read to obtain **matd**. If **matd**=0, the **PURR** run is complete. A tape-end record is written on the **PENDF** file being generated, and the code closes up. For a nonzero **matd**, the input parameters are checked and echoed to the output listing.

With the size of the problem determined, **purr** allocates storage for the elements of the resonance ladder, such as the resonance energies **er**, the neutron widths **gnr**, the fission widths **gfr**, the sampling arrays **es**, **xs**, **fis**, **cap**, and **els**, and the probability table itself (**tabl** and **tval**). Next, it reads through File 2 on the **ENDF** file to get the resonance parameters using **rdf2un**, and it reads through File 3 on the **ENDF** tape to find the background cross sections using **rdf3un**. It then goes to the **PENDF** file and searches for the total and partial heating cross sections that it will need for computing the conditional average for heating (see **rdheat**).

At this point, all the data needed to generate the probability tables are in place. The code sets up a loop over the energies that define the unresolved cross sections. Note that there is an option for debugging called **nunx**. If nonzero, **purr** skips over some of the incident energies, which can give a faster calculation. In practice, use **nunx**=0 to get the full unresolved data. For each energy, **unresx** is called to construct the ladder parameters, infinite-dilution cross sections, and potential scattering. Subroutine **unrest** is called to generate a set of ladders, sample from the ladders, and accumulate the probability table. The resulting probability table for this energy is stored on a scratch file, and the energy loop continues.

The code now continues by writing the new Bondarenko cross sections to the output **PENDF** file using **MF**=2/**MT**=152 and the new probability table to the file using **MF**=2/**MT**=153. It writes a report on this material to the listing, and continues the material loop.

Subroutine **rdf2un** is very similar to the routine in **UNRESR** that reads in unresolved resonance parameter data. All the comments made in the **RECONR** and **UNRESR** sections of this report about the complexities of constructing the energy grid in the unresolved range apply here also. Subroutine **rdf3un** is also very similar to the corresponding routine in **UNRESR**; it reads any background cross sections that may exist in the unresolved range from the input **ENDF** file. The resulting background cross sections are analyzed to see if any of the non-

resonant cross sections overlap into the unresolved range. The inelastic overlap `iinel` can be equal to 51 if only the first inelastic level overlaps the unresolved range, or equal to 4 if more levels overlap. The absorption overlap `iabso` can be equal to 103 if the (n,p) reaction overlaps, or some higher value for another reaction, but only one absorption reaction is allowed to overlap the unresolved. The routine types out “not allowed” messages for overlaps that it can’t handle.

Subroutine `rdheat` extracts the total heating value (MT=301), the elastic heating (MT=302), the fission heating (MT=318), and the capture heating (MT=402) from the input PENDF tape. The results are stored in the array `heat`, indexed by reaction type, energy index, and temperature index. If no total heating value is found on the PENDF tape, a message “no heating found on pendf, ur heating set to zero” will be issued. If a total heating value is found, but the partial heating values are missing, the message will read “no partial heating xsecs found on pendf, ur heating will not selfshield.” For full capabilities, the user should be sure to run [HEATR](#) with partial heating cross sections requested before running *PURR*.

Subroutine `unresx` reads through the resonance data in MF=2/MT=151 on the ENDF tape and extracts the resonance parameters for each resonance sequence that contributes to the unresolved cross sections. These parameters are stored by their sequence index in a set of arrays that are passed to `unrest`. For example, `cgg` contains the gamma widths for the sequences. At the same time, `unresx` uses these parameters to compute the potential scattering cross sections `spot` (a global variable), and the infinitely dilute total, elastic, fission, and capture cross sections. This last is exactly equivalent to the calculation done in [RECONR](#).

Subroutine `ladr2` is the routine that actually constructs a “ladder” of resonances for one particular spin sequence. In the unresolved range, it is not known exactly where a resonance lies on the energy scale or what the resonance widths are for a particular resonance. But the ENDF format does provide expectation values for quantities like the resonance spacing and capture width, and the format specifies the statistical distributions that these quantities should follow. Therefore, `ladr2` can produce a plausible sequence of resonances by starting with a first energy point chosen randomly (to provide an random offset between the various spin sequences). Selected partial widths are then assigned to this resonance using values drawn from the distributions for each type of width (chi-square distributions). A second resonance energy is chosen above the first one using a spacing drawn from the distribution of resonance spacings

(the Wigner distribution). The partial widths are chosen as before, and a third resonance is constructed above the first two. This process continues until the entire energy range specified for the ladder (**elow** to **ehigh**) has been filled. The results are stored in the parameter arrays **er** for energies, **gt** for total widths, **gnr** for neutron widths, **gfr** for fission widths, **ggr** for gamma widths, and **gxr** for competitive widths, for a total of **nr** resonances in this sequence.

Subroutine **unrest** is the core of the calculation of the probability tables. It starts by setting up the energy range for the calculation and printing out the constant values for this energy, namely, the potential scattering cross sections **spot**, the average resonance spacing **dbar**, and the competing cross section **sigx**. It then sets up the loop over the number of ladders requested by the user, **nladr**. For each different ladder, it chooses a random set of energies in the energy range of the ladder to be used to calculate cross sections (it avoids 300 resonances on each end to minimize truncation effects). It then starts up a loop over resonance sequences and generates a ladder for each sequence using **ladr2**. For each of these sequence-specific ladders, it loops over temperature. For each temperature, it loops over all the resonances in the ladder and increments the accumulating cross sections for each point in the energy grid that is contributed to by that resonance. The cross sections are computed by the  $\psi$ - $\chi$  method using the different ranges for the  $w$  function to take advantage of the asymptotic forms, the rational approximations, and the pre-tabulated values. The formulas used here are the same as those used for the **quikw** routine in **UNRESR**. Note that the same set of energies is used for every temperature. This is what preserves the temperature correlations. When the loop over resonances, temperatures, and spin sequences is complete, the code makes a pass through the results to eliminate the negative elastic cross sections that can occur with the Single-Level Breit-Wigner (SLBW) approximation, computes the corresponding infinitely dilute cross sections, and prints out the results for this particular ladder. The infinitely dilute values computed for any given ladder will not equal the proper results defined by the ENDF parameters, but they should fluctuate around the proper values to form a normal distribution. There is a unused option controlled by **nmode=1** that will renormalize the results of each ladder to the proper infinitely dilute values.

Now that we have a set of cross sections samples at various temperatures, the probability table can be generated. When the first ladder comes through, the routine uses it to set up the total cross section values that will define the bins of the table. Then that ladder and each subsequent ladder are used to increment

the cells for the total cross section and the various reaction cross sections. A set of Bondarenko self-shielded cross sections are computed at the same time. This process continues until all the ladders have been processed. The final summary gives the background cross section, the proper infinitely dilute cross section, the average of all the ladders (which should converge to the infinite dilution values when many ladders are used), and the percent standard deviation of the samples for the cross sections. The code then computes and displays the Bondarenko table and the final normalized probability table. As a cross check it also computes the Bondarenko table from the probability table. It should compare well with the Bondarenko table generated by direct sampling if enough ladders have been used.

The last step is to renormalize the probability table and the Bondarenko table to match the proper infinitely dilute cross sections. This is the result that is written to the output PENDF tape in **purr**. The conditional probabilities for heating are added at this time. It is important to note that the values printed on the PURR listing won't be quite the same as those passed on to ACER or other modules that access the PENDF sections MF=2/MT=152 or MF=2/MT=153.

The format used for the specially-defined MT=152, which contains the Bondarenko tables of self-shielded cross sections, is the same as the one described in the [UNRESR](#) chapter. Using the standard ENDF style,

```
[MAT,2,152/ ZA, AWR, LSSF, 0, 0, INTUNR ] HEAD
[MAT,2,152/ TEMZ, 0, NREAC, NSIGZ, NW, NUNR/
      SIGZ(1), SIGZ(2),...,SIGZ(NSIGZ),
      EUNR(1),
      SIGU(1,1,1), SIGU(1,2,1),...,SIGU(1,NSIGZ,1),
      SIGU(2,1,1),...
      ...
      SIGU(NREAC,1,1),...,SIGU(NREAC,NSIGZ,1),
      EUNR(2),...
      <continue for energies through EUNR(NUNR)>
      ...SIGU(NREAC,NSIGZ,NUNR) ] LIST
```

where **NREAC** is always 5 (for the total, elastic, fission, capture, and current-weighted total reactions, in that order), **NSIGZ** is the number of  $\sigma_0$  values, **NUNR** is the number of unresolved energy grid points, and **NW** is given by

```
NW=NSIGZ+NUNR*(1+5*NSIGZ)
```

The format used for the specially-defined MT=153, which contains the probability tables, is

```
[MAT,2,153/ ZA, AWR, 0, 0, 0, NBIN ] HEAD
[MAT,2,153/ TEMZ, 0, LSSF, ICOMP, NW, NUNR/
    EUNR(1),
    PROB(1,1),...,PROB(1,NBIN),
    TOTL(1,1),...,TOTL(1,NBIN),
    ELAS(1,1),...,ELAS(1,NBIN),
    FISS(1,1),...,FISS(1,NBIN),
    CAPT(1,1),...,CAPT(1,NBIN),
    HEAT(1,1),...,HEAT(1,NBIN),
    EUNR(2),...
    <continue for energies through EUNR(NUNR)>
    ...,HEAT(NUNR,NBIN) ] LIST
```

Here NBIN is the number of bins in the probability table, and NUNR is the number of energies in the unresolved energy grid. The total length of the LIST data is

```
NW=(1+6*NBIN)*NUNR
```

There is a section like this added for each temperature TEMZ on the output PENDF tape. In addition, *lssf* is the flag that tells whether the quantities given are cross sections, or whether they are factors to be applied to the corresponding infinitely-dilute cross sections, and ICOMP defines the reactions that compete with the unresolved fluctuations: ICOMP=1000\**iabso*+*iinel*, where *iabso* is the MT number for absorption competition (for example, 103), and *iinel* is the MT number for inelastic competition (either 4 or 51).

The heating values read in by *rdheat* from the input PENDF file are the heat production in eV-barns for the heating reactions found. If none are found, *ihave*=0. If only total heating, MT=301, is found, *ihave*=1. And if all the required partial heating values are found (MT=302, 318, and 402), *ihave*=2.



If `ihave=1` and `lssf=1`, the heating entries in the probability table are set to one, meaning that the infinitely dilute values from the PENDF file will be used in calculations. If `ihave=1` and `lssf=0`, then the total heating read in by `rdheat` will be divided by the total cross section and the same value of heating in eV/reaction will be stored in every bin (no fluctuations for heating). If `ihave=2`, it is possible to add real fluctuations for heating. The partial heating values are subtracted from the total heating to obtain the part of the heating coming from competitive reactions (eV-barns). Then each component of the partial heating is divided by the corresponding infinitely dilute cross sections to get eV/reaction for that component. This quantity is multiplied by the conditional cross section in each bin to get eV-barns for events with the total cross section in this bin, and that value is added into the accumulating heating value. After all the partials have been processed, the result is eV-barns in each bin. For `lssf=1`, this result is divided by the total heating in eV-barns, which gives a fluctuation factor to be used with the normal infinitely dilute heating value from the PENDF file. For `lssf=0`, the result is divided by the average total cross section for the bin to get a heating value in eV/reaction appropriate for use in MCNP as a multiplier for the sampled value of the total cross section.

If the ENDF parameter LSSF is equal to one, the elements of the heating in the probability table are divided by the infinitely dilute heating cross sections to give heating fluctuation factors in each bin. If a total heating value is available on the PENDF file (MT=301), but the partials are missing, the heating elements in the probability table will be filled in with the same non-fluctuating value in each bin.

The coding includes two sections of output statements that are normally commented out. In *PURR*, there is a block of statements that will print out the self-shielded cross sections in a form that can be adapted for the [VIEWR](#) module. In *unrest*, there is a block of coding that will print out [VIEWR](#) input for plotting the probability distribution (see Fig. 69).

### 23.7 Error Messages

```
error in purr***mode conversion between nin and nout not allowed nin
and nout must both be binary (negative) or ASCII (positive).
```

```
error in purr***nbin should be 15 or more
```

The construction of the cross sections bins requires this.

```
error in purr***not enough scratch space
```

The amount of space in the allocatable array **a** has been exceeded. See **maxscr=20000** in the subroutine **purr**.

**error in rdf2un\*\*\*storage exceeded**

The amount of space in the allocatable array **arry** has been exceeded. See the global variable **jx=10000** at the start of the **purm** module.

**error in rdf2un\*\*\*too many ur energy points**

The limit **meunr=150** defined in the global assignments has been exceeded.

**error in unresx\*\*\*illegal naps**

The NAPS parameter on the ENDF file can be 0, 1, or 2 with **nro** equal to 1 only. Check the evaluation.

**error in unresx\*\*\*too many sequences**

The limit of 100 spin sequences allowed in subroutine **unresx** has been exceeded. See **mxns0=100**.

**error in ladr2\*\*\*too many resonances in ladder**

There is a limit of **nermax=1000** resonances in a ladder. This is global variable defined at the start of module **purm** and set in **purr**. It controls the length of several allocatable arrays that are defined in subroutine **purr**, such as **er**, **gnr**, and so on.

**error in rann\*\*\*failed**

The random number generator failed.

**message from purr---reset ibin=1 (or =nsamp), consider ...**

The **nbin** size specified is too large for **PURR**'s internal arrays. Either decrease the input **nbin** or increase the **PURR**'s **nsamp** variable.

## 24 LEAPR

The LEAPR module is used to prepare the scattering law  $S(\alpha, \beta)$ , which describes thermal scattering from bound moderators, in the ENDF-6 format used by [THERMR](#). The original ENDF thermal scattering data[51] was prepared by General Atomics (GA) using the GASKET code[95]. This code has difficulty working with the very large energy and momentum transfers encountered for large incident energy or very low temperatures. For these reasons, LEAPR is based on the British code LEAP+ADDELT originally written by McLatchie at Harwell[96], then implemented by Butland at Winfrith[97], and finally modified to work better for cold moderators as part of the Ph.D. Thesis of D. J. Picton[98]. The code that Dr. Picton provided was modified extensively to fit better into the NJOY environment and to take advantage of modern large computers. This involved massive rearrangement of storage and routines, updating for first FORTRAN-77, then Fortran-90, and extensive editing of the comment cards. The original Edgewood expansion and Short Collision Time (SCT) treatments were removed in favor of using more terms in the phonon expansion and using the simple ENDF SCT formula[8]. In addition, output in ENDF-6 format[8] was provided, the capability to include either coherent or incoherent elastic scattering was added, a major speedup for the diffusion calculation was provided, and a capability to produce a mixed scattering law for materials like BeO and benzene was developed. In order to improve the numerics on short-word computers, the code was changed to use the asymmetric scattering function, the normalization scheme for the phonon expansion was revised, and the discrete-oscillator calculation was rebuilt to take better advantage of the convolution properties of the delta function and to use better Bessel Functions. A complete discussion of the theory used in the code is given below.

LEAPR was used[99] to reevaluate several of the thermal moderator materials from ENDF/B-VI using the original GA physics[51] but extending the alpha and beta ranges for incoherent inelastic scattering. The energy range for coherent scattering was also increased. The code was also used to prepare scattering-law files for several cold moderators of interest for experimental cold-neutron sources[100, 101]. More recently, some of these materials were updated for ENDF/B-VII.0 and additional materials were added. Several of the ENDF/B-VII.0 cases are discussed below as examples of how to run LEAPR.

Acknowledgements are due to Gary Russell of the Los Alamos Neutron Science Center (LANSCE) for motivating this work, to Drew Kornreich of the

University of Arizona for his careful study of the water problem, and to Max Lazo (University of New Mexico, SAIC, and Sandia National Laboratory) for testing and reviewing the code and documentation. In addition, we thank D. J. Picton for sending us his cold-moderator version of LEAPR, Rolf Neef of Julich and Guy Robert of ILL-Grenoble for sending us the initial version of the cold hydrogen treatment, and M. Mattes and J. Keinert of the University of Stuttgart for their help with the liquid hydrogen and deuterium models.

This section describes LEAPR in NJOY 2012.0. It is a new section that was not included in the previous report in this series[3]. It includes a number of changes from the version described in[99] related to the use of Fortran-90 style and memory allocation. Some of the work designed to make LEAPR run on short-word machines is now obsolete, because NJOY2012 is committed to using double precision on short-word machines, or to using long-word computers (64 bits), through the “kind” mechanism of Fortran-90.

## 24.1 Theory

The following discussion of the theories used in the the code is based on the original British documentation and the presentation in a standard reference[102].

**Coherent and Incoherent Scattering.** In practice, the scattering of neutrons from a system of  $N$  particles with a random distribution of spins or isotope types can be expressed as the sum of a coherent part and an incoherent part. The coherent scattering includes the effects from waves that are able to interfere with each other, and the incoherent part depends on a simple sum of noninterfering waves from all the  $N$  particles. (The spin correlations in ortho and para hydrogen violate the assumption of randomness, so liquid hydrogen does not fit into the model described here. A method for treating them will be described below.) The cross sections for coherent and incoherent scattering can be considered to be characteristic properties of the materials. As examples, the scattering from hydrogen is almost completely incoherent, and the scattering from carbon and oxygen is almost completely coherent.

Furthermore, the coherent and incoherent scattering include both elastic and inelastic parts. The elastic scattering takes place with no energy change. It should not be confused with the elastic scattering from a single particle that is familiar for higher neutron energies where the neutron loses energy; thermal elastic scattering can be considered to be scattering from the entire lattice, thus the effective mass of the target is very large, and the neutron does not

lose energy in the scattering process. Thermal inelastic scattering results in an energy loss (gain) for the neutron with a corresponding excitation (deexcitation) of the target. The excitation may correspond to the production of one or more phonons in a crystalline material, to the production of rotations or vibrations in molecules, or to the initiation of atomic or molecular recoil motions in a liquid or gas.

In addition, the coherent inelastic part of the scattering contains both interference effects between waves scattered by different particles and direct terms. It turns out that the direct part for gases, liquids and solids consisting of randomly oriented crystallites has approximately the same form as the incoherent term. The interference is usually neglected.

Therefore, we can usually divide the thermal scattering cross section into three different parts:

- *Coherent elastic.* Important for crystalline solids like graphite or beryllium.
- *Incoherent elastic.* Important for hydrogenous solids like solid methane, polyethylene, and zirconium hydride.
- *Inelastic.* Important for all materials (this category includes both incoherent and coherent inelastic).

The absence of interference in incoherent scattering and the neglect of interference in coherent inelastic scattering allows us to construct thermal scattering laws for “hydrogen in water” or “hydrogen in solid methane” or “oxygen in beryllium oxide”. However, this simplification is not possible in general for coherent elastic scattering in materials with more than one type of atom in the unit cell; for coherent elastic scattering, beryllium oxide must be considered as a unit.

**Inelastic Scattering** It is shown in the standard references[102] that the double differential scattering cross section for thermal neutrons for gases, liquids or solids consisting of randomly ordered microcrystals can be written as

$$\sigma(E \rightarrow E', \mu) = \frac{\sigma_b}{2kT} \sqrt{\frac{E'}{E}} \mathcal{S}(\alpha, \beta), \quad (502)$$

where  $E$  and  $E'$  are the incident and secondary neutron energies in the laboratory system,  $\mu$  is the cosine of the scattering angle in the laboratory,  $\sigma_b$  is the characteristic bound scattering cross section for the material,  $kT$  is the thermal

energy in eV, and  $\mathcal{S}$  is the asymmetric form of the scattering law. The scattering law depends on only two variables: the momentum transfer

$$\alpha = \frac{E' + E - 2\mu\sqrt{E'E}}{AkT}, \quad (503)$$

where  $A$  is the ratio of the scatterer mass to the neutron mass, and the energy transfer

$$\beta = \frac{E' - E}{kT}. \quad (504)$$

Note that  $\beta$  is positive for energy gain and negative for energy loss. Working in the incoherent approximation and the Gaussian approximation, the scattering law can be written

$$\mathcal{S}(\alpha, \beta) = \frac{1}{2\pi} \int_{-\infty}^{\infty} e^{i\beta\hat{t}} e^{-\gamma(\hat{t})} d\hat{t}, \quad (505)$$

where  $\hat{t}$  is time measured in units of  $\hbar/(kT)$  seconds. The function  $\gamma(\hat{t})$  is given by

$$\gamma(\hat{t}) = \alpha \int_{-\infty}^{\infty} P(\beta) \left[ 1 - e^{-i\beta\hat{t}} \right] e^{-\beta/2} d\beta, \quad (506)$$

where

$$P(\beta) = \frac{\rho(\beta)}{2\beta \sinh(\beta/2)}, \quad (507)$$

and where  $\rho(\beta)$  is the frequency spectrum of excitations in the system expressed as a function of  $\beta$ . The spectrum must be normalized as follows:

$$\int_0^{\infty} \rho(\beta) d\beta = 1. \quad (508)$$

The function  $P(\beta)$  defined by Eq.(507) is used directly in LEAPR, and  $\rho(\beta) = \rho(\epsilon/kt)$  is given as a function of  $\epsilon$  in eV. For systems in thermal equilibrium, there is a relationship between upscatter and downscatter called “detail balance” that is a consequence of microscopic reversibility. It requires that

$$\mathcal{S}(\alpha, \beta) = e^{-\beta} \mathcal{S}(\alpha, -\beta). \quad (509)$$

Liquid hydrogen and deuterium violate this condition, as will be described below. In addition, the scattering law satisfies two other important constraints; namely,

normalization,

$$\int_{-\infty}^{\infty} \mathcal{S}(\alpha, \beta) d\beta = 1, \quad (510)$$

and the sum rule

$$\int_{-\infty}^{\infty} \beta \mathcal{S}(\alpha, \beta) d\beta = -\alpha. \quad (511)$$

Actually, ENDF works with the so-called “symmetric”  $S(\alpha, \beta)$ ,

$$S(\alpha, \beta) = e^{\beta/2} \mathcal{S}(\alpha, \beta) \quad (512)$$

which (except for liquid hydrogen or deuterium) satisfies the condition

$$S(\alpha, \beta) = S(\alpha, -\beta). \quad (513)$$

Note that  $\mathcal{S}(\alpha, -\beta)$  for positive  $\beta$  describes the downscatter side of the function, and because it is basically proportional to the cross section, it can be represented by reasonable numbers (say  $10^{-8}$  to 1) for all  $\beta$ . The symmetric  $S(\alpha, \beta)$ , on the other hand, can easily be smaller than  $\mathcal{S}(\alpha, -\beta)$  by factors like  $e^{-\beta/2} \sim e^{-80} \sim 10^{-35}$ , which can cause trouble on short-word machines. This kind of numerical problem is even more severe for cold moderators, where dynamic ranges on the order of  $10^{100}$  occur for  $S(\alpha, \beta)$ . (The user will have to use some caution reading this report, because the typographic symbols for S and script-S are very similar.) By working with  $\mathcal{S}(\alpha, -\beta)$ , LEAPR can do all of its calculations using single-precision variables, even on a short-word machine.

The next step is to decompose the frequency spectrum into a sum of simple spectra

$$\rho(\beta) = \sum_{j=1}^K \rho_j(\beta), \quad (514)$$

where the following possibilities are allowed:

$$\rho_j(\beta) = w_j \delta(\beta_j) \quad \text{discrete oscillator} \quad (515)$$

$$\rho_j(\beta) = \rho_s(\beta) \quad \text{solid-type spectrum} \quad (516)$$

$$\rho_j(\beta) = \rho_t(\beta) \quad \text{translational spectrum} \quad (517)$$

The solid-type spectrum must vary as  $\beta^2$  as  $\beta$  goes to zero, and it must integrate to  $w_s$ , the weight for the solid-type law. The translational spectrum can be either a free-gas law or a diffusion-type spectrum represented with the approximation of Egelstaff and Schofield that will be discussed later. In either case, the spectrum must integrate to  $w_t$ , the translational weight. The sum of all the weights of the partial spectra must equal 1. Defining  $\gamma_j(\hat{t})$  to be the value of  $\gamma$  appropriate for  $\rho_j$ , and  $\mathcal{S}_j$  to be the corresponding partial scattering law, and using the convolution theorem for Fourier transforms, leads to a recursive formula for the scattering law:

$$\mathcal{S}(\alpha, \beta) = \mathcal{S}^{(K)}(\alpha, \beta), \quad (518)$$

where

$$\begin{aligned} \mathcal{S}^{(J)}(\alpha, \beta) &= \frac{1}{2\pi} \int_{-\infty}^{\infty} e^{i\beta\hat{t}} \prod_{j=1}^J e^{-\gamma_j(\hat{t})} d\hat{t} \\ &= \int_{-\infty}^{\infty} \mathcal{S}_J(\alpha, \beta') \mathcal{S}^{(J-1)}(\alpha, \beta - \beta') d\beta'. \end{aligned} \quad (519)$$

As an example of the use of this recursive procedure, consider a case where the desired frequency spectrum is a combination of  $\rho_s$  and two discrete oscillators. First, calculate  $\mathcal{S}^{(1)} = \mathcal{S}_1$  using  $\rho_s$ . Then calculate  $\mathcal{S}_2$  using  $\rho(\beta_1)$ , the distribution for the first discrete oscillator, and convolve  $\mathcal{S}_2$  with  $\mathcal{S}^{(1)}$  to obtain  $\mathcal{S}^{(2)}$ , the composite scattering law for the first two partial distributions. Repeat the process with the second discrete oscillator to obtain  $\mathcal{S}^{(3)}$ , which is equal to  $\mathcal{S}(\alpha, \beta)$  for the full distribution.

**The Phonon Expansion.** Consider first  $\gamma_s(\hat{t})$ , the Gaussian function for solid-type frequency spectra. Expanding the time-dependent part of the exponential gives

$$e^{-\gamma_s(\hat{t})} = e^{-\alpha\lambda_s} \sum_{n=0}^{\infty} \frac{1}{n!} \left[ \alpha \int_{-\infty}^{\infty} P_s(\beta) e^{-\beta/2} e^{-i\beta\hat{t}} d\beta \right]^n, \quad (520)$$

where  $\lambda_s$  is the Debye-Waller coefficient

$$\lambda_s = \int_{-\infty}^{\infty} P_s(\beta) e^{-\beta/2} d\beta. \quad (521)$$



The scattering function becomes

$$\begin{aligned} \mathcal{S}_s(\alpha, \beta) &= e^{-\alpha\lambda_s} \sum_{n=0}^{\infty} \frac{1}{n!} \alpha^n \\ &\times \frac{1}{2\pi} \int_{-\infty}^{\infty} e^{i\beta\hat{t}} \left[ \int_{-\infty}^{\infty} P_s(\beta') e^{-\beta'/2} e^{-i\beta'\hat{t}} d\beta' \right]^n d\hat{t}. \end{aligned} \quad (522)$$

For convenience, define the quantity in the second line of this equation to be  $\lambda_s^n \mathcal{T}_n(\beta)$ . Then clearly,

$$\mathcal{S}_s(\alpha, \beta) = e^{-\alpha\lambda_s} \sum_{n=0}^{\infty} \frac{1}{n!} [\alpha\lambda_s]^n \mathcal{T}_n(\beta), \quad (523)$$

where

$$\mathcal{T}_0(\beta) = \frac{1}{2\pi} \int_{-\infty}^{\infty} e^{i\beta\hat{t}} d\hat{t} = \delta(\beta), \quad (524)$$

and

$$\mathcal{T}_1(\beta) = \int_{-\infty}^{\infty} \frac{P_s(\beta') e^{-\beta'/2}}{\lambda_s} \left\{ \frac{1}{2\pi} \int_{-\infty}^{\infty} e^{i(\beta-\beta')\hat{t}} d\hat{t} \right\} d\beta' = \frac{P_s(\beta) e^{-\beta/2}}{\lambda_s}, \quad (525)$$

In general,

$$\mathcal{T}_n(\beta) = \int_{-\infty}^{\infty} \mathcal{T}_1(\beta') \mathcal{T}_{n-1}(\beta-\beta') d\beta'. \quad (526)$$

The script-T functions obey the relationship  $\mathcal{T}_n(\beta) = e^{-\beta} \mathcal{T}_n(-\beta)$ . In addition, each of the  $\mathcal{T}_n$  functions obeys the following normalization condition:

$$\int_{-\infty}^{\infty} \mathcal{T}_n(\beta) d\beta = 1. \quad (527)$$

It guarantees that Eq.510 will be satisfied by the sum in Eq.523. In LEAPR, the  $\mathcal{T}_n(-\beta)$  functions are precomputed on the input  $\beta$  grid for  $n$  up to some specified maximum value, typically 100. It is then easy to compute the smooth part of  $\mathcal{S}_s(\alpha, -\beta)$  for any sufficiently small value of  $\alpha$  using Eq.523. The corresponding values of  $\mathcal{S}_s(\alpha, \beta)$  can then be obtained by multiplying by  $e^{-\beta}$ . The delta function arising from the “zero-phonon” term is carried forward separately. The normalization in Eq.523 has better numerical properties than the one used in LEAP.

**The Short-Collision-Time Approximation.** For larger values of  $\alpha$ , the expansion of Eq.523 requires too many terms. LEAPR uses the simple Short-Collision-Time (SCT) approximation from ENDF to extend the solid-type scattering law.

$$\mathcal{S}_s(\alpha, -\beta) = \frac{1}{\sqrt{4\pi w_s \alpha \bar{T}_s / T}} \exp \left[ -\frac{(w_s \alpha - \beta)^2}{w_s \alpha \bar{T}_s / T} \right], \quad (528)$$

and

$$\mathcal{S}_s(\alpha, \beta) = e^{-\beta} \mathcal{S}_s(\alpha, -\beta) \quad (529)$$

where  $\beta$  is positive, and where the effective temperature is given by

$$\bar{T}_s = \frac{T}{2w_s} \int_{-\infty}^{\infty} \beta^2 P_s(\beta) e^{-\beta} d\beta. \quad (530)$$

As above,  $w_s$  is the weight for the solid-type spectrum.

**Diffusion and Free-Gas Translation.** The neutron scattering from many important liquids, including water and liquid methane, can be represented using a solid-type spectrum of rotational and vibrational modes combined with a diffusion term. Egelstaff and Schofield have proposed an especially simple model for diffusion called the “effective width model”. It has the advantage of having analytic forms for both  $S(\alpha, \beta)$  and the associated frequency spectrum  $\rho(\beta)$ :

$$\begin{aligned} \mathcal{S}_t(\alpha, \beta) = & \frac{2cw_t\alpha}{\pi} \exp [2c^2w_t\alpha - \beta/2] \\ & \frac{\sqrt{c^2 + .25}}{\sqrt{\beta^2 + 4c^2w_t^2\alpha^2}} K_1 \left\{ \sqrt{c^2 + .25} \sqrt{\beta^2 + 4c^2w_t^2\alpha^2} \right\}, \end{aligned} \quad (531)$$

and

$$\rho(\beta) = w_t \frac{4c}{\pi\beta} \sqrt{c^2 + .25} \sinh(\beta/2) K_1 \left\{ \sqrt{c^2 + .25} \beta \right\}. \quad (532)$$

In these equations,  $K_1(x)$  is a modified Bessel function of the second kind, and the translational weight  $w_t$  and the diffusion constant  $c$  are provided as inputs.

An alternative for the translational part of the distribution is the free-gas law. It is clearly appropriate for a gas of molecules, but it has also been used to

represent the translational component for liquid moderators like water[51]. The scattering law is given by

$$\mathcal{S}_t(\alpha, -\beta) = \frac{1}{\sqrt{4\pi w_t \alpha}} \exp \left[ -\frac{(w_t \alpha - \beta)^2}{4w_t \alpha} \right], \quad (533)$$

and

$$\mathcal{S}_t(\alpha, \beta) = e^{-\beta} \mathcal{S}_t(\alpha, -\beta), \quad (534)$$

with  $\beta$  positive. The free-gas law is used in LEAPR if the diffusion coefficient  $c$  is input as zero.

In LEAPR,  $\mathcal{S}_s(\alpha, \beta)$ , the scattering law for the solid-type modes, is calculated using the phonon expansion as described above. The translational contribution  $\mathcal{S}_t(\alpha, \beta)$  is then calculated using one of the formulas above on a  $\beta$  grid chosen to represent its shape fairly well. The combined scattering law is then obtained by convolution as follows:

$$\mathcal{S}(\alpha, \beta) = \mathcal{S}_t(\alpha, \beta) e^{-\alpha \lambda_s} + \int_{-\infty}^{\infty} \mathcal{S}_t(\alpha, \beta') \mathcal{S}_s(\alpha, \beta - \beta') d\beta'. \quad (535)$$

The first term arises from the delta function in Eq.523, which isn't included in the numerical results for the phonon series calculation. The values for  $\mathcal{S}_t(\beta)$  and  $\mathcal{S}_s(\beta - \beta')$  are obtained from the precomputed functions by interpolation. This makes LEAPR run much faster than LEAP+ADDELT for diffusive cases, because the original code did direct recalculations of the solid-type scattering law for all the desired values of  $\beta - \beta'$ . It also had to take pains to compute  $\mathcal{S}_t$  on a  $\beta$  grid that was commensurate with the input grid. This often resulted in more points for  $\mathcal{S}_t$  than were necessary to obtain useful accuracy for the convolutions.

The effective temperature for a combination of solid-type and translation modes is computed using

$$\overline{T}_s = \frac{w_t T + w_s \overline{T}_s}{w_t + w_s}. \quad (536)$$

**Discrete Oscillators.** Polyatomic molecules normally contain a number of vibrational modes that can be represented as discrete oscillators. The distribution function for one oscillator is given by  $w_i \delta(\beta_i)$ , where  $w_i$  is the fractional weight for mode  $i$ , and  $\beta_i$  is the energy-transfer parameter computed from the mode's vibrational frequency. The corresponding scattering law is given by

$$\begin{aligned}
\mathcal{S}_i(\alpha, \beta) &= e^{-\alpha\lambda_i} \sum_{n=-\infty}^{\infty} \delta(\beta - n\beta_i) I_n \left[ \frac{\alpha w_i}{\beta_i \sinh(\beta_i/2)} \right] e^{-n\beta_i/2} \\
&= \sum_{n=-\infty}^{\infty} A_{in}(\alpha) \delta(\beta - n\beta_i),
\end{aligned} \tag{537}$$

where

$$\lambda_i = w_i \frac{\coth(\beta_i/2)}{\beta_i}. \tag{538}$$

The combination of a solid-type mode (s) with discrete oscillators (1) and (2) would give

$$\mathcal{S}^{(0)}(\alpha, \beta) = \mathcal{S}_s(\alpha, \beta), \tag{539}$$

$$\begin{aligned}
\mathcal{S}^{(1)}(\alpha, \beta) &= \int_{-\infty}^{\infty} \mathcal{S}_1(\alpha, \beta') \mathcal{S}^{(0)}(\alpha, \beta - \beta') d\beta' \\
&= \sum_{n=-\infty}^{\infty} A_{1n}(\alpha) \mathcal{S}^{(0)}(\alpha, \beta - n\beta_1),
\end{aligned} \tag{540}$$

$$\begin{aligned}
\mathcal{S}^{(2)}(\alpha, \beta) &= \int_{-\infty}^{\infty} \mathcal{S}_2(\alpha, \beta') \mathcal{S}^{(1)}(\alpha, \beta - \beta') d\beta' \\
&= \sum_{m=-\infty}^{\infty} A_{2m}(\alpha) \sum_{n=-\infty}^{\infty} A_{1n}(\alpha) \mathcal{S}^{(0)}(\alpha, \beta - n\beta_1 - m\beta_2).
\end{aligned} \tag{541}$$

This process can be continued through  $\mathcal{S}^{(3)}(\alpha, \beta)$ ,  $\mathcal{S}^{(4)}(\alpha, \beta)$ , etc., until all the discrete oscillators have been included. The result has the form

$$\mathcal{S}(\alpha, \beta) = \sum_k W_k(\alpha) \mathcal{S}_s(\alpha, \beta - \beta_k), \tag{542}$$

where the  $\beta_k$  and the associated weights  $W_k$  are easily generated recursively using a procedure that throws out small weights at each step. The Debye-Waller  $\lambda$  for the combined modes is computed using

$$\lambda = \lambda_s + \sum_{i=1}^N \lambda_i. \tag{543}$$

The effective temperature for the combined modes is given by

$$\bar{T}_s = w_t T + w_s \bar{T}_s + \sum_{i=1}^N w_i \frac{\beta_i}{2} \coth\left(\frac{\beta_i}{2}\right) T. \quad (544)$$

If the starting-point scattering law  $\mathcal{S}^{(0)}$  does not contain a translational contribution (true for hydrogenous solids like polyethylene and frozen methane), it is important to remember to include the effects of the “zero-phonon” term  $\exp(-\alpha\lambda_s)\delta(\beta)$ . The code does this by adding in triangular peaks with the proper areas and with their apexes at the  $\beta$  value closest to the  $\beta_k$  values. One of these peaks is at  $\beta=0$ . This peak is not put into the scattering law as a sharp triangle; instead, it is handled as “incoherent elastic” scattering in order to take full advantage of the analytic properties of  $\delta(\beta)$ .

**Incoherent Elastic Scattering.** In hydrogenous solids, there is an elastic (no energy loss) component of scattering arising from the “zero-phonon”, or  $n=0$  term, of Eq.523. In ENDF terminology, this is called the “incoherent elastic” term. Clearly,

$$S_{\text{iel}}(\alpha, \beta) = e^{-\alpha\lambda} \delta(\beta). \quad (545)$$

The corresponding differential scattering cross section is

$$\sigma(E, \mu) = \frac{\sigma_b}{2} e^{-2WE(1-\mu)}, \quad (546)$$

and the integrated cross section is

$$\sigma(E) = \frac{\sigma_b}{2} \left\{ \frac{1 - e^{-4WE}}{2WE} \right\}. \quad (547)$$

In these equations, the Debye-Waller coefficient is given by

$$W = \frac{\lambda}{AkT}, \quad (548)$$

where  $\lambda$  is computed from the input frequency spectrum as shown by Eq.521 and modified by the presence of discrete oscillators (if any) as shown above. LEAPR writes the bound scattering cross section  $\sigma_b$  and the Debye-Waller coefficient  $W$  as a function of temperature into a section of the ENDF-6 output with MF=7 and MT=2.

**Coherent Elastic Scattering.** In solids consisting of coherent scatterers – for example, graphite – the zero-phonon term leads to interference scattering from the various planes of atoms of the crystals making up the solid. Once again, there is no energy loss, and the ENDF term for the process is “coherent elastic scattering”. The differential scattering cross section is given by

$$\sigma_{\text{coh}}(E, \mu) = \frac{\sigma_c}{E} \sum_{E_i < E} f_i e^{-4WE_i} \delta(\mu - \mu_i), \quad (549)$$

where

$$\mu_i = 1 - E_i/E, \quad (550)$$

and the integrated cross section is given by

$$\sigma_{\text{coh}} = \frac{\sigma_c}{E} \sum_{E_i < E} f_i e^{-4WE_i}. \quad (551)$$

In these equations,  $\sigma_c$  is the effective bound coherent scattering cross section for the material,  $W$  is the effective Debye-Waller coefficient,  $E_i$  are the so-called “Bragg Edges”, and the  $f_i$  are related to the crystallographic structure factors.

It can be seen from Eq.551 that the coherent elastic cross section is zero below the first Bragg Edge,  $E_1$  (typically about 2 to 5 meV). It then jumps sharply to a value determined by  $f_1$  and the Debye-Waller term. At higher energies, the cross section drops off as  $1/E$  until  $E=E_2$ . It then takes another jump, and resumes its  $1/E$  drop off. The sizes of the steps in the cross section gradually get smaller, and at high energies there is nothing left but an asymptotic  $1/E$  decrease (typically above 1 to 2 eV). LEAPR stores the quantity  $E\sigma_{\text{coh}}(E)$  as a function of energy and temperature in a section of the ENDF-6 output with MF=7 and MT=2. The cross section is easily recovered from this representation by dividing by  $E$  (this is done in the **THERMR** module of NJOY). The angular distribution of scattered neutrons can be calculated by extracting the  $f_i$  from the steps in  $\sigma_{\text{coh}}(E)$  file by subtraction. This process is carried out automatically in the **GROUPE** module of NJOY.

The calculation of the  $E_i$  and  $f_i$  depends on a knowledge of the crystal structure of the scattering material. The methods used are borrowed from HEXSCAT[31]. In general, the energies of the Bragg edges are given by

$$E_i = \frac{\hbar^2 \tau_i^2}{8m}, \quad (552)$$

where  $\tau_i$  is the length of the vectors of one particular “shell” of the reciprocal lattice, and  $m$  is the neutron mass. The  $f_i$  factors for a material containing a single atomic species are given by

$$f_i = \frac{2\pi\hbar^2}{4mNV} \sum_{\tau_i} |F(\tau)|^2, \quad (553)$$

where the sum extends over all reciprocal lattice vectors of the given length, and the crystallographic structure factor is given by

$$|F(\tau)|^2 = \left| \sum_{j=1}^N e^{i2\pi\phi_j} \right|^2, \quad (554)$$

where  $N$  is the number of atoms in the unit cell,  $\phi_j = \vec{\tau} \cdot \vec{\rho}_j$  are the phases for the atoms, and the  $\vec{\rho}_j$  are their positions. The situation is more complicated for materials containing different atomic species, such as beryllium oxide. In these cases,

$$\sigma_c e^{-2W_{E_i}} = \left| \sum_{j=1}^N \sqrt{\sigma_j} e^{-W_j E_i} e^{i2\pi\phi_j} \right|^2, \quad (555)$$

where the coherent cross section and Debye-Waller factor can be different for each site in the unit cell. The effective coherent cross section is clearly given by

$$\sigma_c = \sum_{j=1}^N \sigma_j. \quad (556)$$

Since LEAPR only works with one material at a time, it doesn’t have access to different values of  $W_j$  for the atoms in the unit cell. Therefore, it assumes that either  $W_j E_i$  is small, or the  $W_j$  doesn’t vary much from site to site. This allows it to calculate the  $f_i$  using

$$|F|^2 = \left| \sum_{j=1}^N \frac{\sqrt{\sigma_j}}{\sqrt{\sigma_c}} e^{-2\pi\phi_j} \right|^2. \quad (557)$$

For hexagonal materials, the lattice is described by the two constants  $a$  and  $c$ . The reciprocal lattice vector lengths are given by

$$\left( \frac{\tau}{2\pi} \right) = \frac{4}{3a^2} (\ell_1^2 + \ell_2^2 + \ell_1 \ell_2) + \frac{1}{c^2} \ell_3^2 \quad (558)$$

where  $\ell_1, \ell_2$ , and  $\ell_3$  run over all the positive and negative integers, including zero. The volume of the unit cell is

$$V = \sqrt{3}a_2c/2. \quad (559)$$

For graphite, there are four atoms in the unit cell at positions[103]

$$(0, 0, 0), \left(-\frac{1}{3}, \frac{1}{3}, 0\right), \left(-\frac{2}{3}, -\frac{1}{3}, \frac{1}{2}\right), \left(-\frac{1}{3}, \frac{1}{3}, \frac{1}{2}\right).$$

These positions give the following phases:

$$\phi_1 = 0, \quad (560)$$

$$\phi_2 = (-\ell_1 + \ell_2)/3, \quad (561)$$

$$\phi_3 = -(2/3)\ell_1 - (1/3)\ell_2 + (1/2)\ell_3, \quad (562)$$

$$\phi_4 = -(1/3)\ell_1 + (1/3)\ell_2 + (1/2)\ell_3. \quad (563)$$

The form factor for graphite becomes

$$|F|^2 = \begin{cases} 6 + 10 \cos[2\pi(\ell_1 - \ell_2)/3] & \ell_3 \text{ even} \\ 4 \sin^2[\pi(\ell_1 - \ell_2)/3] & \ell_3 \text{ odd} \end{cases} \quad (564)$$

For the hexagonal close packed (hcp) structure, which includes beryllium, there are two atoms per unit cell at

$$(0, 0, 0), \left(\frac{1}{3}, \frac{2}{3}, \frac{1}{2}\right),$$

and the form factor for hcp lattices like beryllium becomes

$$|F|^2 = 2 + 2 \cos[2\pi(2\ell_1 + 4\ell_2 + 3\ell_3)/6]. \quad (565)$$

The beryllium oxide lattice consists of two interpenetrating hcp lattices, one for the beryllium atoms, and one for the oxygen. There are four atoms per unit cell with positions

$$(0, 0, 0), \left(\frac{1}{3}, \frac{2}{3}, \frac{1}{2}\right), (0, 0, u), \left(\frac{1}{3}, \frac{2}{3}, u + \frac{1}{2}\right),$$



Using the approximation that the Debye-Waller factor doesn't vary from position to position in the unit cell gives the following expression for the structure factor:

$$|F|^2 = \left(1 + \cos[2\pi(2\ell_1 + 4\ell_2 + 3\ell_3)/6]\right) \left(r_1^2 + 2r_1r_2 \cos(3\pi\ell_3/4)\right), \quad (566)$$

where  $r_1^2$  and  $r_2^2$  are the bound coherent cross sections for beryllium and oxygen, respectively, and the effective coherent cross section,  $\sigma_c$ , is to be taken as 1.

LEAPR contains similar logic to handle face-centered cubic (fcc), *e.g.* aluminum, and body-centered cubic (bcc), *e.g.* iron, lattices. More formulas for the structure factor can be added to the code when needed.

**Liquid Hydrogen and Deuterium.** Materials containing hydrogen (H) or deuterium (D) molecules violate the assumption that spins are distributed randomly that underlies the incoherent approximation used for Eq.523, and an explicitly quantum-mechanical formula is required to take account of the correlations between the spins of two atoms in the same molecule. This problem was considered by Young and Koppel[104]. Changing to our notation, the formulas for the hydrogen molecule (neglecting vibrations) become

$$\begin{aligned} \mathcal{S}_{\text{para}}(\alpha, \beta) &= \sum_{J=0,2,4,\dots} P_J \\ &\times \frac{4\pi}{\sigma_b} \left[ A_{\text{para}} \sum_{J'=0,2,4,\dots} + B_{\text{para}} \sum_{J'=1,3,5,\dots} \right] (2J' + 1) \\ &\times \mathcal{S}_f(w\alpha, \beta + \beta_{JJ'}) \\ &\times \sum_{\ell=|J'-J|}^{J'+J} 4j_\ell^2(y) C^2(JJ'\ell; 00), \end{aligned} \quad (567)$$

and

$$\begin{aligned} \mathcal{S}_{\text{ortho}}(\alpha, \beta) &= \sum_{J=1,3,5,\dots} P_J \\ &\times \frac{4\pi}{\sigma_b} \left[ A_{\text{ortho}} \sum_{J'=0,2,4,\dots} + B_{\text{ortho}} \sum_{J'=1,3,5,\dots} \right] (2J' + 1) \\ &\times \mathcal{S}_f(w\alpha, \beta + \beta_{JJ'}) \\ &\times \sum_{\ell=|J'-J|}^{J'+J} 4j_\ell^2(y) C^2(JJ'\ell; 00). \end{aligned} \quad (568)$$

The coefficients for the even and odd sums are given in the following table:

| Type    | $A(\text{even})$   | $B(\text{odd})$    |
|---------|--------------------|--------------------|
| H para  | $a_c^2$            | $a_i^2$            |
| H ortho | $a_c^2/3$          | $a_c^2 + 2a_i^2/3$ |
| D para  | $3a_i^2/4$         | $a_c^2 + a_i^2/4$  |
| D ortho | $a_c^2 + 5a_i^2/8$ | $3a_i^2/8$         |

Here  $a_c$  and  $a_i$  are the coherent and incoherent scattering lengths (note that the characteristic bound cross section is  $\sigma_b = 4\pi[a_c^2 + a_i^2]$ ),  $P_J$  is the statistical weight factor,  $\beta_{JJ'} = (E'_J - E_J)/kT$  is the energy transfer for a rotational transition,  $j_\ell(x)$  is a spherical Bessel function of order  $\ell$ , and  $C(JJ'\ell; 00)$  is a Clebsch-Gordan coefficient. The parameter  $y$  is given by  $\kappa a/2 = (a/2)\sqrt{4MkT\alpha/2}$ , where  $a$  is the interatomic distance in the molecule. The translational weight  $w$  is 1/2 for H<sub>2</sub> and 1/4 for D<sub>2</sub>. The sums over  $J'$  are treated as operators into order to keep the notation compact.

Young and Koppel assumed that the molecular translations were free, so the equations contain

$$\mathcal{S}_f(\alpha, -\beta) = \frac{1}{\sqrt{4\pi\alpha}} \exp\left[-\frac{(\alpha - \beta)^2}{4\alpha}\right], \quad (569)$$

and

$$\mathcal{S}_f(\alpha, \beta) = e^{-\beta} \mathcal{S}_f(\alpha, -\beta), \quad (570)$$

the free-atom scattering function (with  $\beta$  positive). Note that  $\alpha$  is multiplied by a translational weight of 0.5 or 0.25 when this equation is used in order to make the formula apply to a molecule with mass ratio 2 or 4, respectively.

These formulas as stated are appropriate for a gas of hydrogen or deuterium molecules. In a liquid, there are two additional effects to be considered: interference between the neutron waves scattered from different molecules, and the fact that the recoil of the hydrogen molecule is not really free. First, we will consider the latter effect. Experiments by Egelstaff, Haywood, and Webb at Harwell[105] and Schott at Karlsruhe[106] showed appreciable broadening of the quasi-elastic scattering peak for liquid hydrogen, and both groups ascribed this to diffusive effects. Later, Utsuro of Kyoto University constructed a simple analytic model[107] that included both diffusion and intermolecular vibrations and showed good agreement with experiment. More recently, Keinert and Sax of the University of Stuttgart proposed the model[108] that we follow here.

They suggested that the free translation term in the Young and Koppel formulas be replaced by the superposition of a solid-state like motion and a diffusive law. One can picture a hydrogen molecule bound in a cluster of about 20 molecules and undergoing vibrations similar to those of a hydrogen molecule in a solid. These clumps then diffuse through the liquid (hindered translations) according to the Egelstaff-Schofield effective width model discussed above. The details of the performance of this model will be discussed further in a subsequent section.

As mentioned earlier, waves scattered from different molecules can also interfere. Inter-molecular coherence results when there is a correlation between the positions of nearby molecules. This kind of coherence is described by the “static structure factor”  $S(\kappa)$ . This quantity can be used in an approximation due to Vineyard as follows:

$$\frac{d^2\sigma}{d\Omega d\epsilon} = \frac{d^2\sigma_{\text{coh}}}{d\Omega d\epsilon} S(\kappa) + \frac{d^2\sigma_{\text{incoh}}}{d\Omega d\epsilon} . \quad (571)$$

This is equivalent to using Eqs. 567 and 568 with  $a_c^2$  replaced by  $S(\kappa)a_c^2$  in the calculation of the coefficients  $A$  and  $B$ . The effects of this procedure will be shown below.

**Mixed Moderators.** In some cases, thermal evaluations give the scattering for a principal scatterer as bound in a moderator; for example, H in H<sub>2</sub>O, or Zr in ZrH. The other atoms in the molecule are represented by an analytic law (free-gas O), or by another detailed scattering law (H in ZrH). In other cases, the scattering from the entire molecule is represented in one file. Examples are BeO and benzene in earlier versions of ENDF/B, but only benzene remains as a mixed moderator in ENDF/B-VII.0. The molecular scattering is renormalized to be used with the principal scatterer (Be or H for these cases); the secondary scatterer is assumed to have zero scattering in the thermal range.

Taking BeO as an example, the thermal cross section can be represented as follows:

$$\sigma_{\text{BeO}} = \frac{\sigma_{b,\text{Be}}}{2kT} \sqrt{\frac{E'}{E}} e^{-\beta/2} \left\{ S_{\text{Be}}(\alpha_{\text{Be}}, \beta) + \frac{\sigma_{b,\text{O}}}{\sigma_{b,\text{Be}}} S_{\text{O}}\left(\frac{A_{\text{Be}}}{A_{\text{O}}} \alpha_{\text{Be}}, \beta\right) \right\} , \quad (572)$$

where  $\alpha_{\text{Be}}$  stands for  $\alpha$  computed with the atomic mass ratio for Be,  $A_{\text{Be}}$ . In practice, LEAPR first computes  $S_{\text{Be}}$  using the input  $\alpha$  grid, and then it computes

$S_O$  on a new  $\alpha$  grid obtained by transforming the input grid with the indicated mass ratio. The two parts can now be added up by weighting with the indicated ratio of the bound cross sections. The method for preparing a mixed  $S(\alpha, \beta)$  for BeO is shown in detail below.

## 24.2 Input Instructions

The following listing of input instructions was copied from the comment cards at the beginning of the LEAPR module. It is always a good idea to check the current source file in case there have been changes.

```
!----- user input (free format) -----
!
! card 1 - units
!      nout      endf output unit for thermal file
!
! card 2 - title
!
! card 3 - run control
!      ntempr    number of temperatures (def=1)
!      iprint    print control (0=min, 1=more, 2=most, def=1)
!      nphon     phonon-expansion order (def=100)
!
! card 4 - endf output control
!      mat       endf mat number
!      za        1000*z+a for principal scatterer
!      isabt     sab type (0=s, 1=ss, def=0)
!      ilog      log flag (0=s, 1=log10(s), def=0)
!
! card 5 - principal scatterer control
!      awr       weight ratio to neutron for principal scatterer
!      spr       free atom cross section for principal scatterer
!      npr       number of principal scattering atoms in compound
!      iel       coherent elastic option
!
!               0  none (default)
!               1  graphite
!               2  beryllium
!               3  beryllium oxide
!               4  aluminum
!               5  lead
!               6  iron
```

```

!   ncold   cold hydrogen option
!           0   none (default)
!           1   ortho hydrogen
!           2   para hydrogen
!           3   ortho deuterium
!           4   para deuterium
!   nsk      0   none (default)
!           1   vineyard
!           2   skold
!
! card 6 - secondary scatterer control
!   nss      number of secondary scatterers (0 or 1)
!   b7       secondary scatterer type
!            (0=sct only, 1=free, 2=diffusion)
!   aws      weight ratio to neutron for secondary scatterer
!   sps      free atoms cross section for secondary scatterer
!   mss      number of atoms of this type in the compound
!
! card 7 - alpha, beta control
!   nalpha   number of alpha values
!   nbeta    number of beta values
!   lat      if lat.eq.1, alpha and beta values are scaled
!            by .0253/tev, where tev is temp in ev. (def=0)
!
! card 8 - alpha values (increasing order)
! card 9 - beta values (increasing order)
!
! scatterer loop, do temperature loop for principal scatterer.
!       repeat for secondary scatterer (if any) if b7=0.
!
! temperature loop, repeat cards 10 to 18 for each temperature
!
!   card 10 - temperature (k)
!       a negative value means skip cards 11 to 18,
!       thereby using previous parameters for this temp.
!
!   card 11 -- continuous distribution control
!       delta   interval in ev
!       ni      number of points
!
!   card 12 -- rho(energy) (order of increasing ev)
!

```

```

!      card 13 - continuous distribution parameters
!      twt      translational weight
!      c        diffusion constant (zero for free gas)
!      tbeta    normalization for continuous part
!
!      card 14 - discrete oscillator control
!      nd       number of discrete oscillators
!
!      card 15 - oscillator energies (ev)
!      card 16 - oscillator weights (sum to 1.-tbeta-twt)
!
!      card 17 - pair correlation control (nsk.ne.0 only)
!      nka      number of kappa values
!      dka      kappa increment (inv. angstroms)
!
!      card 18  skappa values in increasing order (inv. ang.)
!
!      card 19  coherent scattering fraction for nsk.eq.2 only
!      cfrac   coherent fraction
!
!      card 20 - file 1 comments, repeat until blank line is read.
!
!-----

```

**Card1.** Card 1 is the standard NJOY units card. The value of **nout** should be a number from 20 up, and it can be either positive (ASCII) or negative (blocked binary).

**Card 2.** Card 2, the title card, is just used to label the input deck and the output listing for the user's convenience. The title string does not go into the output ENDF file.

**Card 3.** Card 3 contains global parameters that control the run. The meaning of **ntempr** is clear. The amount of information printed on the output listing is controlled by **iprint**. The default is 1 (a mid-size listing). If you suspect problems, you can turn on the long listing to see more details. The parameter **nphon** gives the order of the phonon expansion. Usually a fairly large number (such as 100) is suitable. If it is too small, the SCT approximation will be used to excess.

**Card 4.** The ENDF MAT number on Card 4 should be one of the numbers listed in Appendix C of ENDF-102[8]. For the user's convenience, the numbers currently (ENDF/B-VII.1) being used are given in the following table:

| Compound          | MAT | Compound              | MAT |
|-------------------|-----|-----------------------|-----|
| Water             | 1   | Liquid Methane        | 33  |
| Para Hydrogen     | 2   | Solid Methane         | 34  |
| Ortho Hydrogen    | 3   | Polyethylene          | 37  |
| H in ZrH          | 7   | Benzine               | 40  |
| Heavy Water       | 11  | O in BeO              | 46  |
| Para Deuterium    | 12  | O in SiO <sub>2</sub> | 47  |
| Ortho Deuterium   | 13  | O in UO <sub>2</sub>  | 48  |
| Be                | 26  | Al metal              | 53  |
| BeO               | 27  | Fe metal              | 56  |
| Be <sub>2</sub> C | 28  | Zr in ZrH             | 58  |
| Be in BeO         | 29  | UO <sub>2</sub>       | 75  |
| Graphite          | 31  | UC                    | 76  |

Some of these files (Al, Fe, U in UO<sub>2</sub>, and O in UO<sub>2</sub>) were also available in ENDF/B-VII.0 with non-standard material numbers. The appropriate value to be used for **za** is fairly obvious. The parameter **isym** controls whether the output ENDF tape contains the symmetric  $S(\alpha, \beta)$  or the asymmetric  $\mathcal{S}(\alpha, \beta)$ . The second option gives much better numerics, especially on short-word machines, but it is not sanctioned by the ENDF-6 format. Here, **ilog** controls whether the output file contains  $S$  (or  $\mathcal{S}$ ) or  $\log_{10} S$ . Giving the log of  $S$  is the ENDF-sanctioned way of handling very small numbers in File 7.

**Card 5.** The “principal scatterer” may be hard to select for some compounds. For water, it is H. For ZrH, it would be H for **mat**=7 and Zr for **mat**=58. For mixed moderators like BeO, it is usually the light material. The value of **spr** should be chosen by looking at the low-energy limit for MF=3/MT=2 (elastic scattering) on the neutron file to be used with the new evaluation. The value for **npr** would be 2 for H<sub>2</sub>O, or 1 for BeO. The elastic option **iel** would normally be zero, except for solid moderators. Currently, only the five crystalline materials graphite, beryllium, beryllium oxide, FCC aluminum, and BCC iron are supported for coherent elastic scattering. Options for UO<sub>2</sub> and UC need to be added. The current evaluation for U in UO<sub>2</sub> and O in UO<sub>2</sub> uses the Bragg edges from the old UO<sub>2</sub> evaluation divided between the two channels. If **iel**=0 and **twt**=0.0, an incoherent elastic section is automatically added to the ENDF

tape. This normally occurs for hydrogenous solids like polyethylene, ZrH, or frozen methane. The `nscol` option is set to zero, except when a liquid hydrogen or deuterium calculation is desired. The `nsk` parameter is used when intermolecular interference is represented. See Cards 17, 18, and 19.

**Card 6.** The “secondary scatterer” card would be just “0/” for simple materials like graphite or beryllium. The behavior of LEAPR for molecular moderators is determined by the value of B7. The choice B7=0.0 is for mixed moderators like BeO and Benzene. In these cases, the entire  $S(\alpha, \beta)$  for the molecule is given in MF=7/MT=4, and it is intended to be used with the neutron file for the primary scatterer. The secondary scatterer’s cross section, atomic weight ratio, and effective temperature are only used for extending  $S(\alpha, \beta)$  with the SCT approximation (see [THERMR](#)). When B7>0.0, only the scattering law for the primary scatterer is given. The effects of the secondary scatterer are to be included later by using an analytic law. For example, in the water evaluation, the  $S(\alpha, \beta)$  is for H in H<sub>2</sub>O; the oxygen is included later by using a free-gas cross section using the given `sps` and `aws`.

**Cards 7, 8 and 9.** Cards 7-9 are used to define the  $\alpha$  and  $\beta$  grids for the LEAPR run. In the ENDF thermal format, the values for  $S(\alpha, \beta)$  for the higher temperatures are given on the same  $\alpha$  and  $\beta$  grids as for the base temperature, but since  $\alpha$  and  $\beta$  are inversely proportional to  $T$ , only the smaller  $\alpha$  and  $\beta$  values would be seen at higher temperatures. The results for the higher values would normally be zero. This is a waste of space in the fields on the ENDF evaluation. Using LAT=1 will spread the scattering law values for the higher temperatures out, thereby giving a more accurate representation.

The range of  $\beta$  helps determine the high-energy limit for the evaluation. For example, if  $T$  is 296K, a value of  $\beta_{\max}$  of 160 will allow downscatter events of 4 eV to be represented without recourse to the SCT approximation. This implies that pretty good results would be obtained for incident neutrons with energies of 4 eV. If incident energies are limited to  $\beta_{\max}kT$ , the range of  $\alpha$  values that can be obtained using Eq. 503 is limited to  $\alpha_{\max} = 4\beta_{\max}/A$ . The specific points in the  $\alpha$  and  $\beta$  grids are hard to choose. Too many points makes the evaluation expensive to use; too few lead to inaccurate interpolated results. The low  $\beta$  grid should probably have about the same detail as the input  $\rho(\beta)$  in order to reflect all the structure in the frequency distribution. Because of the smoothing effect of the convolutions, the grid can gradually get coarser as  $\beta$  increases. GA



traditionally used a log spacing in this higher region. If translational modes are to be included, a finer  $\beta$  grid for small  $\beta$  may be required to get good results at small  $\alpha$ . If discrete oscillators are included, additional  $\beta$  values might be needed near the values  $\pm n\beta_i$  and their various sums and differences, especially for  $n=1$ . After running LEAPR, the user should examine the results *vs*  $\beta$  printed out on the listing and the results *vs*  $\alpha$  printed out on the ENDF file to see whether the features of  $S(\alpha, \beta)$  are being represented well enough. If the normalization and sum rule checks are not being satisfied well, this may be an indication that the grids are too coarse.

If a secondary scatterer with  $B7=0.0$  is seen, it is necessary to read two entire temperature loops, one for the principal scatterer, and one for the secondary scatterer. See the BeO example below for how this is done.

**Cards 10 through 19.** LEAPR allows you to change the input frequency distribution  $\rho(\epsilon)$  for every temperature, but for many ENDF/B evaluations, it is taken to be energy independent. In those cases, Cards 11-19 are given for the first temperature only. Subsequently, only Card 10 is given to enter the desired temperature value.

The input distribution is given as a function of energy (eV) on a uniform grid. It can be in arbitrary units; it will always be normalized to the value **tbeta**. If a translational term is desired in addition, set **tw** to a number greater than zero. The translational term can be either a free-gas law ( $c=0.0$ ) or a diffusive law ( $c>0.0$ ).

Card 14 is used to enter the number of discrete oscillators desired. Their energies and weights are given on Cards 15 and 16. It is important to obey the restriction

$$w_t + w_s + \sum_{i=1}^{ND} w_i = 1 \quad (573)$$

Of course, if  $nd=0$ , the sum over  $i$  in this equation is omitted.

Card 17 is only given for the liquid hydrogen or liquid deuterium cases. It controls the entry of the pair-correlation function used to account for intermolecular interference at very low neutron energies. There are two options for this: Vineyard and Skold. Card 18 gives the actual values for the pair-correlation function  $S(\kappa)$ . See the liquid hydrogen example below for an example of how this quantity is entered. Card 19 gives the coherent scattering fraction for use with the Skold option. See the D in D2O example for how this is entered.

**Card 20.** The final section of the input deck gives the new comment cards to be added to the section MF=1/MT=451 on the ENDF file generated by LEAPR. If this section is to be a part of a standard library like ENDF/B-VII, there are standard fields that must appear. An example of the appearance of such a formal section will be found in the graphite example below. Note that the comment cards are terminated by an empty card; the number of cards entered is counted by LEAPR.

### 24.3 LEAPR Examples

The examples that follow were chosen for their practical importance and to illustrate several important points.

**The Model for Graphite.** The basic physics for graphite was left unchanged from the original GA evaluation[51]. A concise account appears in the new ENDF File 1 comment cards included in the input deck below. The important changes are the extended  $\alpha$  and  $\beta$  grids, an updated value for the cross section to match the value in ENDF/B-VII.0, and the use of LEAPR itself. The new grids were chosen to allow energies up to 4 eV. Note that  $\alpha$  values are only needed up to  $4\beta_{\max}/A$ . The input deck for the LEAPR graphite run follows:

```
leapr
20
'graphite, endf model (extended) '/
10 1/
31 131./
11.898 4.7392 1 1/
0/
72 96 1/
.01008 .015 .0252 .033 .0504 .0756 .1008 .15
2.52030e-1 .33 5.040600-1 7.560900-1 1.008120+0 1.260150+0 1.512180+0
1.76421e+0 2.016240+0 2.273310+0 2.535520+0 2.802970+0 3.075770+0
3.35401e+0 3.637900+0 3.927330+0 4.222710+0 4.523830+0 4.831110+0
5.14443e+0 5.464110+0 5.790130+0 6.122610+0 6.461850+0 6.807830+0
7.16077e+0 7.520670+0 7.887830+0 8.262340+0 8.644320+0 9.033960+0
9.43136e+0 9.836730+0 1.025060+1 1.067190+1 1.110240+1 1.154090+1
1.19886e+1 1.244520+1 1.291100+1 1.338580+1 14. 15. 16. 17. 18.
19. 20. 22. 24. 26. 28. 30. 32.5 35. 37.5 40. 42.5 45. 47.5
50. 52.5 55. 60. /
0.000000+0 1.008120-1 2.016240-1 3.024360-1 4.032480-1 5.040600-1
```

```

6.048720-1 7.056840-1 8.064960-1 9.073070-1 1.008120+0 1.108930+0
1.209740+0 1.310550+0 1.411370+0 1.512180+0 1.612990+0 1.713800+0
1.814610+0 1.915430+0 2.016240+0 2.117050+0 2.217860+0 2.318670+0
2.419490+0 2.520300+0 2.621110+0 2.721920+0 2.822730+0 2.923540+0
3.024360+0 3.125170+0 3.225980+0 3.326790+0 3.427600+0 3.528420+0
3.629230+0 3.730040+0 3.830850+0 3.931670+0 4.032480+0 4.133290+0
4.243780+0 4.364850+0 4.497620+0 4.643090+0 4.802480+0 4.977190+0
5.168730+0 5.378620+0 5.608670+0 5.73473 5.860800+0 5.99896
6.137130+0 6.28855 6.439970+0 6.60591
6.771840+0 6.95376 7.135670+0 7.33502 7.534380+0 7.75289
7.971400+0 8.21088 8.450360+0 8.975290+0
9.550520+0 1.018100+1 1.087260+1 1.162970+1 1.245930+1 1.336970+1
1.436670+1 1.545950+1 1.665710+1 1.796970+1 1.940930+1 2.098600+1
2.271390+1 2.460820+1 2.668490+1 2.896020+1 3.145330+1 3.418730+1
3.718250+1 4.046590+1 45. 50. 55. 60. 65. 70. 75. 80. /
293.6/
.005485 40/
0. .346613 1.4135 3.03321 3.25901 3.38468 3.48269
3.76397 4.05025 4.84696 7.35744 5.88224 4.63255
4.48287 5.80642 4.63802 4.28503 3.92079 4.91352
5.53836 7.51076 5.31651 5.40525 5.20376 5.3276
7.17251 3.31813 4.50126 5.04663 4.2089 2.91985
4.65109 13.1324 7.25016 6.5662 5.47181 5.06137
5.19813 .457086 0./
0. 0. 1. 0./
0/
-400/
-500/
-600/
-700/
-800/
-1000/
-1200/
-1600/
-2000/
' graphite lanl eval-may05 macfarlane '/
' ref. 4 dist- '/
' ---- endf/b-6 material 31 '/
' ----- thermal neutron scattering data '/
' ----- endf-6 '/
' '/
' temperatures = 293.6, 400, 500, 600, 700, 800, 1000, '/

```

```

'               1200, 1600, 2000 deg k. '//
'   '//
' history '//
' ----- '//
'   '//
' changed temperatures may05'//
'   '//
' this evaluation was generated at the los alamos national '//
' laboratory (apr 1993) using the leapr code. the physical '//
' model is very similar to the one used at general atomic '//
' in 1969 to produce the original endf/b-iii evaluations '//
' (see ref. 1). tighter grids and extended ranges for alpha '//
' and beta were used. a slightly more detailed calculation '//
' of the coherent inelastic scattering was generated. of '//
' course, the various constants were updated to agree with '//
' the endf/b-vi evaluation of natural carbon. '//
'   '//
' theory '//
' ----- '//
' graphite has an hexagonal close-packed crystal structure. the '//
' lattice dynamics is represented using a model with four force '//
' constants (refs.2,3). one force constant is used to describe a '//
' nearest-neighbor central force that binds two hexagonal planes '//
' together, another describes a bond-bending force in an hexagonal '//
' plane, the third is for bond-stretching between nearest neighbors '//
' in a plane, and the fourth corresponds to a restoring force '//
' against bending of the hexagonal plane. the force constants '//
' were evaluated numerically using a very precise fit to the '//
' high and low temperature specific heat and compressibility '//
' of reactor grade graphite. the phonon spectrum was computed '//
' from this model using the root sampling method, and then used '//
' to compute s(alpha,beta). the coherent elastic scattering '//
' cross section was computed using the known lattice '//
' structure and the debye-waller integrals from the lattice '//
' dynamics model. '//
'   '//
' references '//
' ----- '//
' 1. j.u.koppel and d.h.houston, reference manual for endf thermal '//
' neutron scattering data, general atomic report ga-8774 '//
' revised and reissued as endf-269 by the national nuclear '//
' data center, july 1978. '//

```

```

' 2. j.a.young, n.f.wilkner, and d.e.parks, nukleonik '/
'   band 1, 295(1965). '/
' 3. j.a.young and j.u.koppel, j.chem.phys. 42, 357(1965). '/
' 4. r.e.macfarlane, new thermal neutron scattering files for '/
'   endf/b-vi release 2, los alamos national laboratory report '/
'   la-12639-ms (march 1994). '/
'   '/
/
stop

```

The first card tells the code to write the  $S(\alpha, \beta)$  output on unit 20. After the comment card, which is just for the user's convenience and does not go into the output file, comes the global options for the run. Here we see that 10 temperatures and a mid-size listing are desired. The default size for the phonon expansion of 100 is taken. The next card gives the ENDF MAT number to be used and a substitute for ZA.

The next input line gives information for the primary scatterer. In this case, there is only a primary; its ZA is 11.898 and its free scattering cross section is 4.7392 barns. These values come from the ENDF/B-VII.0 carbon evaluation. The next field indicates that there is only one of the primary scatterers in the compound. The coherent elastic option is set to 1, which means that the code obtains its information from the ENDF file. The “secondary scatterer” card just has “0/” for graphite.

The following lines are used to define the  $\alpha$  and  $\beta$  grids for the LEAPR run. Each list is terminated by a “/” character. The graphite case uses 72  $\alpha$  values and 96  $\beta$  values. The high upper limits for  $\alpha$  and  $\beta$  allow for a high energy limit in the calculation. The next field gives the LAT parameter. The frequency distribution was copied directly from the GASKET input in the GA report, except the last point was changed to satisfy LEAPR input restrictions. See Fig. 72.

LEAPR allows you to change the input frequency distribution for every temperature, but this has not been done very often. The new ENDF/B-VII.0 evaluations for H in H<sub>2</sub>O and D in D<sub>2</sub>O are exceptions. In this case, the distribution is not temperature dependent, and the minus sign in front of each subsequent temperature indicates that no additional parameters are to be read for that temperature.

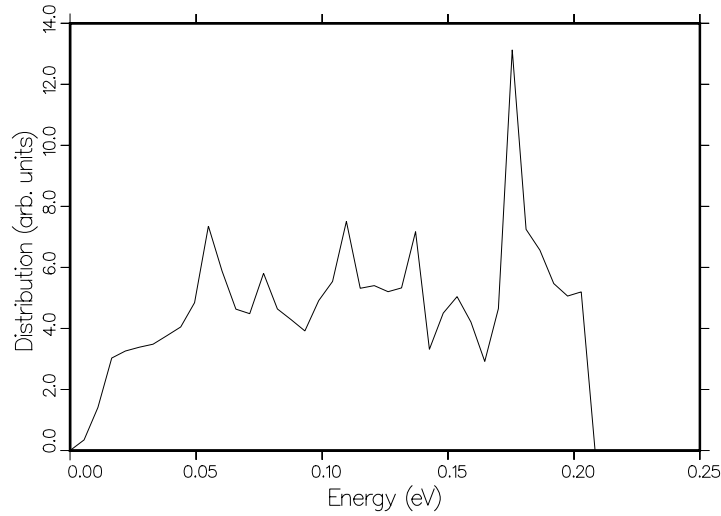


Figure 72: The phonon frequency spectrum  $\rho(\epsilon)$  used for graphite.

The rest of the sample input for graphite gives comment cards to be entered into MF1/MT451 in the new evaluation.

After echoing back the input, the code prints out  $\rho(\beta)$ ,  $P(\beta)$ , and  $\mathcal{T}_1(\beta)$  in normalized form. It then prints out the effective temperature for the SCT approximation and the Debye-Waller factor needed for the coherent scattering cross section calculation. The break points between the phonon expansion and

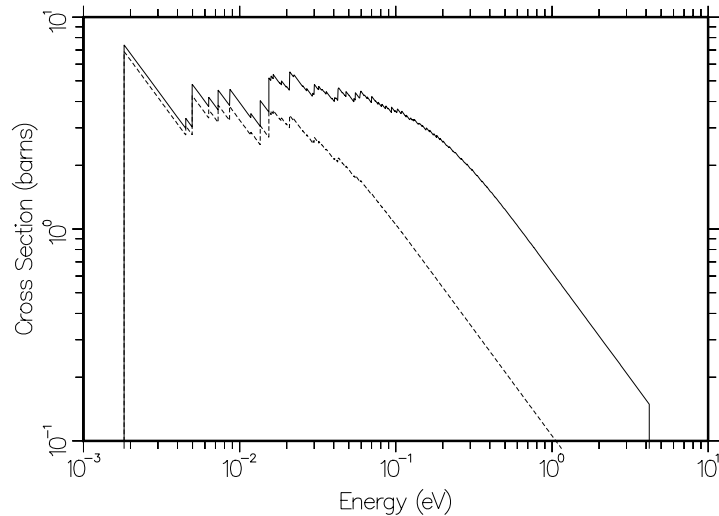


Figure 73: The coherent elastic cross section for graphite at temperatures of 293.6K (solid) and 2000K (dashed) showing the Bragg peaks. Note that the 293.6K cross section near the 4 eV breakpoint is still an appreciable part of the 4.74 barn free cross section.

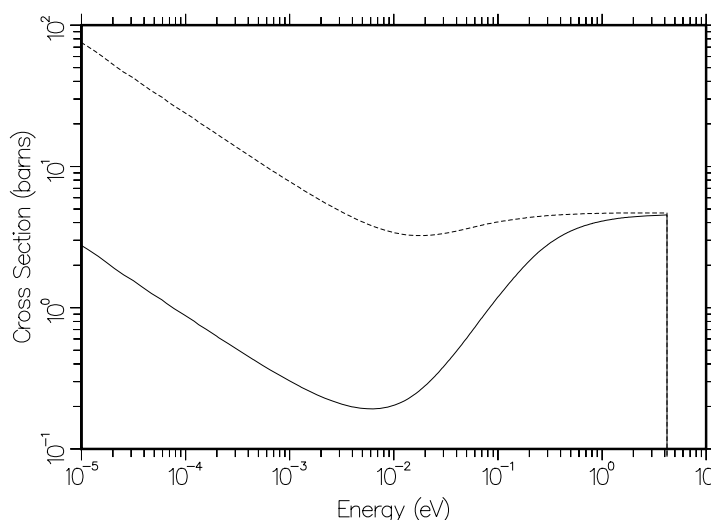


Figure 74: The incoherent inelastic cross section for graphite at temperatures of 293.6K (solid) and 2000K (dashed). A comparison of the two curves near the 4 eV breakpoint shows that the 293.6K cross section still has not reached the 4.74 barn free cross section. However, the sum of the elastic and inelastic components does equal the free value.

the SCT are also shown. LEAPR next computes the  $S(\alpha, \beta)$  function for each  $\alpha$ . For quality control, it displays the results of the normalization and sum rule tests. If these tests are not fairly close to unity, it may be necessary to tighten up the grids used for the calculation. Don't worry about test failures at high values of  $\alpha$ ; the  $\beta$  grid will not extend to high enough values to complete the integral over  $\beta$ .

An examination of the ENDF-6 output on “tape20” will show that both coherent elastic scattering (MF=7/MT=2) and incoherent inelastic scattering (MF=7/MT=4) are included in the new evaluation. As shown in Fig. 73, the coherent scattering extends all the way to 4 eV, which is an improvement over the original GA evaluation. There is also enough range in  $\alpha$  and  $\beta$  grids to compute thermal inelastic cross sections up to 4 eV. See Fig. 74.

**The Model for BeO** This example demonstrates how to prepare a mixed  $S(\alpha, \beta)$ . Actually, the evaluation used in ENDF/B-VII.0 (and later) splits the BeO case into separate parts for Be in BeO and O in BeO. This earlier example is kept here to demonstrate the methods used for preparing mixed moderators.

The basic physics was left unchanged from the GA evaluation of 1969[51]. Note that the following input deck contains both “Be in BeO” and “O in BeO”. The mixing option is selected by the “0.” in the second field of input card 6.

```

leapr
20
'test of BeO in LEAPR'/
1/
27 4009/
8.93478 6.15 1 3/
1 0. 15.858 3.7481 1/
50 80 1/
.252 .504 .756 1.008 1.260 1.512 1.764 2.016 2.268 2.520 2.772 3.024
3.282 3.544 3.813 4.087 4.366 4.652 4.943 5.241 5.545 5.855 6.172 6.495
6.825 7.162 7.507 7.858 8.217 8.583 8.957 9.339 9.729 10.13 10.53 10.95
11.37 11.81 12.25 12.69 13.16 13.63 14.11 14.60 15.10 15.61 16.13 16.66
17.21 17.76/
0. .1513 .3025 .4537 .6049 .7561 .9073 1.059 1.210 1.361 1.512 1.663
1.815 1.966 2.117 2.268 2.419 2.571 2.722 2.873 3.024 3.176 3.327 3.478
3.629 3.780 3.932 4.083 4.241 4.408 4.583 4.766 4.958 5.159 5.371 5.592
5.825 6.069 6.325 6.593 6.875 7.170 7.480 7.805 8.146 8.504 8.879 9.273
9.686 10.12 10.57 11.05 11.55 12.07 12.62 13.20 13.81 14.44 15.11 15.81
16.54 17.31 18.12 18.96 19.85 20.78 21.76 22.78 23.86 24.99 26.17 27.41
28.71 30.08 31.51 33.01 34.59 36.24 37.98 39.80/
296/ Be in BeO
.0016518 84/
0.0 .3 .7 .9 1. 1.2 1.6 2.0 2.2 3.0 3.5 4.5 5.5 6.8 8.0 9.2 10.9 12.9
15.5 18.6 22.0 26.0 30.5 35.0 39.0 40.0 34.0 28.0 26.0 24.4 23.0
21.3 19.8 17.0 14.1 12.0 10.0 9.0 9.0 8.5 7.5 6.0 4.6 3.1 1.6
0.5 0. 0.0 4.0 15.0 38.0 52.0 70.0 105.0 165.0 230.0 200.0 170.0
145.0 136.0 134.0 112.0 96.0 89.0 84.0 75.0 87.0 81.0 66.0 59.0
68.0 105.0 95.0 97.0 135.0 163.0 130.0 111.0 92.0 67.0 45.0 19.0
7.0 0.0/
0. 0. 1./
0/
296/ O in BeO
.0016518 84/
0.0 0.4 0.8 1.0 1.4 2.0 2.5 3.5 4.8 6.2 8.9 11.0 14.0 17.2 21.5 26.5
34.0 40.0 46.0 58.0 60.0 93.0 110.0 129.0 141.0 142.0 125.0 101.0
93.0 92.0 91.0 95.0 95.0 98.0 108.0 93.0 78.0 98.0 112.0 115.0 145.0
160.0 190.0 190.0 120.0 43.0 0.0 0.0 1.0 9.0 19.0 26.0 35.0 48.0 66.0
92.0 82.0 56.0 44.0 35.0 29.0 21.0 15.0 11.5 9.0 8.0 7.0 6.0 5.2
4.5 5.0 5.9 6.0 5.0 4.0 2.5 1.8 1.0 0.50 0.50 0.20 0.0 0.0 0.0/
0. 0. 1. 0./

```



```

0/
*TEST COMMENTS*/
*FOR MF1/MT451 OF BEO*/
/
STOP

```

The output listing for this case starts with the output for the primary scatterer “Be in BeO” and continues with results for the secondary scatterer “O in BeO”. Note that the  $\alpha$  values for the secondary scatterer have been transformed by the atomic weight ratio of the two atoms. This allows us to add the  $S(\alpha, \beta)$  contribution for  $\alpha_i$  from Be in BeO to the contribution for  $\alpha_i$  from O in BeO with only a cross-section weighting. The resulting  $S(\alpha, \beta)$  is intended to be used with the beryllium cross sections. The two frequency distributions are shown in Fig. 75.

The listing includes effective temperatures and Debye-Waller factors for both constituents. The average of the Debye-Waller factors is used in computing the coherent elastic scattering for BeO.

The ENDF output on `tape20` looks pretty much like the results for graphite, except data for two scatterers is given at the start of MF=7/MT=4, and two effective temperatures are given at the end of the section.

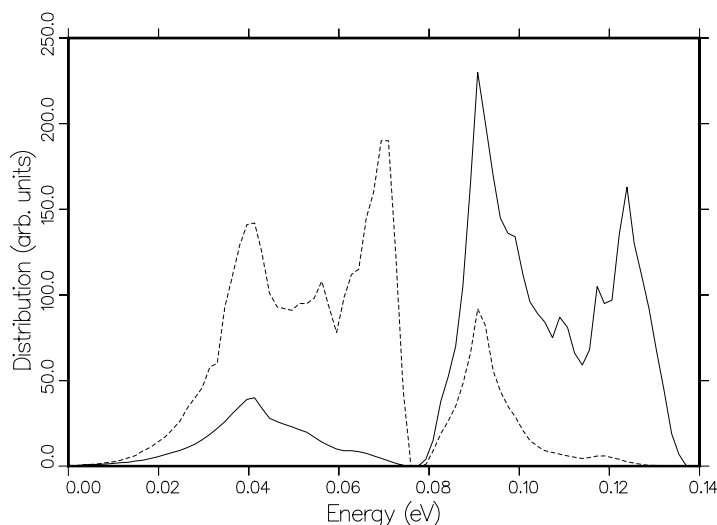


Figure 75: The frequency spectr  $\rho(\epsilon)$  used for Be in BeO (solid) and O in BeO (dashed).

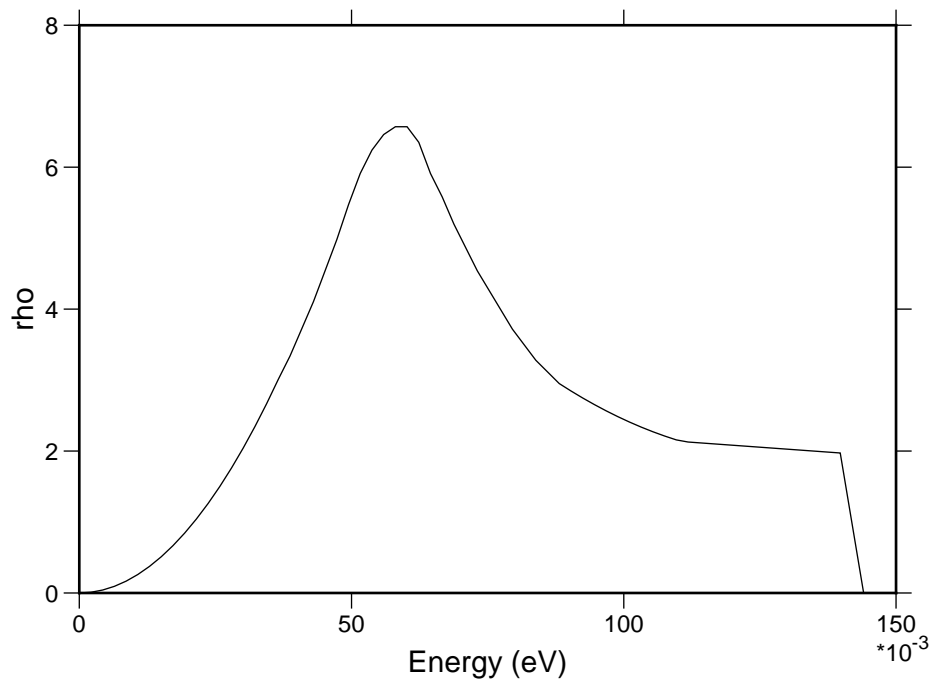


Figure 76: The frequency spectrum used for H in H<sub>2</sub>O for ENDF/B-VII.0.

**The Model for Water.** The current ENDF/B-VII.0 evaluation for the thermal scattering law for H bound in H<sub>2</sub>O is based on recent work done under IAEA auspices[109] with some slight modifications. Mainly, the  $\alpha$  and  $\beta$  grids were extended and enhanced. The temperature grid was modified to be more like the other ENDF/B cases by interpolating in the original distributions. Note that the frequency spectrum is temperature dependent in this input. The 296K spectrum is shown in Fig. 76. In addition, the energy scale of the rotational spectrum was adjusted slightly to improve agreement with experiment in the region between 0.01 eV and 0.1 eV. The final input deck is listed below.

```
leapr
20
' H in H2O, IKE model modified at LANL' /
9 2 200/
1 1001/
0.99917 20.43634 2/ latest Hale values for VII
1 1 1.585751+1 3.842443 1/ oxygen as free gas from VII
187 274 1/ lat=1
.001 .0015 .0025 .0035 .005 .007 .01 .015 .025 .035 .05 .070
```

|         |       |        |        |        |        |               |
|---------|-------|--------|--------|--------|--------|---------------|
| .1      | .125  | .15    | .2     | .25    | .3     | .325          |
| .35     | .375  | .4     | .425   | .45    | .475   | .5            |
| .525    | .55   | .58    | .61    | .65    | .69    | .73           |
| .78     | .83   | .88    | .94    | 1.     | 1.08   | 1.16          |
| 1.24    | 1.33  | 1.43   | 1.54   | 1.66   | 1.79   | 1.94          |
| 2.09    | 2.26  | 2.48   | 2.7127 | 2.89   | 3.11   | 3.38          |
| 3.67    | 3.98  | 4.32   | 4.65   | 5.0    | 5.4255 | 6.            |
| 6.56    | 7.13  | 7.6    | 8.1026 | 8.8    | 9.5    | 10.2          |
| 10.8152 | 11.7  | 12.6   | 13.528 | 14.4   | 15.3   | 16.2051       |
| 17.233  | 18.2  | 18.92  | 20.3   | 21.63  | 22.9   | 24.308        |
| 25.6    | 27.02 | 28.4   | 29.73  | 31.    | 32.41  | 33.44         |
| 34.466  | 36.15 | 37.18  | 38.8   | 40.513 | 41.54  | 42.57         |
| 44.2    | 46.0  | 47.0   | 48.615 | 49.6   | 51.2   | 52.5          |
| 54.41   | 55.2  | 56.72  | 58.4   | 59.80  | 61.2   | 62.51         |
| 63.8    | 65.23 | 66.5   | 67.90  | 68.93  | 70.61  | 71.64         |
| 72.92   | 75.9  | 80.    | 84.    | 89.    | 94.    | 100.          |
| 105.    | 113.  | 120.63 | 126.   | 132.   | 140.   | 147.          |
| 154.    | 162.  | 170.   | 177.   | 184.   | 191.   | 199.          |
| 208.    | 218.  | 227.   | 237.   | 246.   | 255.   | 265.          |
| 275.72  | 284.  | 293.58 | 302.   | 311.   | 320.   | 329.          |
| 338.    | 347.  | 356.   | 365.   | 374.   | 383.   | 392.          |
| 401.    | 410.  | 419.   | 428.   | 437.   | 446.   | 455.          |
| 464.    | 473.  | 482.   | 491.   | 500.   | 509.   | 518.          |
| 527.    | 536.  | 545.   | 554.   | 563.   | 572.   | 581.          |
| 590.    | 597.  | 604.   | 611.   | 618.   | 625.   | 632.9 / alpha |
| 0.0     | 0.005 | 0.01   | 0.015  | 0.020  | 0.025  | 0.030         |
| 0.040   | 0.050 |        |        |        |        |               |
| 0.06    | 0.07  | 0.08   | 0.1    | 0.125  |        |               |
| 0.15    | 0.175 | 0.20   | 0.225  | 0.250  | 0.30   | 0.35          |
| 0.40    | 0.45  |        |        |        |        |               |
| 0.50    | 0.55  | 0.60   | 0.65   | 0.70   | 0.75   | 0.80          |
| 0.85    | 0.90  | 0.95   | 1.0    | 1.05   | 1.10   | 1.15          |
| 1.20    | 1.25  | 1.30   | 1.35   | 1.4    | 1.45   | 1.5           |
| 1.55    | 1.6   | 1.65   | 1.7    | 1.75   | 1.8    | 1.85          |
| 1.9     | 1.95  | 2.0    | 2.05   | 2.1    | 2.15   | 2.2           |
| 2.25    | 2.3   | 2.35   | 2.4    | 2.45   | 2.5    | 2.55          |
| 2.6     | 2.65  | 2.7127 | 2.77   | 2.83   | 2.90   | 2.96          |
| 3.03    | 3.11  | 3.18   | 3.26   | 3.34   | 3.43   | 3.52          |
| 3.61    | 3.71  | 3.81   | 3.92   | 4.03   | 4.14   | 4.26          |
| 4.39    | 4.52  | 4.65   | 4.80   | 4.94   | 5.10   | 5.26          |
| 5.4255  | 5.60  | 5.70   | 5.97   | 6.17   | 6.37   | 6.59          |
| 6.81    | 7.04  | 7.29   | 7.54   | 7.81   | 7.9    | 8.0           |
| 8.103   | 8.2   | 8.28   | 8.37   |        |        |               |
| 8.67    | 8.98  | 9.30   | 9.64   | 10.    | 10.4   | 10.8152       |
| 11.16   | 11.57 | 12.0   | 12.46  | 12.98  | 13.528 | 13.94         |

|                                    |             |              |             |                          |        |        |       |      |
|------------------------------------|-------------|--------------|-------------|--------------------------|--------|--------|-------|------|
| 14.48                              | 15.03       | 15.62        | 16.2051     | 16.8                     | 17.    | 17.233 | 17.5  | 18.2 |
| 18.92                              | 19.4        | 19.95        | 20.7        | 21.63                    | 22.1   |        | 22.66 |      |
| 23.5                               | 24.308      | 24.8         | 25.34       | 26.2                     | 27.02  |        | 27.5  |      |
| 28.05                              | 28.9        | 29.73        | 30.2        | 30.76                    | 31.5   |        | 32.41 |      |
| 32.9                               | 33.44       | 34.          | 34.466      | 35.3                     | 36.15  |        | 36.6  |      |
| 37.18                              | 37.9        | 38.8         | 39.89       | 40.2                     | 40.513 |        | 41.   |      |
| 41.54                              | 42.         | 42.57        | 43.2        | 44.2                     | 45.28  |        | 46.0  |      |
| 47.0                               | 47.99       | 48.3         | 48.615      | 49.6                     | 50.67  |        | 51.2  |      |
| 51.70                              | 52.5        | 53.38        | 53.9        | 54.41                    | 55.2   |        | 56.   |      |
| 56.72                              | 57.12       | 58.4         | 59.80       | 61.2                     | 62.51  |        | 63.8  |      |
| 65.23                              | 66.5        | 67.90        | 68.4        | 68.93                    | 69.8   |        | 70.61 |      |
| 71.1                               | 71.64       | 72.2         | 72.92       | 73.3340                  | 74.    |        | 74.8  |      |
| 75.6                               | 76.4        | 77.2         | 78.         | 78.9                     | 79.8   |        | 80.7  |      |
| 81.6                               | 82.5        | 83.4         | 84.3        | 85.2                     | 86.1   |        | 87.   |      |
| 88.                                | 89.         | 90.          | 91.         | 92.                      | 93.    |        | 94.   |      |
| 95.                                | 96.         | 97.          | 98.         | 99.                      | 100.   |        | 101.2 |      |
| 102.4                              | 103.6       | 104.8        | 106.        | 107.2                    | 108.4  |        | 109.6 |      |
| 110.8                              | 112.        | 113.5        | 115.        | 116.5                    | 118.   |        | 119.5 |      |
| 121.                               | 122.5       | 124.         | 125.5       | 127.                     | 128.5  |        | 130.  |      |
| 132.                               | 134.        | 136.         | 138.        | 140.                     | 142.   |        | 144.  |      |
| 146.                               | 148.        | 150.         | 152.        | 154.                     | 156.   |        | 158.1 | beta |
| 293.6/ temperature (K)             |             |              |             |                          |        |        |       |      |
| 0.00215 68/ frequency distribution |             |              |             |                          |        |        |       |      |
| 0.00000E+00                        | 1.04170E-02 | 4.16710E-02  | 9.37490E-02 | 1.66682E-01              |        |        |       |      |
| 2.60457E-01                        | 3.74972E-01 | 5.10341E-01  | 6.66586E-01 | 8.43707E-01              |        |        |       |      |
| 1.04169E+00                        | 1.26039E+00 | 1.49991E+00  | 1.76047E+00 | 2.04172E+00              |        |        |       |      |
| 2.34379E+00                        | 2.66665E+00 | 3.01045E+00  | 3.33873E+00 | 3.72164E+00              |        |        |       |      |
| 4.10441E+00                        | 4.54222E+00 | 4.98019E+00  | 5.47328E+00 | 5.91196E+00              |        |        |       |      |
| 6.24071E+00                        | 6.45971E+00 | 6.56965E+00  | 6.56980E+00 | 6.35010E+00              |        |        |       |      |
| 5.91059E+00                        | 5.58143E+00 | 5.19738E+00  | 4.86852E+00 | 4.53952E+00              |        |        |       |      |
| 4.26544E+00                        | 3.99124E+00 | 3.71714E+00  | 3.49814E+00 | 3.27889E+00              |        |        |       |      |
| 3.11484E+00                        | 2.95067E+00 | 2.84650E+00  | 2.74784E+00 | 2.65469E+00              |        |        |       |      |
| 2.56706E+00                        | 2.48495E+00 | 2.40835E+00  | 2.33727E+00 | 2.27169E+00              |        |        |       |      |
| 2.21165E+00                        | 2.15711E+00 | 2.12732E+00  | 2.11543E+00 | 2.10353E+00              |        |        |       |      |
| 2.09165E+00                        | 2.07975E+00 | 2.06786E+00  | 2.05596E+00 | 2.04408E+00              |        |        |       |      |
| 2.03218E+00                        | 2.02029E+00 | 2.00839E+00  | 1.99651E+00 | 1.98461E+00              |        |        |       |      |
| 1.97272E+00                        | 9.86360E-01 | 0.00000E+00/ |             |                          |        |        |       |      |
| 0.0192                             | 0.          | .4904        | /           | weights                  |        |        |       |      |
| 2                                  | /           |              |             | discrete oscillators     |        |        |       |      |
| .205                               | .436        | /            |             | oscillator energies (eV) |        |        |       |      |
| .163467                            | .326933     | /            |             | oscillator weights       |        |        |       |      |
| 350./                              |             |              |             |                          |        |        |       |      |

```

0.00215 68/
0.00215 68/
  0.00000E+00  1.01473E-02  4.05927E-02  9.13258E-02  1.62372E-01
  2.53717E-01  3.65283E-01  4.97147E-01  6.49350E-01  8.21883E-01
  1.01473E+00  1.22779E+00  1.46112E+00  1.71490E+00  1.98888E+00
  2.28315E+00  2.59770E+00  2.93259E+00  3.25984E+00  3.63884E+00
  4.02767E+00  4.45671E+00  4.88387E+00  5.34035E+00  5.73991E+00
  6.04488E+00  6.25544E+00  6.34641E+00  6.34077E+00  6.15681E+00
  5.79298E+00  5.49979E+00  5.16054E+00  4.85982E+00  4.56082E+00
  4.31061E+00  4.06087E+00  3.81176E+00  3.60561E+00  3.39981E+00
  3.23731E+00  3.06474E+00  2.95935E+00  2.84908E+00  2.74389E+00
  2.64100E+00  2.54595E+00  2.45437E+00  2.37253E+00  2.29361E+00
  2.22288E+00  2.15259E+00  2.10362E+00  2.07303E+00  2.04091E+00
  2.00986E+00  1.98036E+00  1.95997E+00  1.93780E+00  1.91648E+00
  1.89595E+00  1.87631E+00  1.86017E+00  1.84223E+00  1.82513E+00
  1.80884E+00  8.99437E-01  0.00000E+00/
    0.029135  0.  .485433 /
      2 /
    .205  .436 /
      .161811  .323622 /
400/
0.00215 68/
  0.00000E+00  9.92998E-03  3.97244E-02  8.93749E-02  1.58902E-01
  2.48290E-01  3.57482E-01  4.86523E-01  6.35474E-01  8.04310E-01
  9.93028E-01  1.20154E+00  1.42988E+00  1.67821E+00  1.94634E+00
  2.23432E+00  2.54218E+00  2.86990E+00  3.19677E+00  3.57300E+00
  3.96771E+00  4.38985E+00  4.80833E+00  5.23385E+00  5.60019E+00
  5.88507E+00  6.08865E+00  6.16336E+00  6.15269E+00  5.99938E+00
  5.70048E+00  5.43794E+00  5.13693E+00  4.86008E+00  4.58656E+00
  4.35661E+00  4.12764E+00  3.89978E+00  3.70442E+00  3.50993E+00
  3.34851E+00  3.16838E+00  3.06178E+00  2.94128E+00  2.82550E+00
  2.70924E+00  2.60283E+00  2.49814E+00  2.40685E+00  2.31627E+00
  2.23617E+00  2.15212E+00  2.08649E+00  2.03966E+00  1.98998E+00
  1.94228E+00  1.89751E+00  1.86973E+00  1.83863E+00  1.80911E+00
  1.78107E+00  1.75470E+00  1.73486E+00  1.71165E+00  1.69001E+00
  1.66990E+00  8.25640E-01  0.00000E+00/
    0.0346475  0.  .482676 /
      2 /
    .205  .436 /
      0.160892  0.321784 /
450/
0.00215 68/

```

|             |             |              |             |             |
|-------------|-------------|--------------|-------------|-------------|
| 0.00000E+00 | 9.75410E-03 | 3.90199E-02  | 8.77925E-02 | 1.56087E-01 |
| 2.43887E-01 | 3.51155E-01 | 4.77906E-01  | 6.24218E-01 | 7.90054E-01 |
| 9.75417E-01 | 1.18024E+00 | 1.40455E+00  | 1.64845E+00 | 1.91182E+00 |
| 2.19470E+00 | 2.49715E+00 | 2.81904E+00  | 3.14676E+00 | 3.52166E+00 |
| 3.92356E+00 | 4.34050E+00 | 4.75201E+00  | 5.14878E+00 | 5.48392E+00 |
| 5.75016E+00 | 5.94766E+00 | 6.00672E+00  | 5.99108E+00 | 5.86722E+00 |
| 5.63083E+00 | 5.39736E+00 | 5.13269E+00  | 4.87821E+00 | 4.62866E+00 |
| 4.41770E+00 | 4.20824E+00 | 4.00034E+00  | 3.81484E+00 | 3.63071E+00 |
| 3.46976E+00 | 3.28157E+00 | 3.17338E+00  | 3.04241E+00 | 2.91583E+00 |
| 2.78605E+00 | 2.66813E+00 | 2.55020E+00  | 2.44932E+00 | 2.34697E+00 |
| 2.25742E+00 | 2.15958E+00 | 2.07737E+00  | 2.01447E+00 | 1.94741E+00 |
| 1.88323E+00 | 1.82333E+00 | 1.78821E+00  | 1.74824E+00 | 1.71058E+00 |
| 1.67508E+00 | 1.64202E+00 | 1.61848E+00  | 1.59002E+00 | 1.56386E+00 |
| 1.53993E+00 | 7.56386E-01 | 0.00000E+00/ |             |             |
| 0.0385185   | 0.480741    | /            |             |             |
| 2           | /           |              |             |             |
| .205        | .436        | /            |             |             |
| 0.160247    | 0.320494    | /            |             |             |
| 500./       |             |              |             |             |
| 0.00215     | 68/         |              |             |             |
| 0.00000E+00 | 9.59182E-03 | 3.83708E-02  | 8.63356E-02 | 1.53495E-01 |
| 2.39833E-01 | 3.45330E-01 | 4.69972E-01  | 6.13855E-01 | 7.76930E-01 |
| 9.59202E-01 | 1.16064E+00 | 1.38122E+00  | 1.62104E+00 | 1.88004E+00 |
| 2.15823E+00 | 2.45569E+00 | 2.77222E+00  | 3.10113E+00 | 3.47514E+00 |
| 3.88458E+00 | 4.29687E+00 | 4.70201E+00  | 5.07095E+00 | 5.37579E+00 |
| 5.62401E+00 | 5.81575E+00 | 5.85948E+00  | 5.83894E+00 | 5.74390E+00 |
| 5.56870E+00 | 5.36355E+00 | 5.13433E+00  | 4.90155E+00 | 4.67527E+00 |
| 4.48277E+00 | 4.29224E+00 | 4.10374E+00  | 3.92773E+00 | 3.75358E+00 |
| 3.59291E+00 | 3.39657E+00 | 3.28670E+00  | 3.14529E+00 | 3.00795E+00 |
| 2.86472E+00 | 2.73536E+00 | 2.60427E+00  | 2.49386E+00 | 2.37982E+00 |
| 2.28086E+00 | 2.16936E+00 | 2.07076E+00  | 1.99198E+00 | 1.90775E+00 |
| 1.82730E+00 | 1.75245E+00 | 1.71007E+00  | 1.66134E+00 | 1.61563E+00 |
| 1.57276E+00 | 1.53308E+00 | 1.50587E+00  | 1.47223E+00 | 1.44158E+00 |
| 1.41387E+00 | 6.89143E-01 | 0.00000E+00/ |             |             |
| 0.0417390   | 0.479131    | /            |             |             |
| 2           | /           |              |             |             |
| .205        | .436        | /            |             |             |
| .159710     | .319420     | /            |             |             |
| 550./       |             |              |             |             |
| 0.00215     | 68/         |              |             |             |
| 0.00000E+00 | 9.44225E-03 | 3.77730E-02  | 8.49922E-02 | 1.51106E-01 |
| 2.36096E-01 | 3.39961E-01 | 4.62659E-01  | 6.04301E-01 | 7.64830E-01 |

|             |             |              |             |             |
|-------------|-------------|--------------|-------------|-------------|
| 9.44252E-01 | 1.14257E+00 | 1.35972E+00  | 1.59577E+00 | 1.85074E+00 |
| 2.12460E+00 | 2.41747E+00 | 2.72905E+00  | 3.05951E+00 | 3.43307E+00 |
| 3.85041E+00 | 4.25857E+00 | 4.65785E+00  | 4.99971E+00 | 5.27495E+00 |
| 5.50565E+00 | 5.69192E+00 | 5.72054E+00  | 5.69514E+00 | 5.62848E+00 |
| 5.51353E+00 | 5.33613E+00 | 5.14167E+00  | 4.93008E+00 | 4.72654E+00 |
| 4.55204E+00 | 4.38002E+00 | 4.21047E+00  | 4.04363E+00 | 3.87915E+00 |
| 3.71857E+00 | 3.51397E+00 | 3.40232E+00  | 3.25044E+00 | 3.10232E+00 |
| 2.94564E+00 | 2.80482E+00 | 2.66059E+00  | 2.54064E+00 | 2.41493E+00 |
| 2.30656E+00 | 2.18144E+00 | 2.06653E+00  | 1.97198E+00 | 1.87070E+00 |
| 1.77407E+00 | 1.68437E+00 | 1.63478E+00  | 1.57734E+00 | 1.52363E+00 |
| 1.47343E+00 | 1.42716E+00 | 1.39631E+00  | 1.35749E+00 | 1.32239E+00 |
| 1.29091E+00 | 6.23480E-01 | 0.00000E+00/ |             |             |
| 0.044466    | 0.          | 0.477767     | /           |             |
| 2           | /           |              |             |             |
| .205        | .436        | /            |             |             |
| 0.159256    | 0.318512    | /            |             |             |
| 600./       |             |              |             |             |
| 0.00215     | 68/         |              |             |             |
| 0.00000E+00 | 9.30614E-03 | 3.72301E-02  | 8.37725E-02 | 1.48936E-01 |
| 2.32702E-01 | 3.35086E-01 | 4.56017E-01  | 5.95626E-01 | 7.53841E-01 |
| 9.30674E-01 | 1.12615E+00 | 1.34019E+00  | 1.57282E+00 | 1.82412E+00 |
| 2.09406E+00 | 2.38276E+00 | 2.68985E+00  | 3.02226E+00 | 3.39584E+00 |
| 3.82152E+00 | 4.22611E+00 | 4.62011E+00  | 4.93565E+00 | 5.18198E+00 |
| 5.39565E+00 | 5.57674E+00 | 5.59048E+00  | 5.56024E+00 | 5.52153E+00 |
| 5.46600E+00 | 5.31580E+00 | 5.15545E+00  | 4.96453E+00 | 4.78321E+00 |
| 4.62629E+00 | 4.47234E+00 | 4.32131E+00  | 4.16331E+00 | 4.00819E+00 |
| 3.84750E+00 | 3.63447E+00 | 3.52091E+00  | 3.35849E+00 | 3.19952E+00 |
| 3.02936E+00 | 2.87703E+00 | 2.71964E+00  | 2.59009E+00 | 2.45269E+00 |
| 2.33489E+00 | 2.19614E+00 | 2.06498E+00  | 1.95472E+00 | 1.83644E+00 |
| 1.72372E+00 | 1.61923E+00 | 1.56244E+00  | 1.49632E+00 | 1.43462E+00 |
| 1.37712E+00 | 1.32429E+00 | 1.28978E+00  | 1.24581E+00 | 1.20626E+00 |
| 1.17101E+00 | 5.59371E-01 | 0.00000E+00/ |             |             |
| 0.046537    | 0.          | 0.476732     | /           |             |
| 2           | /           |              |             |             |
| .205        | .436        | /            |             |             |
| 0.158911    | 0.317821    | /            |             |             |
| 650./       |             |              |             |             |
| 0.00215     | 68/         |              |             |             |
| 0.00000E+00 | 9.20968E-03 | 3.68424E-02  | 8.29024E-02 | 1.47390E-01 |
| 2.30283E-01 | 3.31608E-01 | 4.51281E-01  | 5.89440E-01 | 7.46008E-01 |
| 9.20999E-01 | 1.11445E+00 | 1.32627E+00  | 1.55647E+00 | 1.80516E+00 |
| 2.07229E+00 | 2.35801E+00 | 2.66190E+00  | 2.99405E+00 | 3.36630E+00 |

```

3.79437E+00  4.19585E+00  4.58597E+00  4.88805E+00  5.11997E+00
5.32491E+00  5.50293E+00  5.50965E+00  5.47725E+00  5.45177E+00
5.42426E+00  5.28734E+00  5.14353E+00  4.96297E+00  4.79271E+00
4.64457E+00  4.49963E+00  4.35781E+00  4.20453E+00  4.05433E+00
3.89416E+00  3.67795E+00  3.56391E+00  3.39713E+00  3.23364E+00
3.05777E+00  2.90060E+00  2.73760E+00  2.60402E+00  2.46163E+00
2.33984E+00  2.19520E+00  2.05689E+00  1.93967E+00  1.81386E+00
1.69399E+00  1.58295E+00  1.52299E+00  1.45304E+00  1.38783E+00
1.32711E+00  1.27139E+00  1.23530E+00  1.18907E+00  1.14757E+00
1.11069E+00  5.27354E-01  0.00000E+00/
  0.049020  0.    0.47549 /
  2 /
  .205  .436 /
  0.158497      0.316993 /
800./
0.00215 68/
0.00000E+00  9.20968E-03  3.68424E-02  8.29024E-02  1.47390E-01
2.30283E-01  3.31608E-01  4.51281E-01  5.89440E-01  7.46008E-01
9.20999E-01  1.11445E+00  1.32627E+00  1.55647E+00  1.80516E+00
2.07229E+00  2.35801E+00  2.66190E+00  2.99405E+00  3.36630E+00
3.79437E+00  4.19585E+00  4.58597E+00  4.88805E+00  5.11997E+00
5.32491E+00  5.50293E+00  5.50965E+00  5.47725E+00  5.45177E+00
5.42426E+00  5.28734E+00  5.14353E+00  4.96297E+00  4.79271E+00
4.64457E+00  4.49963E+00  4.35781E+00  4.20453E+00  4.05433E+00
3.89416E+00  3.67795E+00  3.56391E+00  3.39713E+00  3.23364E+00
3.05777E+00  2.90060E+00  2.73760E+00  2.60402E+00  2.46163E+00
2.33984E+00  2.19520E+00  2.05689E+00  1.93967E+00  1.81386E+00
1.69399E+00  1.58295E+00  1.52299E+00  1.45304E+00  1.38783E+00
1.32711E+00  1.27139E+00  1.23530E+00  1.18907E+00  1.14757E+00
1.11069E+00  5.27354E-01  0.00000E+00/
  0.049020  0.    0.47549 /
  2 /
  .205  .436 /
  0.158497      0.316993 /
' H(H2O)    IKE,LANL    EVAL-mar06 MacFarlane,Keinert,Mattes    '/
' INDC-NDS-0470      DIST-      '/
'-----ENDF/B-VII      MATERIAL      1      '/
'-----THERMAL NEUTRON SCATTERING DATA      '/
'-----ENDF-6 FORMAT      '/
'      '/
' Temperatures (K)      '/
'      293.6  350  400  450  500  550  600  650  800      '/

```



```

',
',
' This evaluation[1] was generated at IKE in January of 2004 using ',
' the LEAPR module of the NJOY Nuclear Data Processing System[2] ',
' and modified at LANL in March of 2006 to use a temperature grid ',
' more like the other ENDF evaluations and to fit the experimental ',
' data slightly better. The model is improved over the one used ',
' at General Atomics in 1969 to produce the original ENDF/B-III ',
' evaluation[3]. The alpha and beta grids have been extended to ',
' allow for larger incident energies and to properly represent the ',
' features of S(alpha,beta) for the various integrations required. ',
' The physical constants have been updated for ENDF/B-VII to match ',
' the current hydrogen and oxygen evaluations. The LANL changes ',
' include some additional alpha and beta points, interpolating the ',
' rotational energy distributions and translational masses onto ',
' the new temperature grid, and slightly reducing the rotational ',
' energies to improve the energy region between .01 and .1 eV. ',
',
',
' Water is represented by freely moving H2O molecule clusters ',
' with some temperature dependence to the clustering effect. ',
' Each molecule can undergo torsional harmonic oscillations ',
' (hindered rotations) with a broad spectrum of distributed ',
' modes. The excitation spectra were improved over the older ',
' ENDF model, and they are given with a temperature variation. ',
' In addition, there are two internal modes of vibration at ',
' 205 and 436 meV. The stretching mode was reduced from the ',
' older ENDF value of 480 meV to account for the liquid state. ',
' Scattering by the oxygen atoms is not included in the ',
' tabulated scattering law data. It should be taken into ',
' account by adding the scattering for free oxygen of mass 16. ',
',
',
' References ',
' ----- ',
' 1. M.Mattes and J.Keinert, "Thermal Neutron Scattering Data ',
' for the Moderator Materials H2O, D2O, and ZrHx in ENDF-6 ',
' Format and as ACE Library for MCNP(X) Codes," INDC/NDS ',
' report INDC(NDS)-0470 (April 2005). ',
' 2. R.E.MacFarlane, "New Thermal Neutron Scattering Files for ',
' ENDF/B-VI Release 2," Los Alamos National Laboratory report ',
' LA-12639-MS (March 1994). ',
' 3. J.U.Koppel and D.H.Houston, "Reference Manual for ENDF ',
' Thermal Neutron Scattering Data," General Atomic report ',
' GA-8774 revised and reissued as ENDF-269 by the National '

```

```

'      Nuclear Data Center, July 1978.          '/
'                                                  '/
' ----- '/
/  end leapr
stop

```

These  $\alpha$  and  $\beta$  grids extend to rather high values in order to allow calculations of water cross sections to energies on the order of 10 eV.

This run specifies `iprint=2` to get a more detailed output listing. Note that the listing now includes checks for the normalization of the phonon expansion members,  $\mathcal{T}_n$ . It also prints out the values  $S(\alpha, \beta)$ ,  $\mathcal{S}(\alpha, \beta)$ , and  $\mathcal{S}(\alpha, -\beta)$  for each  $\beta$ . Note that only the asymmetric  $S$  for  $-\beta$  is actually used and stored inside the code. The other two versions are computed just before being printed. On a short-word machine, these first two styles of  $S$  may underflow and be printed as zero, even though the last column is nonzero. No accuracy is actually lost at this point.

After the results for the solid-type rotational modes have been printed out, the code starts a print for the convolution of the translational modes with the continuous modes. For each  $\alpha$ , the values for  $S_{\text{free}}$  are printed out, followed by the results of the convolution, and the results of the normalization and sum-rule tests. These results can be examined to see if the  $\beta$  grid seems to be sufficient for the problem. The problem here is that the translational peak is very sharp for small  $\alpha$ , and it is difficult to make the  $\beta$  grid fine enough to represent it well. Some loss in the normalization and sum-rule accuracies must be accepted.

Next, the code shows similar results for the convolution of the discrete oscillators with the current scattering law. Now the problem is that new peaks appear at the  $n\beta_i$  values and their various sums and differences (see Table 29 for examples). For small  $\alpha$ , these peaks are very sharp. A few additional  $\beta$  points can be added near the peaks to improve the results, but it is usually impractical to represent them with full fidelity. Once again, some loss in the accuracy of the checks must be accepted.

Finally, a summary of the effective temperature and Debye-Waller factor is printed out, and the ENDF output file is constructed. The resulting  $S(\alpha, \beta)$  can be plotted using capabilities of the `PLOTR` module. Fig. 77 shows  $S$  vs  $\beta$  for various  $\alpha$  values. The high-energy cutoff of the energy distribution for the rotational modes is visible, as well as the effect of the discrete oscillators. Fig. 78 shows  $S$  vs  $\alpha$  for various  $\beta$  values. Note the singularity at low  $\alpha$  and  $\beta$

Table 29: Discrete oscillator  $\beta$  values and weights for  $\alpha = 1$  for H in H<sub>2</sub>O.

| Beta     | Weight     |
|----------|------------|
| 0.0000   | 9.6160E-01 |
| -8.1026  | 1.9405E-02 |
| -17.2328 | 1.8243E-02 |
| -25.3353 | 3.6814E-04 |
| -16.2051 | 1.9580E-04 |
| -34.4655 | 1.7304E-04 |
| 8.1026   | 5.8752E-06 |
| -33.4379 | 3.7146E-06 |
| -42.5680 | 4.4920E-06 |
| -24.3077 | 1.3171E-06 |
| -51.6983 | 1.0943E-06 |

where the slope changes sign. This is an effect characteristic of the translational modes in liquids.

The neutron emission spectra for incoherent inelastic scattering that results from processing this scattering law is shown in Fig. 79 for several incident ener-

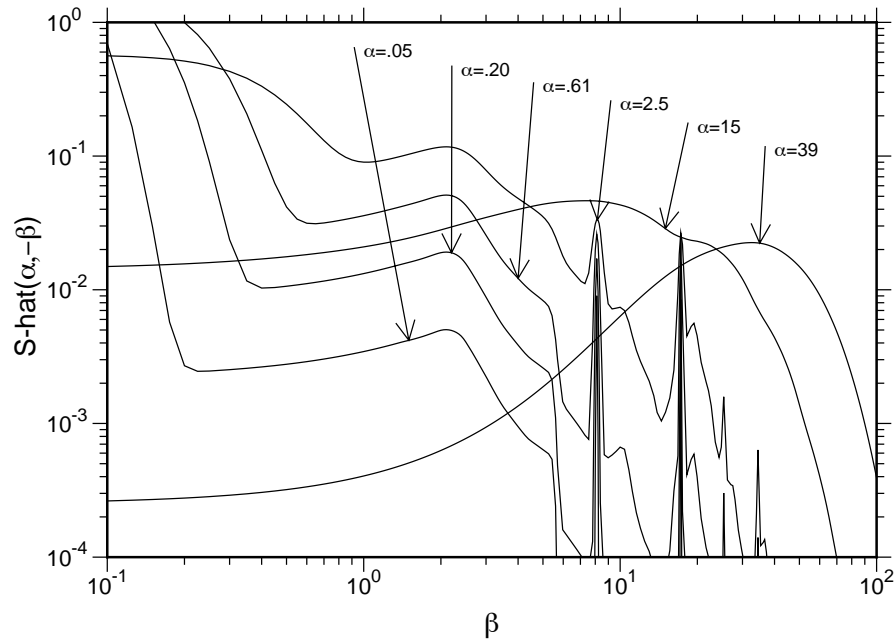


Figure 77:  $\mathcal{S}(\alpha, -\beta)$  for H in H<sub>2</sub>O at room temperature plotted versus  $\beta$  for various values of  $\alpha$ .

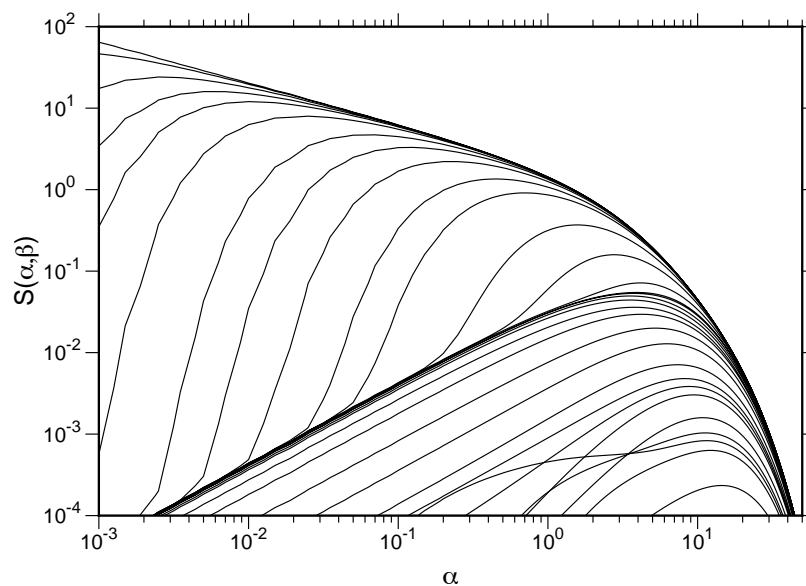


Figure 78:  $\mathcal{S}(\alpha, -\beta)$  vs  $\alpha$  for a number of  $\beta$  values.

gies. For very low incident energies, the neutron gains energy from the rotational modes excited at thermal equilibrium. For higher energies, it is more probable that the neutron will lose energy, and the effects of exciting translational, rotational and vibrational modes are visible. The down-scatter behavior is shown

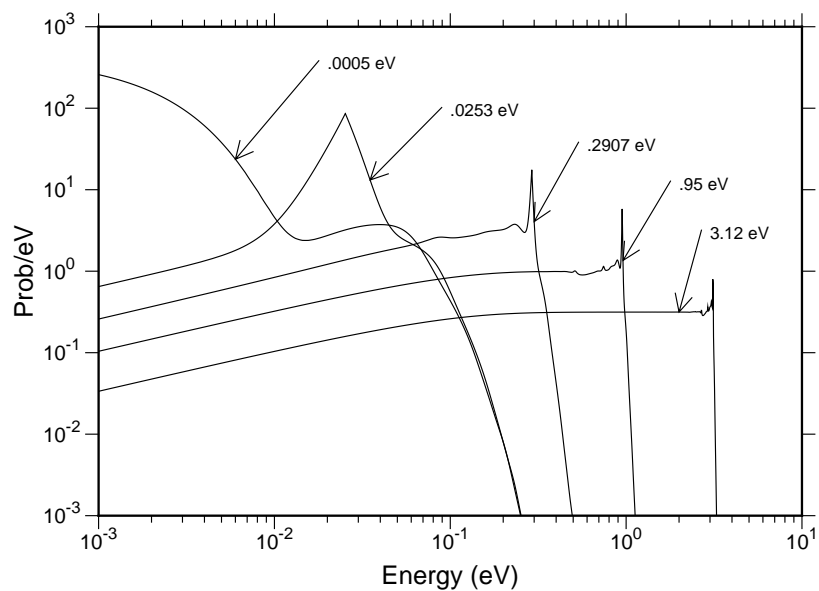


Figure 79: Incoherent inelastic spectra for several incident energies for H in H<sub>2</sub>O.

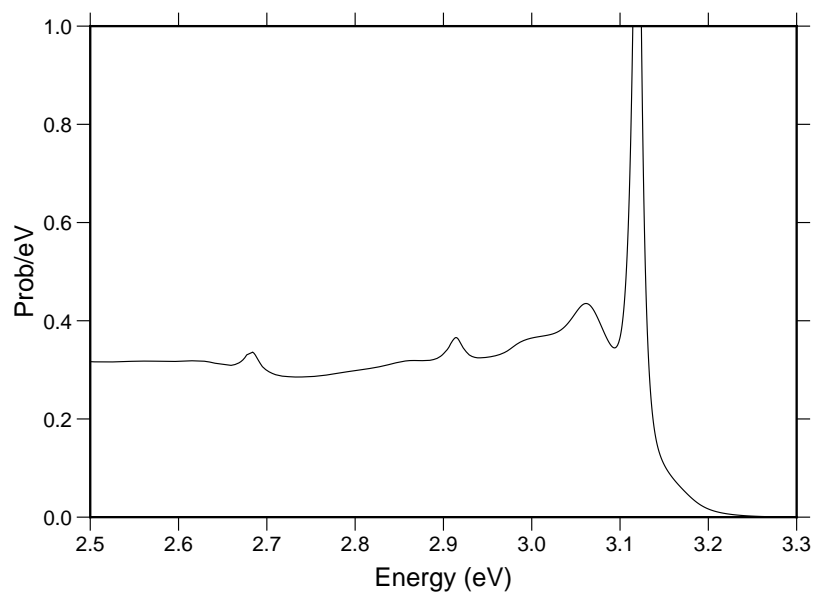


Figure 80: Detailed view of a neutron emission spectrum for inelastic scattering for H in  $\text{H}_2\text{O}$ .

in more detail in Fig. 80. The sharp peak at  $E' = E$  is the quasi-elastic peak coming from the diffusive translations. The next lower hump is from rotational modes, and the other peaks are from vibrational modes.

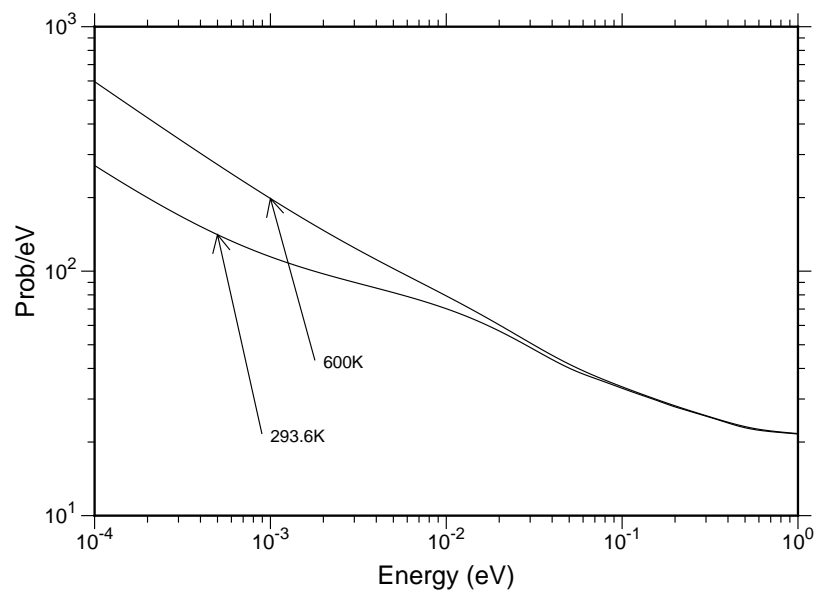


Figure 81: The incoherent inelastic cross section for H in  $\text{H}_2\text{O}$  at two temperatures.

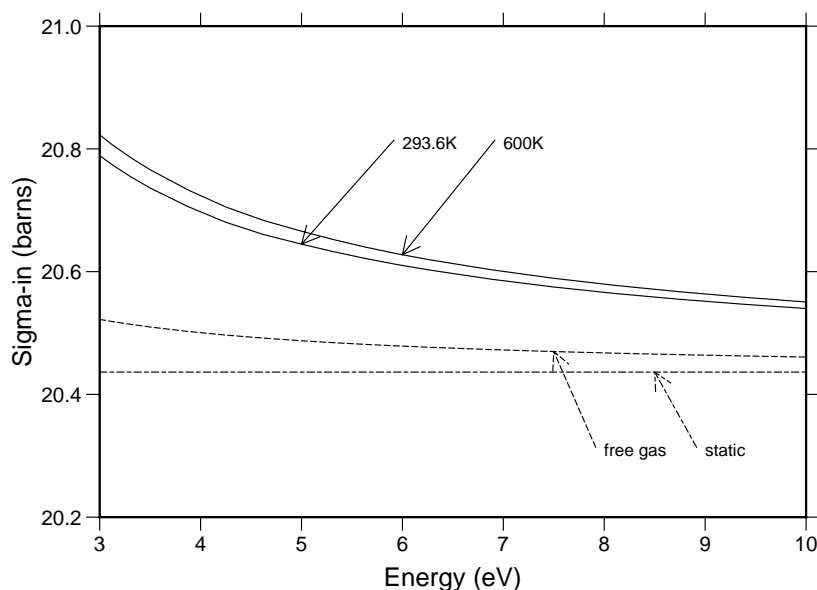


Figure 82: The incoherent inelastic cross section for H in  $\text{H}_2\text{O}$  for higher incident energies showing the static limit (scattering from atoms at rest) and the free-gas cross section.

The integrated cross section is shown in Fig. 81 and Fig. 82 for two temperatures. As the incident energy increases, the cross section begins to approach the free-atom value, as predicted by the theory. In practice, multigroup codes would normally change from the thermal value to the target-at-rest value at some particular break-point energy chosen so that error caused by the additional discontinuity at that energy group was not too significant. Monte Carlo codes normally change from the thermal cross section to the free-gas cross section at some breakpoint energy. There again, it is hoped that the breakpoint can be made high enough to minimize the adverse effects of the discontinuity.

Another approach that has been used in practice is to shift from the thermal cross section to an SCT cross section, that is, a free-gas cross section at a higher temperature than the ambient value. Table 30 shows the effective SCT temperatures for H in  $\text{H}_2\text{O}$ . This approach gives a fairly good integrated cross section versus energy above the thermal cutoff of the scattering law calculation, and it gives a good downscatter spectrum, but the up-scatter is too large.

The angular behavior of thermal scattering is also of interest. For H bound in  $\text{H}_2\text{O}$ , the hydrogen atom is not as free to recoil as the free atom. This makes it look like it has a higher effective mass, and it causes the scattering to be more isotropic on the average. See Fig. 83. However, as Fig. 84 demonstrates, there

Table 30: Effective temperatures for the Short Collision Time approximation for H in H<sub>2</sub>O.

| Temp (°K) | Eff Temp (°K) |
|-----------|---------------|
| 293.6     | 1269          |
| 350       | 1276          |
| 400       | 1289          |
| 450       | 1305          |
| 500       | 1324          |
| 550       | 1344          |
| 600       | 1367          |
| 800       | 1473          |

are still interesting anisotropies seen, especially near  $E' = E$  where translational effects are important.

Fig. 85 gives an overall view of the isotropic part of the scattering distribution for H in H<sub>2</sub>O.

As the description of the evaluation for H in H<sub>2</sub>O demonstrates, ENDF scattering law data are not obtained directly from experimental measurement as that requires more complete differential data than are currently available. Instead,

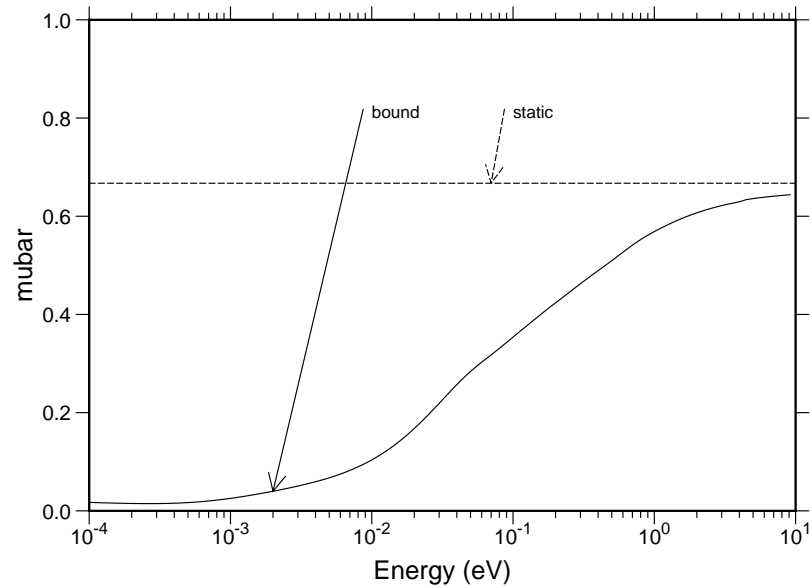


Figure 83: The average scattering cosine for H in H<sub>2</sub>O compared to the static value for scattering from atoms at rest. The effect of the binding of H in H<sub>2</sub>O is to make the scattering more isotropic at thermal energies.

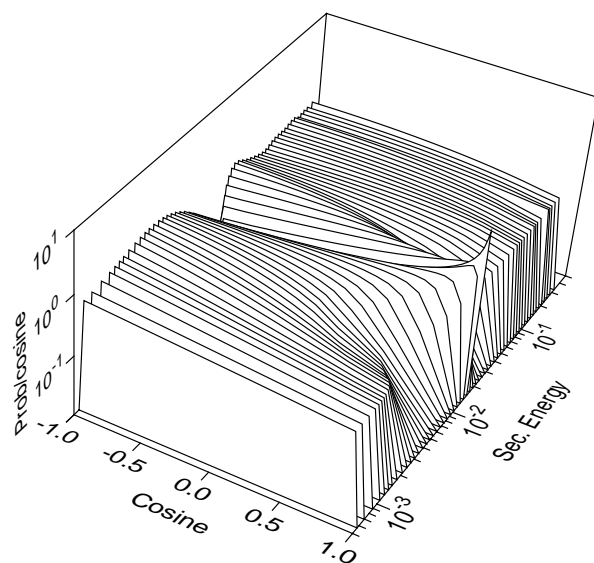


Figure 84: A perspective view of an angle-energy distribution for H in H<sub>2</sub>O.

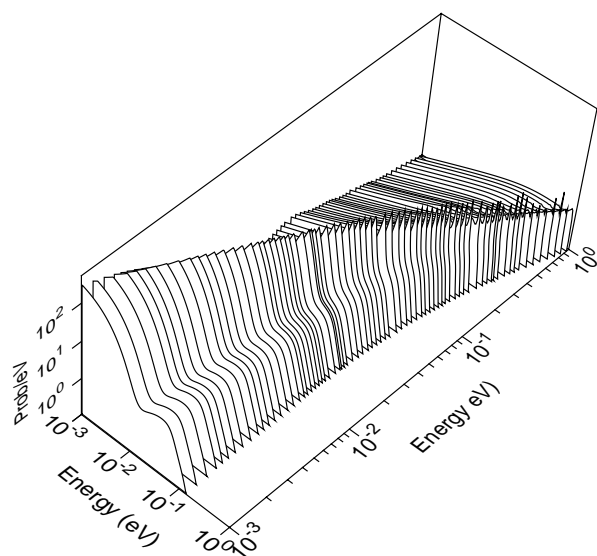


Figure 85: A perspective view of the isotropic part of the incoherent inelastic scattering from H in H<sub>2</sub>O. The variations in the size of the quasi-elastic peak are artifacts of the plotting program.



they are modeled based on various kinds of input data ranging from neutron scattering measurements to optical results. The model results are then compared to the available experimental data to see how good of a job was done with the evaluation. Examples of the comparison of the modeled thermal cross section for water with experiment[110, 111, 112, 113, 114, 115, 116] are shown in Fig. 86 and Fig. 87. Additional comparisons with differential data are shown in the report on the IAEA evaluation[109]. The results are fairly good, except around 300 to 400 meV and below 1 meV. The problem at the lowest energies comes from the failure of the translational model. This part of the distribution is not too important in practice due to effects of detail balance.

**The Model for Solid Methane.** The methane molecule consists of an atom of carbon surrounded by four atoms of hydrogen placed on the corners of a tetrahedron. The carbon atom is at the center of mass of the system; because of its symmetry, the methane molecule is often called a “spherical top”. Optical measurements of methane in the gas phase show four fairly well defined vibrational modes at 162 meV, 190 meV, 361 meV and 374 meV. Following the

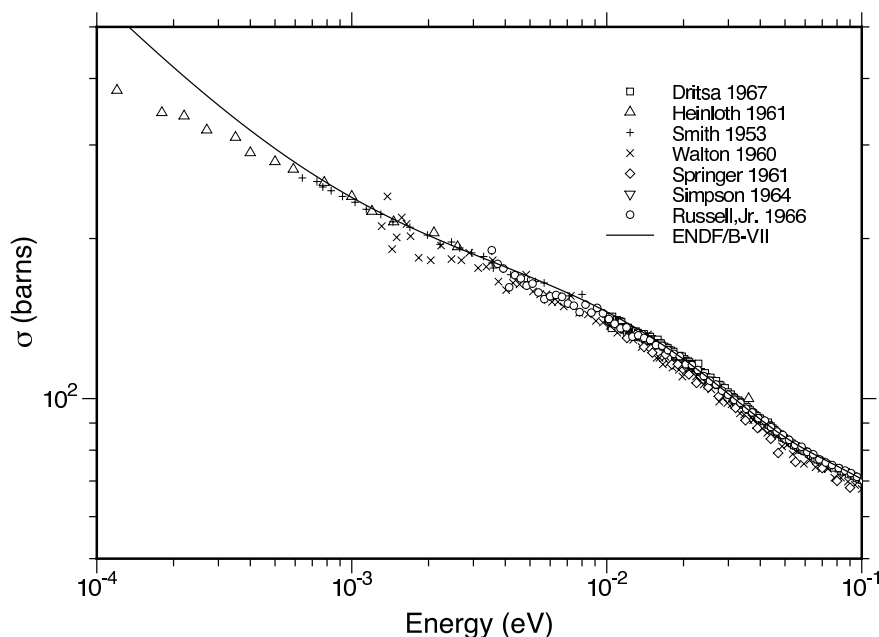


Figure 86: Comparison of the ENDF/B-VII.0 thermal cross section for water at lower incident energies with experimental results for the CSISRS compilation at the the National Nuclear Data Center of the Brookhaven National Laboratory. See the compilation for the references.

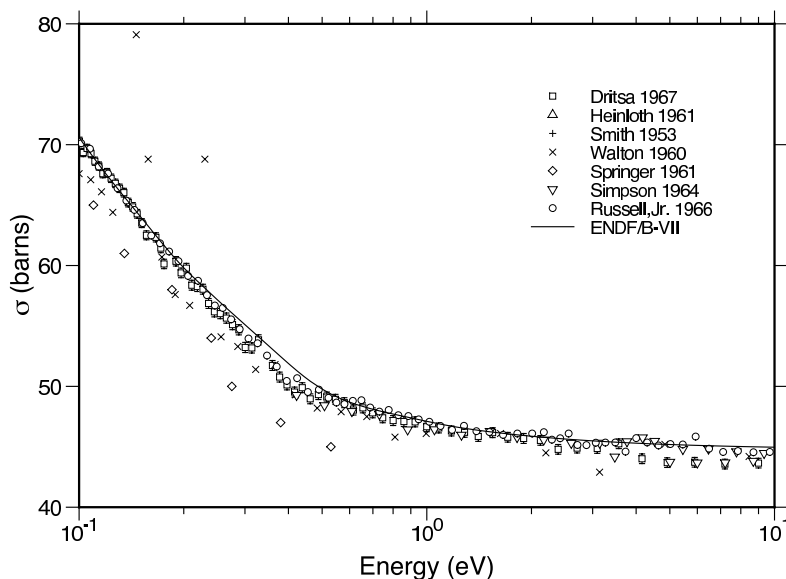


Figure 87: Comparison of the ENDF/B-VII.0 thermal cross section for water at higher incident energies with experimental results for the CSISRS compilation at the the National Nuclear Data Center of the Brookhaven National Laboratory. See the compilation for the references.

lead of Picton, they have been included in this model as discrete oscillators with weights equal to .308, .186, .042, and .144, respectively.

Specific heat measurements in solid methane near one atmosphere show three phases with transitions at 8K and 20.4K. The melting point is about 89K. X-ray measurements show that the carbon atoms are arranged on an fcc lattice for both of the higher two phases; it has been speculated that the phase transition is due to a change in the degree of rotational order, or perhaps due to the onset of a self-diffusion behavior. Because of this interesting question, a series of slow neutron inelastic scattering experiments were carried out with samples in each of the phases[117]. Since hydrogen is an incoherent scatterer, it was possible to analyze the data to obtain a frequency spectrum for hydrogen in solid methane. The results didn't really explain what was happening in the 20K phase transition, but they did provide the data needed for our calculation.

Again following Picton, we chose the spectrum for 22.1K for our model. Instead of using Picton's numbers directly, we digitized the curve from the graph in the reference, plotted it on a large scale, and then smoothed it by hand. Care was taken to use an  $\omega^2$  variation for low energies. The resulting spectrum is shown in Fig. 88. As discussed by Harker and Brugger, the appropriate normalization for this curve is 0.32.

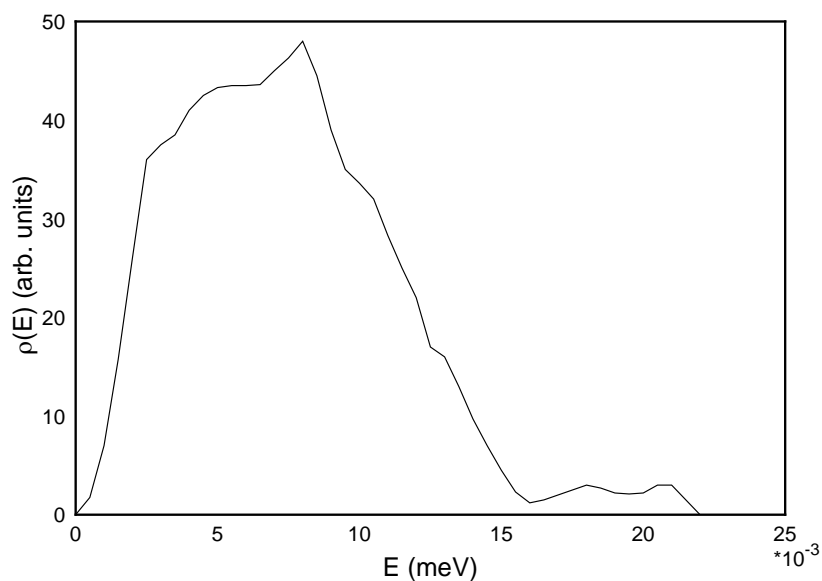


Figure 88: The Harker-Brugger frequency spectrum used for solid methane. Note the quadratic shape at low energies.

This spectrum and the four discrete oscillators were then used to calculate  $S(\alpha, \beta)$  with LEAPR using the  $\alpha$  and  $\beta$  grids of Picton. The input file follows:

```
leapr
26
'solid methane at 22K, Harker & Brugger spectrum'/
1 2/
11 1001./
0.9992 20.36 4/
1 1. 11.898 4.7392 1/
70 80/
.1742 .3488 .4059 .4644 .5215 .6386 .7547 .8703
.9860 1.1601 1.3932 1.6245 1.9148 2.2050 2.6105
3.0177 3.5393 4.1198 4.8740 5.6871 6.6159 7.7760
9.0522 10.6200 12.4187 14.5066 16.9443 19.8464 23.2115
27.0995 31.7421 37.0805 43.4052 50.7168 59.1889 69.6343
81.2403 87.0431 94.0059 101.5493 110.2545 120.1198 129.9834
151.4547 177.5682 188.0122 204.2604 207.1629 209.4831 214.7058
217.0265 220.5090 232.1145 242.5599 261.1291 272.7347 282.0199
287.2413 298.2667 304.6496 311.0342 319.1575 327.2810 331.9236
350. 370. 390. 410. 450. 500./
```

```

0. .1742 .3488 .4059 .4644 .5215 .6386 .7547 .8703
.9860 1.1601 1.3932 1.6245 1.9148 2.2050 2.6105
3.0177 3.5393 4.1198 4.8740 5.6871 6.6159 7.7760
9.0522 10.6200 12.4187 14.5066 16.9443 19.8464 23.2115
27.0995 31.7421 37.0805 43.4052 50.7168 59.1889 69.6343
81.2403 85.451 89.650 94.0059 96.0 100.221 104.6 110.2545
120.1198 129.9834 151.4547 170.90 177.5682 181.6 185.67 190.419
193.8 197.276 200.8 204.2604 207.1629 209.4831 214.7058
217.0265 220.5090 232.1145 242.5599 261.1291 272.7347 282.0199
287.2413 298.2667 304.6496 311.0342 319.1575 327.2810 331.9236
350. 370. 390. 410. 430. 450./
22/
.0005 45/
0. 1.75 7 15.75 26 36 37.5 38.5 41 42.5 43.3 43.5
43.5 43.6 45 46.3 48 44.5 39 35 33.6 32 28.3 25 22 17 16
13 9.7 7 4.5 2.3 1.2 1.5 2 2.5 3 2.7 2.2 2.1 2.2 3 3 1.5
0./
0. 0. .32/
4/
.162 .190 .361 .374/
.308 .186 .042 .144/
* S-CH4 LANL EVAL-NOV92 MACFARLANE*/
* NO REF TO DATE DIST-*/
*----ENDF/B-6 MATERIAL 11*/
*-----THERMAL DATA
*-----ENDF-6*/
* SOLID METHANE AT 22K, SPECTRUM OF HARKER AND BRUGGER.*
/
stop

```

After the calculation, the moments of  $T_n$  and  $S(\alpha, \beta)$  can be checked. The errors should be modest. The output listing for the solid-type part of the problem should be examined carefully to see that the  $\alpha$  and  $\beta$  ranges are sufficient and that the normalization and sum rule checks are reasonably well satisfied. Since this is a solid, there was no translational calculation. In the discrete-oscillator calculation the delta functions for  $\beta > 0$  are put directly into the scattering law as sharp triangles. The  $\beta=0$  peak is converted into incoherent elastic scattering. A listing showing some of the discrete lines is given below:

```

alpha=    2.61050

debye-waller factor=  6.0347e-01

discrete lines
      beta      weight
      0.000  9.8340E-01
     -85.451  9.2531E-03
    -170.903  4.3532E-05
    -100.221  4.7644E-03
    -185.672  4.4830E-05
    -200.441  1.1541E-05
    -190.419  5.6623E-04
    -197.276  1.8739E-03
    -282.728  1.7632E-05
norm check    1.0000
rule check    0.9964

```

The Debye-Waller factor printed here is the one from the solid-type spectrum,  $\lambda_s$ . It defines the total strength of all the discrete lines. All the discrete lines taken together must satisfy the normalization and sum-rule requirements of any scattering law. If the number of discrete lines increases above 100, some of them will begin to be lost, and the checks will begin to decrease below unity. The listing for the discrete-oscillator calculation should show that the grid specified does a reasonable job of satisfying the overall normalization and sum-rule checks. LEAPR automatically prepared an output file in ENDF-6 format. Plots of  $S(\alpha, \beta)$  vs.  $\beta$  for several values of  $\alpha$  are given in Fig. 89.

Next, the new evaluation for  $S(\alpha, \beta)$  can be processed into integrated cross sections and double differential cross sections using the [THERMR](#) module of NJOY. A plot of the integrated cross section is given in Fig. 90, and plots of the outgoing neutron spectrum integrated over angle at several incident energies are given in Fig. 91.

**The Model for Liquid Methane.** This example is for liquid methane at 100K. Once again, we use the four discrete oscillators to represent the molecular vibrations. In addition, we need a continuous frequency distribution to represent the molecular rotations, and a pair of parameters  $d$  and  $c$  to represent

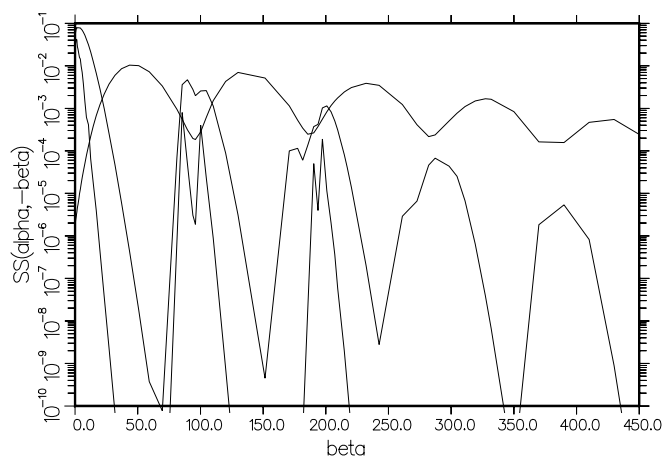


Figure 89:  $\mathcal{S}(\alpha, -\beta)$  for solid methane shown as a function of  $\beta$  for the  $\alpha$  values 0.986 (lowest), 16.94, and 151.45 (highest). The four discrete levels show up as sharp triangles in the lowest curve.

diffusion. This latter component was omitted from the earlier model of Picton, but we felt that it might be needed to obtain a reasonable quasi-elastic peak in the spectrum of scattered neutrons. Therefore, we couldn't use the Picton input directly, and we had to refer to his source[118]. Agrawal and Yip divided the problem into two parts: translations and rotations.

For translations, they proposed a model for  $\gamma(t)$  that matches the expected diffusive behavior at long times and provides an oscillatory behavior at short

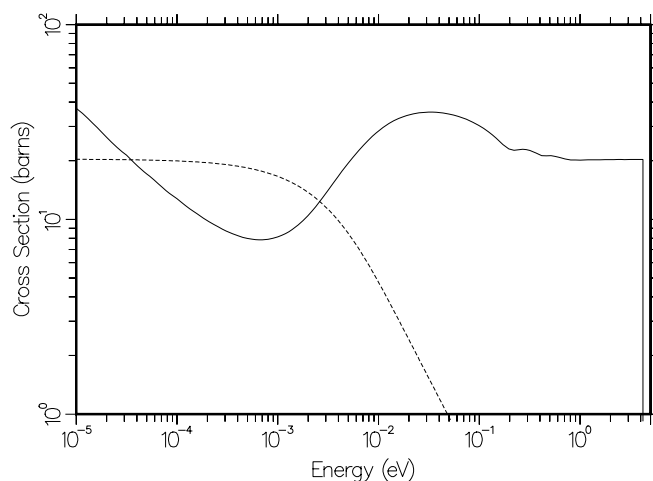


Figure 90: Inelastic (solid) and incoherent elastic (dashed) cross sections for solid methane. The small bumps starting at about 0.2 eV are due to the discrete levels at 0.162 eV, 0.190 eV, 0.361 eV, and 0.374 eV.

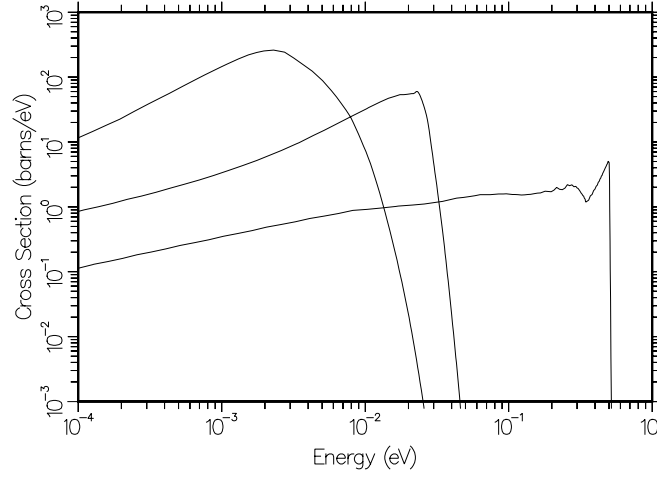


Figure 91: Neutron spectra  $\sigma(E \rightarrow E')$  for solid methane shown as functions of outgoing neutron energy  $E'$  for  $E = 0.0001$  eV,  $0.0253$  eV, and  $0.503$  eV.

times. Each methane molecule is assumed to move in a “cage” formed by its neighbors, and the cage itself is allowed to relax with time. As Agrawal and Yip point out, the molecule will oscillate initially, but gradually as the restoring forces decay into a frictional background, it will go over into diffusive motions. The resulting analytic expression for the frequency spectrum is

$$f_t(\omega) = \frac{2}{\pi} \frac{\omega_0^2/\tau_0}{(\omega^2 - \omega_0^2)^2 + (\omega/\tau_0)^2}. \quad (574)$$

The fact that  $f(\omega)$  is nonzero at  $\omega=0$  indicates that the molecules are capable of diffusion, and in addition,  $f(\omega)$  has a resonant behavior near  $(\omega^2 - \tau_0^2)^{1/2}$ , the characteristic frequency of local oscillations.

For rotations, the argument starts out by recalling that for translations,  $\gamma(t)$  is related to the mean-square displacement  $W(t)$  by

$$\gamma(t) = \kappa^2 W(t), \quad (575)$$

where the magnitude of the wave vector is related to  $\alpha$  by

$$\alpha = \frac{\hbar^2 \kappa^2}{2MkT}. \quad (576)$$

The rotational analog of the mean-square displacement is the mean-square component of the bond length  $\vec{b}$  along the the vector  $\vec{\kappa}$ , or

$$\begin{aligned}
W(t) &= \langle [b_\kappa(t) - b_\kappa(0)]^2 \rangle \\
&= 2 \langle b_\kappa^2 \rangle \left[ 1 - \frac{\langle b_\kappa(t)b_\kappa(0) \rangle}{\langle b_\kappa^2 \rangle} \right] \\
&= \frac{2b^2}{3} [1 - F_1(t)].
\end{aligned} \tag{577}$$

The function  $F_1(t)$  is seen to describe the correlation between a specific direction in the molecule at  $t=0$  with its direction at a later time  $t$ . Therefore, it is called the “dipole correlation function”. The same function appears in the classical limit of the theory of optical line shapes for infrared absorption as presented by Gordon[119]. At frequencies where it is safe to assume that the internal vibrations of different molecules are uncoupled, the shape of a vibrational line depends mostly on the reorientation motions of individual molecules, and the dipole correlation function can be obtained from

$$F_1(t) = \int_{\text{band}} \hat{I}(\omega) \cos \omega t d\omega. \tag{578}$$

Gordon has used this method to compute  $F_1(t)$  for liquid methane at 98K based on the infrared data of Ewing[120]. In order to link this result to neutron scattering, we use the high-temperature classical limit of Eq.506 to express  $W(t)$ ; namely,

$$W(\hat{t}) = \frac{\hbar^2}{2MkT} \int_0^\infty \frac{\rho_r}{\beta^2} [1 - \cos(\beta\hat{t})] d\beta, \tag{579}$$

which can be inverted to obtain

$$\rho_r(\beta) = \frac{2MkT}{\hbar^2} \int_{-\infty}^\infty \frac{d^2\gamma_r}{dt^2} e^{i\beta\hat{t}} d\hat{t}. \tag{580}$$

This limit is justified by noting that  $\beta < 1$  for the rotational modes in liquid methane around 90K. It is now easy to compute  $\rho_r$  by taking two derivatives of the dipole correlation function graphed by Gordon.

The result is shown in Fig. 92, together with the translational frequency distribution discussed above. These numbers were generated by digitizing the curve from Agrawal and Yip, subtracting the translational part, and smoothing the remainder. Agrawal and Yip compared their model with both double-differential and integrated cross sections, with very good agreement.



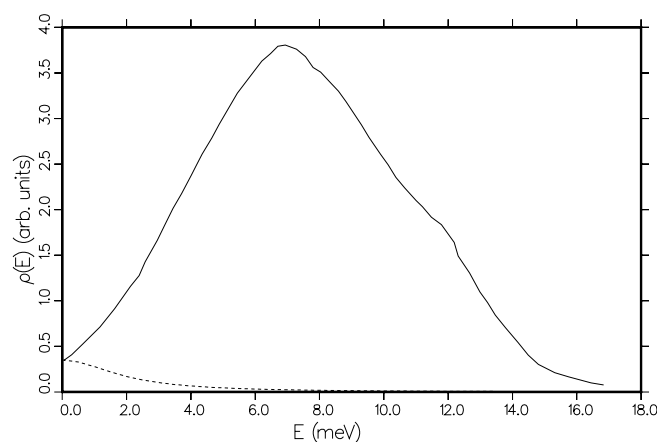


Figure 92: Frequency spectrum for liquid methane (solid) as given by Agrawal and Yip, including an analytic translational part (dashed) and a rotational part based on Gordon's analysis of the optical measurements of Ewing.

Unfortunately, this model does not match the requirements of LEAPR. The only type of frequency distribution that is nonzero at  $\omega=0$  that can be used by the code is the diffusive law of Egelstaff and Schofield, which does not have the short-time oscillatory behavior of Eq. 574. Our main reason for using the diffusion term in our model for liquid methane was to improve the “quasi-elastic” peak, which depends mostly on the small- $\omega$  part of the frequency distribution. Therefore, it seemed reasonable to select diffusion parameters  $d$  and  $c$  that gave a reasonable representation for the full width at half maximum of the quasi-elastic peak, to subtract the result  $f_d$  from the sum of the two curves shown in

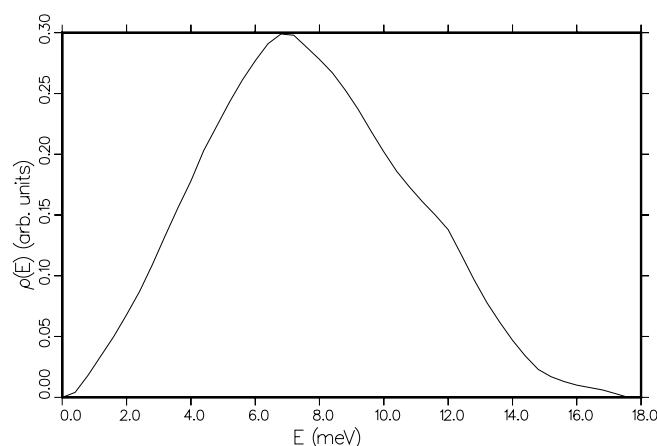


Figure 93: Effective frequency spectrum for methane including both translational and rotational modes, but not including diffusive modes.

Fig. 92, and to use the difference to represent both the translational oscillatory modes and the rotational modes. Fig. 93 shows this breakdown. Once again, there has been some hand smoothing, and the low energy part of the distribution was forced to follow an  $\omega^2$  law. The final breakdown was 1.5% diffusion, 30.5% rotation, and 68% molecular vibrations.

The LEAPR input for liquid methane at 100K is shown below.

```
liquid methane at 100k, modified agrawal & yip model
89 81/
.0387 .0775 .0902 .1032 .1159
.1419 .1677 .1934 .2191 .2578 .3096 .3610
.4255 .4900 .5801 .6706 .7865 .9155 1.0831
1.2638 1.4702 1.7280 2.0116 2.3600 2.7597 3.2237
3.7654 4.4103 5.1581 6.0221 7.0538 8.2401 9.6456
11.2704 13.1531 15.4743 18.0534 19.3429 20.8902 22.5665
24.5010 26.6933 28.8852 33.6566 39.4596 41.7805 45.3912
46.0362 46.5518 47.7124 48.2218 49.0020 51.5810 53.9022
58.0287 60.6077 62.6711 63.8314 66.2815 67.6999 69.1187
70.9239 72.7291 73.7608 78.6611 83.5613 86.1404 90.0089
93.2326 96.4566 98.0039 100.8408 104.4516 109.6097 117.8625
137.8503 140.5583 144.6847 149.5850 161.1907 183.4447 208.7711
237.5941 270.3965 307.7273 350.2124 398.5625 453.5881 516.2107/
0.0 .0387 .0775 .0902
.1032 .1159 .1419 .1677 .1934 .2191 .2578
.3096 .3610 .4255 .4900 .5801 .6706 .7865
.9155 1.0831 1.2638 1.4702 1.7280 2.0116 2.3600
2.7598 3.2237 3.7654 4.4103 5.1581 6.0221 7.0538
8.2401 9.6456 11.2704 13.1531 15.4743 18.0538 19.3429
20.8902 22.5665 24.5010 26.6933 28.8852 33.6566 39.4596
41.7805 45.3912 46.0362 46.5518 47.7124 48.2281 49.0020
51.5810 53.9022 58.0287 60.6077 62.6711 63.8314 66.2815
67.6999 69.1187 70.9239 72.7291 73.7608 78.6611 83.5613
86.1404 90.0089 93.2326 96.4566 98.0039 100.8408 104.4516
109.6097 117.8625 137.8503 140.5583 144.6847 149.5850 161.1907/
100/
1 1/
.00040 45/
0. .004 .018 .034 .050 .068 .087 .109
.133 .156 .178 .203 .223 .243 .261 .277 .291 .299
.298 .288 .278 .267 .253 .237 .219 .202 .186 .173
.161 .150 .138 .118 .097 .078 .062 .047 .034 .023
```

```

      .017 .013 .010 .008 .006 .003 0./
3. 200. 0 0 .32/
4/
      .162 .190 .361 .374/
      .308 .186 .042 .144/
0/
10 1001. 1.008 20.3 1 0 8
L-CH4      LANL      EVAL-FEB88 MACFARLANE
NO REF TO DATE      DIST-
----ENDF/B-6      MATERIAL
-----THERMAL DATA
-----ENDF-6
LIQUID METHANE AT 100k, MODEL OF AGRAWAL AND YIP
AS IMPLEMENTED BY D.J.PICTON,
MODIFIED TO INCLUDE A DIFFUSIVE COMPONENT.

```

LEAPR can be run with this input deck. Once again the moments of  $T_n$  and  $S(\beta)$  can be checked, and no great problems should be seen. These checks help to prove that the  $\epsilon$  grid for the input frequency spectrum and the  $\beta$  grid for calculating  $S$  are reasonable. The user should also check the range of  $\alpha$  and  $\beta$  to be sure that no significant cross section contributions were being cut off. The results should be good for all energy transfers possible with incident neutron energies up to 1 eV. Once again, LEAPR produces an output file in ENDF-6 format. This time, there will be no elastic contribution at all. Plots of  $S(\alpha, \beta)$  versus  $\alpha$  for several values of  $\beta$  with this mode are shown in Fig. 94. Note that

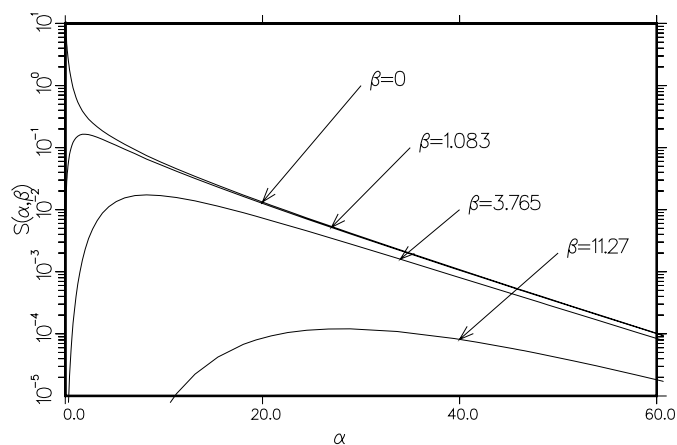


Figure 94:  $S(\alpha, \beta)$  curves for liquid methane. Note the diffusive behavior at low  $\alpha$  and  $\beta$ .

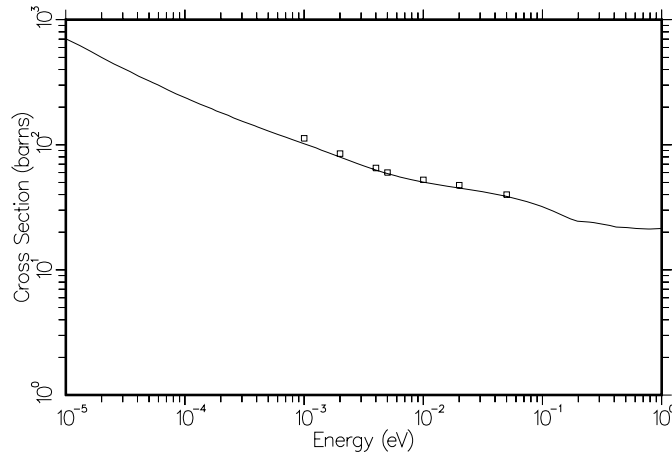


Figure 95: The computed cross section for liquid methane at 100K (solid) is compared to experimental data at 110K (squares) by Whittemore and by Rogalska as quoted by Agrawal and Yip.

the behavior of the curves for small  $\beta$  is quite different than in Fig. 89. This reflects the presence of the diffusive component.

The new evaluation for liquid methane can be run through the [THERMR](#) module of NJOY to produce integrated and differential cross sections. Sample results are given in Figs. 95 and 96. The integrated cross section at 100K is compared with experimental data at 110K that was quoted in the Agrawal and Yip paper.

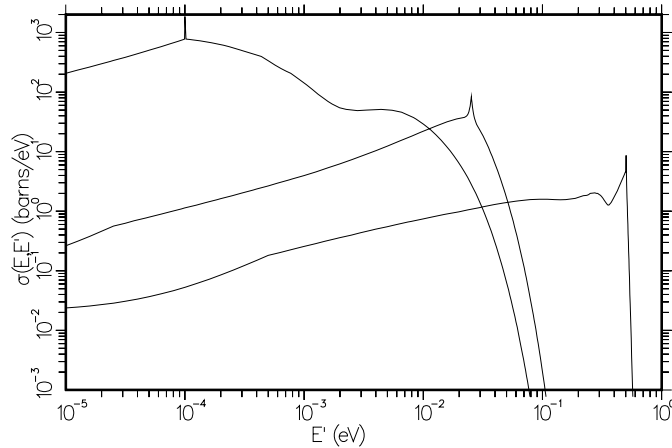


Figure 96: Neutron spectra  $\sigma(E \rightarrow E')$  are shown for  $E = 0.0001$  eV,  $0.0253$  eV, and  $0.503$  eV. Note the sharp quasi-elastic peak that results from the diffusive term in the theory used here.

**The Model for Liquid Hydrogen.** As discussed above, we picture a hydrogen molecule bound in a cluster of about 20 molecules and undergoing vibrations similar to those of a hydrogen molecule in a solid. These clumps then diffuse through the liquid (hindered translations) according to the Egelstaff-Schofield effective width model. This physical situation is described by the Keinert-Sax distribution function shown in Fig. 97. They assumed a weight of 0.025 for the hindered translation, leaving a value of 0.475 for the solid-like distribution. In addition, intermolecular coherence is taken into account using the Vineyard approximation. The static structure factor  $S(\kappa)$  was provided by Keinert and Sax. See Fig. 98.

This model can then be used in LEAPR. Some results for the effective translational  $\mathcal{S}(\alpha, \beta)$  to be used in the Young and Koppel formulas are shown in Figs. 99 and 100. Because of the spin correlations,  $S(\alpha, \beta) \neq S(\alpha, -\beta)$ , and it is necessary to calculate both sides of the function. Similar results for ortho hydrogen are shown in Figs. 101 and 102. These results were then passed to the ENDF output subroutine, which allows for asymmetric scattering functions through the parameter “LASYM” in the ENDF File 7 format (it is in the “L1” position of the head card for MF=7, MT=4). When LASYM=1, the  $\beta$  grid in File 7 starts with  $-\beta_{\max}$  and increases through zero to  $+\beta_{\max}$ . Some examples of energy distributions for this asymmetric case computed by THERMR are shown in Figs. 103 and 104.

A comparison of the computed cross section for para and ortho hydrogen with experiment is shown in Fig. 105.

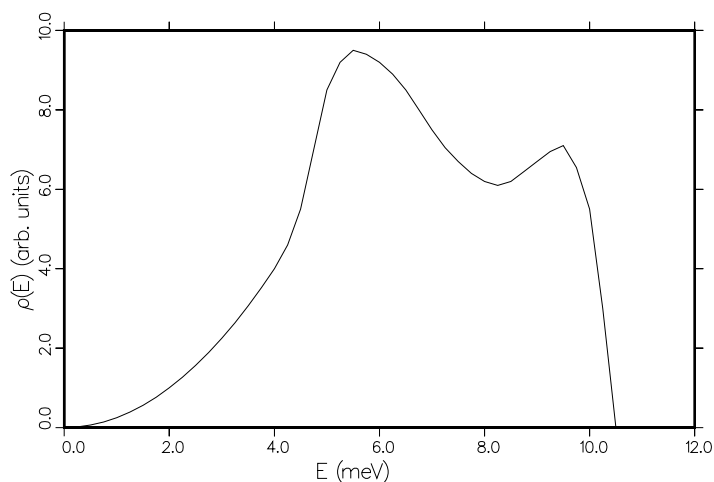


Figure 97: The Keinert-Sax frequency distribution for the effective translational modes of liquid hydrogen.

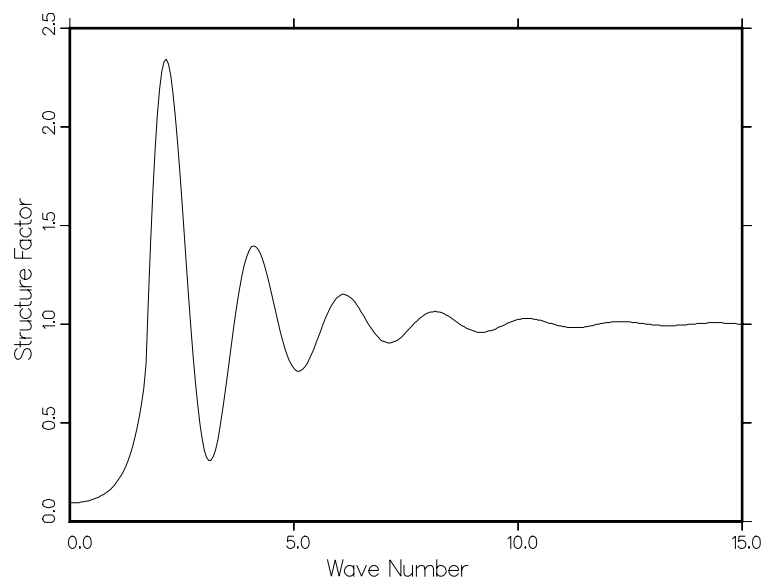


Figure 98: The static structure factor  $S(\kappa)$  for liquid hydrogen.

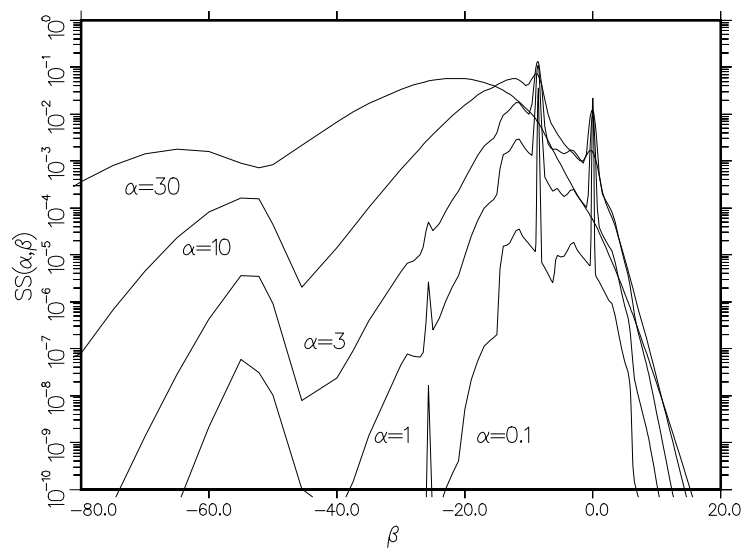


Figure 99: Script-S for para-hydrogen at 20K is shown as a function of  $\beta$  for several  $\alpha$  values.

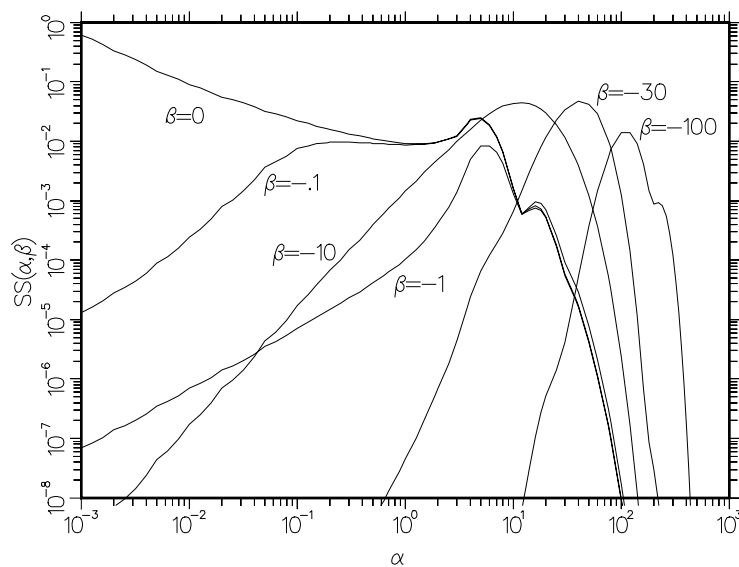


Figure 100: Script-S for para-hydrogen at 20K is shown as a function of  $\alpha$  for several  $\beta$  values corresponding to downscatter.

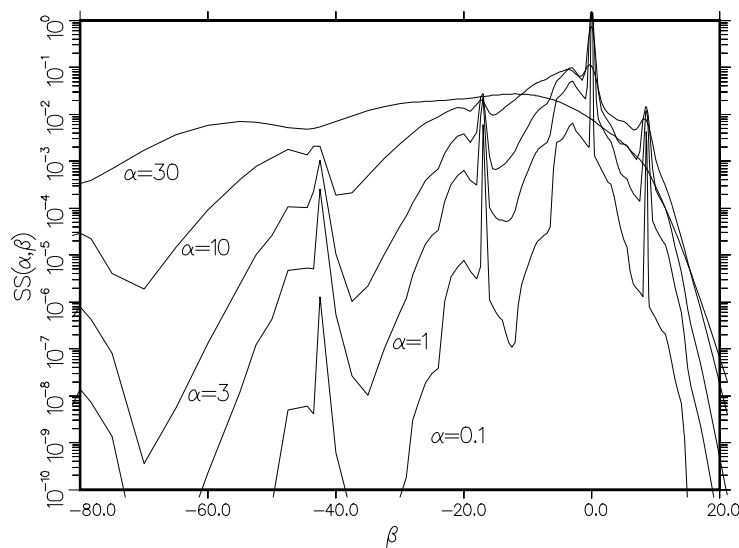


Figure 101: Script-S for ortho-hydrogen at 20K is shown as a function of  $\beta$  for several  $\alpha$  values.

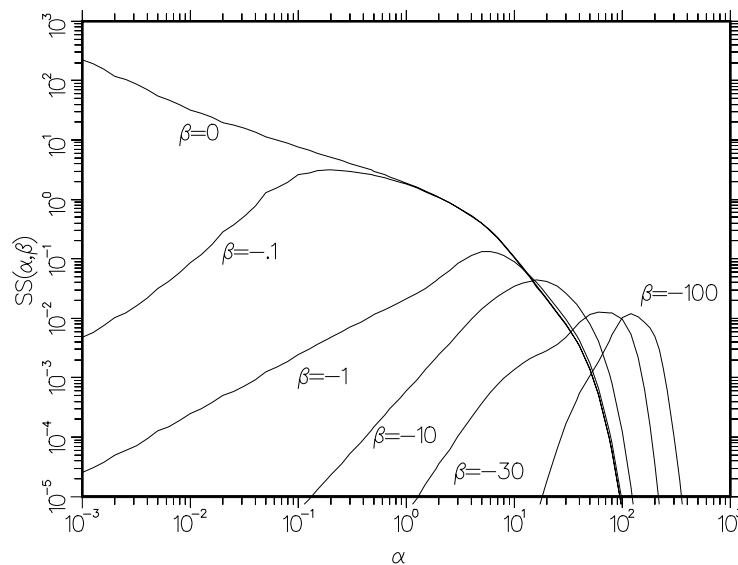


Figure 102: Script-S for ortho-hydrogen at 20K is shown as a function of  $\alpha$  for several  $\beta$  values corresponding to downscatter.

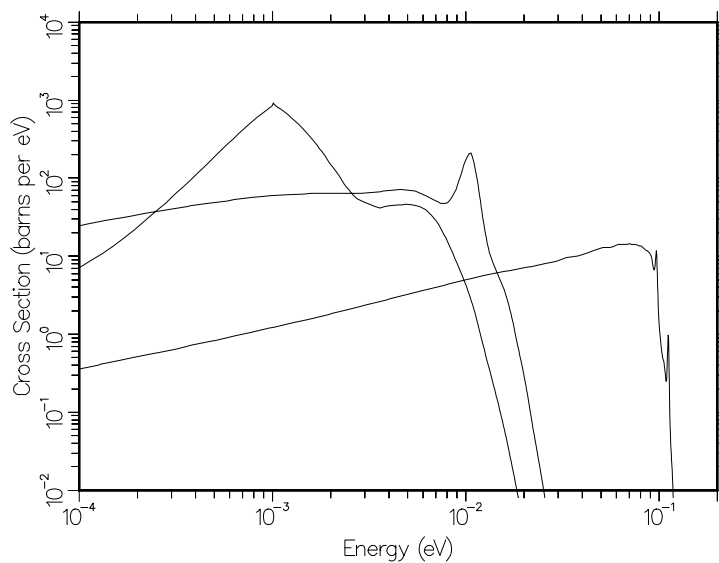


Figure 103: The spectra  $\sigma(E \rightarrow E')$  for liquid para-hydrogen are shown for  $E = 0.0001$  eV, 0.0106 eV, and 0.112 eV.



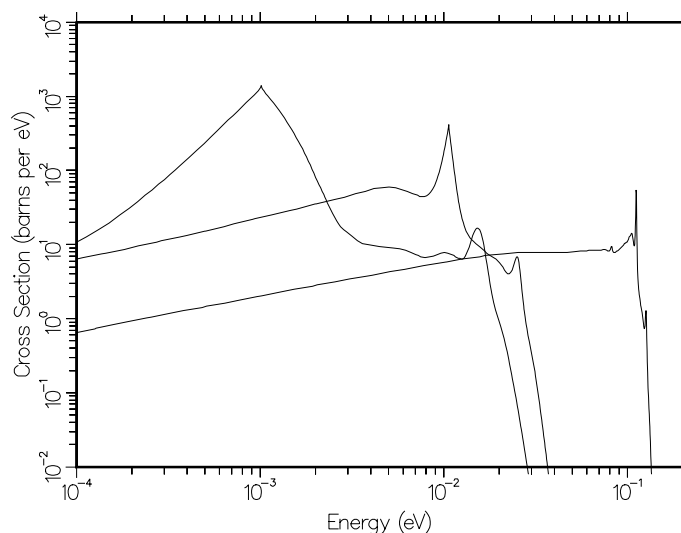


Figure 104: The spectra  $\sigma(E \rightarrow E')$  for liquid ortho-hydrogen are shown for  $E = 0.0001$  eV, 0.0106 eV, and 0.112 eV.

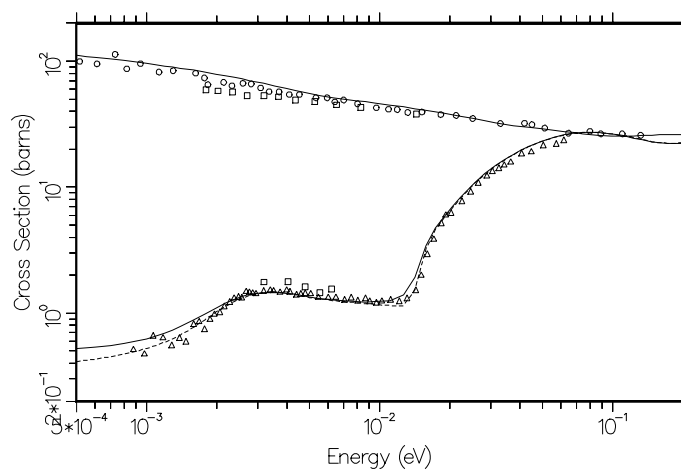


Figure 105: The cross sections for liquid ortho-hydrogen (upper curve) and liquid para-hydrogen (lower curve) at 20K are compared with experimental data[121] due to Squires (gas) at 20K (squares), Whittemore at 20K (circles), and Seiffert at 14K (triangles). The solid curves are at 20K and the dashed curve is at 14K. The sharp drop in the para cross section below 0.05 eV is due to spin coherence, and the second drop below 0.003 eV is due to intermolecular interference.

## 24.4 Coding Details

Subroutine `leapr` is exported by module `leapm`. It follows the standard pattern for an NJOY module in that it starts with a group of comment cards describing the code and giving the input instructions.

LEAPR performs many calculations of exponentials of very small numbers and of products of small numbers. These calculations will lead to underflow conditions on many machines. These underflow events are not intercepted or reset by LEAPR for efficiency. The programmer should use the appropriate system calls or compiler options to suppress these underflow messages and to assure that the system does not generate “Not a Number” (NaN) values that would affect the calculation.

User input is read in using the standard Fortran `READ*`. With the size of the problem determined, storage can be allocated for the `alpha` grid, the `beta` grid, and the `ssm` and `ssp` array (if needed).

Most of the main program consists of the loops over principal and secondary scatterers, and the loop over temperatures. If the mixed-moderator option has been requested, the results for the principal scatterer are written onto a scratch file on unit 10, and the effective temperature and Debye-Waller factor for the principal scatterer are stored in the variables `tempf1` and `dwp1`. The code then loops back to statement 100 to repeat the calculation for the secondary scatterer. Note the global variable `arat`. This is the mass ratio that is used to scale the  $\alpha$  grid for the secondary scatterer in the mixed-moderator calculation. If only one scattering law is being calculated, the code drops through to the ENDF output section.

Inside the temperature loop, LEAPR first reads in the temperature, the continuous frequency distribution, the oscillator data, and the pair correlation function. It then processes the continuous spectrum by calling subroutine `contin`, the translational modes (if any) by calling `trans`, the discrete oscillators (if any) by calling `discre`, and the liquid hydrogen or deuterium option using subroutine `coldh`.

We next look at `contin`. The first part of the calculation is performed by `start`, which prepares and normalizes the functions  $\rho(\beta)$  and  $P(\beta)$ . It also calculates the effective temperature and Debye-Waller  $\lambda$ , and starts the convolution process for the phonon expansion by computing  $\mathcal{T}_1$ . The results printed out at this point refer to the continuous part of the distribution only. The effective temperature and Debye-Waller  $\lambda$  may change as other modes are added.

When **start** returns to **contin**, the continuous part of the scattering law is computed by carrying out the phonon expansion. At any one time, only  $\mathcal{T}_1$ ,  $\mathcal{T}_{\text{last}}$ , and  $\mathcal{T}_{\text{now}}$  have to be kept in memory to carry out the convolution. Note that the number of elements of  $\mathcal{T}_n$  starts out equal to the number of  $\beta$  values in  $\rho$  for  $n=1$ , and then it increases by this number for every subsequent step. Therefore, the maximum sizes for **tlast** and **tnow** are equal to the number of points in the frequency distribution times **nphon**.

Each step of the expansion is handled by the convolution routine **convol**. The input T arrays **tlast** and **t1** contain only the  $-\beta$  part of the asymmetric T functions. This is the part that has the smallest dynamic range, because it is roughly proportional to the cross section. Really small numbers like those that occur on the upscatter side of the asymmetric T function cannot significantly affect the answers. This approach was developed to get good results even on short-word computers that could not represent numbers less than quantities like  $10^{-31}$  or  $10^{-45}$ . This is less of a problem with Fortran-90's "kind" method. Note that **convol** also returns the quantity **ckk**, which is used to check the normalization condition on the  $\mathcal{T}_n$ .

Returning to **contin**, note that the code determines the maximum value of  $\alpha$  that can be used for each  $\beta$  without invoking the SCT approximation. This is done by checking each term that is accumulated into the phonon expansion to see if it is smaller than 0.1% of the accumulating  $\mathcal{S}(\alpha, -\beta)$ . These breakpoints are summarized on the output listing if **iprint**=2. Next, **contin** checks the computed scattering law to see if it satisfies the normalization and sum rule requirements. The scattering law may also be printed out by this loop. Note that the quantity  $\mathcal{S}(\alpha, -\beta)$  is the result actually computed by **contin**. The corresponding upscatter side of  $\mathcal{S}$  and the symmetric  $\mathcal{S}(\alpha, \beta)$  are computed just for the listing. On a short-word machine, these two quantities may underflow to zero, but that doesn't affect the accuracy of subsequent calculations. The denominator of the normalization test with **sum0** is  $1 - \exp(-\alpha\lambda)$  because the delta function that represents the "zero-phonon" term is not included in the calculated scattering law.

When **contin** returns to **leapr**, the  $-\beta$  side of the asymmetric scattering law is safely stored in **ssm** for this temperature. If translational modes have been requested by entering a value greater than zero for **twt**, subroutine **trans** is called. The task here is to convolve a free-gas or diffusive shape with the current scattering law. The approach is to first use **stable** to compute the free-gas or diffusive shape on an appropriate  $\beta$  grid. Then, subroutine **sbfill**

is called to remap the current scattering law onto the same  $\beta$  grid. It is then easy to perform the convolution integral using Simpson's Rule. The final step is to add in the convolution of the "zero-phonon" term, which is a delta function, with the translational term. That step is very easy, because it is only necessary to interpolate for the translational term at the current  $\beta$  value and multiply by  $\exp(-\alpha\lambda)$ . When the loop over  $\beta$  is complete, another  $\beta$  loop is used to check the normalization and sum-rule conditions. Normally, there is some loss in accuracy at this point, because it is impractical to keep the  $\beta$  grid fine enough at small  $\beta$  to represent the very sharp shape of the translational contribution at small  $\alpha$ . When the  $\alpha$  loop is complete, a new value for the effective temperature to be used with the SCT approximation is computed. The Debye-Waller  $\lambda$  remains unchanged.

The next step is to call subroutine **discre** to add the contributions from the discrete oscillators, if any. The keys to this calculation are the routine **bfact**, which generates the terms

$$e^{-\alpha\lambda_i} I_n \left[ \frac{\alpha w_i}{\beta_i \sinh(\beta_i/2)} \right] e^{-n\beta_i/2}, \quad (581)$$

and the routine **sint**, which interpolates for the scattering law at  $\alpha$  and  $\beta - n\beta_i$ . **sint** uses the arrays **bex**, **rdbe**, and **sex**, which are generated by **bfill** and **exts**. These arrays extend the  $\beta$  grid and the  $-\beta$  side of the scattering law over the entire  $\beta$  range needed for the discrete oscillator calculation. This makes it easy for **sint** to interpolate for the scattering law at a given  $\beta$  without having to worry about the asymmetry of the  $\mathcal{S}$  function. The sum given by

$$\sum_{n=-\infty}^{\infty} \cdots, \quad (582)$$

is evaluated by first doing the term with  $n=0$ , then doing the negative  $n$  terms until **add** is less than **tiny** (currently  $1.0 \times 10^{-30}$ ), and finally, doing the positive  $n$  terms until the **add** is less than **tiny**. This entire process is continued until all  $\beta$  and  $\alpha$  values have been processed. The normalization and sum-rule checks are carried out as before. There is usually some loss in the accuracy of these tests at high  $\alpha$ , because the  $\beta$  grid doesn't extend to high enough values to complete the integrals.

New values for the effective temperature and the Debye-Waller  $\lambda$  are also produced by **discre** before it returns to the main processing line in **contin**.

Subroutine **bfact** computes the factors used to weight the various discrete-oscillator contributions to the scattering law. The modified Bessel Functions  $I_0(x)$  and  $I_1(x)$  are computed separately for small  $x$  and large  $x$  to take advantage of the factor  $e^x$  at large  $x$ . It is easier to control the numerics when  $x$  can be combined with  $-\alpha\lambda$  and  $-n\beta_i/2$  in the exponent before computing the factor. The  $I_0(x)$  and  $I_1(x)$  are computed using series expansions; higher orders are generated using reverse recursion[122]. The numerics of the products  $I_n(x)e^x$  is controlled to return all significant values for both  $+$  and  $-n$ , even for large  $x$ . This is an improvement over the original LEAP code.

Subroutine **sint** first checks to see if the requested value of  $\beta$  is in the tabulated range. If not, it computes the scattering law using the SCT expression. Otherwise, the value is computed by finding the appropriate panel in the tabulated function and interpolating on  $\log \mathcal{S}$ . Note that the  $\beta$  grid has been extended over the entire range of negative and positive  $\beta$  values using **bfill** and **exts**.

Subroutine **coldh** is fairly complicated due to the messy details of following the quantum mechanics needed to compute the effects of spin correlation. It starts by setting values for the atomic masses, coherent and incoherent scattering lengths. The fundamental constants needed are available from the **NJOY physics** module. It also sets the translational weight for the free-gas and SCT formulas and the effective temperature ratio **tbart** for the SCT approximation. Of course, all these values depend on whether hydrogen or deuterium are being processed (see **law**). Inside the  $\alpha$  loop, the even and odd  $A$  and  $B$  coefficients are computed for the current molecule from the coherent and incoherent scattering lengths. The next step is to prepare the arrays for **sint**, just as was done in **discre**.

The  $\beta$  loop is complicated by the fact that it is necessary to keep both the  $+\beta$  and  $-\beta$  sides of the scattering function, because the principle of detailed balance doesn't hold for para or ortho phases treated separately. Note that the  $+\beta$  terms go into **ssp**, and the  $-\beta$  terms go into **ssm**. For each value of  $\beta$ , the sums over the even values of  $J'$  and the odd values of  $J'$  are performed separately using **sumh** to retrieve the appropriate sums over Bessel Functions and Clebsch-Gordan coefficients and using **sint** to get the corresponding values of the translational scattering law. A hidden option is available to use the free-gas law instead of the scattering law computed from  $\rho(\beta)$ . One has to change the flag **ifree** to 1.

The **endout** routine begins by merging the principal and secondary scatterer, if the mixed-moderator option was used. It then displays the final values of the

effective temperatures and Debye-Waller coefficients. For comparison with the GA results, the Debye-Waller terms are printed out as  $A\lambda$ . For cases with coherent elastic scattering, subroutine **coher** is called to construct the Bragg edges.

The routine can now start to build up the output ENDF-6 file. It starts by writing the appropriate header cards and the subsection containing the Hollerith description. It then constructs a subsection with MF=7 and MT=2 for incoherent elastic scattering, if present. Note that this section contains the Debye-Waller integral obtained from **dbw**. Next, the code constructs a section with MF=7 and MT=2 for coherent elastic scattering, if present. Because the Bragg edges get very small at high energies, it is possible to thin down the coherent-elastic results slightly. The fractional tolerance for this thinning is set to  $0.9 \times 10^{-7}$ . The final data are output inside a loop over temperature. For mixed-moderator cases, the Debye-Waller integral is computed as the average of the two parts.

The rest of the subroutine outputs the inelastic part. There are a number of variations possible. Normally, the array **ssm** contains the  $-\beta$  side of the asymmetric scattering law. For liquid hydrogen or deuterium, **ssm** contains the  $-\beta$  side of the asymmetric scattering law and **ssp** contains the  $+\beta$  side. These numbers have reasonable values, even on short-word machines. However, the ENDF-6 format normally requires you to give the “symmetric”  $S(\alpha, \beta)$  (it is not really symmetric for liquid hydrogen or deuterium). This function can require that numbers on the order of  $10^{-50}$  be kept, if incident energies as high as 4 eV are needed. For cold moderators, it is necessary to handle numbers on the order of  $10^{-99}$ . For NJOY2012, this is handled by using the Fortran-90 “kind” mechanism.

## 24.5 Error Messages

**error in sjbes\*\*\*argument is invalid...**

There is a problem with the argument to the Bessel functions used for cold hydrogen and deuterium calculations.

**message from sjbes---value is not accurate...**

There is a problem with calculating the Bessel functions.

**error in coh\*\*\*illegal lat**

Currently limited to 1 to 6, for graphite, be, and beo, al, pb, and fe, respectively.

error in coh\*\*\*storage exceeded

Currently limited to `maxb=60 000`, the size of the allocatable array `bragg` in subroutine `leapr`.

error in endout\*\*\*scratch storage exceeded for hollerith...

This refers to the allocatable array `scr` with length `mscr=4000` in subroutine `leapr`.





## 25 GASPR

The GASPR module will add gas production reactions (MT=203-207) to the PENDF file. Any existing gas-production sections on the input PENDF file are removed, and the file directory is updated to show the new reactions. This module can be run anywhere in the PENDF preparation sequence, as long as it is somewhere after [BROADR](#).

This chapter describes GASPR in NJOY 2012.0.

### 25.1 Gas Production

The light products of nuclear reactions – namely, protons, deuterons, tritons,  $^3\text{He}$ 's, and alphas – can accumulate as gases in a nuclear system. The resulting hydrogen, deuterium, tritium,  $^3\text{He}$ , and  $^4\text{He}$  buildup can have important effects on the original material, such as causing embrittlement. In other cases, the gas may even be the desired product, such as in tritium production.

Keeping track of the total production of each gas species is complicated. Gases can sometimes be determined from the MT number for the reaction; for example, an  $(n,\alpha)$  reaction produces one  $^4\text{He}$  per reaction. The gas might be a residual nucleus as in  $^2\text{H}(n,2n)^1\text{H}$  or  $^9\text{Be}(n,2n)2\alpha$ . Sometimes, the ENDF LR flags are used to indicate that the residual nucleus from a reaction breaks up by further particle emission. An example of this is  $^{16}\text{O}(n,n_6)\alpha$  represented using MT=56/LR=22. In other cases, the yield per reaction for the light product may be tabulated directly (and even be fractional) when File 6 is used for the reaction. This is common for the high-energy data (150 MeV) introduced for ENDF/B-VI Release 6. GASPR goes through all the reactions in the evaluation and adds up all these various contributions to get the net production of each of the light species.

The ENDF format assigns the MT values from 203 to 207 to represent the production of hydrogen, deuterium, tritium,  $^3\text{He}$ , and  $^4\text{He}$ , but only a few evaluators have supplied these data in the past. By using GASPR to generate these data at the PENDF stage, a number of possible inconsistencies are avoided. Therefore, when gas-production MT values are found, GASPR removes them in favor of the ones that it calculates.

When the code runs, it prints out a summary of which reactions contribute to the production of each gas. Here is an example for aluminum from ENDF/B-VII.0:

```

mf6,mt5 found

the gas production threshold is  1.8969E+06 ev

found  1038 points

pendf mt   mt203  mt204  mt205  mt206  mt207
-----
   5    ***    ***    ***    0.0    ***
  22    0.0    0.0    0.0    0.0    1.0
  28    1.0    0.0    0.0    0.0    0.0
  32    0.0    1.0    0.0    0.0    0.0
  33    0.0    0.0    1.0    0.0    0.0
  45    1.0    0.0    0.0    0.0    1.0
 103    1.0    0.0    0.0    0.0    0.0
 104    0.0    1.0    0.0    0.0    0.0
 105    0.0    0.0    1.0    0.0    0.0
 107    0.0    0.0    0.0    0.0    1.0
 108    0.0    0.0    0.0    0.0    2.0
 111    2.0    0.0    0.0    0.0    0.0
 112    1.0    0.0    0.0    0.0    1.0
 117    0.0    1.0    0.0    0.0    1.0

*** means that the yield is energy dependent

found 8 temperatures

```

## 25.2 User Input

The following input instructions were copied from the comment cards at the beginning of the GASPR source. It is always a good idea to check the cards in the current version of the program for possible changes.

Users are cautioned that only tape numbers are input. GASPR assumes that the first material read from each tape is the material to be processed. Therefore, if dealing with multi-material tapes [MODER](#) should be run to create a single material tape for input to GASPR.

```

! card 1
!   nendf      unit for endf tape
!   nin        unit for input pendf tape
!   nout       unit for output pendf tape

```

### 25.3 Coding Details

Subroutine `gaspr` is exported by module `gaspm`. The code first checks the directory in File 1 of the ENDF tape to see whether MF=6/MT=5 is present (see `mf6mt5`). If so, it reads through the MT=5 section of File 6 and saves the various light-particle yields in the array `six` using a set of pointers like 1203, 1204, and so on.

GASPR then proceeds to read through the input PENDF tape. It copies all the sections up to point where the gas production sections will be inserted to a scratch file. It then goes through all these reactions computing the direct products and the residual nucleus (with full account of the LR flags) and determines the lowest threshold for gas production. It then goes back through the scratch file again to get the energy grid for the total cross section starting at the threshold (see `egas`). It continues looping over all the reactions on the file, determining again what the direct products and residual nuclei are, and accumulating the gas production values in the array `sgas(particle,energy)`.

When all the reactions have been processed, GASPR goes back and updates the directory in MF=1/MT=451 to reflect the new reactions that have been added. It copies all the reactions on the scratch file to the output PENDF tape. It constructs new MF=3 sections for each of the gas-production reactions that was found. And then it copies the remainder of the input PENDF tape to the output file.

### 25.4 Error Messages

`error in gaspr***npend and noutp must both be ...`

The mode of the PENDF tape must not change, because many of the sections are simply copied.

`error in gaspr***too many gas production energy points.`

Should not occur, `maxg` used to allocate space for `egas(maxg)` and `sgas(5,maxg)` is determined from the input file.



## 26 NJOY Maintenance and Testing

There are several components of the NJOY Quality Assurance system: a detailed code manual (this report), a code maintenance system that keeps track of all the changes made to the code (UPD), a suite of standard test problems to verify installation, and extensive application of the code to find special cases that lead to failures.

### 26.1 Code Maintenance with UPD

NJOY2012 is maintained using a new version of the UPD code[87] that was used for earlier versions of NJOY. The code is similar in concept to the UPDATE code[123] used on Cray and CDC systems. It keeps a history of changes to a computer code that is very useful as part of a Quality Assurance (QA) program. However, UPD is much simpler than UPDATE, thereby facilitating transport from system to system. This transportability is very important, because it ensures that one set of “updates” will produce the same code for compilation on all the target systems. With other systems used in the past, modifications sometimes behaved differently on different systems.

The changes are specified with simple directives that are easy to exchange between various users of the code or other text being maintained. The history mechanism provides a capability to step back to previous versions, and it also provides for detailed explanatory comments on each revision made. UPD includes an option for conditional blocks of text or computer code that can be activated by switches in the input file; this is useful for handling computer system dependency issues. This version differs from the previous version of UPD in the following ways:

- it can construct new updates automatically from the differences between the current edited files and the files defined by the previous updates,
- it only touches files that really change in order to make the best use of code configuration tools like make,
- it has changes to help it manage other kinds of information than Fortran-77 “.f” or Fortran-90 “.f90” files,
- it no longer labels lines after column 72 in order to handle free-format text lines (up to 80 columns allowed),
- conditional blocks are more restrictive, and
- some of its operations are now controlled by command-line options.

The “**\*b**” (insert before) and “**\*comdeck**” directives from previous versions of UPD are no longer supported. The “**\*cpl**”, “**\*lst**”, “**\*noid**”, and “**\*npl**” directives are no longer needed.

The original text, such as a Fortran source, is stored in the file **src**. It is divided up into separate parts by **\*deck name.suf** lines, and each deck is designed to generate an active file **name.suf** and a corresponding listing file **name.lst**. The “name” is limited to 6 characters. The suffix could be **f90** for Fortran-90 code, **tex** for documentation, **bat** for a DOS batch file, or almost any other useful string with no more than 3 characters. Each name must be unique; that is, you cannot have **njoy.f90** and **njoy.bat** both present in the package.

A key feature of UPDATE-type programs is that each line has a label that is permanently associated with that line. In each deck, the first line after the **\*deck** line is labeled **name.2**, the next line is referred to using **name.3**, and so on. The **src** files can also contain **\*if** and **\*endif** lines as described below. These lines are numbered just like any other lines in the **src** file.

Changes to the managed text are given in an input file called **upn**. This file is divided into separate named parts by lines of the form **\*ident name**. The “name” is a string of up to six characters used to construct labels for the new lines. Each ident contains a mixture of UPD directives and new lines of text (such as Fortran statements). The directives are as follows:

**\*i ref**

Insert the lines between the **\*i** directive and the next UPD directive after the location **ref**.

**\*d ref1,ref2**

Delete the lines from **ref1** through **ref2**, and insert the lines between the **\*d** directive and the next UPD directive (if any).

**\*/ text**

Comments on the changes being made (the comments are not inserted into the code)

The line references can have the following forms:

```
name.5
name.5,7
name1.5,name2.6
```

Updates can be made on top of previous updates as long as each line referenced is currently active. Updates are numbered so that the first line after the `*ident name` line is labeled `name.2`. A new `*deck` card with associated text lines can appear in an ident, but changes to the new deck will have to use the ident name until a new resequenced version is prepared.

The ident names are arbitrary, but it is useful to establish some conventions. For example, an ident called `up11` might advance the version name of this code to “UPD 3.11”. Experimental changes, site-dependent changes, or machine-dependent changes can be given other appropriate names.

For quality-assurance reasons, it is important to label source code and output from codes with current version/date information. Codes normally contain version and date information as comments near the beginning of the source file, and they should also provide version and date strings for labeling output files. For flexibility and simplicity, UPD does not provide a standard mechanism for changing version and date inside the text being managed. It is recommended that this information be included in the ident for each update using something like the following:

```
*IDENT UP0
*D VERS.12
    CHARACTER(25)::VERS='    VERS. 2012.0 (12JAN01)'
*IDENT UP1
*/ 11 MAR 12
*/ MAKE SOME GREAT IMPROVEMENT...
*D UP0.3
    CHARACTER(25)::VERS='    VERS. 2012.1 (12MAR11)'
*I NJOY.53
....
```

UPD supports a capability for conditional blocks in the package coding that can be turned on with `*set switch` lines at the beginning of the `upn` file. This capability is useful for handling machine dependencies. Conditional blocks in the `src` or `upn` files have the following very simple form:

```
*IF SWITCH  
  LINE1  
  LINE2  
*ENDIF
```

Nesting of if-endif blocks is not allowed; the effects of nesting or “else” clauses can be achieved by choosing appropriate switch names. In NJOY2012, the following switch can be set if desired:

```
*set ctime
```

`ctime` is used for the CPU timing routine for platforms where the the Fortran `cpu_time` command is not available. If set, the code uses the UNIX `etime` call.

In order to construct modification directives manually, it is necessary to know the line labels. These labels are shown along the left-hand edge of the listings in the `.lst` files. These files provide a handy way to see what changes were made in a region of coding, and they provide a readable version of the code for a notebook. Some `.lst` files give procedure names on the right to make it easier to scan through the listings by eye. The `.lst` files should be printed using a font that allows for 104 columns on the page (8pt). Most of the time, it is not necessary to look at the `.lst` files, because the changes can be constructed automatically with the UPD “revise” option.

UPD provides the following options:

**upd history**

Write the history provided by the “\*/ comment” cards to standard output. The action string “history” can be abbreviated as “h”.

**upd extract**

Extract all the `.suf` files to the current directory. Any files that are present and not different will be left untouched so that a make run will only process the changed or new files. The action string “extract” can be abbreviated as “x”.

**upd list**

Extract `.lst` files for all the decks to the current directory. The action string “list” can be abbreviated as “l”.



**upd revise**

Find all the differences between the edited `.suf` files currently in the working directory and the corresponding files as defined by the current `upn` file. Construct the UPD directives needed to produce the changes and write them into the file `rev`. Remind the user to insert `rev` into the UPN file and to edit the new `*ident` section to provide an appropriate name, version/date information, and detailed descriptive comments. If the new UPN implies further changes to the `.suf` files, run `upd extract`. If new `.lst` files are needed, run `upd list`. The action string “revise” can be abbreviated as “r”.

**upd new**

Make a new SRC file called “new”. This command is used to start a new major version of the package. The action string “new” can be abbreviated as “n”.

To back up to an earlier version of a package, copy your `upn` file to a backup file, delete any `idents` that are not wanted, and run UPD with the “extract” option. This will only affect files that are changed by backing up, so just run `make` to recompile the modified files.

## 26.2 Code Conversion

With Fortran-90, it is no longer necessary to make many changes in NJOY to move from platform to platform. One exception is the CPU timer routine. Some version of Fortran-90 or -95 provide a “cpu time” intrinsic function, and others use a unix-like “etime” call. We have provided the “`*set ctime`” option for the latter platforms.

## 26.3 Standard Test Problems

Another important part of the NJOY revision control procedure is the set of standard test problems used to validate each new version. This kind of systematic testing is also a key part of any QA program. The NJOY test problems also act as examples in helping new users to operate the code system. Brief descriptions of the current set of test problems follow. See the following sections for details.

**Problem 1:** Process one ENDF/B-V isotope through pointwise and multigroup modules. It tests heating and damage calculations, thermal calculations for free-gas carbon and carbon bound in graphite, and multigroup averaging. The full PENDF tape is included in the test comparisons. ENDF/B-V Tape

511 and ENDF/B-III thermal tape T322 are provided in the NJOY2012 package.

**Problem 2:** Process one ENDF/B-IV isotope for a practical CCCC library. It tests resonance reconstruction, Doppler-broadening to several temperatures, self-shielded unresolved cross sections, self-shielded multigroup cross sections, and the CCCC files ISOTXS, BRKOXS, and DLAYXS. Tape 404 is provided in the NJOY2012 package.

**Problem 3:** Process photon interaction cross sections into DTF and MATXS formats. The problem tests photoatomic cross section linearization in [RECONR](#), multigroup averaging in [GAMINR](#), and output formatting in [DTFR](#) and [MATXSR](#). The DLC7E library is provided in the NJOY2012 package.

**Problem 4:** [ERRORR](#) is tested, including the calculation of covariances for fission  $\bar{\nu}$ . Tape 511 is used.

**Problem 5:** This run tests [COVR](#), including the plotting capability. Tape 511 is used. This calculation produces a large number of covariance graphs.

**Problem 6:** Includes a number of 2-D sample problems for [PLOTB](#), and one 3-D case. Plots with special characters, error bars, curve tags, and legend blocks are demonstrated.

**Problem 7:** Prepares an ACE-format library for a fissionable material.

**Problem 8:** Checks the processing of a typical ENDF/B-VI material using Reich-Moore resonances and File 6 for energy-angle distributions through PENDF production and [ACER](#) formatting.

**Problem 9:** Demonstrates the use of [LEAPR](#) to generate a scattering kernel for water. The  $\alpha$  and  $\beta$  ranges have been reduced to make the case run faster with less output.

**Problem 10:** The production of unresolved resonance probability tables for MCNP is demonstrated. [UNRESR](#) and [PURR](#) are both run to allow comparisons of the Bondarenko results, and then [ACER](#) is run to format the results for MCNP.

**Problem 11:** Demonstrates the production of a library for the WIMS reactor lattice code using  $^{238}\text{Pu}$  from ENDF/B-V. PENDF processing, [GROUPE](#), and [WIMSR](#) are all included.

**Problem 12:** Shows how to use [GASPR](#) to generate gas-production data on the PENDF file, including color Postscript plots of the resulting cross sections.

**Problem 13:** Demonstrates the “new” MCNP formats and ACE plotting.

**Problem 14:** Shows how to prepare ACE incident proton data and demonstrates the charged-particle format. The necessary evaluation is provided.

**Problem 15:** Executes [MODER](#)/[RECONR](#)/[BROADR](#)/[GROUPE](#)/[ERRORR](#) (once each for MF31, MF33 and MF34). This job illustrates NJOY's ability to process uncertainty data for  $\bar{\nu}$  (MF31), pointwise cross sections (MF33)

and angular distributions (MF4/MT2 P<sub>1</sub> moment). The “ENDF” input tape is the JENDL-3.3 <sup>238</sup>U evaluation, demonstrating that non-ENDF libraries that conform to the ENDF-6 format can be successfully processed by NJOY. This input tape is provided in the NJOY2012 package.

**Problem 16:** This test job is similar to Problem 15, but it omits the **GROUPR** module, demonstrating that uncertainty data (MF33 & MF34) processing can proceed directly from PENDF input. We also append multiple **COVR** and **VIEWR** inputs to this job to illustrate postscript plot generation for a user-specified set of cross sections (MF33) and automatic plot generation for MF34.

**Problem 17:** This is the longest running job in the NJOY test suite, involving processing of <sup>235,238</sup>U and <sup>239</sup>Pu. The job suite includes **RECONR**, **BROADR**, and **GROUPR** for each nuclide, a **MODER** job to combine the GENDF files and **ERRORR** processing that includes correlations among the isotopes. The necessary JENDL-3.3 input files are provided in the NJOY2012 package.

**Problem 18:** Execute **MODER**/**RECONR**/**BROADR**/**GROUPR**/**ERRORR**/**COVR** and **VIEWR** to process MF35 (spectrum) uncertainty data. The multigroup energy boundaries used in **GROUPR** and **ERRORR** match those used to define the uncertainty data on the input tape and allow for easy comparison of the processed output and the original data. The “ENDF” input file is a composite of ENDF/B-VII.0 <sup>252</sup>Cf decay data (for MF5 & MF35, MT18) and ENDF/B-VII.0 <sup>252</sup>Cf neutron transport data (for all other MF/MT data) and given a dummy MATN of 9999.

**Problem 19:** Tests processing of a Reich-Moore evaluation (<sup>241</sup>Pu) in an ACE file for MCNP. An RM evaluation from ORNL is provided.

**Problem 20:** Tests processing of covariance data from Reich-Moore-Limited resonance parameters using an experimental <sup>35</sup>Cl evaluation from ORNL that is included in the NJOY2012 package.

## 26.4 Test Problem 1

This problem demonstrates how to prepare data for natural carbon as given on the ENDF/B-V “Standards Tape” and one of the ENDF/B-III thermal tapes. We’ve kept on using these old input libraries for this test over all the versions of NJOY for consistency.

The input cards for NJOY are listed below in the form of a UNIX shell script. We normally run this script in a subdirectory called **test**, and the first few cards copy the ENDF general-purpose and thermal data from their normal locations in the next higher directory into the test subdirectory. Note that the data files are assigned the local names **tape20** and **tape26**. The **cat** line starts a “here” file, which continues down to the **eof** line near the end of the input. The NJOY

code is then run using this new input file, and the output file and PENDF file are saved in the names out01, and pend01 for later comparisons with previous runs.

```

echo 'NJOY Test Problem 1'
echo 'getting endf tape 511'
cp ../t511 tape20
echo 'getting thermal tape 322'
cp ../t322 tape26
echo 'running njoy'
ulimit -s 32768
cat>input <<EOF
  moder
  20 -21
  reconr
  -21 -22
  'pendf tape for c-nat from endf/b tape 511'/'
  1306 3/
  .005/
  '6-c-nat from tape 511'/'
  'processed by the njoy nuclear data processing system'/'
  'see original endf/b-v tape for details of evaluation'/'
  0/
  broadr
  -21 -22 -23
  1306 1/
  .005/
  300.
  0/
  heatr
  -21 -23 -22/
  1306 1/
  444
  thermr
  0 -22 -24
  0 1306 8 1 1 0 0 1 221 2
  300.
  .05 1.2/
  thermr
  26 -24 -23
  1065 1306 8 1 2 1 0 1 229 2

```

```

300.
.05 1.2/
groupr
-21 -23 0 -24
1306 3 3 3 3 1 1 1
'carbon in graphite'/
300
1.e10
3 1 'total'/
3 2 'elastic'/
3 4 'inelastic'/
3 51 'discrete inelastic'/
3 -68 'continued'/
3 91 'continuum inelastic'/
3 102 'n,g'/
3 103 '(n,p)'/
3 104 '(n,d)'/
3 107 '(n,a)'/
3 221 'free thermal scattering'/
3 229 'graphite inelastic thermal scattering'/
3 230 'graphite elastic thermal scattering'/
3 251 'mubar'/
3 252 'xi'/
3 253 'gamma'/
3 301 'total heat production'/
3 444 'total damage energy production'/
6 2 'elastic'/
6 51 'discrete inelastic'/
6 -68 'continued'/
6 91 'continuum inelastic'/
6 221 'free thermal scattering'/
6 229 'graphite inelastic thermal scattering'/
6 230 'graphite elastic thermal scattering'/
17 51 'inelastic gamma production'/
16 102 'capture gamma production'/
0/
0/
moder
-23 25
stop
EOF
../xnjoy<input

```

```
echo 'saving output and pendf files'
cp output out01
cp tape25 pend01
```

The first step is to run the [MODER](#) module to convert the ASCII ENDF file to binary mode. Using binary mode will often cut the cost of running NJOY jobs. [RECONR](#) is then used to linearize and unionize the cross sections (no resonance reconstruction is needed for carbon). A tolerance of 0.5% was requested for this linearization. The [BROADR](#) module is used to Doppler-broaden the carbon cross sections to 300K. It is recommended that the same thinning and reconstruction tolerances be used in [BROADR](#) as are used in [RECONR](#).

This NJOY run supplements the original ENDF data with computed values for heating, radiation damage, and thermal scattering. The call to the [HEATR](#) module requests MT444 to get the damage cross section; heating (MT301) is automatically provided. The first of the two [THERMR](#) runs generates thermal scattering data for a carbon free gas at 300K (MT221). The second [THERMR](#) run generates data for graphite (MT229). The “1” in the sixth field on the input card directs the module to use the  $S(\alpha, \beta)$  data from MT1065 on `tape26` in order to compute the inelastic scattering cross section and scattering matrix, the next field of “0” requests  $E, E', \mu$  ordering, and the following “1” directs it to compute the coherent elastic scattering cross section using the built-in parameters for graphite.

When the second [THERMR](#) run has finished, `tape23` contains the complete PENDF tape needed by [GROUPT](#). Multigroup neutron reaction and photon production cross sections are computed using the Los Alamos 30-group structure for neutrons, the Los Alamos 12-group structure for photons, and the CLAW weight function. The scattering order is  $P_3$ . Note that the long-input form is used to specify the list of reactions to be processed. Most users now prefer the automatic input option. The user has to carefully look at the reactions available on the ENDF tape and to consider the additional reactions added by [HEATR](#) and [THERMR](#). Note especially the inclusion of several gas production reactions from the ENDF tape, the thermal reactions MT221 and MT229 from the PENDF tape, and MT301 and MT444 as generated by [HEATR](#) from the PENDF tape. The output is easy to read, but remember that groups are given in the order of increasing energy.

The thermal scattering reactions must also be requested in the scattering

matrix section (MFD=6). MT230 was automatically generated by [THERMR](#) as MT229+1 when coherent elastic scattering for graphite was requested.

Photon production matrices are requested in the lines with `mfd=17` and `mfd=16`. Actually, the use of “17” to denote data given in MF13 on the ENDF tape is no longer required by [GROUPR](#).

As a last step, this problem runs [MODER](#) once more to convert the binary PENDF tape to ASCII mode.

## 26.5 Test Problem 2

The second problem supplements the first by adding resonance reconstruction and output formatting. The ENDF/B-IV material  $^{238}\text{Pu}$  (MAT1050) was originally chosen for this problem because it was freely available and its execution time was fairly small.

```
echo 'NJOY Test Problem 2'
echo 'getting endf tape 404'
cp ../t404 tape20
echo 'running njoy'
cat>input <<EOF
moder
20 -21
reconr
-21 -22
'pendf tape for pu-238 from endf/b-iv tape 404'/
1050 3/
.005/
'94-pu-238 from endf/b tape t404'/
'processed by the njoy nuclear data processing system'/
'see original endf/b-iv tape for details of evaluation'/
0/
broadr
-21 -22 -23
1050 3 0 1 0/
.005/
300. 900. 2100.
0/
moder
-23 33
unresr
```

```

-21 -23 -24
1050 3 7 1
300 900 2100
1.e10 1.e5 1.e4 1000. 100. 10. 1
0/
groupr
-21 -24 0 -25
1050 5 0 4 3 3 7 1
'94-pu-238'/
300. 900. 2100.
1.e10 1.e5 1.e4 1000. 100. 10. 1
.1 0.025 0.8208e06 1.4e06
3 1 'total'/
3 2 'elastic'/
3 16 'n2n'/
3 17 'n3n'/
3 18 'fission'/
3 102 'capture'/
3 251 'mubar'/
3 252 'xi'/
3 253 'gamma'/
3 259 '1/v'/
6 2 'elastic'/
6 16 'n2n'/
6 17 'n,3n'/
6 18 'fission'/
6 51 'discrete inelastic'/
6 -59 'continued'/
6 91 'continuum inelastic'/
0/
3 1 'total'/
3 2 'elastic'/
3 18 'fission'/
3 102 'capture'/
6 2 'elastic'/
0/
3 1 'total'/
3 2 'elastic'/
3 18 'fission'/
3 102 'capture'/
6 2 'elastic'/
0/

```



```

0/
ccccr
-25 26 27 0
1 1 't2lanl njoy'/
'ccccr tests for njoy'/
50 0 1 4 1
pu238 pu238 endfb4 ' 1050 ' 1050 10.89
1 0 50 -1
0 2.3821e02 3.3003e-11 1.7461e-12 0. 1.e10 0.0
3 6
300 900 2100
1.e5 1.e4 1000. 100. 10. 1
moder
-24 28
stop
EOF
../xnjoy<input
echo 'saving output and pendf files'
cp output out02
cp tape28 pend02

```

The [RECONR](#) input is similar to the one in Problem 1, but reading the listing file will demonstrate that [RECONR](#) added about 2700 points to the original grid in the resonance region. After a little thinning, it ended up with about 2800 resonance energy points at 0K for 0.5% reconstruction. The data from [RECONR](#) was then passed to [BROADR](#) for preparation of cross sections at 300, 900, and 2100K. An examination of the output listing shows that some thinning was possible because of the smoothing effect of Doppler broadening; the zero degree grid of 3241 points changed to 2341 points at 2100 degrees.

One of the new features of this run is the call to [UNRESR](#). The user will normally notice that unresolved-resonance parameters are available for a material by reading the introductory information on the ENDF tape, but [UNRESR](#) will return gracefully if no unresolved data are present in the evaluation. The long output from [UNRESR](#) gives a table of the self-shielded cross sections by reaction (vertical) and sigma-zero value (horizontal) for each point of the unresolved-range energy grid. The reactions are flux-weighted total, elastic, fission, capture, and current-weighted total reading from the top down. Heating, damage, and thermal cross sections were omitted for this particular problem. Therefore, the final PENDF tape is on **tape22**, the output from [UNRESR](#).

The **GROUPE** run shown here adds several new features over the one given for Problem 1. First, multiple temperatures and sigma-zero values are specified in order to get tables of self-shielded cross sections for the total, elastic, fission, and capture reactions. It is desirable to use the same sigma-zero grid in **GROUPE** that was used in **UNRESR**, although **GROUPE** will attempt to interpolate if the grids are different. Note that a section of **GROUPE** input is given for 300K with complete coverage of all the reactions, and additional sections are given for the two higher temperatures with only the self-shielded reactions included. An examination of the output listing will show that self-shielded cross sections are given for the low-energy reactions (total, elastic, fission, capture), with group index reading down and sigma-zero value reading across.

Another new feature of this input is the computation of the fission matrix (`mfd=6, mtd=18`). More complicated input may be necessary for other materials. Examination of the output listing will show that **GROUPE** discovered that the fission spectrum shape was constant over the entire energy range; therefore, it only put out a spectrum and a fission-neutron production cross section.

When the **GROUPE** run is complete, the final GENDF tape will be found on `tape25`. This file is used as input to the **CCCCR** module to produce ISOTXS and BRKOXS files for  $^{238}\text{Pu}$ .

## 26.6 Test Problem 3

This problem demonstrates the use of **GAMINR** to prepare photon interaction (or photoatomic) cross sections. It also demonstrates **DTFR**, including plotting, and **MATXS**. For the sake of continuity, this test problem uses a rather old version of the photon interaction files called DLC7E. The MF23 and MF27 parts of these data are written on two separate files. Later libraries have everything on a single file.

```
echo 'NJOY Test Problem 3'
echo 'getting photoatomic tape gam23'
cp ../gam23 tape30
echo 'getting photoatomic tape gam27'
cp ../gam27 tape32
echo 'running njoy'
cat>input <<EOF
  reconr
  30 31
'pendf tape for photon interaction cross sections from dlc7e'/'
```

```

1 1 0
.001/
'1-hydrogen'/
92 1 0
.001/
'92-uranium'/
0/
gaminr
32 31 0 33
1 3 3 4 1
'12 group photon interaction library'/
-1 0/
92
-1 0/
0/
dtfr
33 34 31 36
1 1 0
5 12 4 5 16 1 0
'pheat'
1 621 1
0/
'h' 1 1 0./
'u' 92 1 0./
/
matxsr
0 33 35/
1 't2lanl njoy'/
1 1 1 2
'12-group photon interaction library'/
'g'
12
'gscat'/
1
1
'h' 1 1
'u' 92 92
viewr
36 37/
stop
EOF
../xnjoy<input

```

```
echo 'saving output and plot files'
cp output out03
cp tape37 plot03
```

This run starts with an application of the [RECONR](#) module to linearize and unionize the File 23 cross sections. Of course, there is no resonance reconstruction required here. This [RECONR](#) run demonstrates the use of a material loop; both hydrogen and uranium are processed in one run. [GAMINR](#) is then used to prepare the multigroup photon interaction cross sections, including heating; this run also uses a multimaterial loop. The LANL 12-group photon structure is used. The GENDF tape ([tape33](#)) is processed into two completely different library formats. First, [DTFR](#) is called. This is a rather old output module, but it is still useful for some purposes. For one thing, it automatically produces plots of the multigroup data overlayed with the PENDF data. Examples of the plots are given in the [DTFR](#) chapter of this manual. The MATXS output is more useful, because it can be used in a much more flexible way by the TRANSX code.

## 26.7 Test Problem 4

This problem illustrates several aspects of the calculation of covariances (uncertainties) of multigroup data using [ERRORR](#). The first [ERRORR](#) problem produces, on unit 23, a file of multigroup cross section covariances ([mfcov=33](#)) for all reactions present ([iread=0](#)) in File 33 for  $^{235}\text{U}$ . The group structure employed is identical to the energy grid selected by the evaluator ([ign=19](#)); however, no covariances are produced for cross sections below 1 eV or above 1 keV. The second [ERRORR](#) run adds to the above results a second data set containing multigroup  $\bar{\nu}$  covariances. Note that the use of [mfcov=31](#) dictates that a GENDF file be produced ([ngout=24](#)) prior to the start of [ERRORR](#). In the  $\bar{\nu}$  run, a user-defined group structure is employed ([ign=1](#)).

```
echo 'NJOY Test Problem 4'
echo 'getting endf tape 511'
cp ../t511 tape20
echo 'running njoy...'
cat>input <<EOF
moder
20 -21
```

```

reconr
-21 -22
'u-235 10% pendf for errorr test problem from t511'/
1395/
.10/
0/
errorr
-21 -22 0 23 0/
1395 19 3 1 1/
0 0./
0 33/
1
1.e0 1.e3
groupr
-21 -22 0 24
1395 3 0 3 0 1 1 1
'u-235 multigroup nubar calculation'/
0.
1.e10
3 452 'total nubar'/
0/
0/
errorr
-21 0 24 25 23/
1395 1 2 1 1/
1 0
0 31/
7
1.e0 1.e1 1.e2 1.e3 1.e4 1.e5 1.e6 1.e7
stop
EOF
../xnjoy<input
echo 'saving output'
cp output out04

```

## 26.8 Test Problem 5

This short problem produces multigroup covariances for carbon, again using `ign=19`, but here all cross sections from `1E-5` to `2E7` are treated. The [COVR](#) module reads the binary output file from [ERRORR](#) and produces publication-

quality plots of all reactions for which covariance data exist. This simple problem setup could be used with only a few simple changes for any nuclide, in order to take a quick look at the contents of the covariance files. For applications where the resonance region is of interest, it is necessary to replace the second [MODER](#) step with a resonance reconstruction step using [RECONR](#), as in the previous example.

```
echo 'NJOY Test Problem 5'
echo 'getting endf tape 511'
cp ../t511 tape30
echo 'running njoy...'
cat>input <<EOF
moder
30 -31
moder
-31 -32
errorr
-31 -32 0 33/
1306 19 2 1/
0 0
0 33/
1
1e-5 2e7/
covr
33 0 34/
1/
/
/
1306/
viewr
34 35/
stop
EOF
../xnjoy<input
echo 'saving output and plot files'
cp output out05
cp tape35 plot05
```

## 26.9 Test Problem 6

This test problem demonstrates and tests a number of different kinds of plots using data from ENDF/B-V Tape 511 (the “Standards Tape”). The graphs produced and a detailed discussion of the input cards will be found in the [PLOT](#) chapter of this manual.

```
echo 'NJOY Test Problem 6'
echo 'getting endf tape 511'
cp ../t511 tape30
echo 'running njoy'
cat>input <<EOF
plotr
31/
/
1/
'<endf/b-v carbon'/
'<t>otal <c>ross <s>ection'/
4/
1e3 2e7/
/
.5 10/
/
5 30 1306 3 1/
/
1/
'<endf/b-v carbon'/
'(n,la>) with fake data'/
1 0 2 1 1.3e7 .32/
/
/
/
/
5 30 1306 3 107/
/
'<endf/b-v mat1306'/
2/
0/
-1 0/
'<s>mith & <s>mith 1914'/
0/
```

```

1.1e7 .08 .05 .05/
1.2e7 .10 .05 .05/
1.3e7 .09 .04 .04/
1.4e7 .08 .03 .03/
/
3/
0/
-1 2/
'<b>lack & <b>lue 2008'/
0/
1.15e7 .07 .02 0. .2e6 0./
1.25e7 .11 .02 0. .2e6 0./
1.35e7 .08 .015 0. .2e6 0./
1.45e7 .075 .01 0. .2e6 0./
/
1/
'<endf/b-v carbon'/
'<e>lastic <mf4>'/
-1 2/
/
/
/
/
/
/
5 30 1306 4 2/
/
1/
'<endf/b-v l>i-6'/
'(n,2n)]a >neutron distribution'/
-1 2/
/
/
0 12e6 2e6/
/
/
/
5 30 1303 5 24/
/
1/
'<endf/b-v l>i-6'/
'(n,2n)]a >neutron spectra vs <E>'/

```



```

4 0 2 2/
10. 2.e7/
/
1e-11 1e-6/
'<c>ross <s>ection (barns/e<v>)' /
5 30 1303 5 24 0. 12/
/
'10 <m>e<v>' /
1e3 2e-11 1e2/
2/
5 30 1303 5 24 0. 16/
/
'14 <m>e<v>' /
1e4 2e-10 2e3/
3/
5 30 1303 5 24 0. 20/
/
'20 <m>e<v>' /
1e5 2e-9 4e4/
99/
viewr
31 32/
stop
EOF
../xnjoy<input
echo 'saving plot file'
cp tape32 plot06

```

### 26.10 Test Problem 7

This test problem demonstrates the preparation of ACE format libraries for the MCNP continuous-energy Monte Carlo code. The material selected for processing was  $^{235}\text{U}$  from ENDF/B-V. The [GROUPE](#) run is included to make a 30x20 photon production matrix for [ACER](#). This is an obsolete method for handling photon production for MCNP – nowadays, people use the “Detailed Photon Production” option. This old test problem is kept for consistency with the testing in previous versions of NJOY.

```

echo 'NJOY Test Problem 7'

```

```
echo 'getting endf tape 511'
cp ../t511 tape20
echo 'running njoy...'
cat>input <<EOF
moder
20 -21
reconr
-21 -22
'pendf tape for u-235 from endf/b-v tape 511' /
1395 3 /
.005 /
'92-u-235 from endf/b-v tape 511 ' /
'processed by the njoy nuclear data processing system' /
'see original endf/b-v tape for details of evaluation' /
0 /
broadr
-21 -22 -23
1395 1 0 1 0 /
.005 /
300.
0 /
heatr
-21 -23 -24/
1395/
moder
-24 28
groupr
-21 -24 0 -25
1395 3 2 9 0 1 1 1 /
'u-235 from tape 511' /
300.
1.0e10
16 /
0 /
0 /
acer
-21 -24 -25 26 27 /
1/
'njoy test problem 7'/
1395 300. /
0/
/
```

```

    stop
EOF
../xnjoy<input
echo 'saving output, pendf, and ace files'
cp output out07
cp tape26 ace07
cp tape28 pend07

```

### 26.11 Test Problem 8

This problem was added to the NJOY testing suite to verify the processing of a typical ENDF/B-VI material with Reich-Moore resonances and File 6 energy-angle distributions. The  $^{61}\text{Ni}$  evaluation is from ORNL, and the file is included in the NJOY package. The normal processing sequence is used. The [GROUPE](#) run is included to provide additional output for comparing to standard results or to older testing results. An [ACER](#) run is also included.

```

echo 'NJOY Test Problem 8'
echo 'getting endf tape for ni-61'
cp ../eni61 tape20
cat>input <<EOF
  moder
  20 -21
  reconr
  -21 -22
  'pendf tape for endf/b-vi.1 28-ni-61a'/'
  2834 1 0 /
  .01/
  '28-ni-61a from endf/b-vi.1 t124 (hetrick,fu;ornl)'/
  0/
  broadr
  -21 -22 -23
  2834 1/
  .01/
  300/
  0/
  heatr
  -21 -23 -24/
  2834 6 0 1 0 2/
  302 303 304 402 443 444

```

```

moder
-24 28
groupr
-21 -24 0 -22
2834 3 3 9 4 1 1 1
'ni61a endf/b-vi.1 30x12'/
300
1e10
3/
3 251 'mubar'/
3 252 'xi'/
3 253 'gamma'/
3 259 '1/v'/
6/
16/
0/
0/
acer
-21 -24 0 25 26
1 1 1/
'28-ni-61a from endf-vi.1'/
2834 300./
0/
/
stop
EOF
echo "running njoy"
../xnjoy<input
echo 'saving output and pendf files'
cp output out08
cp tape28 pend08

```

### 26.12 Test Problem 9

This example demonstrates and tests the use of the [LEAPR](#) module to generate thermal scattering data. The material is  $^1\text{H}$  to be used with  $^{16}\text{O}$  for a problem requiring water. The run starts out with the familiar use of [RECONR](#) and [BROADR](#) to construct the basic cross sections at 296K. [LEAPR](#) is then used to generate an  $S(\alpha, \beta)$  scattering kernel on **tape24**. Shortened  $\alpha$  and  $\beta$  grids are used for compactness. The [THERMR](#) module is then run using **tape24** as input

to add the thermal scattering cross section and scattering data to the PENDF tape on **tape23**. The new PENDF tape is on **tape25**, and it can be used as input to **GROUPR** for a multigroup library or to **ACER** for an MCNP Monte Carlo library.

```

echo 'NJOY Test Problem 9'
echo 'getting endf tape 511'
cp ../t511 tape20
echo 'running njoy'
cat>input <<EOF
  moder
  20 -21
  reconr
  -21 -22
  'pendf tape for h-1 from endf/b tape 511'/
  1301 3/
  .005/
  '1-h-1 from tape 511'/
  'processed by the njoy nuclear data processing system'/
  'see original endf/b-v tape for details of evaluation'/
  0/
  broadr
  -21 -22 -23
  1301 1/
  .005/
  296.
  0/
  leapr
  24
  'h in h2o, shortened endf model'/
  1 1/
  101 1001./
  0.99917 20.449 2 0 0/
  1 1. 15.85316 3.8883 1/
  65 75 1/
  .01008 .015 .0252 .033 0.050406
  .0756 0.100812 0.151218 0.201624 0.252030 0.302436 0.352842
  0.403248 0.453654 0.504060 0.554466 0.609711 0.670259 0.736623
  0.809349 0.889061 0.976435 1.072130 1.177080 1.292110 1.418220
  1.556330 1.707750 1.873790 2.055660 2.255060 2.473520 2.712950
  2.975460 3.263080 3.578320 3.923900 4.302660 4.717700 5.172560

```

```

5.671180 6.217580 6.816500 7.472890 8.192280 8.980730 9.844890
10.79190 11.83030 12.96740 14.21450 15.58150 17.07960 18.72080
20.52030 22.49220 24.65260 27.02160 29.61750 32.46250 35.58160
38.99910 42.74530 46.85030 50.0/
0.000000 0.006375 0.012750 0.025500 0.038250 0.051000 0.065750
.0806495 0.120974 0.161299 0.241949 0.322598 0.403248 0.483897
0.564547 0.645197 0.725846 0.806496 0.887145 0.967795 1.048440
1.129090 1.209740 1.290390 1.371040 1.451690 1.532340 1.612990
1.693640 1.774290 1.854940 1.935590 2.016240 2.096890 2.177540
2.258190 2.338840 2.419490 2.500140 2.580790 2.669500 2.767090
2.874450 2.992500 3.122350 3.265300 3.422470 3.595360 3.785490
3.994670 4.224730 4.477870 4.756310 5.062580 5.399390 5.769970
6.177660 6.626070 7.119240 7.661810 8.258620 8.915110 9.637220
10.43200 11.30510 12.26680 13.32430 14.48670 15.76600 17.17330
18.72180 20.42450 22.29760 24.35720 25.0/
296/
.00255 67/
  0 .0005 .001 .002 .0035 .005 .0075 .01 .013 .0165 .02 .0245
  .029 .034 .0395 .045 .0506 .0562 .0622 .0686 .075 .083 .091
  .099 .107 .115 .1197 .1214 .1218 .1195 .1125 .1065 .1005 .09542
  .09126 .0871 .0839 .0807 .07798 .07574 .0735 .07162 .06974
  .06804 .06652 .065 .0634 .0618 .06022 .05866 .0571 .05586
  .05462 .0535 .0525 .0515 .05042 .04934 .04822 .04706 .0459
  .04478 .04366 .04288 .04244 .042 0./
0.055556 0. 0.444444 0./ for diffusion, use 120. for second number
2/
.205 .48/
.166667 .333333/
' h(h2o) thermal scattering '/
' '/
' temperatures = 296 deg k. '/
' '/
' shortened version of the endf/b-vi.4 evaluation for '/
' hydrogen in water. the energy transfer is limited to '/
' 0.625 ev. this is only for njoy testing, not for '/
' real applications. '/
/
thermr
24 -23 -25
101 1301 8 1 2 1 0 1 222 2
296.
.05 .625

```

```

stop
EOF
../xnjoy<input
echo 'saving output and pendf files'
cp output out09
cp tape24 pend09

```

### 26.13 Test Problem 10

This case was constructed to demonstrate unresolved resonance range processing for MCNP libraries. It starts with linearization, unionization, resonance reconstruction, and Doppler broadening to 300, 900, and 2100K. The [UNRESR](#) module is run to generate one version of the self-shielded unresolved range cross sections on MF=2/MT152 to [tape24](#) for the three temperatures and seven values of the background cross section  $\sigma_0$ . Then the [PURR](#) module is run to generate probability tables on MF=2/MT153 of the PENDF tape and an alternate set of self-shielded cross sections. Actually, once [PURR](#) has run, the MT152 values for [UNRESR](#) are overwritten with the [PURR](#) values. Both methods are provided on this run to allow them to be compared. Finally, [ACER](#) is run to format the data for MCNP.

```

echo 'NJOY Test Problem 10'
echo 'getting endf tape 404'
cp ../t404 tape20
echo 'running njoy'
cat>input <<EOF
  moder
  20 -21
  reconr
  -21 -22
  'pendf tape for pu-238 from endf/b-iv tape 404'/
  1050 3/
  .005/
  '94-pu-238 from endf/b tape t404'/
  'processed by the njoy nuclear data processing system'/
  'see original endf/b-iv tape for details of evaluation'/
  0/
  broadr
  -21 -22 -23

```

```

1050 3 0 1 0/
.005/
300. 900. 2100.
0/
unresr
-21 -23 -24
1050 3 7 1
300 900 2100
1.e10 1.e5 1.e4 1000. 100. 10. 1
0/
purr
-21 -24 -25
1050 3 7 20 4/
300 900 2100
1.e10 1.e5 1.e4 1000. 100. 10. 1
0/
acer
-21 -25 0 26 27/
1/
'njoy test problem 10'/
1050 300./
/
/
moder
-25 28
stop
EOF
../xnjoy<input
echo 'saving output, ace, and pendf files'
cp output out10
cp tape26 ace10
cp tape28 pend10

```

### 26.14 Test Problem 11

This case demonstrates and tests the construction of a multigroup library for the WIMS reactor physics code. Here, we will need thermal data, so the [THERMR](#) module is included in the processing path. Once the [GROUPR](#) module has been run, [WIMSR](#) is used for the final formatting.



```
echo 'NJOY Test Problem 11'
echo 'getting endf tape 404'
cp ../t404 tape20
echo 'running njoy'
cat>input <<EOF
  moder
  20 -21
  reconr
  -21 -22
  'pendf tape for pu-238 from endf/b-iv tape 404' /
  1050 3 /
  .005 /
  '94-pu-238 from endf/b tape t404' /
  'processed by the njoy nuclear data processing system' /
  'see original endf/b-iv tape for details of evaluation' /
  0 /
  broadr
  -21 -22 -23
  1050 3 0 1 0 /
  .005 /
  300. 900. 2100.
  0 /
  unresr
  -21 -23 -24
  1050 3 7 1
  300 900 2100
  1.e10 1.e5 1.e4 1000. 100. 10. 1
  0 /
  thermr
  0 -24 -25
  0 1050 8 3 1 0 0 1 221 0
  300. 900. 2100.
  .05 4.2
  groupr
  -21 -25 0 -26
  1050 9 0 5 3 3 7 1
  '94-pu-238' /
  300. 900. 2100.
  1.e10 1.e5 1.e4 1000. 100. 10. 1
  3 1 'total' /
```

```

3 2 'elastic'/
3 16 'n2n'/
3 17 'n3n'/
3 18 'fission'/
3 102 'capture'/
3 221 'free gas thermal'/
6 2 'elastic'/
6 16 'n2n'/
6 17 'n,3n'/
6 18 'fission'/
6 51 'discrete inelastic'/
6 -59 'continued'/
6 91 'continuum inelastic'/
6 221 'free gas thermal'/
0/
3 1 'total'/
3 2 'elastic'/
3 18 'fission'/
3 102 'capture'/
3 221 'free gas thermal'/
6 2 'elastic'/
6 221 'free gas thermal'/
0/
3 1 'total'/
3 2 'elastic'/
3 18 'fission'/
3 102 'capture'/
3 221 'free gas thermal'/
6 2 'elastic'/
6 221 'free gas thermal'/
0/
0/
wimsr
-26 27
1/
1050 1 1050./
3 7 1e10 3 10.890 221 0/
1. 1. 1. 1. 1. 1. 1. 1. 1. 1. 1. 1. 1./
stop
EOF
../xnjoy<input
echo 'saving output and wims files'

```

```
cp output out11
cp tape27 wims11
```

### 26.15 Test Problem 12

This case was constructed to demonstrate the methods for adding gas production to a processing stream. The [GASPR](#) module doesn't require any special input. We then use the [PLOT](#)R and [VIEW](#)R modules to graph the gas production reactions using color Postscript. The gas production reactions have special MT values in the range 203 to 207. They can also be fed into GROUPT for multigroup applications and [ACER](#) for MCNP Monte Carlo libraries.

```
echo 'NJOY Test Problem 12'
echo 'getting endf tape for ni-61'
cp ../eni61 tape20
cat>input <<EOF
  reconr
  20 21
  'pendf tape for endf/b-vi.1 28-ni-61a' /
  2834 1 0 /
  .01/
  '28-ni-61a from endf/b-vi.1 t124 (hetrick,fu;ornl)' /
  0/
  gaspr
  20 21 22
  plotr
  23/
  1 1 .3 2/
  1 3/
  '<endf/b-vi n>i-61' /
  '<r>esonance <c>ross <s>ections' /
  2 0 3 1 23e3 5e2/
  .5e4 3e4 .5e4/
  /
  1e-3 1e3/
  /
  6 22 2834 3 2/
  0 0 0 3 2/
  'elastic' /
  2/
```

```

6 22 2834 3 102/
0 0 0 1 2/
'capture'/
1 7/
'<endf/b-vi n>i-61'/
'<g>as <p>roduction'/
1 0 3 1/
0 2e7 5e6/
/
/
/
6 22 2834 3 203 0./
0 0 0 1 2/
'hydrogen'/
2/
6 22 2834 3 207 0./
0 0 0 2 2/
'helium-4'/
99/
viewr
23 24
stop
EOF
echo "running njoy"
../xnjoy<input
echo 'saving output, pendf, and plot files'
cp output out12
cp tape22 pend12
cp tape24 plot12

```

### 26.16 Test Problem 13

This test problem was constructed when Reich-Moore resonance processing and File 6 energy-angle distributions began to be used in ENDF/B files. The sample evaluation for  $^{61}\text{Ni}$  was generated at ORNL, and it is provided in the NJOY package. Note that [HEATR](#) and [GASPR](#) are included to satisfy the expectations for a complete ACE library. Two [ACER](#) runs are used here. The first one generates an ACE library on **tape26**. The second one reads in this new ACE file, does a series of consistency checks, provides an eye-readable listing, and makes a large set of color Postscript plots showing the various reaction cross

sections and distributions. This is a part of the QA procedure for ACE libraries. The file `tape36` output by [VIEWR](#) is the plot file in Postscript format.

```

echo 'NJOY Test Problem 13'
echo 'getting endf tape for ni-61'
cp ../eni61 tape20
cat>input <<EOF
  moder
  20 -21
  reconr
  -21 -22
  'pendf tape for endf/b-vi.1 28-ni-61a'/'
  2834 1 0 /
  .01/
  '28-ni-61a from endf/b-vi.1 t124 (hetrick,fu;ornl)'/
  0/
  broadr
  -21 -22 -23
  2834 1/
  .01/
  300/
  0/
  heatr
  -21 -23 -24/
  2834 6 0 1 0 2/
  302 303 304 402 443 444
  gaspr
  -21 -24 -25
  moder
  -25 28
  acer
  -21 -25 0 26 27
  1 0 1/
  '28-ni-61a endf-vi.1 njoy99'/'
  2834 300./
  /
  /
  acer
  0 26 33 34 35
  7 1 2/
  '28-ni-61a endf-vi.1 njoy99'/'

```

```

viewr
33 36/
stop
EOF
echo "running njoy"
../xnjoy<input
echo 'saving output, pendf, ace, and plot files'
cp output out13
cp tape28 pend13
cp tape26 ace13
cp tape36 plot13

```

### 26.17 Test Problem 14

This case demonstrates and tests processing for incident charged particles, specifically, protons on  $^{14}\text{N}$ . It is not necessary to run reconstruction or Doppler broadening, so the evaluation is read directly into [ACER](#). A copy of the ENDF/B file is used as the PENDF input. Once again, two [ACER](#) runs are used: one to generate the ACE file, and one to do the checks and make color Postscript plots.

```

echo 'NJOY Test Problem 14'
echo 'getting endf tape for p+n14'
cp ../epn14 tape20
cp tape20 tape21
cat>input <<EOF
acer
20 21 0 31 32
1 0 1/
'proton + 7-n-14 apt la150 njoy99 mcnp' /
725 0./
/
/
acer
0 31 33 34 35
7 1 2/
'proton + 7-n-14 apt la150 njoy99 mcnp' /
viewr
33 36/
stop

```

```

EOF
echo "running njoy"
../xnjoy<input
echo 'saving output, ace, and plot files'
cp output out14
cp tape31 ace14
cp tape36 plot14

```

### 26.18 Test Problem 15

This test problem exercises the [ERRORR](#) routines used to process MF31 ( $\bar{\nu}$ ), MF33 (cross sections) and MF34 (MF4/MT2 P<sub>1</sub> component only) uncertainty data. We use the JENDL-3.3 <sup>238</sup>U evaluation for input, demonstrating that non-ENDF/B libraries that conform to the ENDF-6 format can be processed by NJOY. The job includes a standard [MODER](#)/[RECONR](#)/[BROADR](#)/[GROUPR](#) sequence to create Doppler broadened PENDF and group-averaged GENDF tapes followed by a sequence of [ERRORR](#) jobs; one for each MF value to be processed. Use of [GROUPR](#) to process  $\bar{\nu}$  (MF=3, MT=whatever MF=31 sections are present) is a pre-requisite for MF=31 processing with [ERRORR](#). The first [ERRORR](#) job processes MF=31 data (specified via the second item on the third input line (corresponding to card 7 in the [ERRORR](#) input description)). The first input line specifies the various input and output files; [tape21](#) for a binary ENDF tape, [tape91](#) for a GENDF tape and [tape25](#) for the [ERRORR](#) output tape in this instance. The material number, multigroup energy structure and weighting function options are specified on the second input line. This input line could have been terminated here, as the fourth and fifth items, related to printing and selection of relative rather than absolute covariances, are given their default values. Users will notice that the group structure and weighting function options differ from those specified in the [GROUPR](#) input preceding [ERRORR](#). NJOY will not flag this as an error, but it is not recommended practice. The third input card (corresponding to card 7 in the [ERRORR](#) input, since `ngout.ne.0`, and we are dealing with ENDF-6 format data), specifies `iread=0` meaning that all MF=31 (the second item on this input card) MT values found on the ENDF input tape will be processed. The remaining items on this card are not germane to MF=31 processing and could have been omitted. Additional [ERRORR](#) jobs process the cross section uncertainties (MF=33) and elastic scattering Legendre (P<sub>1</sub> only) moment uncertainty (MF=34) using a combination

of ENDF and GENDF input tapes. Separate output files (`tape25`, `tape26` and `tape27`) are created with these three `ERRORR` executions. These are ASCII files that may be viewed in any text editor or saved for use in a subsequent NJOY job, such as `COVR`/`VIEWR` for plot generation.

```

echo 'NJOY Test Problem 15'
echo 'getting JENDL-3.3 U-238'
cp ../J33U238 tape20
echo 'running njoy'
ulimit -s 32768
cat>input <<EOF
moder
  20 -21 /
reconr
  -21 -22 /
  'processing of U-238 of jendl-3.3.'
9237 0 0 /
0.001 /
0 /
broadr
  -21 -22 -23 /
9237 1 0 0 0 /
0.001 /
300. /
0 /
groupr
  -21 -23 0 91 /
9237 3 0 2 1 1 1 1 /
'test'
300. /
1.0e10 /
3 /
3 251 'mubar' /
3 252 'xi' /
3 452 'nu' /
3 455 'nu' /
3 456 'nu' /
5 18 'xi' /
0 /
0 /
--

```



```

-- process mf31
errorr
  -21 0 91 25 0 0 /
9237 3 6 1 1 /
1 300./
0 31 1 1 -1 /
--
-- process mf33
errorr
  -21 0 91 26 0 0 /
9237 3 6 1 1 /
1 300./
0 33 1 1 -1 /
--
-- process mf34
errorr
  -21 0 91 27 0 0 /
9237 3 6 1 1 /
1 300./
0 34 1 1 -1 /
--
-- make mf31 plot file
covr
  25 0 35 /
  1 /
  /
  /
  9237 /
--
-- make mf33 plot file.
covr
  26 0 36 /
  1 /
  /
  1 14 /
9237 1 9237 1 /
9237 1 9237 2 /
9237 2 9237 2 /
9237 2 9237 4 /
9237 2 9237 16 /
9237 2 9237 17 /
9237 2 9237 18 /

```

```

9237  2  9237 102 /
9237  4  9237  4 /
9237 16  9237 16 /
9237 17  9237 17 /
9237 18  9237 18 /
9237 18  9237 102 /
9237 102  9237 102 /
--
-- make mf34 plot file.
covr
27 0 37 /
1 /
/
/
9237 /
--
-- make mf31 postscript file.
viewr
35 45 /
--
-- make mf33 postscript file.
viewr
36 46 /
--
-- make mf34 postscript file.
viewr
37 47 /
stop
EOF
../xnjoy<input
echo 'saving output file'
cp output out15
cp tape45 plot15-31
cp tape46 plot15-33
cp tape47 plot15-34

```

### 26.19 Test Problem 16

This test problem is similar to test 15, but we omit [GROUPE](#) and only process cross section (MF=33) and  $P_1$  moment (MF=34) uncertainties with [ERRORR](#).

As stated in the previous problem, **GROU**PR execution is required when using **ERRORR** to process MF=31 data but, as shown here, is not required to process MF=33 or MF=34 uncertainty data. We also append **COVR** and **VIEWR** to this job to demonstrate Postscript plot generation. The first **COVR** job reads **tape26**, the **ERRORR** MF=33 processed output tape and will create **tape36** containing the appropriate plot commands that **VIEWR** uses to create a Postscript formatted **tape46**. Additional **COVR** input includes **icolor=1** (card 2) to specify color plots, and a user-specified number of plots, **ncase=14**, on the third (card 3a) input card. This is followed by 14 occurrences of card 4. The second **COVR** job reads the **ERRORR** output tape created from MF=34 processing and creates all possible plots as we use the default input values for the variables defined by the third input card. In reality there will only be a single plot since MF=34 processing is only performed for the elastic scattering (MF=4/MT=2)  $P_1$  Legendre moment. The output of this **COVR** job, **tape37** is fed to **VIEWR**, which generates a Postscript formatted file, **tape47**.

```

echo 'NJOY Test Problem 16'
echo 'getting JENDL-3.3 U-238'
cp ../J33U238 tape20
echo 'running njoy'
ulimit -s 32768
cat>input <<EOF
moder
20 -21 /
reconr
-21 -22 /
'processing of U-238 of jendl-3.3.'
9237 0 0 /
0.001 /
0 /
broadr
-21 -22 -23 /
9237 1 0 0 0 /
0.001 /
300. /
0 /
--
-- process mf33 with internal group averaging
-- since there is no groupr input tape
errorr

```

```

-21 -23 0 26 0 0 /
9237 3 6 1 1 /
0 300. /
0 33 1 /
--
-- process mf34
errorr
-21 -23 0 27 0 0 /
9237 3 6 1 1 /
0 300. /
0 34 1 1 /
--
-- make mf33 plot file.
covr
26 0 36 /
1 /
/
1 14 /
9237 1 9237 1 /
9237 1 9237 2 /
9237 2 9237 2 /
9237 2 9237 4 /
9237 2 9237 16 /
9237 2 9237 17 /
9237 2 9237 18 /
9237 2 9237 102 /
9237 4 9237 4 /
9237 16 9237 16 /
9237 17 9237 17 /
9237 18 9237 18 /
9237 18 9237 102 /
9237 102 9237 102 /
--
-- make mf34 plot file.
covr
27 0 37 /
1 /
/
/
9237 /
--
-- make mf33 postscript file.

```

```

viewr
 36 46 /
--
-- make mf34 postscript file.
viewr
 37 47 /
stop
EOF
../xnjoy<input
echo 'saving output file'
cp output out16
cp tape46 plot16-33
cp tape47 plot16-34

```

## 26.20 Test Problem 17

Test problem 17 is the longest running job in the NJOY test suite, involving processing of  $^{235,238}\text{U}$  and  $^{239}\text{Pu}$ . We start with a standard sequence of [RECONR](#)/[BROADR](#)/[GROUPR](#) for each of these nuclides. Three separate GENDF files are created ([tape91](#), [tape92](#), and [tape93](#)) by these [GROUPR](#) executions, followed by a [MODER](#) job that merges the three GENDF files onto a single GENDF tape. [MODER](#)s card 1 [nin=2](#) option is specified, followed by multiple card 3 input to accomplish this merge. [ERRORR](#) begins with the standard input and output tape specifications on card 1 and the material number, multigroup and weighting function specification on card 2. As we've included an GENDF tape as part of the input and we're dealing with ENDF-6 formatted data, the third input card corresponds to card 7 in the [ERRORR](#) input description. Here we specify [iread=2](#), indicating that additional MAT/MT data are to be included over those found on the original ENDF input ([tape21](#)). This additional input follows on the fourth and fifth input cards, corresponding to repeated use of card 10 from the [ERRORR](#) input description. Based upon this additional input, the effect of  $^{235}\text{U}$  ([mat=9228](#)) and  $^{239}\text{Pu}$  ([mat=9437](#)) MT=18 uncertainties are included when processing  $^{238}\text{U}$  ([mat=9237](#)) uncertainties.

```

echo 'NJOY Test Problem 17'
echo 'getting JENDL-3.3 U-238'
cp ../J33U238 tape21
echo 'getting JENDL-3.3 U-235'

```

```
cp ../J33U235 tape22
echo 'getting JENDL-3.3 Pu-239'
cp ../J33Pu239 tape23
echo 'running njoy'
ulimit -s 32768
cat>input <<EOF
  reconr
  21 41 /
  'processing jendl-3.3 238u.' /
  9237 0 0 /
  0.001 /
  0 /
  broadr
  21 41 31 /
  9237 1 0 0 0 /
  0.001 /
  300. /
  0 /
  reconr
  22 42 /
  'processing jendl-3.3 235u.' /
  9228 0 0 /
  0.001 /
  0 /
  broadr
  22 42 32 /
  9228 1 0 0 0 /
  0.001 /
  300. /
  0 /
  reconr
  23 43 /
  'processing jendl-3.3 239pu.' /
  9437 0 0 /
  0.001 /
  0 /
  broadr
  23 43 33 /
  9437 1 0 0 0 /
  0.001 /
  300. /
  0 /
```

```

groupr
21 31 0 91 /
9237 3 0 6 1 1 1 0 /
'u-238' /
300. /
1.0e10 /
3 /
3 251 'mubar' /
3 252 'xi' /
3 452 'nu' /
3 455 'nu' /
3 456 'nu' /
5 18 'xi' /
0 /
0 /
groupr
22 32 0 92 /
9228 3 0 6 1 1 1 0 /
'u-235' /
300. /
1.0e10 /
3 /
0 /
0 /
groupr
23 33 0 93 /
9437 3 0 6 1 1 1 0 /
'pu-239' /
300. /
1.0e10 /
3 /
0 /
0 /
moder
2 99 /
'merge u235, u-238 and pu-239' /
92 9228 /
91 9237 /
93 9437 /
0 /
errorr
21 0 99 26 0 /

```

```

9237 3 6 1 /
1 300./
2 33 1 1 -1 /
9228 18 /
9437 18 /
0 /
stop
EOF
../xnjoy<input
echo 'saving output file'
cp output out17

```

## 26.21 Test Problem 18

This test problem exercises the [ERRORR](#) spectrum uncertainty processing routines followed by a [COVR/VIEWR](#) job to produce plots of these data. There are no spectrum uncertainty data in the ENDF/B-VII.0 neutron transport files, but such data are provided for the spontaneous fission of  $^{252}\text{Cf}$  in the ENDF/B-VII.0 decay file. Therefore a fictitious transport file has been created containing MF5 and MF35, MT18 data from the decay file with the remaining MF/MT data coming from the transport file. This tape serves as the ENDF input to a [MODER/RECONR/ BROADR/GROUPR/ ERRORR/COVR/ VIEWR](#) job.

This job could have started at [GROUPR](#) with MF5/MT18 processing. The multigroup user input mimics the energy structure appearing in the MF35/MT18 input tape and was chosen to allow easy comparison of the final calculated uncertainty with the corresponding data provided in MF1/MT451 by the evaluator. The [GROUPR](#) GENDF output file resides on `tape91` which along with the original ENDF input (`tape20`) are input to [ERRORR](#). The [ERRORR](#) output will go on `tape28`. This tape will contain the results of processing MATN 9999 for the user-specified multigroup structure with no weighting function (based upon the `ign=1`, `iwt=2` options specified on card 2). The third line in the [ERRORR](#) input (really card 7 in the [ERRORR](#) input description) specifies processing MF35 data for an incident neutron energy of 1.23 MeV (based upon the `-1`, `1.23e6` values appearing as the fourth and fifth items on this input card). The remaining input identifies the user-specified multigroup structure. After [ERRORR](#), we pass `tape28` to [COVR](#), where the appropriate plot commands are generated to produce the correlation matrix plot, the spectrum plot, and the uncertainty plot. Card 2 (`icolor`) requests a color contour plot, and card 3 sets the lower (x-axis)



energy limit to 1 keV with default values used for the other input parameters. Card 5 specifies the `mat` number for the material of interest. Finally, [VIEWR](#) reads the [COVR](#) output file, `tape38`, and produces a postscript-formatted file, `tape39`.

```

echo 'NJOY Test Problem 18'
echo 'getting endf tape for e7 cf252'
cp ../DCf252 tape20
echo 'running njoy'
cat>input <<EOF
--
-- Copy ascii input to binary.
moder
  20 -21 /
--
-- Resonance reconstruction, to 0.1%.
reconr
  -21 -22 /
  'processing e70 252Cf with decay mf5/mt18 & mf35/mt18'
  9999 0 0 /
  0.001 /
  0 /
--
-- Doppler broaden to 300K.
broadr
  -21 -22 -23 /
  9999 1 0 0 0 /
  0.001 /
  300. /
  0 /
--
-- Group average, 300K with mf35 group structure.
-- - All file 3 cross sections plus fission spectrum.
groupr
  -21 -23 0 91 /
  9999 1 0 2 1 1 1 1 /
  'test'
  300. /
  1.0e10 /
  71 / # of groups, energy boundaries follow:
  1.000000-5 1.500000+4 3.500000+4 5.500000+4 7.500000+4

```

```

9.500000+4 1.150000+5 1.350000+5 1.650000+5 1.950000+5
2.250000+5 2.550000+5 3.050000+5 3.550000+5 4.050000+5
4.550000+5 5.050000+5 5.550000+5 6.050000+5 6.550000+5
7.050000+5 7.550000+5 8.050000+5 8.550000+5 9.050000+5
9.550000+5 1.050000+6 1.150000+6 1.250000+6 1.350000+6
1.450000+6 1.550000+6 1.650000+6 1.750000+6 1.850000+6
1.950000+6 2.150000+6 2.350000+6 2.550000+6 2.750000+6
2.950000+6 3.250000+6 3.550000+6 3.850000+6 4.150000+6
4.450000+6 4.750000+6 5.050000+6 5.550000+6 6.050000+6
6.550000+6 7.050000+6 7.550000+6 8.050000+6 8.550000+6
9.050000+6 9.550000+6 1.005000+7 1.055000+7 1.105000+7
1.155000+7 1.205000+7 1.255000+7 1.305000+7 1.355000+7
1.405000+7 1.460000+7 1.590000+7 1.690000+7 1.790000+7
1.910000+7 2.000000+7
3 /
5 18 'chi' /
0 /
0 /
--
-- ERRORJ, mf35
errorr
20 0 91 28 0 0 /
9999 1 2 1 1 /
1 300./
0 35 1 1 -1 1.23e6 /
71 / # of groups, energy boundaries follow:
1.000000-5 1.500000+4 3.500000+4 5.500000+4 7.500000+4
9.500000+4 1.150000+5 1.350000+5 1.650000+5 1.950000+5
2.250000+5 2.550000+5 3.050000+5 3.550000+5 4.050000+5
4.550000+5 5.050000+5 5.550000+5 6.050000+5 6.550000+5
7.050000+5 7.550000+5 8.050000+5 8.550000+5 9.050000+5
9.550000+5 1.050000+6 1.150000+6 1.250000+6 1.350000+6
1.450000+6 1.550000+6 1.650000+6 1.750000+6 1.850000+6
1.950000+6 2.150000+6 2.350000+6 2.550000+6 2.750000+6
2.950000+6 3.250000+6 3.550000+6 3.850000+6 4.150000+6
4.450000+6 4.750000+6 5.050000+6 5.550000+6 6.050000+6
6.550000+6 7.050000+6 7.550000+6 8.050000+6 8.550000+6
9.050000+6 9.550000+6 1.005000+7 1.055000+7 1.105000+7
1.155000+7 1.205000+7 1.255000+7 1.305000+7 1.355000+7
1.405000+7 1.460000+7 1.590000+7 1.690000+7 1.790000+7
1.910000+7 2.000000+7
--

```

```

-- make plot file.
covr
  28 0 38 /
  1 /
  1.e3 /
  /
  9999 /
--
-- make postscript file.
viewr
  38 39 /
stop
EOF
../xnjoy<input
echo 'saving output, ace, and pendf files'
cp output out18
cp tape39 plot18

```

## 26.22 Test Problem 19

The input file for this test is an evaluation for  $^{241}\text{Pu}$  using Reich-Moore resonance parameters.

```

echo 'NJOY Test Problem 19'
echo 'getting endf tape for e6 pu241c'
cp ../e6pu241c tape20
echo 'running njoy'
cat>input <<EOF
moder
20 -21
reconr
-21 -22
'pendf tape for pu-241 from endf/b-vi.3'/
9443 3/
.02/
'94-pu-241 from endf/b-vi.3'/
'processed by the njoy nuclear data processing system'/
'see original endf/b-iv tape for details of evaluation'/
0/
broadr

```

```

-21 -22 -23
9443 3 0 1 0/
.02/
293.6 900. 2100.
0/
unresr
-21 -23 -24
9443 3 7 1
293.6 900 2100
1.e10 1.e5 1.e4 1000. 100. 10. 1
0/
heatr
-21 -24 -25/
9443 3/
302 318 402
purr
-21 -25 -26
9443 3 7 20 4/
293.6 900 2100
1.e10 1.e5 1.e4 1000. 100. 10. 1
0/
acer
-21 -26 0 27 28/
1/
'njoy test problem 19'/
9443 293.6/
/
/
moder
-26 29
stop
EOF
../xnjoy<input
echo 'saving output, ace, and pendf files'
cp output out19
cp tape27 ace19
cp tape29 pend19

```

It starts with a normal [RECONR](#) run using 2% reconstruction for economy. The output file will disclose that Reich-Moore resonances were processed. The rest of the run follows the pattern of the previous examples.

### 26.23 Test Problem 20

The input file for this case is an experimental evaluation from ORNL for  $^{35}\text{Cl}$  that uses the Reich-Moore-Limited (RML) format for its resonance parameters (lrf=7 in MF2/MT151) and for the covariances between resonance parameters (MF32). Utilizing the multi-channel capabilities of the RML representation, resonance cross sections and their covariances also include the first two inelastic levels (MT=51 and 52) in addition to the normal elastic and capture channels.

```

echo 'NJOY Test Problem 20'
echo 'getting cl35rml'
cp ../cl35rml tape20
echo 'running njoy'
ulimit -s 32768
cat>input <<EOF
errorr
  999      /  option to insert dummy file 33 data
+20 +21 /  input & output tapes
   1      /  mt to insert,
   2      /  continue mt list ...
102      /
600      /
   0      /  terminate mt list with zero
reconr
+21 +22 /
'processing cl35 with rml'
1725 0 0 /
0.01 /
0 /
broadr
+20 +22 +23 /
1725 1 0 0 0 /
0.01 /
293.6 /
0 /
groupr
+20 +23 0 +91 /
1725 4 0 2 1 1 1 1 /
'test of cl35 with rml'
293.6 /
1.0e10 /

```

```

3 /
3 251 'mubar' /
3 252 'xi' /
0 /
0 /
errorr
+21 0 +91 +25 0 0 /
1725 4 2 1 1 /
1 293.6/
0 33 1 1 -1 /
covr
+25 0 +26 /
1 /
.01 /
1 /
1725 /
viewr
+26 +27
stop
EOF
../xnjoy<input
echo 'saving output file'
cp output out20
cp tape23 pend20
cp tape27 plot20

```

The reconr output from this run will show that it used the RML methods and it will list the reactions treated with resonance methods (MT=2, 51, 52, 102). **BROADR** and **GROUPE** are used in the normal way, **ERRORR** and **COVR** are then run to produce the covariances and prepare plots of the results.

## 26.24 Application of the NJOY System

There are not enough standard test problems to exercise all the many options that evaluators manage to use. Therefore, the next step in testing is to run NJOY on many different evaluations. This has included running all the materials in the ENDF/B-VII.0 neutron, thermal, photoatomic, photonuclear, and charged-particle sublibraries through to MCNP “ACE” files followed by short MCNP runs to make sure the data have no obvious flaws that prevent the code from running. The output files were examined for error messages and other

indications of problems. This process also produces a useful set of plots that can be scanned for possible problems. The plots from some of these tests are available on the web. Browse to <http://t2.lanl.gov> and select the “Nuclear Information Service (NIS)”, “Data area” and “US ENDF/B Libraries” links. Look in “ENDF/B-VII Neutron Data,” “ENDF/B-VII Thermal Scattering Data,” “ENDF/B-VII Proton Data,” and “ENDF/B-VII Photonuclear Data. Similar plots from the recently released ENDF/B-VII.1 library will become available in the near future.

As discussed in the [HEATR](#) section of this report, NJOY has the capability to examine ENDF-format evaluations for energy balance problems that show up for nuclear heating calculations. These tests can also reveal problems with the processing on occasion. A large set of results, including plots, can be found on the web. As before, browse to <http://t2.lanl.gov>, again select the “Nuclear Information Service (NIS)”, “Data area” and “US ENDF/B Libraries” links, but now scroll down to “Energy Balance of ENDF/B-VII.1,” and click on “summary.” This page lists the materials with their problems and provides links to the plots.

Another test of the processing code comes from running criticality benchmarks such as those defined in the ICSBEP Handbook[124] using the processed data libraries. If results are consistent, it gives some confidence that the libraries don’t contain severe errors. Table [31](#) shows some benchmark results using ENDF/B-VII.0 data processed with NJOY and used by MCNP5. The results are calculated  $k_{\text{eff}}$  values divided by the evaluated model  $k_{\text{eff}}$  value (C/E).

Similarly, we can calculate criticality benchmarks using multigroup libraries with a discrete-ordinates transport code. The Los Alamos PARTISN code was used with data prepared using TRANSX. Table [32](#) shows results for a selection of fast critical assemblies using three different group structures. Comparing these results with the previous table shows that multigroup methods can compare favorably with Monte Carlo when using high-accuracy libraries. IMF007h is a 2-D cylindrical homogenized model for Bigten. Table [33](#) shows results for two of the thermal solution criticals from Table [31](#). Once again, the results are satisfactory. These kinds of tests provide some confidence that the multigroup processing in NJOY2012 is working properly and is consistent with the Monte Carlo processing.

As a further verification of NJOY processing, it is useful to do intercomparisons with other processing systems. Over the years, we have periodically compared NJOY results from [RECONR](#) and [BROADR](#) with the PREPRO sys-

Table 31: Criticality benchmark results from MCNP5 using NJOY processed ENDF/B-VII.0 Cross Sections

| Critical          | $k_{\text{eff}}$ C/E | Description                                        |
|-------------------|----------------------|----------------------------------------------------|
| HMF001 Godiva     | 0.99986              | sphere of $^{235}\text{U}$                         |
| PMF001 Jezebel    | 1.00006              | sphere of $^{239}\text{Pu}$                        |
| UMF001 Jezebel-23 | 0.99970              | sphere of $^{233}\text{U}$                         |
| HMF028 Flattop-25 | 1.00277              | $^{235}\text{U}$ core, $^{nat}\text{U}$ reflector  |
| PMF006 Flattop-Pu | 1.00105              | $^{239}\text{Pu}$ core, $^{nat}\text{U}$ reflector |
| UMF006 Flattop-23 | 0.99937              | $^{233}\text{U}$ core, $^{nat}\text{U}$ reflector  |
| IMF007s Bigten    | 0.99995              | 10% enr. U core, $^{nat}\text{U}$ refl.            |
| HST042-02         | 1.00028              | HEU in nitrate solution                            |
| HST042-03         | 1.00065              | HEU in nitrate solution                            |
| HST042-05         | 1.00019              | HEU in nitrate solution                            |
| LCT006-01         | 0.99995              | low enriched $\text{UO}_2$ lattice                 |
| LCT006-02         | 1.00052              | low enriched $\text{UO}_2$ lattice                 |
| LCT006-03         | 1.00036              | low enriched $\text{UO}_2$ lattice                 |

Table 32: Benchmark Results for Fast Criticals Using ENDF/B-VII.0 Multigroup Libraries and TRANSX/PARTISN

| Critical          | $k_{\text{eff}}$ C/E |         |         |         |
|-------------------|----------------------|---------|---------|---------|
|                   | MCNP                 | 30 gp   | 80 gp   | 187 gp  |
| HMF001 Godiva     | 0.99986              | 1.00234 | 1.00091 | 1.00025 |
| PMF001 Jezebel    | 1.00006              | 1.00060 | 1.00047 | 1.00036 |
| UMF001 Jezebel-23 | 0.99970              | 1.00115 | 1.00024 | 0.99992 |
| HMF028 Flattop-25 | 1.00277              | 1.00349 | 1.00343 | 1.00295 |
| PMF006 Flattop-Pu | 1.00105              | 1.00126 | 1.00147 | 1.00134 |
| UMF006 Flattop-23 | 0.99937              | 1.00126 | 1.00010 | 0.99971 |
| IMF007h Bigten    | 1.00005              |         | 1.00022 | 1.00001 |

Table 33: Benchmark Results for Thermal Criticals Using ENDF/B-VII.0 Multigroup Libraries and TRANSX/PARTISN.

| Critical  | $k_{\text{eff}}$ C/E |         |         |
|-----------|----------------------|---------|---------|
|           | MCNP                 | 69 gp   | 187 gp  |
| HST042-03 | 1.00065              | 0.99931 | 0.99958 |
| HST042-05 | 1.00019              | 0.99946 | 0.99935 |



tem of D. E. Cullen[125], especially when new features have been added to the ENDF system. We recently did a number of comparisons with ORNL results to verify the new capabilities for resonance reconstruction and covariance processing imported from the ORNL SAMMY code. In some cases, these comparisons have been extended to multiple laboratories. An example of that is a recent comparison of unresolved resonance range processing[126]. This study suggests that more work is needed in the unresolved resonance range.

The comparisons described above were on cross sections. It is also useful to do multilab comparisons on integral results. As an example, a LANL-LLNL comparison[127] shows that we can get good agreement for the fast criticals Godiva, Jezebel, and Jezebel-23. Another recent multilab comparison involving LANL, LLNL, ANL, and the CEA demonstrated reasonable results for the softer spectrum of the Bigten critical assembly[128].



## References

- [1] R. E. MacFarlane and R. M. Boicourt, “NJOY: A Neutron and Photon Processing System,” *Trans. Am. Nucl. Soc.* **22**, 720 (1975).
- [2] R. E. MacFarlane, D. W. Muir, and R. M. Boicourt, “The NJOY Nuclear Data Processing System, Volume 1: User’s Manual,” Los Alamos National Laboratory report LA-9303-M, Vol. I (ENDF-324), (May 1982). R. E. MacFarlane, D. W. Muir, and R. M. Boicourt, “The NJOY Nuclear Data Processing System, Volume II: The NJOY, RECONR, BROADR, HEATR, and THERMR Modules,” Los Alamos National Laboratory report LA-9303-M, Vol. II (ENDF-324) (May 1982). R. E. MacFarlane and D. W. Muir, “The NJOY Nuclear Data Processing System, Volume III: The GROUPE, GAMINR, and MODER Modules,” Los Alamos National Laboratory report LA-9303-M, Vol. III (ENDF-324) (October 1987). D. W. Muir and R. E. MacFarlane, “The NJOY Nuclear Data Processing System, Volume IV: The ERRORR and COVR Modules,” Los Alamos National Laboratory report LA-9303-M, Vol. IV (ENDF-324) (December 1985).
- [3] R. E. MacFarlane and D. W. Muir, “The NJOY Nuclear Data Processing System, Version 91,” Los Alamos National Laboratory report LA-12740-M (1994).
- [4] R. E. MacFarlane and A. C. Kahler, “Methods for Processing ENDF/B-VII with NJOY,” *Nuclear Data Sheets*, **111**, 2739–2890 (2010).
- [5] For an online tutorial on NJOY, see <http://t2.lanl.gov>, and follow links to the “Nuclear Information Service (NIS)”, “Training area” and “NJOY” which leads to “Understanding NJOY,” Los Alamos National Laboratory report LA-UR-00-1538 (March 2000).
- [6] M. B. Chadwick *et al.*, “ENDF/B-VII.0: Next Generation Evaluated Nuclear Data Library for Nuclear Science and Technology,” *Nuclear Data Sheets*, **107**, 2931–3060 (2006).
- [7] M. B. Chadwick *et al.*, “ENDF/B-VII.1 Nuclear Data for Science and Technology: Cross Sections, Covariances, Fission Product Yields and Decay Data,” *Nuclear Data Sheets*, **112**, 2887–2996 (2011).
- [8] M. Herman and A. Trkov, Eds., ENDF-6 Formats Manual, Data Formats and Procedures for the Evaluated Nuclear Data File ENDF/B-VI and ENDF/B-VII, Brookhaven National Laboratory report BNL-90365-2009 (ENDF-102) (June 2009). For the latest version of this report, see <http://www.nndc.bnl.gov> and take the ENDF tab to ENDF-6 Formats Manual.
- [9] For an online tutorial on the ENDF formats, see <http://t2.lanl.gov>, and follow links to the “Nuclear Information Service (NIS)”, “Training area” and “ENDF” which leads to “An Introduction to the ENDF Formats,” Los Alamos National Laboratory report LA-UR-98-1779 (January 1998).

- [10] R. D. O'Dell, "Standard Interface Files and Procedures for Reactor Physics Codes, Version IV," Los Alamos Scientific Laboratory report LA-6941-MS (September 1977).
- [11] R. E. MacFarlane, "TRANSX-CTR: A Code for Interfacing MATXS Cross-Section Libraries to Nuclear Transport Codes for Fusion Systems Analysis," Los Alamos National Laboratory report LA-9863-MS (February 1984).
- [12] W. W. Engle, Jr., "A Users Manual for ANISN, A One-Dimensional Discrete Ordinates Transport Code with Anisotropic Scattering," Oak Ridge Gaseous Diffusion Plant Computing Technology Center report K-1693 (1967).
- [13] R. D. O'Dell, F. W. Brinkley, Jr., D. R. Marr, and R. E. Alcouffe, "Revised User's Manual for ONEDANT: A Code Package for One-Dimensional, Diffusion-Accelerated, Neutral-Particle Transport," Los Alamos National Laboratory report LA-9184-M, Rev. (December 1989).
- [14] R. E. Alcouffe, F. W. Brinkley, D. R. Marr, and R. D. O'Dell, "User's Guide for TWODANT: A Code Package for Two-Dimensional, Diffusion-Accelerated, Neutral-Particle Transport," Los Alamos National Laboratory report LA-10049 Revised (February 1990).
- [15] K. L. Derstine, "DIF3D: A Code to Solve One-, Two-, and Three-Dimensional Finite-Difference Diffusion Theory Problems," Argonne National Laboratory report ANL-82-64 (April 1984).
- [16] R. E. Alcouffe, R. S. Baker, J. A. Dahl, S. A. Turner, and R. C. Ward, "PARTISN: A Time-Dependent, Parallel Neutral Particle Transport Code System," Los Alamos National Laboratory report LA-UR-05-3925 (Revised May 2005).
- [17] X-5 Monte Carlo Team, "MCNP—A General Monte Carlo N-Particle Transport Code, Version 5," Los Alamos National Laboratory report LA-UR-03-1987 (April 2003).
- [18] J. R. Askew, F. J. Fayers, and P. B. Kemshell, "A General Description of the Lattice Code WIMS," *J. Brit. Nucl. Energy Soc.* 5, 564 (1966).
- [19] Userinput information may be found on the NJOY homepage, found under the "Nuclear Information Service (NIS)", "Codes" and "NJOY" links at <http://t2.lanl.gov>.
- [20] C. R. Weisbin, P. D. Soran, R. E. MacFarlane, D. R. Harris, R. J. LaBauve, J. S. Hendricks, J. E. White, and R. B. Kidman, "MINX, A Multigroup Interpretation of Nuclear X-Sections from ENDF/B," Los Alamos Scientific Laboratory report LA-6486-MS (ENDF-237) (September 1976).
- [21] D. J. Dudziak, R. E. Seamon, and D. V. Susco, "LAPHAN0: A Multigroup Photon-Production Matrix and Source Code for ENDF," Los Alamos Scientific Laboratory report LA-4750-MS (ENDF-156) (January 1972).
- [22] K. D. Lathrop, "GAMLEG—A FORTRAN Code to Produce Multigroup Cross Sections for Photon Transport Calculations," Los Alamos Scientific Laboratory report LA-3267 (April 1965).

- [23] K. D. Lathrop, “DTF-IV, A FORTRAN Program for Solving the Multi-group Transport Equation with Anisotropic Scattering,” Los Alamos Scientific Laboratory report LA-3373 (November 1965).
- [24] R. J. LaBauve, C. R. Weisbin, R. E. Seamon, M. E. Battat, D. R. Harris, P. G. Young, and M. M. Klein, “PENDF: A Library of Nuclear Data for Monte Carlo Calculations Derived from Data in the ENDF/B Format,” Los Alamos Scientific Laboratory report LA-5687 (October 1974).
- [25] O. Ozer, Ed. “Description of the ENDF/B Processing Codes and Retrieval Subroutines,” Brookhaven National Laboratory report BNL-50300 (ENDF-11) (June 1971).
- [26] D. E. Cullen, “Program SIGMA1 (Version 74-1),” Lawrence Livermore Laboratory report UCID-16426 (January 1974).
- [27] R. E. Schenter, J. L. Baker, and R. B. Kidman, “ETOX, A Code to Calculate Group Constants for Nuclear Reactor Calculations,” Battelle Northwest Laboratory report BNWL-1002 (1969).
- [28] B. M. Carmichael, “Standard Interface Files and Procedures for Reactor Physics Codes, Version III,” Los Alamos Scientific Laboratory report LA-5486-MS (1974).
- [29] M. A. Abdou, C. W. Maynard, and R. Q. Wright, “MACK: A Computer Program to Calculate Neutron Energy Release Parameters (Fluence to Kerma Factors) and Multigroup Neutron Reaction Cross Sections from Nuclear Data in ENDF Format,” Oak Ridge National Laboratory report ORNL-TM-3994 (1973).
- [30] H. C. Honek and D. R. Finch, “FLANGE-II (Version 71-1), A Code to Process Thermal Neutron Data from an ENDF/B Tape,” E. I. DuPont de Nemours and Co. Savannah River Laboratory report DP-1278 (1971).
- [31] Y. D. Naliboff and J. U. Koppel, “HEXSCAT, Coherent Elastic Scattering of Neutrons by Hexagonal Lattices,” General Atomic report GA-6026 (1964).
- [32] R. E. MacFarlane, R. J. Barrett, D. W. Muir, and R. M. Boicourt, “NJOY: A Comprehensive ENDF/B Processing System,” in A Review of Multigroup Nuclear Cross-Section Processing, Proceedings of a Seminar-Workshop, Oak Ridge, Tennessee, March 14-16, 1978,” Oak Ridge National Laboratory report ORNL/RSIC-41 (October 1978).
- [33] R. E. MacFarlane, “Introducing NJOY89,” in Proceedings of the Seminar on NJOY and Themis, 20-21 June 1989, OECD/NEA Data Bank, Saclay, France (1989). See also “Nuclear Theory and Application Progress Report, January 1, 1989—April 1, 1990,” pp. 21-38, Los Alamos National Laboratory report LA-11972-PR (December 1990).
- [34] Go Chiba, “ERRORJ, A Code to Process Neutron-Nuclide Reaction Covariance, Version 2.3,” JAEA-Data/Code 2007-007, March 2007.

- [35] N.M.Larson, "Updated Users Guide for SAMMY: Multilevel R-Matrix Fits to Neutron Data Using Bayes Equations," Oak Ridge National Laboratory report ORNL/TM-9179/R8 (October 2008).
- [36] B. J. Toppel, A. L. Rago, and D. M. O'Shea, "MC<sup>2</sup>, A Code to Calculate Multigroup Cross Sections," Argonne National Laboratory report ANL-7318 (1967).
- [37] H. Henryson II, B. J. Toppel, and C. G. Stenberg, "MC<sup>2</sup>-2: A Code to Calculate Fast Neutron Spectra and Multigroup Cross Sections," Argonne National Laboratory report ANL-8144 (ENDF-239) (1976).
- [38] I. I. Bondarenko, Ed., *Group Constants for Nuclear Reactor Calculations* (Consultants Bureau, New York, 1964).
- [39] R. B. Kidman, "Cross Section Structure Factor Interpolation Schemes," Hanford Engineering Development Laboratory report HEDL-TME-71-40 (1971).
- [40] R. E. MacFarlane, "TRANSX 2: A Code for Interfacing MATXS Cross-Section Libraries to Nuclear Transport Codes," Los Alamos National Laboratory report LA-12312-MS (July 1992).
- [41] D. W. Muir, "Gamma Rays, Q-Values, and Kerma Factors," Los Alamos Scientific Laboratory report LA-6258-MS (March 1976).
- [42] R. E. MacFarlane, "Energy Balance of ENDF/B-V," *Trans. Am. Nucl. Soc.* **33**, 681 (1979). See also R. E. MacFarlane, "Energy Balance of ENDF/B-V.2," Minutes of the Cross Section Evaluation Working Group (available from the National Nuclear Data Center, Brookhaven National Laboratory, Upton, NY) (May 1984).
- [43] T. A. Gabriel, J. D. Amburgy, and N. M. Greene, "Radiation-Damage Calculations: Primary Knock-On Atom Spectra, Displacement Rates, and Gas Production Rates," *Nucl. Sci. Eng.* **61**, 21 (1976).
- [44] D. G. Doran, "Neutron Displacement Cross Sections for Stainless Steel and Tantalum Based on a Linhard Model," *Nucl. Sci. Eng.* **49**, 130 (1972).
- [45] L. R. Greenwood and R. K. Smither, "Displacement Damage Calculations with ENDF/B-V," in Proceedings of the Advisory Group Meeting on Nuclear Data for Radiation Damage Assessment and Reactor Safety Aspects, October 12-16, 1981, IAEA, Vienna, Austria (October 1981).
- [46] M. T. Robinson, in *Nuclear Fusion Reactors* (British Nuclear Energy Society, London, 1970).
- [47] J. Lindhard, V. Nielsen, M. Scharff, and P. V. Thomsen, *Kgl. Dansk, Vidensk. Selsk, Mat-Fys. Medd.* **33** (1963).
- [48] R. E. MacFarlane, D. W. Muir, and F. M. Mann, "Radiation Damage Calculations with NJOY," *J. Nucl. Materials* **122** and **123**, 1041 (1984).
- [49] R. E. MacFarlane and D. G. Foster, Jr., "Advanced Nuclear Data for Radiation Damage Calculations," *J. Nucl. Materials* **122** and **123**, 1047 (1984).

- [50] R. Kinsey, Ed., “ENDF-102, Data Formats and Procedures for the Evaluated Nuclear Data File, ENDF,” Brookhaven National Laboratory report BNL-NCS-50496 (ENDF-102) 2nd Edition (ENDF/B-V) (October 1979).
- [51] J. U. Koppel and D. H. Houston, “Reference Manual for ENDF Thermal Neutron Scattering Data,” General Atomic report GA-8774 revised and reissued as ENDF-269 by the National Nuclear Data Center, Brookhaven National Laboratory (1978).
- [52] G. I. Bell and S. Glasstone, *Nuclear Reactor Theory* (Van Nostrand Reinhold, New York, 1970).
- [53] R. W. Hardie and W. W. Little, Jr., “1DX, A One-Dimensional Diffusion Code for Generating Effective Nuclear Cross Sections,” Battelle Northwest Laboratory report BNWL-954 (1969).
- [54] R. E. MacFarlane, “ENDF/B-IV and -V Cross Sections for Thermal Power Reactor Analysis,” in Proc. Intl. Conf. of Nuclear Cross Sections for Technology, Knoxville, TN (October 22-26 1979), National Bureau of Standards Publication 594 (September 1980).
- [55] G. I. Bell, G. E. Hansen, and H. A. Sandmeier, “Multitable Treatments of Anisotropic Scattering in  $S_N$  Multigroup Transport Calculations,” Nucl. Sci. Eng. 28, 376 (1967).
- [56] M. Abramowitz and I. Stegun, *Handbook of Mathematical Functions* (Dover Publications, New York, 1965).
- [57] D. G. Madland, “New Fission Neutron Spectrum Representation for ENDF,” Los Alamos National Laboratory report LA-9285-MS (ENDF-321) (April 1982).
- [58] C. Kalbach and F. M. Mann, “Phenomenology of Continuum Angular Distributions. I. Systematics and Parameterization,” Phys. Rev. C. 23, 112 (1981).
- [59] C. Kalbach, “Systematics of Continuum Angular Distributions: Extensions to Higher Energies,” Phys. Rev. C. 37, 2350 (1988).
- [60] P. G. Young and E. D. Arthur, “GNASH: A Preequilibrium Statistical Nuclear Model Code for Calculation of Cross Sections and Emission Spectra,” Los Alamos Scientific Laboratory report LA-6947 (1977).
- [61] R. E. MacFarlane, “ENDF/B-V Cross-Section Library for Reactor Cell Analysis,” Electric Power Research Institute report EPRI NP-3418 (February 1984).
- [62] R. B. Kidman and R. E. MacFarlane, “LIB-IV, A Library of Group Constants for Nuclear Reactor Calculations,” Los Alamos Scientific Laboratory report LA-6260-MS (1976).
- [63] G. Lehner, “Reaction Rates and Energy Spectra for Nuclear Reactions in High Energy Plasmas,” Z. Physik **232**, 174 (1970).

- [64] D. E. Nagle, W. E. Quinn, W. B. Riesenfeld, and W. Leland, "Ion Temperature in Scylla, as Determined from the Reaction  $D(d,p)T$ ," *Phys. Rev. Letters* **3**, 318 (1959).
- [65] N. Jarmie and J. D. Seagrave (Eds.), "Charged Particle Cross Sections," Los Alamos Scientific Laboratory report LA-2014 (1956).
- [66] D. W. Muir, "Sensitivity of Neutron Multigroup Cross Sections to Thermal Broadening of the Fusion Peak," Proc. 1st Topical Meeting on the Technology of Controlled Nuclear Fusion, San Diego, Calif., April 1974, CONF-740402-P2, p.166 (1975).
- [67] R. W. Roussin, J. R. Knight, J. H. Hubbell, and R. J. Howerton, "Description of the DLC-99/HUGO Package of Photon Interaction Data in ENDF/B-V Format," Oak Ridge National Laboratory report ORNL/RSIC-46 (ENDF-335) (December 1983).
- [68] J. H. Hubbell, Wm. J. Viegle, E. A. Briggs, R. T. Brown, D. T. Cromer, and R. J. Howerton, "Atomic Form Factors, Incoherent Scattering Functions, and Photon Scattering Cross Sections," *J. Phys. Chem. Ref. Data* **4**, 471 (1975).
- [69] S. A. W. Gerstl, D. J. Dudziak, and D. W. Muir, "Cross Section Sensitivity and Uncertainty Analysis with Application to a Fusion Reactor," *Nucl. Sci. Eng.* **62**, 137 (January 1977).
- [70] W. A. Reupke, D. W. Muir, and J. N. Davidson, "Consistency of Neutron Cross-Section Data,  $S_n$  Calculations, and Measured Tritium Production for a 14-MeV Neutron-Driven Sphere of Natural-Lithium Deuteride," *Nucl. Sci. Eng.* **82**, 416 (December 1982).
- [71] D. W. Muir, "Evaluation of Correlated Data Using Partitioned Least Squares: A Minimum-Variance Derivation," *Nucl. Sci. and Eng.* **101**, 88-93 (January 1989).
- [72] C. R. Weisbin, E. M. Oblow, J. Ching, J. E. White, R. Q. Wright, and J. Drischler, "Cross Section and Method Uncertainties: The Application of Sensitivity Analysis to Study Their Relationship in Radiation Transport Benchmark Problems," Oak Ridge National Laboratory report ORNL-TM-4847 (ENDF-218) (August 1975). (See especially Chapter IV.)
- [73] J. D. Smith III, "Processing ENDF/B-V Uncertainty Data into Multigroup Covariance Matrices," Oak Ridge National Laboratory report ORNL/TM-7221 (ENDF-295) (June 1980).
- [74] P. G. Young, "Evaluation of  $n + {}^7\text{Li}$  Reactions using Variance-Covariance Techniques," *Trans. Am. Nucl. Soc.* **39**, 272 (1981).
- [75] P. G. Young, J. W. Davidson, and D. W. Muir, "Evaluation of the  ${}^7\text{Li}(n,n't){}^4\text{He}$  Cross Section for ENDF/B-VI and Application to Uncertainty Analysis," *Fusion Tech.* **15**, 440-448 (1989).
- [76] D. W. Muir and R. J. LaBauve, "COVFILS: A 30-Group Covariance Library Based on ENDF/B-V," Los Alamos National Laboratory report LA-8733-MS (ENDF-306) (March 1981).



- [77] D. W. Muir, "COVFILS-2: Neutron Data and Covariances for Sensitivity and Uncertainty Analysis," *Fusion Tech.* **10** (3), Part 2B, 1461 (November 1986).
- [78] S. A. W. Gerstl, "SENSIT: A Cross-Section and Design Sensitivity and Uncertainty Analysis Code," Los Alamos Scientific Laboratory report LA-8498-MS (August 1980).
- [79] M. J. Embrechts, "SENSIT-2D: A Two-Dimensional Cross-Section Sensitivity and Uncertainty Analysis Code," Los Alamos National Laboratory report LA-9515-MS (October 1982).
- [80] D. W. Muir, R. E. MacFarlane, and R. M. Boicourt, "Multigroup Processing of ENDF/B Dosimetry Covariances," Proc. 4th ASTM-EURATOM Symp. on Reactor Dosimetry, Gaithersburg, Maryland, March 22-26, 1982, NUREG/CP-0029 (CONF-820321), p. 655 (1982).
- [81] R. J. Barrett and R. E. MacFarlane, "Coupled Neutron and Photon Cross Sections for Transport Calculations," Los Alamos Scientific Laboratory report LA-7808-MS (April 1979).
- [82] R. E. MacFarlane and R. B. Kidman, "LINX and BINX: CCCC Utility Codes for the MINX Multigroup Processing Code," Los Alamos Scientific Laboratory report LA-6219-MS (February 1976).
- [83] "CINX: Collapsed Interpretation of Nuclear X Sections," Los Alamos Scientific Laboratory report LA-6287-MS (April 1976).
- [84] W. J. Davis, M. B. Yarbrough, and A. B. Bortz, "SPHINX: A One Dimensional Diffusion and Transport Nuclear Cross Section Processing Code," Westinghouse Advanced Reactors Division report WARD-XS-3045-17 (August 1977).
- [85] C. L. Cowan, B. A. Hutchins, and J. E. Turner, "TDOWN – A Code to Generate Composition and Spatially Dependent Cross Sections," General Electric report GEAP-13740 (August 1971).
- [86] R. J. LaBauve, T. R. England, D. C. George, R. E. MacFarlane, and W. B. Wilson, "DANDE—A Linked Code System for Core Neutronics/Depletion Analysis," Los Alamos National Laboratory report LA-10412-MS (June 1985).
- [87] R. E. MacFarlane and D. C. George, "UPD: A Portable Version-Control Program," Los Alamos National Laboratory report LA-12057-MS (April 1991).
- [88] Y. Farawila, Y. Gohar, and C. Maynard, "KAOS/LIB-V: A Library of Nuclear Response Functions Generated by KAOS-V Code From ENDF/B-V and Other Data Files" Argonne National Laboratory report ANL/FPP/TM-241 (April 1989).
- [89] E. D. Cashwell, J. R. Neergaard, W. M. Taylor, and G. D. Turner, "MCN: A Neutron Monte Carlo Code," Los Alamos Scientific Laboratory report LA-4751 (January 1972).

- [90] E. D. Cashwell, J. R. Neergaard, C. J. Everett, R. G. Schrandt, W. M. Taylor, and G. D. Turner, "Monte Carlo Photon Codes MCG and MCP," Los Alamos Scientific Laboratory report LA-5157-MS (March 1973).
- [91] C. J. Everett and E. D. Cashwell, "MCP Code Fluorescence-Routine Revision," Los Alamos Scientific Laboratory report LA-5240-MS (May 1973).
- [92] Adobe Systems Incorporated, *Postscript Language Reference Manual*, Addison-Wesley Publishing Company, 1985.
- [93] L. B. Levitt, "The Probability Table Method for Treating Unresolved Resonances in Monte Carlo Criticality Calculations," *Trans. Am. Nucl. Soc.* 14, 648 (1971).
- [94] R. E. Prael and L. J. Milton, "A User's Manual for the Monte Carlo Code VIM," Argonne National Laboratory report FRA-TM-84 (1976). Also, R. Blomquist, "VIM continuous energy Monte Carlo transport code," in Proc. Inter. Conf. on Mathematics, Computations, Reactor Physics and Environmental Analysis, Portland, OR, April 30 – May 4, 1995.
- [95] J. U. Koppel, J. R. Triplett, and Y. D. Naliboff, "GASKET: A Unified Code for Thermal Neutron Scattering," General Atomics report GA-7417 (Rev.) (March 1967).
- [96] R. C. F. McLatchie, 1962, unpublished.
- [97] A. T. Butland, "LEAP and ADDELTA, A Users Guide to Two Complementary Codes on the ICL-470 for Calculating The Scattering Law From a Phonon Frequency Function," Atomic Energy Establishment Winfrith report AEEW-M-1200, 1973.
- [98] D. J. Picton, personal communication to G. J. Russell, 1987.
- [99] R. E. MacFarlane, "New Thermal Neutron Scattering Files for ENDF/B-VI Release 2," Los Alamos National Laboratory report LA-12639-MS (1994).
- [100] R. E. MacFarlane, "Cold Moderator Scattering Kernels," in *Advanced Neutron Sources 1988, Proceedings of the 10th Meeting of the International Collaboration on Advanced Neutron Sources (ICANS-X) held at Los Alamos, 3-7 October 1988*, Institute of Physics Conferences Series Number 97 (Institute of Physics, Bristol and New York, 1988), p.157.
- [101] R. E. MacFarlane, "Cold Moderator Scattering Kernels," presented at the International Workshop on Cold Neutron Sources, March 5-8, 1990, Los Alamos, New Mexico, Los Alamos National Laboratory report LA-12146-C (August 1991).
- [102] D. E. Parks, M. S. Nelkin, J. R. Beyster, and N. F. Wikner, *Slow Neutron Scattering and Thermalization*, W. A. Benjamin, Inc. (New York, 1970).
- [103] R. W. G. Wyckoff, *Crystal Structures*, John Wiley & Sons, New York, London, 1963.
- [104] J. A. Young and J. U. Koppel, *Phys. Rev.* 135, A603(1964).
- [105] P. A. Egelstaff, B. C. Haywood, and F. J. Webb, *Proc. Phys. Soc.*, 90, 681(1967).

- [106] Wolfgang Schott, Z. Physik 231, 243(1970).
- [107] Masahiko Utsuro, Z. Physik B 27, 111(1977).
- [108] J. Keinert and J. Sax, "Investigation of Neutron Scattering Dynamics in Liquid Hydrogen and Deuterium for Cold Neutron Sources," Kerntechnik 51, 19 (1987).
- [109] M. Mattes and J. Keinert, "Thermal Neutron Scattering Data for the Moderator Materials H<sub>2</sub>O, D<sub>2</sub>O and ZrHx in ENDF-6 Format and as ACE Library for MCNP(X)", IAEA INDC(NDS)-0470, April 2005.
- [110] M. Dritsa, report from misc. OECD countries to EANDC, No. 63, 1967.
- [111] K. Heinloth, Zeitschrift fur Physik **163**, 218 (1961).
- [112] R. R. Smith, private communication held at BNL, 1953.
- [113] W. Walton, private communication held at BNL, 1960.
- [114] V. T. Springer, Nucleonik **3**, 110 (1961).
- [115] O. D. Simpson, J. Nuclear Instruments and Methods **30**, 293 (1964).
- [116] J. L. Russell, Jr., General Atomic report 7581, 1966.
- [117] Y. D. Harker and R. M. Brugger, "Investigation of the Low-Temperature Phase Transitions in Solid Methane by Slow Neutron Inelastic Scattering," J. Chem. Phys. 46, 2201(1967).
- [118] A. K. Agrawal and S. Yip, "Slow-Neutron Scattering by Molecular Liquids," Nucl. Sci. Eng. 37, 368(1969).
- [119] R. G. Gordon, J. Chem. Phys. 43, 1307(1965).
- [120] G. E. Ewing, J. Chem. Phys. 40, 179(1964).
- [121] These data were obtained from the paper of Keinert and Sax[108] and converted to the numbers shown by subtracting the hydrogen absorption cross section. The ortho cross sections were converted from normal <sup>2</sup>H cross sections using the theoretical ortho and para cross sections to produce a conversion factor. The original references are G. L. Squires and A. T. Stewart, Proc. Roy. Soc. A230, 19(1955), W. L. Whittemore and A. W. McReynolds, "Differential Neutron Thermalization," General Atomic report GA-2505 (1961), and W. D. Seiffert, "Messung der Streuquerschnitte von flüssigem und festem Wasserstoff, Deuterium, und Deuteriumhydrid für thermische Neutronen," EUR-5566d (1970).
- [122] W. H. Press, B. P. Flannery, Saul A. Teukolsky, and William T. Vetterling, *Numerical Recipes in C*, Cambridge University Press, 1988.
- [123] "UPDATE, VERSION 1, Reference Manual," Revision 11/23/81, Control Data Corporation report 60449900 (November 1981).
- [124] J. B. Briggs, *et al*, "International Handbook of Evaluated Criticality Safety Benchmark Experiments," Tech. Rep. NEA/NSC/DOC(95)04/I, Nuclear Energy Agency, Paris, France, 2004. Note that this Handbook is updated annually.

- [125] D. E. Cullen, “PREPRO 2007: 2007 ENDF/B Pre-Processing Codes,” IAEA-NDS-39, Rev. 13, Nuclear Data Section, International Atomic Energy Agency, Vienna, Austria.
- [126] J. C. Sublet, R. N. Blomquest, S. Goluoglu, and R. E. MacFarlane, “Unresolved Resonance Range Cross Section Probabiliy and Self Shielding Factors,” CEA-R-6227 (July 2009).
- [127] D. E. Cullen, P. Brown, E. Lent, R. MacFarlane, and S. McKinley, “Criticality Calculations Using LANL and LLNL Neutron Transport Codes,” Lawrence Livermore National Laboratory report UCRL-TR-237333 (November 22, 2007).
- [128] R. E. MacFarlane, R. M. Blomquist (ANL), D. E. Cullen (LLNL), and J. C. Sublet (CEA), “A Code Comparison Study for the Bigten Critical Assembly,” Los Alamos National Laboratory report LA-UR-08-4668 (August 2008).

## Index

- $S(\alpha, \beta)$ , [4](#), [165](#), [169](#), [512](#), [513](#), [647](#)
- $\psi\chi$  broadening, [10](#), [43](#), [51](#), [54](#), [56](#),  
[57](#), [69](#), [76](#), [103](#), [635](#)
- $\sigma_0$ , [95](#), [193](#), [473](#), [553](#), [733](#)
  - $\sigma_0$  interpolation, [107](#), [108](#)
- 12-group structure, [730](#), [736](#)
- 1DX, [193](#)
- 30-group structure, [730](#)
- 30x12 library, [10](#)
- 4-group structure, [235](#)
- 69-group structure, [553](#)
- 94-group structure, [507](#)
  
- a10, [37](#)
- a11, [39](#)
- bpart, [70](#)
- ACE consistency checks, [510](#)
- ACE dosimetry data, [11](#)
- ACE format, [6](#), [495](#), [499](#), [741](#)
  - Type 1, [518](#)
  - Type 2, [518](#)
  - Type 3, [518](#)
- ACE photoatomic data, [11](#)
- ACE quality assurance, [510](#)
- acecpe, [532](#), [533](#)
- acedos, [537](#)
- acefc, [497](#)
- acelcp, [509](#), [535](#)
- acelf5, [501](#), [533](#)
- acelf6, [533](#)
- acelod, [500](#), [501](#), [527](#), [531](#)
- acelpp, [535](#)
- acensd, [501](#), [532](#), [533](#)
- aceout, [535](#)
- acephn, [517](#), [539](#)
- acepho, [516](#), [538](#)
  
- aceprt, [535](#)
- ACER, [2](#), [6](#), [9–11](#), [13–16](#), [64](#), [187](#),  
[226](#), [228](#), [495](#), [604](#), [620](#)
  - ACER input, [519](#)
- acer, [527](#)
- ACER quality assurance, [515](#)
- ACER thinning
  - integral fraction, [497](#)
  - point removal, [497](#)
- acesix, [511](#), [513](#), [514](#), [536](#)
- acetop, [527](#)
- ad3d, [600](#)
- adaptive reconstruction, [87](#)
- Adler-Adler, [45](#), [51](#), [54](#), [57](#), [68](#)
- AEE/Winfirth, [553](#)
- afend, [26](#), [40](#)
- Aguilar, [12](#)
- ajku, [105](#), [113](#), [114](#)
- amend, [26](#), [40](#)
- anabar, [154](#), [155](#)
- anadam, [154](#), [155](#)
- anased, [220](#), [264](#)
- angle-energy distributions, [504](#)
- angular distributions, [62](#), [500](#), [691](#)
- ANISN, [6](#)
- anlyzd, [66](#)
- aplots, [510](#)
- Arcilla, [16](#)
- Argonne National Laboratory
  - ANL, [102](#), [114](#), [399](#)
- ascale, [601](#)
- ascalv, [616](#), [617](#)
- asend, [26](#), [40](#)
- atend, [26](#), [40](#)
- atomic form factors, [4](#), [271](#), [517](#)

- atomic screening, [217](#)
- atomic weight ratio
  - AWR, [45](#)
- axis2, [616](#), [619](#)
- axis3, [619](#)
- bach, [226](#), [259](#)
- bachaa, [502](#), [534](#)
- background cross section, [193](#)
- background R-matrix, [60](#)
- backspace, [22](#)
- band, [485](#)
- banner, [33](#)
- Barrett, [9](#)
- BBC, [471](#)
- Be, [513](#)
- Bell factors, [196](#)
- benzine, [513](#), [647](#)
- BeO, [513](#), [647](#), [663](#), [669](#), [675](#)
- bfact, [712](#), [713](#)
- bfile3, [86–88](#)
- bfill, [712](#)
- Bhat, [51](#)
- BINX, [399](#)
- blocked binary, [20](#), [25](#), [373](#)
- Boicourt, [9](#)
- Boltzmann constant, [54](#), [78](#), [169](#)
- Bondarenko method, [4](#), [93](#), [187](#), [192](#), [201](#), [473](#), [631](#)
- bootstrap, [90](#)
- bound atom scattering cross section, [169](#)
- BOXER format, [5](#), [354](#)
- Bragg edges, [166](#), [209](#), [514](#), [658](#)
- brkdat, [436](#), [437](#)
- BRKOXS, [2](#), [5](#), [228](#), [403](#), [419](#), [474](#), [734](#)
- broadn, [87](#)
- BROADR, [1](#), [3](#), [9](#), [13](#), [14](#), [21](#), [45](#), [54](#), [69](#), [77](#), [122](#), [173](#), [175](#), [190](#), [191](#), [235](#), [264](#), [497](#), [717](#), [730](#), [733](#)
- BROADR input, [88](#)
- broadr, [85](#)
- Brookhaven National Laboratory
  - BNL, [9](#), [51](#)
- bsigma, [87](#)
- Butland, [647](#)
- calcem, [170](#), [175](#), [177](#), [179](#)
- capdam, [152–154](#), [158](#)
- capture heating, [118](#)
- cbrkxs, [432](#), [436](#)
- CCCC, [9](#), [489](#)
- CCCC format, [449](#)
- CCCC-III, [9](#), [399](#), [449](#)
- CCCC-IV, [5](#), [10](#), [399](#), [449](#)
- CCCC interface files, [399](#)
- CCCCR, [2](#), [5](#), [10](#), [21](#), [187](#), [228](#), [399](#), [474](#), [734](#)
- CCCCR input, [440](#)
- ccccr, [431](#)
- cclip, [621](#)
- cdlyxs, [432](#), [438](#)
- change, [536](#)
- channel radius, [52](#)
- channel spin, [55](#)
- charged-particle cross sections, [11](#), [476](#)
- charw, [621](#)
- chi-square distributions, [64](#), [631](#)
- Chiba, [15](#), [16](#)
- CINX, [399](#)
- circle, [621](#)
- cisotx, [432](#)
- CLAW library

- CLAW-III, 382
- CLAW-IV, 382
- CLAW weight function, 730
- closz, 22, 37
- cm2lab, 257, 258
- cmatxs, 481
- coh, 175, 176
- coher, 714
- coherent cross section, 166, 514
- coherent elastic, 4, 165, 166, 209, 475, 514, 647–649, 657
- colaps, 300
- cold moderators, 647
- coldh, 710, 713
- collision-probability method, 489, 553
- commenting, 8
- competitive width, 51, 65
- complementary error function, 80, 88
- complex probability integral, 111, 114
- conbar, 152, 154
- CONT, 23
- contin, 710
- contio, 25
- conver, 158, 218, 252, 263
- convol, 711
- convr, 507, 528
- corr, 357
- correlations, 286
- Coulomb channels, 62
- Coulomb scattering, 217, 476
- coupled energy-angle distributions, 4
- coupled sets, 208
- covard, 357
- covariance libraries, 5
- covariance plotting, 10
- covariances, 2, 9, 283, 353, 736
- covcal, 301, 306, 307
- covout, 307
- COVR, 2, 5, 10, 311, 326, 353, 604, 737
  - COVR input, 358
- cptab, 530
- critical points, 215
- cross, 70
- csaa, 57, 68
- CSEWG, 507
- cshyb, 68
- CSISRS compilation, 693
- csmlbw, 55, 68
- csmlbw2, 56, 69
- csrmat, 58, 68
- cssammy, 60, 68, 70
- csslbw, 51, 68
- csunr1, 64, 67
- csunr2, 64
- Cullen, 16, 77
- cumulative probability distributions, 501
- current weighting, 94
- curv2, 616, 620
- curv3, 617, 620
- damage, 1, 3, 248
- damage energy, 12
- damage energy production, 120, 126
- Dancoff corrections, 196
- DANDE, 400
- data adjustment, 284
- data flow, 1, 3
- dater, 30, 36
- dchr, 621

- Debye-Waller coefficient, 657
- Debye-Waller factor, 166, 174
- delayed chi, 203
- delayed fission, 203
- delayed-neutron spectra, 187, 473
- delayed-neutron yield, 203, 473
- delayed-neutrons, 4, 477
- DeLeege, 12, 13
- desammy, 60, 70
- detail balance, 650
- df, 153–155
- DICT, 24
- dictio, 26
- DIF3D, 6, 399
- diffusion, 654, 663
- diffusion constant, 204
- diffusion singularity, 687
- direct heating, 116
- disbar, 152, 153
- discre, 710, 712
- discrete oscillators, 655, 686
- discrete-ordinates transport, 5, 205, 379
- disgam, 158, 159
- displa, 251, 255
- DLAYXS, 2, 5, 228, 403, 426, 477
- DLC7E, 734
- dldata, 438, 439
- Doppler-broadening, 1, 3, 45, 77, 81
- dosfix, 538
- dosimetry, 515, 537
- dosout, 518, 537
- dosprt, 537
- DP, 454
- DPA, 119, 191
- depend, 397
- drawh, 619, 621
- dsym, 621
- DTF, 8
- DTF format, 449
- DTF-IV, 2, 379
- dtfout, 397
- DTFR, 2, 5, 9, 187, 228, 353, 379, 604, 734, 736
  - DTFR input, 391
- dtfr, 396
- Dunford, 11, 51
- dynamic data storage, 9
- dynamic storage allocation, 7
- ed3d, 600
- effective temperature, 654, 655, 657, 690
- Electric Power Research Institute, *see* EPRI
- elemental cross sections, 623
- elemental heating, 117
- eliminated width, 60
- emerge, 69
- ENDF, 1, 3, 373, 575
  - ENDF format, 23
  - ENDF-6 format, 11, 43, 51, 589
  - ENDF standards tape, 727
  - ENDF/B, 44
  - ENDF/B-III, 1, 179
  - ENDF/B-IV, 1, 10, 731
  - ENDF/B-V, 1, 117, 727
  - ENDF/B-VI, 1, 11, 647
  - ENDF/B-VII, 1, 83, 90, 132, 187, 227, 647, 675
- endfr, 617, 619
- endout, 713
- endp, 616, 618, 621
- endw, 616, 618



- energy balance consistency, 115, 125, 134
- energy-angle data, 11, 501
- energy-balance checks, 3
- energy-balance heating, 3, 117, 625
- energy-dependent Q, 118, 135
- epithermal, 187, 489
- EPRI, 9, 228, 237, 547
  - EPRI-CELL, 6, 9, 10, 228, 547
  - EPRI-CPM, 6, 9, 228, 547
- equally probable bins, 501
- equally probable events, 513
- equally probably cosines, 515
- equivalence principle, 196
- equivalence theory, 473, 553, 555
- erbar, 616, 617
- erfc function, 29
  - erfc, 29
- error, 31, 36
- ERRORJ, 15, 16, 292, 297, 312
- ERRORR, 2, 5, 9, 10, 15, 17, 70, 187, 214, 228, 283, 353, 355, 373, 736, 737
  - ERRORR input, 314
- escape cross section, 195
- ETOPL, 8, 9, 500
- ETOX, 9, 93, 101
- evaporation spectrum, 501
- experimental data, 586
- exponential integral, 29
  - e1, 29
- exts, 712
- f6cm, 158, 258
- f6ddx, 158, 225, 258, 259
- f6dis, 158
- f6lab, 224, 258, 260
- f6psp, 158, 225, 258
- Fast Breeder Reactor Program, 9, 399
- fatal error messages, 30
- feed function, 4, 212
- File 6, 3, 11, 132, 214, 501, 590, 591
- File 7, 11, 169, 209
- fillh, 620, 621
- finda, 152, 158, 253
- findf, 23, 40, 66, 600
- findg, 483
- first, 527
- fission chi, 202, 473
- fission matrix, 202, 473, 558, 734
- fission neutron yield, 202
- fission Q, 121
- fission source, 201
- fission, steady-state, 203, 473
- fix6, 530
- FIXER, 572
- fixl7, 601
- FLANGE-II, 9, 165
- fluctuation integrals, 96
- fluorescence, 517
- flux calculator, 4, 10, 187, 192, 198, 241, 489, 553, 623
- Forrest, 9
- frame2, 616, 619
- free atom scattering cross section, 169, 690
- free gas, 4, 169, 512, 654, 662
- free-form input, 7, 9
- frequency spectrum, 650
- funky, 88
- fusion peak, 239
- gambar, 158, 159
- GAMINR, 2, 4, 9, 208, 214, 228, 271, 456, 734, 736

- GAMINR input, 276
- GAMLEG, 8, 271
- gamout, 507, 531
- gamsun, 531
- gas production, 2, 4, 717
- GASPR, 2, 4, 12, 717
  - GASPR input, 718
- Gauss-Jacobi quadrature, 105
- Gauss-Legendre quadrature, 131, 153, 224
- Gaussian quadrature, 215
- gdone, 616, 620
- gend, 618, 620
- GENDF, 4, 21, 187, 228, 251, 276, 320, 373, 382, 575, 600, 604, 734
- General Electric, 399
- genflx, 251, 253
- gengpg, 253
- gengpn, 252
- genunr, 67, 69
- genwtf, 241, 253
- getaed, 254, 257, 262
- getco, 215, 262
- getdis, 215, 217, 218, 257, 261
- getff, 212, 215, 251, 256
- getfle, 153, 215, 256, 261, 262
- getflx, 212, 255
- getgfl, 256, 262
- getgyl, 263
- getmf6, 224, 257
- getsed, 154, 256, 264
- getsig, 212, 255, 263
- getsix, 152, 156
- getunr, 242, 253, 255, 256
- getwtf, 241, 253, 255
- gety, 628
- gety1, 28, 41, 152, 158, 253, 628
- gety2, 28, 41, 158
- gety6, 601
- getyld, 154, 255, 256
- gg3d, 601
- gheat, 158
- GNASH, 225, 227, 502
- gnwtf, 276
- gpanel, 276
- gplot, 616, 620
- gral, 29, 40
- graphite, 513, 670, 730
- grid2, 619
- grid3, 619
- gridd, 300
- grist, 300
- group structures, 4, 235, 271
- group-to-group fission, 4
- group-to-group matrices, 190
- GROUPR, 2, 4, 9–11, 13, 15, 16, 21, 64, 67, 69, 95, 108, 131, 132, 154, 158, 168, 172, 187, 276, 320, 353, 373, 382, 386, 452, 489, 507, 547, 553, 623, 631, 658, 730, 734
  - GROUPR input, 230
- grouppr, 251
- grpav, 300
- gset, 620
- gtff, 276
- gtflx, 276
- gtsig, 276
- h6cm, 132, 157
- h6ddx, 157
- h6dis, 157
- h6psp, 157
- Hale, 15

- Hancock, 9
- Harris, 9
- hatch, 620
- hconvr, 151, 158
- hdatio, 25
- heating, 1, 3
- HEATR, 1, 3, 9–13, 15, 115, 190, 191, 226, 453, 604, 637, 730
  - HEATR input, 132
  - HEATR output, 136
- heatr, 150
- heavy water, 513
- heterogeneity, 195
- HEXSCAT, 9, 165, 167
- hgtfle, 153
- hgtyld, 154
- hinit, 150
- histod, 397
- hnab, 264
- hnabb, 88
- hname, 483
- hout, 159
- hunky, 88
- Hwang, 65
- Hybrid R-Function, 11, 45, 59
  - HRF, 45, 51, 59, 68
- IAEA, 517, 678
- iel, 175, 177
- iheat, 539
- ilist, 113
- in-sequence overlap, 98
- incoherent elastic, 4, 165, 174, 209, 475, 515, 647–649, 657
- incoherent inelastic, 4, 168, 210, 647, 649
- incomplete gamma function, 29
  - gami, 29
- incomplete probability integral, 80
- indx, 152, 153
- infinite dilution, 193
- init, 251, 254
- init2, 616, 618
- init3, 617, 619
- initp, 616–618
- input
  - ACER, 519
  - BROADR, 88
  - CCCCR, 440
  - COVR, 358
  - DTFR, 391
  - ERRORR, 314
  - GAMINR, 276
  - GASPR, 718
  - GROUPR, 230
  - HEATR, 132
  - LEAPR, 664
  - MATXSR, 477
  - MIXR, 623
  - MODER, 373
  - NJOY, 20
  - PLOTR, 592
  - POWR, 547
  - RECONR, 71
  - RESXSR, 493
  - THERMR, 181
  - UNRESR, 109
  - VIEWR, 604
  - WIMSR, 560
- input instructions, 8
- intega, 29, 40, 517
- integral thinning, 49
- intermediate resonance effects, 489, 553, 554, 623
- intermediate resonances, 187

- intermolecular interference, 663, 668, 669
- interpolation, 44–46
  - linear interpolation, 45
  - nonlinear interpolation, 45
- INTG, 24
- intgio, 26
- intr, 114
- intrf, 114
- inverse-velocity, 187
- inverted stack, 46, 87
- IR  $\lambda$ , 554
- ismooth, 227
- isolated resonances, 97
- isomtx, 434
- ISOTXS, 2, 5, 228, 403, 404, 449, 734
- isxdat, 432
- J values
  - duplicate  $J$  values, 55
- JEF-2, 11
- JEFF, 1
- JENDL, 1
- KAERI, 518
- Kalbach systematics, 225, 502
- Kalbach-Mann systematics, 225, 502
- Keinert, 648
- KERMA, 3, 9, 116, 191, 248, 271, 453
  - direct KERMA, 11
  - kinematic KERMA, 3, 11
  - negative KERMA, 117
- kernel broadening, 3, 54, 77
- Kidman, 108
- kinematic heating tests, 118
- kinematic limits, 123, 143
- Klein-Nishina, 272, 517
- Knolls Atomic Power Laboratory
  - KAPL, 51
- Kornreich, 647
- LaBauve, 9
- ladr2, 641
- LAPHANO, 8
- Larson, 13, 17
- Lawrence Livermore National Laboratory
  - LLNL, 9, 504
- Lazo, 648
- LEAPR, 2, 12, 14, 15, 647, 647
  - LEAPR input, 664
- leapr, 710
- Legendre polynomials, 29
- legndb, 617
- legndr, 29, 41
- Levine factors, 196
- Levitt, 631
- LIB-IV, 239, 399
- linearization, 46
- linking modules, 19
- LINUX, 399
- liquid hydrogen, 648, 650, 661, 668, 669
- LIST, 23
- listio, 25
- l12lab, 224, 257, 260
- loada/finda, 27, 37, 176
- Lobatto quadrature, 214, 255, 275
- Los Alamos National Laboratory
  - LANL, 9, 102, 227, 399, 518, 736
- Lubitz, 12, 13, 51
- Lubitz-Rose method, 55
- lunion, 68, 69

- MacFarlane, 9
- MACK, 9
- Madland, 15
- Madland-Nix law, 221
- Magnetic Fusion Energy Program, 10
- math
  - complementary error function, 80
  - erfc function, 29
  - exponential integral, 29
  - incomplete gamma function, 29
  - incomplete probability integral, 80
  - Legendre polynomials, 29
- matrix, 482, 485
- matshd, 357
- Mattes, 10, 12, 15, 648, 678
- MATXS, 5, 228
  - data type names, 451
  - particle names, 451
  - photoatomic cross sections, 456
  - reaction names, 451
  - thermal cross sections, 456
- MATXS format, 2, 11, 400, 449, 458
- MATXS/TRANSX, 5, 10, 379, 382
- MATXS1, 10
- MATXSR, 2, 5, 9, 14, 21, 187, 208, 228, 353, 449, 734
  - MATXSR input, 477
- matxsr, 480
- Maxwell-Boltzmann function, 78
- Maxwellian fission spectrum, 501
- MC2, 93, 101, 114
- MC2-2, 102
- McLatchie, 647
- MCN, 497
- MCNP, 2, 6, 9–12, 14, 15, 495, 631, 741
- MCPOINT, 9
- measurement vs theory, 693
- mess, 31, 36
- mfchk, 252
- mfchk2, 252
- MINX, 8, 25, 215, 399
- mixed moderators, 663, 675
- MIXR, 2, 6, 11, 623
  - MIXR input, 623
- MODER, 2, 5, 228, 320, 373, 730, 738
  - MODER input, 373
- modules
  - acecm, 496
  - acedo, 515, 537
  - acefc, 496, 527
  - acem, 496, 527
  - acepa, 496, 516, 538
  - acepn, 496, 517, 539
  - aceth, 496, 511, 536
  - broadm, 85
  - ccccm, 431
  - dtfm, 396
  - endf, 23, 25, 26, 28, 37, 66, 628
  - gaminm, 276
  - gaspm, 719
  - graph, 603, 616, 618
  - groupm, 251
  - heatm, 150
  - leapm, 710
  - locale, 33, 34
  - mainio, 35
  - math, 88
  - mathm, 29, 41
  - mixm, 628

- modem, [373](#)
- physics, [35](#), [713](#)
- plotm, [599](#)
- purrm, [639](#)
- reconm, [65](#)
- samm, [60](#), [66](#), [67](#), [69](#), [70](#)
- thrmm, [174](#)
- unresm, [111](#)
- util, [22](#), [27](#), [29](#), [30](#), [35](#)
- version, [33](#), [34](#)
- viewm, [616](#)
- wimsr, [565](#)
- Monte Carlo, [2](#), [10](#), [45](#), [495](#), [631](#), [741](#)
  - continuous-energy Monte Carlo, [45](#)
- moreio, [25](#)
- moveh, [621](#)
- MT
  - MT152, [108](#), [112](#)
  - MT203 – 207, [4](#)
  - MT221 – 250, [4](#)
  - MT442, [15](#)
  - MT443, [3](#)
  - MT444, [3](#)
- mtxdat, [481](#), [482](#)
- Muir, [9](#), [10](#), [241](#)
- mult, [402](#)
- Multi-Level Breit-Wigner, [45](#), [55](#)
  - GH MLBW method, [51](#), [56](#), [69](#)
  - MLBW, [45](#), [51](#), [54–56](#), [58](#), [68–70](#), [312](#)
- multigroup cross sections, [4](#), [190](#)
- mxproc, [437](#)
- namer, [251](#), [252](#)
- narrow resonance approximation, [192](#), [253](#), [553](#)
- narrow resonances, [187](#), [489](#)
- National Nuclear Data Center
  - NNDC, [51](#), [693](#)
- nclip, [621](#)
- ncurve, [621](#)
- NEA Data Bank, [10](#)
- Neef, [648](#)
- negative cross sections, [54](#)
- newp, [618](#), [620](#)
- nextr, [251](#)
- nheat, [151](#), [152](#)
- NJOY, [1](#)
- NJOY 10/81, [10](#)
- NJOY 6/83, [11](#)
- NJOY 77, [10](#)
- NJOY input, [20](#)
- NJOY2010, [16](#)
- NJOY2012, [16](#), [19](#)
- NJOY78, [10](#)
- NJOY89, [11](#)
- NJOY91, [11](#), [19](#)
- NJOY94, [12](#), [13](#)
- NJOY97, [13](#), [14](#)
- NJOY99, [14](#), [16](#)
- NNDC, *see* National Nuclear Data Center
- npage, [20](#), [33](#)
- nsyse, [20](#)
- nsysi, [20](#)
- nsyso, [20](#)
- nuclear amplitude expansion, [217](#)
- nuclear heating, [115](#)
- nuclear plus interference, [217](#)
- Oak Ridge National Laboratory
  - ORNL, [9](#), [62](#), [102](#), [293](#), [503](#), [769](#)
- ONEDANT, [6](#), [399](#)
- openz, [22](#), [37](#)
- ortho deuterium, [662](#)

- ortho hydrogen, [169](#), [662](#)
- Ozer, [9](#)
- p1scat, [568](#)
- p1sout, [568](#)
- paging, [84](#)
- pair correlation function, [669](#)
- panel, [214](#), [215](#), [254](#), [256](#)
- Panini, [13](#)
- para deuterium, [662](#)
- para hydrogen, [169](#), [662](#)
- partial fission, [203](#), [472](#)
- PARTISN, [6](#)
- parts, [257](#)
- Paul Scherer Institute, [10](#)
- pbrkxs, [432](#), [438](#)
- pdlyxs, [432](#), [439](#)
- Pelloni, [10](#), [13](#)
- PENDF, [3](#), [21](#), [25](#), [43](#), [45](#), [64](#), [67](#),  
[77](#), [79](#), [85](#), [90](#), [115](#), [122](#), [150](#),  
[165](#), [175](#), [191](#), [251](#), [276](#), [320](#),  
[373](#), [489](#), [497](#), [513](#), [527](#), [575](#),  
[604](#), [717](#), [728](#)
- penetrabilities, [52](#)
- penetrability factor, [61](#)
- phase shifts, [53](#), [61](#)
- phase-space distributions, [225](#), [504](#),  
[535](#)
- phnfix, [517](#), [542](#)
- phnout, [518](#)
- phofix, [516](#), [539](#)
- phonon expansion, [652](#)
- phoout, [518](#), [539](#)
- phoprt, [539](#)
- photoatomic, [4](#), [271](#), [456](#), [479](#), [516](#)
  - coherent, [272](#), [517](#)
  - incoherent, [272](#), [517](#)
  - KERMA, [274](#)
  - pair production, [273](#), [517](#)
  - photoelectric, [273](#), [517](#)
- photon interaction cross sections,  
[207](#), [516](#), [734](#)
- photon production, [506](#)
- photon transport, [207](#)
- photonuclear data, [517](#)
- photonuclear reactions, [271](#)
- Picton, [647](#), [648](#)
- pisotx, [432](#), [436](#)
- ploted, [397](#)
- plotnn, [397](#)
- plotp, [398](#)
- PLOTR, [2](#), [6](#), [11](#), [12](#), [14](#), [16](#), [575](#),  
[604](#), [739](#)
  - PLOTR input, [592](#)
- plotr, [599](#)
- plotting, [353](#), [575](#), [603](#), [625](#), [734](#),  
[736](#), [738](#), [739](#)
  - 2-D plots, [576](#)
  - 3-D plots, [587](#)
  - contour plots, [356](#)
  - correlation matrix, [356](#)
  - covariance data, [353](#)
  - standard deviation, [356](#)
- pointwise cross sections, [3](#), [4](#)
- poly2, [618](#), [620](#)
- poly3, [620](#)
- polyethylene, [174](#), [513](#), [515](#)
- Postscript plots, [12](#), [379](#)
- potential scattering, [55](#), [95](#)
- POWR, [2](#), [6](#), [9](#), [228](#), [547](#)
  - POWR input, [547](#)
- ppsammy, [60](#), [67](#), [70](#)
- preequilibrium fraction, [225](#), [502](#)
- press, [355](#)
- prinxs, [432](#)

- probability distribution for total, 633
- probability tables, 2, 11, 508, 631
- prompt fission, 203
- ptleg, 500, 530
- ptleg2, 501, 533, 534
- pttab, 500, 530
- pttab2, 501, 533
- PURR, 2, 6, 11–13, 16, 67, 105, 190, 191, 194, 242, 508, 631
  - PURR input, 638
- purrr, 639
- Q-value, 45
- Quality Assurance
  - QA, 721, 725
- quickw, 66, 69
- quikw, 114
- R-function, 58, 59
- R-matrix, 58, 60, 70
- radiation damage, 10, 115, 119, 625
- rdelas, 175
- rdf2aa, 67
- rdf2bw, 67
- rdf2hy, 67
- rdf2u0, 67
- rdf2u1, 67
- rdf2u2, 67
- rdf2un, 640
- rdf3un, 640
- rdfil2, 67
- rdheat, 640, 641
- rdsammy, 60, 67, 70
- rdunf2, 112, 113
- rdunf3, 112, 113
- reciprocity theorem, 195
- recoil distributions, 129
- RECONR, 1, 3, 9–11, 13, 14, 17, 21, 43, 77, 79, 81, 86, 87, 91, 108, 114, 122, 190, 191, 212, 235, 276, 320, 497, 529, 730, 733, 736
  - RECONR input, 71
- reconr, 65
- recout, 67, 69
- redundant reactions, 43, 66
- REED, 402
- Reich-Moore, 11, 45, 57
  - RM, 45, 51, 58, 59, 64, 68, 70, 312, 767
- Reich-Moore-Limited, 45, 60
  - RML, 45, 51, 59, 60, 62, 64, 66, 68, 70, 293, 313, 769
- repoz, 22, 37
- RESEND, 9, 51
- residual cross section expansion, 218
- resint, 565
- resolved resonance range, 44
- resolved-unresolved overlap, 106
- resonance angular distributions, 51, 59, 70
- resonance integral check, 49
- resonance integrals, 553, 554
- resonance interference, 201, 623
- resonance overlap, 98
- resonance parameters, 43, 292
- resonance reconstruction, 1, 3, 9, 43, 46
- resonance shift factors, 54
- restart, 21, 90
- resxs, 68, 69
- RESXS format, 489
- RESXSR, 2, 6, 489
  - RESXSR input, 493



- rget, 620
- RITE, 402
- rname, 601
- Robert, 648
- Robinson partition function, 126
- Rose, 51
- RSICC, 382
- rsiout, 566
- ruin, 65
- ruinb, 251
- ruinbr, 436
- ruinis, 432
- ruinm, 481
- Russell, 647
- Rutherford formula, 217
- $S_N$  transport, 205, 379
- s2sammy, 60, 66, 70
- SAMMY, 60
- Sartori, 10
- sbfill, 711
- scana, 28, 37
- scattering law, 169, 650
- scattering radius, 52
- SCT, *see* short collision time
- Seamon, 9, 12
- second-chance fission, 472
- self-shielding, 1, 3, 93, 95, 192, 235, 473, 489, 553, 631, 733, 734
- sensitivity analysis, 283, 353
- sensitivity systems, 5
- separation energy, 226, 502
- sequence-sequence overlap, 98
- set2d, 616
- set3d, 616, 617
- setr, 70
- shift factor, 61
- short collision time, 169, 647, 654
- shuffl, 435
- shufl, 485
- sig, 170, 177–179
- sigc, 304
- sigcoh, 176
- sigfig, 30, 37, 355
- sigl, 170, 177, 178
- sigma, 68
- SIGMA1, 9, 77, 88
- significant figures, 3, 30, 48, 77, 355
- sigp, 70
- sigu, 178
- sigunr, 68
- Single-Level Breit-Wigner, 51, 635
  - SLBW, 45, 51, 54, 57, 59, 64, 68–70, 312, 635
- sint, 712, 713
- sixbar, 152, 155, 156
- skiprz, 22, 37
- Skold, 669
- SLATEC, 88
- smooth cross sections, 44
- smoothing, 227, 506
- Soran, 9
- SPHINX, 399
- spin group, 60
- sqrt(E) shape, 227
- ssum, 620
- stable, 711
- stand, 309
- start, 710
- static structure factor, 663
- stopping power, 217, 476
- stounr, 242, 251, 256
- stripv, 621
- structured programming, 9
- summation cross sections, 3, 43, 45,

- 86
- summation reactions, 66
- TAB1, 24, 86
- tab1io, 25
- TAB2, 24
- tab2io, 25
- tabbar, 154–156
- tabdam, 154, 155
- tabsqr, 159
- tagit, 617
- TAPEID, 23, 65
- target-at-rest cross section, 690
- tabsq6, 156
- TDOWN, 399
- temperature correlations, 637
- terp, 176, 177
- terp1, 28, 40, 154, 158
- terpa, 28, 40, 154, 155, 177, 255, 264
- testing
  - Problem 01, 727
  - Problem 02, 731
  - Problem 03, 734
  - Problem 04, 736
  - Problem 05, 737
  - Problem 06, 739
  - Problem 07, 741
  - Problem 08, 743
  - Problem 09, 744
  - Problem 10, 747
  - Problem 11, 748
  - Problem 12, 751
  - Problem 13, 752
  - Problem 14, 754
  - Problem 15, 755
  - Problem 16, 758
  - Problem 17, 761
  - Problem 18, 764
  - Problem 19, 767
  - Problem 20, 769
  - test problems, 725
- text2, 620
- text3, 620
- thermal constants, 83
- thermal cross sections, 165, 475, 511
- thermal energy grid, 171
- thermal inelastic, 165, 512
- thermal MT numbers, 475, 524, 564
- thermal parameters, 77
- thermal reconstruction tolerance, 51, 77
- thermal scattering, 2, 647
- THERMR, 2–4, 9–11, 15, 17, 165, 190, 191, 209, 386, 513, 515, 547, 647, 658, 730
- THERMR input, 181
- thermr, 174
- thinb, 87, 88
- thnwrt, 438
- Thomson cross section, 272, 517
- thresholds, 45
- thrfix, 511, 536
- thrlod, 514, 536
- throu, 518, 536
- thrp, 536
- timer, 30, 36
- to fend, 23, 39
- to mend, 23, 39
- topfil, 500, 530, 534
- to send, 23, 39
- to tend, 23, 39
- tpend, 175, 177, 179
- tpidio, 25
- trans, 710, 711

- trans3, [619](#)
- transport approximations, [206](#)
- transport tables, [379](#)
- transw, [618](#)
- TRANSX, [2](#), [6](#), [10](#), [14](#), [193](#), [208](#), [237](#),  
[449](#), [489](#)
- TRANSX-2, [108](#)
- TRANSX-CTR, [108](#)
- Trkov, [12](#), [13](#), [15](#), [16](#)
- two-body kinematics, [214](#)
- two-body scattering, [500](#)
- TWODANT, [6](#)
- txtlen, [620](#)
- typen, [536](#)
- typewriter font, [8](#)
- uncertainties, [286](#)
- union grid, [3](#), [6](#), [9](#), [43](#), [489](#), [497](#)
- uniong, [300](#)
- unionx, [497](#), [500](#), [528](#)
- unresl, [113](#)
- unresolved  $\sigma_0$  range, [107](#)
- unresolved energy grid, [46](#), [106](#)
- unresolved resonance range, [1–3](#), [11](#),  
[44](#), [46](#), [64](#), [93](#), [194](#), [508](#), [631](#)
- UNRESR, [1](#), [3](#), [9](#), [67](#), [69](#), [93](#), [190](#),  
[191](#), [194](#), [242](#), [631](#), [633](#), [635](#),  
[733](#)
- UNRESR input, [109](#)
- UNRESR output, [110](#)
- unresr, [111](#)
- unrest, [642](#)
- unresx, [641](#)
- UPD, [401](#), [721](#)
- upscatter, [475](#)
- user grid, [46](#)
- uunfac, [114](#)
- uw, [111](#), [114](#)
- uwtab, [111](#), [114](#)
- UXSR, [102](#), [105](#), [107](#)
- vday, [20](#)
- vect2, [619](#)
- vect3, [619](#)
- vector, [482](#), [483](#)
- vers, [20](#)
- VIEWR, [2](#), [5](#), [6](#), [12](#), [134](#), [160](#), [357](#),  
[379](#), [397](#), [510](#), [542](#), [575](#), [600](#),  
[603](#)
- VIEWR input, [604](#)
- viewr, [603](#), [616](#)
- VIM, [631](#)
- Vineyard, [663](#), [669](#), [705](#)
- Want\_Angular\_Dist, [64](#), [67](#), [70](#)
- Want\_Partial\_Derivs, [70](#)
- Want\_SAMRML\_BW, [66](#), [70](#)
- Want\_SAMRML\_RM, [64](#), [66](#), [70](#)
- warning messages, [30](#)
- water, [182](#), [513](#), [677](#)
- Watt fission spectrum, [501](#)
- wclock, [30](#), [36](#)
- Weapons Program, [9](#)
- weight functions, [4](#), [235](#), [271](#)
- weighting flux, [191](#), [285](#), [623](#)
- Weisbin, [9](#)
- Westinghouse, [399](#)
- White, [12](#), [13](#), [15](#)
- wide, [67](#), [106](#), [113](#)
- Wigner distributions, [631](#)
- Wigner rational approximation, [195](#)
- wimout, [568](#)
- WIMS, [11](#), [553](#)
- WIMS-D, [2](#), [6](#), [553](#), [572](#)
- WIMS-E, [2](#), [6](#), [553](#)
- WIMS format, [569](#)

WIMSR, [2](#), [6](#), [11](#), [12](#), [187](#), [489](#), [553](#)

WIMSR input, [560](#)

window, [618](#)

wmunit, [565](#)

Wright, [10](#)

WRITER, [572](#)

wrtmtx, [435](#)

wtab, [66](#)

xinvrs, [619](#)

xscale, [619](#)

xseco, [567](#)

xsecs, [566](#)

xsproc, [437](#)

yinvrs, [619](#)

yscale, [619](#)

zirconium hydride, [174](#), [513](#), [515](#)

zscale, [619](#)